

**REPRODUCIBLE COPY  
(FACILITY CASEFILE COPY)**

*Sup #77-16261*  
*N77-17000*

NASA CR-145046

**SUPERSONIC PRESSURE MEASUREMENTS AND COMPARISON  
OF THEORY TO EXPERIMENT FOR AN ARROW-WING  
CONFIGURATION**

**Marjorie E. Manro**

**November 1976**

**Prepared under contract NAS1-14141 by**

**Boeing Commercial Airplane Company  
P.O. Box 3707  
Seattle, Washington 98124**

**for**

**NASA**

National Aeronautics and  
Space Administration



1. Report No <b>NASA CR-145046</b>		2. Government Accession No.		3. Recipient's Catalog No.	
4. Title and Subtitle <b>SUPERSONIC PRESSURE MEASUREMENTS AND COMPARISON OF THEORY TO EXPERIMENT FOR AN ARROW-WING CONFIGURATION</b>				5. Report Date <b>November 1976</b>	
				6. Performing Organization Code	
7. Author(s) <b>Marjorie E. Manro</b>				8. Performing Organization Report No. <b>D6-44224</b>	
9. Performing Organization Name and Address <b>Boeing Commercial Airplane Company P.O. Box 3707 Seattle, Washington 98124</b>				10. Work Unit No. <b>743-01-12-02</b>	
				11. Contract or Grant No. <b>NAS1-14141</b>	
12. Sponsoring Agency Name and Address <b>Langley Research Center National Aeronautics and Space Administration Washington, D.C. 20546</b>				13. Type of Report and Period Covered <b>Contractor Report</b>	
				14. Sponsoring Agency Code	
15. Supplementary Notes <b>Technical monitor, Percy J. Bobbitt; Theoretical Aerodynamics Branch, NASA Langley Research Center, Hampton, Virginia. Experimental and attached flow theory pressure data are available on magnetic tape. Final report.</b>					
16. Abstract  <p><b>A wind tunnel test of an arrow-wing-body configuration consisting of flat and twisted wings, as well as leading- and trailing-edge control surface deflections, has been conducted at Mach numbers from 1.54 to 2.50 to provide an experimental pressure data base for comparison with theoretical methods. Theory-to-experiment comparisons of detailed pressure distributions have been made using a state-of-the-art inviscid-flow, constant-pressure-panel method. The purpose of these comparisons was to delineate conditions under which this theory is valid for both flat and twisted wings.</b></p> <p><b>This report supplements an earlier test program at Mach numbers from 0.40 to 1.1 using the same models. The results of the entire subsonic-transonic investigation are summarized in NASA CR-2610 with a discussion of both the experimental results and theory-to-experiment comparisons. NASA CR-132727 presents more detailed results of the experimental phase of the program for the base configuration (flat wing) and the effects of wing twist, leading-edge shape, and the leading-edge droop. The effects of full- and partial-span trailing-edge control surface deflection and partial-span leading-edge control surface deflection are presented in NASA CR-132728. NASA CR-132729 presents more detailed comparisons of the experimental pressure data with the results of attached flow methods.</b></p>					
17. Key Words (Suggested by Author(s)) <b>Aeroelasticity Experimental pressure distributions Aerodynamic theory Arrow-wing configuration Wind tunnel test</b>				18. Distribution Statement  <b>Unclassified-unlimited</b>  <b>Subject Category 02</b>	
19. Security Classif. (of this report) <b>Unclassified</b>		20. Security Classif. (of this page) <b>Unclassified</b>		21. No. of Pages <b>691</b>	
				22. Price*	



**Page  
Intentionally  
Left Blank**

# CONTENTS

	Page
SUMMARY .....	1
INTRODUCTION .....	1
SYMBOLS .....	3
EXPERIMENTAL TASK .....	5
Wind Tunnel Models .....	5
Flat Wing .....	5
Twisted Wing .....	5
Body .....	5
Wing-Body Intersection .....	7
Pressure Orifice Locations .....	7
Design and Construction .....	7
Wind Tunnel Capabilities .....	16
Tests and Data Acquisition .....	17
Data Tape Description .....	19
Experimental Data .....	19
Base Configuration .....	21
Effect of Leading-Edge Shape .....	21
Effect of Wing Twist .....	21
Effect of Leading-Edge Droop .....	21
Effect of Full-Span Trailing-Edge Control Surface Deflection .....	22
Effect of Partial-Span Trailing-Edge Control Surface Deflection .....	22
Effect of Mach Number .....	22
THEORY COMPARISON TASK .....	23
Attached Flow Theory-FLEXSTAB .....	23
Theory-to-Experiment Comparisons .....	23
Base Configuration .....	25
Twisted Wing .....	25
Leading-Edge Droop .....	26
Full-Span Trailing-Edge Control Surface Deflection .....	26
Partial-Span Trailing-Edge Control Surface Deflection .....	26
Effect of Mach Number .....	26
Empirical Corrections .....	26
CONCLUDING REMARKS .....	28
APPENDIX A-Detailed Test Log .....	29
APPENDIX B-Data Reduction and Presentation .....	45
APPENDIX C-Summary of Subsonic-Transonic Program .....	57
REFERENCES .....	71

## TABLES

No.		Page
1	Wing Half-Thickness Distribution, Percent Chord .....	6
2	Wing Pressure Orifice Locations, Percent Local Chord .....	8
3	Body Pressure Orifice Locations .....	15
4	Summary of Test Conditions by Run Number.....	18
5	Summary of Experimental Data Presentations by Figure Number .....	20
6	Summary of FLEXSTAB Conditions by Run Number .....	24
7	Summary of FLEXSTAB-to-Experiment Comparisons by Figure Number .....	25
A-1	Experimental Data Test Point Log. Twisted Wing, Rounded Leading Edge; L.E. Deflection, Full span = $0.0^\circ$ .....	30
A-2	Experimental Data Test Point Log. Flat Wing, Rounded Leading Edge; L.E. Deflection, Full Span = $5.1^\circ$ ; T.E. Deflection, Full Span = $0.0^\circ$ .....	32
A-3	Experimental Data Test Point Log. Flat Wing, Rounded Leading Edge; L.E. Deflection, Full Span = $0.0^\circ$ .....	33
A-4	Experimental Data Test Point Log. Flat Wing, Sharp Leading Edge; T.E. Deflection, Full Span = $0.0^\circ$ .....	38
A-5	FLEXSTAB Test Point Log. Twisted Wing, Rounded Leading Edge; L.E. Deflection, Full Span = $0.0^\circ$ .....	39
A-6	FLEXSTAB Test Point Log. Flat Wing, Rounded Leading Edge; L.E. Deflection, Full Span = $5.1^\circ$ ; T.E. Deflection, Full Span = $0.0^\circ$ .....	40
A-7	FLEXSTAB Test Point Log. Flat Wing, Rounded Leading Edge; L.E. Deflection, Full Span = $0.0^\circ$ .....	41
B-1	Integration Constants .....	54
C-1	Summary of Subsonic/Transonic Test Conditions by Run Number .....	59
C-2	Summary of Subsonic/Transonic FLEXSTAB Conditions by Run Number .....	67



# FIGURES

No.		Page
1	General Arrangement and Characteristics .....	72
2	Spanwise Twist Distribution for the Model Wing .....	73
3	Pressure Orifice Locations .....	74
4	Control Surface Bracket Details .....	75
5	Schematic of 9-by-7-ft Leg of NASA Ames Unitary Wind Tunnel .....	76
6	Data Acquisition and Reduction System-9-by-7-ft Leg of Ames Unitary Wind Tunnel .....	77
7	Wing Tunnel Model-Flat Wing, Rounded L.E. ....	78
8	Wind Tunnel Model-Twisted Wing .....	78
9	Model Installation in 9-by-7-ft Leg of NASA Ames Unitary Wind Tunnel .....	79
10	Wing Experimental Data-Effect of Angle of Attack; Flat Wing, Rounded L.E.; L.E. Deflection, Full Span = $0.0^\circ$ ; T.E. Deflection, Full Span = $0.0^\circ$ ; M = 1.54 .....	80
11	Wing Experimental Data-Effect of Angle of Attack; Flat Wing, Rounded L.E.; L.E. Deflection, Full Span = $0.0^\circ$ ; T.E. Deflection, Full Span = $0.0^\circ$ ; M = 1.70 .....	90
12	Wing Experimental Data-Effect of Angle of Attack; Flat Wing, Rounded L.E.; L.E. Deflection, Full Span = $0.0^\circ$ ; T.E. Deflection, Full Span = $0.0^\circ$ ; M = 2.10 .....	100
13	Wing Experimental Data-Effect of Angle of Attack; Flat Wing, Rounded L.E.; L.E. Deflection, Full Span = $0.0^\circ$ ; T.E. Deflection, Full Span = $0.0^\circ$ ; M = 2.50 .....	110
14	Wing Experimental Data-Effect of Angle of Attack; Flat Wing, Sharp L.E.; L.E. Deflection, Full Span = $0.0^\circ$ ; T.E. Deflection, Full Span = $0.0^\circ$ ; M = 1.70 .....	120
15	Wing Experimental Data-Effect of Angle of Attack; Flat Wing, Sharp L.E.; L.E. Deflection, Full Span = $0.0^\circ$ ; T.E. Deflection, Full Span = $0.0^\circ$ ; M = 2.50 .....	130
16	Wing Experimental Data-Effect of L.E. Shape With Angle of Attack; Flat Wing; L.E. Deflection, Full Span = $0.0^\circ$ ; T.E. Deflection, Full Span = $0.0^\circ$ ; M = 1.70 .....	140
17	Wing Experimental Data-Effect of Angle of Attack; Twisted Wing, Rounded L.E.; L.E. Deflection, Full Span = $0.0^\circ$ ; T.E. Deflection, Full Span = $0.0^\circ$ ; M = 1.60 .....	152
18	Wing Experimental Data-Effect of Angle of Attack; Twisted Wing, Rounded L.E.; L. E. Deflection, Full Span = $0.0^\circ$ ; T.E. Deflection, Full Span = $0.0^\circ$ ; M = 1.70 .....	162
19	Wing Experimental Data-Effect of Angle of Attack; Twisted Wing, Rounded L.E.; L. E. Deflection, Full Span = $0.0^\circ$ ; T.E. Deflection, Full Span = $0.0^\circ$ ; M = 1.90 .....	172
20	Wing Experimental Data-Effect of Angle of Attack; Twisted Wing, Rounded L.E.; L.E. Deflection, Full Span = $0.0^\circ$ ; T.E. Deflection, Full Span = $0.0^\circ$ ; M = 2.10 .....	182

## FIGURES (Continued)

No.	Page
21	Wing Experimental Data—Effect of Angle of Attack; Twisted Wing, Rounded L.E.; L.E. Deflection, Full Span = $0.0^\circ$ ; T.E. Deflection, Full Span = $0.0^\circ$ ; M = 2.50 ..... 192
22	Wing Experimental Data—Effect of Wing Twist With Angle of Attack; Rounded L.E.; L.E. Deflection, Full Span = $0.0^\circ$ ; T.E. Deflection, Full Span = $0.0^\circ$ ; M = 1.70 ..... 202
23	Wing Experimental Data—Effect of Wing Twist With Angle of Attack; Rounded L.E.; L.E. Deflection, Full Span = $0.0^\circ$ ; T.E. Deflection, Full Span = $0.0^\circ$ ; M = 2.50 ..... 214
24	Wing Experimental Data—Effect of Full Span L. E. Deflection With Angle of Attack; Flat Wing; Rounded L.E.; T.E. Deflection, Full Span = $0.0^\circ$ ; M = 1.70 ..... 226
25	Wing Experimental Data—Effect of Full Span L.E. Deflection With Angle of Attack; Flat Wing; Sharp L.E.; T.E. Deflection, Full Span = $0.0^\circ$ ; M = 1.70 ..... 238
26	Wing Experimental Data—Effect of Full Span T.E. Deflection With Angle of Attack; Flat Wing, Rounded L.E.; L.E. Deflection, Full Span = $0.0^\circ$ ; M = 1.70 ..... 250
27	Wing Experimental Data—Effect of Full Span T.E. Deflection With Angle of Attack; Flat Wing, Rounded L.E.; L.E. Deflection, Full Span = $0.^\circ$ ; M = 2.50 ..... 268
28	Wing Experimental Data—Effect of Full Span T.E. Deflection With Angle of Attack; Twisted Wing, Rounded L.E.; L.E. Deflection, Full Span = $0.0^\circ$ ; M = 1.70 ..... 286
29	Wing Experimental Data—Effect of Partial Span T. E. Deflection With Angle of Attack; Flat Wing, Rounded L.E.; L.E. Deflection, Full Span = $0.0^\circ$ ; T.E. Deflection, Outboard = $0.0^\circ$ ; M = 1.70 ..... 298
30	Wing Experimental Data—Effect of Partial Span T. E. Deflection With Angle of Attack; Flat Wing, Rounded L.E.; L.E. Deflection Full Span = $0.0^\circ$ ; T.E. Deflection, Outboard = $0.0^\circ$ ; M = 2.10 ..... 300
31	Wing Experimental Data—Effect of Partial Span T. E. Deflection With Angle of Attack; Flat Wing, Rounded L.E.; L.E. Deflection, Full Span = $0.0^\circ$ ; T.E. Deflection, Outboard = $0.0^\circ$ ; M = 2.50 ..... 302
32	Wing Experimental Data—Effect of Partial Span T.E. Deflection With Angle of Attack; Flat Wing, Rounded L.E.; L.E. Deflection, Full Span = $0.0^\circ$ ; T.E. Deflection, Inboard = $0.0^\circ$ ; M = 1.70 ..... 304
33	Wing Experimental Data—Effect of Partial Span T.E. Deflection With Angle of Attack; Flat Wing, Rounded L.E.; L.E. Deflection, Full Span = $0.0^\circ$ ; T.E. Deflection, Inboard = $0.0^\circ$ ; M = 2.10 ..... 306
34	Wing Experimental Data—Effect of Partial Span T.E. Deflection With Angle of Attack; Flat Wing, Rounded L.E.; L.E. Deflection, Full Span = $0.0^\circ$ ; T.E. Deflection, Inboard = $0.0^\circ$ ; M = 2.50 ..... 308
35	Wing Experimental Data—Effect of Partial Span T.E. Deflection With Angle of Attack; Flat Wing, Rounded L.E.; L.E. Deflection, Full Span = $0.0^\circ$ ; M = 1.70 ..... 310

## FIGURES (Continued)

No.	Page
36	Wing Experimental Data—Effect of Partial Span T.E. Deflection With Angle of Attack; Flat Wing, Rounded L.E.; L.E. Deflection, Full Span = 0.0°; M = 2.10 ..... 312
37	Wing Experimental Data—Effect of Partial Span T.E. Deflection With Angle of Attack; Flat Wing, Rounded L.E.; L.E. Deflection, Full Span = 0.0°; M = 2.50 ..... 314
38	Body Surface Longitudinal Pressure Distributions—Effect of Angle of Attack; Flat Wing, Rounded L.E.; L.E. Deflection, Full Span = 0.0°; T.E. Deflection, Full Span = 0.0°; M = 1.54 ..... 316
39	Body Surface Longitudinal Pressure Distributions—Effect of Angle of Attack; Flat Wing, Rounded L.E.; L.E. Deflection, Full Span = 0.0°; T.E. Deflection, Full Span = 0.0°; M = 1.70 ..... 318
40	Body Surface Longitudinal Pressure Distributions—Effect of Angle of Attack; Flat Wing, Rounded L.E.; L.E. Deflection, Full Span = 0.0°; T.E. Deflection, Full Span = 0.0°; M = 2.10 ..... 320
41	Body Surface Longitudinal Pressure Distributions—Effect of Angle of Attack; Flat Wing, Rounded L.E.; L.E. Deflection, Full Span = 0.0°; T.E. Deflection, Full Span = 0.0°; M = 2.50 ..... 322
42	Body Surface Longitudinal Pressure Distributions—Effect of Angle of Attack; Flat Wing, Sharp L.E.; L.E. Deflection, Full Span = 0.0°; T.E. Deflection, Full Span = 0.0°; M = 1.70 ..... 324
43	Body Surface Longitudinal Pressure Distributions—Effect of Angle of Attack; Twisted Wing, Rounded L.E.; L.E. Deflection, Full Span = 0.0°; T.E. Deflection, Full Span = 0.0°; M = 1.60 ..... 326
44	Body Surface Longitudinal Pressure Distributions—Effect of Angle of Attack; Twisted Wing, Rounded L.E.; L.E. Deflection, Full Span = 0.0°; T.E. Deflection, Full Span = 0.0°; M = 1.70 ..... 328
45	Body Surface Longitudinal Pressure Distributions—Effect of Angle of Attack; Twisted Wing, Rounded L.E.; L.E. Deflection, Full Span = 0.0°; T.E. Deflection, Full Span = 0.0°; M = 1.90 ..... 330
46	Body Surface Longitudinal Pressure Distributions—Effect of Angle of Attack; Twisted Wing, Rounded L.E.; L.E. Deflection, Full Span = 0.0°; T.E. Deflection, Full Span = 0.0°; M = 2.10 ..... 332
47	Body Surface Longitudinal Pressure Distributions—Effect of Angle of Attack; Twisted Wing, Rounded L.E.; L.E. Deflection, Full Span = 0.0°; T.E. Deflection, Full Span = 0.0°; M = 2.50 ..... 334
48	Wing Experimental Data—Effect of Mach Number and Angle of Attack; Flat Wing, Rounded L.E.; L.E. Deflection, Full Span = 0.0°; T.E. Deflection, Full Span = 0.0° ..... 336
49	Wing Experimental Data—Effect of Mach Number and Angle of Attack; Flat Wing, Sharp L.E.; L.E. Deflection, Full Span = 0.0°; T.E. Deflection, Full Span = 0.0° ..... 372
50	Wing Experimental Data—Effect of Mach Number and Angle of Attack; Twisted Wing, Rounded L.E.; L.E. Deflection, Full Span = 0.0°; T.E. Deflection, Full Span = 0.0° ..... 388



## FIGURES (Continued)

No.	Page
51	Wing Experimental Data—Effect of Mach Number and Angle of Attack; Flat Wing, Rounded L.E.; L.E. Deflection, Full Span = $5.1^\circ$ ; T.E. Deflection, Full Span = $0.0^\circ$ ..... 404
52	Wing Experimental Data—Effect of Mach Number and Angle of Attack; Flat Wing, Rounded L.E.; L.E. Deflection, Full Span = $0.0^\circ$ ; T.E. Deflection, Full Span = $8.3^\circ$ ..... 420
53	Wing Experimental Data—Effect of T.E. Control Surface Deflection With Mach Number and Angle of Attack; Flat Wing, Rounded L.E.; L.E. Deflection, Full Span = $0.0^\circ$ ..... 436
54	Paneling for FLEXSTAB Computer Program ..... 451
55	Wing Theory-to-Experiment Comparison—Flat Wing, Rounded L.E.; L.E. Deflection, Full Span = $0.0^\circ$ ; T.E. Deflection, Full Span = $0.0^\circ$ ; M = 1.70 ..... 452
56	Wing Theory-to-Experiment Comparison—Flat Wing, Rounded L.E.; L.E. Deflection, Full Span = $0.0^\circ$ ; T.E. Deflection, Full Span = $0.0^\circ$ ; M = 2.10 ..... 470
57	Wing Theory-to-Experiment Comparison—Flat Wing, Rounded L.E.; L.E. Deflection, Full Span = $0.0^\circ$ ; T.E. Deflection, Full Span = $0.0^\circ$ ; M = 2.50 ..... 488
58	Body Theory-to-Experiment Comparison—Flat Wing, Rounded L.E.; L.E. Deflection, Full Span = $0.0^\circ$ ; T.E. Deflection, Full Span = $0.0^\circ$ ; M = 1.70 ..... 506
59	Body Theory-to-Experiment Comparison—Flat Wing, Rounded L.E.; L.E. Deflection, Full Span = $0.0^\circ$ ; T.E. Deflection, Full Span = $0.0^\circ$ ; M = 2.10 ..... 510
60	Body Theory-to-Experiment Comparison—Flat Wing, Rounded L.E.; L.E. Deflection, Full Span = $0.0^\circ$ ; T.E. Deflection, Full Span = $0.0^\circ$ ; M = 2.50 ..... 514
61	Wing Theory-to-Experiment Comparison—Twisted Wing, Rounded L.E.; L.E. Deflection, Full Span = $0.0^\circ$ ; T.E. Deflection, Full Span = $0.0^\circ$ ; M = 1.70 ..... 518
62	Wing Theory-to-Experiment Comparison—Twisted Wing, Rounded L.E.; L.E. Deflection, Full Span = $0.0^\circ$ ; T.E. Deflection, Full Span = $0.0^\circ$ ; M = 2.10 ..... 536
63	Wing Theory-to-Experiment Comparison—Twisted Wing, Rounded L.E.; L.E. Deflection, Full Span = $0.0^\circ$ ; T.E. Deflection, Full Span = $0.0^\circ$ ; M = 2.50 ..... 554
64	Wing Theory-to-Experiment Comparison—Flat Wing, Rounded L.E.; L.E. Deflection, Full Span = $5.1^\circ$ ; T.E. Deflection, Full Span = $0.0^\circ$ ; M = 1.70 ..... 572
65	Wing Theory-to-Experiment Comparison—Flat Wing, Rounded L.E.; L.E. Deflection, Full Span = $0.0^\circ$ ; T.E. Deflection, Full Span = $8.3^\circ$ ; M = 2.10 ..... 590

## FIGURES (Concluded)

No.	Page
66 Wing Theory-to-Experiment Comparison-Flat Wing, Rounded L.E.; L.E. Deflection, Full Span = $0.0^\circ$ ; T.E. Deflection, Outboard = $0.0^\circ$ ; M = 2.10 .....	608
67 Wing Theory-to-Experiment Comparison-Flat Wing, Rounded L.E.; L.E. Deflection, Full Span = $0.0^\circ$ ; T.E. Deflection, Inboard = $0.0^\circ$ ; M = 2.10 .....	626
68 Wing Theory-to-Experiment Comparison-Effect of Mach Number and Angle of Attack; Flat Wing, Rounded L.E.; L.E. Deflection, Full Span = $0.0^\circ$ ; T.E. Deflection, Full Span = $0.0^\circ$ .....	644
69 Wing Theory-to-Experiment Comparison-Effect of Mach Number and Angle of Attack; Twisted Wing, Rounded L.E.; L.E. Deflection, Full Span = $0.0^\circ$ ; T.E. Deflection, Full Span = $0.0^\circ$ .....	650
70 Wing Theory-to-Experiment Comparison-Effect of Mach Number and Angle of Attack; Flat Wing, Rounded L.E.; L.E. Deflection, Full Span = $0.0^\circ$ ; T.E. Deflection, Full Span = $8.3^\circ$ .....	656
71 Pseudo Aeroelastic Predictions; Rounded L.E.; L.E. Deflection, Full Span = $0.0^\circ$ ; T.E. Deflection, Full Span = $0.0^\circ$ ; M = 2.10 .....	662
B-1 Codes Used to Interpolate and Extrapolate .....	46
C-1 Boeing Transonic Wind Tunnel .....	58
C-2 Model in Boeing Transonic Wind Tunnel-Flat Wing, Rounded L.E.; L.E. Deflection, Full Span = $0.0^\circ$ ; T.E. Deflection, Full Span = $0.0^\circ$ .....	62
C-3 Model in Boeing Transonic Wind Tunnel-Twisted Wing, Rounded L.E.; L.E. Deflection, Full Span = $0.0^\circ$ ; T. E. Deflection, Full Span = $4.1^\circ$ .....	63
C-4 Model Installation in Boeing Transonic Wind Tunnel .....	64
C-5 Paneling for FLEXSTAB Computer Program, M = 1.05 and 1.11 .....	66

# **SUPERSONIC PRESSURE MEASUREMENTS AND COMPARISON OF THEORY TO EXPERIMENT FOR AN ARROW-WING CONFIGURATION**

Marjorie E. Manro  
Boeing Commercial Airplane Company

## **SUMMARY**

A wind tunnel test of an arrow-wing body configuration consisting of flat and twisted wings, as well as a variety of leading- and trailing-edge control surface deflections, has been conducted primarily at Mach numbers of 1.70, 2.10, and 2.50 to provide an experimental pressure data base for comparison with theoretical methods. Some data were also obtained at  $M = 1.54$ , 1.60, and 1.90. Theory-to-experiment comparisons of detailed pressure distributions have been made using a state-of-the-art inviscid-flow, constant-pressure-panel computer program. The purpose of these comparisons was to delineate conditions under which this theory is valid for both flat and twisted wings.

This report supplements an earlier test program at Mach numbers from 0.40 to 1.1 using the same models. These data have been reported in NASA CR-2610, NASA CR-132727, NASA CR-132728, and NASA CR-132729 (refs. 1 through 4).

## **INTRODUCTION**

Accurate analytical techniques for predicting the magnitude and distribution of aeroelastic loads are required in order to design, in an optimum manner, the structure of large flexible aircraft. Uncertainties in the characteristics of loads may result in an improper accounting for aeroelastic effects, leading to understrength or overweight designs and unacceptable fatigue life. Moreover, correct prediction of loads and the resultant structural deformations is essential to the determination of control power requirements, control surface moments, and aircraft stability and control characteristics. The alternative to the development of satisfactory analytical techniques is exorbitantly expensive, time-consuming wind tunnel testing for each aircraft configuration. In addition, the ability to perform meaningful parametric or tradeoff studies is severely limited by the lack of accurate prediction techniques.



In the structural design of an aircraft, wind tunnel pressure tests on a single wing shape (with twist and camber) are extrapolated by means of an aeroelastic solution to obtain the load distributions for all other elastically deformed shapes of that wing. In this process, equations are used that relate the changes in local pressure to changes in structural deformation. Methods for high aspect ratio wings at subsonic speeds are well developed and have been substantiated by flight tests. However, for thin, highly swept wings, where various nonlinear phenomena become important, no satisfactory methods are available. Until such tools are developed the need will remain for wind tunnel test programs simulating each flight design condition on the flexible airplane.

The purpose of this study was to obtain some of the required experimental data for a highly swept, thin wing at supersonic Mach numbers and, at the same time, to provide comparisons with a state-of-the-art attached-flow method. The study was viewed as a two-part effort consisting of an experimental task and a theory comparison task.

The objective of the experimental task was to provide measured load distributions on an uncambered and untwisted wing as well as on a model deformed to simulate a representative twist distribution. Both models have deflectable trailing-edge control surfaces; the flat wing also has deflectable leading-edge control surfaces. These load distributions were used in the theoretical task to assess the adequacy of a linear constant-pressure-panel method.

The models chosen for this study combined a slender body with wings having a leading-edge sweep of  $71.2^\circ$  and a thickness of 3.3% (see fig. 1). Model components included both flat and twisted wings, deflectable full-span and half-span leading- and trailing-edge control surfaces, and both rounded and sharp leading edges. The tests were conducted in the 9- by 7-ft leg of the NASA Ames Unitary Wind Tunnel at Mach numbers from 1.54 to 2.50 with angles of attack from  $-8^\circ$  to  $+15^\circ$ . The measurements included pressure data on both the wing and body, as well as total force and moment data.

The theoretical calculations were carried out using FLEXSTAB, a state-of-the-art linear-flow technique, to predict detailed pressures over both the flat and twisted wings. Comparisons were made of theoretical and experimental pressures for both wings with and without deflected control surfaces.

The results of the various aerodynamic calculations and theory-to-experiment comparisons have been used to point out areas where linear theory is inadequate for design, and to examine combined theoretical and empirical approaches to aeroelastic design based on lifting- surface solutions.

## SYMBOLS

<b>b</b>	wingspan, cm
<b>BL</b>	buttock line, cm; distance outboard from model plane of symmetry
<b>bpi</b>	bits per inch
<b>c</b>	section chord length, cm
<b><math>\bar{c}</math>, M.A.C.</b>	mean aerodynamic chord length, cm
<b><math>C_B</math></b>	surface bending moment coefficient referenced to $y_{ref}$ ; positive wingtip up
<b><math>C_c</math></b>	section chord force coefficient; positive aft
<b><math>C_m</math></b>	section pitching moment coefficient referenced to section leading edge; positive leading edge up
<b><math>C_{m.25c}</math></b>	section pitching moment coefficient referenced to section 0.25c; positive leading edge up
<b><math>C_M</math></b>	surface pitching moment coefficient, referenced to 0.25 M.A.C.; positive leading edge up
<b><math>C_n</math></b>	section normal force coefficient; positive up
<b><math>C_N</math></b>	surface normal force coefficient; positive up
<b><math>C_p</math></b>	pressure coefficient = $\frac{\text{measured pressure} - \text{reference pressure}}{q}$
<b>D</b>	body diameter, cm
<b>M</b>	Mach number
<b>MS</b>	model station, cm; measured aft along the body centerline from the nose
<b><math>p_s</math></b>	static pressure, kN/m <sup>2</sup>
<b><math>p_t</math></b>	total pressure, kN/m <sup>2</sup>
<b>q</b>	dynamic pressure, kN/m <sup>2</sup>
<b>S</b>	reference area used for surface coefficients, cm <sup>2</sup>
<b><math>S_h</math></b>	area of streamwise strip associated with a pressure station, cm <sup>2</sup> ; used in summation of section force coefficients (app. B)

$x,y,z$	general coordinates for distances in the longitudinal, lateral, and vertical directions, respectively.
$y_{ref}$	distance outboard of model centerline of the bending moment reference point, cm
$\alpha$	corrected angle of attack, degrees; the angle between the wing root chord and the relative wind measured in the model plane of symmetry; includes compensation for sting deflection, tunnel flow angularities, and wall effects; positive nose up with respect to relative wind
$\alpha_{sec}$	wing twist angle relative to wing reference plane, degrees; positive leading edge up
$\Delta C_p$	increment between adjacent lines on isobars
$\delta$	control surface deflection, degrees; positive leading edge down for leading edge (see exception in app. B) and trailing edge down for trailing edge
$\eta$	fraction of wing semispan, $y/(b/2)$
$\Lambda$	sweep angle, degrees; measured from a line perpendicular to the model centerline, positive aft
$\phi$	angle defining location of pressure orifices on the surface of the cylindrical body at a constant MS, degrees; measured from the top of the body
Subscripts:	
L.E.	leading-edge control surface
r	wing root
s	referenced to segment of local chord
T.E.	trailing-edge control surface



## **EXPERIMENTAL TASK**

### **WIND TUNNEL MODELS**

The configuration chosen for this study was a thin, low aspect ratio, highly swept wing mounted below the centerline of a high fineness ratio body. The general arrangement and characteristics of the model are shown in figure 1. Two complete wings were constructed, one with no camber or twist and one with no camber but with a spanwise twist variation. Deflectable control surfaces were available on these wings.

#### **FLAT WING**

The mean surface of the flat wing is the wing reference plane. The nondimensional wing thickness distributions, shown in table 1, deviate slightly from a constant for all streamwise sections to maintain a finite thickness of 0.0254 cm (0.01 in.) at the trailing edge (a manufacturing requirement). The wing was designed with a full-span, 25% chord, trailing-edge control surface. Sets of fixed angle brackets allowed streamwise deflections of  $\pm 4.1^\circ$ ,  $\pm 8.3^\circ$ ,  $\pm 17.7^\circ$ , and  $\pm 30.2^\circ$ , as well as  $0.0^\circ$ . A removable full-span leading-edge control surface (15% of streamwise chord) could be placed in an undeflected position and also drooped  $5.1^\circ$  and  $12.8^\circ$  with fixed angle brackets. Both the leading- and trailing-edge control surfaces extended from the side of the body ( $0.087 b/2$ ) to the wingtip and were split near midspan ( $0.570 b/2$ ). Both the inboard and outboard portions of the control surfaces could be deflected separately and were rotated about points in the wing reference plane. An additional leading-edge control surface for this wing was constructed with a sharp ( $20^\circ$  included angle) leading edge to examine the effects of leading-edge shape. The surface ordinates and slopes of this leading-edge segment were continuous with those of the flat wing at the leading-edge hingeline (table 1). The sharp leading edge was smoothly faired from  $0.180 b/2$  into the fixed portion of the rounded leading edge at  $0.090 b/2$ .

#### **TWISTED WING**

The mean surface of the twisted wing was generated by rotating the streamwise section chord lines about the 75% local chord points (trailing-edge control surface hingeline). The spanwise variation of twist is shown in figure 2. The hingeline was straight and located in the wing reference plane at its inboard end ( $0.087 b/2$ ) and 2.261 cm (0.890 in.) above the wing reference plane at the wingtip. The airfoil thickness distribution (table 1) and the trailing-edge control surface location and available deflections were identical to those of the flat wing.

#### **BODY**

The body was circular in cross section and had a straight centerline. The body geometry is shown in figure 1. The sting was an integral part of the model body.

Table 1.—Wing Half-Thickness Distribution, Percent Chord

x/c, percent chord	0 b/2	0.09 b/2	0.20 b/2	0.35 b/2	0.50 b/2	0.65 b/2	0.80 b/2	0.93 b/2	1.00 b/2
Flat wing with rounded leading edge and twisted wing									
.0000	.0000	.0000	.0000	.0000	.0000	.0000	.0000	.0000	.0000
.1250	.3359	.3359	.3359	.3359	.3360	.3360	.3360	.3362	.3364
.2500	.4506	.4506	.4506	.4506	.4507	.4507	.4508	.4509	.4512
.5000	.6064	.6064	.6064	.6064	.6065	.6065	.6066	.6068	.6072
.7500	.7247	.7247	.7247	.7248	.7248	.7249	.7250	.7253	.7258
1.0000	.8182	.8182	.8182	.8183	.8183	.8184	.8185	.8188	.8194
1.5000	.9520	.9520	.9520	.9521	.9522	.9523	.9525	.9530	.9538
2.5000	1.1191	1.1191	1.1192	1.1192	1.1194	1.1195	1.1199	1.1206	1.1219
5.0000	1.3448	1.3448	1.3449	1.3450	1.3453	1.3456	1.3462	1.3475	1.3497
8.5000	1.4809	1.4809	1.4811	1.4813	1.4816	1.4822	1.4832	1.4855	1.4892
10.0000	1.5195	1.5196	1.5197	1.5200	1.5204	1.5210	1.5222	1.5250	1.5293
12.5000	1.5444	1.5445	1.5447	1.5450	1.5456	1.5463	1.5479	1.5514	1.5568
15.0000	1.5630	1.5631	1.5634	1.5638	1.5644	1.5654	1.5673	1.5715	1.5781
17.5000	1.5720	1.5722	1.5724	1.5729	1.5737	1.5748	1.5770	1.5821	1.5898
20.0000	1.5813	1.5815	1.5818	1.5823	1.5832	1.5845	1.5871	1.5929	1.6018
30.0000	1.6214	1.6217	1.6222	1.6230	1.6242	1.6262	1.6301	1.6389	1.6522
40.0000	1.6398	1.6402	1.6408	1.6419	1.6435	1.6462	1.6514	1.6630	1.6807
45.0000	1.6282	1.6286	1.6293	1.6305	1.6324	1.6354	1.6413	1.6544	1.6742
50.0000	1.5901	1.5906	1.5914	1.5927	1.5948	1.5981	1.6046	1.6192	1.6412
60.0000	1.4344	1.4350	1.4359	1.4375	1.4400	1.4440	1.4518	1.4692	1.4956
65.0000	1.3121	1.3127	1.3137	1.3155	1.3181	1.3225	1.3310	1.3498	1.3784
70.0000	1.1627	1.1634	1.1644	1.1663	1.1692	1.1739	1.1831	1.2034	1.2341
72.5000	1.0792	1.0799	1.0810	1.0830	1.0860	1.0908	1.1003	1.1213	1.1532
75.0000	.9921	.9928	.9940	.9960	.9991	1.0041	1.0139	1.0357	1.0686
77.5000	.9006	.9013	.9025	.9046	.9078	.9129	.9231	.9456	.9796
80.0000	.8069	.8077	.8089	.8111	.8143	.8197	.8302	.8534	.8885
85.0000	.6132	.6140	.6153	.6176	.6211	.6268	.6379	.6626	.6999
90.0000	.4156	.4165	.4178	.4203	.4240	.4300	.4418	.4679	.5074
95.0000	.2153	.2162	.2177	.2202	.2241	.2305	.2430	.2706	.3122
100.0000	.0113	.0123	.0138	.0165	.0206	.0273	.0405	.0695	.1134
Sharp leading edge									
.0000	.0000	.0000	.0000	.0000	.0000	.0000	.0000	.0000	.0000
.1250	.3359	.3359	.0293	.0307	.0329	.0364	.0433	.0585	.0815
.2500	.4506	.4506	.0557	.0580	.0614	.0670	.0781	.1024	.1392
.5000	.6064	.6064	.0998	.1021	.1055	.1111	.1222	.1465	.1833
.7500	.7247	.7247	.1439	.1462	.1496	.1552	.1663	.1906	.2274
1.0000	.8182	.8182	.1880	.1903	.1937	.1993	.2103	.2347	.2715
1.5000	.9520	.9520	.2761	.2784	.2818	.2875	.2985	.3229	.3596
2.5000	1.1191	1.1191	.4524	.4547	.4581	.4638	.4748	.4992	.5359
5.0000	1.3448	1.3448	.8933	.8956	.8990	.9046	.9156	.9400	.9768
8.5000	1.4809	1.4809	1.3413	1.3429	1.3453	1.3493	1.3570	1.3741	1.4001
10.0000	1.5195	1.5196	1.4547	1.4559	1.4578	1.4609	1.4669	1.4803	1.5007
12.5000	1.5444	1.5445	1.5203	1.5210	1.5221	1.5238	1.5272	1.5347	1.5461
15.0000	1.5630	1.5631	1.5634	1.5638	1.5644	1.5654	1.5673	1.5715	1.5781

## WING-BODY INTERSECTION

The wing reference plane was located 3.149 cm (1.240 in.) below and parallel to (zero incidence) the body centerline. The apex (extension of the wing leading edge to the centerline) of the wing was located 33.496 cm (13.187 in.) aft of the model nose.

## PRESSURE ORIFICE LOCATIONS

All pressure orifices were located on the left side of the model and distributed as shown in figure 3 and tables 2 and 3. Both the flat wing with rounded leading edge and the twisted wing had 214 orifices with seven spanwise pressure stations of 31 or 30 chordwise orifices each. One of these orifices was located at the leading edge; the remainder were distributed so that upper and lower surface orifices were located at the same chordwise locations. The orifice locations on the sharp leading edge were identical except that the leading-edge orifice at each spanwise station was omitted. The 83 orifices on the body were located at 15 stations along the length of the model. At each station, orifices were located at angles of  $0^\circ$ ,  $45^\circ$ ,  $90^\circ$ ,  $135^\circ$ , and  $180^\circ$  measured from the top of the body. In the area of the wing-body intersection, the orifices that are nominally identified as being at  $135^\circ$  and  $180^\circ$  were located on the wing lower surface at the same lateral location as the orifices at  $45^\circ$  and  $0^\circ$ , respectively. Eight additional orifices were placed close to the juncture of the body with the wing upper surface.

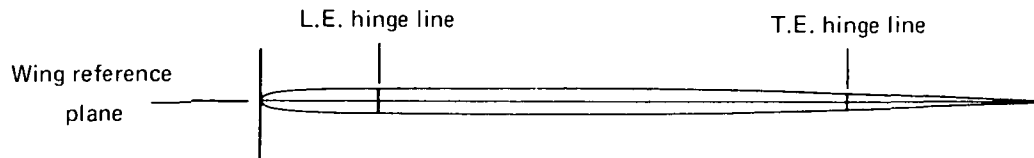
## DESIGN AND CONSTRUCTION

The objectives of this study dictated that the contours and physical characteristics of the flat and twisted wings be as nearly identical as possible. The model was constructed of steel to minimize aeroelastic deflections and to provide strength for potential future testing to a Mach number of 3.0. The aft body was flared approximately  $4^\circ$  from 194.310 cm (76.500 in.) aft of the nose to provide the required safety factor on predicted loads (see fig. 1). The model size was selected as the best compromise between potential tunnel blockage and adequate room to install orifices in the model.

A computerized lofting program was used to provide the wing definition. This definition was then used to machine the model components using numerically controlled machines. The tolerance on the contour was  $+0.1524$ ,  $-0.0$  mm ( $+0.006$ ,  $-0.0$  in.). The leading- and trailing-edge control surfaces were cut from the wings after they had been machined to final contour. Cuts were made along the 15% chord line of the twisted wing to simulate the removable leading edge of the flat wing in order to duplicate more closely the elastic characteristics of the flat wing (see fig. 4). Fixed angle brackets, arranged as shown in figure 4, were used to obtain the required control surface deflections with all pivot points located midway between the upper and lower surfaces at the hingelines. The brackets were also machined on numerically controlled machines. The same sets of trailing-edge brackets were used on both the flat and twisted wings, and the same sets of leading-edge brackets were used for both the rounded and sharp leading edges.

Table 2.—Wing Pressure Orifice Locations, Percent Local Chord

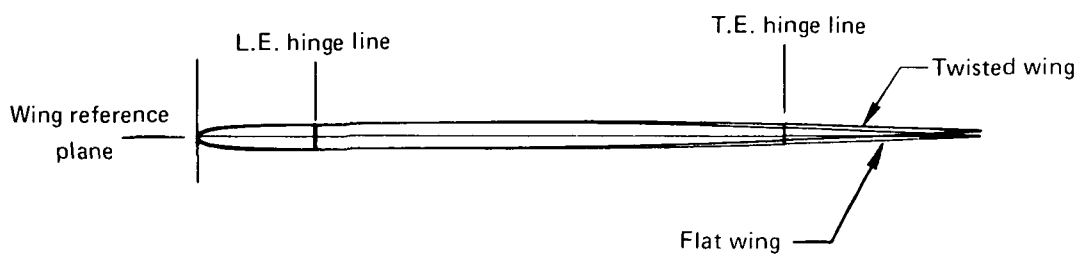
(a) Section at  $0.09 \frac{b}{2}$ , chord = 102.89 cm



Nominal	Flat wing, $\alpha_{\text{sec}} = 0.0^\circ$				Twisted wing, $\alpha_{\text{sec}} = -0.01^\circ$	
	Rounded leading edge		Sharp leading edge		Rounded leading edge	
	Upper surface	Lower surface	Upper surface	Lower surface	Upper surface	Lower surface
0.00	0.00		---	---	0.00	
2.50	2.45	2.59	2.61	2.54	2.26	2.26
5.00	4.95	5.07	5.06	5.03	4.76	4.76
8.50	8.45	8.53	8.59	8.58	8.40	8.26
11.30	---	---	---	11.31	---	---
12.25	---	---	---	---	12.23	12.27
12.50	12.45	12.55	12.58	---	---	---
17.50	17.49	17.62			17.59	17.66
20.00	19.94	20.08			20.03	20.03
30.00	29.92	30.09			29.98	29.89
45.00	45.00	45.07			44.96	44.89
60.00	59.98	60.08			60.01	59.97
70.00	70.03	70.13			70.05	69.95
72.50	72.55	72.60			72.58	72.51
77.50	77.53	77.62			77.56	77.51
85.00	85.11	85.14			85.03	85.00
90.00	90.10	90.10			90.04	89.98
95.00	95.09	95.05			94.96	94.98

Table 2.—(Continued)

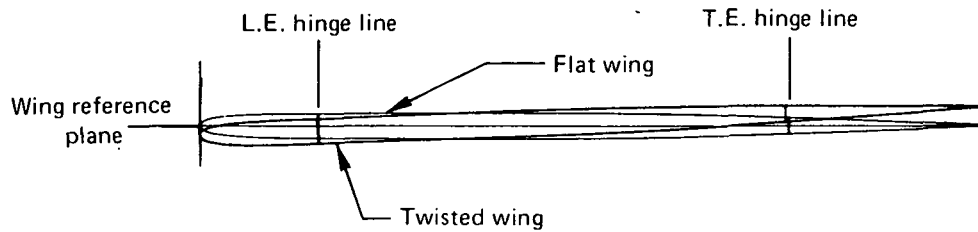
(b) Section at  $0.20 \frac{b}{2}$ , chord = 91.80 cm



Nominal	Flat wing, $\alpha_{\text{sec}} = 0.0^\circ$				Twisted wing, $\alpha_{\text{sec}} = -0.47^\circ$	
	Rounded leading edge		Sharp leading edge		Rounded leading edge	
	Upper surface	Lower surface	Upper surface	Lower surface	Upper surface	Lower surface
0.00	0.00		---	---	0.00	
2.50	2.59	2.69	2.62	2.65	2.52	2.42
5.00	5.05	5.00	5.14	5.14	5.00	4.93
8.50	8.54	8.59	8.67	8.62	8.52	8.40
11.40	---	---	---	11.37	---	---
12.50	12.54	12.49	12.63	---	12.53	12.42
17.50	17.63	17.61			17.65	17.52
20.00	20.08	20.07			20.00	19.90
30.00	30.04	30.09			30.02	29.89
45.00	45.08	45.09			45.03	44.92
60.00	60.02	60.13			60.03	59.91
70.00	70.11	70.13			70.06	69.96
72.50	72.63	72.61			72.55	72.50
77.50	77.59	77.65			77.59	77.52
85.00	85.07	85.13			85.02	85.00
90.00	90.14	90.11			90.07	89.97
95.00	95.14	95.10			95.05	95.08

Table 2.—(Continued)

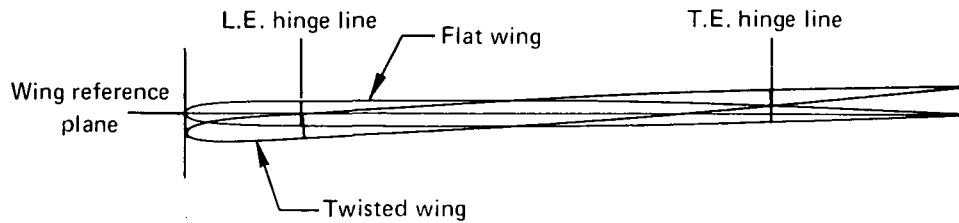
(c) Section at  $0.35 \frac{b}{2}$ , chord = 76.69 cm



Nominal	Flat wing, $\alpha_{\text{sec}} = 0.0^\circ$				Twisted wing, $\alpha_{\text{sec}} = -1.70^\circ$	
	Rounded leading edge		Sharp leading edge		Rounded leading edge	
	Upper surface	Lower surface	Upper surface	Lower surface	Upper surface	Lower surface
0.00	0.00		---	---	0.00	
2.50	2.45	2.59	2.59	2.58	2.39	2.33
5.00	4.93	5.07	5.11	5.04	5.12	4.78
8.50	8.60	8.54	8.65	8.63	8.49	8.32
10.50	---	---	---	10.46	---	---
11.00	---	11.03	---	---	---	---
12.50	12.37	---	12.57	---	12.50	12.33
17.50	17.64	17.63			17.54	17.53
20.00	20.00	20.09			19.94	19.84
30.00	30.01	30.10			29.88	29.87
45.00	44.99	45.09			44.96	44.79
60.00	60.03	60.08			59.97	59.89
70.00	70.07	70.08			70.03	69.90
72.50	72.55	72.58			72.56	72.44
77.50	77.60	77.61			77.54	77.51
85.00	85.11	85.14			85.08	84.96
90.00	90.06	90.09			89.89	89.89
95.00	95.07	95.09			94.95	94.86

Table 2.—(Continued)

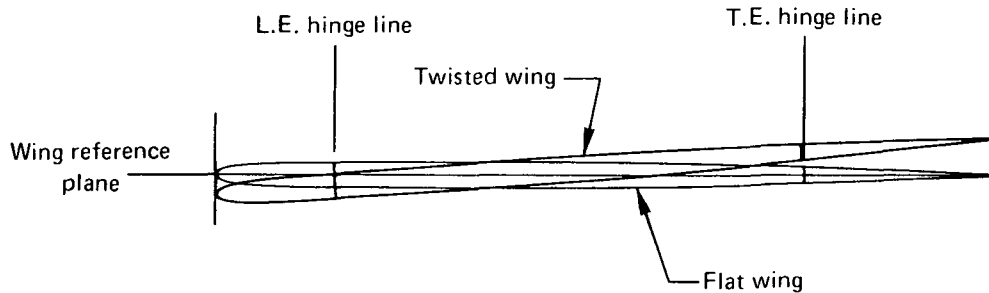
(d) Section at  $0.50 \frac{b}{2}$ , chord = 61.57 cm



Nominal	Flat wing, $\alpha_{sec} = 0.0^\circ$				Twisted wing, $\alpha_{sec} = -2.85^\circ$	
	Rounded leading edge		Sharp leading edge		Rounded leading edge	
	Upper surface	Lower surface	Upper surface	Lower surface	Upper surface	Lower surface
0.00	0.00		---	---	0.00	
2.50	2.47	2.53	2.69	2.60	2.44	2.38
5.00	4.99	4.95	5.13	5.06	4.92	4.80
8.50	8.48	8.38	8.66	8.61	8.46	8.38
10.10	---	---	---	10.14	---	---
11.10	---	11.08	---	---	---	---
12.50	12.39	---	12.61	---	12.50	12.31
17.50	17.64	17.52			17.54	17.24
20.00	19.98	19.97			19.92	19.83
30.00	30.07	30.06			29.91	29.85
45.00	44.98	45.06			45.00	44.85
60.00	59.97	60.00			59.95	59.92
70.00	70.07	70.10			70.03	69.88
72.50	72.65	72.61			72.56	72.44
77.50	77.66	77.65			77.61	77.43
85.00	85.19	85.18			84.85	84.90
90.00	90.22	90.12			89.93	89.93
95.00	95.05	94.94			94.88	94.93

Table 2.—(Continued)

(e) Section at  $0.65 \frac{b}{2}$ , chord = 46.46 cm



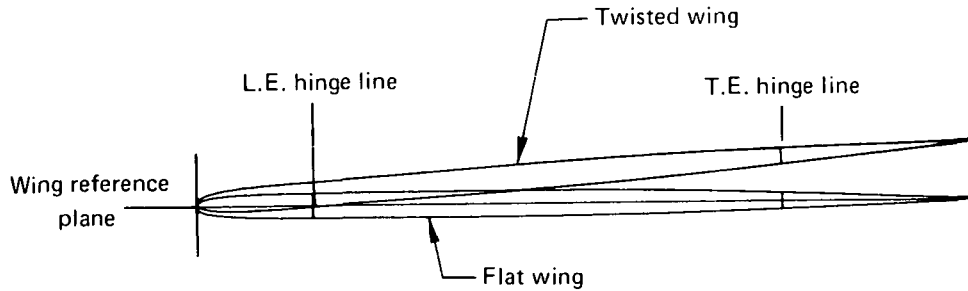
Nominal	Flat wing, $\alpha_{\text{sec}} = 0.0^\circ$				Twisted wing, $\alpha_{\text{sec}} = -3.59^\circ$	
	Rounded leading edge		Sharp leading edge		Rounded leading edge	
	Upper surface	Lower surface	Upper surface	Lower surface	Upper surface	Lower surface
0.00	0.00		---	---	0.00	
2.50	2.56	2.66	2.49	2.38	2.18	2.49
5.00	5.06	5.12	4.94	4.95	4.76	5.01
8.50	8.55	8.55	8.46	8.40	8.32	8.45
12.20	---	---	12.12	9.90 (a)	12.21	---
12.60	12.57	---	---	---	---	12.44 (a)
17.50	17.60	17.65			17.24	17.44
20.00	20.17	20.11			19.70	19.88
30.00	30.05	30.11			30.26	29.73
45.00	45.16	45.23			44.75	44.89
60.00	60.13	60.13			59.81	59.87
70.00	69.89	70.12			69.92	69.90
72.50	72.59	72.69			72.38	72.49
77.50	77.74	77.76			77.22	77.49
85.00	85.25	85.32			84.79	84.93
90.00	90.22	90.21			89.70	89.92
95.00	95.13	95.27			95.12	94.86

(a) These orifices were not available in the previous test.



Table 2.—(Continued)

(f) Section at  $0.80 \frac{b}{2}$ , chord = 31.35 cm

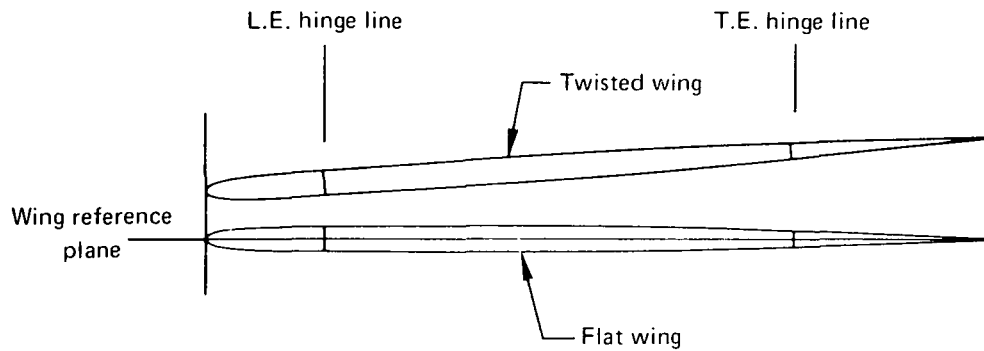


Nominal	Flat wing, $\alpha_{\text{sec}} = 0.0^\circ$				Twisted wing, $\alpha_{\text{sec}} = -3.84^\circ$	
	Rounded leading edge		Sharp leading edge		Rounded leading edge	
	Upper surface	Lower surface	Upper surface	Lower surface	Upper surface	Lower surface
0.00	0.00		---	---	0.00	
2.50	2.55	2.47	2.50	2.46	2.33	2.43
5.00	5.01	5.02	5.01	4.93	4.86	4.74
8.50	8.55	8.59	8.58	8.41	8.32	8.41 (a)
12.50	12.50	---	12.58	---	12.47	12.43
17.50	17.53	17.57			17.36	17.47
20.00	20.16	20.13			19.79	19.82
30.00	30.00	30.11			29.83	29.83
45.00	44.91	45.15			44.81	44.91
60.00	59.94	60.10			59.80	59.92
70.00	70.06	70.11			69.89	69.87
72.50	72.61	72.60			72.22	72.39
77.50	77.73	77.72			77.29	77.41
85.00	85.25	85.18			84.80	84.95
90.00	90.20	90.34			90.62	90.03
95.00	95.41	95.49			95.71	95.00

(a) This orifice was not available in the previous test.

Table 2. — (Concluded)

(g) Section at  $0.93 \frac{b}{2}$ , chord = 18.25 cm



Nominal	Flat wing, $\alpha_{\text{sec}} = 0.0^\circ$				Twisted wing, $\alpha_{\text{sec}} = -4.14^\circ$	
	Rounded leading edge		Sharp leading edge		Rounded leading edge	
	Upper surface	Lower surface	Upper surface	Lower surface	Upper surface	Lower surface
0.00	0.00		---	---	0.00	
2.51	1.70	1.81	2.12	1.86	1.74	2.59
5.00	4.38	4.68	4.72	4.52	4.41	4.65
8.50	7.89	8.24	8.21	8.06	7.92	8.23
11.59	---	---	---	9.48 (a)	11.59	---
12.25	12.33	---	12.19	---	---	12.36 (a)
17.50	17.36	16.60			16.60	17.49
20.00	19.78	19.81			19.58	19.96
30.00	29.67	29.00			29.17	29.62
45.00	44.70	44.80			44.12	44.44
60.00	59.68	59.47			59.18	59.71
70.00	69.69	70.33			68.99	69.31
72.50	72.15	71.89			71.59	72.01
77.50	77.38	77.31			76.80	77.12
85.00	84.62	84.90			84.54	84.82
90.00	89.51	89.81			89.21	89.74
95.00	94.46	94.68			94.41	94.56

(a) These orifices were not available in the previous test.

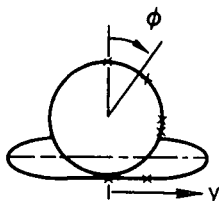


Table 3.— Body Pressure Orifice Locations

Nominal locations	x/L, percent body length														
	4.5	7.5	11.0	14.5	21.8	25.0	33.0	39.0	50.0	55.0	60.0	64.0	70.0	75.5	80.0
$\phi = 0.0^\circ$	0.0	0.0	0.0	0.0	0.0	0.0	0.0	0.0	0.0	0.0	0.0	0.0	0.0	0.0	0.0
$\phi = 45.0^\circ$	44.3	44.3	44.5	44.7	44.4	44.8	45.0	44.8	45.0	44.8	44.8	45.0	44.8	45.0	44.8
$\phi = 90.0^\circ$	90.0	89.9	90.5	90.3	90.4	89.9	90.1	90.2	90.2	90.0	89.9	89.9	89.8	90.1	89.8
$\phi \approx 110.0^\circ$	---	---	---	---	110.2	110.0	110.1	110.1	110.2	116.8	119.9	124.2	---	---	---
Body, $\phi = 135.0^\circ$ Flat wing, $y = 3.094$ cm Twisted wing, $y = 3.094$ cm	136.1	135.3	135.0	135.2	3.025 3.132	3.028 3.106	3.028 3.048	3.056 3.048	3.071 3.005	3.056 2.926	3.043 3.094	3.045 3.094	134.6	134.5	134.8
Body, $\phi = 180.0^\circ$ Flat wing, $y = 0.0$ cm Twisted wing, $y = 0.0$ cm	180.0	180.0	180.0	180.0	-.018 .020	-.030 -.008	-.064 -.041	.081 -.043	-.048 -.056	180.0	180.0	180.0	180.0	180.0	180.0

Pressure tubing used in this model was 1.016-mm (0.040-in.) o.d. Monel with a 0.1524-mm (0.006-in.) wall thickness. The major channels for wing pressure tubing were machined into the surface. The detailed grooves required to route tubing from the orifices to these channels were cut by hand. The pressure orifices were installed normal to and flush with the local surface. After installation of the pressure tubing, the surfaces were brought back to contour with solder. The tubing for body pressure orifices was run through the hollow center of the model body rather than in grooves in the outside contour. Tubing from all the orifices was routed through the hollow body to the scanivalves located in the body nose. Wiring from the scanivalves was routed through the body to the sting.

The nose portion of the body was removable to provide access to the fifteen 24-position scanivalves. Figure 1 shows the aft body location of the strain gages used to measure normal force and pitching moment.

### WIND TUNNEL CAPABILITIES

The 9- by 7-ft supersonic leg of the NASA Ames Unitary Wind Tunnel is a continuous-flow, closed-return, variable-density facility with an operating range of Mach number from 1.54 to 2.50. A schematic is shown in figure 5. The tunnel is equipped with an asymmetric, sliding-block nozzle and a flexible upper plate; variation of the test section Mach number is achieved by translating, in the streamwise direction, the fixed contour block that forms the floor of the nozzle. For this test, the Reynolds number was selected as  $8.65 \times 10^6$  based on the mean aerodynamic chord ( $\bar{c}$ ) of this model. The test section is 2.74 by 2.13 by 5.49 m (9 by 7 by 18 ft).

The tunnel air is driven by an 11-stage, axial-flow compressor powered by four variable-speed, wound-rotor induction motors with a combined output of 134 280 kW (180 000 hp). Four  $850 \text{ m}^3$  (30 000  $\text{ft}^3$ ) spherical storage tanks provide dry air for tunnel pressurization. The temperature is controlled by aftercooling.

The data acquisition system is comprised of a Beckman 210 analog-digital recorder and a minicomputer. Output from the Beckman 210 is converted to an acceptable format and transmitted by the minicomputer to an IBM 360 computer located in the AMES Research Center central computer facility for processing and preparation of final data. This flow is illustrated in figure 6.

The angle of attack of the reference point (0.25 M.A.C. for this model) for a sting-mounted model is a combination of the input angle at the base of the sting and an increment due to sting deflection. The input angle of attack at the base of the sting is accurate within 0.02 deg.

Sting deflections due to load were determined during the calibration of the strain gages mounted on the integral sting body of the model. The corrections for sting deflection are based on the normal force and pitching moment loads obtained during wind-on data acquisition. The sting deflection was taken into account when setting test angles of attack to minimize the variation in final angle of attack for the various model configurations. Only a crude calibration of the normal force and pitching moment gages

was obtained since the force and pitching moment measurements were used primarily for calculating sting deflection. Comparison with the integrated pressure results indicates that both force and moment measurements may be about 10% low, which could yield a maximum error in final angle of attack of 0.1 deg.

The model was instrumented with fifteen 24-position scanivalves. Each scanivalve contained a 103.42-kN/m<sup>2</sup> (15-psi) differential Statham, variable-resistance, unbonded strain gage transducer. These transducers are calibrated against a high accuracy standard and, if placed in a temperature-controlled environment, will read with an accuracy of  $\pm 0.1\%$  of full scale. For this test, the transducers were located inside the model. Based on the maximum temperature measured in the test section, the accuracy of pressure measurements for this test is better than  $\pm 0.3\%$ .

## TESTS AND DATA ACQUISITION

Table 4 lists the 13 configurations that were tested. Photographs of two of these are shown in figures 7 and 8; a diagram of the model installation in the test section is shown in figure 9. Pressure and total force data were obtained at Mach numbers of 1.70, 2.10, and 2.50 for all configurations. Table 4 shows the run numbers for each Mach number and configuration for which these data were obtained. A detailed listing of all test points is given in appendix A.

The initial plan for the test specified Mach 1.60 as the lowest Mach number. Using the Schlieren system, the shock wave reflected from the wall of the tunnel at this Mach number was observed to impinge on the wingtip. The low Mach number was then changed to 1.70. Because of the rather large gap between the highest Mach number in the subsonic/transonic test (1.11) and the basic low Mach number for this test (1.70), it was decided to run the lowest possible Mach number for this tunnel (1.54) for the basic configuration despite the shock impingement on the wing tip.

Test angles of attack were from  $-8^\circ$  to  $+14^\circ$  in  $2^\circ$  increments and  $+15^\circ$ . A trip strip of No. 60 carborundum grit (6 to 8 grains per cm) was used throughout the test. On the body, the trip strip was 0.32 cm (0.125 in.) wide and placed 2.54 cm (1 in.) from the nose. On the wing, it was 0.32 cm (0.125 in.) wide from the side of the body to the midspan control surface break ( $0.57 b/2$ ) and tapered to 0.16 cm (0.0625 in.) wide at the wingtip. On the upper surface of the wing, the trip strip was placed at 15% chord; on the lower surface, it was placed just aft of the leading-edge control surface brackets (see fig. 4).

The pressure data were recorded through the use of fifteen 24-position scanivalves located in the fore body of the model. Pressure transducers in the scanivalves measured the differential pressure between the local surface pressures and a known reference pressure. Signals from the scanivalves, force and moment data, tunnel parameters, and model attitude angle were recorded on the Beckman 210 analog-digital recorder and reduced by the Ames staff.

Final data (pressure coefficients, tunnel parameters, and model attitude) were merged on magnetic tapes, with appropriate configuration and test point identification for integration and plotting of these data.

Table 4.—Summary of Test Conditions by Run Number.  
Reynolds Number =  $8.65 \times 10^6$

Leading-edge deflection, deg	Mach number	Trailing-edge deflection, deg							
		Full span				Outboard (inboard = 0.0)		Inboard (outboard = 0.0)	
		8.3	4.1	0.0	-4.1	8.3	4.1	8.3	4.1
Flat wing, rounded L.E.									
Full span = 0.0	1.543			19					
	1.70	26	37	20	44	23	40	30	34
	2.10	27	38	21	45	24	41	31	35
	2.50	28	39	22	46	25	42	32	36
Full span = 5.1	1.70			16					
	2.10			17					
	2.50			18					
Flat wing, sharp L.E.									
Full span = 0.0	1.70			51					
	2.10			52					
	2.50			53					
Full span = 5.1	1.70			48					
	2.10			49					
	2.50			50					
Twisted wing, rounded L.E.									
Full span = 0.0	1.60			1					
	1.70	11		3					
	1.90			4, 6					
	2.10	12		9					
	2.50	13		10					

A detailed description of the data editing and integration procedure and the data presentation are included in appendix B.

## **DATA TAPE DESCRIPTION**

The experimental data were recorded on seven-track unlabeled tapes written by the Boeing Computer Services CDC 6600 computer. The tapes were written in binary (odd parity) mode at a density of 556 bpi. The first file of each tape and any program files are BCD (formatted) information. The data files are binary.

A description of each of the tape files follows.

- First file of each tape (BCD format with 80-column records).—This file contains an identification of the test and model and describes the content of the remaining files.
- Program files (BCD).—These files contain the source code of FORTRAN IV programs that may be used to provide listings of user-selected items in the data files.
- Data files (binary).—The first record contains geometry pertinent to the data that will follow (i.e., for pressure data, the spanwise location of each section and the arrays of  $x/c$  for which  $C_p$ 's are listed; for integrated data, geometric constants used in the integrations). The remaining records each contain data for one test point. A list defining all test points is in appendix A.

Questions regarding the availability of these data should be addressed to Mr. Percy J. Bobbitt of the NASA Langley Research Center.

## **EXPERIMENTAL DATA**

The experimental data are summarized and discussed in this section. The effect on loading of wing twist, leading-edge shape, leading-edge droop, and both full-span and partial-span trailing edge control surface deflection are shown in figures 10 through 47. As mentioned earlier, this model has also been tested at subsonic and transonic Mach numbers as reported in references 1 through 4 and summarized in appendix C. The total range of Mach numbers for which experimental data are available is now 0.40 to 2.50. Figures 48 through 53 show the effect of Mach number on the experimental data. Table 5 summarizes the data presented. The presentations include:

- Wing upper and lower surface isobars
- Wing upper and lower surface chordwise pressure distributions
- Wing net chordwise pressure distributions
- Wing spanload distributions

- Wing section aerodynamic characteristics
- Wing aerodynamic characteristics
- Body longitudinal pressure distributions

The experimental data are available for all 13 configurations tested at Mach numbers of 1.70, 2.10, and 2.50. In addition, data for the basic flat wing configuration are available at  $M = 1.54$  and for the twisted wing at  $M = 1.60$  and 1.90. Data presentations include all available Mach numbers for these two configurations. The effects of leading- and trailing-edge control surface deflection are shown for selected Mach numbers.

The pressure data of the wing and body were integrated to obtain total normal force and pitching moment. These integrated data and the strain gage measurements are listed in the test point log in appendix A. The difference of approximately 10% between the two is probably due largely to the previously mentioned crude calibration of the strain gages in the tunnel.

*Table 5.—Summary of Experimental Data Presentations by Figure Number*

	Mach number						
	1.54	1.60	1.70	1.90	2.10	2.50	0.40-2.50
Wing							
Base configuration	10		11		12	13	48
Sharp leading edge			14			15	49
Effect of L.E. shape			16				
Twisted wing		17	18	19	20	21	50
Effect of wing twist			22			23	
Effect of L.E. droop							
Rounded L.E.			24				51
Sharp L.E.			25				
Full span T.E. deflection							
Flat wing			26			27	52, 53
Twisted wing			28				
Partial span T.E. deflection							
Inboard (outboard = $0^\circ$ )			29		30	31	
Outboard (inboard = $0^\circ$ )			32		33	34	
Combinations			35		36	37	
Body							
Base configuration	38		39		40	41	
Sharp leading edge			42				
Twisted wing		43	44	45	46	47	



## BASE CONFIGURATION

Figures 10 through 13 show the wing experimental data for the base configuration (flat wing with rounded leading edge and zero control surface deflection). Results are presented for Mach numbers of 1.54, 1.70, 2.10, and 2.50. The data include wing isobars, chordwise pressure distributions, spanload distributions, and section aerodynamic characteristics.

At the lower Mach numbers, an examination of the isobars<sup>1</sup> and chordwise pressure distributions shows that the flow on the upper surface separates near the leading edge and forms a spiral vortex at relatively low angles of attack ( $4^\circ$ ). As angle of attack increases, this vortex moves inboard and becomes the predominant influence on the pressure distributions. The section characteristics do not show as strong a vortex at supersonic speeds as at the subsonic Mach numbers (ref. 1). At the higher Mach numbers the vortex formation becomes masked as the pressures approach an absolute vacuum. The apparent presence of a strong vortex at  $M = 2.5$  on the isobars is due to the increased density of lines. The  $\Delta C_p$  has been reduced to 0.010 for this Mach number and is 0.025 for the lower Mach numbers.

## EFFECT OF LEADING-EDGE SHAPE

Data are shown in figures 14 and 15 for the flat wing with sharp leading edge. Figure 16 compares data for the rounded and sharp leading edges at Mach 1.70. The effect of leading-edge shape is small at these Mach numbers as was noted at transonic Mach numbers in reference 1.

## EFFECT OF WING TWIST

Data for the twisted wing are shown in figures 17 through 21; comparisons with the flat wing data are shown in figures 22 and 23. The washout of the twisted wing ( $4.5^\circ$  at the wingtip) delays the start of vortex formation. At the highest angles of attack the twisted wing data looks much like the flat as the flow phenomena on this model overshadow the effect of twist.

## EFFECT OF LEADING-EDGE DROOP

The effect of leading-edge droop is shown in figure 24 for the rounded leading edge and in figure 25 for the sharp leading edge. Data are shown only for Mach number = 1.70 as the incremental effects are typical of the data at  $M = 2.10$  and 2.50.

---

<sup>1</sup>The  $\Delta C_p$  noted on each of the isobars refers to the increment in pressure level between adjacent isobar lines. These  $\Delta C_p$  increments are automatically selected within the plot program based on maximum and minimum pressure levels. These increments should be carefully noted when plots are compared for several angles of attack since they may vary.

## **EFFECT OF FULL-SPAN TRAILING-EDGE CONTROL SURFACE DEFLECTION**

The effects of full-span trailing-edge control surface deflection are shown in figures 26 and 27 for the flat wing and in figure 28 for the twisted wing. At  $0^\circ$  angle of attack and for these relatively small trailing-edge deflections, the chordwise pressure distributions are typical of moderately swept wings. At an angle of attack of  $8^\circ$ , the outboard wing pressure distributions more closely resemble the effects of change in angle of attack rather than control surface deflection. The deflection of the control surface induces loading over the full chord on the outboard portion of the wing.

## **EFFECT OF PARTIAL-SPAN TRAILING-EDGE CONTROL SURFACE DEFLECTION**

The effect of partial-span trailing-edge control surface deflection is illustrated in figures 29 through 37 with spanload distributions. When only the inboard segment is deflected, it is interesting to note that this deflection also affects the loading on the outboard wing (figs. 29-31). In contrast, the outboard segment is very ineffective and the loadings on the outboard wing are not increased appreciably over deflecting the inboard segment only.

## **BODY PRESSURE DISTRIBUTIONS**

Figures 38 through 47 show the body longitudinal pressure distributions. The basic configuration (flat wing with rounded leading edge and zero control surface deflection) is shown in figures 38 through 41. The influence of wing configuration change (wing twist and leading-edge shape) is small at these Mach numbers.

## **EFFECT OF MACH NUMBER**

The effect of Mach number on the integrated section and surface characteristics of this model is shown in figures 48 through 53. Figure 48 is data for the basic configuration. In addition to the integrated data, this figure includes plots of pressures at individual orifices, which further emphasize the nonlinearity of these data throughout the entire range of Mach numbers available. Data for the sharp leading-edge configuration are shown in figure 49, for the twisted wing in figure 50, for the flat wing with rounded leading edge drooped in figure 51, and for the flat wing with trailing-edge control surface deflected in figure 52. Figure 53 illustrates the effect of Mach number for various trailing-edge control surface deflections.

## **THEORY COMPARISON TASK**

### **ATTACHED FLOW THEORY-FLEXSTAB**

Theoretical predictions of pressure distributions based on attached potential flow were obtained using the unified subsonic/supersonic panel technique of FLEXSTAB, which was developed by Boeing under NASA-Ames sponsorship (see refs. 5 and 6). This method provides detailed surface pressure distributions, and therefore the data were interpolated to the orifice locations on the model and then integrated with the methods described for the experimental data (see app. B). These data are also recorded on magnetic tapes. Enquiries regarding the availability of these data should be addressed to Mr. Percy J. Bobbitt of the NASA Langley Research Center. A listing of all available data points is included in appendix A.

The FLEXSTAB system of digital computer programs uses linear theory to evaluate the static and dynamic stability, the inertial and aerodynamic loading, and the resulting elastic deformations of aircraft configurations. The aerodynamic module contained in the FLEXSTAB system is based on the constant-pressure-panel method developed by Woodward (refs. 7 and 8) to solve the linearized potential-flow equations for supersonic and subsonic speeds with planar boundary conditions. The usual small-perturbation assumptions are made. The severity of the preceding limitations is a function of the configuration and the flight conditions.

Figure 54 shows the distribution of panels used in the analysis of this configuration. Line sources and doublets are distributed along the longitudinal axis of the body to simulate its thickness and lifting effects. Source panels are placed in the plane of the wing to simulate its thickness. To account for the wing lifting effects and interference effects between the wing and body, constant pressure vortex panels are placed in the plane of the wing and on a shell around the body. This "interference" shell serves to cancel the normal velocity components on the body induced by the wing.

The configuration was represented by 50 line singularities, 168 interference panels, and 160 wing panels. For the wing, panel edges were chosen to coincide with control surface hingelines and midspan breaks. The resulting panel arrangement has panels of nearly equal width and, in the chordwise direction, panel edges are at constant percent chord with closer spacing at the leading edge and the hingelines. The linearized boundary conditions employed by the method permitted control surface deflections to be treated as boundary condition changes and therefore repaneling of the wing was not required. Table 6 summarizes the configurations and Mach numbers for which solutions were obtained.

### **THEORY-TO-EXPERIMENT COMPARISONS**

The ability of FLEXSTAB to predict the experimental data are discussed in this section. Test results at  $M = 1.70$ ,  $2.10$ , and  $2.50$  are compared with the attached-flow method FLEXSTAB in figures 55 through 67 for the flat and twisted wings; included are the effects of leading- and trailing-edge control surface deflections. The comparisons include

Table 6.—Summary of FLEXSTAB Conditions by Run Number

Leading-edge deflection, deg	Mach number	Trailing-edge deflection, deg							
		Full span				Outboard (inboard = 0.0)		Inboard (outboard = 0.0)	
		8.3	4.1	0.0	-4.1	8.3	4.1	8.3	4.1
Flat wing, rounded L.E.									
Full span = 0.0	1.543			19					
	1.70	(26)	(37)	(20)	(44)	(23)	(40)	(30)	(34)
	2.10	(27)	(38)	(21)	(45)	(24)	(41)	(31)	(35)
	2.50	(28)	(39)	(22)	(46)	(25)	(42)	(32)	(36)
Full span = 5.1	1.70			(16)					
	2.10			(17)					
	2.50			(18)					
Flat wing, sharp L.E.									
Full span = 0.0	1.70			51					
	2.10			52					
	2.50			53					
Full span = 5.1	1.70			48					
	2.10			49					
	2.50			50					
Twisted wing, rounded L.E.									
Full span = 0.0	2.60			1					
	1.70	(11)		(3)					
	1.90			4, 6					
	2.10	(12)		(9)					
	2.50	(13)		(10)					

○ FLEXSTAB solution available

Note: On the data tapes and in the tables of appendix A, the above run numbers have been incremented by 1 000 to give the FLEXSTAB results unique identification.

pressure distributions and integrated section and surface aerodynamic characteristics. FLEXSTAB predictions are available for the full range of Mach numbers (0.40 through 2.50) for which experimental data are available (see app. C). Figures 68 through 70 compare FLEXSTAB predictions and experiment results as a function of Mach number. Table 7 summarizes the data presented.

*Table 7.—Summary of FLEXSTAB-to-Experiment Comparisons by Figure Number*

	Mach number			
	1.70	2.10	2.50	0.40-2.50
Wing				
Base configuration	55	56	57	68
Twisted wing	61	62	63	69
Full span L.E. droop	64			
Full span T.E. deflection		65		70
Partial span T.E. deflection				
Inboard (outboard = 0°)		66		
Outboard (inboard = 0°)		67		
Body				
Base configuration	58	59	60	

On all these figures the experimental data are identified on the plots with the test number ARC 137. On the plots of surface pressure distributions, the lower surface pressure distributions are indicated by double symbols.

## BASE CONFIGURATION

Figures 55 through 57 give comparisons of the wing data for the base configuration. FLEXSTAB predicts the pressure distributions quite well on the most inboard station throughout the angle-of-attack range. At the midspan stations, the experimental data show some evidence of vortex formation that is not predicted by theory. In contrast, examination of the integrated section and surface coefficients in parts g, h, and j of these figures would indicate good agreement over the majority of the wing for most of the angle-of-attack range. This phenomenon highlights a familiar problem, that of evaluating aerodynamic theories by comparisons only with experimental force data.

Body longitudinal pressure distributions for FLEXSTAB and experiment are compared in figures 58 through 60. These data are typical of the ability of FLEXSTAB to predict pressure distributions on the body. Predictions are reasonably good up to an angle of attack of 8°.

## TWISTED WING

FLEXSTAB is compared to experiment for the twisted wing configuration in figures 61 through 63. The agreement is similar to that for the flat wing although the range in angle of attack for this agreement is slightly shifted due to the washout of the wingtip.

## LEADING-EDGE DROOP

Figure 64 shows data for the leading edge drooped  $5.1^\circ$  at  $M = 1.70$ . The FLEXSTAB prediction seems somewhat better at an angle of attack of  $4^\circ$  than it did for the flat wing, as the drooped leading edge delays somewhat the formation of the vortex. These data are typical of those at the other Mach numbers.

## FULL-SPAN TRAILING-EDGE CONTROL SURFACE DEFLECTION

The effect of full-span trailing-edge control surface deflection of  $8.3^\circ$  is shown in figure 65 for a Mach number of 2.10. FLEXSTAB overpredicts the pressures on the deflected surface at all angles of attack. At  $4^\circ$  angle of attack, the experimental upper surface pressure distributions on the outboard wing have already lost most of the characteristic increased pressure on the control surface. As angle of attack increases, the distribution on the entire upper surface becomes almost constant as vacuum pressure is approached. The results at  $M = 2.50$  are similar. At  $M = 1.70$  (not shown), however, the comparisons were extremely bad, probably because the trailing-edge hinge line is in the area of transition between subsonic and supersonic trailing edge at this Mach number.

## PARTIAL-SPAN TRAILING-EDGE CONTROL SURFACE DEFLECTION

Figures 66 and 67 show, respectively, comparisons for inboard and outboard trailing-edge control surface deflection at Mach 2.10. The conclusions are the same as described previously for the full-span deflection.

## EFFECT OF MACH NUMBER

Figures 68 and 69 show, for the flat and twisted wings, respectively, a comparison of the FLEXSTAB predictions and the experimental data over the entire Mach number range. These plots emphasize the inability of linear theory to predict the load distribution on this arrow-wing configuration. Near the wing root and at low angles of attack, FLEXSTAB can predict the load distributions but not outboard or at high angles of attack.

Figure 70 shows a similar comparison for the flat wing with trailing-edge control surface deflected  $8.3^\circ$ . The predictions show the tendency of FLEXSTAB to overpredict the loading on the control surface even at this relatively small deflection. On the outboard stations the extreme discontinuity in the section pitching moment coefficients at  $M = 1.70$  illustrates the effect of the transition between subsonic and supersonic trailing edge at this Mach number.

## EMPIRICAL CORRECTIONS

The comparisons of the preceding sections indicate that for many conditions, FLEXSTAB does not give adequate results for detail design. In practice, theory is often used to increment wind tunnel data from a rigid model to account for the elastic effects of the actual airframe. An example of this procedure is shown in figure 71 for  $M = 2.10$

and several angles of attack. Here experimental data for the flat wing (rigid model) is taken and a theoretically calculated increment due to the known twist of the model (supposed elastic deformation) is added to it. The result is compared with the twisted wing data at the same angle of attack (deformed airframe). Although this method is typically used for net pressures, this figure includes upper and lower surface pressures so that the parts can be examined. There are significant differences between the flat wing data, theoretically corrected for twist, and the twisted wing results at the outboard stations for all angles of attack shown. This difference is also evident in the upper surface pressure distributions. The predictions of the lower surface pressure distributions are quite reasonable for all angles of attack.

This example is indicative of the types of problems that must be overcome for highly swept back wings before a reliable prediction scheme is available for aerodynamic increments due to elasticity. Improper accounting for aeroelastic effects because of uncertainties in the theoretical methods may result in understrength or overweight designs. In addition, the correct prediction of loads and the resultant structural deformation is essential to the determination of aircraft stability and control characteristics. These results indicate that the use of empirical corrections in the aeroelastic solution to calculate flexible airplane loads is extremely risky, and much research is necessary to develop a reliable method of using such corrections.

## CONCLUDING REMARKS

The data obtained in this contract supplement the subsonic/transonic data from the earlier contract. The large vortex observed at the subsonic Mach numbers becomes weaker as the Mach number increases. The effect of wing twist is similar at all Mach numbers, although the effect on the wing upper surface pressures at the higher supersonic Mach numbers and at high angles of attack is masked as the pressures approach a vacuum.

The attached potential flow method FLEXSTAB yields good agreement with experimental data for this configuration only over a limited range of conditions at low angles of attack. These analyses are generally adequate for the evaluation of a cruise configuration at 1-g (load factor one) conditions. At critical structural and control design conditions, which usually involve large angles of attack and/or large control surface deflections, the attached flow theory is completely inadequate. Attempts to introduce empirical corrections to improve this situation have been unsatisfactory.

It would appear that development and implementation of a general three-dimensional boundary-layer method are needed. There is an evident lack of theoretical tools necessary to predict critical design conditions on low aspect ratio configurations that are dominated by nonlinear flow phenomena. Empirical methods to improve this capability are also lacking. Much research is still necessary in developing the theoretical and empirical techniques before confidence can be acquired in the prediction of aerodynamic loads on highly swept, low aspect ratio, flexible airplanes.

Boeing Commercial Airplane Company  
P. O. Box 3707  
Seattle, Washington 98124  
July 31, 1976



## **APPENDIX A**

### **DETAILED TEST LOG**

All test points for which pressure and force data were recorded are listed in tables A-1 through A-4. These tables include normal force and pitching moment coefficients obtained from strain gage measurements and by integrating the pressure data. Each test point is identified as a unique number within the test by the analysis number, where:

$$\text{ANALYSIS NUMBER} = 100 (\text{RUN NUMBER}) + \text{POSITION IN RUN}$$

Tables A-5 through A-7 list the points at which predicted pressure data are available from FLEXSTAB. For convenience, 1000 has been added to the run number of the corresponding experimental condition to obtain the theoretical test point number.

Table A-1.—Experimental Data Test Point Log. Twisted Wing, Rounded Leading Edge;  
L.E. Deflection, Full Span =  $0.0^\circ$

(a) T.E. Deflection, Full Span =  $0.0^\circ$

Analysis number	Mach number	Dynamic pressure, $\text{kN/m}^2$ (psf)	Angle of attack, deg	Angle of sideslip, deg	Normal force coefficient, bal (integ press.)	Pitching moment coefficient, bal (integ press.)
101	1.601	38.2(798)	-8.03	.05	-.308(-.342)	.097(.107)
102	1.601	38.7(808)	-5.95	.07	-.243(-.269)	.082(.088)
103	1.601	38.7(808)	-3.97	.08	-.180(-.199)	.066(.070)
104	1.601	38.7(808)	-1.96	.09	-.116(-.129)	.049(.050)
105	1.601	39.1(816)	2.03	.11	.010(.015)	.013(.006)
106	1.601	39.1(817)	3.95	.12	.071(.080)	-.005(-.012)
107	1.601	39.1(817)	7.83	.14	.207(.228)	-.042(-.053)
108	1.601	39.0(814)	9.80	.13	.273(.301)	-.059(-.069)
109	1.601	38.7(808)	.02	.08	-.052(-.058)	.031(.029)
301	1.700	38.4(801)	-8.00	.04	-.297(-.334)	.096(.105)
302	1.700	38.4(801)	-5.97	.08	-.238(-.265)	.082(.087)
303	1.700	38.4(801)	-3.93	.08	-.175(-.194)	.066(.069)
304	1.700	38.4(802)	-1.95	.09	-.112(-.126)	.048(.050)
305	1.700	38.4(802)	-.00	.08	-.051(-.057)	.031(.029)
306	1.700	38.4(801)	2.00	.11	.010(.012)	.013(.008)
307	1.700	38.4(802)	4.08	.12	.075(.083)	-.006(-.012)
308	1.700	38.4(801)	4.08	.12	.076(.083)	-.007(-.012)
309	1.700	38.3(801)	5.86	.13	.138(.151)	-.025(-.032)
310	1.700	38.4(801)	7.89	.14	.206(.227)	-.043(-.051)
311	1.700	38.4(801)	9.72	.15	.265(.294)	-.058(-.067)
312	1.700	38.4(801)	11.69	.17	.325(.360)	-.071(-.082)
313	1.700	38.4(801)	13.58	.18	.384(.422)	-.083(-.097)
314	1.700	38.4(801)	14.52	.18	.411(.453)	-.088(-.103)
401	1.900	37.7(787)	-8.03	.02	-.276(-.305)	.089(.094)
402	1.900	37.7(787)	-5.98	.06	-.221(-.242)	.076(.078)
403	1.900	37.6(785)	-4.04	.07	-.167(-.183)	.062(.064)
404	1.900	37.7(788)	-1.96	.08	-.106(-.115)	.046(.045)
405	1.900	37.8(790)	.15	.08	-.042(-.045)	.028(.025)
406	1.900	37.9(792)	2.18	.10	.014(.018)	.012(.007)
407	1.900	37.9(792)	4.03	.12	.072(.078)	-.006(-.010)
408	1.900	38.0(793)	5.77	.11	.128(.139)	-.022(-.027)
409	1.900	38.4(803)	5.89	.11	.131(.142)	-.021(-.028)
410	1.900	38.2(799)	5.89	.11	.132(.143)	-.023(-.028)

Analysis number	Mach number	Dynamic pressure, $\text{kN/m}^2$ (psf)	Angle of attack, deg	Angle of sideslip, deg	Normal force coefficient, bal (integ press.)	Pitching moment coefficient, bal (integ press.)
601	1.900	37.4(782)	3.94	.12	.071(.075)	-.008(-.009)
602	1.900	37.4(782)	5.92	.13	.135(.144)	-.028(-.029)
603	1.900	37.4(782)	7.88	.14	.195(.211)	-.044(-.045)
604	1.900	37.4(782)	9.86	.20	.251(.271)	-.058(-.059)
605	1.900	37.4(782)	11.73	.17	.305(.329)	-.069(-.072)
606	1.900	37.4(782)	13.63	.18	.355(.389)	-.079(-.086)
607	1.900	37.6(785)	14.55	.18	.380(.417)	-.084(-.091)
608	1.900	37.7(788)	.01	.07	-.044(-.051)	.024(.027)
609	1.900	37.9(791)	1.87	.11	.011(.010)	.008(.009)
901	2.101	36.7(766)	-8.12	-.70	-.252(-.286)	.077(.086)
902	2.101	36.7(766)	-6.04	-.66	-.201(-.229)	.064(.072)
903	2.101	36.7(766)	-4.01	-.65	-.149(-.171)	.052(.058)
904	2.101	36.8(770)	-2.02	-.64	-.097(-.112)	.039(.043)
905	2.101	36.8(770)	.00	-.65	-.041(-.048)	.024(.025)
906	2.101	36.8(770)	2.00	-.62	.014(.014)	.008(.007)
907	2.101	36.8(770)	3.98	-.61	.074(.079)	-.010(-.011)
908	2.101	36.9(771)	5.96	-.60	.133(.144)	-.027(-.029)
909	2.101	37.0(773)	7.89	-.59	.188(.204)	-.042(-.044)
910	2.101	37.0(773)	9.80	-.53	.240(.260)	-.054(-.057)
911	2.101	37.0(773)	11.75	-.56	.290(.315)	-.065(-.069)
912	2.101	37.0(773)	13.66	-.55	.338(.370)	-.074(-.081)
913	2.101	37.0(773)	14.57	-.56	.361(.394)	-.079(-.086)
1001	2.501	33.7(705)	-8.14	.21	-.221(-.248)	.067(.075)
1002	2.501	33.7(705)	-6.09	.24	-.176(-.199)	.056(.064)
1003	2.501	33.7(705)	-4.05	.25	-.131(-.149)	.045(.051)
1004	2.501	33.7(705)	-2.01	.27	-.084(-.098)	.034(.038)
1005	2.501	33.7(705)	-.01	.25	-.037(-.045)	.022(.024)
1006	2.501	33.7(705)	1.99	.29	.013(.013)	.008(.007)
1007	2.501	33.8(705)	3.95	.30	.067(.070)	-.010(-.010)
1008	2.501	33.8(705)	5.94	.30	.117(.124)	-.024(-.024)
1009	2.501	33.8(705)	7.90	.32	.165(.172)	-.035(-.036)
1010	2.501	33.8(705)	9.84	.33	.208(.221)	-.045(-.046)
1011	2.501	33.7(705)	11.75	.35	.252(.268)	-.054(-.055)
1012	2.501	33.8(705)	13.64	.36	.292(.313)	-.062(-.064)
1013	2.501	33.8(705)	14.56	.36	.315(.336)	-.067(-.068)

Table A-1.—(Concluded)

(b) T.E. Deflection, Full Span = 8.3°

Analysis number	Mach number	Dynamic pressure, kN/m <sup>2</sup> (psf)	Angle of attack, deg	Angle of sideslip, deg	Normal force coefficient, bal (integ press.)	Pitching moment coefficient, bal (integ press.)
1101	1.700	38.3(800)	-8.15	.04	-.219(-.241)	.040(.041)
1102	1.700	38.4(801)	-6.05	.08	-.160(-.176)	.027(.026)
1103	1.700	38.4(801)	-4.02	.09	-.100(-.107)	.013(.007)
1104	1.700	38.4(802)	-2.02	.10	-.038(-.037)	-.004(-.013)
1105	1.700	38.4(802)	.02	.08	.026(.033)	-.023(-.033)
1106	1.700	38.4(801)	1.99	.11	.086(.100)	-.041(-.053)
1107	1.700	38.4(801)	5.93	.12	.213(.236)	-.077(-.090)
1108	1.700	38.4(801)	7.87	.13	.274(.306)	-.091(-.105)
1109	1.700	38.4(801)	9.82	.14	.330(.372)	-.103(-.118)
1110	1.700	38.4(801)	11.71	.20	.381(.431)	-.109(-.120)
1111	1.700	38.4(801)	13.64	.15	.435(.487)	-.119(-.137)
1112	1.700	38.4(801)	14.55	.16	.464(.512)	-.125(-.140)
1113	1.700	38.4(801)	3.95	.11	.146(.164)	-.057(-.069)
1201	2.100	37.2(778)	-8.11	-.69	-.196(-.220)	.040(.041)
1202	2.100	37.2(777)	-6.21	-.65	-.150(-.169)	.030(.029)
1203	2.100	37.2(778)	-6.08	-.66	-.147(-.165)	.029(.029)
1204	2.100	37.2(777)	-4.07	-.64	-.098(-.108)	.018(.014)
1205	2.100	37.2(778)	-1.94	-.63	-.041(-.042)	.003(-.004)
1206	2.100	37.2(778)	.00	-.65	.012(.016)	-.012(-.019)
1207	2.100	37.3(778)	.00	-.65	.012(.016)	-.012(-.019)
1208	2.100	37.3(778)	2.03	-.62	.070(.082)	-.030(-.039)
1209	2.100	37.3(778)	3.98	-.62	.128(.144)	-.046(-.056)
1210	2.100	37.3(778)	5.94	-.61	.185(.207)	-.063(-.073)
1211	2.100	37.3(778)	7.89	-.60	.238(.266)	-.076(-.087)
1212	2.100	37.3(778)	9.83	-.59	.288(.320)	-.087(-.099)
1213	2.100	37.3(778)	11.73	-.58	.334(.370)	-.095(-.108)
1214	2.100	37.3(778)	13.63	-.57	.376(.422)	-.101(-.117)
1215	2.100	37.3(778)	14.54	-.57	.396(.445)	-.103(-.120)
1301	2.501	34.3(716)	-8.13	.22	-.175(-.200)	.038(.041)
1302	2.501	34.3(716)	-6.13	.26	-.134(-.153)	.028(.030)
1303	2.501	34.3(716)	-4.08	.27	-.089(-.102)	.018(.017)
1304	2.501	34.3(716)	-2.11	.27	-.046(-.052)	.008(.005)
1305	2.501	34.6(723)	.01	.26	.004(.006)	-.005(-.010)
1306	2.501	34.7(725)	1.92	.29	.053(.062)	-.019(-.027)
1307	2.501	34.7(725)	3.92	.29	.108(.121)	-.036(-.044)
1308	2.501	34.8(727)	5.89	.30	.157(.175)	-.050(-.059)
1309	2.501	34.8(727)	7.86	.31	.200(.225)	-.059(-.071)
1310	2.501	34.8(726)	9.78	.32	.242(.272)	-.068(-.080)
1311	2.501	34.8(727)	11.70	.33	.278(.318)	-.072(-.089)
1312	2.501	34.8(726)	13.58	.34	.321(.364)	-.081(-.097)
1313	2.501	34.8(726)	14.49	.33	.342(.386)	-.086(-.101)

Table A-2.—Experimental Data Test Point Log. Flat Wing, Rounded Leading Edge;  
L.E. Deflection, Full Span =  $5.1^\circ$ ; T.E. Deflection, Full Span =  $0.0^\circ$

Analysis number	Mach number	Dynamic pressure, $\text{kN/m}^2$ (psf)	Angle of attack, deg	Angle of sideslip, deg	Normal force coefficient, bal (integ press.)	Pitching moment coefficient, bal (integ press.)
1601	1.700	37.6(786)	-8.10	.06	-.260(-.295)	.069(.076)
1602	1.700	37.6(786)	-6.07	.06	-.197(-.223)	.053(.058)
1603	1.700	37.6(786)	-3.98	.09	-.131(-.147)	.035(.037)
1604	1.700	37.6(786)	-1.98	.10	-.067(-.074)	.018(.016)
1605	1.700	37.6(786)	.02	.08	-.006(-.002)	.001(-.006)
1606	1.700	37.6(786)	2.01	.11	.054(.068)	-.016(-.026)
1607	1.700	37.6(786)	3.99	.11	.120(.138)	-.038(-.048)
1608	1.700	37.6(786)	5.98	.13	.188(.208)	-.059(-.068)
1609	1.700	37.7(788)	7.90	.12	.253(.278)	-.077(-.087)
1610	1.700	37.8(789)	9.85	.13	.312(.340)	-.091(-.101)
1611	1.700	37.7(787)	9.85	.13	.312(.340)	-.091(-.100)
1612	1.700	37.6(786)	11.78	.15	.370(.406)	-.103(-.113)
1613	1.700	37.6(786)	13.68	.16	.426(.465)	-.114(-.126)
1614	1.700	37.6(786)	14.58	.17	.450(.494)	-.118(-.131)
1701	2.100	36.3(758)	-8.14	-.69	-.223(-.257)	.059(.064)
1702	2.100	36.3(758)	-6.09	-.65	-.172(-.199)	.046(.049)
1703	2.100	36.3(758)	-4.03	-.64	-.117(-.137)	.032(.033)
1704	2.100	36.3(758)	-2.03	-.63	-.062(-.072)	.017(.016)
1705	2.100	36.3(758)	-.02	-.65	-.007(-.008)	.001(-.004)
1706	2.100	36.3(758)	2.02	-.62	.049(.063)	-.014(-.025)
1707	2.100	36.3(758)	3.99	-.61	.106(.124)	-.032(-.042)
1708	2.100	36.3(758)	5.91	-.60	.162(.183)	-.048(-.058)
1709	2.100	36.3(758)	7.89	-.59	.220(.241)	-.064(-.071)
1710	2.100	36.3(758)	9.85	-.58	.272(.298)	-.076(-.083)
1711	2.100	36.3(759)	11.75	-.56	.320(.349)	-.086(-.093)
1712	2.100	36.3(759)	13.64	-.55	.369(.404)	-.096(-.104)
1713	2.100	36.3(759)	14.57	-.55	.392(.428)	-.100(-.108)
1801	2.499	33.6(702)	-8.14	.21	-.197(-.225)	.055(.056)
1802	2.499	33.6(702)	-6.12	.25	-.156(-.175)	.046(.044)
1803	2.499	33.6(702)	-4.05	.26	-.112(-.123)	.035(.030)
1804	2.499	33.6(701)	-2.04	.27	-.061(-.067)	.020(.015)
1805	2.499	33.6(701)	-.09	.25	-.008(-.011)	.003(-.001)
1806	2.499	33.6(702)	1.89	.29	.047(.049)	-.015(-.019)
1807	2.499	33.6(702)	4.04	.29	.098(.107)	-.029(-.034)
1808	2.499	33.6(702)	5.97	.30	.145(.158)	-.041(-.046)
1809	2.499	34.0(709)	7.90	.31	.190(.206)	-.052(-.057)
1810	2.499	33.9(709)	11.76	.34	.278(.302)	-.071(-.077)
1811	2.499	34.0(709)	13.64	.35	.320(.349)	-.079(-.086)
1812	2.499	34.0(709)	14.57	.35	.339(.373)	-.082(-.091)
1813	2.499	34.0(709)	9.82	.33	.235(.254)	-.062(-.067)

Table A-3.—Experimental Data Test Point Log. Flat Wing, Rounded Leading Edge;  
L.E. Deflection, Full Span = 0.0°

(a) T.E. Deflection, Full Span = 0.0°

Analysis number	Mach number	Dynamic pressure, kN/m <sup>2</sup> (psf)	Angle of attack, deg	Angle of sideslip, deg	Normal force coefficient, bal (integ press.)	Pitching moment coefficient, bal (integ press.)
1901	1.543	37.6(785)	-8.10	.05	-.276(-.296)	.081(.083)
1902	1.543	37.7(788)	-6.08	.08	-.205(-.220)	.061(.063)
1903	1.543	37.9(793)	-4.04	.09	-.131(-.144)	.040(.041)
1904	1.543	37.9(793)	-2.00	.10	-.062(-.067)	.019(.018)
1905	1.543	38.1(795)	-.07	.08	-.001(-.002)	.002(-.001)
1906	1.543	37.9(791)	2.03	.12	.066(.075)	-.018(-.025)
1907	1.543	38.1(796)	4.05	.12	.135(.149)	-.039(-.047)
1908	1.543	38.1(796)	6.01	.13	.204(.225)	-.058(-.067)
1909	1.543	38.2(797)	7.97	.13	.271(.297)	-.075(-.085)
1910	1.543	38.2(797)	9.88	.18	.335(.370)	-.091(-.101)
1911	1.543	38.3(800)	11.84	.15	.395(.436)	-.104(-.115)
1912	1.543	38.3(799)	13.75	.15	.455(.501)	-.116(-.129)
1913	1.543	38.3(799)	14.66	.15	.484(.533)	-.122(-.136)
2001	1.700	38.6(806)	-8.09	.05	-.260(-.284)	.076(.080)
2002	1.700	38.6(806)	-8.09	.05	-.261(-.284)	.077(.090)
2003	1.700	38.6(807)	-6.08	.08	-.196(-.214)	.059(.061)
2004	1.700	38.6(806)	-4.05	.09	-.129(-.140)	.040(.040)
2005	1.700	38.6(807)	-2.00	.10	-.057(-.065)	.017(.018)
2006	1.700	38.6(806)	.04	.08	.004(.004)	-.001(-.003)
2007	1.700	38.6(806)	2.04	.12	.066(.073)	-.019(-.024)
2008	1.700	38.6(806)	4.04	.12	.132(.145)	-.038(-.046)
2009	1.700	38.6(806)	6.00	.13	.196(.215)	-.056(-.064)
2010	1.700	38.6(806)	7.88	.13	.255(.280)	-.071(-.079)
2011	1.700	38.6(806)	9.80	.14	.314(.345)	-.085(-.093)
2012	1.700	38.6(806)	11.71	.15	.371(.408)	-.097(-.108)
2013	1.700	38.6(806)	13.61	.17	.427(.469)	-.109(-.121)
2014	1.700	38.6(805)	14.52	.16	.454(.499)	-.114(-.128)
2101	2.101	37.2(777)	-8.14	-.68	-.228(-.250)	.066(.067)
2102	2.101	37.2(777)	-6.07	-.65	-.167(-.191)	.048(.052)
2103	2.101	37.2(777)	-4.08	-.65	-.111(-.127)	.033(.035)
2104	2.101	37.2(777)	-2.08	-.63	-.055(-.064)	.017(.017)
2105	2.101	37.2(777)	.00	-.65	.003(.003)	.001(-.002)
2106	2.101	37.2(777)	2.00	-.62	.060(.068)	-.016(-.021)
2107	2.101	37.2(777)	4.02	-.62	.117(.132)	-.032(-.039)
2108	2.101	37.2(777)	5.84	-.61	.169(.189)	-.046(-.053)
2109	2.101	37.2(777)	7.79	-.61	.221(.244)	-.060(-.066)
2110	2.101	37.2(777)	9.77	-.60	.272(.301)	-.072(-.079)
2112	2.101	37.2(777)	13.58	-.58	.368(.407)	-.092(-.102)
2113	2.101	37.2(778)	14.51	-.57	.391(.432)	-.097(-.107)
2114	2.101	37.2(777)	11.70	-.53	.322(.353)	-.082(-.090)

Analysis number	Mach number	Dynamic pressure, kN/m <sup>2</sup> (psf)	Angle of attack, deg	Angle of sideslip, deg	Normal force coefficient, bal (integ press.)	Pitching moment coefficient, bal (integ press.)
2201	2.499	34.5(720)	-8.15	.22	-.193(-.219)	.053(.058)
2202	2.499	34.5(720)	-8.15	.22	-.194(-.220)	.054(.059)
2203	2.499	34.4(719)	-6.14	.26	-.148(-.169)	.042(.046)
2204	2.499	34.5(720)	-4.06	.27	-.101(-.116)	.031(.033)
2205	2.499	34.4(719)	-2.09	.27	-.052(-.061)	.017(.018)
2206	2.499	34.4(719)	-.02	.25	.001(-.001)	.002(.000)
2207	2.499	34.4(719)	1.95	.28	.052(.058)	-.013(-.017)
2208	2.499	34.4(719)	4.05	.28	.104(.115)	-.028(-.032)
2209	2.499	34.4(719)	5.84	.29	.145(.161)	-.038(-.043)
2210	2.499	34.5(720)	7.69	.30	.188(.207)	-.048(-.053)
2211	2.499	34.4(719)	9.64	.31	.232(.255)	-.058(-.064)
2212	2.499	34.4(719)	9.75	.32	.235(.257)	-.059(-.065)
2213	2.499	34.4(719)	11.63	.32	.276(.304)	-.067(-.074)
2214	2.499	34.4(719)	13.51	.32	.319(.349)	-.077(-.083)
2215	2.499	34.4(719)	14.43	.31	.341(.372)	-.082(-.087)

Table A-3.—(Continued)

(b) T.E. Deflection, Inboard =  $0.0^\circ$ , Outboard =  $8.3^\circ$ 

Analysis number	Mach number	Dynamic pressure, $\text{kN/m}^2$ (psf)	Angle of attack, deg	Angle of sideslip, deg	Normal force coefficient, bal (integ press.)	Pitching moment coefficient, bal (integ press.)
2301	1.700	37.9(791)	-8.11	.05	-.245(-.272)	.062(.068)
2302	1.700	37.9(792)	-6.12	.09	-.181(-.203)	.044(.048)
2303	1.700	37.8(789)	-4.11	.09	-.111(-.123)	.022(.023)
2304	1.700	37.8(790)	-2.06	.10	-.043(-.047)	.002(-.001)
2305	1.700	37.8(790)	-.01	.08	.019(.022)	-.016(-.021)
2306	1.700	37.8(790)	1.99	.11	.080(.091)	-.033(-.042)
2307	1.700	37.8(790)	4.00	.11	.144(.161)	-.052(-.061)
2308	1.700	37.8(790)	5.85	.12	.203(.223)	-.066(-.075)
2309	1.700	37.8(790)	7.83	.12	.264(.292)	-.080(-.091)
2310	1.700	37.8(790)	9.75	.13	.322(.358)	-.094(-.105)
2311	1.700	37.8(790)	11.66	.14	.379(.420)	-.106(-.119)
2312	1.700	37.8(790)	13.57	.15	.435(.481)	-.117(-.131)
2313	1.700	37.8(790)	14.57	.14	.464(.514)	-.124(-.139)
2401	2.101	37.0(773)	-8.16	-.68	-.218(-.241)	.056(.058)
2402	2.101	37.0(772)	-6.13	-.64	-.162(-.183)	.040(.043)
2403	2.101	37.0(772)	-4.08	-.64	-.101(-.117)	.022(.024)
2404	2.101	36.9(771)	-2.11	-.63	-.043(-.051)	.005(.004)
2405	2.101	36.8(769)	-.03	-.65	.014(.017)	-.012(-.017)
2406	2.101	36.9(770)	1.99	-.62	.072(.081)	-.028(-.034)
2407	2.101	36.9(771)	4.00	-.62	.127(.143)	-.043(-.050)
2408	2.101	36.9(771)	5.92	-.61	.180(.202)	-.057(-.064)
2409	2.101	36.9(771)	7.89	-.60	.233(.258)	-.070(-.077)
2410	2.101	36.9(771)	9.84	-.59	.283(.314)	-.082(-.090)
2411	2.101	37.0(773)	11.75	-.58	.331(.366)	-.092(-.101)
2412	2.101	37.0(773)	13.63	-.57	.378(.421)	-.101(-.113)
2413	2.101	37.0(773)	14.56	-.57	.400(.445)	-.106(-.118)
2501	2.499	34.1(713)	-8.17	.22	-.187(-.212)	.046(.051)
2502	2.499	34.1(713)	-6.15	.25	-.141(-.162)	.034(.039)
2503	2.499	34.1(713)	-4.08	.26	-.091(-.106)	.021(.024)
2504	2.499	34.1(713)	-2.11	.27	-.042(-.051)	.007(.008)
2505	2.499	34.1(713)	-.04	.25	.010(.011)	-.008(-.011)
2506	2.499	34.1(713)	1.93	.28	.061(.069)	-.023(-.028)
2507	2.499	34.1(713)	4.03	.28	.112(.125)	-.036(-.042)
2508	2.499	34.1(713)	5.92	.29	.156(.173)	-.047(-.053)
2509	2.499	34.1(713)	7.92	.30	.202(.223)	-.058(-.065)
2510	2.499	34.1(713)	9.83	.32	.245(.271)	-.068(-.075)
2511	2.499	34.1(713)	11.77	.34	.288(.318)	-.077(-.085)
2512	2.499	34.1(713)	13.63	.35	.331(.362)	-.087(-.094)
2513	2.499	34.1(713)	14.55	.35	.352(.385)	-.091(-.098)

(c) T.E. Deflection, Full Span =  $8.3^\circ$ 

Analysis number	Mach number	Dynamic pressure, $\text{kN/m}^2$ (psf)	Angle of attack, deg	Angle of sideslip, deg	Normal force coefficient, bal (integ press.)	Pitching moment coefficient, bal (integ press.)
2601	1.700	37.4(781)	-8.07	.04	-.176(-.191)	.020(.017)
2602	1.700	37.4(781)	-6.07	.08	-.114(-.125)	.004(.001)
2603	1.700	37.5(782)	-4.07	.09	-.051(-.051)	-.014(-.022)
2604	1.700	37.4(782)	-2.03	.10	.016(.023)	-.034(-.044)
2605	1.700	37.4(782)	-.03	.08	.075(.089)	-.051(-.063)
2606	1.700	37.4(782)	1.95	.11	.135(.154)	-.068(-.081)
2607	1.700	37.6(786)	3.96	.12	.200(.224)	-.086(-.101)
2608	1.700	37.6(786)	5.90	.12	.259(.288)	-.101(-.115)
2609	1.700	37.6(786)	7.85	.13	.318(.354)	-.114(-.129)
2610	1.700	37.6(786)	9.80	.14	.374(.416)	-.125(-.140)
2611	1.700	37.8(790)	11.71	.15	.425(.469)	-.133(-.148)
2612	1.700	37.8(790)	13.61	.15	.476(.526)	-.140(-.156)
2613	1.700	37.8(790)	14.51	.16	.501(.552)	-.144(-.160)
2701	2.101	36.0(752)	-8.11	-.69	-.164(-.188)	.024(.024)
2702	2.101	36.0(752)	-6.02	-.67	-.112(-.127)	.010(.008)
2703	2.101	36.0(752)	-4.04	-.64	-.057(-.061)	-.004(-.011)
2704	2.101	36.1(755)	-2.07	-.63	-.001(.002)	-.021(-.029)
2705	2.101	36.2(756)	-.01	-.65	.057(.068)	-.038(-.048)
2706	2.101	36.2(756)	2.00	-.62	.114(.131)	-.054(-.065)
2707	2.101	36.2(756)	4.00	-.61	.171(.194)	-.070(-.082)
2708	2.101	36.2(756)	5.92	-.61	.223(.253)	-.083(-.097)
2709	2.101	36.2(756)	7.88	-.60	.274(.308)	-.095(-.109)
2710	2.101	36.2(756)	9.83	-.59	.322(.360)	-.105(-.119)
2711	2.101	36.2(755)	11.74	-.58	.367(.412)	-.114(-.129)
2712	2.101	36.2(755)	13.61	-.57	.412(.460)	-.121(-.137)
2713	2.101	36.2(755)	14.51	-.51	.435(.484)	-.125(-.142)
2801	2.499	33.8(706)	-8.14	.21	-.147(-.170)	.023(.024)
2802	2.499	34.0(709)	-6.09	.25	-.103(-.119)	.012(.012)
2803	2.499	33.9(709)	-4.00	.26	-.055(-.064)	.000(-.002)
2804	2.499	33.9(709)	-2.03	.27	-.007(-.008)	-.013(-.018)
2805	2.499	33.9(709)	-.07	.25	.043(.049)	-.028(-.035)
2806	2.499	34.0(710)	2.04	.28	.097(.111)	-.044(-.053)
2807	2.499	34.1(712)	4.02	.29	.148(.163)	-.059(-.066)
2808	2.499	34.1(712)	5.93	.30	.191(.212)	-.068(-.077)
2809	2.499	34.1(712)	7.87	.31	.235(.260)	-.079(-.089)
2810	2.499	34.1(712)	9.79	.32	.277(.306)	-.088(-.099)
2811	2.499	34.1(712)	11.73	.34	.318(.353)	-.095(-.108)
2812	2.499	34.1(712)	13.57	.33	.358(.397)	-.103(-.116)
2813	2.499	34.1(712)	14.54	.35	.381(.421)	-.108(-.120)

Table A-3.—(Continued)

(d) T.E. Deflection, Inboard =  $8.3^\circ$ , Outboard =  $0.0^\circ$ 

Analysis number	Mach number	Dynamic pressure, kN/m <sup>2</sup> (psf)	Angle of attack, deg	Angle of sideslip, deg	Normal force coefficient, bal (integ press.)	Pitching moment coefficient, bal (integ press.)
3001	1.699	36.6(764)	-8.05	.04	-.186(-.201)	.029(.027)
3002	1.699	36.6(765)	-6.04	.07	-.125(-.137)	.015(.012)
3003	1.699	36.6(765)	-4.06	.08	-.066(-.068)	-.000(-.006)
3004	1.699	36.6(765)	-2.02	.09	-.001(-.003)	-.019(-.026)
3005	1.699	36.6(764)	-.06	.08	.061(.072)	-.036(-.046)
3006	1.699	37.4(781)	-.15	.08	.056(.066)	-.034(-.045)
3007	1.699	37.4(781)	2.02	.11	.122(.138)	-.054(-.065)
3008	1.699	37.4(781)	4.06	.12	.189(.211)	-.074(-.087)
3009	1.699	37.6(785)	5.99	.13	.251(.279)	-.091(-.105)
3010	1.699	37.7(787)	7.91	.13	.310(.343)	-.105(-.119)
3011	1.699	37.7(787)	9.87	.15	.366(.408)	-.116(-.132)
3012	1.699	37.7(787)	11.76	.15	.417(.462)	-.124(-.140)
3013	1.699	37.7(787)	13.66	.16	.467(.517)	-.132(-.148)
3014	1.699	37.7(787)	14.59	.18	.494(.544)	-.136(-.152)
3101	2.100	36.1(755)	-8.11	-.69	-.173(-.195)	.032(.033)
3102	2.100	36.2(755)	-6.08	-.65	-.120(-.136)	.019(.016)
3103	2.100	36.2(755)	-4.04	-.65	-.068(-.075)	.007(.002)
3104	2.100	36.2(755)	-2.07	-.64	-.014(-.013)	-.008(-.014)
3105	2.100	36.1(755)	-.06	-.65	.044(.052)	-.025(-.033)
3106	2.100	36.2(755)	2.01	-.62	.101(.116)	-.042(-.051)
3107	2.100	36.1(755)	4.01	-.62	.159(.182)	-.059(-.071)
3108	2.100	36.1(755)	5.82	-.61	.211(.239)	-.074(-.086)
3109	2.100	36.1(755)	7.77	-.60	.262(.294)	-.086(-.099)
3110	2.100	36.1(755)	9.74	-.59	.310(.348)	-.096(-.109)
3111	2.100	36.2(755)	11.63	-.58	.354(.397)	-.103(-.118)
3112	2.100	36.1(755)	13.56	-.55	.399(.446)	-.111(-.126)
3113	2.100	36.1(755)	14.49	-.55	.423(.471)	-.115(-.131)
3114	2.100	36.1(755)	5.94	-.61	.215(.243)	-.074(-.087)
3115	2.100	36.1(755)	7.92	-.59	.266(.299)	-.087(-.099)
3116	2.100	36.1(755)	9.88	-.58	.313(.351)	-.096(-.109)
3117	2.100	36.1(755)	11.77	-.57	.358(.402)	-.104(-.119)
3118	2.100	36.1(755)	13.66	-.56	.402(.449)	-.111(-.126)
3119	2.100	36.1(755)	14.59	-.55	.425(.474)	-.116(-.131)
3201	2.499	34.0(709)	-8.13	.20	-.155(-.177)	.030(.032)
3202	2.499	33.9(709)	-6.11	.24	-.111(-.127)	.019(.020)
3203	2.499	34.0(709)	-4.09	.26	-.067(-.077)	.010(.008)
3204	2.499	33.9(709)	-2.06	.26	-.019(-.021)	-.003(-.006)
3205	2.499	33.9(709)	.02	.25	.033(.039)	-.018(-.024)
3206	2.499	33.9(709)	1.98	.28	.085(.096)	-.033(-.041)
3207	2.499	33.9(709)	4.06	.29	.138(.154)	-.049(-.057)
3208	2.499	33.9(709)	5.96	.30	.182(.203)	-.060(-.068)
3209	2.499	33.9(709)	7.91	.31	.226(.251)	-.070(-.080)
3210	2.499	34.2(714)	9.85	.32	.268(.298)	-.079(-.090)
3211	2.499	34.2(715)	11.78	.34	.309(.344)	-.087(-.099)
3212	2.499	34.2(715)	13.65	.36	.350(.389)	-.095(-.107)
3213	2.499	34.2(714)	14.56	.35	.372(.411)	-.099(-.111)

(e) T.E. Deflection, Inboard =  $4.1^\circ$ , Outboard =  $0.0^\circ$ 

Analysis number	Mach number	Dynamic pressure, kN/m <sup>2</sup> (psf)	Angle of attack, deg	Angle of sideslip, deg	Normal force coefficient, bal (integ press.)	Pitching moment coefficient, bal (integ press.)
3401	1.700	37.1(774)	-8.06	.04	-.216(-.238)	.047(.050)
3402	1.700	37.9(791)	-8.18	.03	-.219(-.242)	.048(.051)
3403	1.700	37.9(791)	-6.13	.07	-.157(-.173)	.032(.034)
3404	1.700	37.9(792)	-4.17	.08	-.096(-.104)	.017(.015)
3405	1.700	37.9(791)	-2.11	.09	-.031(-.031)	-.001(-.006)
3406	1.700	38.6(806)	-.06	.08	.034(.042)	-.020(-.028)
3407	1.700	38.6(806)	2.04	.11	.097(.110)	-.038(-.048)
3408	1.700	38.6(806)	4.05	.12	.163(.182)	-.058(-.069)
3409	1.700	38.6(806)	6.00	.13	.228(.251)	-.076(-.087)
3410	1.700	38.6(806)	7.95	.14	.288(.317)	-.091(-.102)
3411	1.700	38.6(806)	9.90	.15	.345(.381)	-.103(-.115)
3412	1.700	38.6(806)	11.81	.16	.399(.441)	-.112(-.126)
3413	1.700	38.6(806)	13.72	.18	.453(.498)	-.121(-.136)
3414	1.700	38.6(806)	14.63	.18	.479(.526)	-.127(-.141)
3501	2.100	37.2(777)	-8.14	-.70	-.194(-.221)	.045(.048)
3502	2.100	37.2(777)	-6.07	-.66	-.141(-.162)	.031(.033)
3503	2.100	37.2(777)	-4.03	-.65	-.087(-.100)	.018(.018)
3504	2.100	37.2(777)	-2.06	-.64	-.033(-.037)	.003(.000)
3505	2.100	37.2(777)	.01	-.65	.025(.029)	-.013(-.018)
3506	2.100	37.2(777)	.01	-.65	.024(.029)	-.013(-.018)
3507	2.100	37.2(777)	2.04	-.62	.083(.095)	-.030(-.038)
3508	2.100	37.2(777)	4.03	-.61	.141(.160)	-.048(-.056)
3509	2.100	37.2(777)	5.92	-.61	.195(.219)	-.062(-.072)
3510	2.100	37.2(777)	7.89	-.60	.247(.275)	-.075(-.084)
3511	2.100	37.2(777)	9.85	-.59	.297(.329)	-.086(-.096)
3512	2.100	37.5(783)	11.76	-.58	.343(.381)	-.094(-.106)
3513	2.100	37.5(784)	13.64	-.57	.389(.431)	-.103(-.115)
3514	2.100	37.5(784)	14.57	-.57	.412(.455)	-.107(-.119)
3601	2.500	34.5(721)	-8.14	.21	-.172(-.195)	.040(.043)
3602	2.500	34.6(722)	-6.13	.25	-.128(-.147)	.029(.032)
3603	2.500	34.6(722)	-4.06	.26	-.082(-.095)	.018(.020)
3604	2.500	34.6(722)	-2.09	.27	-.035(-.041)	.006(.005)
3605	2.500	34.6(722)	-.02	.25	.018(.020)	-.009(-.013)
3606	2.500	34.6(723)	-.02	.25	.017(.020)	-.009(-.013)
3607	2.500	34.6(723)	1.95	.28	.068(.078)	-.024(-.030)
3608	2.500	34.6(723)	4.04	.29	.122(.135)	-.039(-.045)
3609	2.500	34.6(723)	5.94	.30	.166(.184)	-.051(-.057)
3610	2.500	34.7(724)	7.89	.30	.211(.232)	-.061(-.069)
3611	2.500	34.8(726)	9.81	.31	.254(.279)	-.071(-.079)
3612	2.500	34.8(727)	11.76	.33	.295(.325)	-.078(-.087)
3613	2.500	34.8(727)	13.62	.34	.337(.369)	-.087(-.095)
3614	2.500	34.8(727)	14.53	.34	.359(.391)	-.092(-.099)

Table A-3.—(Continued)

(f) T.E. Deflection, Full Span =  $4.1^\circ$ 

Analysis number	Mach number	Dynamic pressure, kN/m <sup>2</sup> (psf)	Angle of attack, deg	Angle of sideslip, deg	Normal force coefficient, bal (integ press.)	Pitching moment coefficient, bal (integ press.)
3701	1.700	37.6(786)	-8.08	.05	-.210(-.234)	.042(.045)
3702	1.700	37.6(785)	-6.09	.08	-.148(-.165)	.026(.027)
3703	1.700	37.6(785)	-4.08	.09	-.086(-.092)	.010(.006)
3704	1.700	37.6(785)	-2.01	.10	-.019(-.018)	-.010(-.016)
3705	1.700	37.6(785)	-.02	.08	.041(.050)	-.028(-.037)
3706	1.700	37.6(785)	1.95	.11	.103(.116)	-.046(-.056)
3707	1.700	37.6(785)	3.96	.11	.168(.188)	-.065(-.077)
3708	1.700	38.5(805)	5.92	.12	.231(.255)	-.081(-.093)
3709	1.700	38.6(805)	7.86	.13	.290(.321)	-.095(-.107)
3710	1.700	38.6(806)	9.82	.14	.348(.383)	-.107(-.119)
3711	1.700	38.6(806)	11.72	.15	.401(.444)	-.116(-.131)
3712	1.700	38.6(806)	13.63	.16	.455(.501)	-.126(-.140)
3713	1.700	38.6(807)	14.52	.16	.481(.529)	-.131(-.146)
3801	2.101	37.4(781)	-8.13	-.69	-.190(-.216)	.041(.044)
3802	2.101	37.4(781)	-6.10	-.65	-.137(-.157)	.027(.028)
3803	2.101	37.4(781)	-4.06	-.64	-.083(-.094)	.013(.011)
3804	2.101	37.4(781)	-2.09	-.63	-.027(-.029)	-.003(-.007)
3805	2.101	37.4(781)	-.01	-.65	.031(.037)	-.019(-.026)
3806	2.101	37.4(781)	2.00	-.62	.089(.102)	-.037(-.045)
3807	2.101	37.4(781)	4.01	-.61	.147(.166)	-.053(-.063)
3808	2.101	37.4(781)	5.93	-.60	.199(.225)	-.067(-.077)
3809	2.101	37.7(788)	7.90	-.60	.252(.281)	-.080(-.090)
3810	2.101	37.7(787)	9.86	-.59	.301(.334)	-.090(-.101)
3811	2.101	37.6(786)	11.76	-.57	.348(.386)	-.099(-.112)
3812	2.101	37.6(786)	13.64	-.56	.394(.438)	-.108(-.121)
3813	2.101	37.6(786)	14.55	-.50	.417(.461)	-.112(-.124)
3901	2.499	34.6(723)	-8.14	.22	-.168(-.192)	.036(.040)
3902	2.499	34.6(724)	-6.13	.25	-.124(-.143)	.025(.028)
3903	2.499	34.6(723)	-4.06	.26	-.077(-.090)	.014(.015)
3904	2.499	34.6(723)	-2.09	.27	-.029(-.035)	.001(-.000)
3905	2.499	35.0(731)	-.02	.25	.023(.026)	-.014(-.018)
3906	2.499	35.0(731)	1.95	.28	.074(.084)	-.029(-.036)
3907	2.499	35.0(731)	4.04	.29	.126(.140)	-.043(-.050)
3908	2.499	35.0(731)	5.94	.30	.170(.189)	-.054(-.061)
3909	2.499	35.0(731)	7.89	.30	.215(.237)	-.065(-.073)
3910	2.499	35.0(731)	9.81	.32	.258(.283)	-.074(-.083)
3911	2.499	35.0(731)	11.66	.33	.297(.328)	-.082(-.091)
3912	2.499	35.0(731)	13.52	.34	.339(.372)	-.090(-.100)
3913	2.499	35.0(731)	14.44	.33	.362(.394)	-.096(-.103)

(g) T.E. Deflection, Inboard =  $0.0^\circ$ , Outboard =  $4.1^\circ$ 

Analysis number	Mach number	Dynamic pressure, kN/m <sup>2</sup> (psf)	Angle of attack, deg	Angle of sideslip, deg	Normal force coefficient, bal (integ press.)	Pitching moment coefficient, bal (integ press.)
4001	1.700	38.1(795)	-8.20	.06	-.252(-.284)	.066(.075)
4002	1.700	38.1(795)	-5.97	.10	-.182(-.205)	.047(.054)
4003	1.700	38.0(794)	-1.93	.11	-.050(-.055)	.009(.008)
4004	1.700	38.0(794)	-.01	.09	.010(.010)	-.008(-.012)
4005	1.700	38.0(794)	2.02	.12	.072(.079)	-.026(-.032)
4006	1.700	38.0(793)	4.04	.12	.136(.151)	-.045(-.053)
4007	1.700	38.0(794)	5.97	.13	.198(.218)	-.061(-.069)
4008	1.700	38.0(794)	7.92	.13	.260(.285)	-.076(-.085)
4009	1.700	38.0(794)	9.83	.14	.318(.351)	-.090(-.099)
4010	1.700	38.0(793)	11.78	.15	.376(.416)	-.103(-.114)
4011	1.700	38.0(794)	13.71	.14	.434(.478)	-.114(-.127)
4012	1.700	38.0(793)	14.57	.15	.459(.507)	-.120(-.134)
4013	1.700	38.0(793)	-3.97	.10	-.116(-.130)	.029(.031)
4101	2.101	37.0(773)	-8.03	-.67	-.214(-.246)	.055(.062)
4102	2.101	37.0(773)	-5.91	-.63	-.159(-.185)	.041(.047)
4103	2.101	37.0(773)	-3.97	-.63	-.105(-.123)	.027(.030)
4104	2.101	37.0(773)	-1.99	-.62	-.048(-.056)	.011(.010)
4105	2.101	37.0(773)	.07	-.65	.010(.010)	-.006(-.009)
4106	2.101	37.0(773)	2.08	-.61	.067(.075)	-.023(-.027)
4107	2.101	37.0(772)	4.09	-.61	.123(.139)	-.038(-.044)
4108	2.101	37.0(773)	6.01	-.60	.177(.199)	-.052(-.059)
4109	2.101	37.0(772)	7.98	-.60	.230(.254)	-.066(-.072)
4110	2.101	37.0(773)	9.94	-.59	.281(.311)	-.078(-.084)
4111	2.101	37.0(772)	11.84	-.58	.329(.364)	-.088(-.096)
4112	2.101	37.0(772)	13.73	-.58	.376(.417)	-.098(-.107)
4113	2.101	37.0(772)	14.65	-.59	.399(.442)	-.102(-.113)
4114	2.101	37.0(772)	-6.03	-.63	-.162(-.189)	.042(.049)
4201	2.499	34.4(719)	-8.07	.23	-.188(-.216)	.048(.055)
4202	2.499	34.4(719)	-6.06	.27	-.144(-.166)	.037(.043)
4203	2.499	34.4(719)	-3.98	.27	-.095(-.111)	.025(.029)
4204	2.499	34.4(719)	-2.01	.28	-.047(-.055)	.012(.013)
4205	2.499	34.4(719)	.06	.26	.006(.005)	-.004(-.005)
4206	2.499	34.4(719)	2.02	.29	.057(.063)	-.019(-.023)
4207	2.499	34.4(719)	4.12	.29	.108(.120)	-.033(-.037)
4208	2.499	34.4(719)	6.02	.30	.153(.168)	-.044(-.048)
4209	2.499	34.4(719)	7.97	.30	.198(.217)	-.055(-.059)
4210	2.499	34.4(719)	9.84	.31	.240(.262)	-.064(-.070)
4211	2.499	34.4(719)	11.80	.32	.283(.311)	-.074(-.080)
4212	2.499	34.4(719)	13.66	.32	.326(.356)	-.083(-.089)
4213	2.499	34.4(719)	14.55	.38	.347(.378)	-.087(-.092)
4214	2.499	34.4(719)	4.03	.29	.109(.117)	-.033(-.036)



Table A-3.—(Concluded)

(h) T.E. Deflection, Full Span =  $-4.1^\circ$ 

Analysis number	Mach number	Dynamic pressure, $\text{kN/m}^2$ (psf)	Angle of attack, deg	Angle of sideslip, deg	Normal force coefficient, bal (integ press.)	Pitching moment coefficient, bal (integ press.)
4401	1.700	36.7(767)	-7.99	.05	-.289(-.330)	.094(.112)
4402	1.700	36.9(770)	-6.02	.08	-.229(-.262)	.079(.094)
4403	1.700	37.0(772)	-8.11	.04	-.293(-.335)	.095(.113)
4404	1.700	37.0(772)	-3.98	.09	-.164(-.190)	.063(.075)
4405	1.700	37.0(772)	-1.94	.10	-.099(-.116)	.044(.053)
4406	1.700	37.5(783)	.09	.09	-.035(-.048)	.026(.034)
4407	1.700	37.5(782)	2.07	.12	.027(.022)	.008(.011)
4408	1.700	37.2(778)	3.96	.12	.087(.089)	-.010(-.008)
4409	1.700	37.3(779)	6.03	.13	.153(.164)	-.027(-.029)
4410	1.700	37.3(779)	7.92	.15	.213(.230)	-.042(-.045)
4411	1.700	37.5(782)	9.85	.16	.275(.296)	-.058(-.060)
4412	1.700	37.5(783)	11.78	.17	.334(.362)	-.071(-.077)
4413	1.700	37.5(782)	13.71	.19	.392(.425)	-.083(-.091)
4414	1.700	37.5(783)	14.59	.19	.419(.456)	-.090(-.099)
4501	2.101	36.2(756)	-8.11	-.69	-.249(-.288)	.080(.092)
4502	2.101	36.2(755)	-5.98	-.65	-.194(-.228)	.066(.078)
4503	2.101	36.2(755)	-3.94	-.64	-.138(-.164)	.052(.061)
4504	2.101	36.2(755)	-1.88	-.63	-.080(-.098)	.035(.042)
4505	2.101	36.1(755)	.04	-.64	-.024(-.035)	.019(.024)
4506	2.101	36.1(755)	2.05	-.61	.034(.031)	.003(.004)
4507	2.101	36.9(771)	4.11	-.60	.091(.098)	-.013(-.015)
4508	2.101	37.0(772)	6.06	-.60	.143(.158)	-.026(-.029)
4509	2.101	37.0(772)	8.00	-.58	.196(.214)	-.039(-.043)
4510	2.101	37.0(772)	9.97	-.57	.248(.270)	-.051(-.055)
4511	2.101	37.0(772)	11.86	-.55	.296(.323)	-.061(-.066)
4512	2.101	37.0(772)	13.76	-.54	.344(.377)	-.071(-.078)
4513	2.101	37.0(772)	14.68	-.54	.367(.401)	-.076(-.083)
4514	2.101	37.0(772)	-1.99	-.63	-.083(-.101)	.038(.043)
4515	2.101	37.0(772)	7.93	-.58	.196(.212)	-.039(-.043)
4516	2.101	37.0(772)	9.89	-.58	.247(.267)	-.051(-.055)
4517	2.101	37.0(772)	11.78	-.56	.294(.320)	-.061(-.066)
4518	2.101	37.0(772)	13.68	-.54	.342(.374)	-.071(-.077)
4519	2.101	37.0(772)	14.61	-.54	.366(.399)	-.075(-.082)
4601	2.499	34.1(712)	-8.04	.22	-.213(-.247)	.069(.078)
4602	2.499	34.1(712)	-6.03	.25	-.167(-.198)	.056(.066)
4603	2.499	34.1(712)	-3.95	.26	-.119(-.145)	.044(.053)
4604	2.499	34.1(712)	-1.99	.27	-.071(-.089)	.031(.038)
4605	2.499	34.1(712)	.06	.26	-.017(-.029)	.015(.020)
4606	2.499	34.1(712)	2.03	.29	.034(.030)	.001(.002)
4607	2.499	34.1(712)	4.13	.30	.084(.088)	-.012(-.014)
4608	2.499	34.1(712)	6.02	.31	.127(.136)	-.022(-.025)
4609	2.499	34.1(711)	7.97	.32	.172(.184)	-.033(-.036)
4610	2.499	34.1(712)	9.89	.33	.216(.231)	-.043(-.047)
4611	2.499	34.1(711)	11.83	.34	.259(.279)	-.052(-.057)
4612	2.499	34.1(711)	13.69	.35	.301(.324)	-.061(-.066)
4613	2.499	34.1(711)	14.60	.35	.322(.345)	-.065(-.069)

Table A-4.—Experimental Data Test Point Log. Flat Wing, Sharp Leading Edge; T.E. Deflection,  
Full Span = 0.0°

(a) L.E. Deflection, Full Span = 5.1°

Analysis number	Mach number	Dynamic pressure, kN/m <sup>2</sup> (psf)	Angle of attack, deg	Angle of sideslip, deg	Normal force coefficient, bal (integ press.)	Pitching moment coefficient, bal (integ press.)
4801	1.700	36.8(768)	-8.10	.05	-.267(-.301)	.070(.074)
4802	1.700	36.8(769)	-6.01	.08	-.201(-.227)	.054(.057)
4803	1.700	36.8(769)	-4.04	.09	-.137(-.155)	.036(.036)
4804	1.700	36.8(769)	-1.96	.10	-.068(-.079)	.017(.016)
4805	1.700	36.6(764)	.04	.09	-.003(-.003)	-.002(-.006)
4806	1.700	36.6(764)	2.00	.12	.058(.066)	-.020(-.026)
4807	1.700	36.6(763)	3.96	.13	.120(.135)	-.039(-.048)
4808	1.700	36.6(764)	5.94	.14	.183(.208)	-.058(-.070)
4809	1.700	36.6(764)	7.91	.15	.247(.281)	-.075(-.089)
4810	1.700	36.6(763)	9.81	.16	.307(.345)	-.091(-.102)
4811	1.700	36.7(767)	11.75	.18	.367(.416)	-.104(-.117)
4812	1.700	37.2(777)	13.71	.19	.427(.474)	-.116(-.125)
4813	1.700	37.3(778)	14.58	.19	.453(.502)	-.121(-.130)
4901	2.101	36.3(757)	-8.07	-.68	-.228(-.267)	.060(.063)
4902	2.101	36.2(757)	-5.98	-.64	-.174(-.206)	.046(.049)
4903	2.101	36.2(756)	-4.10	-.64	-.123(-.146)	.033(.034)
4904	2.101	36.2(756)	-2.02	-.63	-.064(-.077)	.017(.016)
4905	2.101	36.2(756)	.05	-.65	-.003(-.005)	-.001(-.005)
4906	2.101	36.2(756)	2.00	-.61	.052(.060)	-.017(-.024)
4907	2.101	36.2(756)	3.98	-.60	.106(.121)	-.033(-.041)
4908	2.101	36.2(756)	5.92	-.59	.157(.179)	-.047(-.056)
4909	2.101	36.2(756)	7.89	-.58	.212(.238)	-.062(-.070)
4910	2.101	36.2(756)	9.81	-.56	.264(.295)	-.074(-.082)
4911	2.101	36.2(756)	11.77	-.55	.316(.355)	-.085(-.093)
4912	2.101	36.2(756)	13.68	-.54	.367(.411)	-.095(-.104)
4913	2.101	36.2(756)	14.55	-.53	.391(.437)	-.101(-.109)
5001	2.499	33.4(698)	-8.13	.22	-.200(-.231)	.053(.056)
5002	2.499	33.4(698)	-6.05	.26	-.154(-.180)	.042(.044)
5003	2.499	33.4(698)	-4.01	.26	-.108(-.127)	.030(.031)
5004	2.499	33.4(698)	-2.01	.28	-.059(-.069)	.017(.015)
5005	2.499	33.5(699)	.05	.26	-.006(-.006)	.001(-.003)
5006	2.499	33.5(699)	2.00	.29	.042(.050)	-.013(-.019)
5007	2.499	33.5(699)	4.06	.30	.091(.105)	-.026(-.034)
5008	2.499	33.5(699)	5.94	.31	.135(.152)	-.038(-.046)
5009	2.499	33.5(699)	7.87	.32	.179(.203)	-.049(-.058)
5010	2.499	33.5(699)	9.78	.34	.224(.254)	-.060(-.068)
5011	2.499	33.5(699)	11.66	.36	.270(.302)	-.071(-.077)
5012	2.499	33.5(699)	13.69	.37	.318(.354)	-.081(-.087)
5013	2.499	33.5(699)	14.62	.37	.339(.378)	-.085(-.091)
5014	2.499	33.5(699)	11.84	.39	.275(.307)	-.071(-.078)

(b) L.E. Deflection, Full Span = 0.0°

Analysis number	Mach number	Dynamic pressure, kN/m <sup>2</sup> (psf)	Angle of attack, deg	Angle of sideslip, deg	Normal force coefficient, bal (integ press.)	Pitching moment coefficient, bal (integ press.)
5101	1.700	37.5(783)	-8.07	.03	-.256(-.292)	.072(.080)
5102	1.700	37.9(792)	-5.98	.06	-.190(-.214)	.056(.059)
5103	1.700	37.9(792)	-3.97	.08	-.125(-.144)	.037(.041)
5104	1.700	37.9(792)	-1.93	.09	-.059(-.066)	.017(.018)
5105	1.700	38.1(795)	.12	.10	.004(.005)	-.001(-.004)
5106	1.700	38.1(796)	2.07	.11	.063(.072)	-.019(-.024)
5107	1.700	38.1(797)	4.08	.12	.128(.148)	-.040(-.047)
5108	1.700	38.1(797)	5.92	.13	.190(.215)	-.057(-.064)
5109	1.700	38.1(796)	7.90	.13	.254(.286)	-.073(-.081)
5110	1.700	38.1(796)	9.82	.14	.314(.353)	-.087(-.096)
5111	1.700	38.1(796)	11.73	.16	.371(.415)	-.098(-.107)
5112	1.700	38.1(796)	13.65	.17	.429(.479)	-.110(-.121)
5113	1.700	38.1(796)	14.54	.16	.456(.508)	-.115(-.127)
5201	2.101	37.2(777)	-8.05	-.70	-.221(-.258)	.061(.068)
5202	2.101	37.2(777)	-6.02	-.66	-.167(-.196)	.048(.054)
5203	2.101	37.2(777)	-3.97	-.65	-.111(-.129)	.033(.036)
5204	2.101	37.2(777)	-2.00	-.64	-.055(-.065)	.017(.018)
5205	2.101	37.2(777)	.00	-.64	.002(.002)	.000(-.002)
5206	2.101	37.2(777)	2.08	-.62	.059(.067)	-.017(-.021)
5207	2.101	37.2(777)	4.07	-.61	.115(.134)	-.034(-.040)
5208	2.101	37.2(777)	5.89	-.61	.167(.191)	-.048(-.054)
5209	2.101	37.2(777)	7.85	-.60	.221(.251)	-.061(-.068)
5210	2.101	37.2(777)	9.83	-.58	.274(.308)	-.074(-.080)
5211	2.101	37.2(777)	11.72	-.57	.322(.362)	-.083(-.090)
5212	2.101	37.2(777)	13.62	-.57	.369(.415)	-.092(-.101)
5213	2.101	37.2(777)	14.54	-.57	.393(.440)	-.098(-.105)
5301	2.499	34.7(724)	-8.06	.20	-.193(-.223)	.052(.059)
5302	2.499	34.7(724)	-6.05	.25	-.147(-.171)	.041(.047)
5303	2.499	34.7(724)	-3.97	.25	-.099(-.115)	.029(.033)
5304	2.499	34.7(724)	-1.98	.26	-.051(-.060)	.016(.018)
5305	2.499	34.7(724)	.05	.26	-.000(-.000)	.001(-.001)
5306	2.499	34.7(724)	2.02	.28	.049(.056)	-.014(-.018)
5307	2.499	34.7(724)	4.11	.29	.100(.113)	-.028(-.032)
5308	2.499	34.6(724)	6.00	.30	.146(.166)	-.040(-.045)
5309	2.499	34.6(724)	7.96	.30	.192(.216)	-.051(-.055)
5310	2.499	34.6(724)	9.83	.36	.238(.267)	-.063(-.068)
5311	2.499	34.6(724)	11.82	.33	.281(.312)	-.071(-.075)
5312	2.499	34.6(724)	13.68	.34	.323(.356)	-.079(-.083)
5313	2.499	34.6(724)	14.59	.34	.343(.380)	-.083(-.087)

Table A-5.—FLEXSTAB Test Point Log. Twisted Wing, Rounded Leading Edge;  
L.E. Deflection, Full Span = 0.0°

(a) T.E. Deflection, Full Span = 0.0°

Analysis number	Mach number	Dynamic pressure, kN/m <sup>2</sup> (psf)	Angle of attack, deg	Normal force coefficient, bal (integ press.)	Pitching moment coefficient, bal (integ press.)
100301	1.70		-8.00	(-.348)	(.1110)
100302	1.70		-5.97	(-.275)	(.090)
100303	1.70		-3.93	(-.201)	(.070)
100304	1.70		-1.95	(-.130)	(.050)
100305	1.70		-.00	(-.060)	(.030)
100306	1.70		2.00	(.012)	(.010)
100307	1.70		4.08	(.087)	(-.011)
100308	1.70		4.08	(.087)	(-.011)
100309	1.70		5.86	(.151)	(-.028)
100310	1.70		7.89	(.224)	(-.049)
100311	1.70		9.72	(.290)	(-.067)
100312	1.70		11.69	(.360)	(-.087)
100313	1.70		13.58	(.428)	(-.106)
100314	1.70		14.52	(.462)	(-.115)
100901	2.10		-8.12	(-.323)	(.103)
100902	2.10		-6.04	(-.253)	(.084)
100903	2.10		-4.01	(-.186)	(.065)
100904	2.10		-2.02	(-.120)	(.046)
100905	2.10		.00	(-.053)	(.027)
100906	2.10		2.00	(.014)	(.008)
100907	2.10		3.98	(.079)	(-.010)
100908	2.10		5.96	(.145)	(-.029)
100909	2.10		7.89	(.209)	(-.047)
100910	2.10		9.80	(.273)	(-.065)
100911	2.10		11.75	(.337)	(-.083)
100912	2.10		13.66	(.401)	(-.101)
100913	2.10		14.57	(.431)	(-.109)
101001	2.50		-8.14	(-.294)	(.091)
101002	2.50		-6.09	(-.232)	(.074)
101003	2.50		-4.05	(-.171)	(.058)
101004	2.50		-2.01	(-.109)	(.042)
101005	2.50		-.01	(-.048)	(.025)
101006	2.50		1.99	(.012)	(.009)
101007	2.50		3.95	(.072)	(-.007)
101008	2.50		5.94	(.132)	(-.023)
101009	2.50		7.90	(.191)	(-.038)
101010	2.50		9.84	(.250)	(-.054)
101011	2.50		11.75	(.308)	(-.069)
101012	2.50		13.64	(.365)	(-.085)
101013	2.50		14.56	(.393)	(-.092)

(b) T.E. Deflection, Full Span = 8.3°

Analysis number	Mach number	Dynamic pressure, kN/m <sup>2</sup> (psf)	Angle of attack, deg	Normal force coefficient, bal (integ press.)	Pitching moment coefficient, bal (integ press.)
101101	1.70		-8.15	(-.217)	(.013)
101102	1.70		-6.05	(-.142)	(-.008)
101103	1.70		-4.02	(-.069)	(-.028)
101104	1.70		-2.02	(.003)	(-.048)
101105	1.70		.02	(.076)	(-.068)
101106	1.70		1.99	(.147)	(-.088)
101107	1.70		5.93	(.288)	(-.127)
101108	1.70		7.87	(.358)	(-.147)
101109	1.70		9.82	(.428)	(-.166)
101110	1.70		11.71	(.496)	(-.185)
101111	1.70		13.64	(.565)	(-.204)
101112	1.70		14.55	(.598)	(-.213)
101113	1.70		3.95	(.217)	(-.108)
101201	2.10		-8.11	(-.235)	(.042)
101202	2.10		-6.21	(-.172)	(.024)
101203	2.10		-6.08	(-.168)	(.023)
101204	2.10		-4.07	(-.101)	(.004)
101205	2.10		-1.94	(-.031)	(-.016)
101206	2.10		.00	(.034)	(-.034)
101207	2.10		.00	(.034)	(-.034)
101208	2.10		2.03	(.101)	(-.053)
101209	2.10		3.98	(.166)	(-.071)
101210	2.10		5.94	(.231)	(-.089)
101211	2.10		7.89	(.295)	(-.108)
101212	2.10		9.83	(.360)	(-.126)
101213	2.10		11.73	(.423)	(-.144)
101214	2.10		13.63	(.486)	(-.161)
101215	2.10		14.54	(.516)	(-.170)
101301	2.50		-8.13	(-.225)	(.042)
101302	2.50		-6.13	(-.165)	(.026)
101303	2.50		-4.08	(-.103)	(.010)
101304	2.50		-2.11	(-.043)	(-.006)
101305	2.50		.01	(.021)	(-.023)
101306	2.50		1.92	(.079)	(-.038)
101307	2.50		3.92	(.139)	(-.054)
101308	2.50		5.89	(.199)	(-.070)
101309	2.50		7.86	(.258)	(-.086)
101310	2.50		9.78	(.316)	(-.102)
101311	2.50		11.70	(.375)	(-.117)
101312	2.50		13.58	(.431)	(-.132)
101313	2.50		14.49	(.459)	(-.139)

Table A-6.—FLEXSTAB Test Point Log. Flat Wing, Rounded Leading Edge; L.E. Deflection,  
Full Span =  $5.1^\circ$ ; T.E. Deflection, Full Span =  $0.0^\circ$

Analysis number	Mach number	Dynamic pressure, $\text{kN/m}^2$ (psf)	Angle of attack, deg	Normal force coefficient, bal (integ press.)	Pitching moment coefficient, bal (integ press.)
101601	1.70		-8.10	(-.294)	(.076)
101602	1.70		-6.07	(-.221)	(.055)
101603	1.70		-3.98	(-.146)	(.034)
101604	1.70		-1.98	(-.074)	(.014)
101605	1.70		.02	(-.002)	(-.005)
101606	1.70		2.01	(.069)	(-.025)
101607	1.70		3.99	(.140)	(-.045)
101608	1.70		5.98	(.212)	(-.065)
101609	1.70		7.90	(.281)	(-.084)
101610	1.70		9.85	(.351)	(-.104)
101611	1.70		9.85	(.351)	(-.104)
101612	1.70		11.78	(.420)	(-.123)
101613	1.70		13.68	(.488)	(-.142)
101614	1.70		14.58	(.520)	(-.151)
101701	2.10		-8.14	(-.274)	(.070)
101702	2.10		-6.09	(-.206)	(.051)
101703	2.10		-4.03	(-.137)	(.032)
101704	2.10		-2.03	(-.071)	(.013)
101705	2.10		-.02	(-.005)	(-.006)
101706	2.10		2.02	(.063)	(-.025)
101707	2.10		3.99	(.128)	(-.043)
101708	2.10		5.91	(.192)	(-.061)
101709	2.10		7.89	(.258)	(-.080)
101710	2.10		9.85	(.323)	(-.098)
101711	2.10		11.75	(.386)	(-.116)
101712	2.10		13.64	(.448)	(-.133)
101713	2.10		14.57	(.479)	(-.142)
101801	2.50		-8.14	(-.250)	(.058)
101802	2.50		-6.12	(-.189)	(.042)
101803	2.50		-4.05	(-.126)	(.025)
101804	2.50		-2.04	(-.065)	(.009)
101805	2.50		-.09	(-.006)	(-.007)
101806	2.50		1.99	(.056)	(-.023)
101807	2.50		4.04	(.118)	(-.040)
101808	2.50		5.97	(.177)	(-.056)
101809	2.50		7.90	(.235)	(-.071)
101810	2.50		11.76	(.352)	(-.102)
101811	2.50		13.64	(.409)	(-.117)
101812	2.50		14.57	(.437)	(-.125)
101813	2.50		9.82	(.293)	(-.086)

Table A-7.—FLEXSTAB Test Point Log. Flat Wing, Rounded Leading Edge;  
L.E. Deflection, Full Span = 0.0°

(a) T.E. Deflection, Full Span = 0.0°

Analysis number	Mach number	Dynamic pressure, kN/m <sup>2</sup> (psf)	Angle of attack, deg	Normal force coefficient, bal (integ press.)	Pitching moment coefficient, bal (integ press.)
102001	1.70		-8.09	(-.292)	(.081)
102002	1.70		-8.09	(-.292)	(.081)
102003	1.70		-6.08	(-.219)	(.061)
102004	1.70		-4.05	(-.146)	(.041)
102005	1.70		-2.00	(-.073)	(.021)
102006	1.70		.04	(.001)	(.000)
102007	1.70		2.04	(.073)	(-.020)
102008	1.70		4.04	(.145)	(-.040)
102009	1.70		6.00	(.215)	(-.060)
102010	1.70		7.88	(.283)	(-.078)
102011	1.70		9.80	(.352)	(-.098)
102012	1.70		11.71	(.420)	(-.117)
102013	1.70		13.61	(.489)	(-.136)
102014	1.70		14.52	(.521)	(-.145)
102101	2.10		-8.14	(-.270)	(.076)
102102	2.10		-6.07	(-.201)	(.057)
102103	2.10		-4.08	(-.135)	(.038)
102104	2.10		-2.08	(-.069)	(.019)
102105	2.10		.00	(.000)	(-.000)
102106	2.10		2.00	(.067)	(-.019)
102107	2.10		4.02	(.134)	(-.038)
102108	2.10		5.84	(.194)	(-.055)
102109	2.10		7.79	(.259)	(-.073)
102110	2.10		9.77	(.325)	(-.092)
102111	2.10		11.66	(.387)	(-.109)
102112	2.10		13.58	(.451)	(-.127)
102113	2.10		14.51	(.482)	(-.136)
102114	2.10		11.70	(.389)	(-.110)
102201	2.50		-8.15	(-.246)	(.065)
102202	2.50		-8.15	(-.246)	(.065)
102203	2.50		-6.14	(-.185)	(.049)
102204	2.50		-4.06	(-.122)	(.033)
102205	2.50		-2.09	(-.062)	(.017)
102206	2.50		-.02	(.000)	(-.000)
102207	2.50		1.95	(.060)	(-.016)
102208	2.50		4.05	(.124)	(-.033)
102209	2.50		5.84	(.178)	(-.047)
102210	2.50		7.69	(.234)	(-.062)
102211	2.50		9.64	(.293)	(-.078)
102212	2.50		9.75	(.296)	(-.079)
102213	2.50		11.63	(.353)	(-.094)
102214	2.50		13.51	(.410)	(-.109)
102215	2.50		14.43	(.438)	(-.117)

(b) T.E. Deflection, Inboard = 0.0°, Outboard = 8.3°

Analysis number	Mach number	Dynamic pressure, kN/m <sup>2</sup> (psf)	Angle of attack, deg	Normal force coefficient, bal (integ press.)	Pitching moment coefficient, bal (integ press.)
102301	1.70		-8.11	(-.262)	(.052)
102302	1.70		-6.12	(-.190)	(.033)
102303	1.70		-4.11	(-.118)	(.012)
102304	1.70		-2.06	(-.044)	(-.008)
102305	1.70		-.01	(.029)	(-.029)
102306	1.70		1.99	(.101)	(-.048)
102307	1.70		4.00	(.173)	(-.069)
102308	1.70		5.85	(.240)	(-.087)
102309	1.70		7.83	(.311)	(-.107)
102310	1.70		9.75	(.380)	(-.126)
102311	1.70		11.66	(.449)	(-.145)
102312	1.70		13.57	(.517)	(-.164)
102313	1.70		14.57	(.553)	(-.174)
102401	2.10		-8.16	(-.251)	(.057)
102402	2.10		-6.13	(-.183)	(.038)
102403	2.10		-4.08	(-.115)	(.019)
102404	2.10		-2.11	(-.050)	(.001)
102405	2.10		-.03	(.019)	(-.019)
102406	2.10		1.99	(.086)	(-.038)
102407	2.10		4.00	(.153)	(-.056)
102408	2.10		5.92	(.217)	(-.074)
102409	2.10		7.89	(.282)	(-.093)
102410	2.10		9.84	(.347)	(-.111)
102411	2.10		11.75	(.410)	(-.129)
102412	2.10		13.63	(.473)	(-.147)
102413	2.10		14.56	(.504)	(-.155)
102501	2.50		-8.17	(-.231)	(.051)
102502	2.50		-6.15	(-.170)	(.035)
102503	2.50		-4.08	(-.107)	(.018)
102504	2.50		-2.11	(-.048)	(.002)
102505	2.50		-.04	(.015)	(-.014)
102506	2.50		1.93	(.075)	(-.030)
102507	2.50		4.03	(.138)	(-.047)
102508	2.50		5.92	(.195)	(-.062)
102509	2.50		7.92	(.256)	(-.078)
102510	2.50		9.83	(.314)	(-.094)
102511	2.50		11.77	(.373)	(-.109)
102512	2.50		13.63	(.429)	(-.124)
102513	2.50		14.55	(.457)	(-.132)

Table A-7.—(Continued)

(c) T.E. Deflection, Full Span =  $8.3^\circ$ 

Analysis number	Mach number	Dynamic pressure, $\text{kN/m}^2$ (psf)	Angle of attack, deg	Normal force coefficient, bal (integ press.)	Pitching moment coefficient, bal (integ press.)
102601	1.70		-8.07	(-.155)	(-.017)
102602	1.70		-6.07	(-.084)	(-.037)
102603	1.70		-4.07	(-.012)	(-.057)
102604	1.70		-2.03	(.061)	(-.078)
102605	1.70		-.03	(.133)	(-.098)
102606	1.70		1.95	(.204)	(-.117)
102607	1.70		3.96	(.276)	(-.137)
102608	1.70		5.90	(.346)	(-.157)
102609	1.70		7.85	(.416)	(-.176)
102610	1.70		9.80	(.486)	(-.196)
102611	1.70		11.71	(.555)	(-.215)
102612	1.70		13.61	(.623)	(-.234)
102613	1.70		14.51	(.655)	(-.243)
102701	2.10		-8.11	(-.182)	(.015)
102702	2.10		-6.02	(-.113)	(-.005)
102703	2.10		-4.04	(-.047)	(-.023)
102704	2.10		-2.07	(.018)	(-.042)
102705	2.10		-.01	(.086)	(-.061)
102706	2.10		2.00	(.153)	(-.080)
102707	2.10		4.00	(.219)	(-.098)
102708	2.10		5.92	(.283)	(-.116)
102709	2.10		7.88	(.348)	(-.135)
102710	2.10		9.83	(.413)	(-.153)
102711	2.10		11.74	(.476)	(-.171)
102712	2.10		13.61	(.538)	(-.188)
102713	2.10		14.51	(.568)	(-.197)
102801	2.50		-8.14	(-.177)	(.017)
102802	2.50		-6.09	(-.115)	(.001)
102803	2.50		-4.00	(-.052)	(-.016)
102804	2.50		-2.03	(.008)	(-.032)
102805	2.50		-.07	(.067)	(-.048)
102806	2.50		2.04	(.131)	(-.065)
102807	2.50		4.02	(.191)	(-.081)
102808	2.50		5.93	(.249)	(-.096)
102809	2.50		7.87	(.307)	(-.112)
102810	2.50		9.79	(.366)	(-.127)
102811	2.50		11.73	(.424)	(-.143)
102812	2.50		13.57	(.480)	(-.157)
102813	2.50		14.54	(.509)	(-.165)

(d) T.E. Deflection, Inboard =  $8.3^\circ$ , Outboard =  $0.0^\circ$ 

Analysis number	Mach number	Dynamic pressure, $\text{kN/m}^2$ (psf)	Angle of attack, deg	Normal force coefficient, bal (integ press.)	Pitching moment coefficient, bal (integ press.)
103001	1.70		-8.05	(-.186)	(.012)
103002	1.70		-6.04	(-.113)	(-.008)
103003	1.70		-4.06	(-.042)	(-.028)
103004	1.70		-2.02	(.031)	(-.048)
103005	1.70		.06	(.106)	(-.069)
103006	1.70		-1.15	(.098)	(-.067)
103007	1.70		2.02	(.176)	(-.089)
103008	1.70		4.06	(.249)	(-.109)
103009	1.70		5.99	(.319)	(-.128)
103010	1.70		7.91	(.388)	(-.147)
103011	1.70		9.87	(.458)	(-.167)
103012	1.70		11.76	(.526)	(-.186)
103013	1.70		13.66	(.594)	(-.205)
103014	1.70		14.59	(.628)	(-.214)
103101	2.10		-8.11	(-.202)	(.034)
103102	2.10		-6.08	(-.135)	(.015)
103103	2.10		-4.04	(-.067)	(-.004)
103104	2.10		-2.07	(-.002)	(-.023)
103105	2.10		-.06	(.065)	(-.042)
103106	2.10		2.01	(.134)	(-.061)
103107	2.10		4.01	(.200)	(-.080)
103108	2.10		5.82	(.260)	(-.097)
103109	2.10		7.77	(.325)	(-.115)
103110	2.10		9.74	(.390)	(-.133)
103111	2.10		11.63	(.453)	(-.151)
103112	2.10		13.56	(.517)	(-.169)
103113	2.10		14.49	(.548)	(-.178)
103114	2.10		5.94	(.264)	(-.098)
103115	2.10		7.92	(.330)	(-.116)
103116	2.10		9.88	(.395)	(-.135)
103117	2.10		11.77	(.457)	(-.152)
103118	2.10		13.66	(.520)	(-.170)
103119	2.10		14.59	(.551)	(-.179)
103201	2.50		-8.13	(-.192)	(.031)
103202	2.50		-6.11	(-.131)	(.015)
103203	2.50		-4.09	(-.070)	(-.001)
103204	2.50		-2.06	(-.008)	(-.017)
103205	2.50		.02	(.059)	(-.034)
103206	2.50		1.98	(.114)	(-.050)
103207	2.50		4.06	(.177)	(-.067)
103208	2.50		5.96	(.235)	(-.082)
103209	2.50		7.91	(.294)	(-.098)
103210	2.50		9.85	(.352)	(-.113)
103211	2.50		11.78	(.411)	(-.129)
103212	2.50		13.65	(.467)	(-.144)
103213	2.50		14.56	(.495)	(-.151)

Table A-7.—(Continued)

(e) T.E. Deflection, Inboard =  $4.1^\circ$ , Outboard =  $0.0^\circ$

Analysis number	Mach number	Dynamic pressure, $\text{kN/m}^2$ (psf)	Angle of attack, deg	Normal force coefficient, bal (integ press.)	Pitching moment coefficient, bal (integ press.)
103401	1.70		-8.06	(-.239)	(.047)
103402	1.70		-8.18	(-.243)	(.048)
103403	1.70		-6.13	(-.169)	(.028)
103404	1.70		-4.17	(-.099)	(.008)
103405	1.70		-2.11	(-.025)	(-.013)
103406	1.70		.06	(.053)	(-.034)
103407	1.70		2.04	(.124)	(-.054)
103408	1.70		4.05	(.197)	(-.074)
103409	1.70		6.00	(.267)	(-.094)
103410	1.70		7.95	(.337)	(-.113)
103411	1.70		9.90	(.407)	(-.133)
103412	1.70		11.81	(.476)	(-.152)
103413	1.70		13.72	(.544)	(-.171)
103414	1.70		14.63	(.577)	(-.180)
103501	2.10		-8.14	(-.237)	(.055)
103502	2.10		-6.07	(-.168)	(.036)
103503	2.10		-4.03	(-.101)	(.017)
103504	2.10		-2.06	(-.035)	(-.002)
103505	2.10		.01	(.034)	(-.021)
103506	2.10		.01	(.034)	(-.021)
103507	2.10		2.04	(.101)	(-.040)
103508	2.10		4.03	(.167)	(-.059)
103509	2.10		5.92	(.230)	(-.076)
103510	2.10		7.89	(.295)	(-.095)
103511	2.10		9.85	(.360)	(-.113)
103512	2.10		11.76	(.424)	(-.131)
103513	2.10		13.64	(.486)	(-.149)
103514	2.10		14.57	(.517)	(-.158)
103601	2.50		-8.14	(-.219)	(.049)
103602	2.50		-6.13	(-.158)	(.032)
103603	2.50		-4.06	(-.095)	(.016)
103604	2.50		-2.09	(-.036)	(-.000)
103605	2.50		-.02	(.027)	(-.017)
103606	2.50		-.02	(.027)	(-.017)
103607	2.50		1.95	(.087)	(-.033)
103608	2.50		4.04	(.150)	(-.050)
103609	2.50		5.94	(.207)	(-.065)
103610	2.50		7.89	(.266)	(-.081)
103611	2.50		9.81	(.325)	(-.096)
103612	2.50		11.76	(.384)	(-.112)
103613	2.50		13.62	(.440)	(-.127)
103614	2.50		14.53	(.467)	(-.134)

(f) T.E. Deflection, Full Span =  $4.1^\circ$

Analysis number	Mach number	Dynamic pressure, $\text{kN/m}^2$ (psf)	Angle of attack, deg	Normal force coefficient, bal (integ press.)	Pitching moment coefficient, bal (integ press.)
103701	1.70		-8.08	(-.224)	(.032)
103702	1.70		-6.09	(-.152)	(.012)
103703	1.70		-4.08	(-.080)	(-.008)
103704	1.70		-2.01	(-.006)	(-.028)
103705	1.70		-.02	(.066)	(-.046)
103706	1.70		1.95	(.136)	(-.068)
103707	1.70		3.96	(.209)	(-.088)
103708	1.70		5.92	(.279)	(-.108)
103709	1.70		7.86	(.349)	(-.127)
103710	1.70		9.82	(.419)	(-.147)
103711	1.70		11.72	(.488)	(-.166)
103712	1.70		13.63	(.556)	(-.185)
103713	1.70		14.52	(.588)	(-.194)
103801	2.10		-8.13	(-.227)	(.046)
103802	2.10		-6.10	(-.159)	(.027)
103803	2.10		-4.06	(-.092)	(.008)
103804	2.10		-2.09	(-.026)	(-.011)
103805	2.10		-.01	(.043)	(-.030)
103806	2.10		2.00	(.110)	(-.049)
103807	2.10		4.01	(.176)	(-.068)
103808	2.10		5.93	(.240)	(-.086)
103809	2.10		7.90	(.306)	(-.104)
103810	2.10		9.86	(.371)	(-.123)
103811	2.10		11.76	(.434)	(-.141)
103812	2.10		13.64	(.496)	(-.158)
103813	2.10		14.55	(.526)	(-.167)
103901	2.50		-8.14	(-.211)	(.041)
103902	2.50		-6.13	(-.151)	(.025)
103903	2.50		-4.06	(-.088)	(.009)
103904	2.50		-2.09	(-.028)	(-.007)
103905	2.50		-.02	(.034)	(-.024)
103906	2.50		1.95	(.094)	(-.040)
103907	2.50		4.04	(.157)	(-.057)
103908	2.50		5.94	(.215)	(-.072)
103909	2.50		7.89	(.274)	(-.088)
103910	2.50		9.81	(.332)	(-.103)
103911	2.50		11.66	(.388)	(-.118)
103912	2.50		13.52	(.444)	(-.133)
103913	2.50		14.44	(.472)	(-.140)

Table A-7.—(Concluded)

(g) T.E. Deflection, Inboard =  $0.0^\circ$ , Outboard =  $4.1^\circ$ 

Analysis number	Mach number	Dynamic pressure, $\text{kN/m}^2$ (psf)	Angle of attack, deg	Normal force coefficient, bal (integ press.)	Pitching moment coefficient, bal (integ press.)
104001	1.70		-8.20	(-.280)	(.068)
104002	1.70		-5.57	(-.200)	(.046)
104003	1.70		-1.93	(-.055)	(.005)
104004	1.70		-.01	(.014)	(-.014)
104005	1.70		2.02	(.087)	(-.034)
104006	1.70		4.04	(.160)	(-.054)
104007	1.70		5.97	(.229)	(-.074)
104008	1.70		7.92	(.299)	(-.093)
104009	1.70		9.83	(.368)	(-.112)
104010	1.70		11.78	(.438)	(-.132)
104011	1.70		13.71	(.507)	(-.151)
104012	1.70		14.57	(.538)	(-.160)
104013	1.70		-3.97	(-.128)	(.026)
104101	2.10		-8.03	(-.257)	(.066)
104102	2.10		-5.91	(-.186)	(.046)
104103	2.10		-3.57	(-.122)	(.028)
104104	2.10		-1.59	(-.056)	(.009)
104105	2.10		-.07	(.012)	(-.010)
104106	2.10		2.08	(.079)	(-.029)
104107	2.10		4.09	(.146)	(-.048)
104108	2.10		6.01	(.210)	(-.066)
104109	2.10		7.98	(.275)	(-.084)
104110	2.10		9.94	(.340)	(-.103)
104111	2.10		11.84	(.403)	(-.120)
104112	2.10		13.73	(.466)	(-.138)
104113	2.10		14.65	(.497)	(-.147)
104114	2.10		-6.03	(-.190)	(.047)
104201	2.50		-8.07	(-.236)	(.058)
104202	2.50		-6.06	(-.175)	(.041)
104203	2.50		-3.98	(-.112)	(.025)
104204	2.50		-2.01	(-.052)	(.009)
104205	2.50		-.06	(.010)	(-.008)
104206	2.50		2.02	(.070)	(-.024)
104207	2.50		4.12	(.133)	(-.041)
104208	2.50		6.02	(.191)	(-.056)
104209	2.50		7.97	(.250)	(-.072)
104210	2.50		9.84	(.307)	(-.087)
104211	2.50		11.80	(.366)	(-.102)
104212	2.50		13.66	(.422)	(-.117)
104213	2.50		14.55	(.449)	(-.125)
104214	2.50		4.03	(.131)	(-.040)

(h) T.E. Deflection, Full Span =  $-4.1^\circ$ 

Analysis number	Mach number	Dynamic pressure, $\text{kN/m}^2$ (psf)	Angle of attack, deg	Normal force coefficient, bal (integ press.)	Pitching moment coefficient, bal (integ press.)
104401	1.70		-7.99	(-.355)	(.129)
104402	1.70		-6.02	(-.284)	(.110)
104403	1.70		-8.11	(-.359)	(.130)
104404	1.70		-3.98	(-.211)	(.089)
104405	1.70		-1.94	(-.138)	(.069)
104406	1.70		-.09	(-.065)	(.048)
104407	1.70		2.07	(.007)	(.029)
104408	1.70		3.96	(.074)	(.010)
104409	1.70		6.03	(.149)	(-.011)
104410	1.70		7.92	(.217)	(-.030)
104411	1.70		9.85	(.286)	(-.049)
104412	1.70		11.78	(.356)	(-.068)
104413	1.70		13.71	(.425)	(-.088)
104414	1.70		14.59	(.457)	(-.096)
104501	2.10		-8.11	(-.312)	(.106)
104502	2.10		-5.98	(-.241)	(.086)
104503	2.10		-3.94	(-.174)	(.067)
104504	2.10		-1.88	(-.105)	(.048)
104505	2.10		-.04	(-.042)	(.030)
104506	2.10		2.05	(.025)	(.011)
104507	2.10		4.11	(.094)	(-.008)
104508	2.10		6.06	(.159)	(-.026)
104509	2.10		8.00	(.223)	(-.045)
104510	2.10		9.97	(.288)	(-.063)
104511	2.10		11.86	(.351)	(-.081)
104512	2.10		13.76	(.414)	(-.099)
104513	2.10		14.68	(.445)	(-.107)
104514	2.10		-1.99	(-.109)	(.049)
104515	2.10		7.93	(.220)	(-.044)
104516	2.10		9.89	(.286)	(-.062)
104517	2.10		11.78	(.348)	(-.080)
104518	2.10		13.68	(.411)	(-.098)
104519	2.10		14.61	(.442)	(-.107)
104601	2.50		-8.04	(-.276)	(.089)
104602	2.50		-6.03	(-.216)	(.072)
104603	2.50		-3.95	(-.153)	(.056)
104604	2.50		-1.99	(-.093)	(.040)
104605	2.50		-.06	(-.031)	(.023)
104606	2.50		2.03	(.028)	(.007)
104607	2.50		4.13	(.092)	(-.010)
104608	2.50		6.02	(.149)	(-.025)
104609	2.50		7.97	(.208)	(-.040)
104610	2.50		9.89	(.266)	(-.056)
104611	2.50		11.83	(.325)	(-.072)
104612	2.50		13.69	(.381)	(-.087)
104613	2.50		14.60	(.409)	(-.094)



## **APPENDIX B**

### **DATA REDUCTION AND PRESENTATION**

#### **DATA EDITING AND INTEGRATION PROCEDURE**

##### **DATA EDITING**

Some cases were encountered with these data where the methods of data editing available within the integration programs were not adequate. Because the plotting program assumes that geometry for all configurations is the same and the chordwise location of orifices on the various model parts was not absolutely identical, points were added as required. Therefore, some interpolations or extrapolations using selected orifices were done before the integration program was used. The row of orifices on the body at the wing-body intersection was extended in front of the wing and aft of the wing by interpolating between the orifices located at  $90^\circ$  and  $135^\circ$ .

Several methods were introduced into the integration program to replace or add data points to account for:

- Plugged or leaking orifices or bad data points
- Extrapolating the data to leading and trailing edges
- Hingeline discontinuities in the pressure data

These procedures were selected by code for each point. The codes are described in the following list and are illustrated in figure B-1. An additional use of these codes is to ensure that only measured pressure data ( $CODE_1 = 0$ ) are identified with symbols on the plots.

IF  $CODE_1 = 0$ , use pressure as entered on tape (measured pressure)

= 20, use as entered on tape (previously replaced value)

= 1, interpolate from adjacent points

= 2, extrapolate from two preceding points

= 3, extrapolate from two following points

= 4, set equal to preceding point

= 5, set equal to following point

= 6, interpolate using points (i-2) and (i+1)

= 7, interpolate using points (i-1) and (i+2)

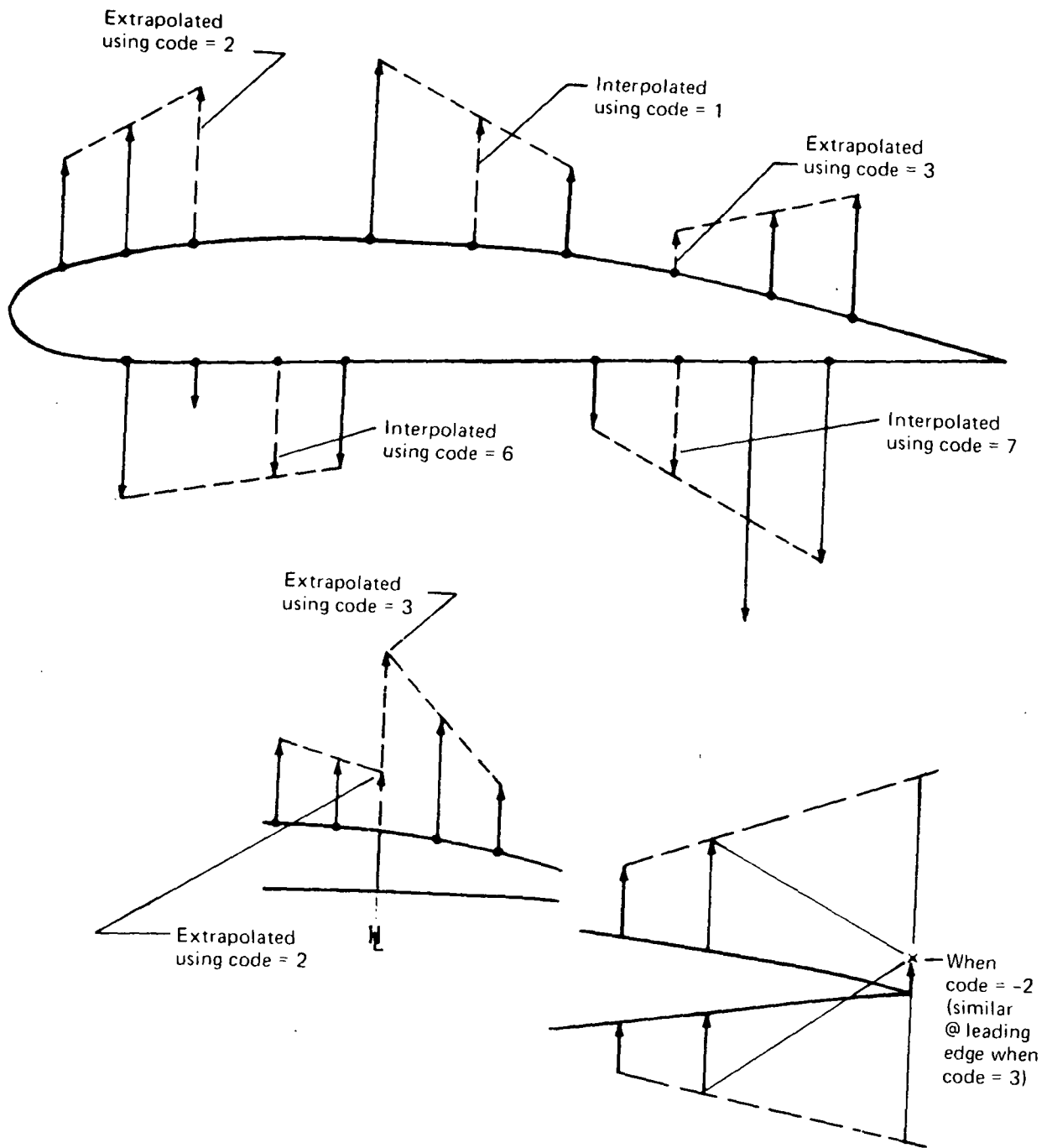


Figure B-1.—Codes Used To Interpolate and Extrapolate

IF CODE<sub>i</sub> = negative of above, evaluate as above but average with corresponding point on opposite surface—used for leading and trailing edges of section only

where

i identifies the position of the point from the leading edge of the upper or lower surface per section

Editing of the pressure data is done in the following order:

1. Each section is done separately.
2. Each surface (upper or lower) per section is done in the following sequence:
  - a. Starting at leading edge, points with codes of 1, 2, and 4
  - b. Starting at trailing edge, points with codes of 3, 5, 6, and 7
3. Leading- and trailing-edge points with negative codes are evaluated. Upper and lower surface codes need not both be negative and need not be the same negative code.

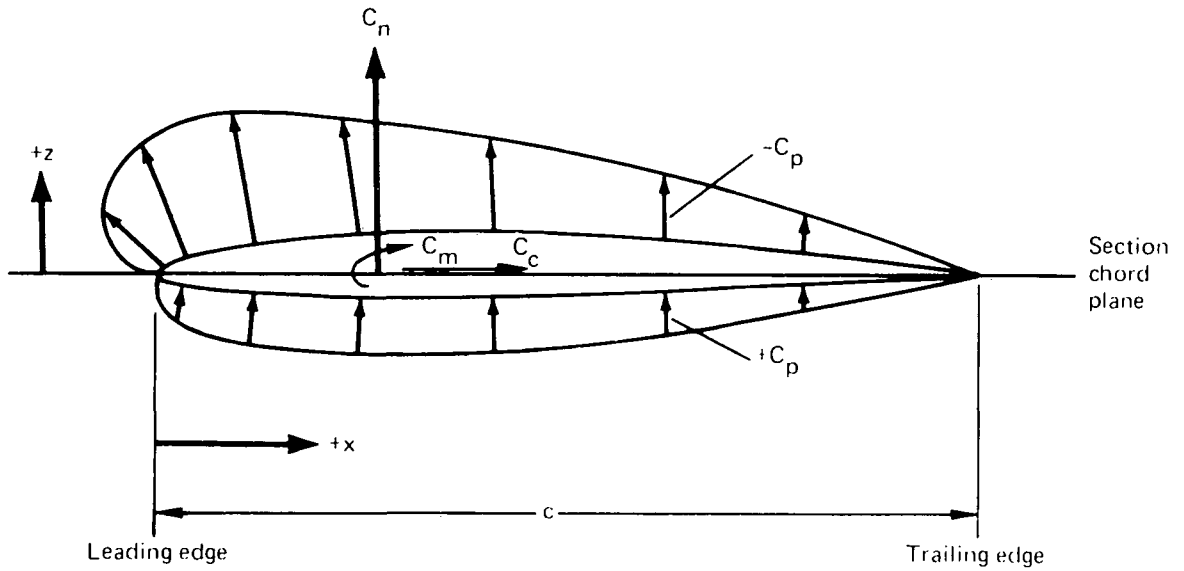
## **CALCULATION OF NET PRESSURE COEFFICIENTS**

The net lift distribution on the section is calculated by:

$$C_{p,net} = C_{p,lower} - C_{p,upper} \quad (B-1)$$

## **INTEGRATION OF PRESSURE DATA**

To account for the effects on integrated coefficients of the deflected control surfaces, each streamwise section (of which there are NSECT) is divided into segments (of which there are NSEG). These segments are the leading-edge control surface, wing box, and trailing-edge control surface. The upper and lower surfaces of each are integrated separately over the number of points available ((number of orifices + 2) = NP1) and are based on the segment chord length  $c$ . Sign conventions are shown in the following sketch. The equations, which use a rectangular integration process, follow.



### Segment Coefficients

Integration of the pressures for each segment per surface per section is the first step.

- Normal force coefficient  $C_{n,s}$

$$C_{n,s} = 0.5 \sum_{i=2}^{NP1} \left[ (C_p)_i + (C_p)_{i-1} \right] \left[ \left( \frac{x}{c} \right)_i - \left( \frac{x}{c} \right)_{i-1} \right] \quad (B-2)$$

$$C_{n,s,net} = C_{n,s,lower} - C_{n,s,upper} \quad (B-3)$$

- Chord force coefficient  $C_{c,s}$

$$C_{c,s} = 0.5 \sum_{i=2}^{NP1} \left[ (C_p)_i + (C_p)_{i-1} \right] \left[ \left( \frac{z}{c} \right)_i - \left( \frac{z}{c} \right)_{i-1} \right] \quad (B-4)$$

$$C_{c,s,net} = C_{c,s,upper} - C_{c,s,lower} \quad (B-5)$$

- Pitching moment coefficient about segment leading edge  $C_{m,s}$

$$C_{m,s} = 0.5 \sum_{i=2}^{NP1} \left[ (C_p)_i + (C_p)_{i-1} \right] \left[ \frac{x}{c}_{i-1} + \frac{\left(\frac{x}{c}\right)_i - \left(\frac{x}{c}\right)_{i-1}}{2.0} \right] \left[ \left(\frac{x}{c}\right)_i - \left(\frac{x}{c}\right)_{i-1} \right]$$

$$= 0.25 \sum_{i=2}^{NP1} \left[ (C_p)_i + (C_p)_{i-1} \right] \left[ \left(\frac{x}{c}\right)_i^2 - \left(\frac{x}{c}\right)_{i-1}^2 \right] \quad (B-6)$$

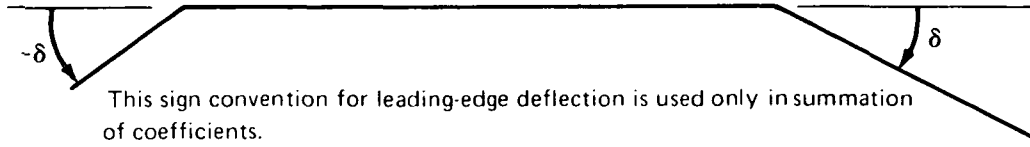
$$C_{m,s,net} = C_{m,s,upper} - C_{m,s,lower} \quad (B-7)$$

- Pitching moment coefficient about 0.25c of segment  $C_{m,0.25c,s}$

$$C_{m,0.25c,s} = C_{m,s} + 0.25 C_{n,s} \quad (B-8)$$

### Section Coefficients

Total section coefficients are obtained by summing the segment coefficients, taking into account segment deflections as defined in the following sketch and segment chord lengths. These coefficients are based on the section chord length  $c_T$ .



- Normal force coefficient  $C_n$

$$C_n = \sum_{j=1}^{NSEG} (C_{n,s})_j \left(\frac{c_s}{c}\right)_j \cos \delta_j - \sum_{j=1}^{NSEG} (C_{c,s})_j \left(\frac{c_s}{c}\right)_j \sin \delta_j \quad (B-9)$$

- Pitching moment coefficient about section leading edge  $C_m$

$$C_m = \sum_{j=1}^{NSEG} (C_{m,s})_j \left(\frac{c_s}{c}\right)_j^2 + \left[ (C_{n,s})_1 (1.0 - \cos \delta_1) + (C_{c,s})_1 \sin \delta_1 \right] \left(\frac{c_s}{c}\right)_1^2$$

$$- \sum_{j=2}^{NSEG} \left[ (C_{n,s})_j \cos \delta_j - (C_{c,s})_j \sin \delta_j \right] \left(\frac{c_s}{c}\right)_j \left[ \frac{x_{L.E.,s} - x_{L.E.}}{c} \right]_j \quad (B-10)$$

where

$c_s$  is segment chord, cm

$c$  is section chord, cm

$\delta$  is deflection of segment relative to section chord plane, leading edge up, degrees

$x_{L.E.,s}$  is leading edge of segment, cm

$x_{L.E.}$  is leading edge of section, cm

- Pitching moment coefficient about 0.25c of section  $C_{m.25c}$

$$C_{m.25c} = C_m + 0.25 C_n \quad (B-11)$$

### Total Surface Coefficients

To obtain total surface coefficients, the assumption is made that the section coefficients apply for a finite distance on both sides of each row of orifices. The equations for total surface coefficients are as follows:

- Normal force coefficient  $C_N$

$$C_N = \frac{1}{S} \sum_{k=1}^{NSECT} (C_n)_k (S_h)_k \quad (B-12)$$

- Bending moment coefficient  $C_B$

$$C_B = \frac{1}{S(b/2)} \sum_{k=1}^{NSECT} (C_n)_k (S_h^y)_k \quad (B-13)$$

- Pitching moment coefficient about 0.25 M.A.C.  $C_M$

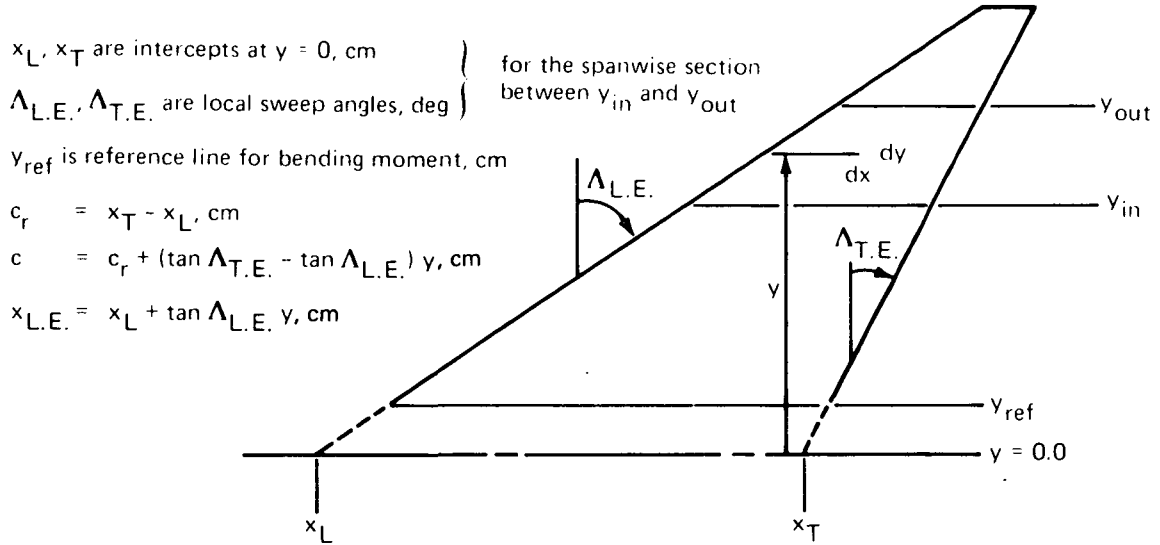
$$C_M = \frac{1}{Sc} \sum_{k=1}^{NSECT} \left\{ (C_m)_k (S_h^c)_k + (C_n)_k (S_h)_k \left[ x_{ref} - (x_{L.E.})_k \right] \right\} \quad (B-14)$$

where

- $c$  is reference chord for pitching moment, cm
- $x_{ref}$  is reference station for pitching moment, cm (0.25 M.A.C.)
- $x_{L.E.}$  is leading edge of section chord, cm
- $b/2$  is reference length for bending moment, cm

### DETERMINATION OF GEOMETRIC CONSTANTS REQUIRED FOR INTEGRATION

To obtain total surface coefficients, the assumption is made that the section coefficients apply for a finite distance on both sides of each row of orifices. The input geometry required to calculate the areas, and products of area and length required for the summation of total surface coefficients, are shown in the following sketch.



#### ● Section area:

$$\begin{aligned}
 S_h &= \int_{y_{in}}^{y_{out}} \int_{x_L + \tan \Lambda_{L.E.} y}^{x_T + \tan \Lambda_{T.E.} y} dy dx \\
 &= c_r (y_{out} - y_{in}) + 0.5 (\tan \Lambda_{T.E.} - \tan \Lambda_{L.E.}) (y_{out}^2 - y_{in}^2) \quad (B-15)
 \end{aligned}$$

- **Product of section area and mean chord:**

$$\begin{aligned}
 S_{hc} &= \int_{y_{in}}^{y_{out}} \int_{x_L + \tan \Lambda_{L.E.} y}^{x_T + \tan \Lambda_{T.E.} y} c \, dy \, dx \\
 &= c_r^2 (y_{out} - y_{in}) + c_r (\tan \Lambda_{T.E.} - \tan \Lambda_{L.E.}) (y_{out}^2 - y_{in}^2) \\
 &\quad + \frac{(\tan \Lambda_{T.E.} - \tan \Lambda_{L.E.})^2}{3.0} (y_{out}^3 - y_{in}^3)
 \end{aligned} \tag{B-16}$$

- **Product of section area and moment arm:**

$$\begin{aligned}
 S_{hy} &= \int_{y_{in}}^{y_{out}} \int_{x_L + \tan \Lambda_{L.E.} y}^{x_T + \tan \Lambda_{T.E.} y} (y - y_{ref}) \, dy \, dx \\
 &= \frac{c_r - (\tan \Lambda_{T.E.} - \tan \Lambda_{L.E.}) y_{ref}}{2.0} (y_{out}^2 - y_{in}^2) \\
 &\quad + \frac{\tan \Lambda_{T.E.} - \tan \Lambda_{L.E.}}{3.0} (y_{out}^3 - y_{in}^3) - c_r y_{ref} (y_{out} - y_{in})
 \end{aligned} \tag{B-17}$$

- **Product of section area and leading-edge coordinate:**

$$\begin{aligned}
 S_{hx} &= \int_{y_{in}}^{y_{out}} \int_{x_L + \tan \Lambda_{L.E.} y}^{x_T + \tan \Lambda_{T.E.} y} x_{L.E.} \, dy \, dx \\
 &= x_L c_r (y_{out} - y_{in}) + \frac{\tan \Lambda_{L.E.} c_r + x_L (\tan \Lambda_{T.E.} - \tan \Lambda_{L.E.})}{2.0} (y_{out}^2 - y_{in}^2) \\
 &\quad + \tan \Lambda_{L.E.} \frac{(\tan \Lambda_{T.E.} - \tan \Lambda_{L.E.})}{3.0} (y_{out}^3 - y_{in}^3)
 \end{aligned} \tag{B-18}$$

- **Total surface reference area:**

$$S = \sum_{k=1}^{NSECT} (S_h)_k \tag{B-19}$$



- M.A.C. and X coordinate of M.A.C. leading edge:

$$\bar{c} = \frac{1}{S} \sum_{k=1}^{N_{SECT}} (S_h^c)_k \quad (B-20)$$

$$x_{L.E.,M.A.C.} = \frac{1}{S} \sum_{k=1}^{N_{SECT}} (S_h^x)_k \quad (B-21)$$

The required integration constants for the wing and body are shown in table B-1.

## DATA PRESENTATION

Computer programs were used to generate plots in order to minimize the amount of manual labor. The following sections describe the forms of data presentation used in this report.

### PRESSURE COEFFICIENTS

Chordwise distributions of upper surface, lower surface, and net (lower-upper) pressure coefficients are plotted as a function of local  $x/c$ . Any interpolated or extrapolated values are used in fairing the lines, but only actual measured values are plotted as symbols. In cases where the measurement at a particular orifice was not valid for a particular test point, the symbol is not shown on the plot either for local surface or net distributions. Longitudinal pressure distributions of surface pressures are presented for the body.

The variation of net pressure coefficients with angle of attack at specific orifice locations is compared with theoretical predictions.

Isobar plots are drawn on the surface planform after interpolating the pressure coefficients from the input locations (for this model all interpolated and extrapolated data from the integration program were used) to a more dense rectangular grid of streamwise lines (orifice stations are retained) and constant percent chord lines. This is a linear interpolation and extrapolation process which ignores the presence of all discontinuities such as deflected control surfaces. The final isobars in the regions near such discontinuities will therefore be inaccurate.

Each set of four adjacent points in the rectangular grid is treated in turn and a fifth point is added to form four triangles as shown in the following sketch. The pressure coefficient at the center point is calculated by averaging the outer four.

The values of pressure coefficient which will be mapped are determined by marking off a series of specified increments above and below zero, up to the maximum and minimum pressure coefficients which exist in the rectangular grid. The upper and lower surfaces are treated separately and can have different increments between isobars.

Table B-1.—Integration Constants

Reference area = 3128.45 cm<sup>2</sup>

M.A.C. = 75.311 cm

Half Span = 50.80 cm

Pitching moment referenced to 0.25 M.A.C.

Bending moment referenced to  $0.086 \frac{b}{2}$  ( $y_{ref}$  4.374 cm)

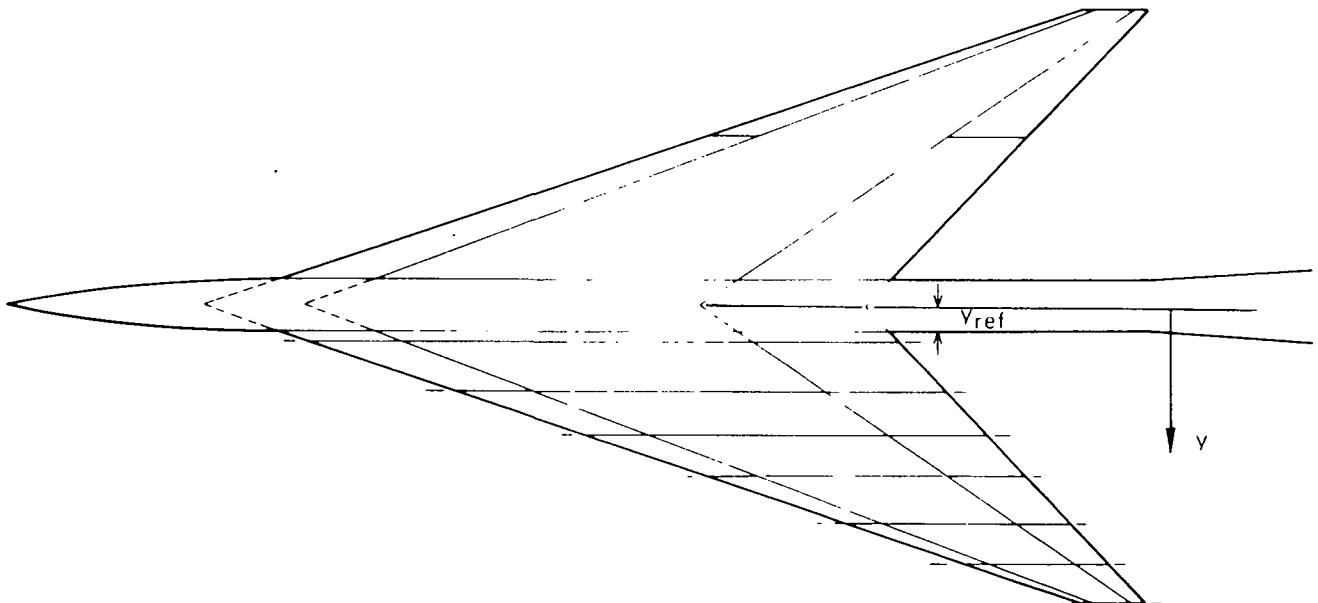
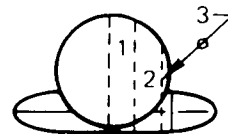
L.E. of M.A.C. @ B.S. 87.760 cm

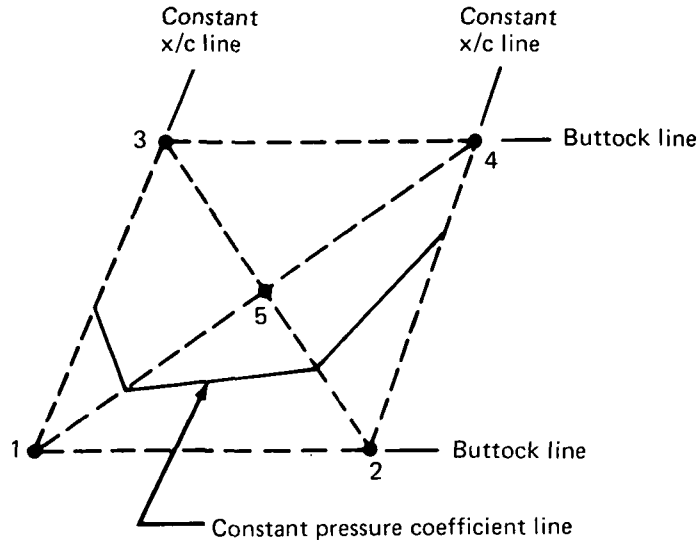
Wing

$2y/b$	$\frac{\Delta y}{(b/2)}$	Area, cm <sup>2</sup>	Area • chord, cm <sup>3</sup>	Area • ( $y - y_{ref}$ ), cm <sup>3</sup>
0.09	0.0425	219.69	22 357.	167.
0.20	0.1575	733.51	67 415.	4 206.
0.35	0.1500	580.54	44 374.	7 857.
0.50	0.1400	437.93	27 084.	9 148.
0.65	0.1600	377.64	17 722.	10 729.
0.80	0.1300	210.35	6 794.	7 528.
0.93	0.1400	129.79	2 487.	5 505.

Body

Longitudinal section	Area, cm <sup>2</sup>	Area • L, cm <sup>3</sup>
1	356.61	81 258.
2	504.32	114 916.
3	70.94	16 164.





The isobars are drawn by checking each triangle to determine if the pressure coefficients at the ends of any triangle side are above and below the desired value, in which case the isobar must cross that triangle side. The location of the crossing is found by linear interpolation between the end points, and when two adjacent triangle sides are found to contain the desired pressure coefficient a small segment of the isobar is drawn. As each set of four points is processed, the whole isobar will be constructed from many of these small segments. A letter symbol identifying the pressure coefficient value is generated wherever an isobar crosses one of the rows of orifices.

## SECTION AND SPANWISE LOADING CHARACTERISTICS

Section aerodynamic coefficients  $C_n$  and  $C_m$  are presented as a function of angle of attack.

The spanwise loading is illustrated by plots of the loading parameters  $C_n c / \bar{c}$  and  $C_{m.25c} c^2 / \bar{c}^2$  along the span of the surfaces.

## TOTAL SURFACE CHARACTERISTICS

The total surface coefficients  $C_N$ ,  $C_M$  and  $C_B$  are shown as a function of angle of attack.

**Page  
Intentionally  
Left Blank**

## **APPENDIX C**

### **SUMMARY OF SUBSONIC-TRANSONIC PROGRAM**

Prior to the present work, this model was tested at subsonic and transonic Mach numbers in the Boeing Transonic Wind Tunnel. The Mach number range was 0.40 to 1.11 with angle of attack varying from  $-8^\circ$  to  $+16^\circ$  in  $2^\circ$  increments. A total of 54 configurations were tested. Theoretical predictions of the pressure distributions were made using both attached- and detached-flow theories. A detailed report of these data is available in reference 1 through 4. A brief description of the test and the theoretical data included in this report is given in the following sections.

#### **WIND TUNNEL CAPABILITIES**

The Boeing Transonic Wind Tunnel (BTWT) is a continuous-flow, closed-circuit, single-return facility with an operating range of Mach number from 0.0 to nearly 1.2. The test section is 2.438 by 3.658 by 4.420 m (8 by 12 by 14.5 ft) with 11.0% of the wall area in slots. The tunnel layout is shown in figure C-1. The tunnel stagnation pressure is atmospheric.

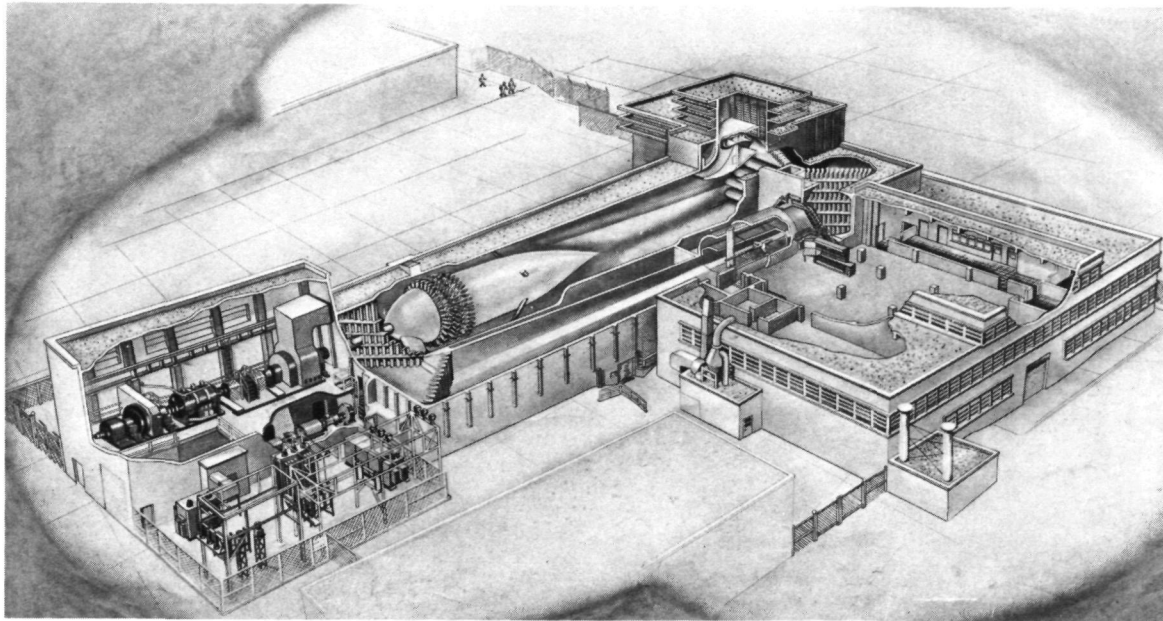
The Boeing wind tunnel data system provides the capabilities of real-time test data acquisition, feedback control computation, and display. The data system consists of an Astrodata acquisition subsystem and a computing subsystem that uses a Xerox data system (XDS 9300) digital computer. The Astrodata system acquires signals from the sensors, conditions them, and passes them directly to the computer. On-line programs provide for preparation of magnetic tapes for plotting or interfacing with off-line programs.

#### **TESTS AND DATA ACQUISITION**

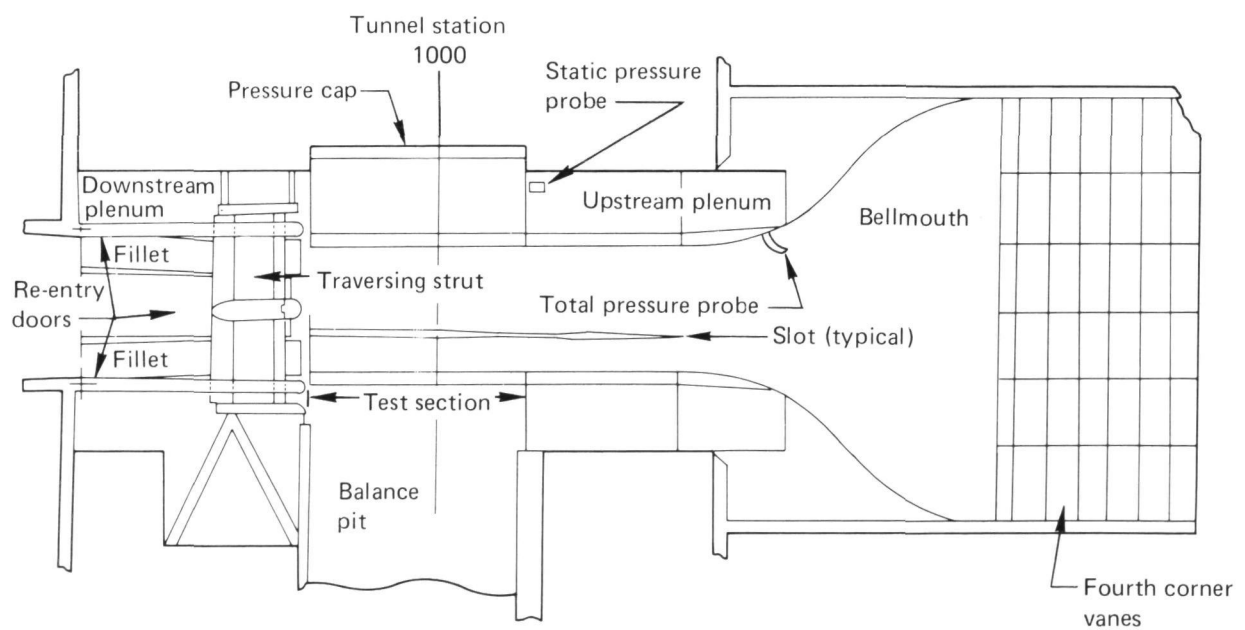
Table C-1 shows the 54 configurations that were tested. Photographs of some are shown in figures C-2 and C-3 and a diagram of the model installation in the BTWT is shown in figure C-4. Pressure and total force data were obtained at Mach numbers of 0.40, 0.70, 0.85, 0.95, and 1.05 for all configurations and at Mach numbers of 1.00 and 1.11 for selected configurations.

The angle of attack of the reference point (0.25 M.A.C. for this model) was determined from several increments. The input angle of attack is determined by an encoder mounted in the strut. This angle is then modified by the effects of sting deflection, up-flow, and wall corrections. The corrections for sting deflection are based on the normal force and pitching moment loads obtained during wind-on data acquisition. The sting deflection was taken into account when setting test angles of attack to minimize the variation in final angle of attack for the various model configurations.

The pressure data were recorded through the use of fifteen 24-position scanivalves located in the fore body of the model. Pressure transducers in the scanivalves measured the differential pressure between the local surface pressures and tunnel total pressure.



(a) Schematic



(b) Test Section

Figure C-1.—Boeing Transonic Wind Tunnel

Table C-1.—Summary of Subsonic/Transonic Test Conditions by Run Number

Leading edge deflection, deg	Mach no.	Trailing edge deflection, deg															
		Full Span								Outboard (inboard = 0.0)				Inboard (outboard = 0.0)			
		30.2	17.7	8.3	4.1	0.0	-4.1	-8.3	-17.7	-30.2	17.7	8.3	-8.3	-17.7	17.7	8.3	-8.3
Flat wing, rounded leading edge, trip strip off																	
Full span = 0.0	0.40					10											
	0.70					15											
	0.85					7											
	0.95					16											
	1.05					14											
	1.11					9											
Flat wing, rounded leading edge, trip strip on																	
Full span = 0.0	0.40	37	32	46	48	21,269	55	78	66	75	280	275			252	259	
	0.70	34	29	43	50	23,263	57	80	63	72	277	271			248	255	
	0.85	36	31	45	52	25,267	59	82	65, 69	74	279	274			250	258	
	0.95	35	30	44	51	24,266	58	81	64, 68	73	278	273			249	257	
	1.00					268											
	1.05	33	28	42	49	22,264	56	79	62	71	276	272			247	256	
1.11			40	47	20,262	54	77				270				254		
Inboard =0.0 Outboard=5.1	0.40					223					215	209	196	202	246	241	235
	0.70					218					211	205	192	198	243	237	231
	0.85					221					214	208	195	201	245	240	233
	0.95					220					213	207	194	200	244	239	232
	1.05					219					212	206	193	199	242	238	230
	1.11					217					210	204	191	197		236	

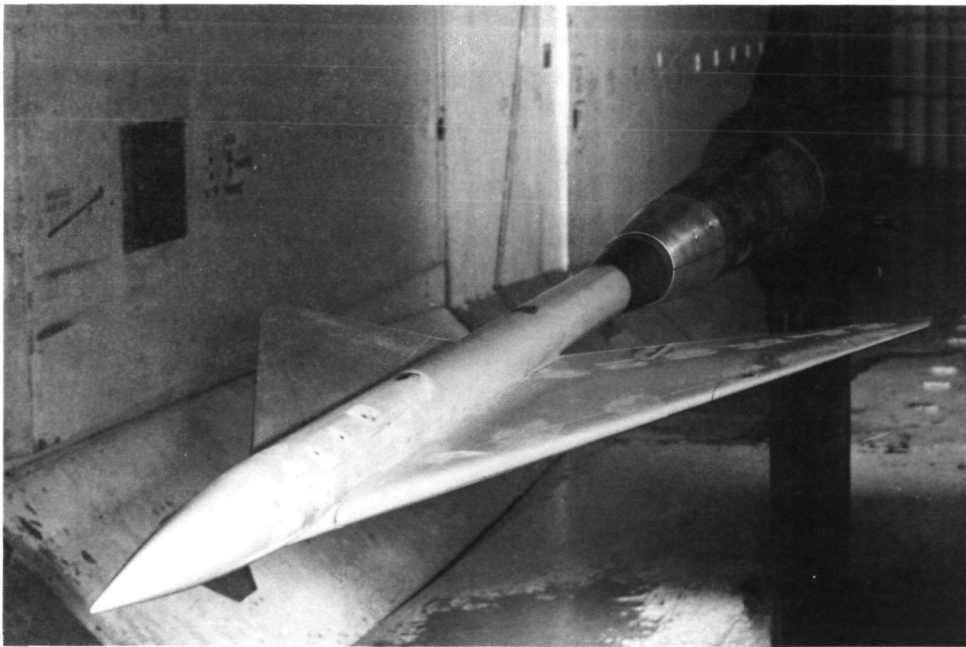
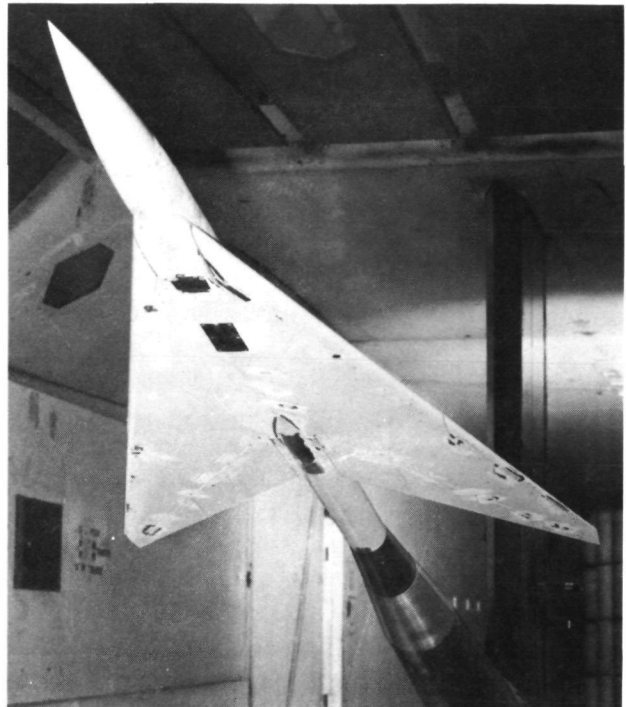
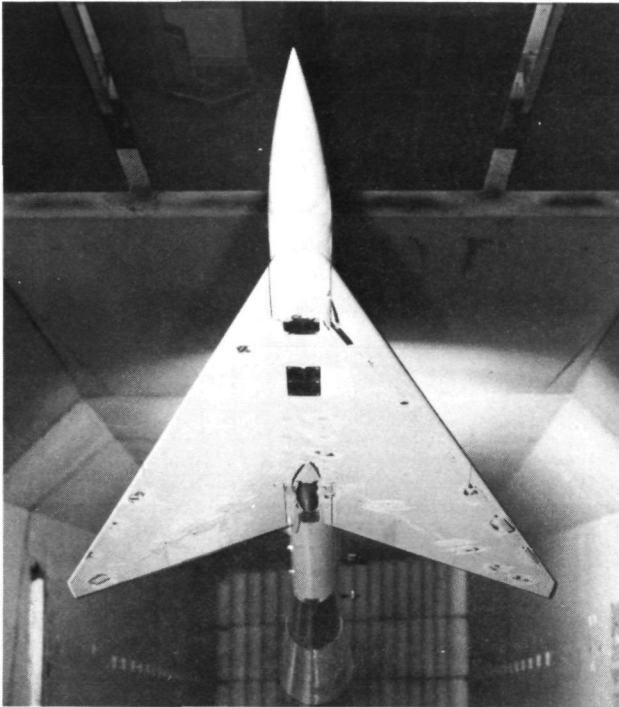
Table C-1.—(Continued)

Leading edge deflection, deg	Mach no.	Trailing edge deflection, deg															
		Full span									Outboard (inboard = 0.0)				Inboard (outboard = 0.0)		
		30.2	17.7	8.3	4.1	0.0	-4.1	-8.3	-17.7	-30.2	17.7	8.3	-8.3	-17.7	17.7	8.3	-8.3
Flat wing, rounded leading edge, trip strip on																	
Inboard =5.1 Outboard=0.0	0.40					319					286	313			329	324	
	0.70					315					283	311			326	321	
	0.85					318					285	312			328	323	
	0.95					317					284	310			327	322	
	1.05					316					282	308			325	320	
	1.11					314											
Full span = 5.1	0.40		177	149	138	183		189	132								
	0.70		173	145	140	179		185	134								
	0.85		175	148	142	182		188	136								
	0.95		174	147	141	181		187	135								
	1.05		172	146	139	180		186	133								
	1.11			144	137	178		184	131								
Full span=12.8	0.40		118	115	109	98		85	126								
	0.70		121	112	105	100		87	128								
	0.85		123	114	108	102		89	130								
	0.95		122	113	107	101		88	129								
	1.05		120	111	106	99		86	127								
	1.11		116		104	97		84	124								

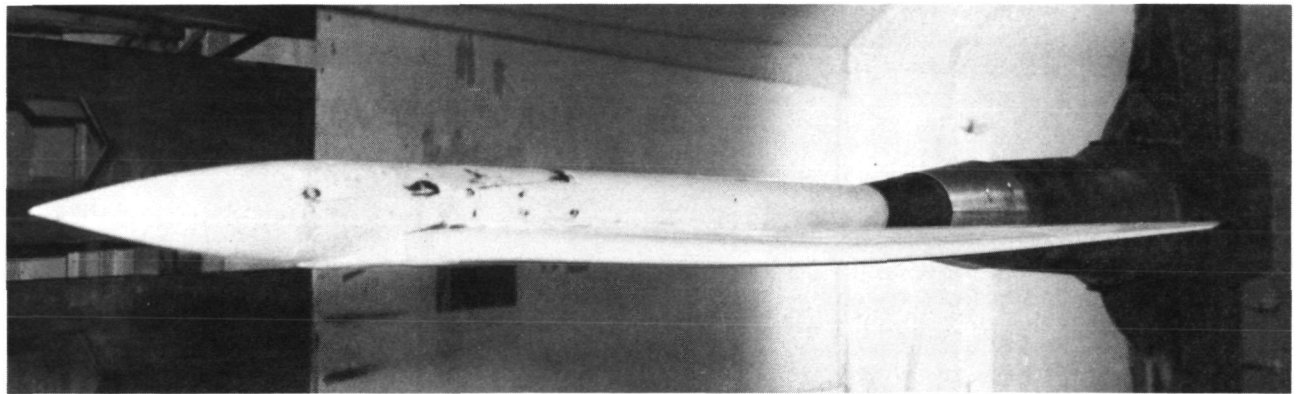
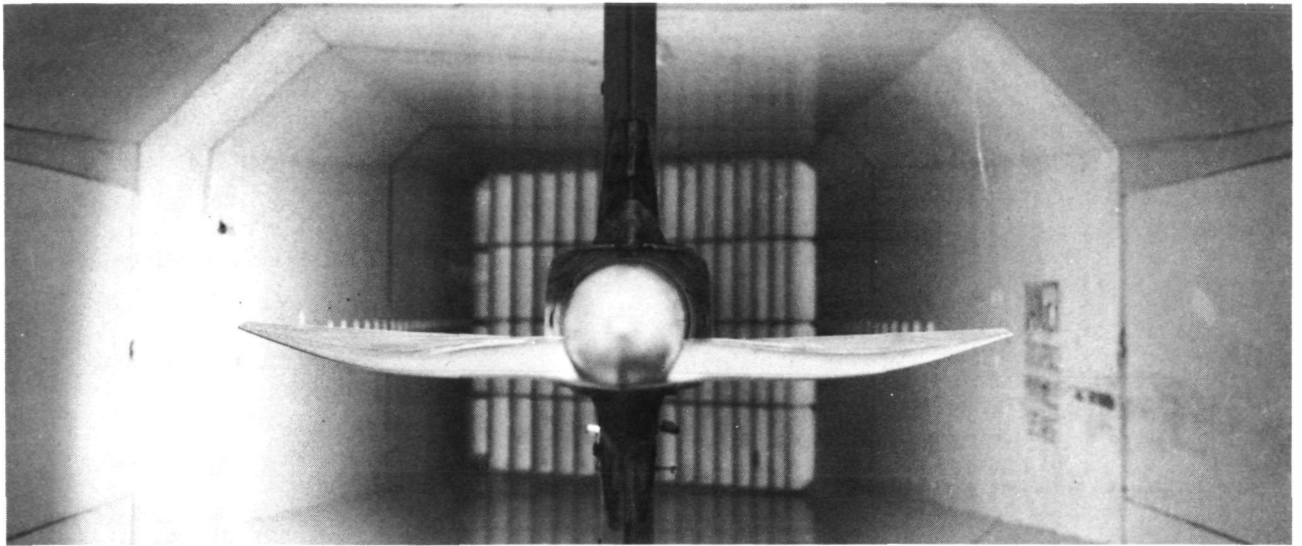


Table C-1. — (Concluded)

Leading edge deflection, deg	Mach no.	Trailing edge deflection, deg																
		Full span									Outboard (inboard = 0.0)				Inboard (outboard = 0.0)			
		30.2	17.7	8.3	4.1	0.0	-4.1	-8.3	-17.7	-30.2	17.7	8.3	-8.3	-17.7	17.7	8.3	-8.3	-17.7
Flat wing , sharp leading edge, trip strip on																		
Full span= 0.0	0.40					368												
	0.70					366												
	0.85					372												
	0.95					374												
	1.00					373												
	1.05					367												
	1.11					365												
Flat wing, twisted trailing edge, rounded leading edge, trip strip on																		
Full span= 0.0	0.40		352	347	342	337		358	363									
	0.70		349	344	339	333		354	360									
	0.85		351	346	341	336		356	362									
	0.95		350	345	340	335		357	361									
	1.05		348	343	338	334		353	359									
	1.11					332												
	Twisted wing, rounded leading edge, trip strip on																	
Full span= 0.0	0.40	427	422	416	411	450		435	442									
	0.70	424	419	413	408	445		432	439									
	0.85	426	421	415	410	449		434	441									
	0.95	425	420	414	409	447		433	440									
	1.00					448												
	1.05	423	418	412	407	446		431	438									
	1.10					444												



*Figure C-2.—Model in Boeing Transonic Wind Tunnel—Flat Wing, Rounded L.E.;  
L.E. Deflection, Full Span =  $0.0^{\circ}$ ; T.E. Deflection, Full Span =  $0.0^{\circ}$*



*Figure C-3.—Model in Boeing Transonic Wind Tunnel—Twisted Wing, Rounded L.E.;  
L.E. Deflection, Full Span =  $0.0^\circ$ ; T.E. Deflection, Full Span =  $4.1^\circ$*

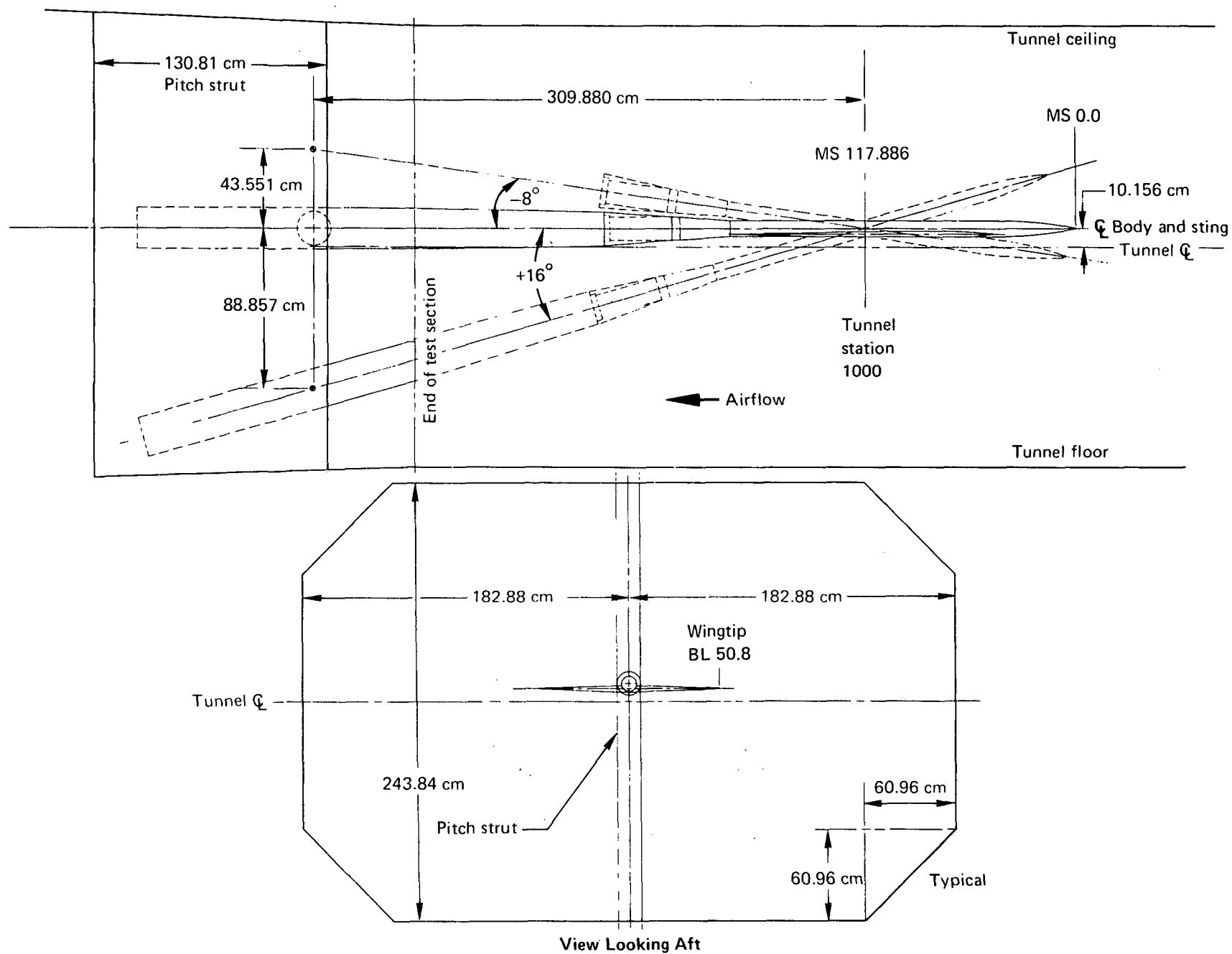


Figure C-4.—Model Installation in Boeing Transonic Wind Tunnel

Signals from the scanivalves, force and moment data, tunnel parameters, and model attitude angle were recorded on the Astrodata system and reduced using the XDS 9300 computer.

Final data (pressure coefficients, tunnel parameters, and model attitude) were merged on magnetic tapes, with appropriate configuration and test point identification for integration and plotting of these data.

### **FLEXSTAB THEORETICAL PREDICTIONS**

The FLEXSTAB program has been described in the main portion of this document. The same paneling was used for the wing throughout the Mach number range. The "interference" shell on the body was paneled differently for Mach numbers of 1.05 and 1.11 because of numerical instabilities associated with the solution. The number of interference panels was greatly increased (from 168 to 330) as shown in figure C-5. Table C-2 shows the combinations of Mach number and configuration for which data are available.

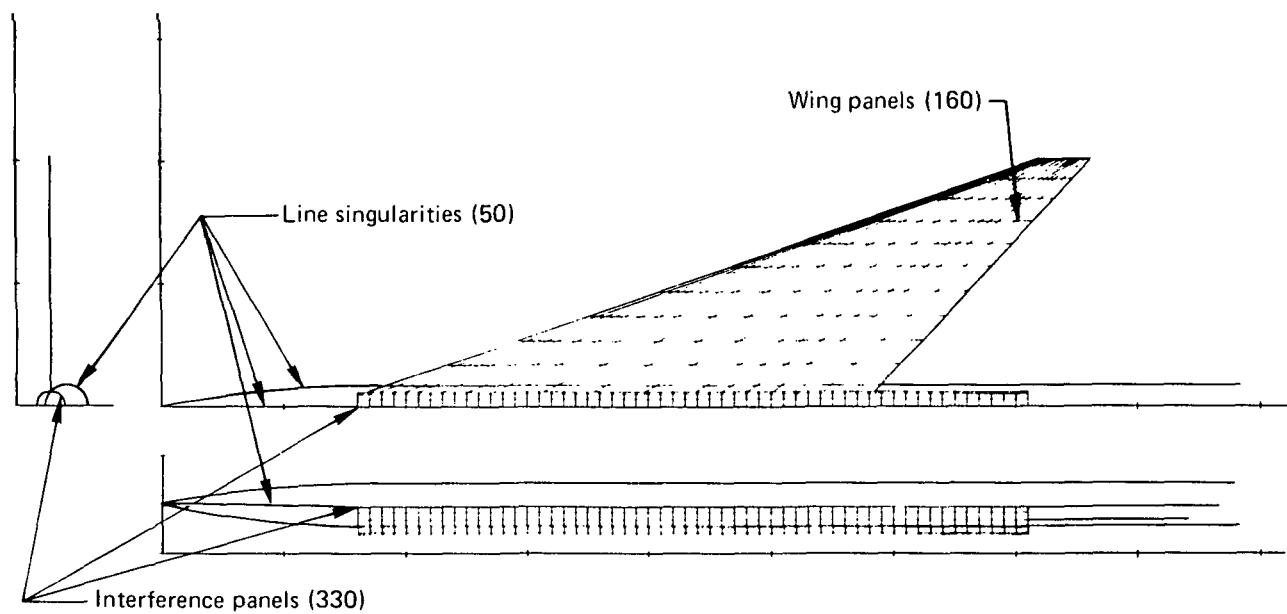


Figure C-5.—Paneling for FLEXSTAB Computer Program,  $M = 1.05$  and  $1.11$

Table C-2.—Summary of Subsonic/Transonic FLEXSTAB Conditions by Number

Leading edge deflection, deg	Mach no.	Trailing edge deflection, deg																
		Full span									Outboard (inboard = 0.0)				Inboard (outboard = 0.0)			
		30.2	17.7	8.3	4.1	0.0	-4.1	-8.3	-17.7	-30.2	17.7	8.3	-8.3	-17.7	17.7	8.3	-8.3	-17.7
Flat wing, rounded leading edge, trip strip off																		
Full span = 0.0	0.40					10												
	0.70					15												
	0.85					7												
	0.95					16												
	1.05					14												
	1.11					9												
Flat wing, rounded leading edge, trip strip on																		
Full span = 0.0	0.40	37	(32)	(46)	48	21(269)	55	(78)	(66)	75	280	275			252	259		
	0.70	34	(29)	(43)	50	23(263)	57	(80)	(63)	72	277	271			248	255		
	0.85	36	(31)	(45)	52	25(267)	59	(82)	(65)	69	74	(279)	(274)		(250)	(258)		
	0.95	35	(30)	(44)	51	24(266)	58	(81)	(64)	68	73	278	273		249	257		
	1.00					(268)												
	1.05	33	(28)	(42)	49	22(264)	56	(79)	(62)	71	276	272			247	256		
	1.11			(40)	47	20(262)	54	(77)				270				254		
Inboard =0.0 Outboard=5.1	0.40					223					215	209	196	202	246	241	235	229
	0.70					218					211	205	192	198	243	237	231	228
	0.85					(221)					(214)	(208)	(195)	(201)	(245)	(240)	(233)	(227)
	0.95					220					213	207	194	200	244	239	232	226
	1.05					219					212	206	193	199	242	238	230	224
	1.11					217					210	204	191	197		236		

○ FLEXSTAB solution available

Note: On the data tapes and in the tables of appendix A, the above run numbers have been incremented by 1 000 to give the FLEXSTAB results unique identification.

Table C-2.-(Continued)

Leading edge deflection, deg	Mach no.	Trailing edge deflection, deg															
		Full span									Outboard (inboard = 0.0)				Inboard (outboard = 0.0)		
		30.2	17.7	8.3	4.1	0.0	-4.1	-8.3	-17.7	-30.2	17.7	8.3	-8.3	-17.7	17.7	8.3	-8.3
Flat wing, rounded leading edge, trip strip on																	
Inboard =5.1 Outboard=0.0	0.40					319					286	313			329	324	
	0.70					315					283	311			326	321	
	0.85					318					285	312			328	323	
	0.95					317					284	310			327	322	
	1.05					316					282	308			325	320	
	1.11					314											
Full span =5.1	0.40		177	149	138	183		189	132								
	0.70		173	145	140	179		185	134								
	0.85		175	148	142	182		188	136								
	0.95		174	147	141	181		187	135								
	1.05		172	146	139	180		186	133								
	1.11			144	137	178		184	131								
Full span=12.8	0.40		118	115	109	98		85	126								
	0.70		121	112	105	100		87	128								
	0.85		123	114	108	102		89	130								
	0.95		122	113	107	101		88	129								
	1.05		120	111	106	99		86	127								
	1.11		116		104	97		84	124								

○ FLEXSTAB solution available

Note: On the data tapes and in the tables of appendix A, the above run numbers have been incremented by 1 000 to give the FLEXSTAB results unique identification.



Table C-2. —(Concluded)

Leading edge deflection, deg	Mach no.	Trailing edge deflection, deg															
		Full span								Outboard (inboard = 0.0)				Inboard (outboard = 0.0)			
		30.2	17.7	8.3	4.1	0.0	-4.1	-8.3	-17.7	-30.2	17.7	8.3	-8.3	-17.7	17.7	8.3	-8.3
Flat wing , sharp leading edge, trip strip on																	
Full span=0.0	0.40					368											
	0.70					366											
	0.85					372											
	0.95					374											
	1.00					373											
	1.05					367											
	1.11					365											
Flat wing, twisted trailing edge, rounded leading edge, trip strip on																	
Full span=0.0	0.40		(352)	(347)	342	(337)		(358)	(363)								
	0.70		349	344	339	333		354	360								
	0.85		(351)	(346)	341	(336)		(356)	(362)								
	0.95		350	345	340	335		357	361								
	1.05		(348)	(343)	338	(334)		(353)	(359)								
	1.11					332											
	Twisted wing, rounded leading edge, trip strip on																
Full span=0.0	0.40	427	(422)	(416)	411	(450)		(435)	(442)								
	0.70	424	(419)	(413)	408	(445)		(432)	(439)								
	0.85	426	(421)	(415)	410	(449)		(434)	(441)								
	0.95	425	(420)	(414)	409	(447)		(433)	(440)								
	1.00					(448)											
	1.05	423	(418)	(412)	407	(446)		(431)	(438)								
	1.10					(444)											

○ FLEXSTAB solution available

Note: On the data tapes and in the tables of appendix A, the above run numbers have been incremented by 1 000 to give the FLEXSTAB results unique identification.

**Page  
Intentionally  
Left Blank**

## REFERENCES

1. Manro, Marjorie E.; Manning, Kenneth J. R.; Hallstaff, Thomas H.; and Rogers, John T.: *Transonic Pressure Measurements and Comparison of Theory to Experiment for an Arrow-Wing Configuration: Summary Report*. NASA CR-2610, 1975.
2. Manro, Marjorie E.; Manning, Kenneth J. R.; Hallstaff, Thomas H.; and Rogers, John T.: *Transonic Pressure Measurements and Comparison of Theory to Experiment for an Arrow-Wing Configuration, Volume I: Experimental Data Report-Base Configuration and Effects of Wing Twist and Leading-Edge Configuration*. NASA CR-132727, 1975.
3. Manro, Marjorie E.; Manning, Kenneth J. R.; Hallstaff, Thomas H.; and Rogers, John T.: *Transonic Pressure Measurements and Comparison of Theory to Experiment for an Arrow-Wing Configuration, Volume II: Experimental Data Report-Effects of Control Surface Deflection*. NASA CR-132728, 1975.
4. Manro, Marjorie E.; Manning, Kenneth J. R.; Hallstaff, Thomas H.; and Rogers, John T.: *Transonic Pressure Measurements and Comparison of Theory to Experiment for an Arrow-Wing Configuration, Volume III: Data Report-Comparison of Attached Flow Theories to Experiment*. NASA CR-132729, 1975.
5. Tinoco, E. N.; and Mercer, J. E.: *FLEXSTAB-A Summary of the Functions and Capabilities of the NASA Flexible Airplane Analysis Computer System*. NASA CR-2564, October 1974.
6. Dusto, A. R., et al.: *A Method for Predicting the Stability Characteristics of an Elastic Airplane, Volume 1: FLEXSTAB Theoretical Manual*. NASA CR-114712, 1974.
7. Woodward, F. A.; Tinoco, E. N.; and Larsen, J. W.: *Analysis and Design of Supersonic Wing-Body Combinations, Including Flow Properties in the Near Field, Part 1: Theory and Application*. NASA CR-73106, 1967.
8. Woodward, F. A.: "Analysis and Design of Wing-Body Combinations at Subsonic and Supersonic Speeds." *J. Aircraft*, vol. 5, no. 6, Nov.-Dec. 1968, pp. 528-534.

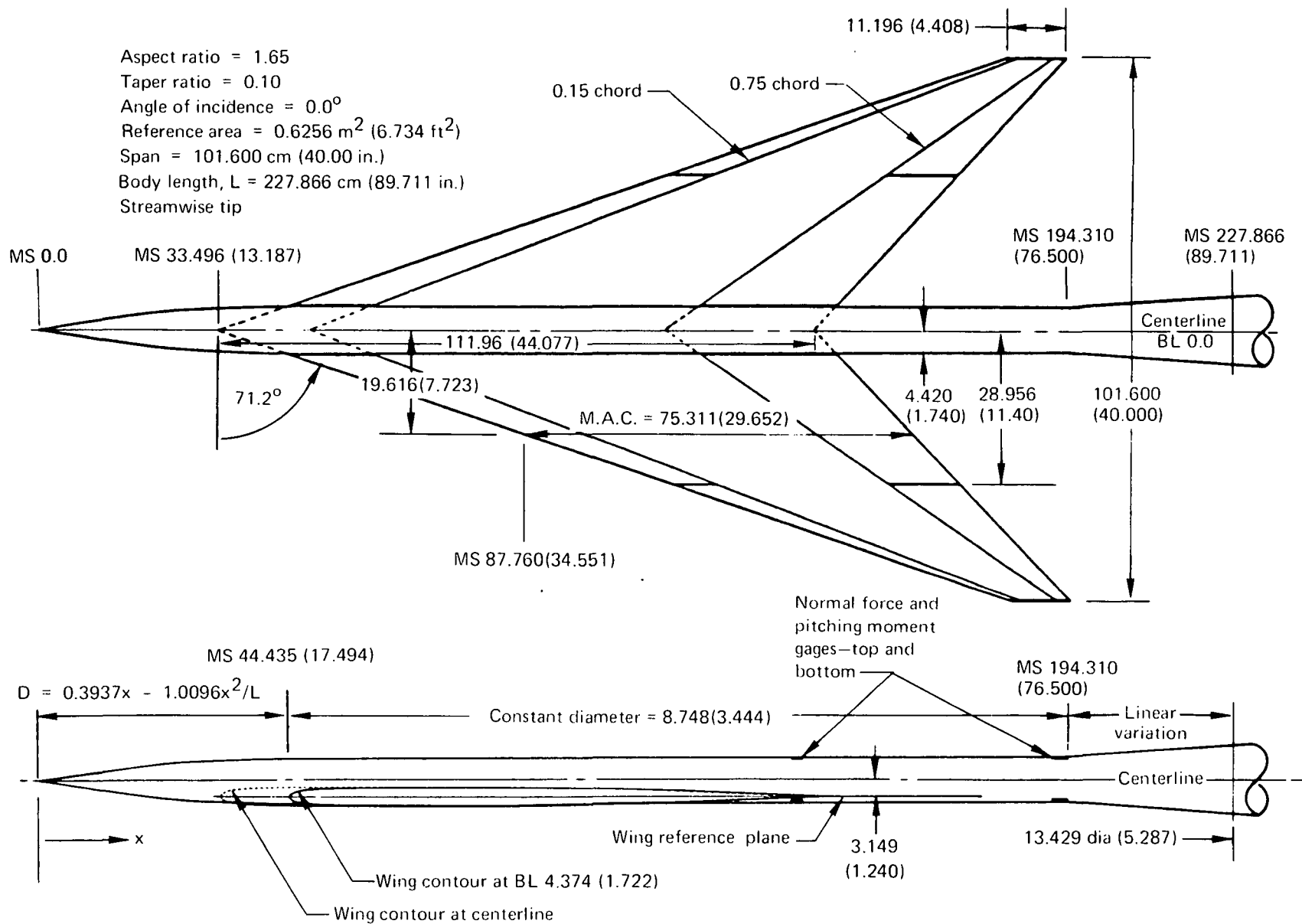


Figure 1.—General Arrangement and Characteristics

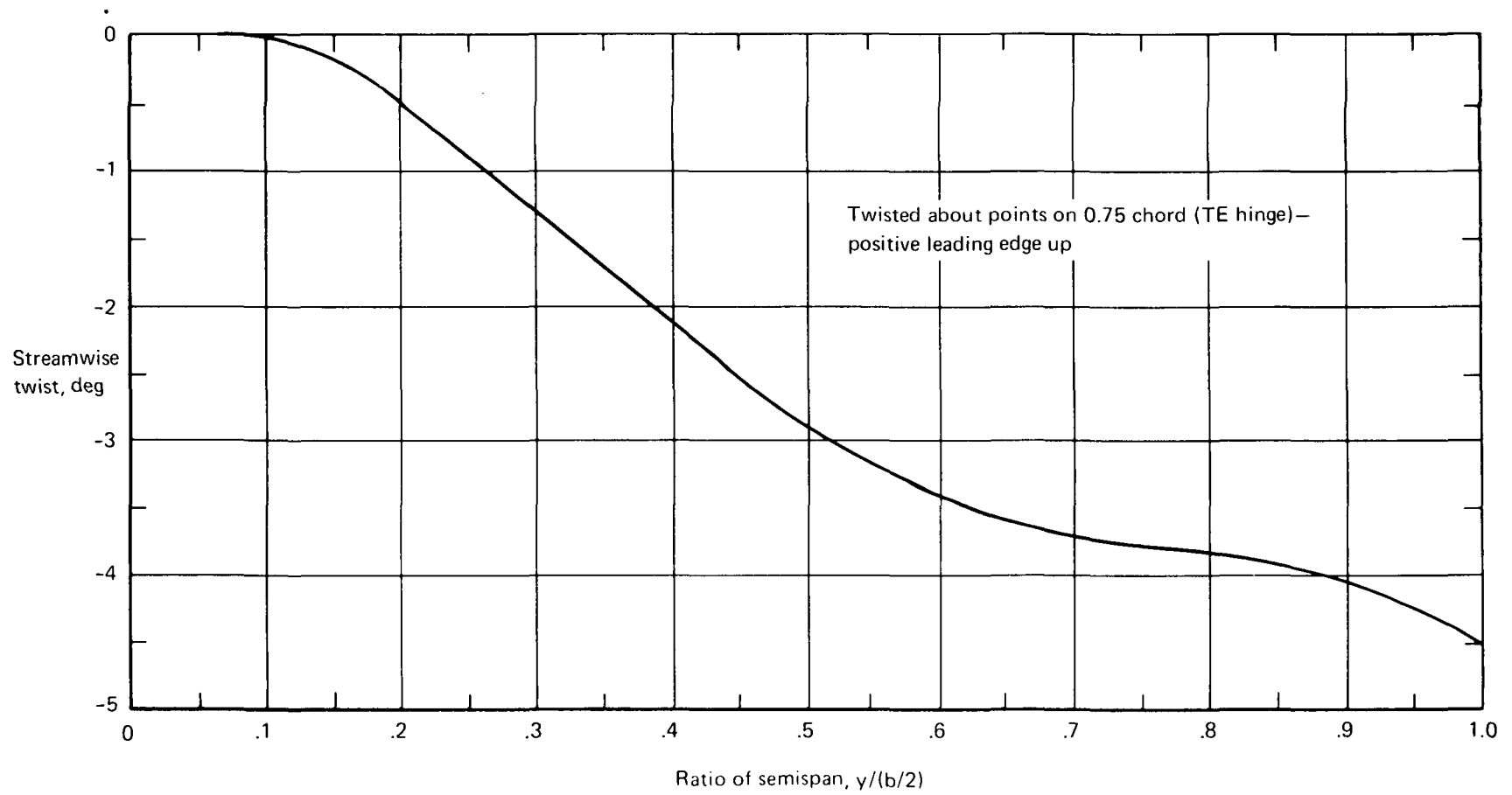


Figure 2.—Spanwise Twist Distribution for the Model Wing

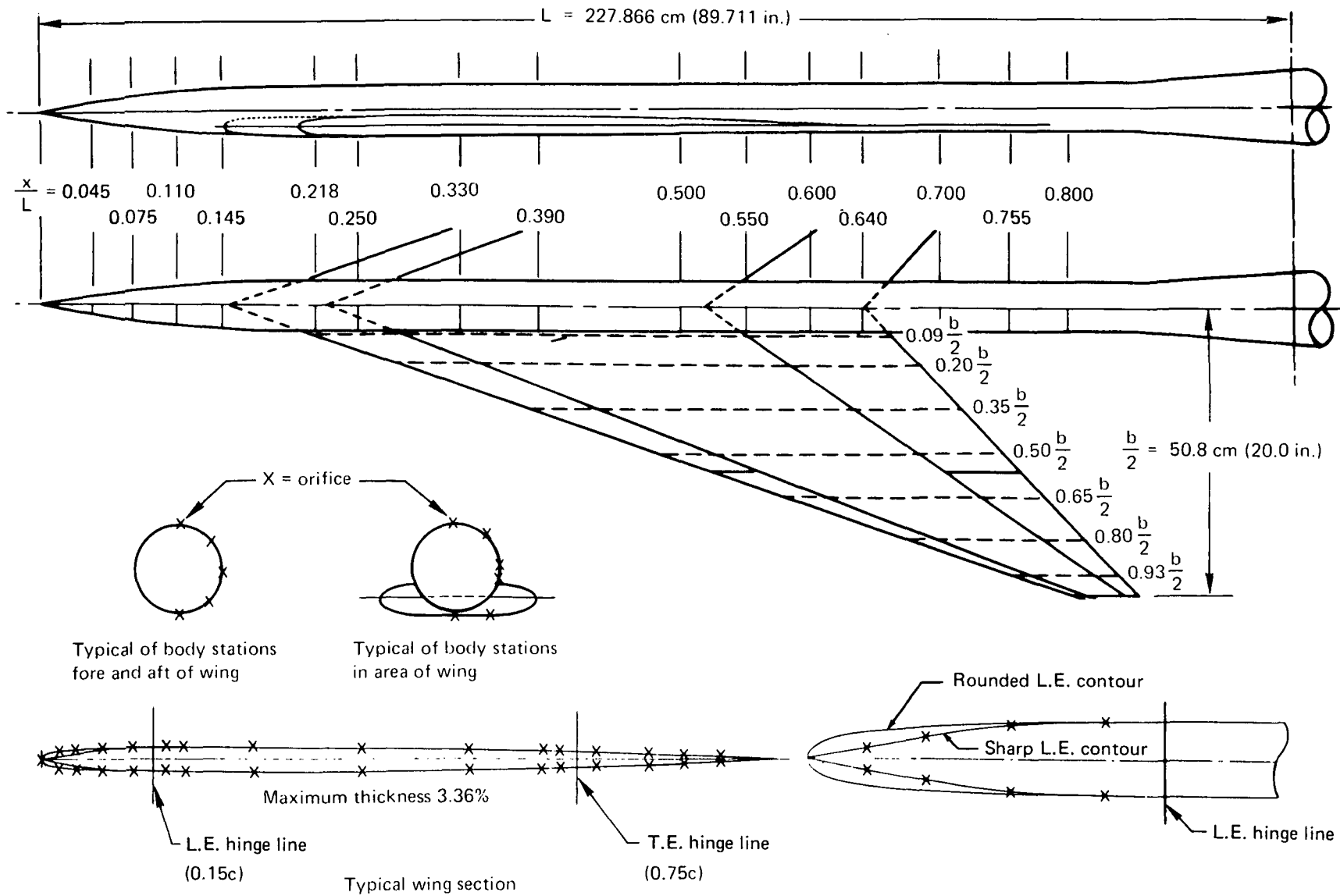


Figure 3.—Pressure Orifice Locations

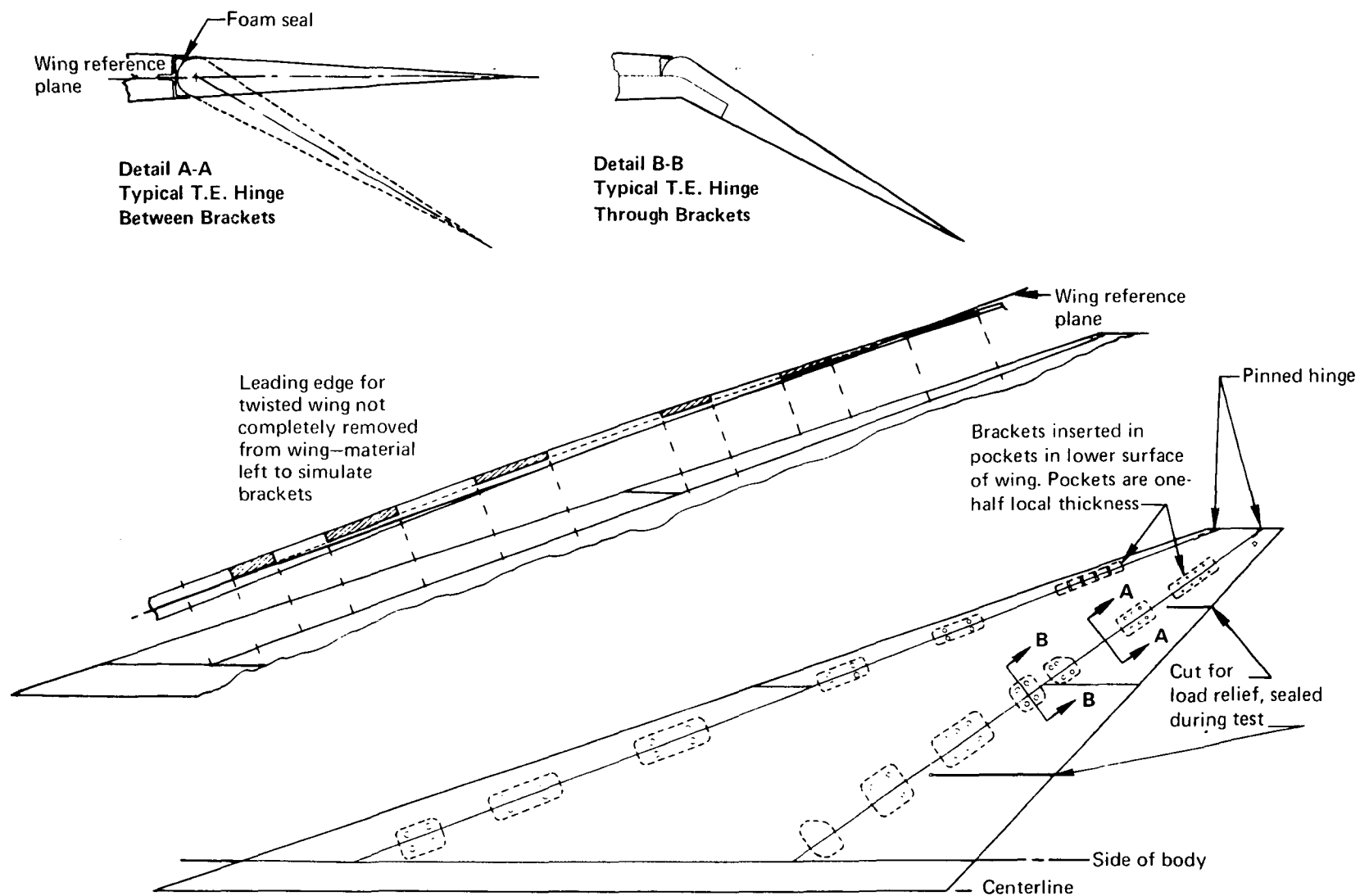


Figure 4.—Control Surface Bracket Details

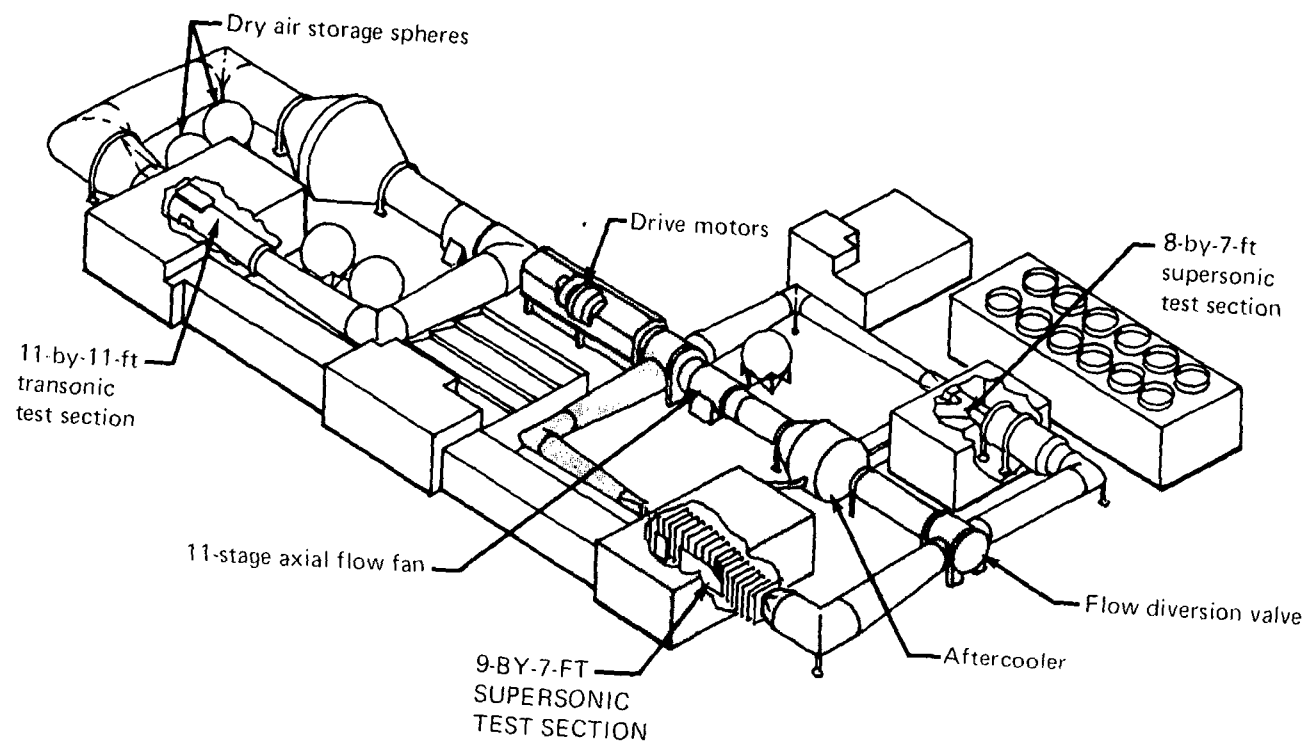
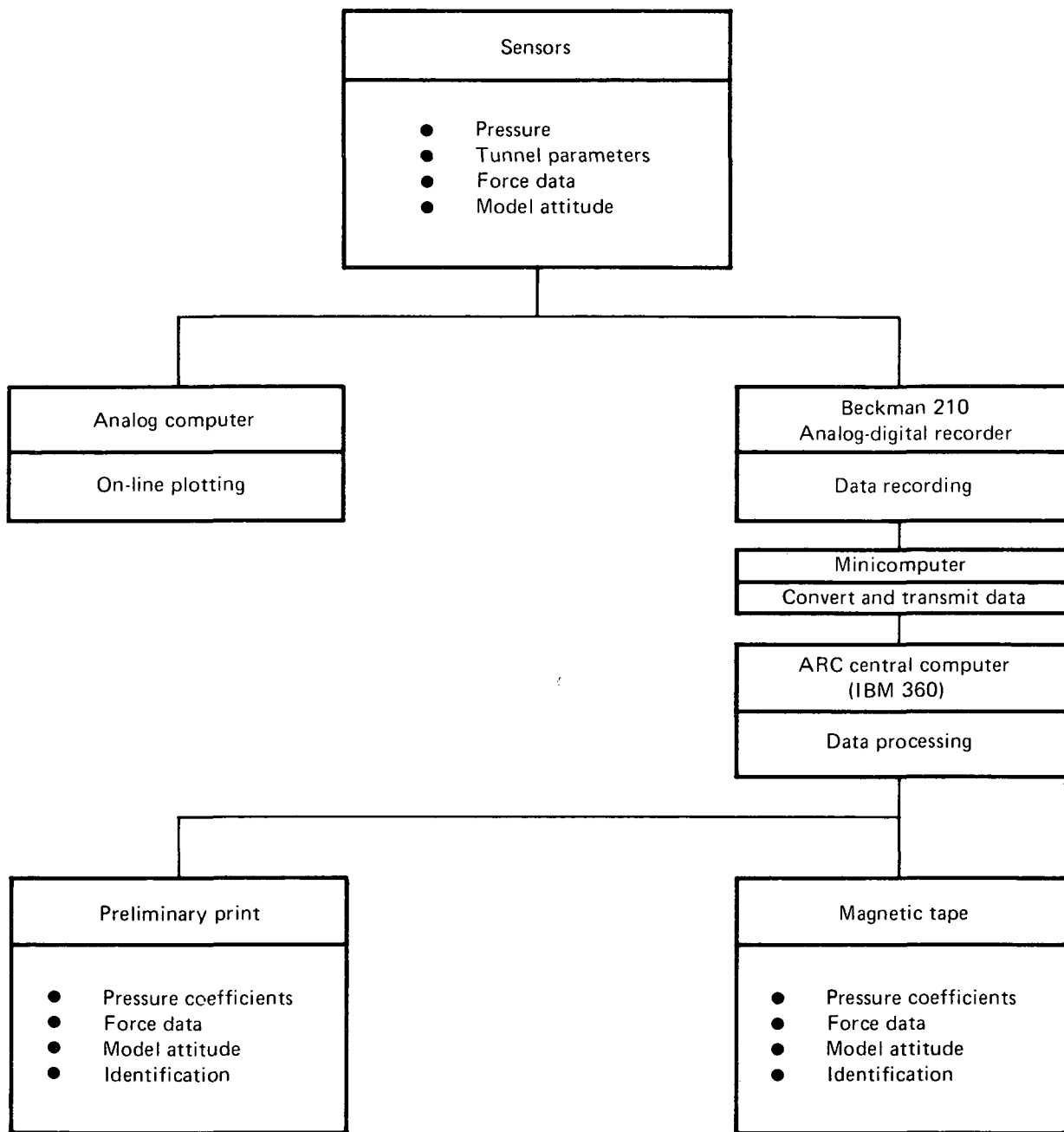
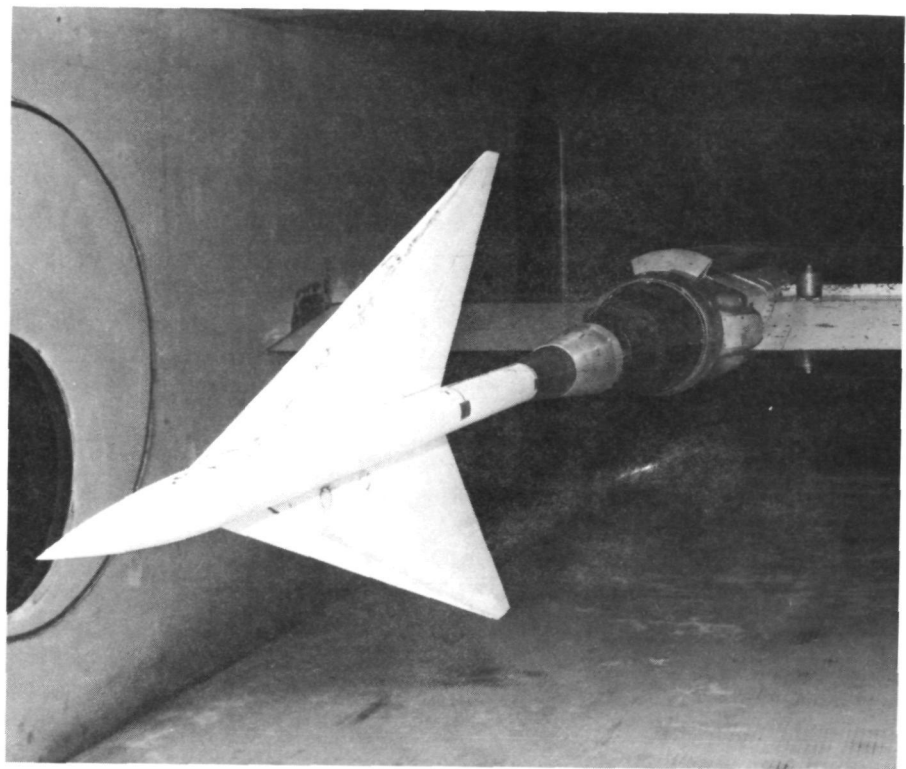
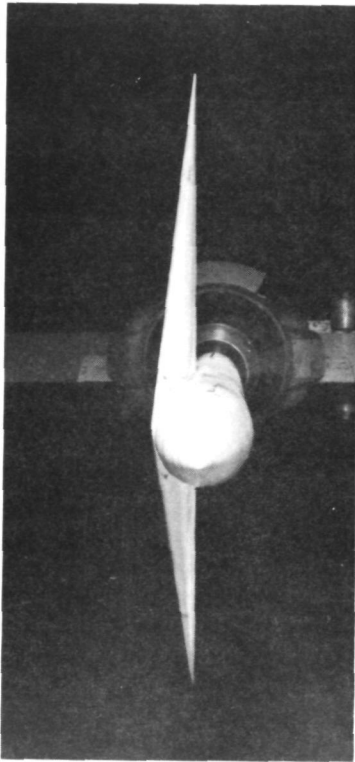


Figure 5.—Schematic of 9-by-7-ft Leg of NASA Ames Unitary Wind Tunnel





*Figure 6.—Data Acquisition and Reduction System—9-by-7-ft Leg of Ames Unitary Wind Tunnel*



*Figure 7.—Wind Tunnel Model—Flat Wing, Rounded L.E.*

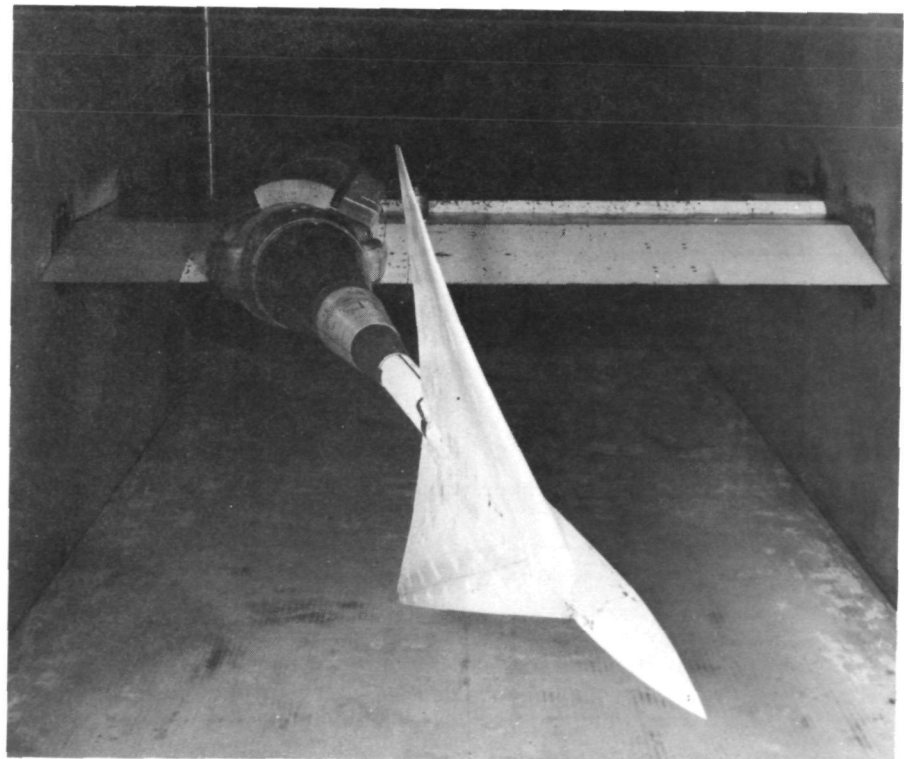
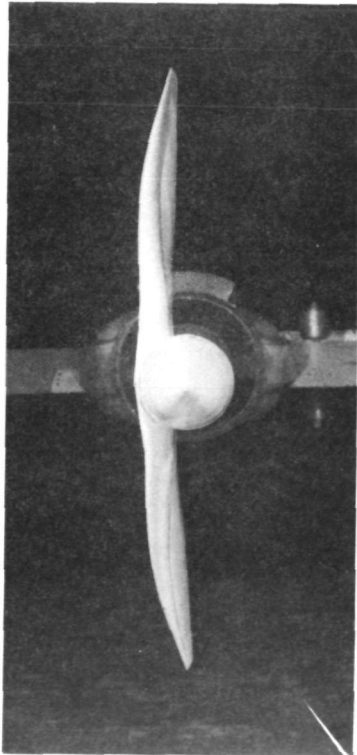
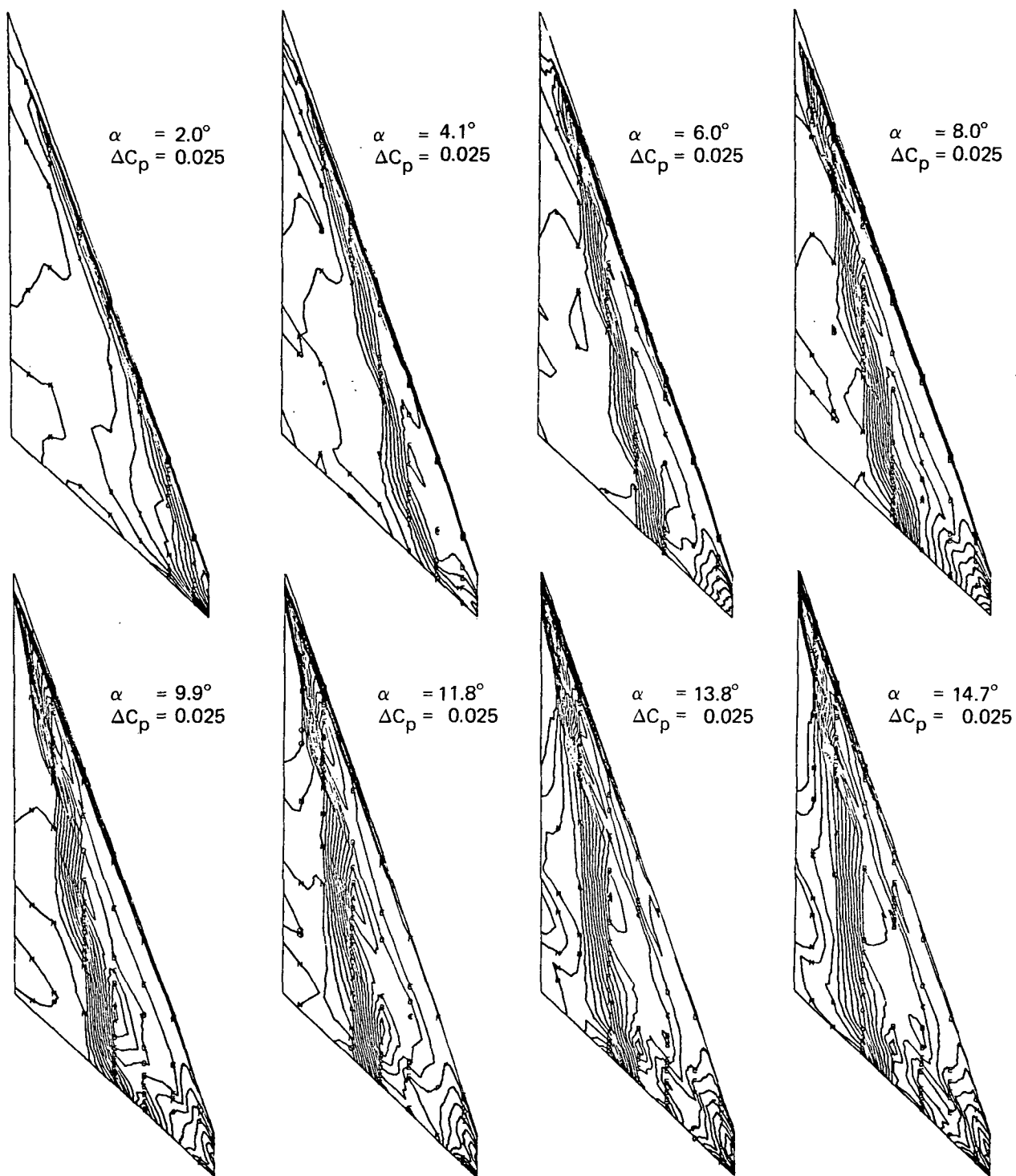


*Figure 8.—Wind Tunnel Model—Twisted Wing*

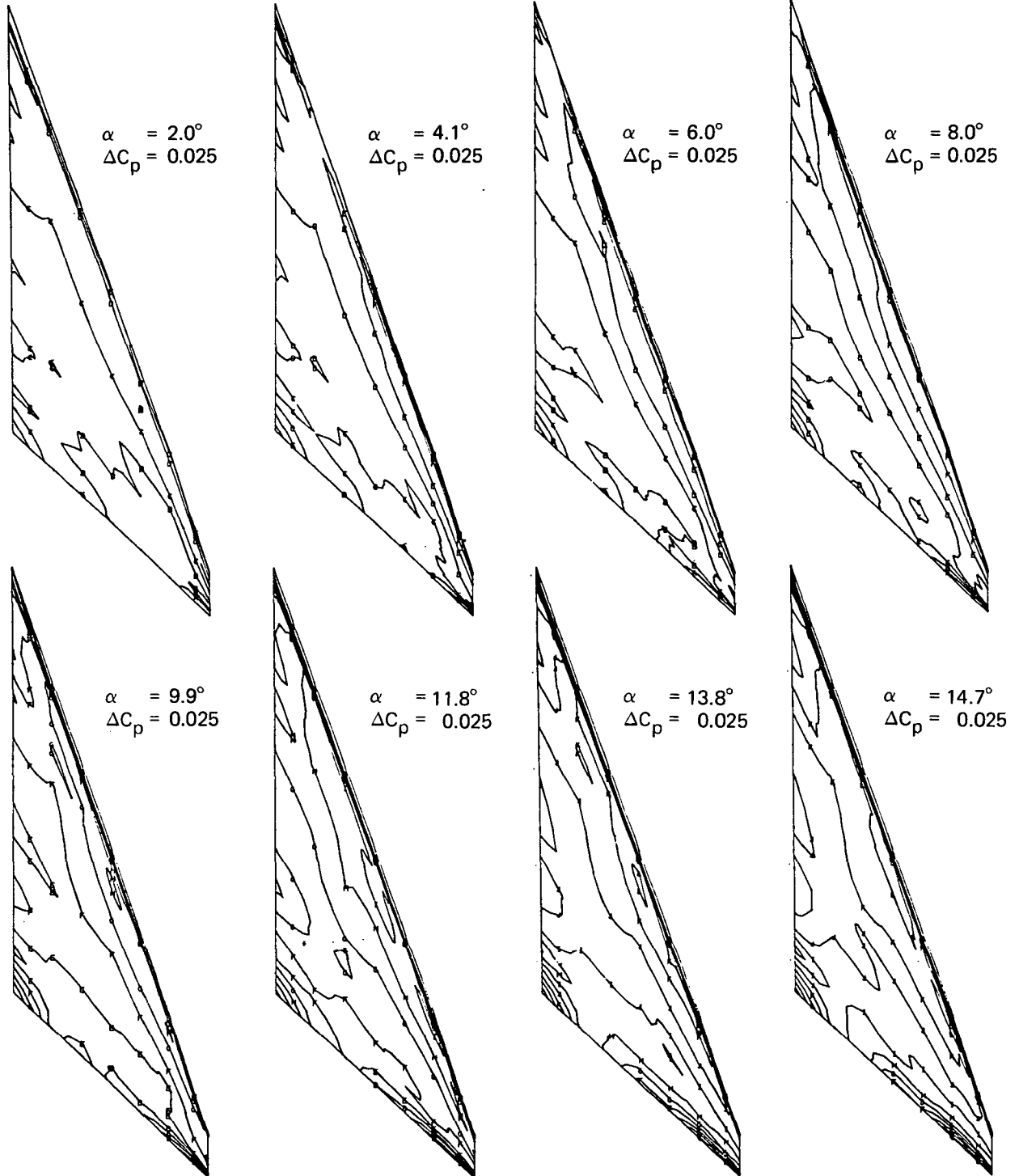




Note:  $\Delta C_p$  = increment between adjacent isobars

(a) Upper Surface Isobars

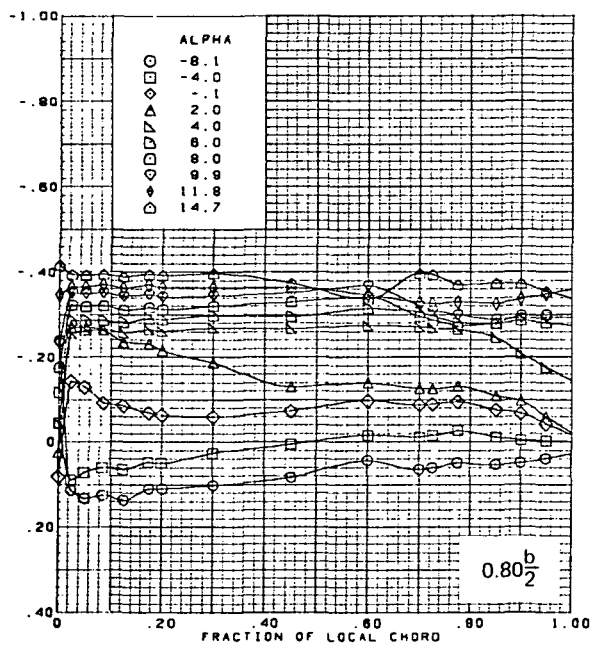
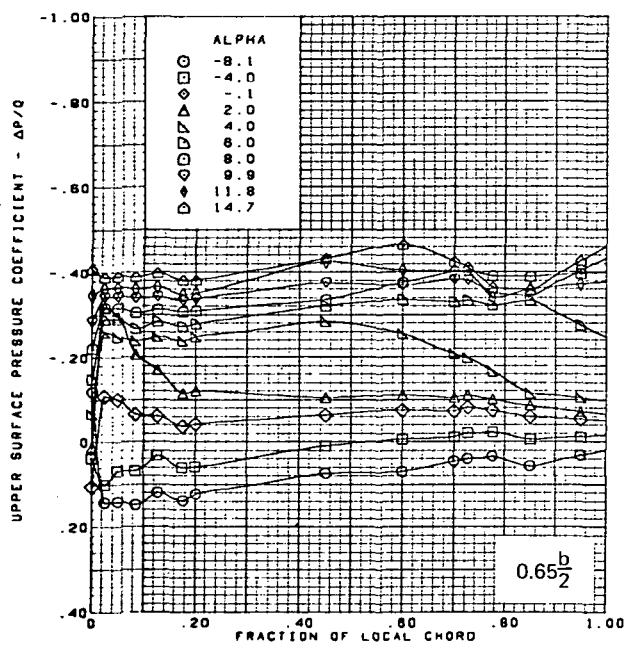
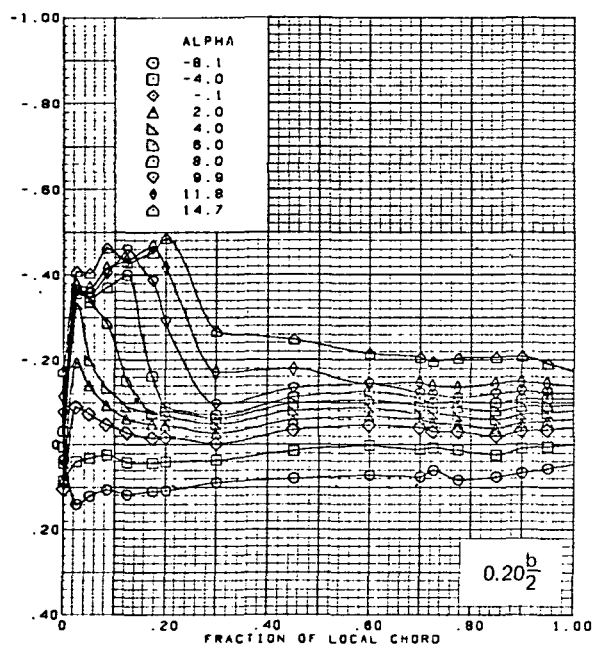
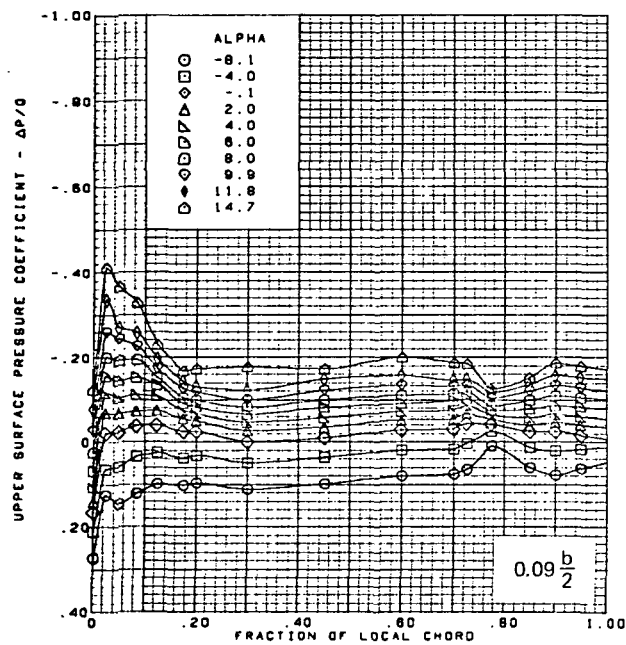
Figure 10.—Wing Experimental Data—Effect of Angle of Attack; Flat Wing, Rounded L.E.; L.E. Deflection, Full Span =  $0.0^\circ$ ; T.E. Deflection, Full Span =  $0.0^\circ$ ;  $M = 1.54$



Note:  $\Delta C_p$  = increment between adjacent isobars

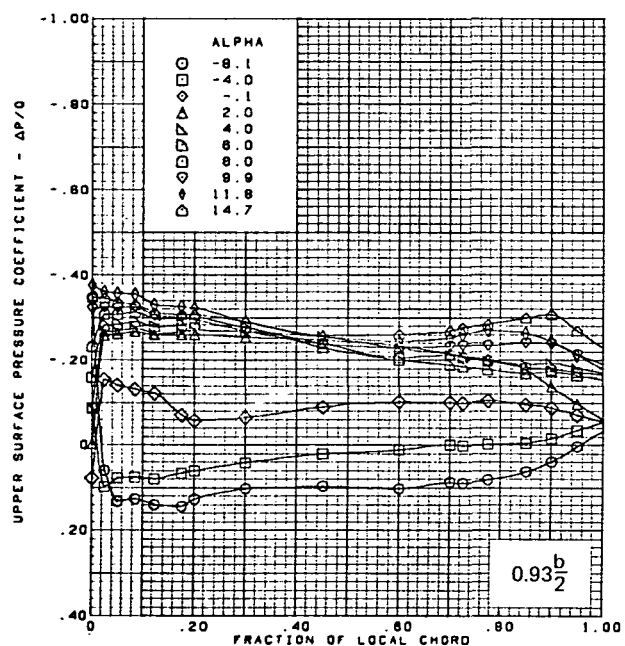
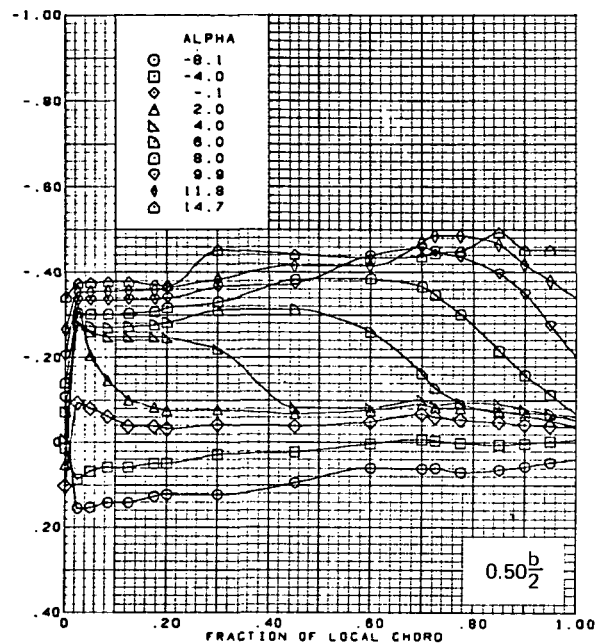
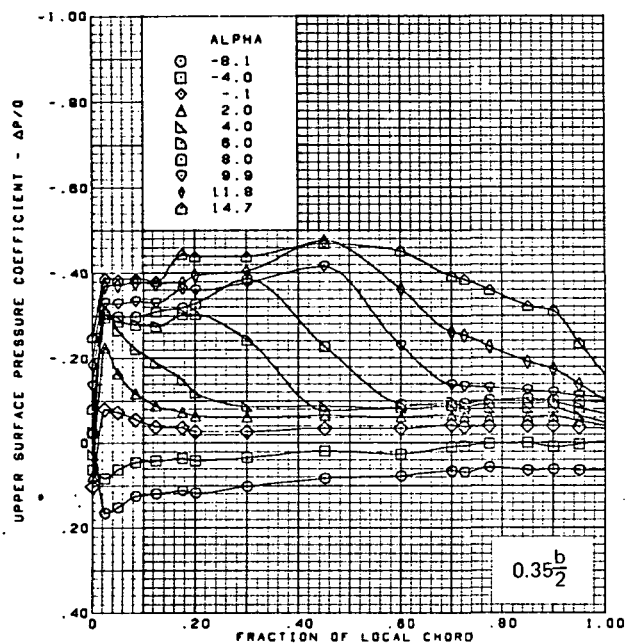
(b) Lower Surface Isobars

Figure 10.—(Continued)



(c) Upper Surface Chordwise Pressure Distributions

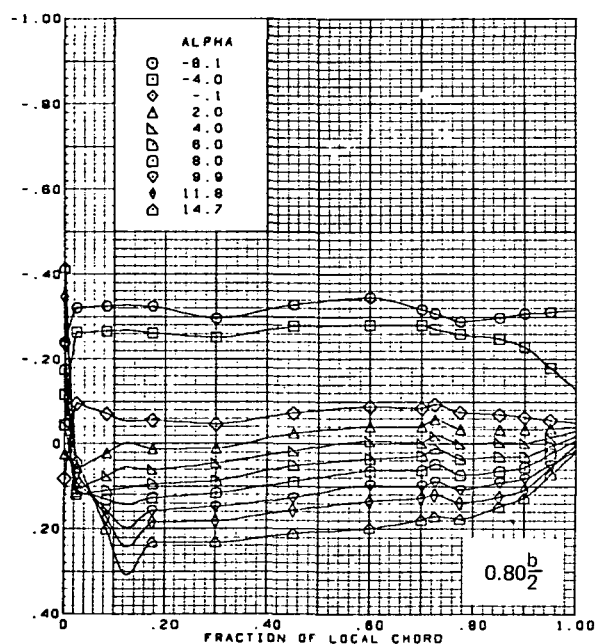
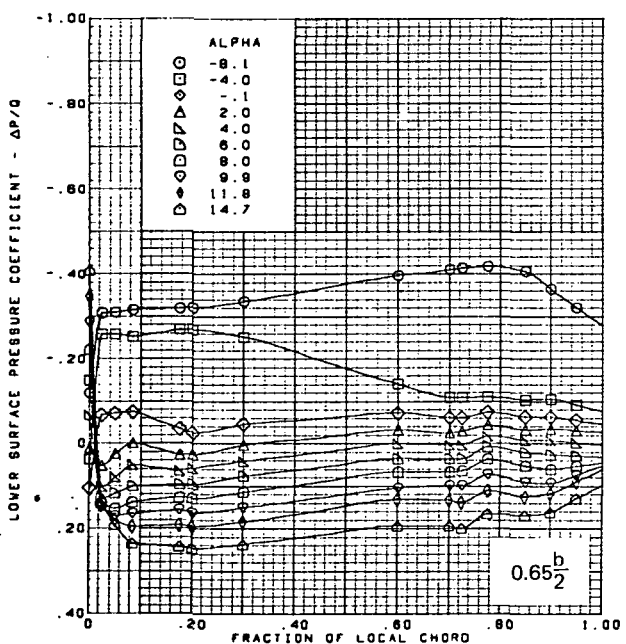
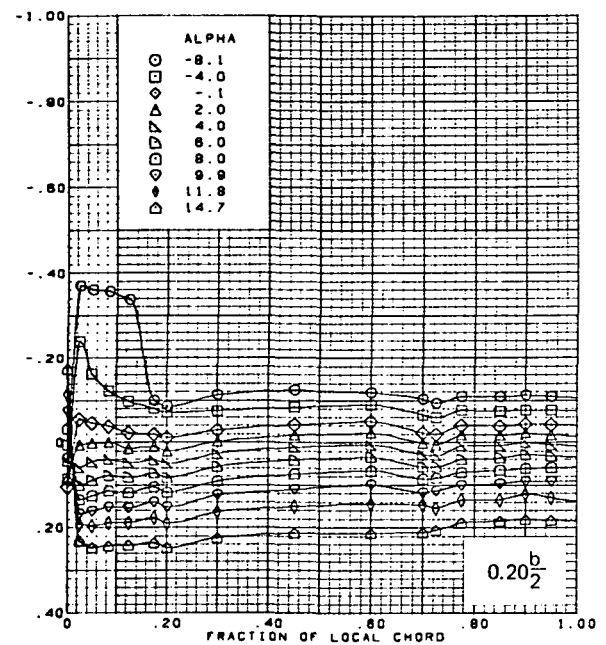
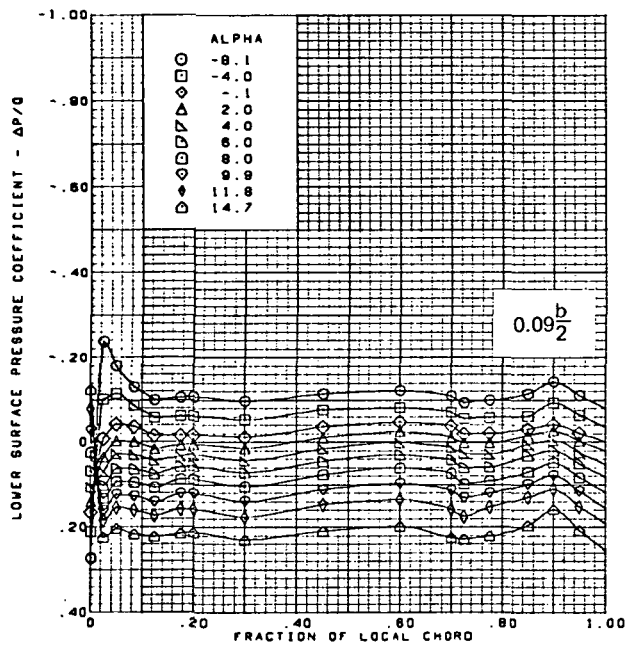
Figure 10.—(Continued)



$M = 1.54$  (run 19)  
 Flat wing, rounded L.E.  
 L.E. deflection, full span =  $0.0^\circ$   
 T.E. deflection, full span =  $0.0^\circ$   
 Note:  $C_{p, \text{vacuum}} = -0.60$

(c) (Concluded)

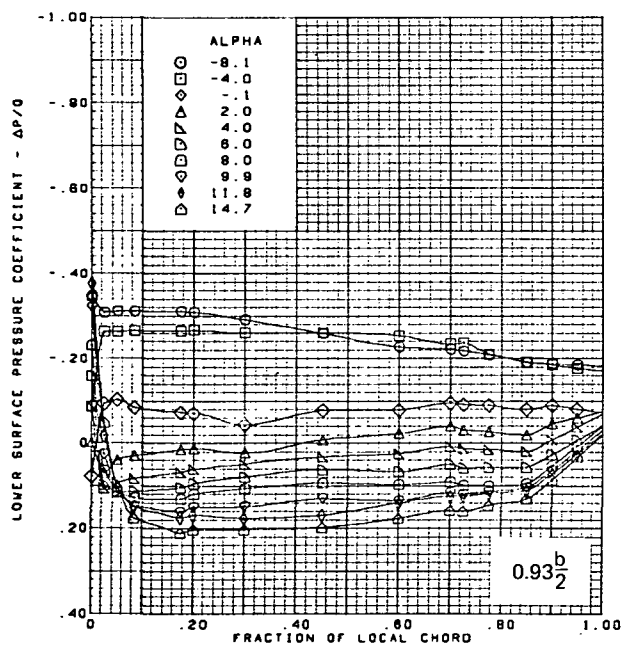
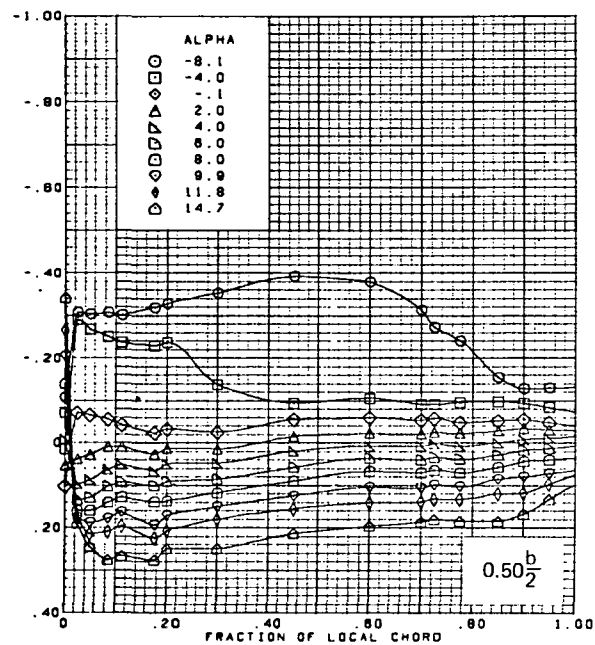
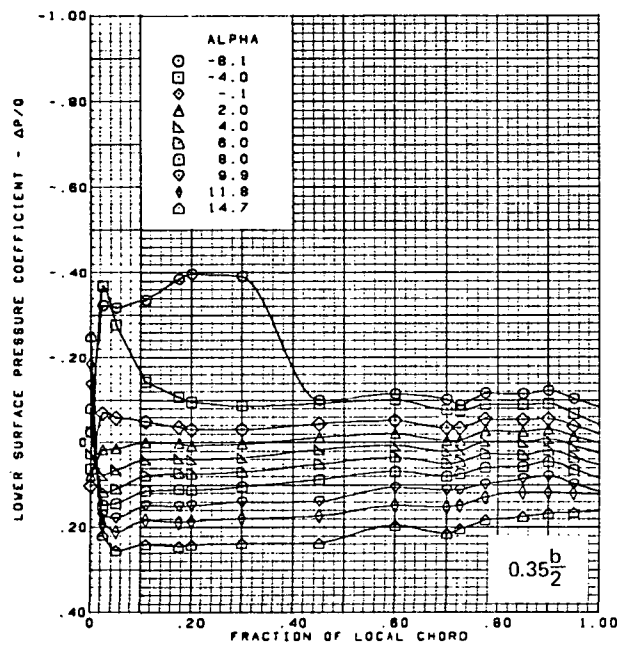
Figure 10.—(Continued)



(d) Lower Surface Chordwise Pressure Distributions

Figure 10.—(Continued)



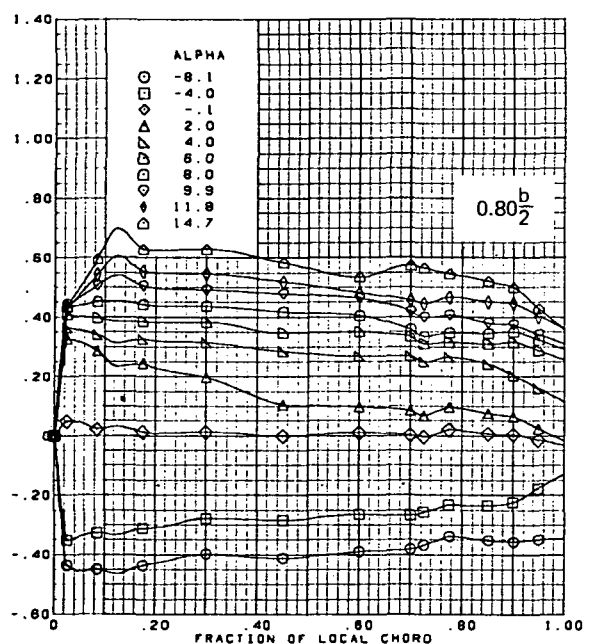
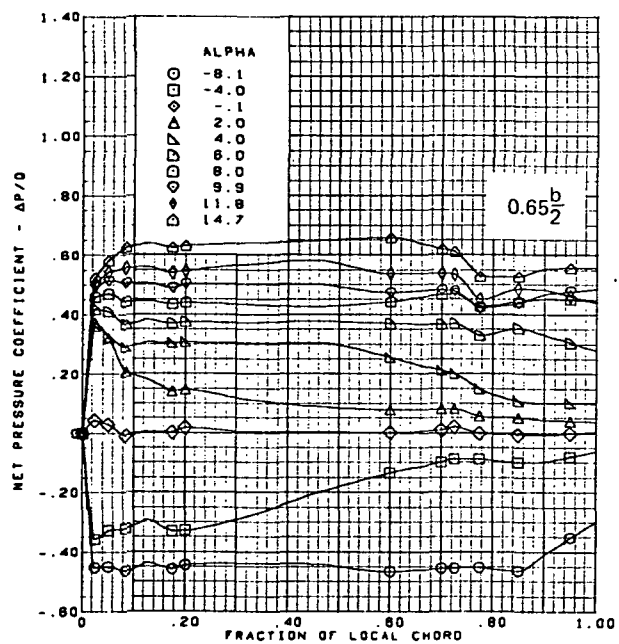
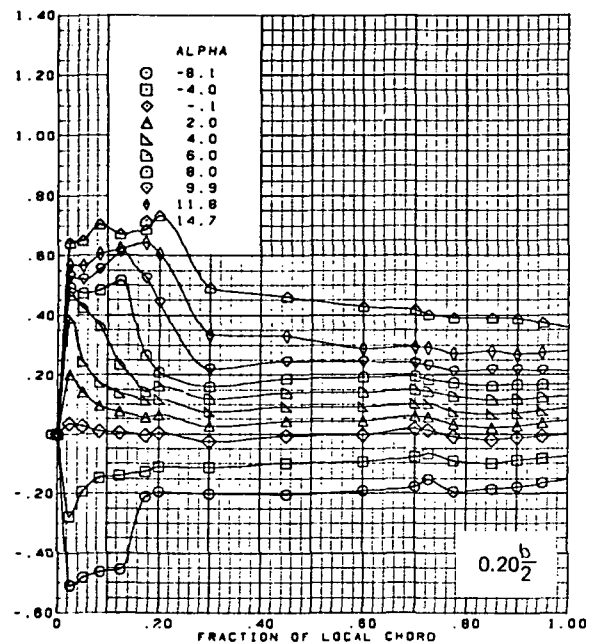
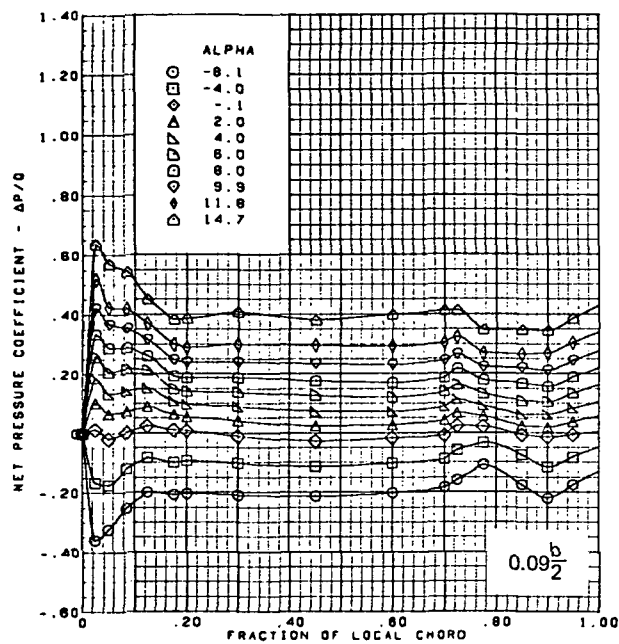


$M = 1.54$  (run 19)  
 Flat wing, rounded L.E.  
 L.E. deflection, full span =  $0.0^\circ$   
 T.E. deflection, full span =  $0.0^\circ$

Note:  $C_{p, \text{vacuum}} = -0.60$

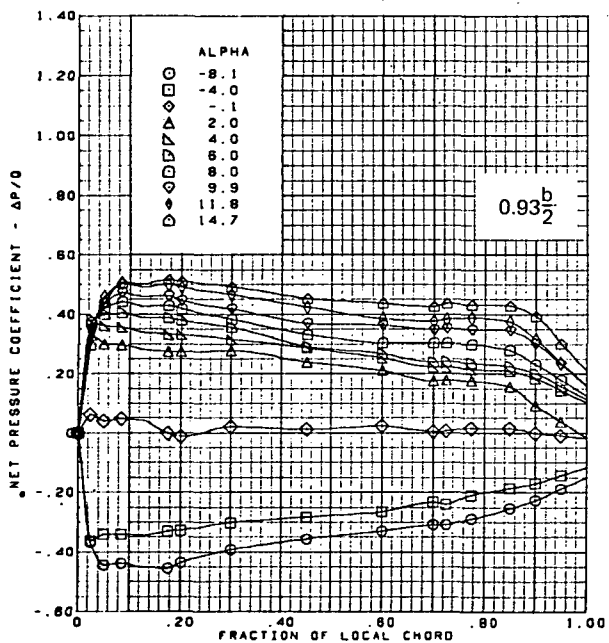
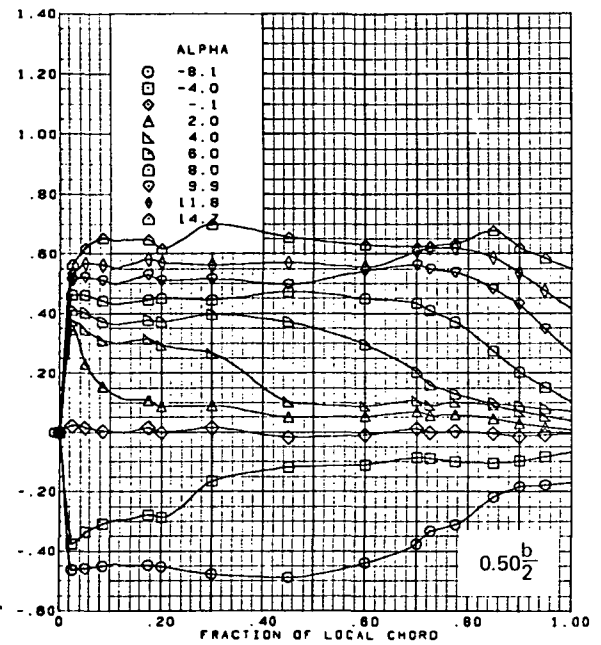
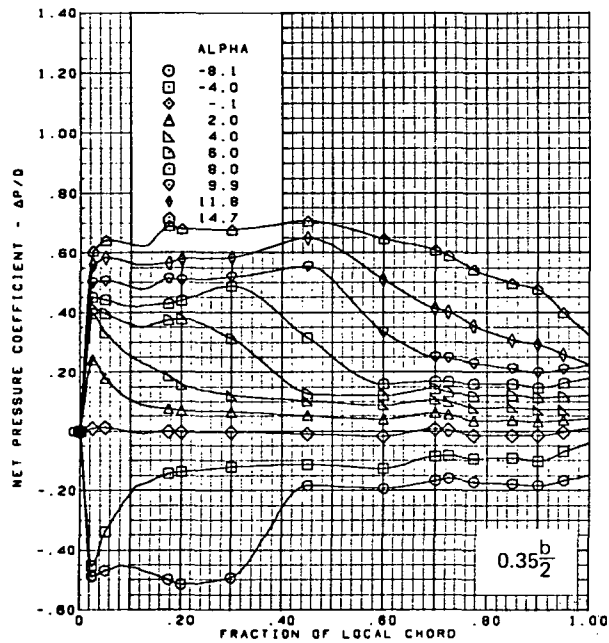
(d) (Concluded)

Figure 10.—(Continued)



(e) Net Chordwise Pressure Distributions

Figure 10.—(Continued)

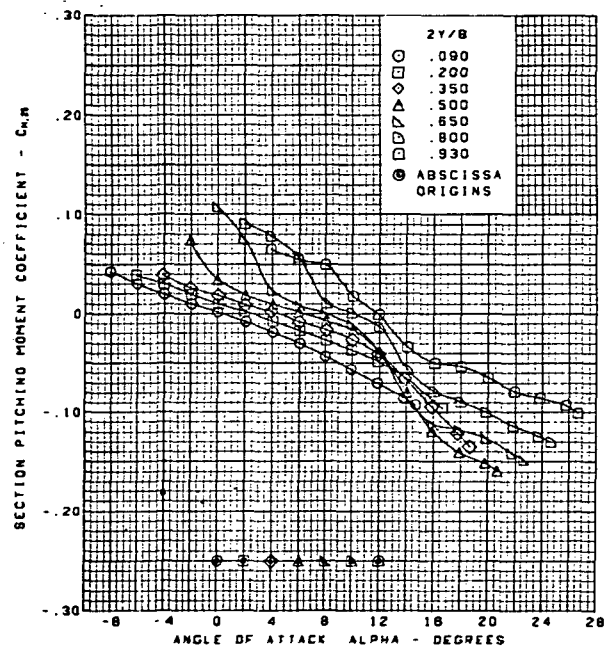
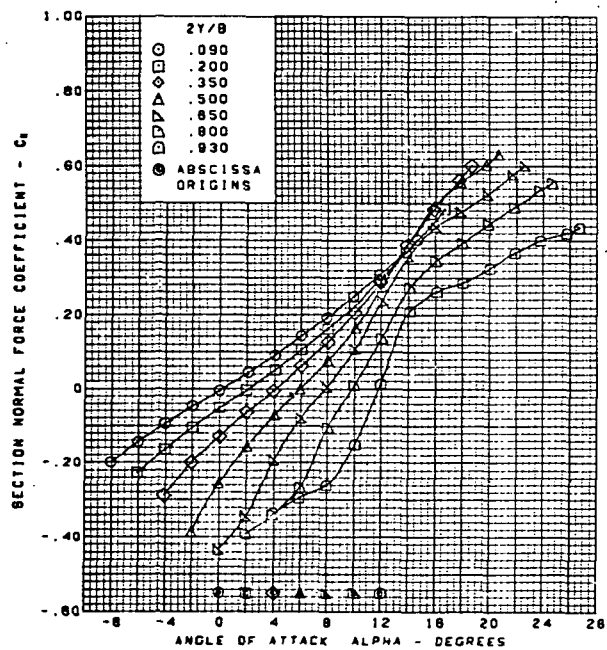
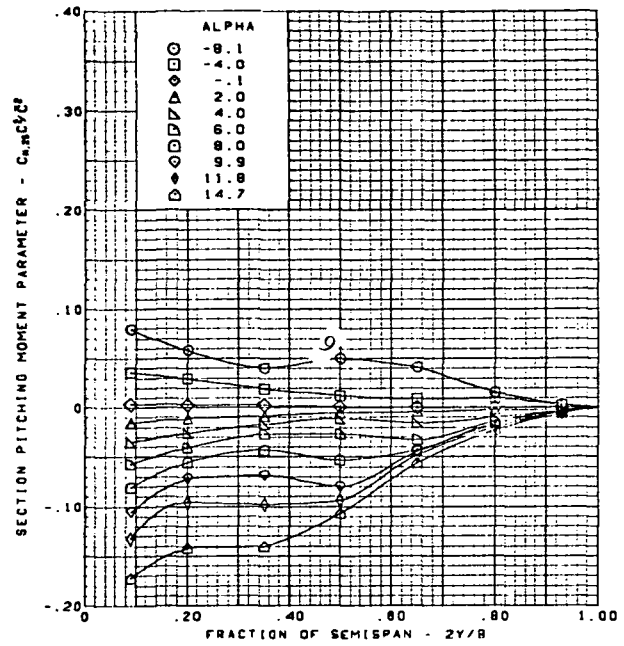
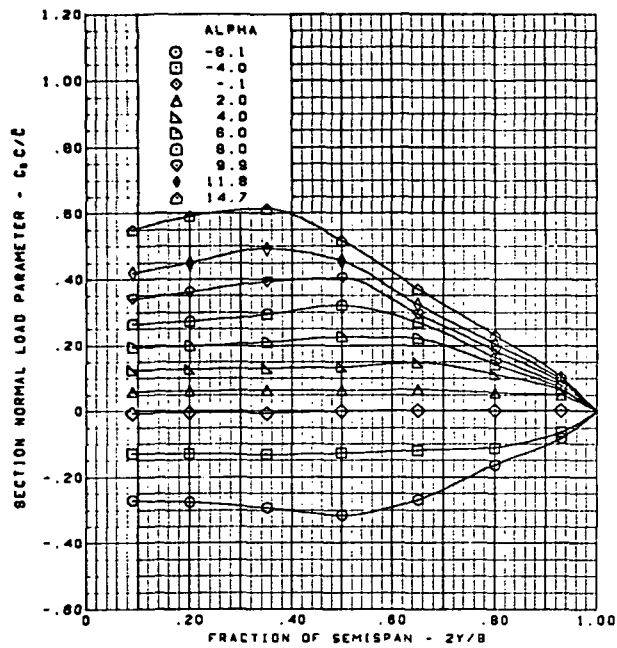


$M = 1.54$  (run 19)  
 Flat wing, rounded L.E.  
 L.E. deflection, full span =  $0.0^\circ$   
 T.E. deflection, full span =  $0.0^\circ$

(e) (Concluded)

Figure 10.—(Continued)

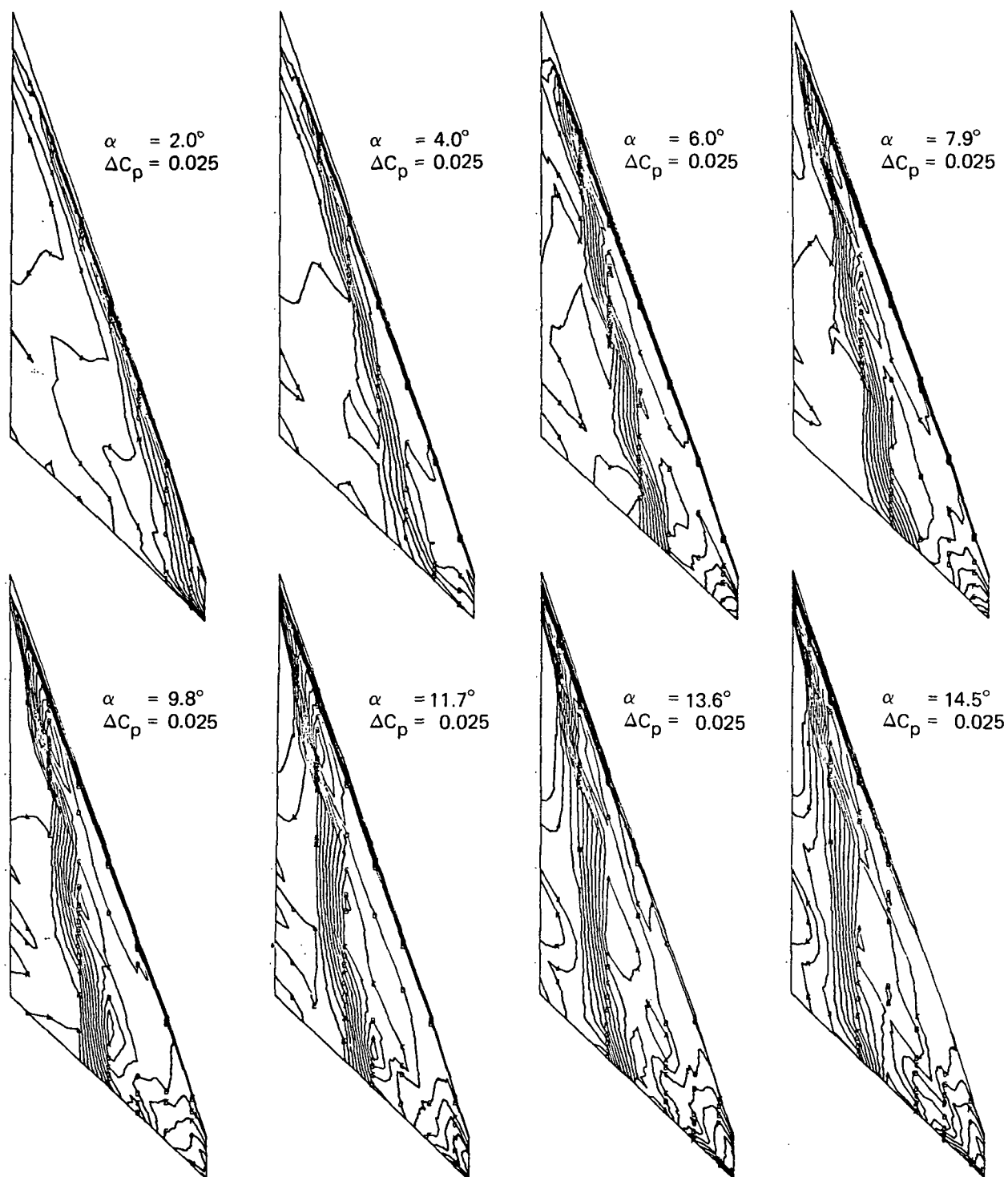
**Page  
Intentionally  
Left Blank**



M = 1.54 (run 19)  
 Flat wing, rounded L.E.  
 L.E. deflection, full span =  $0.0^\circ$   
 T.E. deflection, full span =  $0.0^\circ$

(f) Spanload Distributions and Section Aerodynamic Coefficients

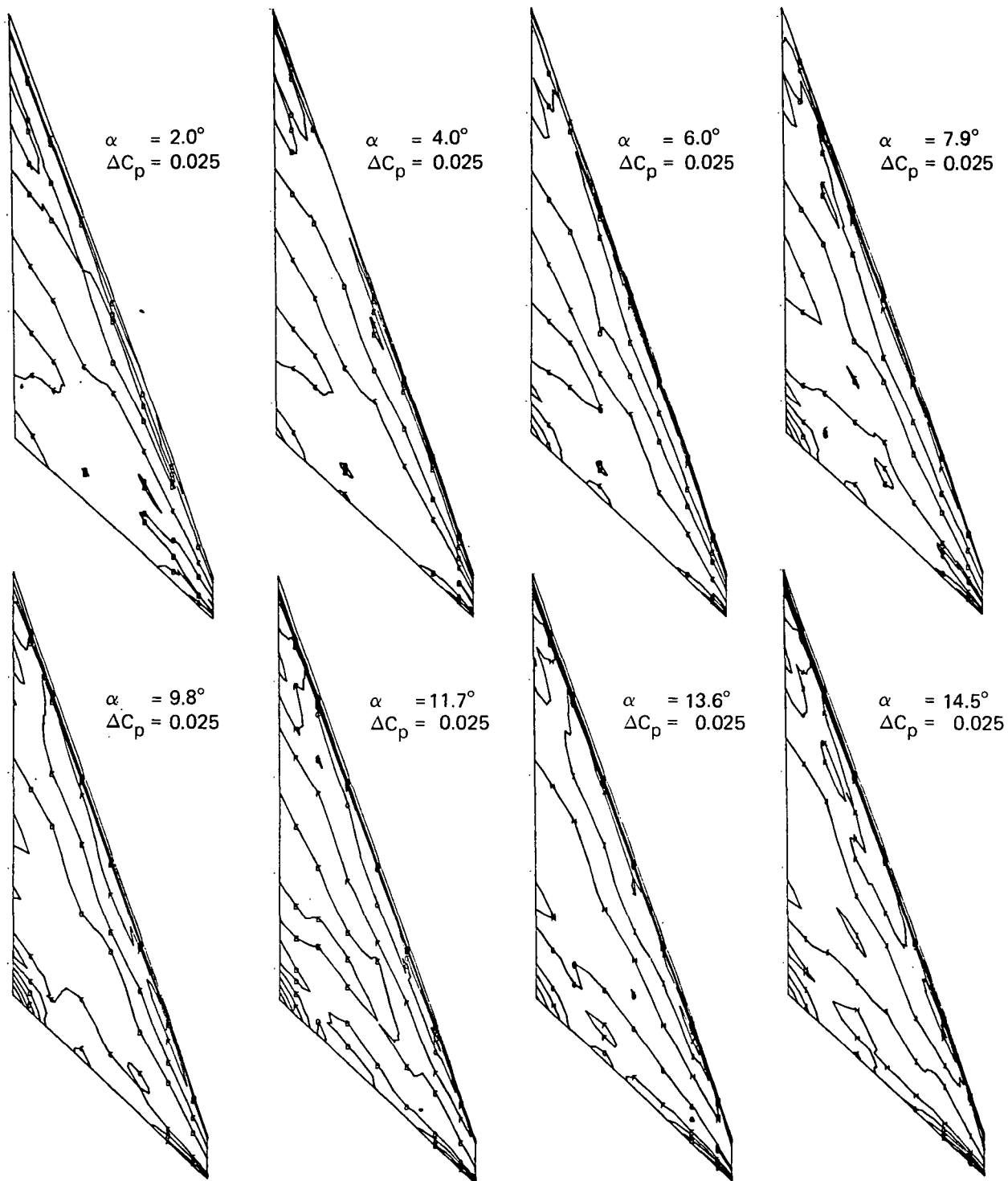
Figure 10.—(Concluded)



Note:  $\Delta C_p$  = increment between adjacent isobars

(a) Upper Surface Isobars

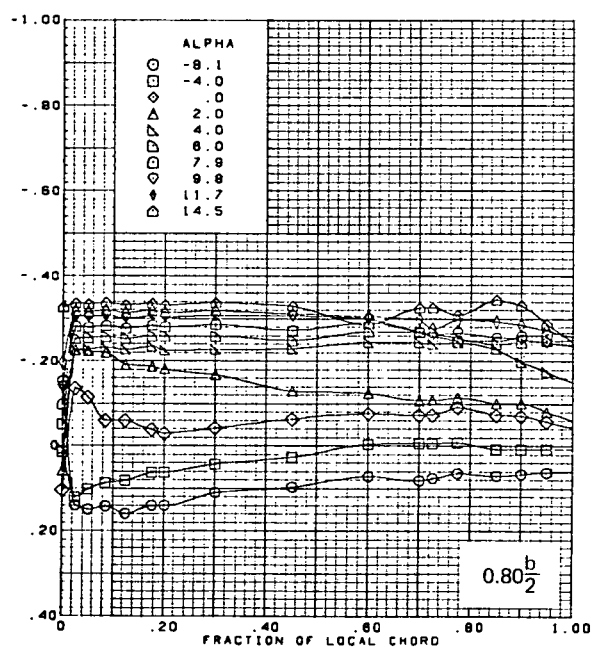
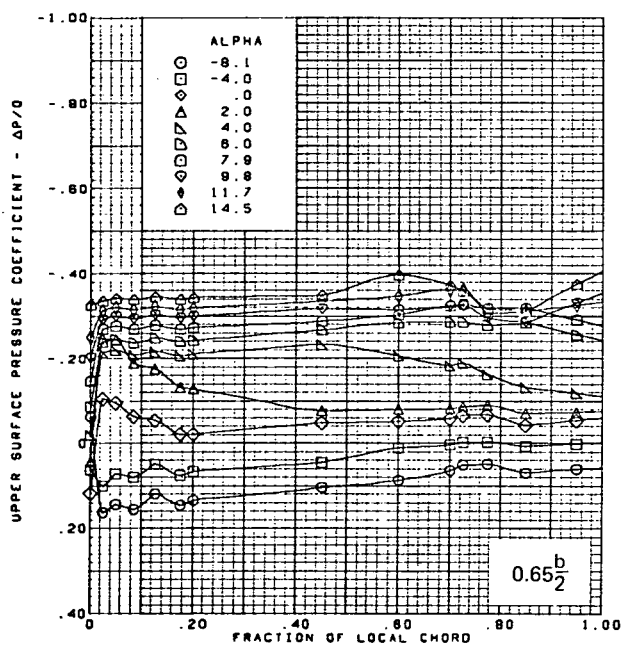
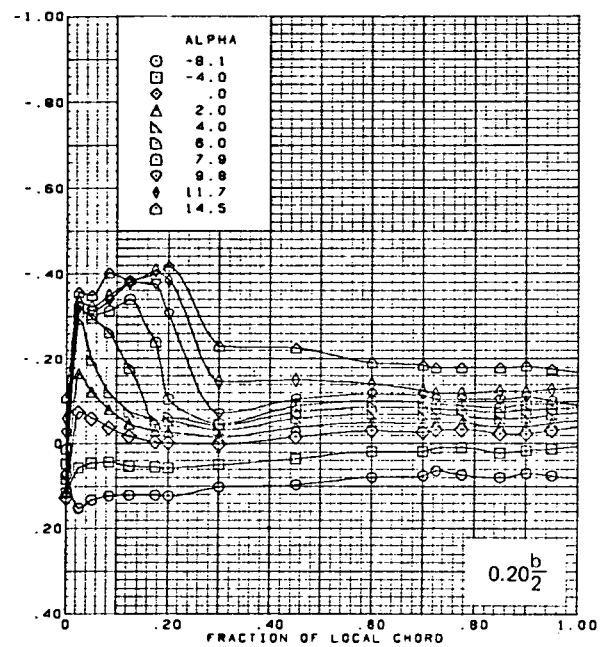
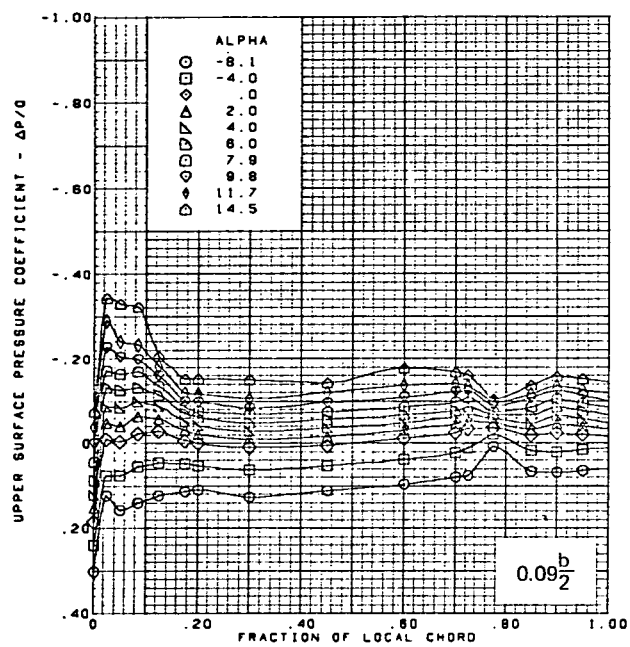
Figure 11.—Wing Experimental Data—Effect of Angle of Attack; Flat Wing, Rounded L.E.; L.E. Deflection, Full Span =  $0.0^\circ$ ; T.E. Deflection, Full Span =  $0.0^\circ$ ;  $M = 1.70$



Note:  $\Delta C_p$  = increment between adjacent isobars

(b) Lower Surface Isobars

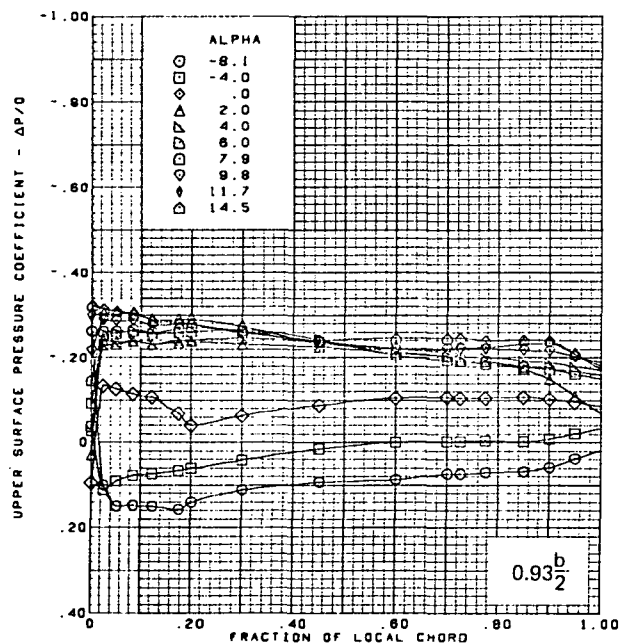
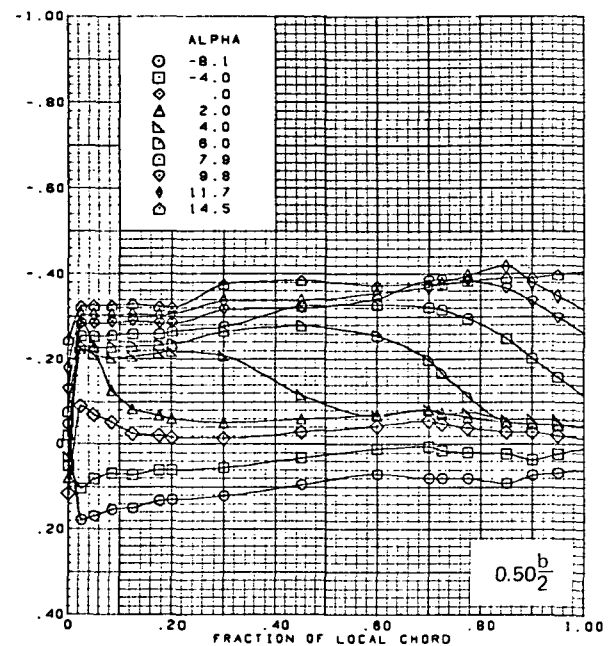
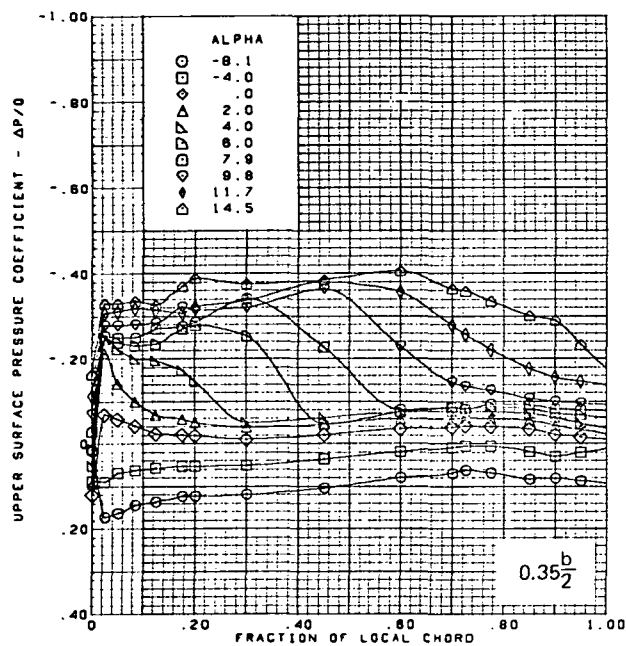
Figure 11.—(Continued)



(c) Upper Surface Chordwise Pressure Distributions

Figure 11.—(Continued)

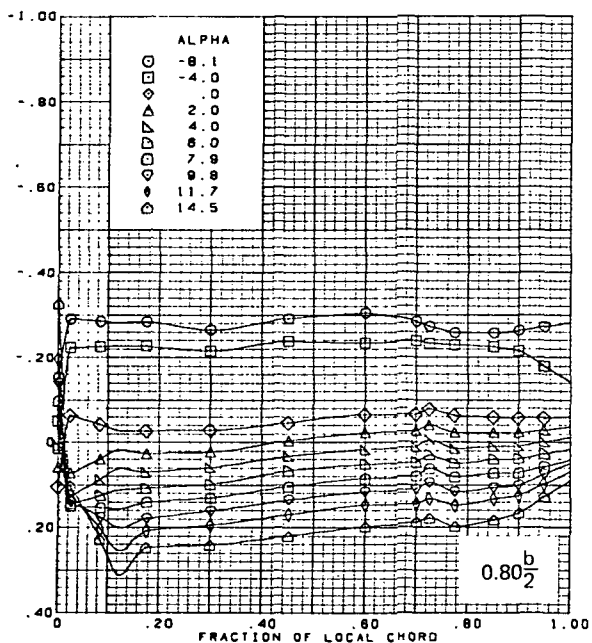
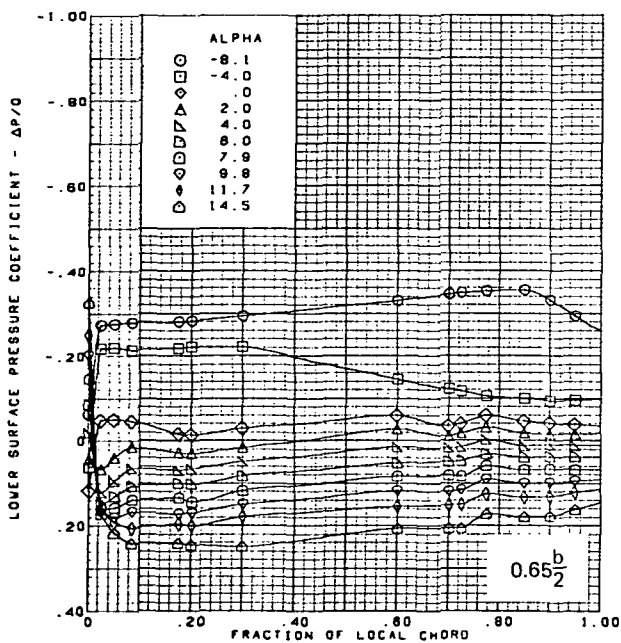
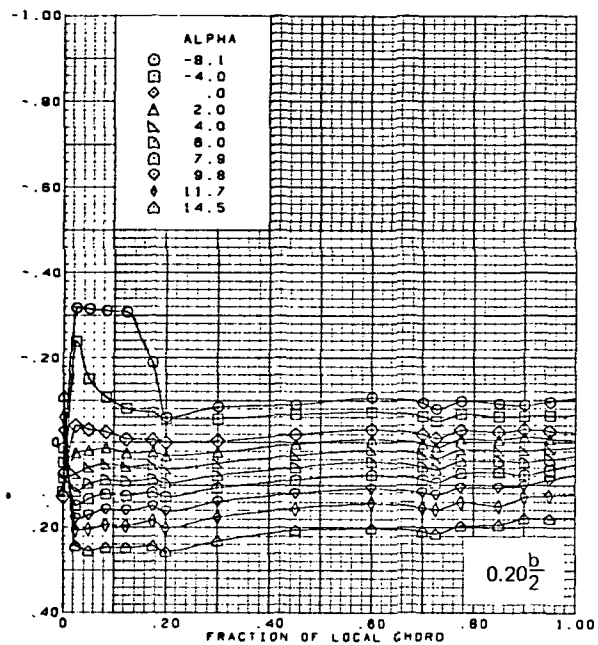
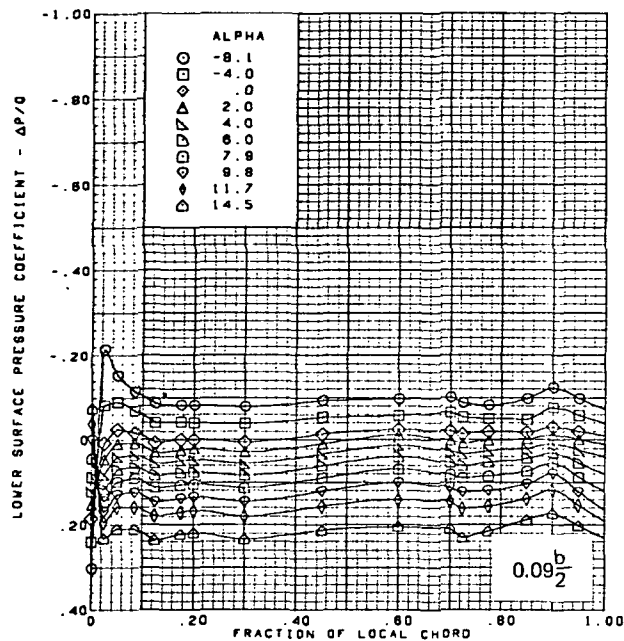




$M = 1.70$  (run 20)  
 Flat wing, rounded L.E.  
 L.E. deflection, full span =  $0.0^\circ$   
 T.E. deflection, full span =  $0.0^\circ$   
 Note:  $C_{p, \text{vacuum}} = -0.49$

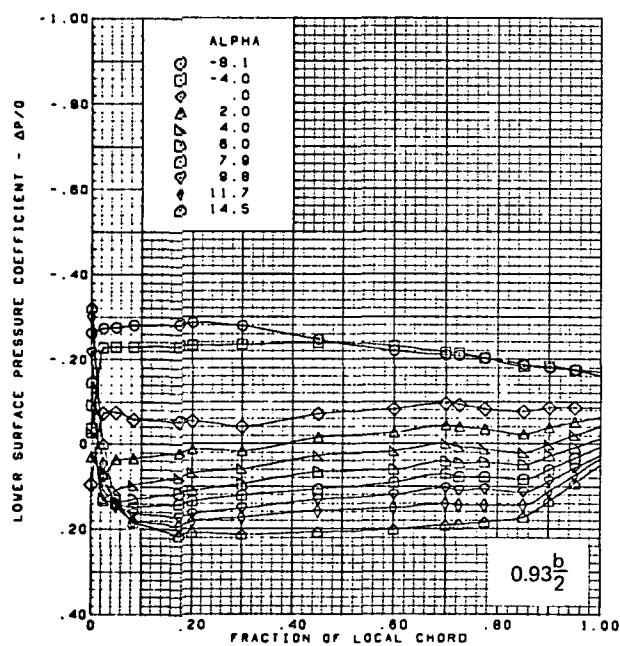
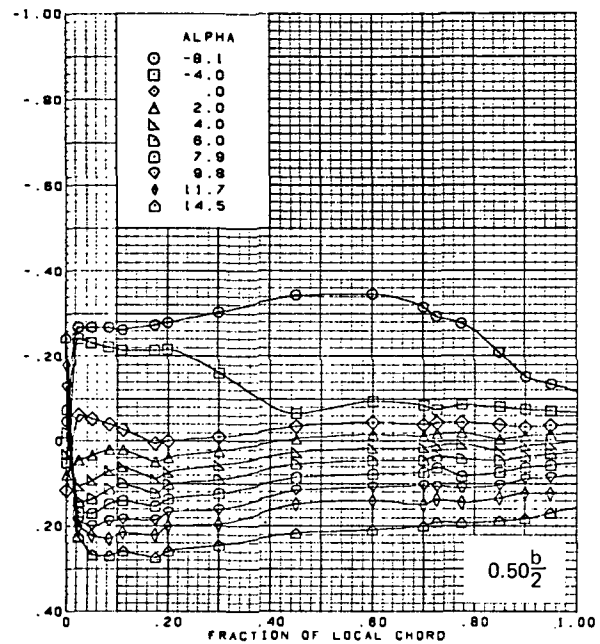
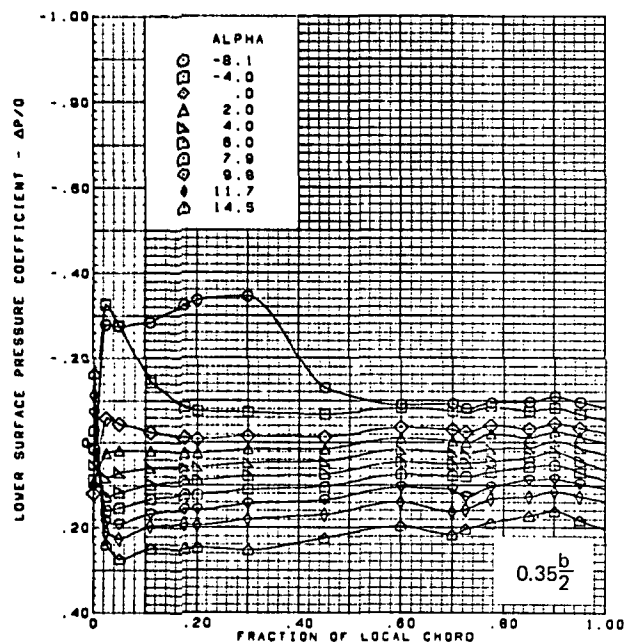
(c) (Concluded)

Figure 11.—(Continued)



(d) Lower Surface Chordwise Pressure Distributions

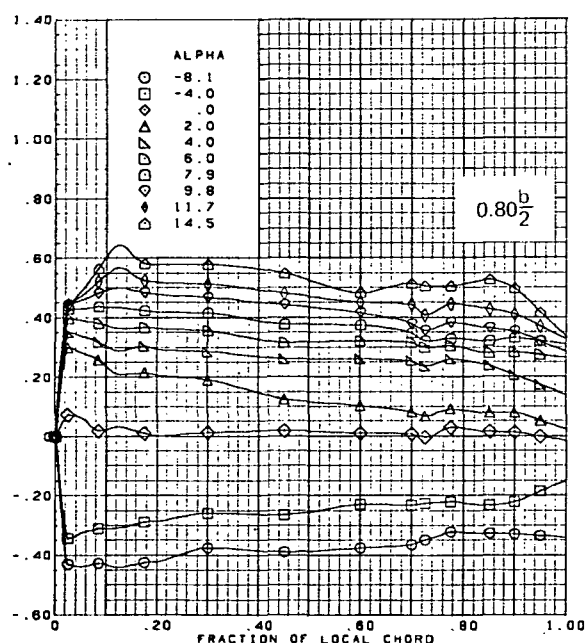
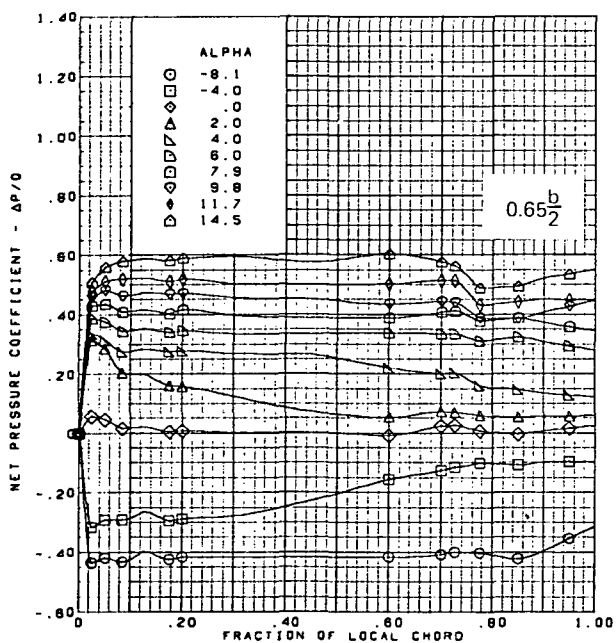
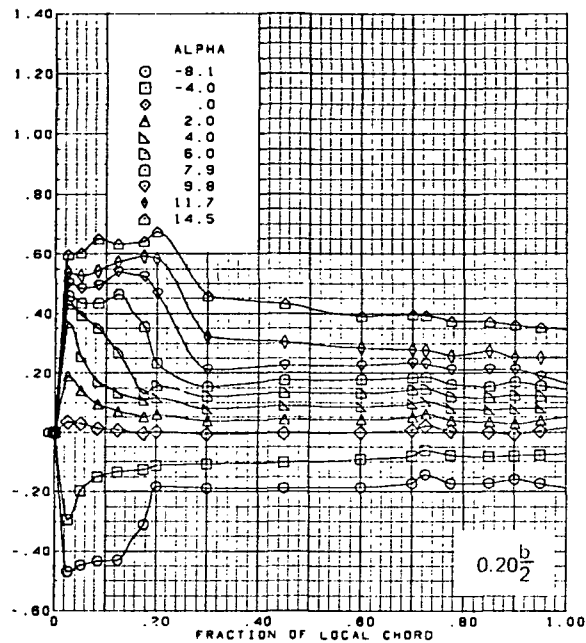
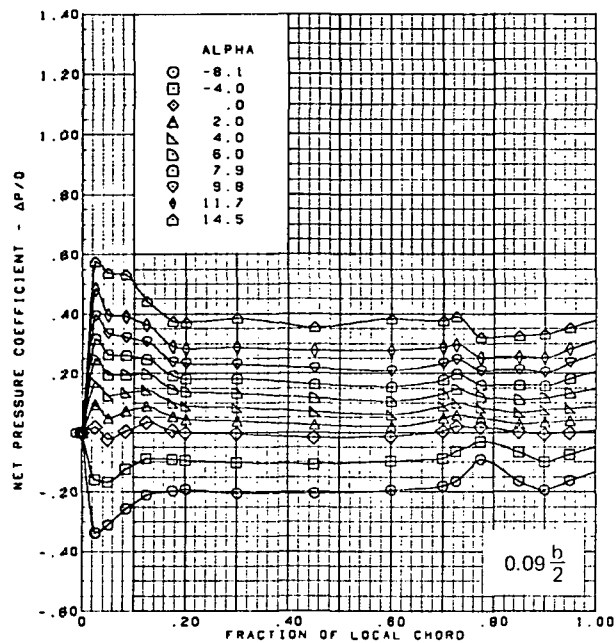
Figure 11.—(Continued)



$M = 1.70$  (run 20)  
 Flat wing, rounded L.E.  
 L.E. deflection, full span =  $0.0^\circ$   
 T.E. deflection, full span =  $0.0^\circ$   
 Note:  $C_{p, \text{vacuum}} = -0.49$

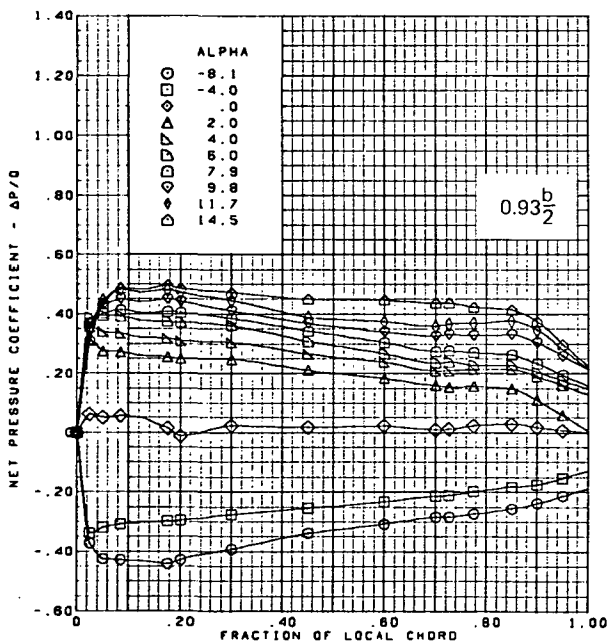
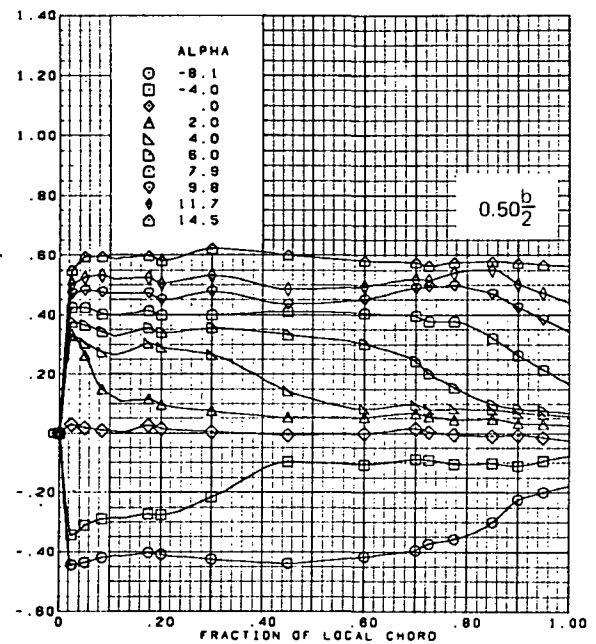
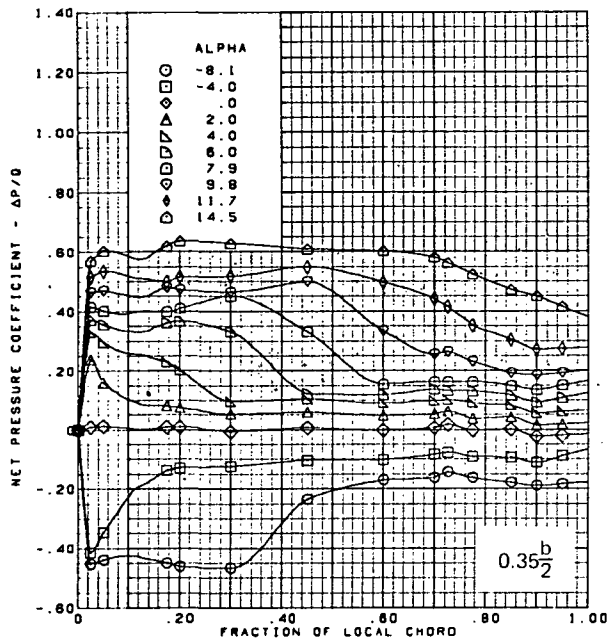
(d) (Concluded)

Figure 11.—(Continued)



(e) Net Chordwise Pressure Distributions

Figure 11.—(Continued)

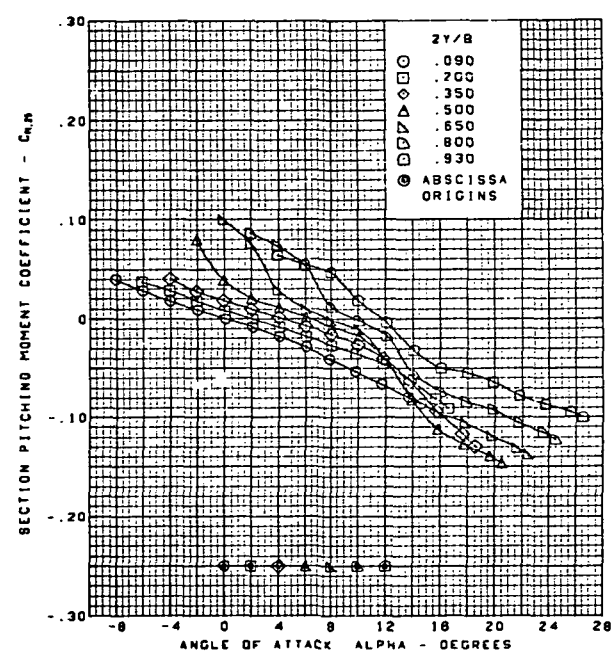
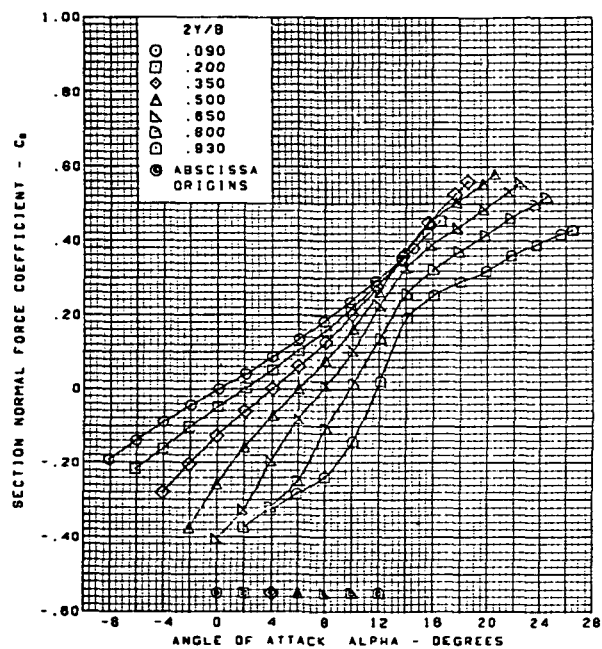
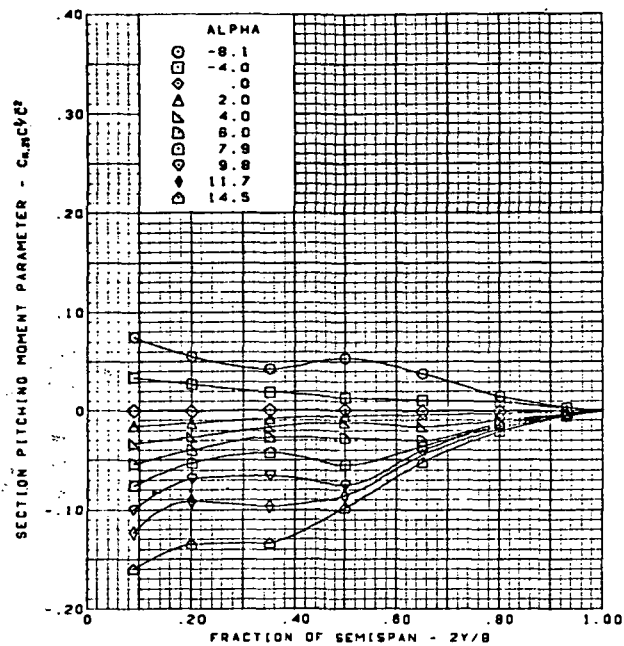
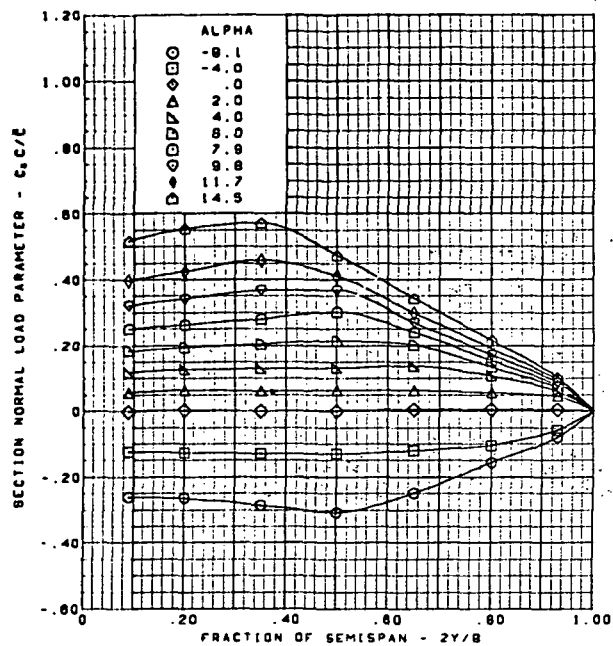


$M = 1.70$  (run 20)  
 Flat wing, rounded L.E.  
 L.E. deflection, full span =  $0.0^\circ$   
 T.E. deflection, full span =  $0.0^\circ$

(e) (Concluded)

Figure 11.—(Continued)

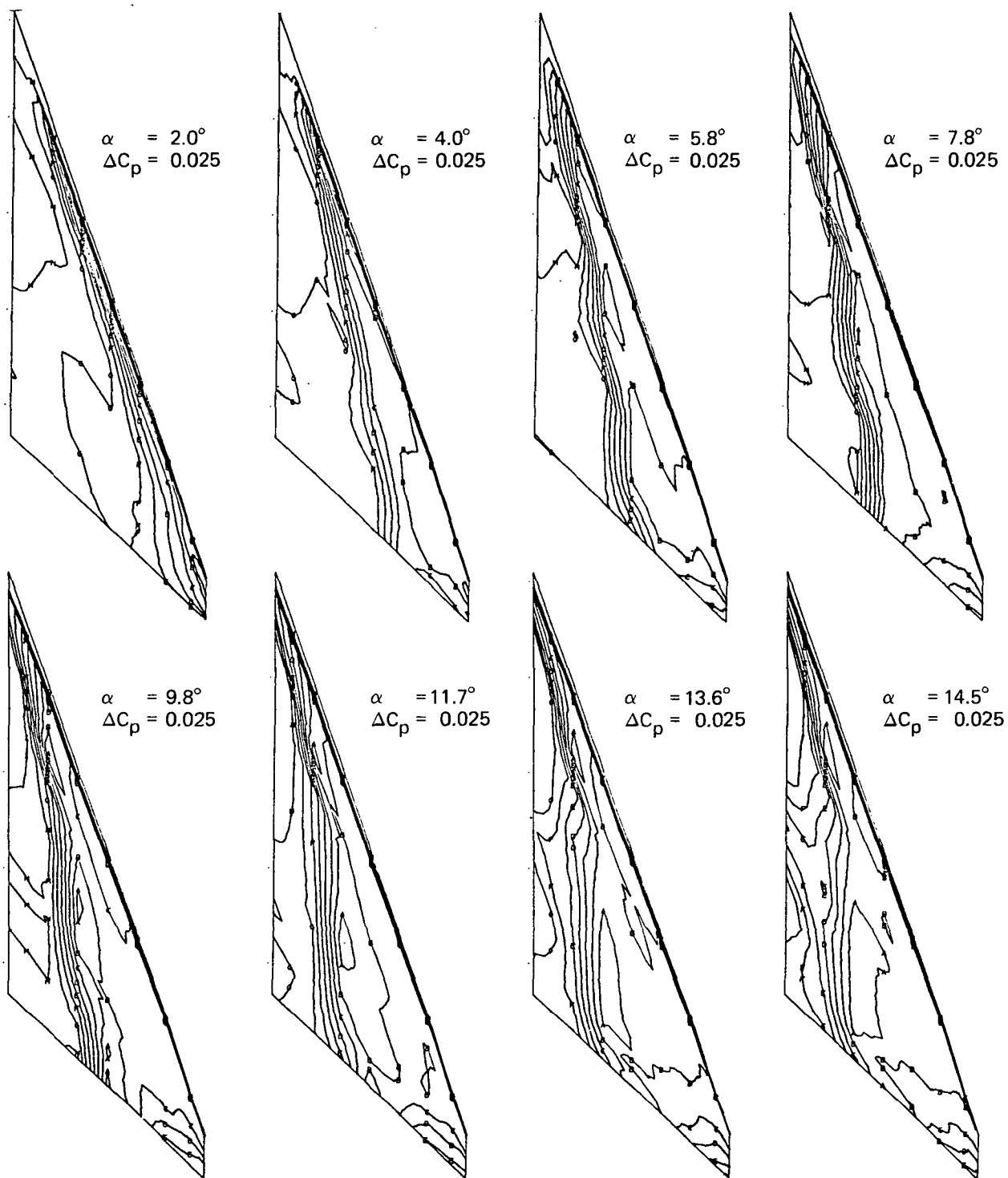
**Page  
Intentionally  
Left Blank**



$M = 1.70$  (run 20)  
 Flat wing, rounded L.E.  
 L.E. deflection, full span =  $0.0^\circ$   
 T.E. deflection, full span =  $0.0^\circ$

(f) Spanload Distributions and Section Aerodynamic Coefficients

Figure 11.—(Concluded)

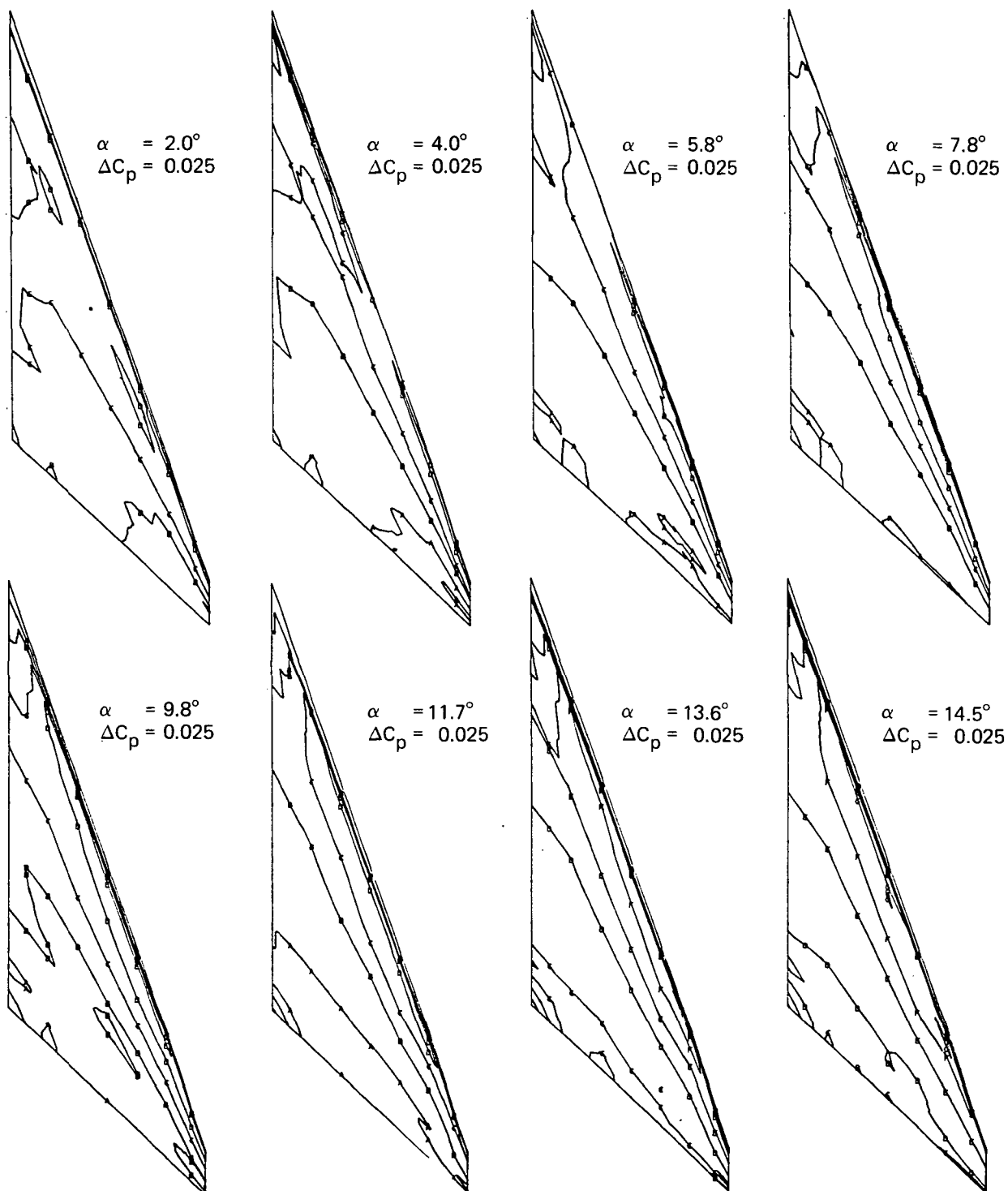


Note:  $\Delta C_p$  = increment between adjacent isobars

(a) Upper Surface Isobars

Figure 12.—Wing Experimental Data—Effect of Angle of Attack; Flat Wing, Rounded L.E.; L.E. Deflection, Full Span = 0.0°; T.E. Deflection, Full Span = 0.0°;  $M = 2.10$

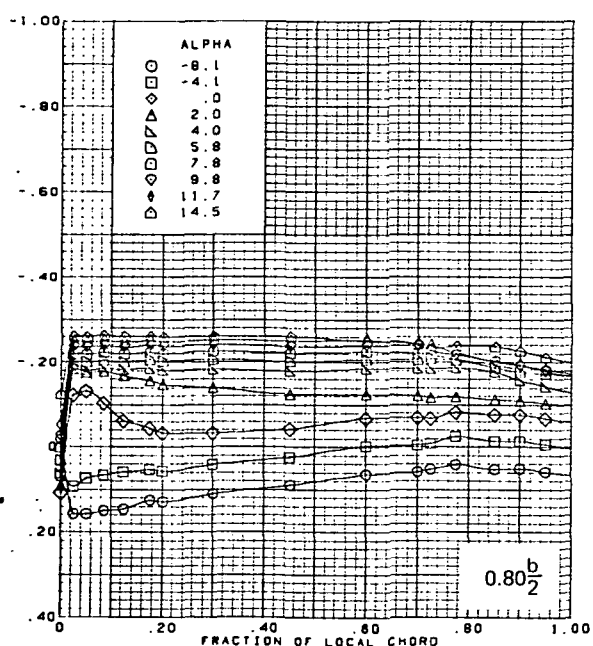
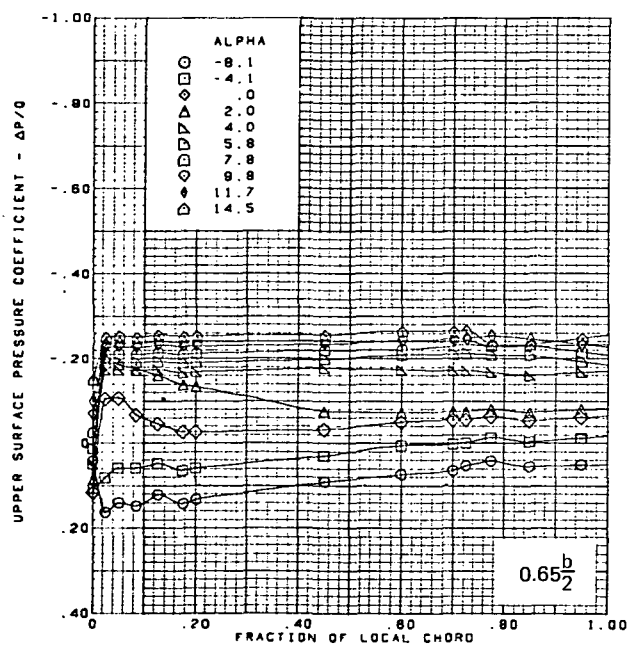
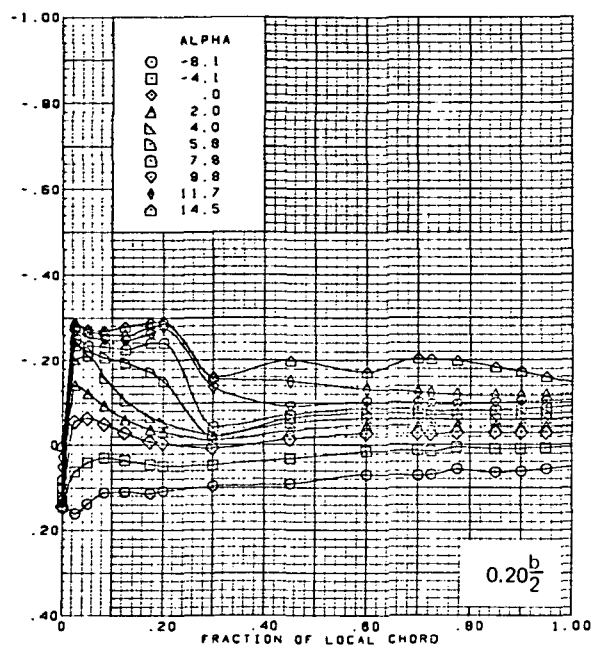
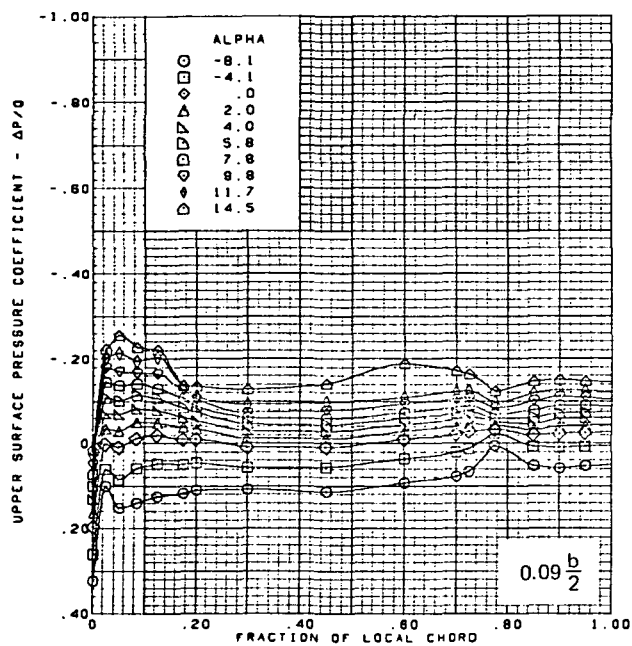




Note:  $\Delta C_p$  = increment between adjacent isobars

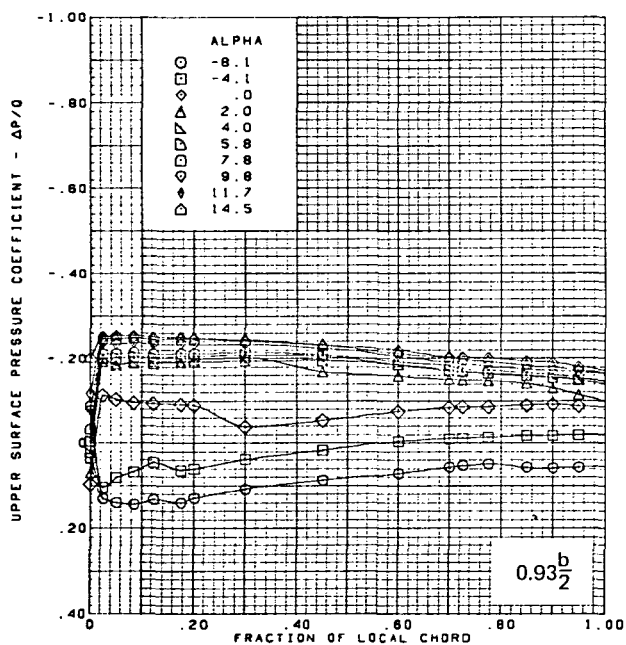
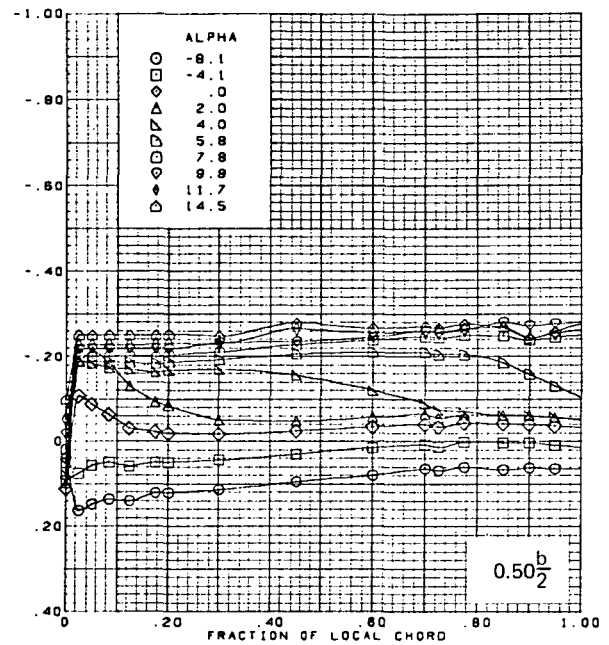
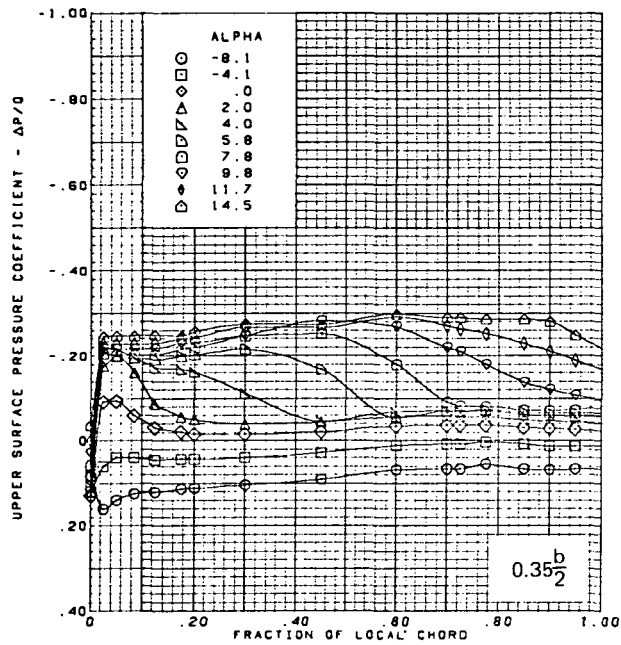
(b) Lower Surface Isobars

Figure 12.—(Continued)



(c) Upper Surface Chordwise Pressure Distributions

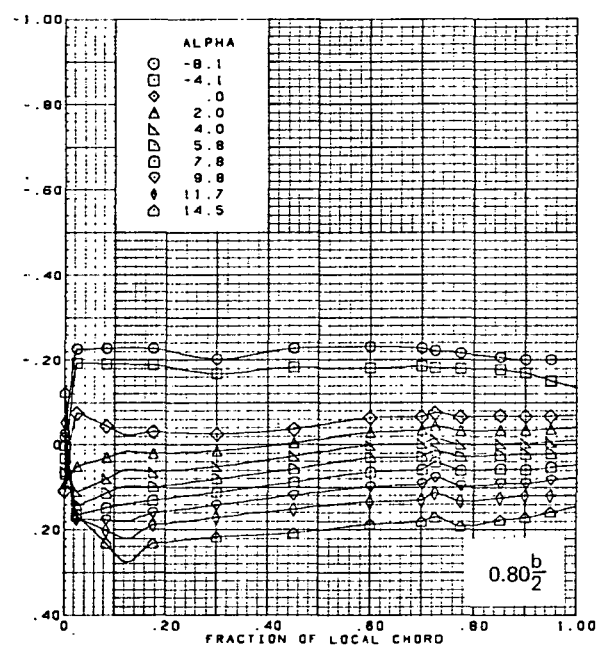
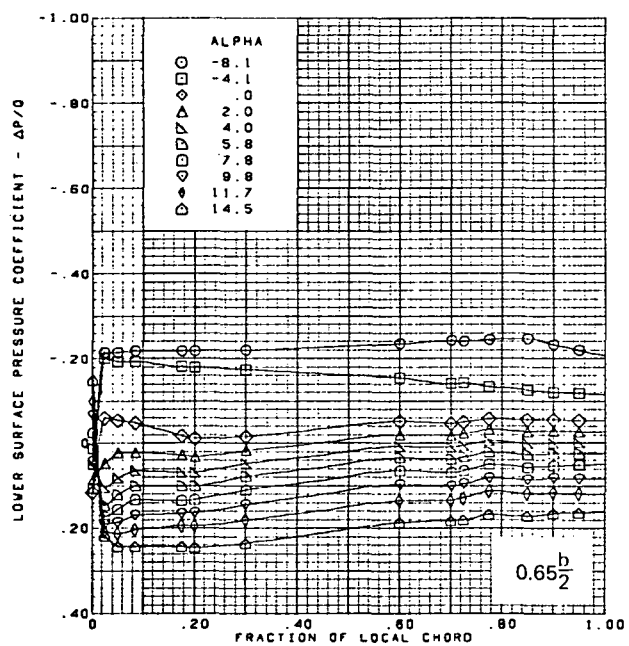
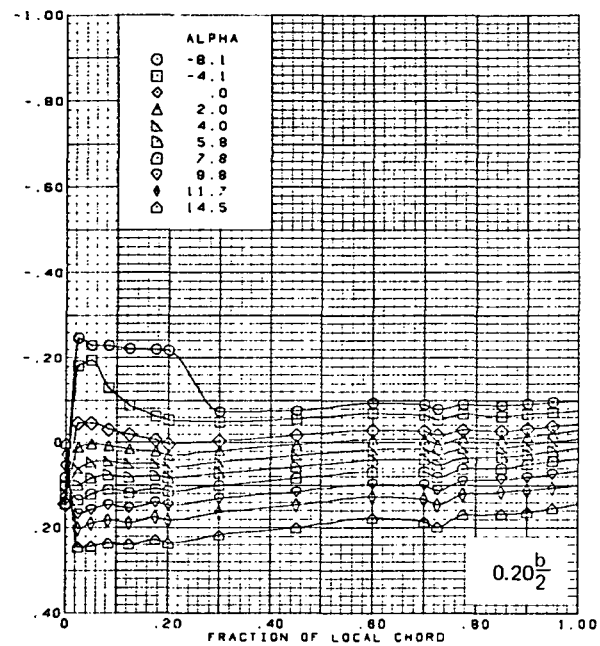
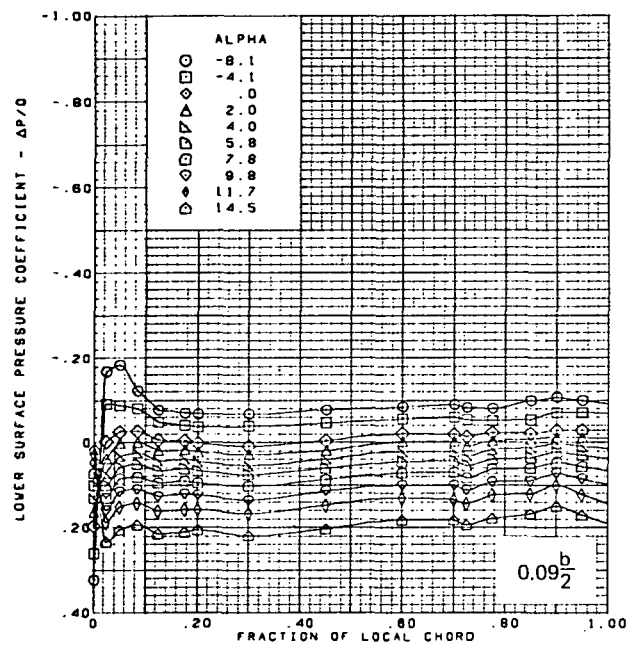
Figure 12.—(Continued)



$M = 2.10$  (run 21)  
 Flat wing, rounded L.E.  
 L.E. deflection, full span =  $0.0^\circ$   
 T.E. deflection, full span =  $0.0^\circ$   
 Note:  $C_{p, \text{vacuum}} = -0.32$

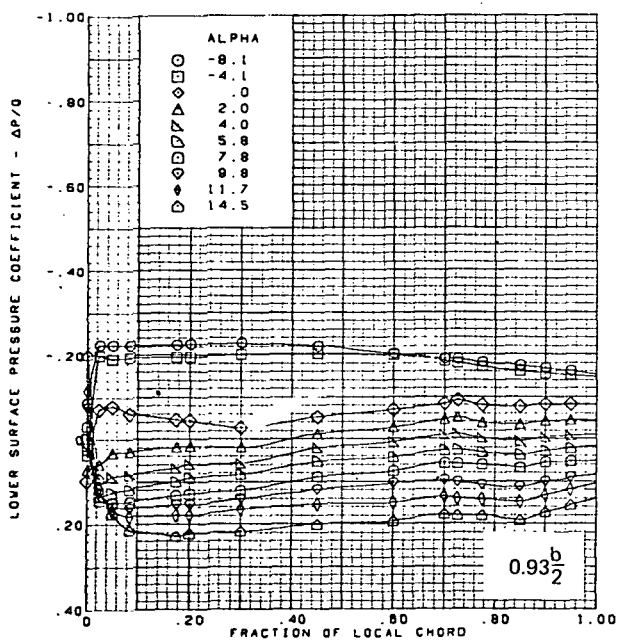
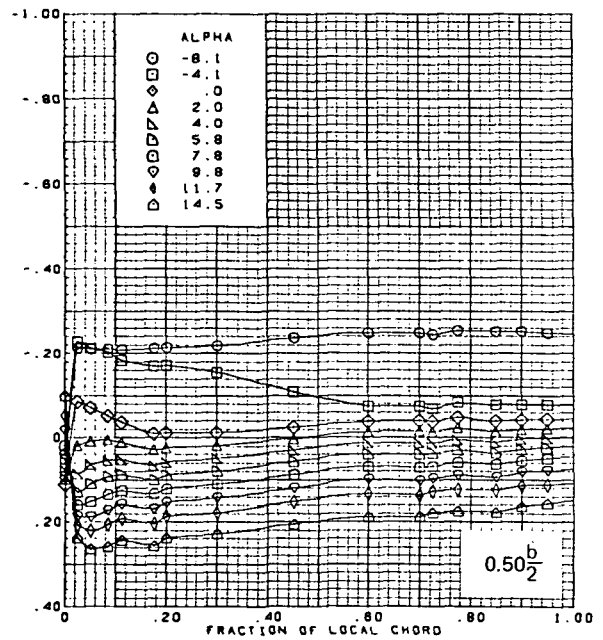
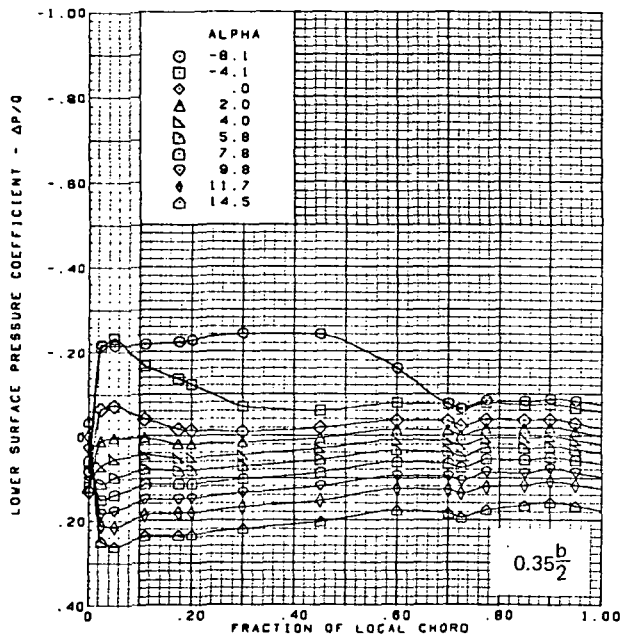
(c)(Concluded)

Figure 12.—(Continued)



(d) Lower Surface Chordwise Pressure Distributions

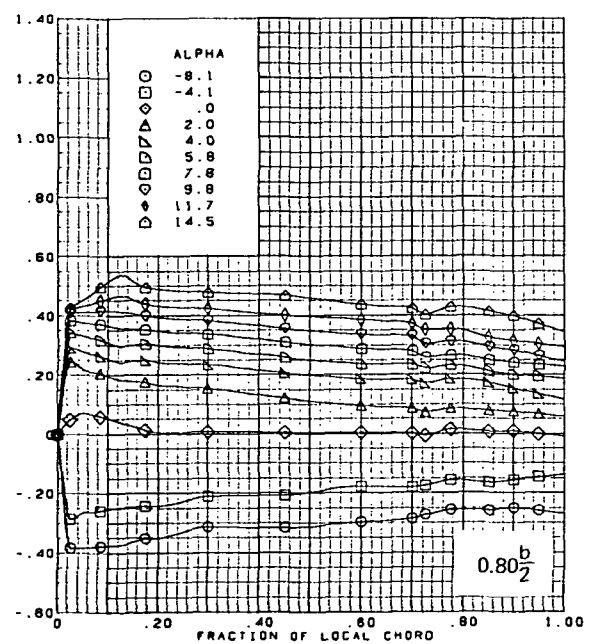
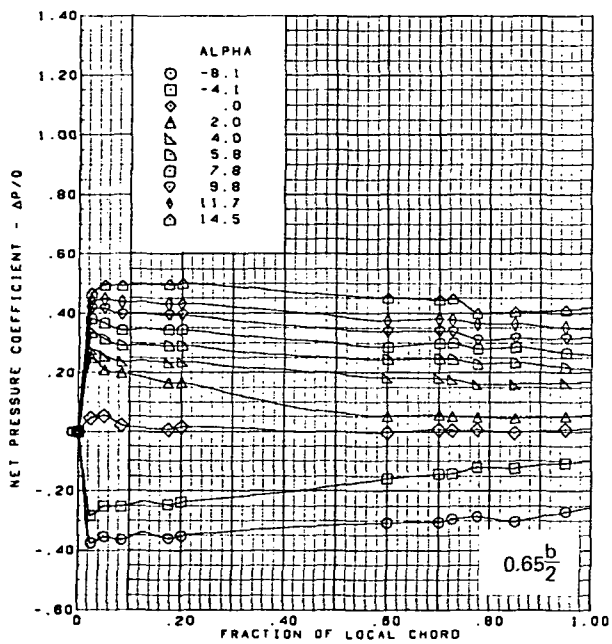
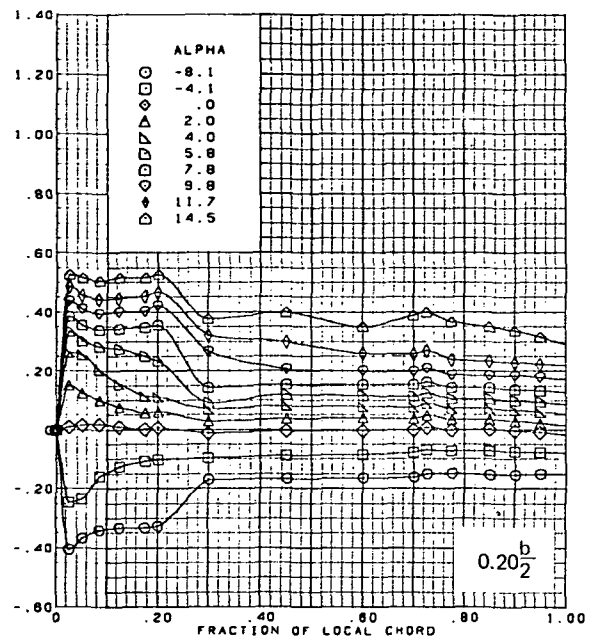
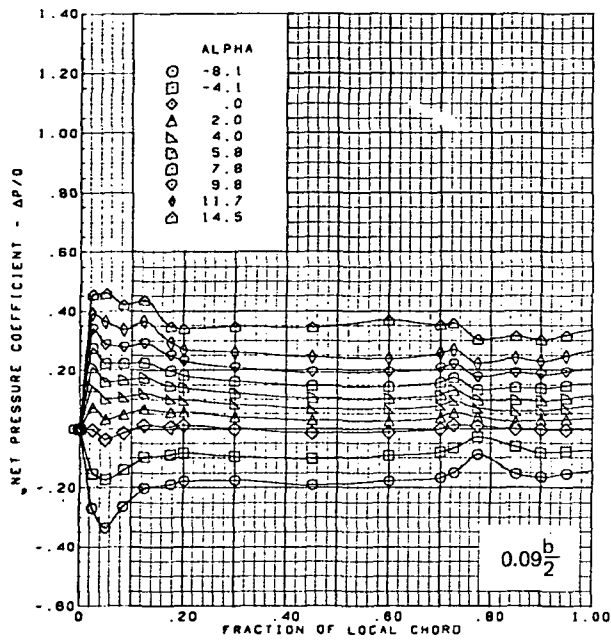
Figure 12.—(Continued)



$M = 2.10$  (run 21)  
 Flat wing, rounded L.E.  
 L.E. deflection, full span =  $0.0^\circ$   
 T.E. deflection, full span =  $0.0^\circ$   
 Note:  $C_{p, \text{vacuum}} = -0.32$

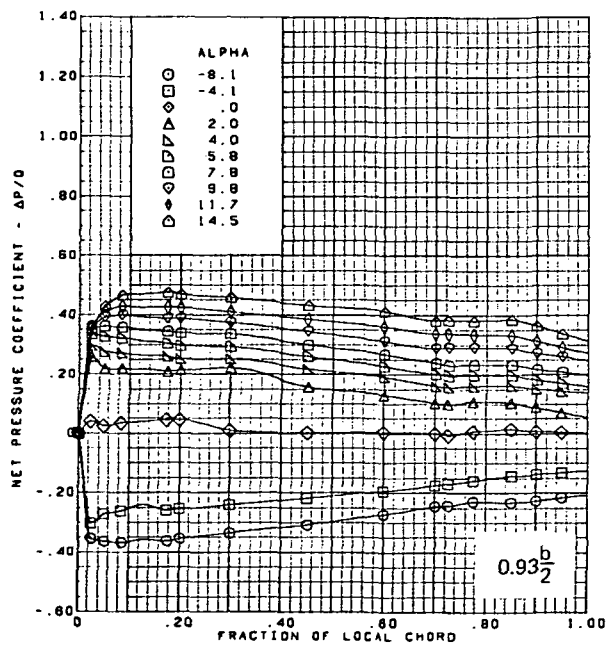
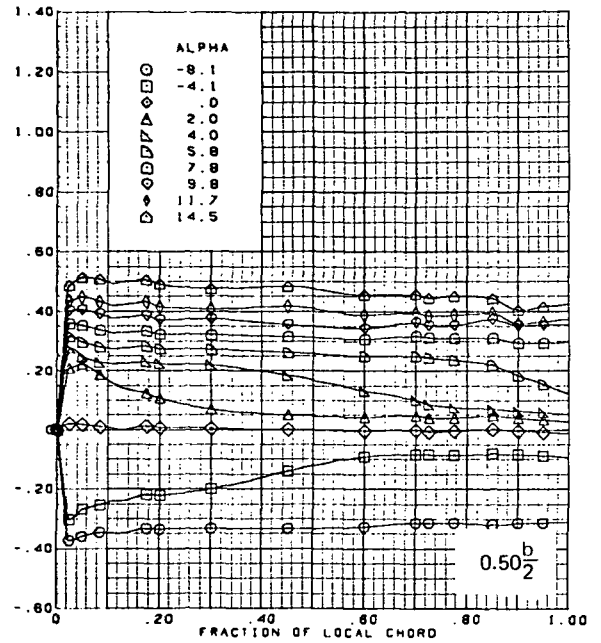
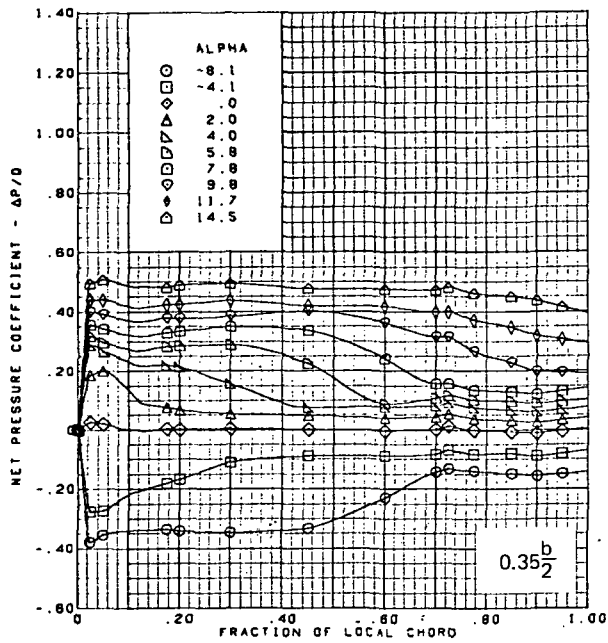
(d) (Concluded)

Figure 12.—(Continued)



(e) Net Chordwise Pressure Distributions

Figure 12.—(Continued)



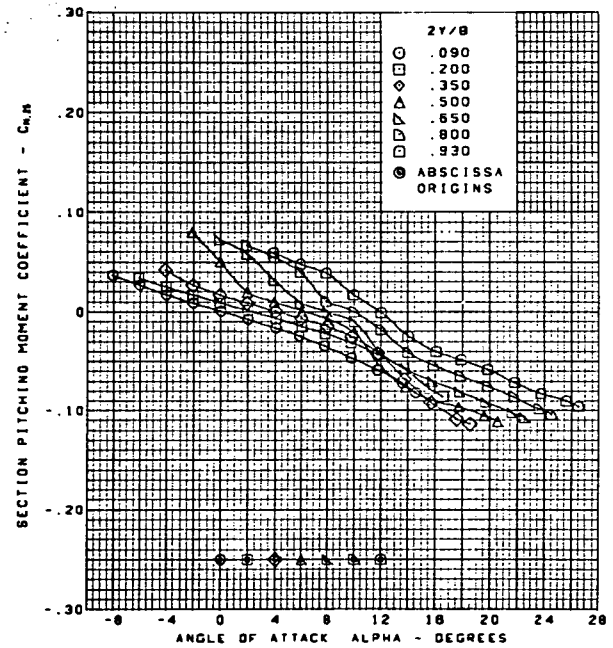
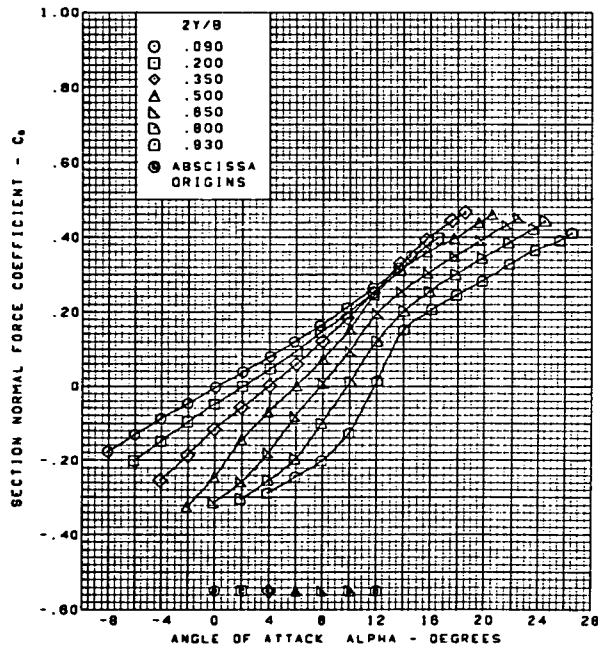
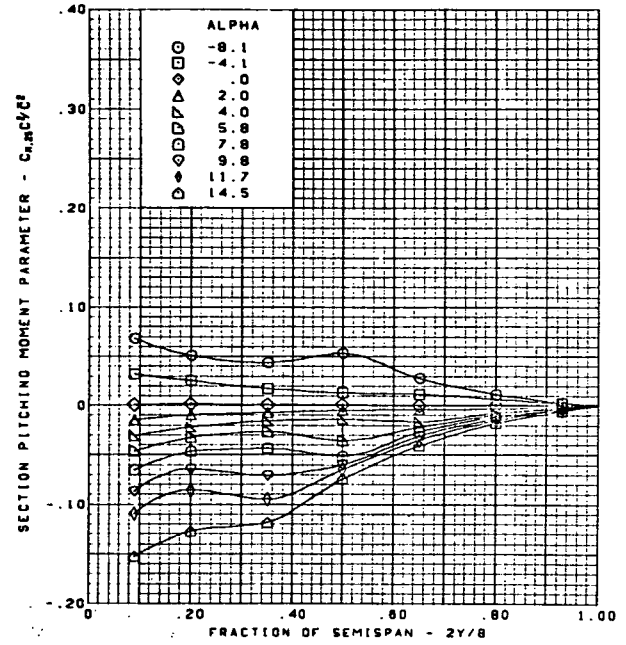
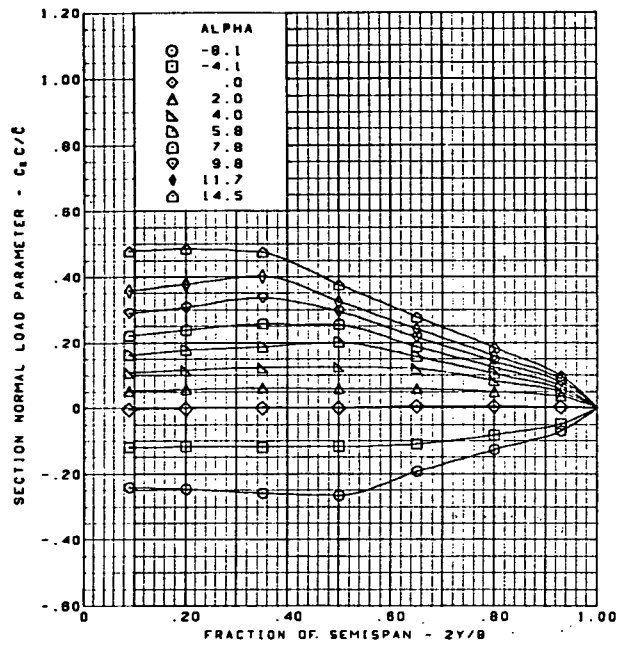
$M = 2.10$  (run 21)  
 Flat wing, rounded L.E.  
 L.E. deflection, full span =  $0.0^\circ$   
 T.E. deflection, full span =  $0.0^\circ$

(e) (Concluded)

Figure 12.—(Continued)

**Page  
Intentionally  
Left Blank**

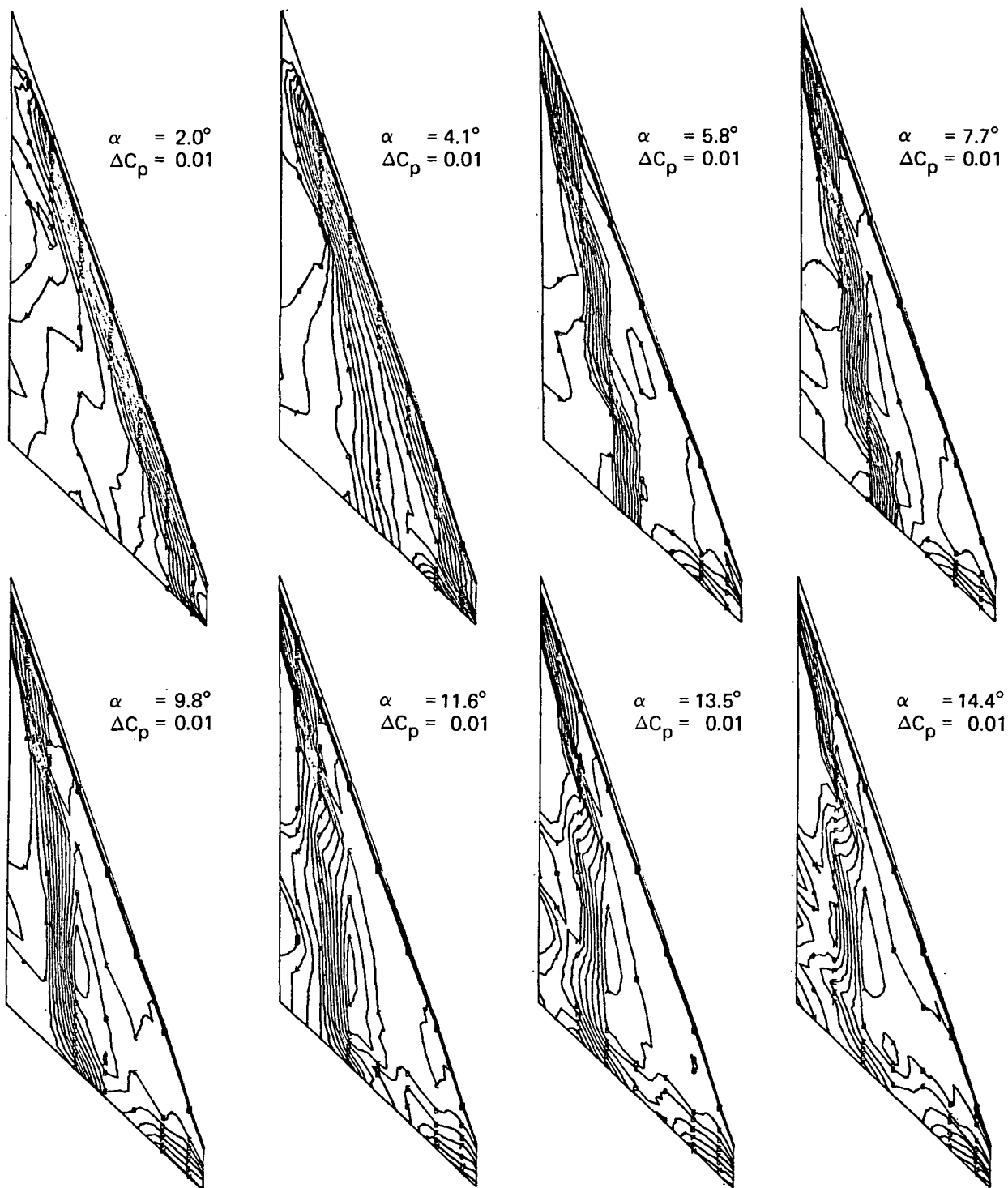




$M = 2.10$  (run 21)  
 Flat wing, rounded L.E.  
 L.E. deflection, full span =  $0.0^\circ$   
 T.E. deflection, full span =  $0.0^\circ$

(f) Spanload Distributions and Section Aerodynamic Coefficients

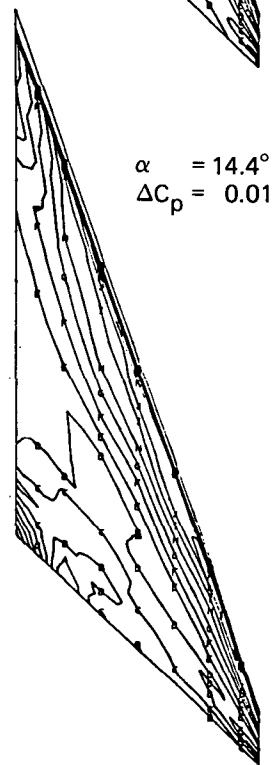
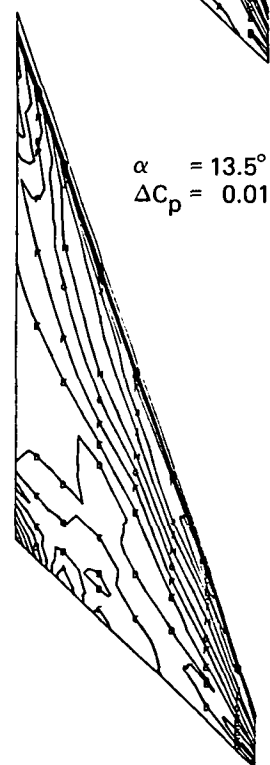
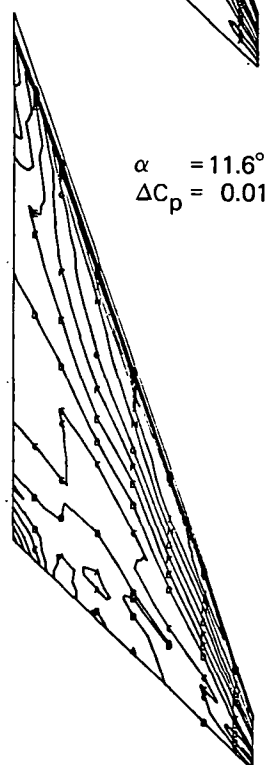
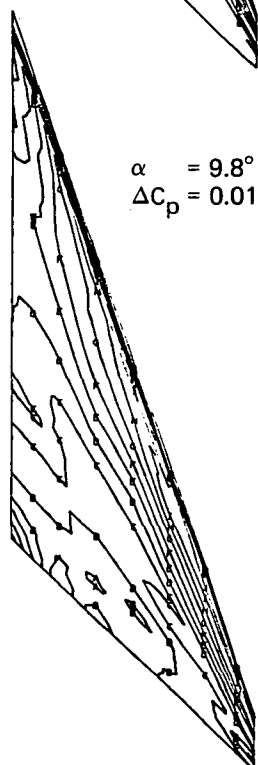
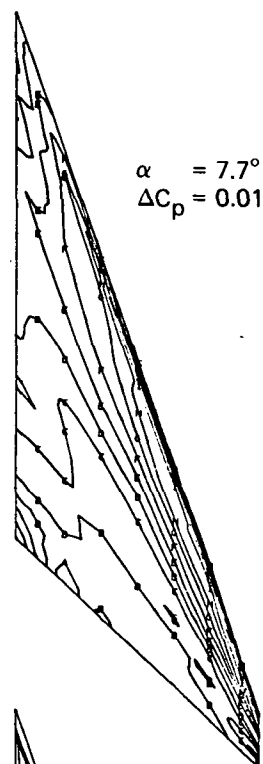
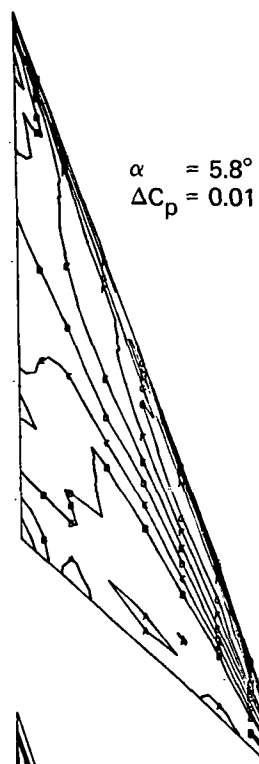
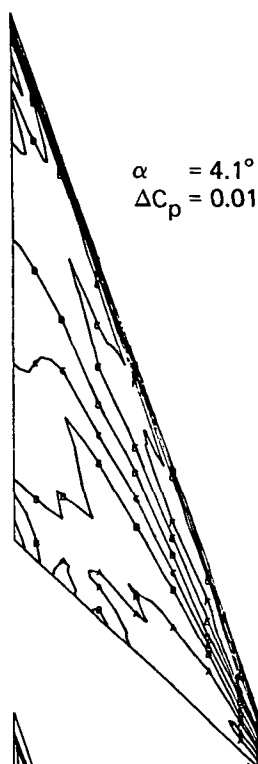
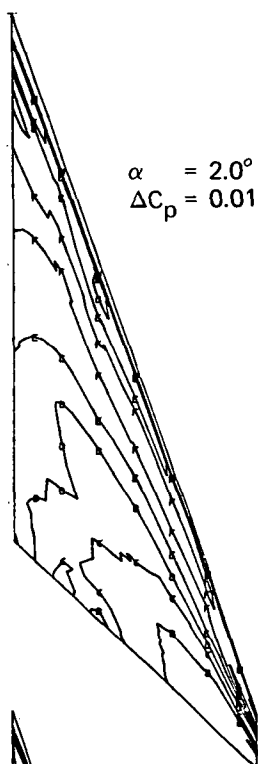
Figure 12.—(Concluded)



Note:  $\Delta C_p$  = increment between adjacent isobars

(a) Upper Surface Isobars

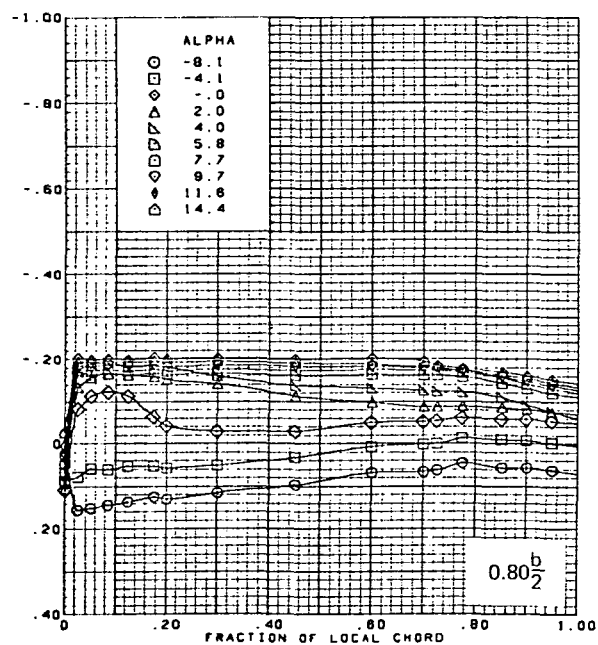
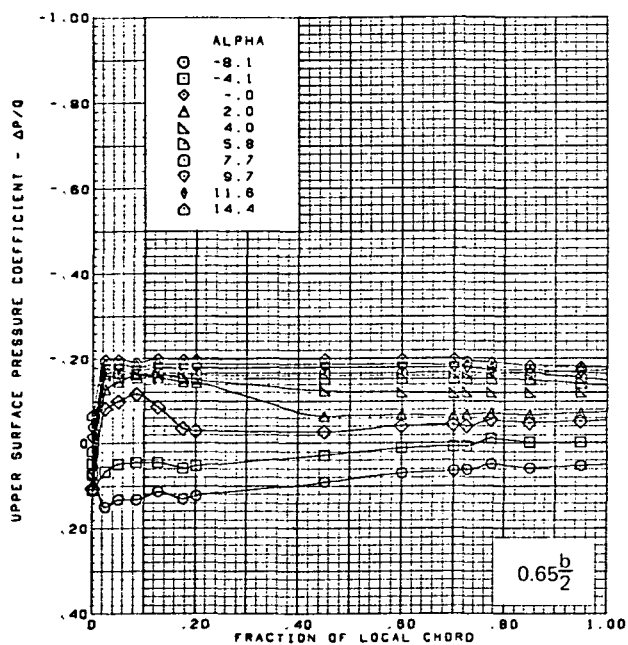
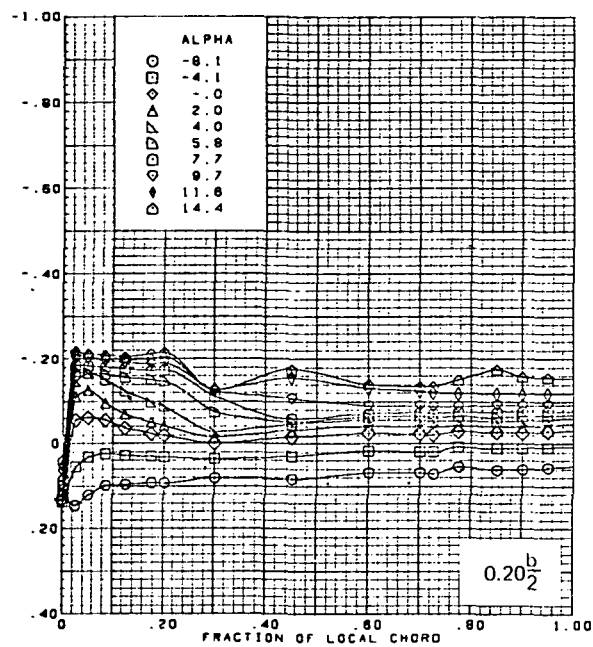
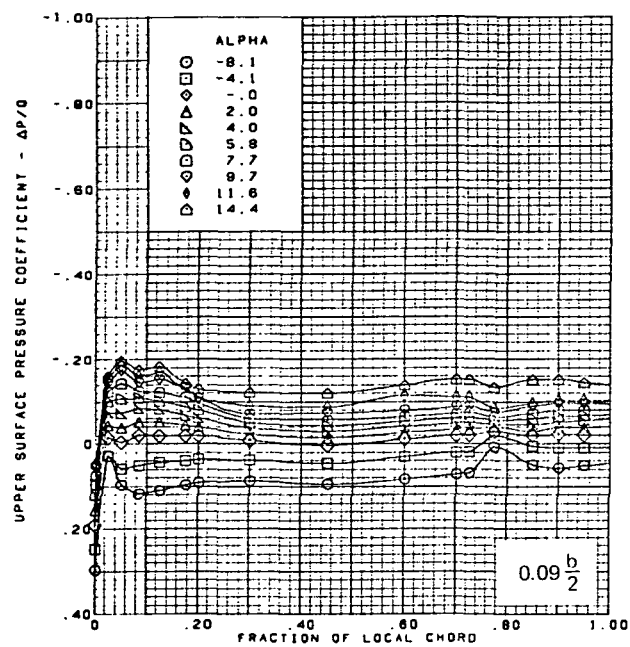
Figure 13.—Wing Experimental Data—Effect of Angle of Attack; Flat Wing, Rounded L.E.; L.E. Deflection, Full Span =  $0.0^\circ$ ; T.E. Deflection, Full Span =  $0.0^\circ$ ;  $M = 2.50$



Note:  $\Delta C_p$  = increment between adjacent isobars

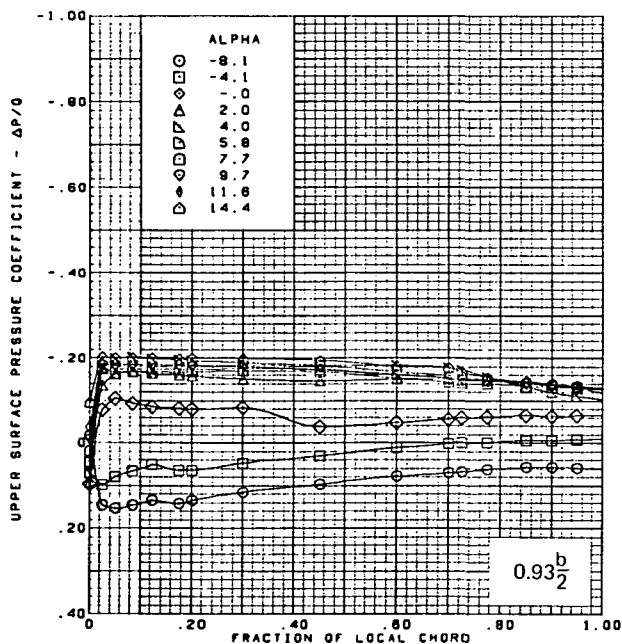
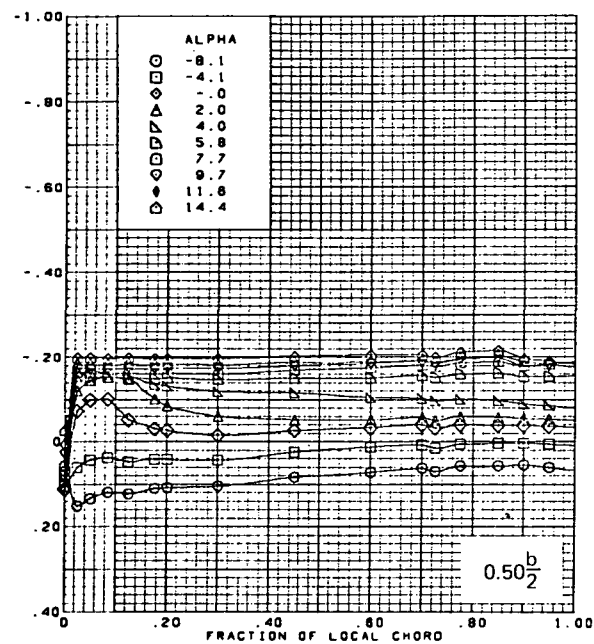
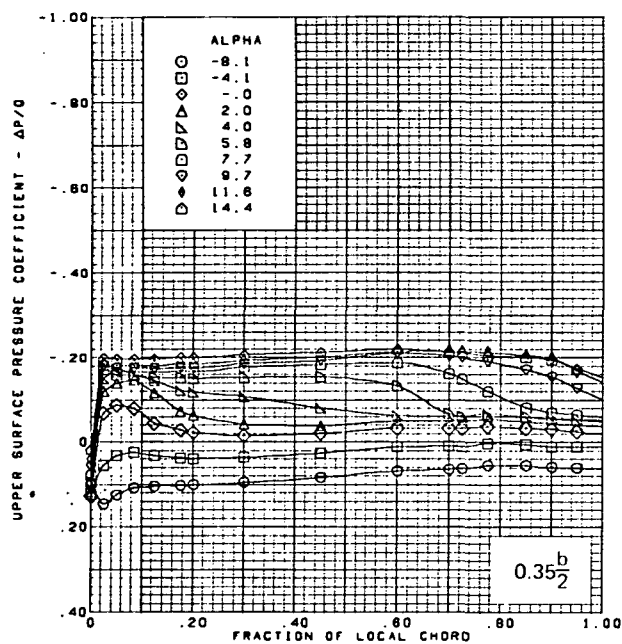
(b) Lower Surface Isobars

Figure 13.—(Continued)



(c) Upper Surface Chordwise Pressure Distributions

Figure 13.—(Continued)

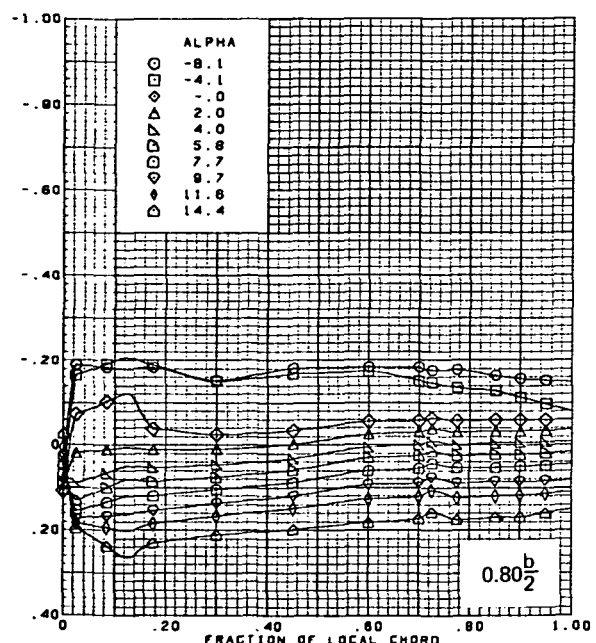
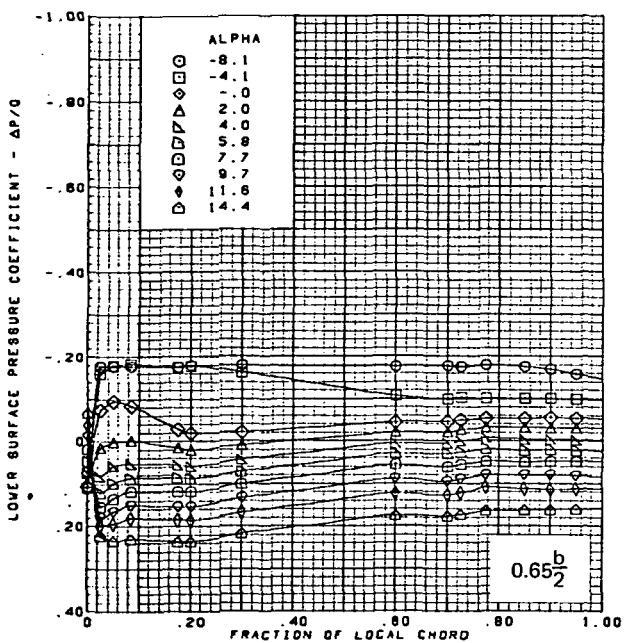
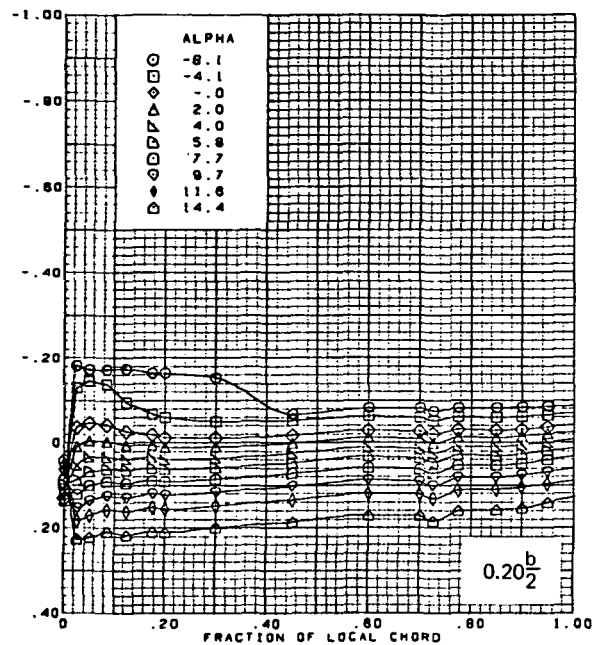
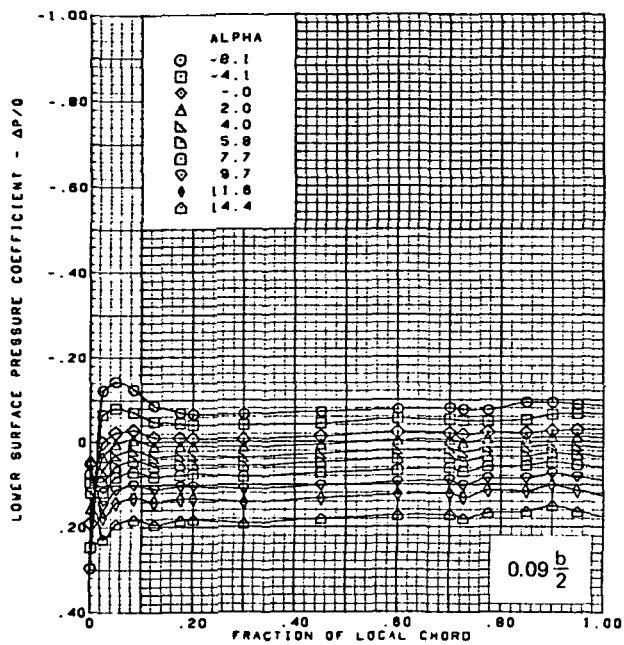


M = 2.50 (run 22)  
 Flat wing, rounded L.E.  
 L.E. deflection, full span =  $0.0^\circ$   
 T.E. deflection, full span =  $0.0^\circ$

Note:  $C_{p, \text{vacuum}} = -0.23$

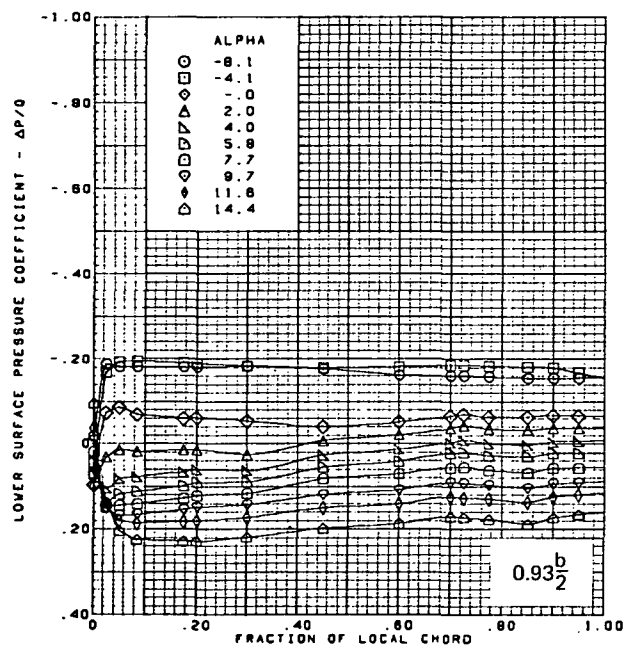
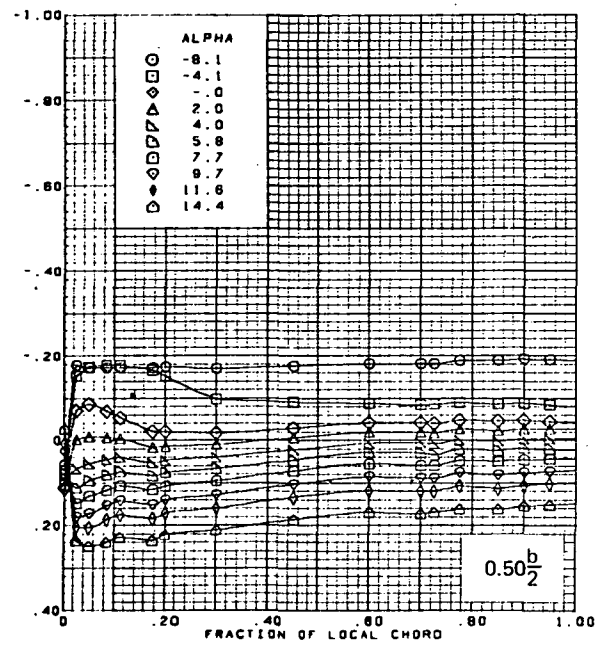
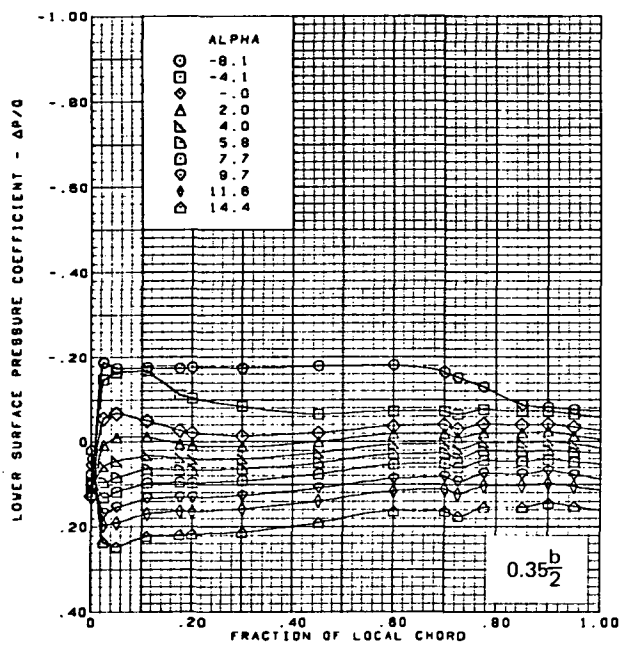
(c) (Concluded)

Figure 13.—(Continued)



(d) Lower Surface Chordwise Pressure Distributions

Figure 13.—(Continued)

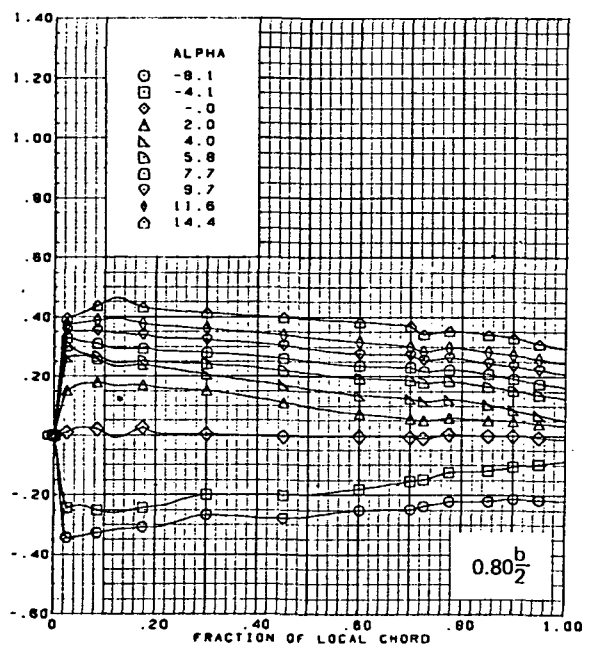
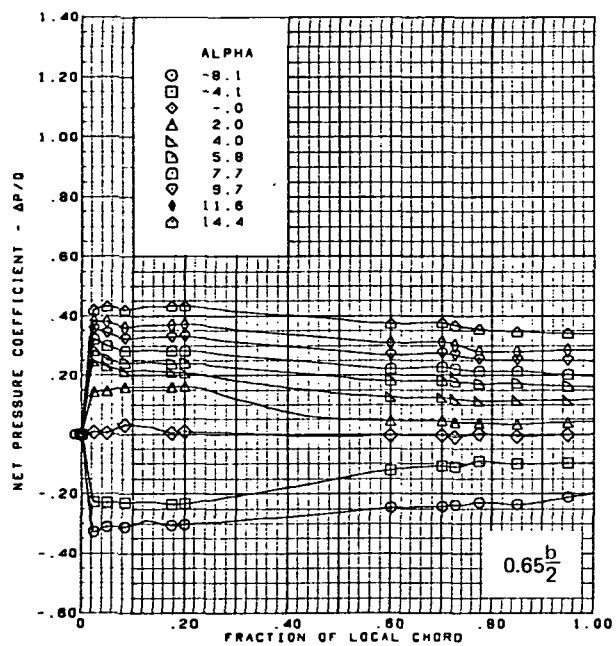
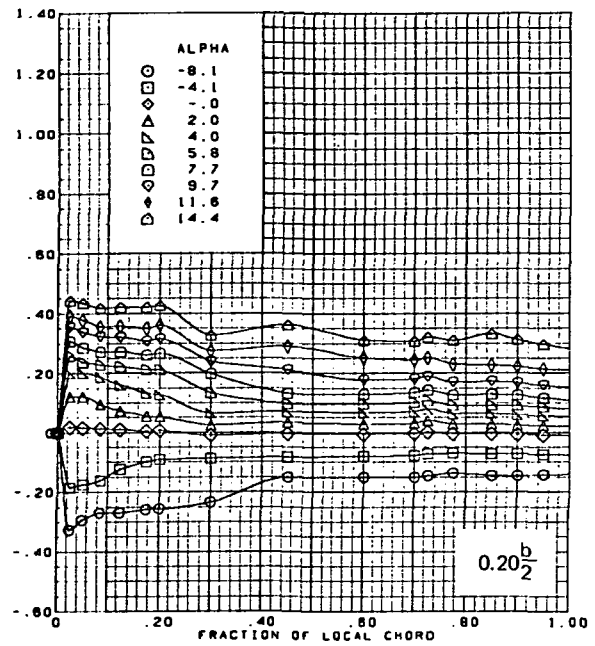
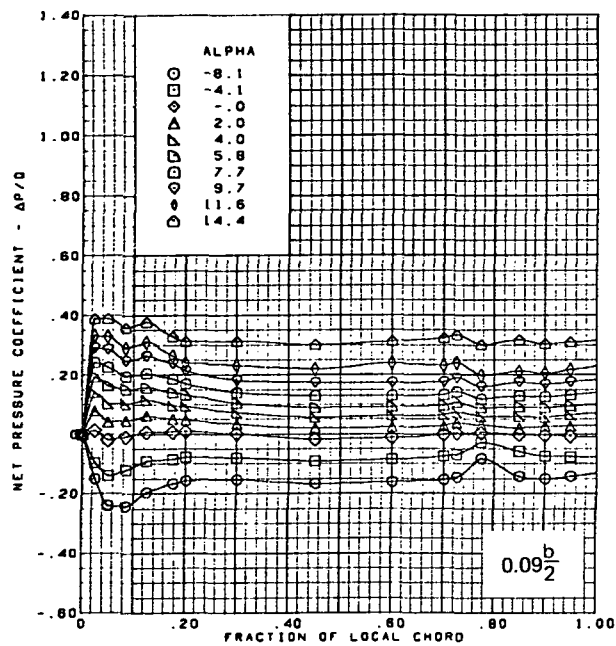


M = 2.50 (run 22)  
 Flat wing, rounded L.E.  
 L.E. deflection, full span =  $0.0^\circ$   
 T.E. deflection, full span =  $0.0^\circ$

Note:  $C_{p, \text{vacuum}} = -0.23$

(d) (Concluded)

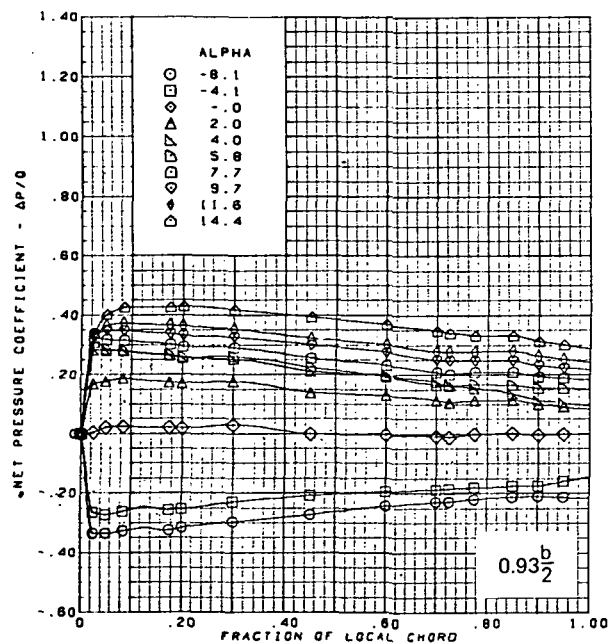
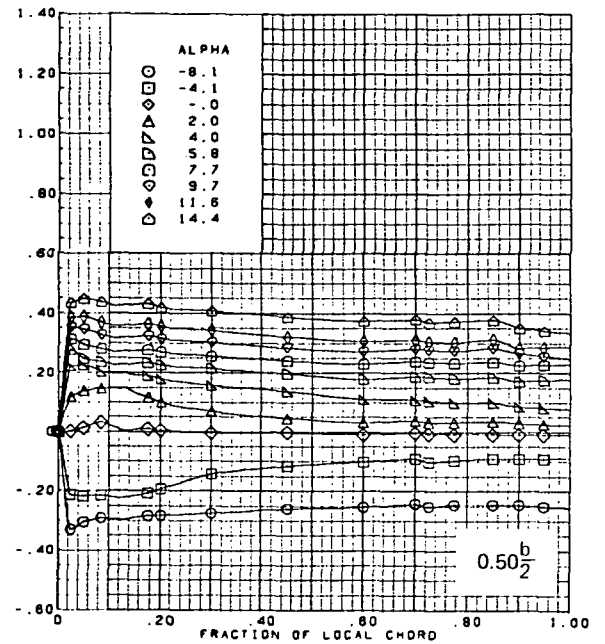
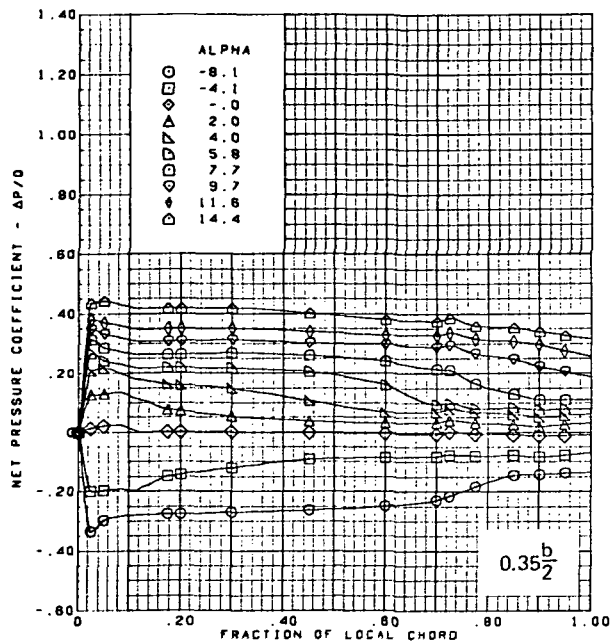
Figure 13.—(Continued)



(e) Net Chordwise Pressure Distributions

Figure 13.—(Continued)



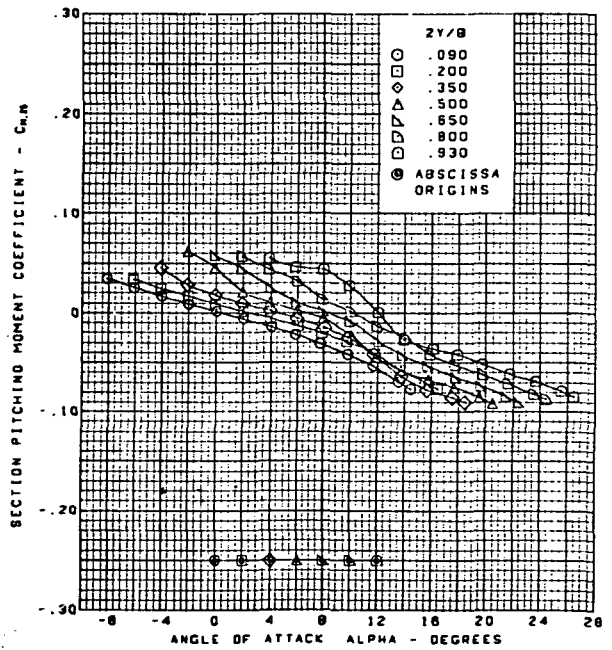
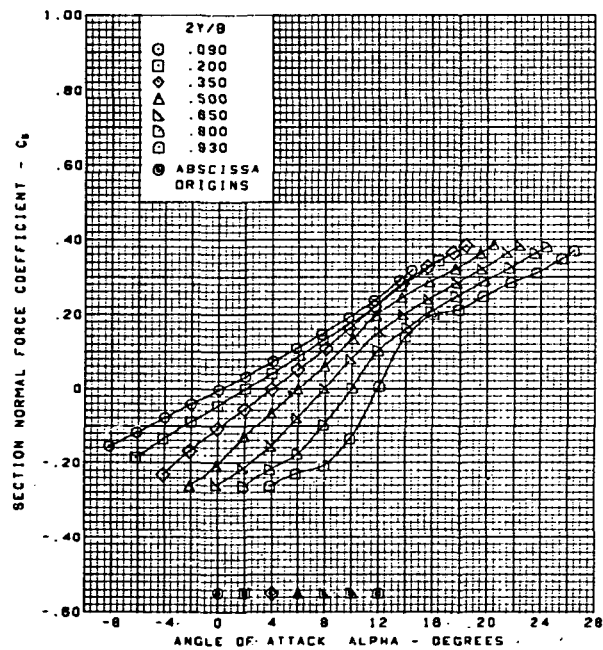
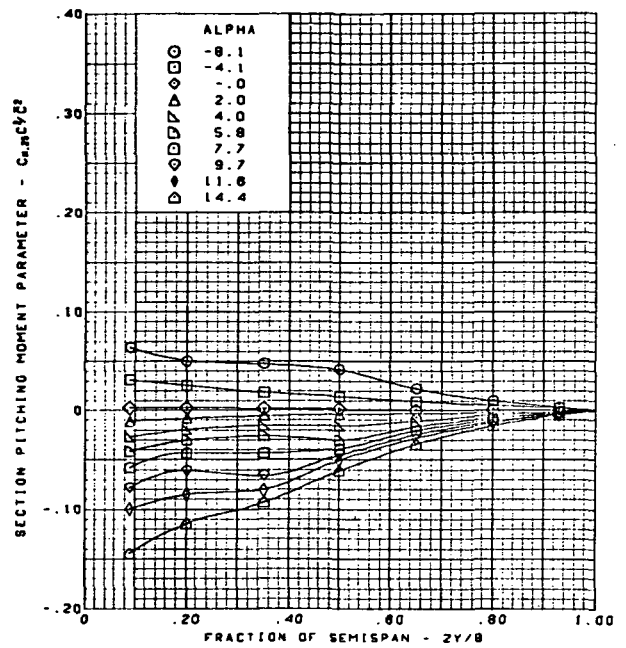
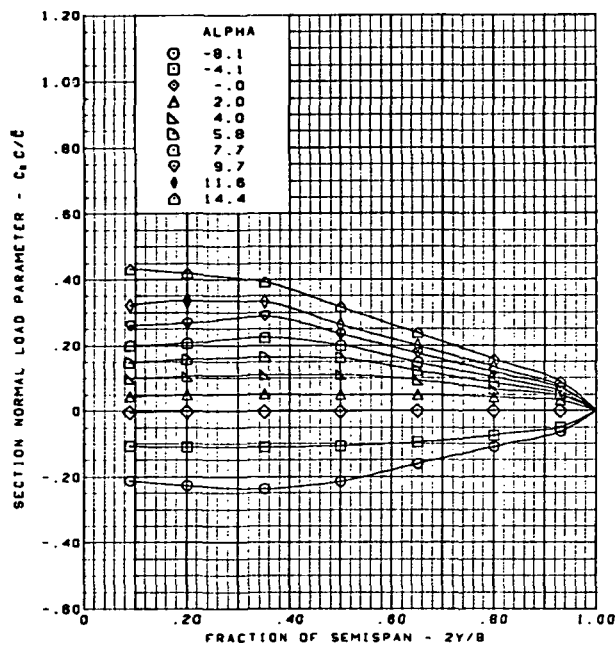


M = 2.50 (run 22)  
 Flat wing, rounded L.E.  
 L.E. deflection, full span =  $0.0^\circ$   
 T.E. deflection, full span =  $0.0^\circ$

(e) (Concluded)

Figure 13.—(Continued)

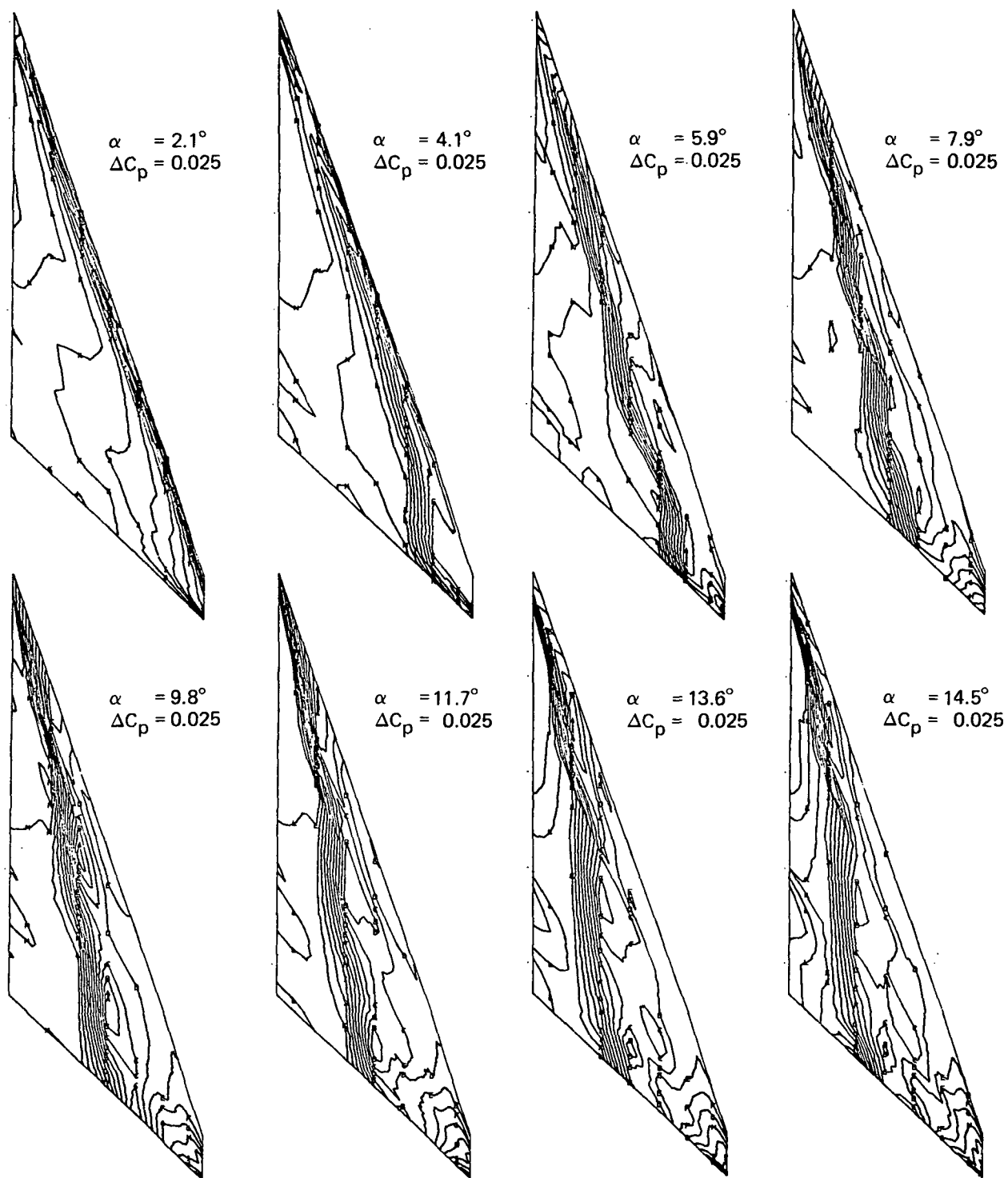
**Page  
Intentionally  
Left Blank**



$M = 2.50$  (run 22)  
 Flat wing, rounded L.E.  
 L.E. deflection, full span =  $0.0^\circ$   
 T.E. deflection, full span =  $0.0^\circ$

(f) Spanload Distributions and Section Aerodynamic Coefficients

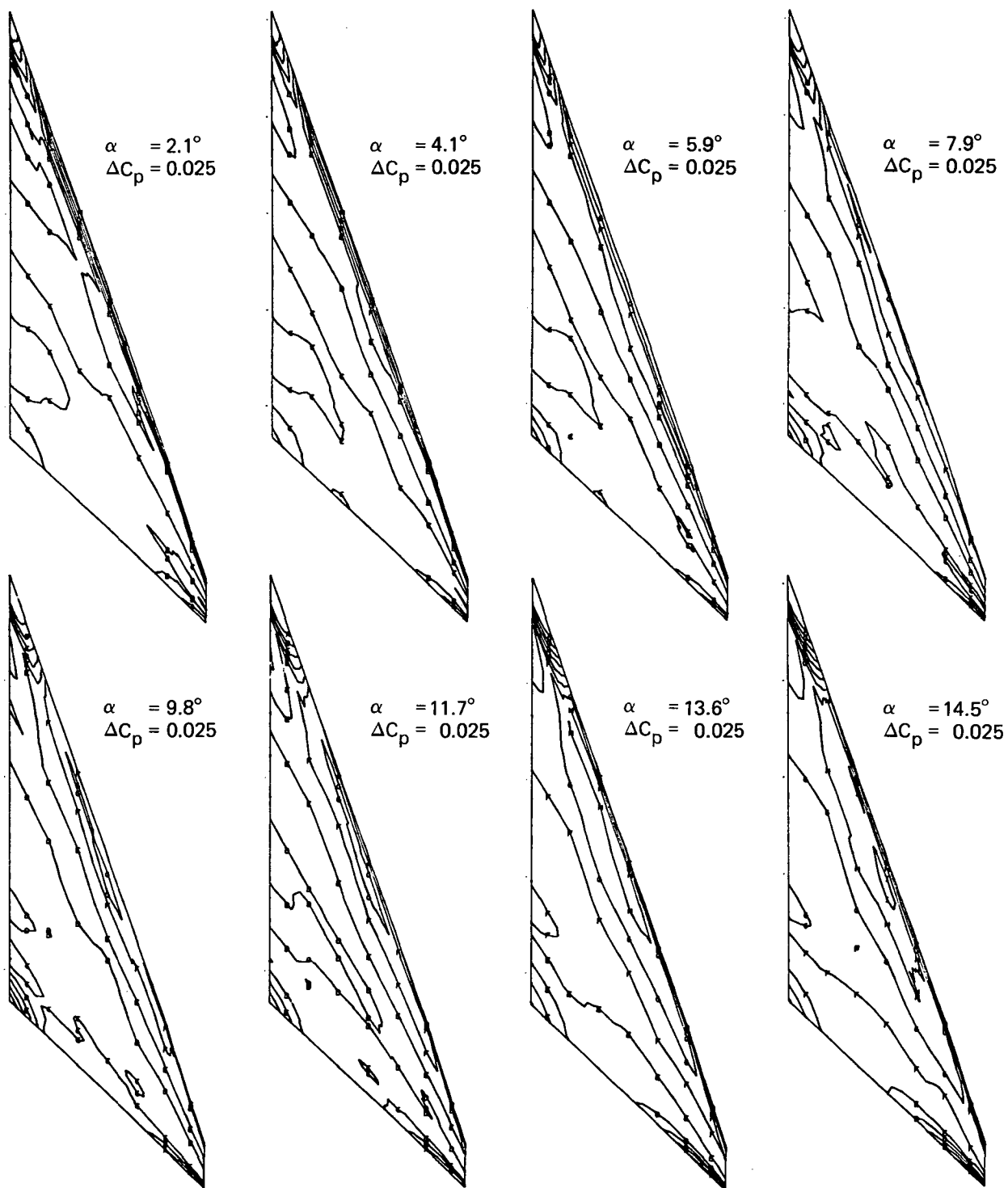
Figure 13.—(Concluded)



Note:  $\Delta C_p$  = increment between adjacent isobars

(a) Upper Surface Isobars

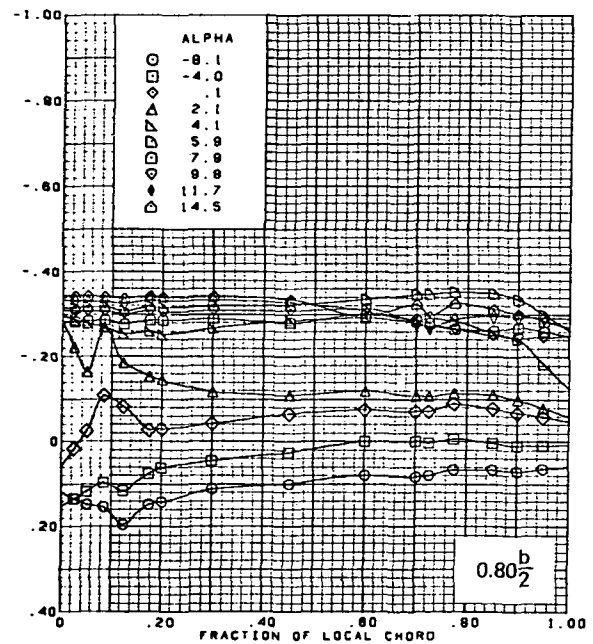
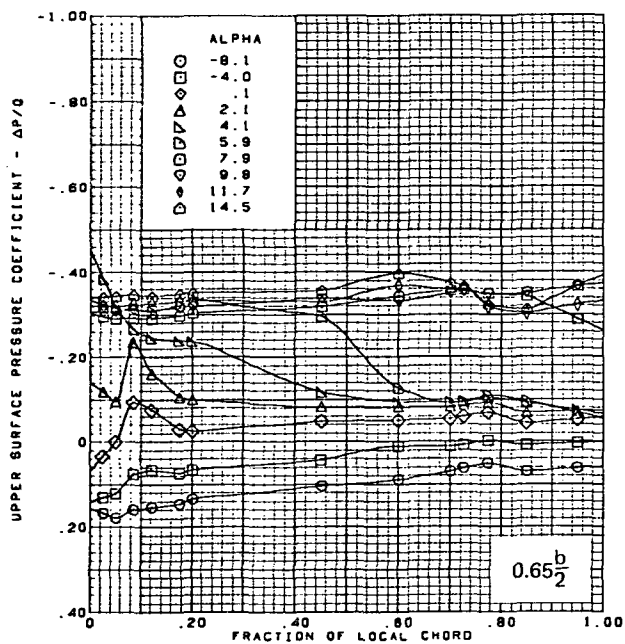
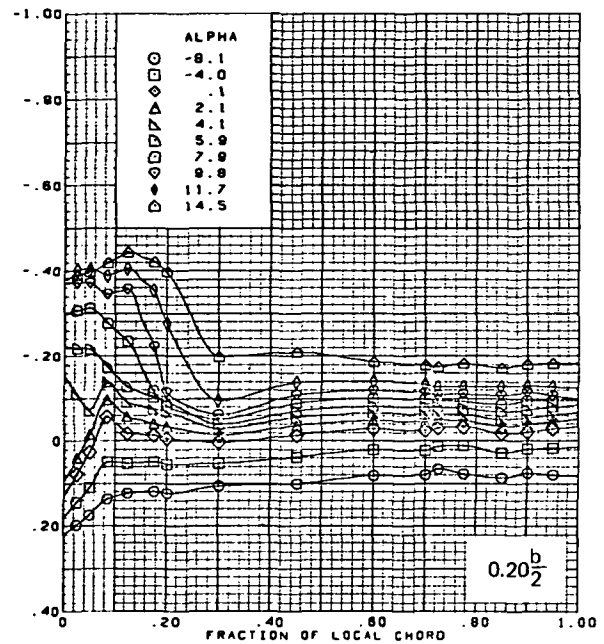
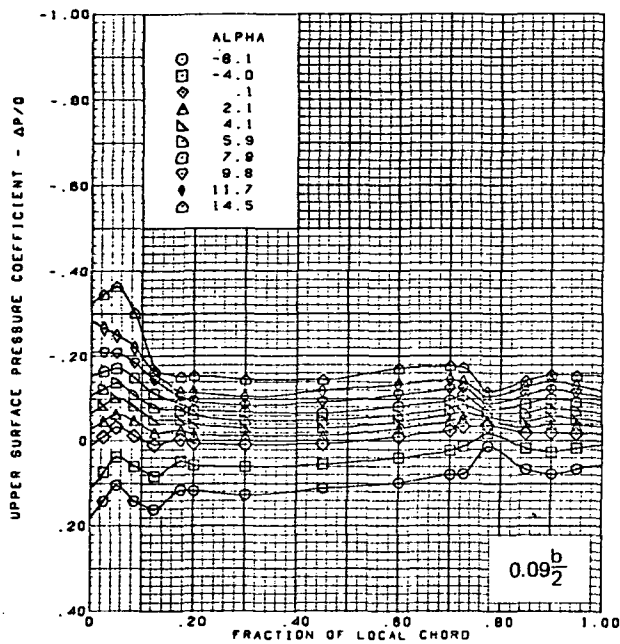
Figure 14.—Wing Experimental Data—Effect of Angle of Attack; Flat Wing, Sharp L.E.; L.E. Deflection, Full Span =  $0.0^\circ$ ; T.E. Deflection, Full Span =  $0.0^\circ$ ;  $M = 1.70$



Note:  $\Delta C_p$  = increment between adjacent isobars

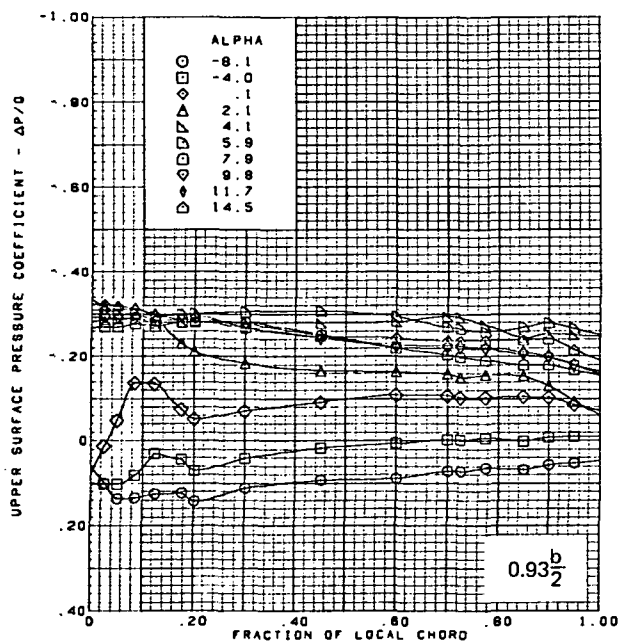
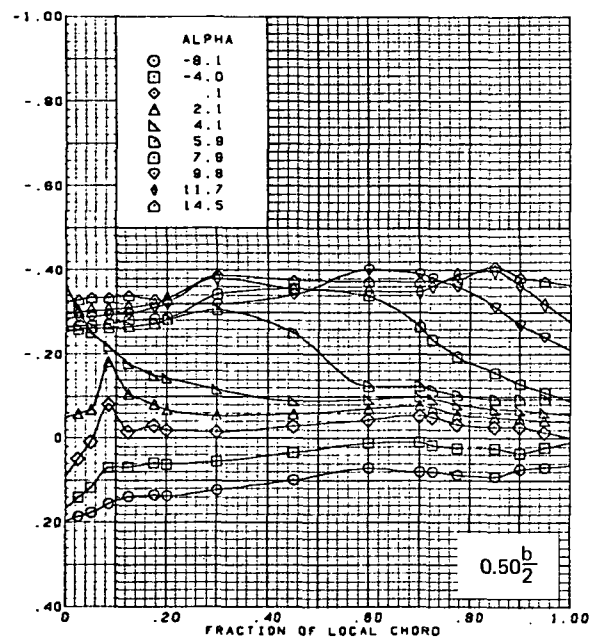
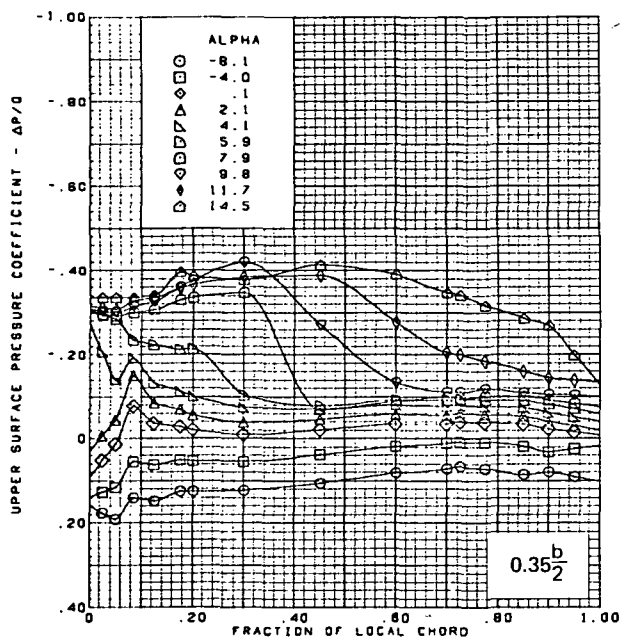
(b) Lower Surface Isobars

Figure 14.—(Continued)



(c) Upper Surface Chordwise Pressure Distributions

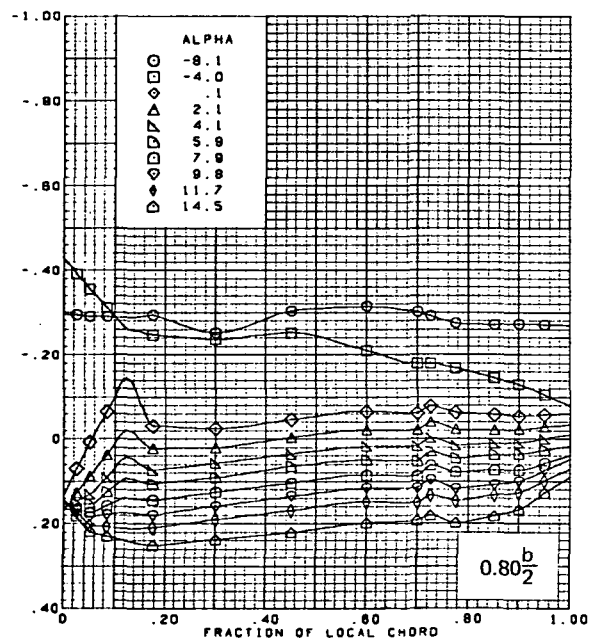
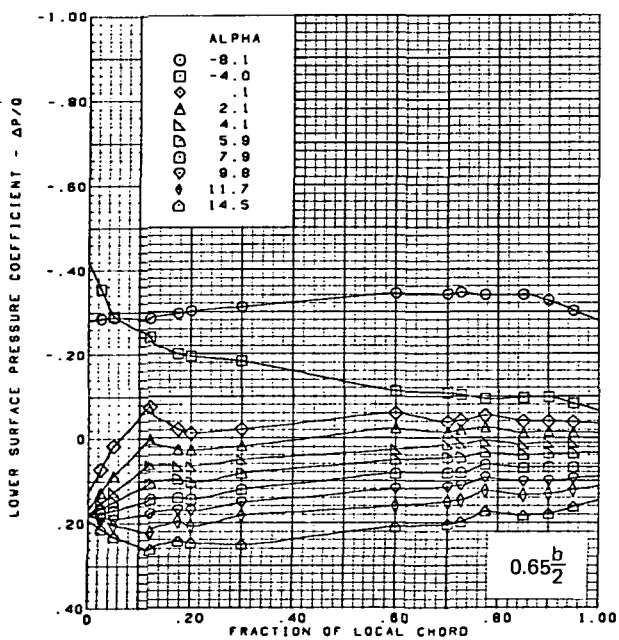
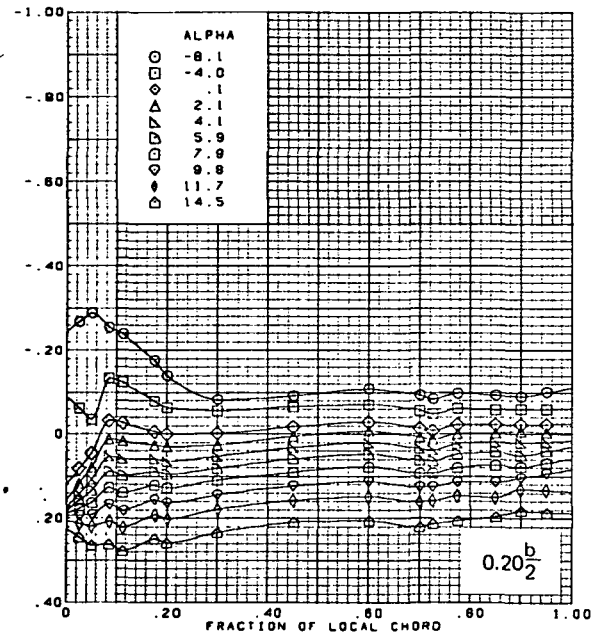
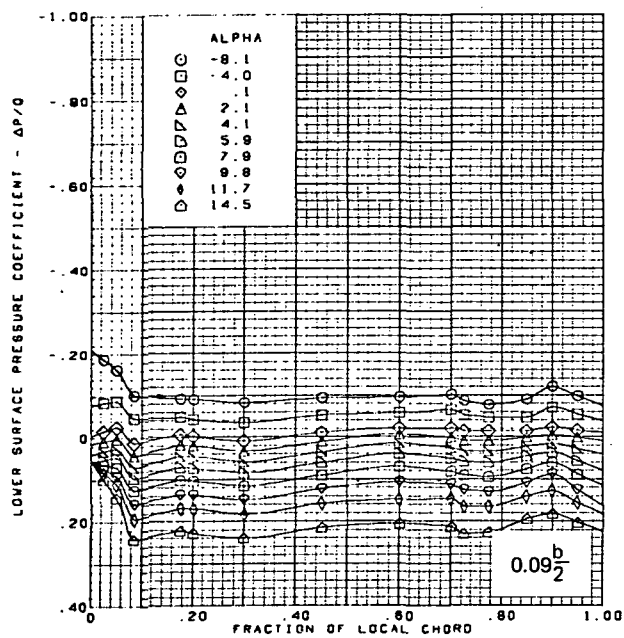
Figure 14.—(Continued)



$M = 1.70$  (run 51)  
 Flat wing, sharp L.E.  
 L.E. deflection, full span =  $0.0^\circ$   
 T.E. deflection, full span =  $0.0^\circ$   
 Note:  $C_{p, \text{vacuum}} = -0.49$

(c) (Concluded)

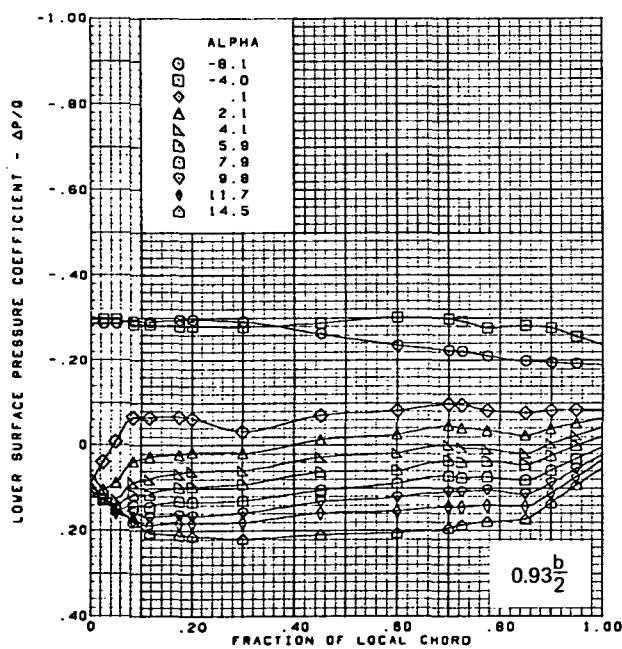
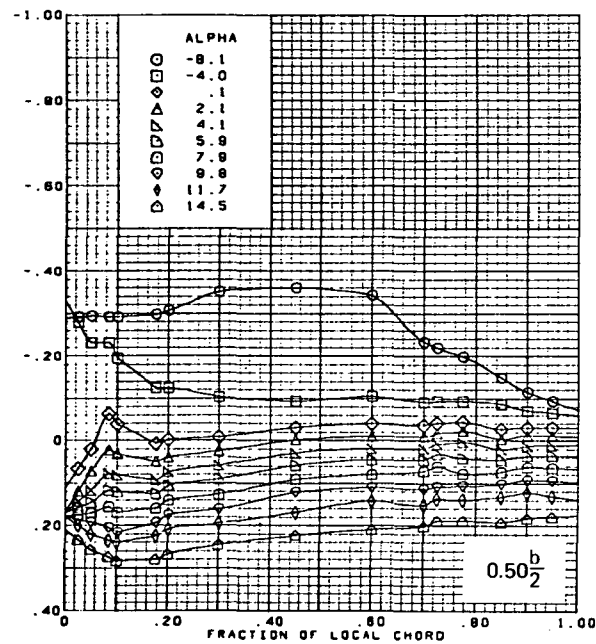
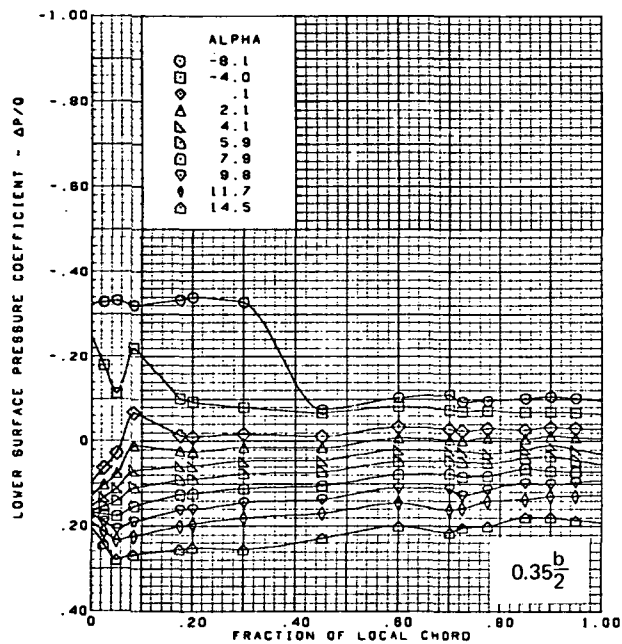
Figure 14.—(Continued)



(d) Lower Surface Chordwise Pressure Distributions

Figure 14.—(Continued)

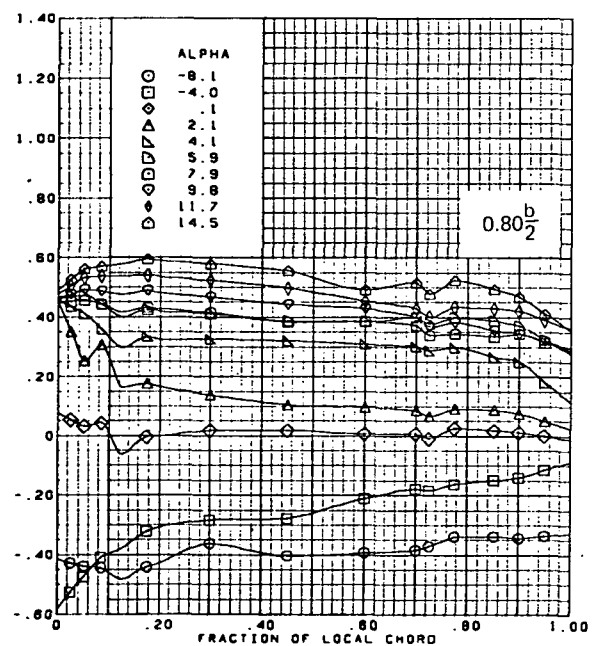
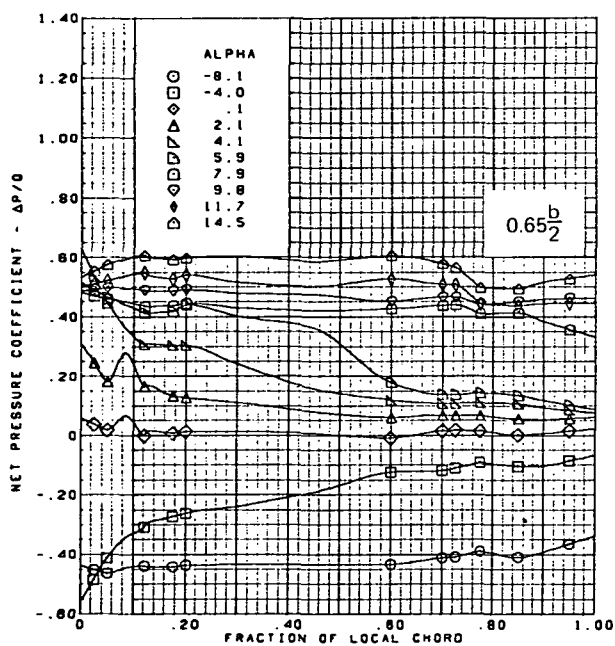
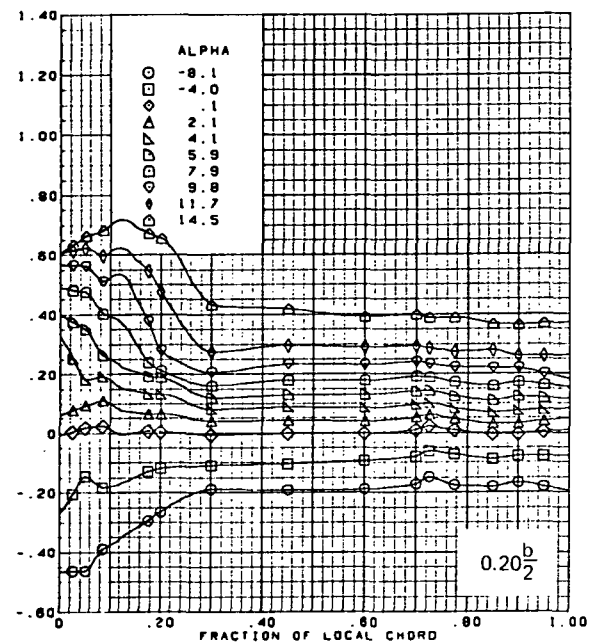
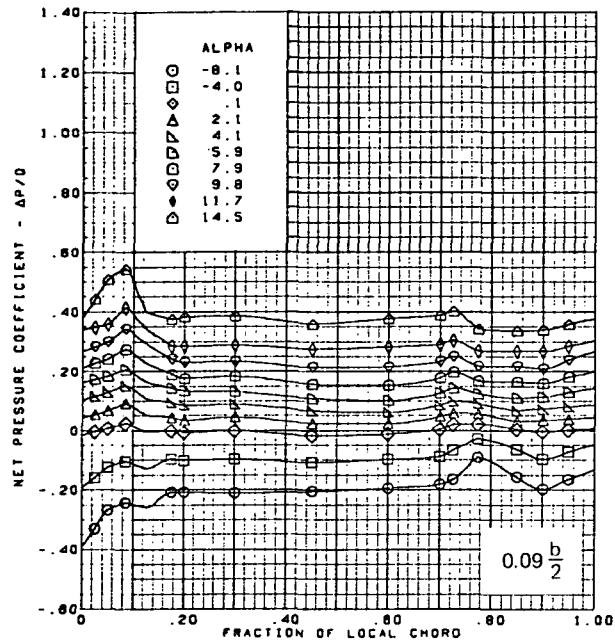




$M = 1.70$  (run 51)  
 Flat wing, sharp L.E.  
 L.E. deflection, full span =  $0.0^\circ$   
 T.E. deflection, full span =  $0.0^\circ$   
 Note:  $C_{p, \text{vacuum}} = -0.49$

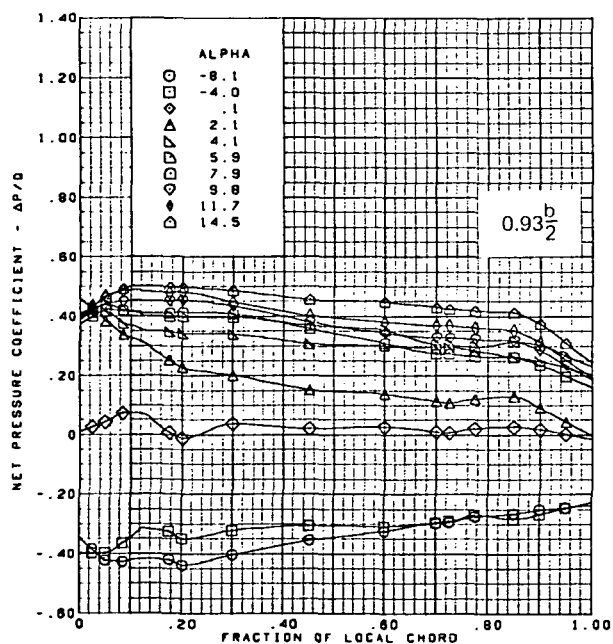
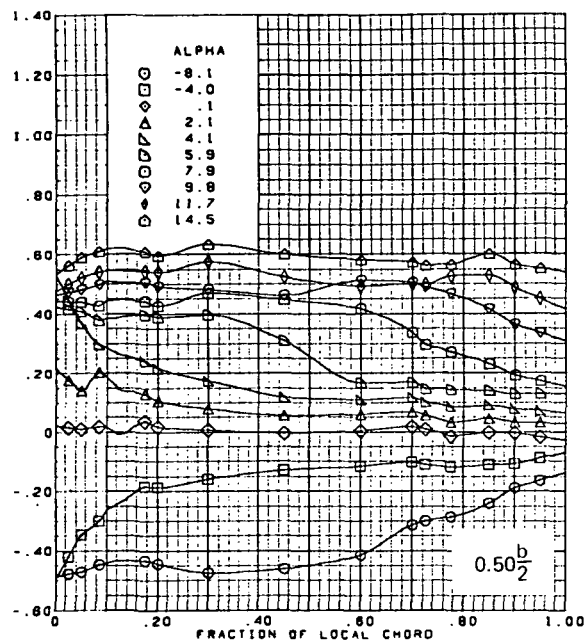
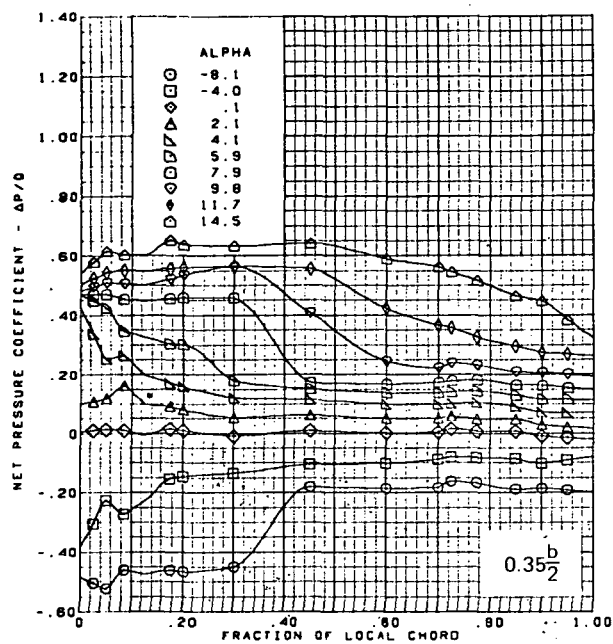
(d) (Concluded)

Figure 14. —(Continued)



(e) Net Chordwise Pressure Distributions

Figure 14.-(Continued)

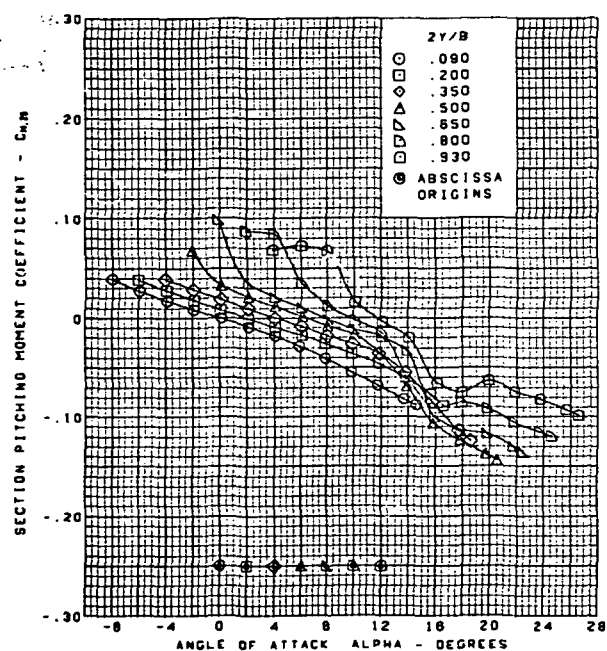
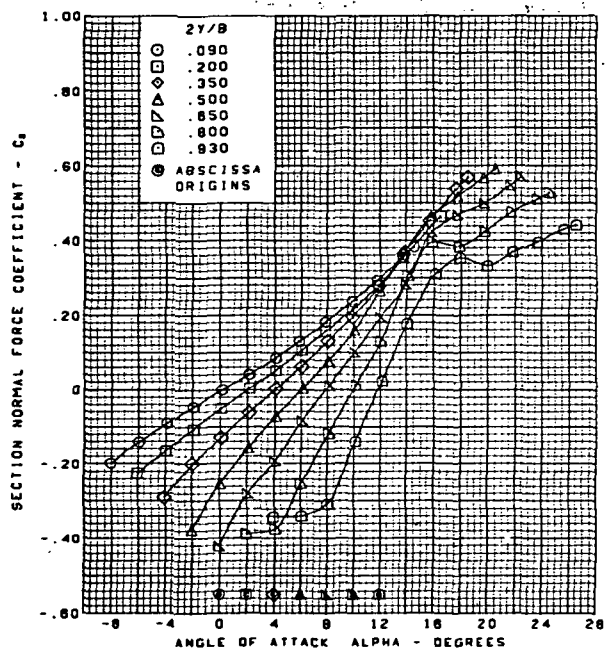
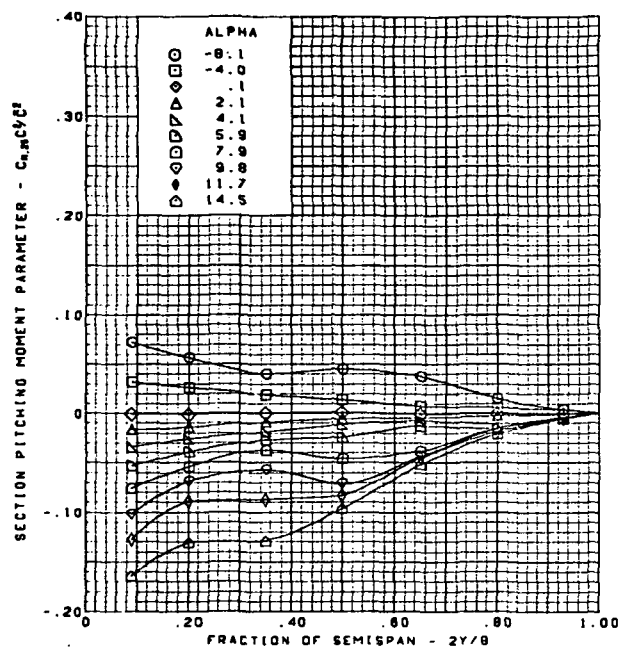
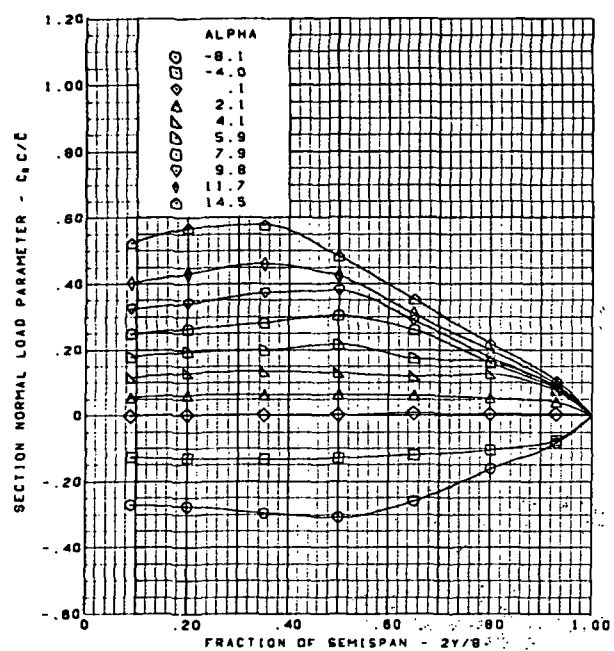


M = 1.70 (run 51)  
 Flat wing, sharp L.E.  
 L.E. deflection, full span =  $0.0^\circ$   
 T.E. deflection, full span =  $0.0^\circ$

(e) (Concluded)

Figure 14.—(Continued)

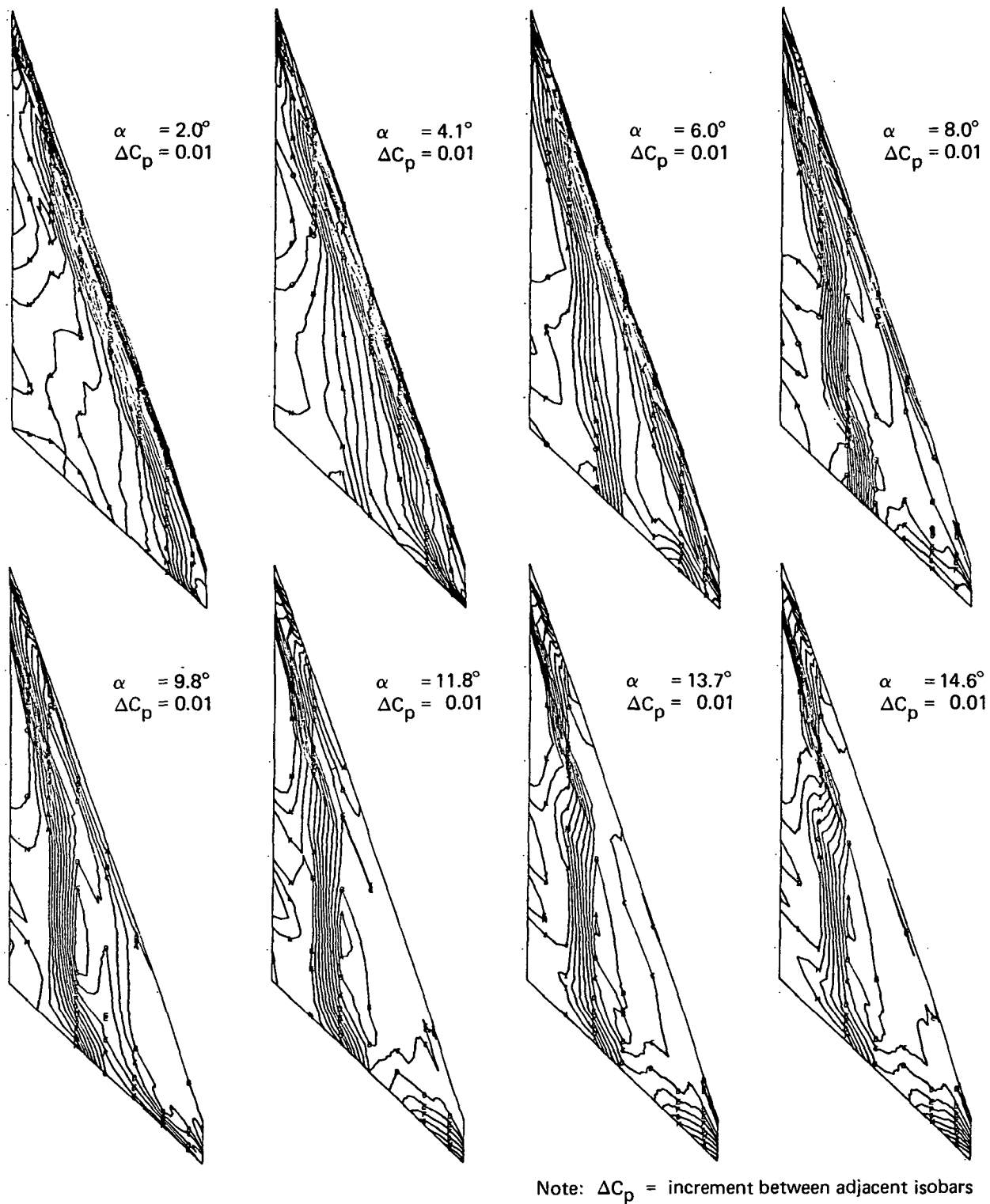
**Page  
Intentionally  
Left Blank**



$M = 1.70$  (run 51)  
 Flat wing, sharp L.E.  
 L.E. deflection, full span =  $0.0^\circ$   
 T.E. deflection, full span =  $0.0^\circ$

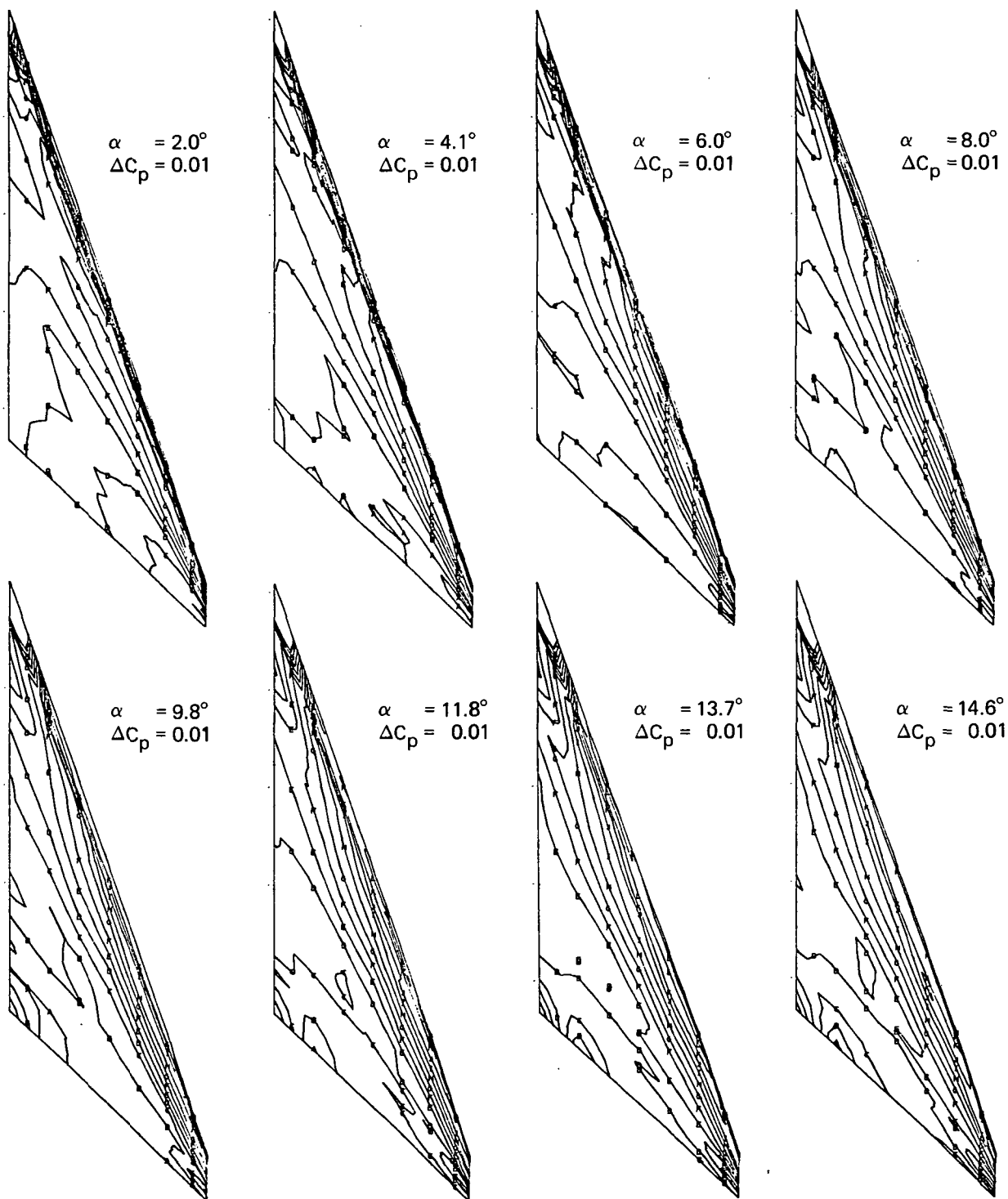
(f) Spanload Distributions and Section Aerodynamic Coefficients

Figure 14.—(Concluded)



(a) Upper Surface Isobars

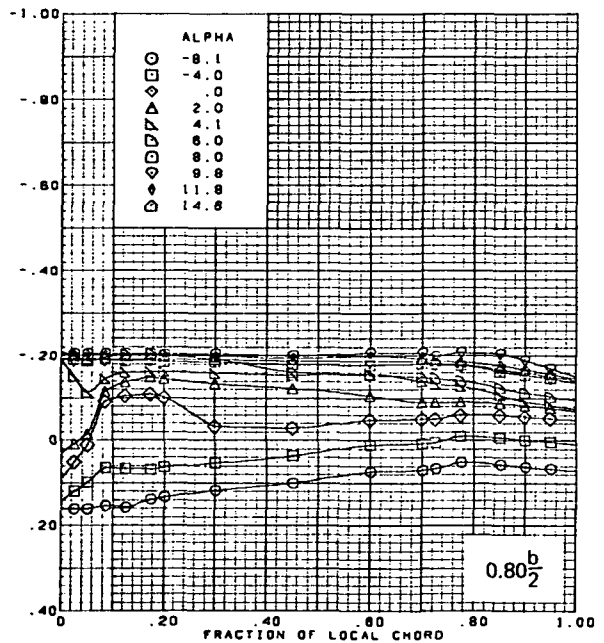
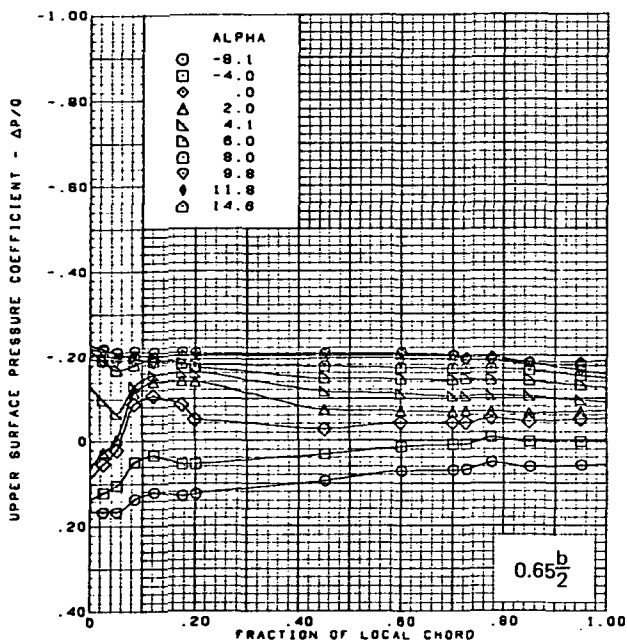
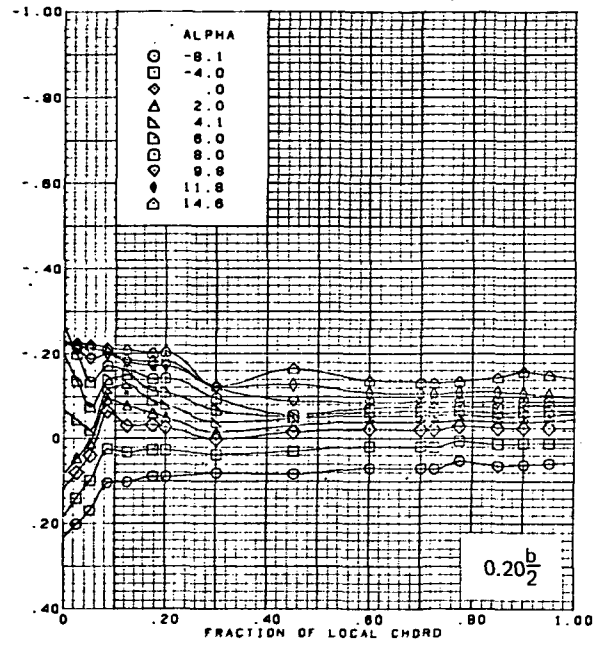
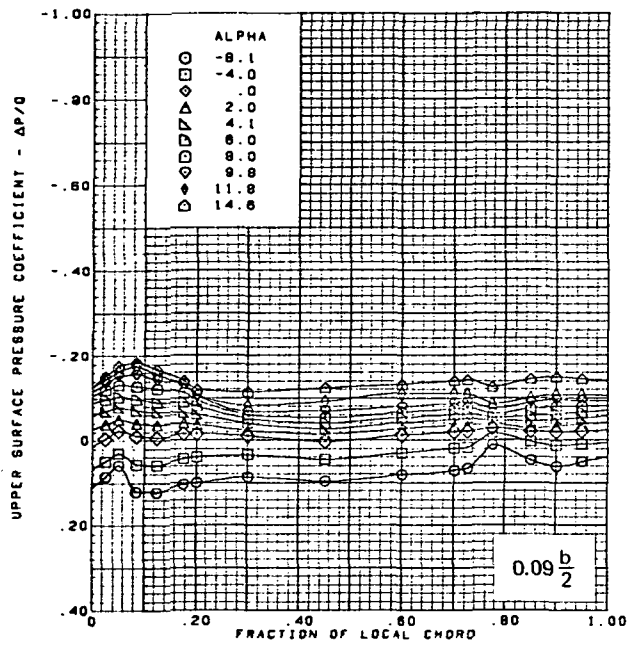
Figure 15.—Wing Experimental Data—Effect of Angle of Attack; Flat Wing, Sharp L.E.; L.E. Deflection, Full Span =  $0.0^\circ$ ; T.E. Deflection, Full Span =  $0.0^\circ$ ;  $M = 2.50$



Note:  $\Delta C_p$  = increment between adjacent isobars

(b) Lower Surface Isobars

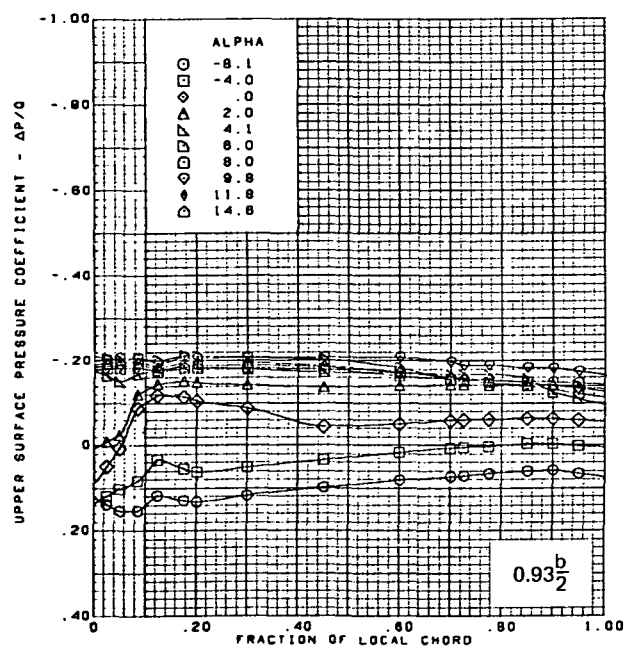
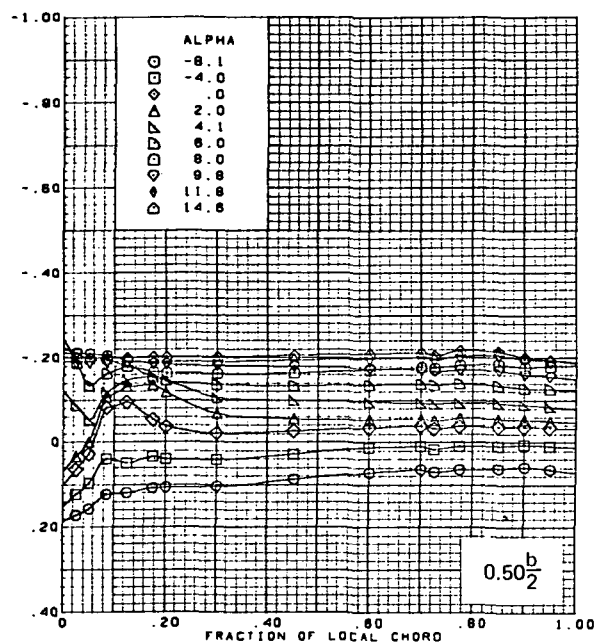
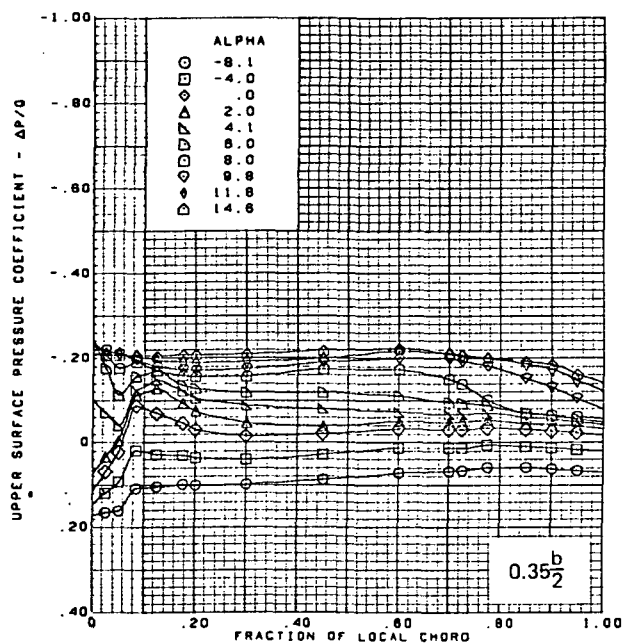
Figure 15.—(Continued)



(c) Upper Surface Chordwise Pressure Distributions

Figure 15.—(Continued)

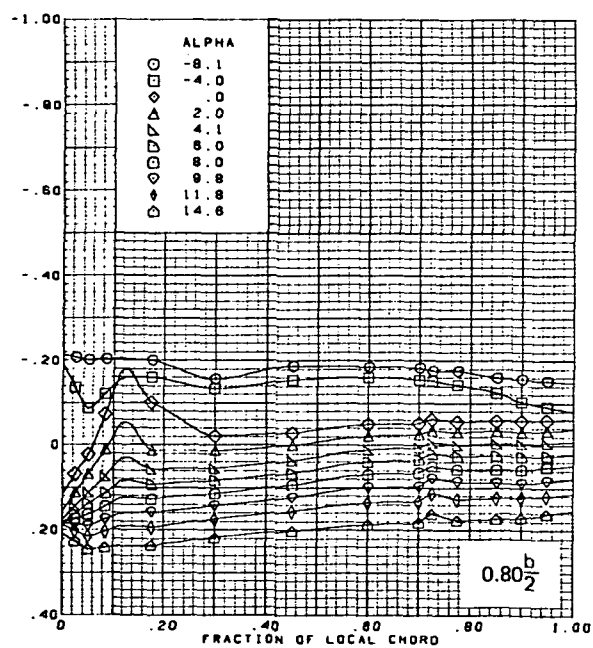
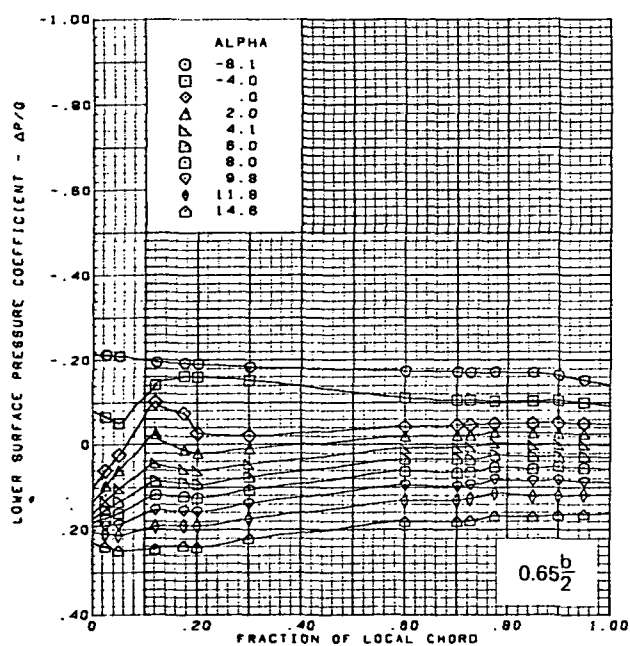
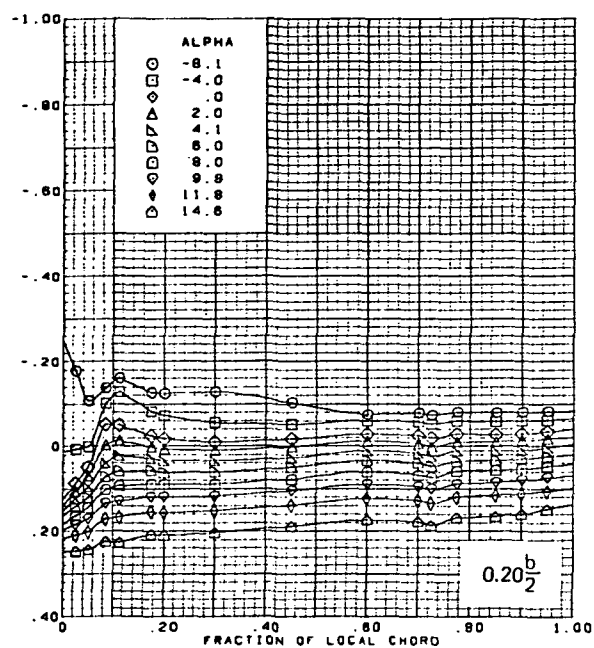
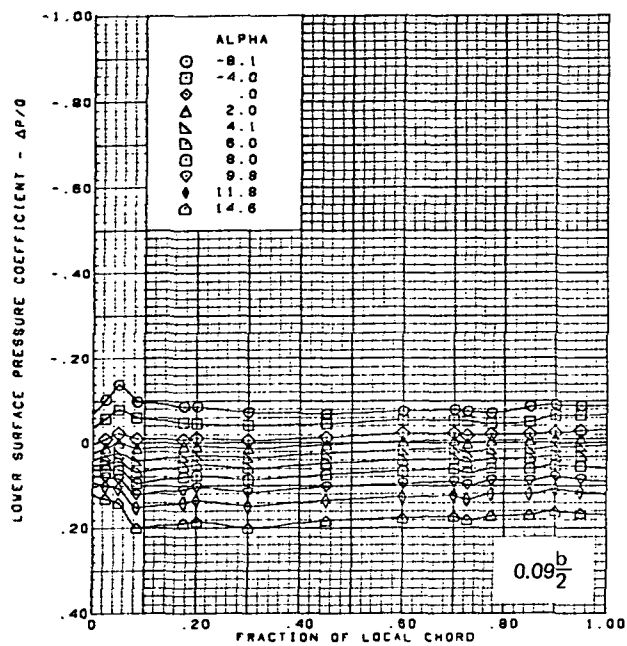




$M = 2.50$  (run 53)  
 Flat wing, sharp L.E.  
 L.E. deflection, full span =  $0.0^\circ$   
 T.E. deflection, full span =  $0.0^\circ$   
 Note:  $C_{p, \text{vacuum}} = -0.23$

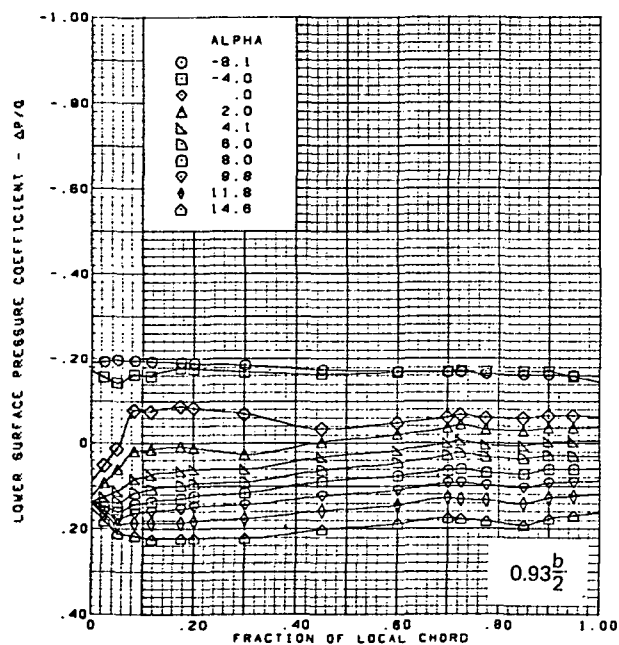
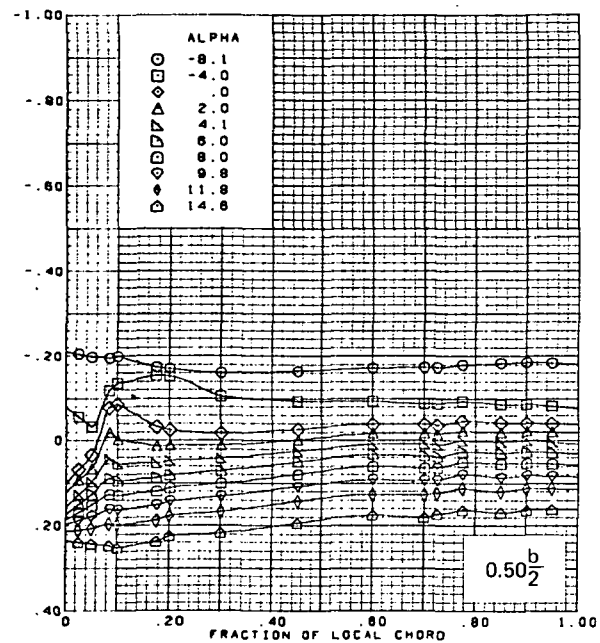
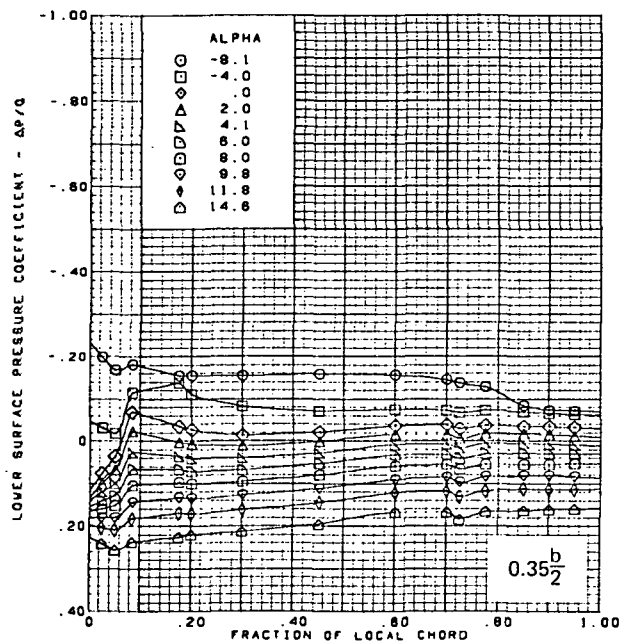
(c) (Concluded)

Figure 15.—(Continued)



(d) Lower Surface Chordwise Pressure Distributions

Figure 15. —(Continued)

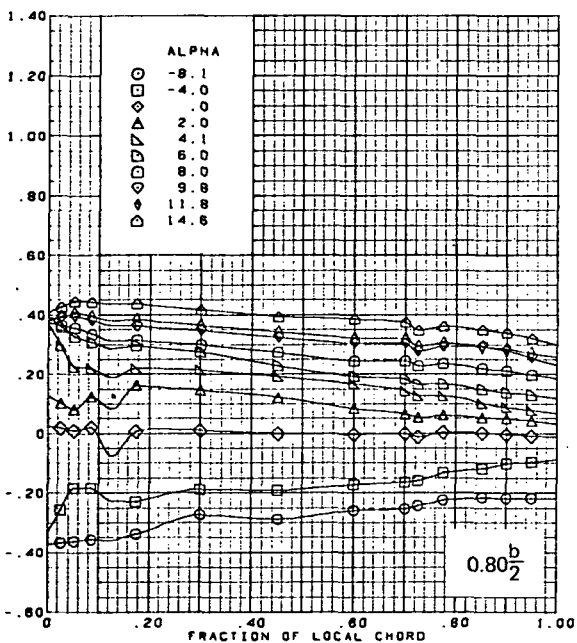
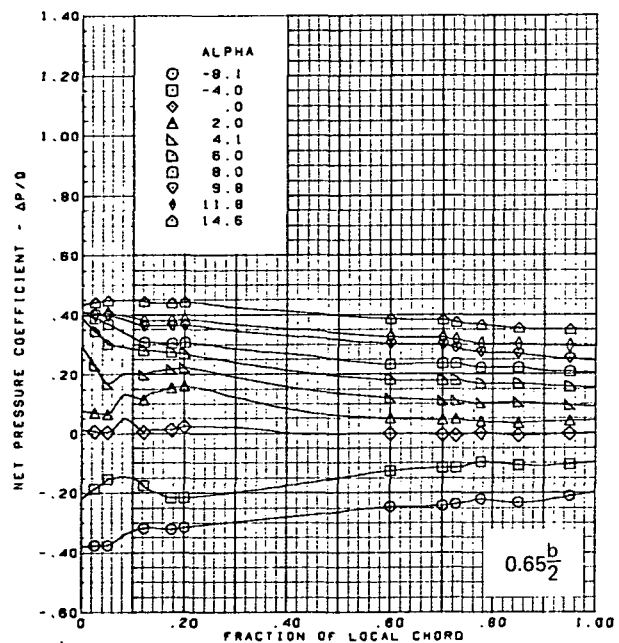
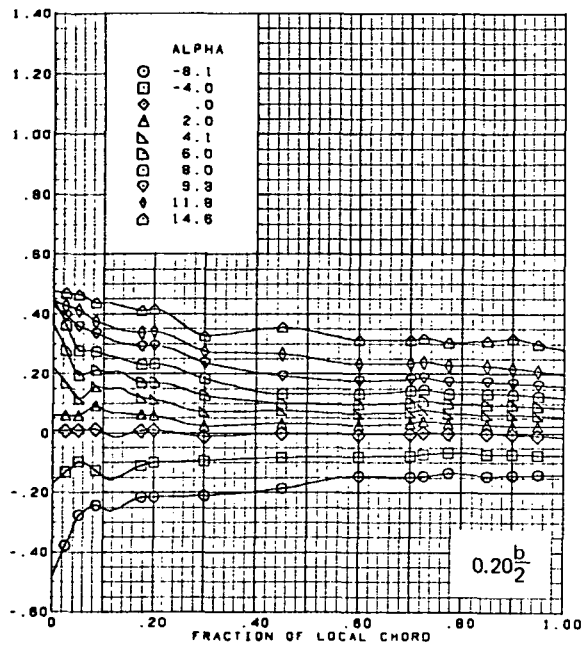
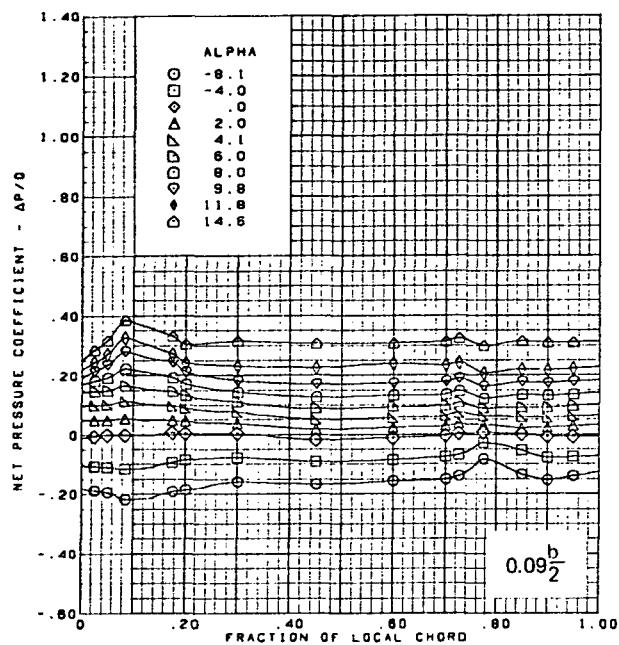


$M = 2.50$  (run 53)  
 Flat wing, sharp L.E.  
 L.E. deflection, full span  $\approx 0.0^\circ$   
 T.E. deflection, full span  $\approx 0.0^\circ$

Note:  $C_{p, \text{vacuum}} = -0.23$

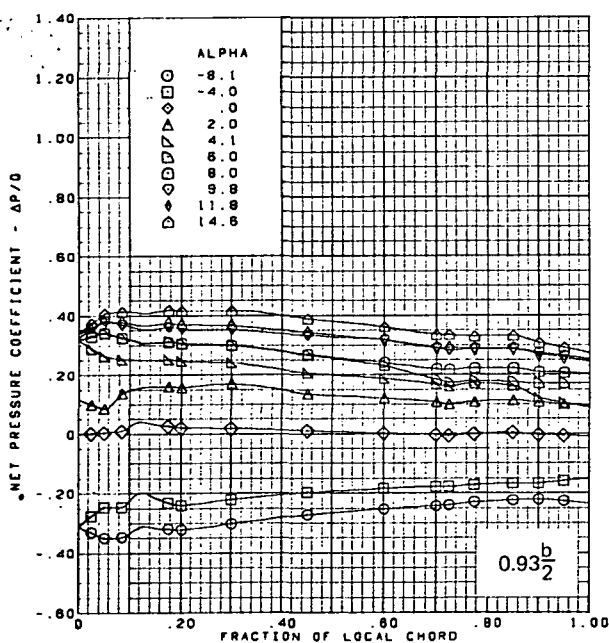
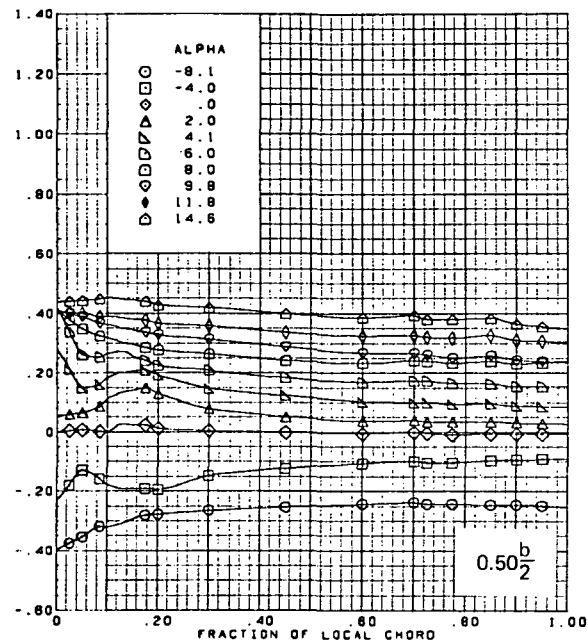
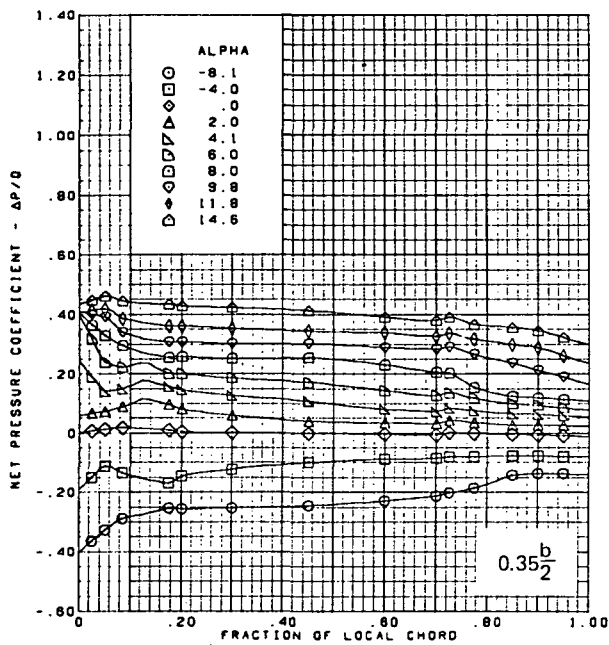
(d) (Concluded)

Figure 15.—(Continued)



(e) Net Chordwise Pressure Distributions

Figure 15. —(Continued)

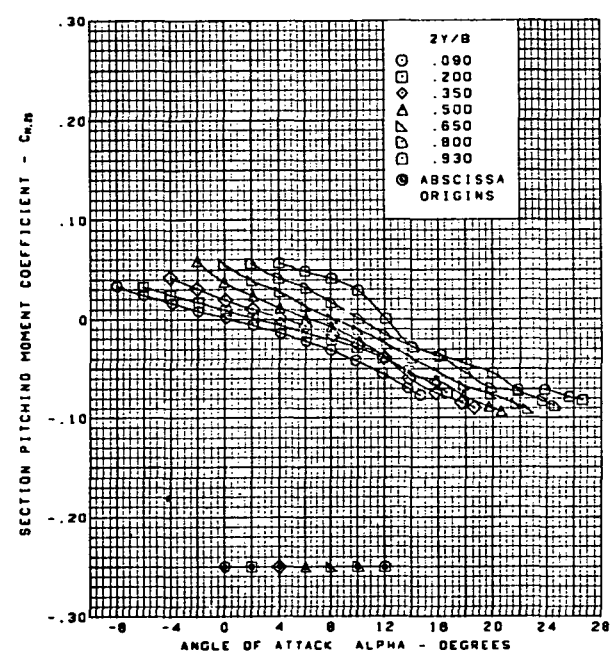
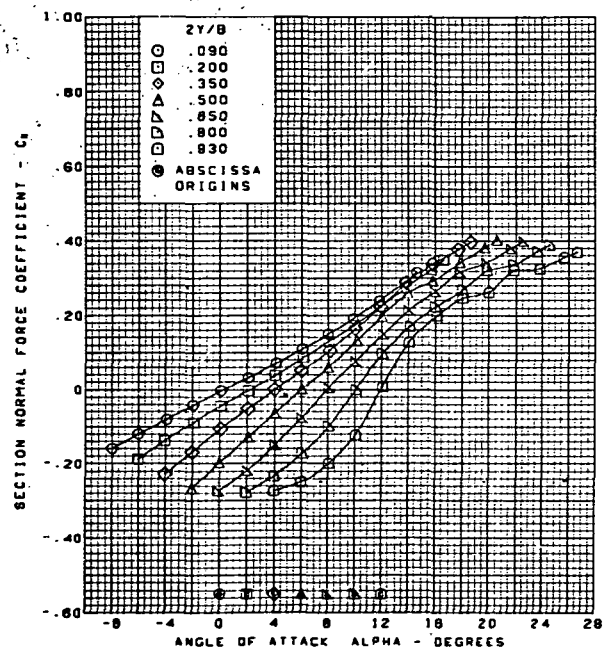
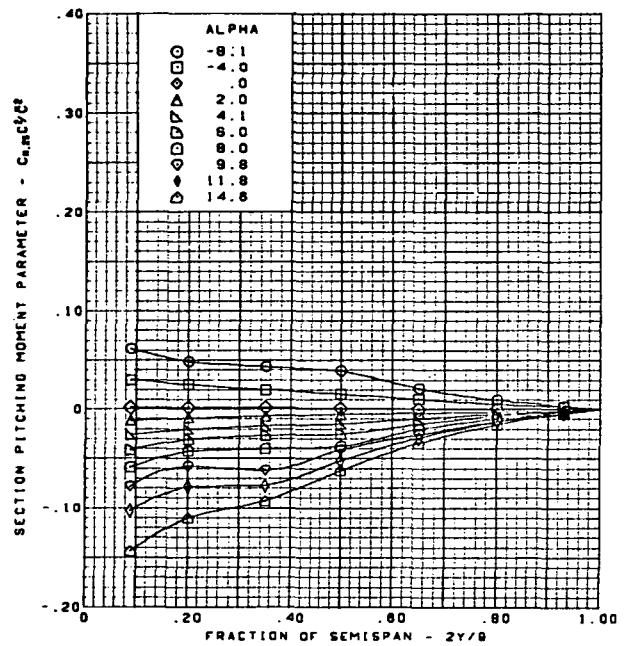
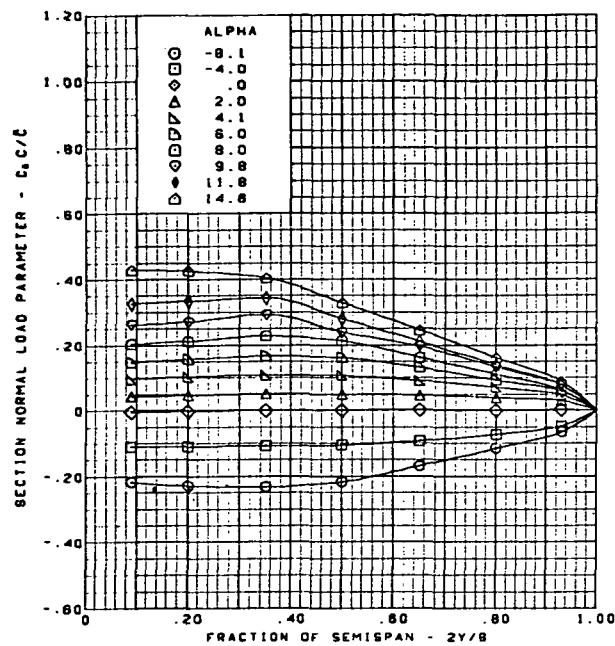


$M = 2.50$  (run 53)  
 Flat wing, sharp L.E.  
 L.E. deflection, full span =  $0.0^\circ$   
 T.E. deflection, full span =  $0.0^\circ$

(e) (Concluded)

Figure 15. —(Continued)

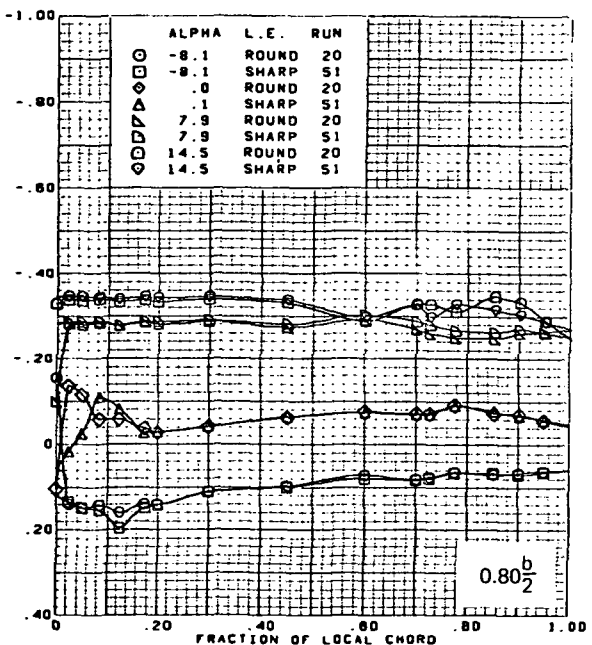
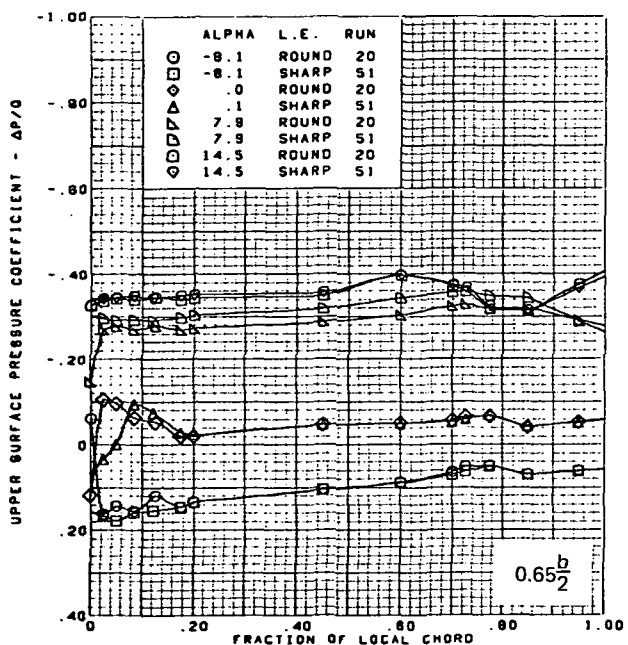
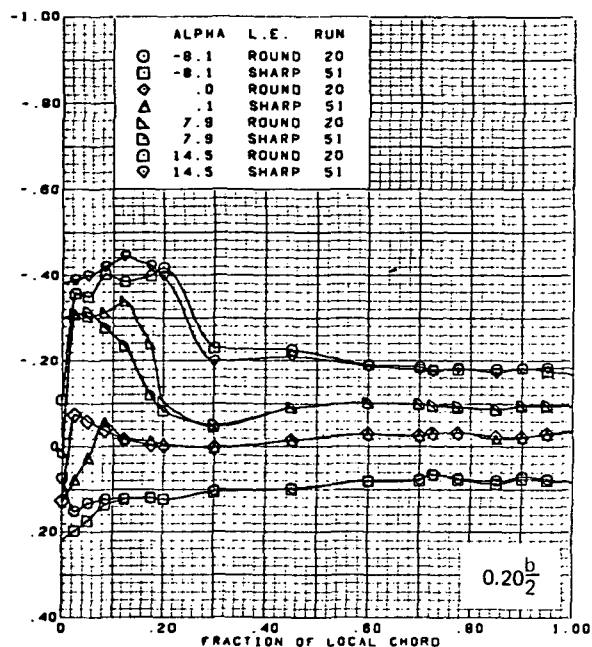
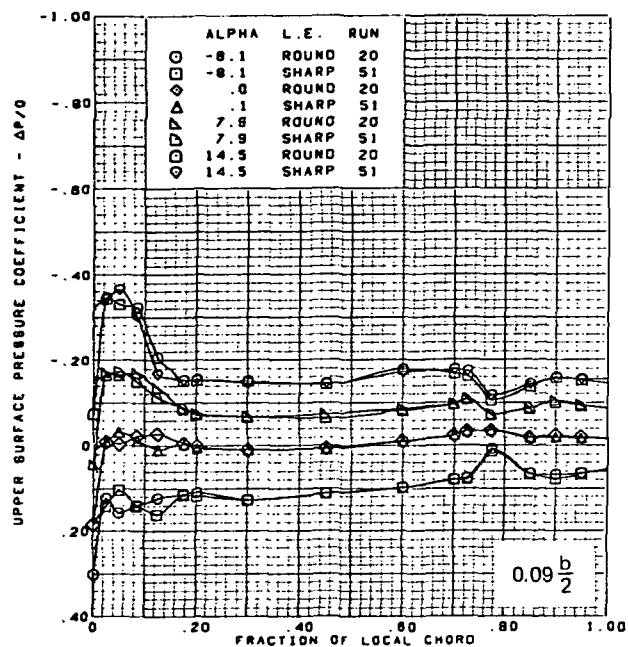
**Page  
Intentionally  
Left Blank**



$M = 2.50$  (run 53)  
 Flat wing, sharp L.E.  
 L.E. deflection, full span =  $0.0^\circ$   
 T.E. deflection, full span =  $0.0^\circ$

(f) Spanload Distributions and Section Aerodynamic Coefficients

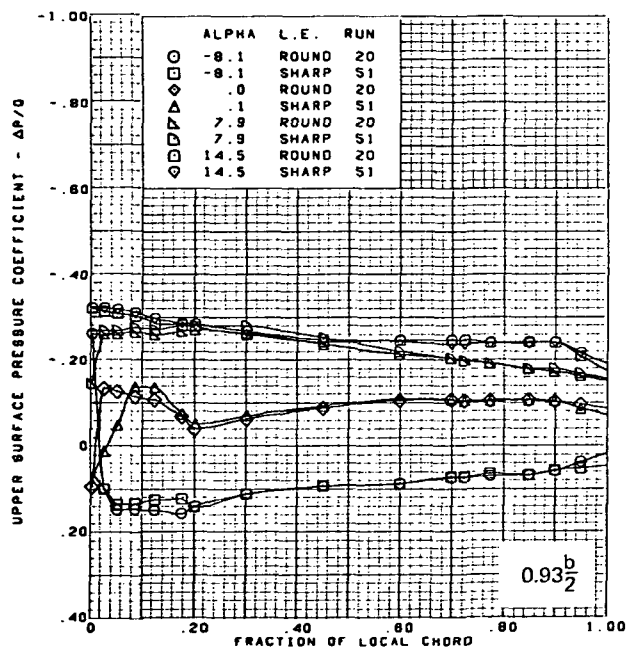
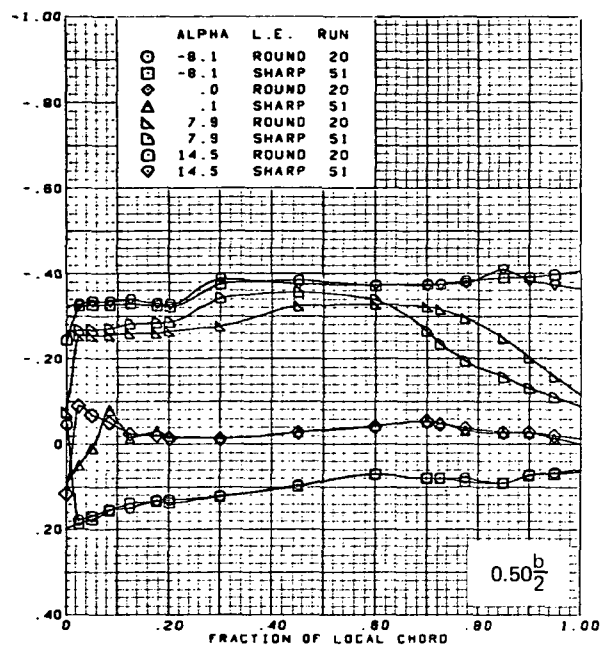
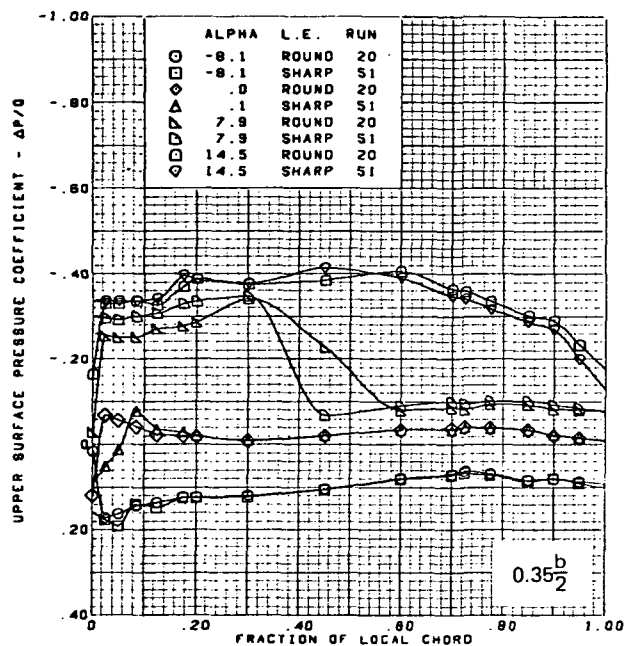
Figure 15.—(Concluded)



(a) Upper Surface Chordwise Pressure Distributions

Figure 16.—Wing Experimental Data—Effect of L.E. Shape With Angle of Attack; Flat Wing; L.E. Deflection, Full Span = 0.0°; T.E. Deflection, Full Span = 0.0°;  $M = 1.70$



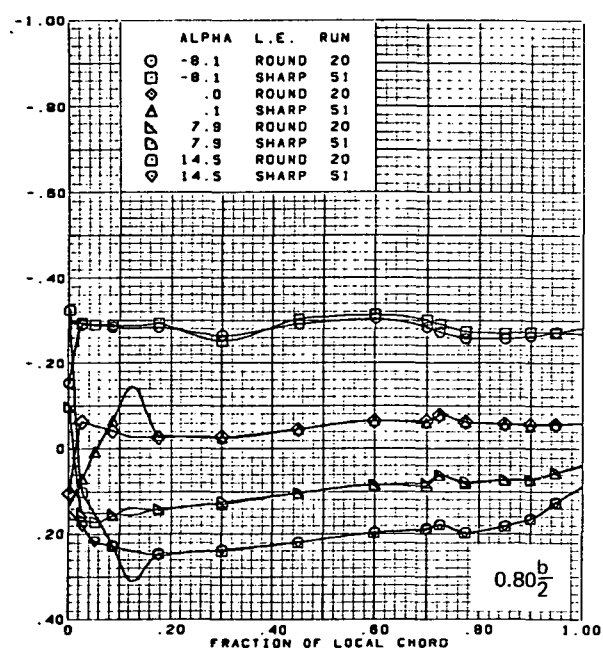
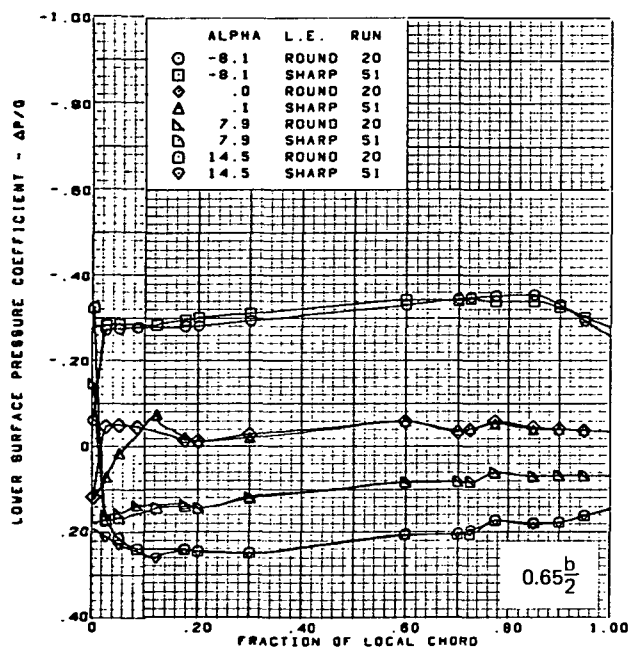
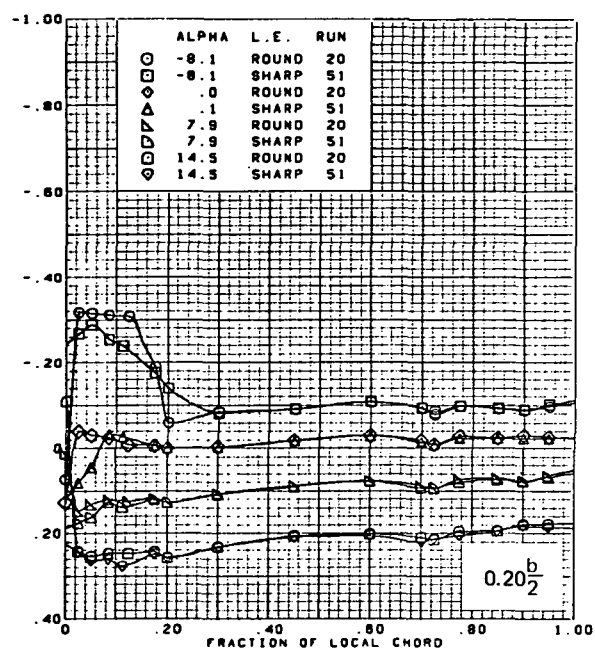
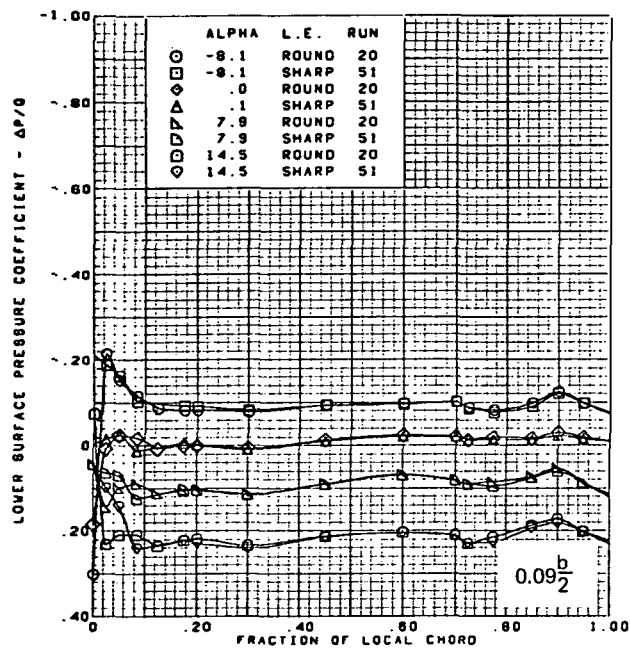


M = 1.70  
 Flat wing  
 L.E. deflection, full span =  $0.0^\circ$   
 T.E. deflection, full span =  $0.0^\circ$

Note:  $C_{p, \text{vacuum}} = -0.49$

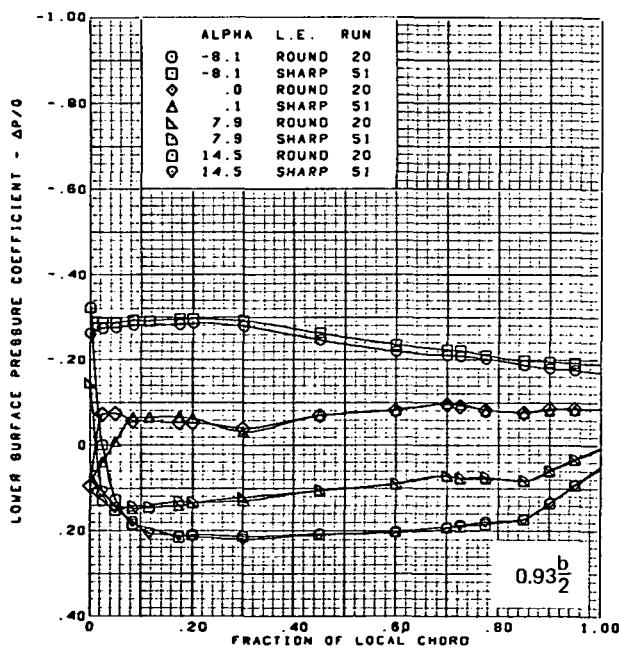
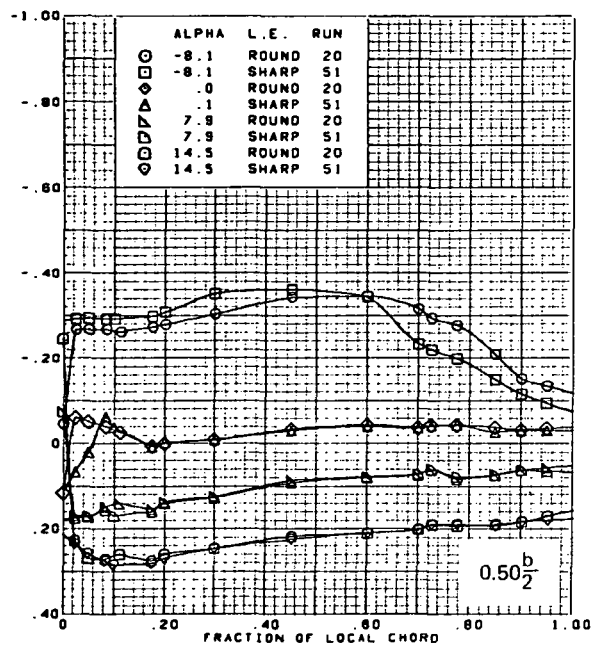
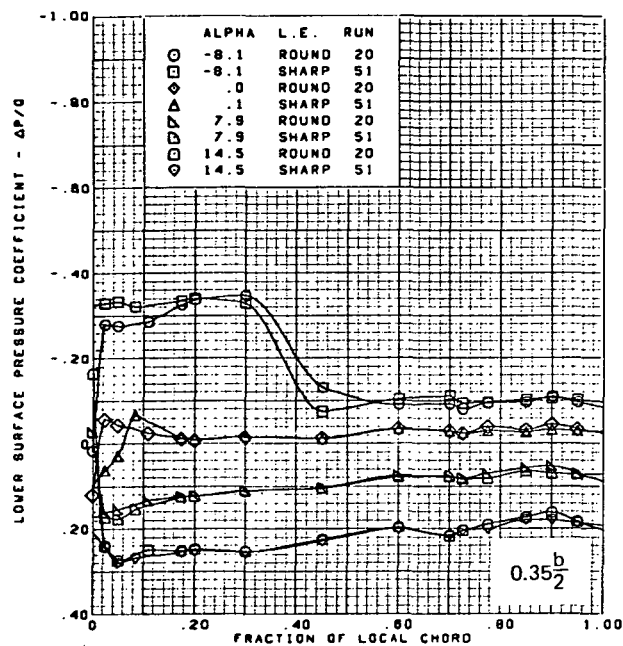
(a) (Concluded)

Figure 16.—(Continued)



(b) Lower Surface Chordwise Pressure Distributions

Figure 16.—(Continued)

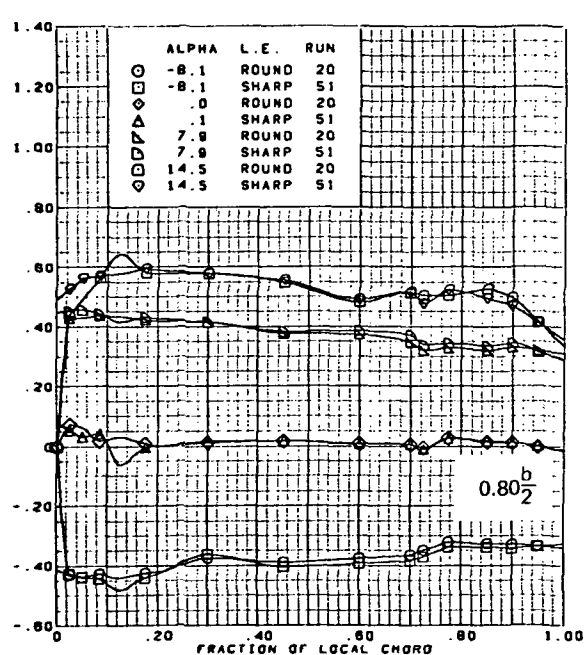
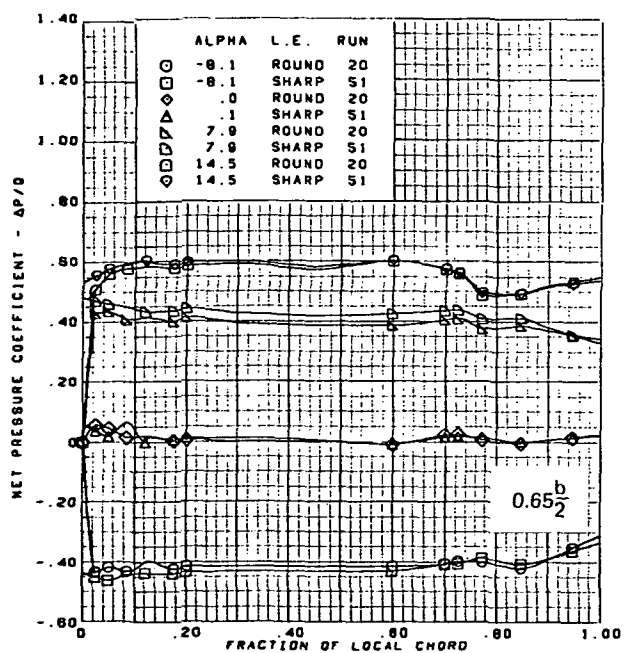
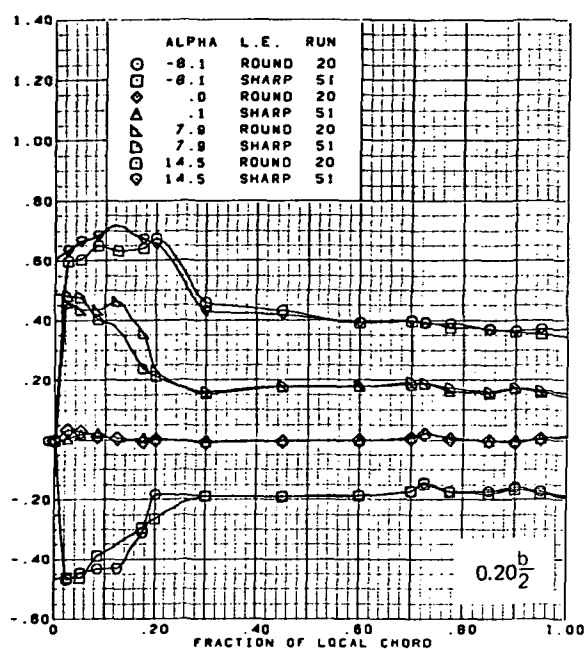
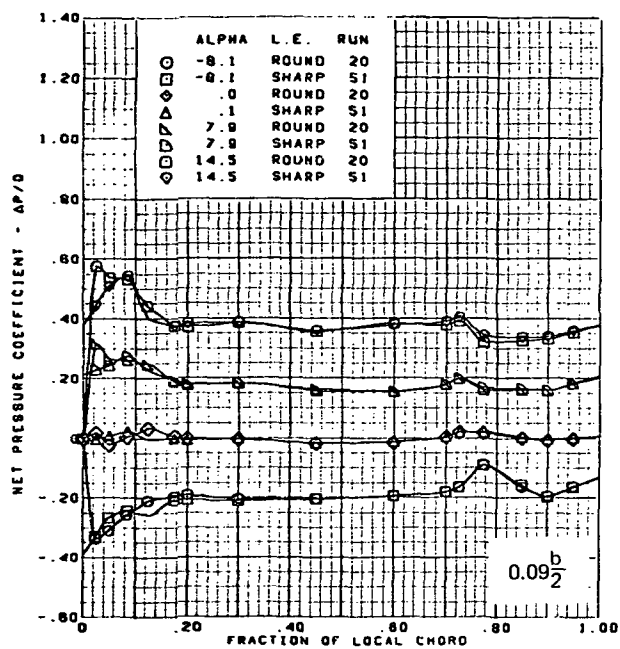


M = 1.70  
 Flat wing  
 L.E. deflection, full span =  $0.0^\circ$   
 T.E. deflection, full span =  $0.0^\circ$

Note:  $C_{p, \text{vacuum}} = -0.49$

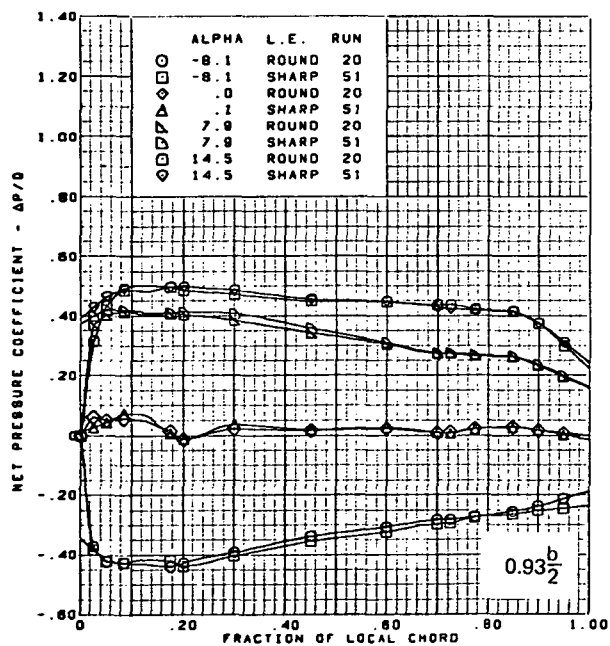
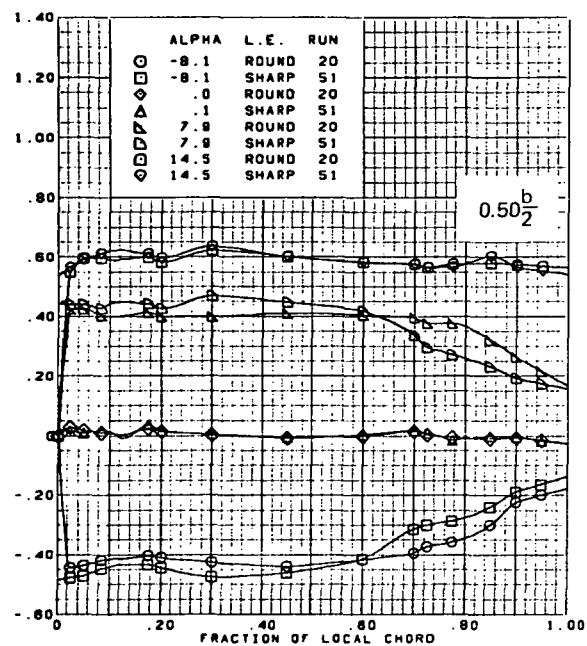
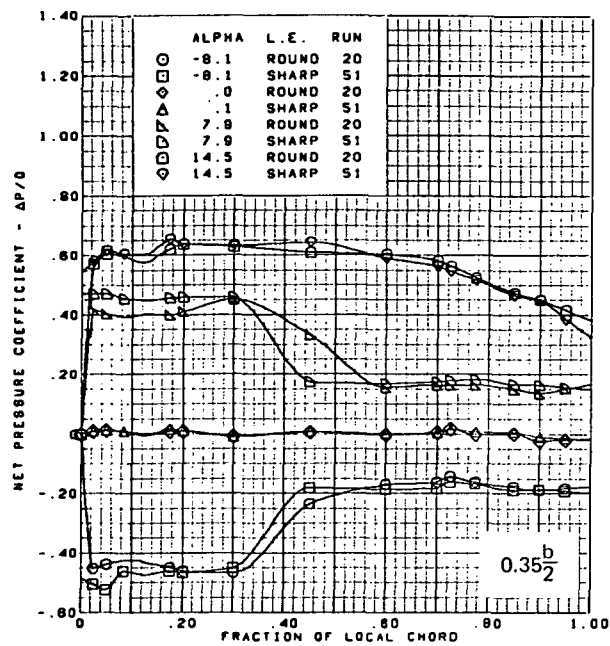
(b) (Concluded)

Figure 16.—(Continued)



(c) Net Chordwise Pressure Distributions

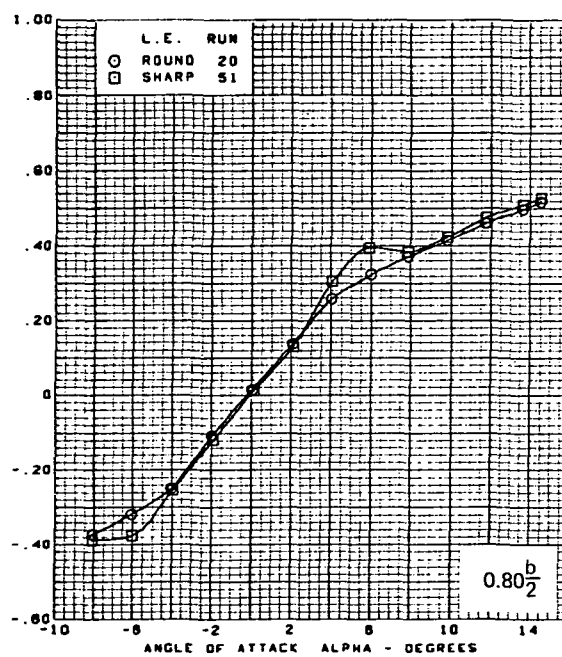
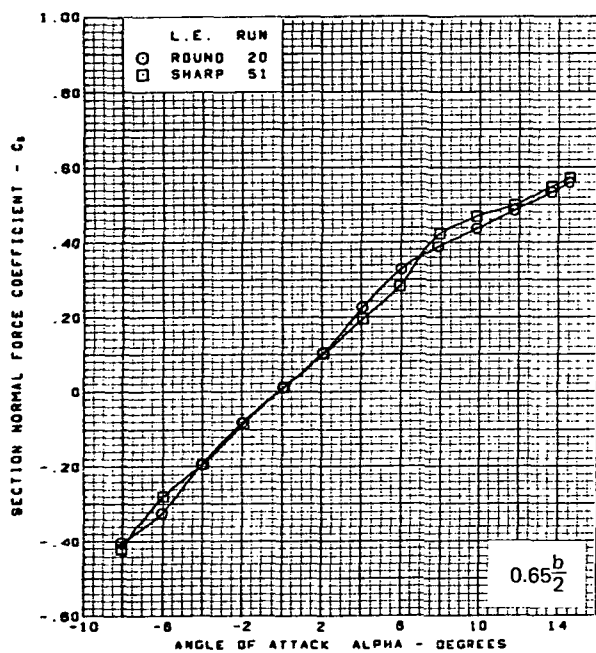
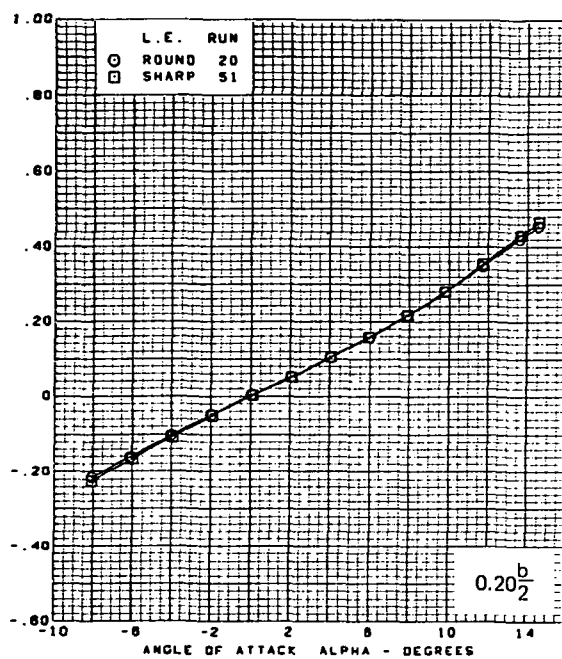
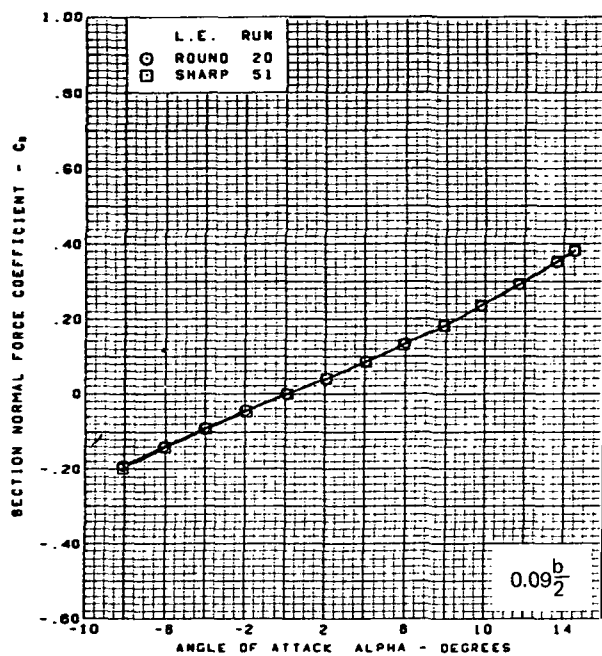
Figure 16.—(Continued)



$M = 1.70$   
 Flat wing  
 $L.E. \text{ deflection, full span} = 0.0^\circ$   
 $T.E. \text{ deflection, full span} = 0.0^\circ$

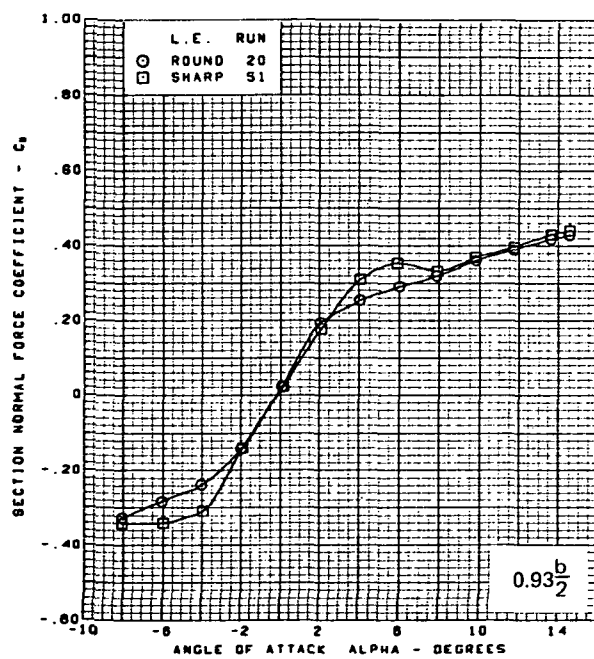
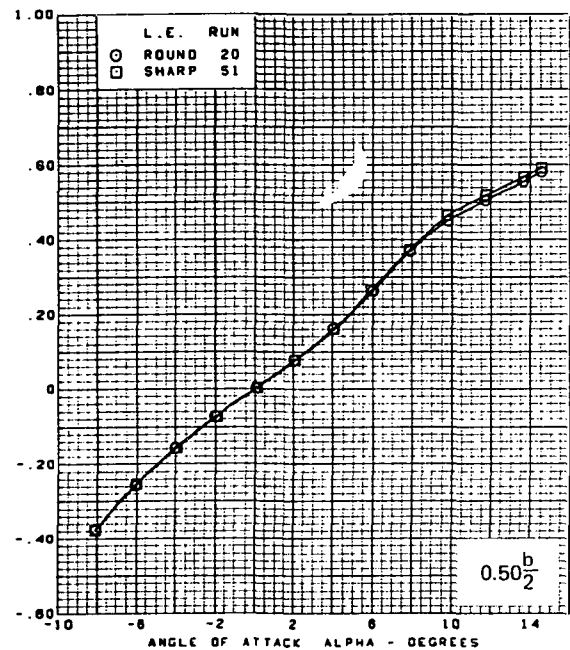
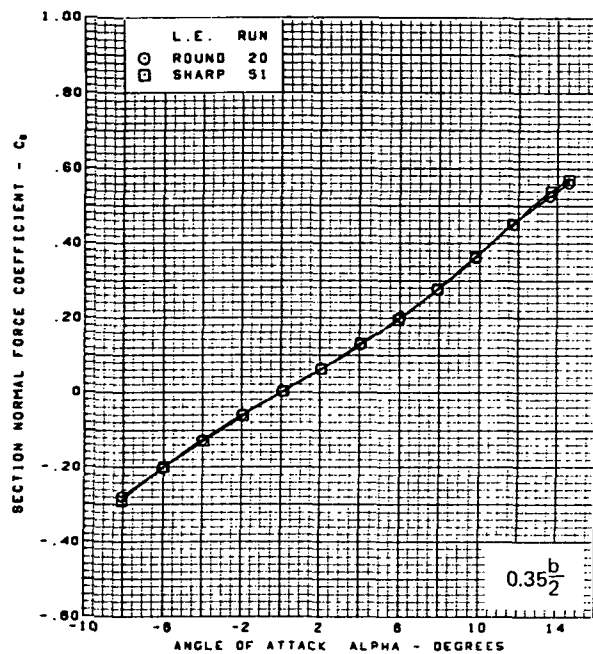
(c) (Concluded)

Figure 16.—(Continued)



(d) Section Aerodynamic Coefficients—Normal Force

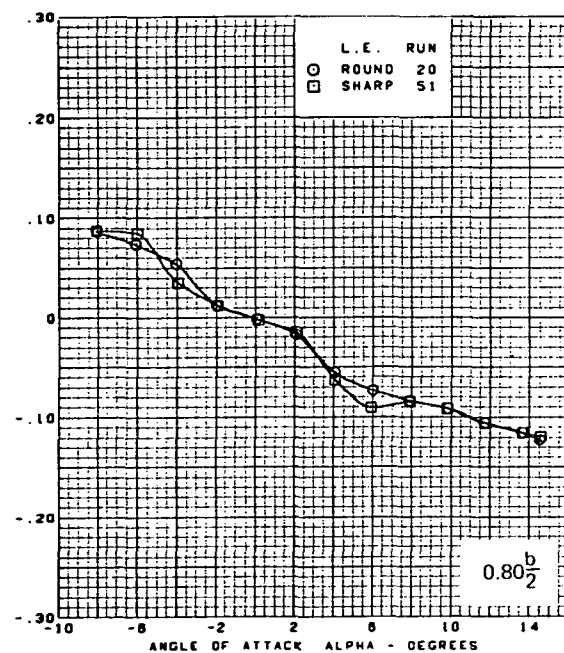
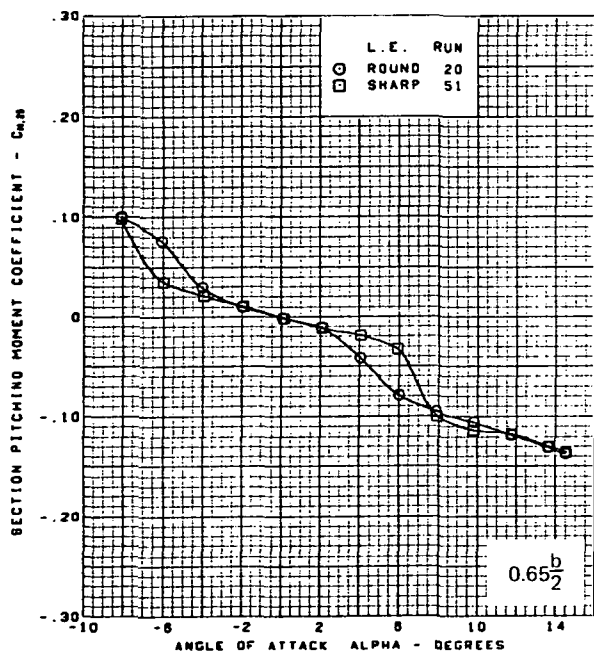
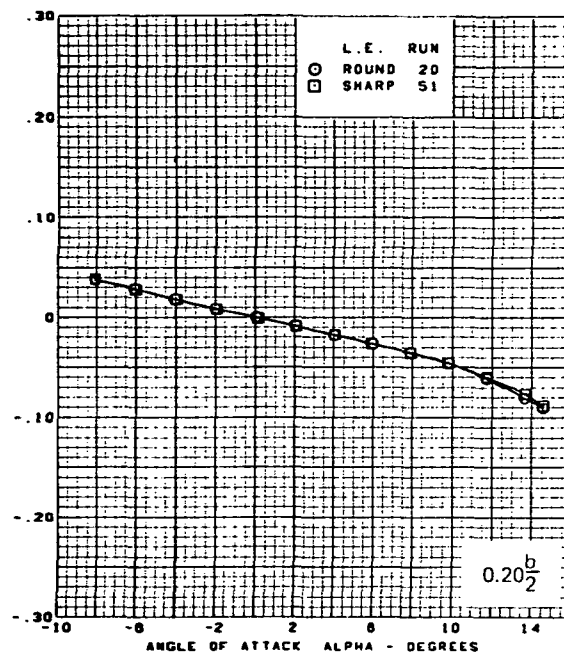
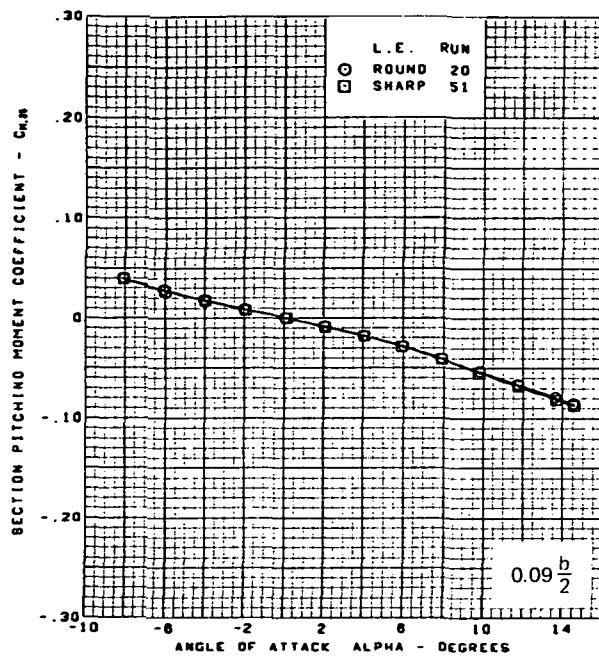
Figure 16.—(Continued)



M = 1.70  
Flat wing  
L.E. deflection, full span = 0.0°  
T.E. deflection, full span = 0.0°

(d) (Concluded)

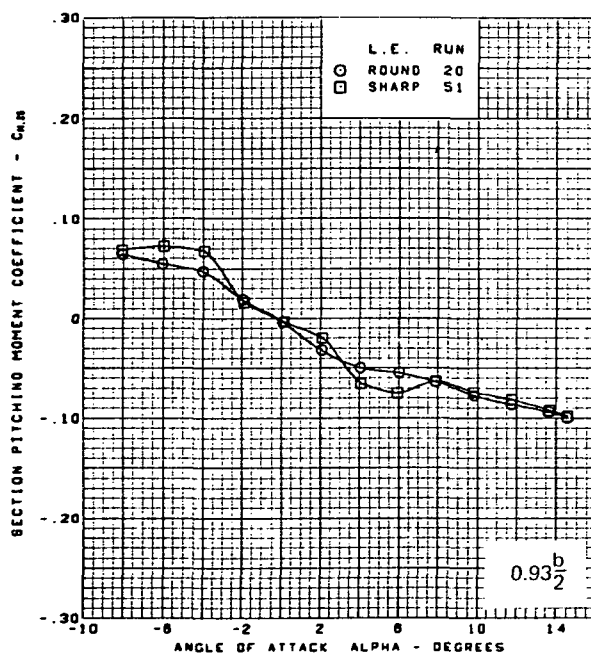
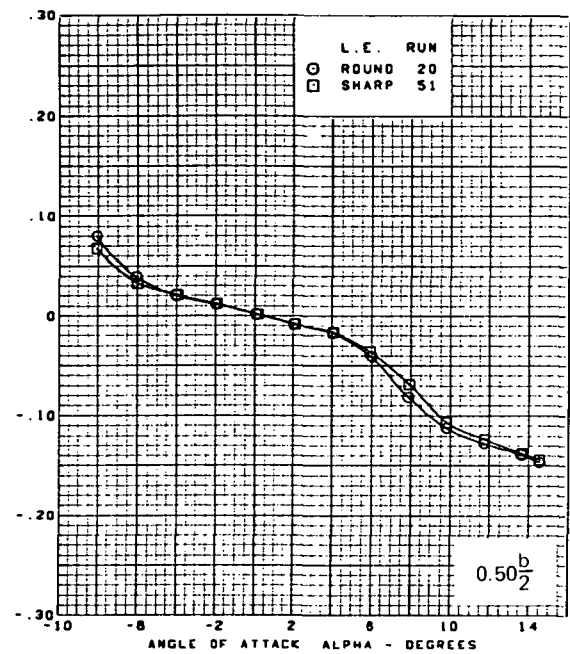
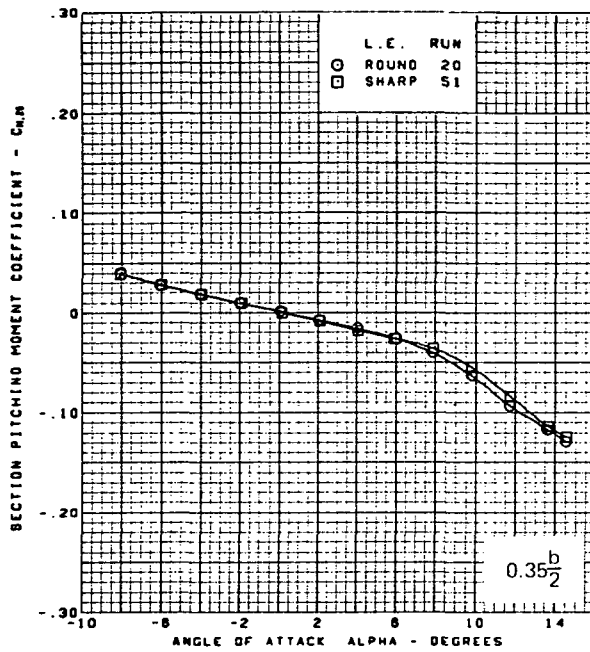
Figure 16.—(Continued)



(e) Section Aerodynamic Coefficients—Pitching Moment

Figure 16.—(Continued)

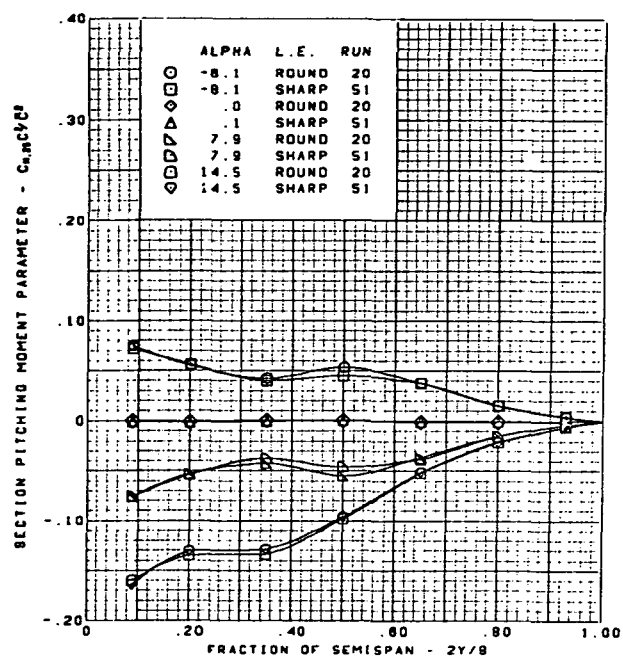
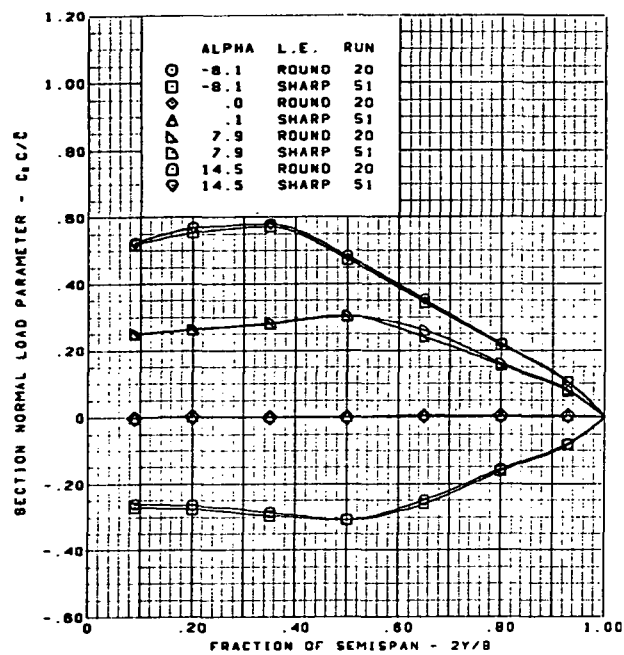




M = 1.70  
 Flat wing  
 L.E. deflection, full span =  $0.0^\circ$   
 T.E. deflection, full span =  $0.0^\circ$

(e) (Concluded)

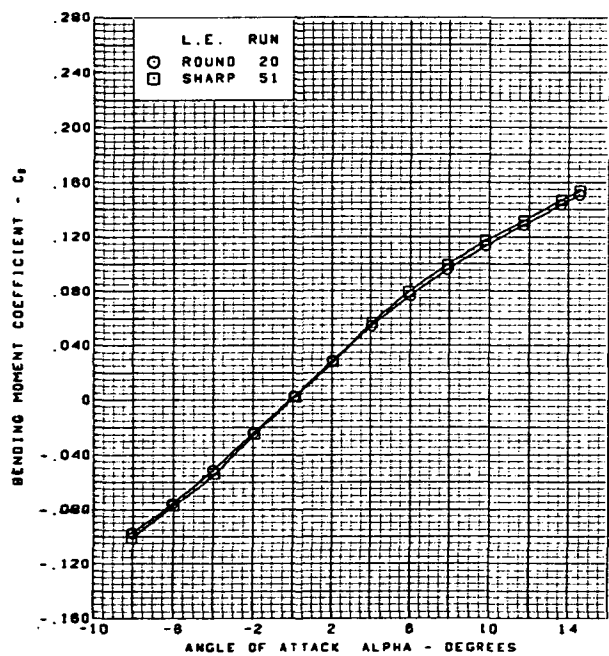
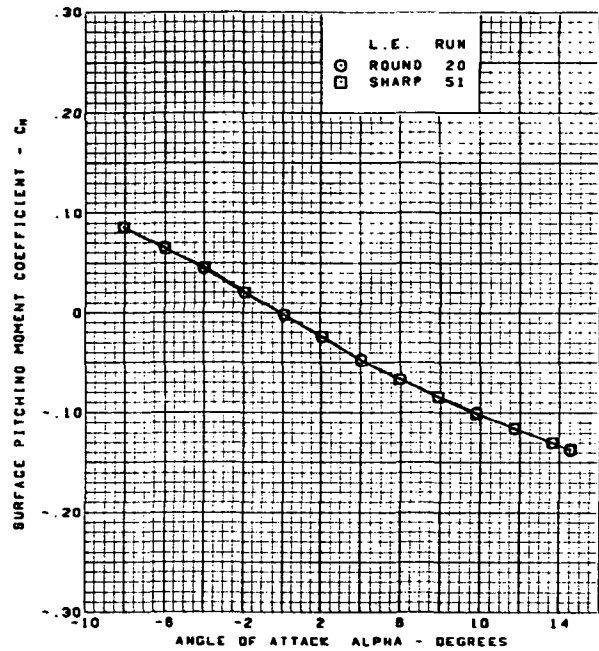
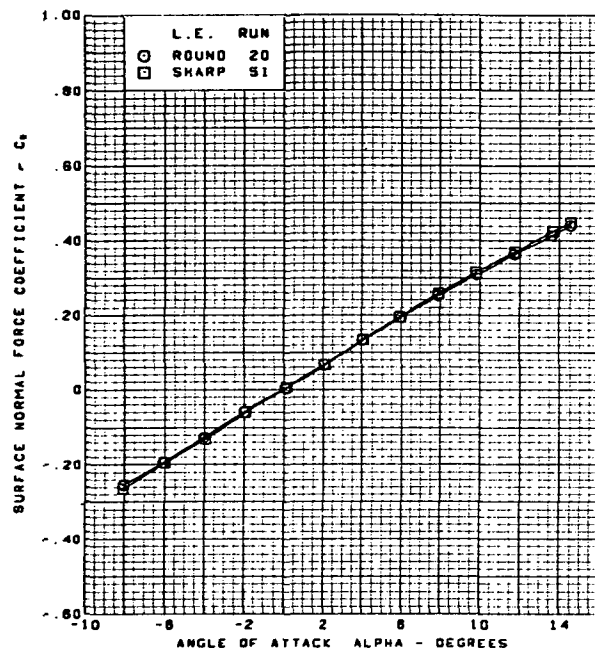
Figure 16.—(Continued)



$M = 1.70$   
 Flat wing  
 L.E. deflection, full span =  $0.0^\circ$   
 T.E. deflection, full span =  $0.0^\circ$

(f) Spanload Distributions

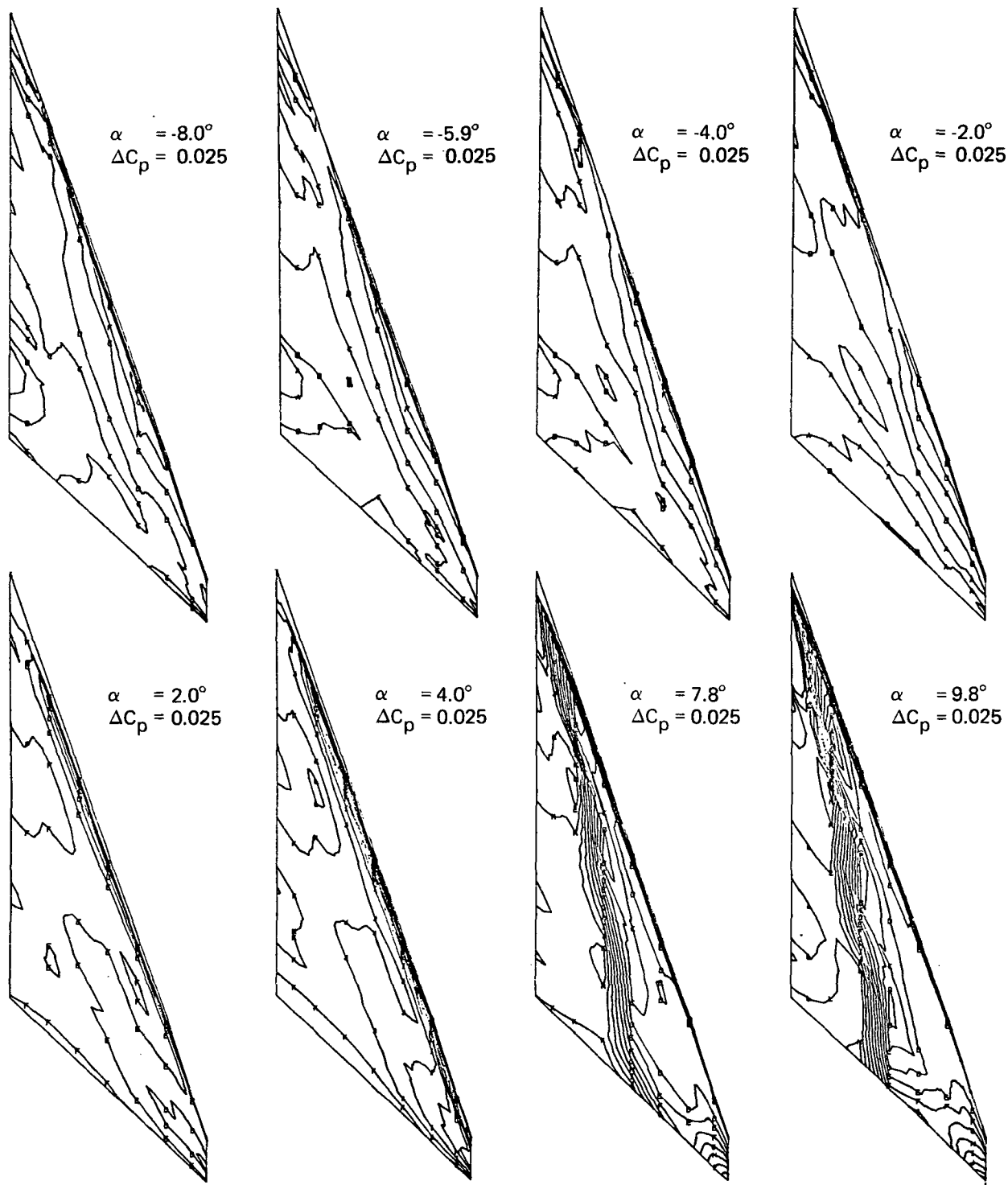
Figure 16.—(Continued)



$M = 1.70$   
 Flat wing  
 L.E. deflection, full span =  $0.0^\circ$   
 T.E. deflection, full span =  $0.0^\circ$

(g) Wing Aerodynamic Coefficients

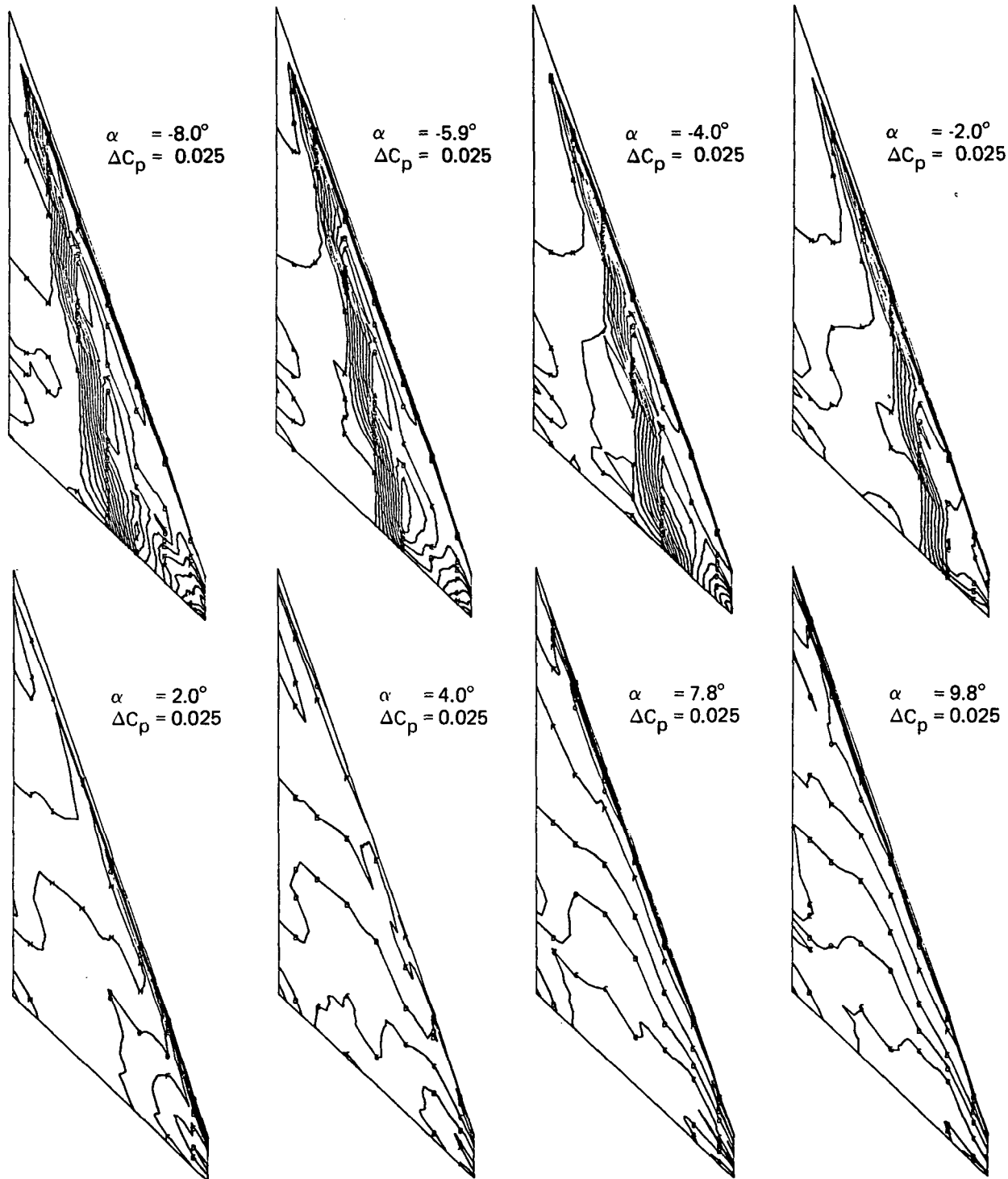
Figure 16.—(Concluded)



Note:  $\Delta C_p$  = increment between adjacent isobars

(a) Upper Surface Isobars

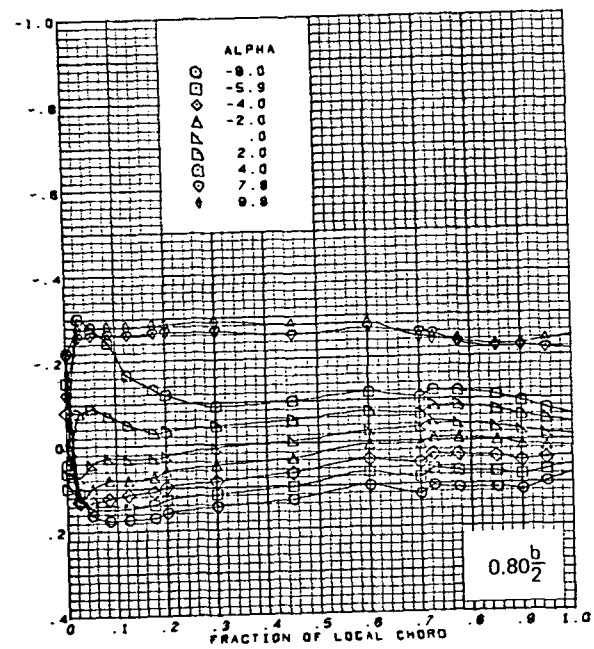
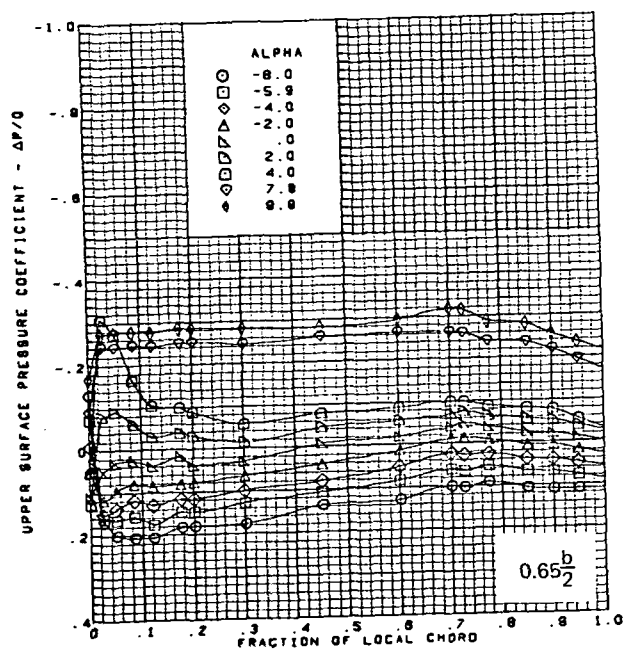
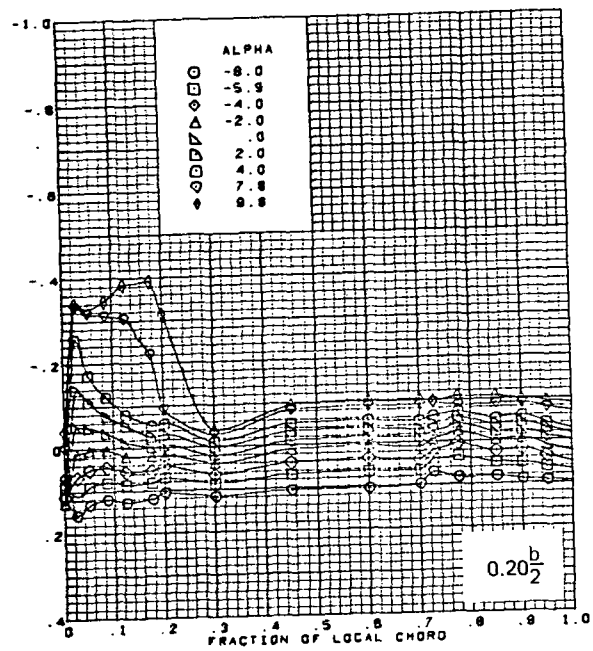
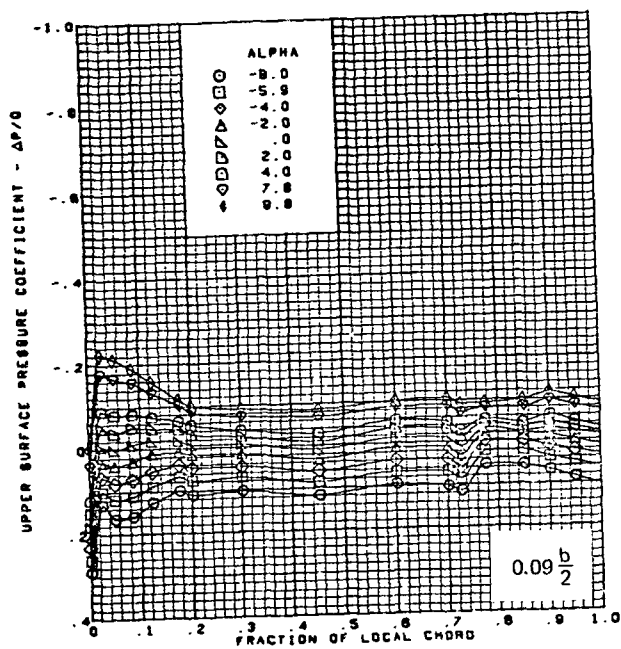
Figure 17.—Wing Experimental Data—Effect of Angle of Attack; Twisted Wing, Rounded L.E.;  
 L.E. Deflection, Full Span =  $0.0^\circ$ ; T.E. Deflection, Full Span =  $0.0^\circ$ ;  $M = 1.60$



Note:  $\Delta C_p$  = increment between adjacent isobars

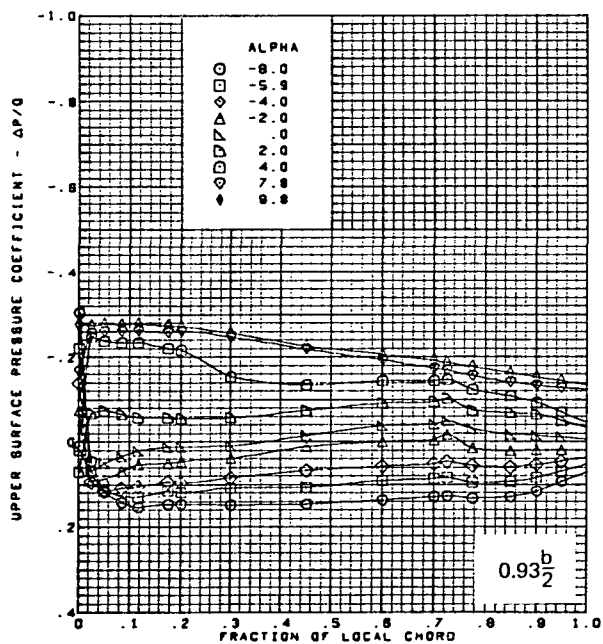
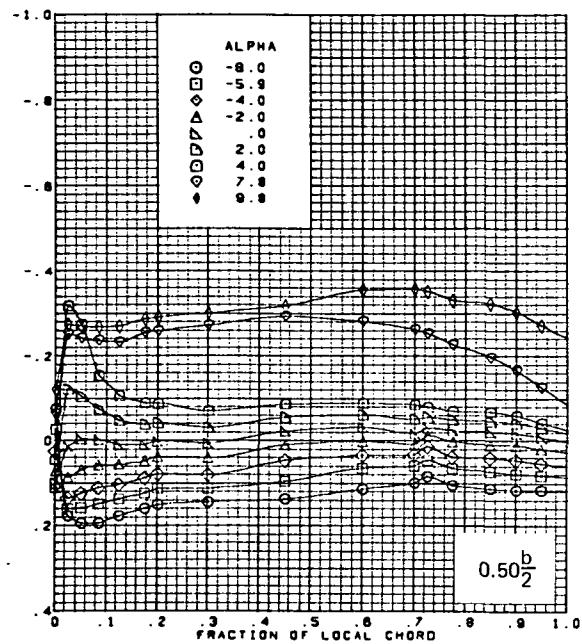
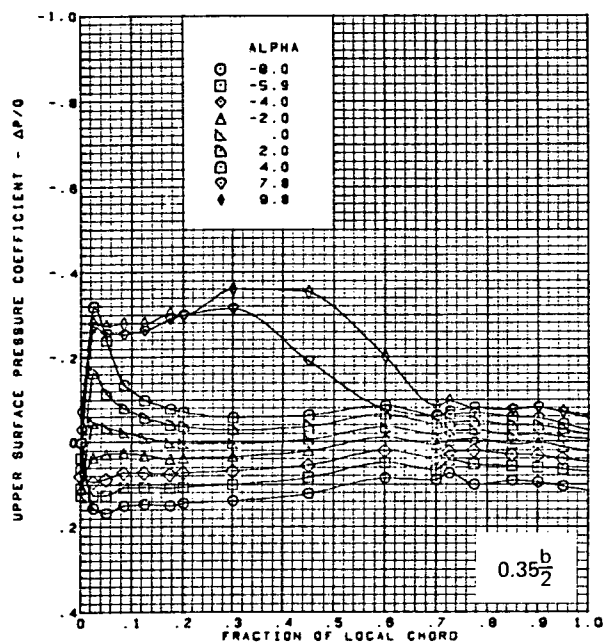
(b) Lower Surface Isobars

Figure 17.—(Continued)



(c) Upper Surface Chordwise Pressure Distributions

Figure 17.—(Continued)

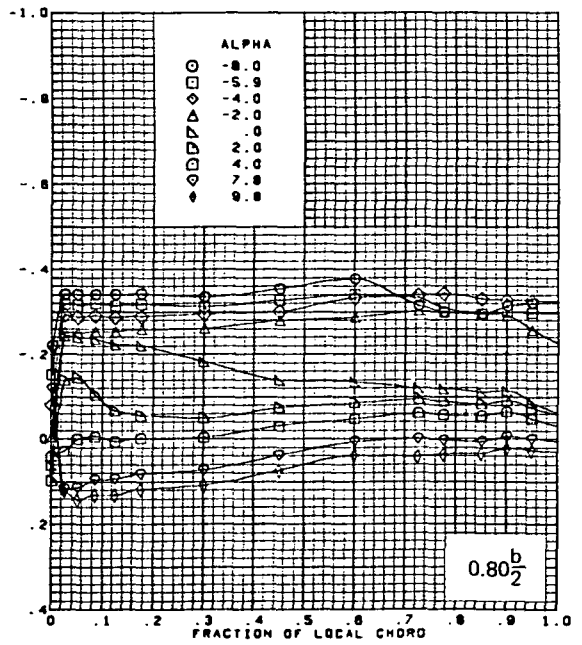
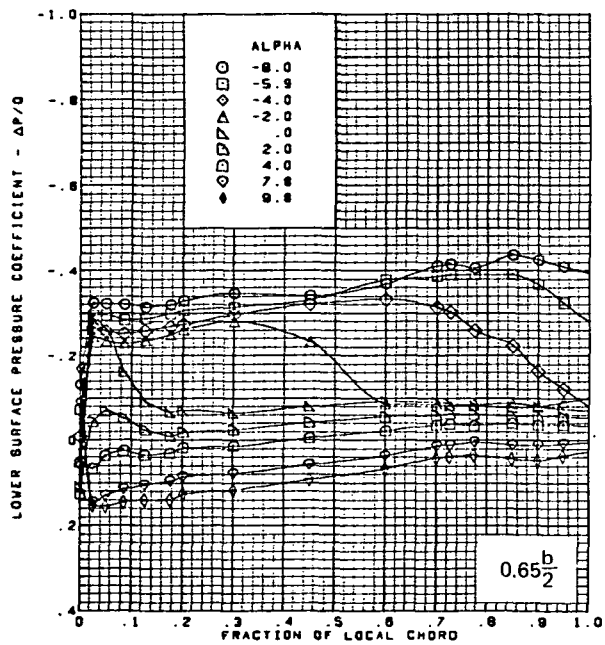
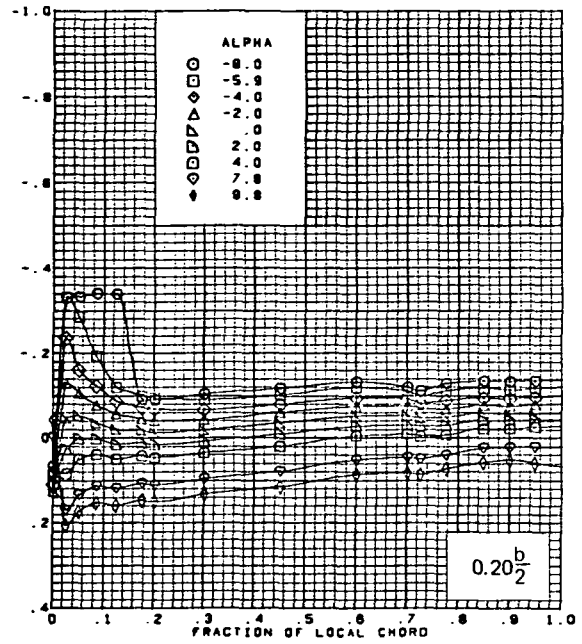
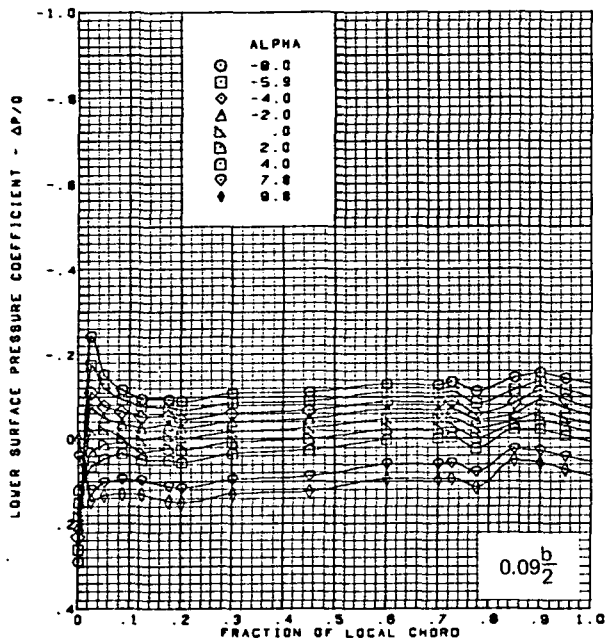


$M = 1.60$  (run 1)  
 Twisted wing, rounded L.E.  
 L.E. deflection, full span =  $0.0^\circ$   
 T.E. deflection, full span =  $0.0^\circ$

Note:  $C_{p, \text{vacuum}} = -0.56$

(c) (Concluded)

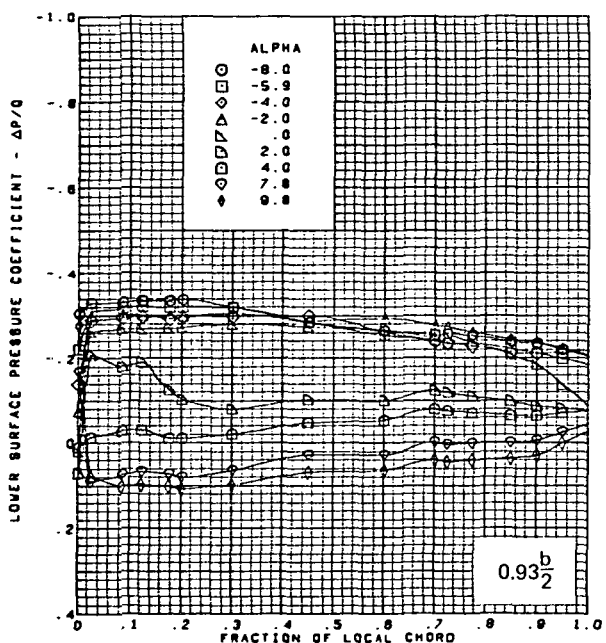
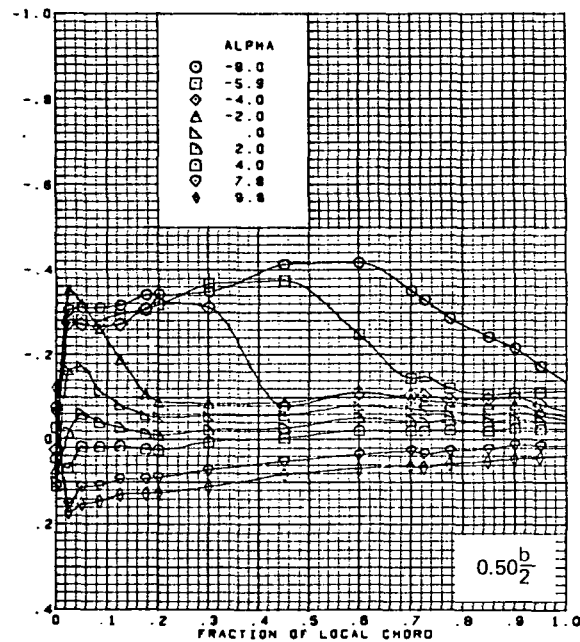
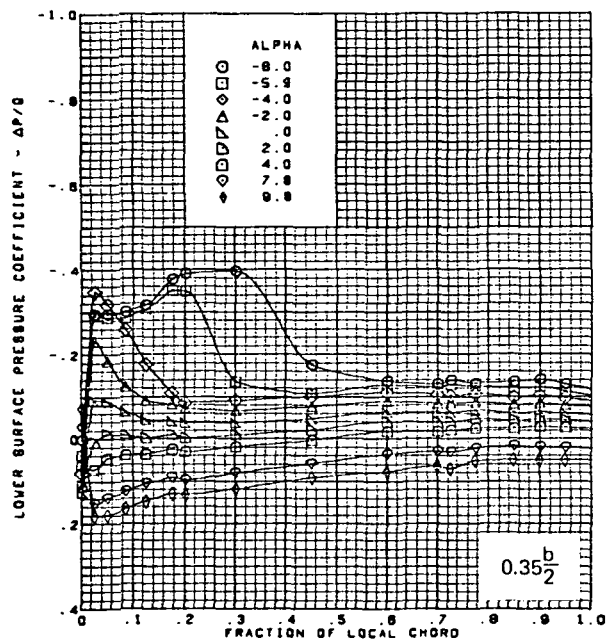
Figure 17.—(Continued)



(d) Lower Surface Chordwise Pressure Distributions

Figure 17.—(Continued)



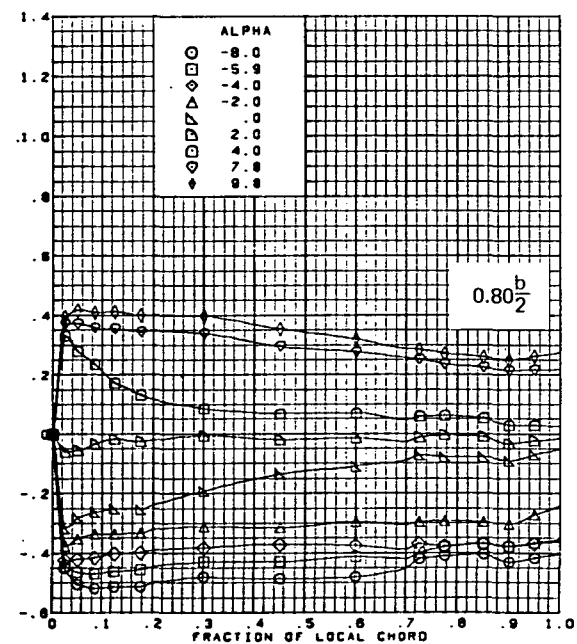
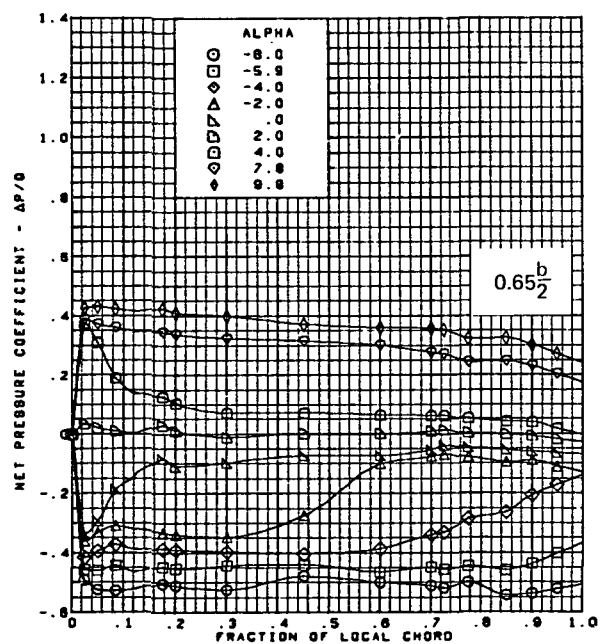
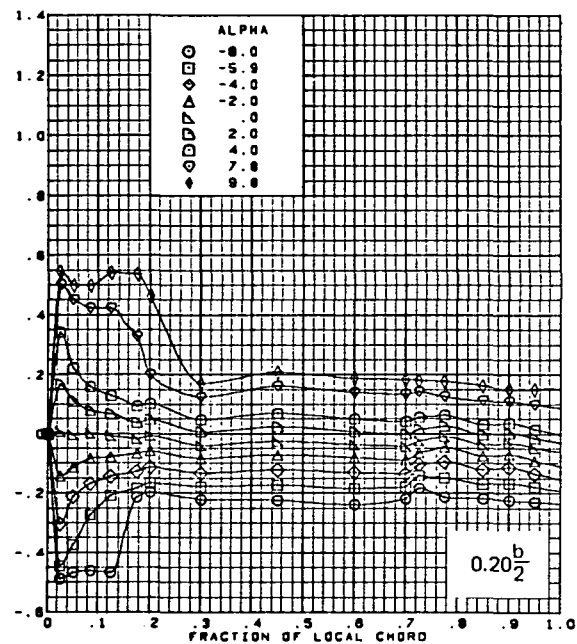
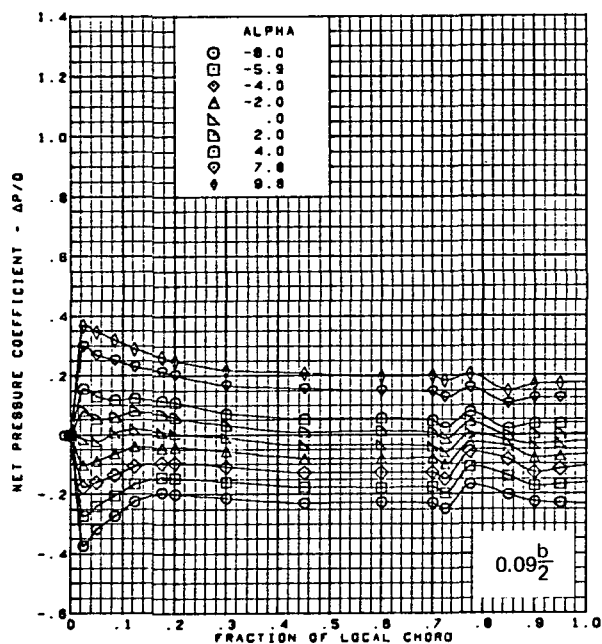


$M = 1.60$  (run 1)  
 Twisted wing, rounded L.E.  
 L.E. deflection, full span =  $0.0^\circ$   
 T.E. deflection, full span =  $0.0^\circ$

Note:  $C_{p, \text{vacuum}} = -0.56$

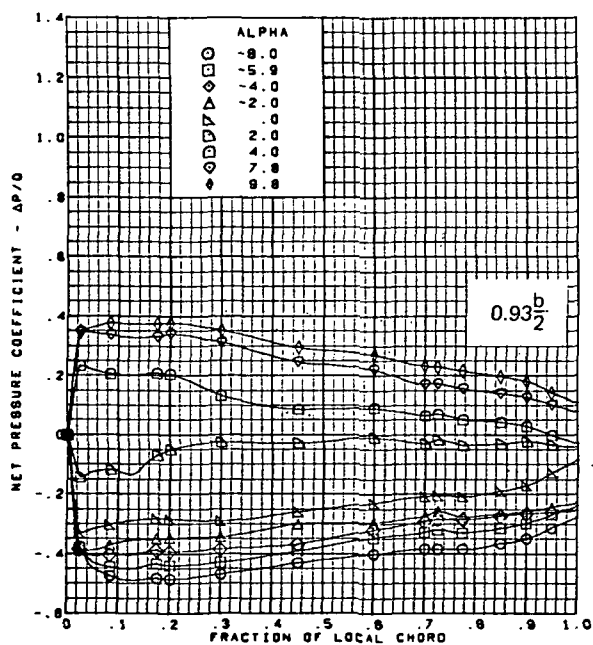
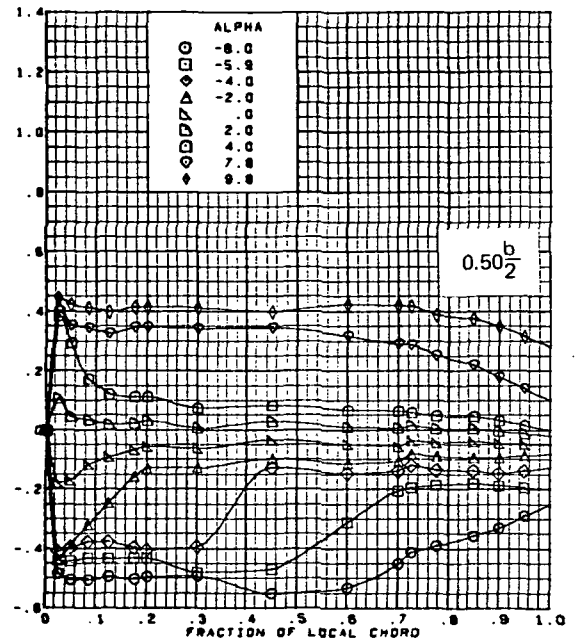
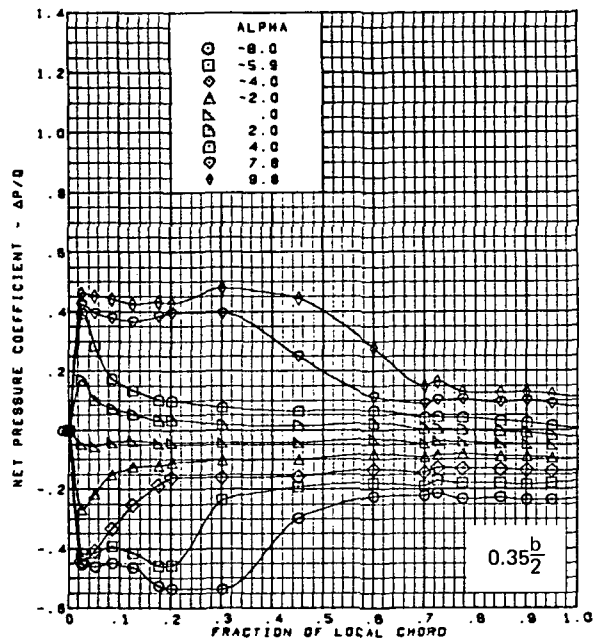
(d) (Concluded)

Figure 17.—(Continued)



(e) Net Chordwise Pressure Distributions

Figure 17.—(Continued)

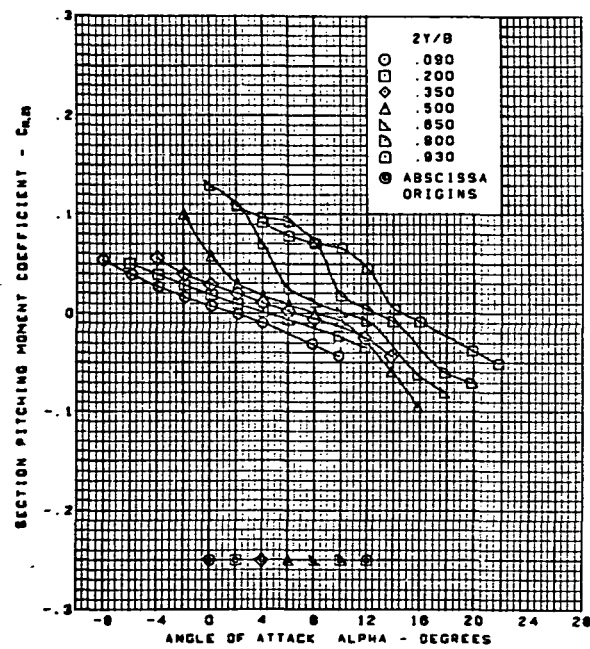
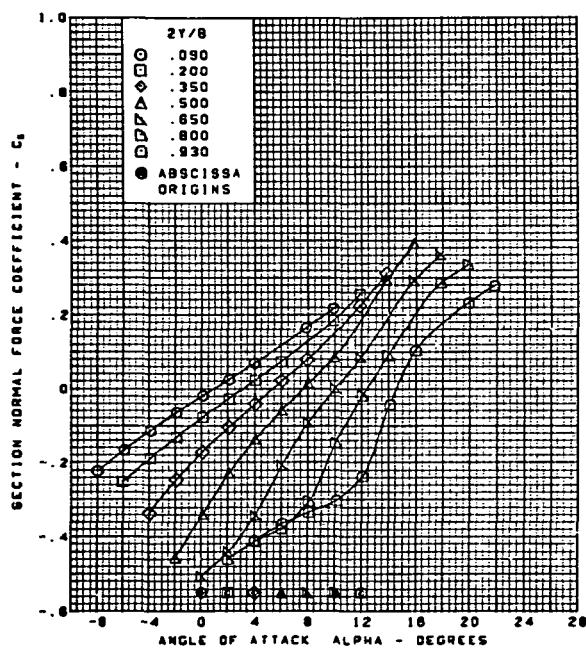
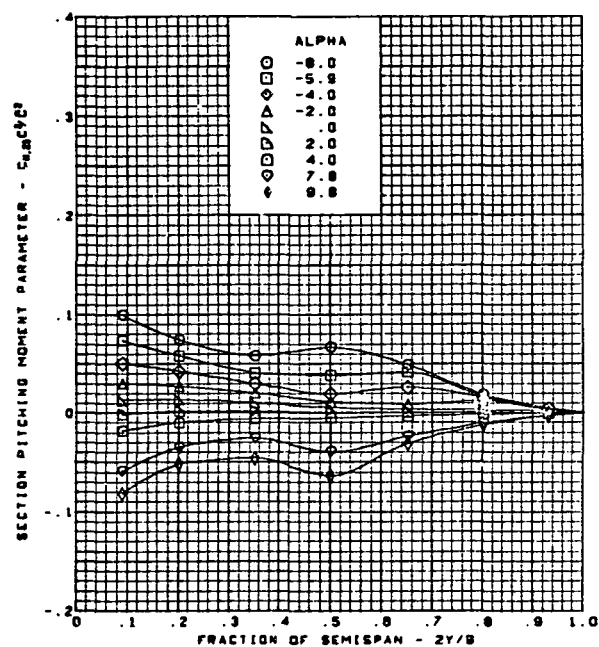
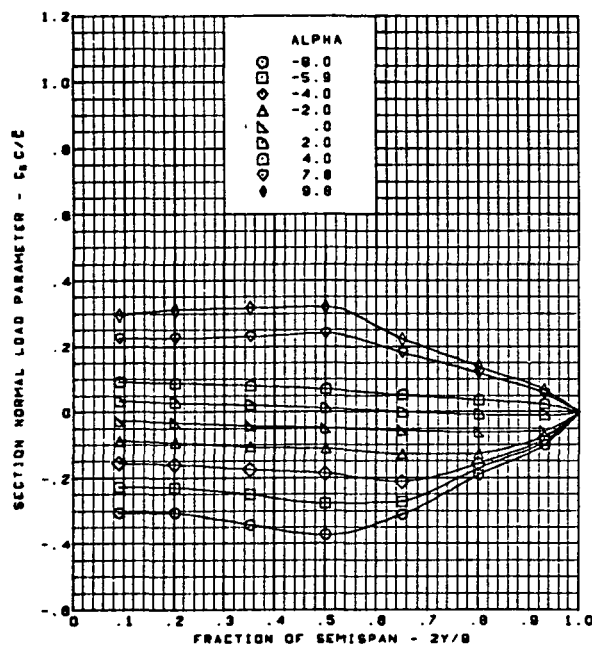


M = 1.60 (run 1)  
 Twisted wing, rounded L.E.  
 L.E. deflection, full span =  $0.0^\circ$   
 T.E. deflection, full span =  $0.0^\circ$

(e) (Concluded)

Figure 17.—(Continued)

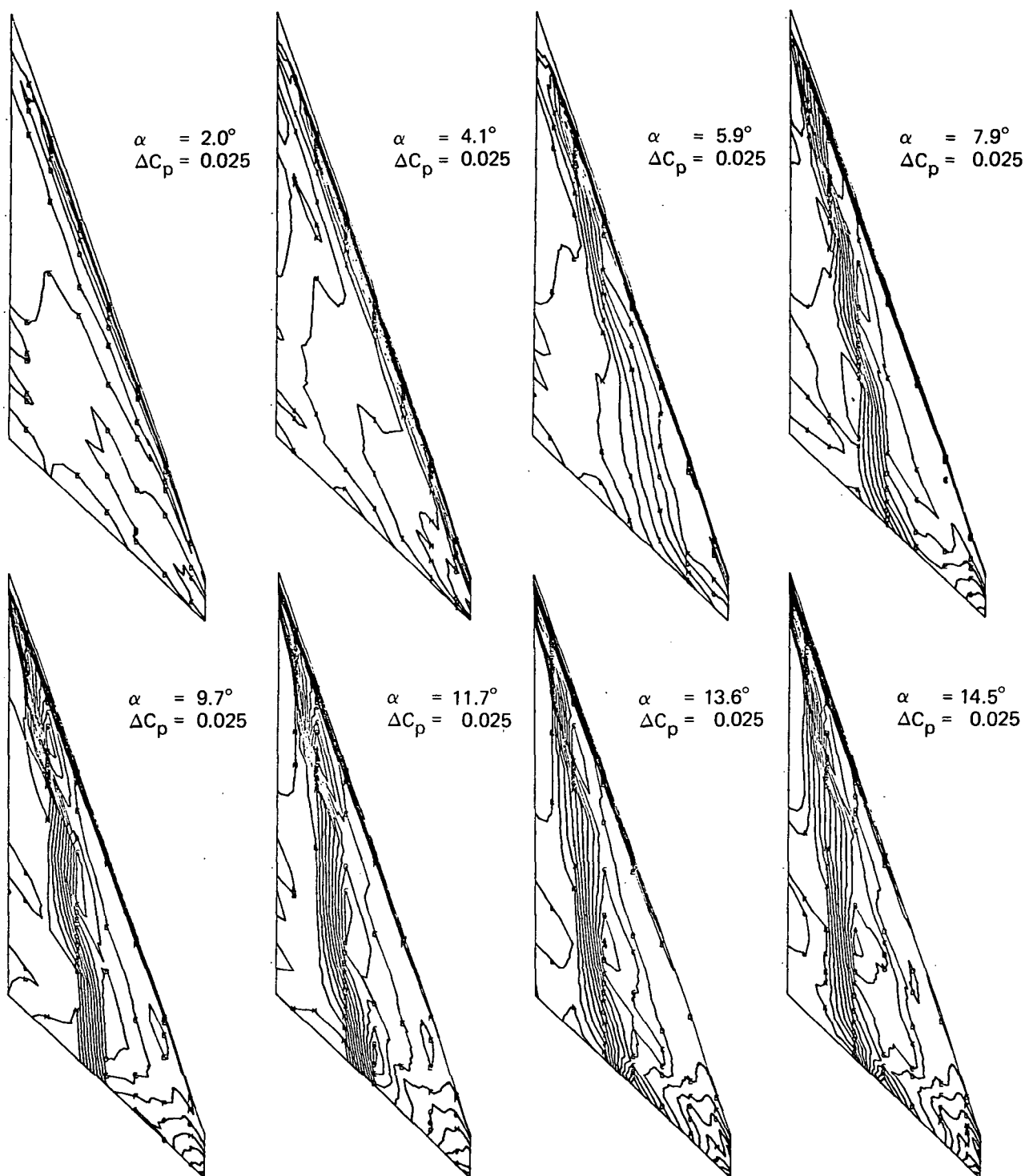
**Page  
Intentionally  
Left Blank**



$M = 1.60$  (run 1)  
 Twisted wing, rounded L.E.  
 L.E. deflection, full span =  $0.0^\circ$   
 T.E. deflection, full span =  $0.0^\circ$

(f) Spanload Distributions and Section Aerodynamic Coefficients

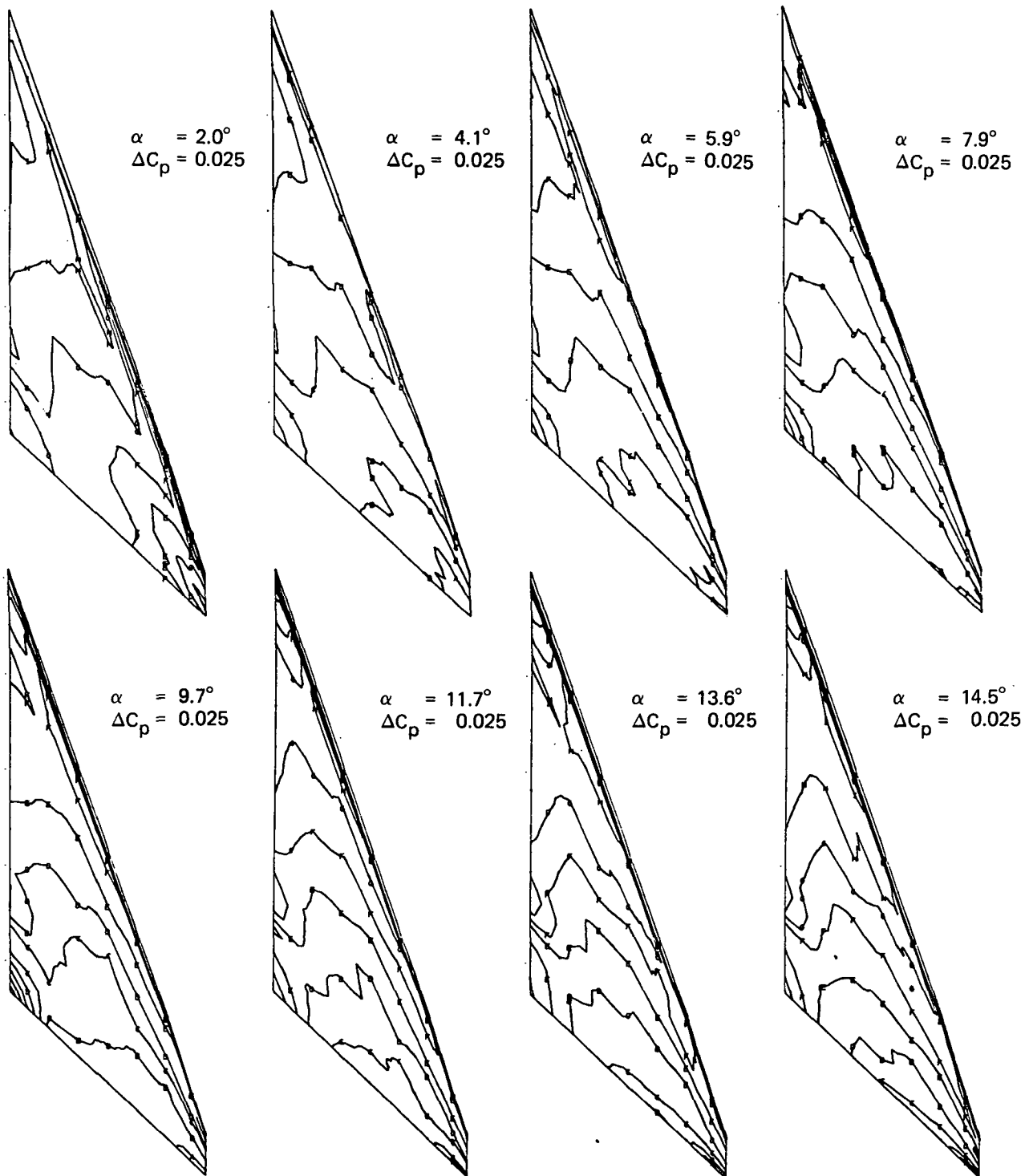
Figure 17.—(Concluded)



Note:  $\Delta C_p$  = increment between adjacent isobars

(a) Upper Surface Isobars

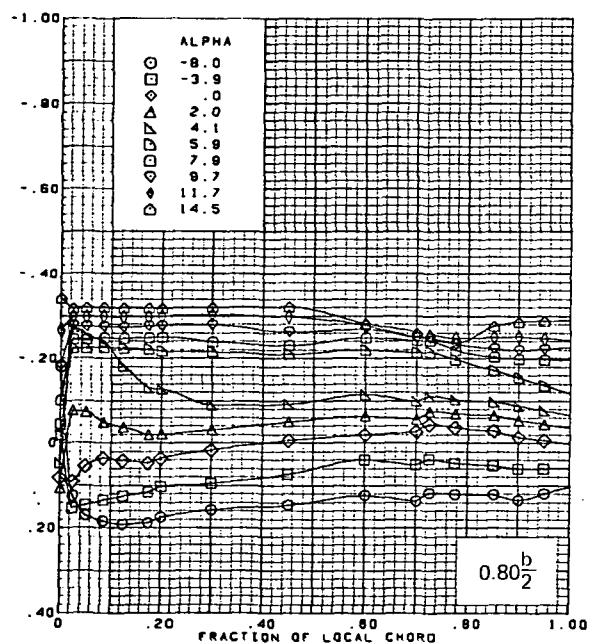
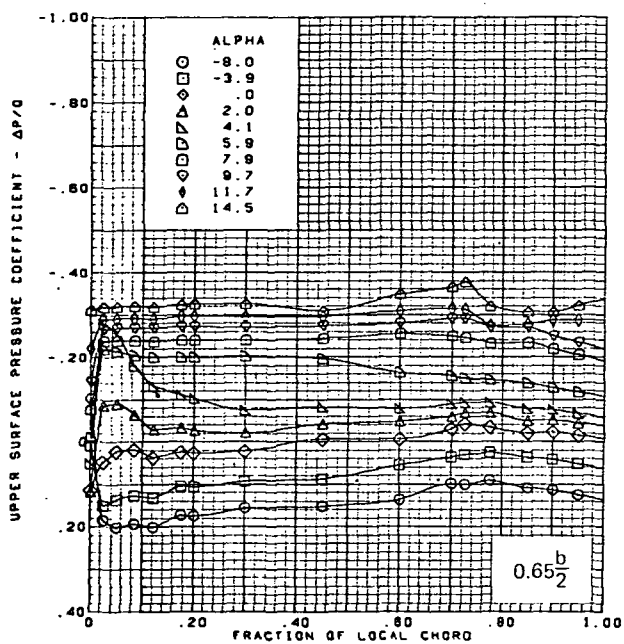
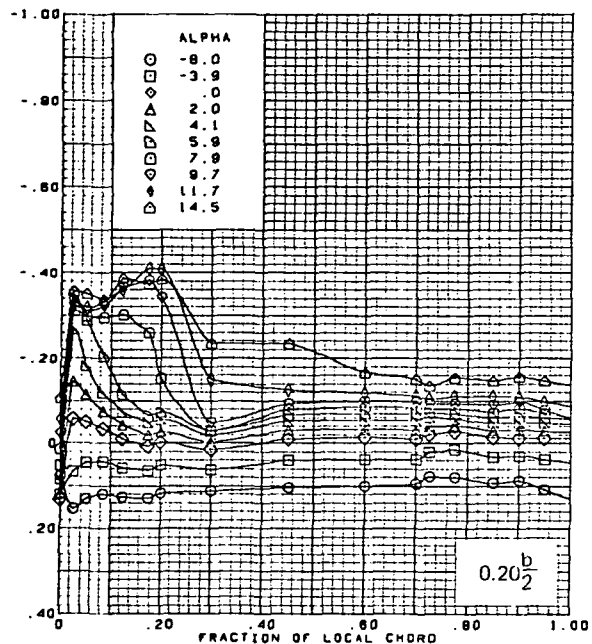
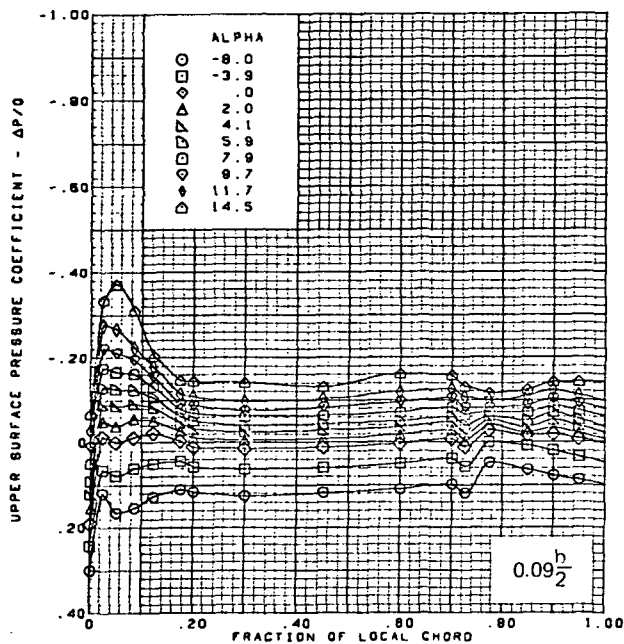
Figure 18.—Wing Experimental Data—Effect of Angle of Attack; Twisted Wing, Rounded L.E.;  
 L.E. Deflection, Full Span =  $0.0^\circ$ ; T.E. Deflection, Full Span =  $0.0^\circ$ ;  $M = 1.70$



Note:  $\Delta C_p$  = increment between adjacent isobars

(b) Lower Surface Isobars

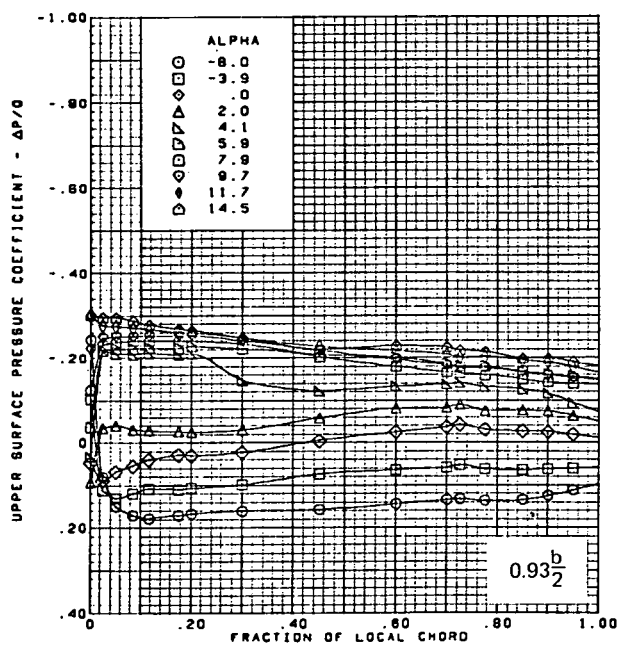
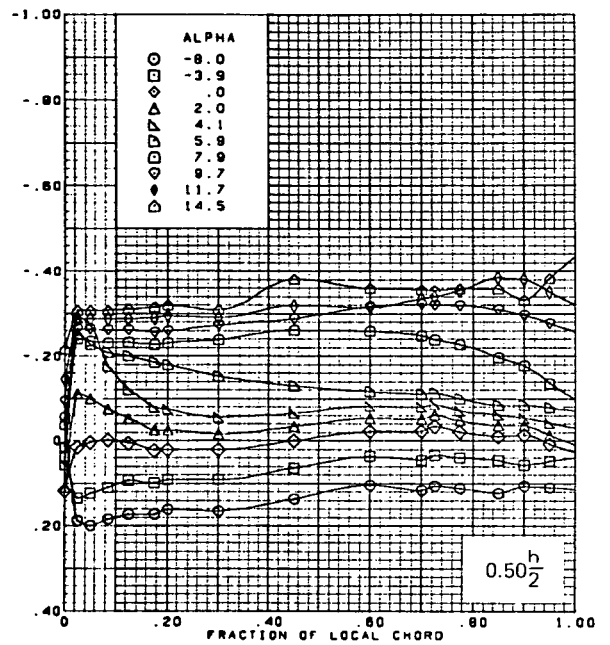
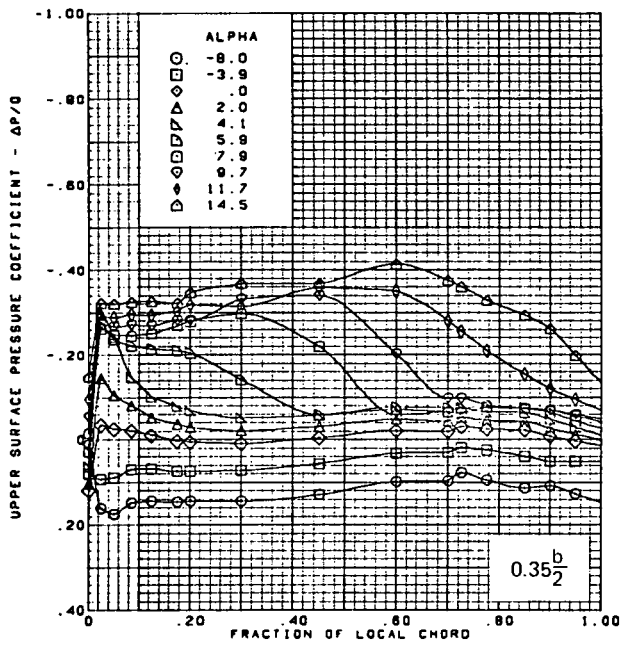
Figure 18.—(Continued)



(c) Upper Surface Chordwise Pressure Distributions

Figure 18.—(Continued)



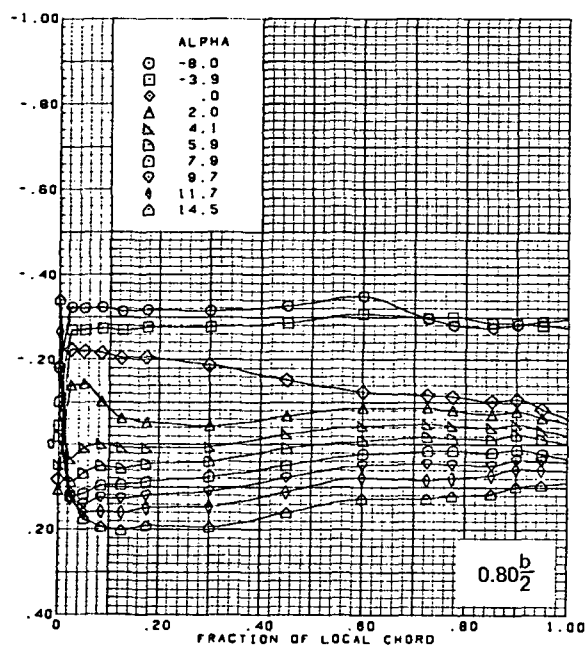
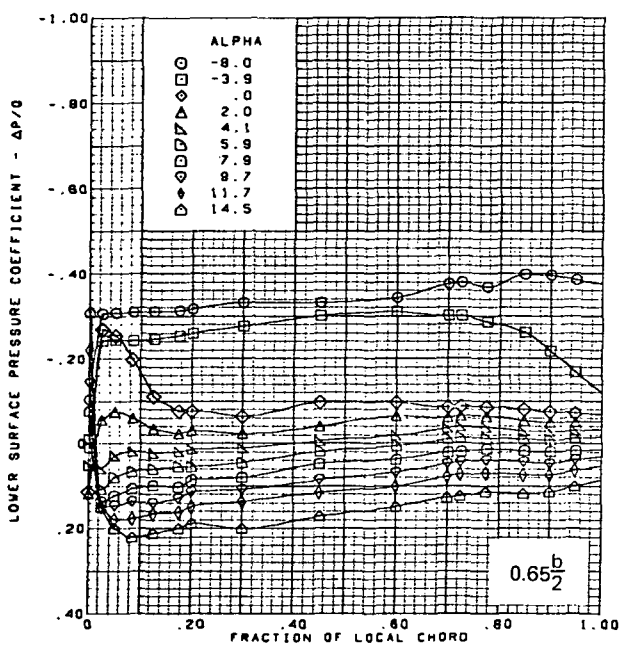
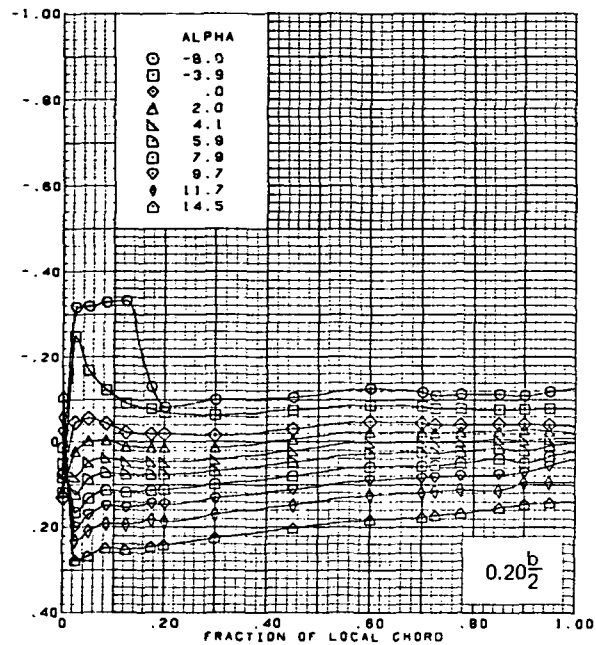
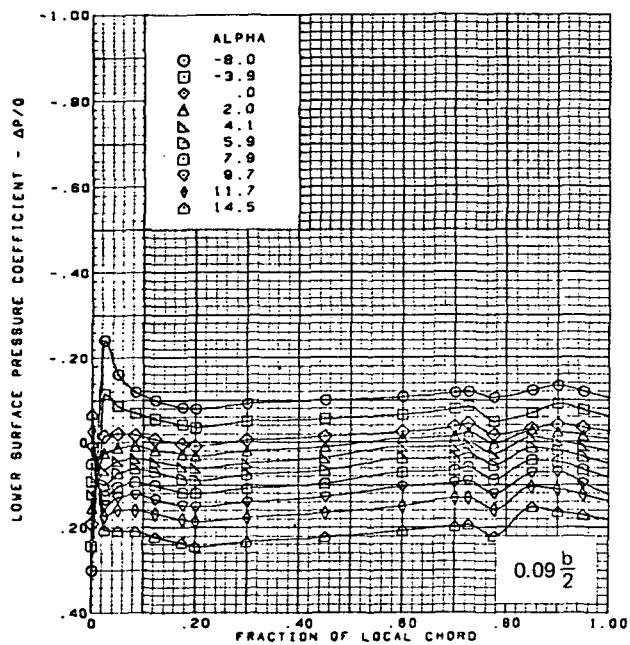


M = 1.70 (run 3)  
 Twisted wing, rounded L.E.  
 L.E. deflection, full span =  $0.0^\circ$   
 T.E. deflection, full span =  $0.0^\circ$

Note:  $C_{p, \text{vacuum}} = -0.49$

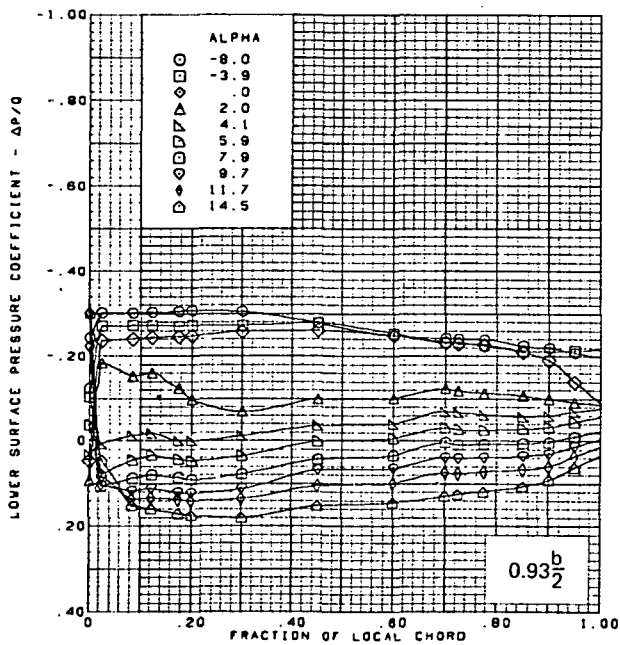
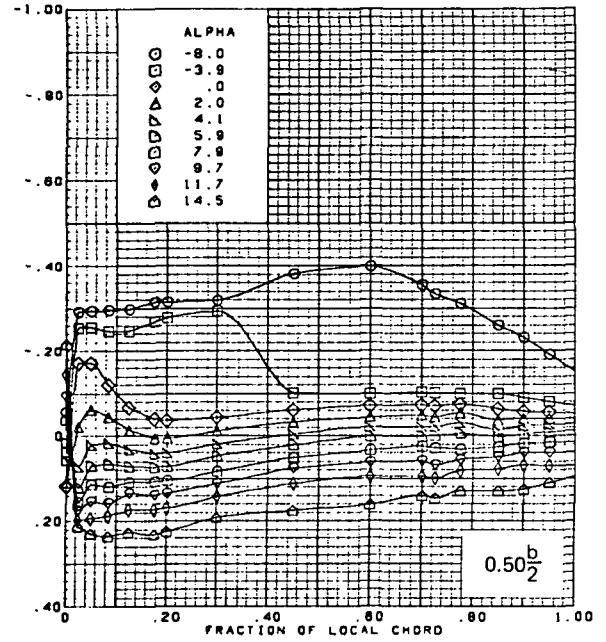
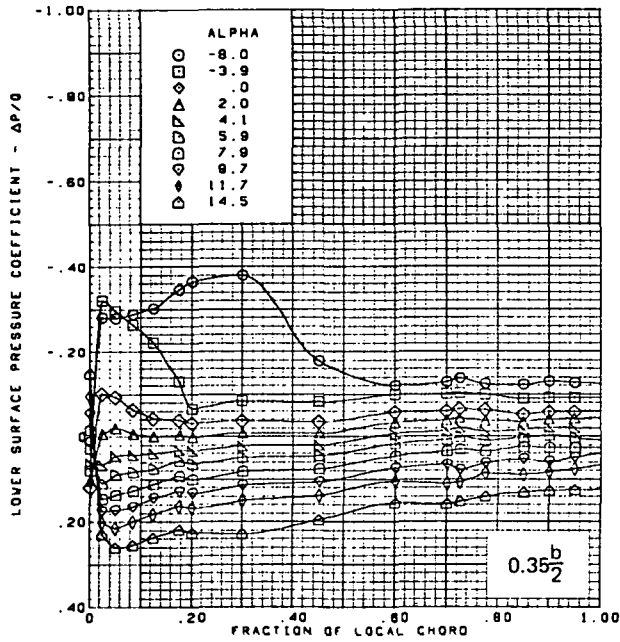
(c) (Concluded)

Figure 18.—(Continued)



(d) Lower Surface Chordwise Pressure Distributions

Figure 18.—(Continued)

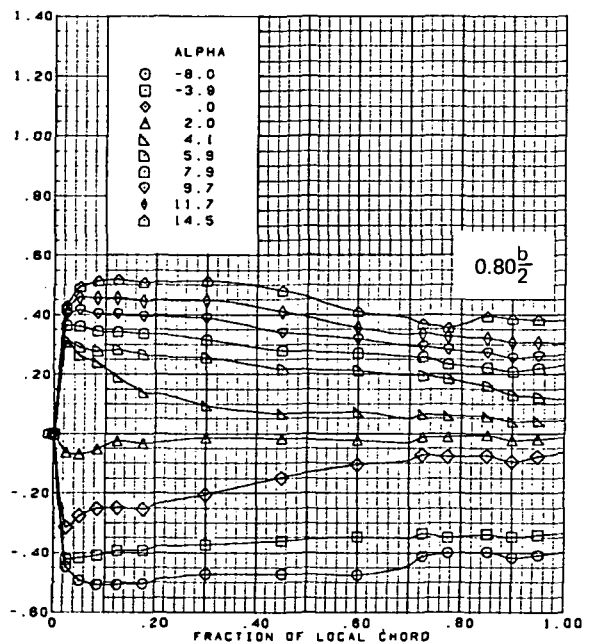
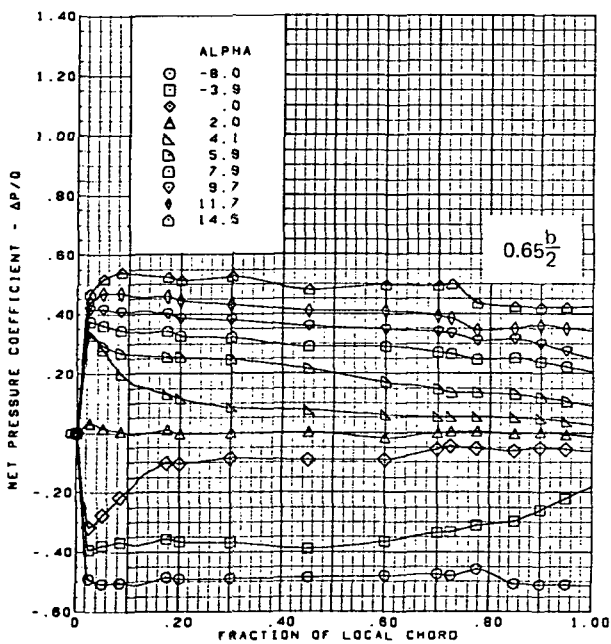
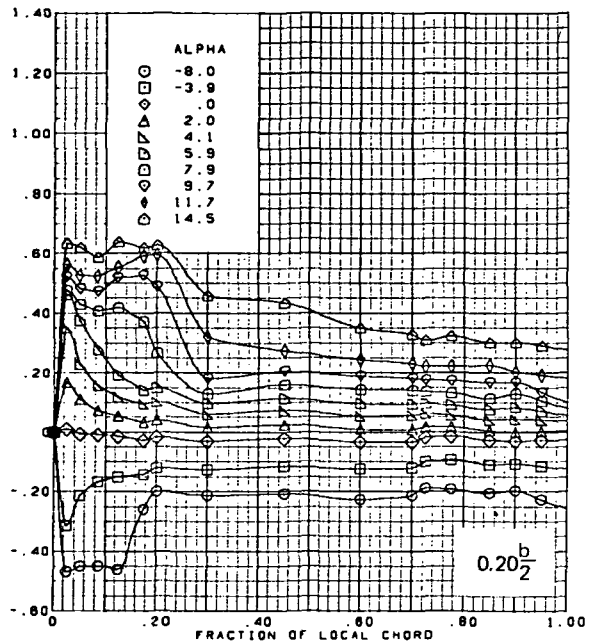
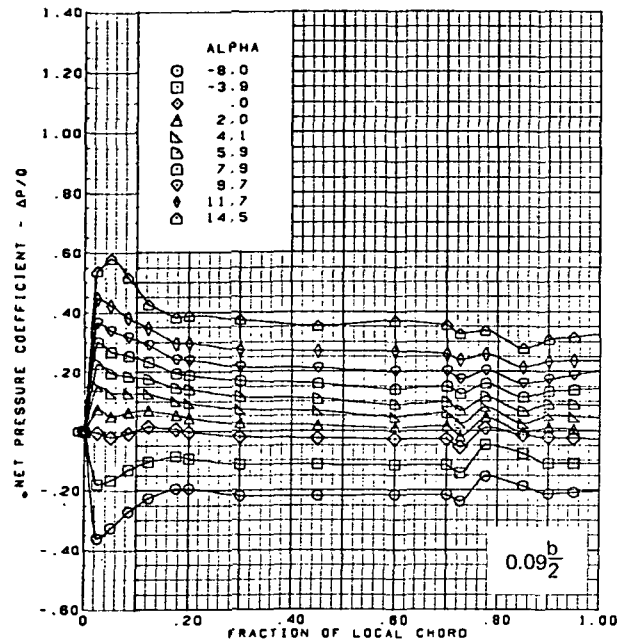


$M = 1.70$  (run 3)  
 Twisted wing, rounded L.E.  
 L.E. deflection, full span =  $0.0^\circ$   
 T.E. deflection, full span =  $0.0^\circ$

Note:  $C_{p, \text{vacuum}} = -0.49$

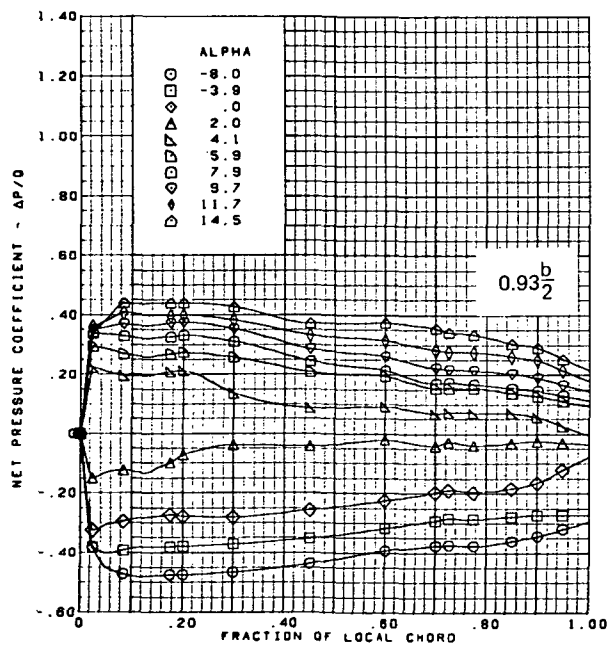
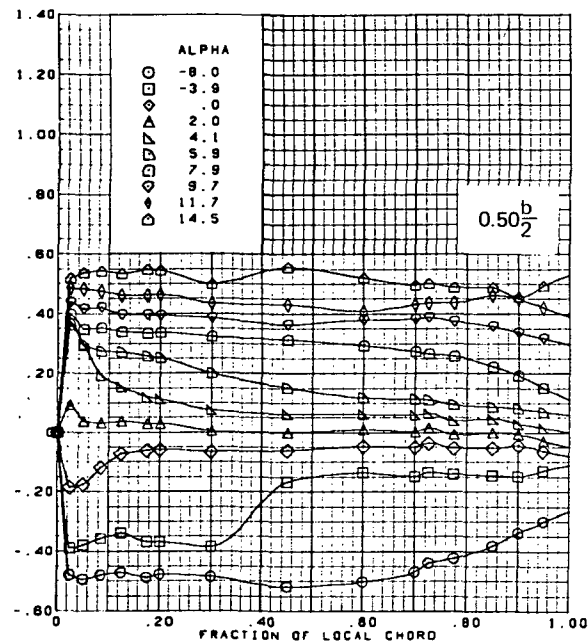
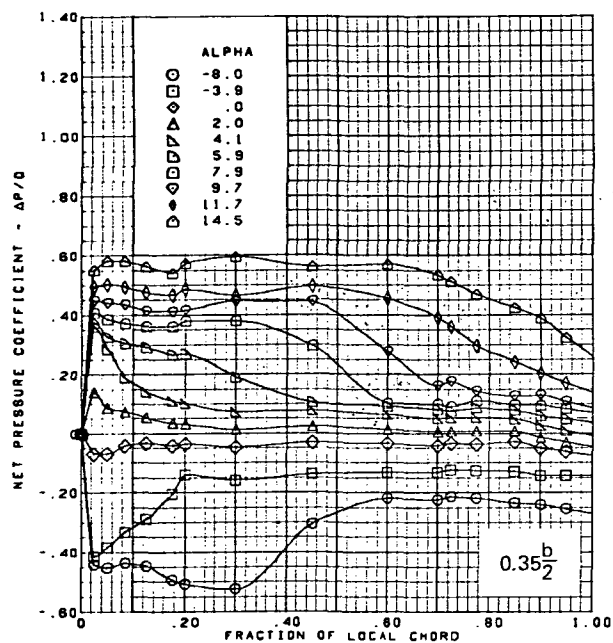
(d) (Concluded)

Figure 18.—(Continued)



(e) Net Chordwise Pressure Distributions

Figure 18.—(Continued)

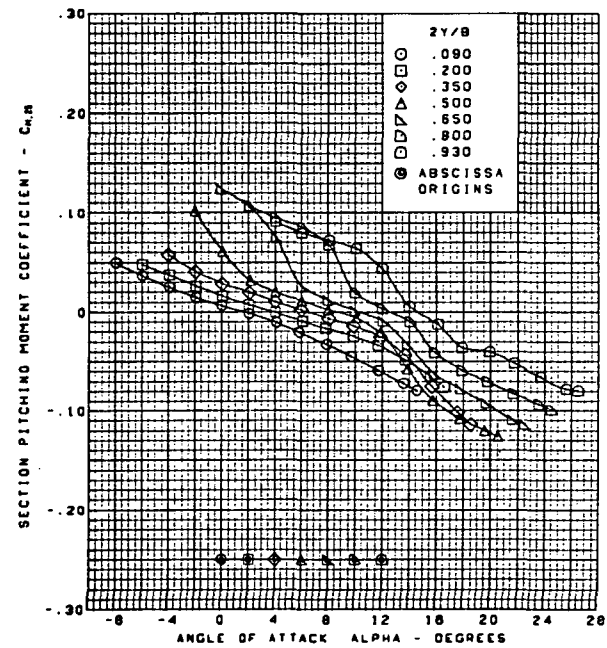
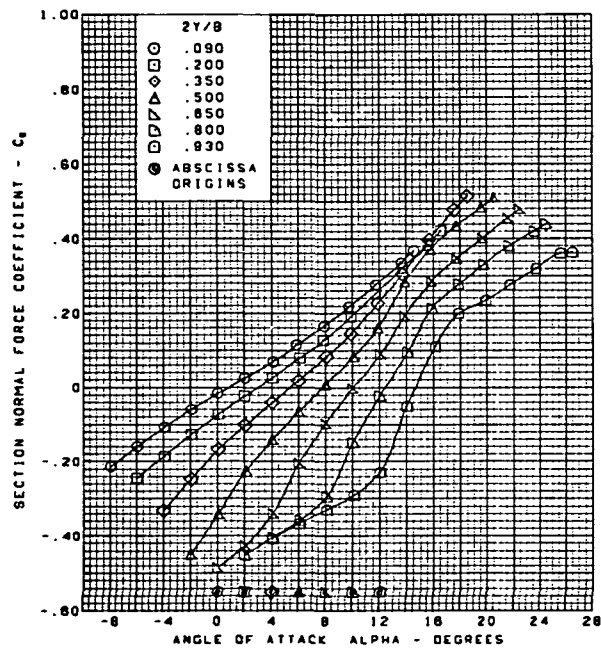
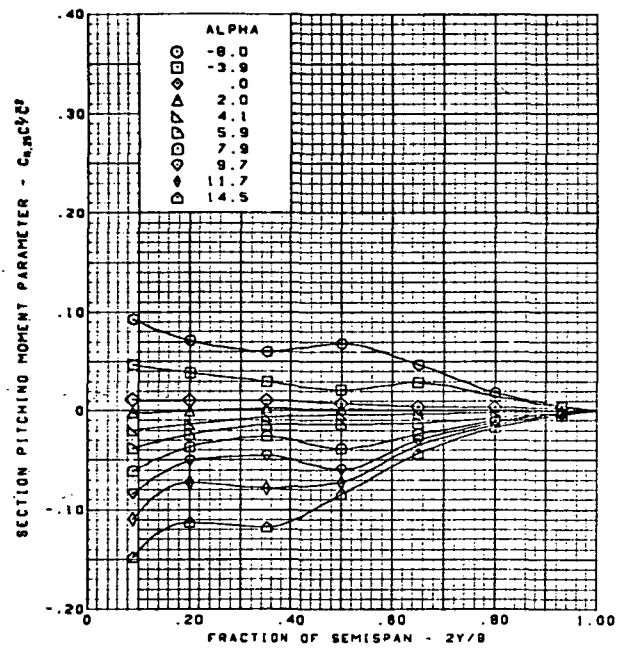
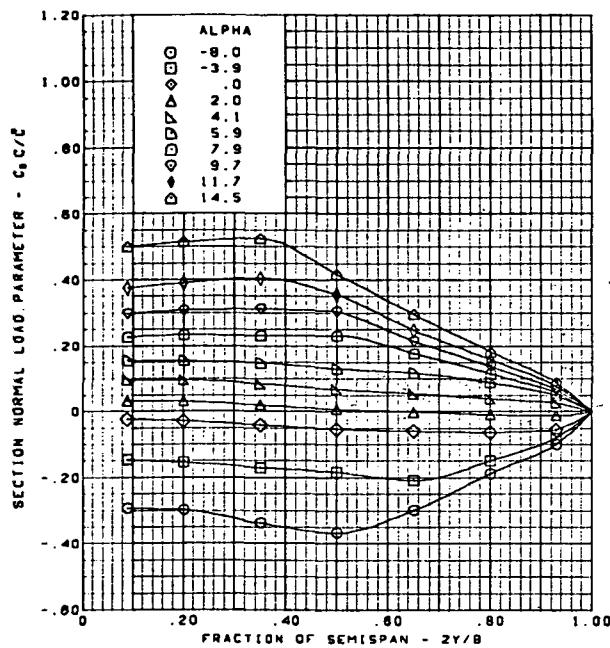


$M = 1.70$  (run 3)  
 Twisted wing, rounded L.E.  
 L.E. deflection, full span =  $0.0^\circ$   
 T.E. deflection, full span =  $0.0^\circ$

(e) (Concluded)

Figure 18.—(Continued)

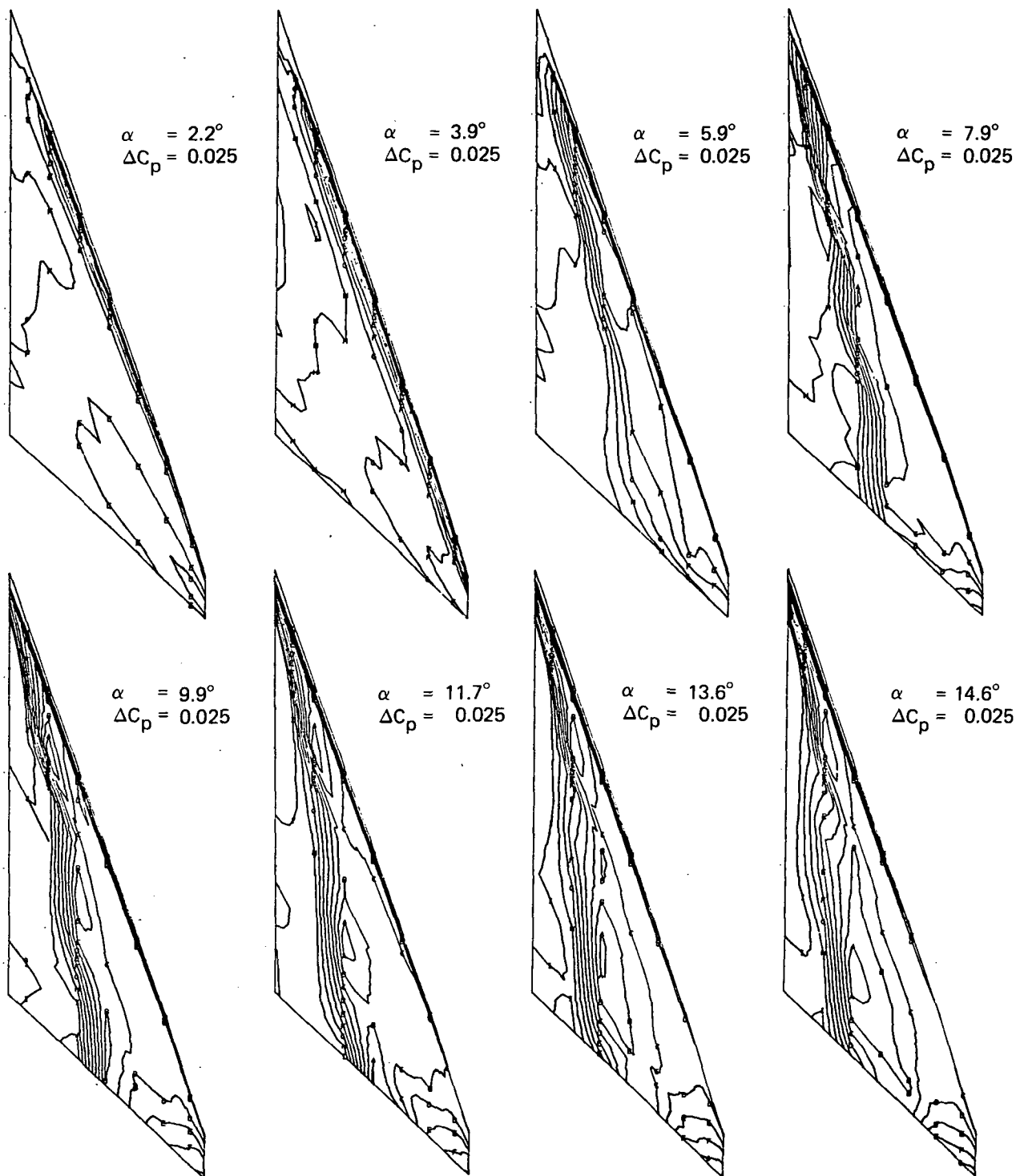
**Page  
Intentionally  
Left Blank**



M = 1.70 (run 3)  
 Twisted wing, rounded L.E.  
 L.E. deflection, full span =  $0.0^\circ$   
 T.E. deflection, full span =  $0.0^\circ$

(f) Spanload Distributions and Section Aerodynamic Coefficients

Figure 18.—(Concluded)

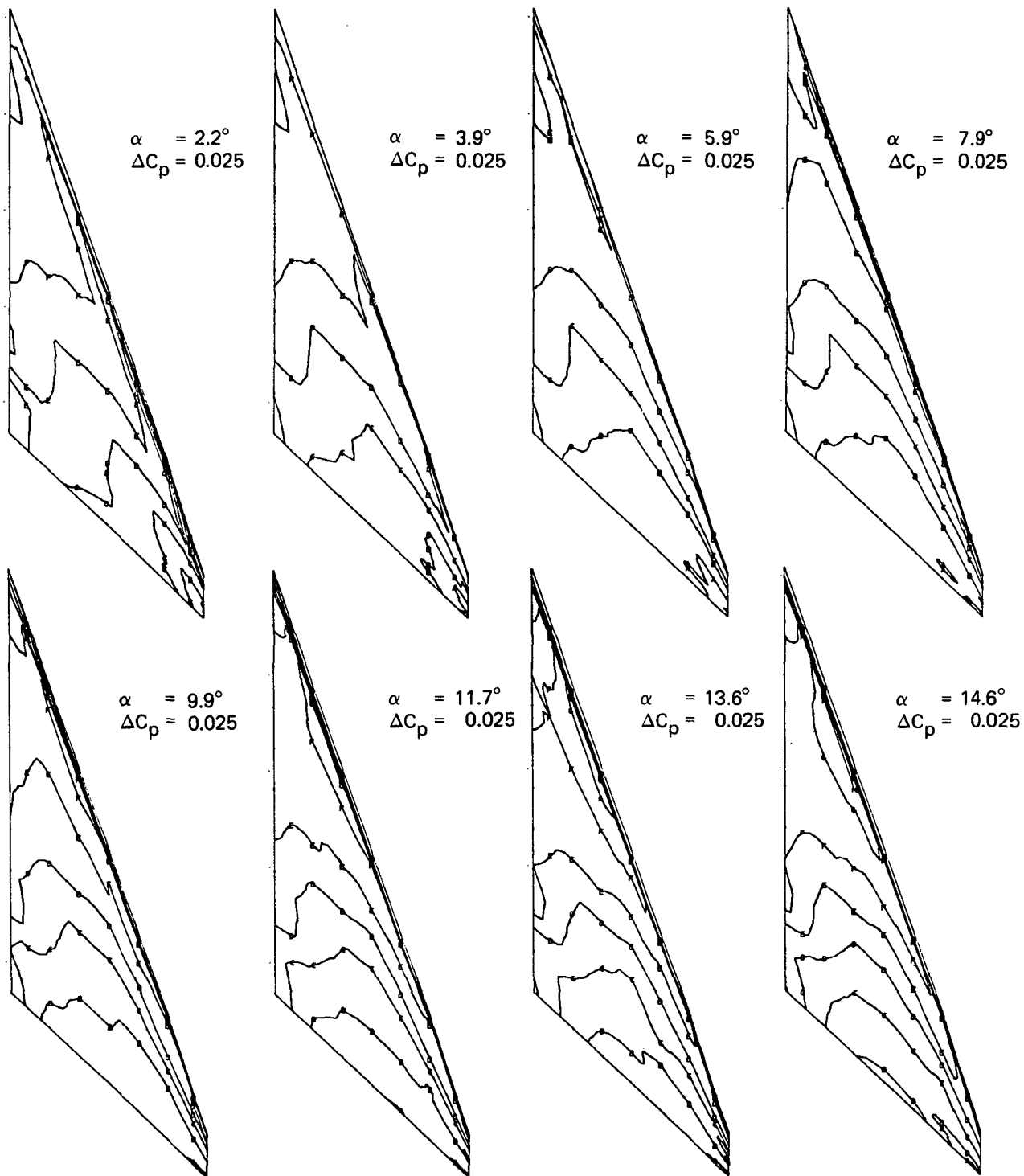


Note:  $\Delta C_p$  = increment between adjacent isobars

(a) Upper Surface Isobars

Figure 19.—Wing Experimental Data—Effect of Angle of Attack; Twisted Wing, Rounded L.E.;  
 L.E. Deflection, Full Span =  $0.0^\circ$ ; T.E. Deflection, Full Span =  $0.0^\circ$ ;  $M = 1.90$

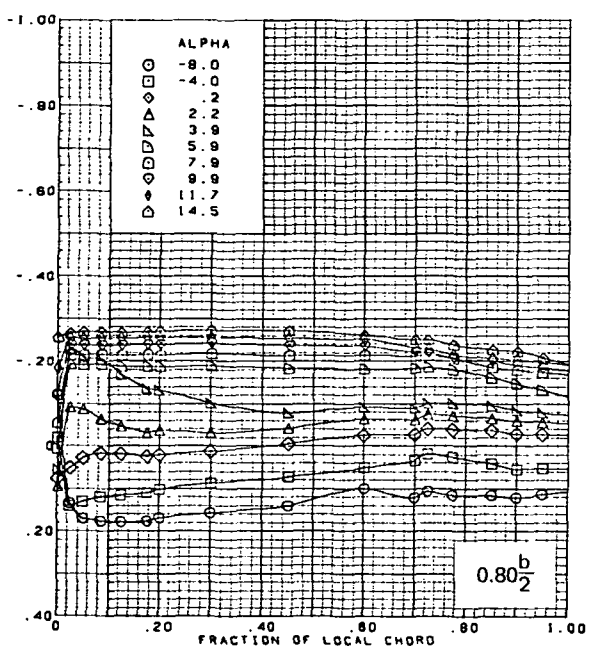
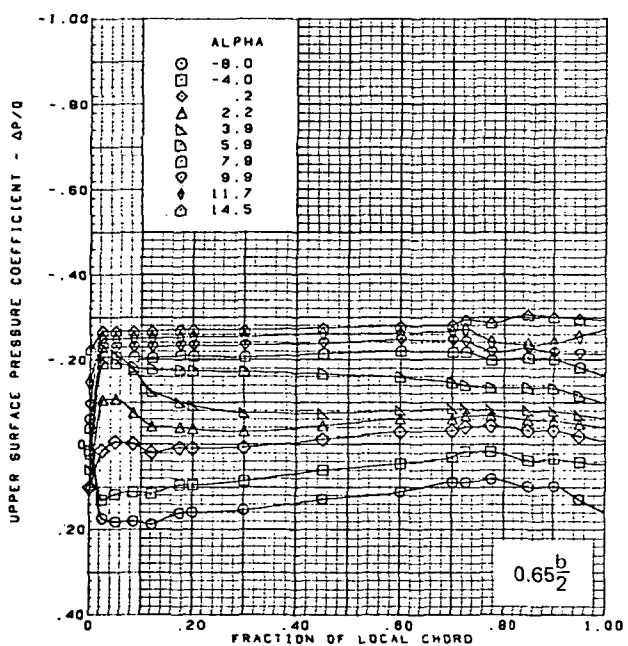
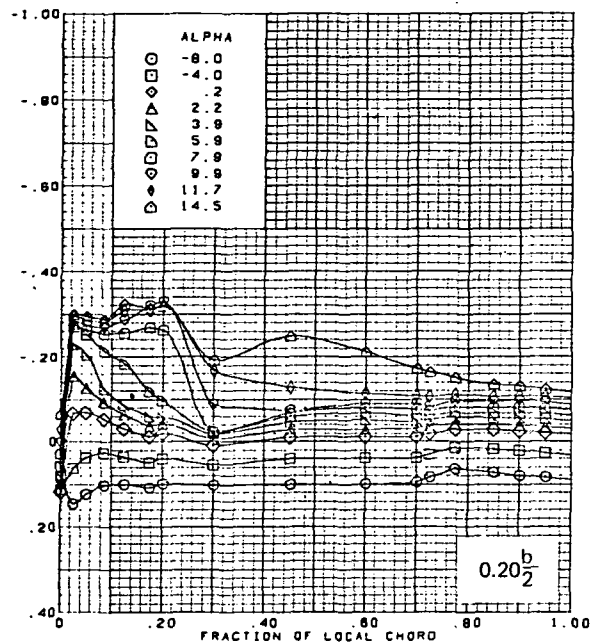
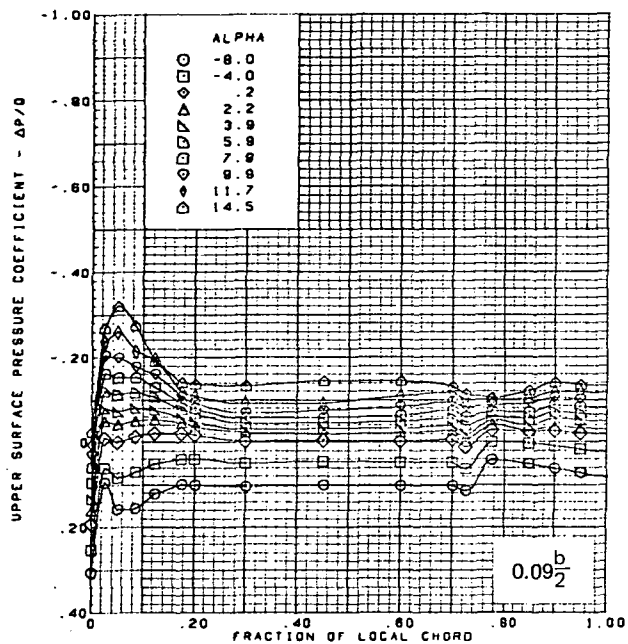




Note:  $\Delta C_p$  = increment between adjacent isobars

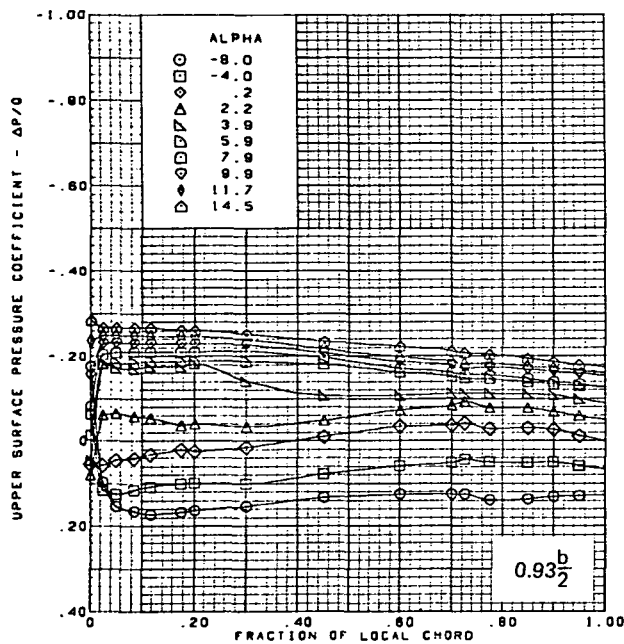
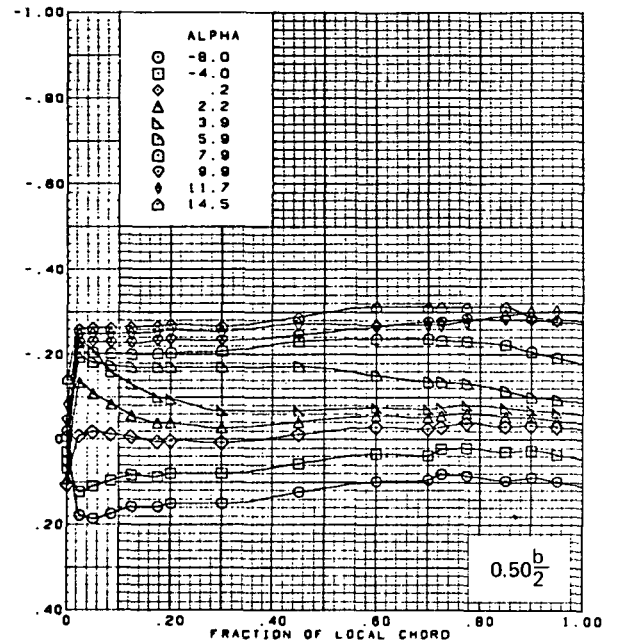
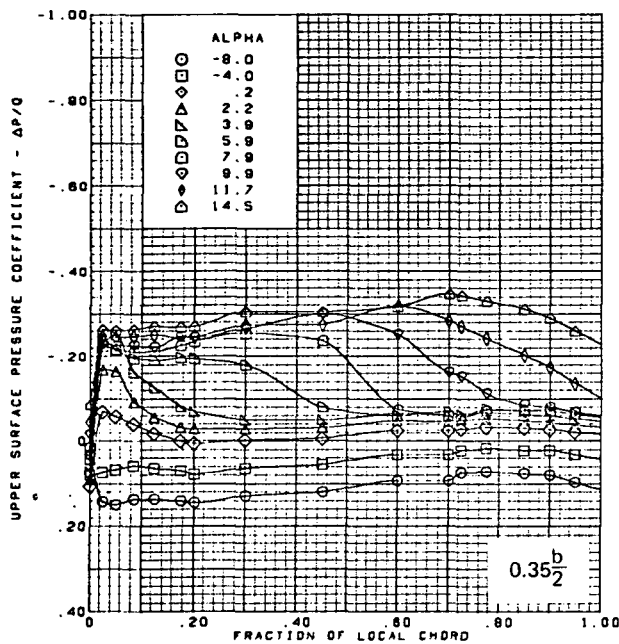
(b) Lower Surface Isobars

Figure 19.—(Continued)



(c) Upper Surface Chordwise Pressure Distributions

Figure 19.—(Continued)

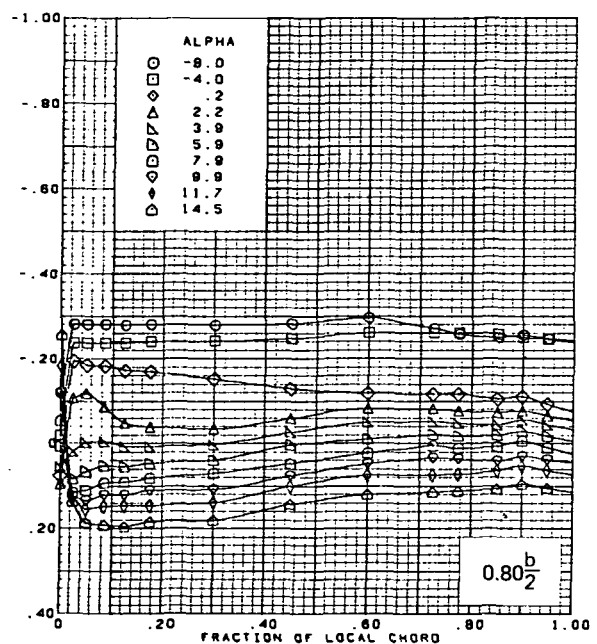
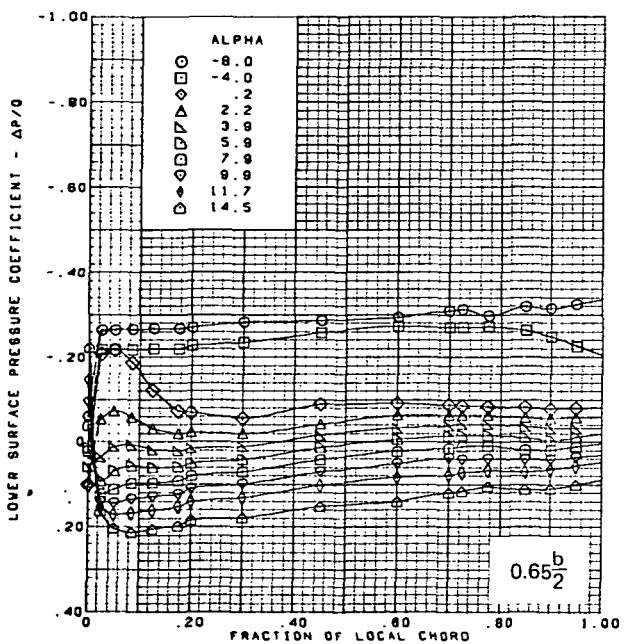
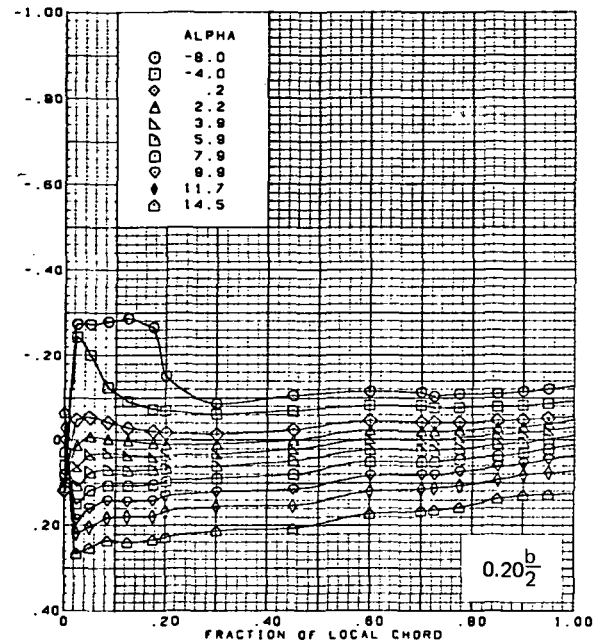
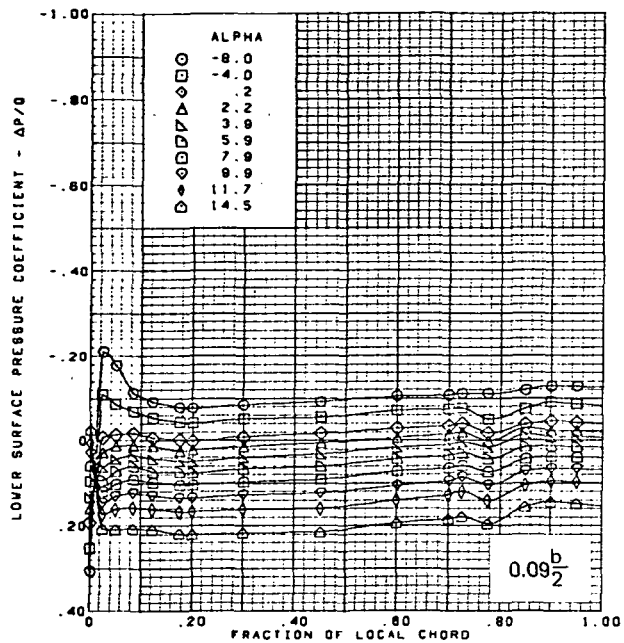


$M = 1.90$  (run 4,6)  
 Twisted wing, rounded L.E.  
 L.E. deflection, full span =  $0.0^\circ$   
 T.E. deflection, full span =  $0.0^\circ$

Note:  $C_{p, \text{vacuum}} = -0.40$

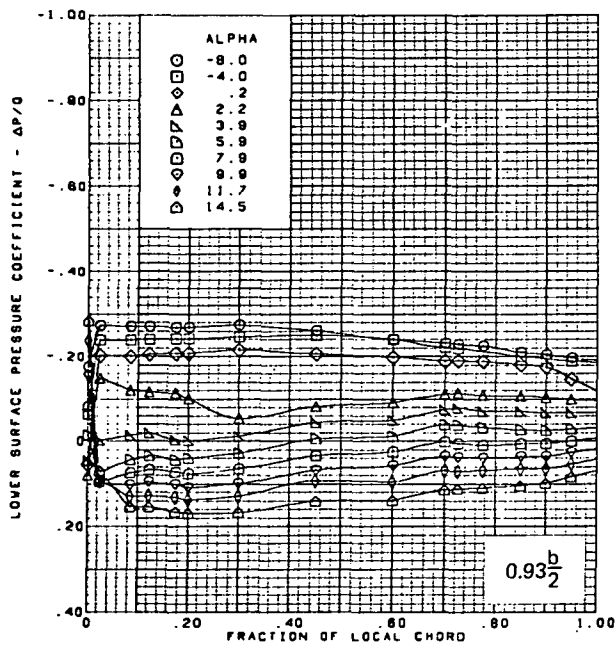
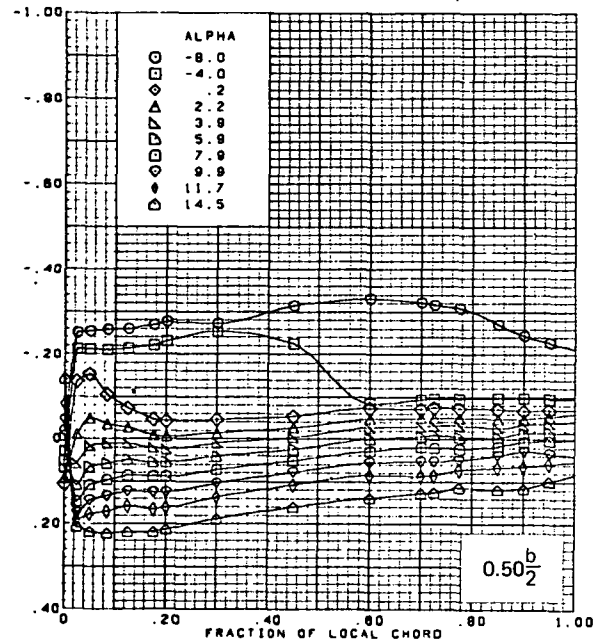
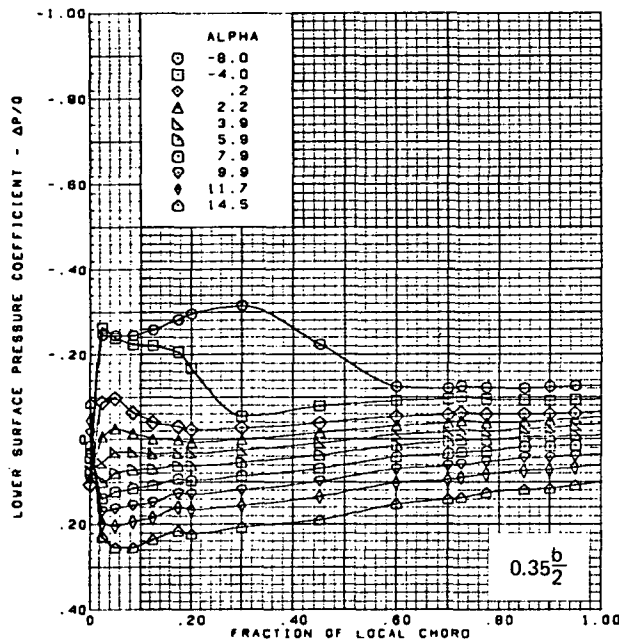
(c) (Concluded)

Figure 19.—(Continued)



(d) Lower Surface Chordwise Pressure Distributions

Figure 19.—(Continued)

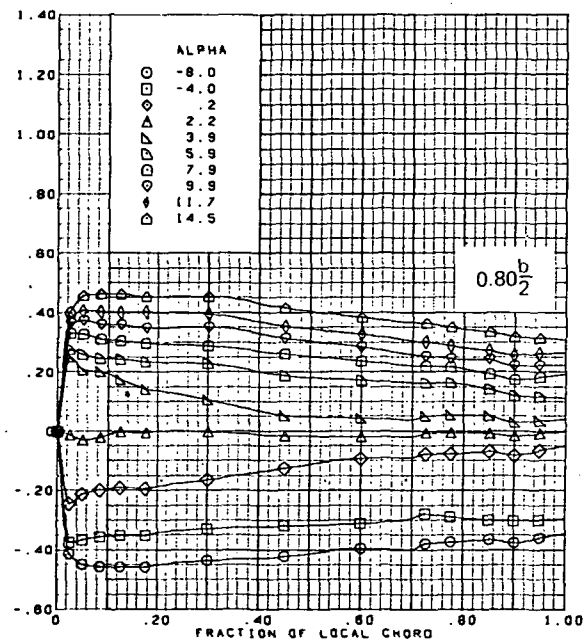
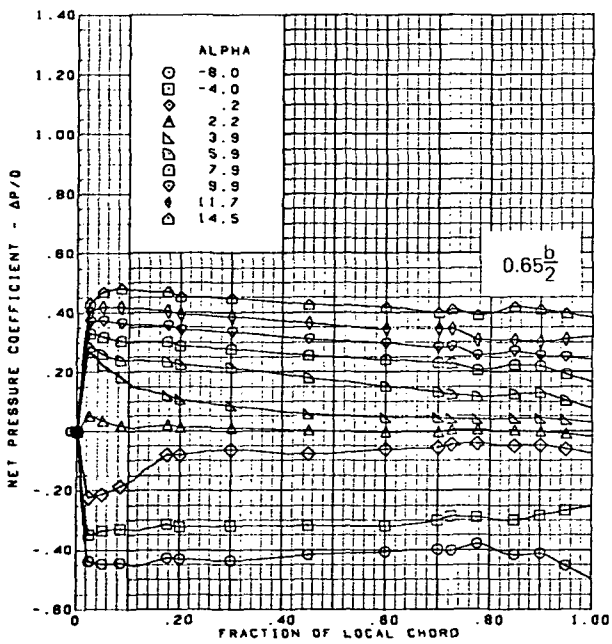
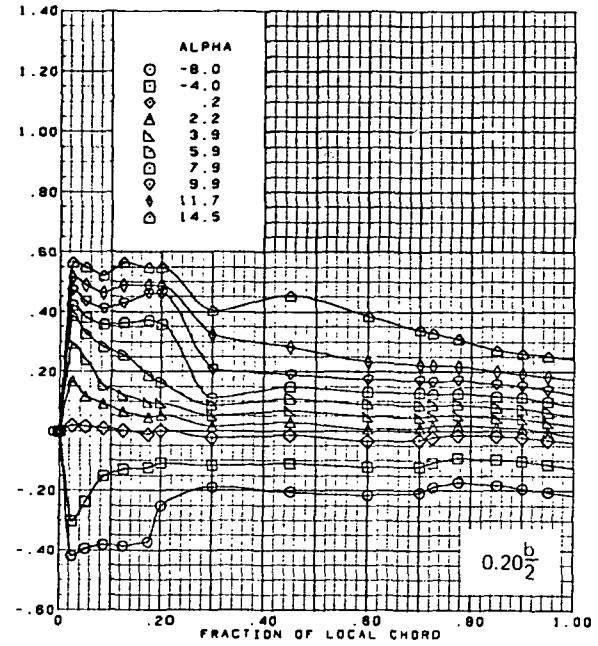
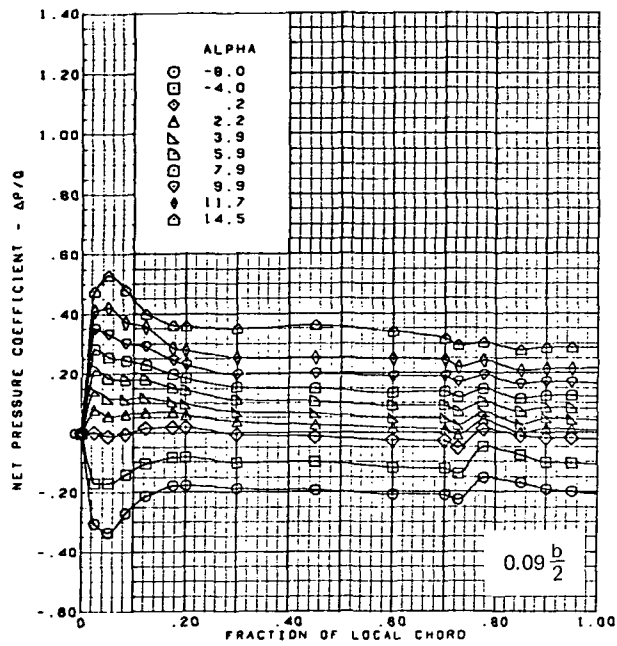


$M = 1.90$  (run 4,6)  
 Twisted wing, rounded L.E.  
 L.E. deflection, full span =  $0.0^\circ$   
 T.E. deflection, full span =  $0.0^\circ$

Note:  $C_{p, \text{vacuum}} = -0.40$

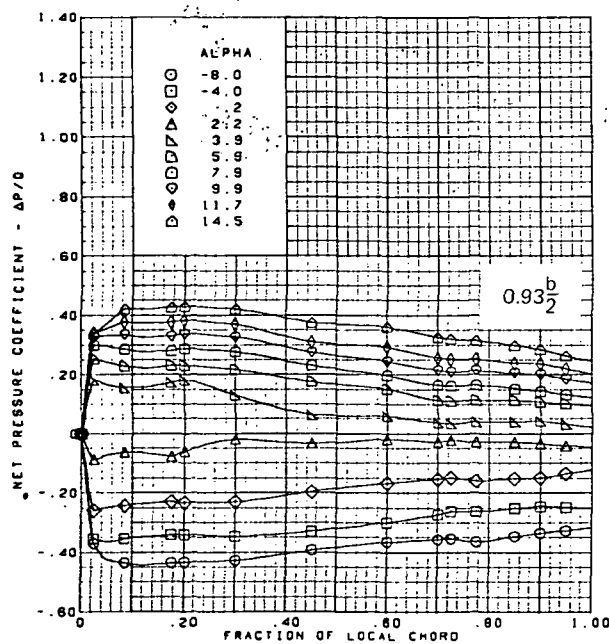
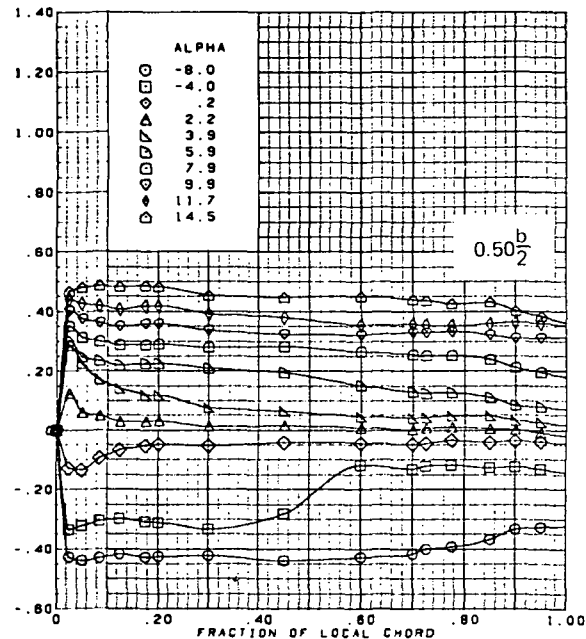
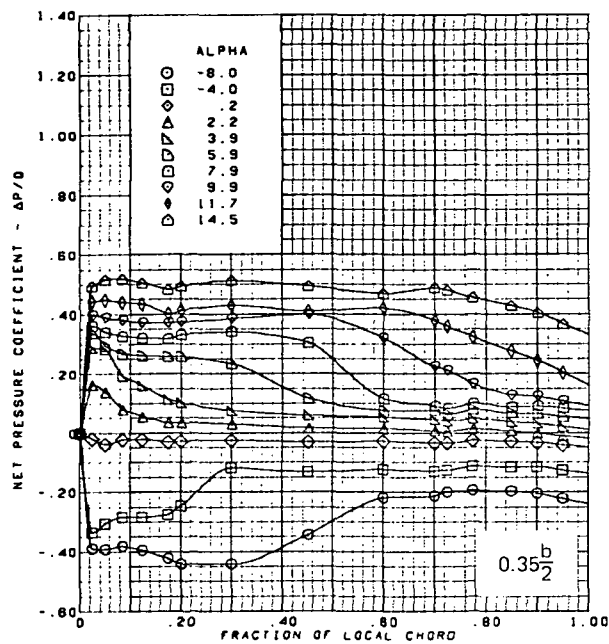
(d) (Concluded)

Figure 19.—(Continued)



(e) Net Chordwise Pressure Distributions

Figure 19.—(Continued)



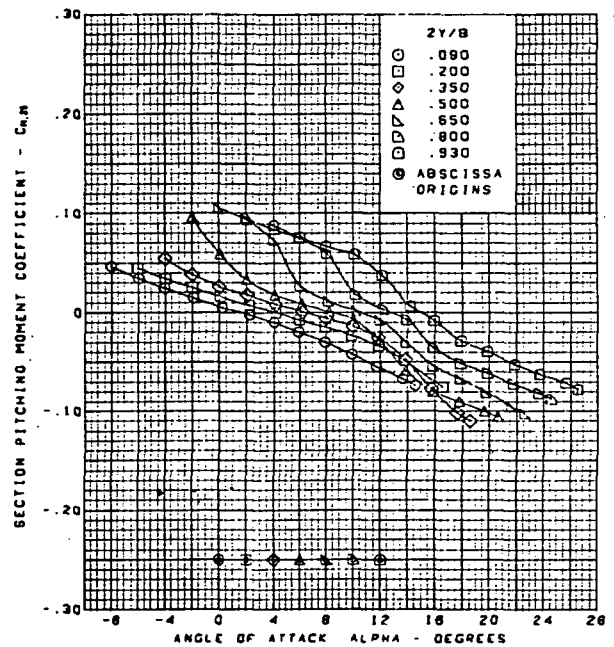
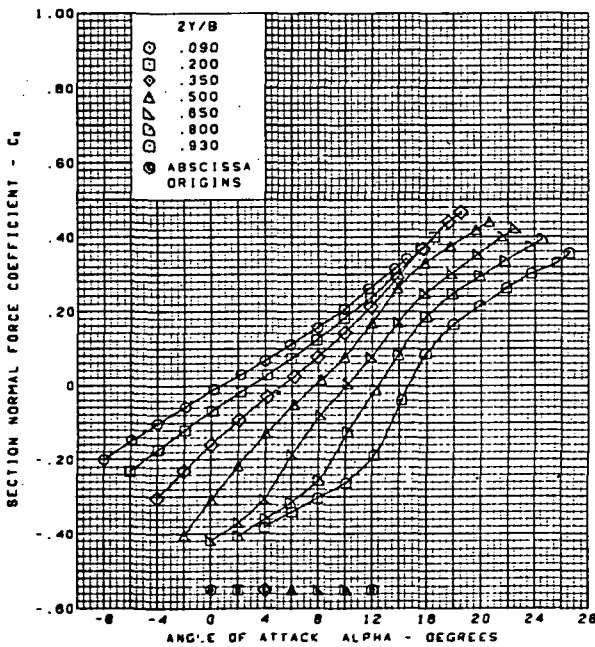
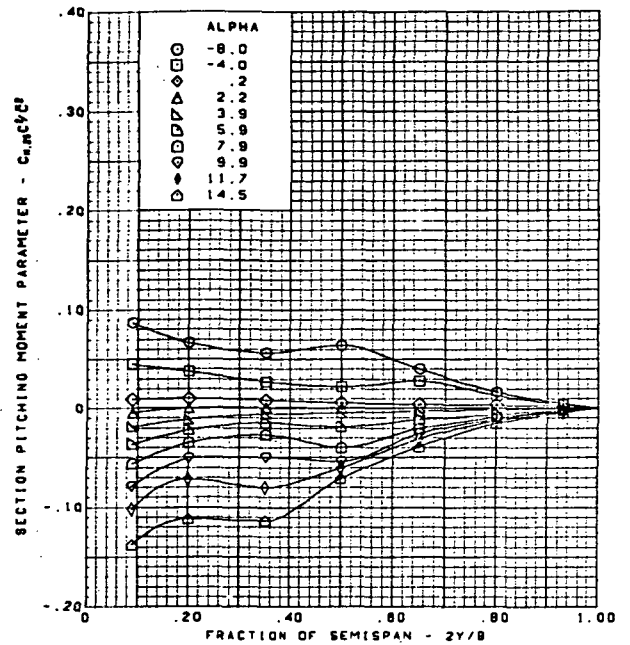
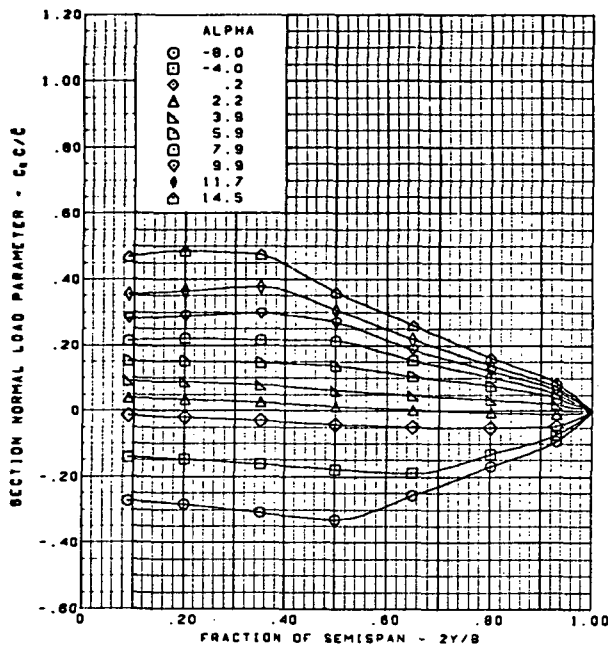
$M = 1.90$  (run 4,6)  
 Twisted wing, rounded L.E.  
 L.E. deflection, full span =  $0.0^\circ$   
 T.E. deflection, full span =  $0.0^\circ$

(e) (Concluded)

Figure 19.—(Continued)

**Page  
Intentionally  
Left Blank**

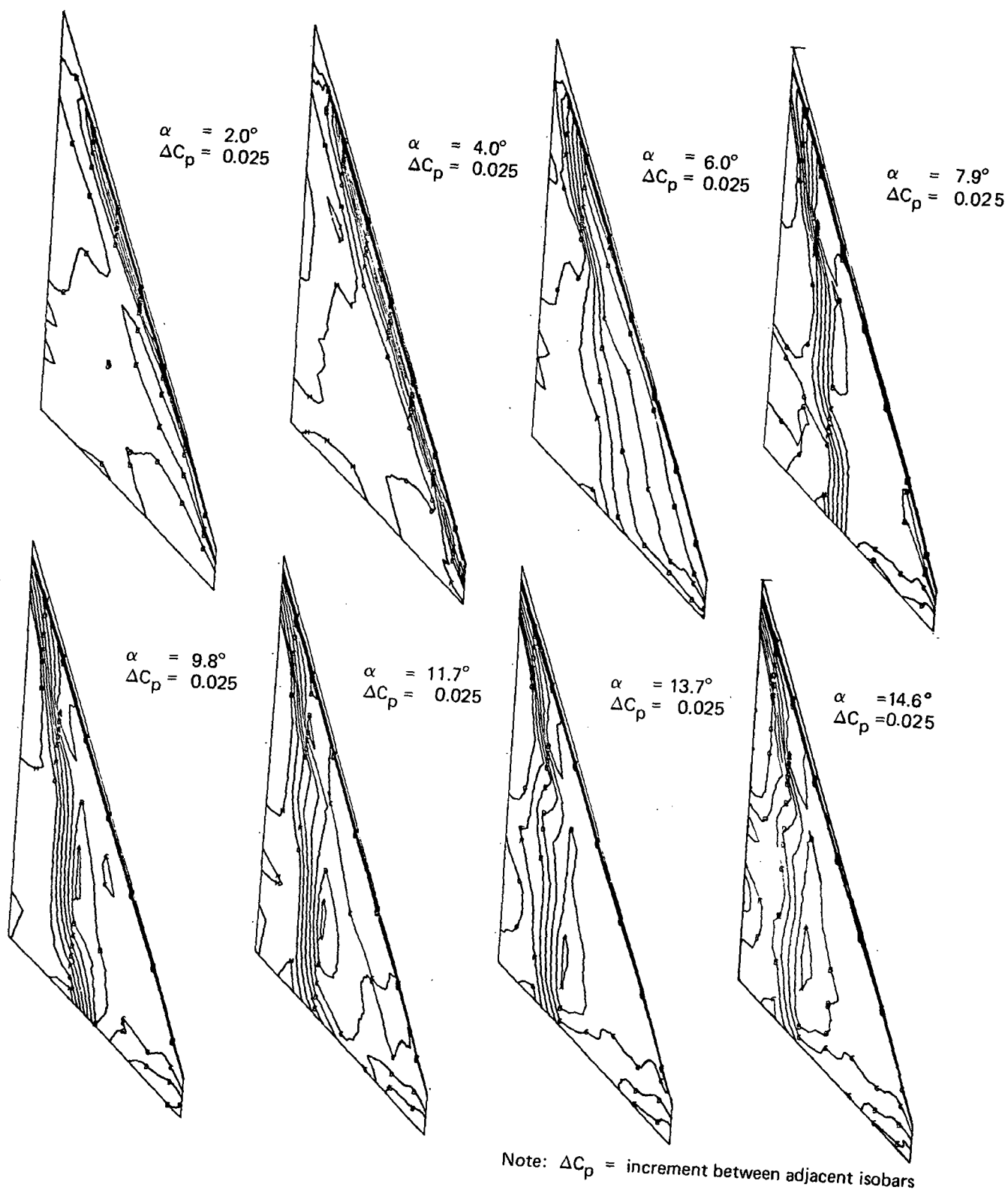




$M = 1.90$  (run 4,6)  
 Twisted wing, rounded L.E.  
 L.E. deflection, full span =  $0.0^\circ$   
 T.E. deflection, full span =  $0.0^\circ$

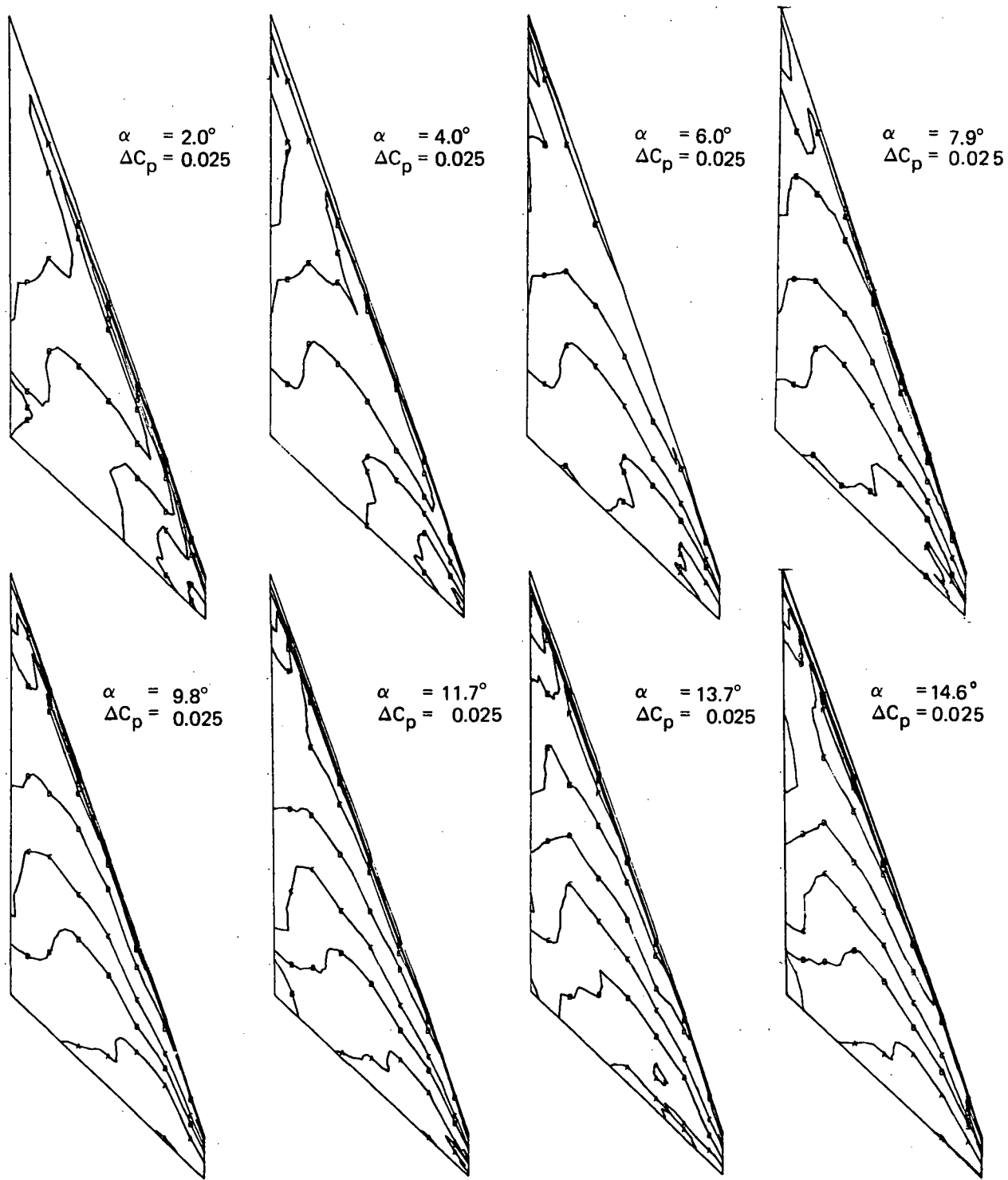
(f) Spanload Distributions and Section Aerodynamic Coefficients

Figure 19.—(Concluded)



(a) Upper Surface Isobars

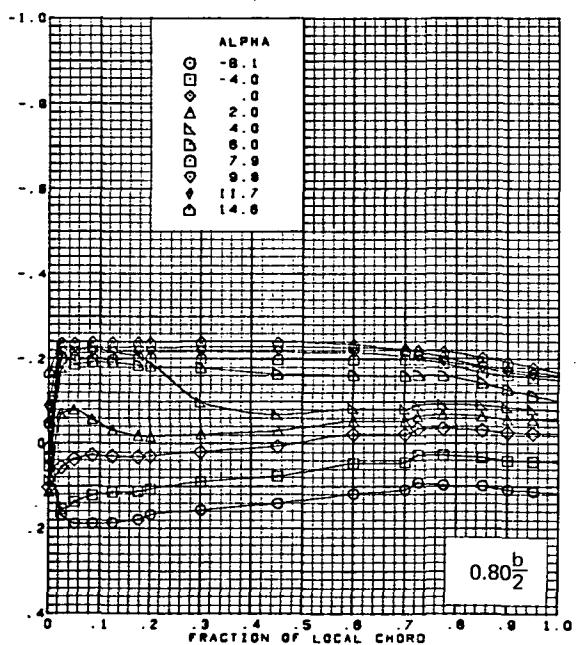
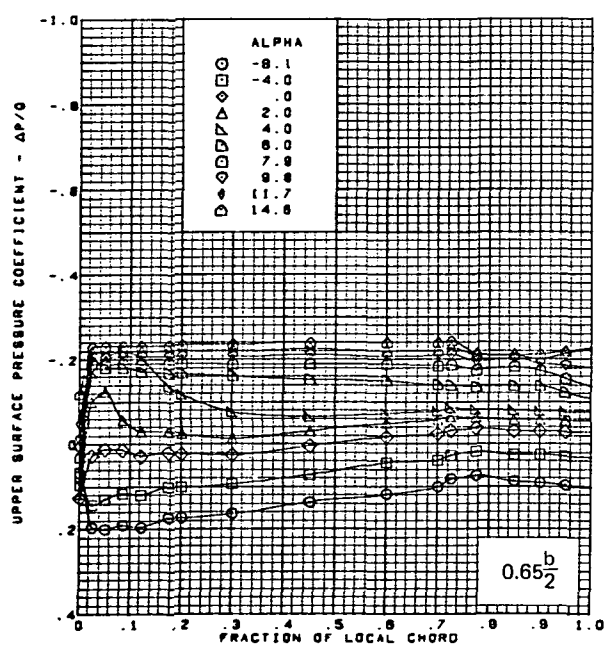
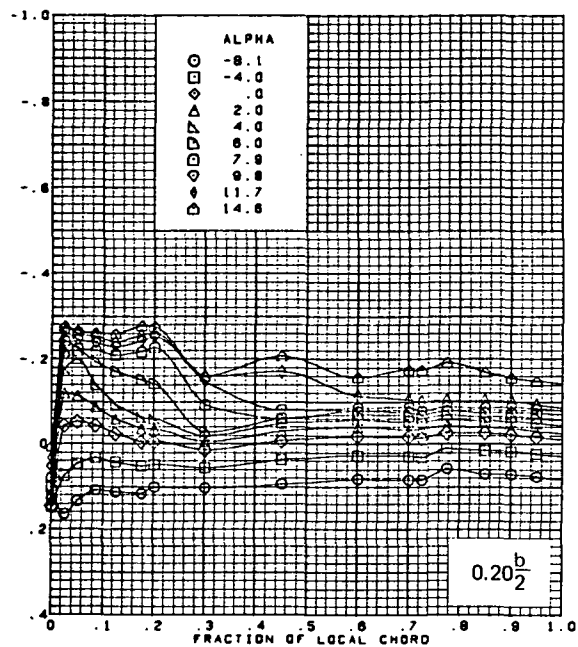
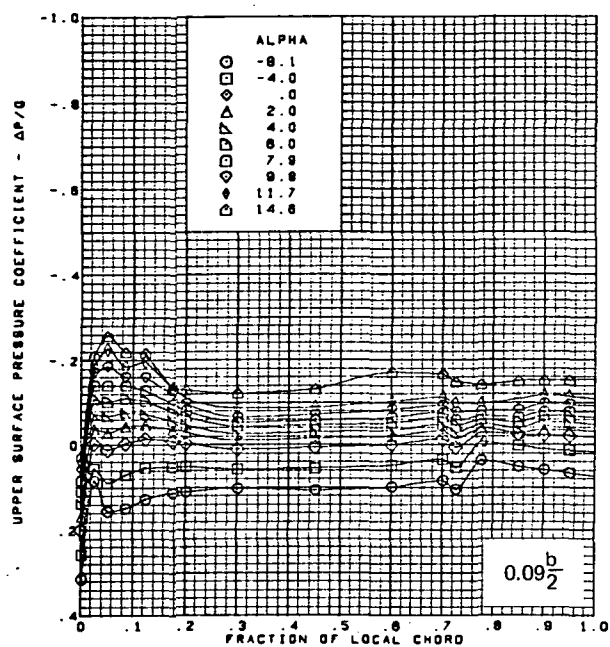
Figure 20.—Wing Experimental Data—Effect of Angle of Attack; Twisted Wing, Rounded L.E.;  
 L.E. Deflection, Full Span =  $0.0^\circ$ ; T.E. Deflection, Full Span =  $0.0^\circ$ ;  $M = 2.10$



Note:  $\Delta C_p$  = increment between adjacent isobars

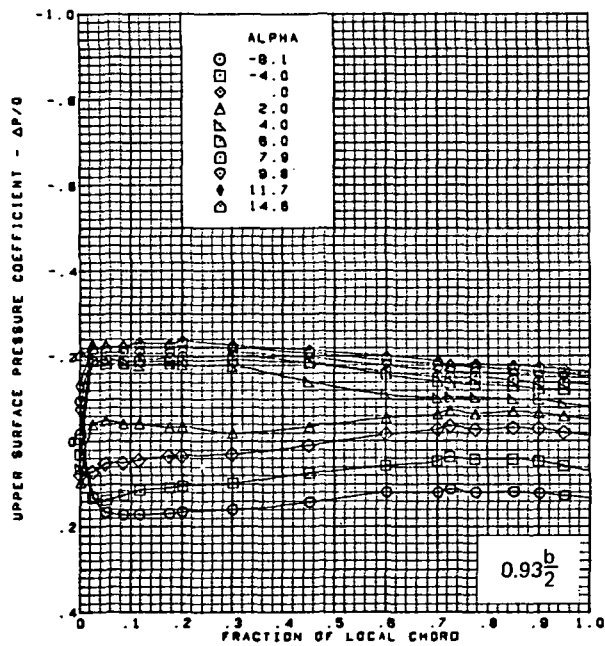
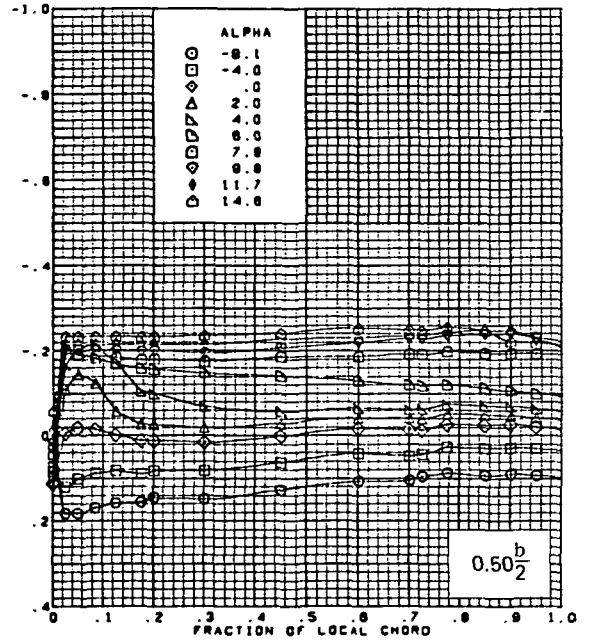
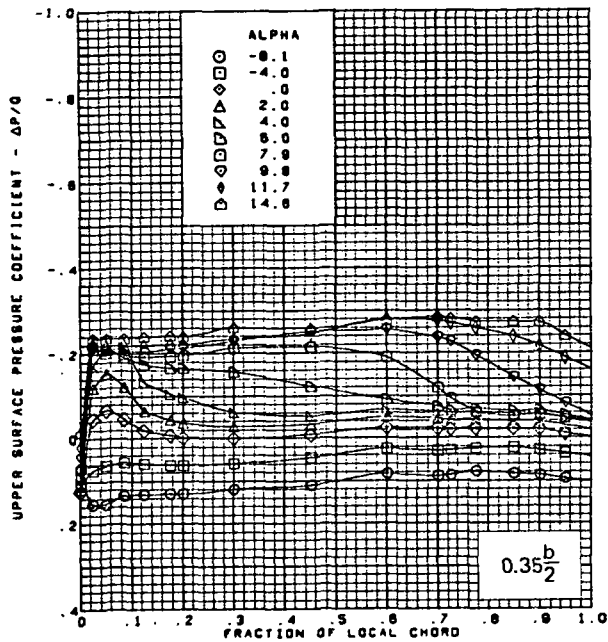
(b) Lower Surface Isobars

Figure 20.—(Continued)



(c) Upper Surface Chordwise Pressure Distributions

Figure 20.—(Continued)

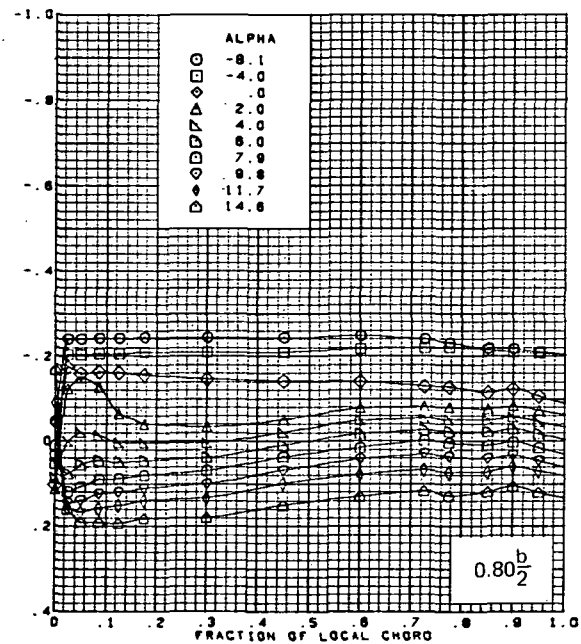
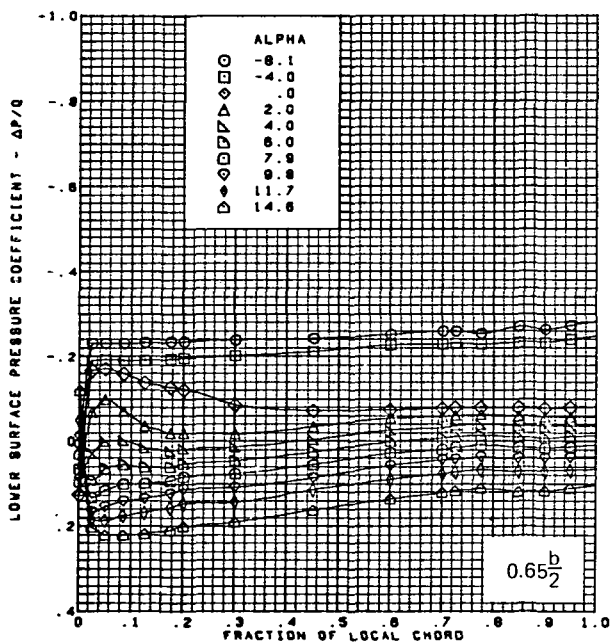
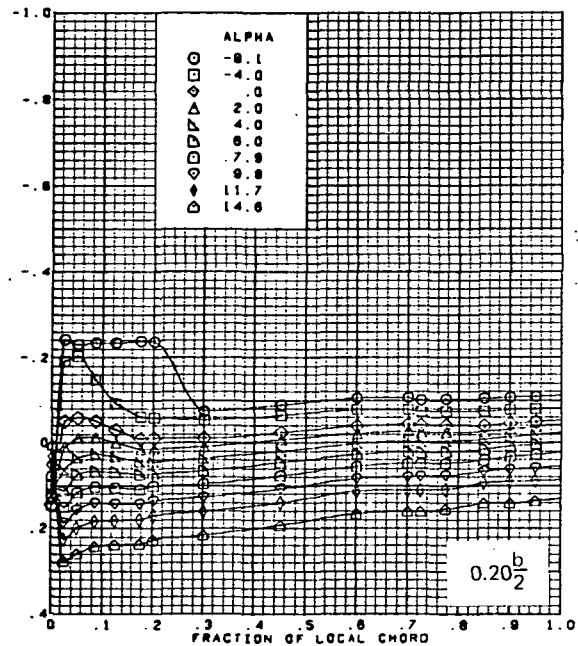
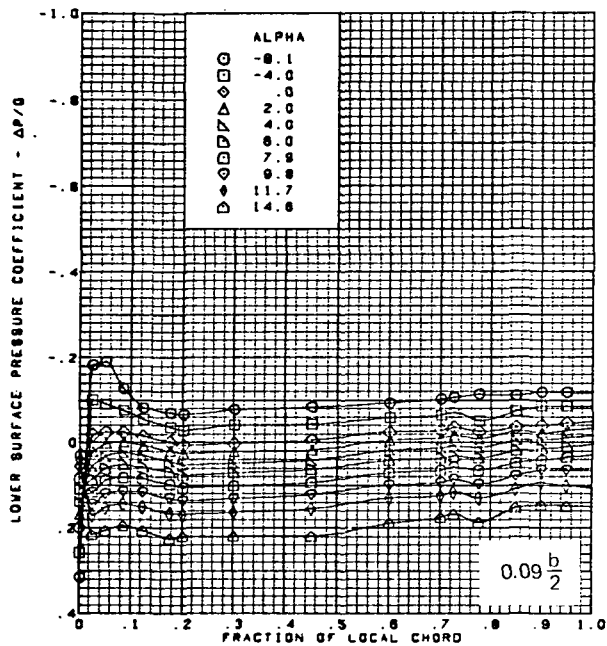


M = 2.10 (run 9)  
 Twisted wing, rounded L.E.  
 L.E. deflection, full span =  $0.0^\circ$   
 T.E. deflection, full span =  $0.0^\circ$

Note:  $C_{p, \text{vacuum}} = -0.32$

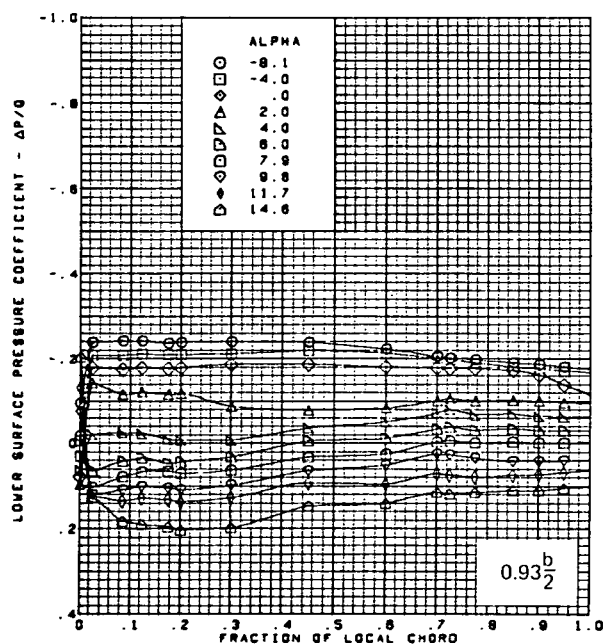
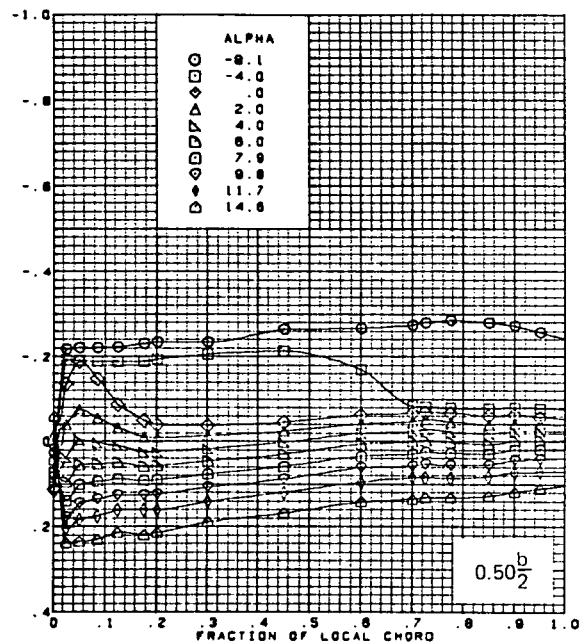
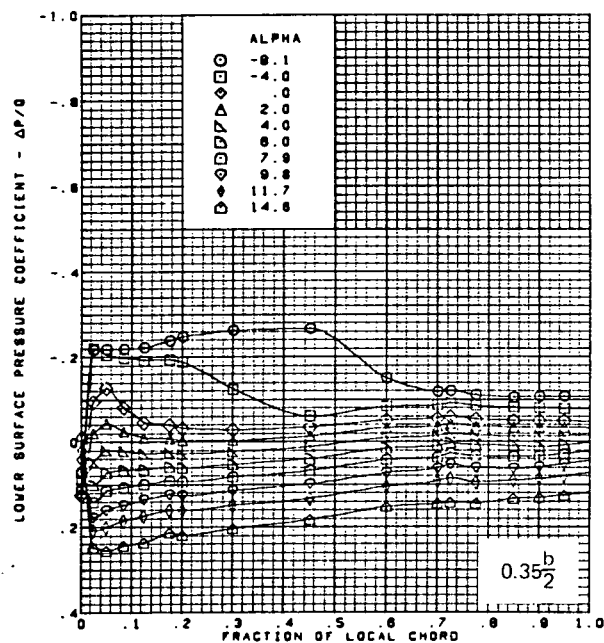
(c) (Concluded)

Figure 20.—(Continued)



(d) Lower Surface Chordwise Pressure Distributions

Figure 20.—(Continued)

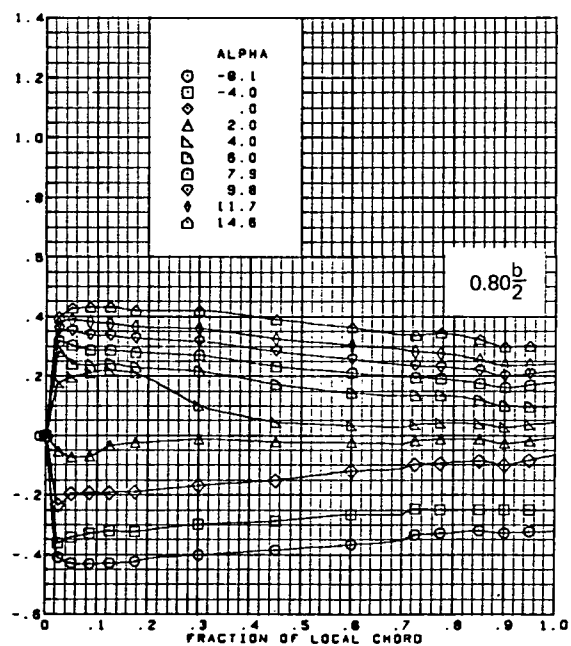
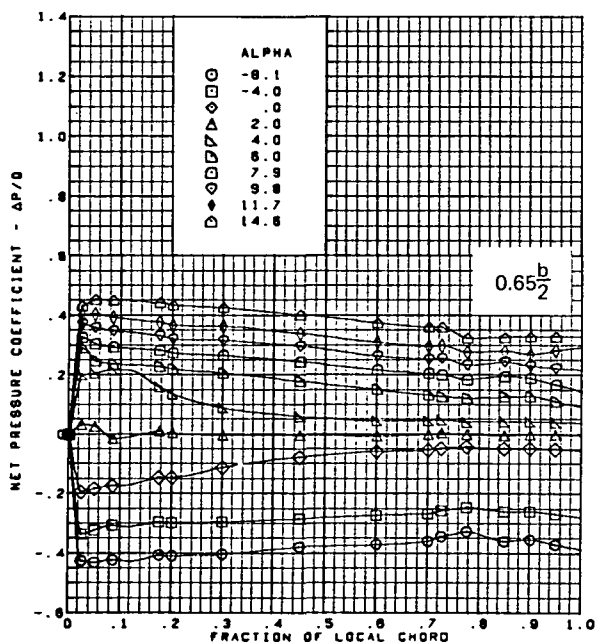
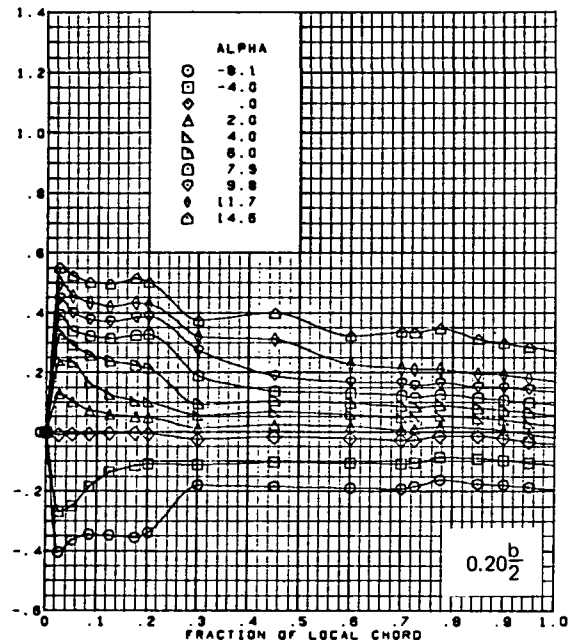
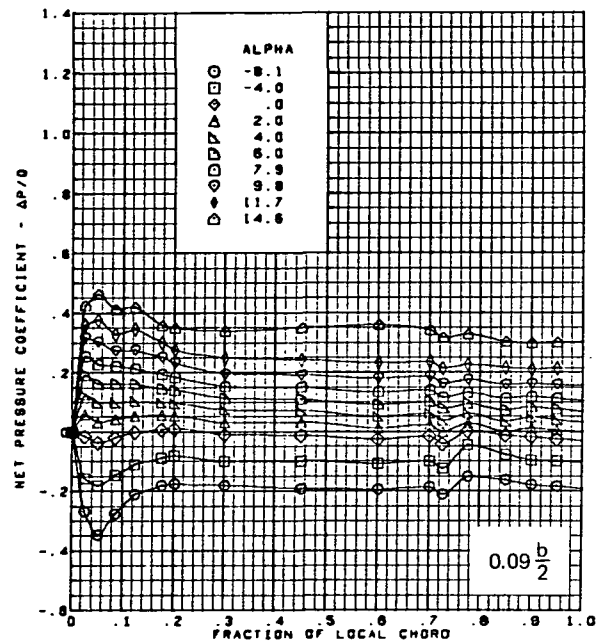


M = 2.10 (run 9)  
 Twisted wing, rounded L.E.  
 L.E. deflection, full span =  $0.0^\circ$   
 T.E. deflection, full span =  $0.0^\circ$

Note:  $C_{p, \text{vacuum}} = -0.32$

(d) (Concluded)

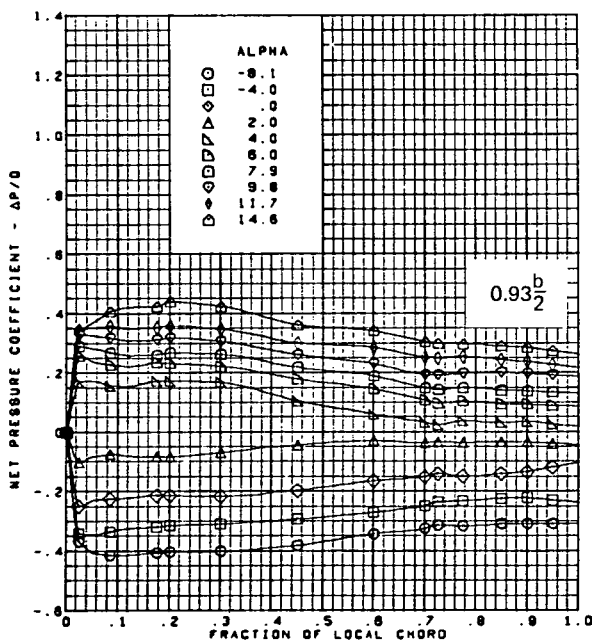
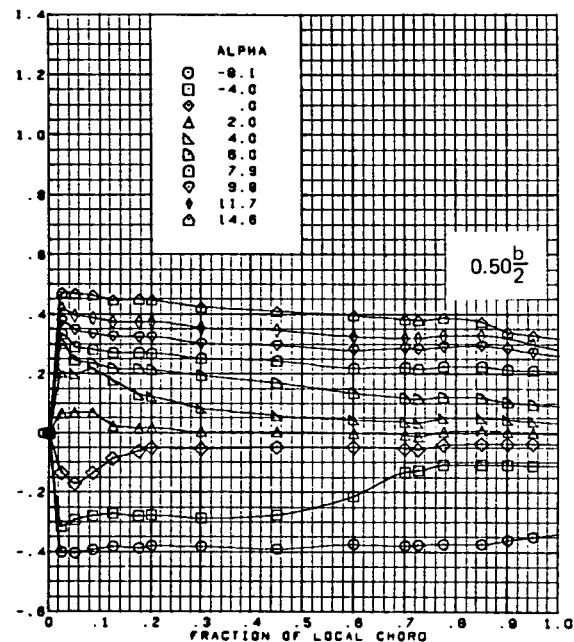
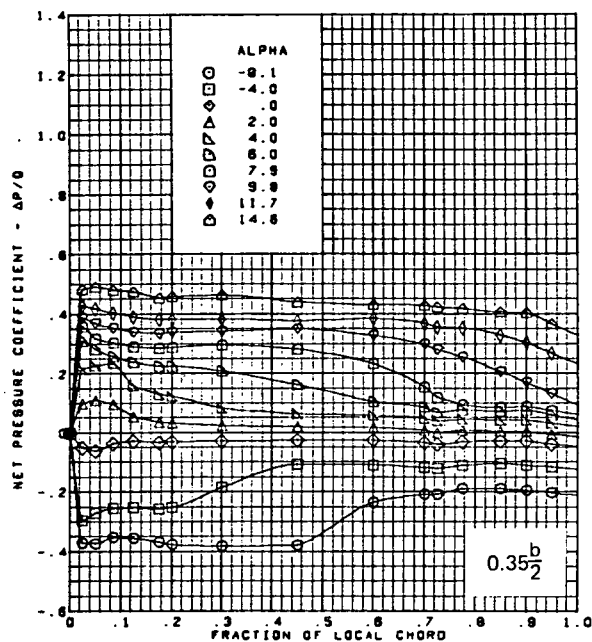
Figure 20.—(Continued)



(e) Net Chordwise Pressure Distributions

Figure 20.—(Continued)



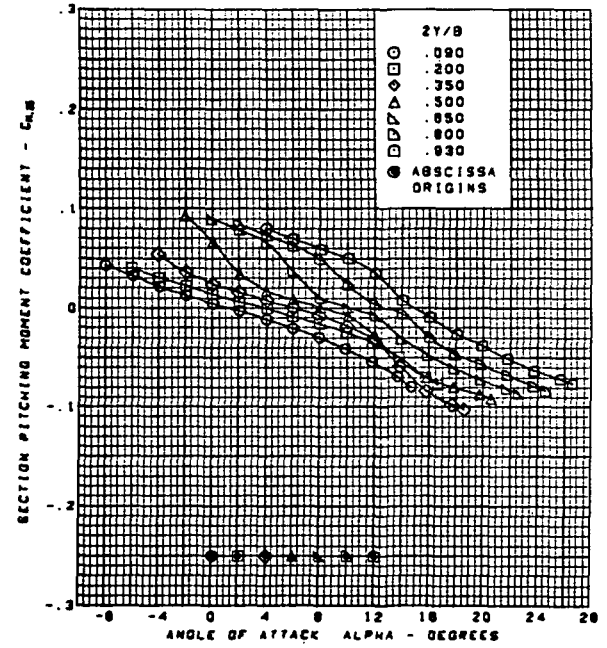
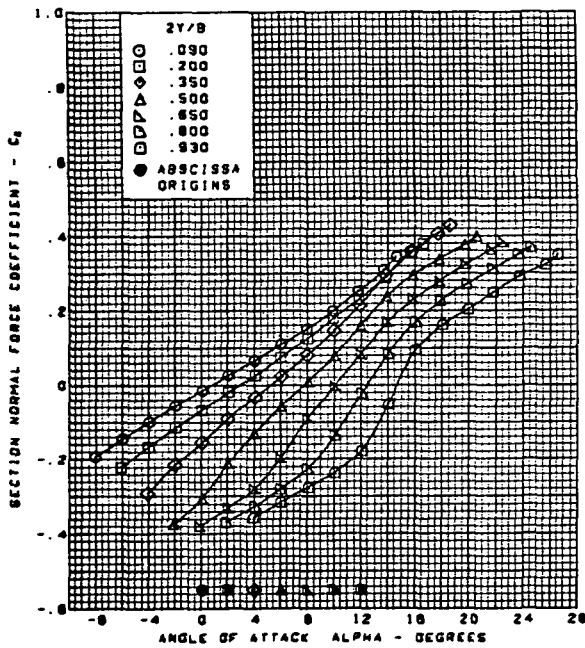
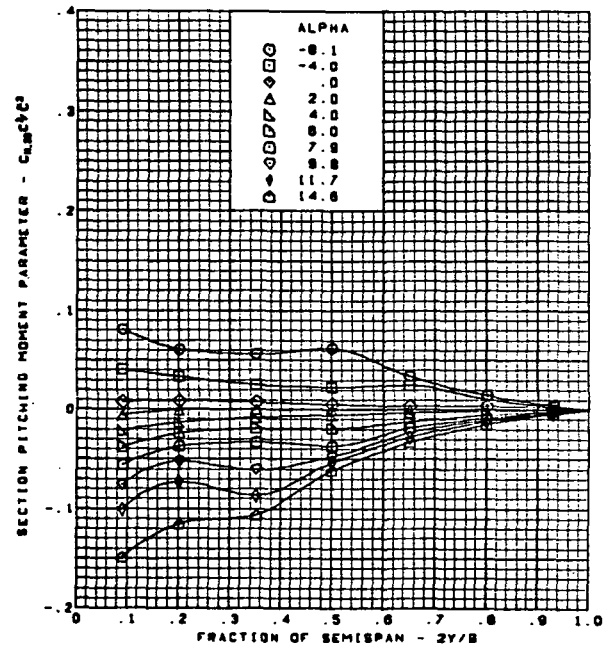
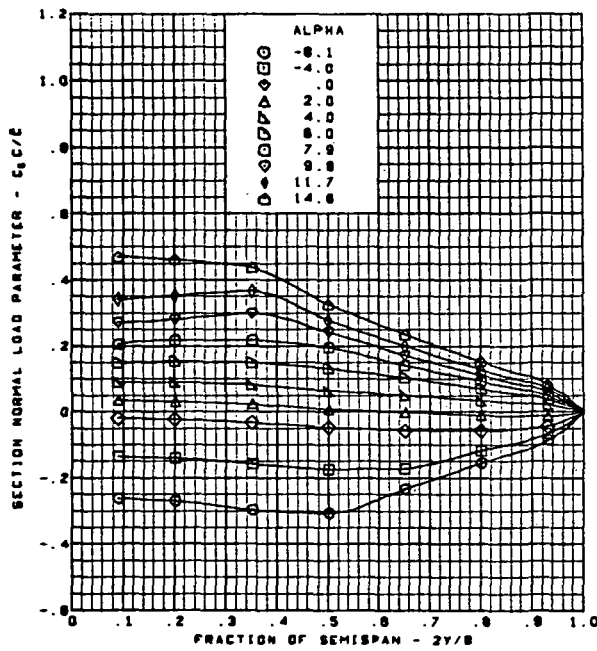


M = 2.10 (run 9)  
 Twisted wing, rounded L.E.  
 L.E. deflection, full span =  $0.0^\circ$   
 T.E. deflection, full span =  $0.0^\circ$

(e) (Concluded)

Figure 20.—(Continued)

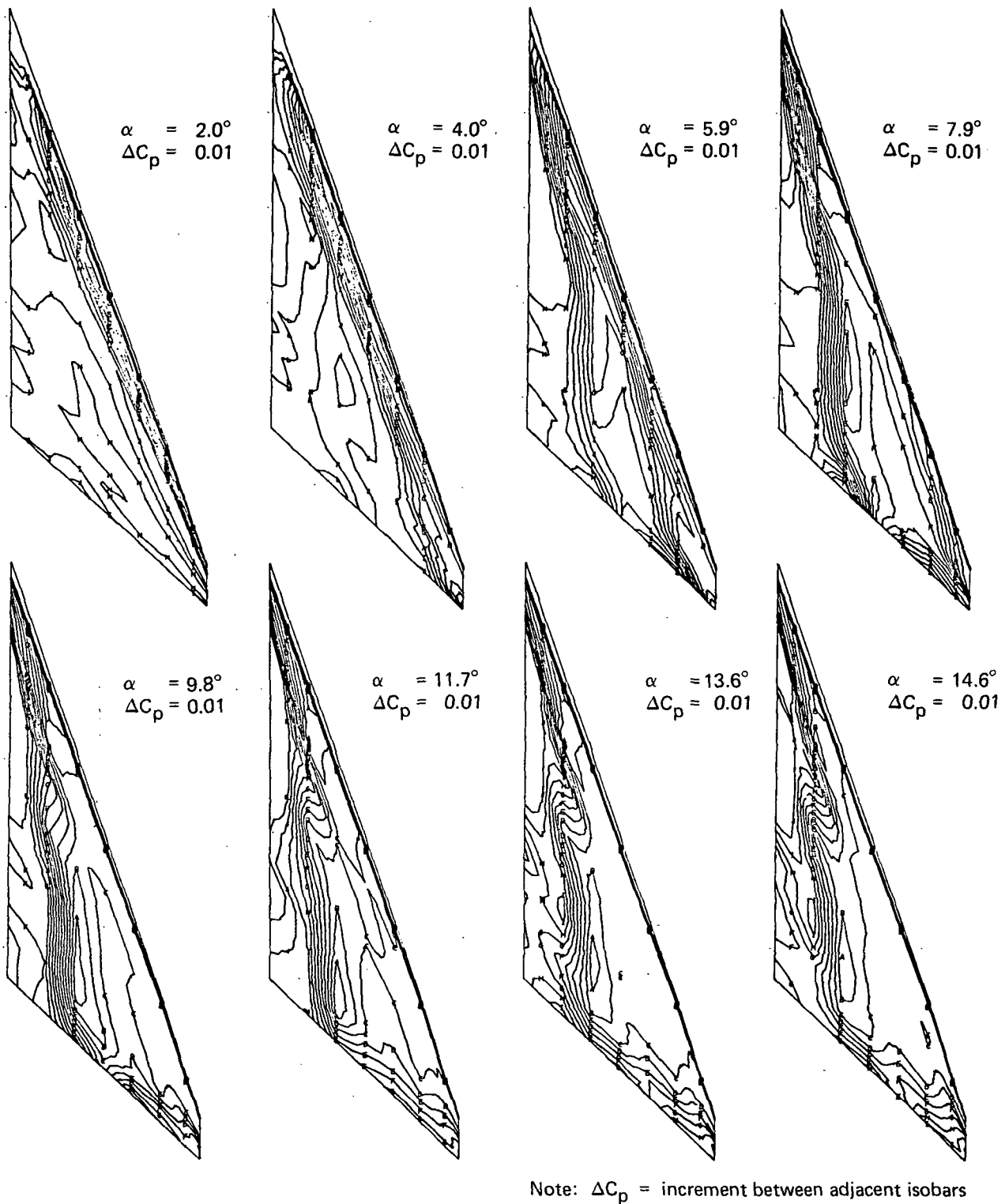
**Page  
Intentionally  
Left Blank**



M = 2.10 (run 9)  
 Twisted wing, rounded L.E.  
 L.E. deflection, full span =  $0.0^\circ$   
 T.E. deflection, full span =  $0.0^\circ$

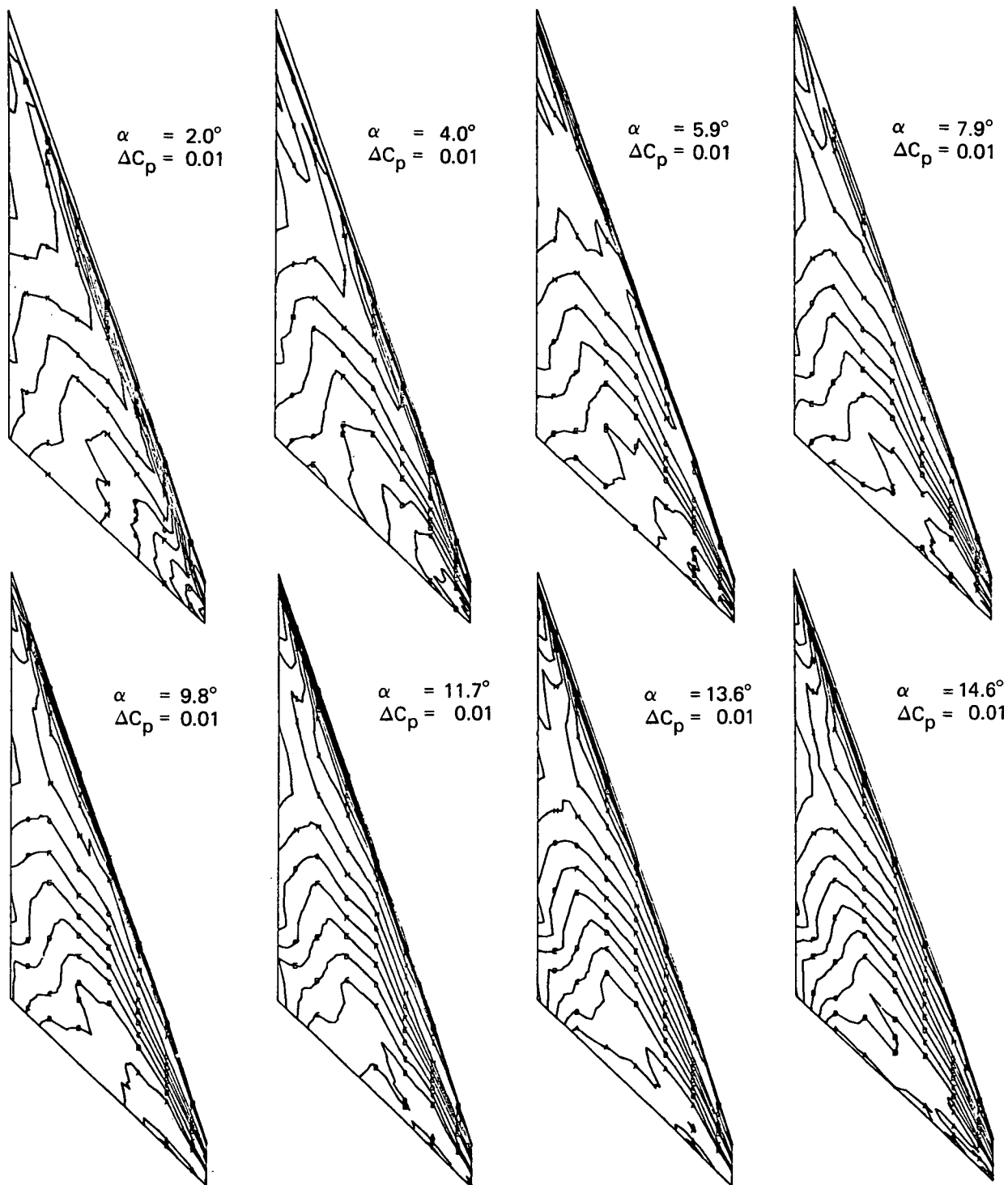
(f) Spanload Distributions and Section Aerodynamic Coefficients

Figure 20.—(Concluded)



(a) Upper Surface Isobars

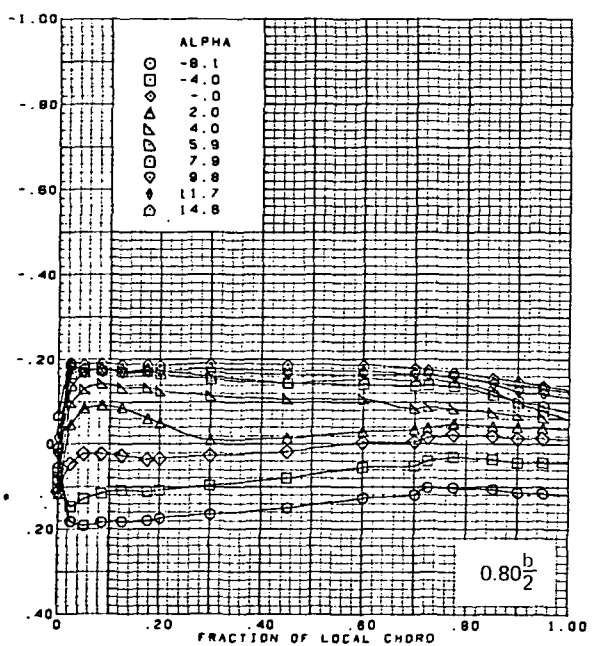
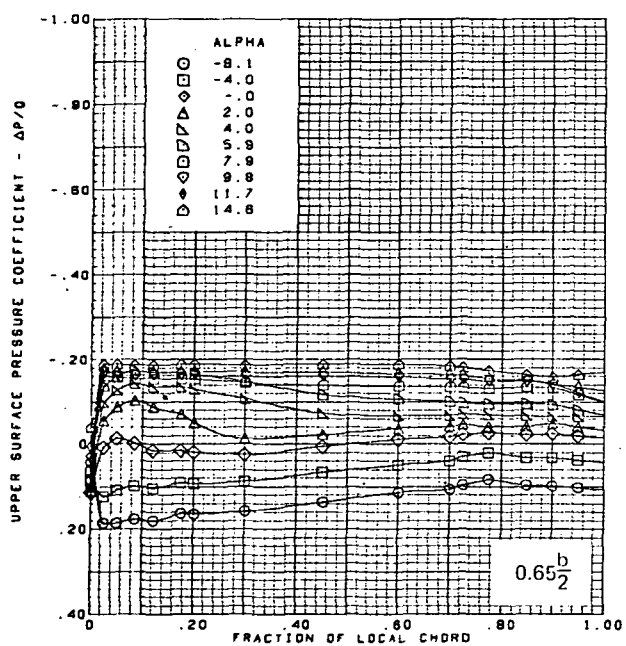
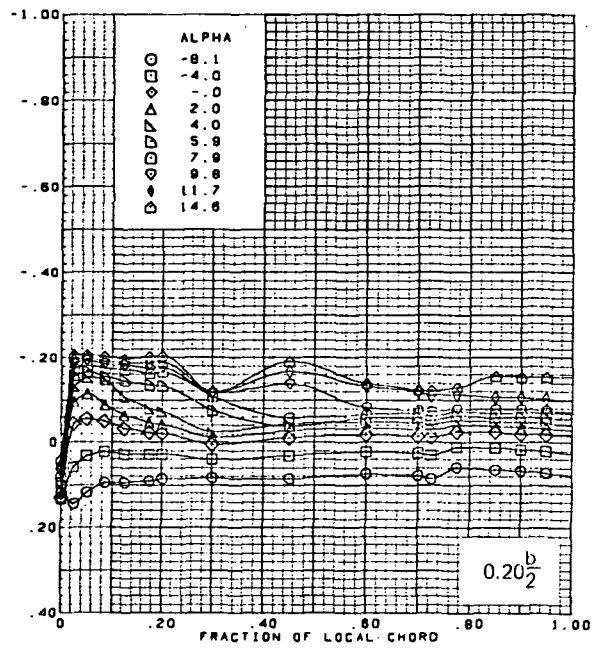
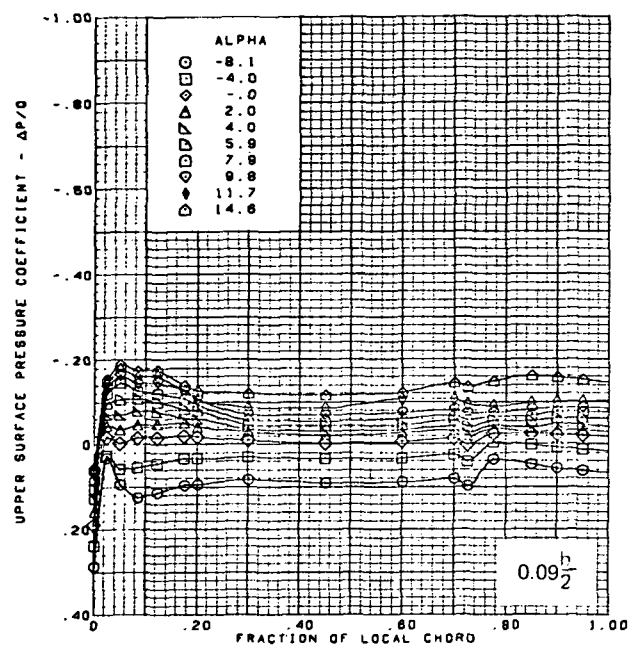
Figure 21.—Wing Experimental Data—Effect of Angle of Attack; Twisted Wing, Rounded L.E.;  
 L.E. Deflection, Full Span =  $0.0^\circ$ ; T.E. Deflection, Full Span =  $0.0^\circ$ ;  $M = 2.50$



Note:  $\Delta C_p$  = increment between adjacent isobars

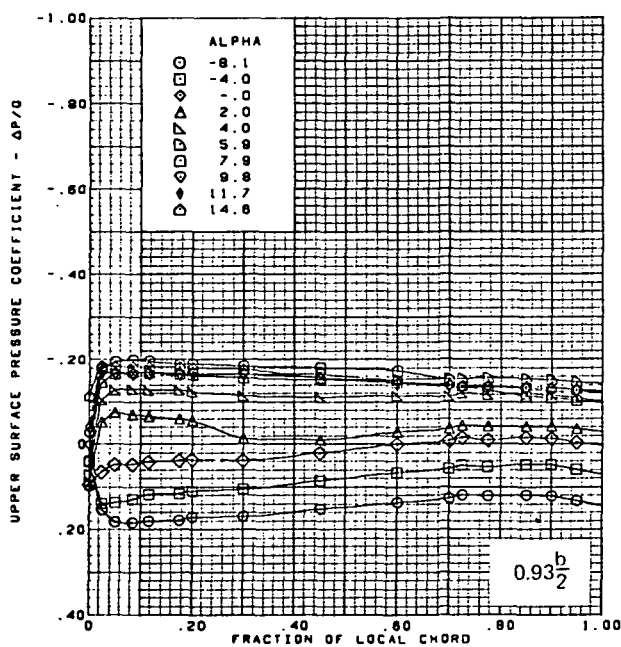
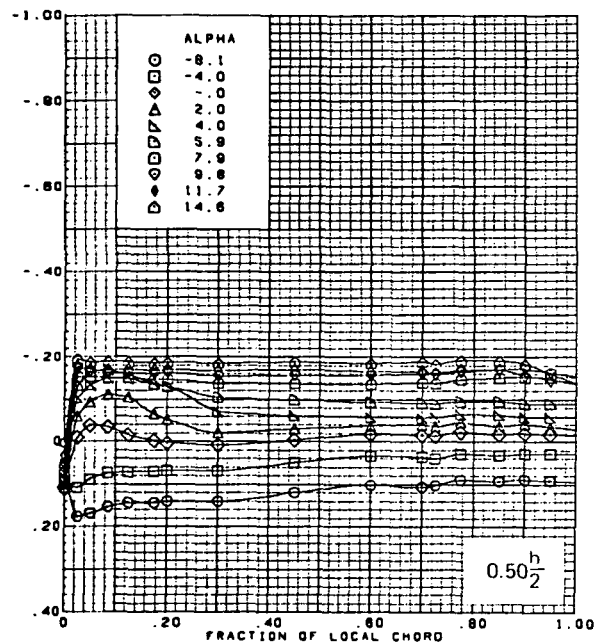
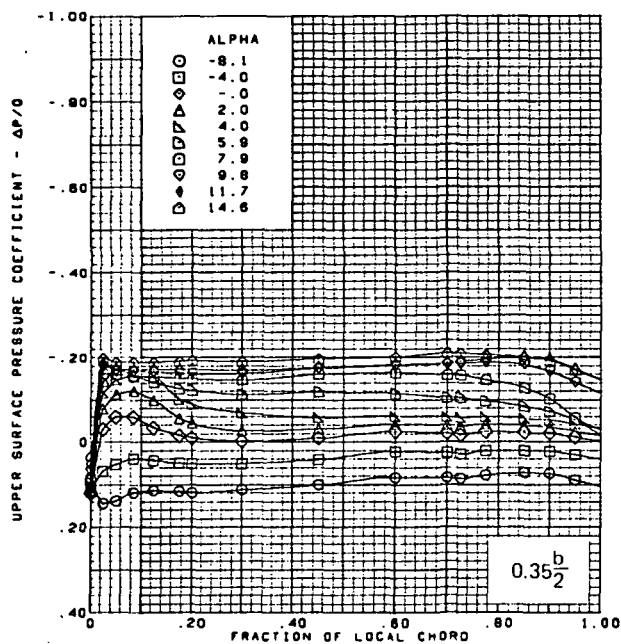
(b) Lower Surface Isobars

Figure 21.—(Continued)



(c) Upper Surface Chordwise Pressure Distributions

Figure 21.—(Continued)

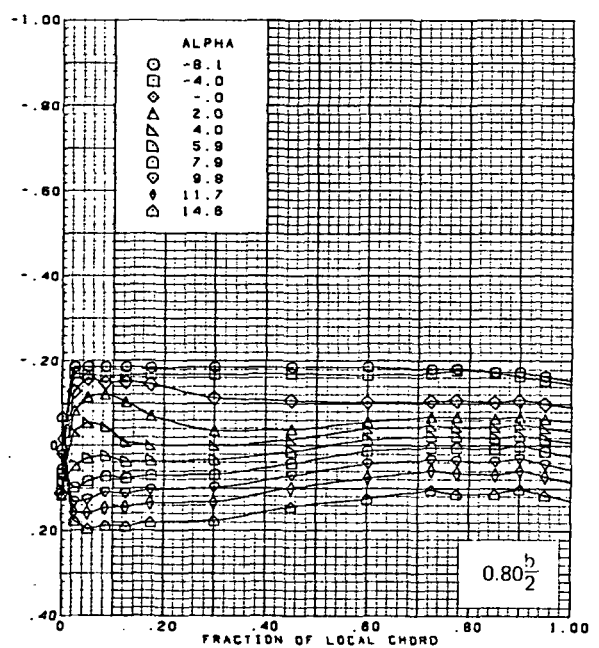
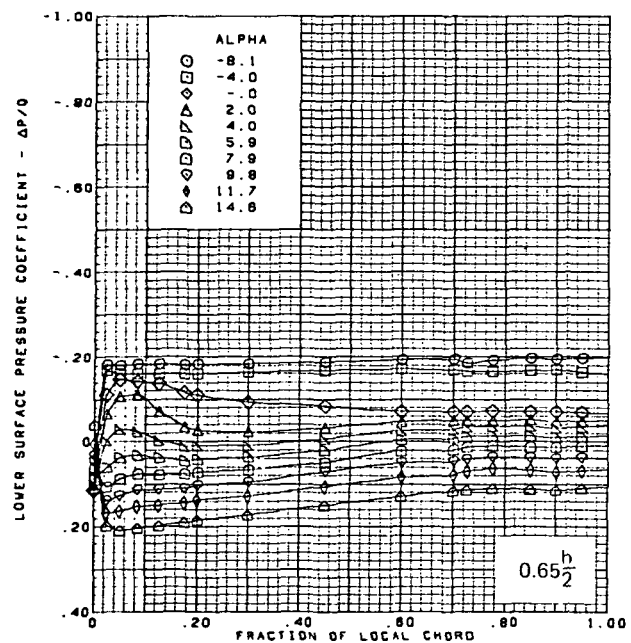
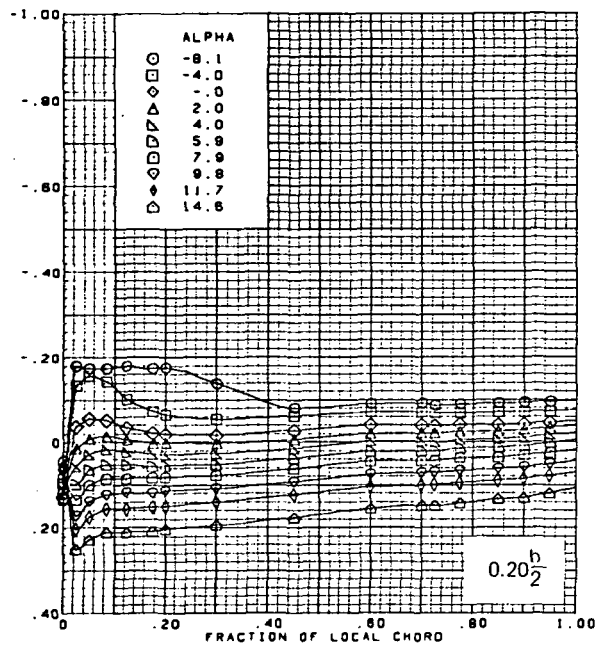
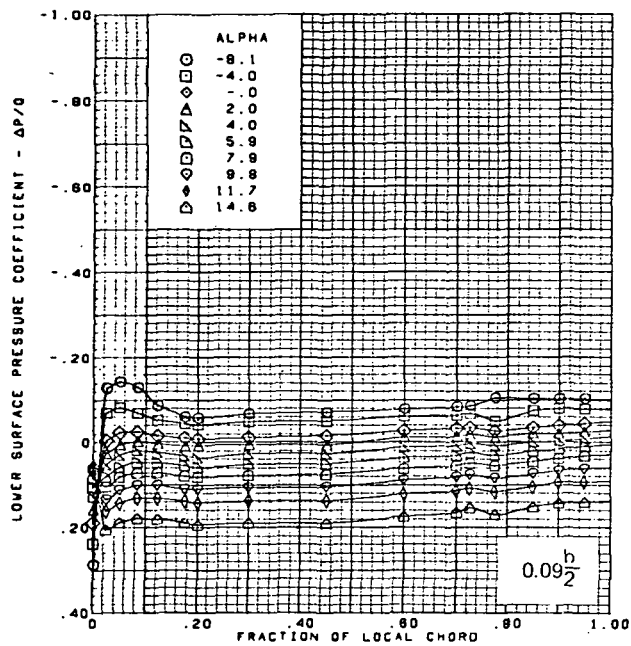


$M = 2.50$  (run 10)  
 Twisted wing, rounded L.E.  
 L.E. deflection, full span =  $0.0^\circ$   
 T.E. deflection, full span =  $0.0^\circ$

Note:  $C_{p, \text{vacuum}} = -0.23$

(c) (Concluded)

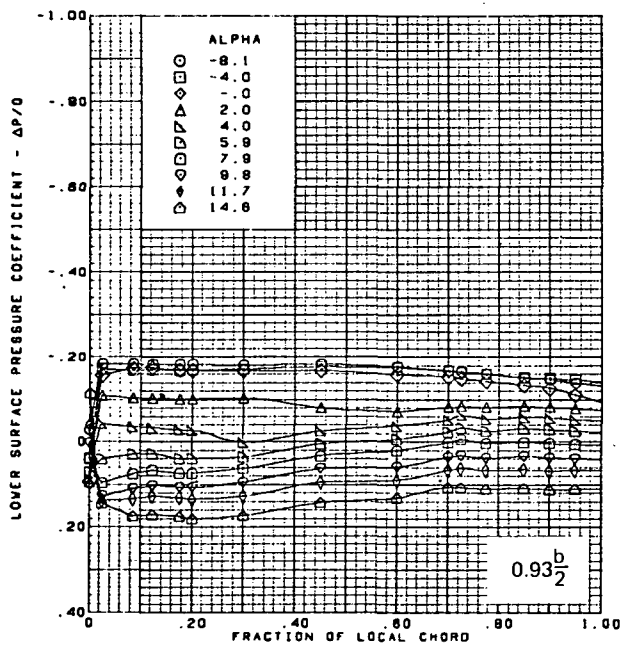
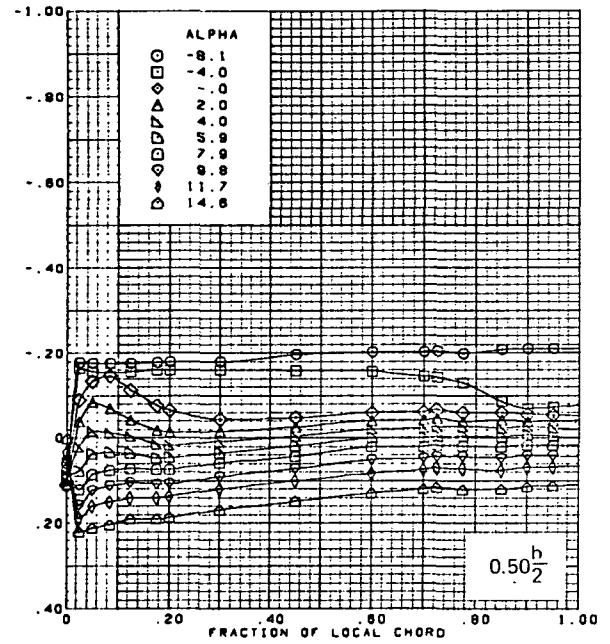
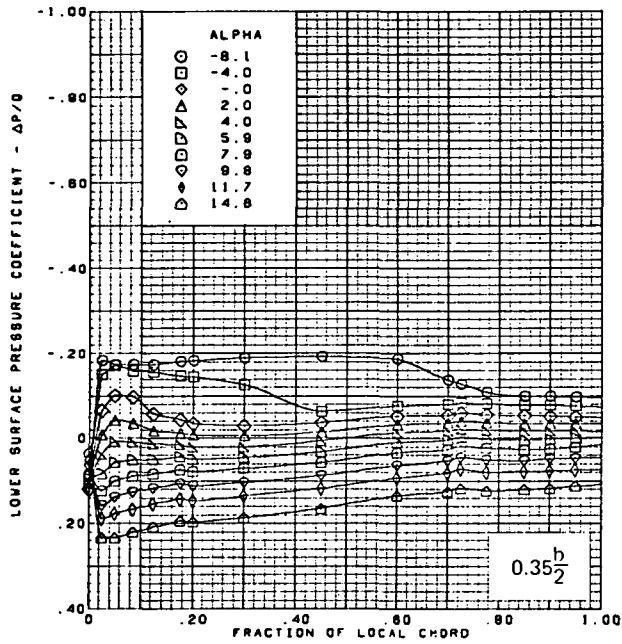
Figure 21.—(Continued)



(d) Lower Surface Chordwise Pressure Distributions

Figure 21.—(Continued)

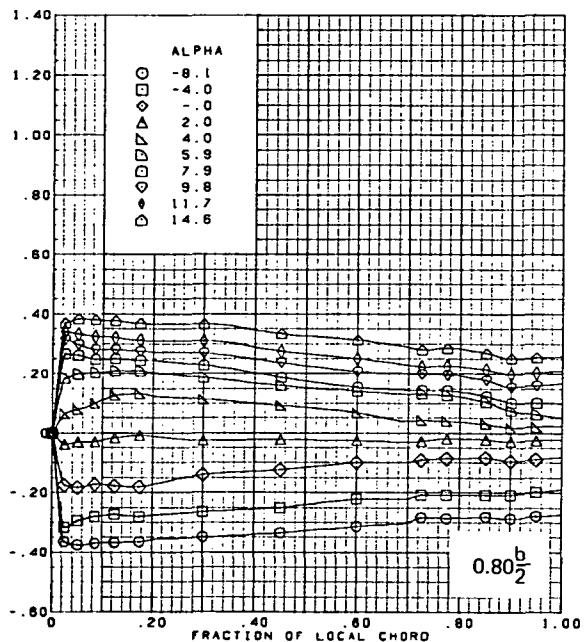
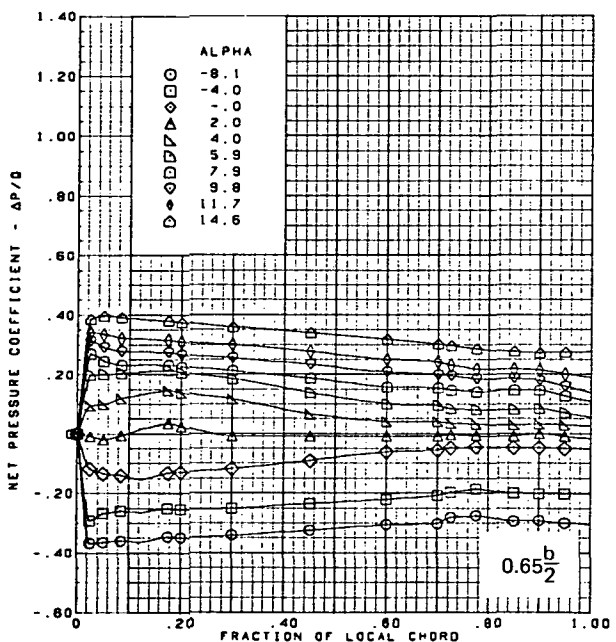
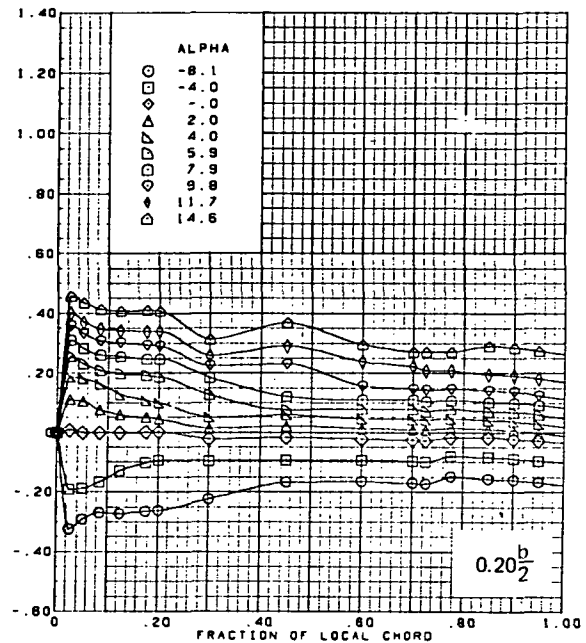
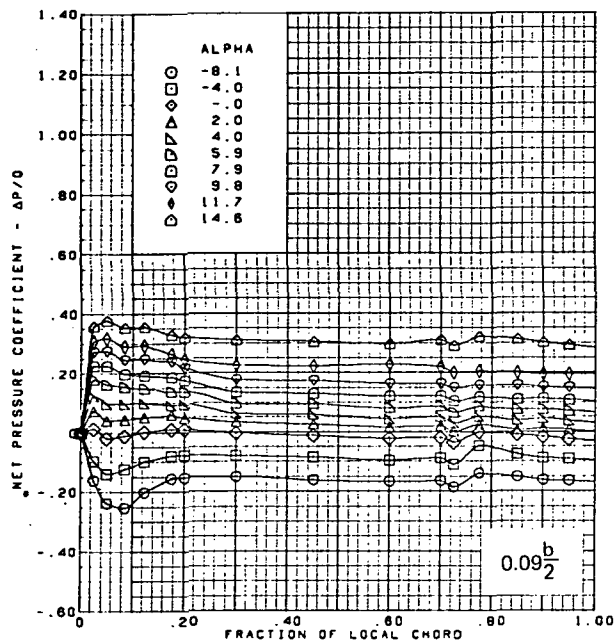




$M = 2.50$  (run 10)  
 Twisted wing, rounded L.E.  
 L.E. deflection, full span =  $0.0^\circ$   
 T.E. deflection, full span =  $0.0^\circ$   
 Note:  $C_{p, \text{vacuum}} = -0.23$

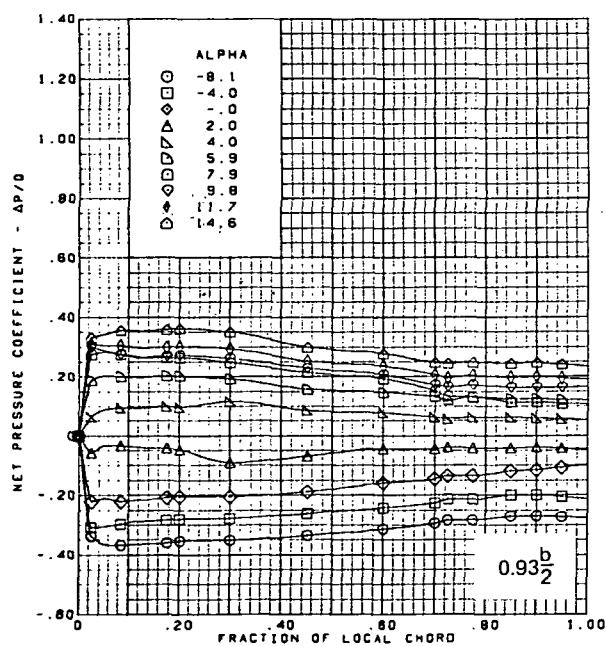
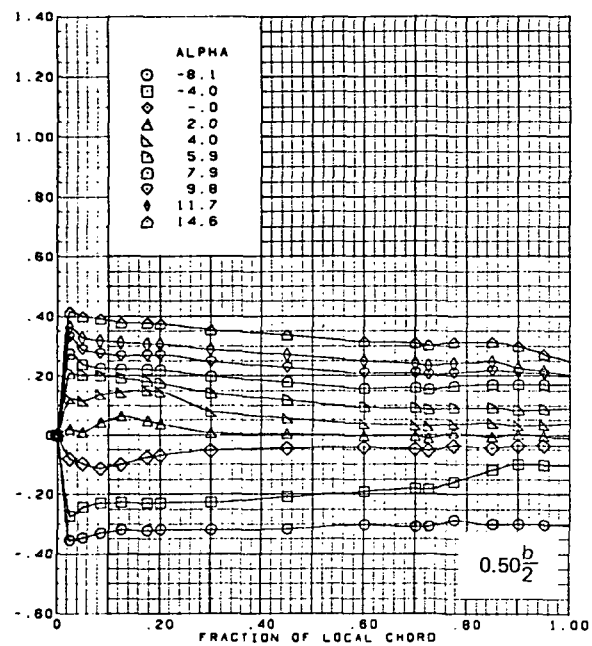
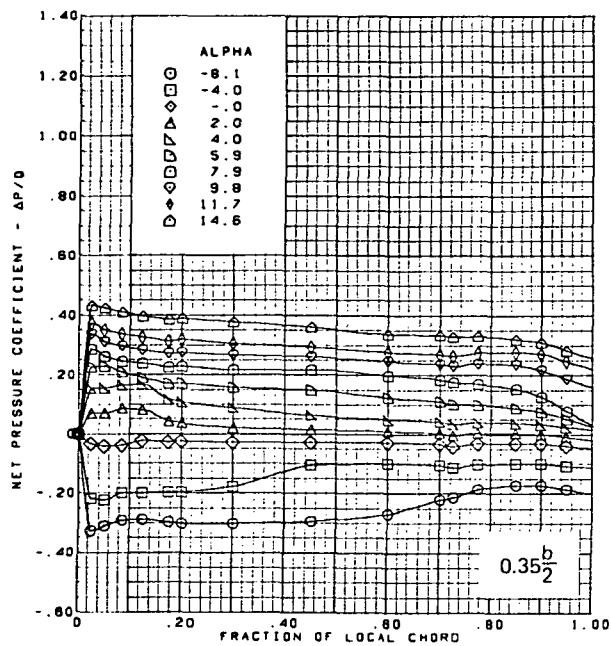
(d) (Concluded)

Figure 21.—(Continued)



(e) Net Chordwise Pressure Distributions

Figure 21.—(Continued)

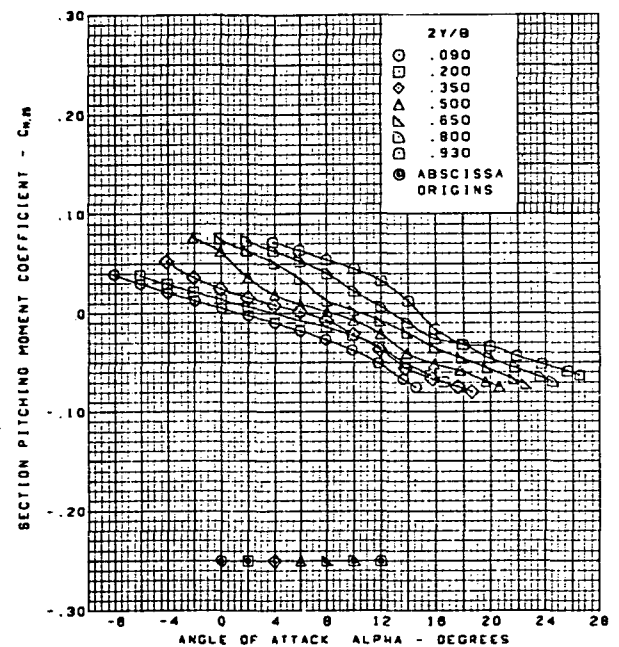
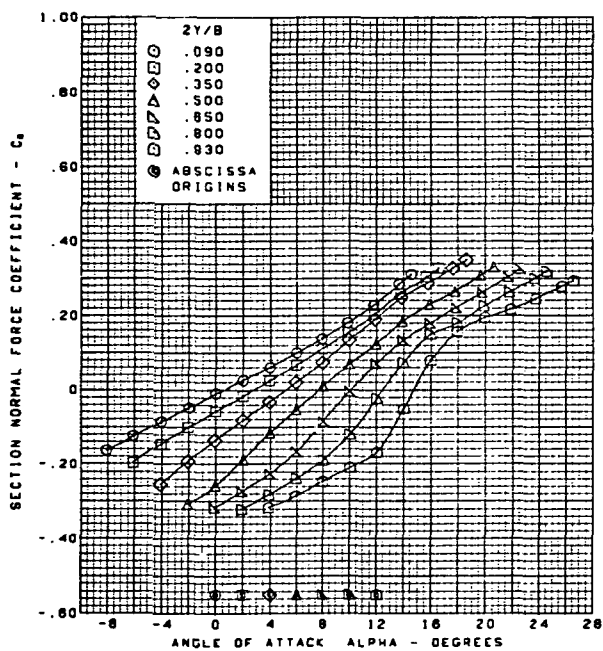
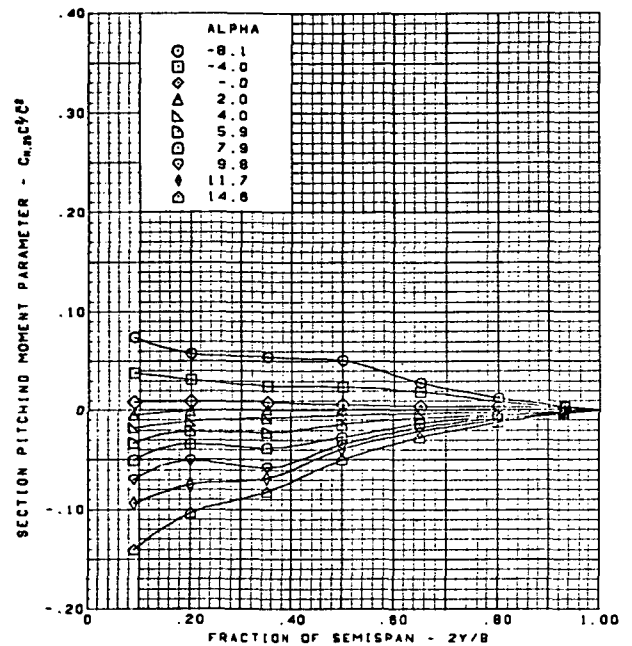
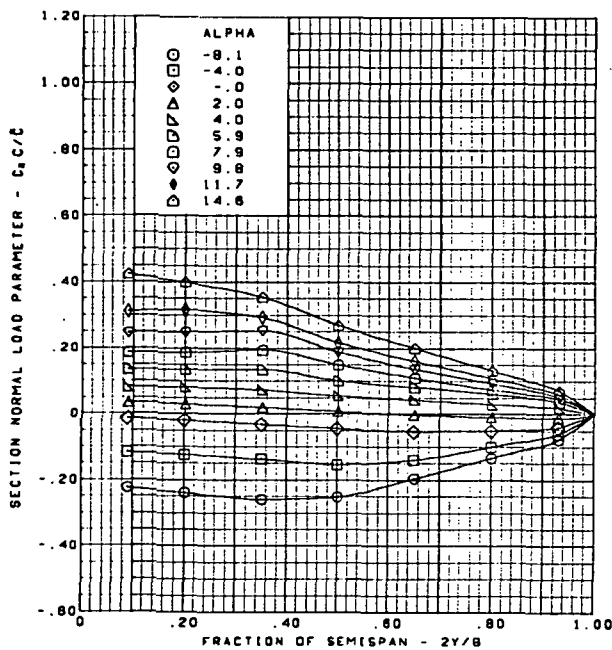


M = 2.50 (run 10)  
 Twisted wing, rounded L.E.  
 L.E. deflection, full span =  $0.0^\circ$   
 T.E. deflection, full span =  $0.0^\circ$

(e) (Concluded)

Figure 21.—(Continued)

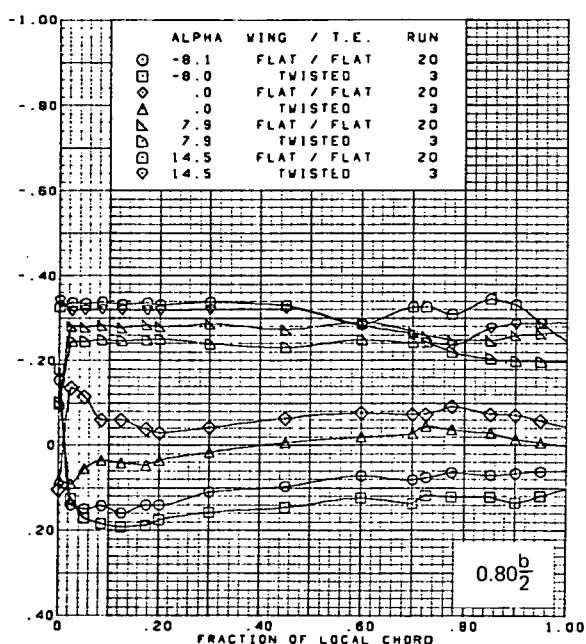
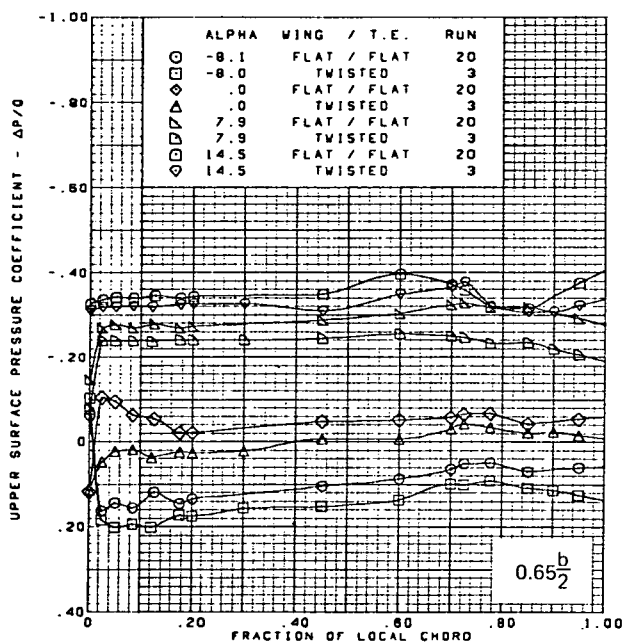
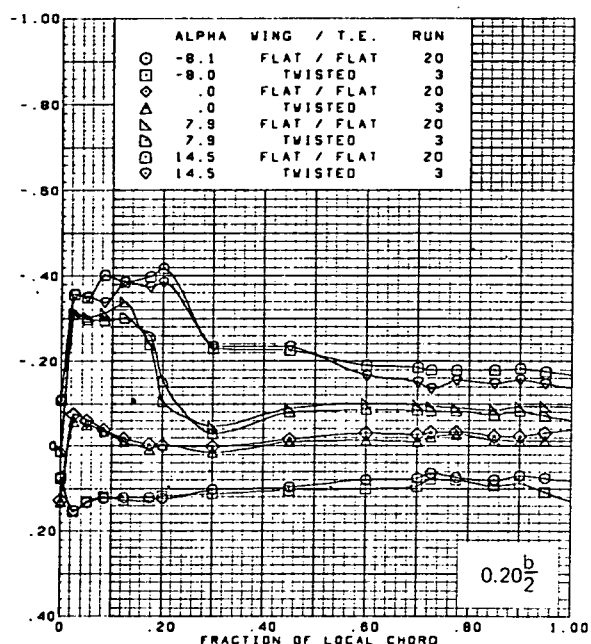
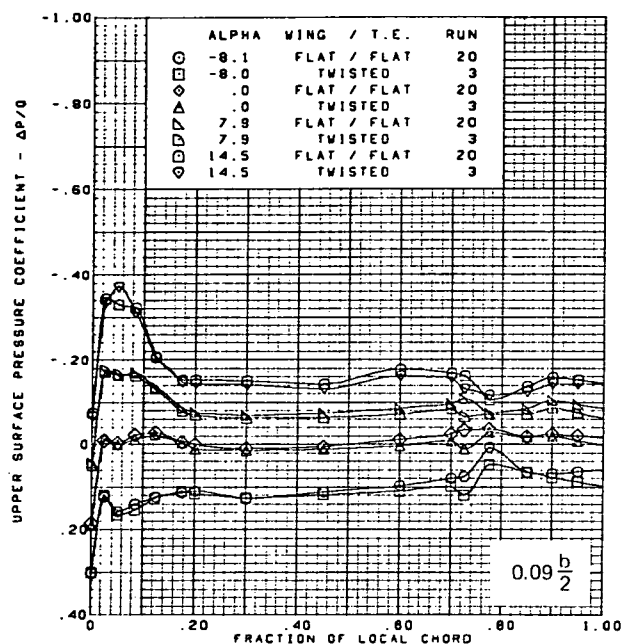
**Page  
Intentionally  
Left Blank**



$M = 2.50$  (run 10)  
 Twisted wing, rounded L.E.  
 L.E. deflection, full span =  $0.0^\circ$   
 T.E. deflection, full span =  $0.0^\circ$

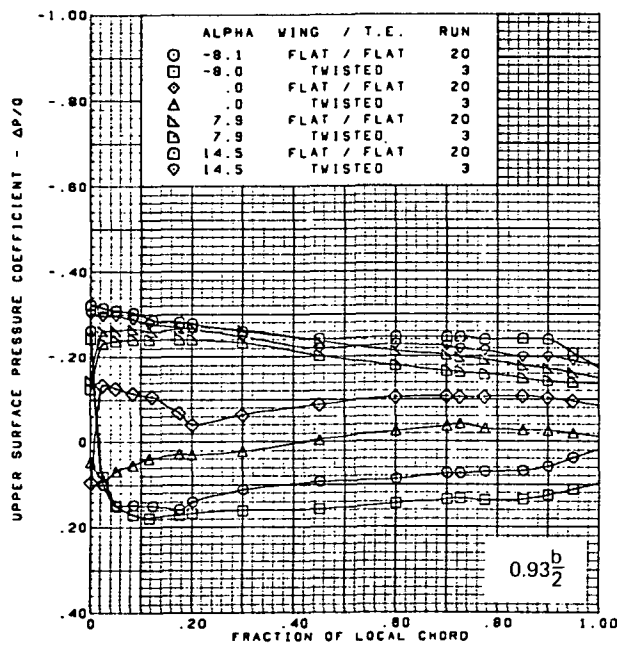
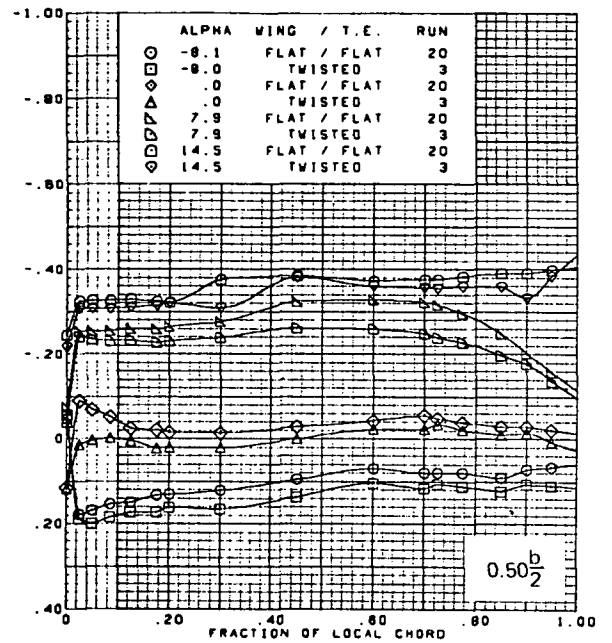
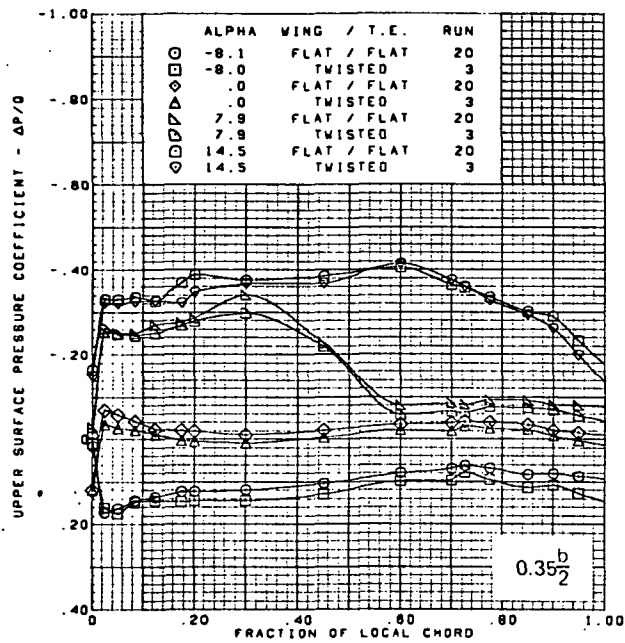
(f) Spanload Distributions and Section Aerodynamic Coefficients

Figure 21.—(Concluded)



(a) Upper Surface Chordwise Pressure Distributions

Figure 22.—Wing Experimental Data—Effect of Wing Twist With Angle of Attack; Rounded L.E.; L.E. Deflection, Full Span = 0.0°; T.E. Deflection, Full Span = 0.0°;  $M = 1.70$

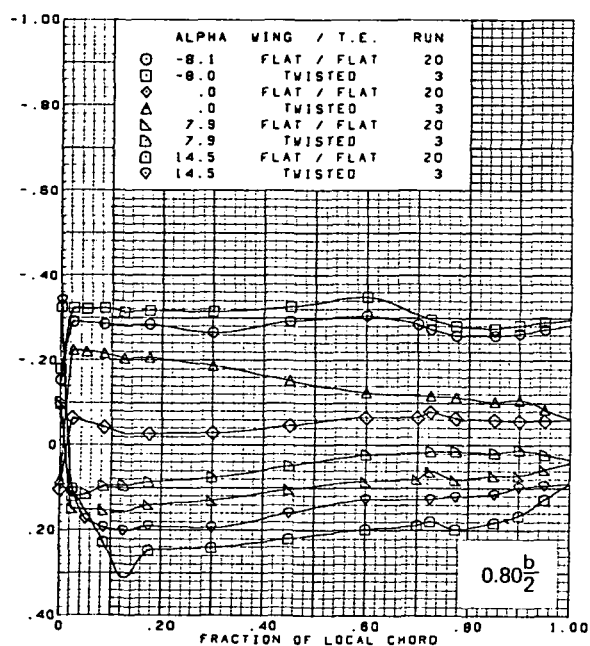
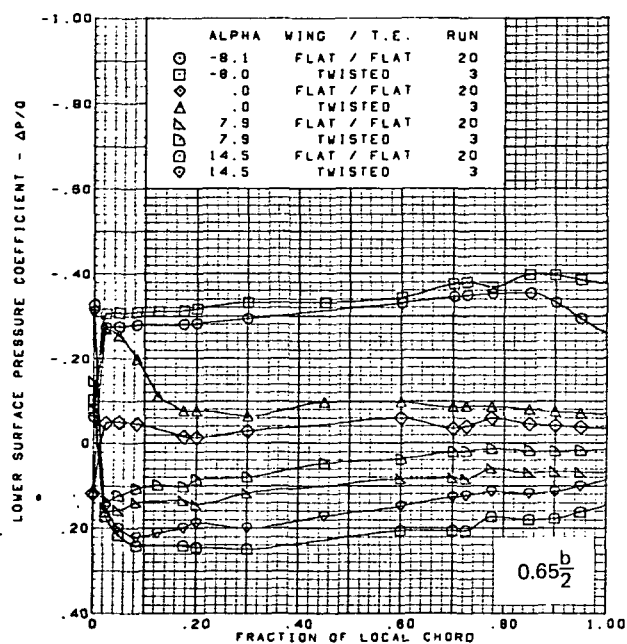
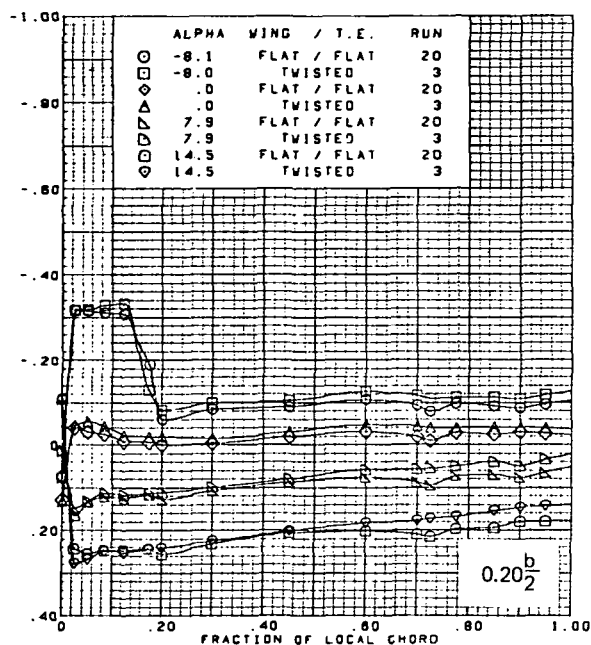
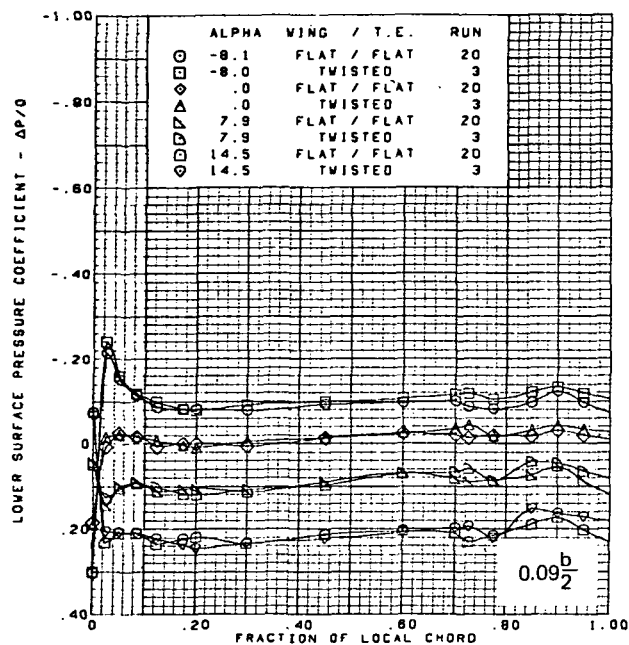


M = 1.70  
 Rounded L.E.  
 L.E. deflection, full span =  $0.0^\circ$   
 T.E. deflection, full span =  $0.0^\circ$

Note:  $C_{p, \text{vacuum}} = -0.49$

(a) (Concluded)

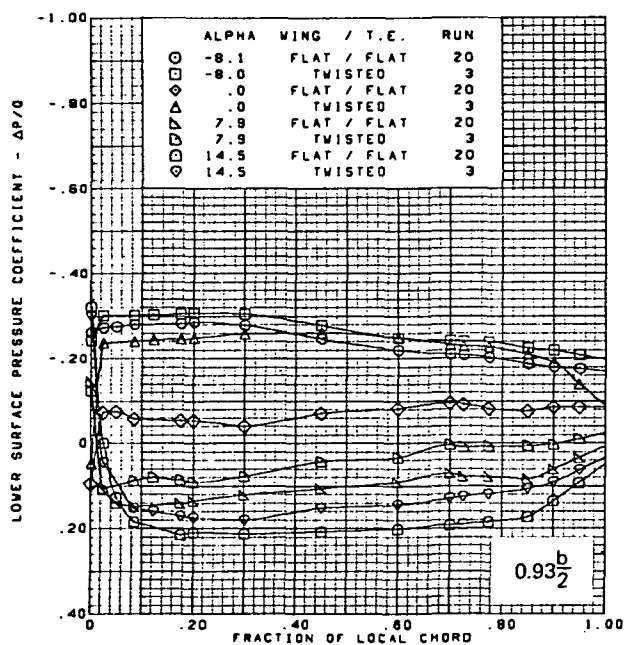
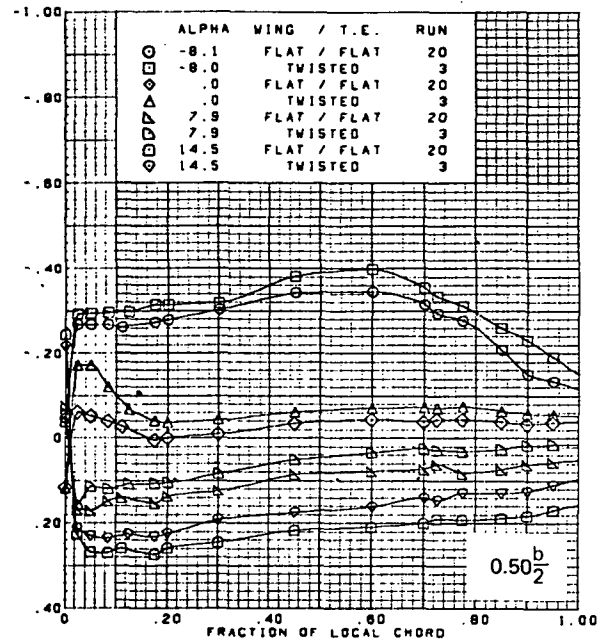
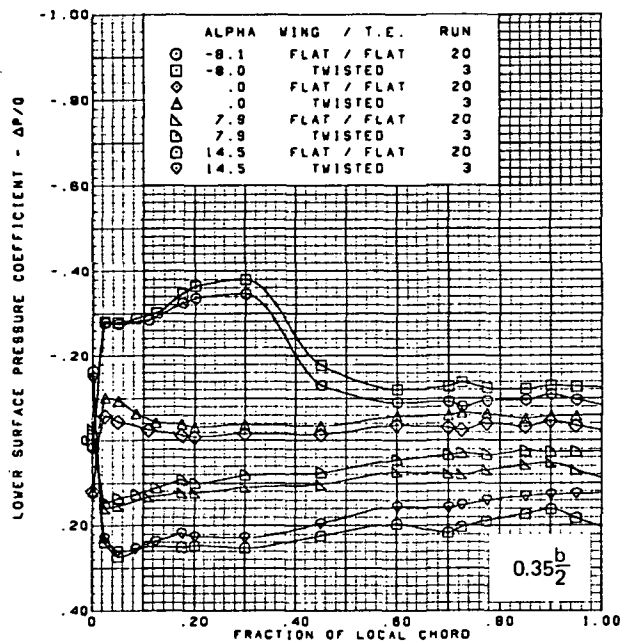
Figure 22.—(Continued)



(b) Lower Surface Chordwise Pressure Distributions

Figure 22.—(Continued)



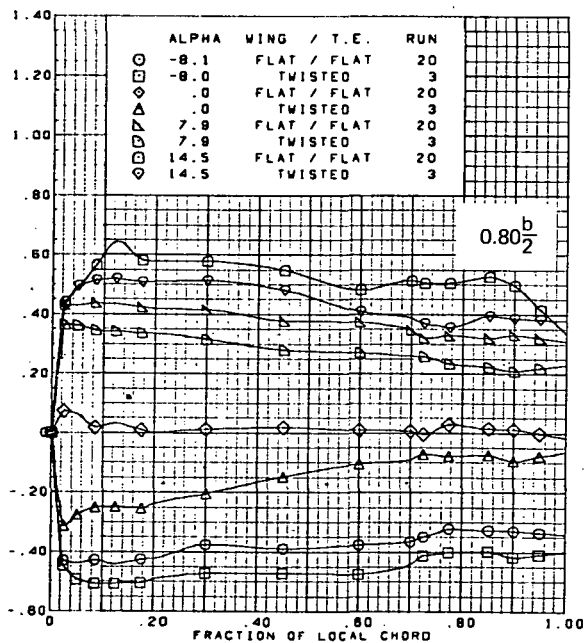
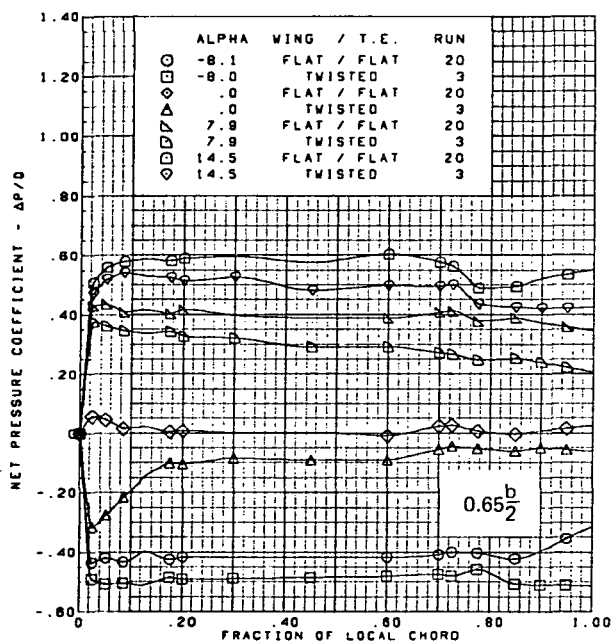
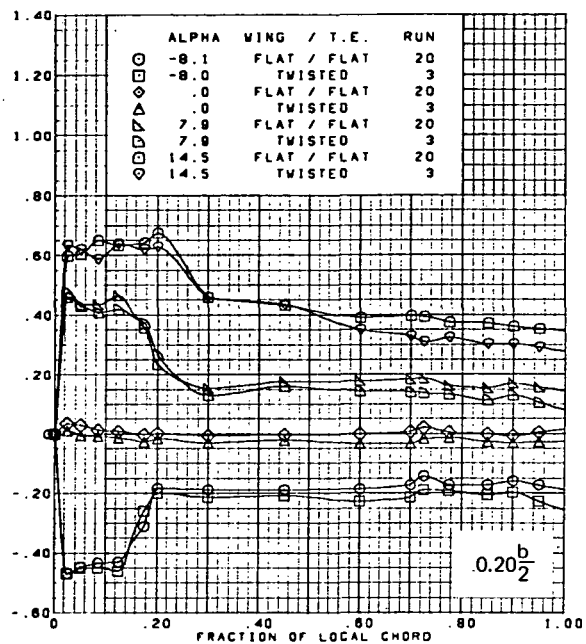
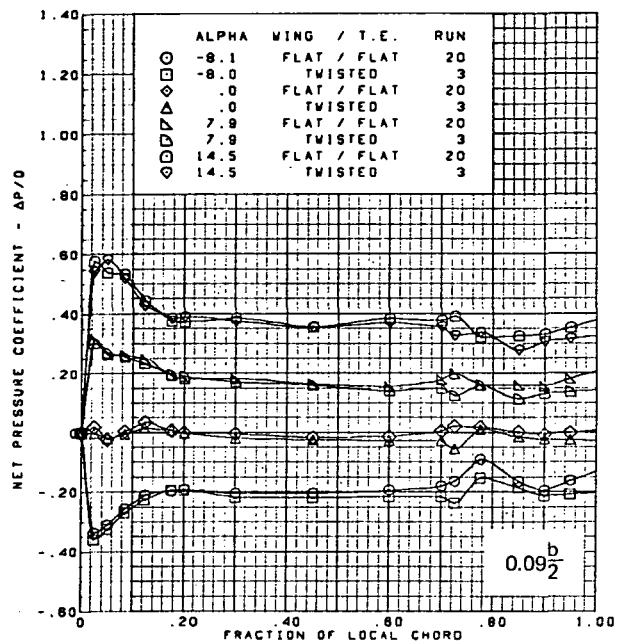


M = 1.70  
 Rounded L.E.  
 L.E. deflection, full span =  $0.0^\circ$   
 T.E. deflection, full span =  $0.0^\circ$

Note:  $C_{p, \text{vacuum}} = -0.49$

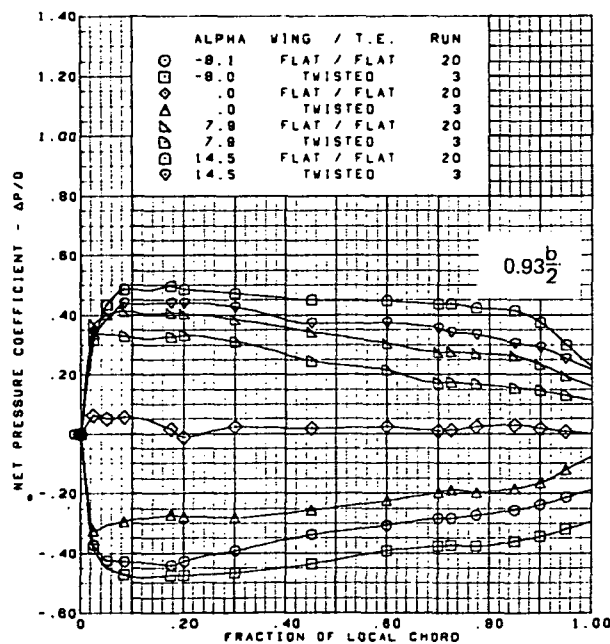
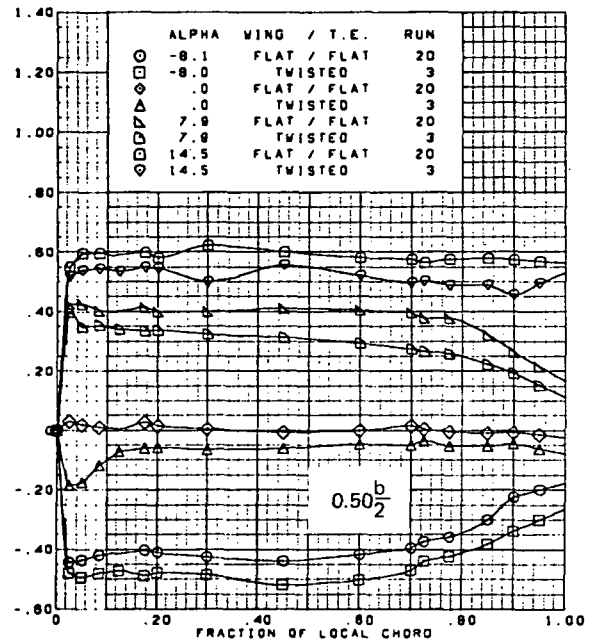
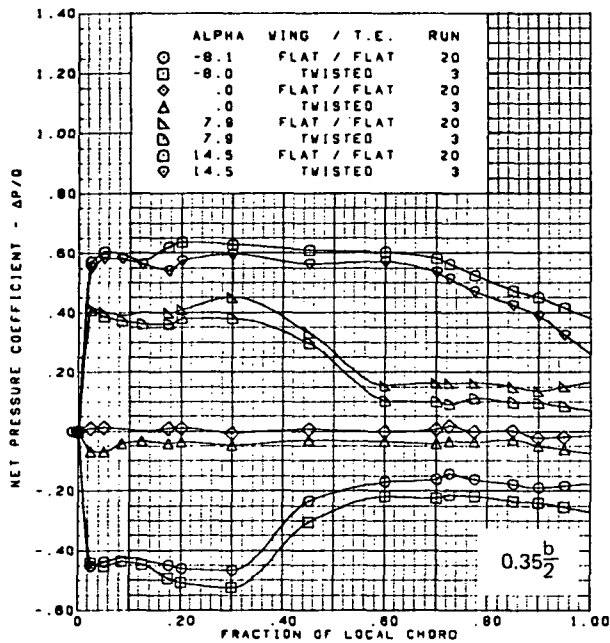
(b) (Concluded)

Figure 22.—(Continued)



(c) Net Chordwise Pressure Distributions

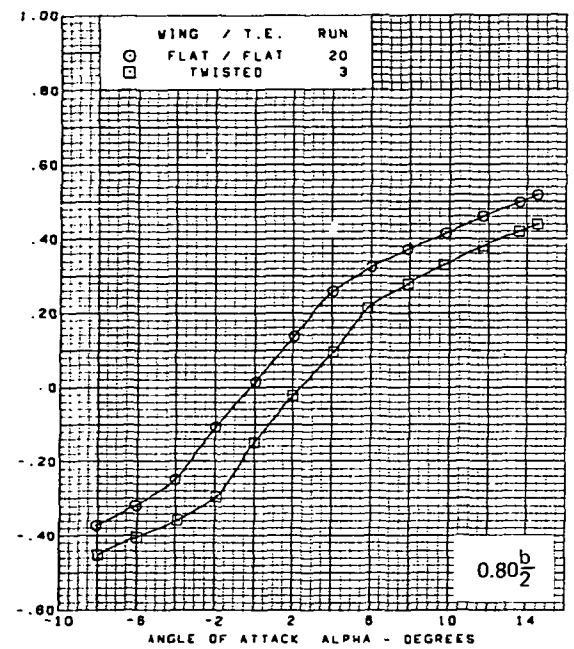
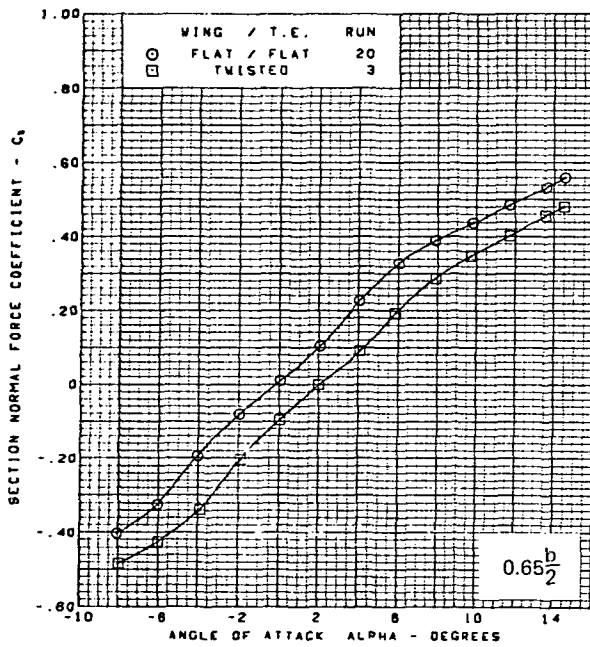
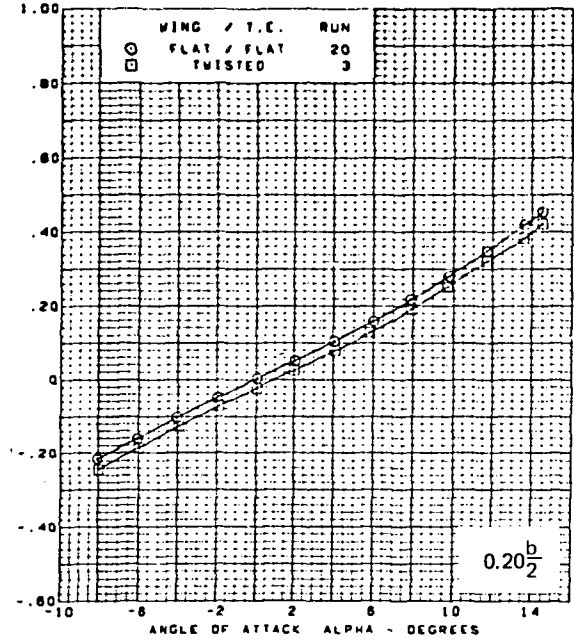
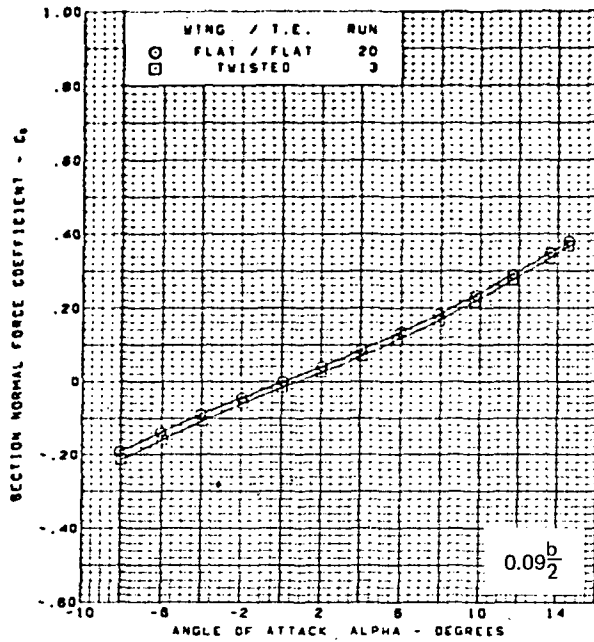
Figure 22.—(Continued)



M = 1.70  
 Rounded L.E.  
 L.E. deflection, full span = 0.0°  
 T.E. deflection, full span = 0.0°

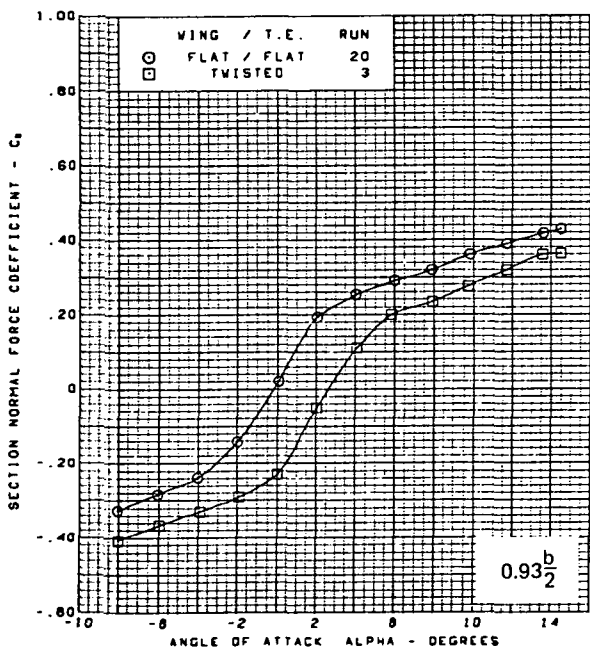
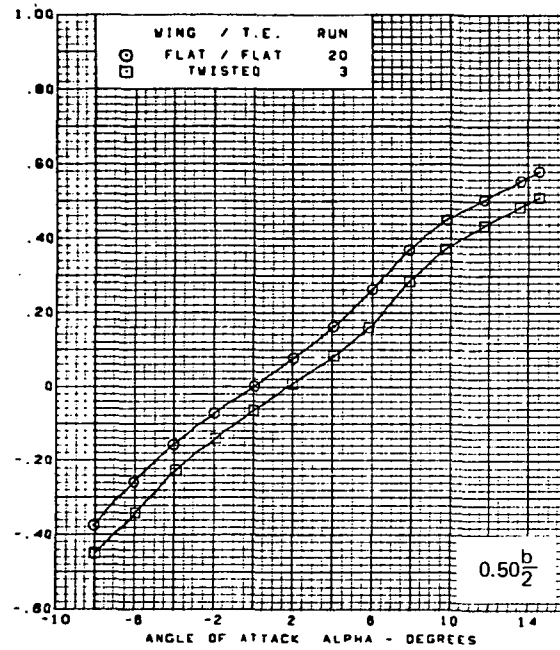
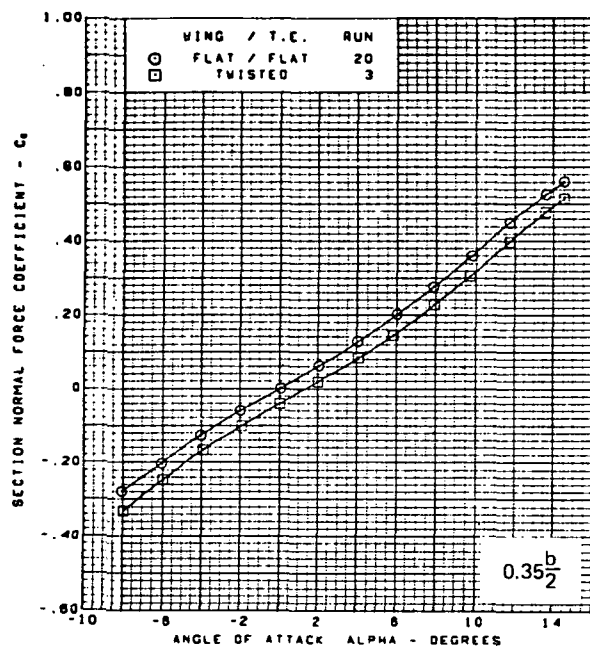
(c) (Concluded)

Figure 22.—(Continued)



(d) Section Aerodynamic Coefficients—Normal Force

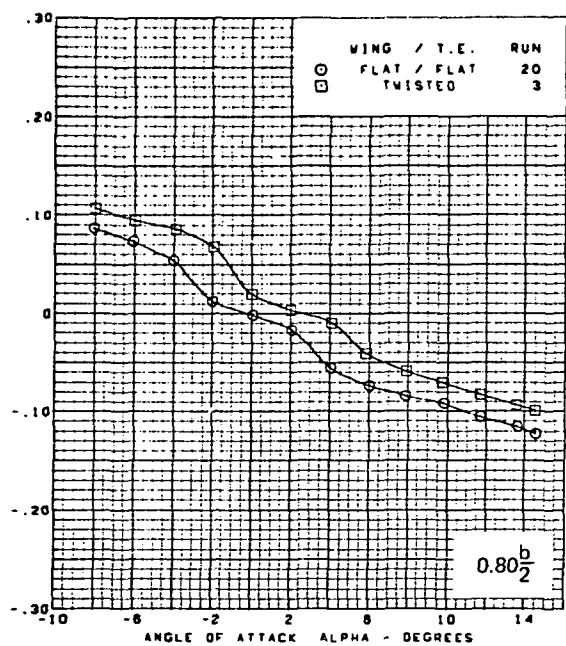
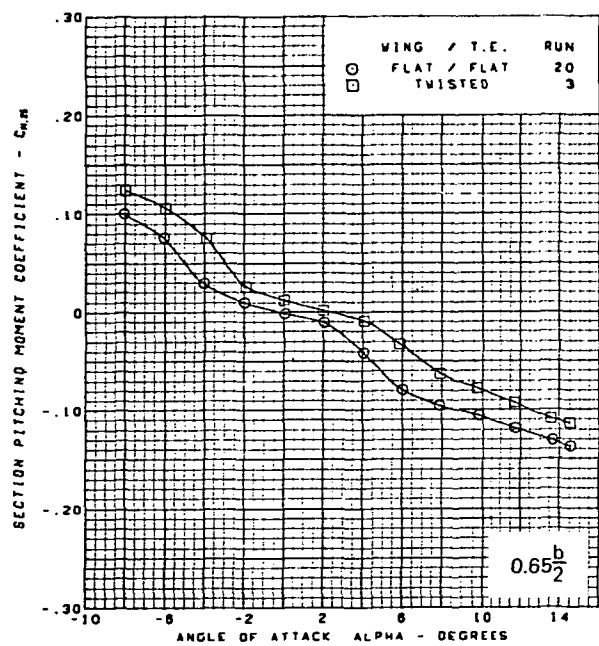
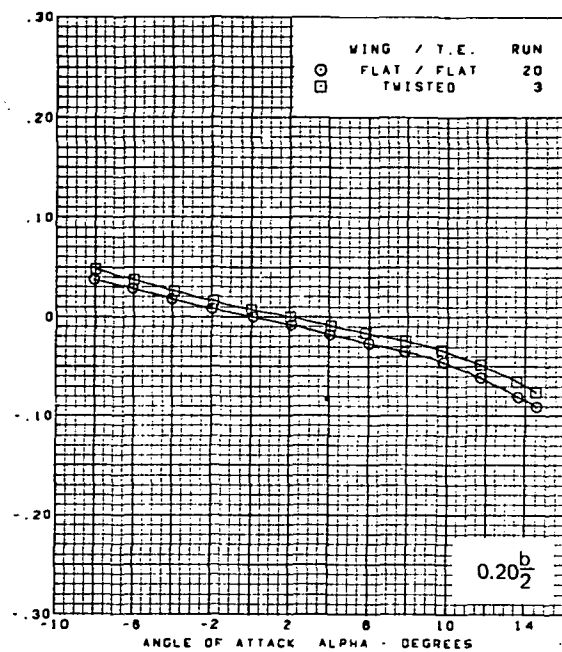
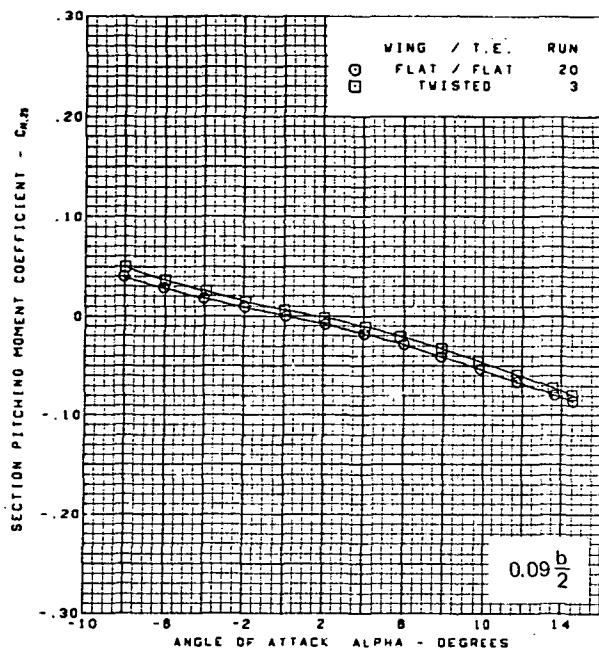
Figure 22.—(Continued)



M = 1.70  
 Rounded L.E.  
 L.E. deflection, full span =  $0.0^\circ$   
 T.E. deflection, full span =  $0.0^\circ$

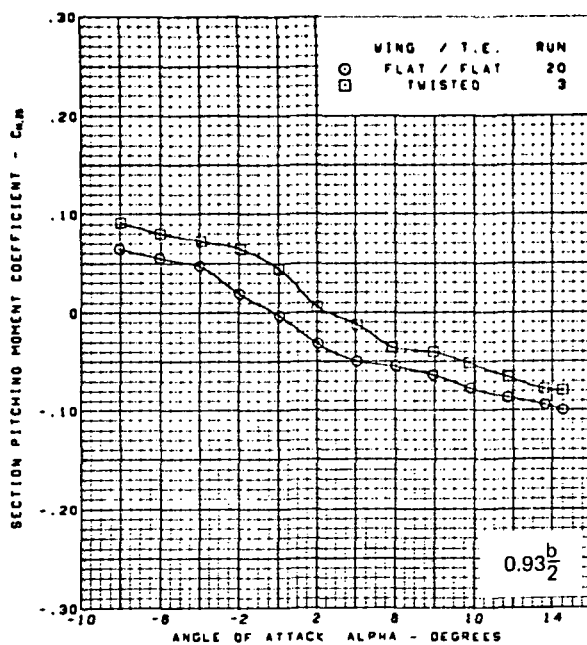
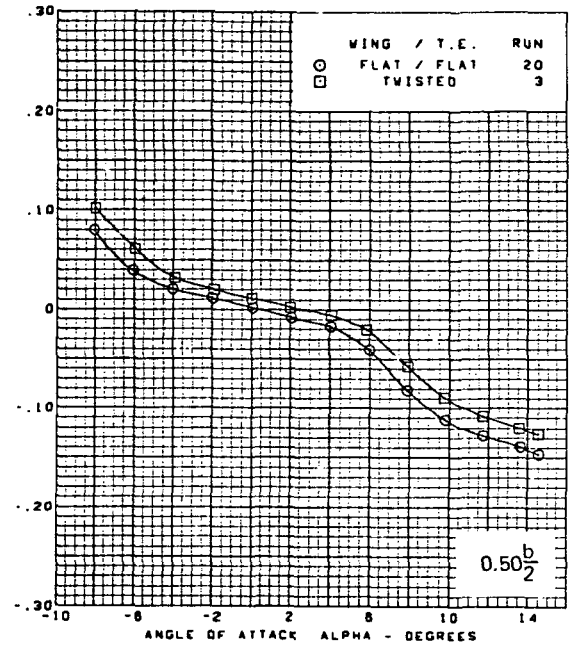
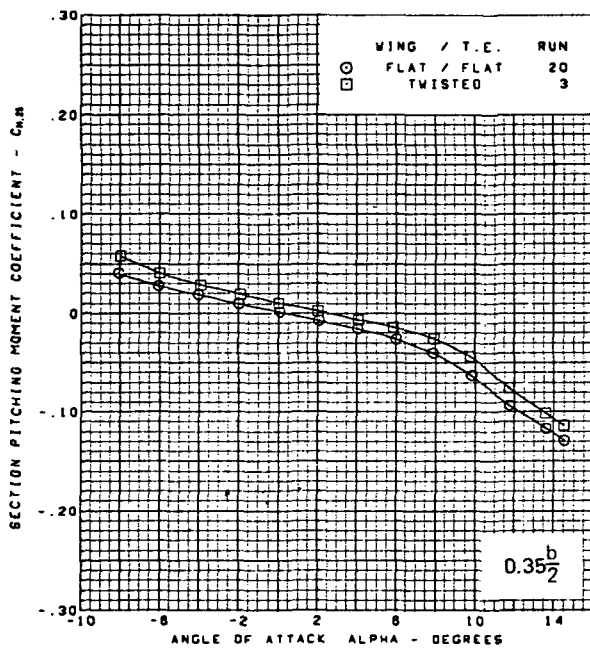
(d) (Concluded)

Figure 22.—(Continued)



(e) Section Aerodynamic Coefficients—Pitching Moment

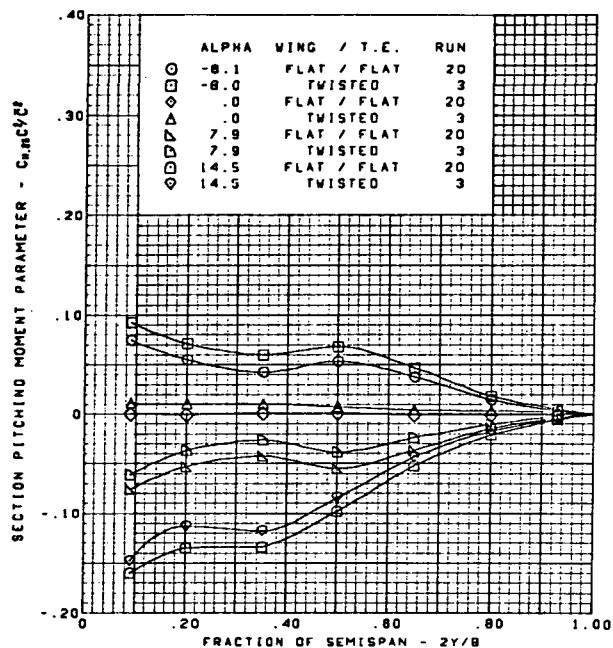
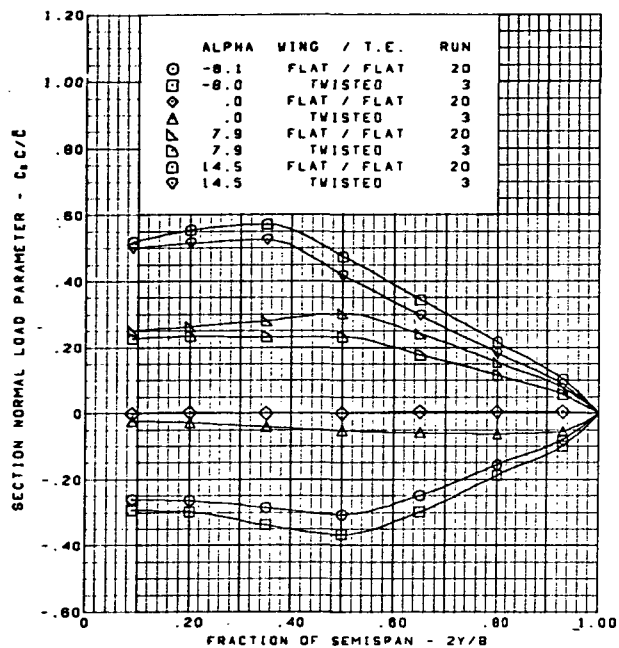
Figure 22.—(Continued)



M = 1.70  
 Rounded L.E.  
 L.E. deflection, full span =  $0.0^\circ$   
 T.E. deflection, full span =  $0.0^\circ$

(e) (Concluded)

Figure 22.—(Continued)

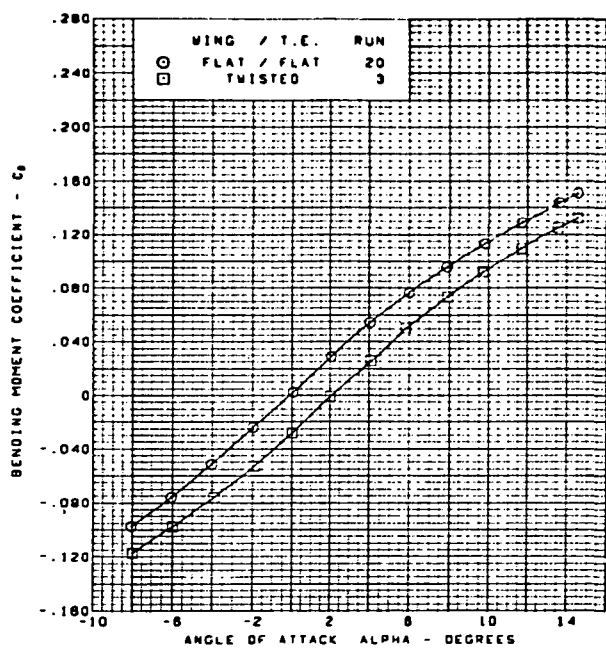
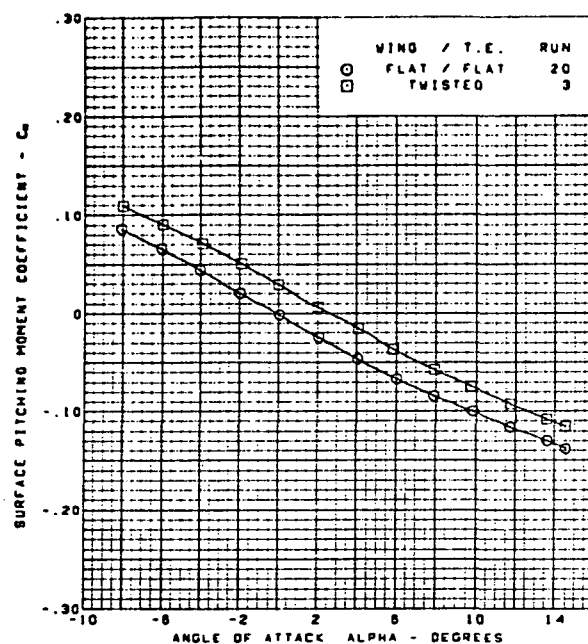
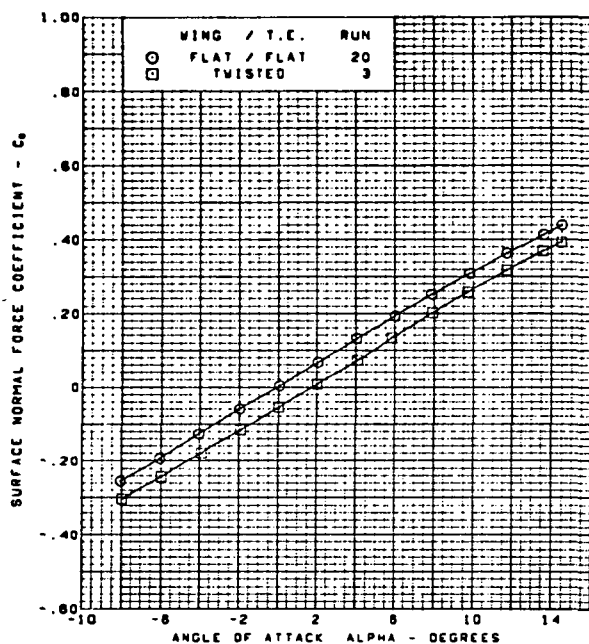


$M = 1.70$   
 Rounded L.E.  
 L.E. deflection, full span =  $0.0^\circ$   
 T.E. deflection, full span =  $0.0^\circ$

(f) Spanload Distributions

Figure 22.—(Continued)

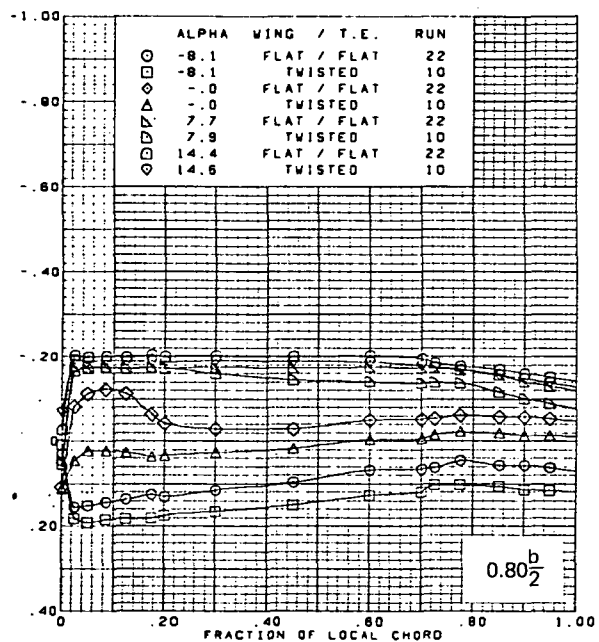
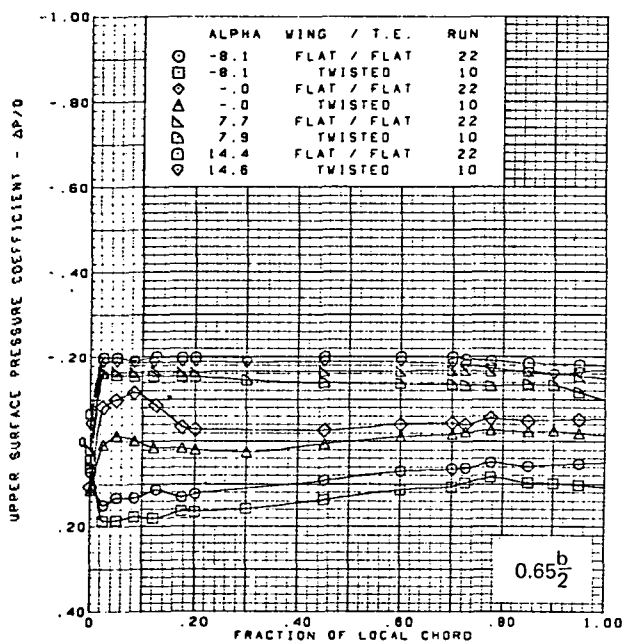
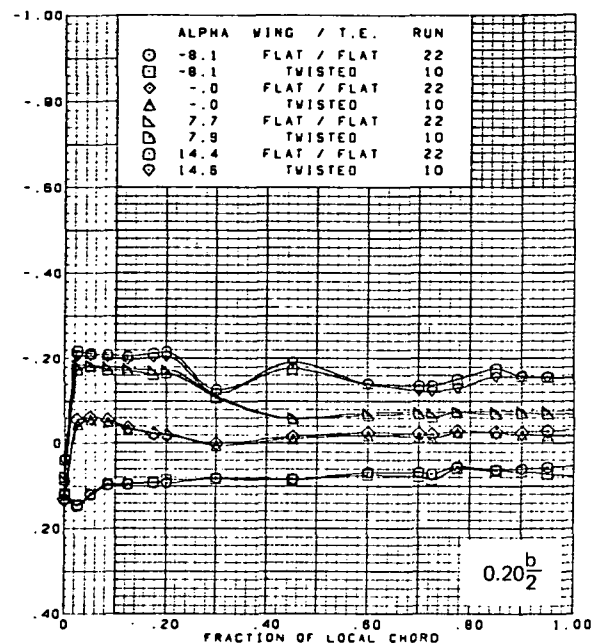
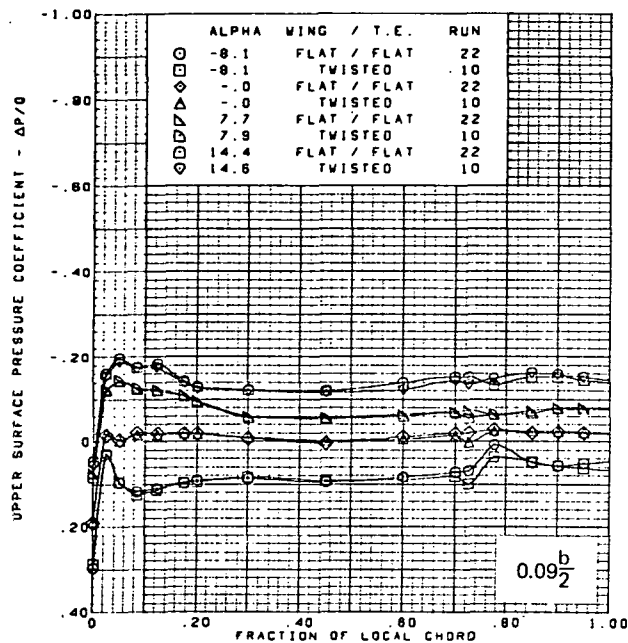




$M = 1.70$   
 Rounded L.E.  
 L.E. deflection, full span =  $0.0^\circ$   
 T.E. deflection, full span =  $0.0^\circ$

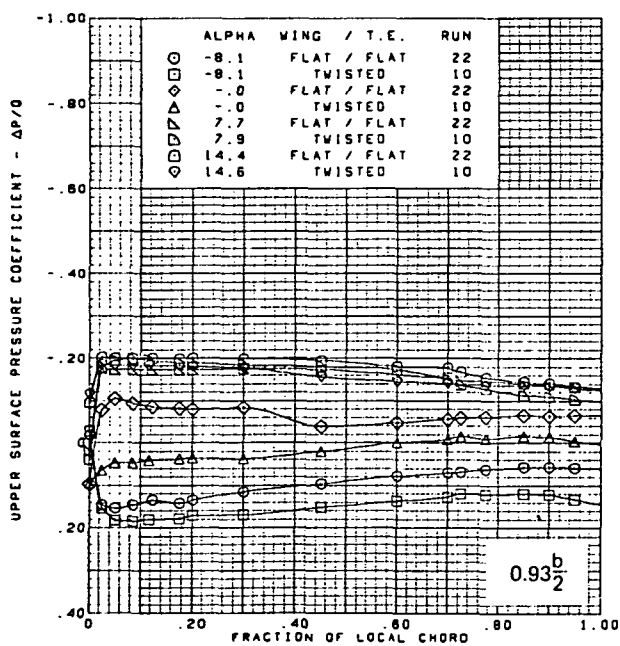
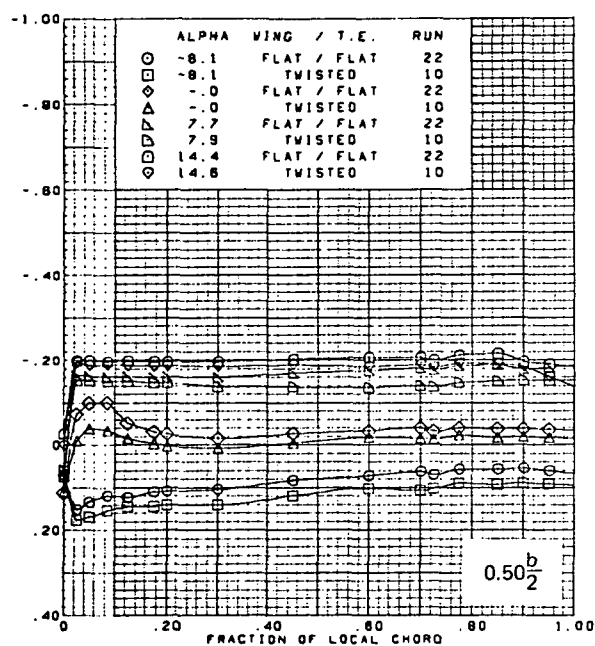
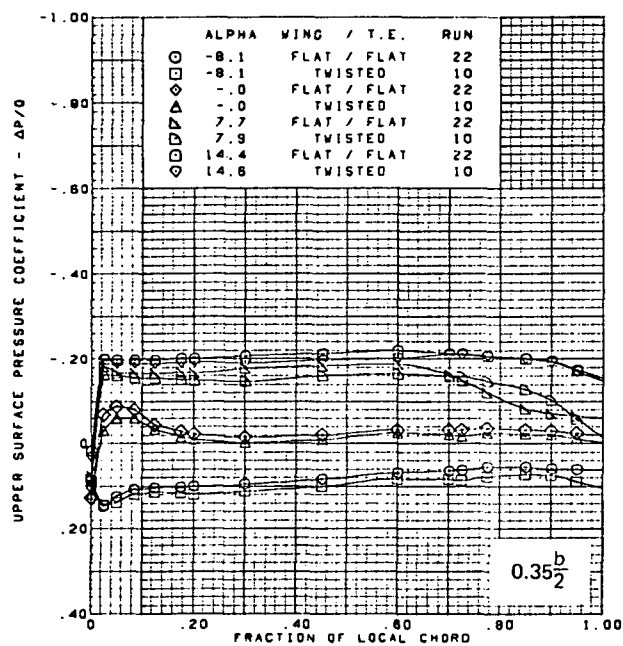
(g) Wing Aerodynamic Coefficients

Figure 22.—(Concluded)



(a) Upper Surface Chordwise Pressure Distributions

Figure 23.—Wing Experimental Data—Effect of Wing Twist With Angle of Attack; Rounded L.E.; L.E. Deflection, Full Span = 0.0°; T.E. Deflection, Full Span = 0.0°;  $M = 2.50$

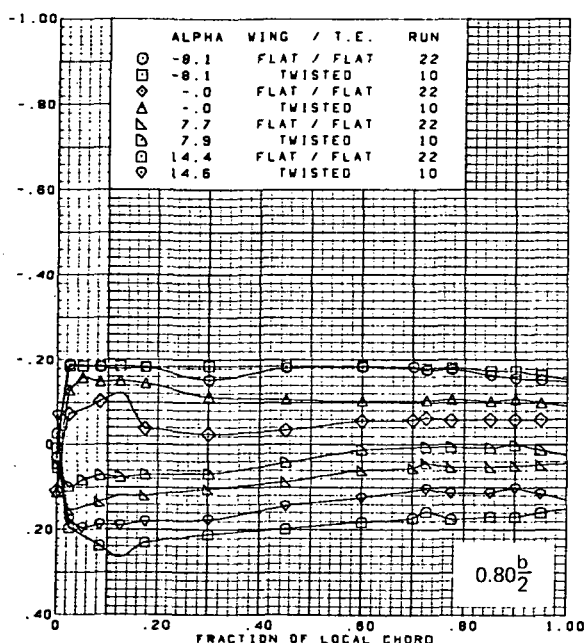
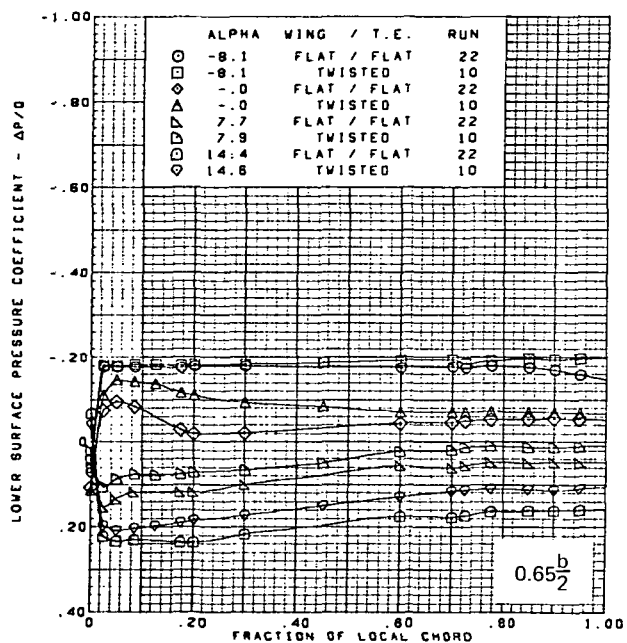
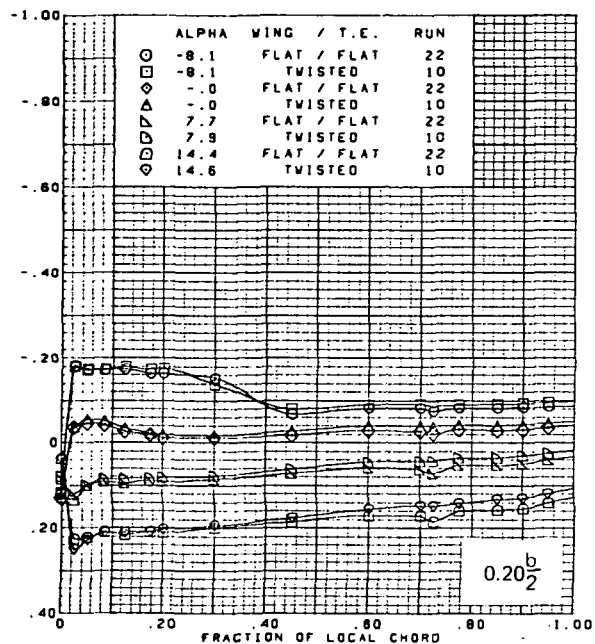
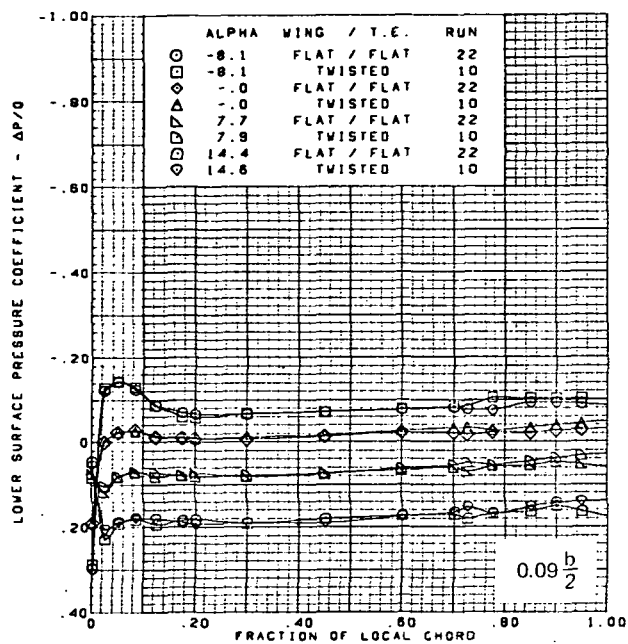


M = 2.50  
 Rounded L.E.  
 L.E. deflection, full span = 0.0°  
 T.E. deflection, full span = 0.0°

Note:  $C_{p, \text{vacuum}} = -0.23$

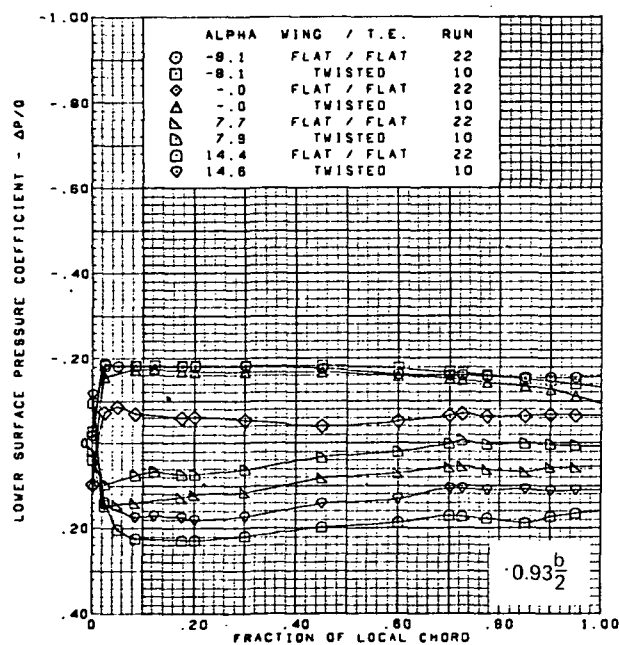
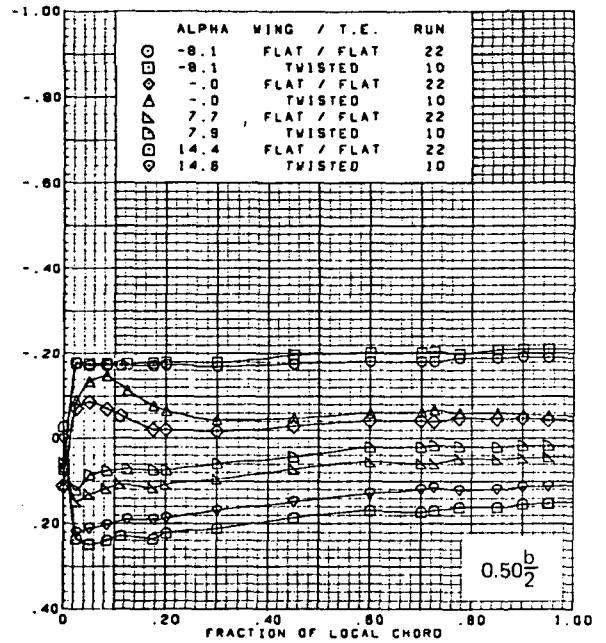
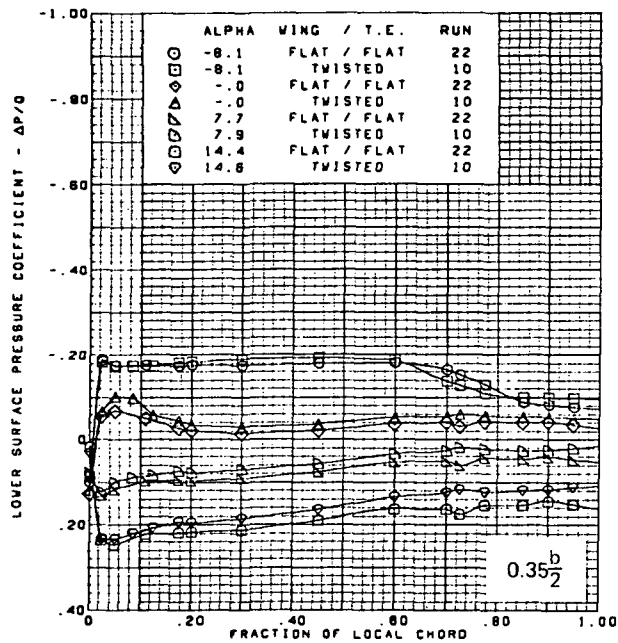
(a) (Concluded)

Figure 23.—(Continued)



(b) Lower Surface Chordwise Pressure Distributions

Figure 23.—(Continued)

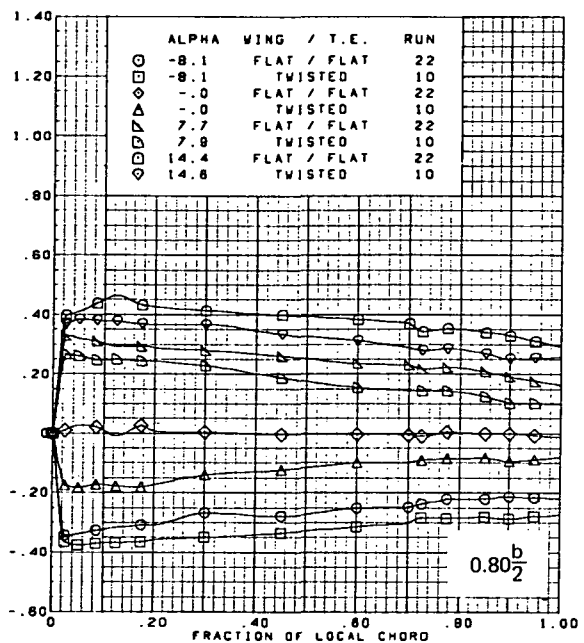
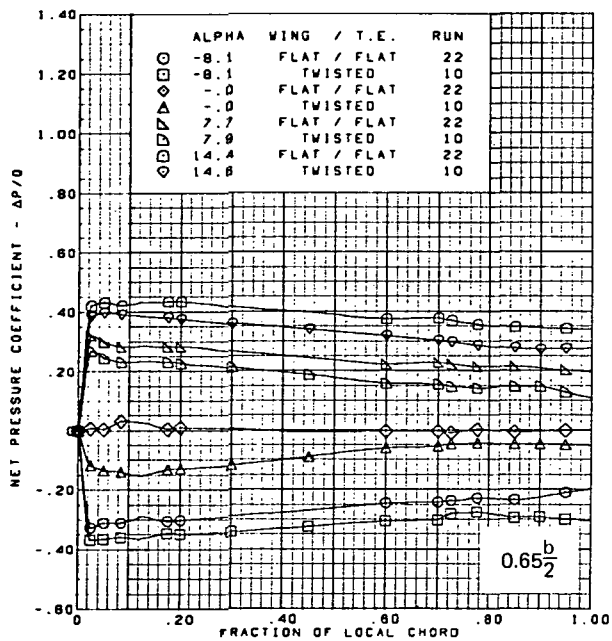
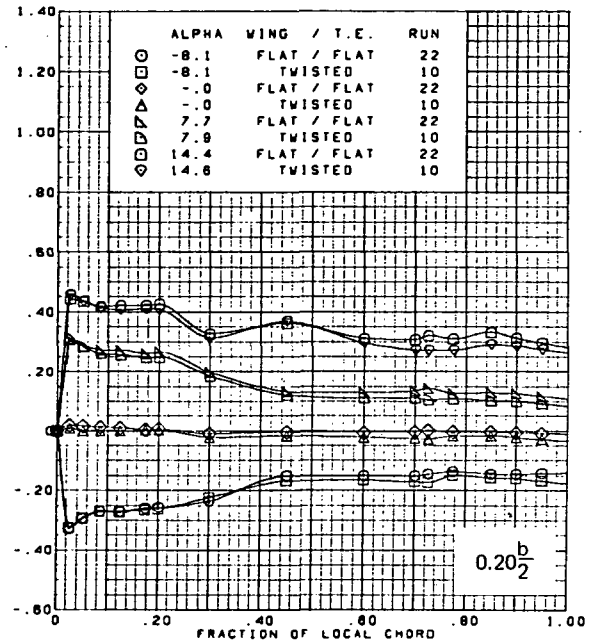
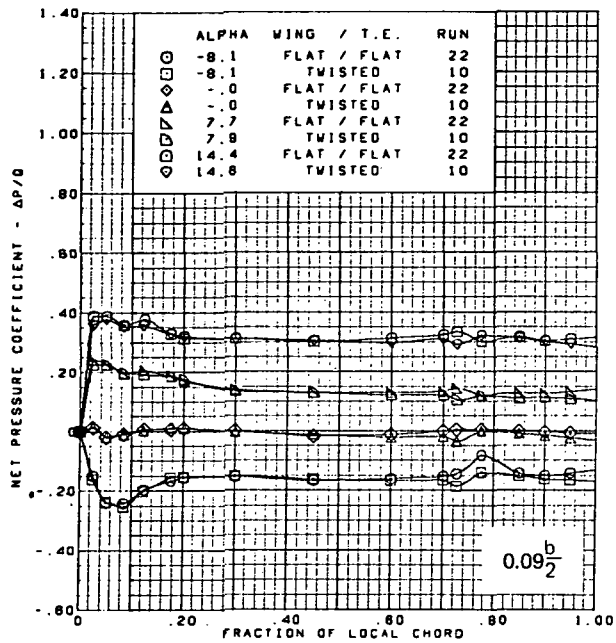


M = 2.50  
 Rounded L.E.  
 L.E. deflection, full span =  $0.0^\circ$   
 T.E. deflection, full span =  $0.0^\circ$

Note:  $C_{p, \text{vacuum}} = -0.23$

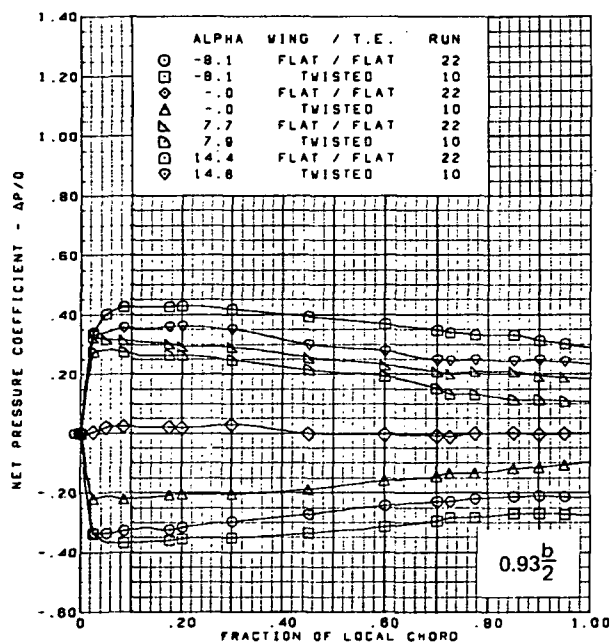
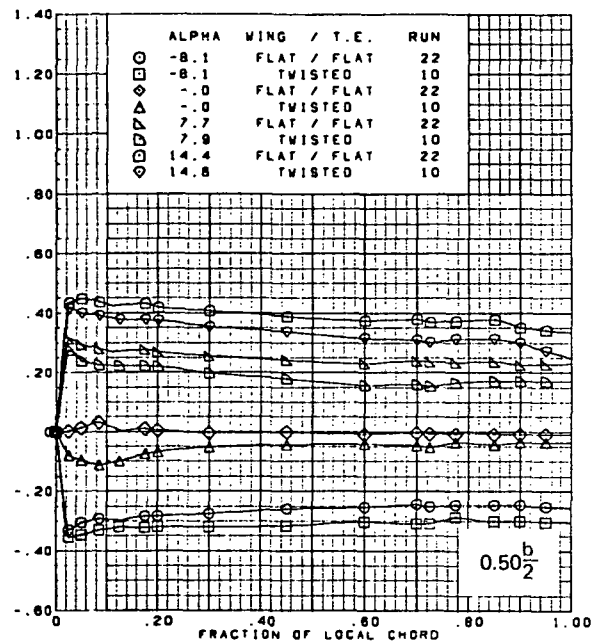
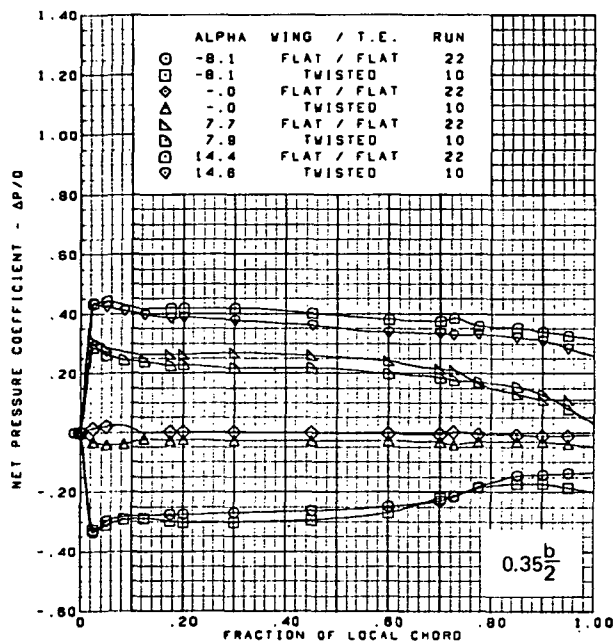
(b) (Concluded)

Figure 23.—(Continued)



(c) Net Chordwise Pressure Distributions

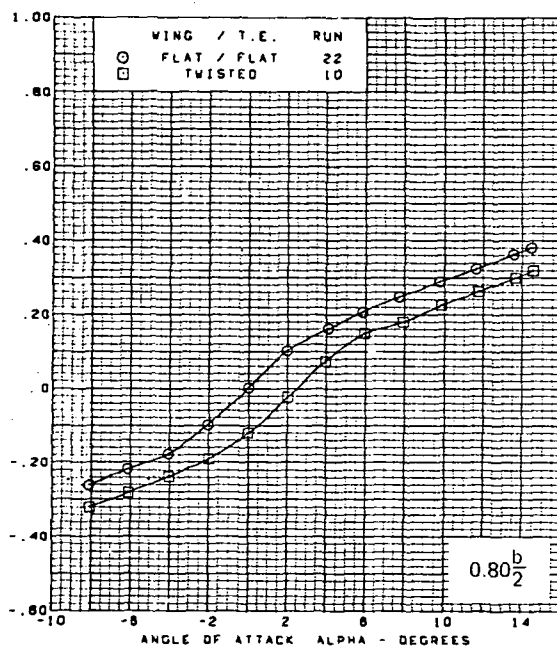
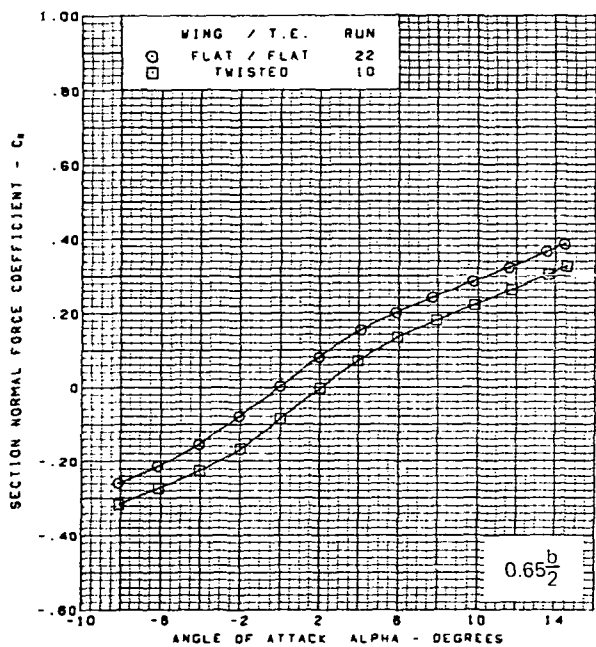
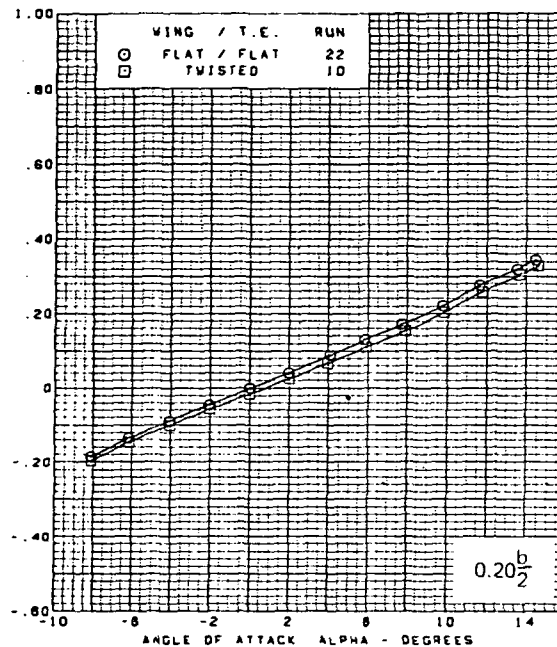
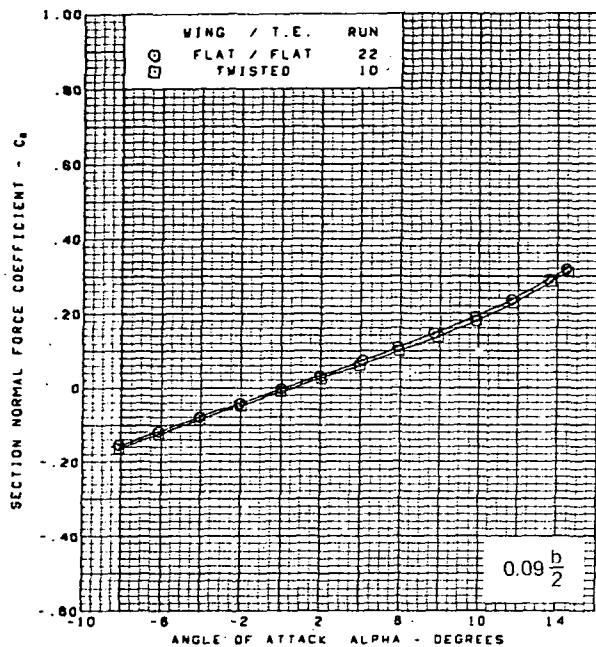
Figure 23.—(Continued)



$M = 2.50$   
 Rounded L.E.  
 L.E. deflection, full span =  $0.0^\circ$   
 T.E. deflection, full span =  $0.0^\circ$

(c) (Concluded)

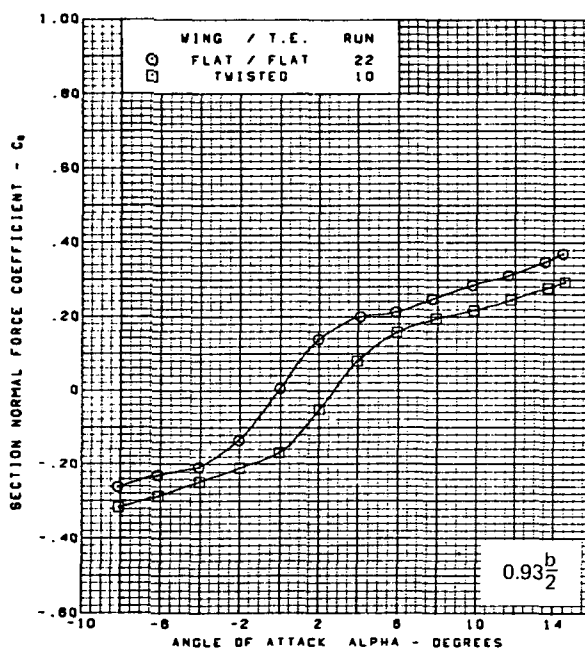
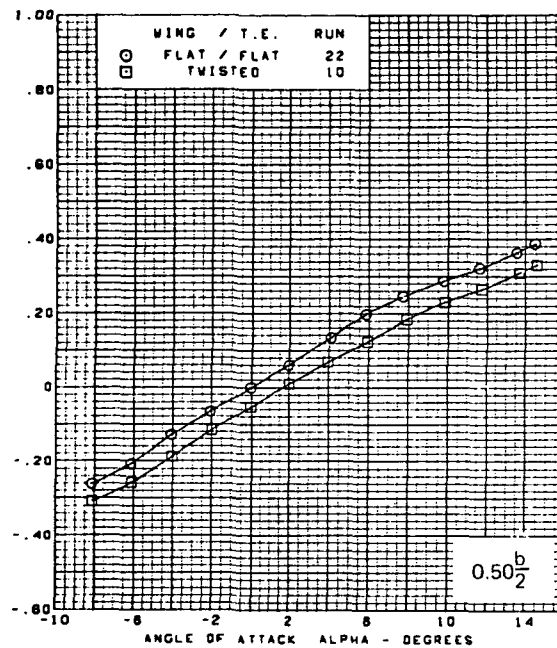
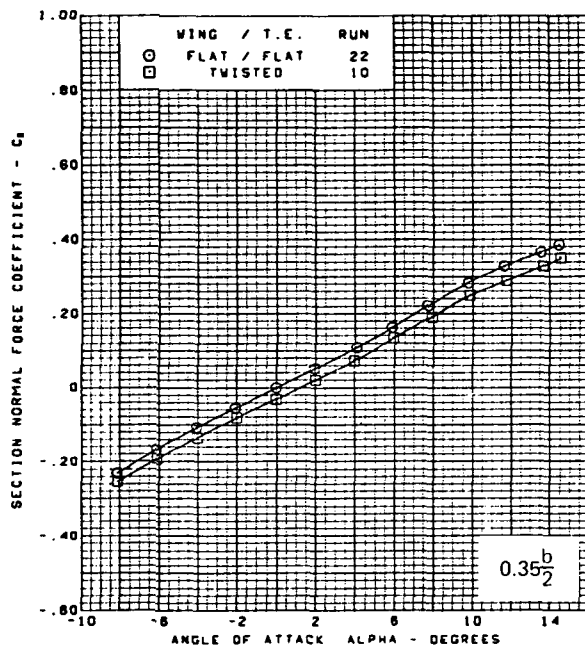
Figure 23.—(Continued)



(d) Section Aerodynamic Coefficients—Normal Force

Figure 23.—(Continued)

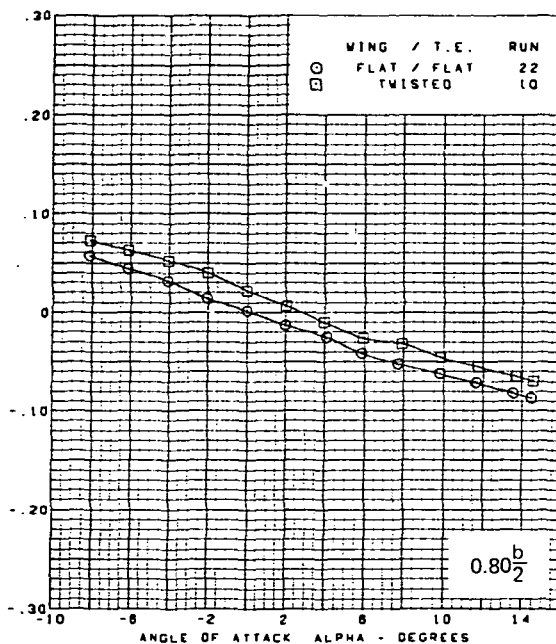
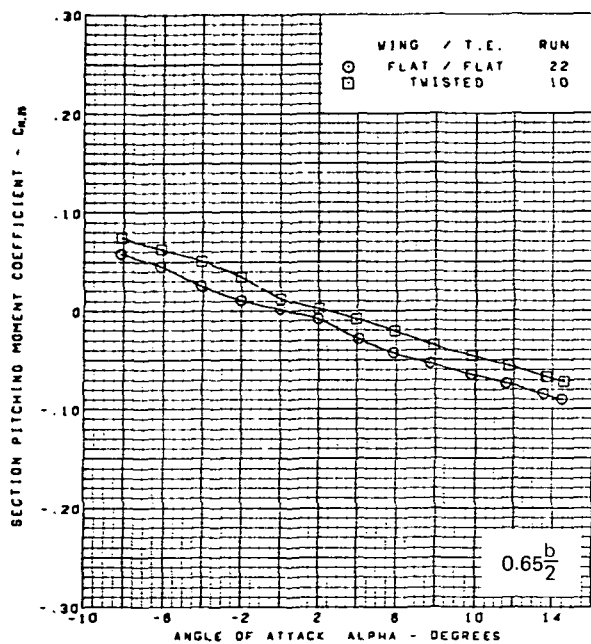
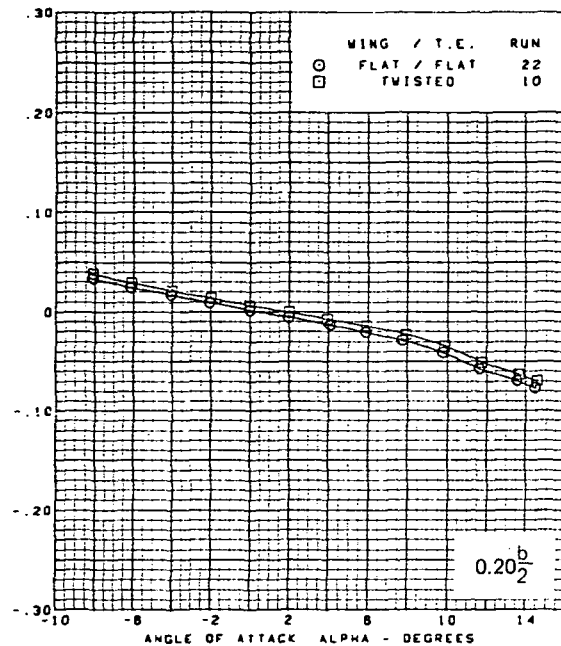
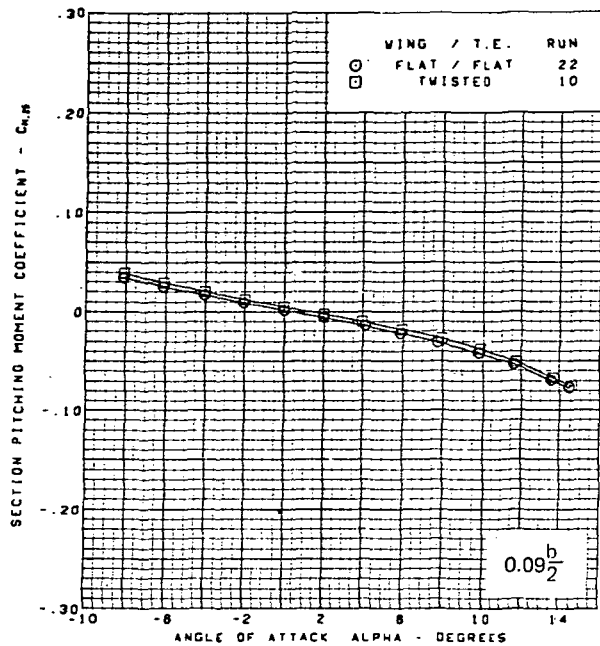




M = 2.50  
 Rounded L.E.  
 L.E. deflection, full span =  $0.0^\circ$   
 T.E. deflection, full span =  $0.0^\circ$

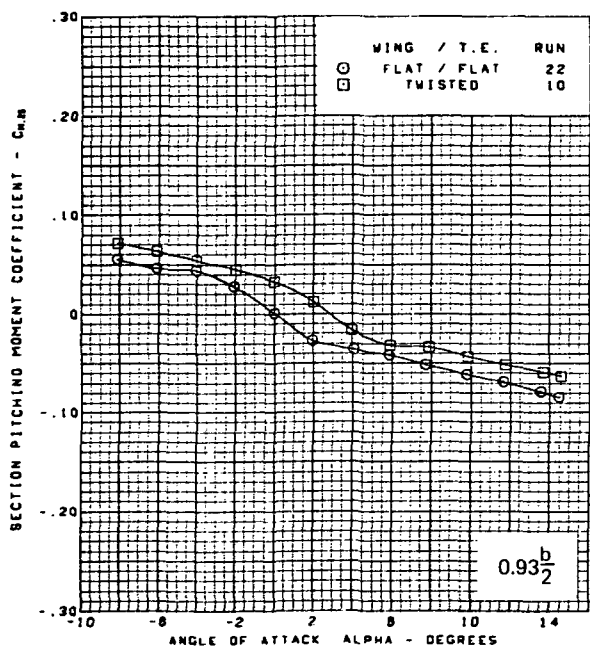
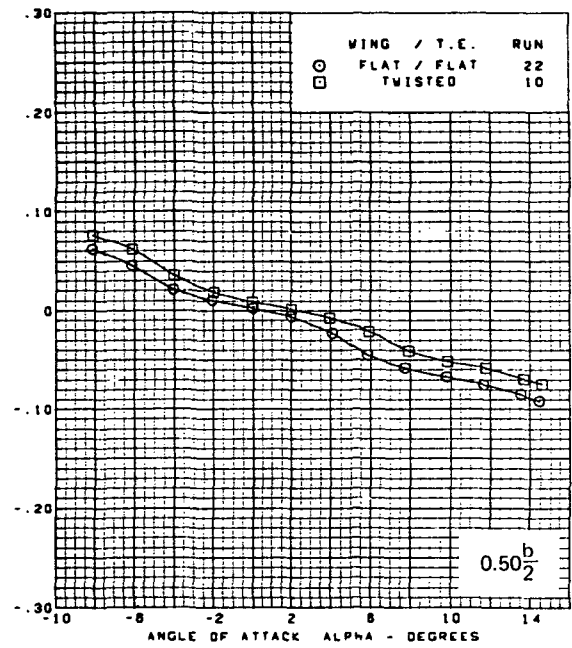
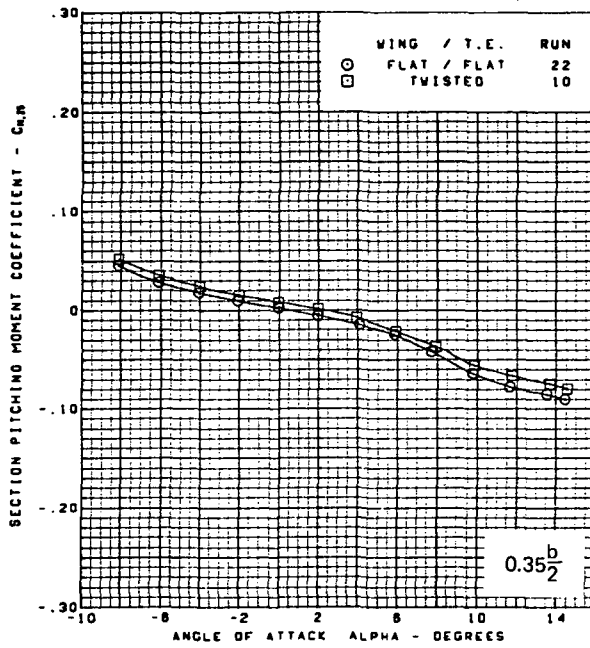
(d) (Concluded)

Figure 23.—(Continued)



(e) Section Aerodynamic Coefficients—Pitching Moment

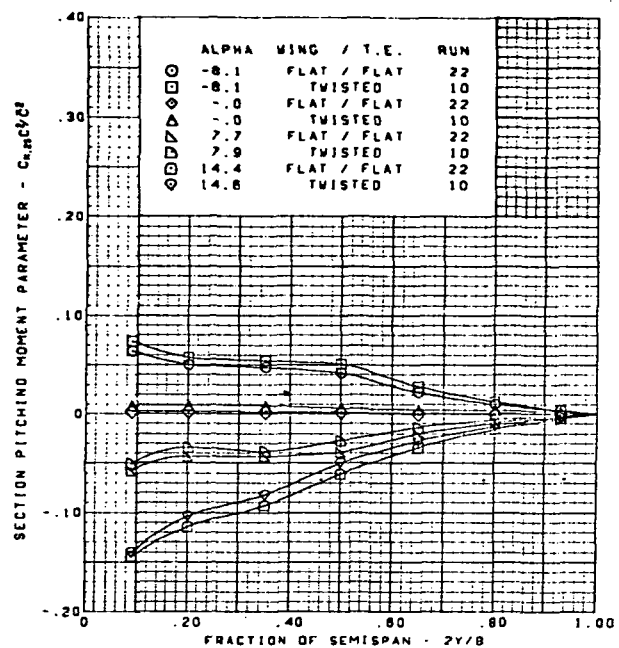
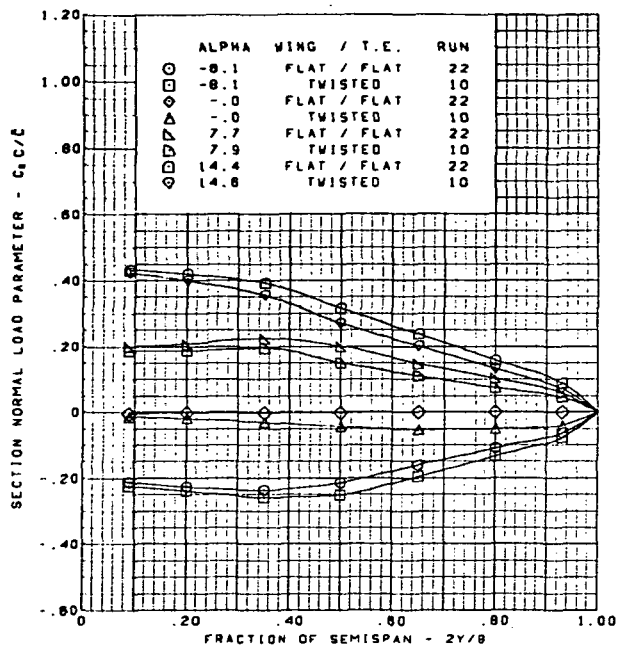
Figure 23.—(Continued)



M = 2.50  
 Rounded L.E.  
 L.E. deflection, full span =  $0.0^\circ$   
 T.E. deflection, full span =  $0.0^\circ$

(e) (Concluded)

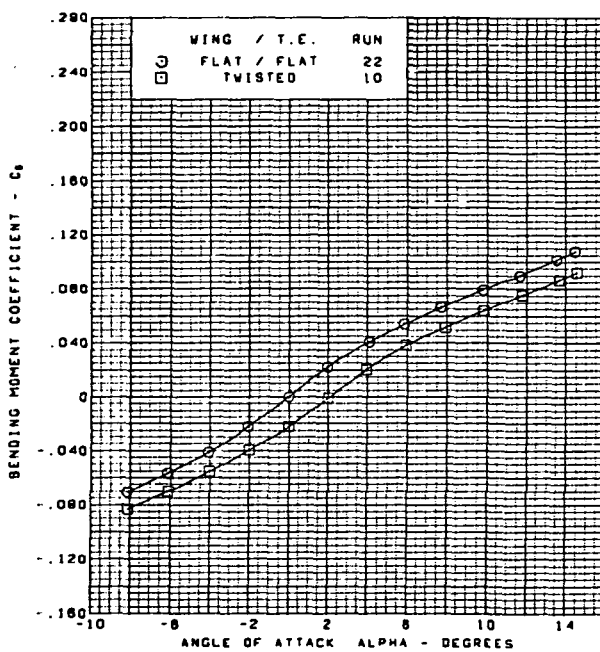
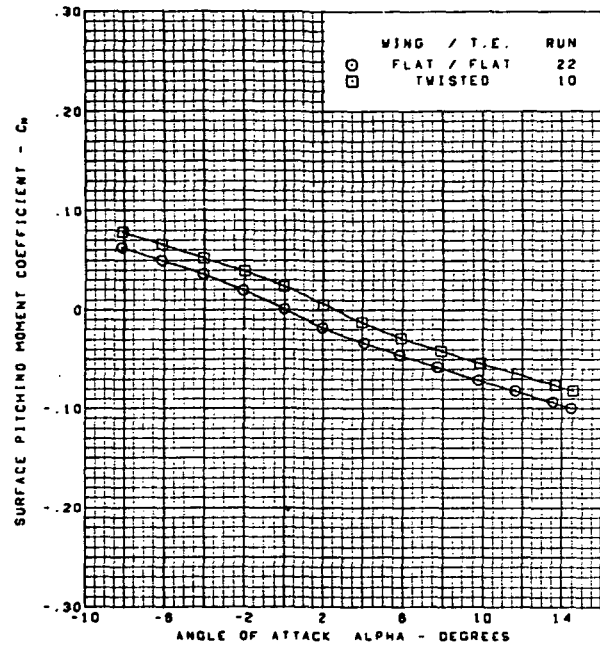
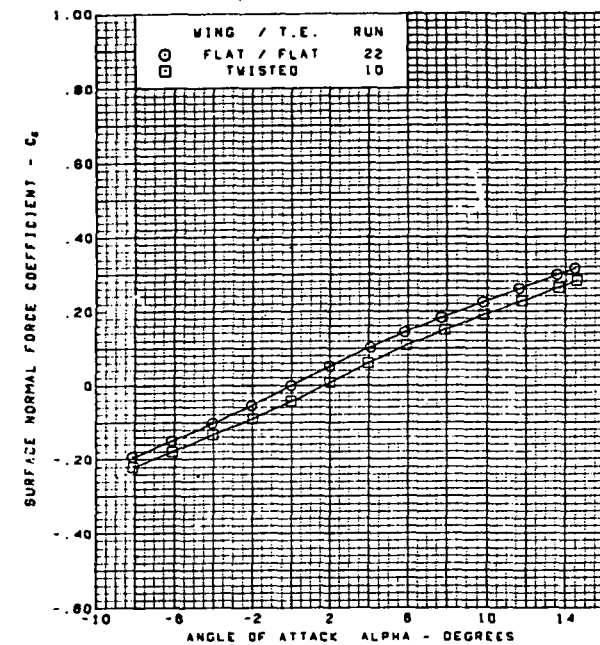
Figure 23.—(Continued)



$M = 2.50$   
 Rounded L.E.  
 L.E. deflection, full span =  $0.0^\circ$   
 T.E. deflection, full span =  $0.0^\circ$

(f) Spanload Distributions

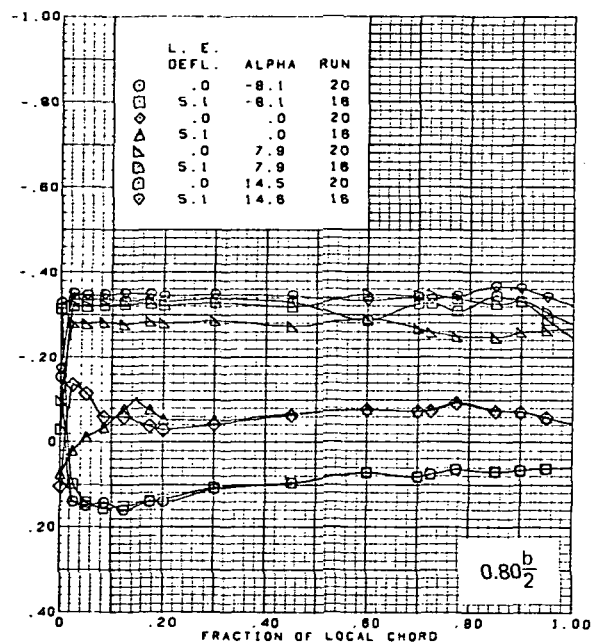
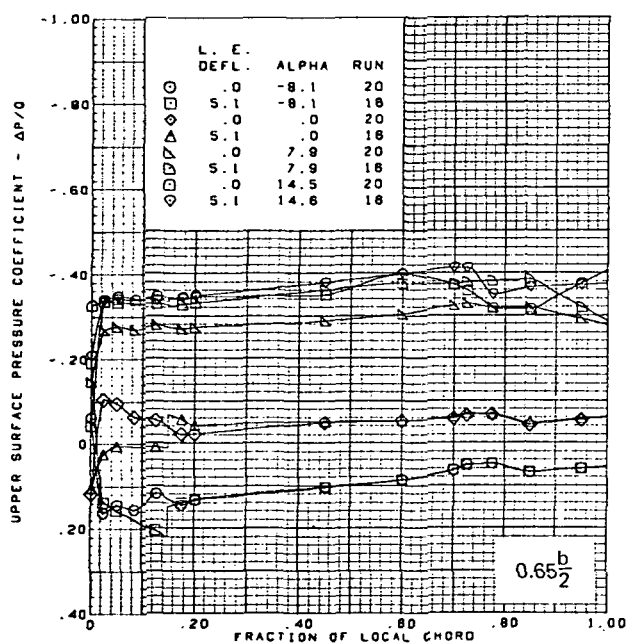
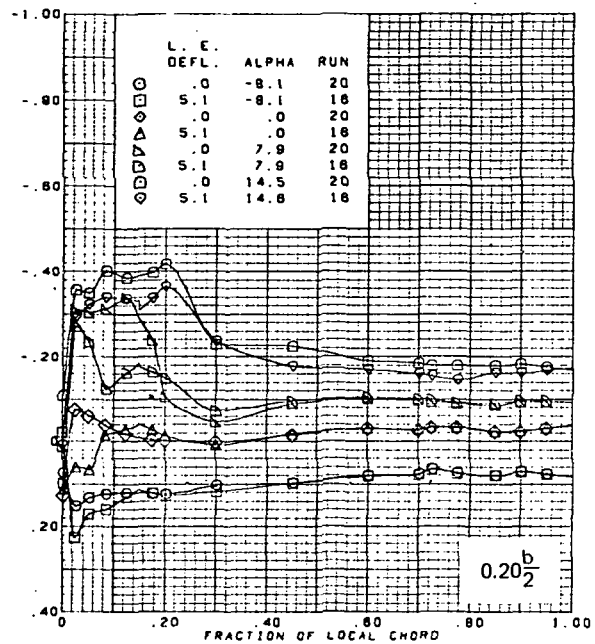
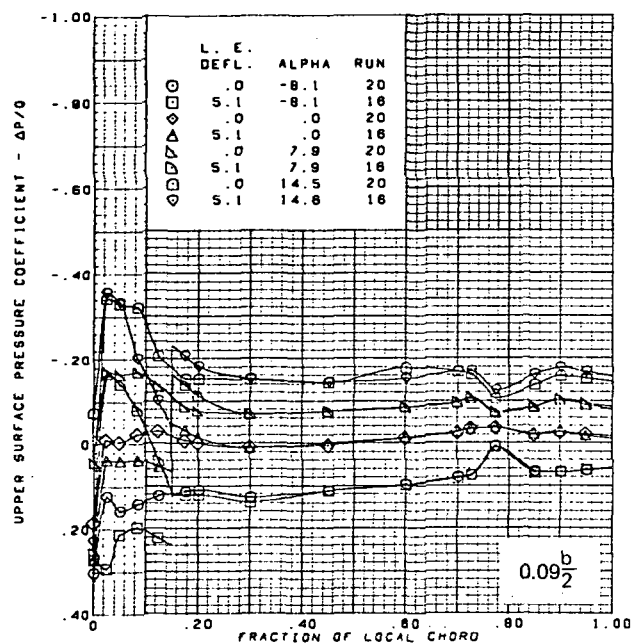
Figure 23.—(Continued)



$M = 2.50$   
 Rounded L.E.  
 L.E. deflection, full span =  $0.0^\circ$   
 T.E. deflection, full span =  $0.0^\circ$

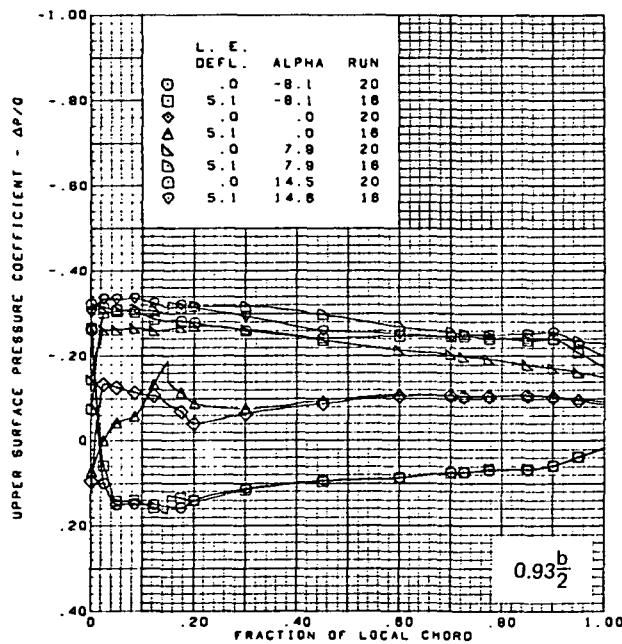
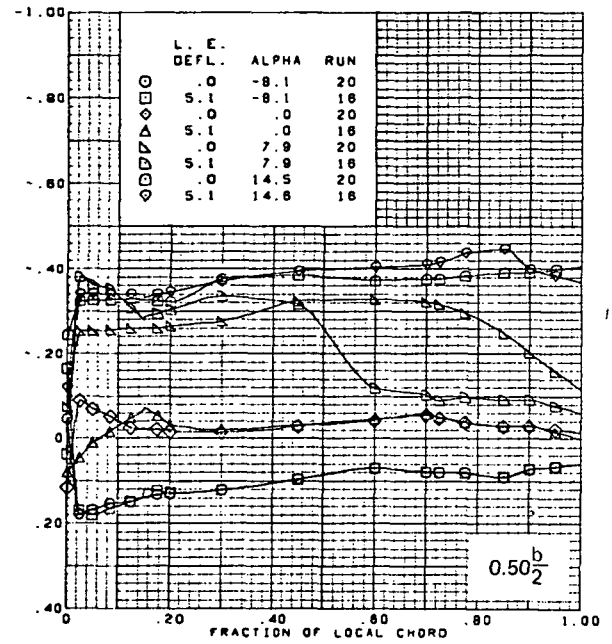
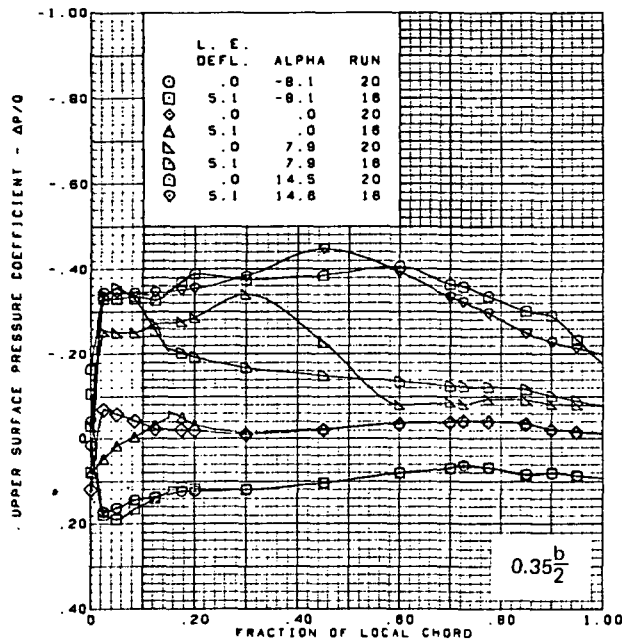
(g) Wing Aerodynamic Coefficients

Figure 23.—(Concluded)



(a) Upper Surface Chordwise Pressure Distributions

Figure 24.—Wing Experimental Data—Effect of Full Span L.E. Deflection With Angle of Attack; Flat Wing; Rounded L.E.; T.E. Deflection, Full Span =  $0.0^\circ$ ;  $M = 1.70$

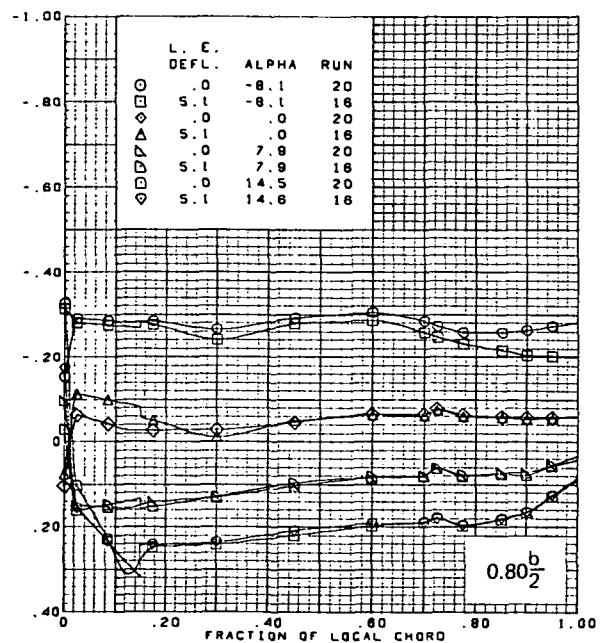
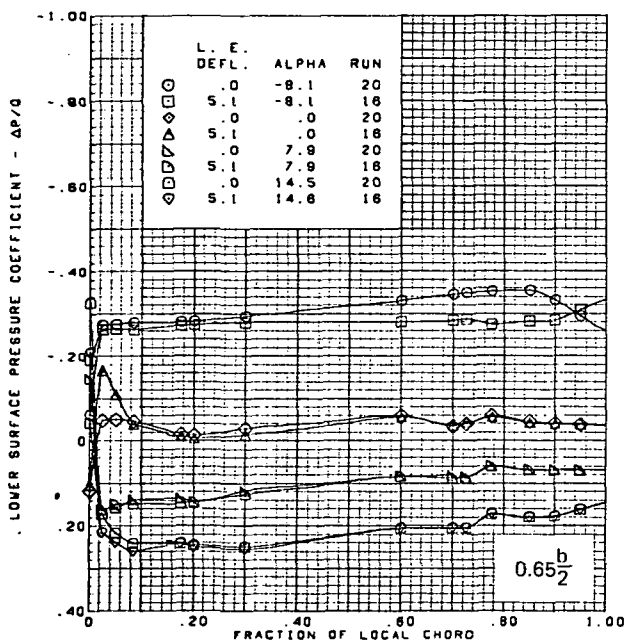
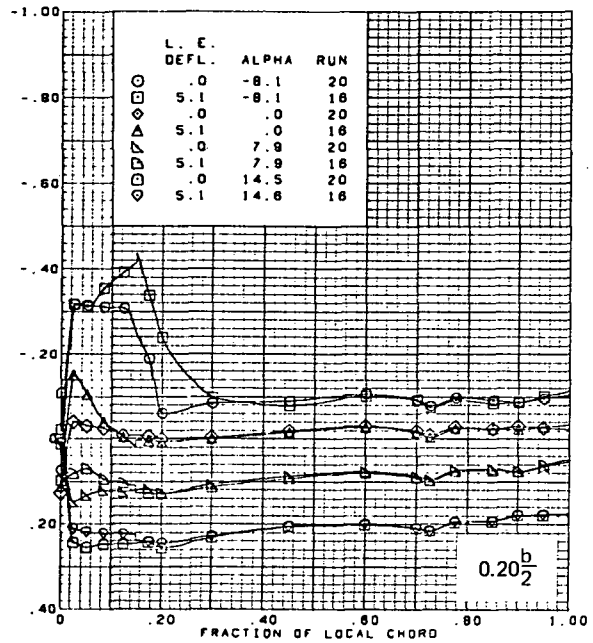
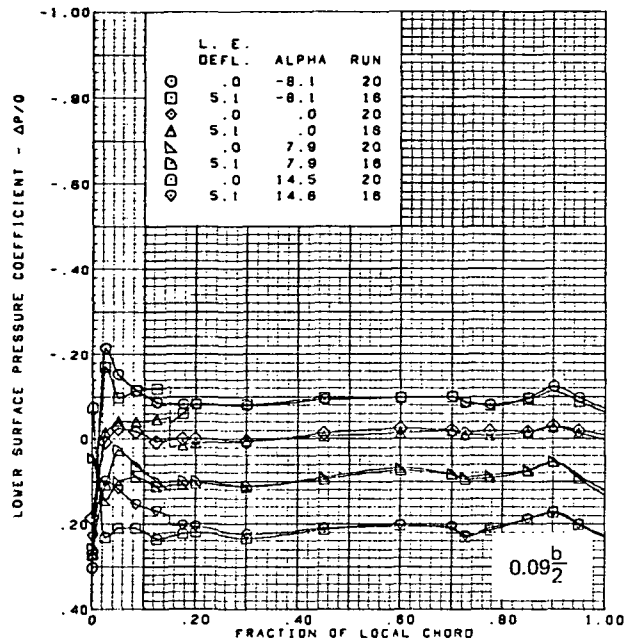


M = 1.70  
 Flat wing, rounded L.E.  
 T.E. deflection, full span = 0.0°

Note:  $C_{p, \text{vacuum}} = -0.49$

(a) (Concluded)

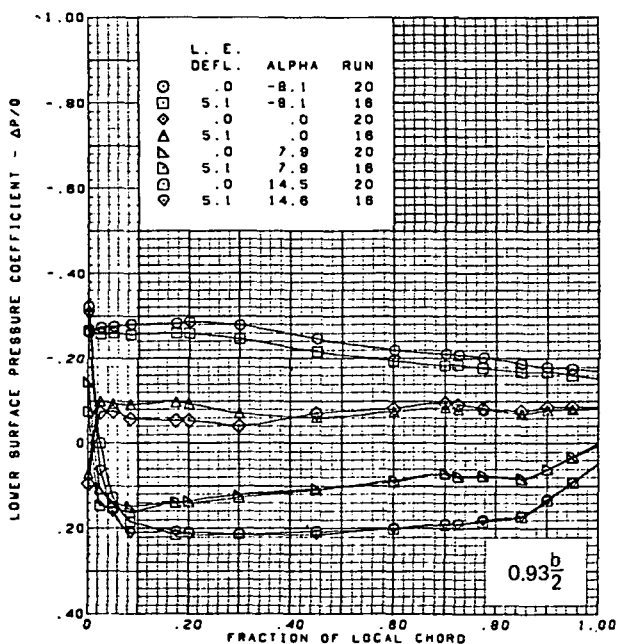
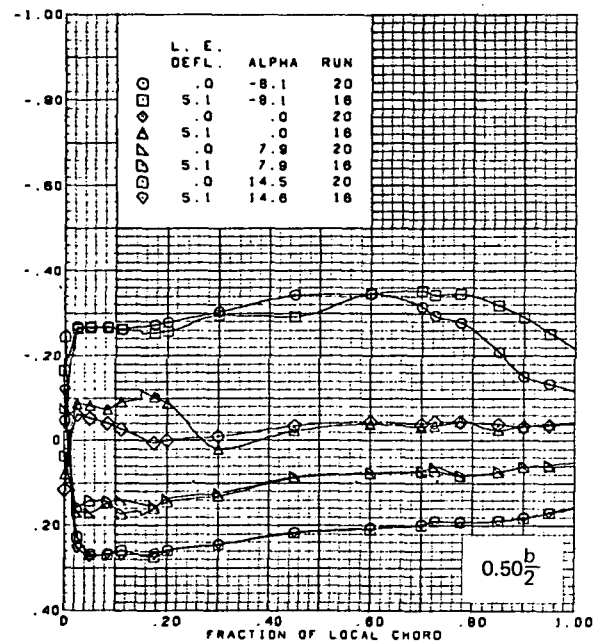
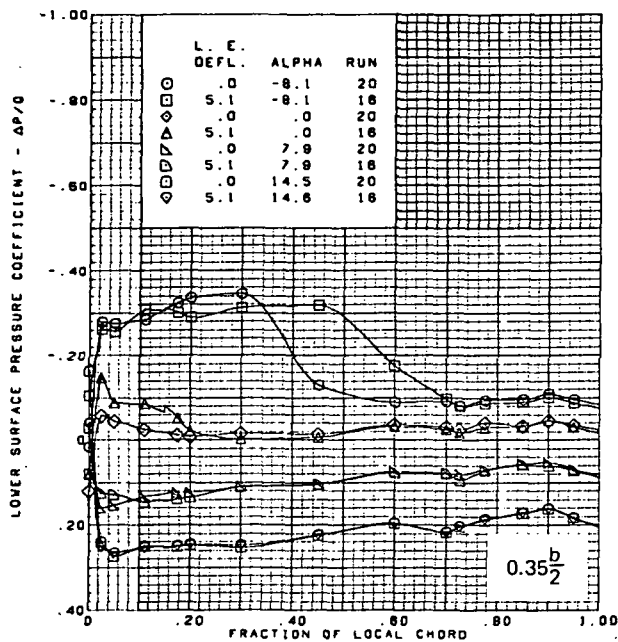
Figure 24.—(Continued)



(b) Lower Surface Chordwise Pressure Distributions

Figure 24.—(Continued)



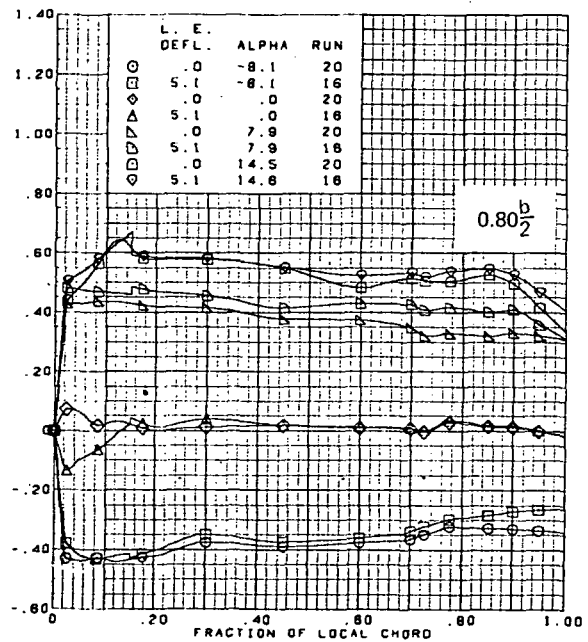
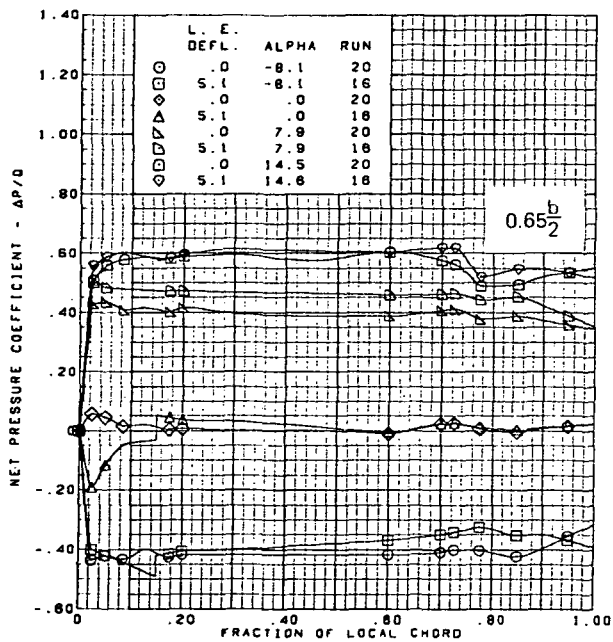
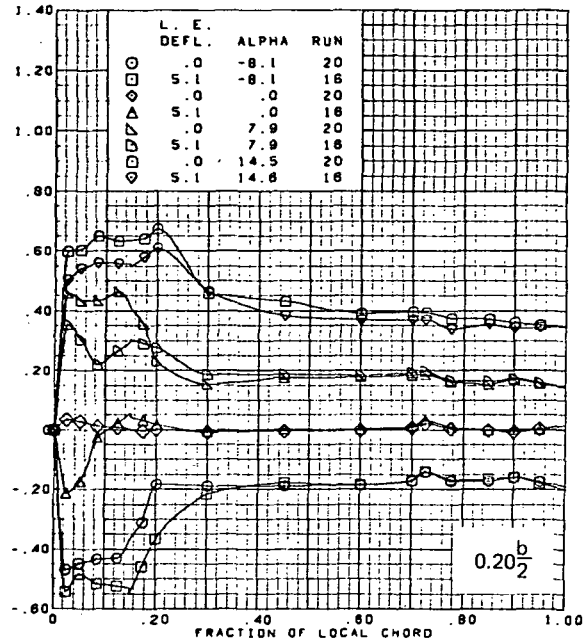
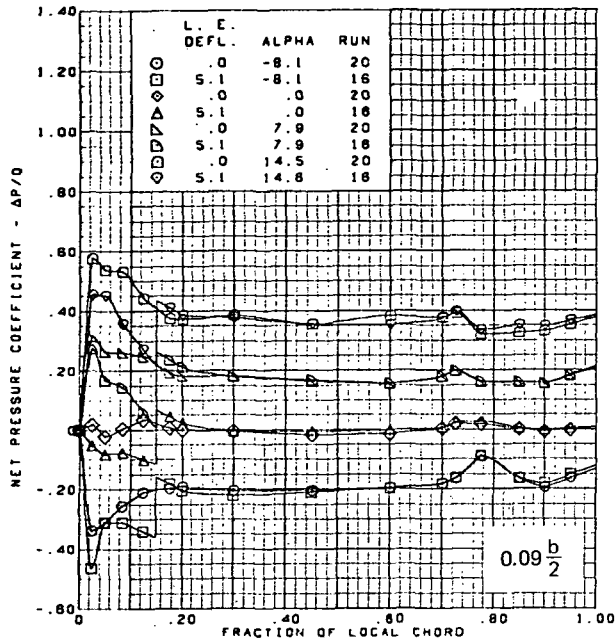


M = 1.70  
 Flat wing, rounded L.E.  
 T.E. deflection, full span = 0.0°

Note:  $C_{p, \text{vacuum}} = -0.49$

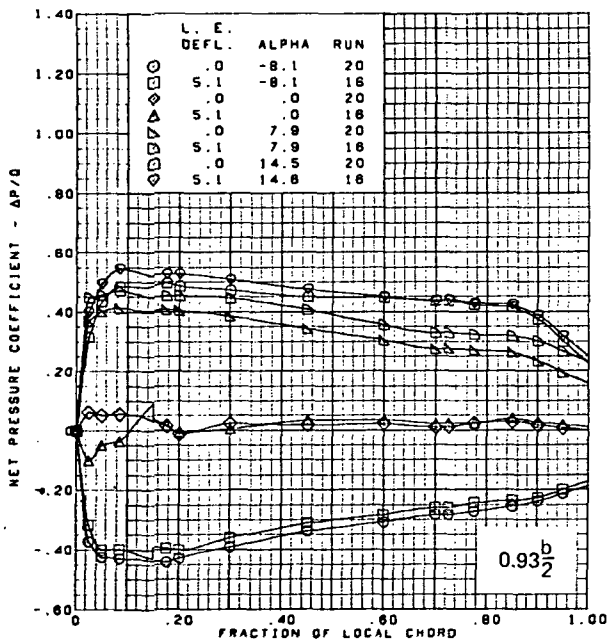
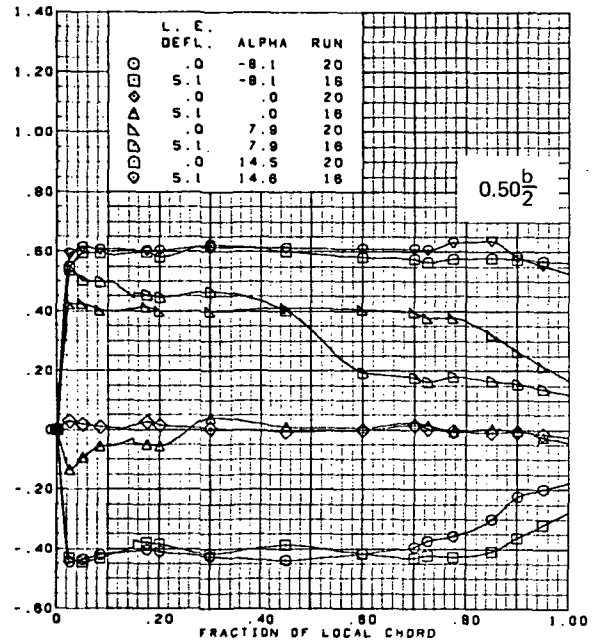
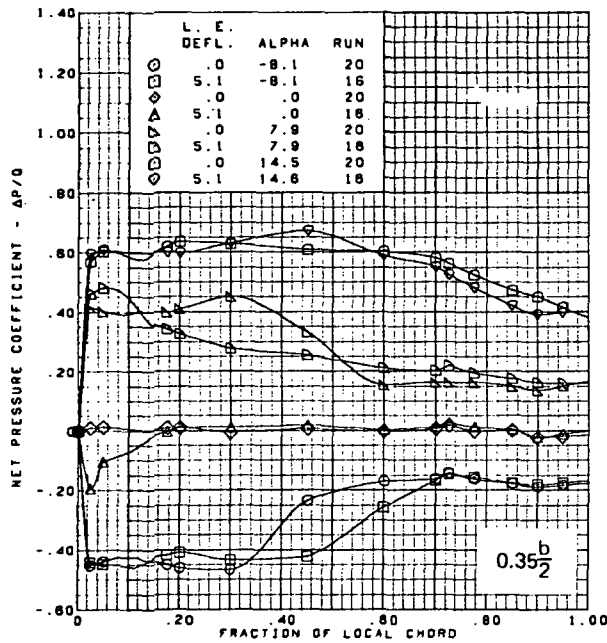
(b) (Concluded)

Figure 24.—(Continued)



(c) Net Chordwise Pressure Distributions

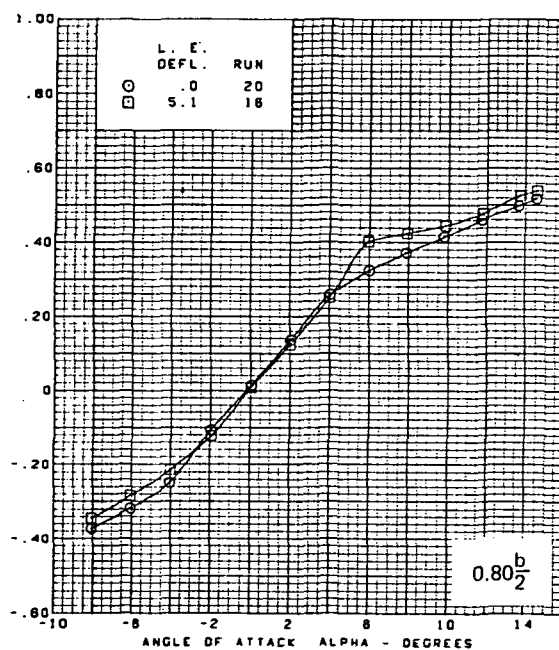
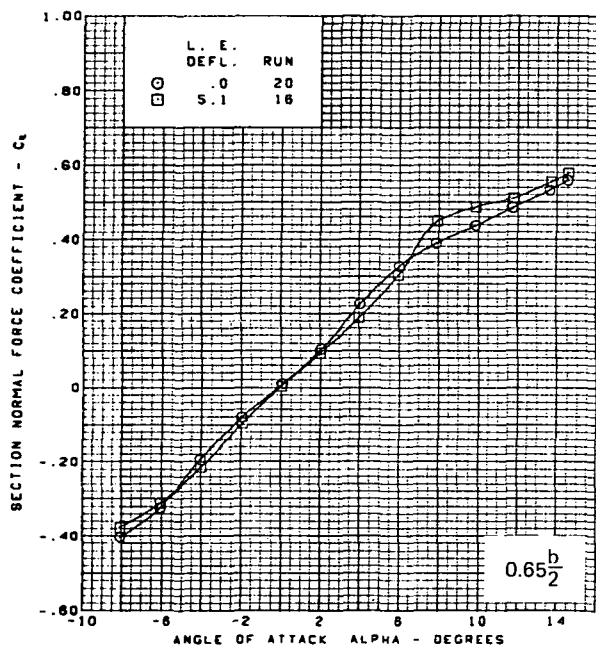
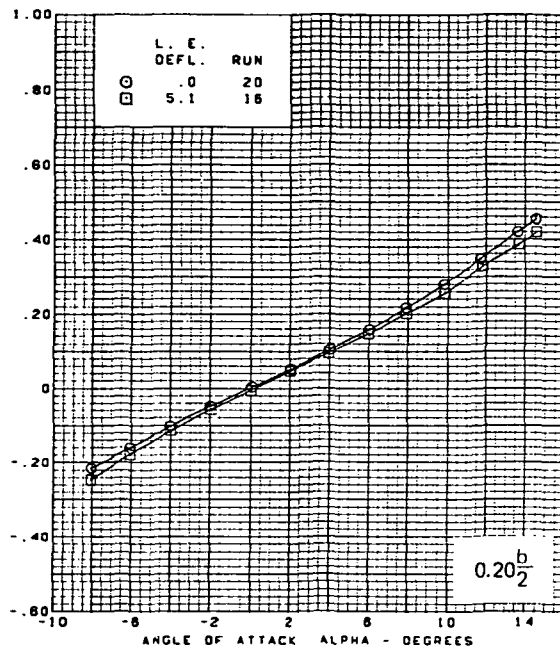
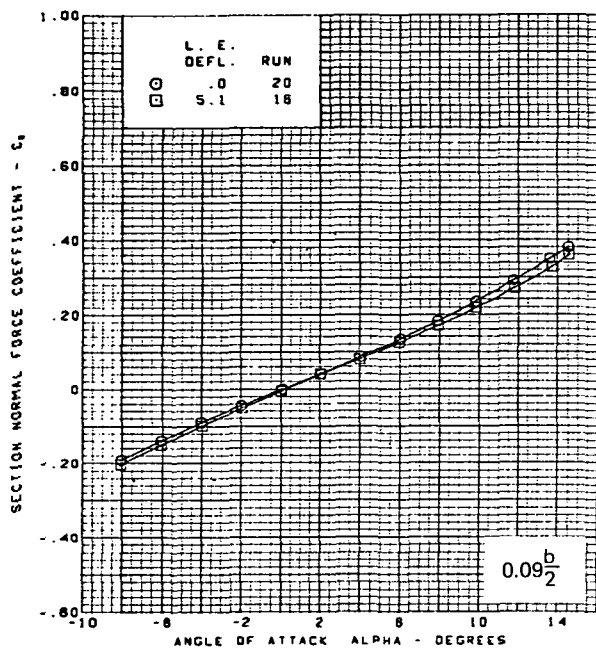
Figure 24.—(Continued)



M = 1.70  
 Flat wing, rounded L.E.  
 T.E. deflection, full span = 0.0°

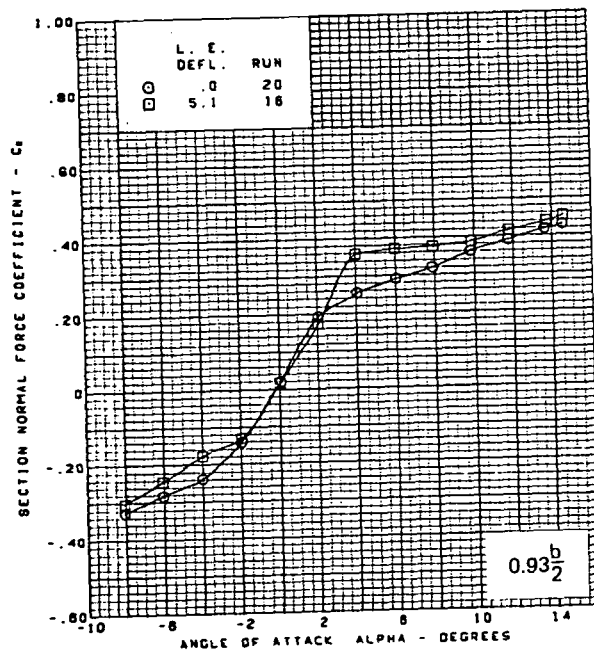
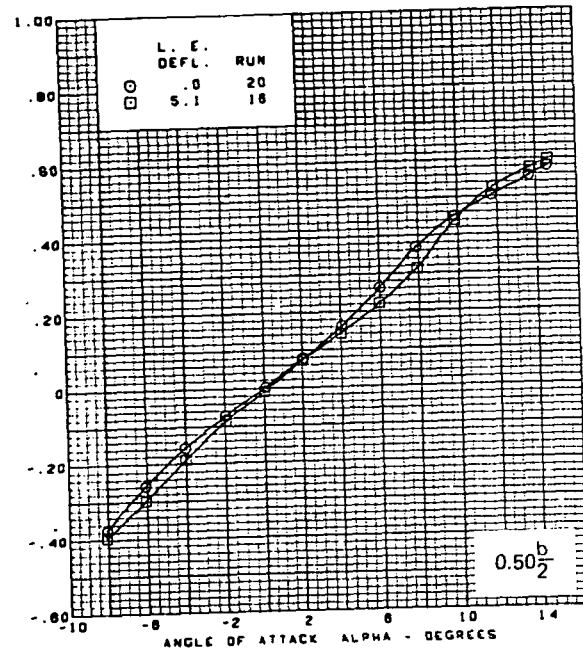
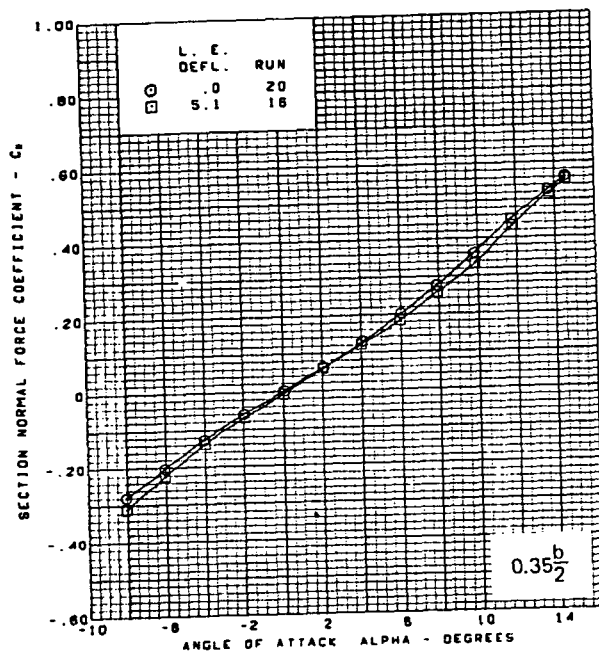
(c) (Concluded)

Figure 24.—(Continued)



(d) Section Aerodynamic Coefficients—Normal Force

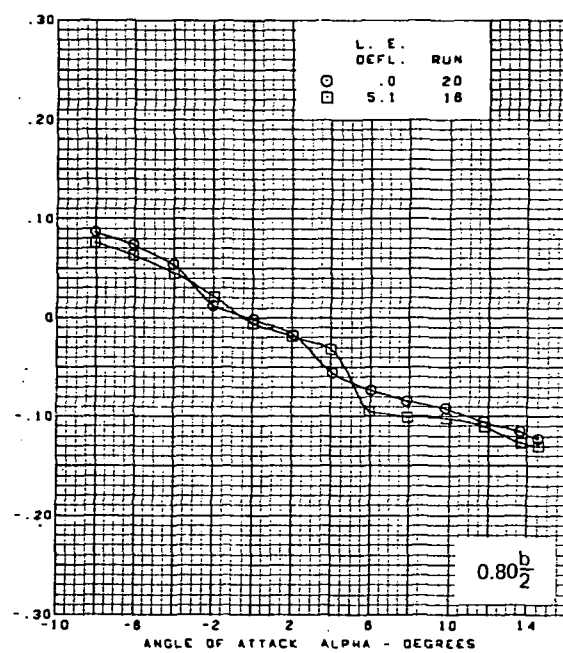
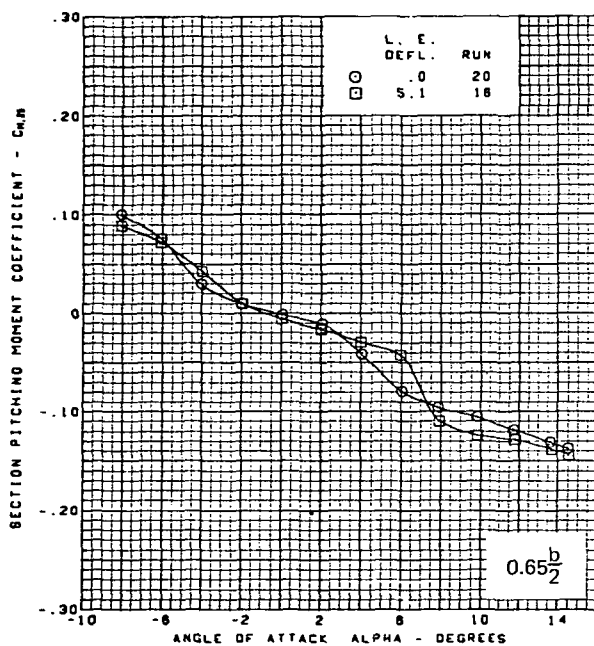
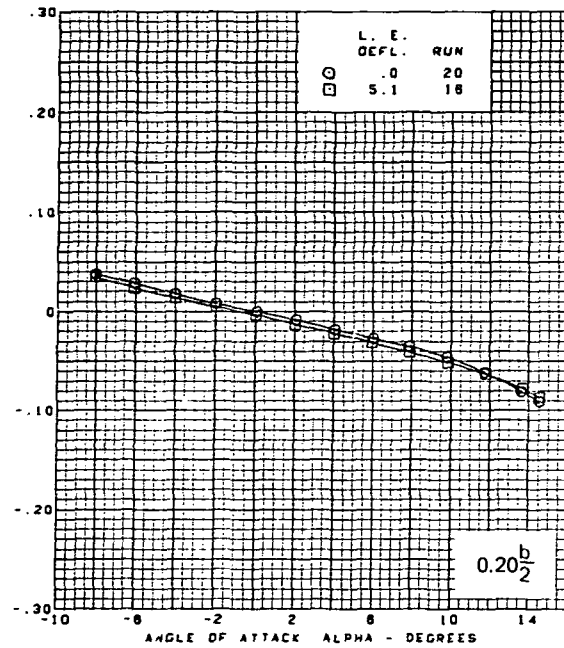
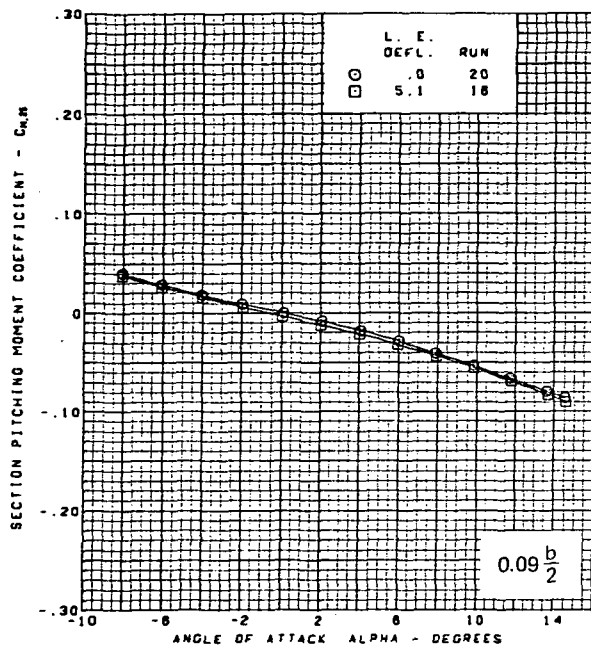
Figure 24.—(Continued)



M = 1.70  
 Flat wing, rounded L.E.  
 T.E. deflection, full span = 0.0°

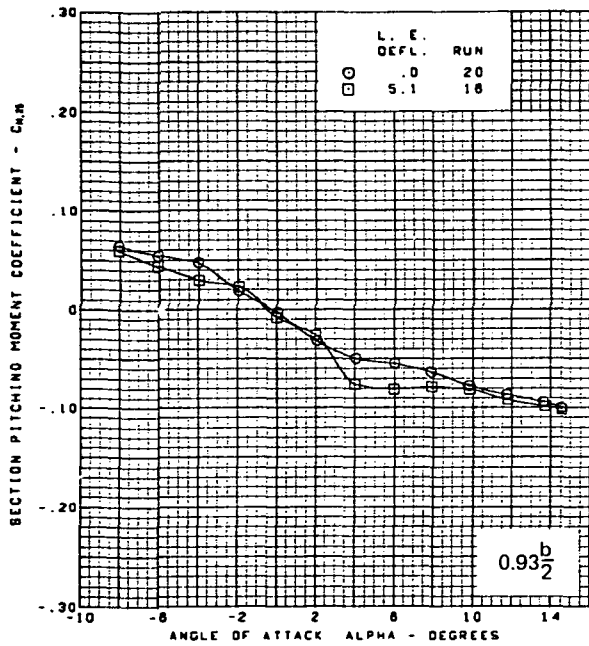
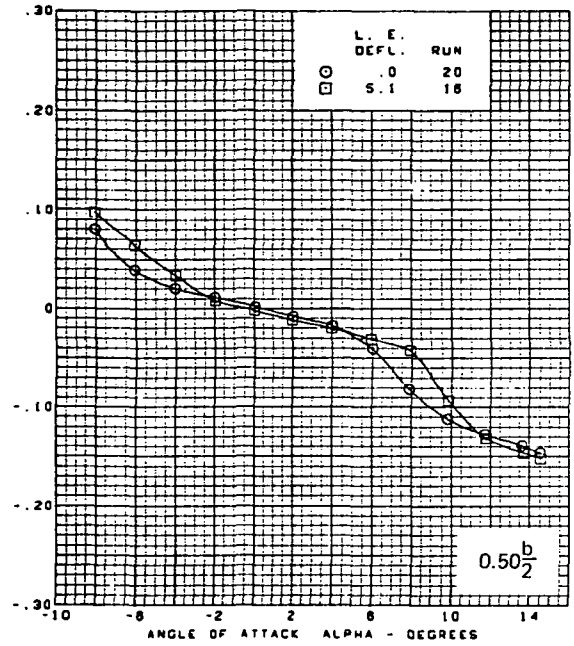
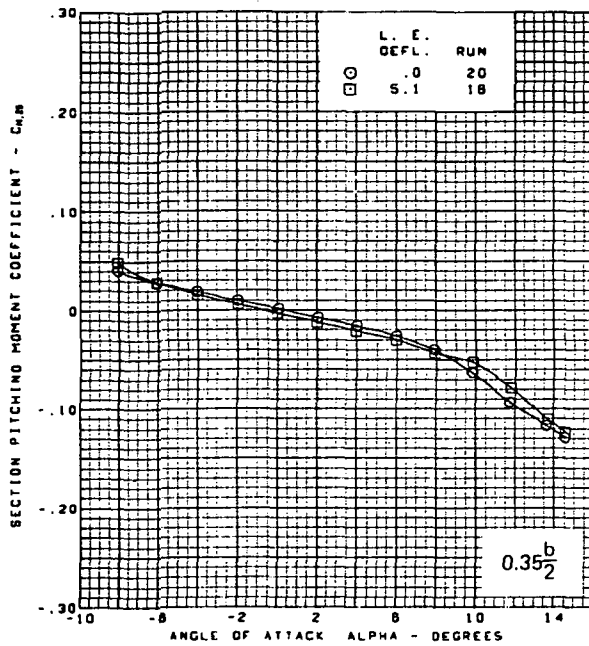
(d) (Concluded)

Figure 24.—(Continued)



(e) Section Aerodynamic Coefficients—Pitching Moment

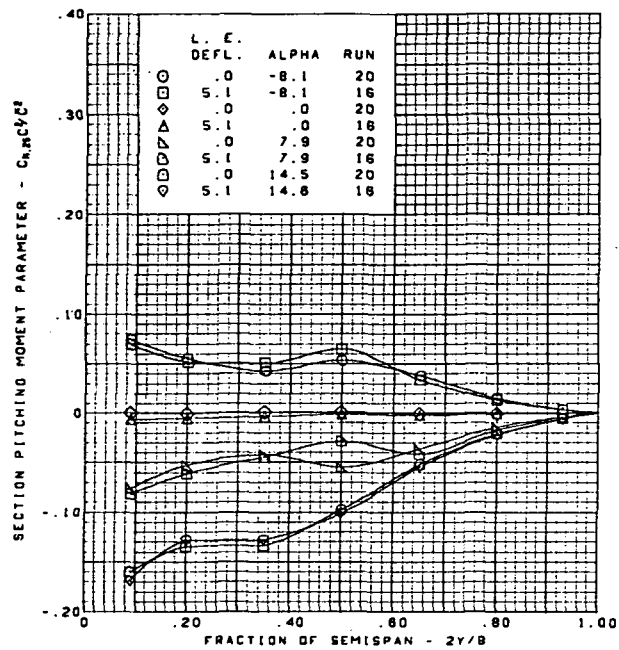
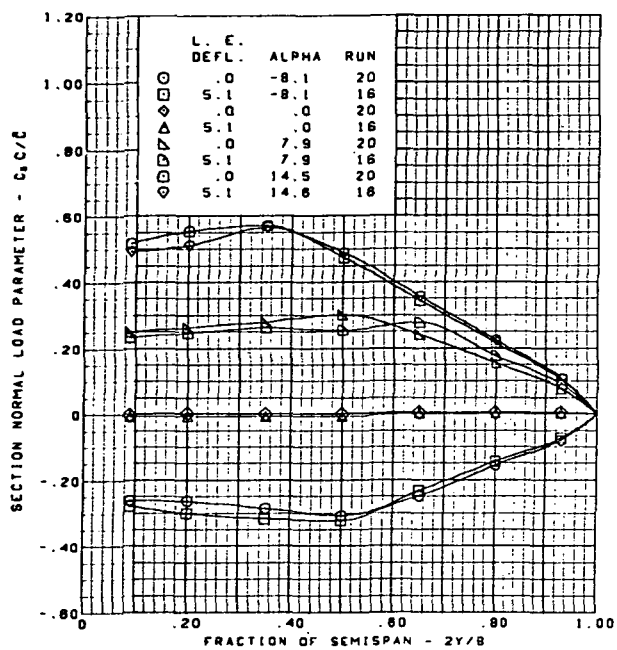
Figure 24.—(Continued)



$M = 1.70$   
 Flat wing, rounded L.E.  
 T.E. deflection, full span =  $0.0^\circ$

(e) (Concluded)

Figure 24.—(Continued)

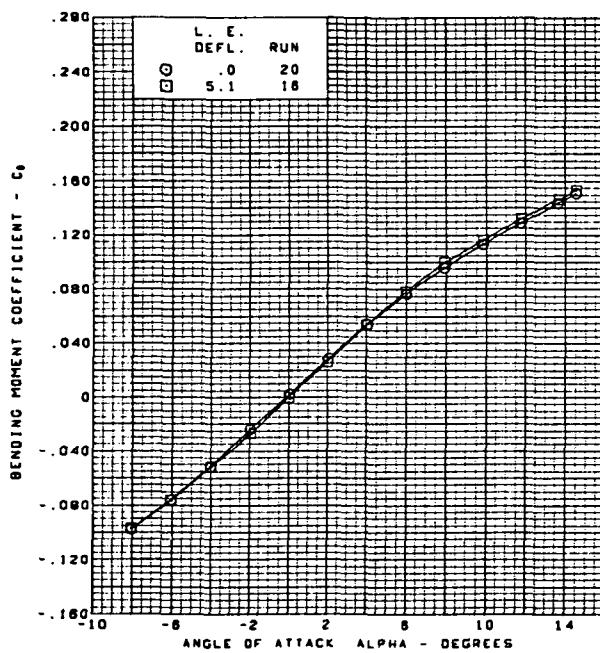
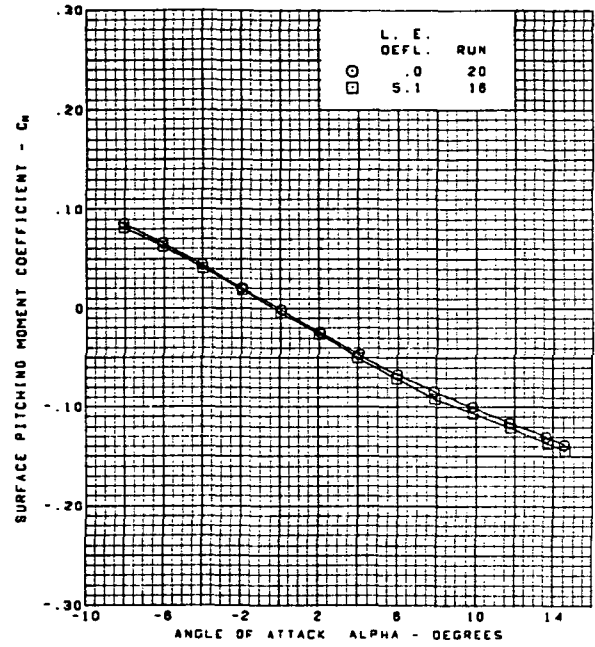
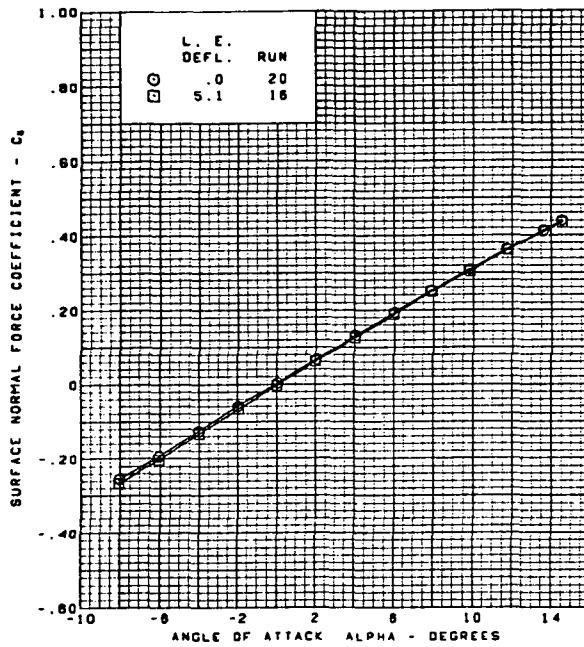


$M = 1.70$   
 Flat wing, rounded L.E.  
 T.E. deflection, full span =  $0.0^\circ$

(f) Spanload Distributions

Figure 24.—(Continued)

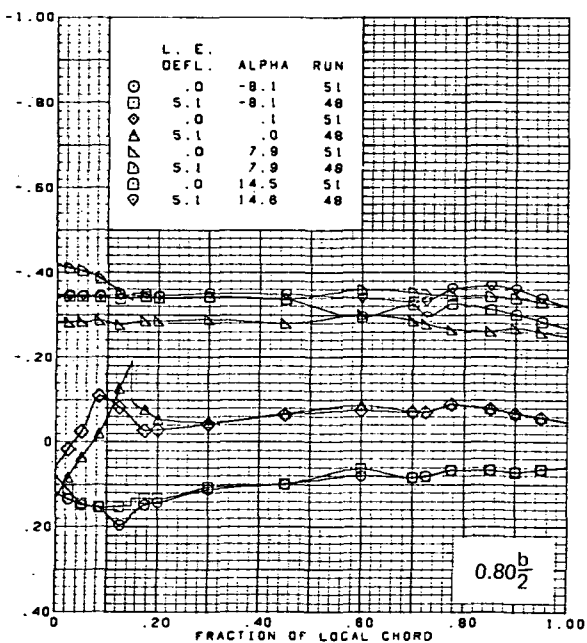
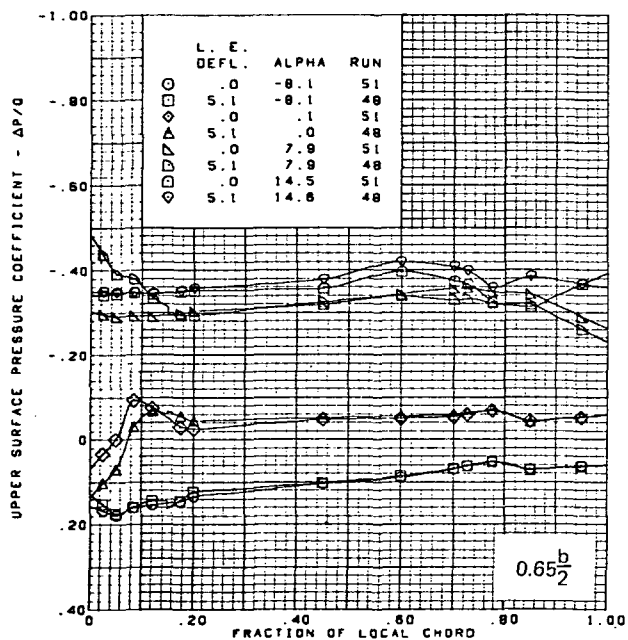
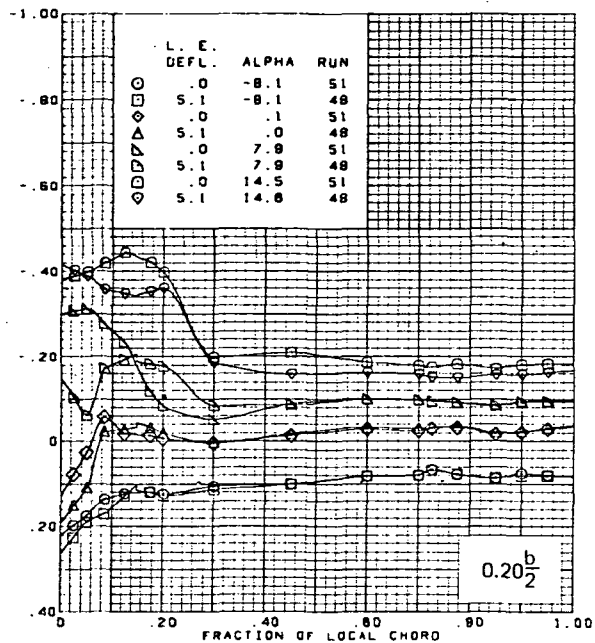
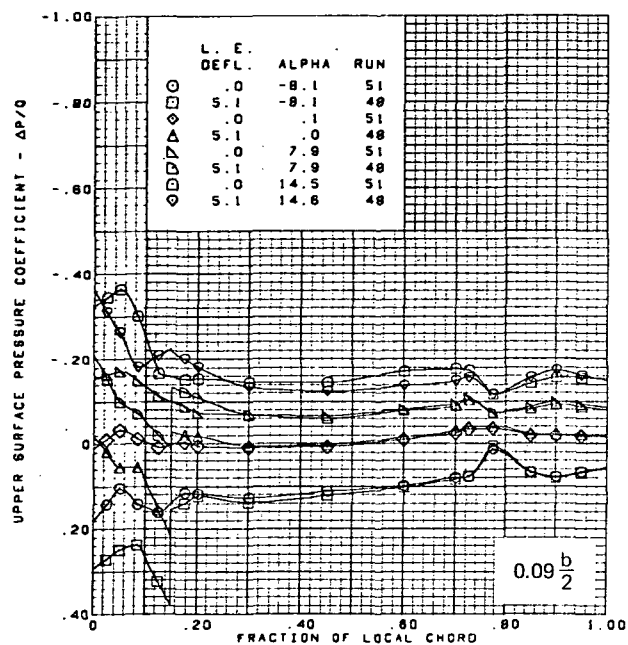




M = 1.70  
 Flat wing, rounded L.E.  
 T.E. deflection, full span = 0.0°

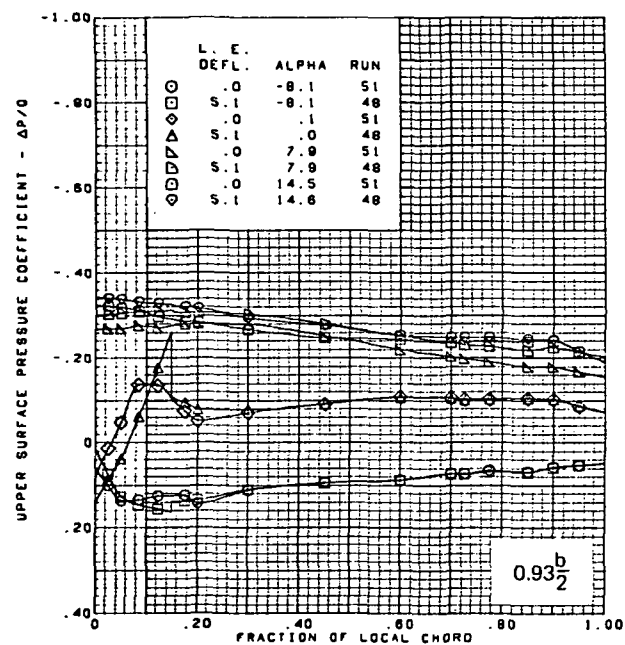
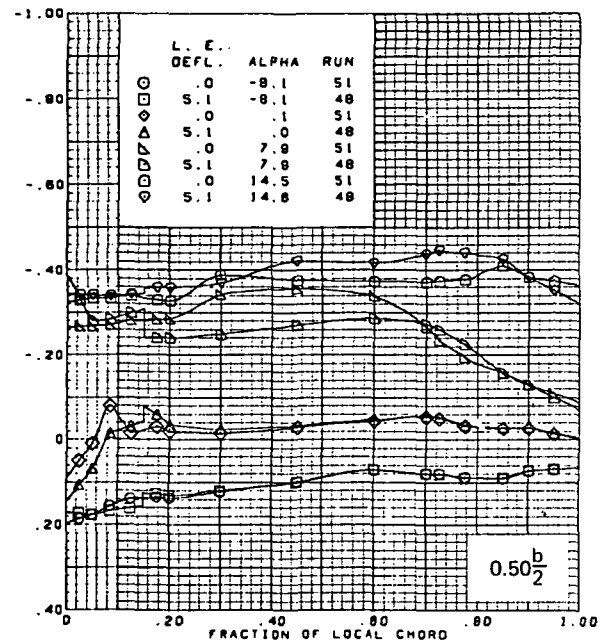
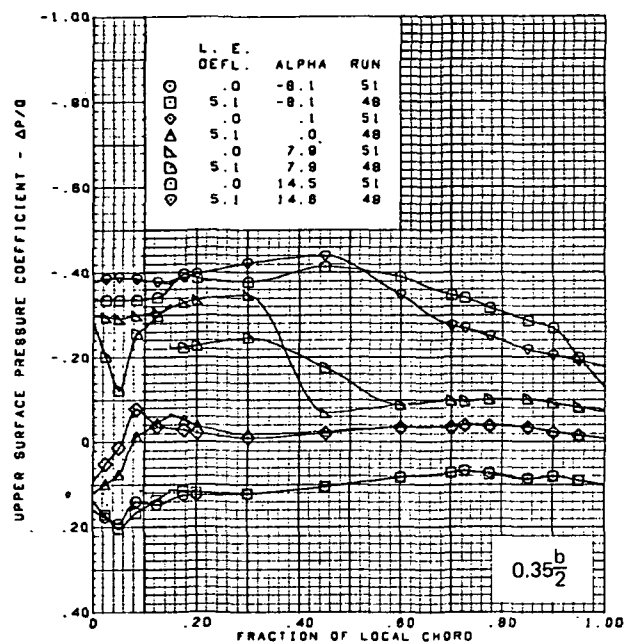
(g) Wing Aerodynamic Coefficients

Figure 24.—(Concluded)



(a) Upper Surface Chordwise Pressure Distributions

Figure 25.—Wing Experimental Data—Effect of Full Span L.E. Deflection With Angle of Attack;  
Flat Wing; Sharp L.E.; T.E. Deflection, Full Span =  $0.0^\circ$ ;  $M = 1.70$

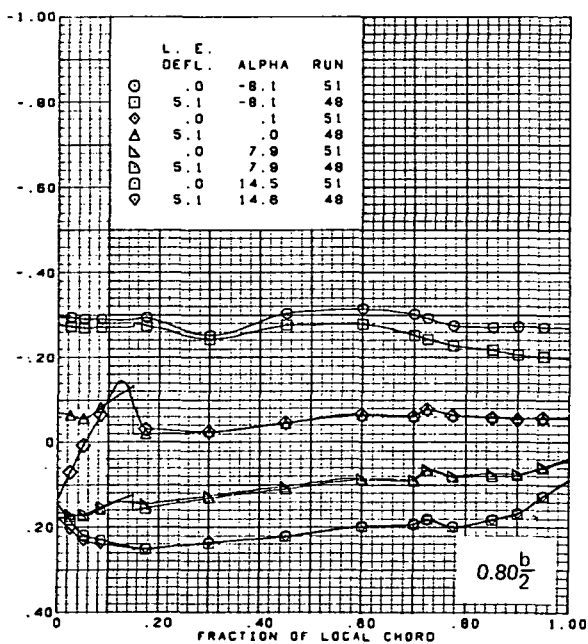
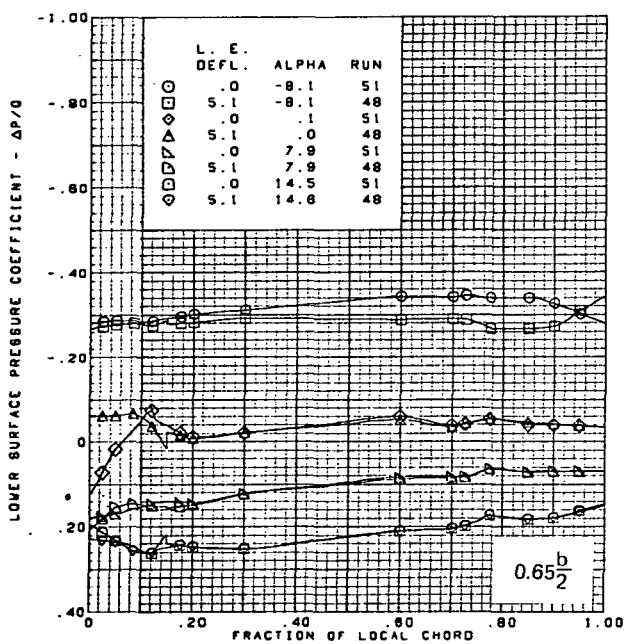
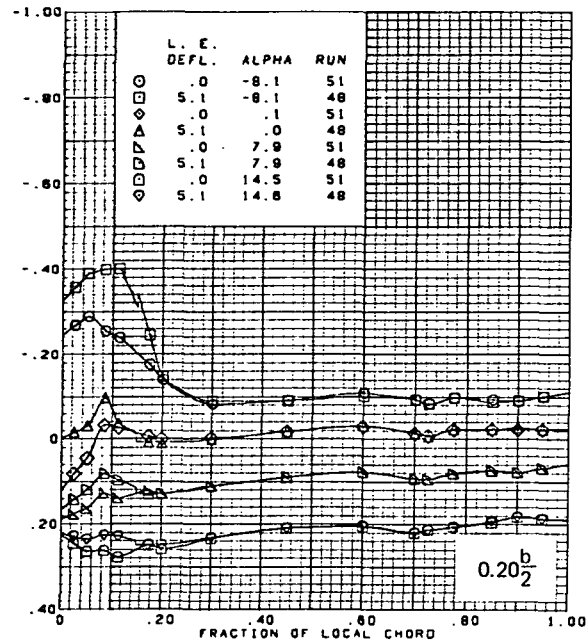
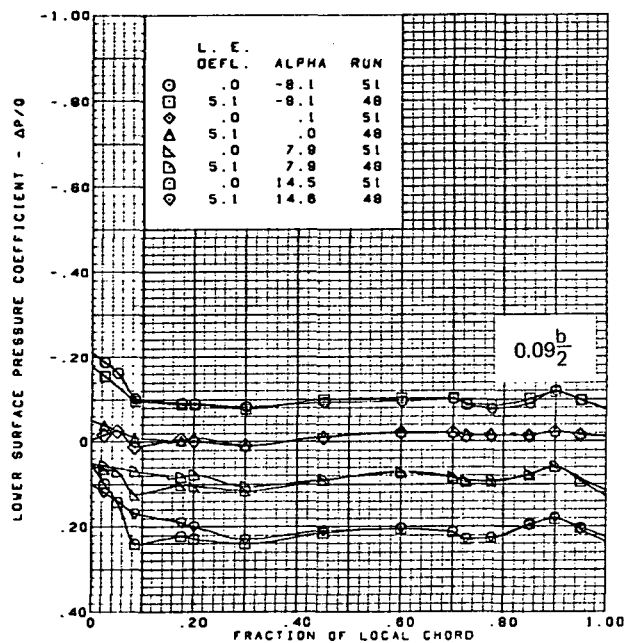


M = 1.70  
 Flat wing, sharp L.E.  
 T.E. deflection, full span = 0.0°

Note:  $C_{p, \text{vacuum}} = -0.49$

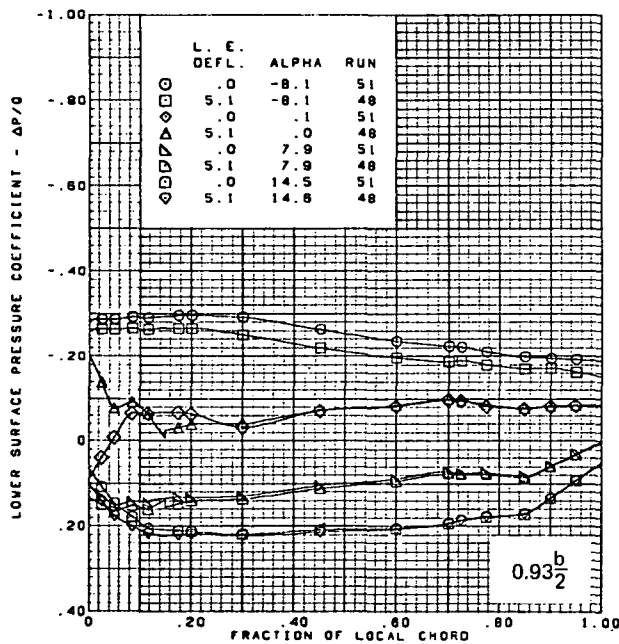
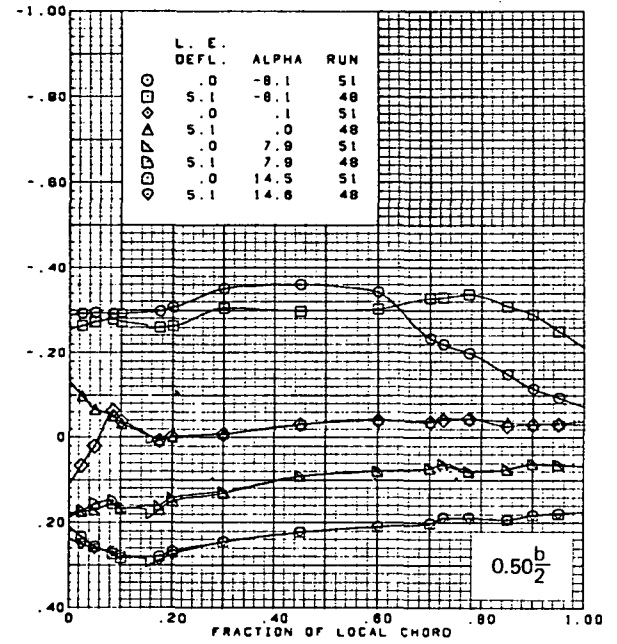
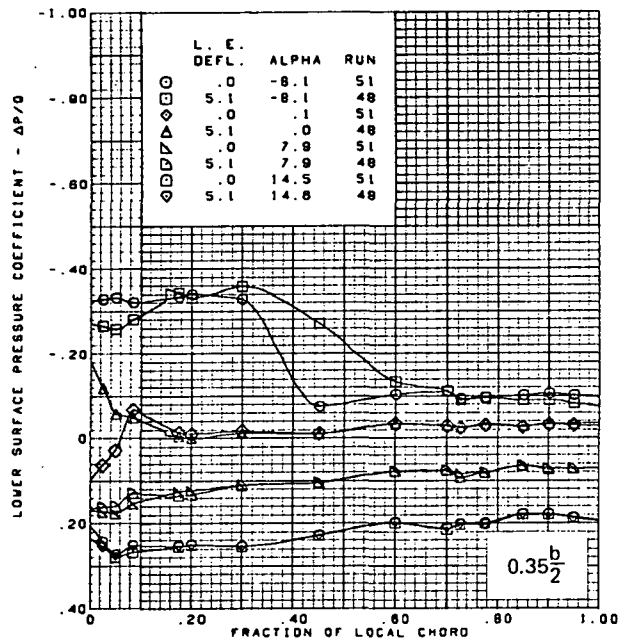
(a) (Concluded)

Figure 25.—(Continued)



(b) Lower Surface Chordwise Pressure Distributions

Figure 25.—(Continued)

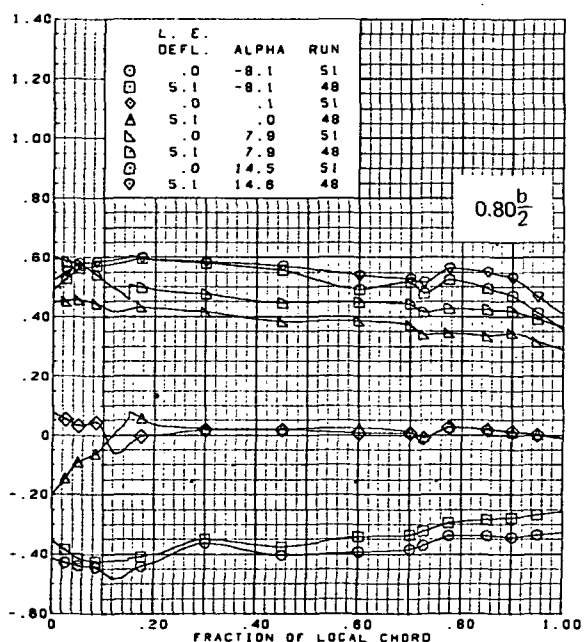
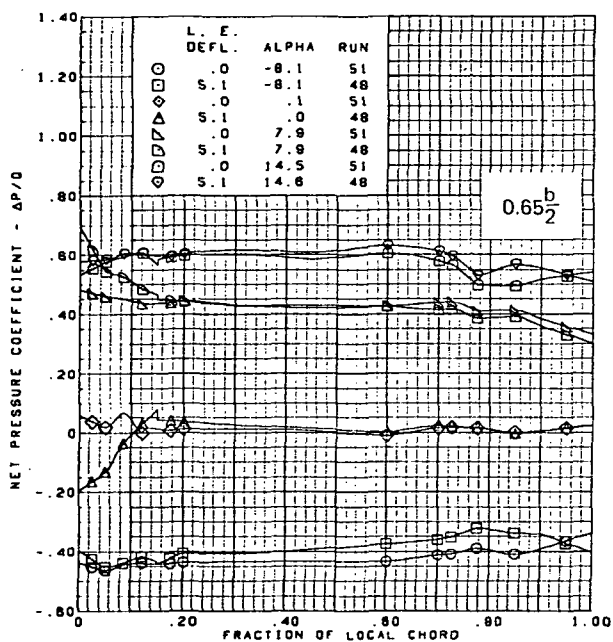
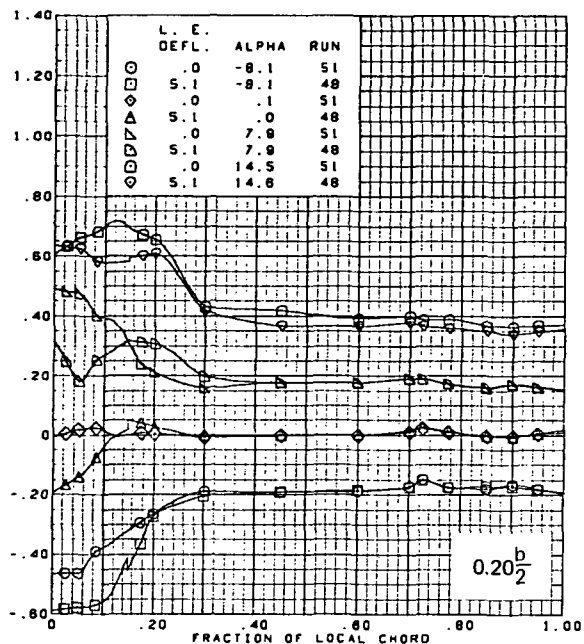
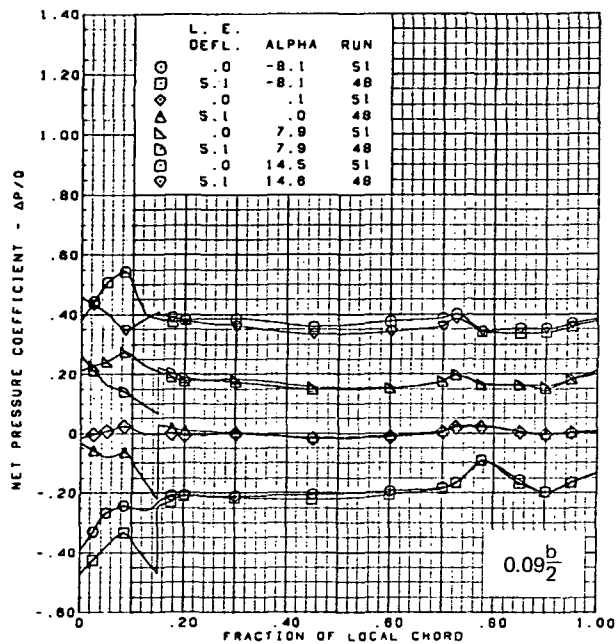


M = 1.70  
 Flat wing, sharp L.E.  
 T.E. deflection, full span =  $0.0^\circ$

Note:  $C_{p, \text{vacuum}} = -0.49$

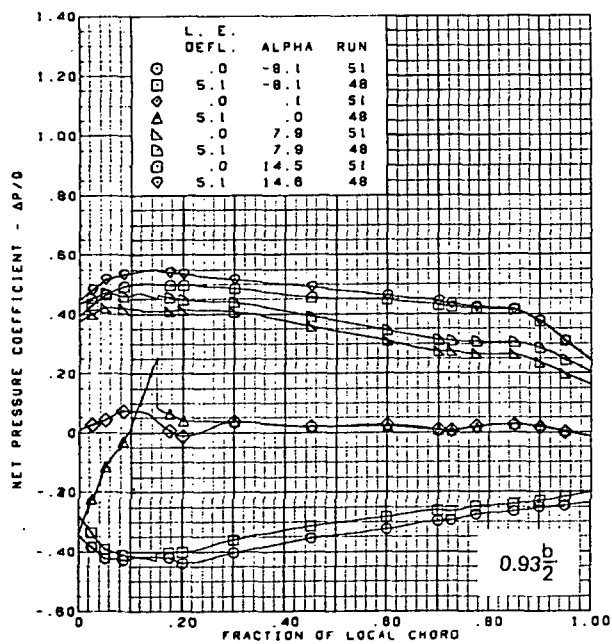
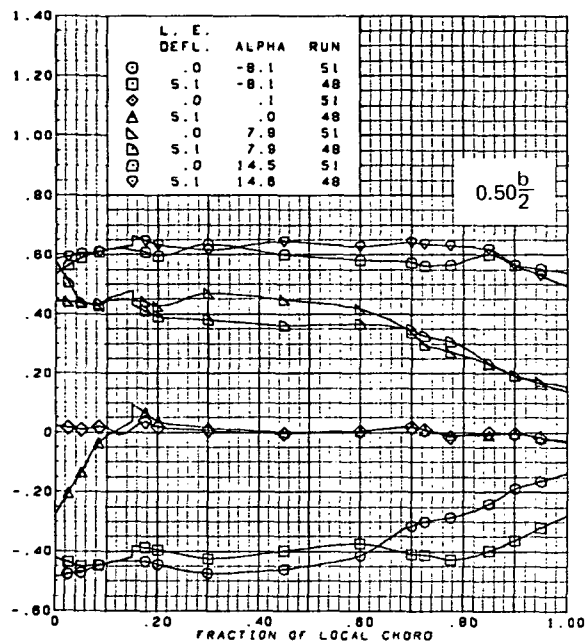
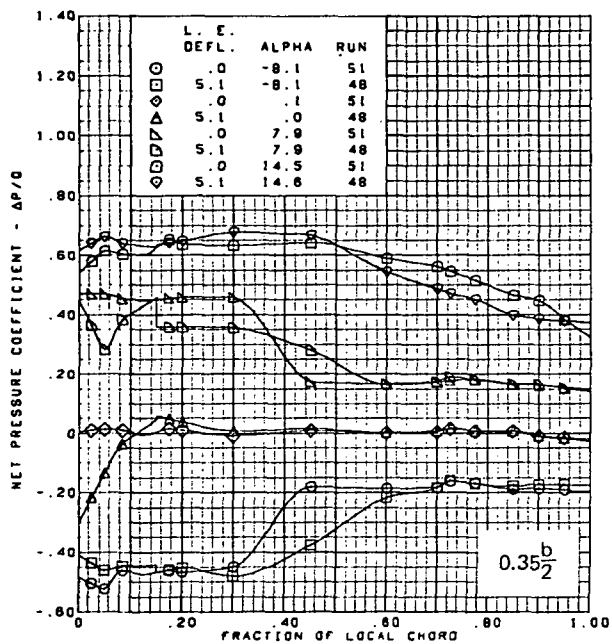
(b) (Concluded)

Figure 25.—(Continued)



(c) Net Chordwise Pressure Distributions

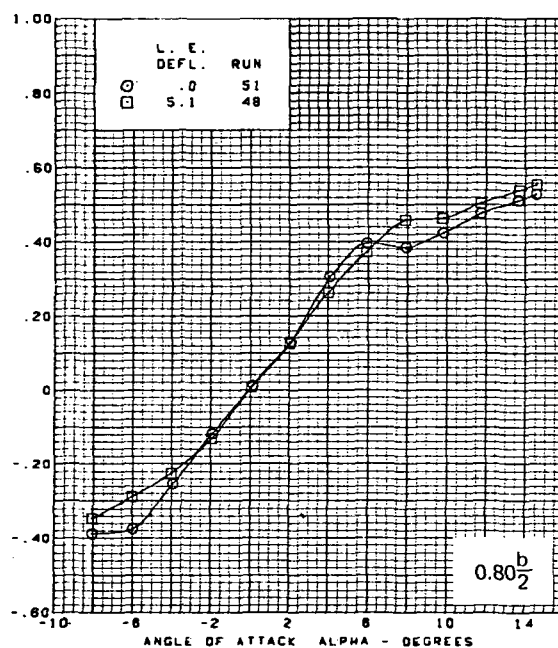
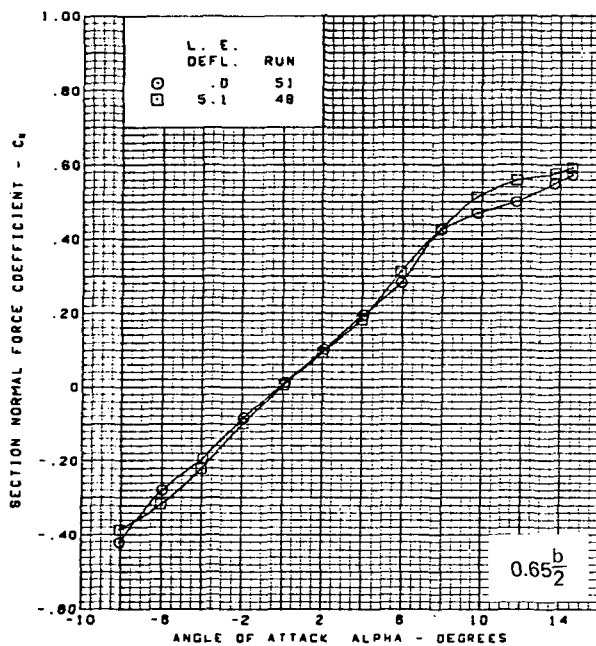
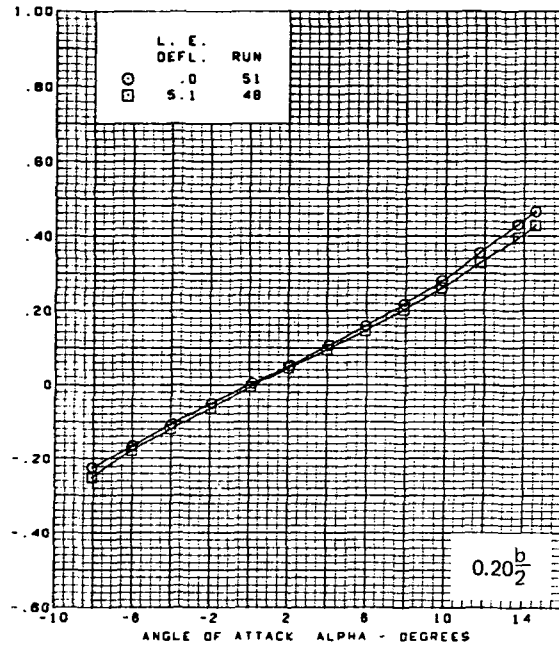
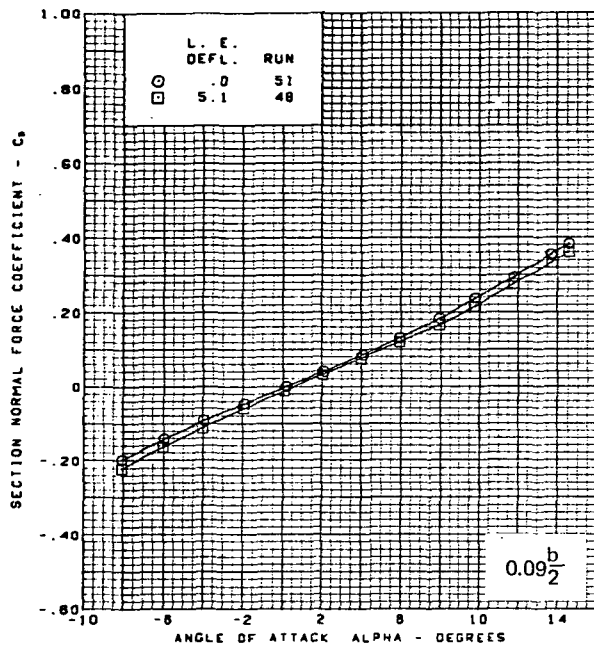
Figure 25.—(Continued)



$M = 1.70$   
 Flat wing, sharp L.E.  
 T.E. deflection, full span =  $0.0^\circ$

(c) (Concluded)

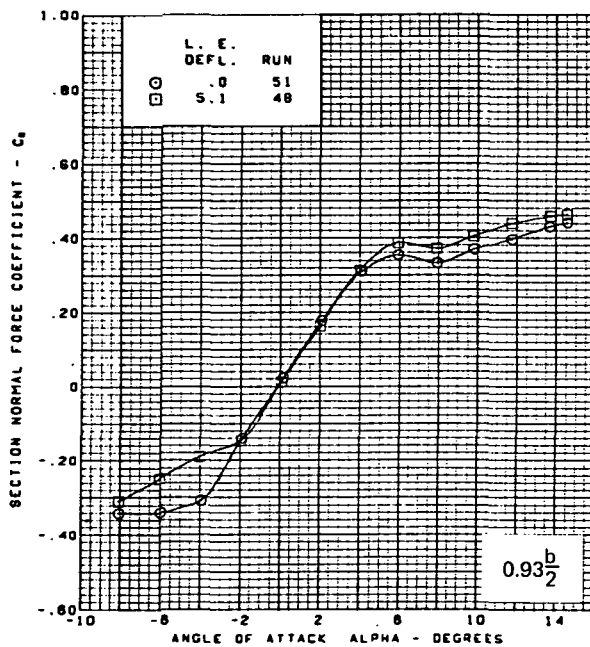
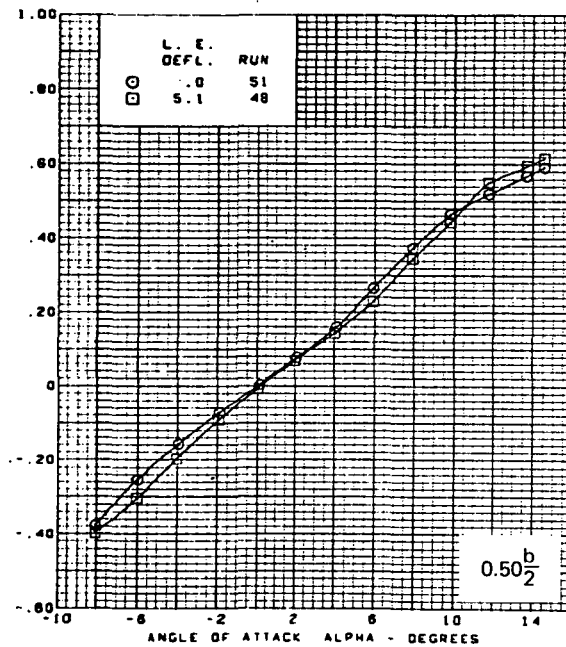
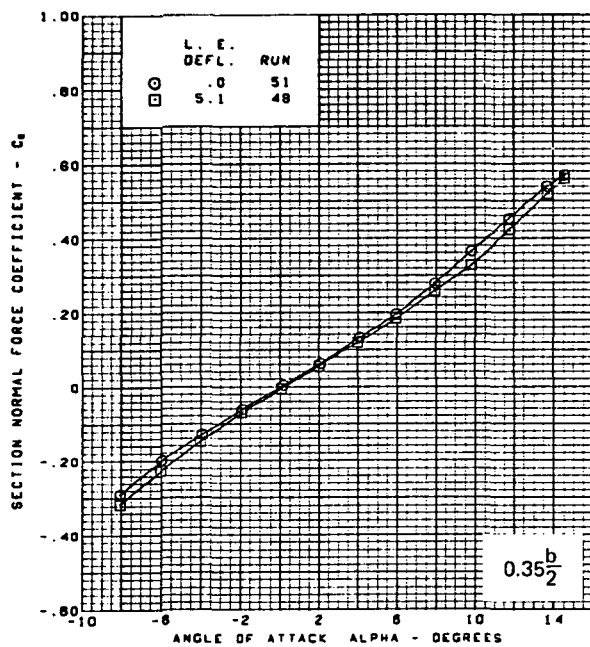
Figure 25.—(Continued)



(d) Section Aerodynamic Coefficients—Normal Force

Figure 25.—(Continued)

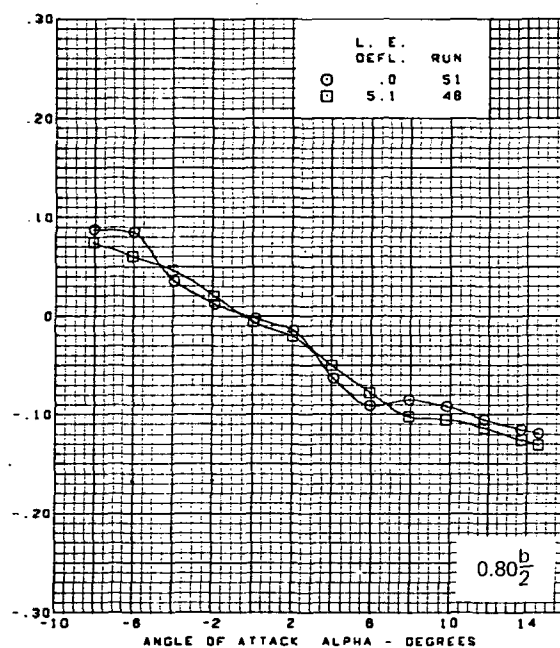
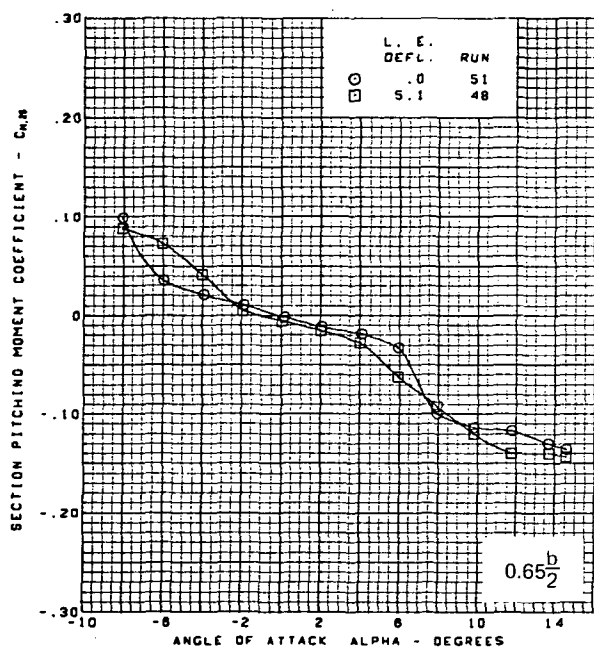
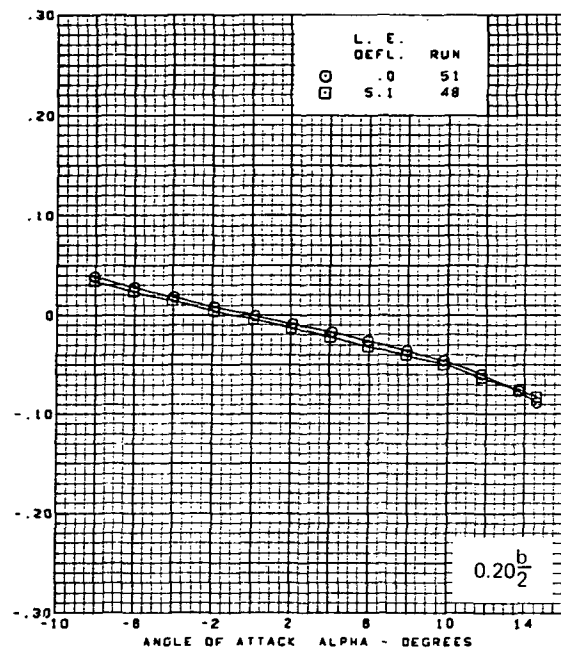
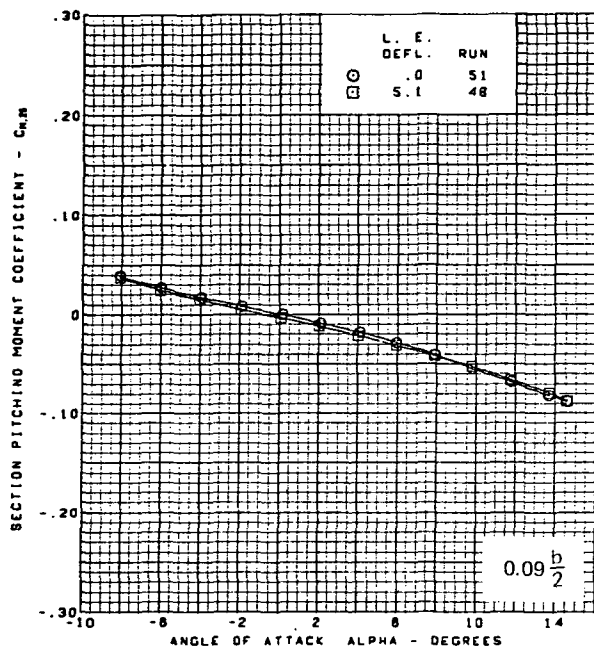




M = 1.70  
 Flat wing, sharp L.E.  
 T.E. deflection, full span = 0.0°

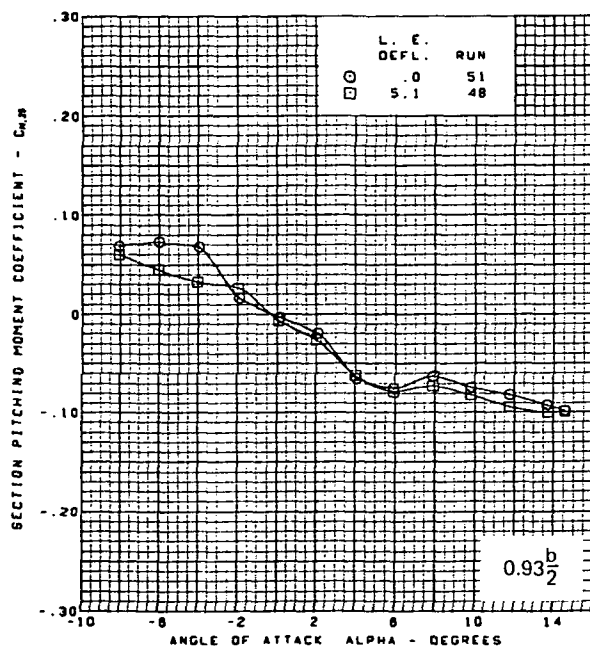
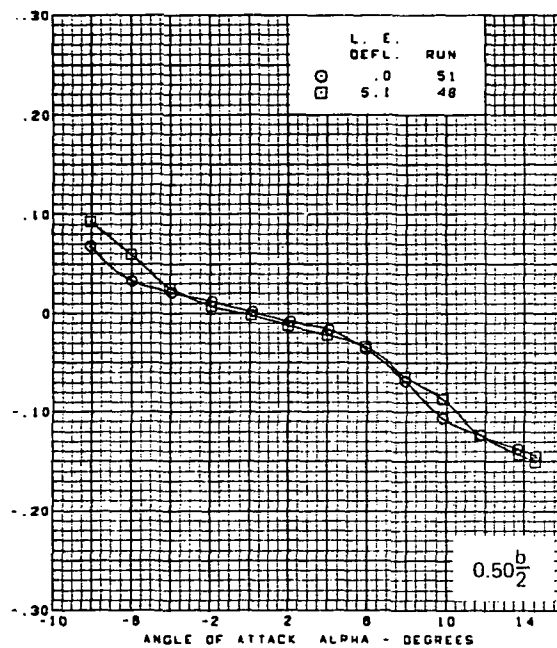
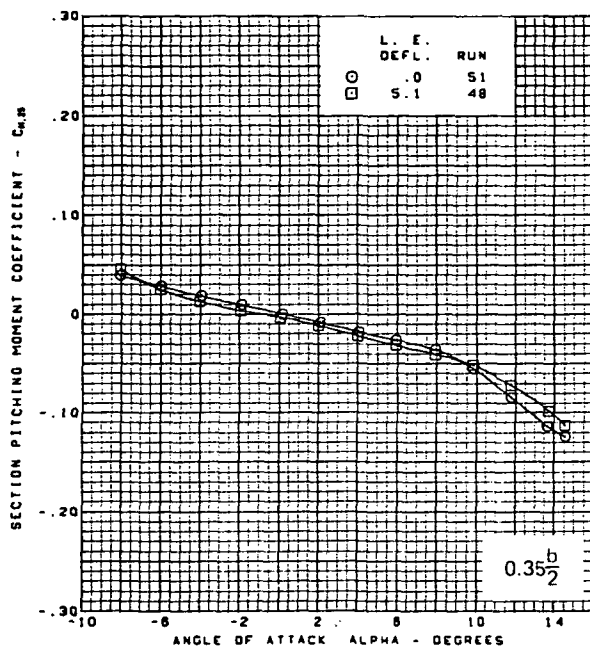
(d) (Concluded)

Figure 25.—(Continued)



(e) Section Aerodynamic Coefficients—Pitching Moment

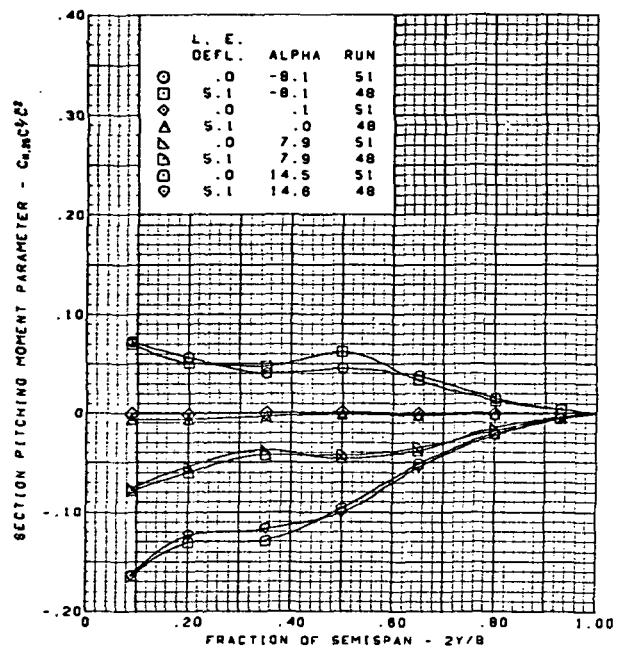
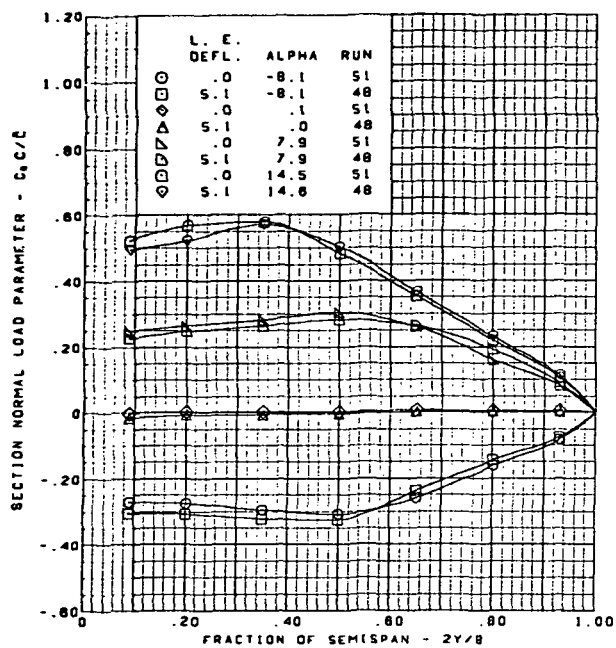
Figure 25.—(Continued)



M = 1.70  
 Flat wing, sharp L.E.  
 T.E. deflection, full span = 0.0°

(e) (Concluded)

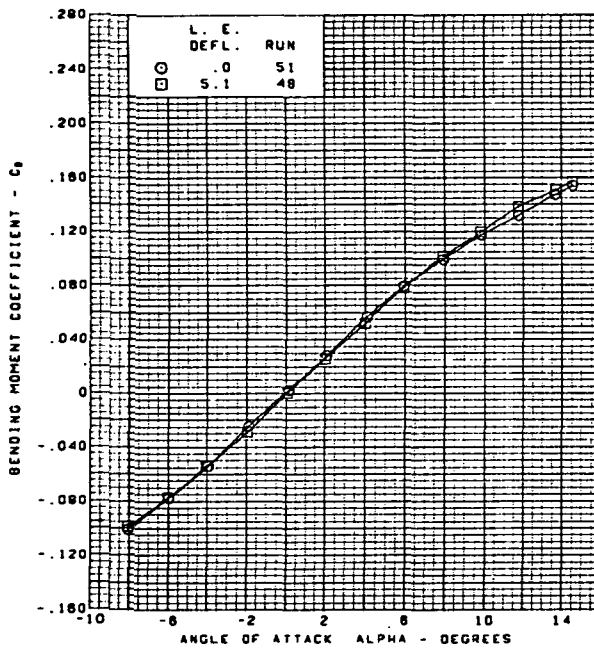
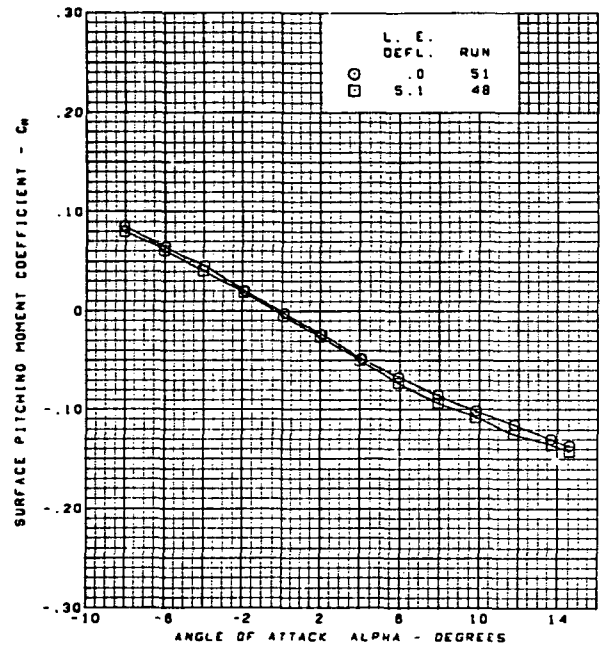
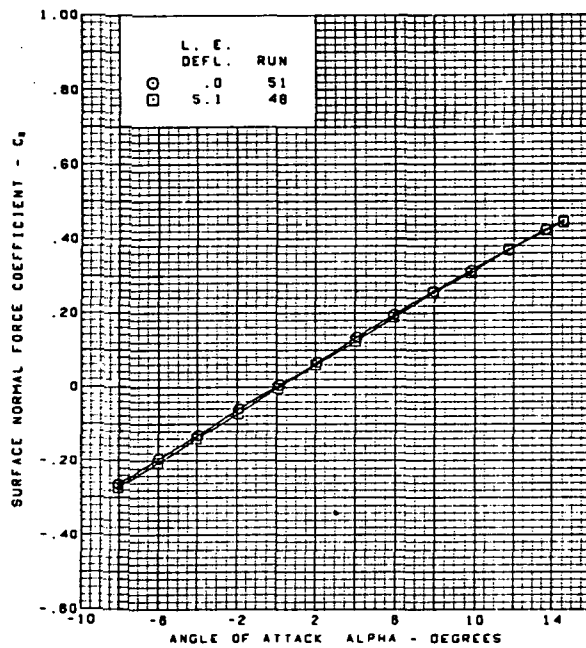
Figure 25.—(Continued)



M = 1.70  
 Flat wing, sharp L.E.  
 T.E. deflection, full span = 0.0°

(f) Spanload Distributions

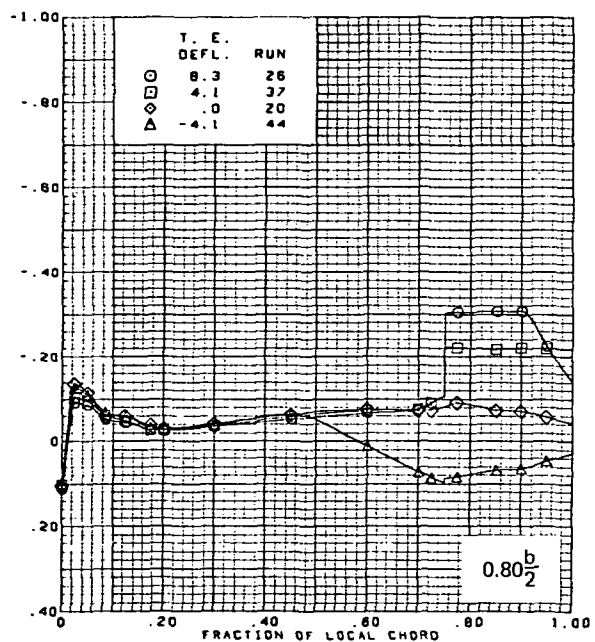
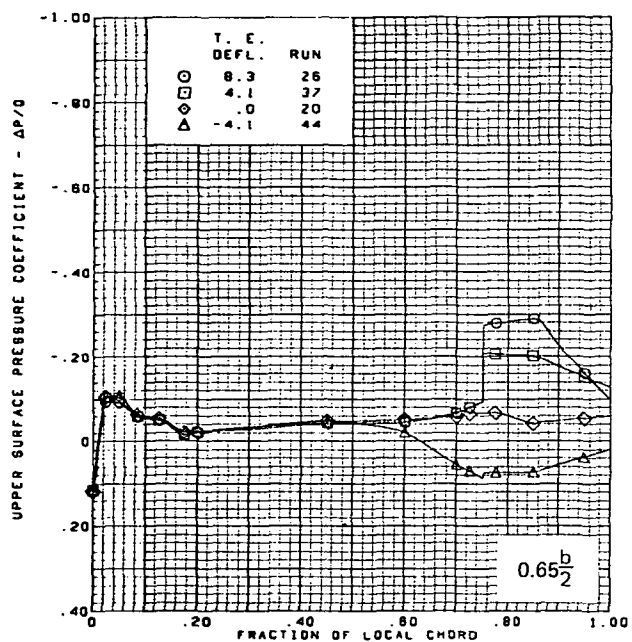
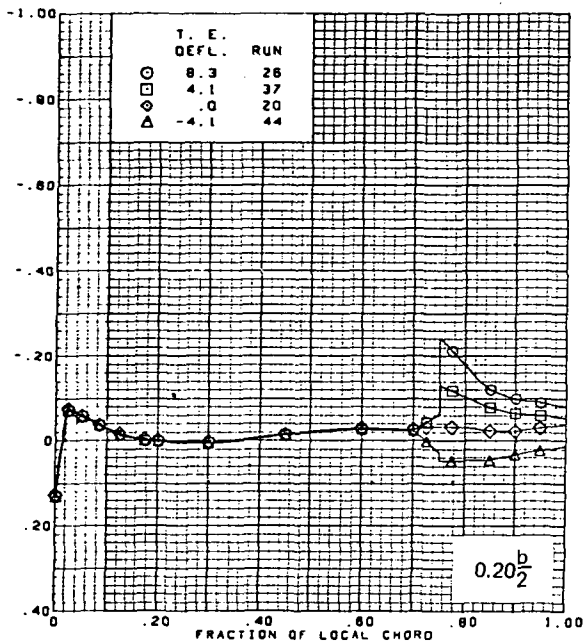
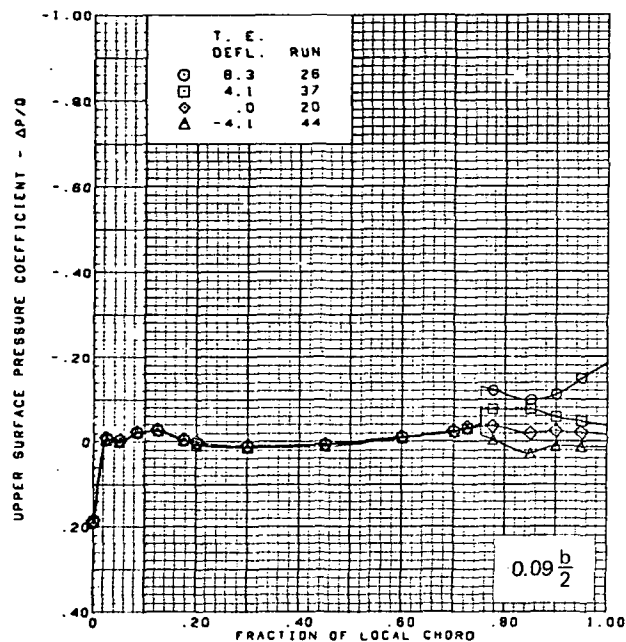
Figure 25.—(Continued)



$M = 1.70$   
 Flat wing, sharp L.E.  
 T.E. deflection, full span =  $0.0^\circ$

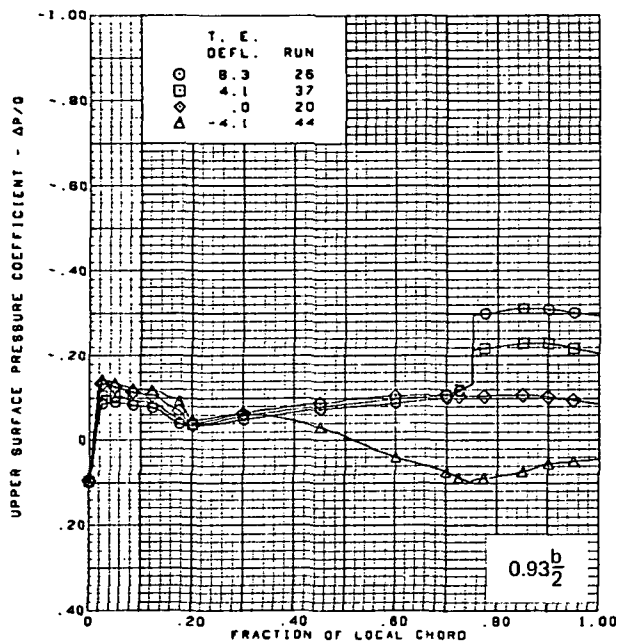
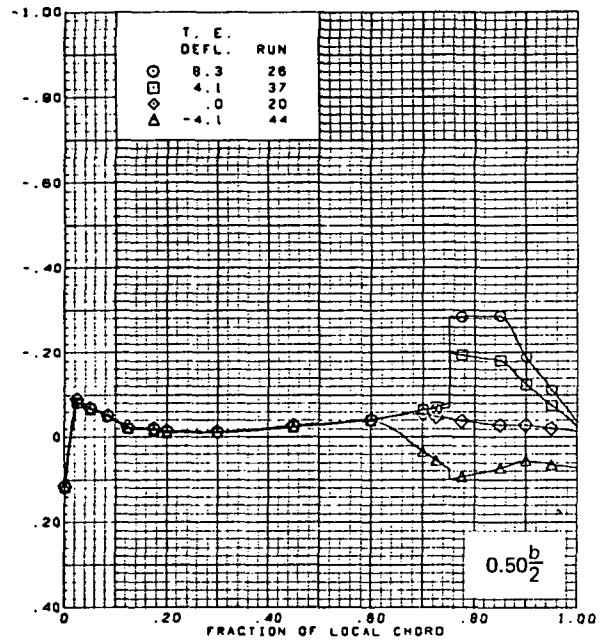
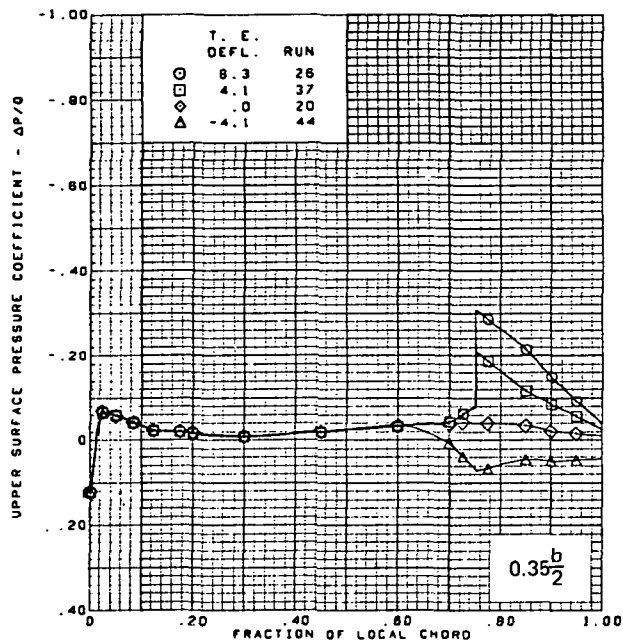
(g) Wing Aerodynamic Coefficients

Figure 25.—(Concluded)



(a) Upper Surface Chordwise Pressure Distributions,  $\alpha = 0^\circ$

Figure 26.—Wing Experimental Data—Effect of Full Span T.E. Deflection With Angle of Attack; Flat Wing; Rounded L.E.; L.E. Deflection, Full Span =  $0.0^\circ$ ;  $M = 1.70$

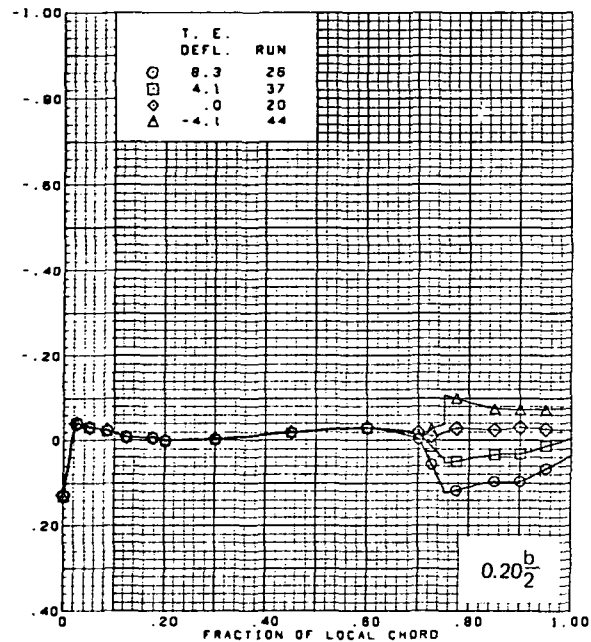
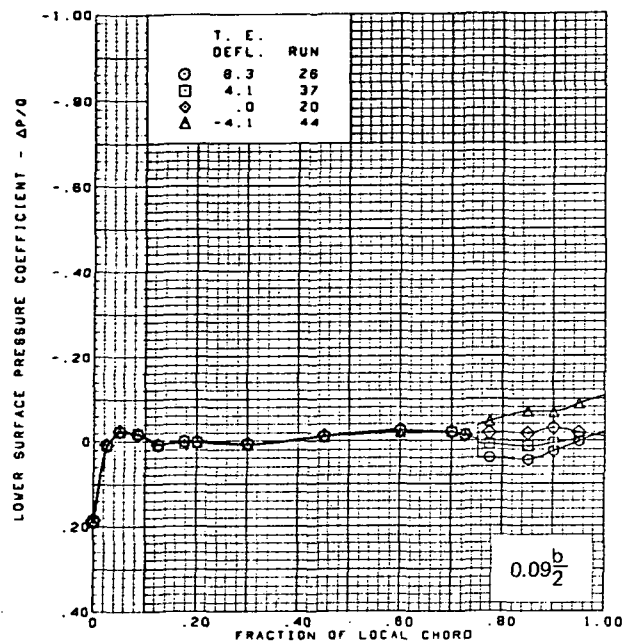


$M = 1.70$   
 $\alpha = 0^\circ$   
 Flat wing, rounded L.E.  
 L.E. deflection, full span =  $0.0^\circ$

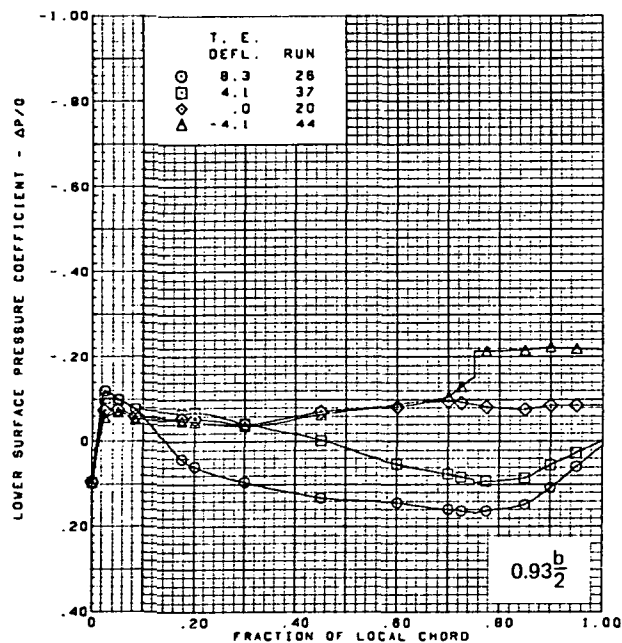
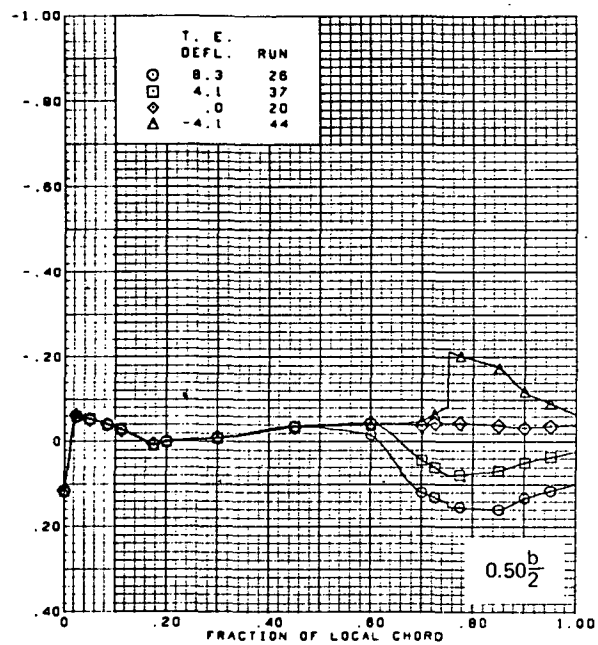
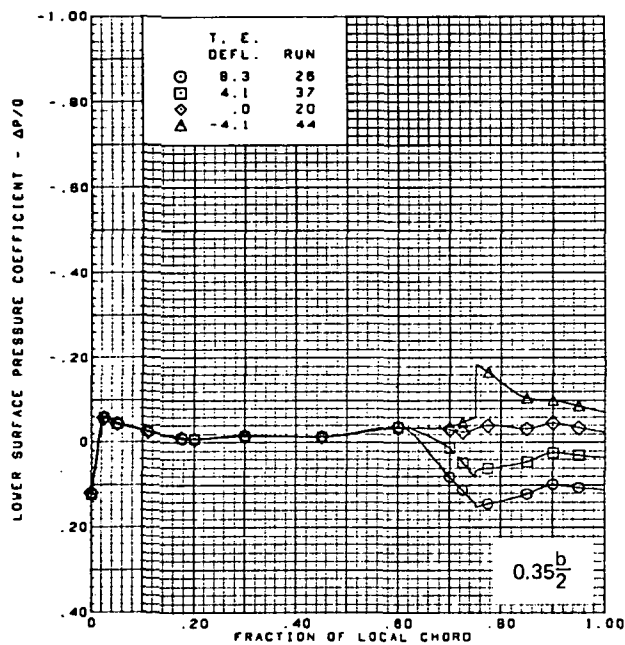
Note:  $C_{p, \text{vacuum}} = -0.49$

(a) (Concluded)

Figure 26.—(Continued)





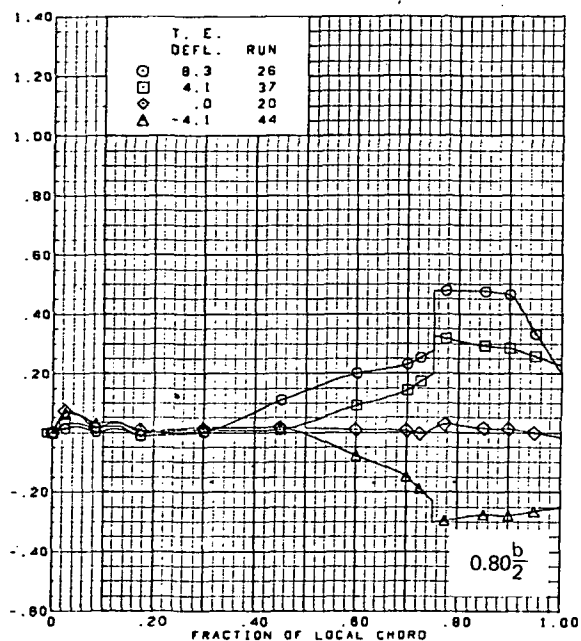
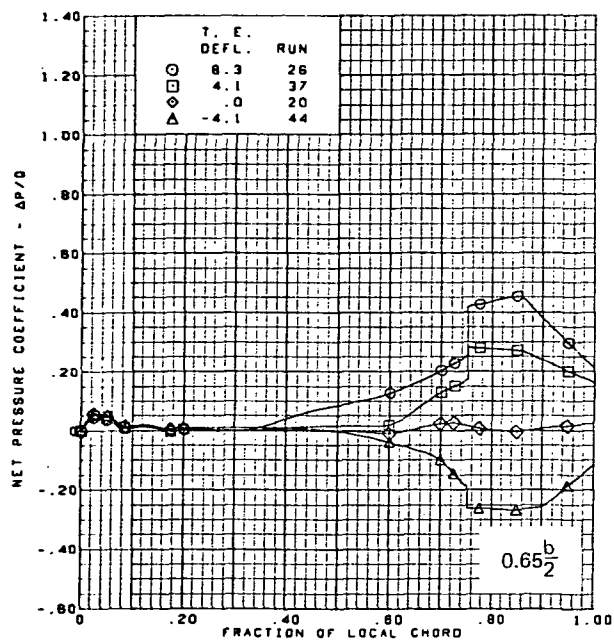
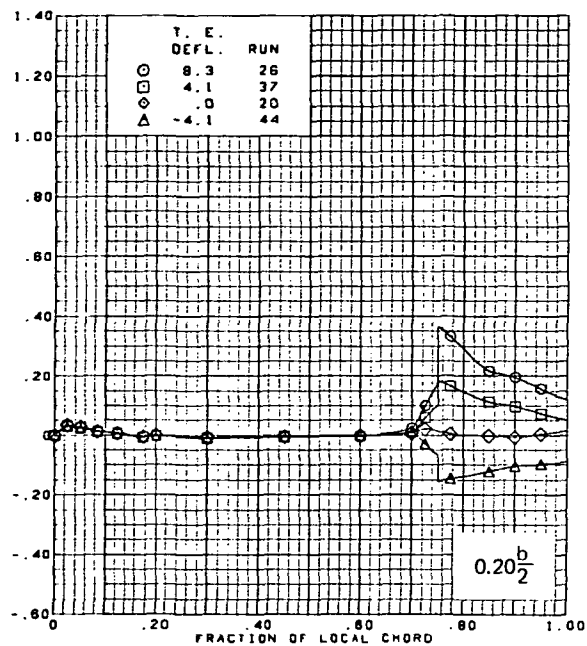
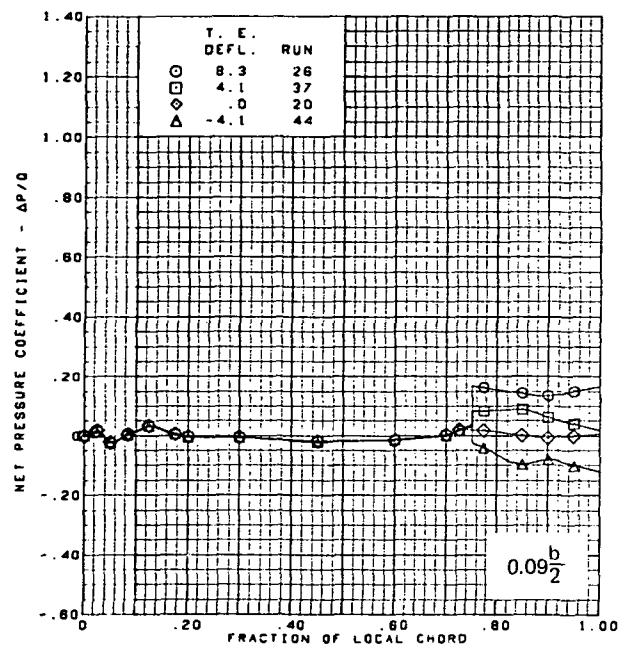


$M = 1.70$   
 $\alpha = 0^\circ$   
 Flat wing, rounded L.E.  
 L.E. deflection, full span =  $0.0^\circ$

Note:  $C_{p, \text{vacuum}} = -0.49$

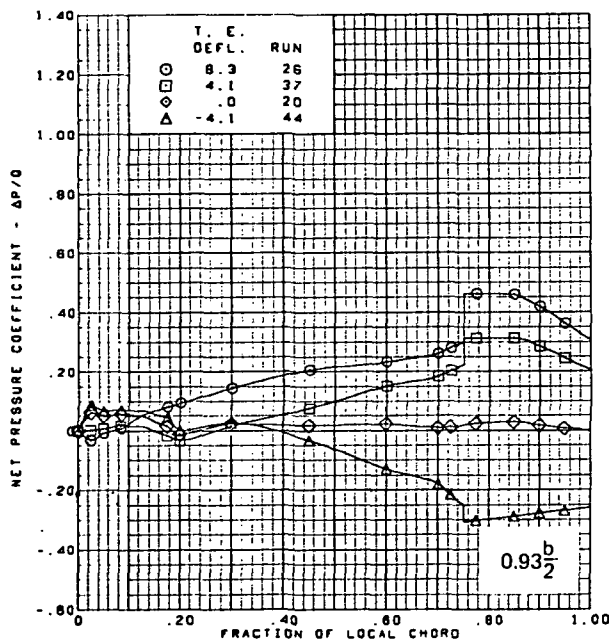
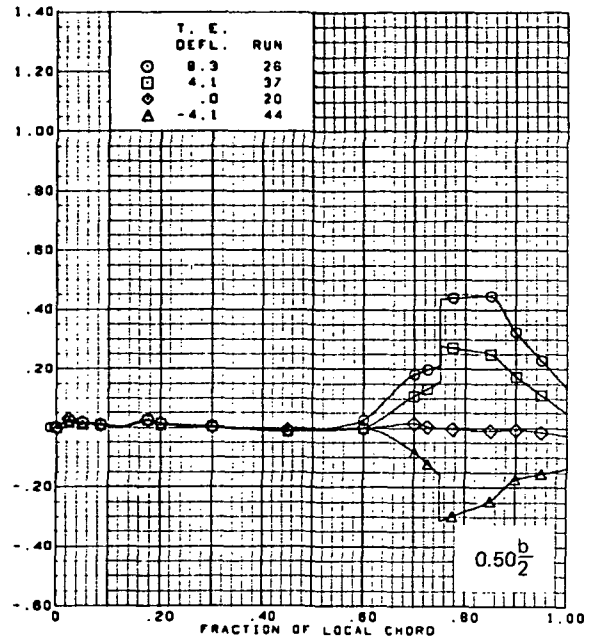
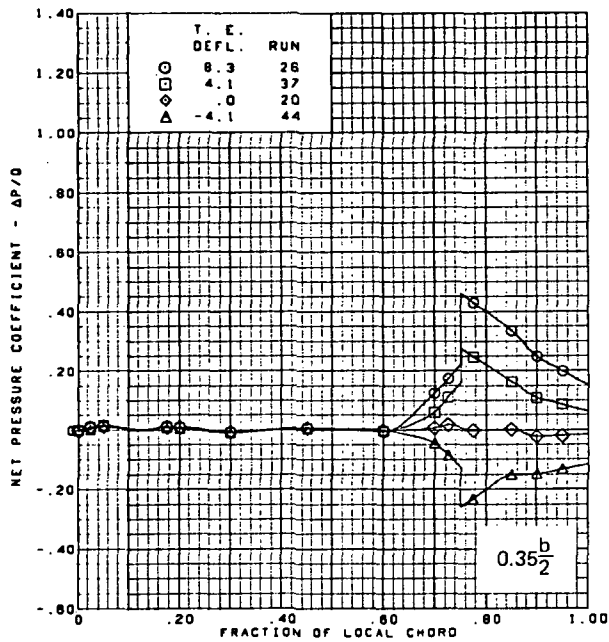
(b) (Concluded)

Figure 26.—(Continued)



(c) Net Chordwise Pressure Distributions,  $\alpha = 0^\circ$

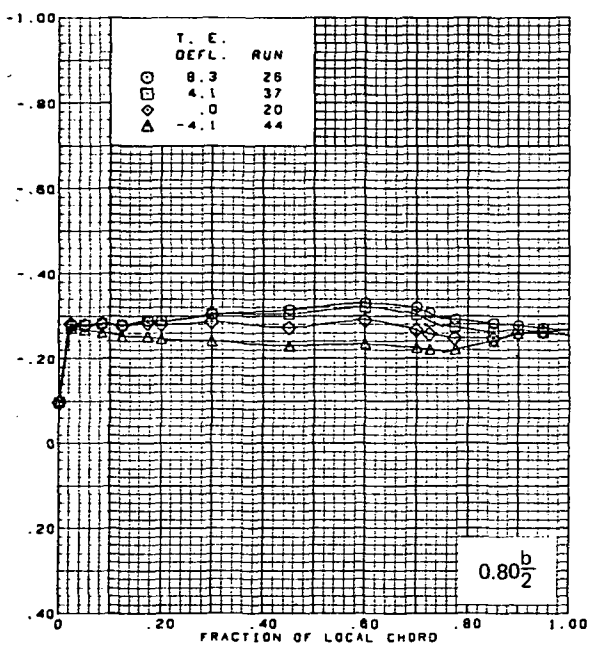
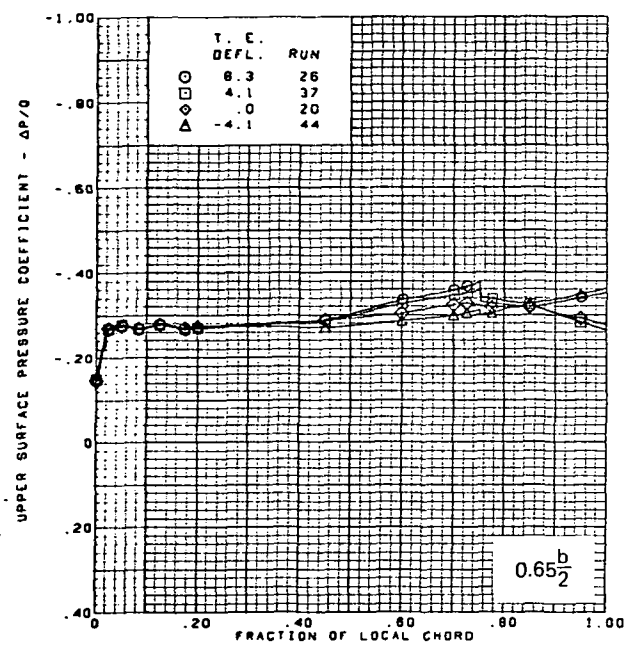
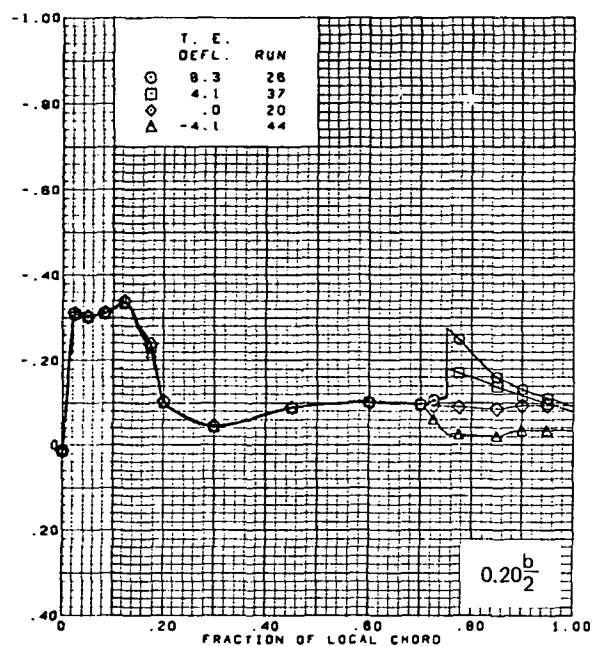
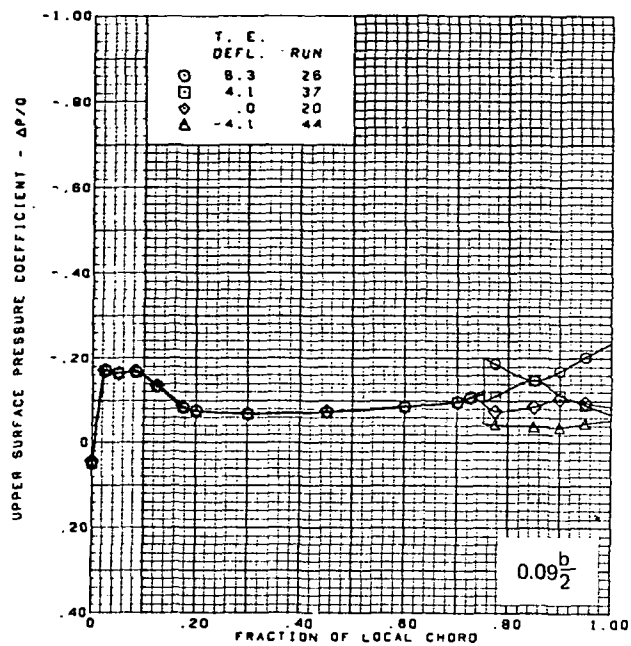
Figure 26.—(Continued)



$M = 1.70$   
 $\alpha = 0^\circ$   
 Flat wing, rounded L.E.  
 L.E. deflection, full span =  $0.0^\circ$

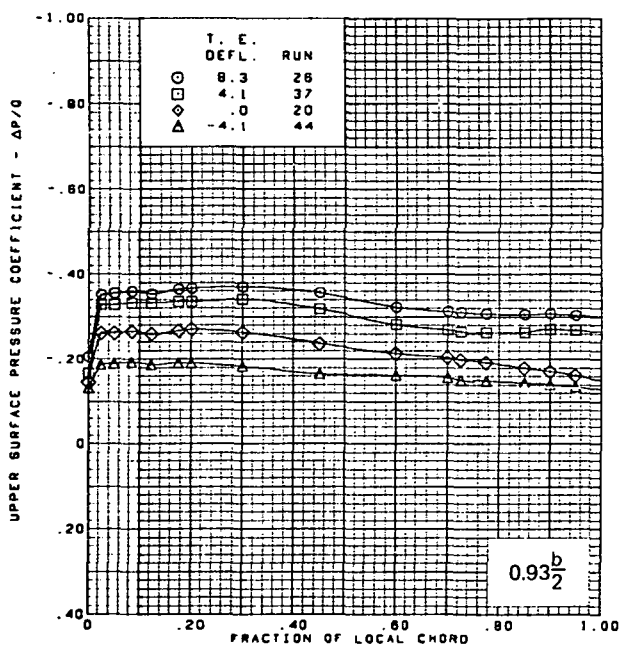
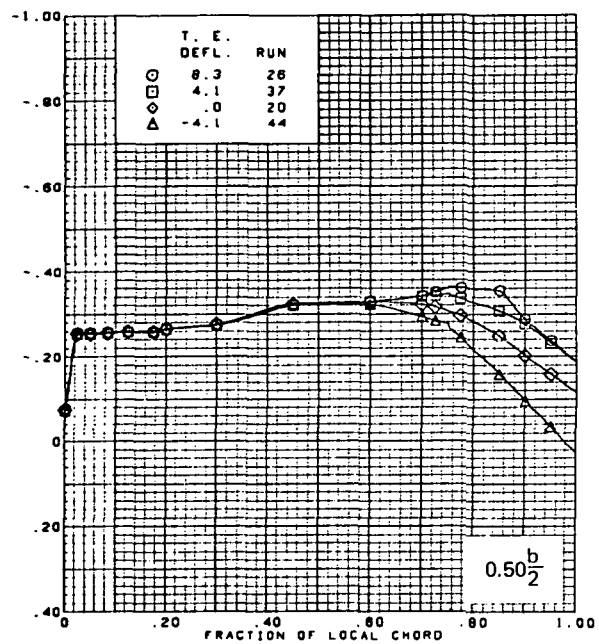
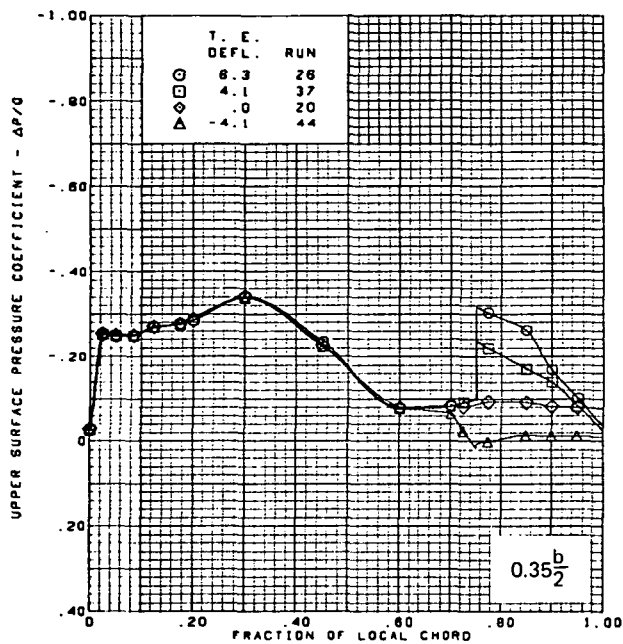
(c) (Concluded)

Figure 26.—(Continued)



(d) Upper Surface Chordwise Pressure Distributions.  $\alpha = 8^\circ$

Figure 26.—(Continued)

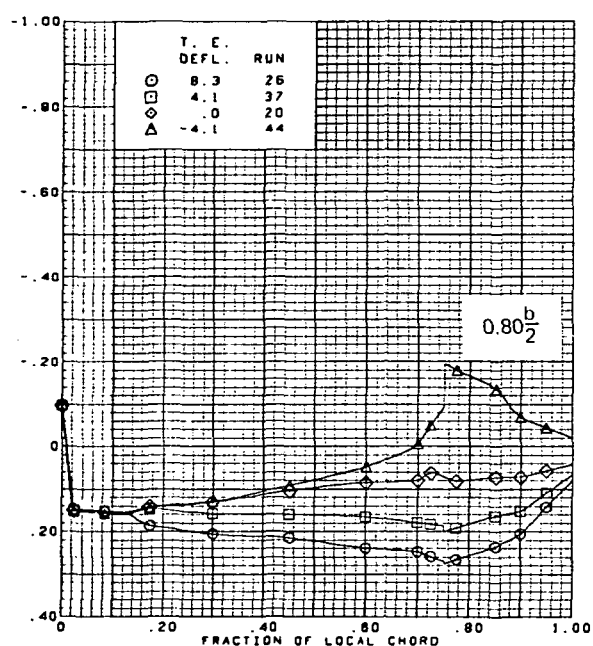
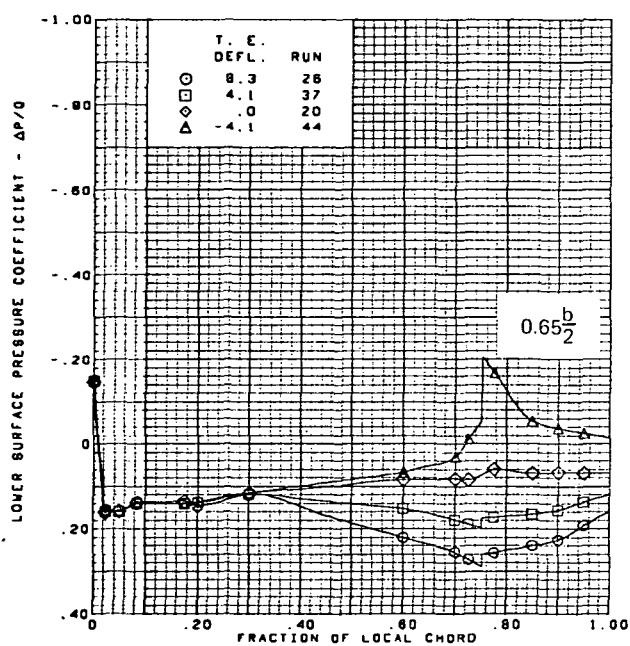
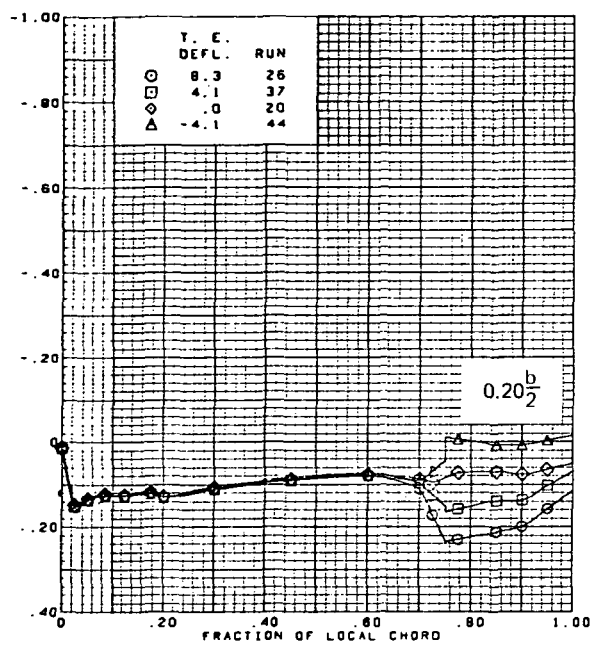
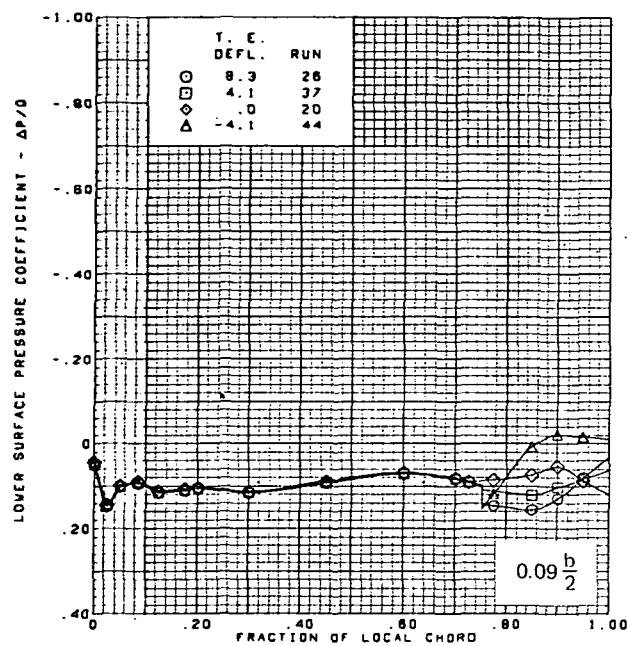


$M = 1.70$   
 $\alpha = 8^\circ$   
 Flat wing, rounded L.E.  
 L.E. deflection, full span =  $0.0^\circ$

Note:  $C_{p, \text{vacuum}} = -0.49$

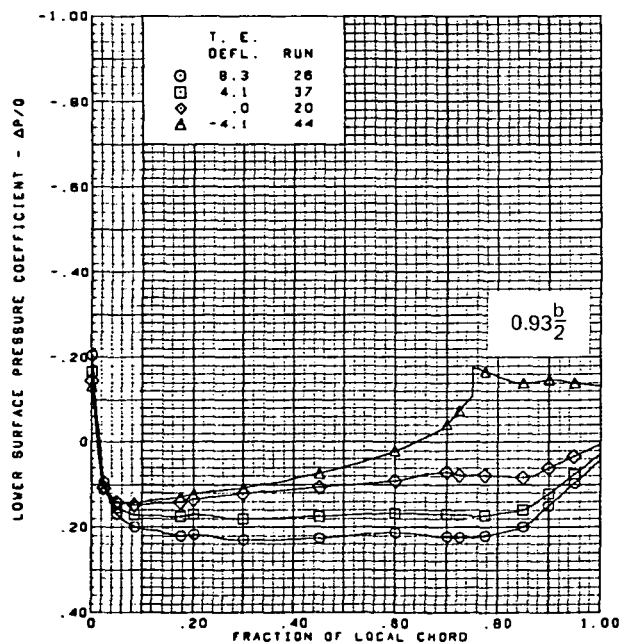
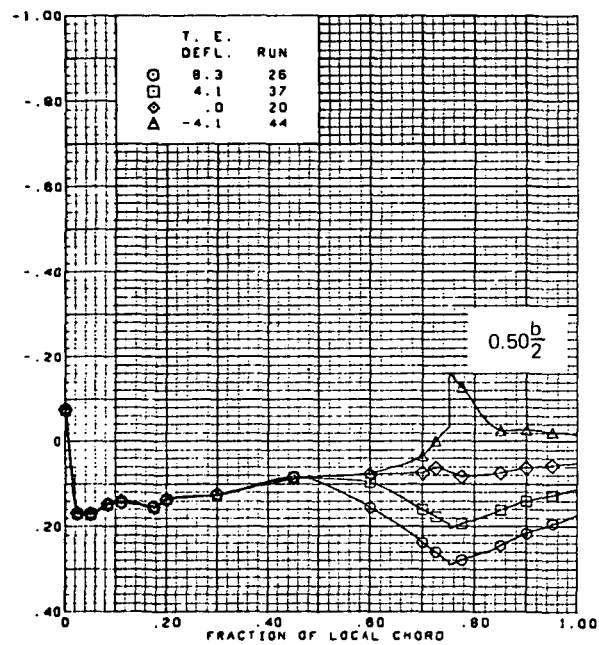
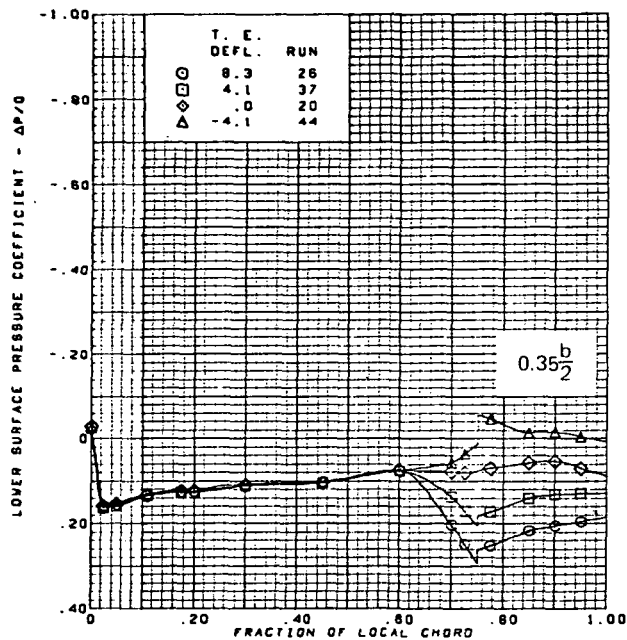
(d) (Concluded)

Figure 26.—(Continued)



(e) Lower Surface Chordwise Pressure Distributions,  $\alpha = 8^\circ$

Figure 26.—(Continued)

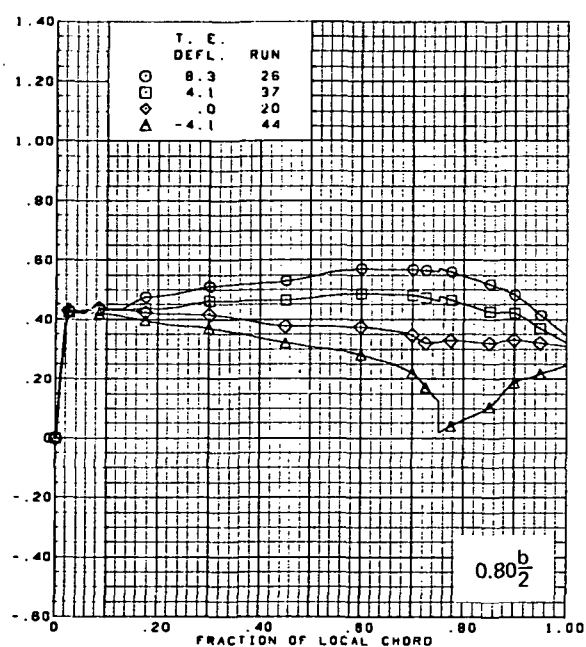
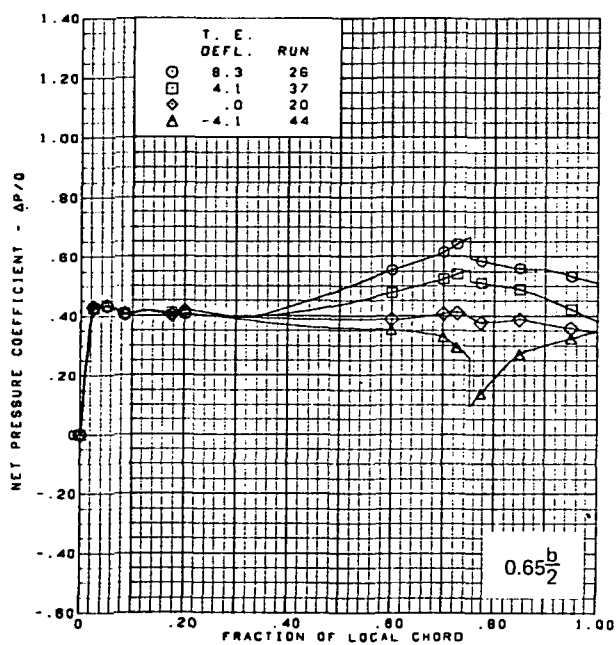
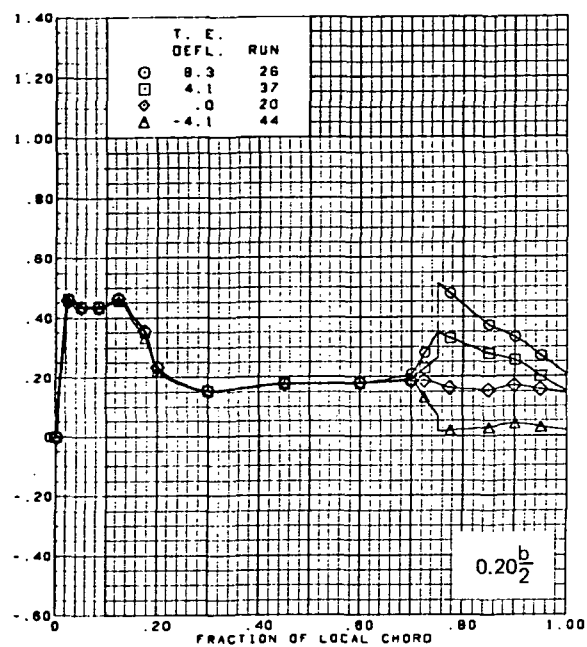
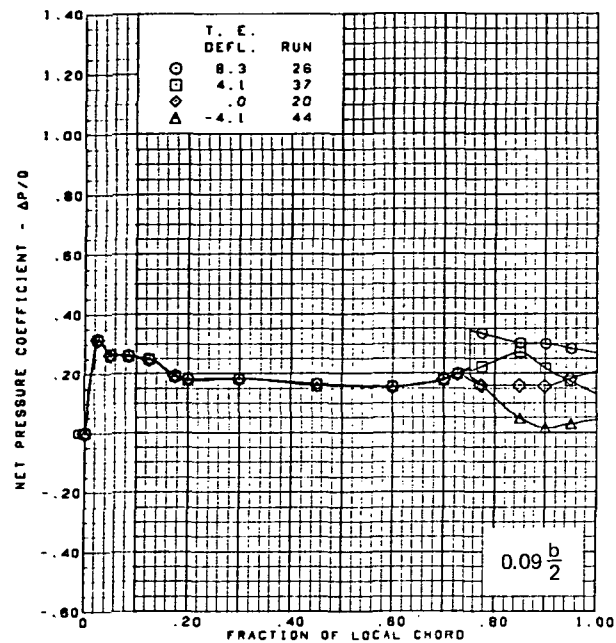


$M = 1.70$   
 $\alpha = 8^\circ$   
 Flat wing, rounded L.E.  
 L.E. deflection, full span =  $0.0^\circ$

Note:  $C_{p, \text{vacuum}} = -0.49$

(e) (Concluded)

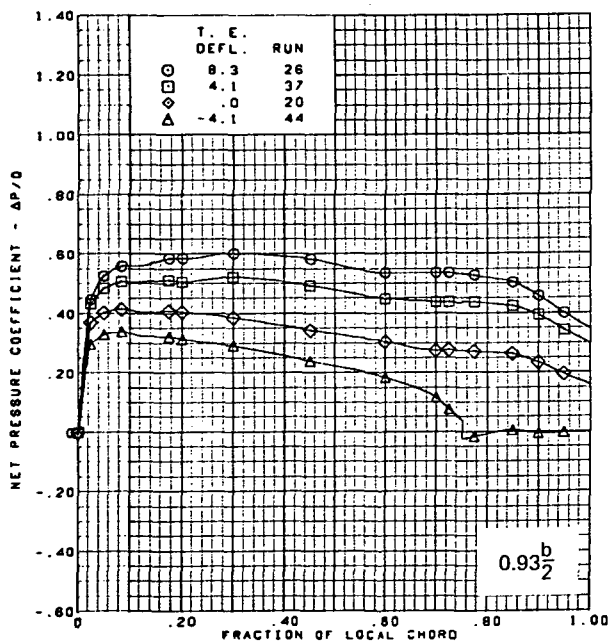
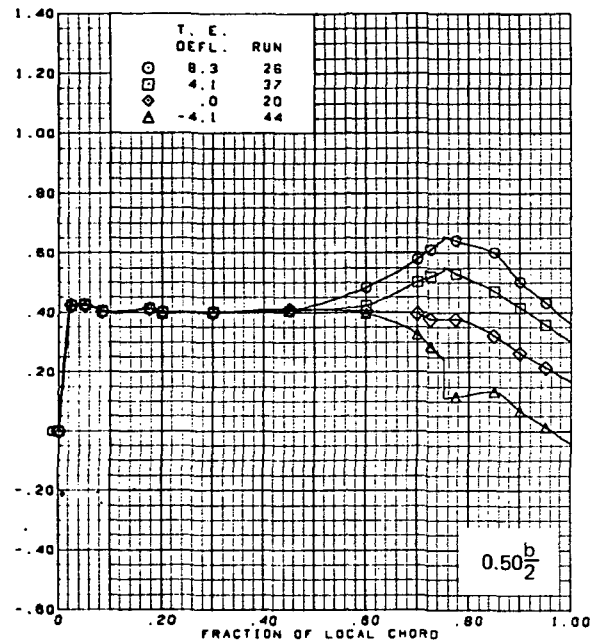
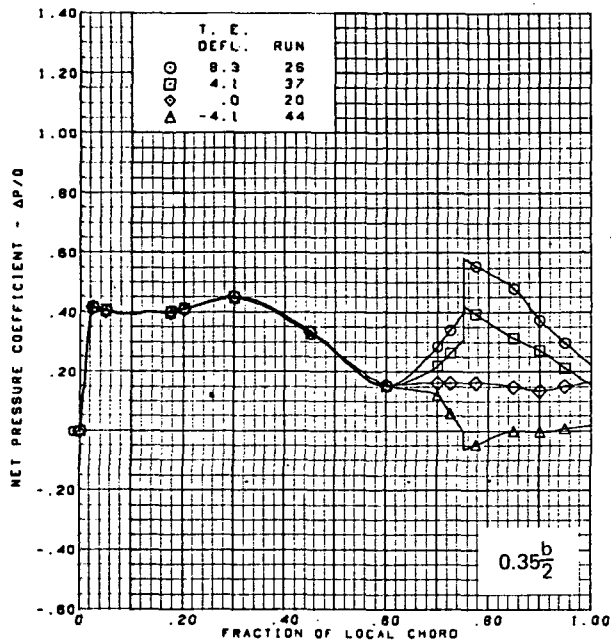
Figure 26.—(Continued)



(f) Net Chordwise Pressure Distributions,  $\alpha = 8^\circ$

Figure 26.—(Continued)

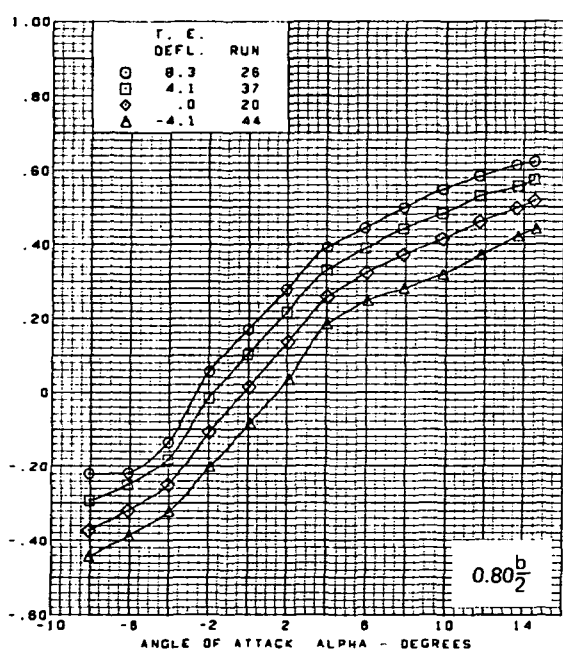
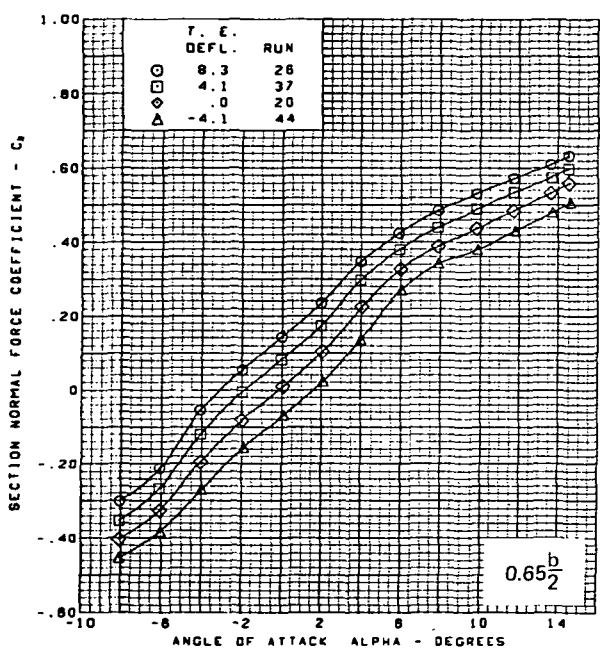
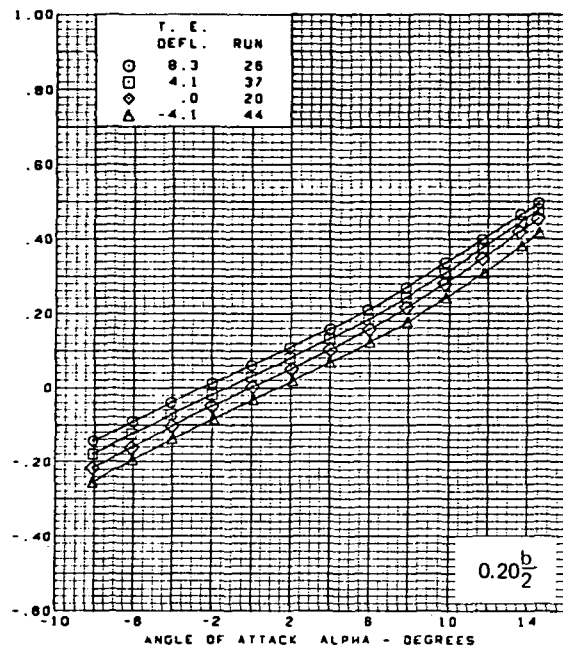
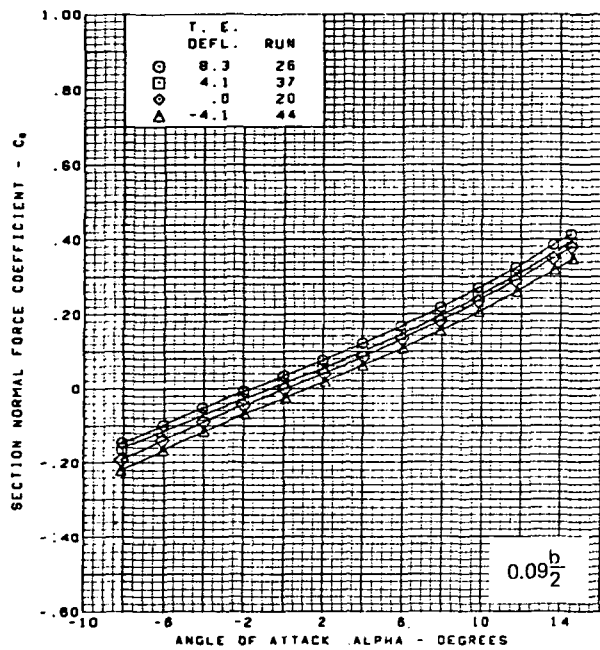




$M = 1.70$   
 $\alpha = 8^\circ$   
 Flat wing, rounded L.E.  
 L.E. deflection, full span =  $0.0^\circ$

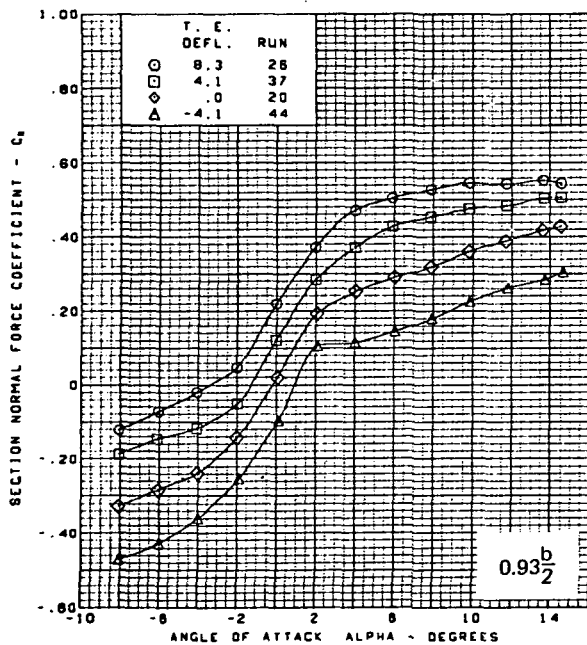
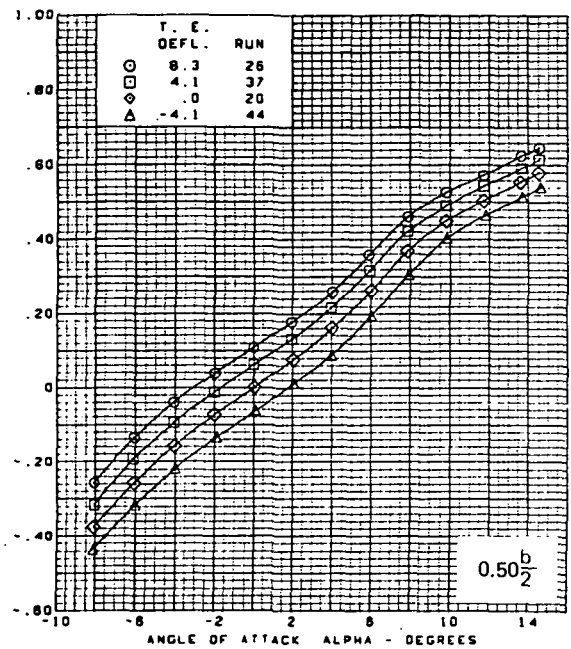
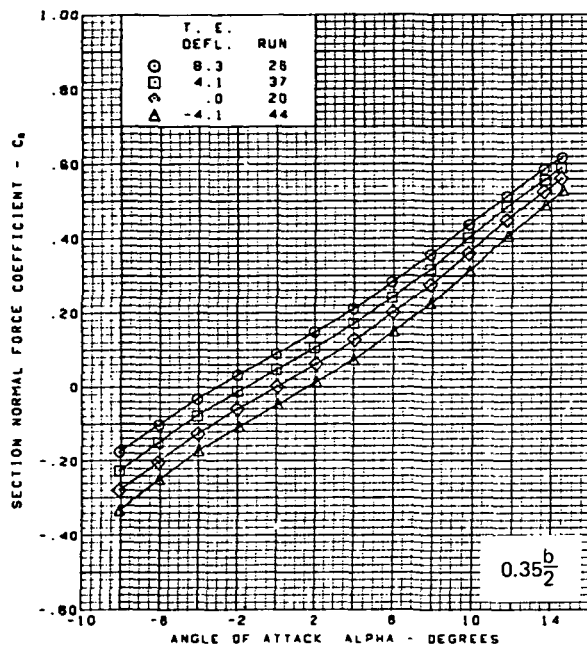
(f) (Concluded)

Figure 26.—(Continued)



(g) Section Aerodynamic Coefficients—Normal Force

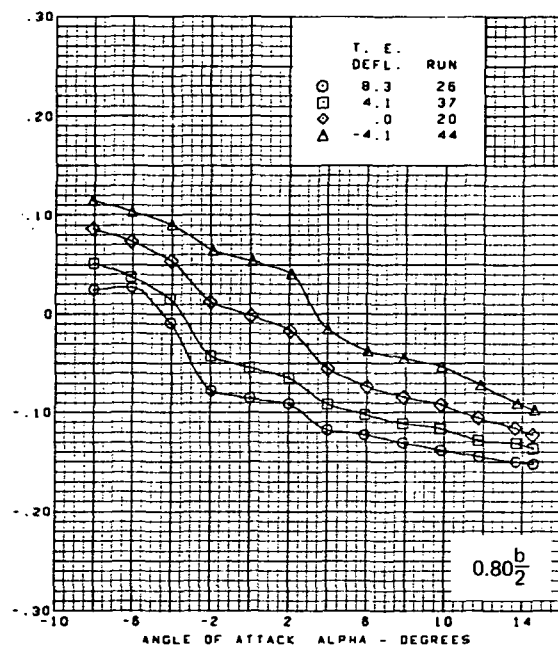
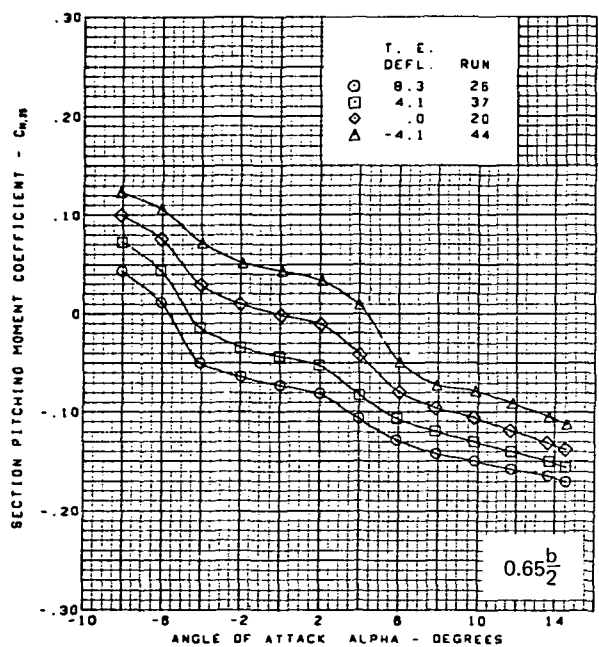
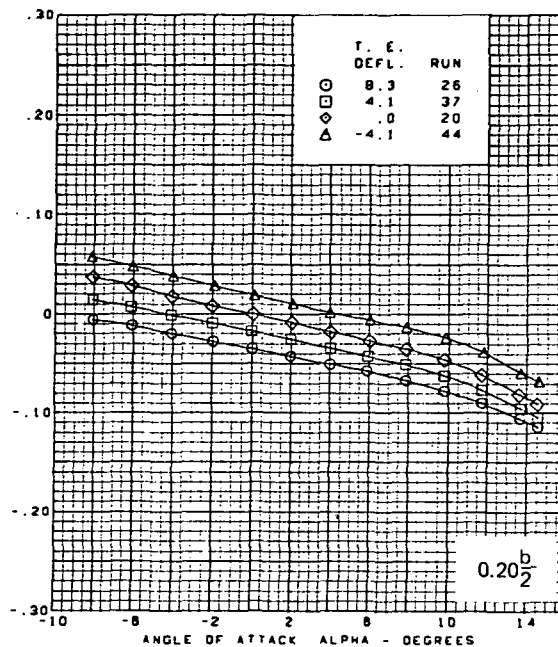
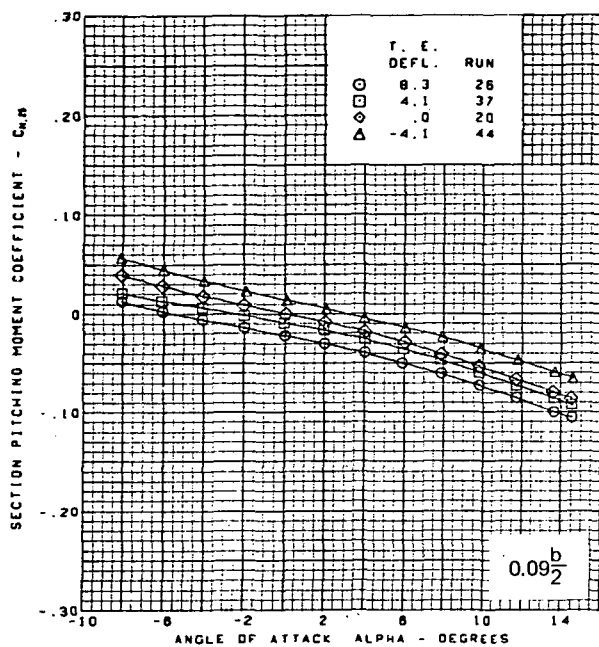
Figure 26.—(Continued)



M = 1.70  
 Flat wing, rounded L.E.  
 L.E. deflection, full span = 0.0°

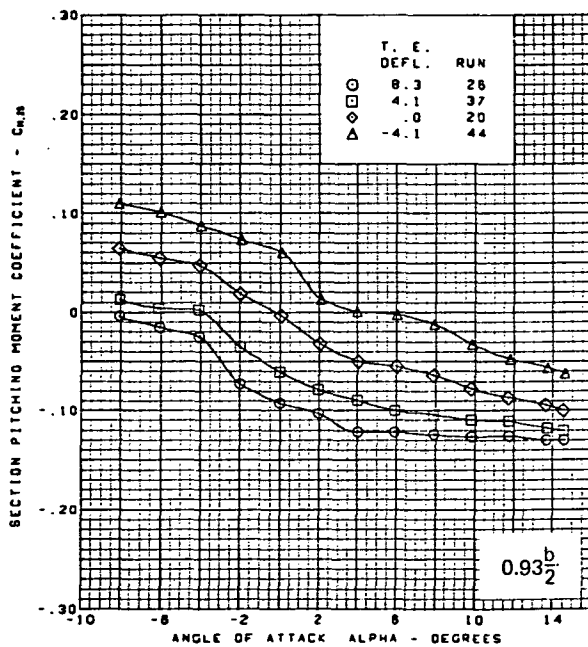
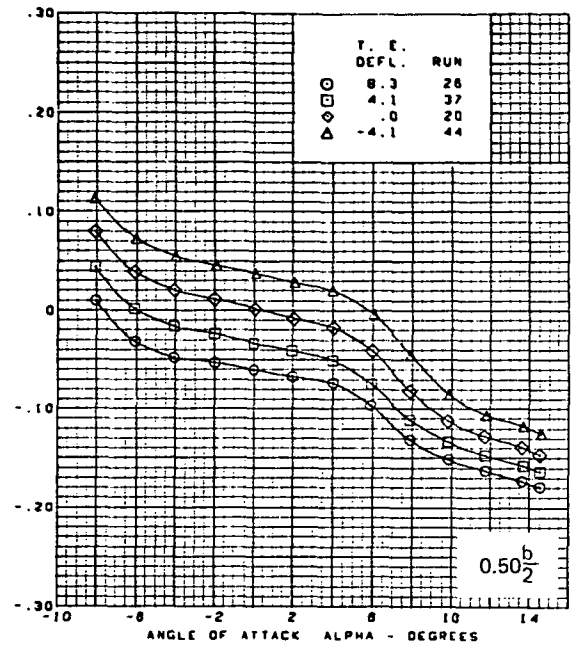
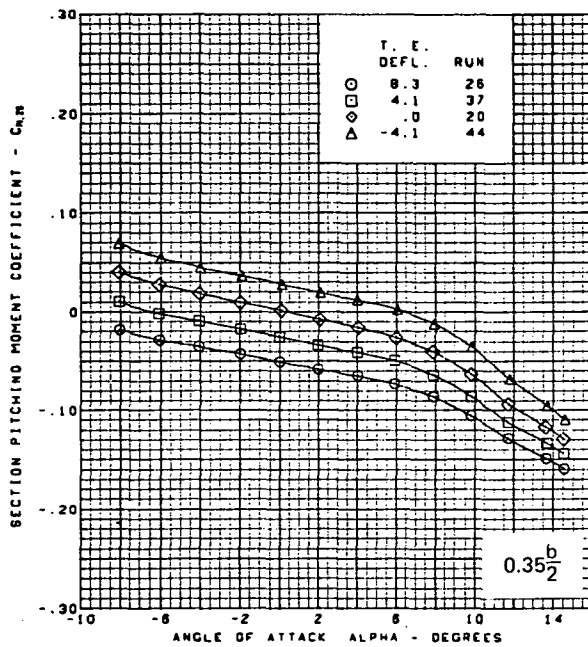
(g) (Concluded)

Figure 26.—(Continued)



(h) Section Aerodynamic Coefficients—Pitching Moment

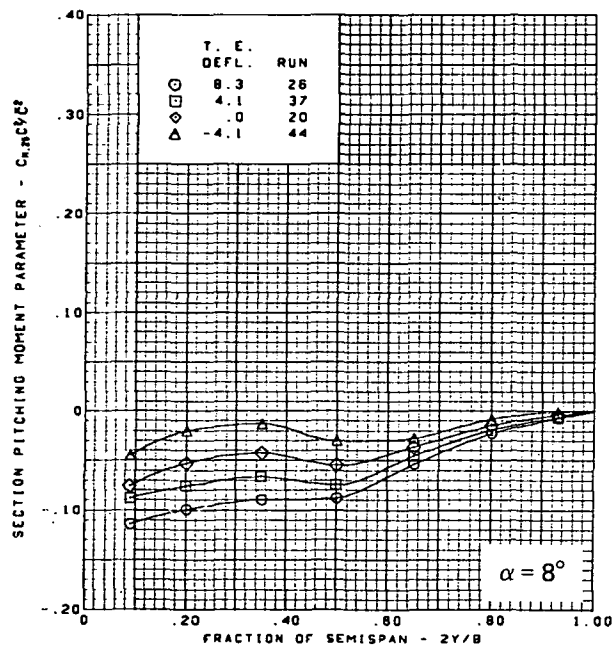
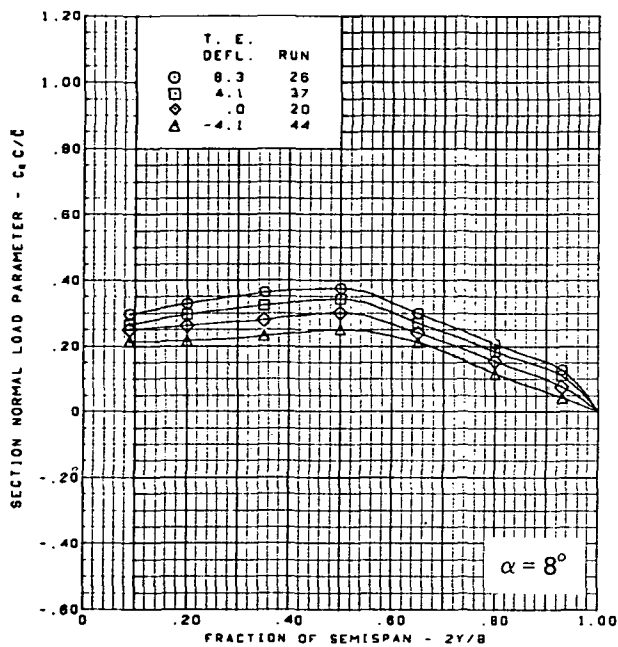
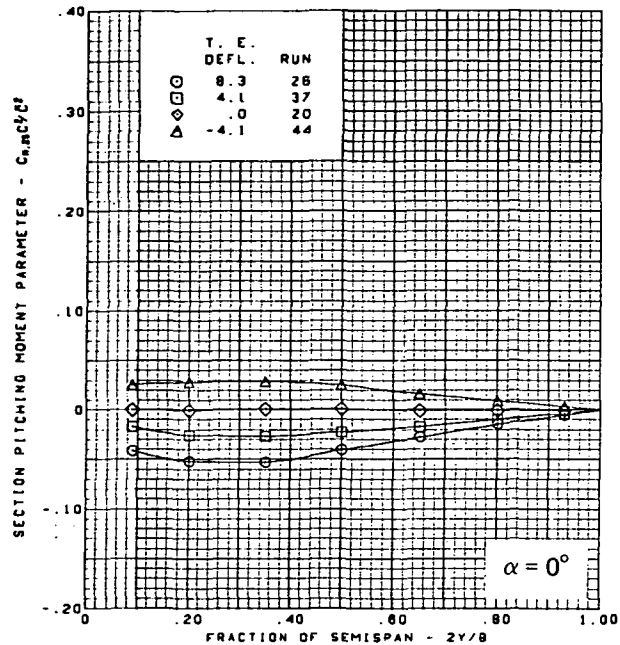
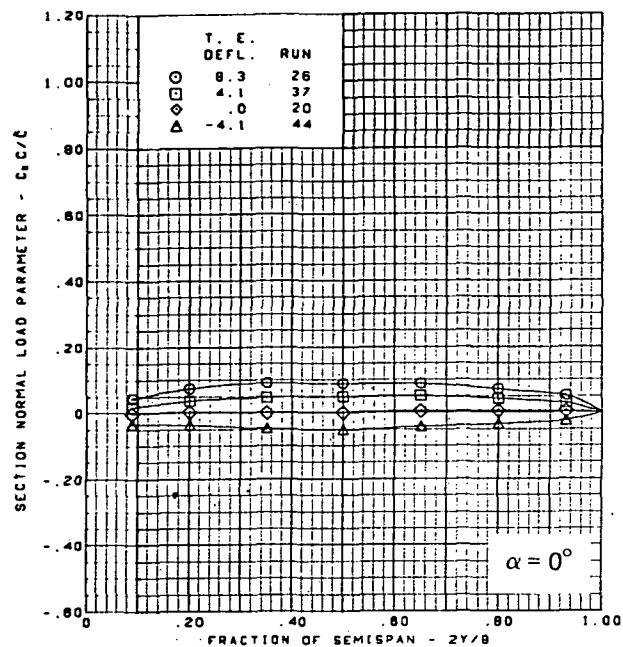
Figure 26.—(Continued)



$M = 1.70$   
 Flat wing, rounded L.E.  
 L.E. deflection, full span =  $0.0^\circ$

(h) (Concluded)

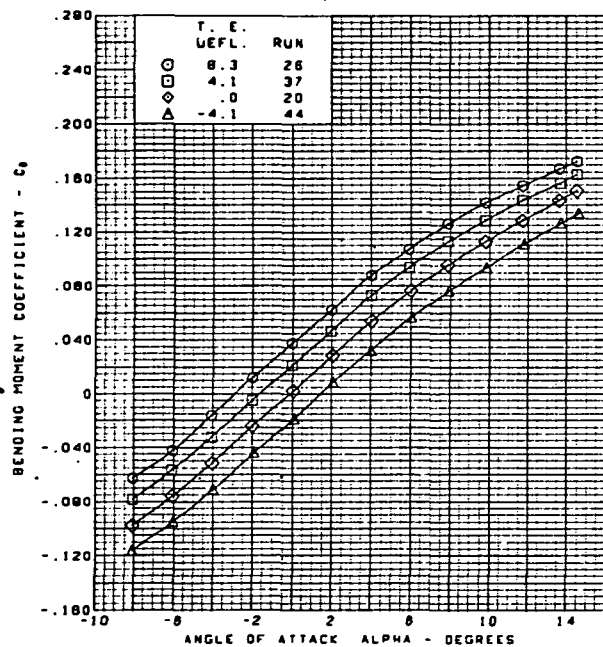
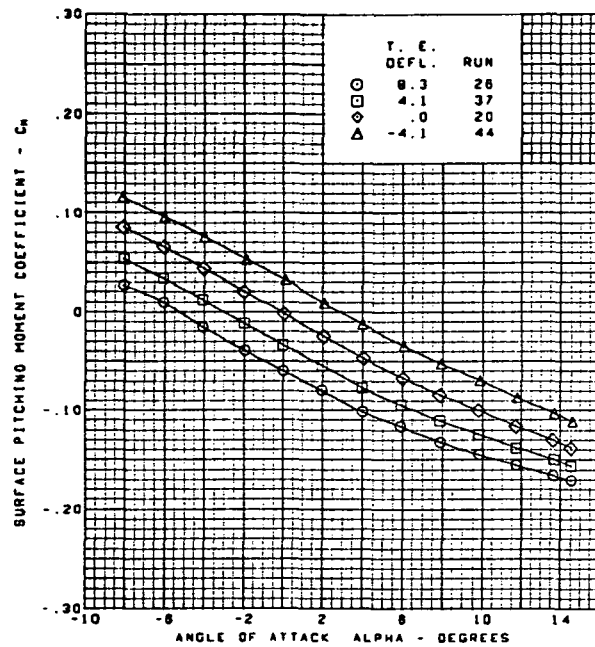
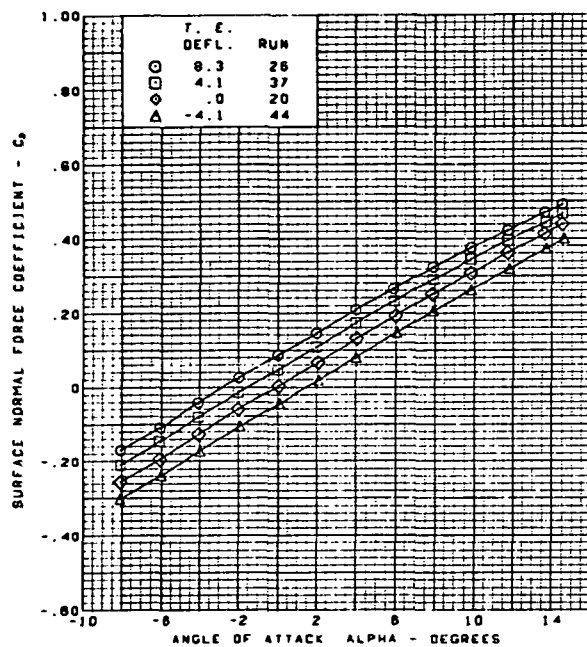
Figure 26.—(Continued)



$M = 1.70$   
 Flat wing, rounded L.E.  
 L.E. deflection, full span =  $0.0^\circ$

(i) Spanload Distributions

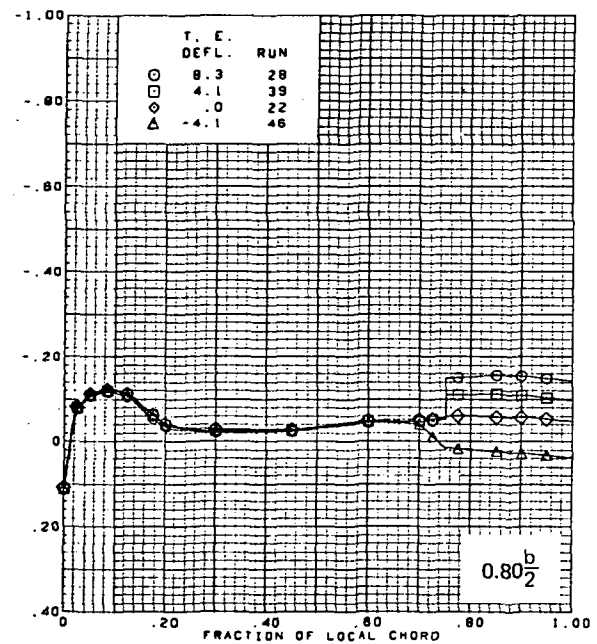
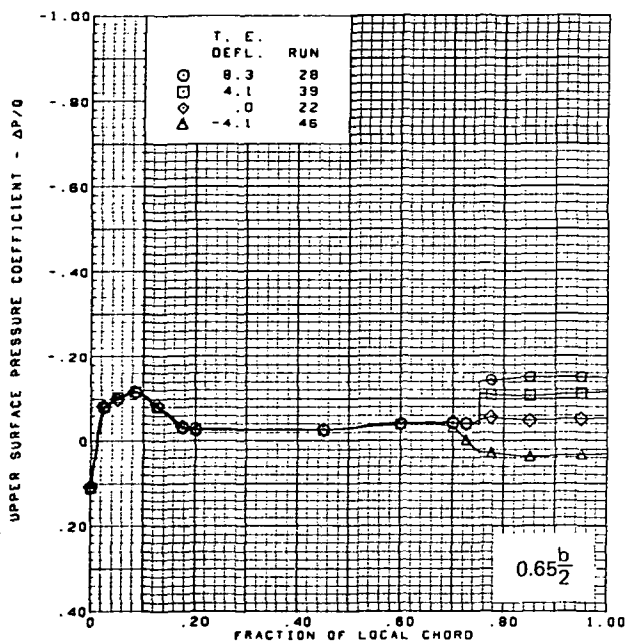
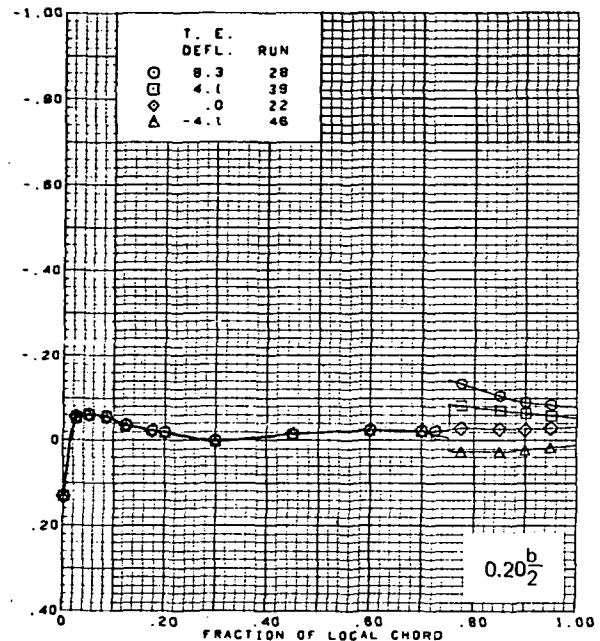
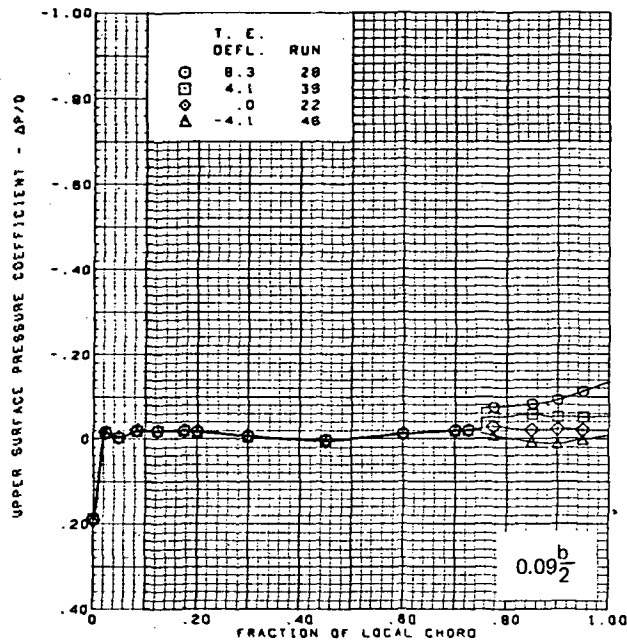
Figure 26.—(Continued)



$M = 1.70$   
 Flat wing, rounded L.E.  
 L.E. deflection, full span =  $0.0^\circ$

(j) Wing Aerodynamic Coefficients

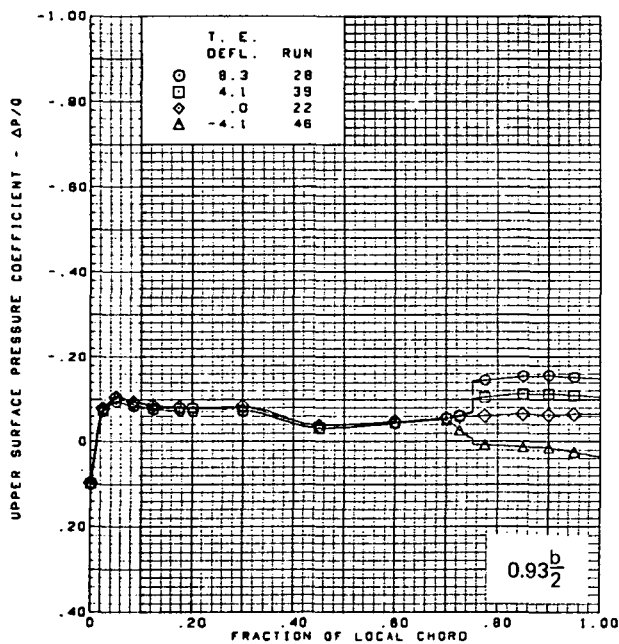
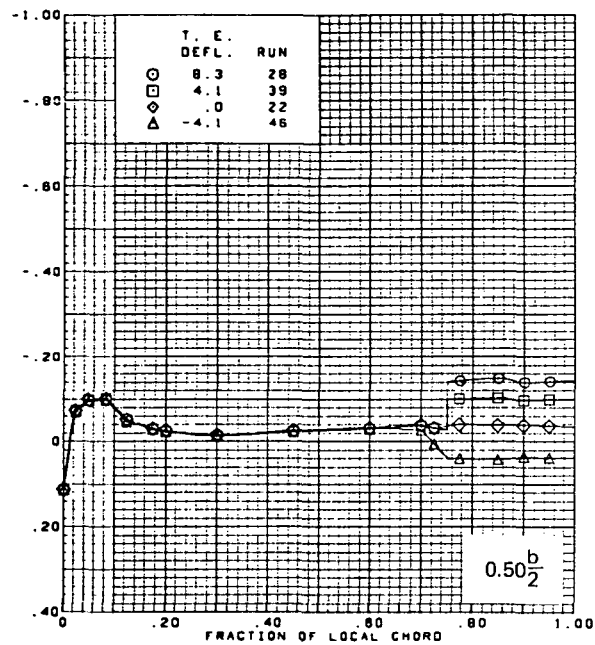
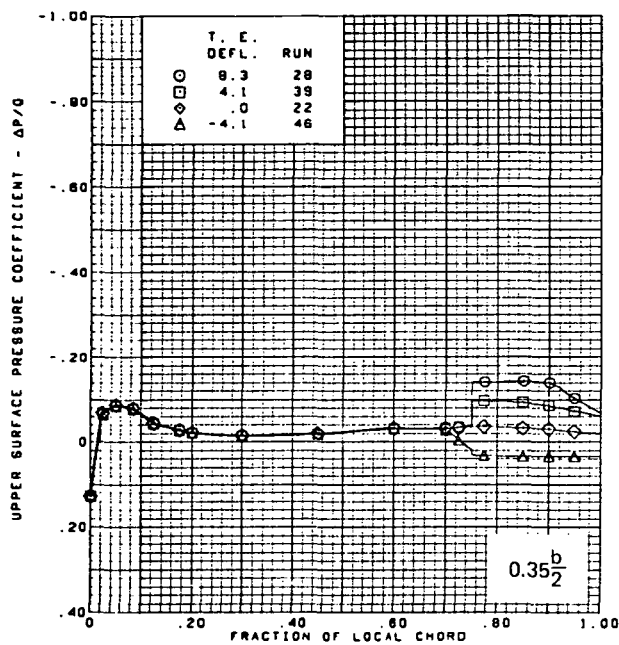
Figure 26.—(Concluded)



(a) Upper Surface Chordwise Pressure Distributions,  $\alpha = 0^\circ$

Figure 27.—Wing Experimental Data—Effect of Full Span T.E. Deflection With Angle of Attack; Flat Wing, Rounded L.E.; L.E. Deflection, Full Span =  $0.0^\circ$ ;  $M = 2.50$



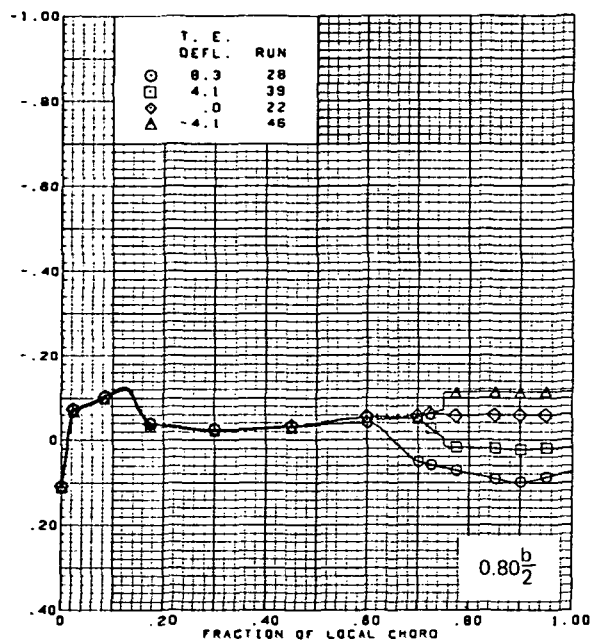
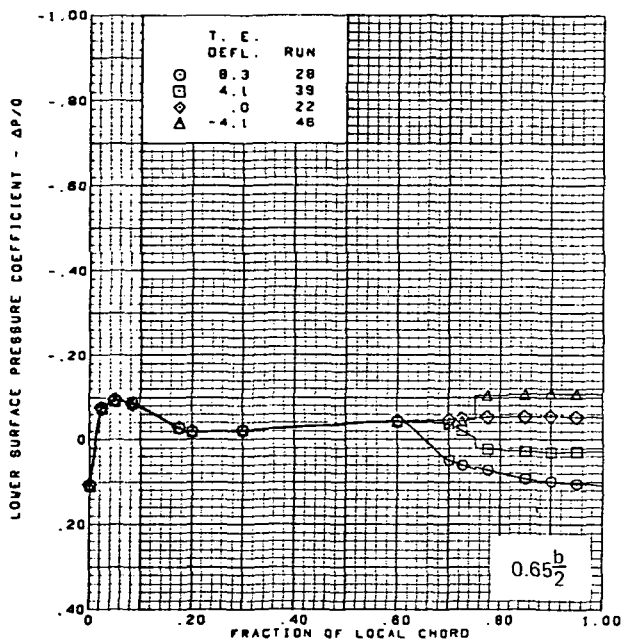
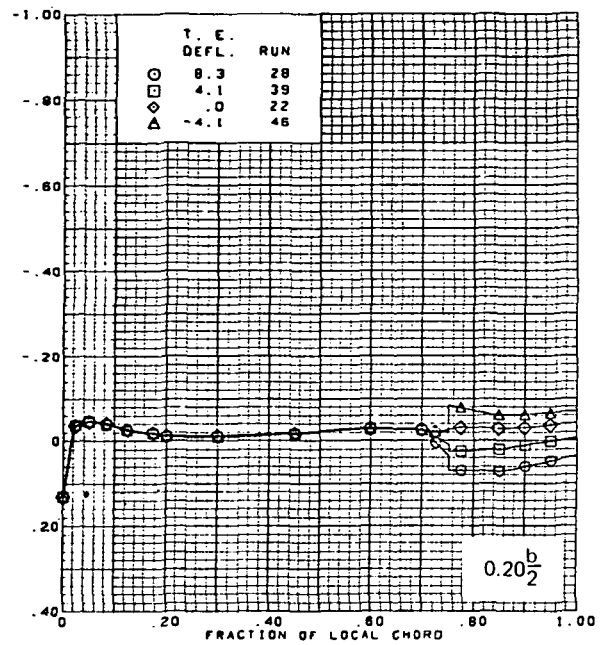
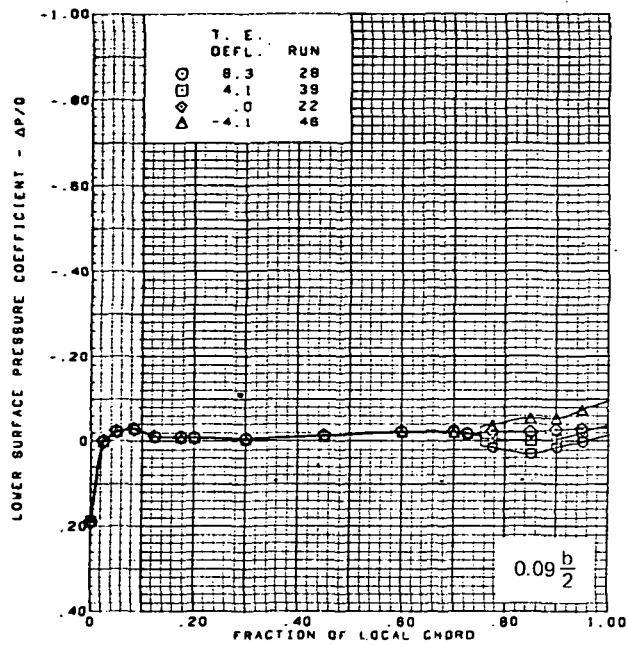


$M = 2.50$   
 $\alpha = 0^\circ$   
 Flat wing, rounded L.E.  
 L.E. deflection, full span =  $0.0^\circ$

Note:  $C_{p, \text{vacuum}} = -0.23$

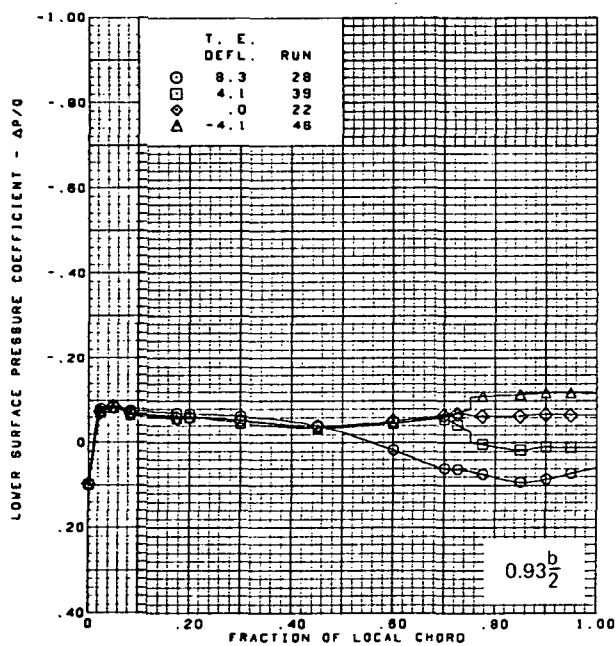
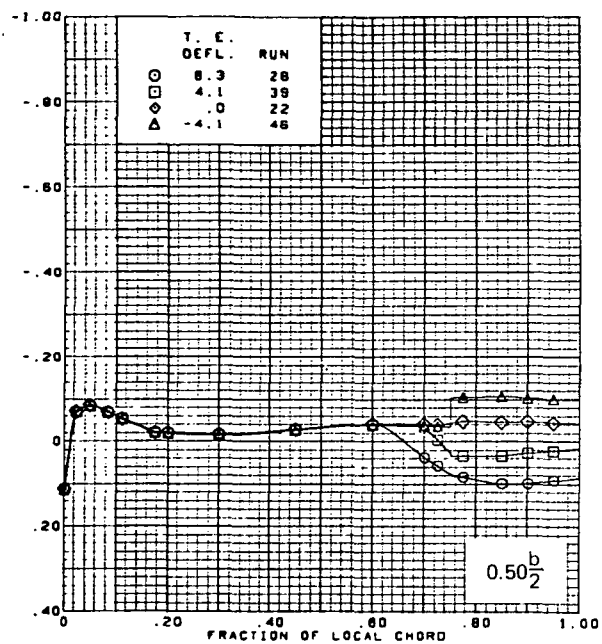
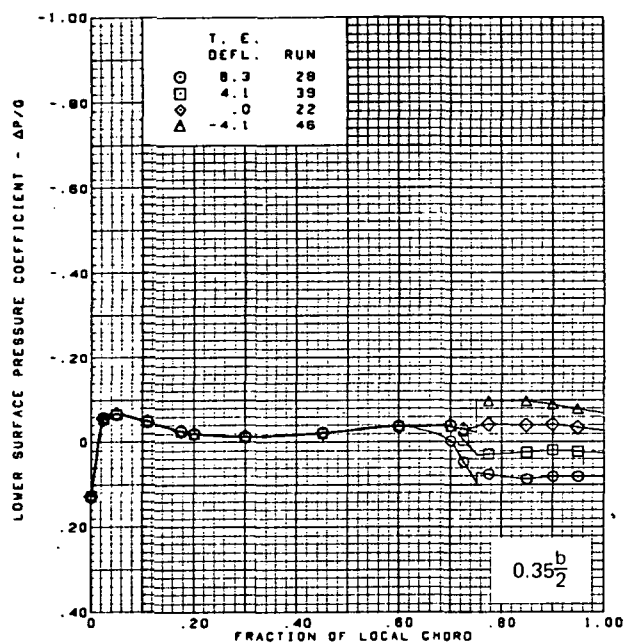
(a) (Concluded)

Figure 27.—(Continued)



(b) Lower Surface Chordwise Pressure Distributions,  $\alpha = 0^\circ$

Figure 27.—(Continued)

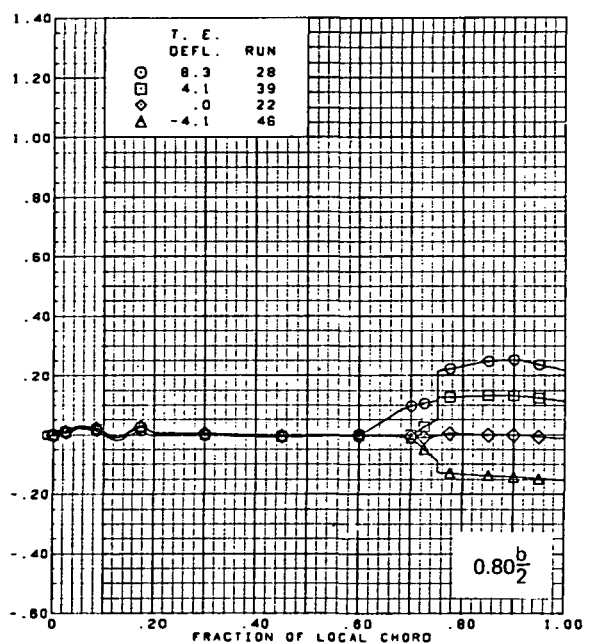
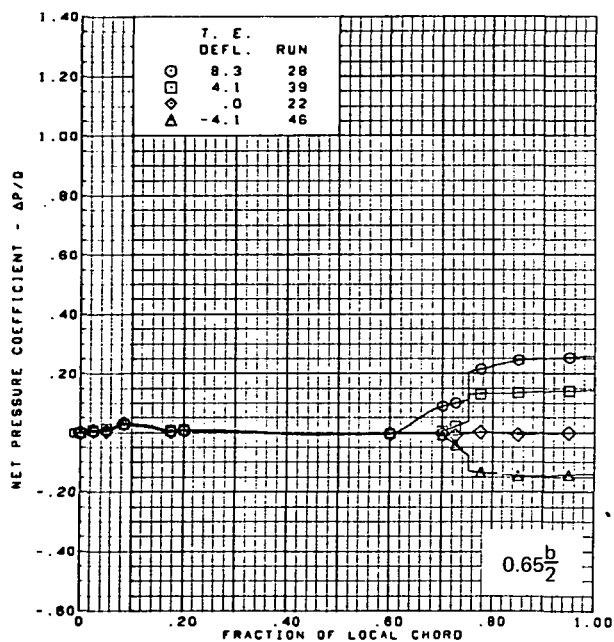
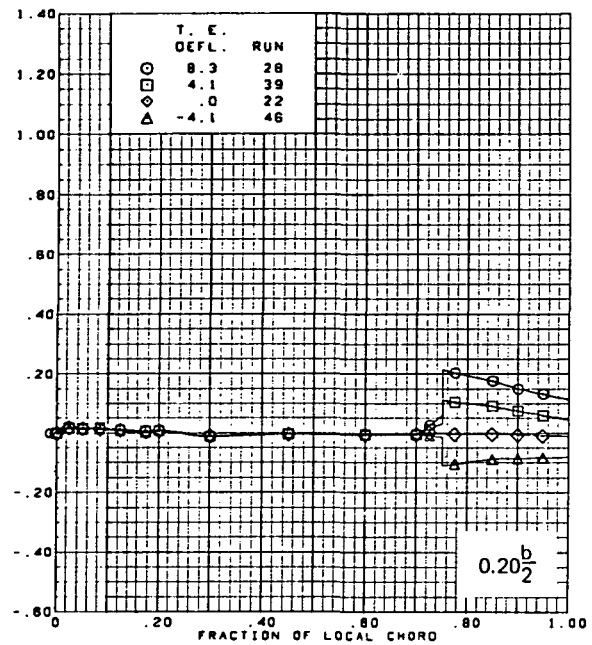
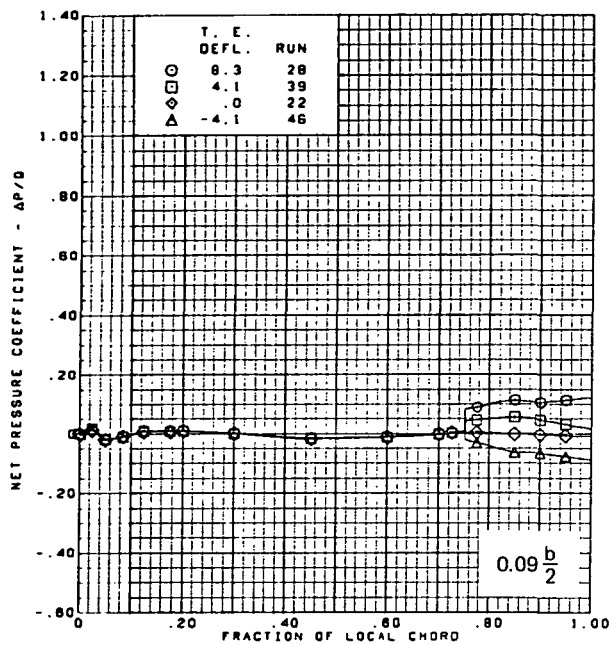


$M = 2.50$   
 $\alpha = 0^\circ$   
 Flat wing, rounded L.E.  
 L.E. deflection, full span =  $0.0^\circ$

Note:  $C_{p, \text{vacuum}} = -0.23$

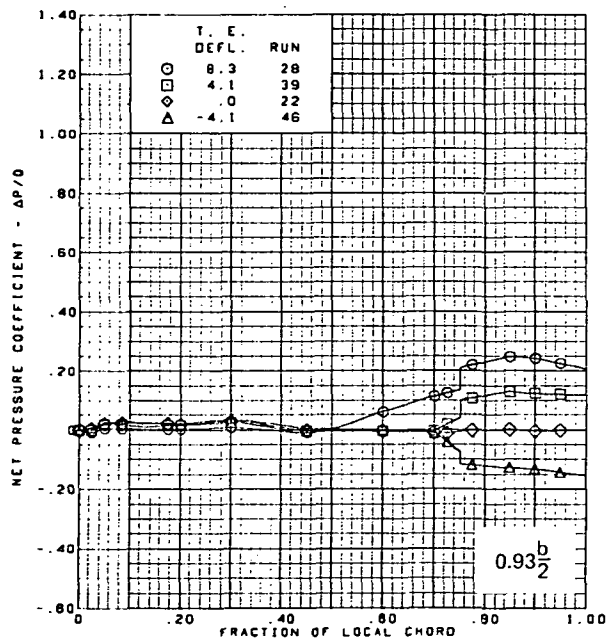
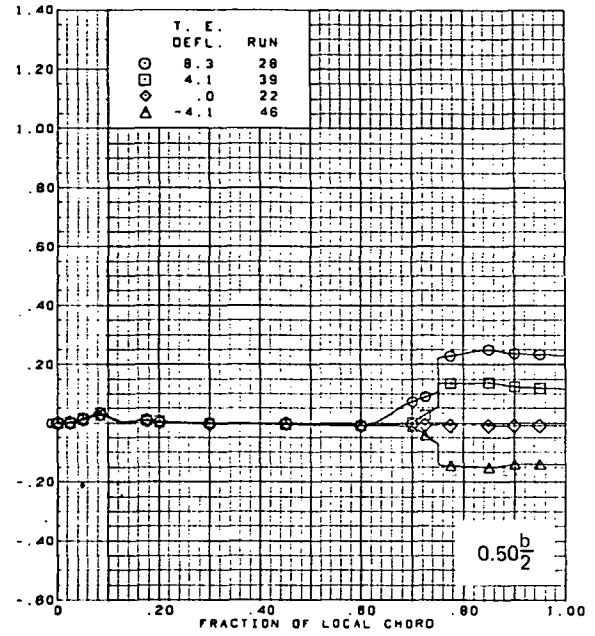
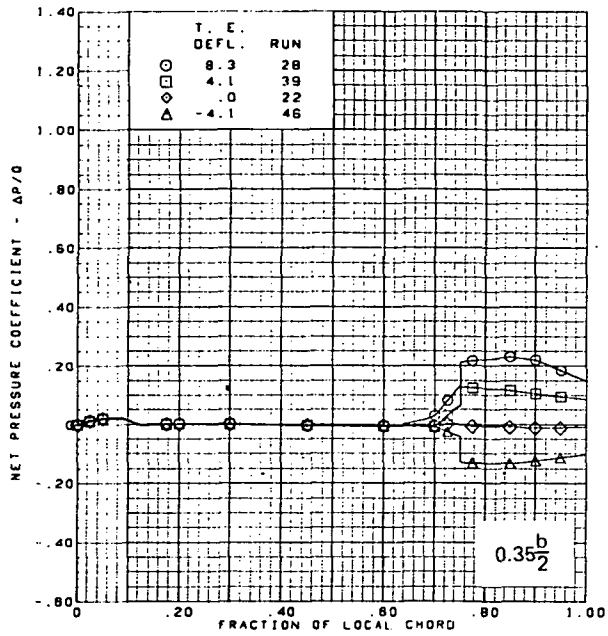
(b) (Concluded)

Figure 27.—(Continued)



(c) Net Chordwise Pressure Distributions,  $\alpha = 0^\circ$

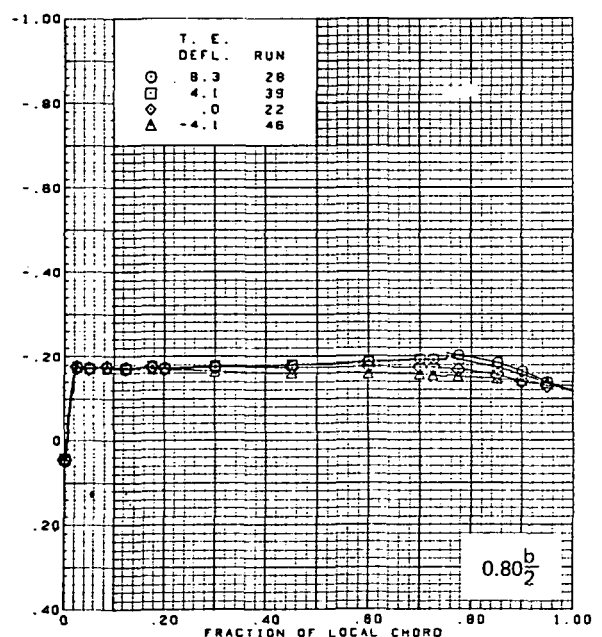
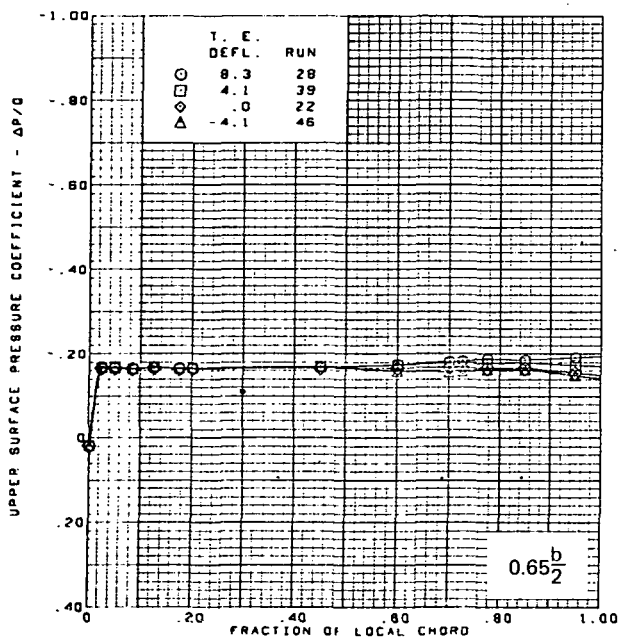
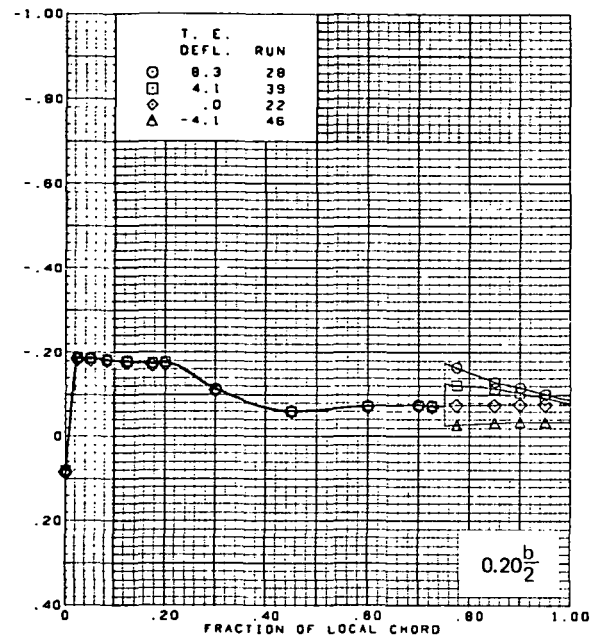
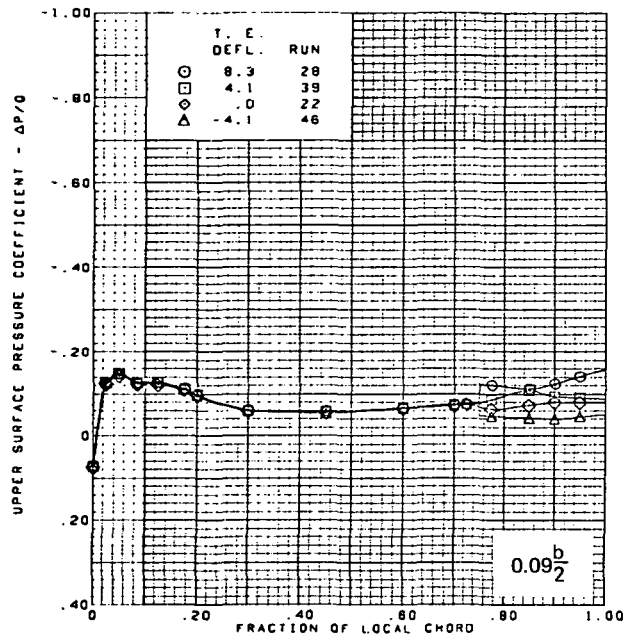
Figure 27.—(Continued)



$M = 2.50$   
 $\alpha = 0^\circ$   
 Flat wing, rounded L.E.  
 L.E. deflection, full span =  $0.0^\circ$

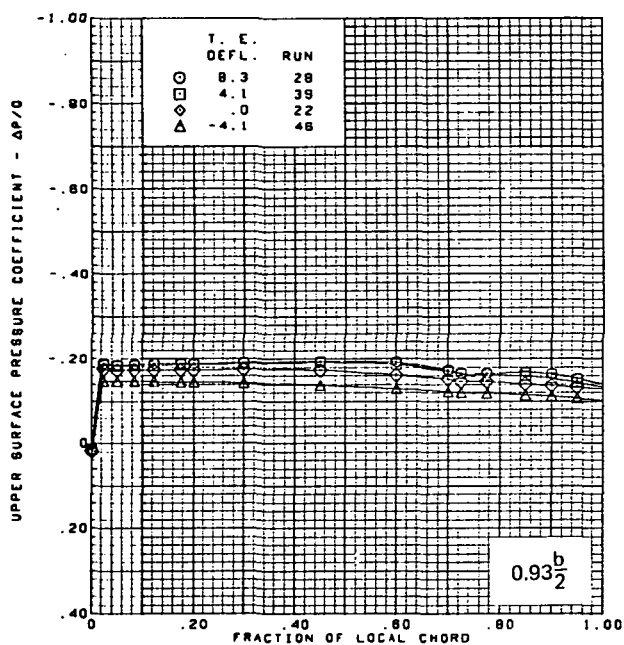
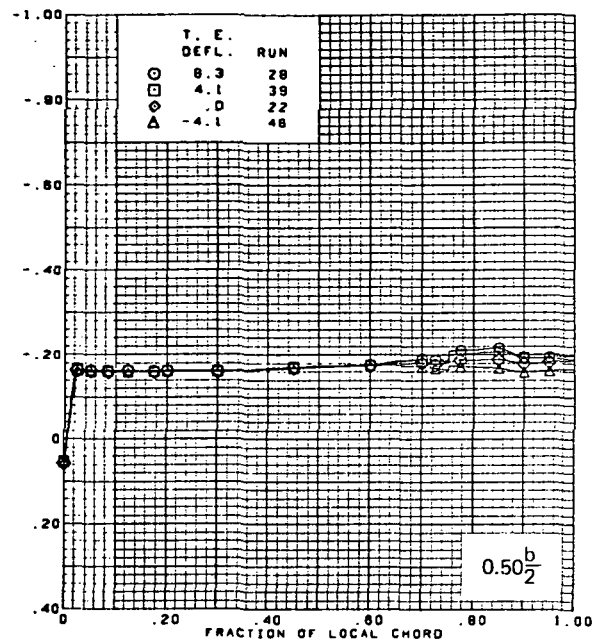
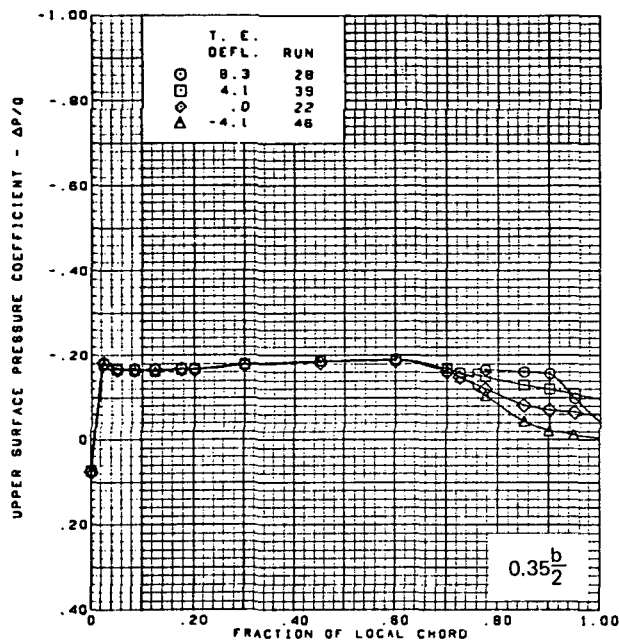
(c) (Concluded)

Figure 27.—(Continued)



(d) Upper Surface Chordwise Pressure Distributions,  $\alpha = 8^\circ$

Figure 27.—(Continued)

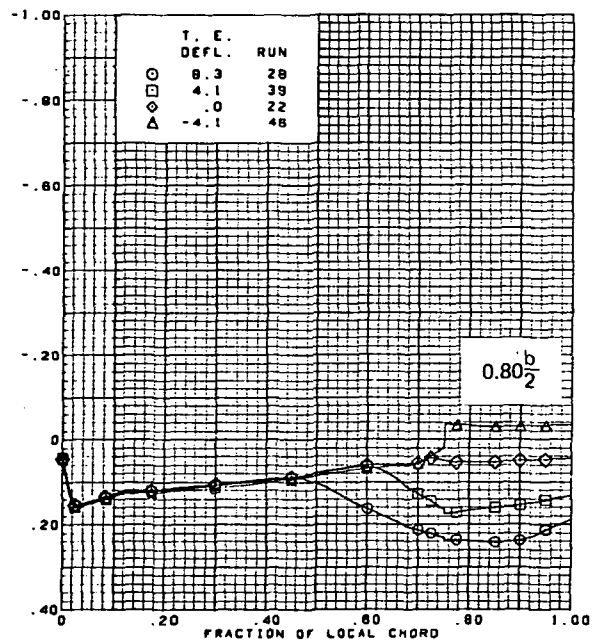
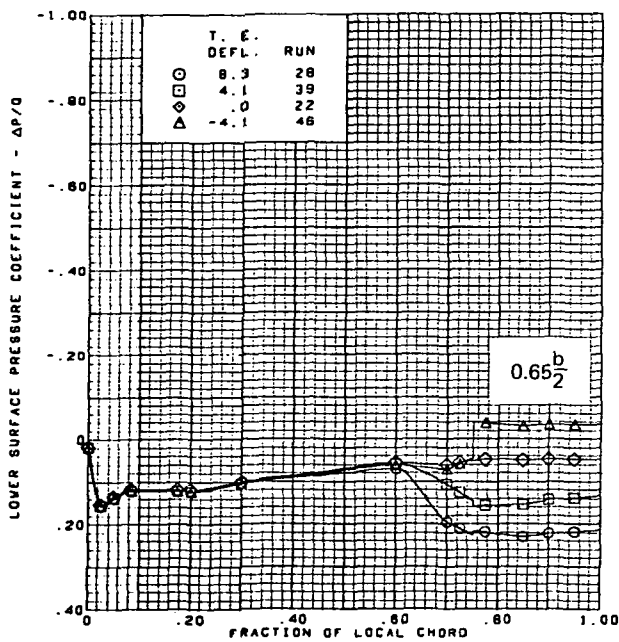
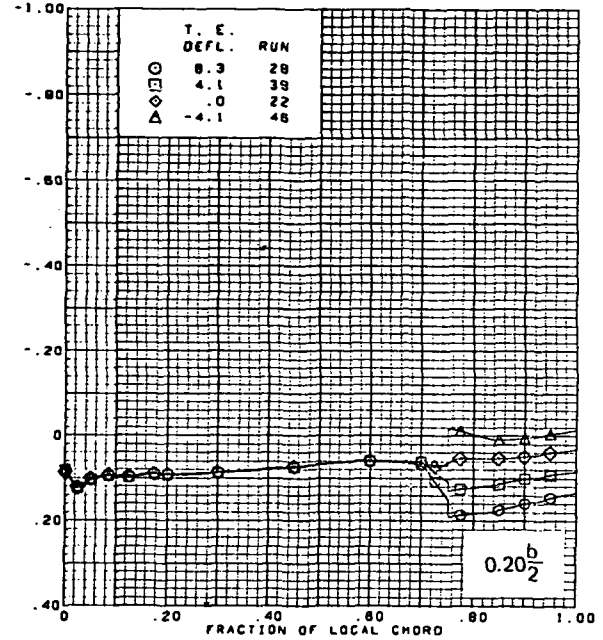
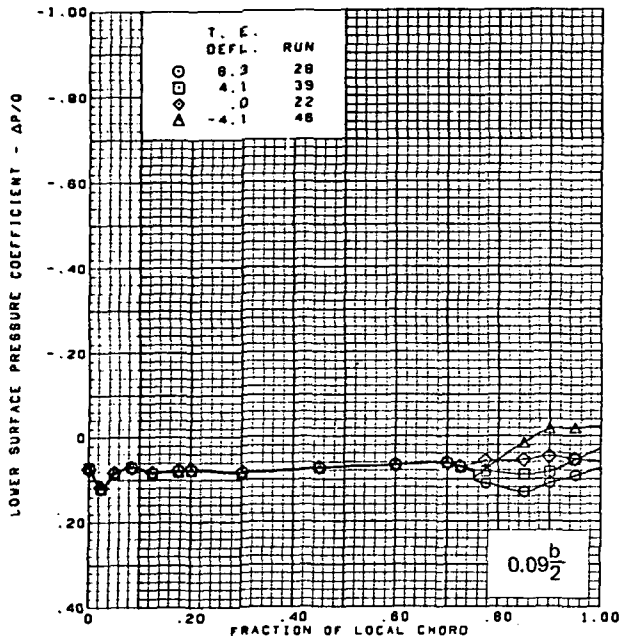


$M = 2.50$   
 $\alpha = 8^\circ$   
 Flat wing, rounded L.E.  
 L.E. deflection, full span =  $0.0^\circ$

Note:  $C_{p, \text{vacuum}} = -0.23$

(d) (Concluded)

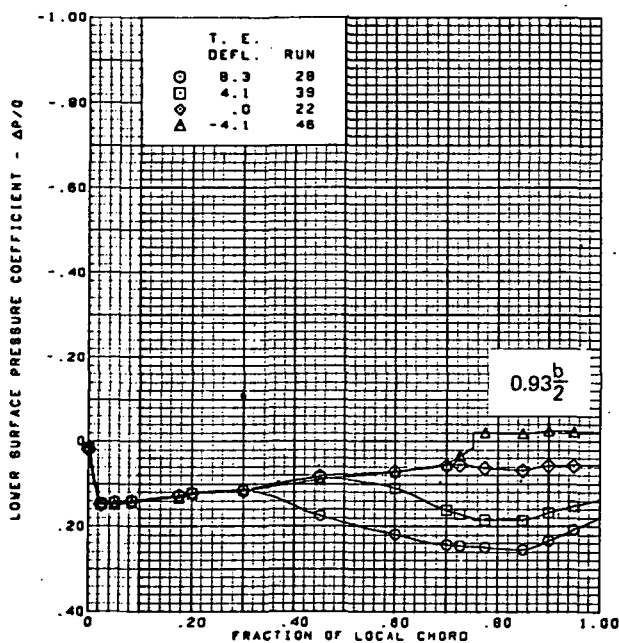
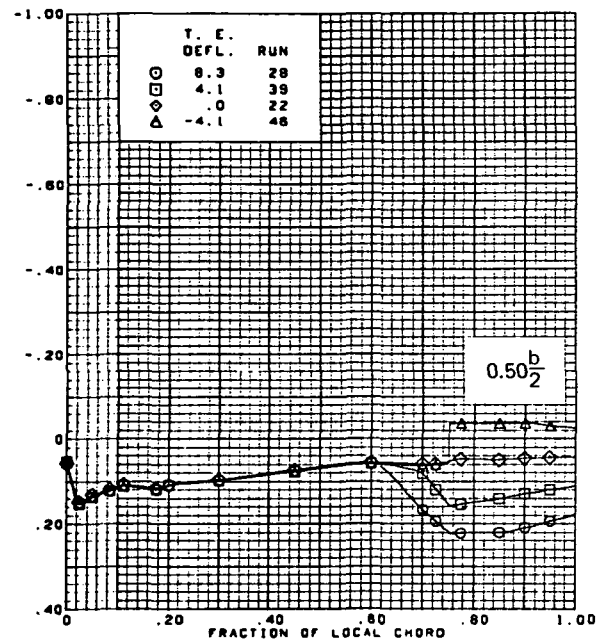
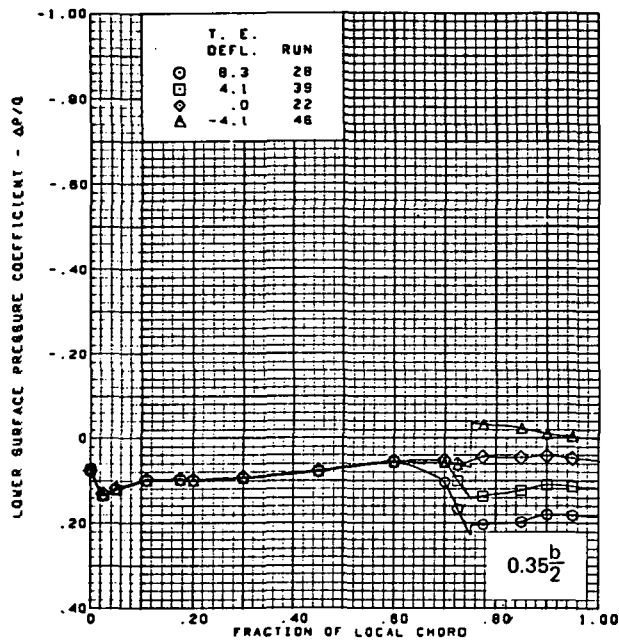
Figure 27.—(Continued)



(e) Lower Surface Chordwise Pressure Distributions,  $\alpha = 8^\circ$

Figure 27.—(Continued)



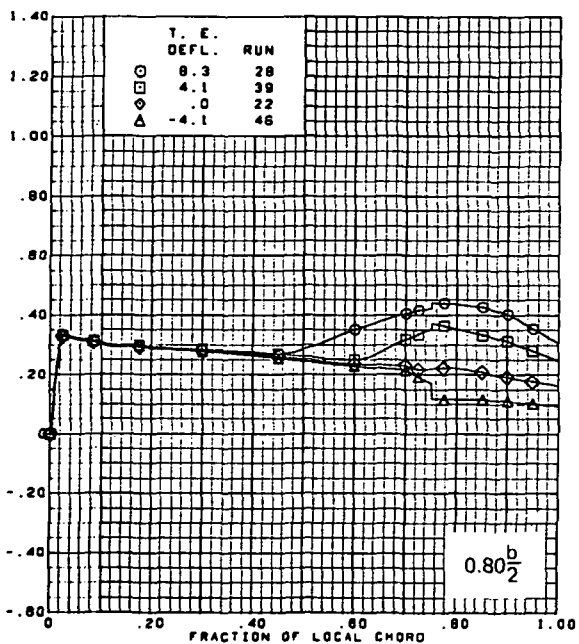
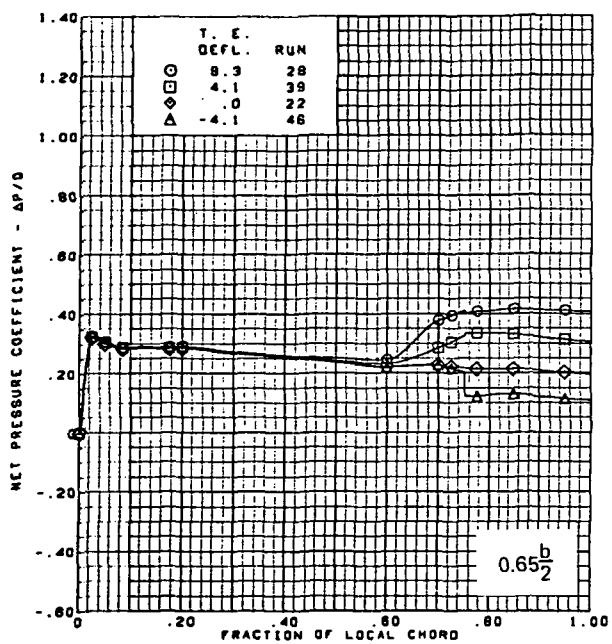
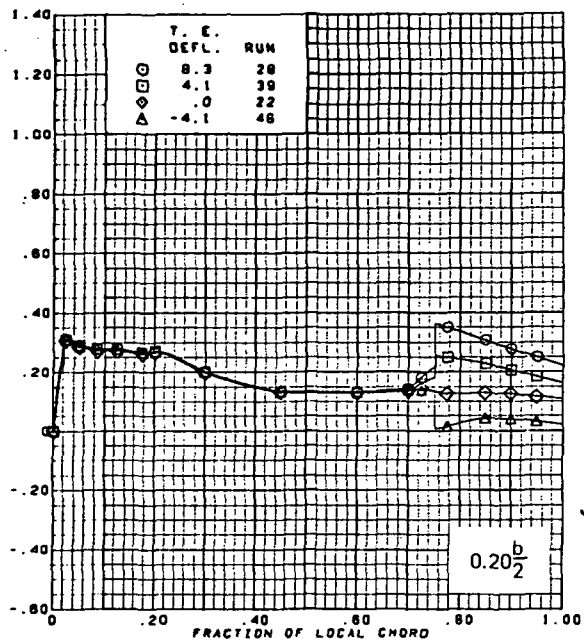
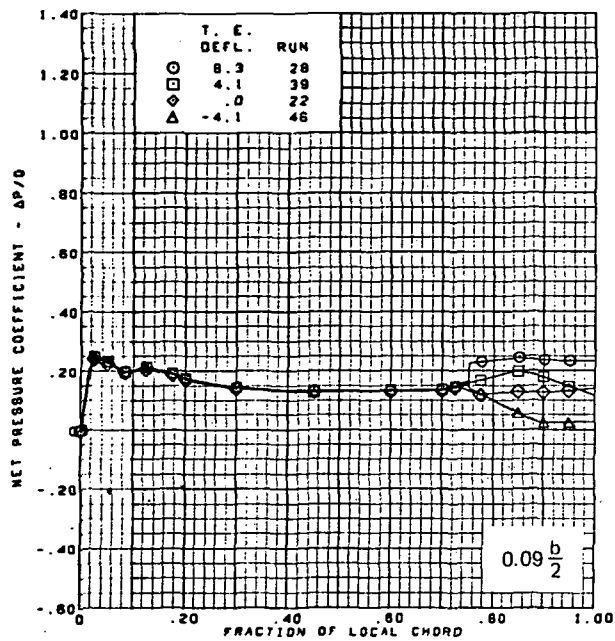


$M = 2.50$   
 $\alpha = 8^\circ$   
 Flat wing, rounded L.E.  
 L.E. deflection, full span =  $0.0^\circ$

Note:  $C_{p, \text{vacuum}} = -0.23$

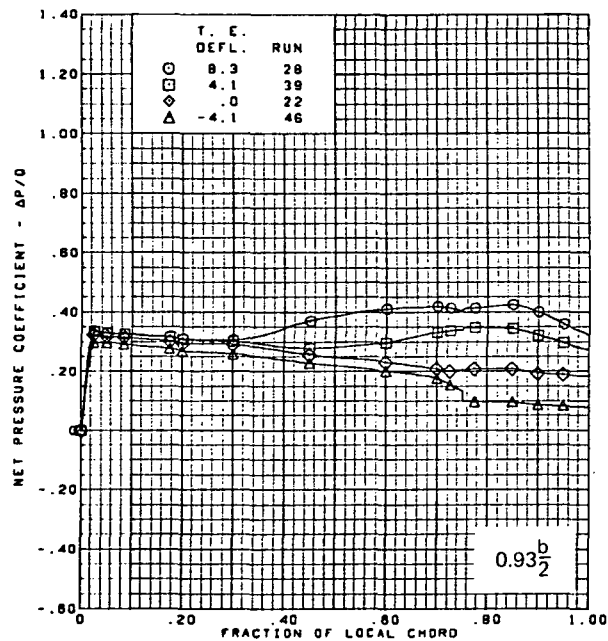
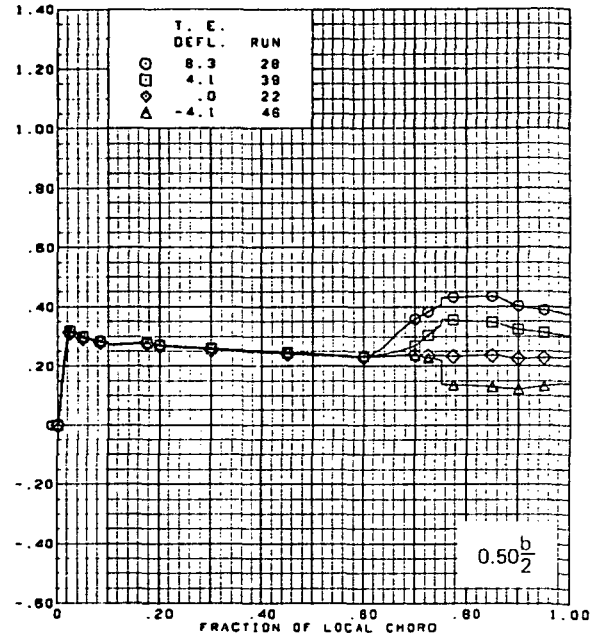
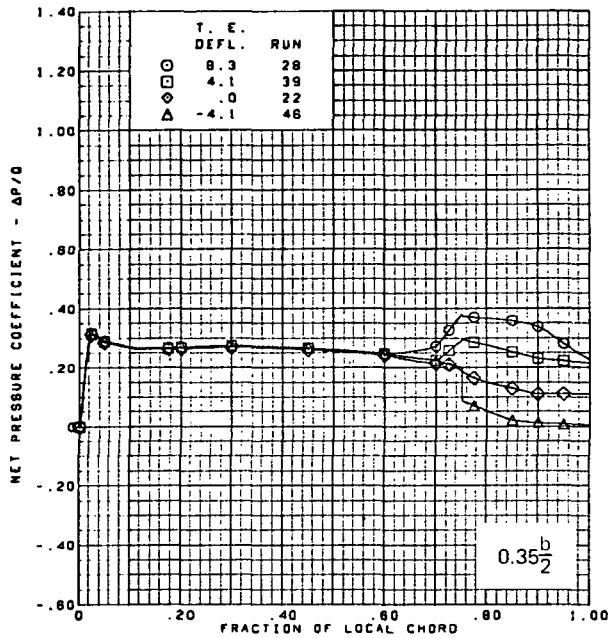
(e) (Concluded)

Figure 27.—(Continued)



(f) Net Chordwise Pressure Distributions,  $\alpha = 8^\circ$

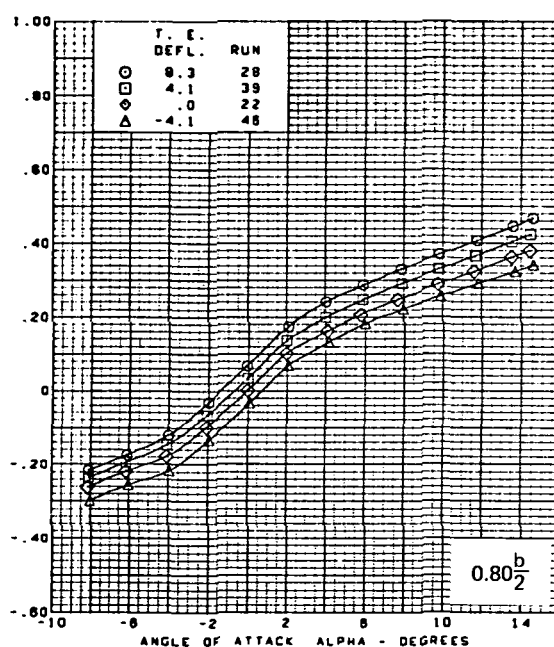
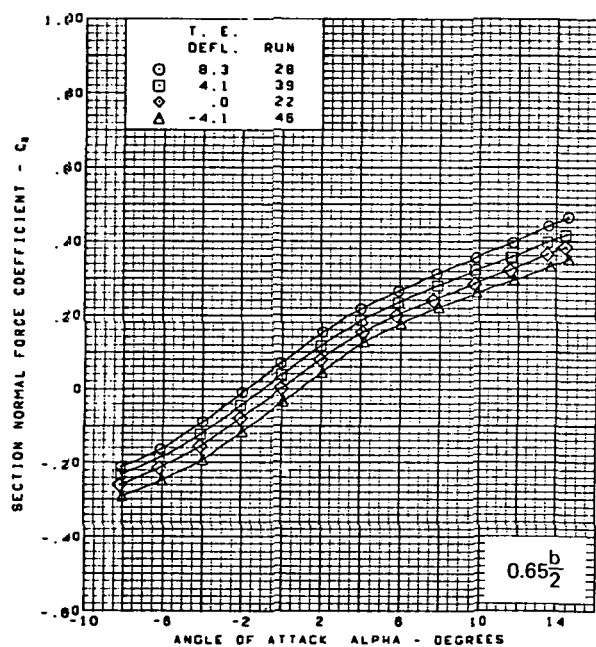
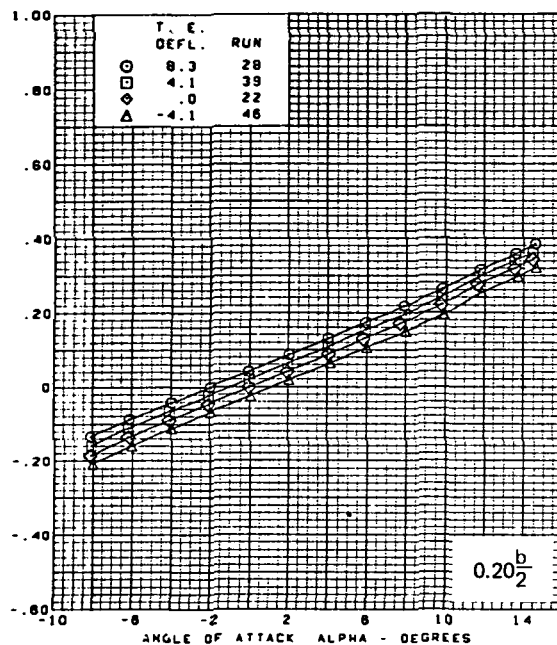
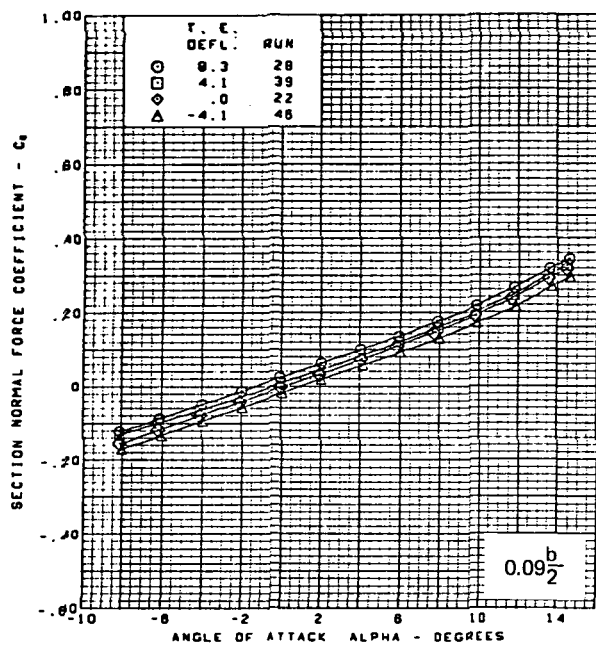
Figure 27.—(Continued)



$M = 2.50$   
 $\alpha = 8^\circ$   
 Flat wing, rounded L.E.  
 L.E. deflection, full span =  $0.0^\circ$

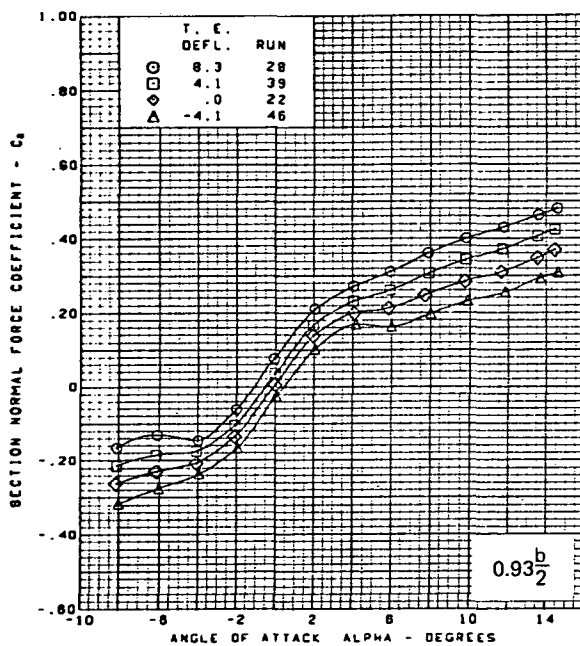
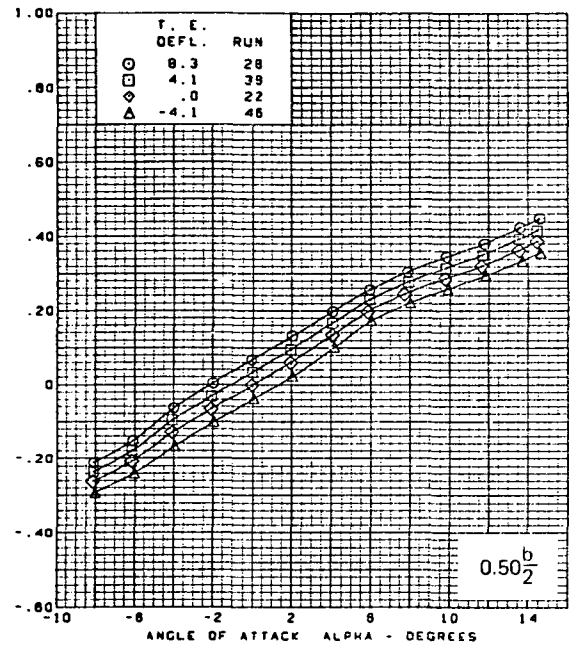
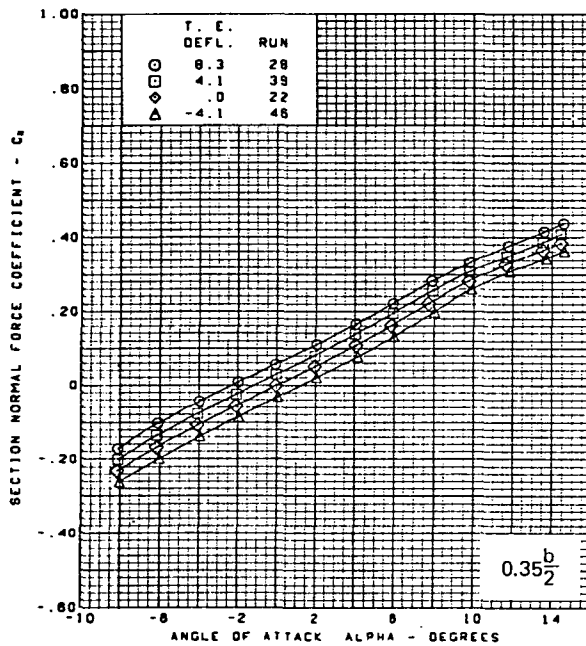
(f) (Concluded)

Figure 27.—(Continued)



(g) Section Aerodynamic Coefficients—Normal Force

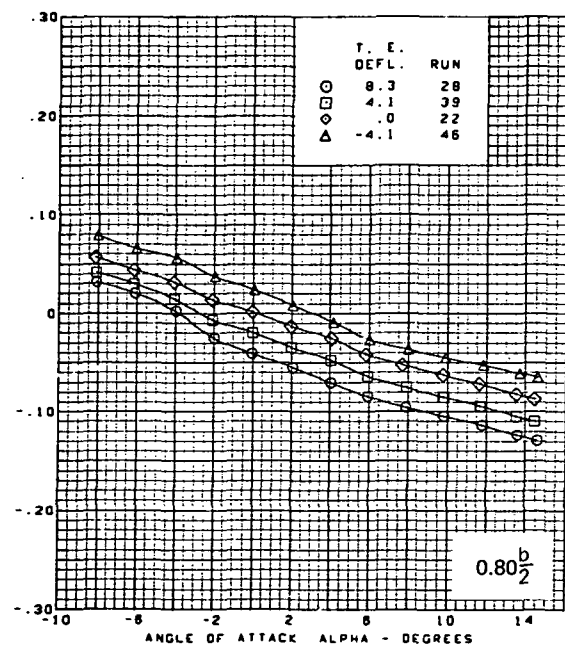
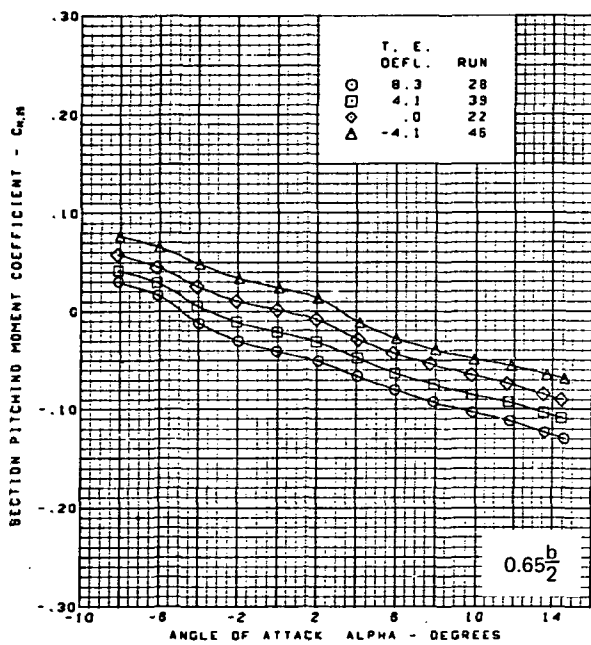
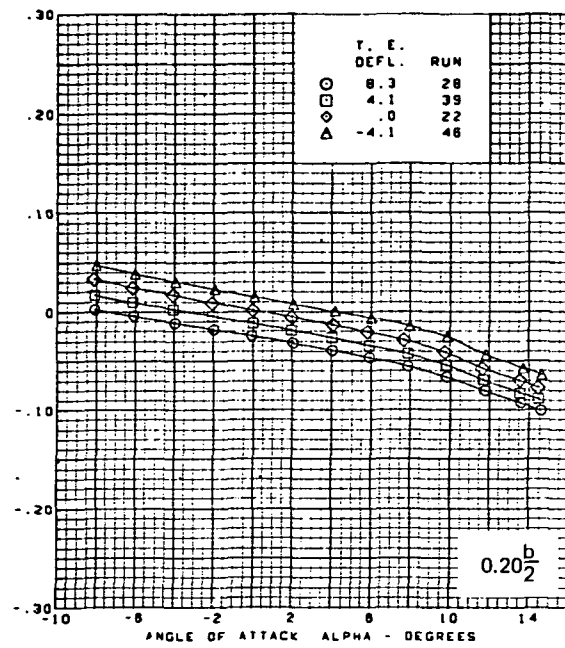
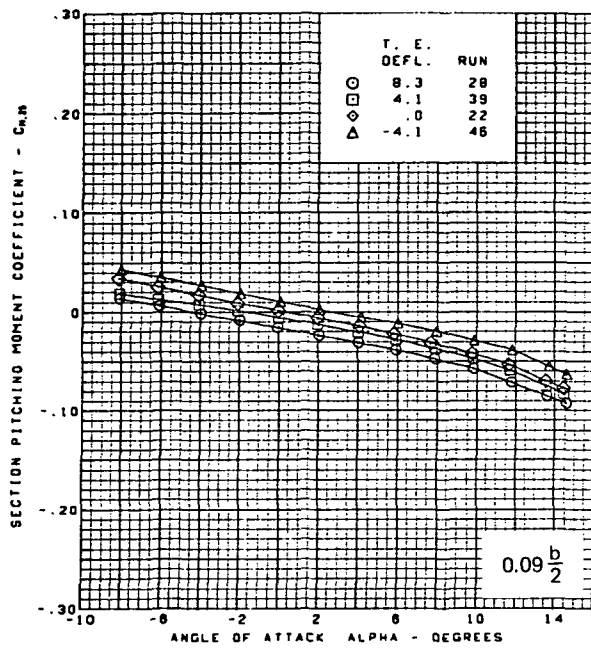
Figure 27.—(Continued)



M = 2.50  
 Flat wing, rounded L.E.  
 L.E. deflection, full span = 0.0°

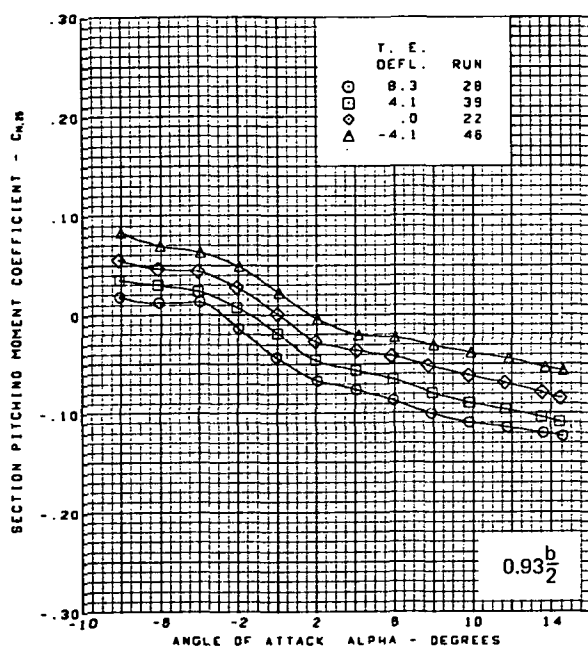
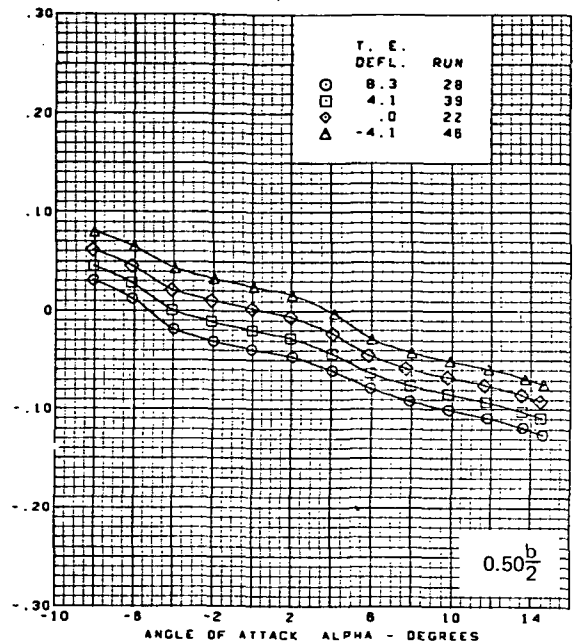
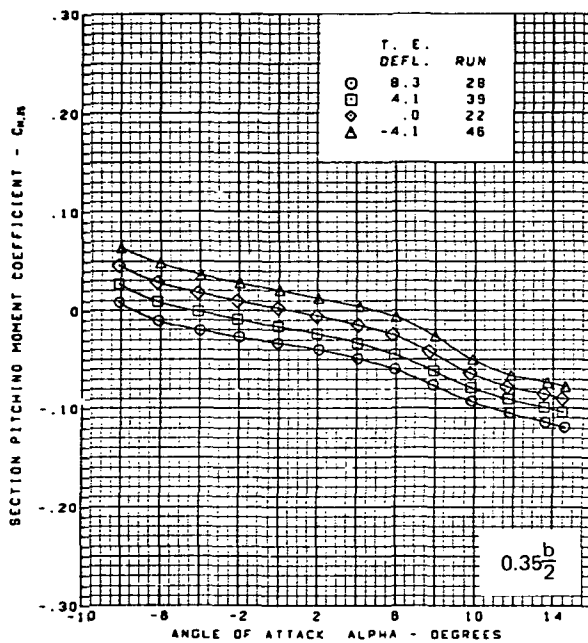
(g) (Concluded)

Figure 27.—(Continued)



(h) Section Aerodynamic Coefficients—Pitching Moment

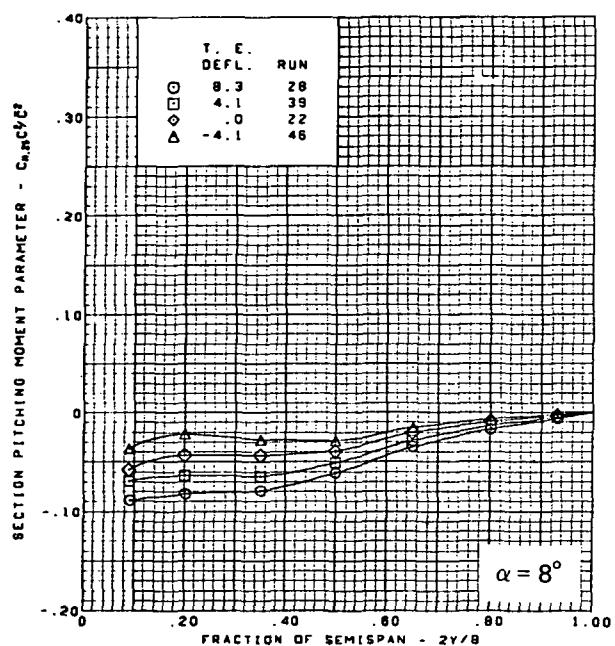
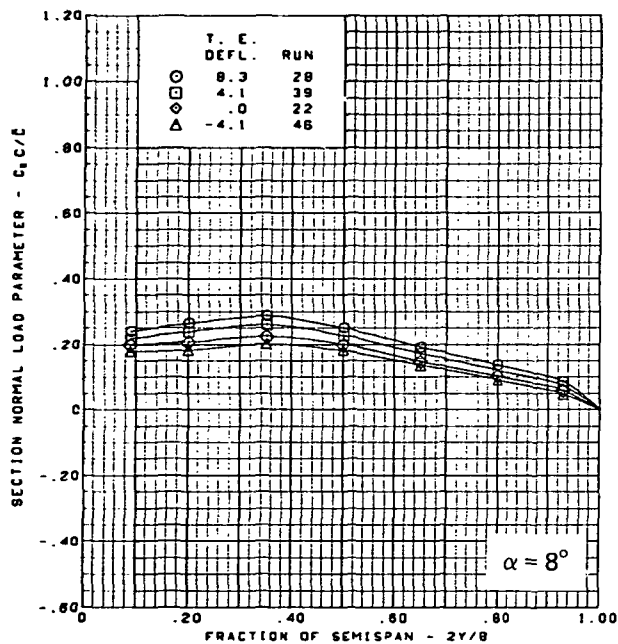
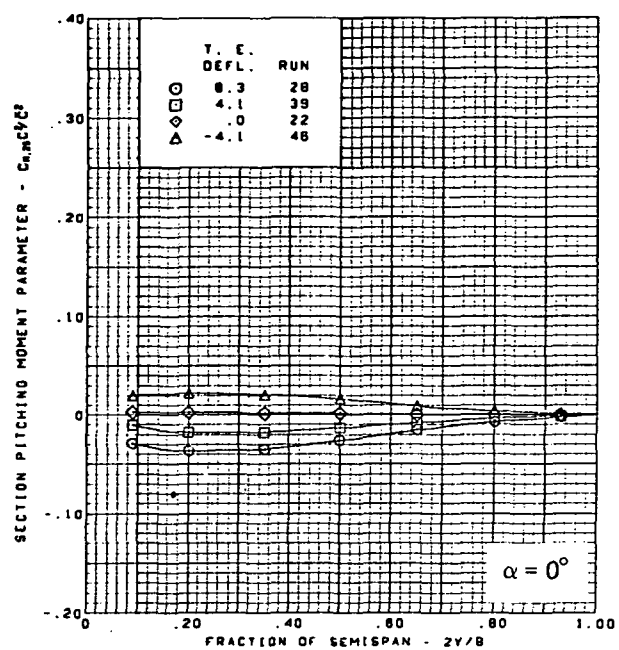
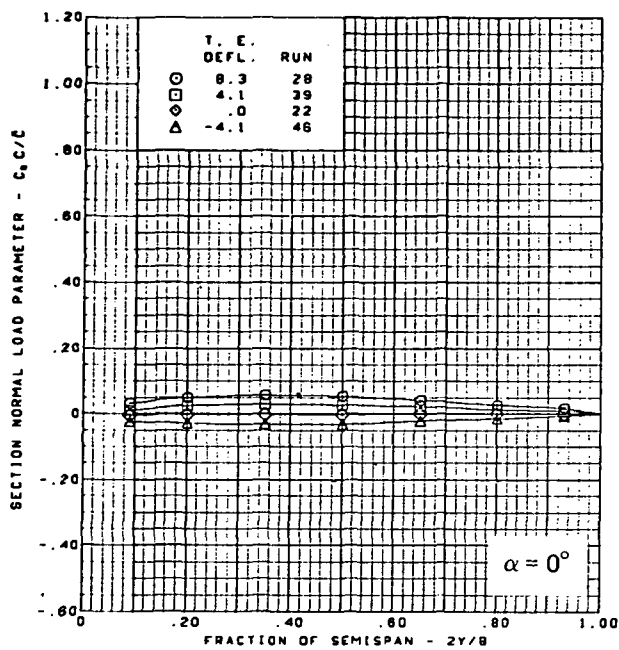
Figure 27.—(Continued)



M = 2.50  
 Flat wing, rounded L.E.  
 L.E. deflection, full span = 0.0°

(h) (Concluded)

Figure 27.—(Continued)

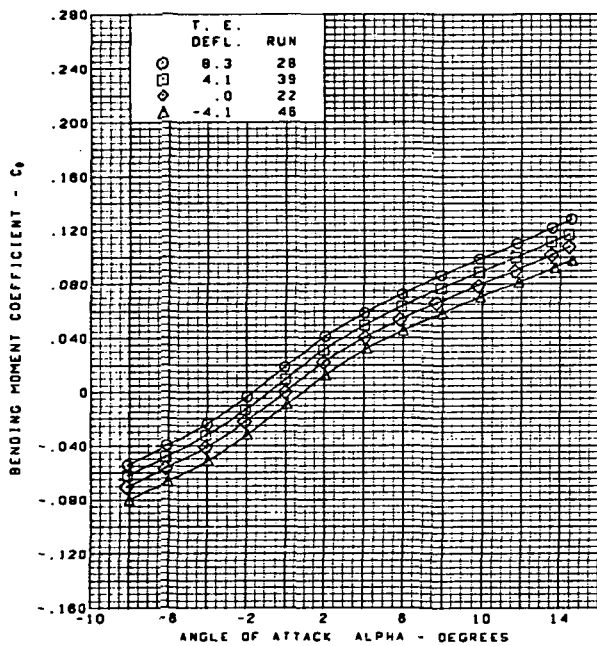
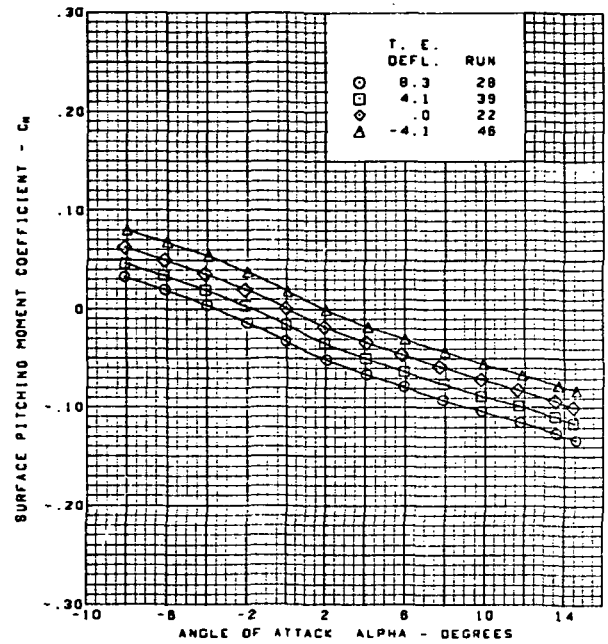
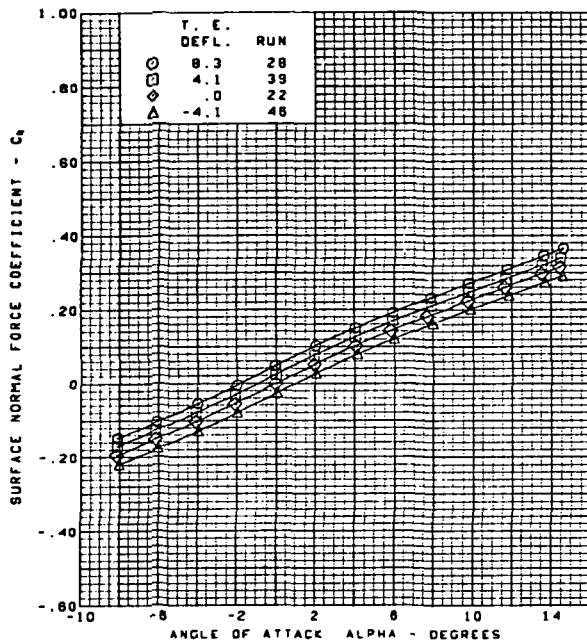


$M = 2.50$   
 Flat wing, rounded L.E.  
 L.E. deflection, full span =  $0.0^\circ$

(i) Spanload Distributions

Figure 27.—(Continued)

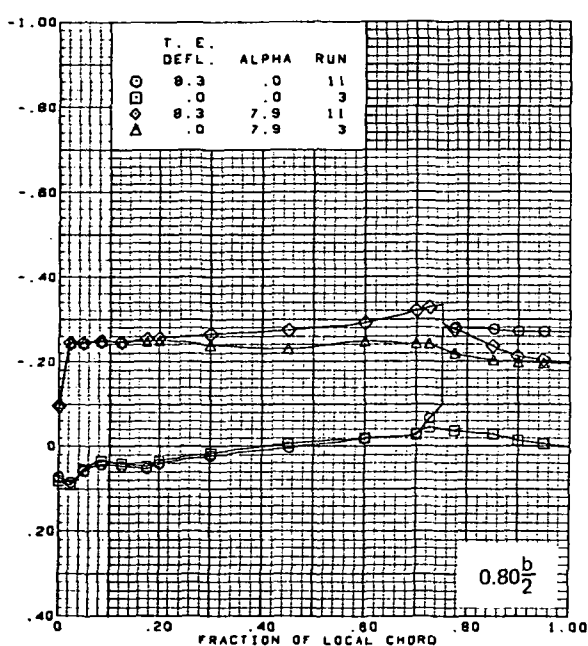
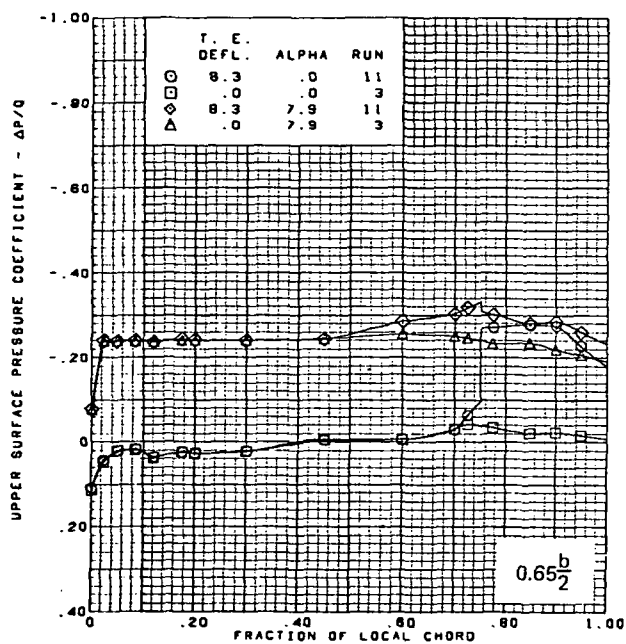
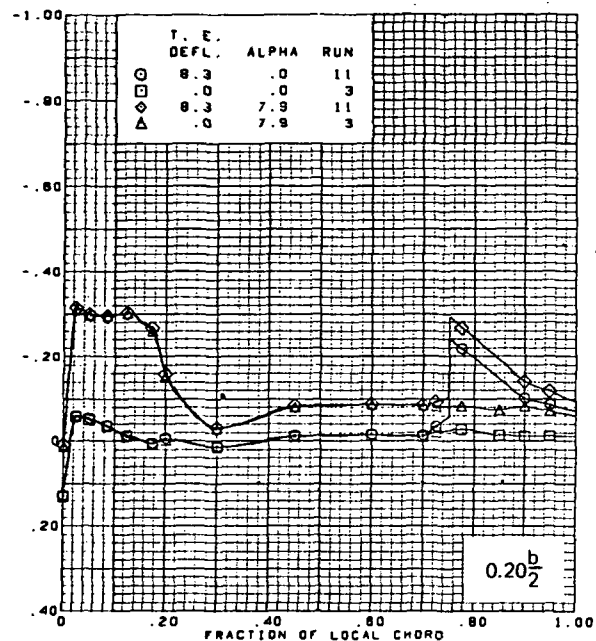
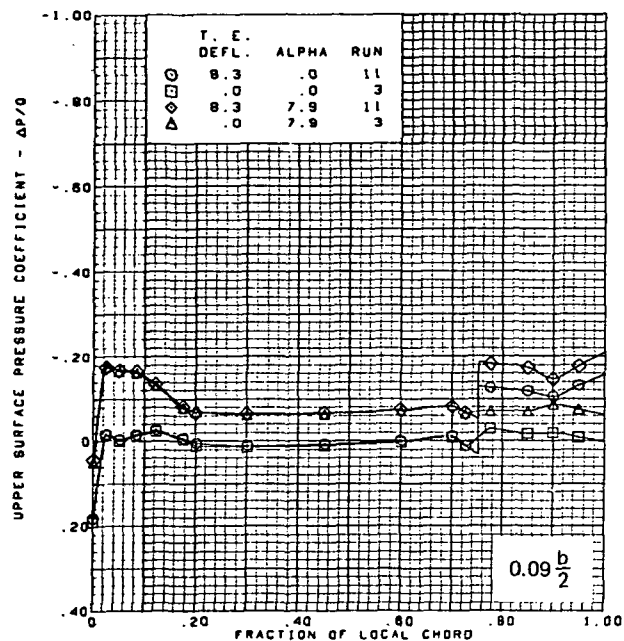




$M = 2.50$   
 Flat wing, rounded L.E.  
 L.E. deflection, full span =  $0.0^\circ$

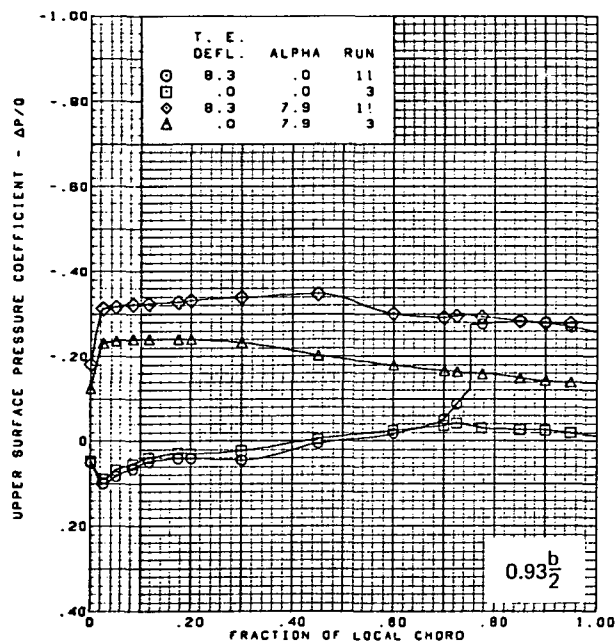
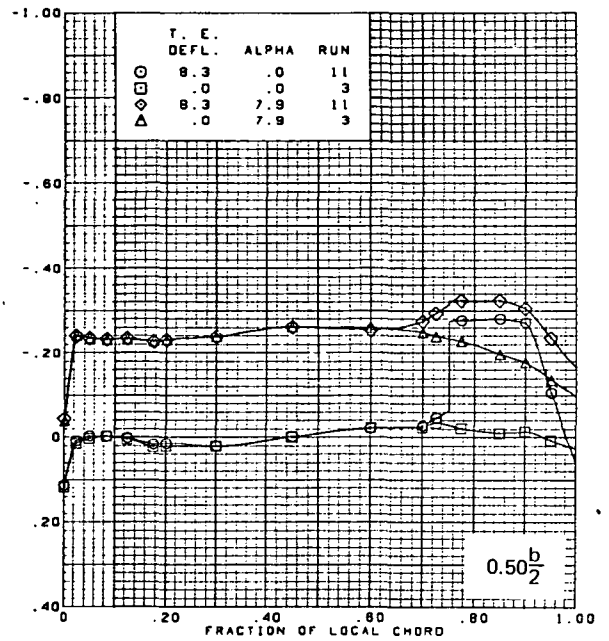
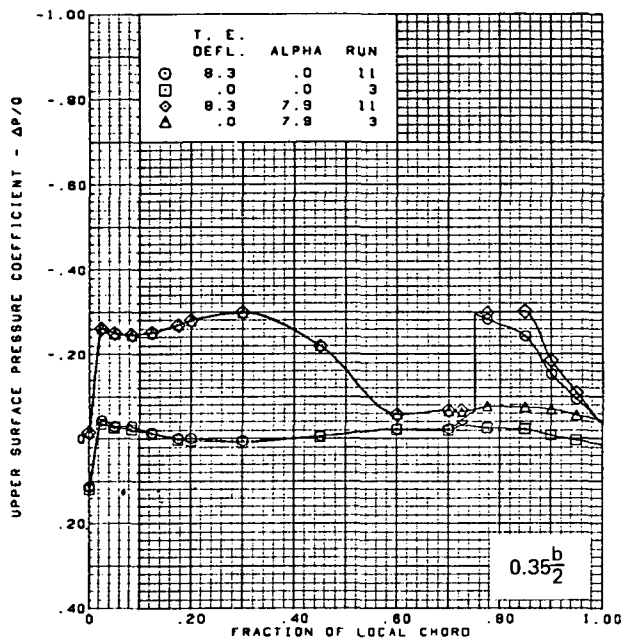
(j) Wing Aerodynamic Coefficients

Figure 27.—(Concluded)



(a) Upper Surface Chordwise Pressure Distributions

Figure 28.—Wing Experimental Data—Effect of Full Span T.E. Deflection With Angle of Attack; Twisted Wing, Rounded L.E.; L.E. Deflection, Full Span = 0.0°;  $M = 1.70$

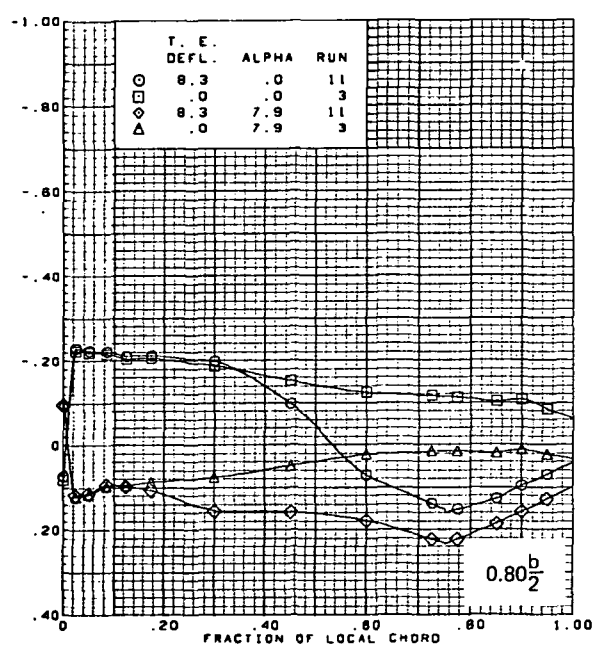
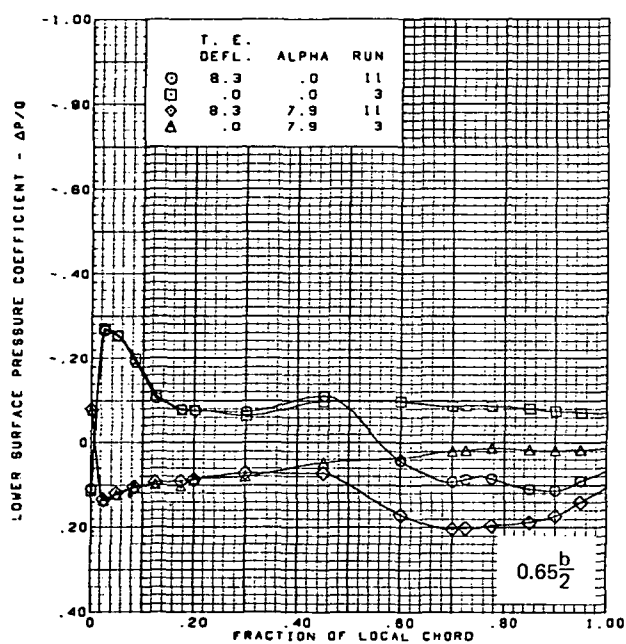
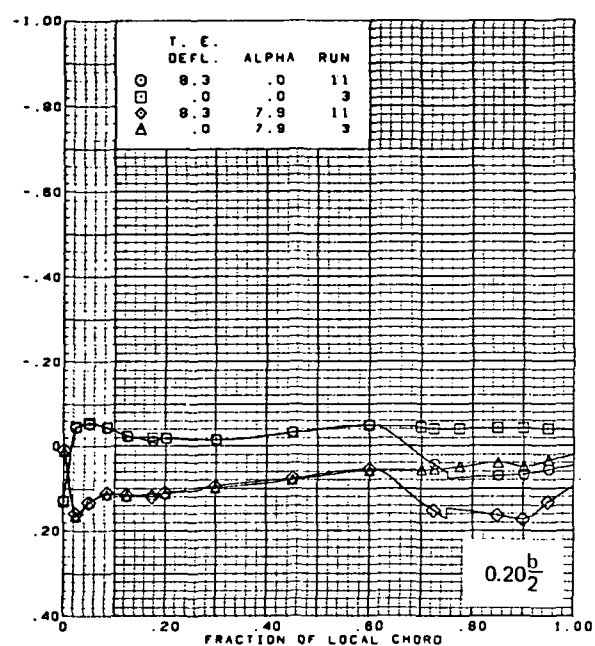
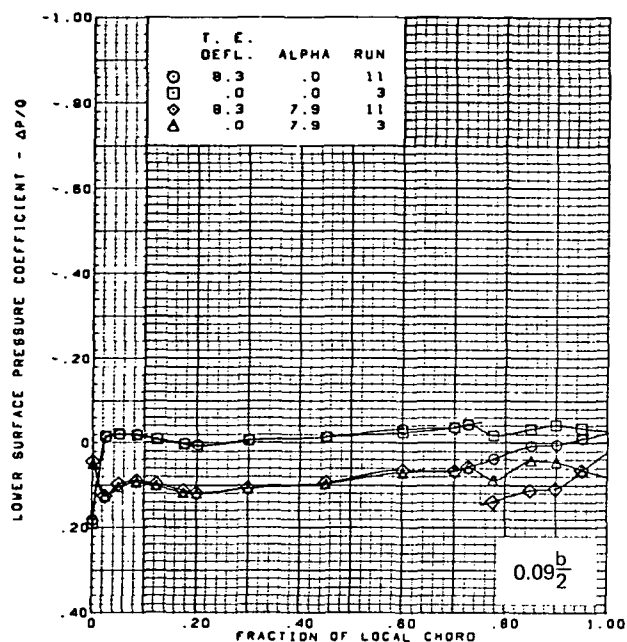


$M = 1.70$   
 Twisted wing, rounded L.E.  
 L.E. deflection, full span =  $0.0^\circ$

Note:  $C_{p, \text{vacuum}} = -0.49$

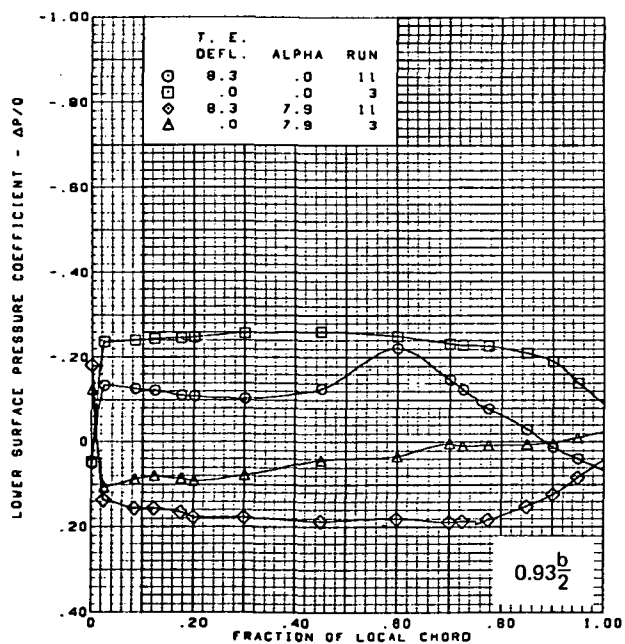
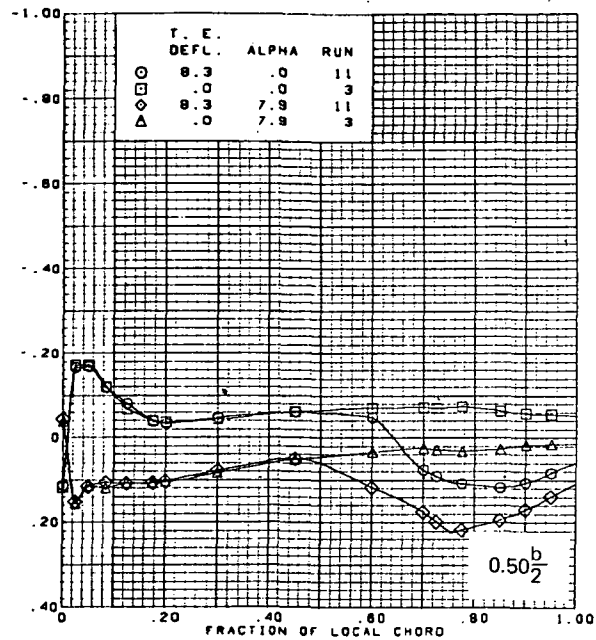
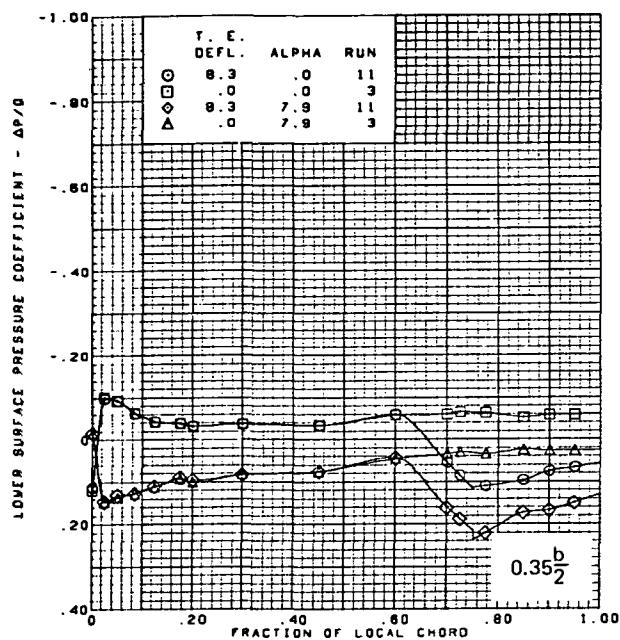
(a) (Concluded)

Figure 28.—(Continued)



(b) Lower Surface Chordwise Pressure Distributions

Figure 28.—(Continued)

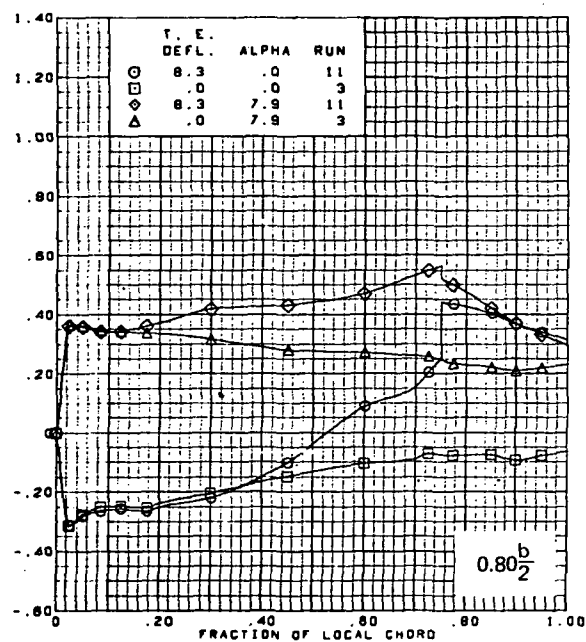
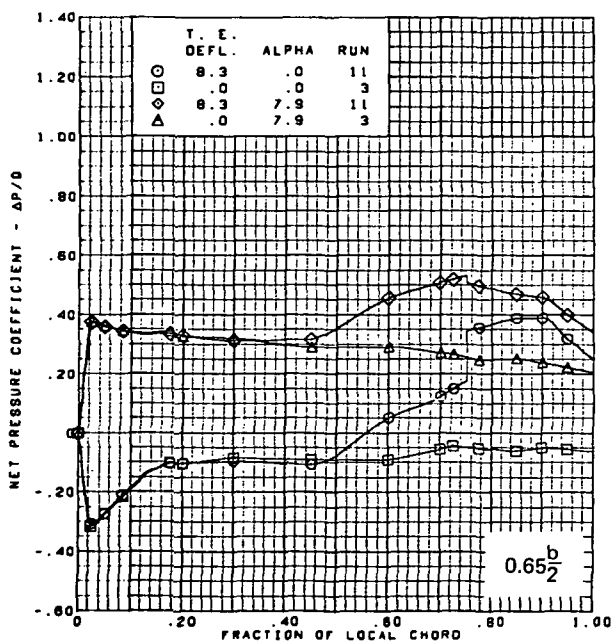
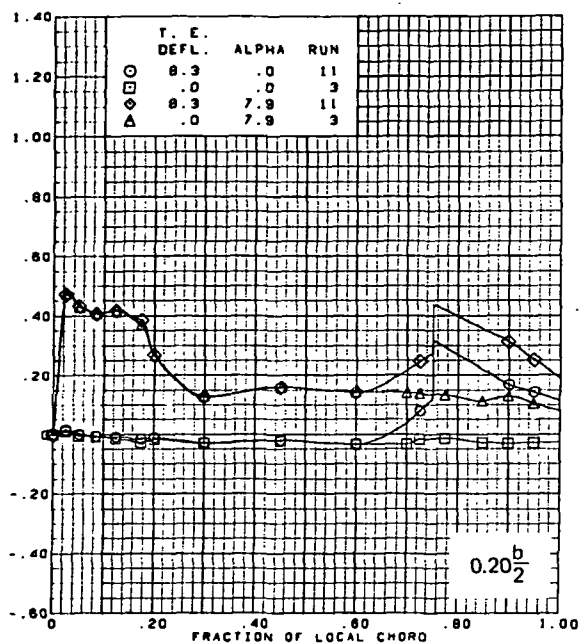
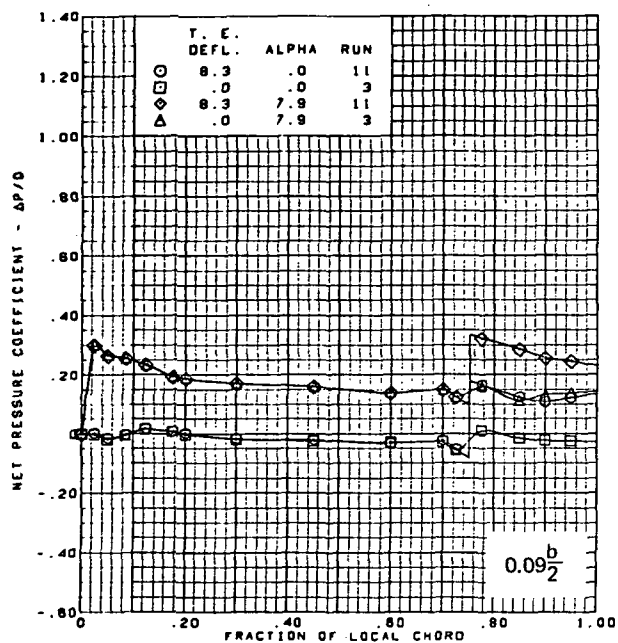


$M = 1.70$   
 Twisted wing, rounded L.E.  
 L.E. deflection, full span =  $0.0^\circ$

Note:  $C_{p, \text{vacuum}} = -0.49$

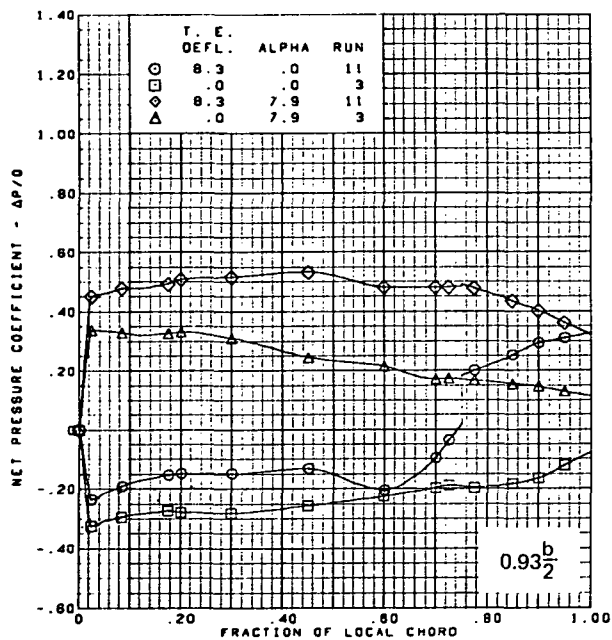
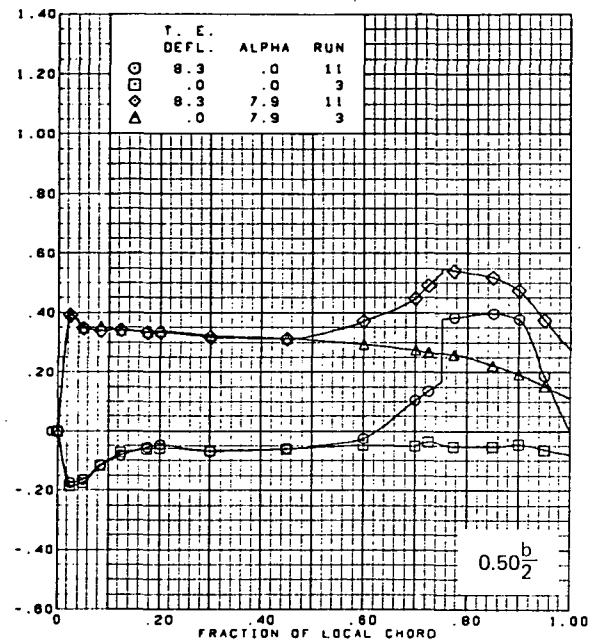
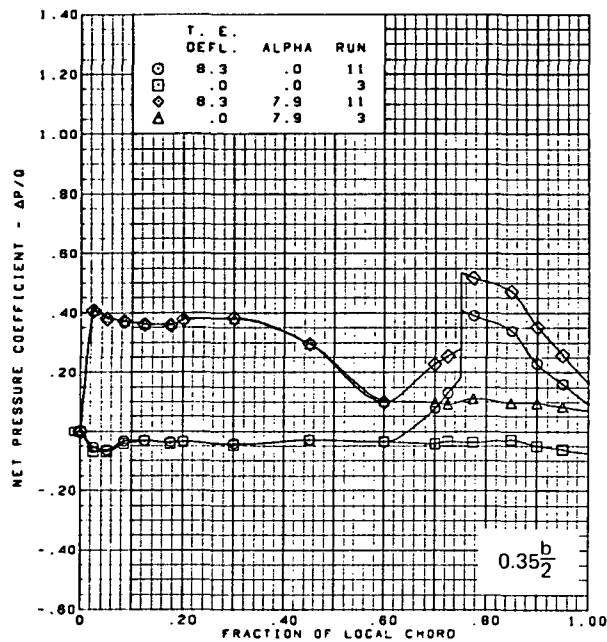
(b) (Concluded)

Figure 28.—(Continued)



(c) Net Chordwise Pressure Distributions

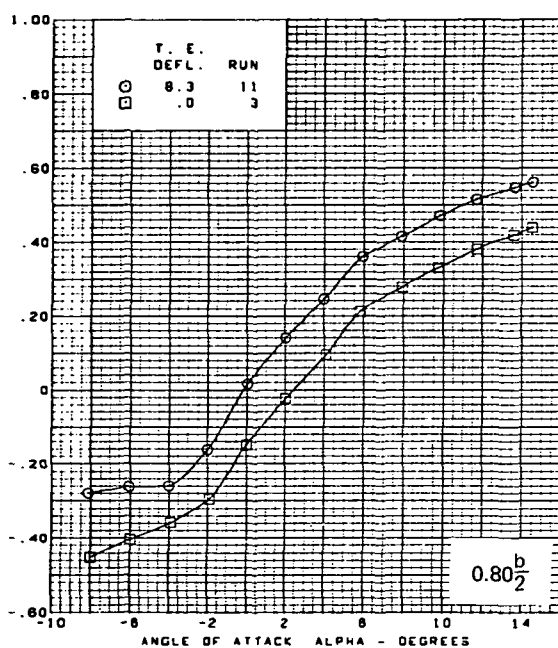
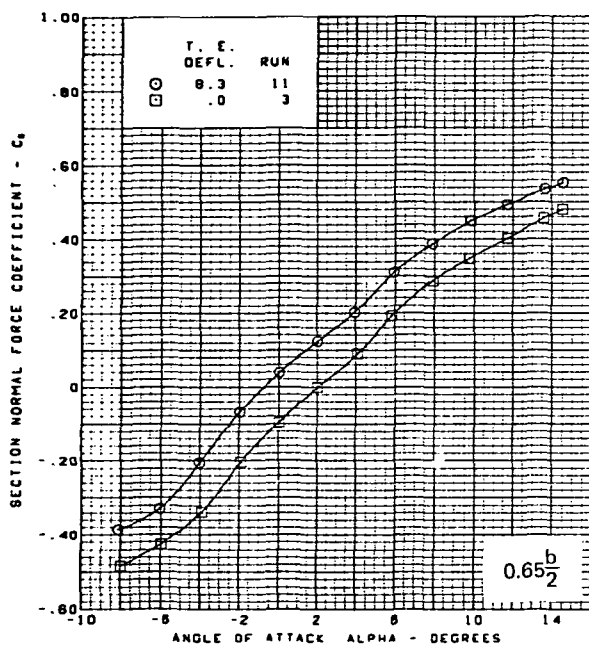
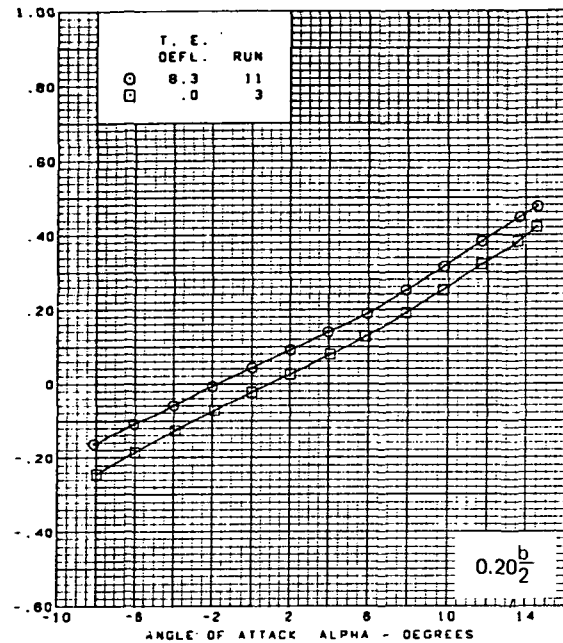
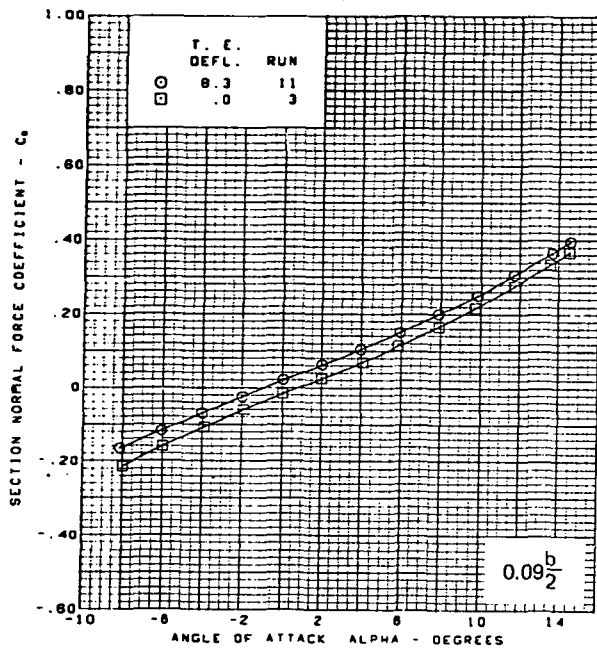
Figure 28.—(Continued)



M = 1.70  
Twisted wing, rounded L.E.  
L.E. deflection, full span =  $0.0^\circ$

(c) (Concluded)

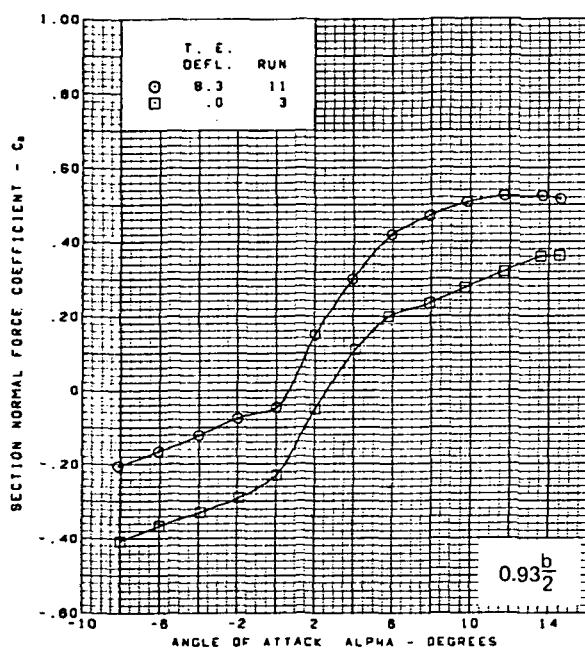
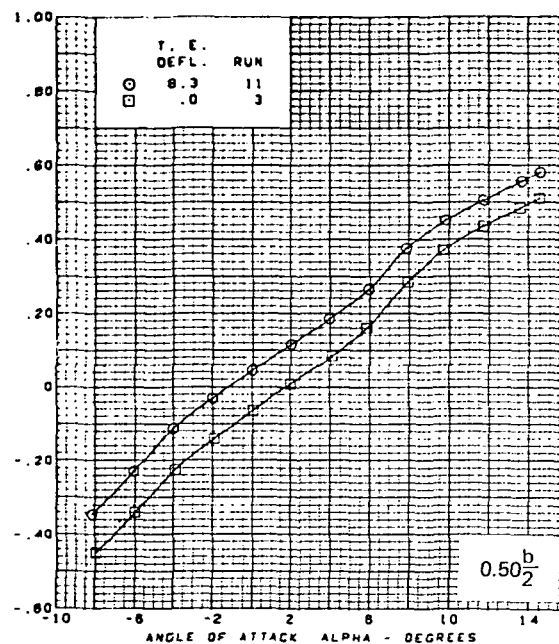
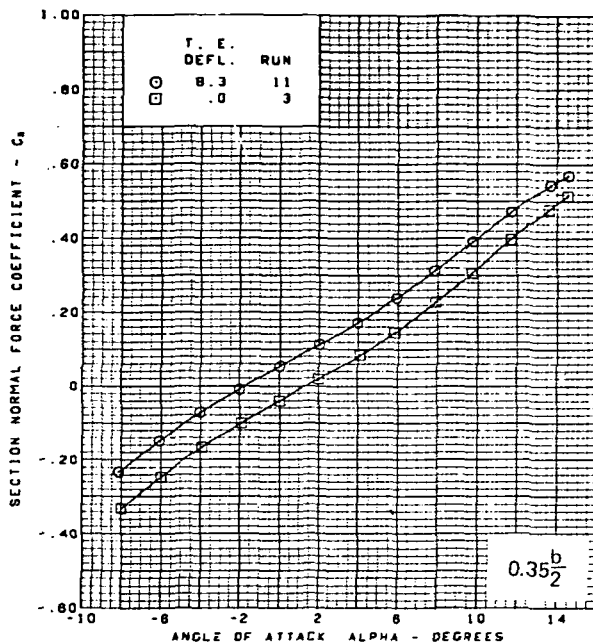
Figure 28.—(Continued)



(d) Section Aerodynamic Coefficients—Normal Force

Figure 28.—(Continued)

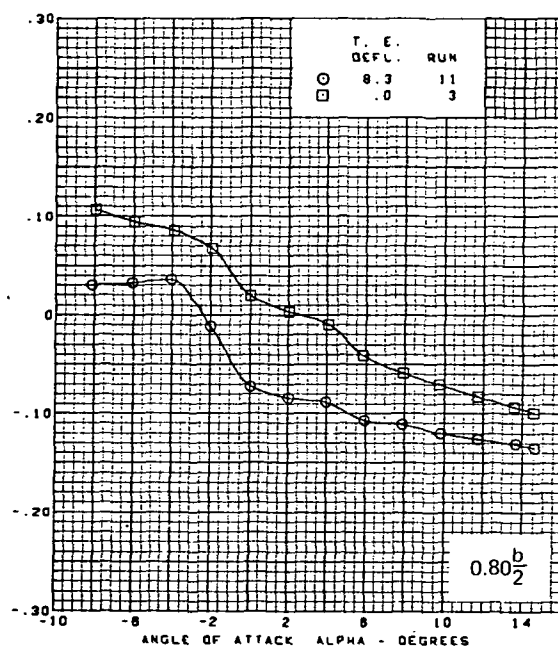
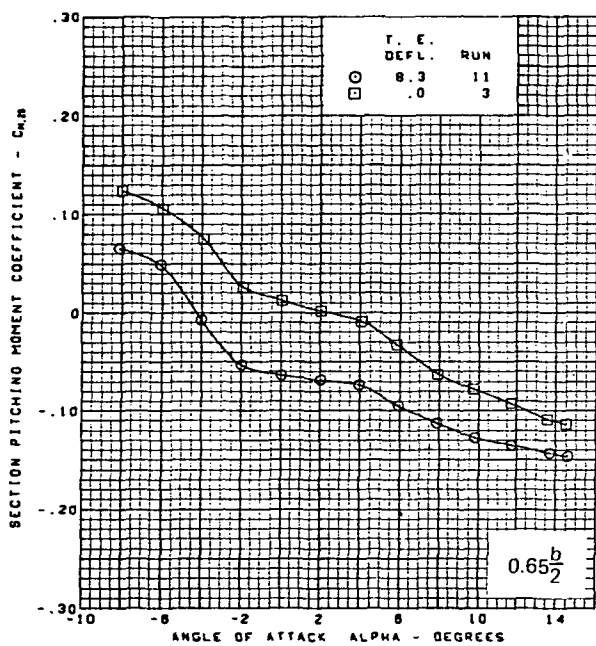
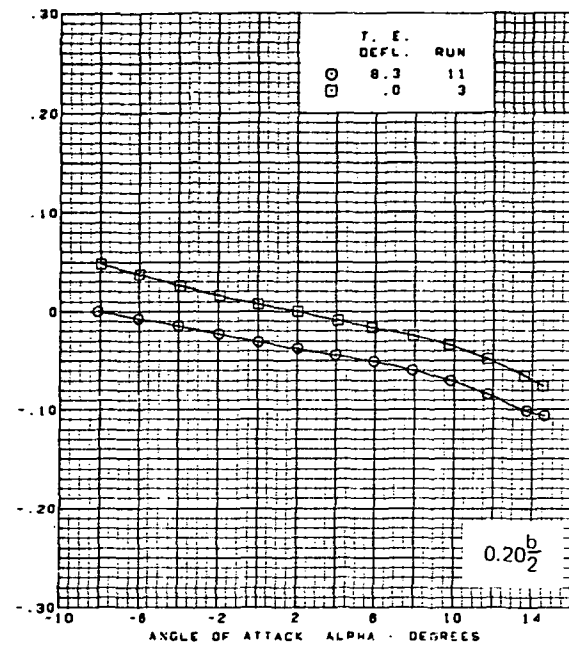
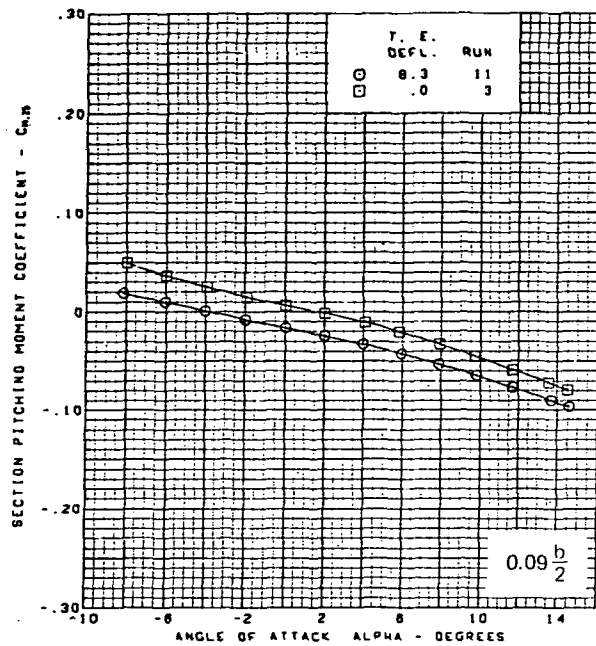




$M = 1.70$   
 Twisted wing, rounded L.E.  
 L.E. deflection, full span =  $0.0^\circ$

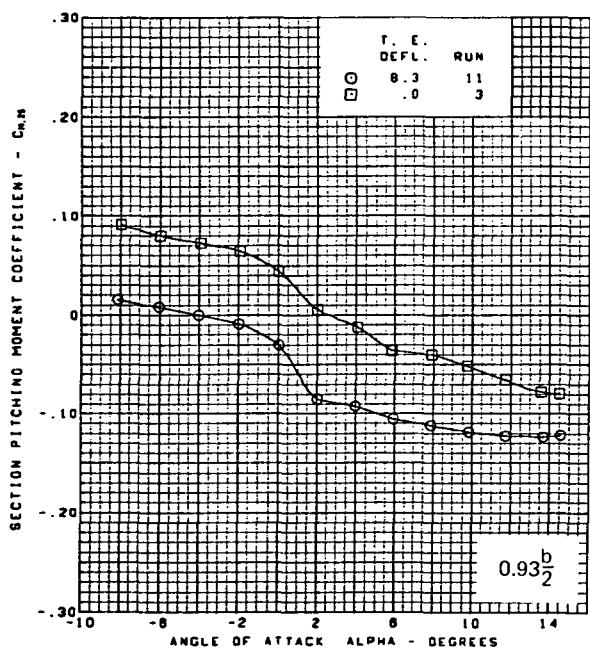
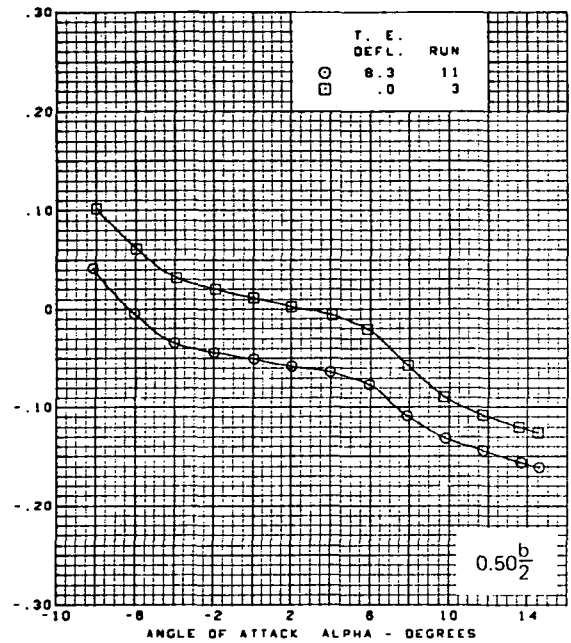
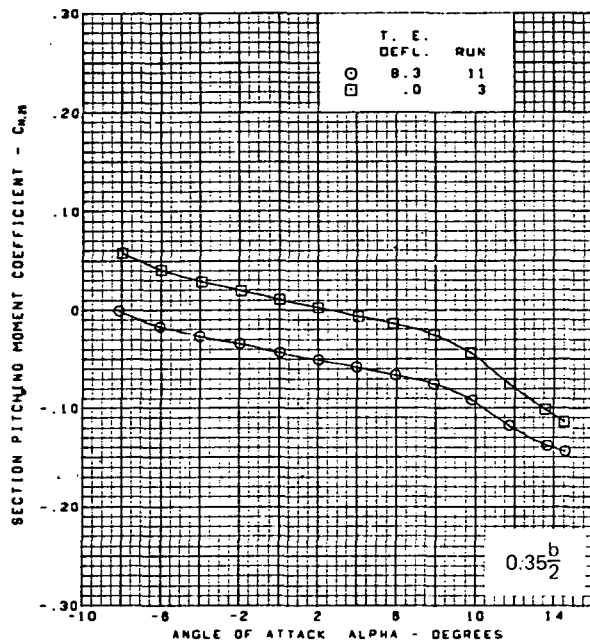
(d) (Concluded)

Figure 28.—(Continued)



(e) Section Aerodynamic Coefficients—Pitching Moment

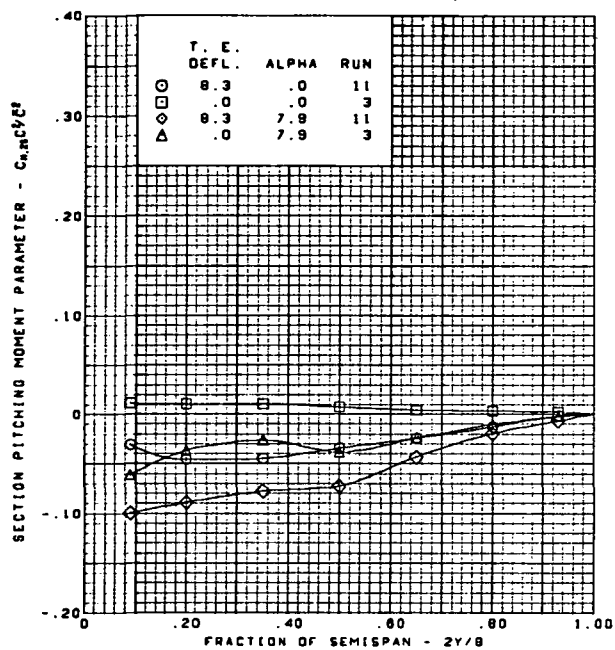
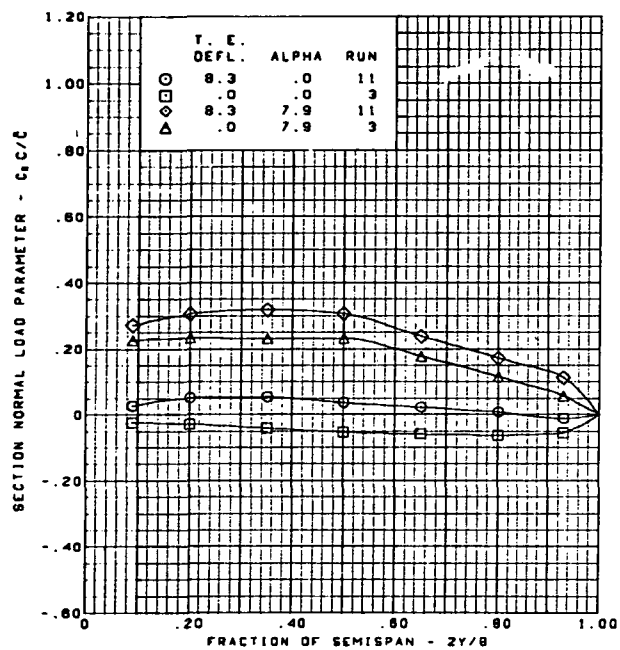
Figure 28.—(Continued)



$M = 1.70$   
 Twisted wing, rounded L.E.  
 L.E. deflection, full span =  $0.0^\circ$

(e) (Concluded)

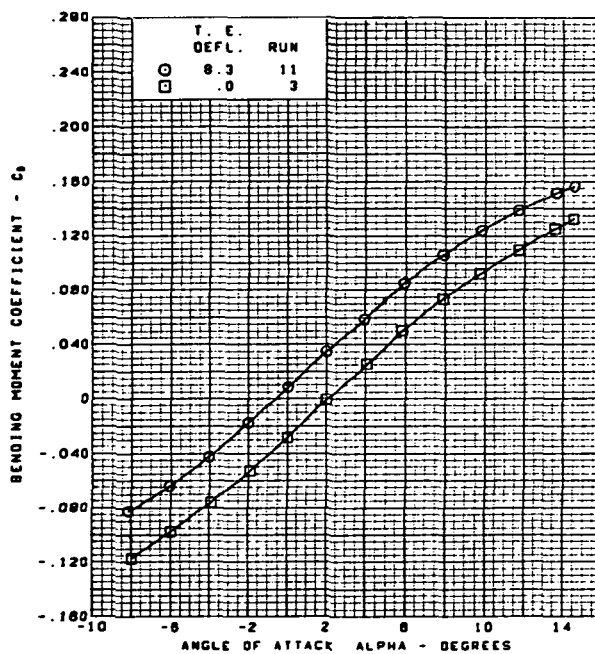
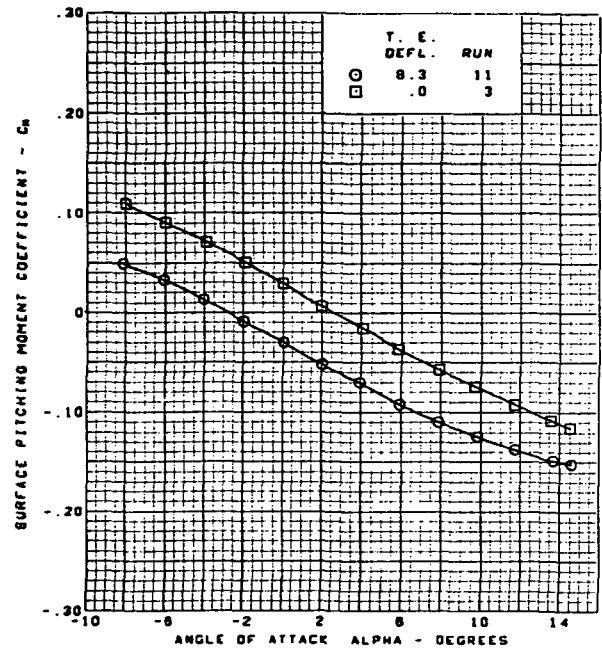
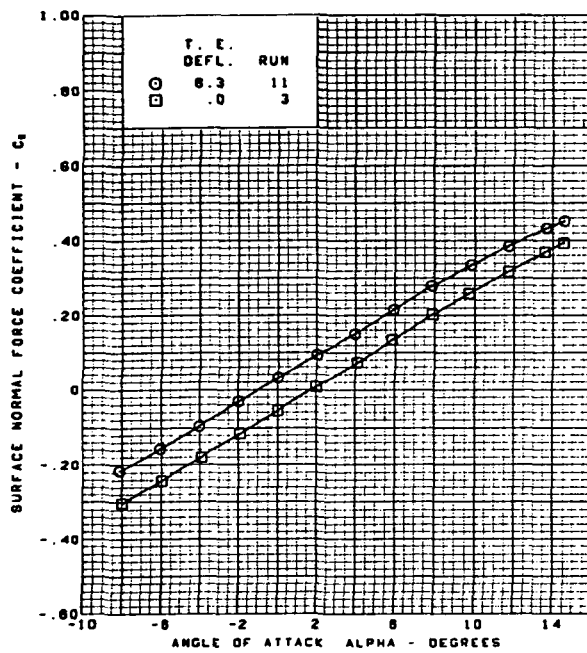
Figure 28.—(Continued)



M = 1.70  
 Twisted wing, rounded L.E.  
 L.E. deflection, full span = 0.0°

(f) Spanload Distributions

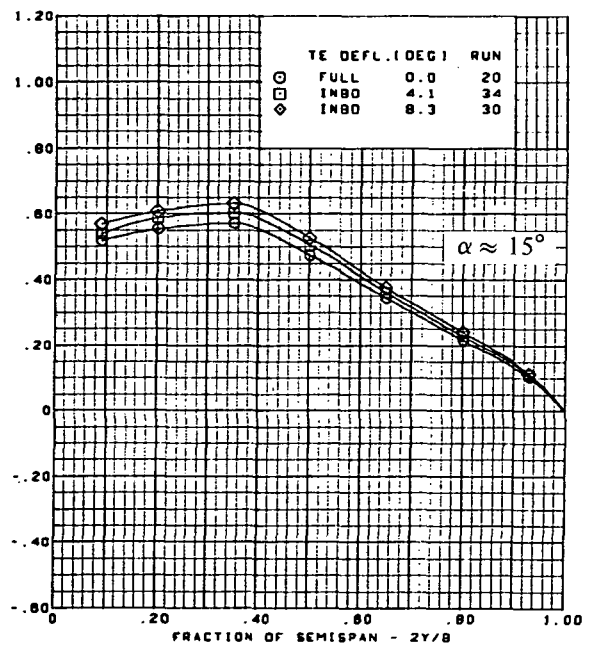
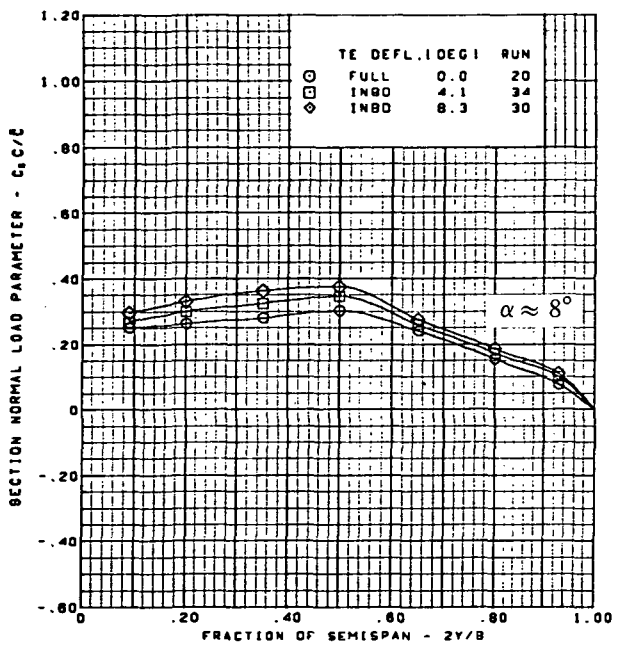
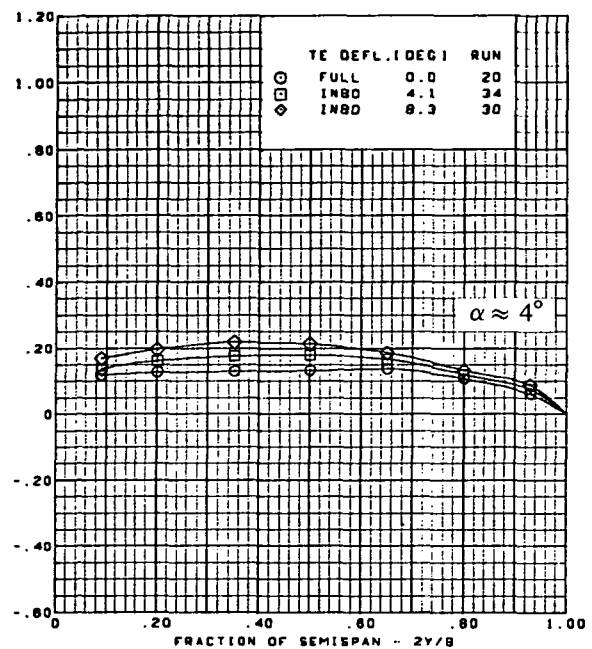
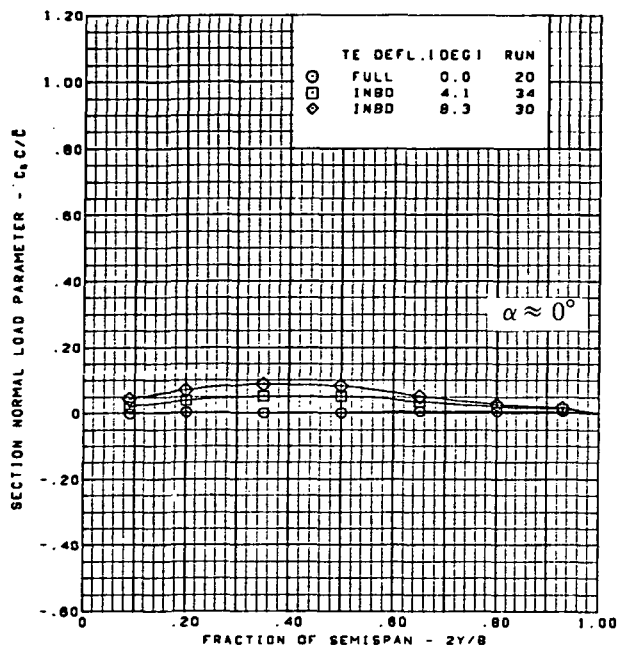
Figure 28.—(Continued)



$M = 1.70$   
 Twisted wing, rounded L.E.  
 L.E. deflection, full span =  $0.0^\circ$

(g) Wing Aerodynamic Coefficients

Figure 28.—(Concluded)



$M = 1.70$

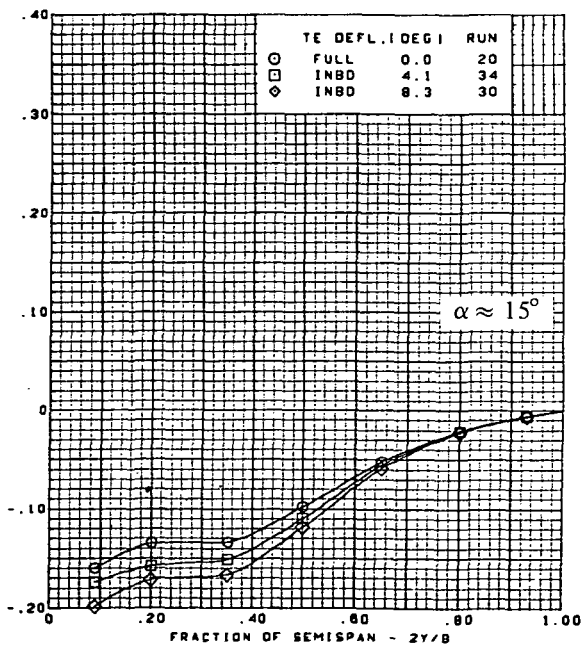
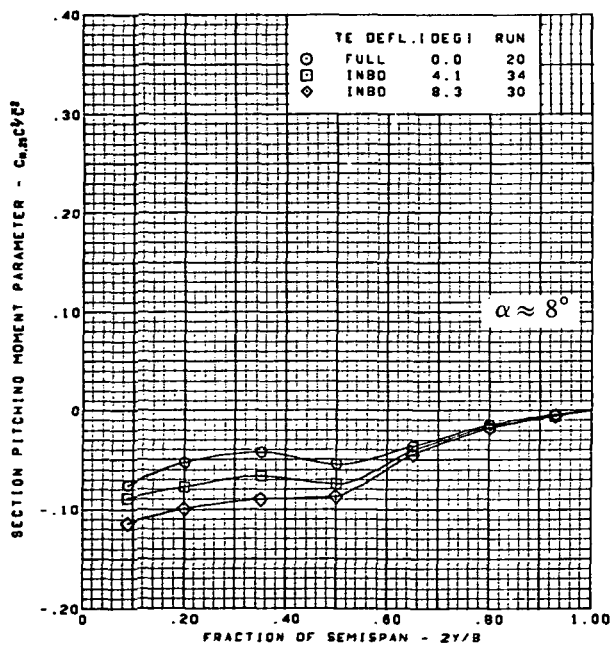
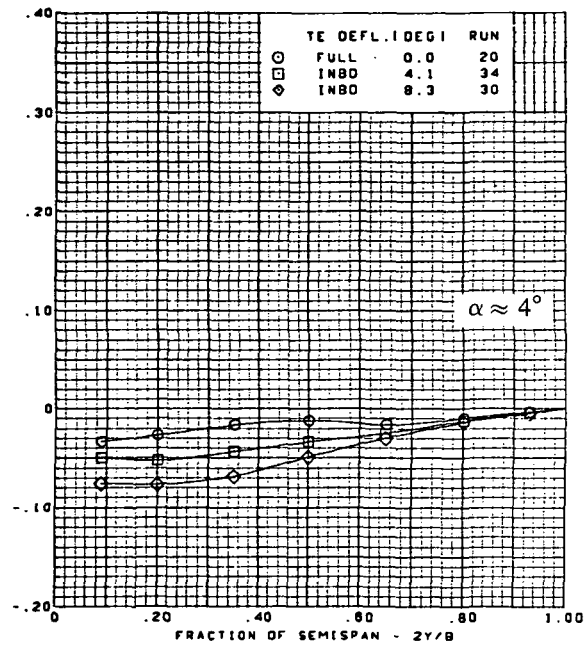
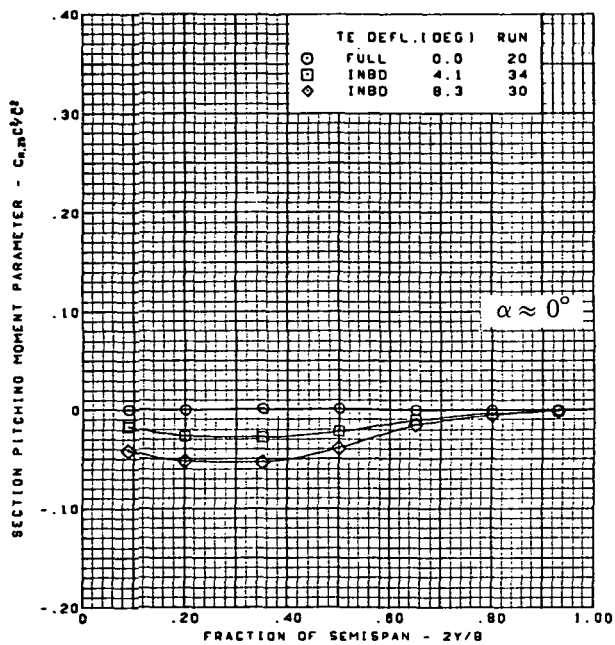
Flat wing, rounded L.E.

L. E. deflection, full span =  $0.0^\circ$

T.E. deflection, outboard =  $0.0^\circ$

(a) Spanload Distributions—Normal Force

Figure 29.—Wing Experimental Data—Effect of Partial Span T.E. Deflection With Angle of Attack; Flat Wing, Rounded L.E.; L.E. Deflection, Full Span =  $0.0^\circ$ ; T.E. Deflection, Outboard =  $0.0^\circ$ ;  $M = 1.70$



$M = 1.70$

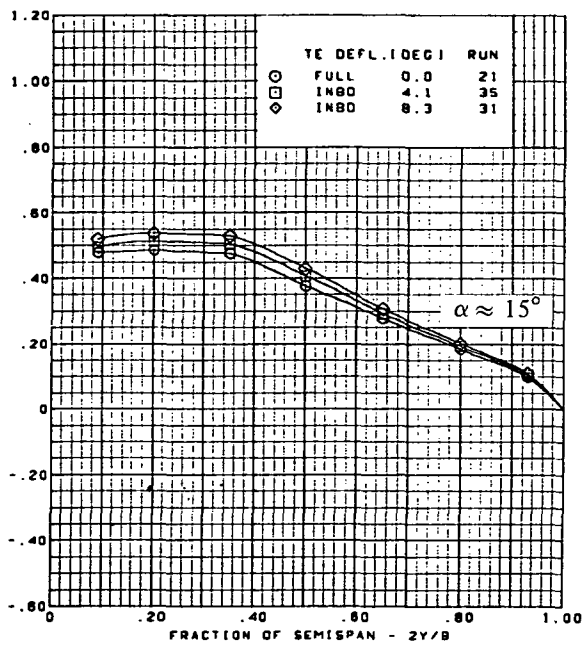
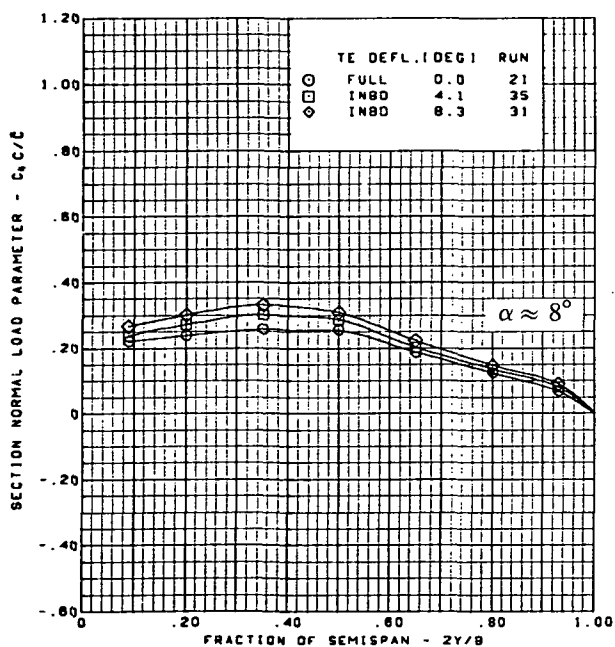
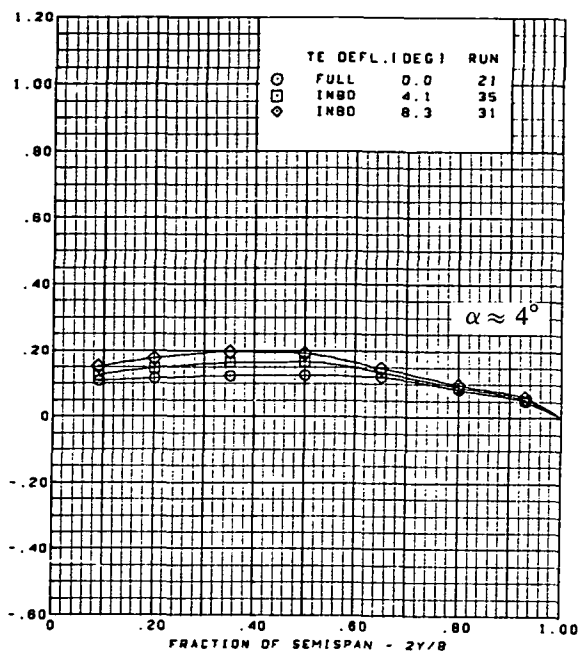
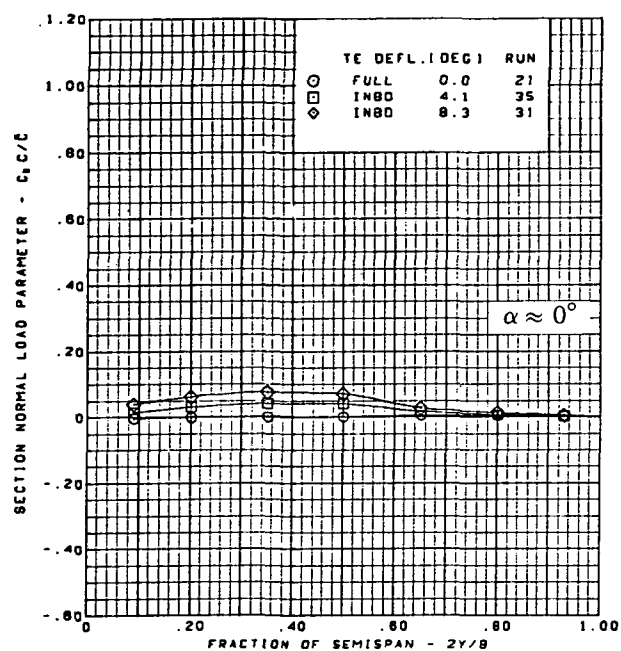
Flat wing, rounded L.E.

L.E. deflection, full span =  $0.0^\circ$

T.E. deflection, outboard =  $0.0^\circ$

(b) Spanload Distributions—Pitching Moment

Figure 29.—(Concluded)



$M = 2.10$

Flat wing, rounded L.E.

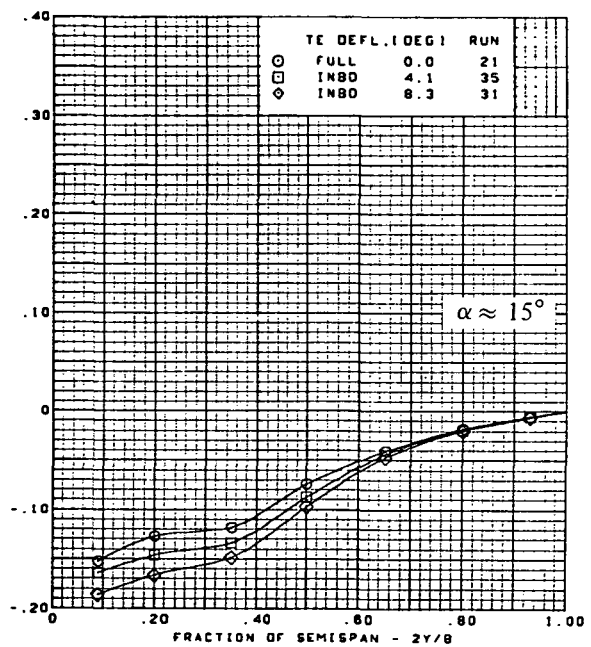
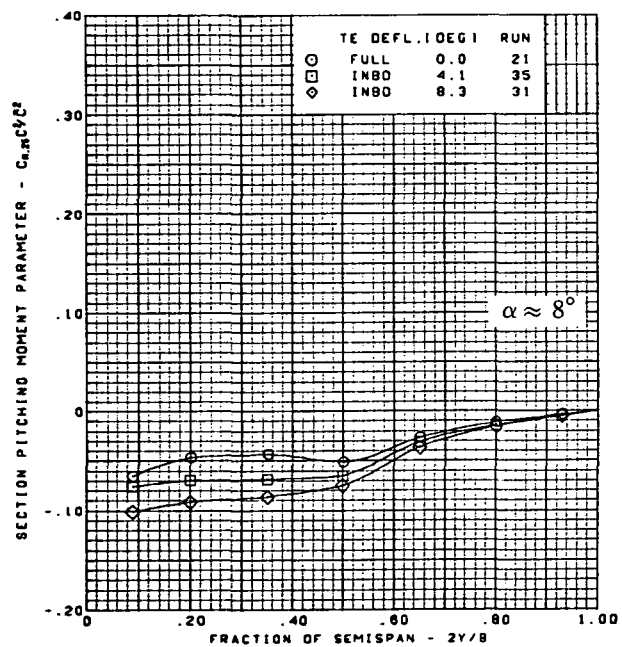
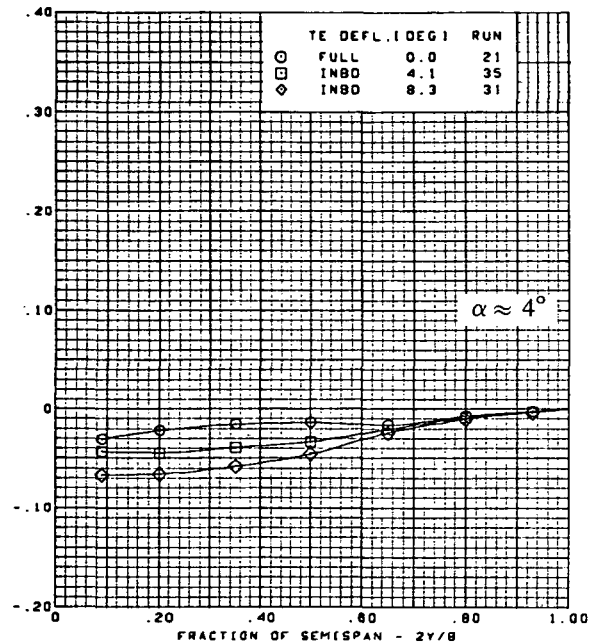
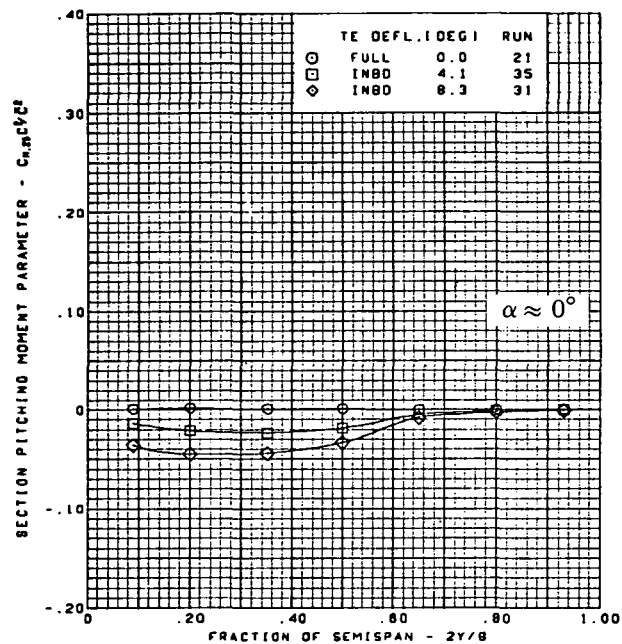
L.E. deflection, full span =  $0.0^\circ$

T.E. deflection, outboard =  $0.0^\circ$

(a) Spanload Distributions—Normal Force

Figure 30.—Wing Experimental Data—Effect of Partial Span T.E. Deflection With Angle of Attack; Flat Wing, Rounded L.E.; L.E. Deflection, Full Span =  $0.0^\circ$ ; T.E. Deflection, Outboard =  $0.0^\circ$ ;  $M = 2.10$

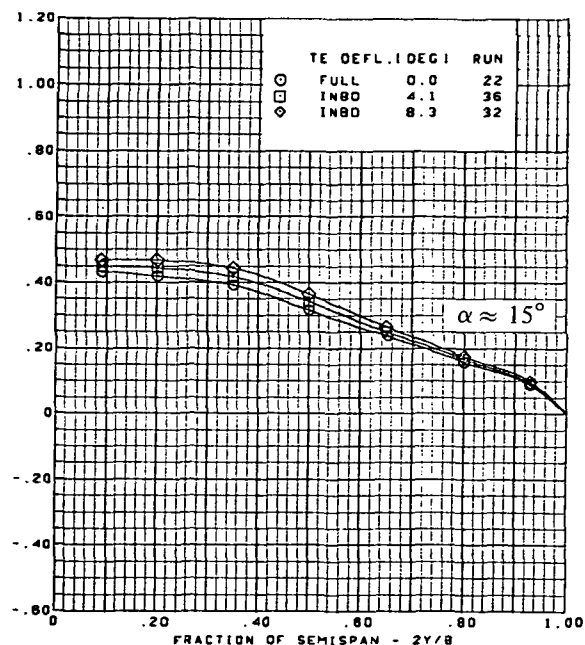
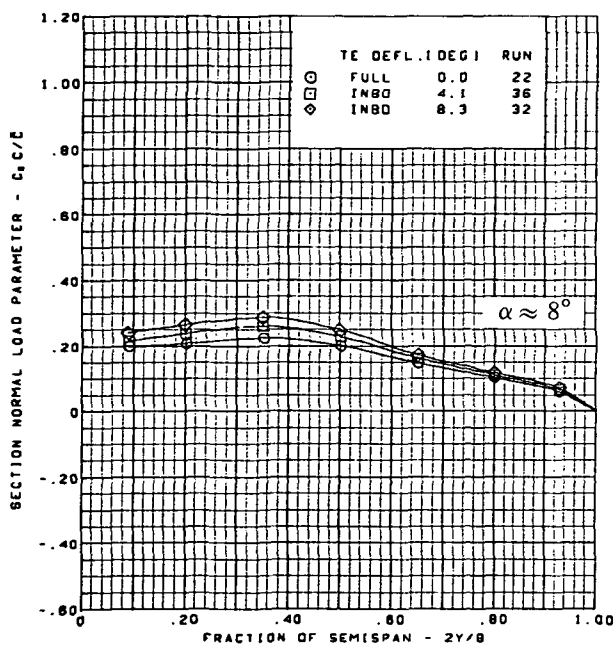
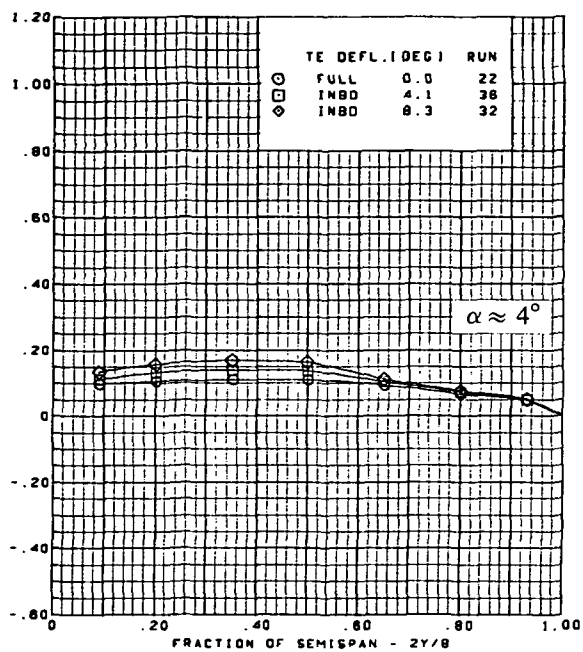
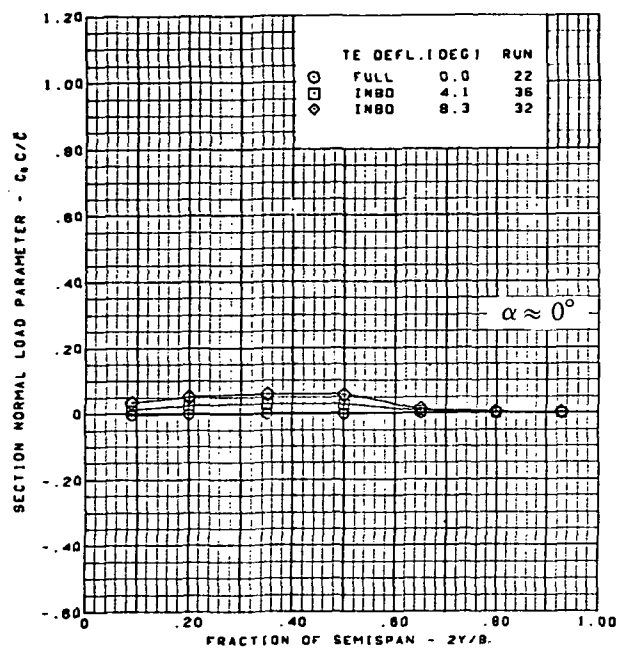




$M = 2.10$   
 Flat wing, rounded L.E.  
 L.E. deflection, full span =  $0.0^\circ$   
 T.E. deflection, outboard =  $0.0^\circ$

(b) Spanload Distributions—Pitching Moment

Figure 30.—(Concluded)



$M = 2.50$

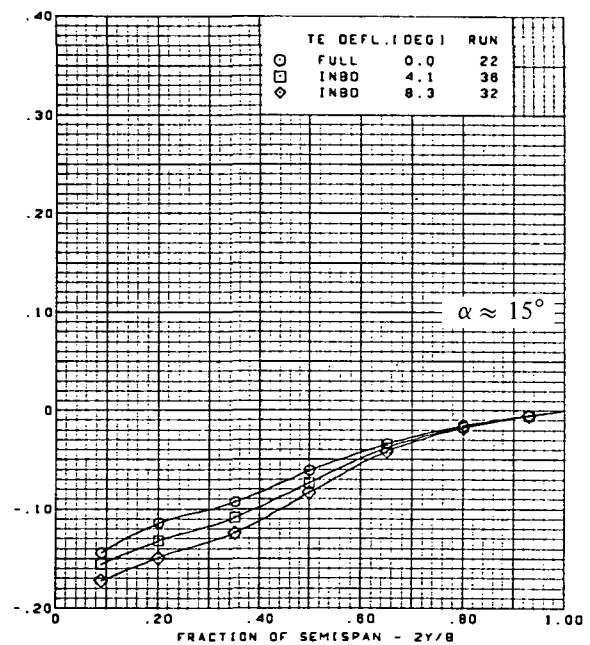
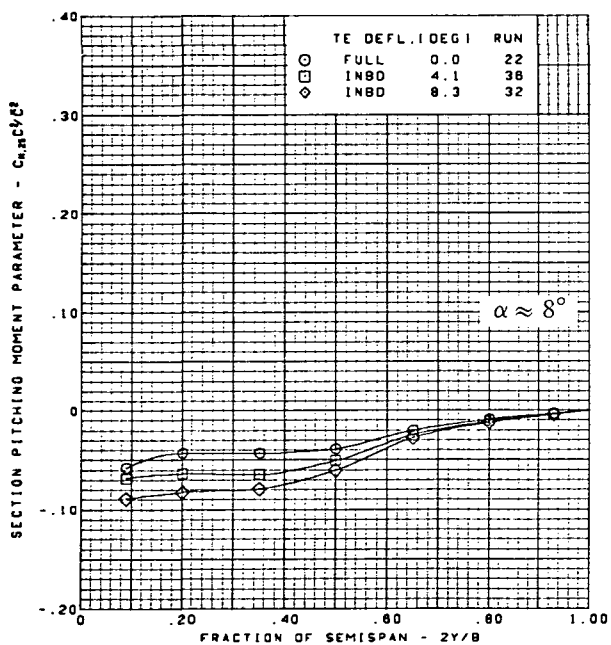
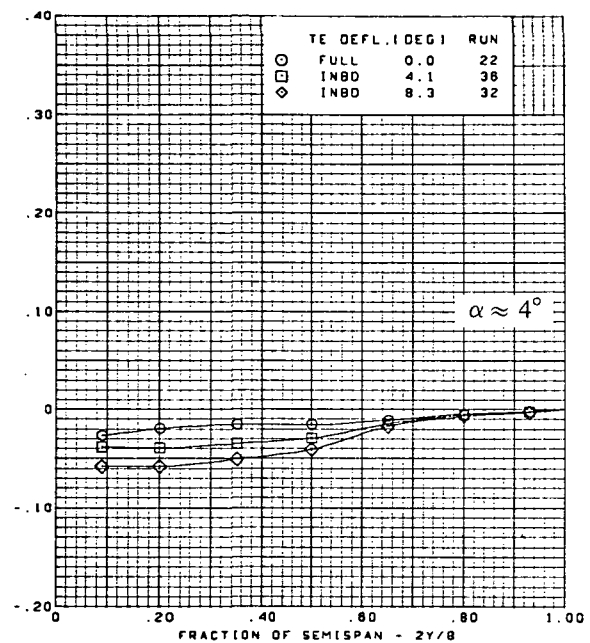
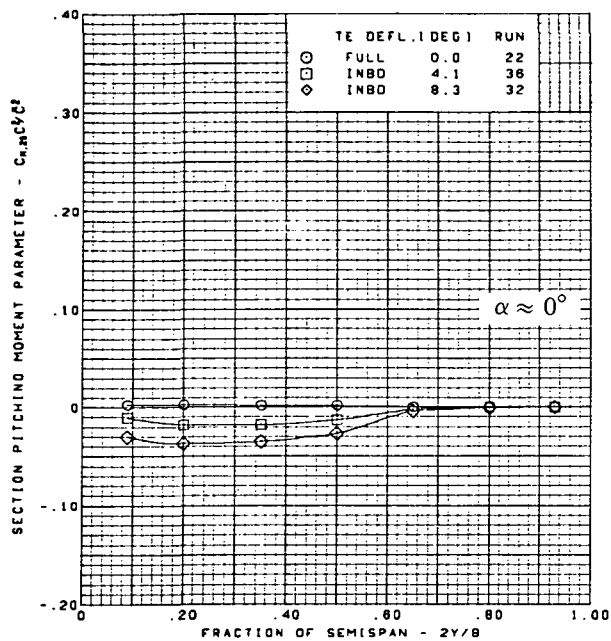
Flat wing, rounded L.E.

L.E. deflection, full span =  $0.0^\circ$

T.E. deflection, outboard =  $0.0^\circ$

(a) Spanload Distributions—Normal Force

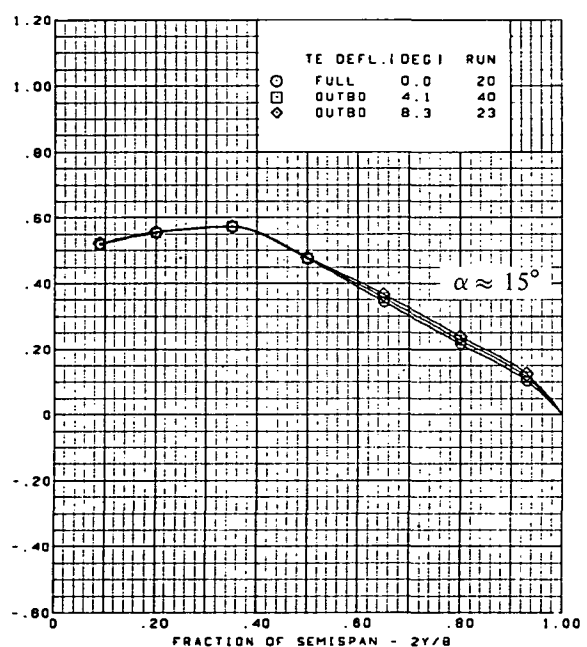
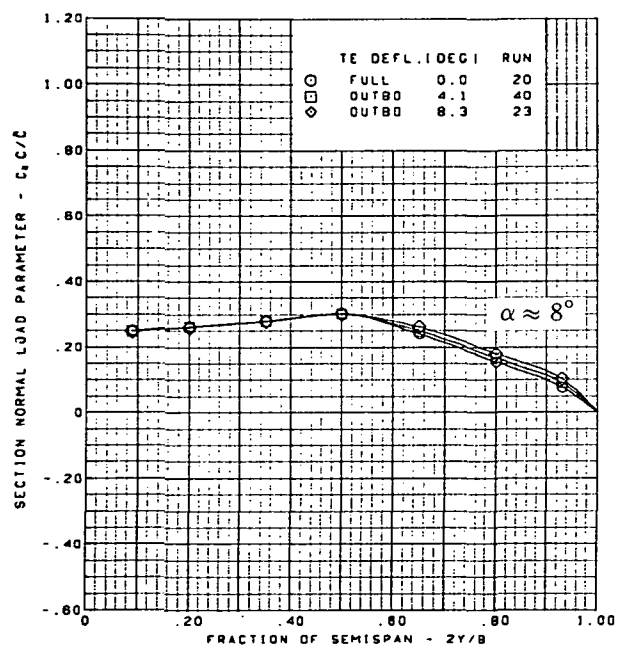
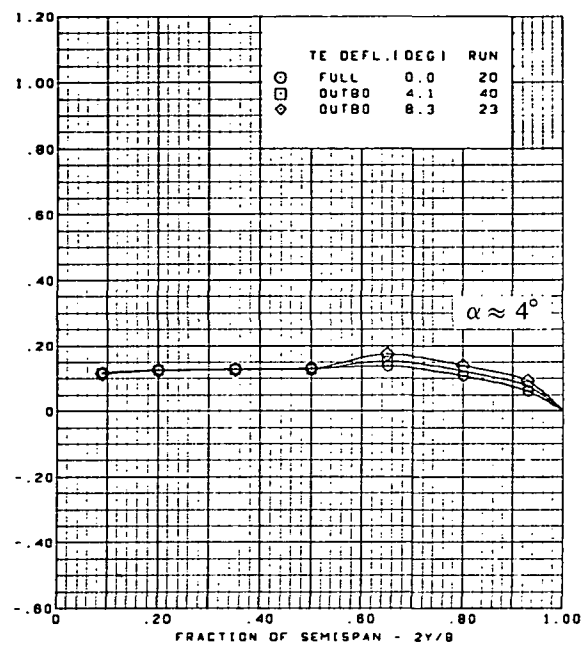
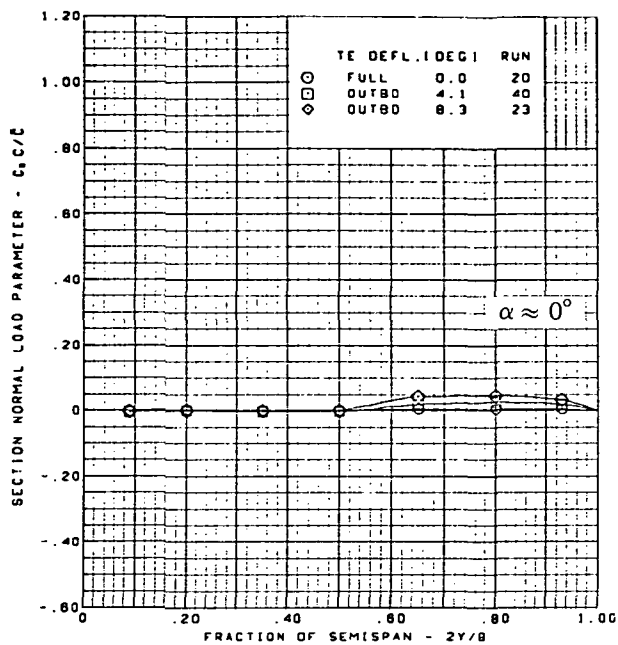
Figure 31.—Wing Experimental Data—Effect of Partial Span T.E. Deflection With Angle of Attack; Flat Wing, Rounded L.E.; L.E. Deflection, Full Span =  $0.0^\circ$ ; T.E. Deflection, Outboard =  $0.0^\circ$ ;  $M = 2.50$



$M = 2.50$   
 Flat wing, rounded L.E.  
 L.E. deflection, full span =  $0.0^\circ$   
 T.E. deflection, outboard =  $0.0^\circ$

(b) Spanload Distributions—Pitching Moment

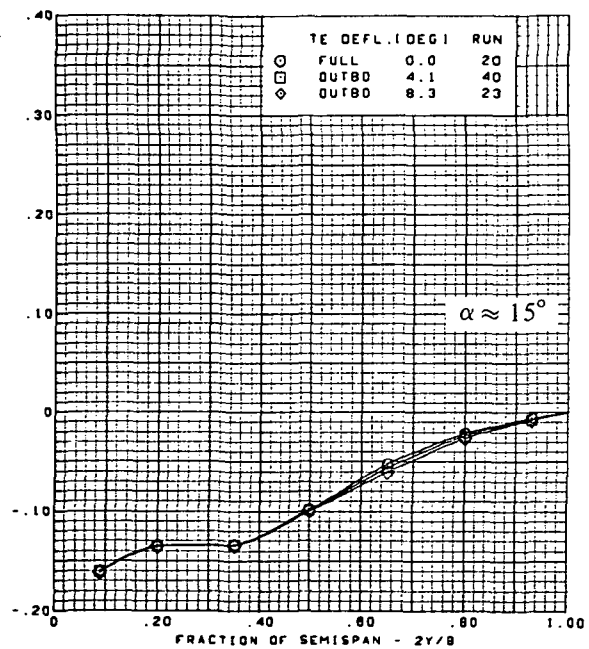
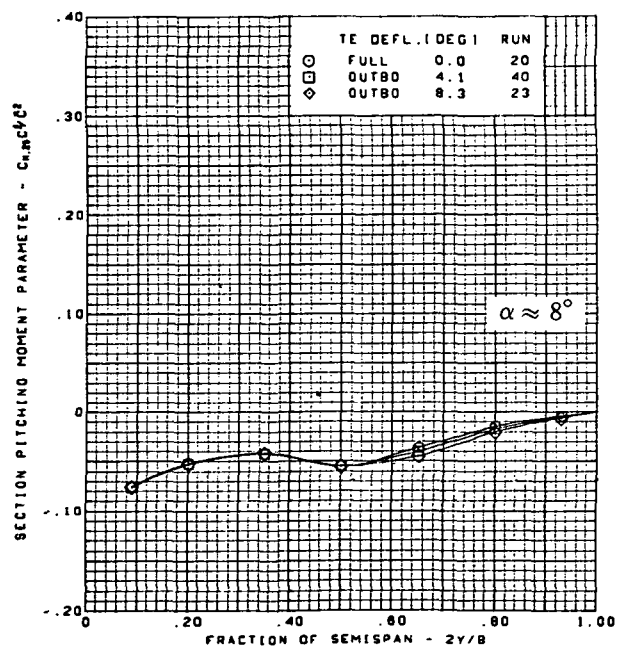
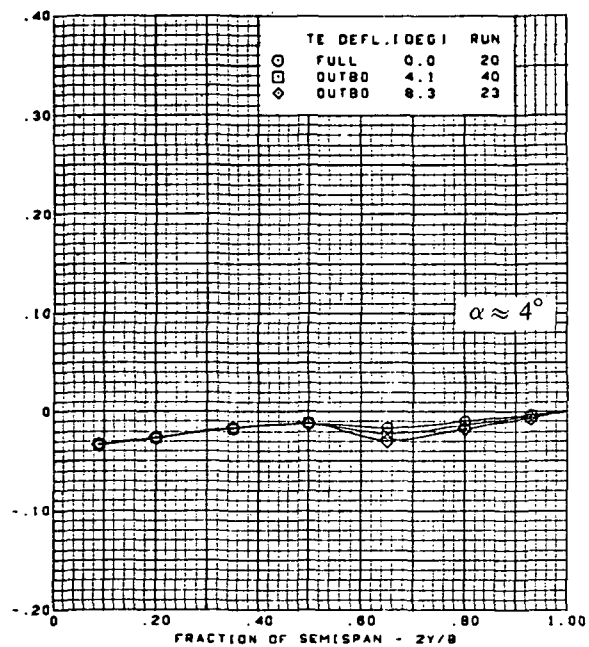
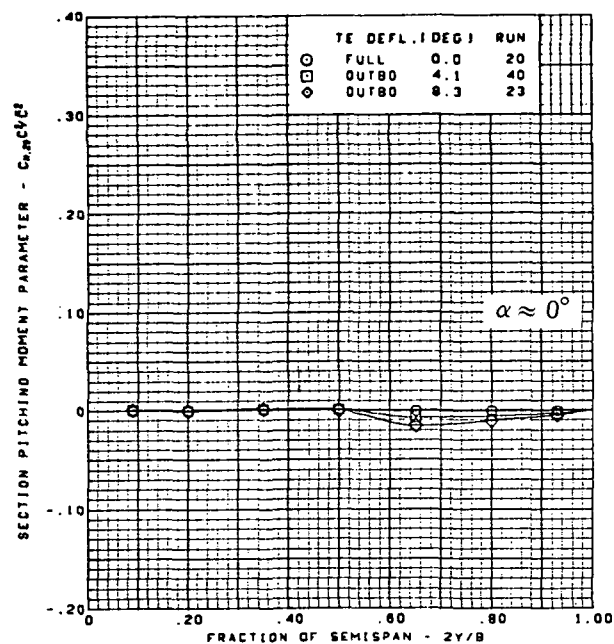
Figure 31.—(Concluded)



$M = 1.70$   
 Flat wing, rounded L.E.  
 L.E. deflection, full span =  $0.0^\circ$   
 T.E. deflection, inboard =  $0.0^\circ$

(a) Spanload Distributions—Normal Force

Figure 32.—Wing Experimental Data—Effect of Partial Span T.E. Deflection With Angle of Attack;  
 Flat Wing, Rounded L.E.; L.E. Deflection, Full Span =  $0.0^\circ$ ; T.E. Deflection,  
 Inboard =  $0.0^\circ$ ;  $M = 1.70$



$M = 1.70$

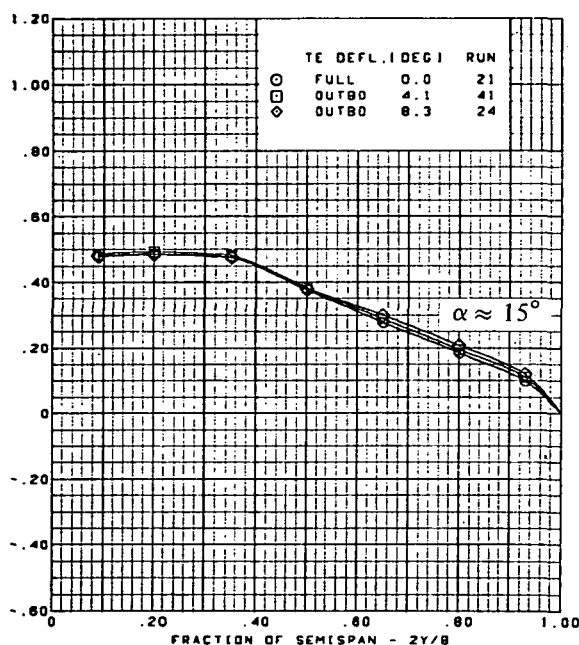
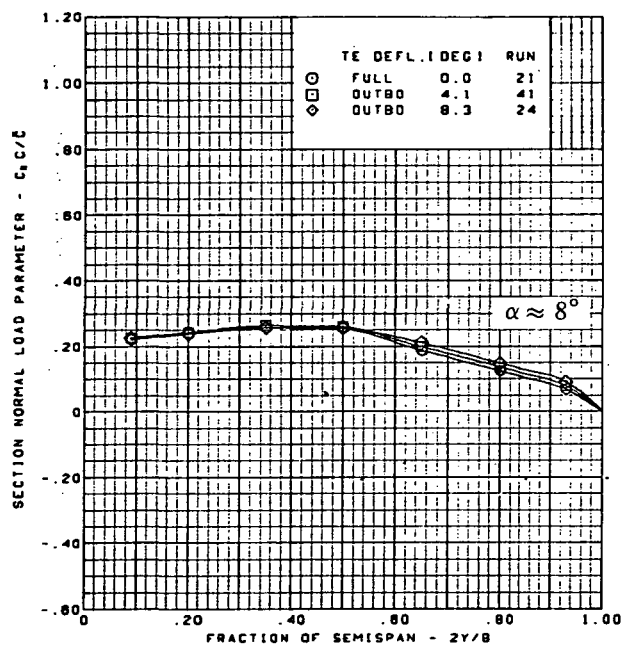
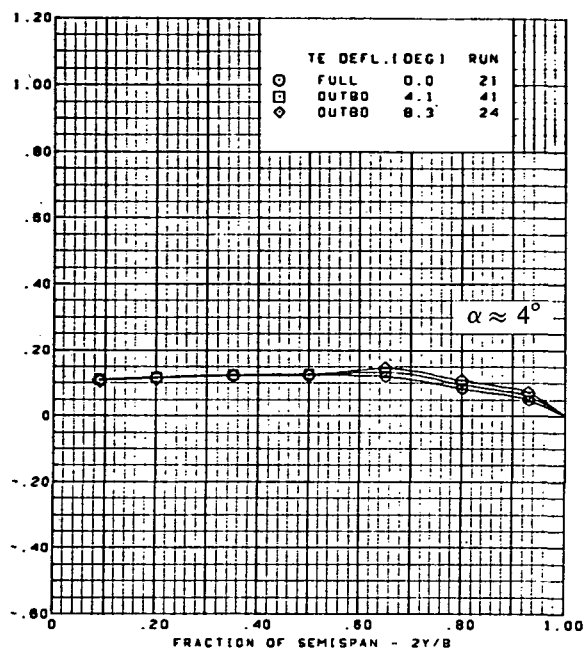
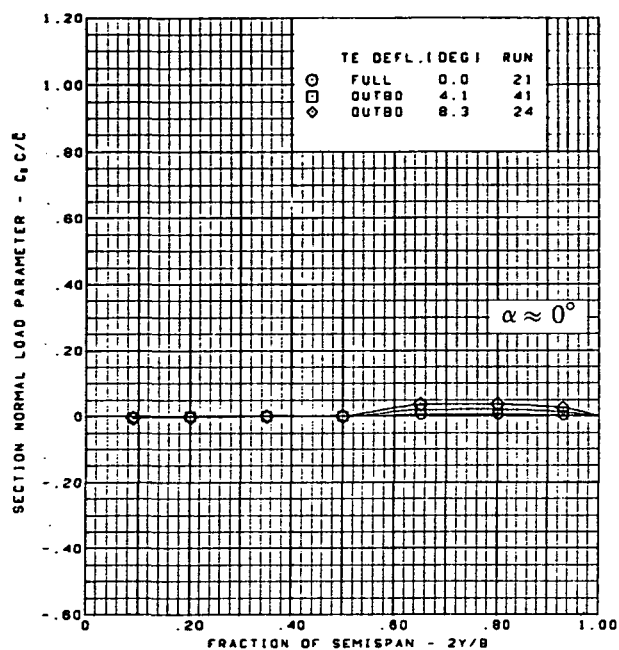
Flat wing, rounded L.E.

L.E. deflection, full span =  $0.0^\circ$

T.E. deflection, inboard =  $0.0^\circ$

(b) Spanload Distributions—Pitching Moment

Figure 32.—(Concluded)



$M = 2.10$

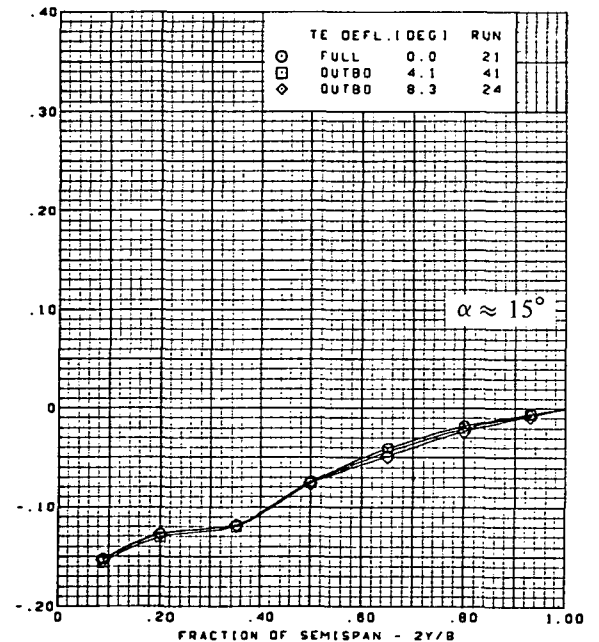
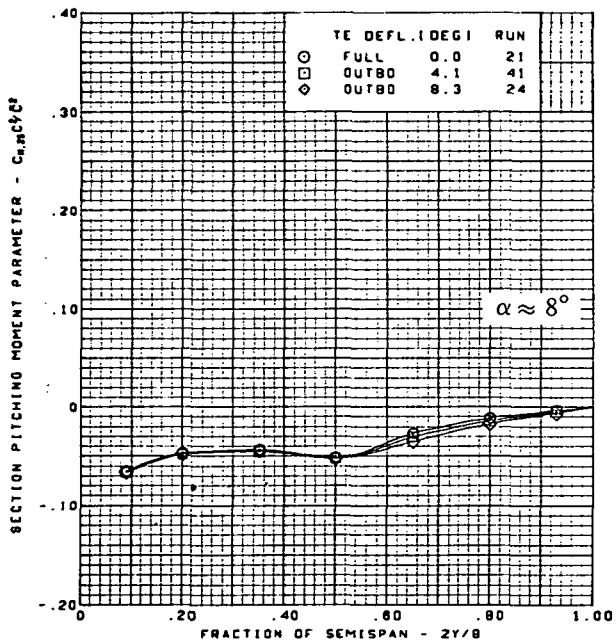
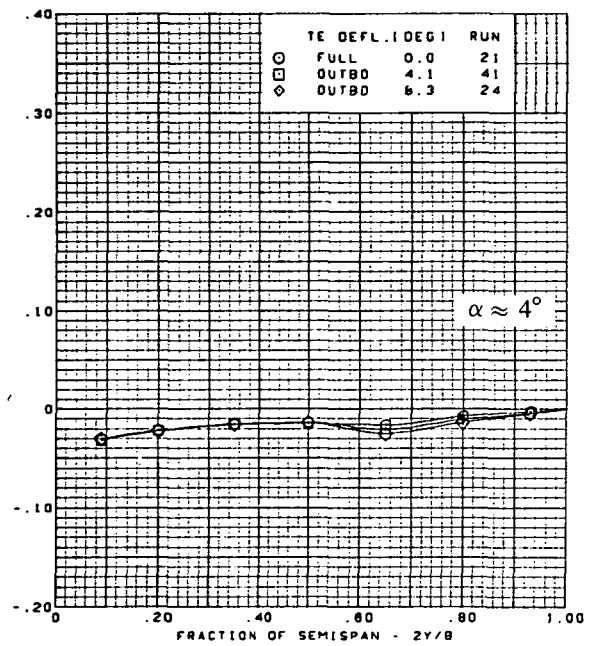
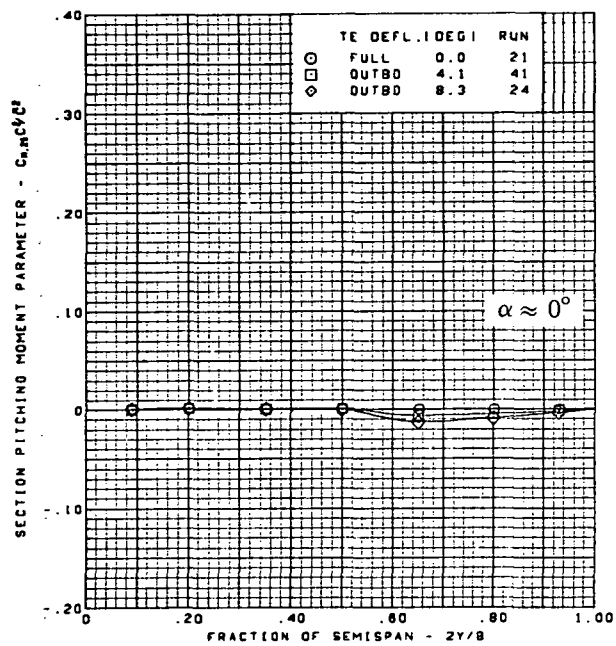
Flat wing, rounded L.E.

L.E. deflection, full span =  $0.0^\circ$

T.E. deflection, inboard =  $0.0^\circ$

(a) Spanload Distributions—Normal Force

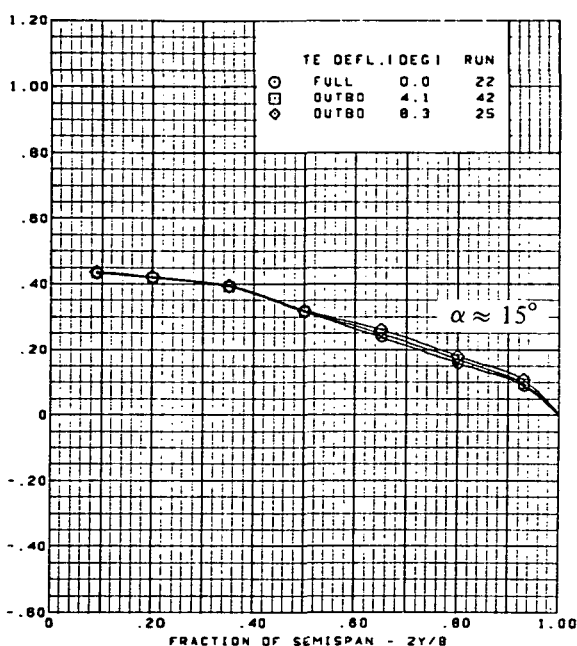
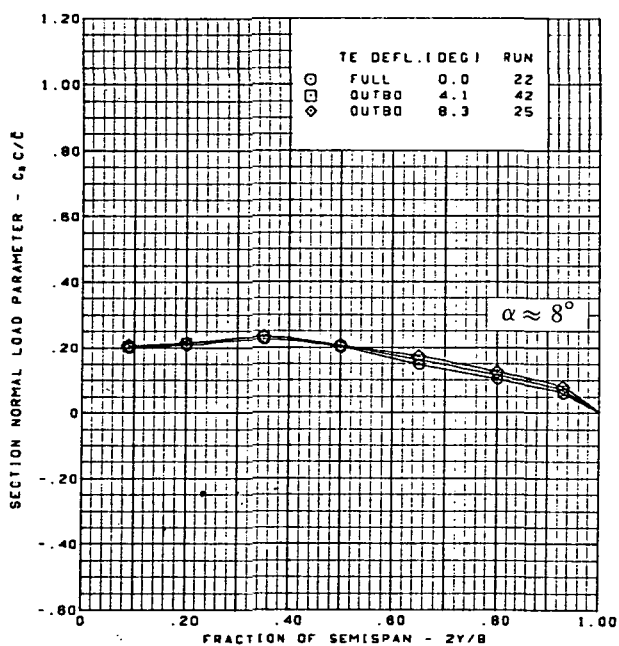
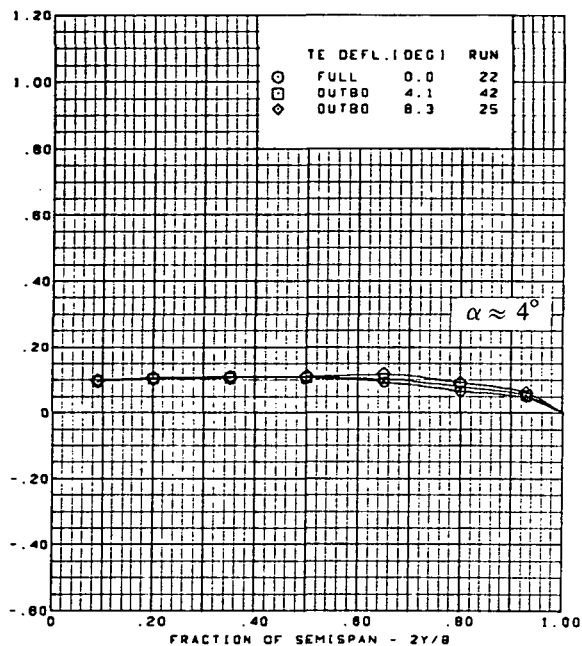
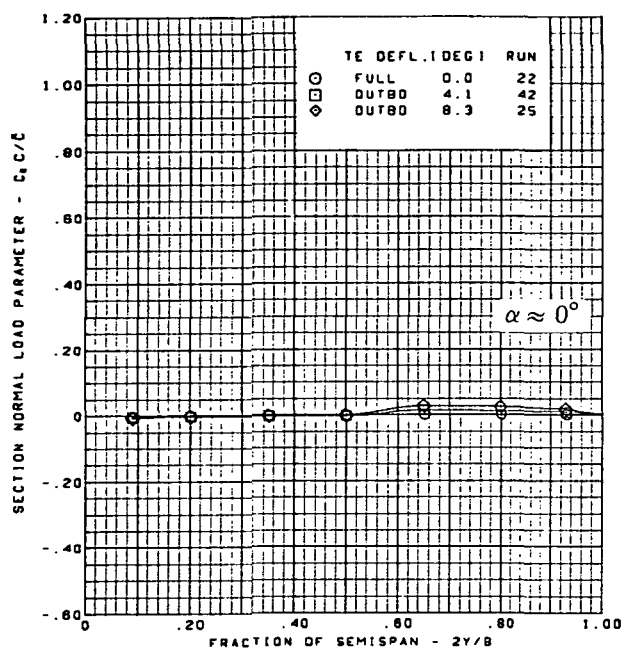
Figure 33.—Wing Experimental Data—Effect of Partial Span T.E. Deflection With Angle of Attack; Flat Wing, Rounded L.E.; L.E. Deflection, Full Span =  $0.0^\circ$ ; T.E. Deflection, Inboard =  $0.0^\circ$ ;  $M = 2.10$



M = 2.10  
 Flat wing, rounded L.E.  
 L.E. deflection, full span =  $0.0^\circ$   
 T.E. deflection, inboard =  $0.0^\circ$

(b) Spanload Distributions—Pitching Moment

Figure 33.—(Concluded)



$M = 2.50$

Flat wing, rounded L.E.

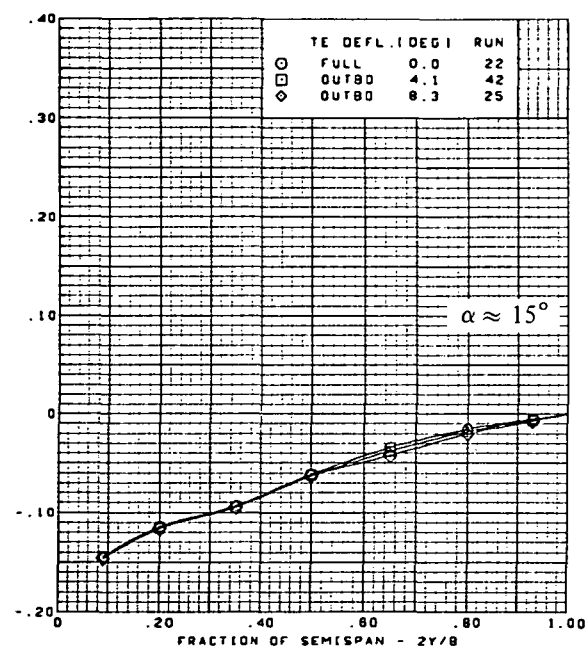
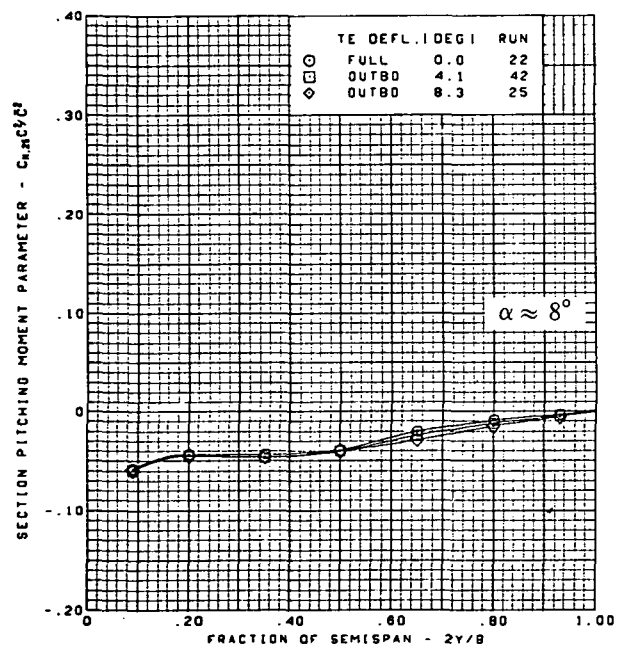
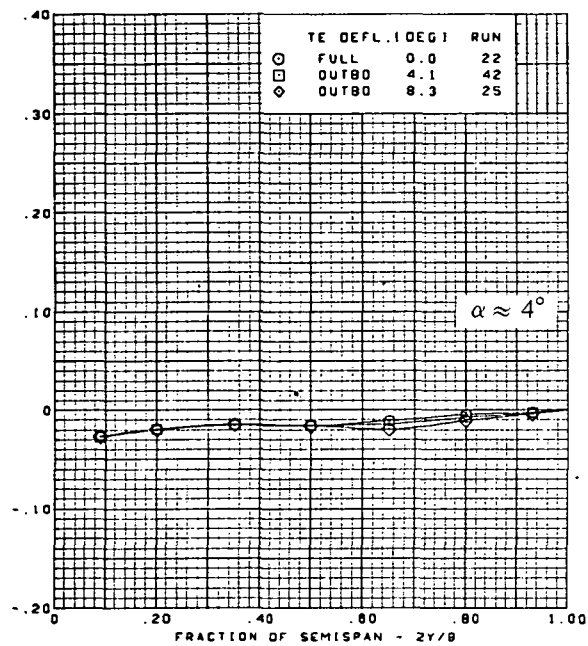
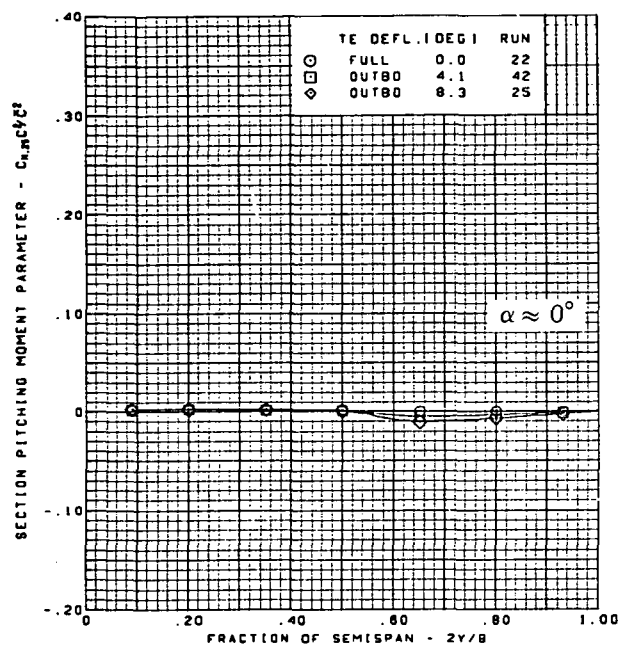
L.E. deflection, full span =  $0.0^\circ$

T.E. deflection, inboard =  $0.0^\circ$

(a) Spanload Distributions—Normal Force

Figure 34.—Wing Experimental Data—Effect of Partial Span T.E. Deflection With Angle of Attack; Flat Wing, Rounded L.E.; L.E. Deflection, Full Span =  $0.0^\circ$ ; T.E. Deflection, Inboard =  $0.0^\circ$ ;  $M = 2.50$





$M = 2.50$

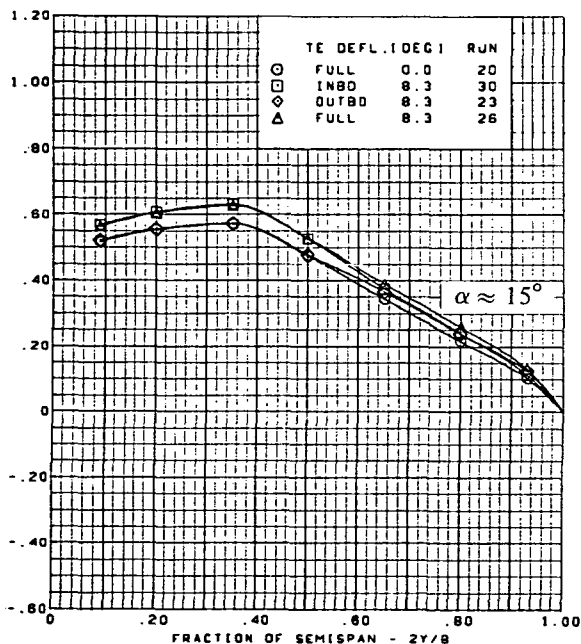
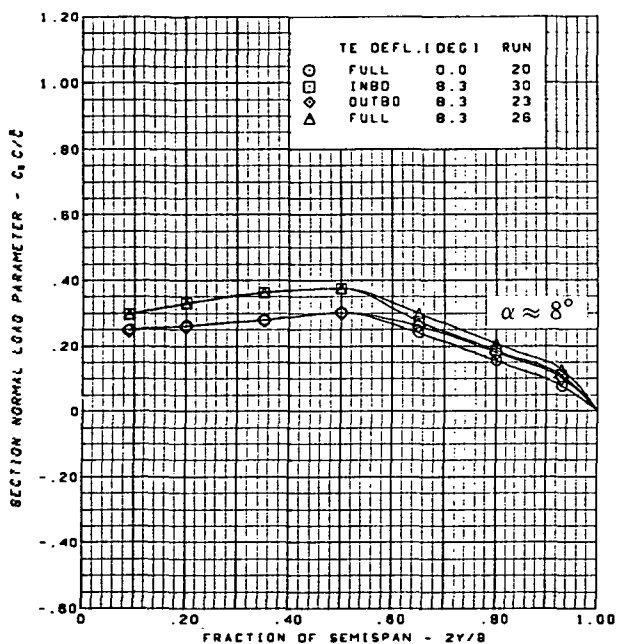
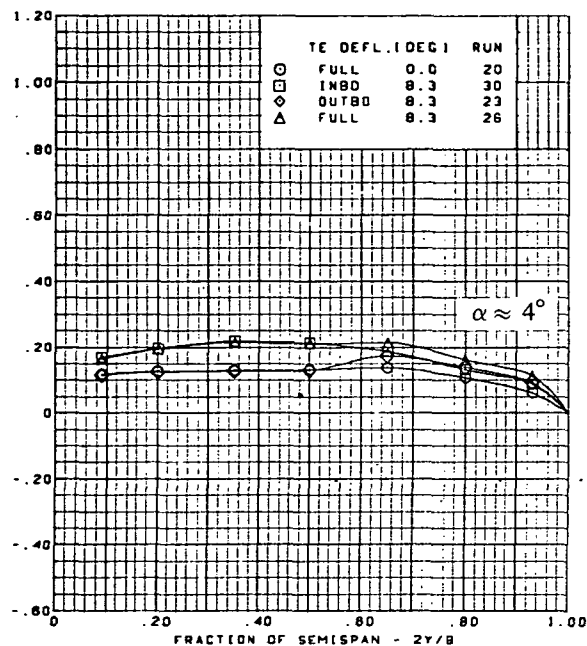
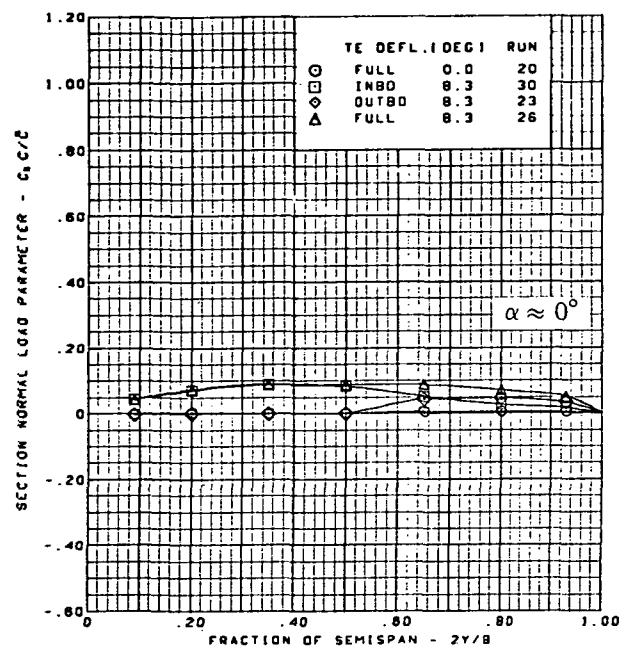
Flat wing, rounded L.E.

L.E. deflection, full span =  $0.0^\circ$

T.E. deflection, inboard =  $0.0^\circ$

(b) Spanload Distributions—Pitching Moment

Figure 34.—(Concluded)



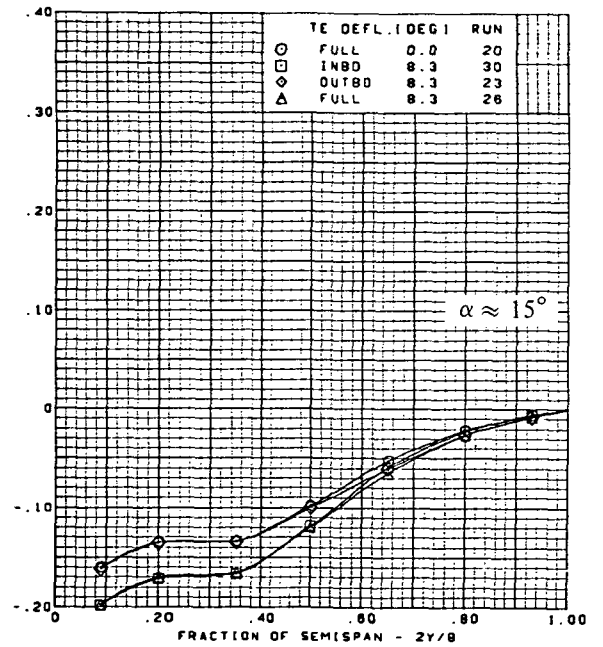
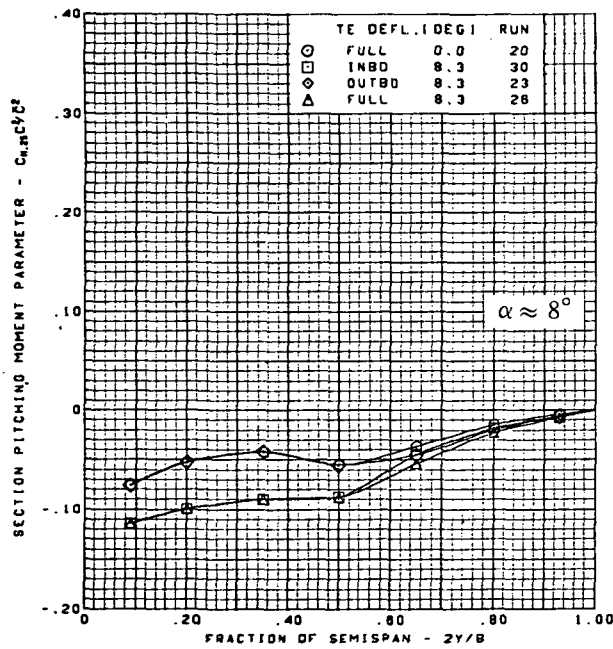
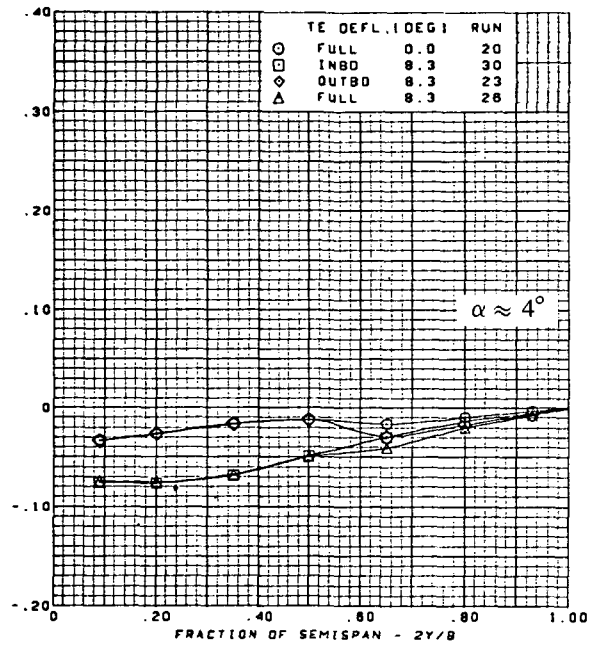
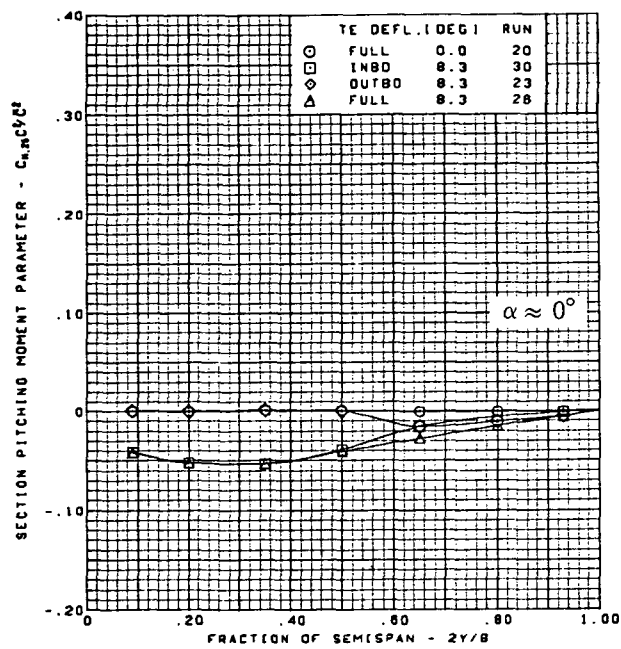
$M = 1.70$

Flat wing, rounded L.E.

L.E. deflection, full span =  $0.0^\circ$

(a) Spanload Distributions—Normal Force

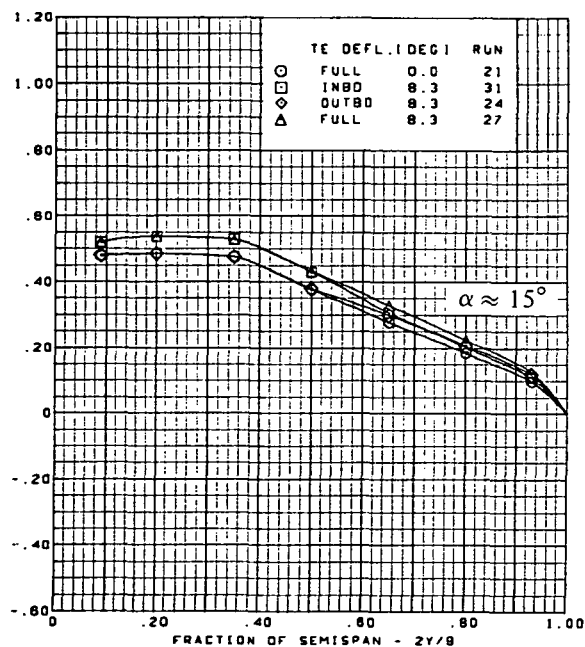
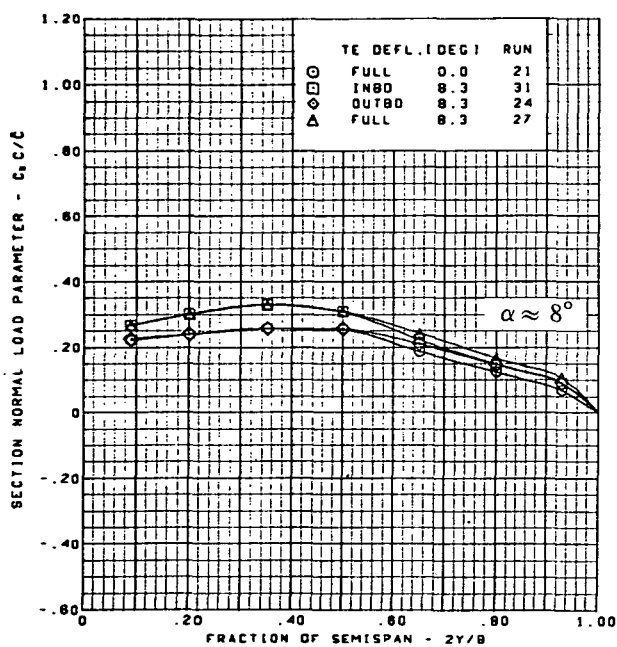
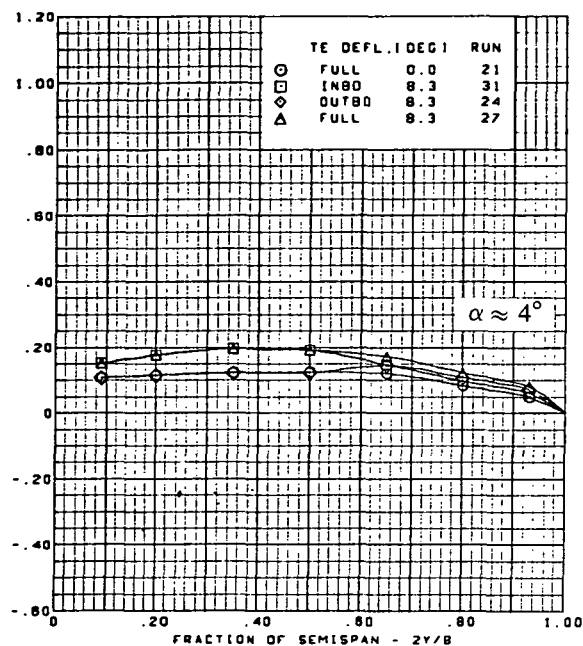
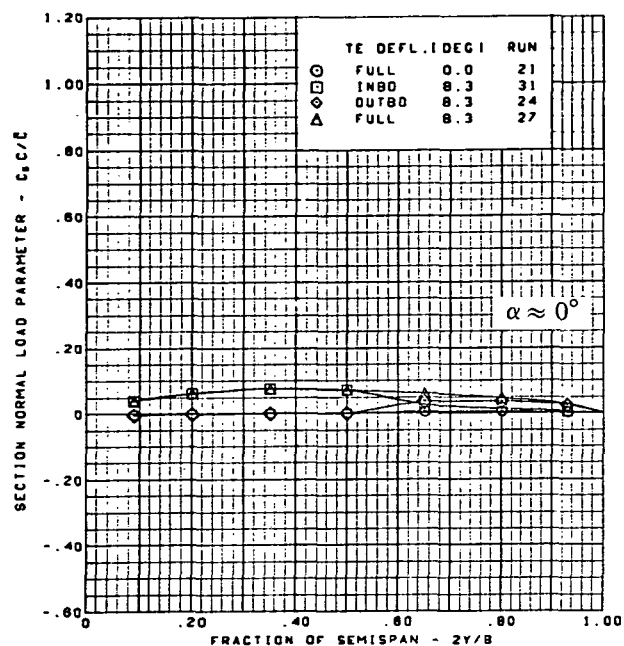
Figure 35.—Wing Experimental Data—Effect of Partial Span T.E. Deflection With Angle of Attack; Flat Wing, Rounded L.E.; L.E. Deflection, Full Span =  $0.0^\circ$ ;  $M = 1.70$



$M = 1.70$   
 Flat wing, rounded L.E.  
 L.E. deflection, full span =  $0.0^\circ$

(b) Spanload Distributions—Pitching Moment

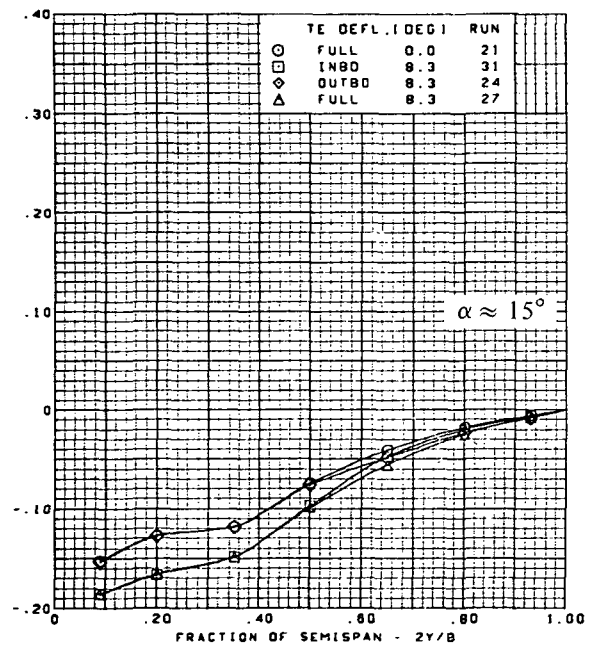
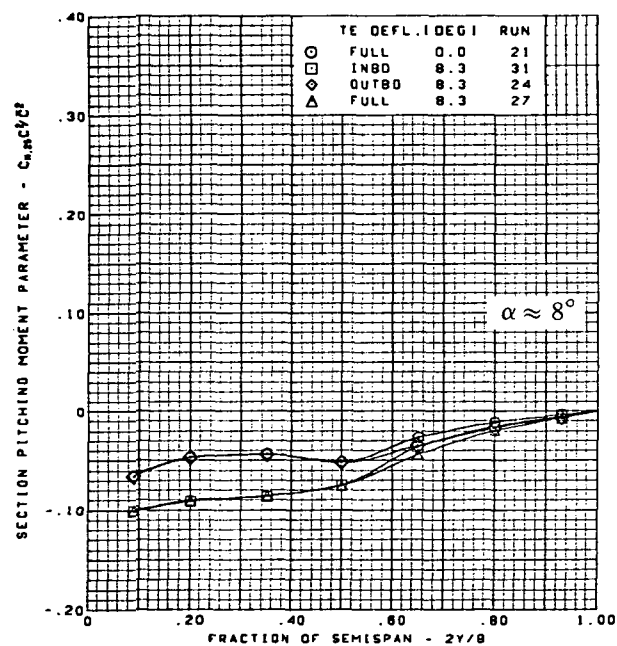
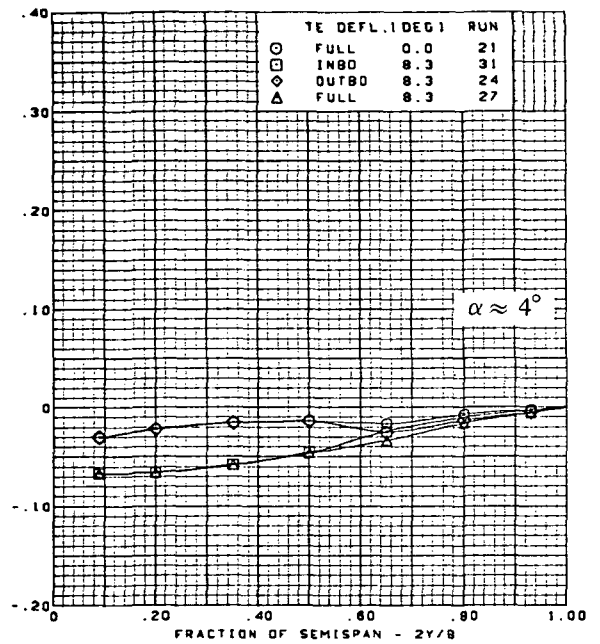
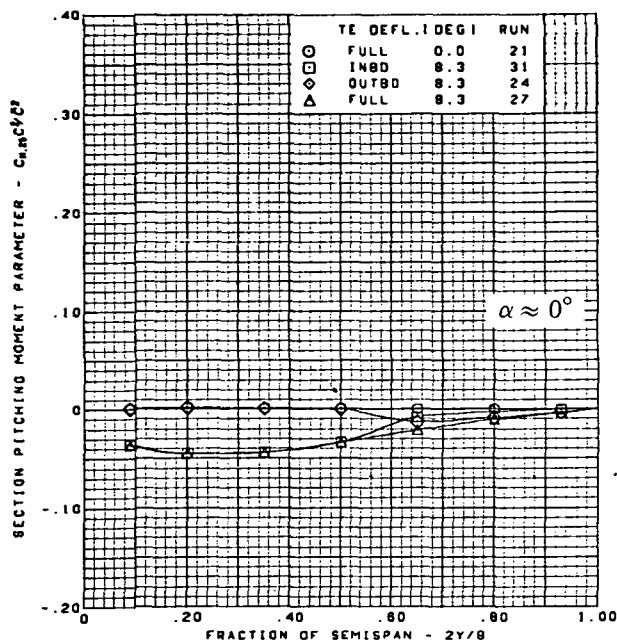
Figure 35.—(Concluded)



M = 2.10  
 Flat wing, rounded L.E.  
 L.E. deflection, full span =  $0.0^\circ$

(a) Spanload Distributions—Normal Force

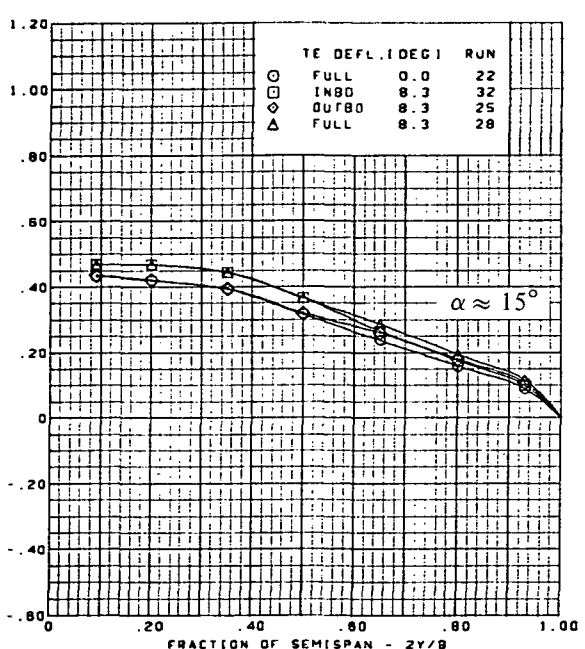
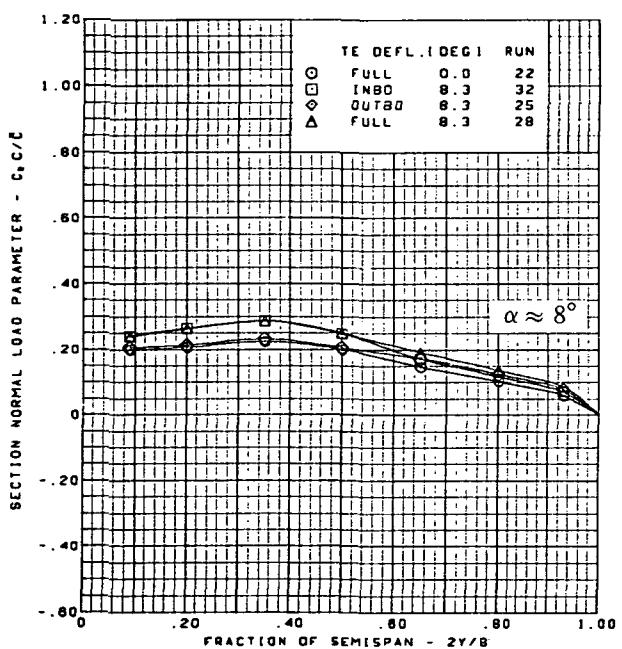
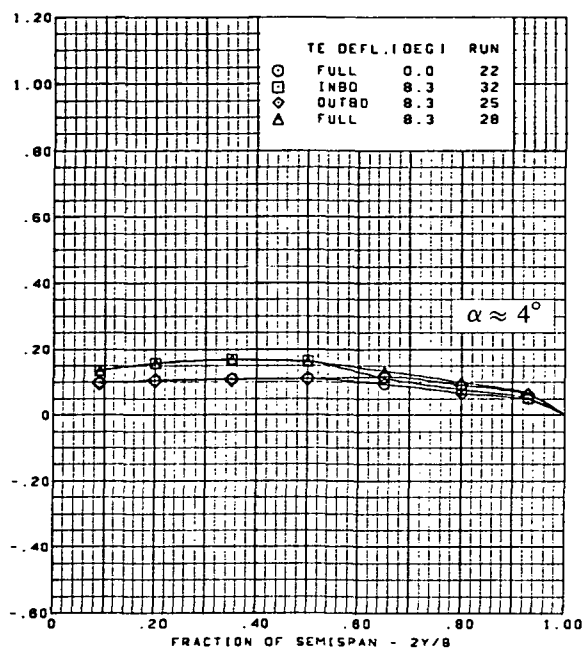
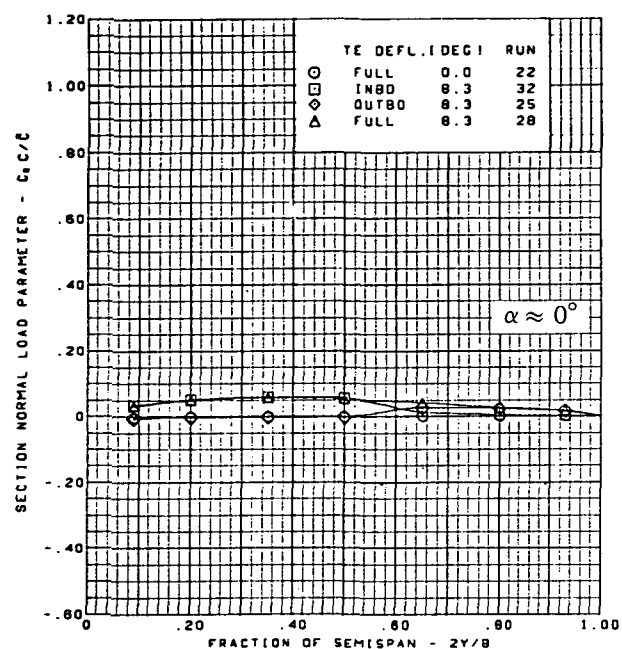
Figure 36.—Wing Experimental Data—Effect of Partial Span T.E. Deflection With Angle of Attack;  
 Flat Wing, Rounded L.E.; L.E. Deflection, Full Span =  $0.0^\circ$ ; M = 2.10



$M = 2.10$   
 Flat wing, rounded L.E.  
 L.E. deflection, full span =  $0.0^\circ$

(b) Spanload Distributions—Pitching Moment

Figure 36.—(Concluded)



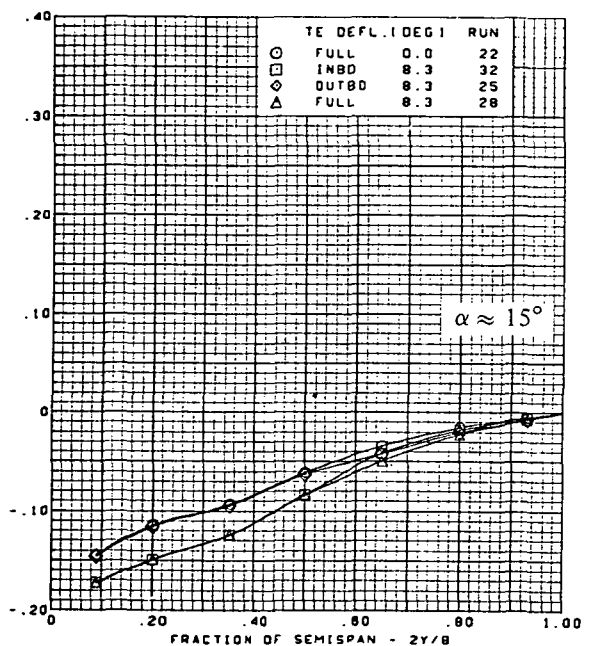
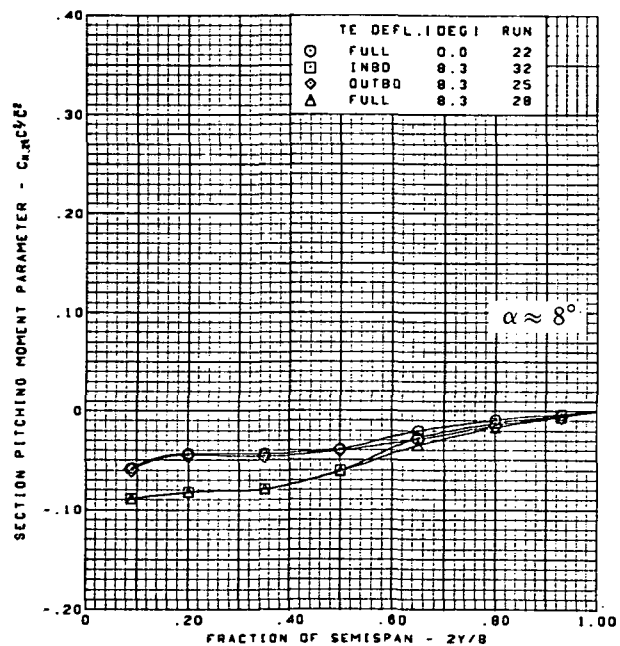
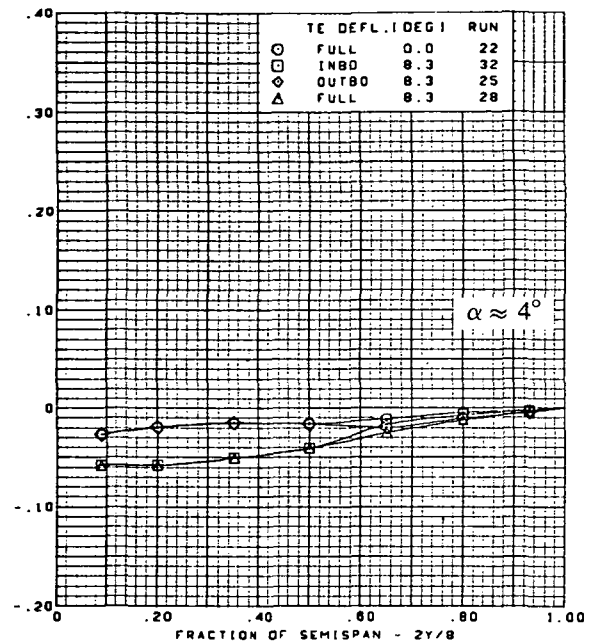
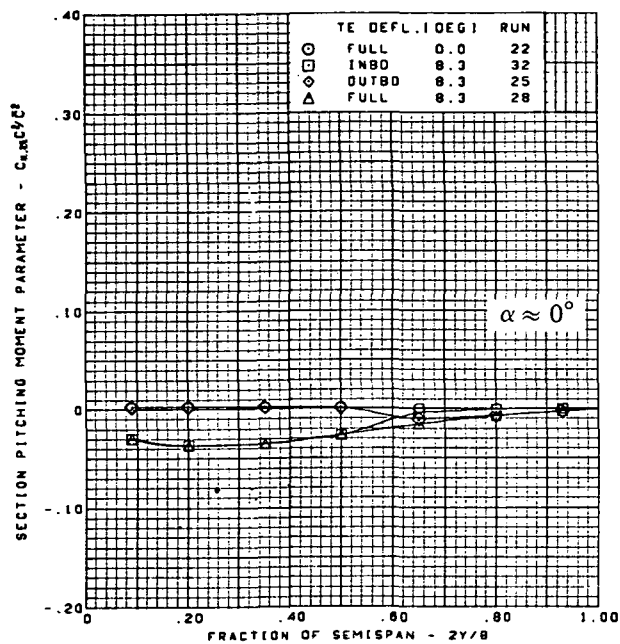
$M = 2.50$

Flat wing, rounded L.E.

L.E. deflection, full span =  $0.0^\circ$

(a) Spanload Distributions—Normal Force

Figure 37.—Wing Experimental Data—Effect of Partial Span T.E. Deflection With Angle of Attack; Flat Wing, Rounded L.E.; L.E. Deflection, Full Span =  $0.0^\circ$ ;  $M = 2.50$



M = 2.50  
 Flat wing, rounded L.E.  
 L.E. deflection, full span  $\approx 0.0^\circ$

(b) Spanload Distributions—Pitching Moment

Figure 37.—(Concluded)

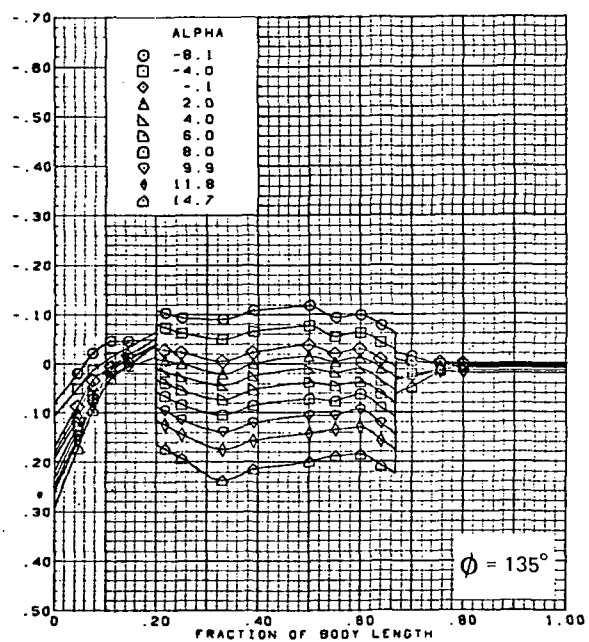
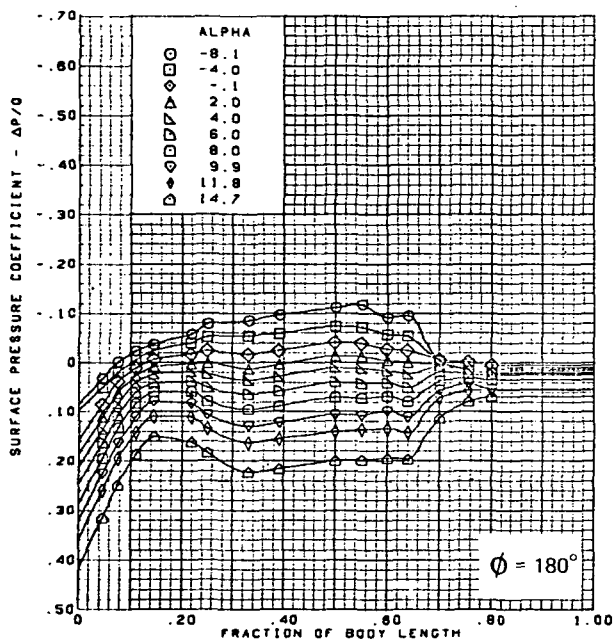
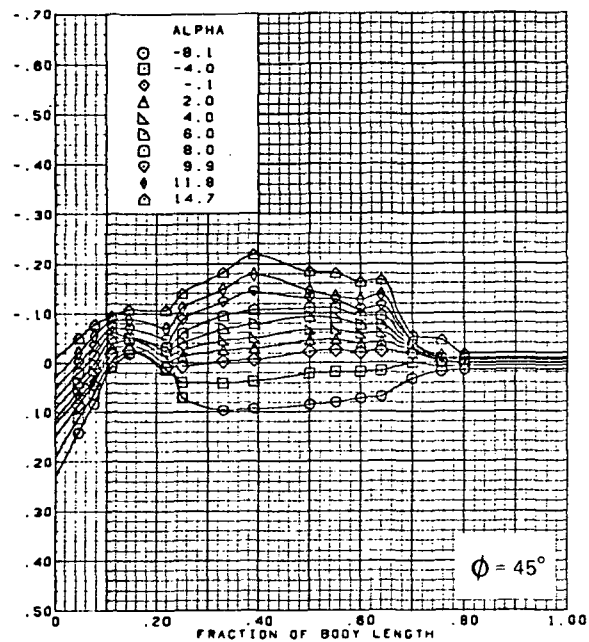
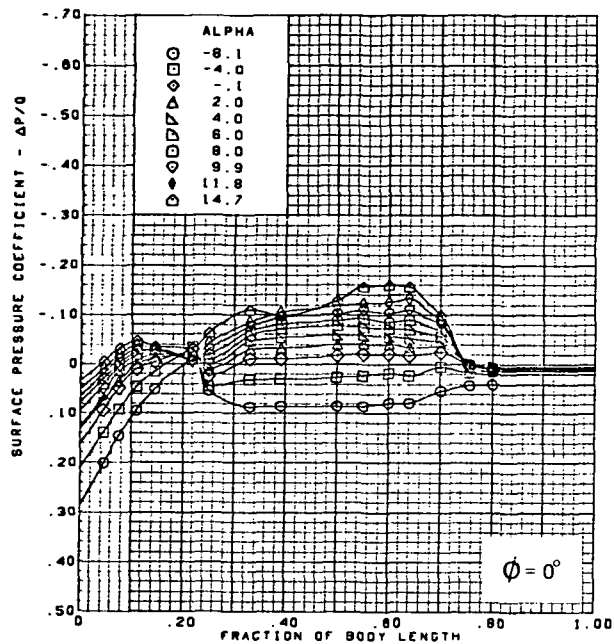
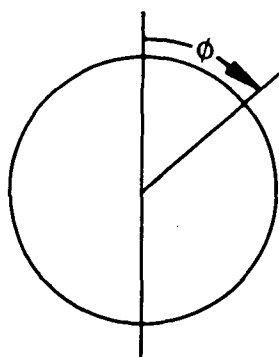
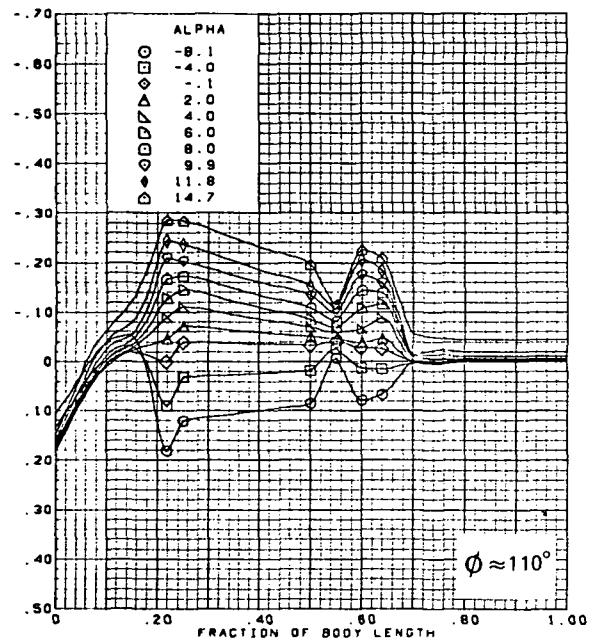
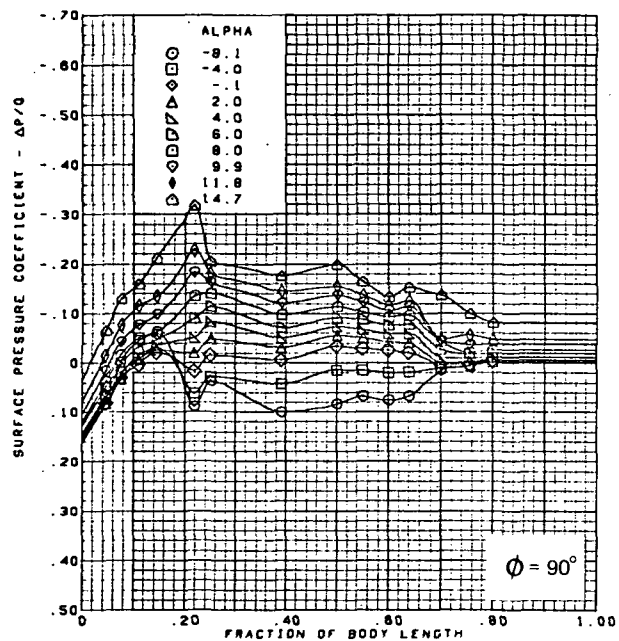


Figure 38.—Body Surface Longitudinal Pressure Distributions—Effect of Angle of Attack; Flat Wing, Rounded L.E.; L.E. Deflection, Full Span =  $0.0^\circ$ ; T.E. Deflection, Full Span =  $0.0^\circ$ ;  $M = 1.54$





M = 1.54 (run 19)  
 Flat wing, rounded L.E.  
 L.E. deflection, full span =  $0.0^\circ$   
 T.E. deflection, full span =  $0.0^\circ$

Note:  $C_{p, \text{vacuum}} = -0.60$

Figure 38.—(Concluded)

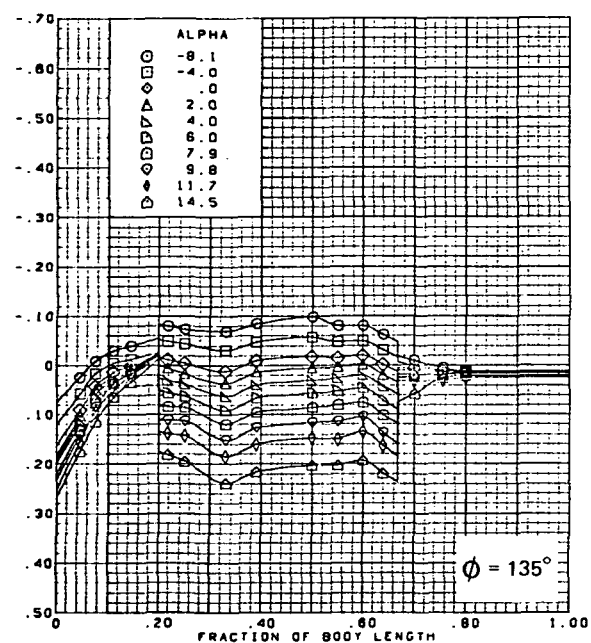
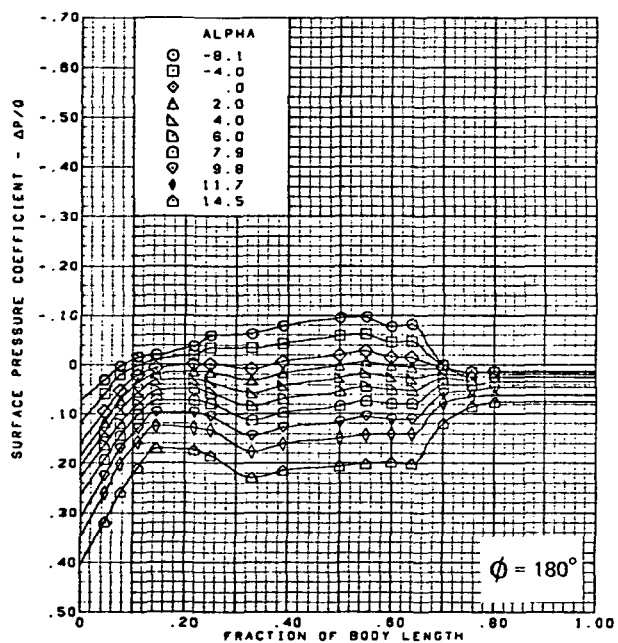
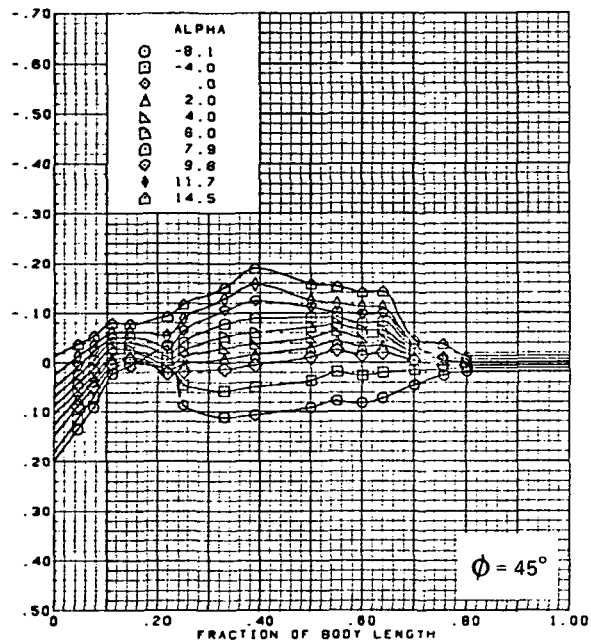
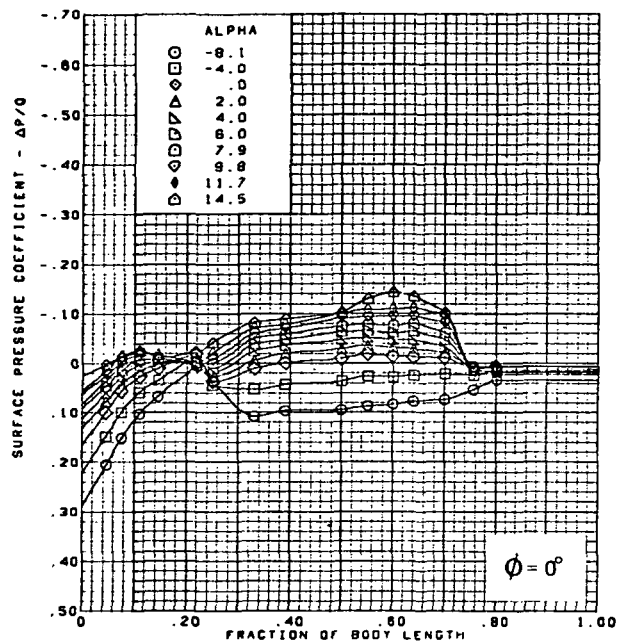
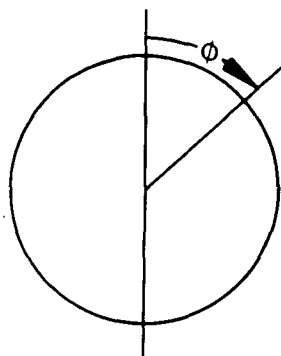
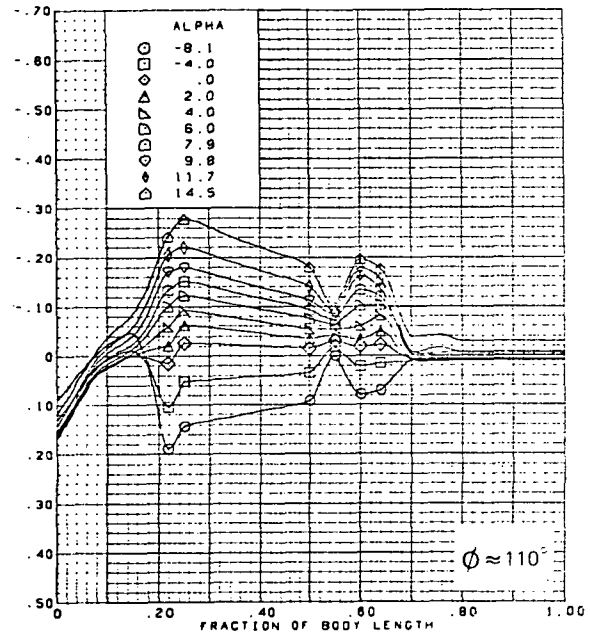
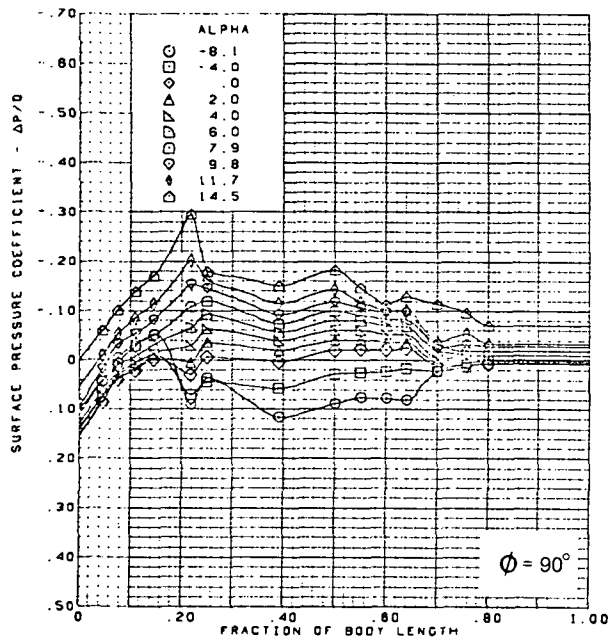


Figure 39.—Body Surface Longitudinal Pressure Distributions—Effect of Angle of Attack; Flat Wing, Rounded L.E.; L.E. Deflection, Full Span = 0.0°; T.E. Deflection, Full Span = 0.0°;  $M = 1.70$



M = 1.70 (run 20)  
 Flat wing, rounded L.E.  
 L.E. deflection, full span =  $0.0^\circ$   
 T.E. deflection, full span =  $0.0^\circ$

Note:  $C_{p, \text{vacuum}} = -0.49$

Figure 39.—(Concluded)

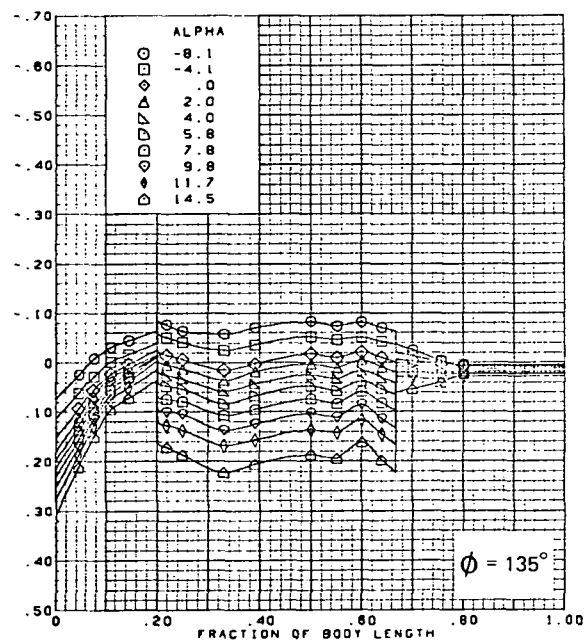
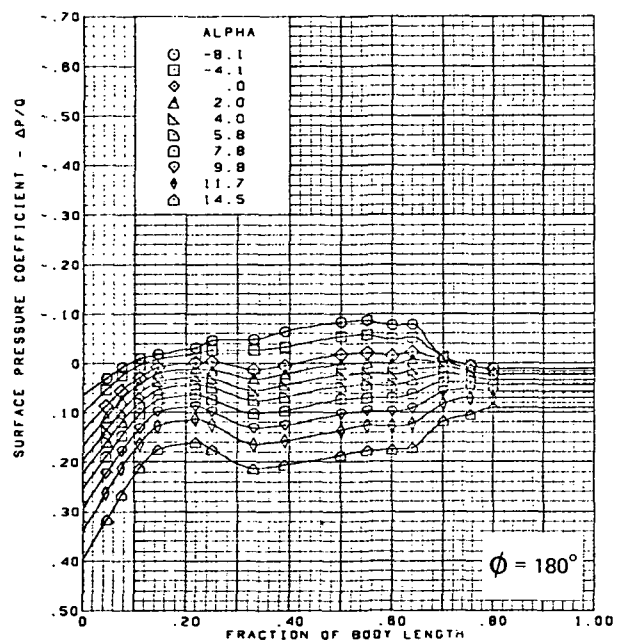
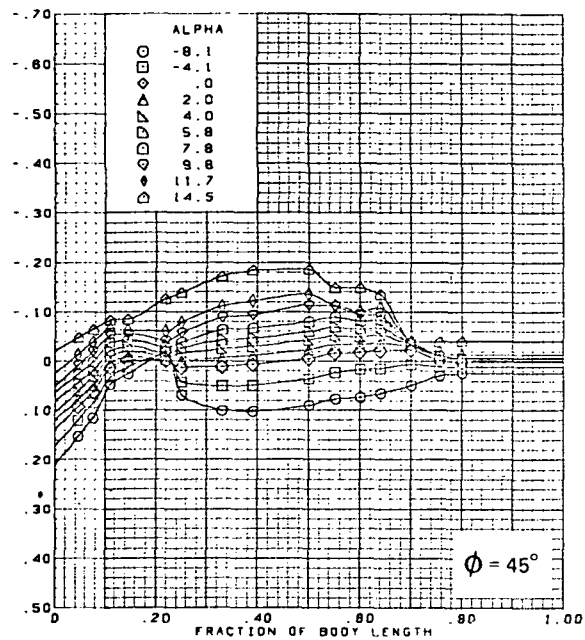
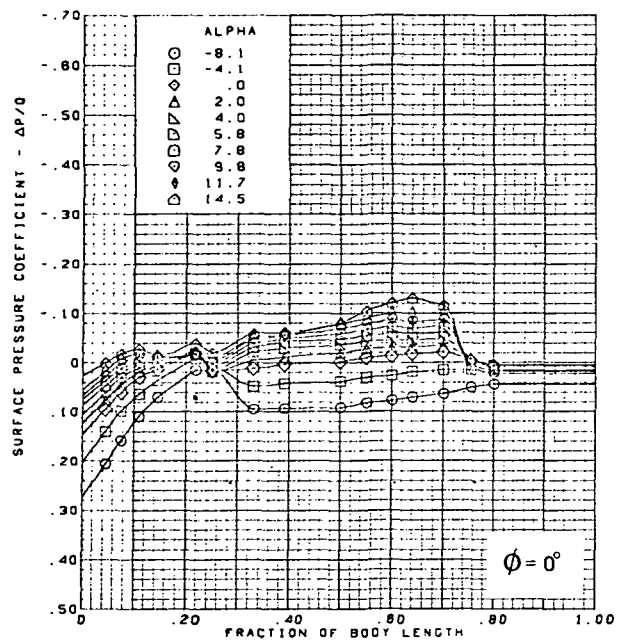
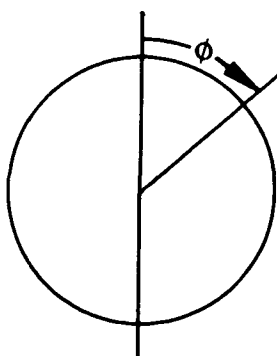
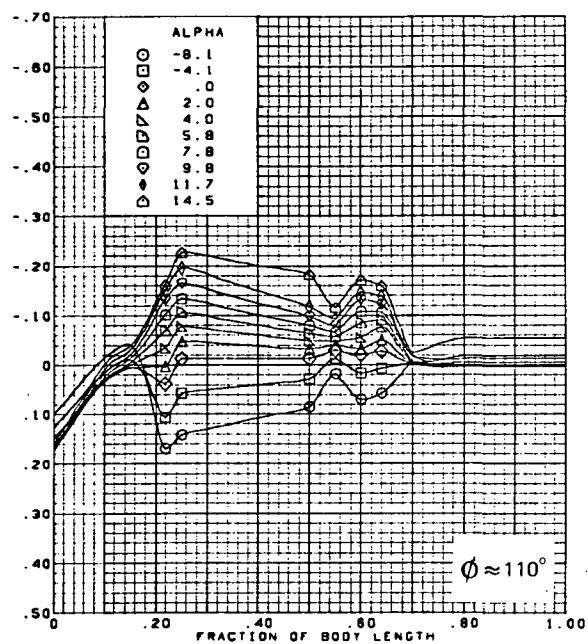
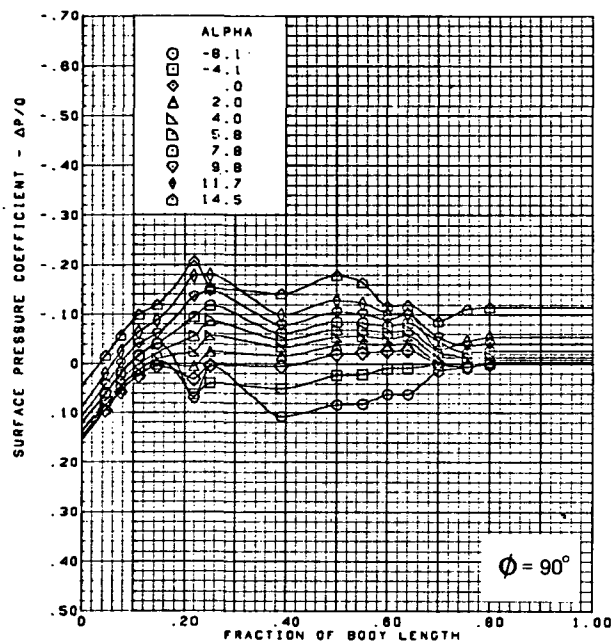


Figure 40.—Body Surface Longitudinal Pressure Distributions—Effect of Angle of Attack; Flat Wing, Rounded L.E.; L.E. Deflection, Full Span =  $0.0^\circ$ ; T.E. Deflection, Full Span =  $0.0^\circ$ ;  $M = 2.10$



M = 2.10 (run 21)  
 Flat wing, rounded L.E.  
 L.E. deflection, full span =  $0.0^\circ$   
 T.E. deflection, full span =  $0.0^\circ$

Note:  $C_{p, \text{vacuum}} = -0.32$

Figure 40.—(Concluded)

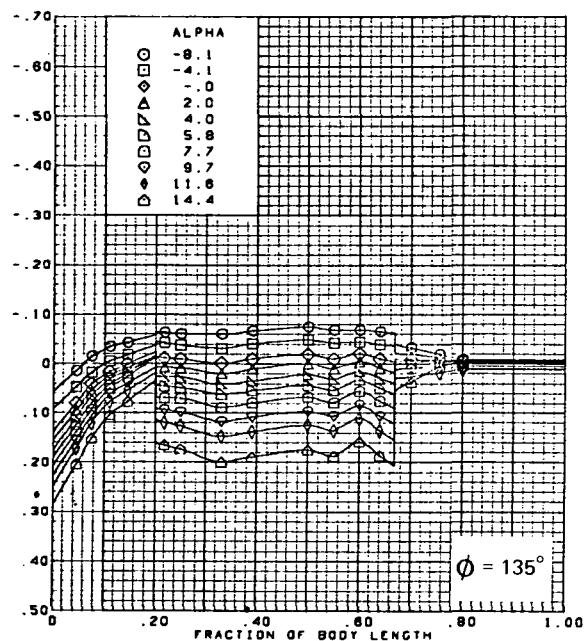
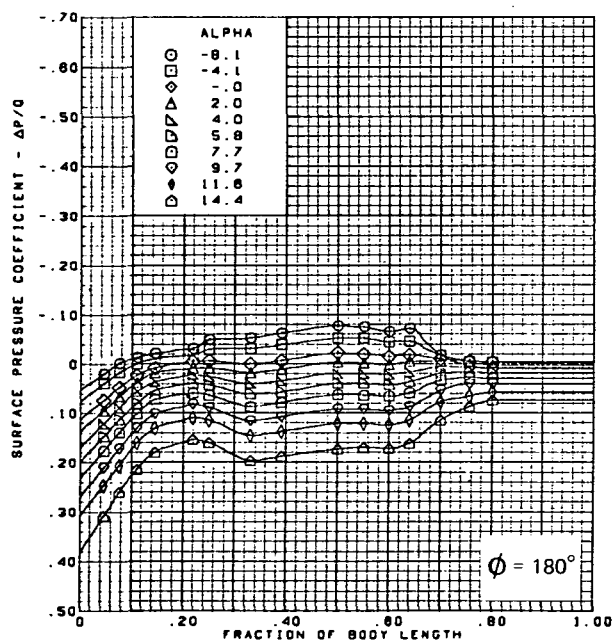
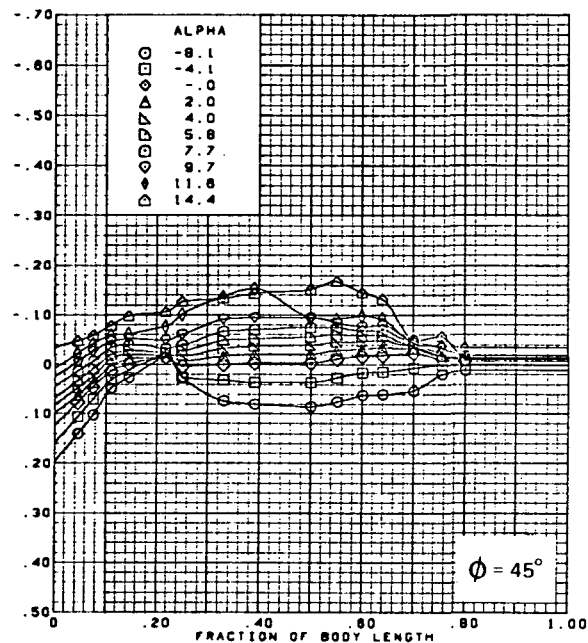
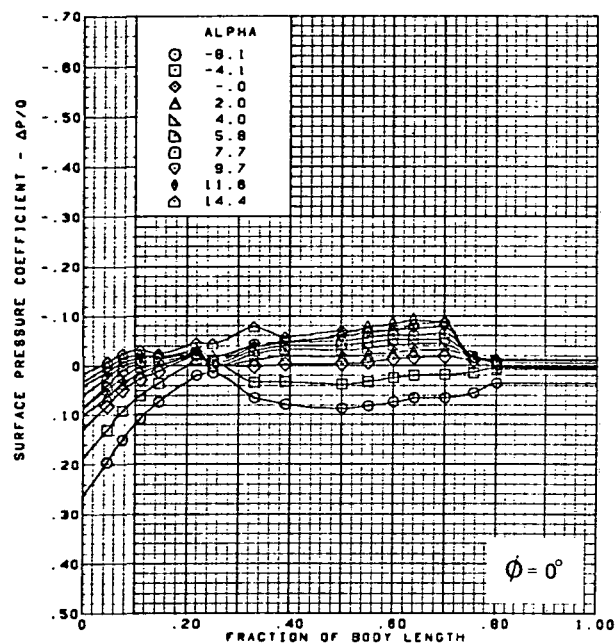
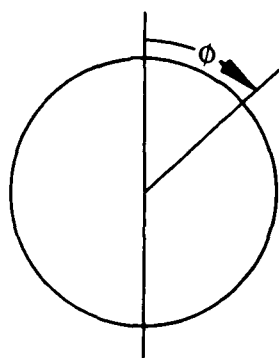
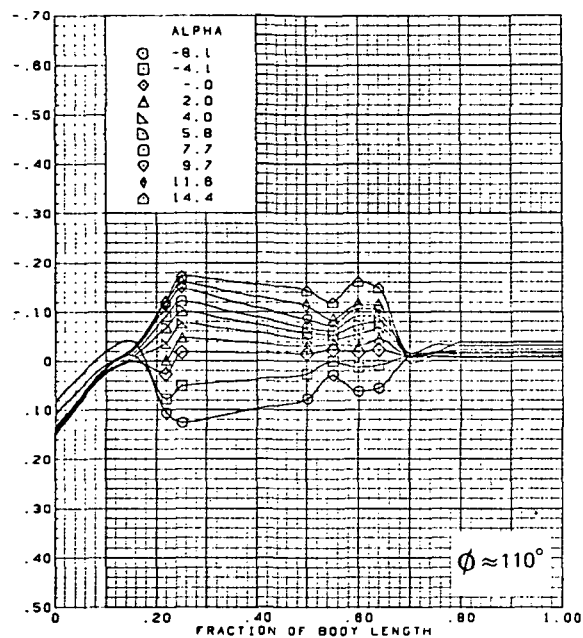
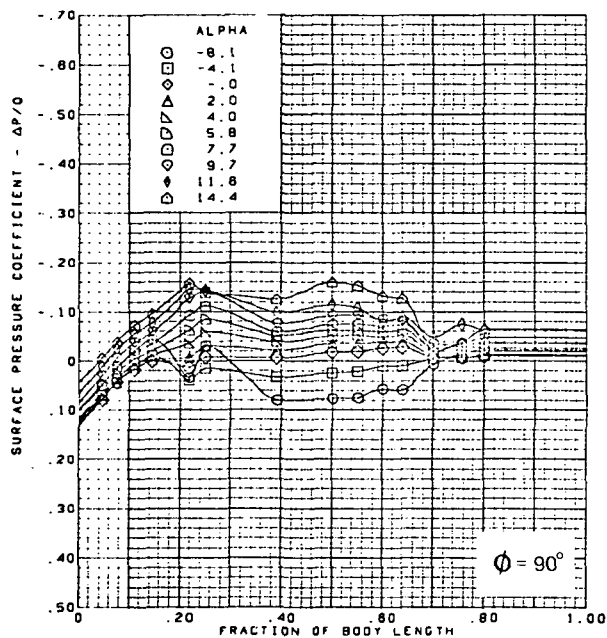


Figure 41.—Body Surface Longitudinal Pressure Distributions—Effect of Angle of Attack; Flat Wing, Rounded L.E.; L.E. Deflection, Full Span =  $0.0^\circ$ ; T.E. Deflection, Full Span =  $0.0^\circ$ ;  $M = 2.50$



$M = 2.50$  (run 22)  
 Flat wing, rounded L.E.  
 L.E. deflection, full span =  $0.0^\circ$   
 T.E. deflection, full span =  $0.0^\circ$

Note:  $C_{p, \text{vacuum}} = -0.23$

Figure 41.—(Concluded)

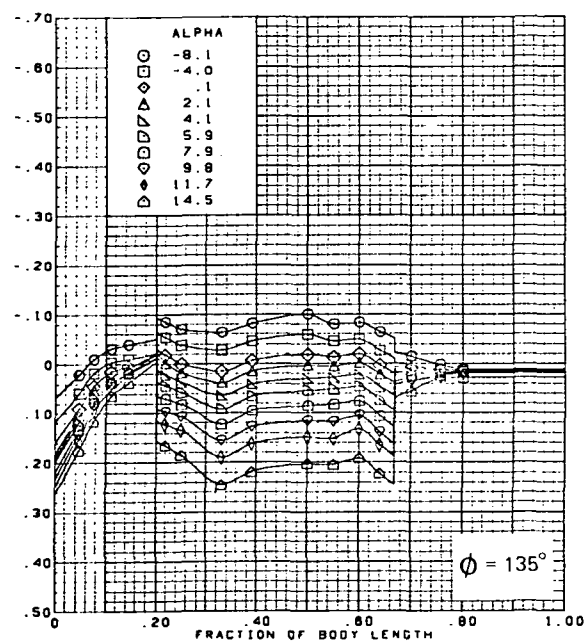
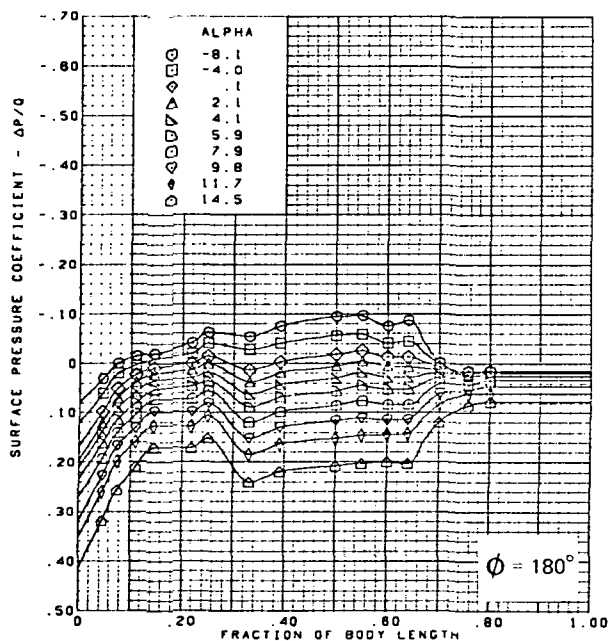
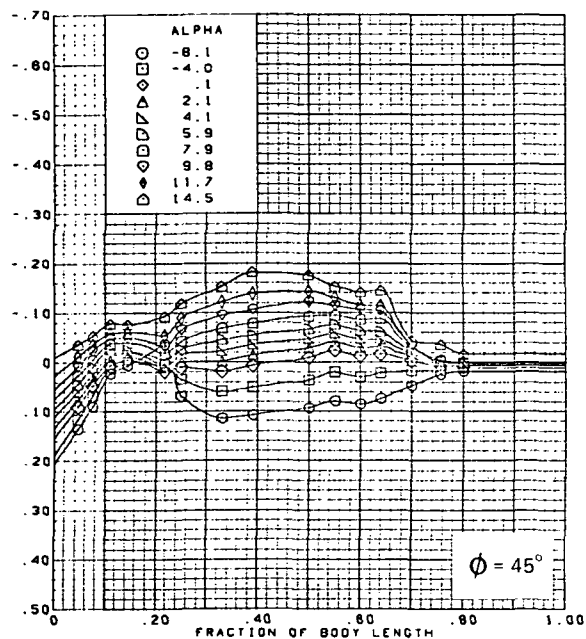
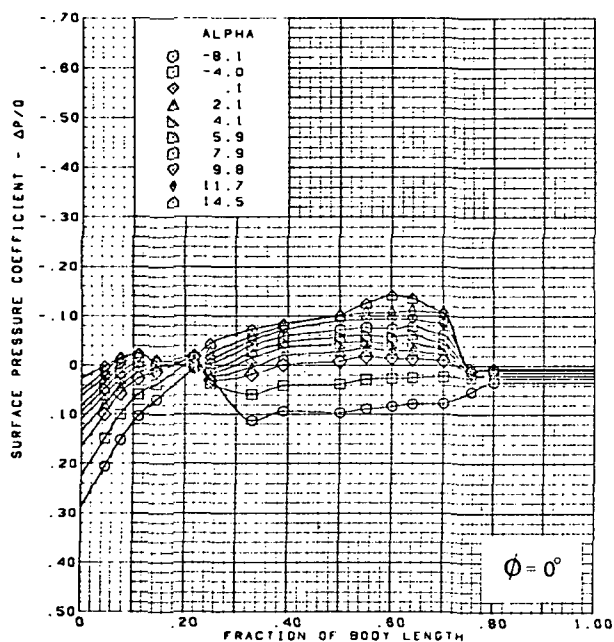
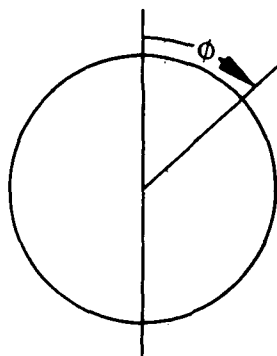
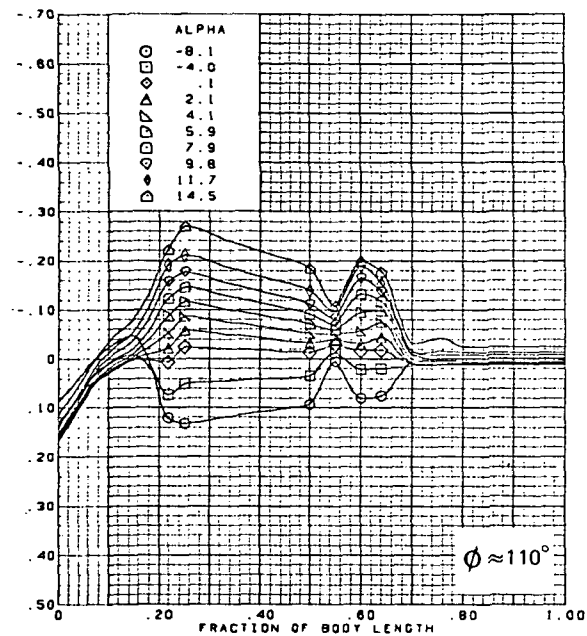
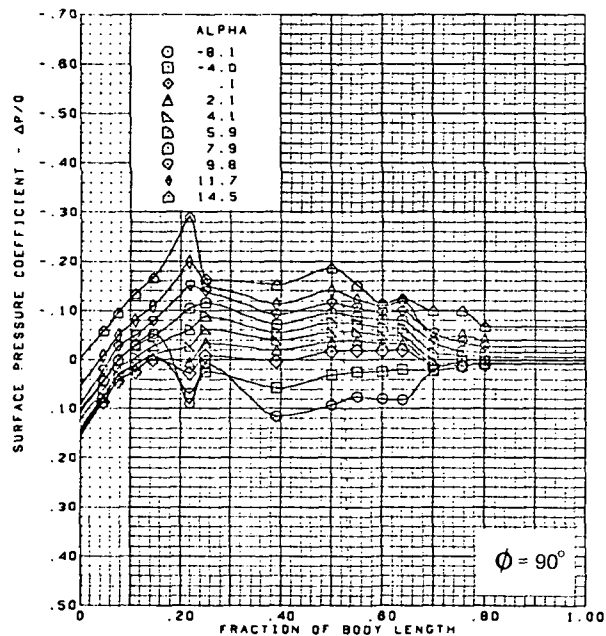


Figure 42.—Body Surface Longitudinal Pressure Distributions—Effect of Angle of Attack; Flat Wing, Sharp L.E.; L.E. Deflection, Full Span =  $0.0^\circ$ ; T.E. Deflection, Full Span =  $0.0^\circ$ ;  $M = 1.70$





$M = 1.70$  (run 51)  
 Flat wing, sharp L.E.  
 L.E. deflection, full span =  $0.0^\circ$   
 T.E. deflection, full span =  $0.0^\circ$

Note:  $C_{p, \text{vacuum}} = -0.49$

Figure 42.—(Concluded)

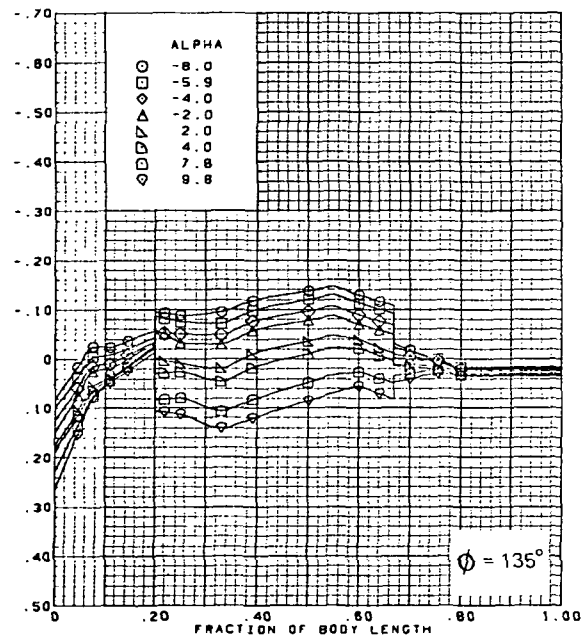
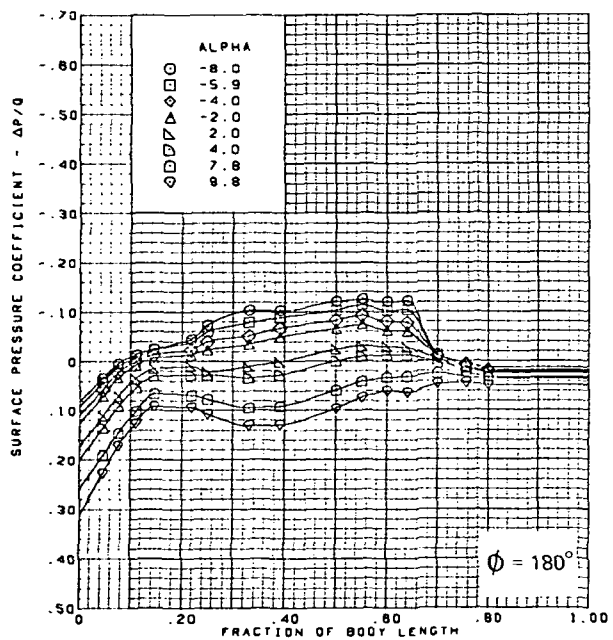
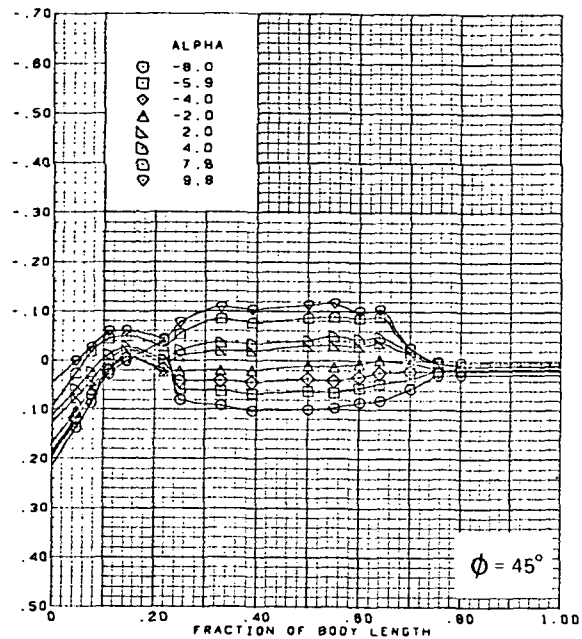
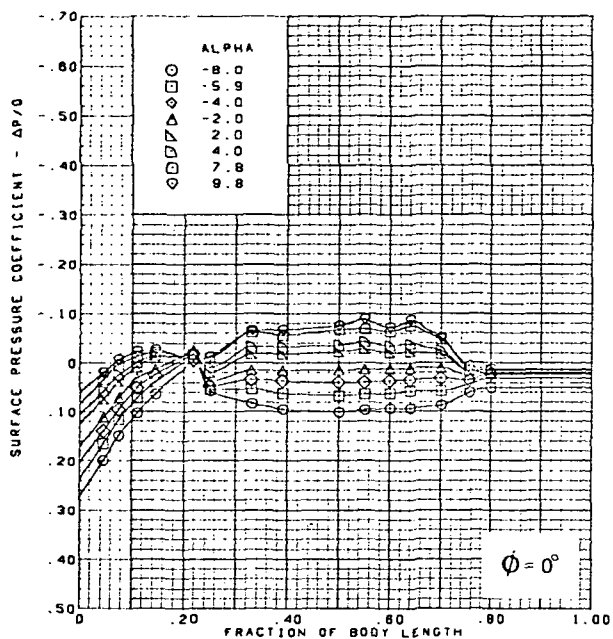
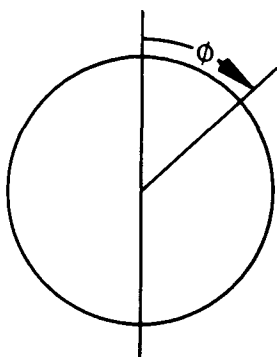
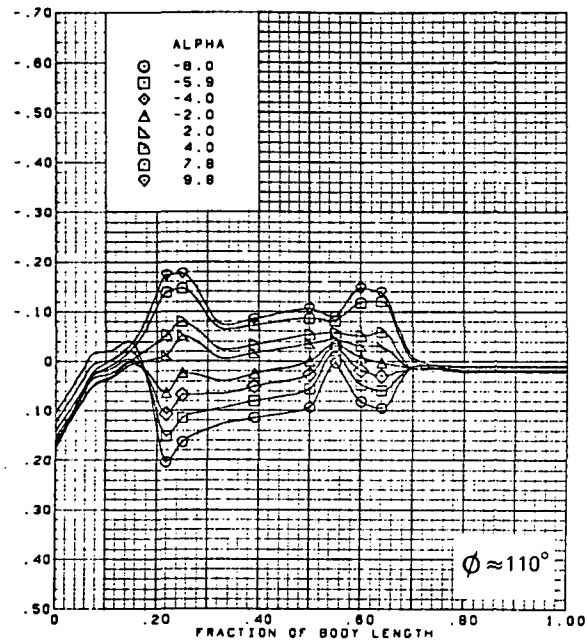
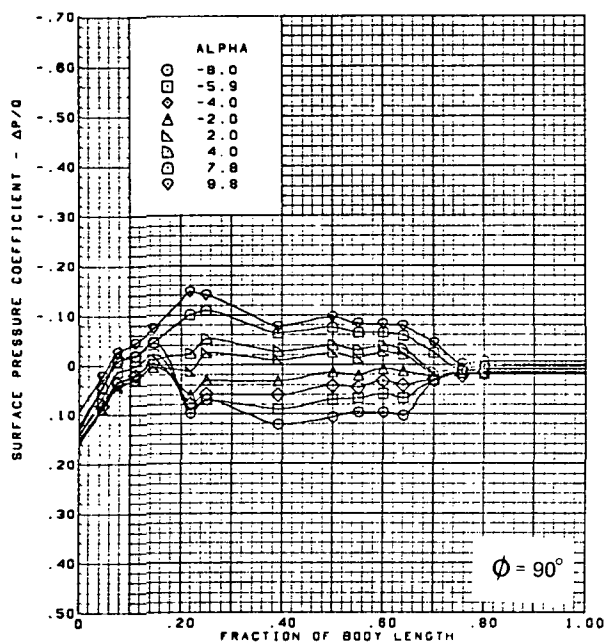


Figure 43.—Body Surface Longitudinal Pressure Distributions—Effect of Angle of Attack; Twisted Wing, Rounded L.E.; L.E. Deflection, Full Span =  $0.0^\circ$ ; T.E. Deflection, Full Span =  $0.0^\circ$ ;  $M = 1.60$



$M = 1.60$  (run 1)  
 Twisted wing, rounded L.E.  
 L.E. deflection, full span =  $0.0^\circ$   
 T.E. deflection, full span =  $0.0^\circ$

Note:  $C_{p, \text{vacuum}} = -0.56$

Figure 43.—(Concluded)

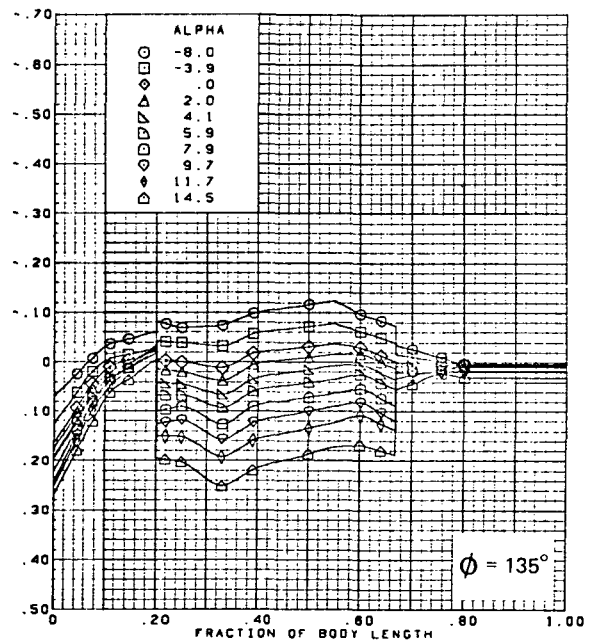
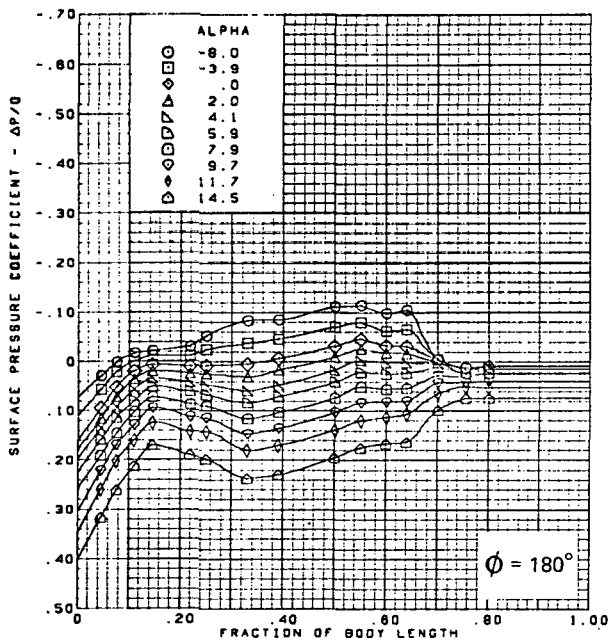
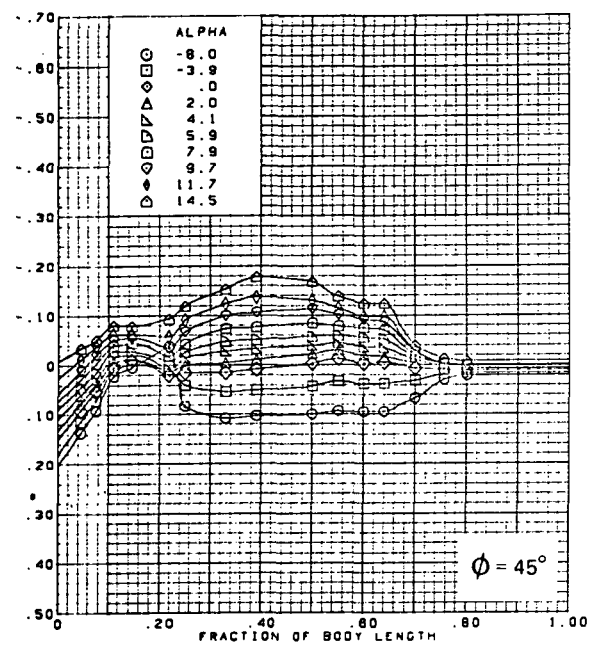
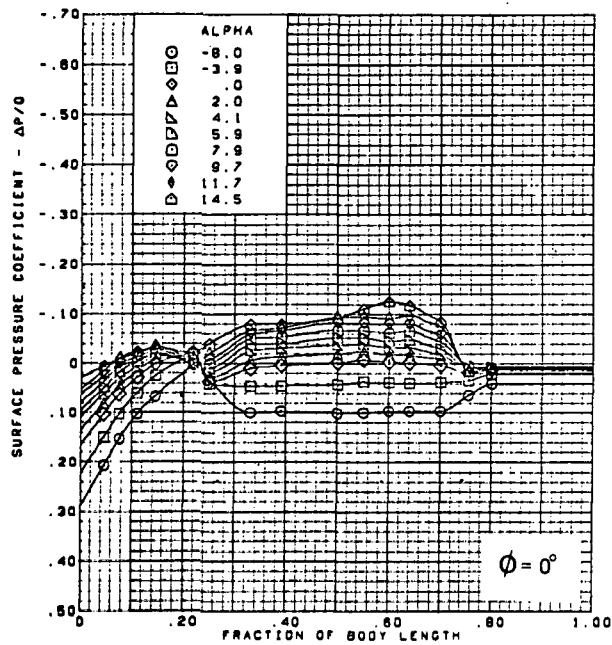
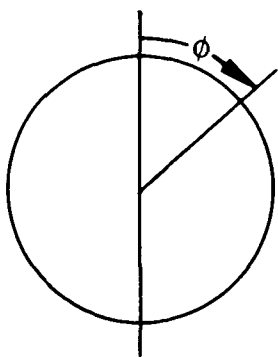
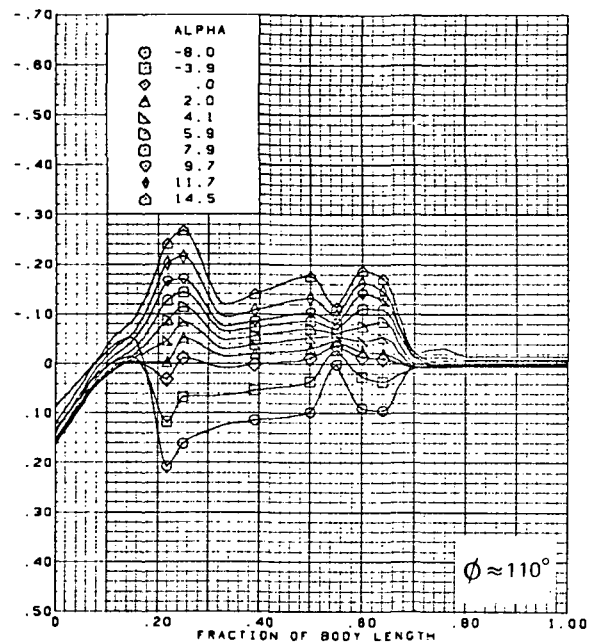
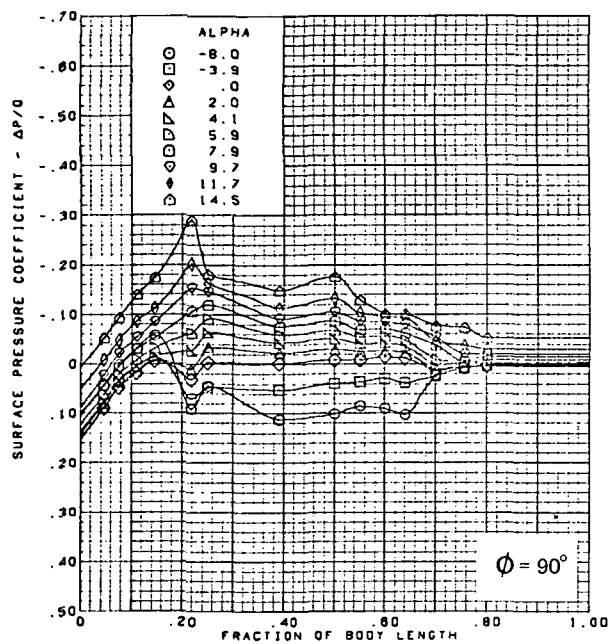


Figure 44.—Body Surface Longitudinal Pressure Distributions—Effect of Angle of Attack;  
Twisted Wing, Rounded L.E.; L.E. Deflection, Full Span =  $0.0^\circ$ ; T.E. Deflection,  
Full Span =  $0.0^\circ$ ;  $M = 1.70$



M = 1.70 (run 3)  
 Twisted wing, rounded L.E.  
 L.E. deflection, full span =  $0.0^\circ$   
 T.E. deflection, full span =  $0.0^\circ$

Note:  $C_{p, \text{vacuum}} = -0.49$

Figure 44.—(Concluded)

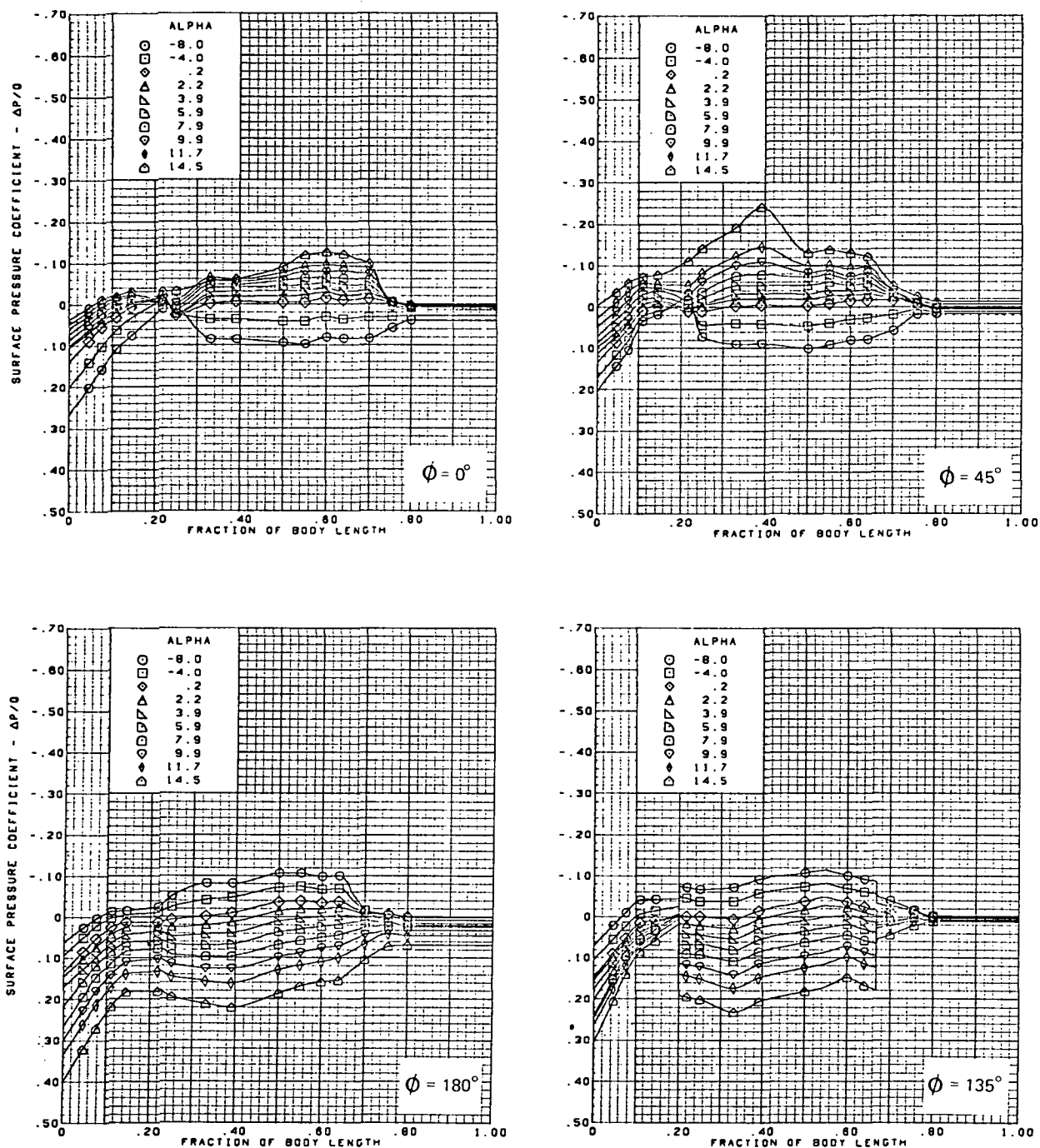
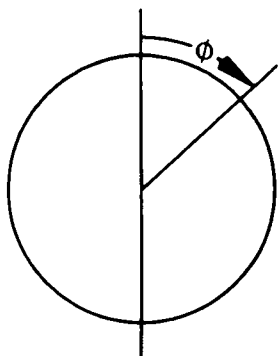
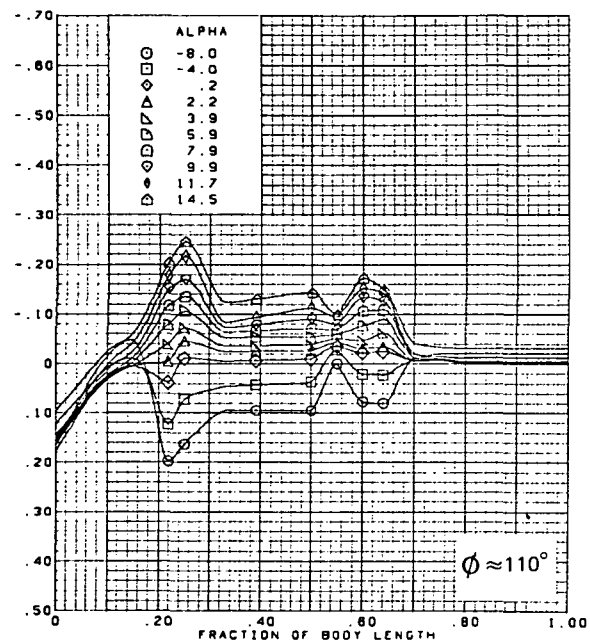
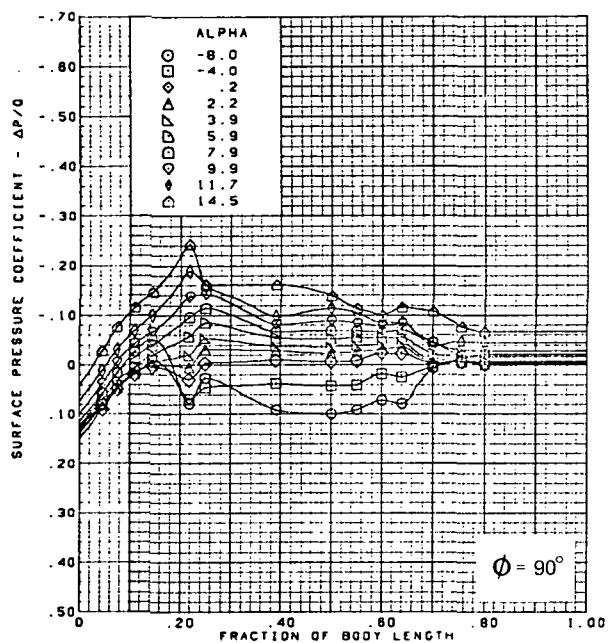


Figure 45.—Body Surface Longitudinal Pressure Distributions—Effect of Angle of Attack;  
Twisted Wing, Rounded L.E.; L.E. Deflection, Full Span =  $0.0^\circ$ ; T.E. Deflection,  
Full Span =  $0.0^\circ$ ;  $M = 1.90$



M = 1.90 (run 4,6)  
 Twisted wing, rounded L.E.  
 L.E. deflection, full span =  $0.0^\circ$   
 T.E. deflection, full span =  $0.0^\circ$

Note:  $C_{p, \text{vacuum}} = -0.40$

Figure 45.—(Concluded)

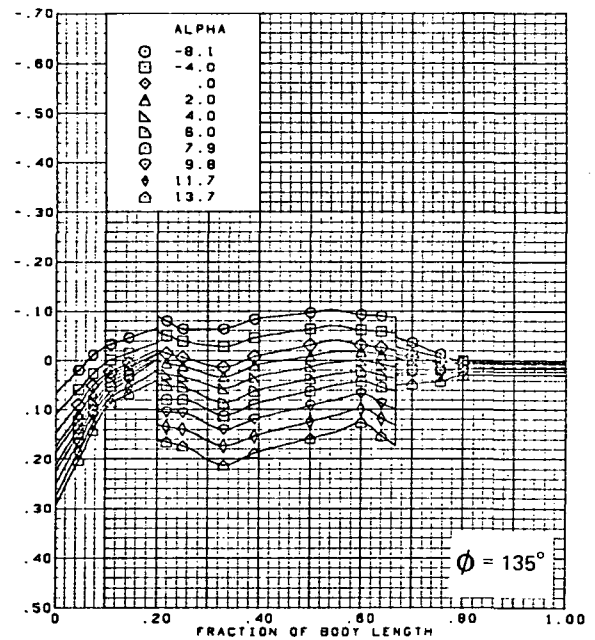
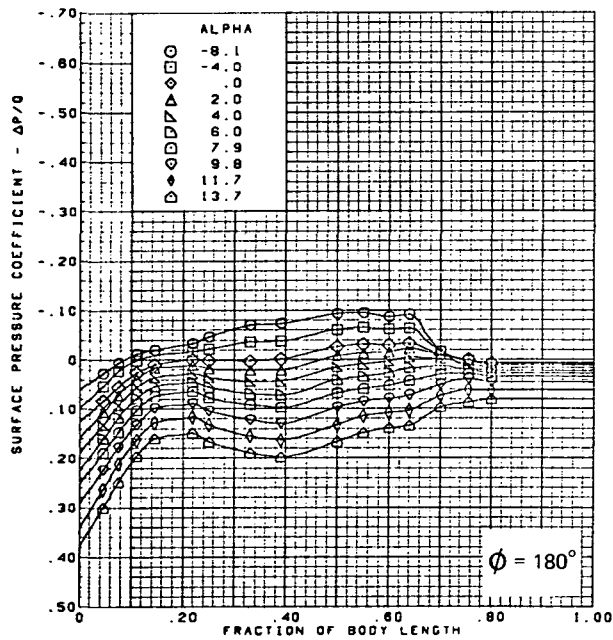
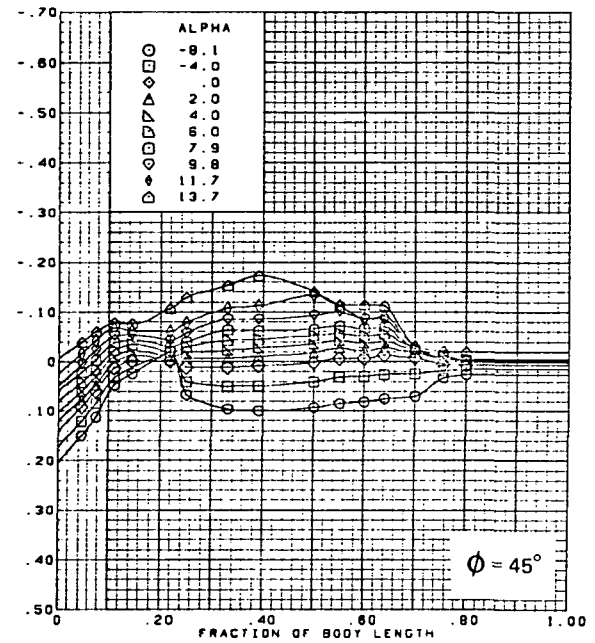
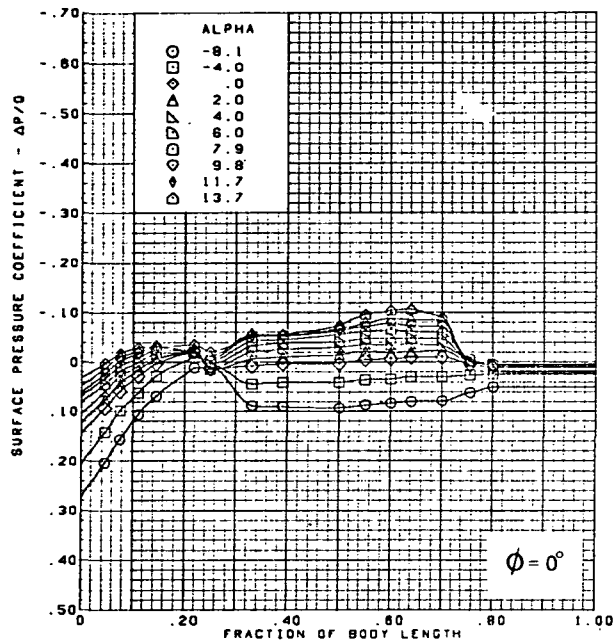
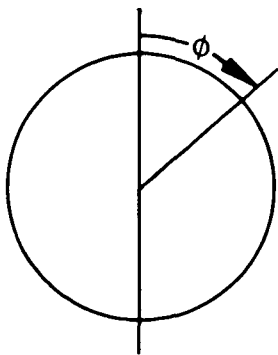
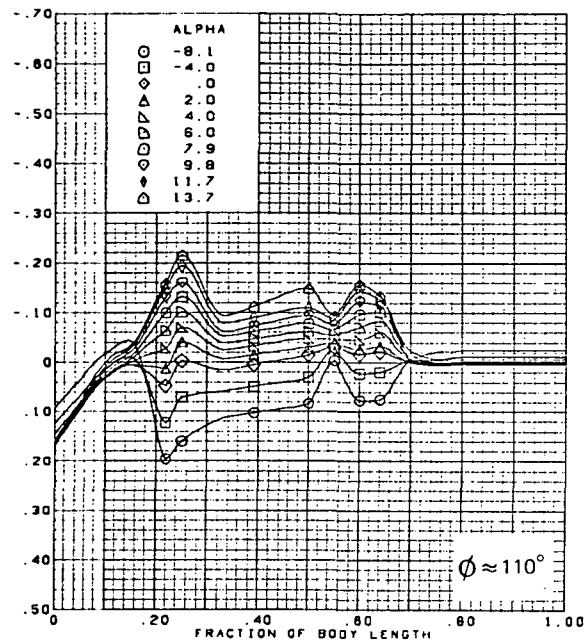
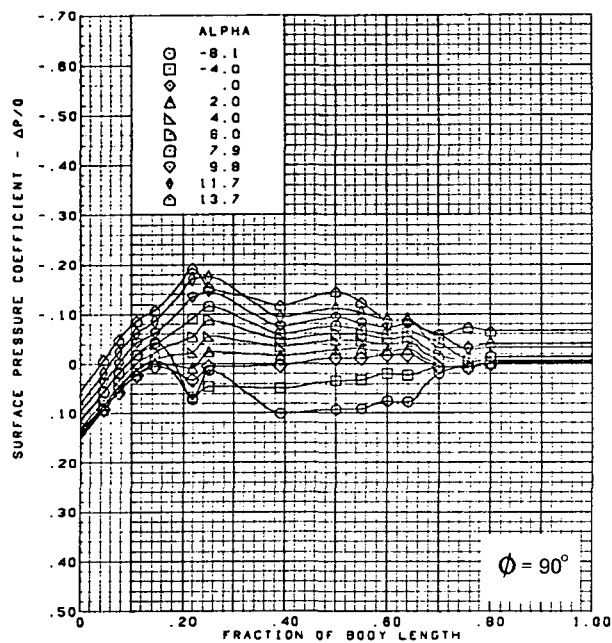


Figure 46.—Body Surface Longitudinal Pressure Distributions—Effect of Angle of Attack; Twisted Wing, Rounded L.E.; L.E. Deflection, Full Span =  $0.0^\circ$ ; T.E. Deflection, Full Span =  $0.0^\circ$ ;  $M = 2.10$





$M = 2.10$  (run 9)  
 Twisted wing, rounded L.E.  
 L.E. deflection, full span =  $0.0^\circ$   
 T.E. deflection, full span =  $0.0^\circ$

Note:  $C_{p, \text{vacuum}} = -0.32$

Figure 46.—(Concluded)

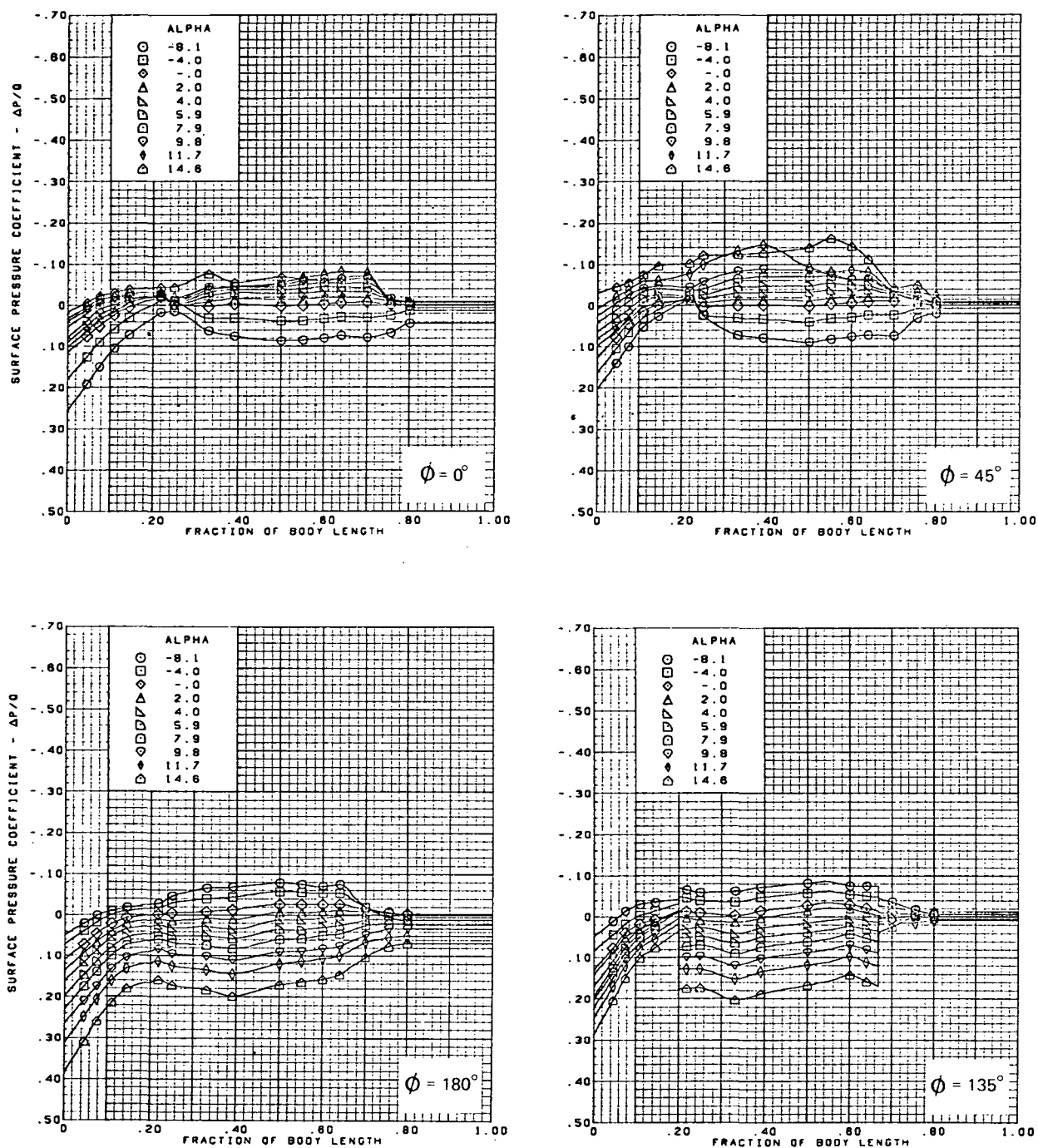
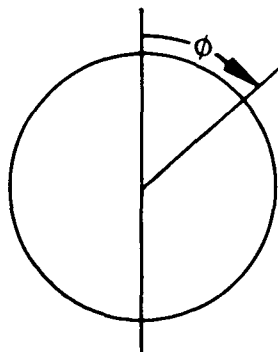
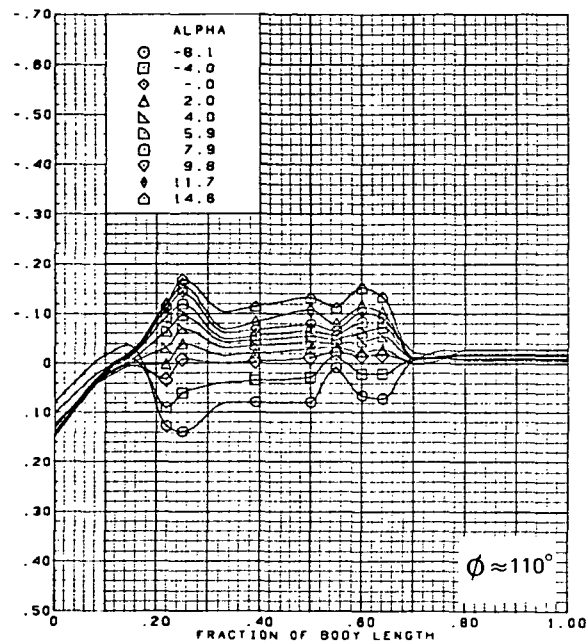
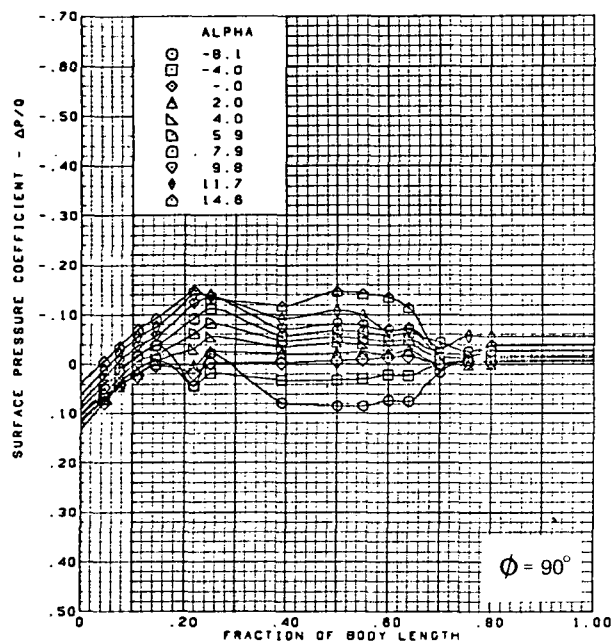


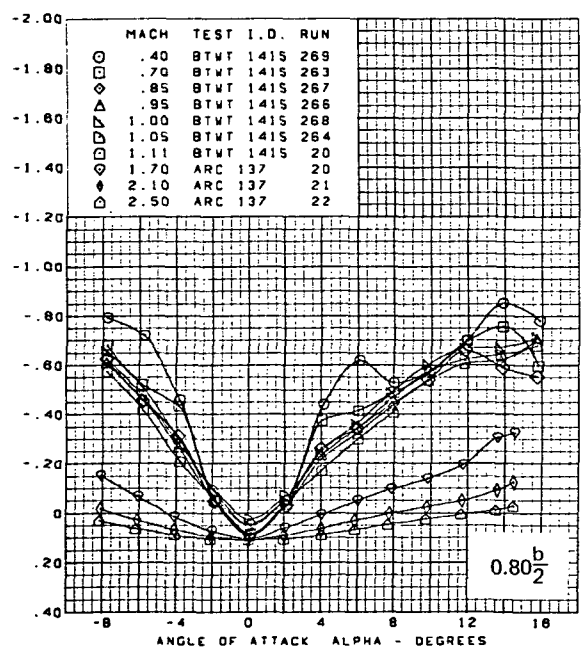
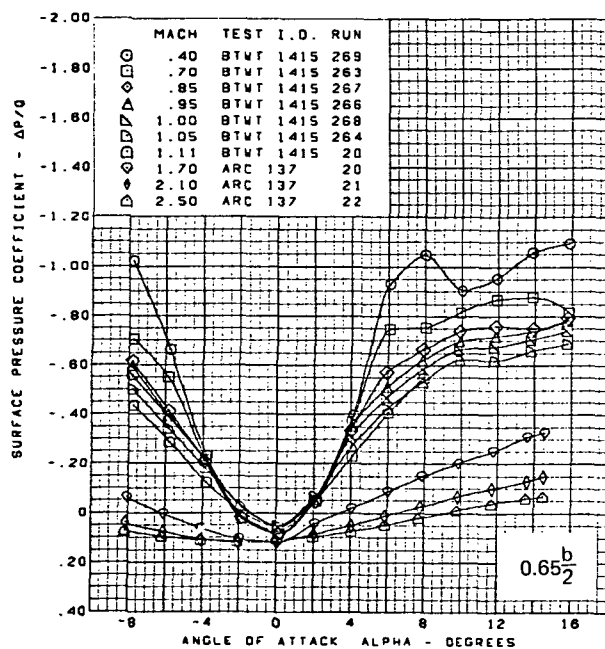
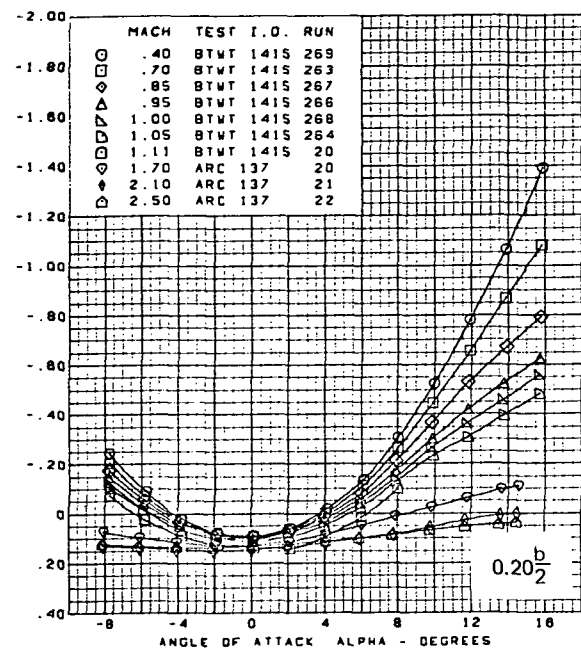
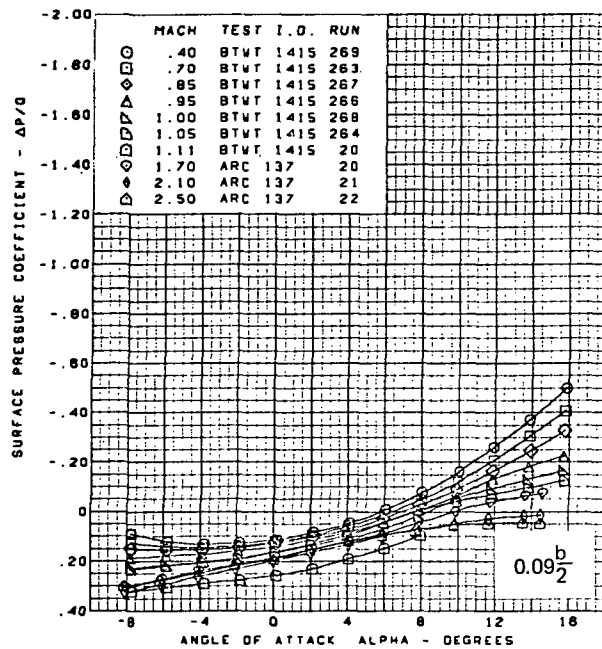
Figure 47.—Body Surface Longitudinal Pressure Distributions—Effect of Angle of Attack; Twisted Wing, Rounded L.E.; L.E. Deflection, Full Span =  $0.0^\circ$ ; T.E. Deflection, Full Span =  $0.0^\circ$ ;  $M = 2.50$



M = 2.50 (run 10)  
 Twisted wing, rounded L.E.  
 L.E. deflection, full span =  $0.0^\circ$   
 T.E. deflection, full span =  $0.0^\circ$

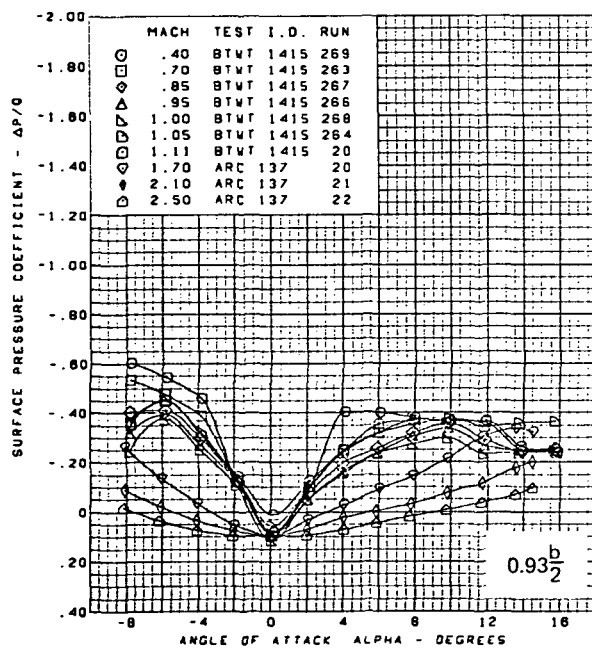
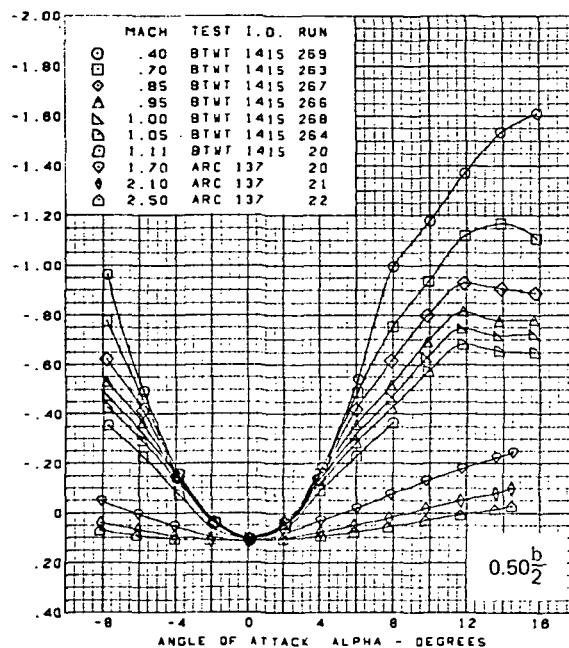
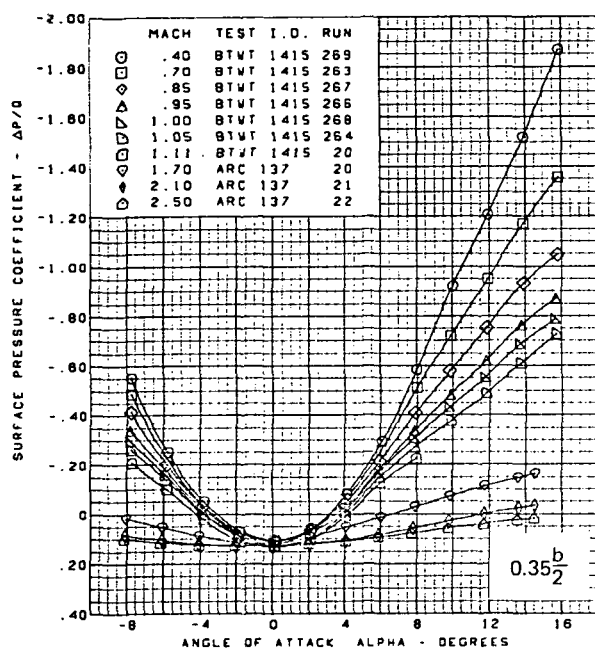
Note:  $C_{p, \text{vacuum}} = -0.23$

Figure 47.—(Concluded)

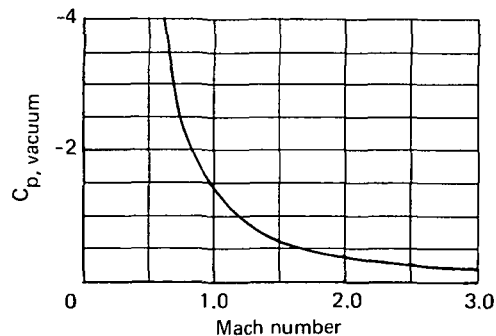


(a) Leading Edge Pressure

Figure 48.—Wing Experimental Data—Effect of Mach Number and Angle of Attack; Flat Wing, Rounded L.E.; L.E. Deflection, Full Span =  $0.0^\circ$ ; T.E. Deflection, Full Span =  $0.0^\circ$

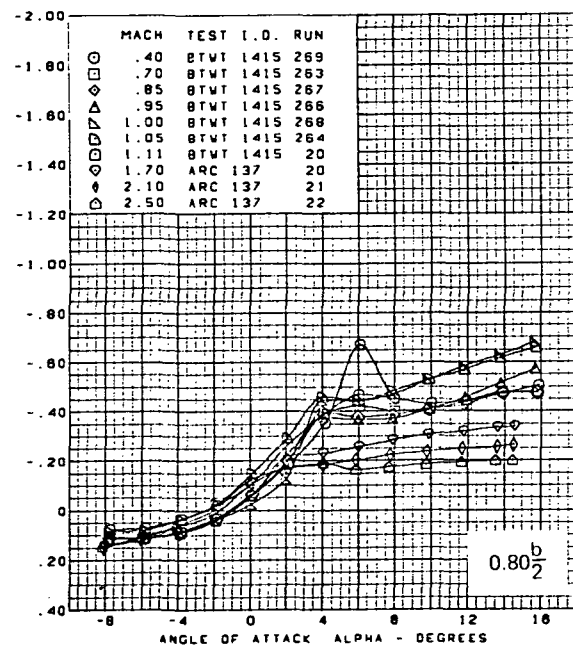
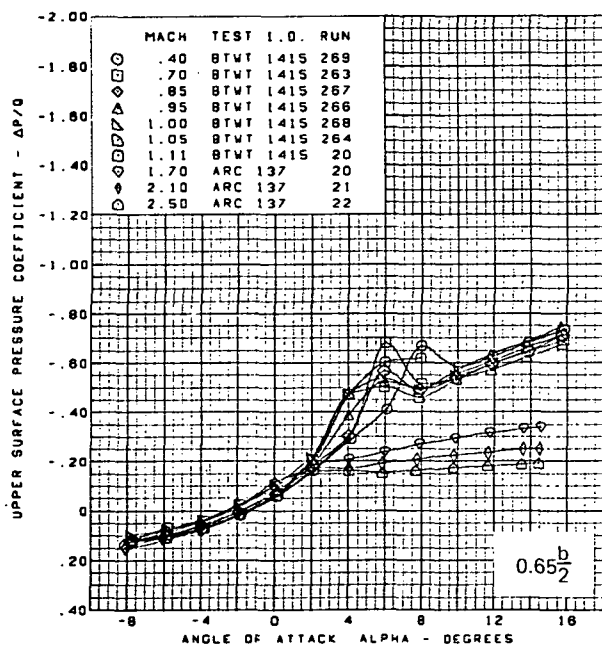
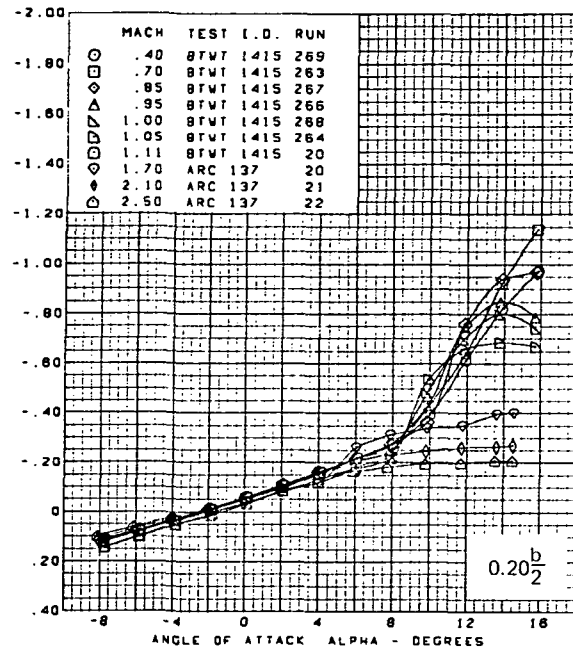
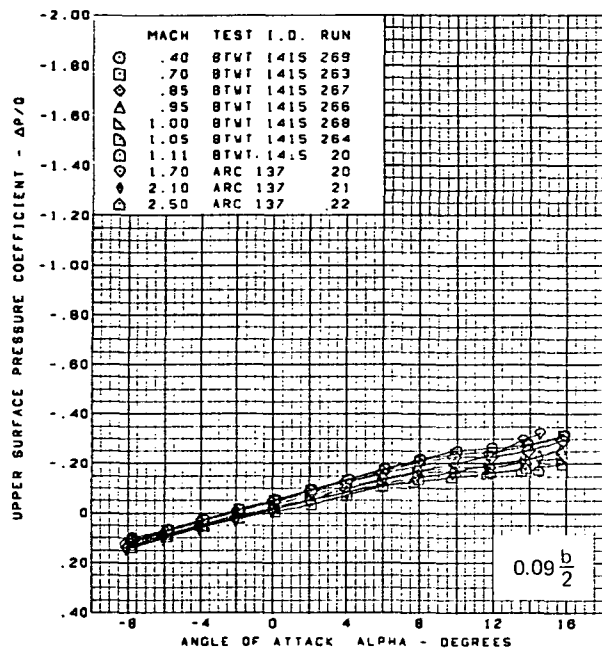


Flat wing, rounded L.E.  
 L.E. deflection, full span =  $0.0^\circ$   
 T.E. deflection, full span =  $0.0^\circ$



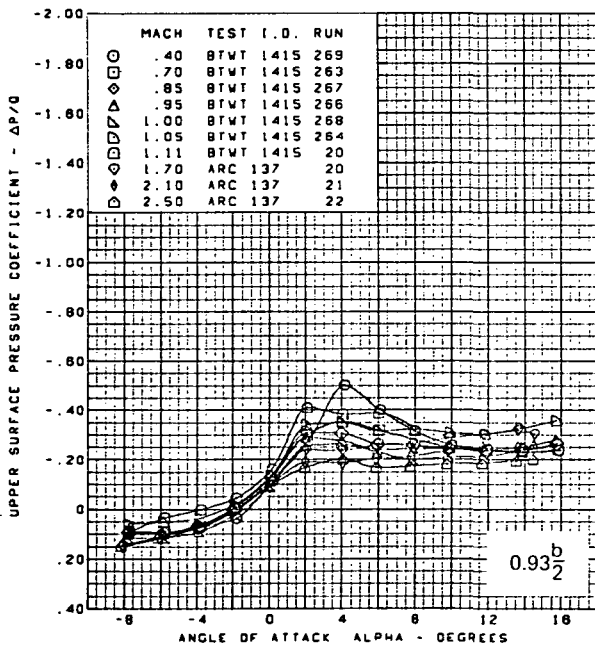
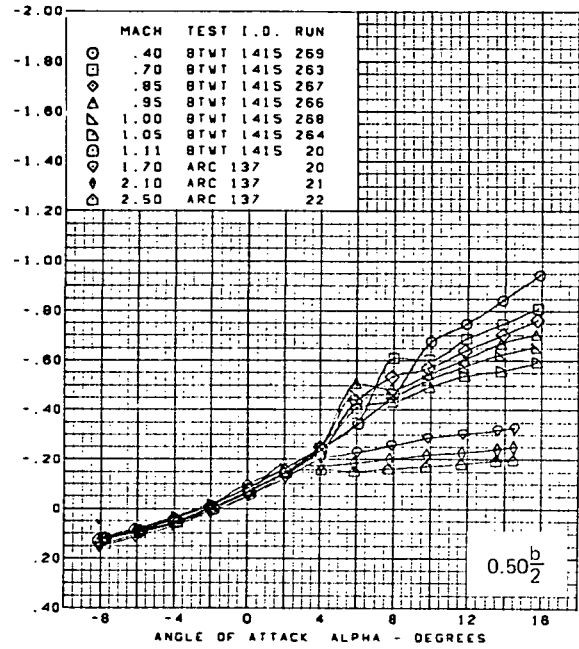
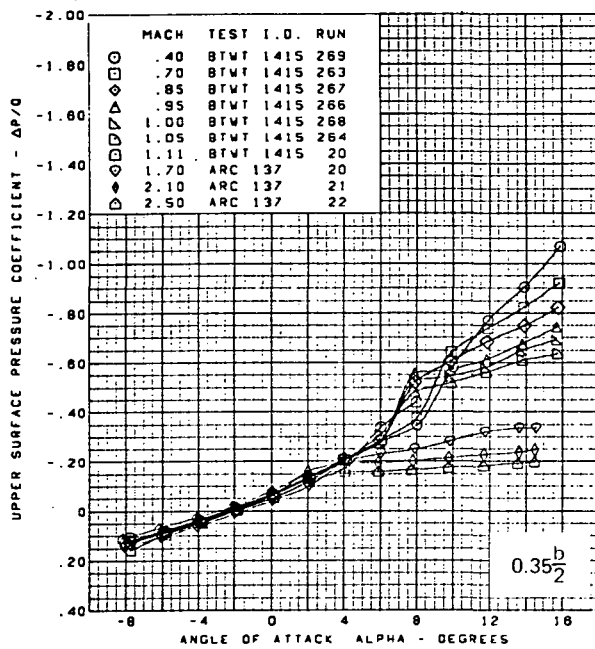
(a) (Concluded)

Figure 48.—(Continued)

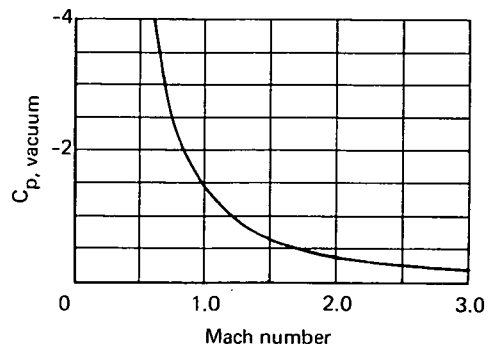


(b) Upper Surface Pressure at  $0.085 \frac{x}{c}$

Figure 48.—(Continued)

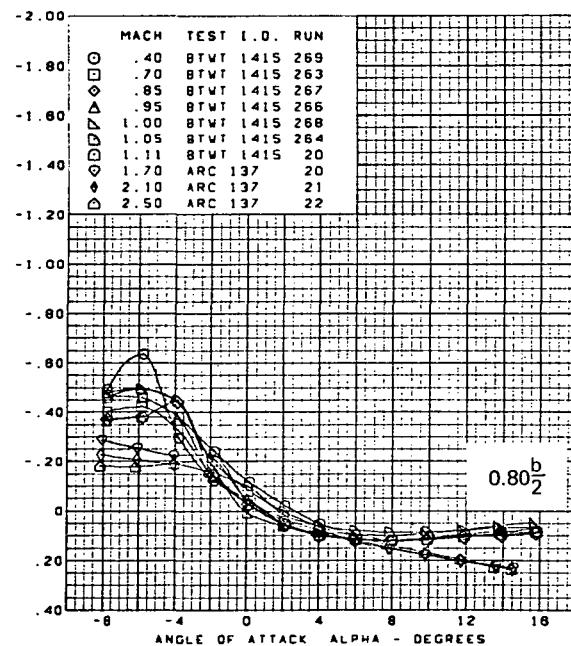
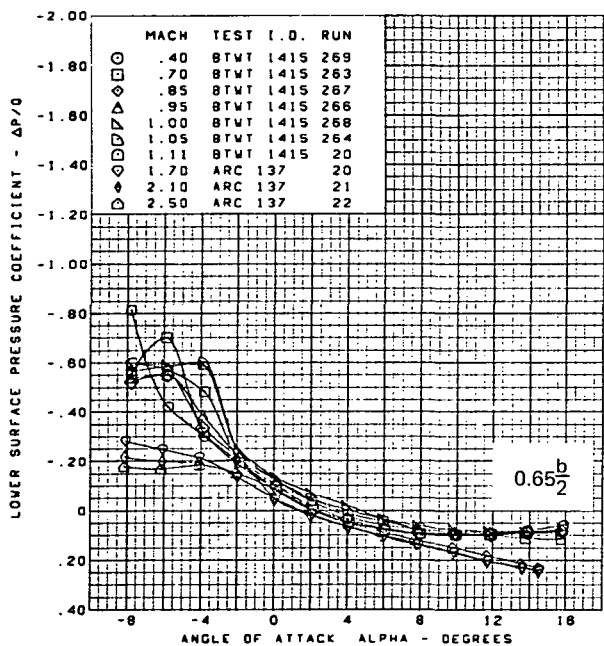
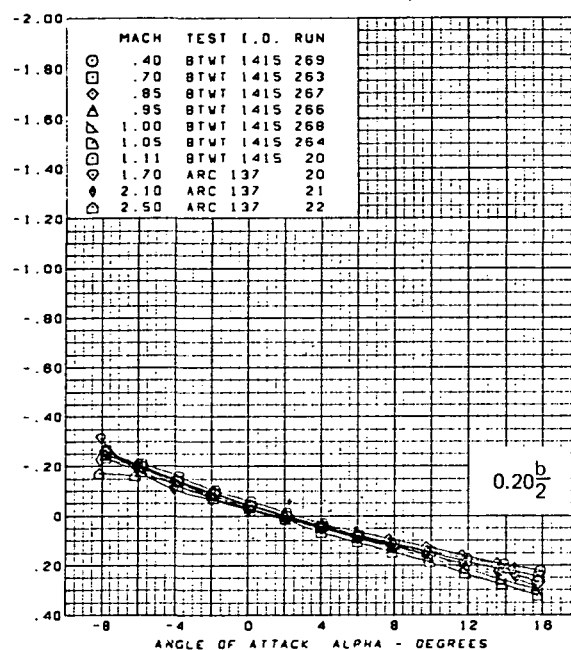
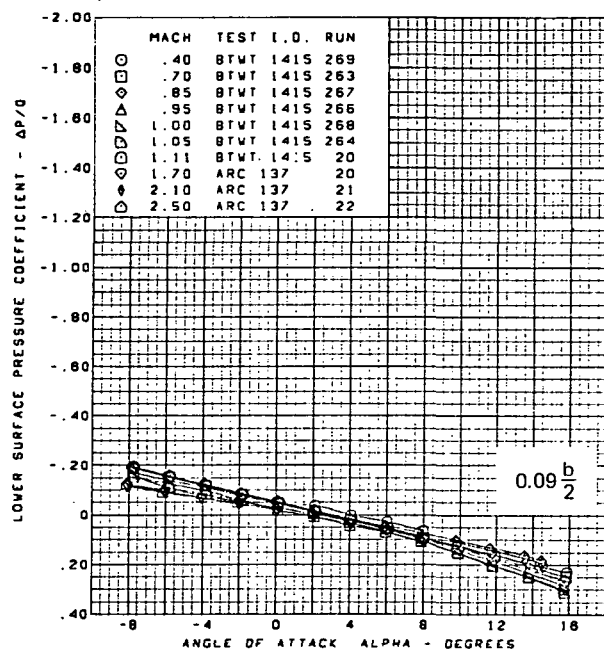


Flat wing, rounded L.E.  
 L.E. deflection, full span =  $0.0^\circ$   
 T.E. deflection, full span =  $0.0^\circ$



(b) (Concluded)

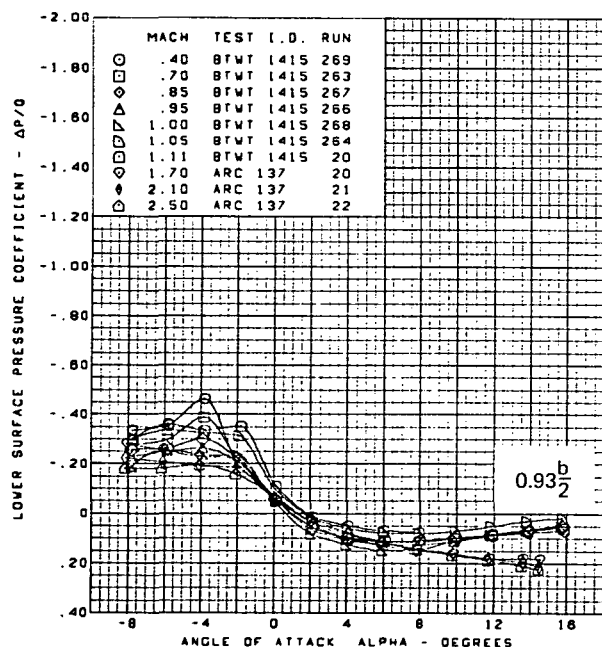
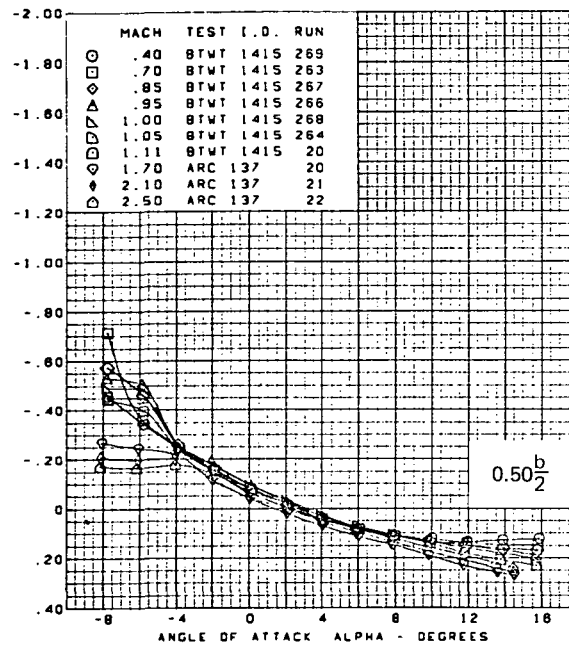
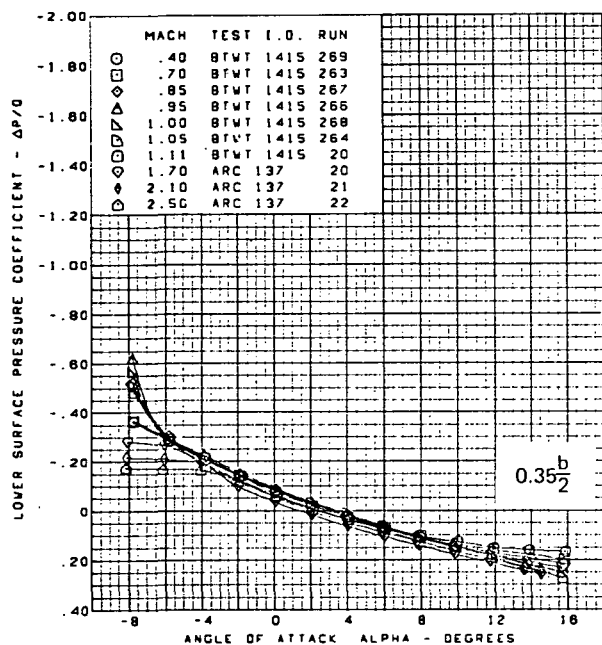
Figure 48.—(Continued)



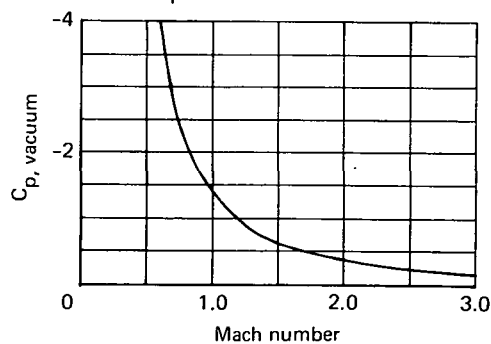
(c) Lower Surface Pressure at  $0.085 \frac{x}{c}$

Figure 48.—(Continued)



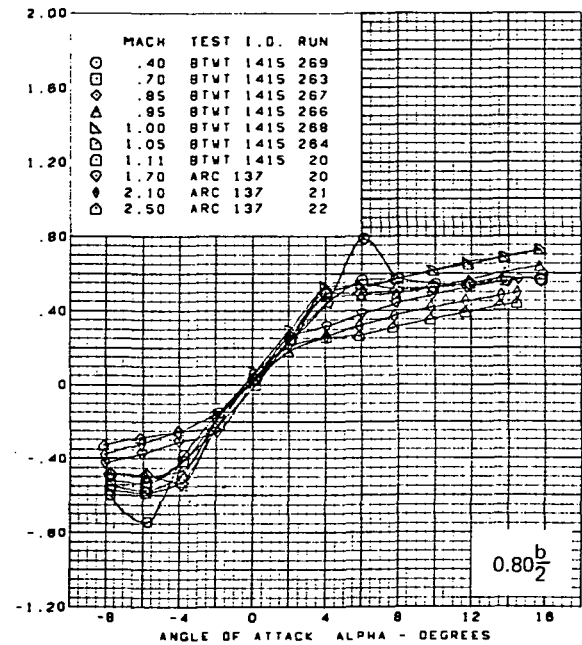
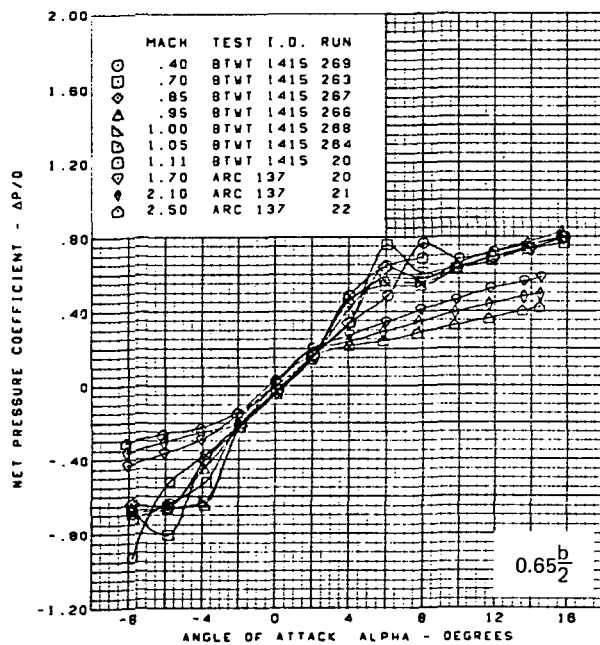
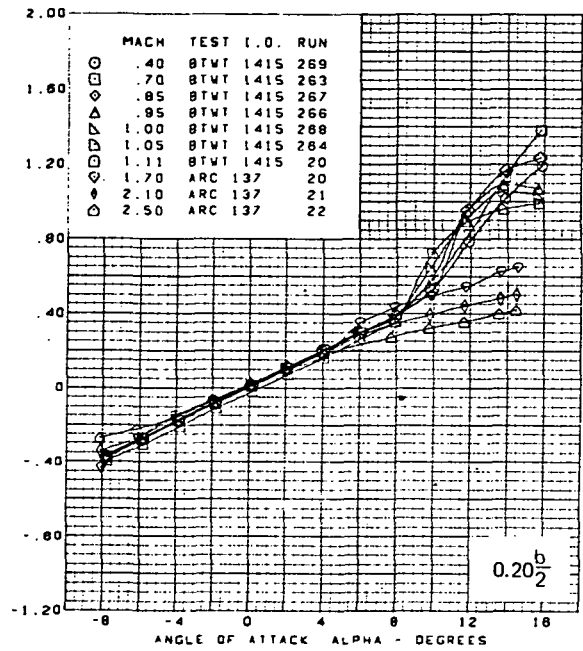
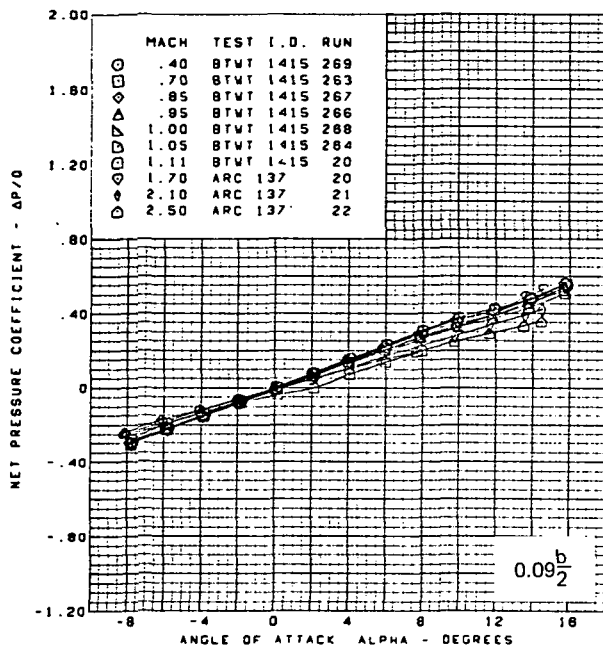


Flat wing, rounded L.E.  
 L.E. deflection, full span =  $0.0^\circ$   
 T.E. deflection, full span =  $0.0^\circ$



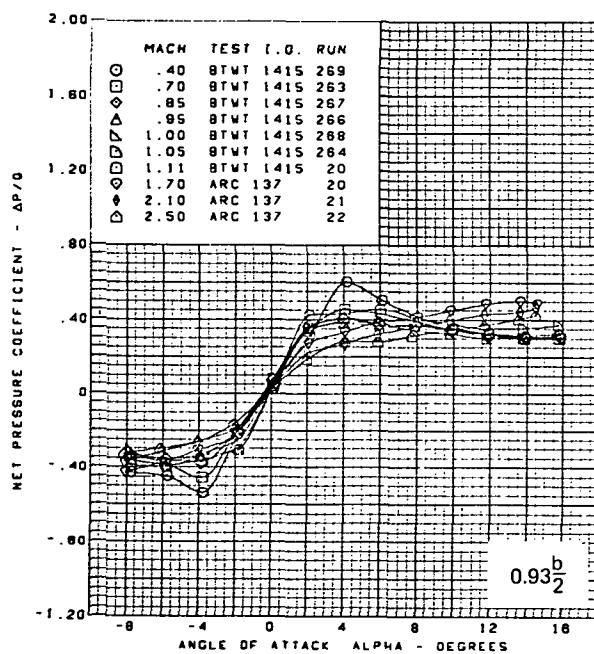
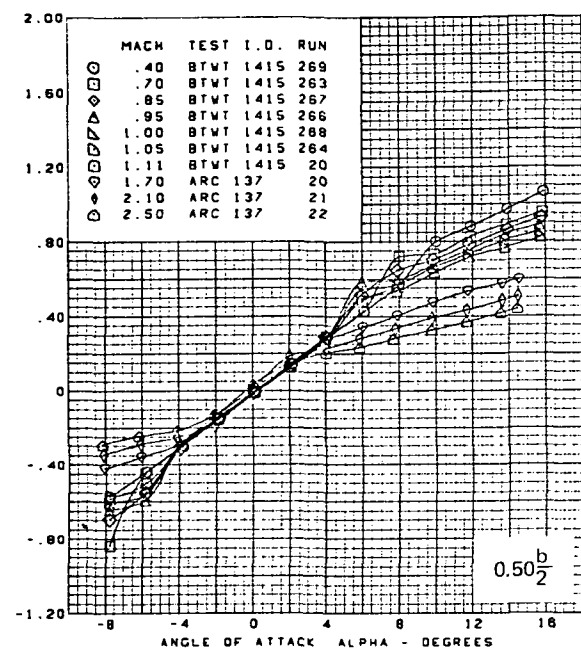
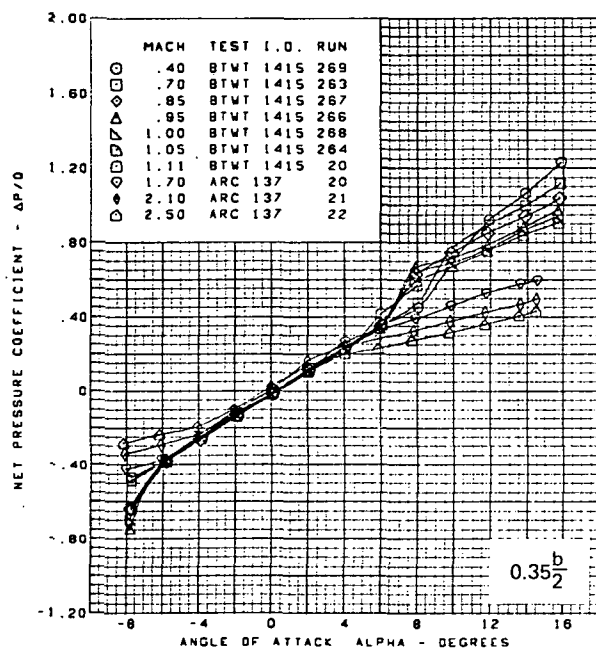
(c) (Concluded)

Figure 48.—(Continued)



(d) Net Pressure at  $0.085 \frac{x}{c}$

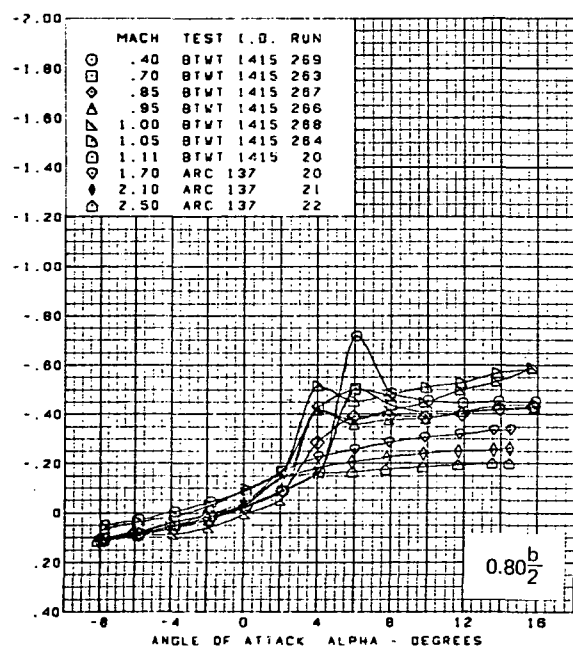
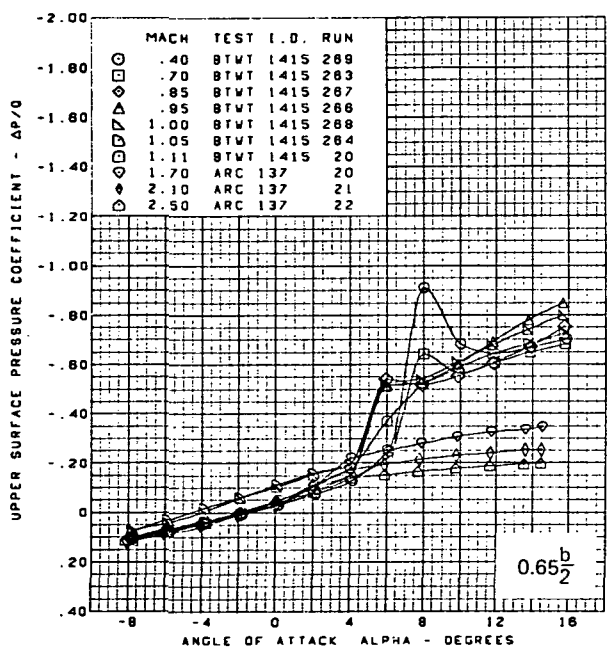
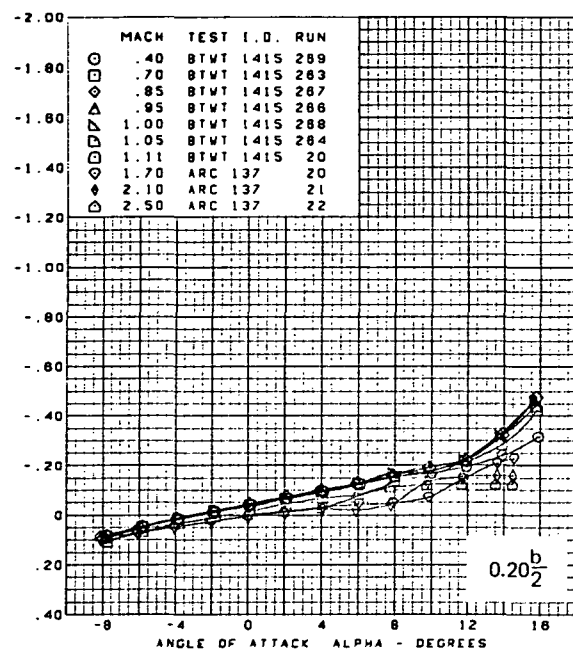
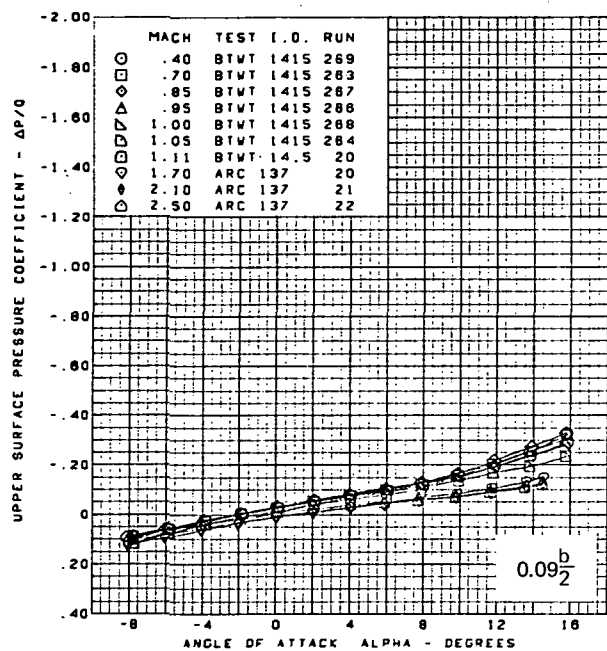
Figure 48.—(Continued)



Flat wing, rounded L.E.  
 L.E. deflection, full span =  $0.0^\circ$   
 T.E. deflection, full span =  $0.0^\circ$

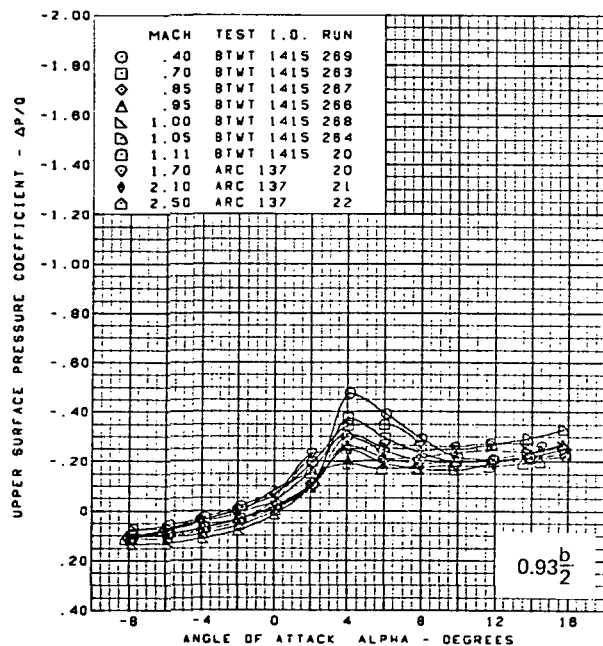
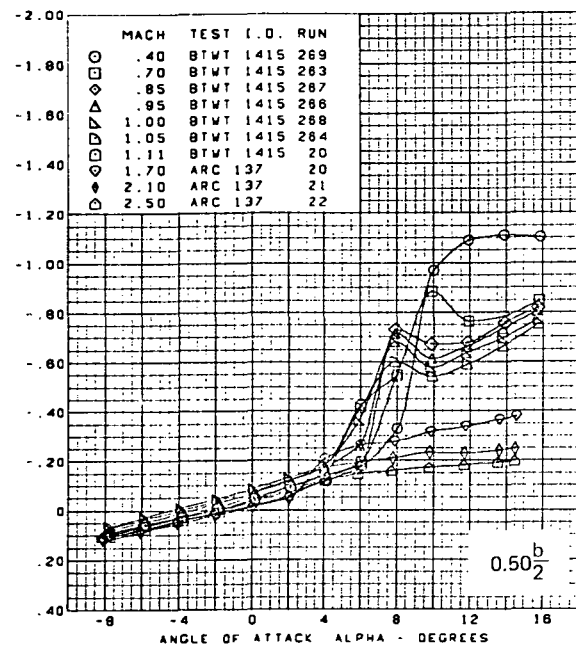
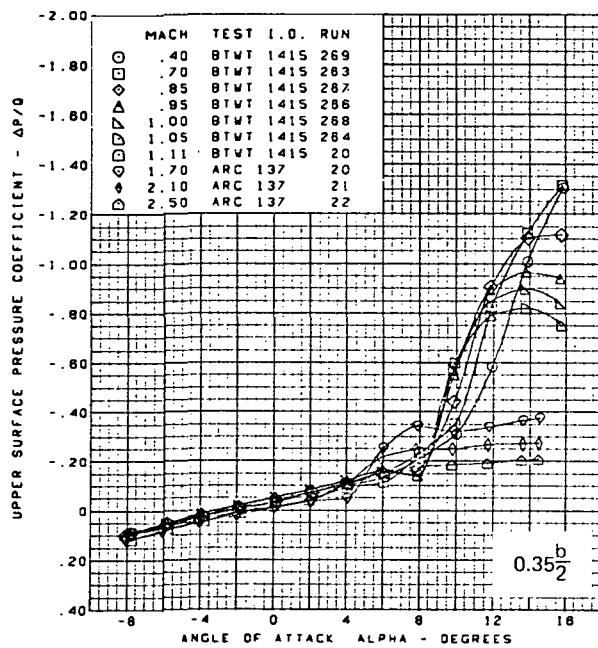
(d) (Concluded)

Figure 48.—(Continued)

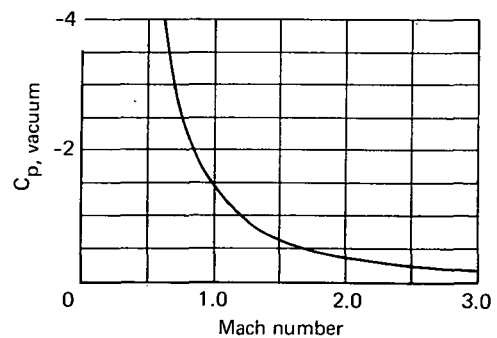


(e) Upper Surface Pressure at  $0.300 \frac{x}{c}$

Figure 48. — (Continued)

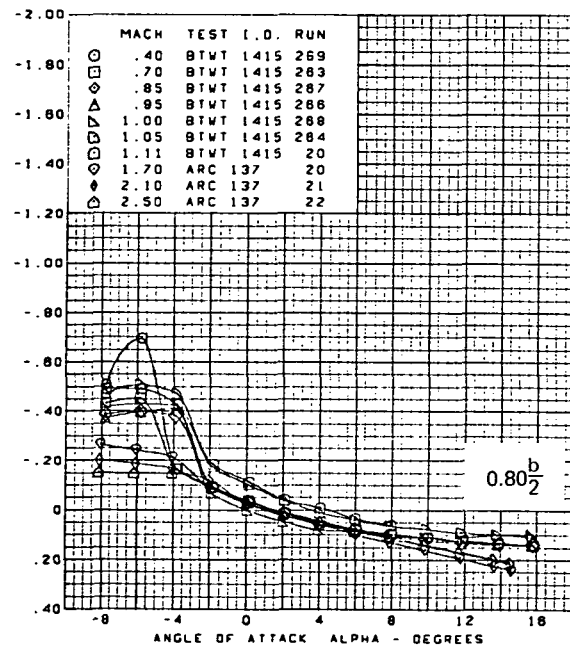
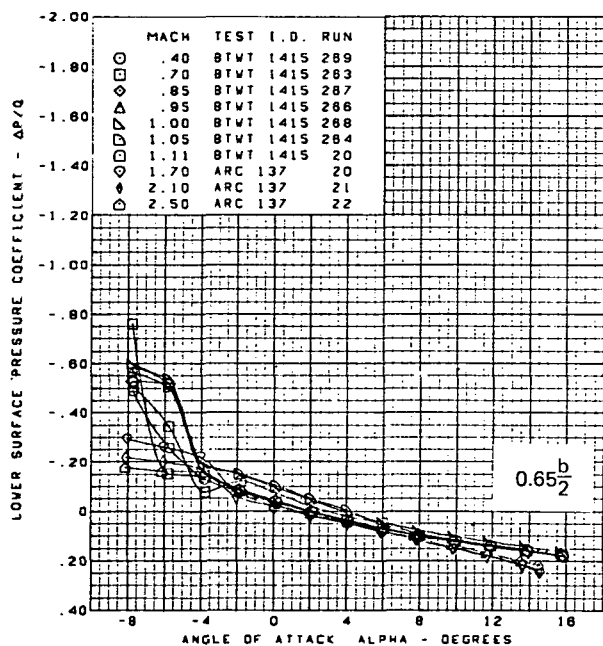
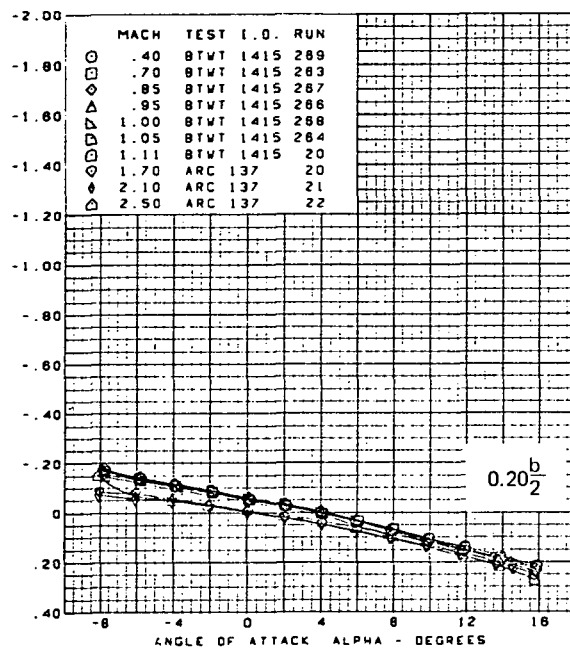
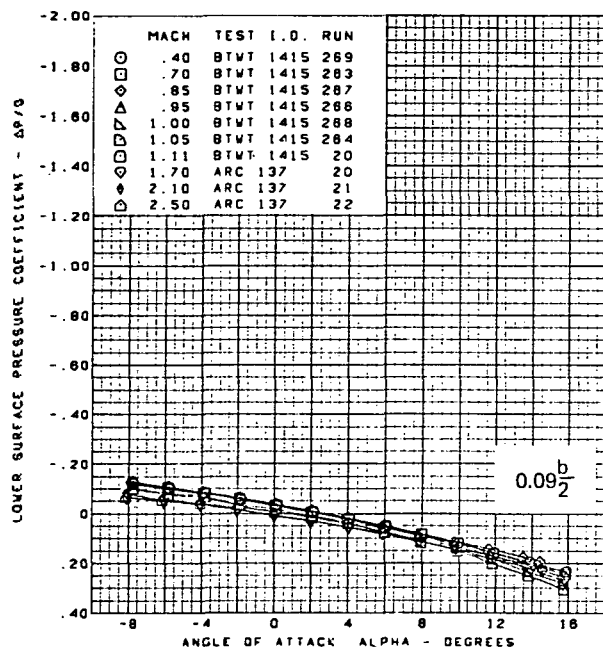


Flat wing, rounded L.E.  
 L.E. deflection, full span =  $0.0^\circ$   
 T.E. deflection, full span =  $0.0^\circ$



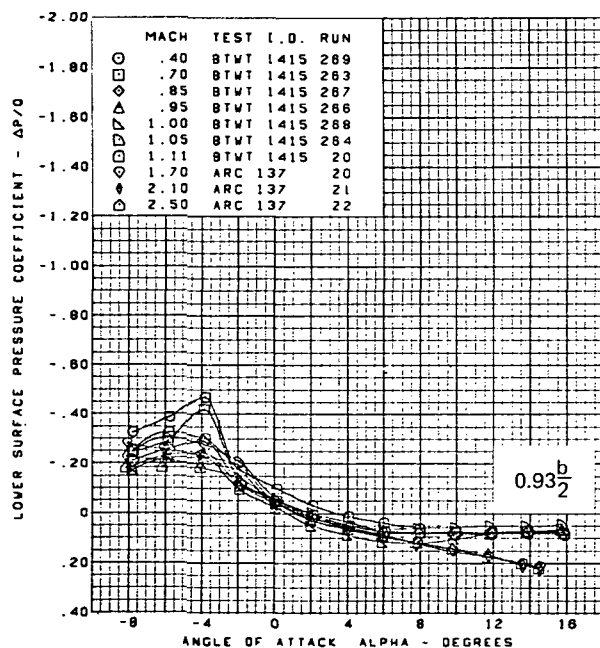
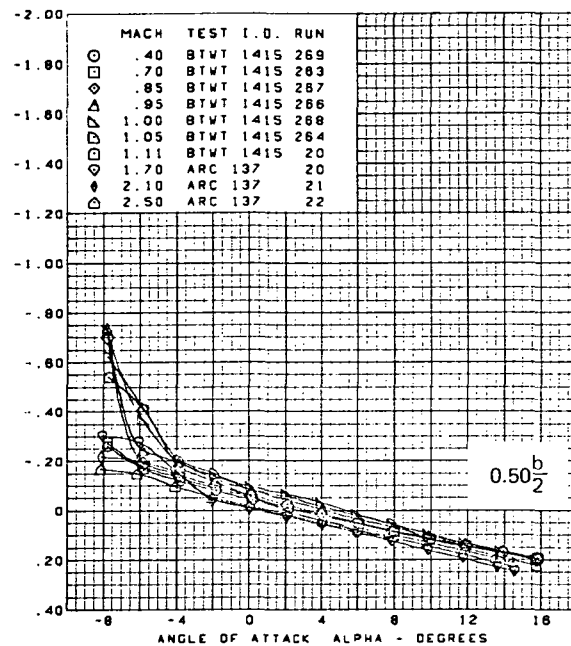
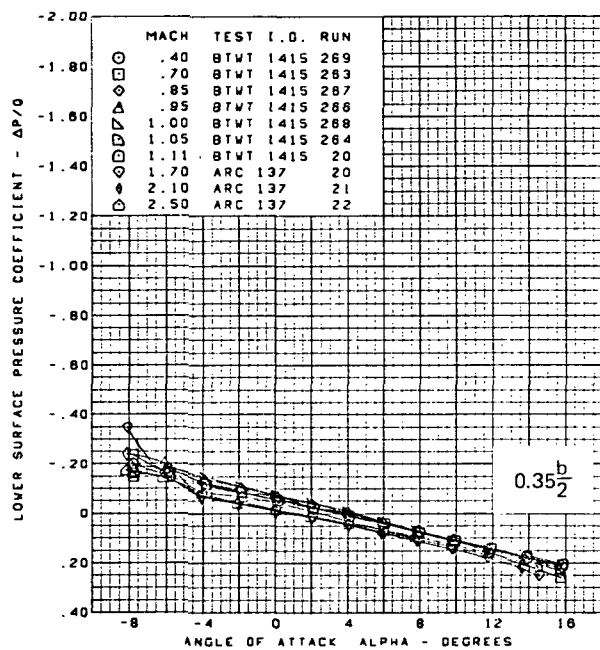
(e) (Concluded)

Figure 48.—(Continued)

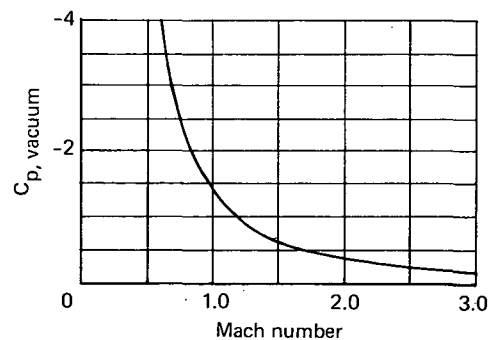


(f) Lower Surface Pressure at  $0.300 \frac{x}{c}$

Figure 48.—(Continued)

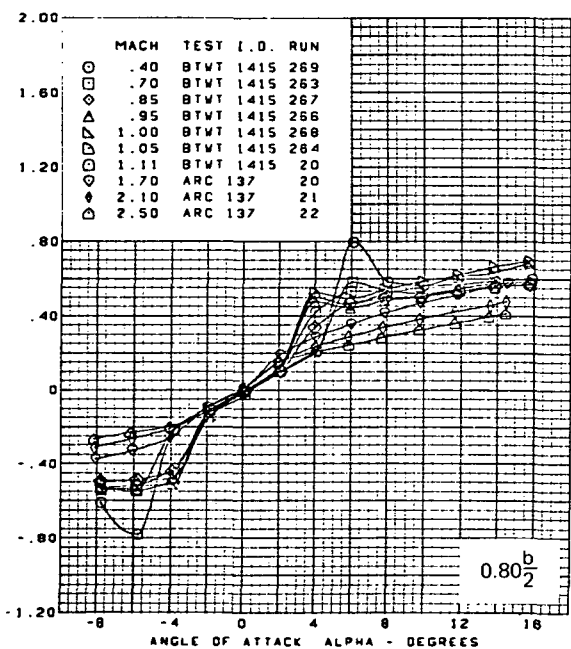
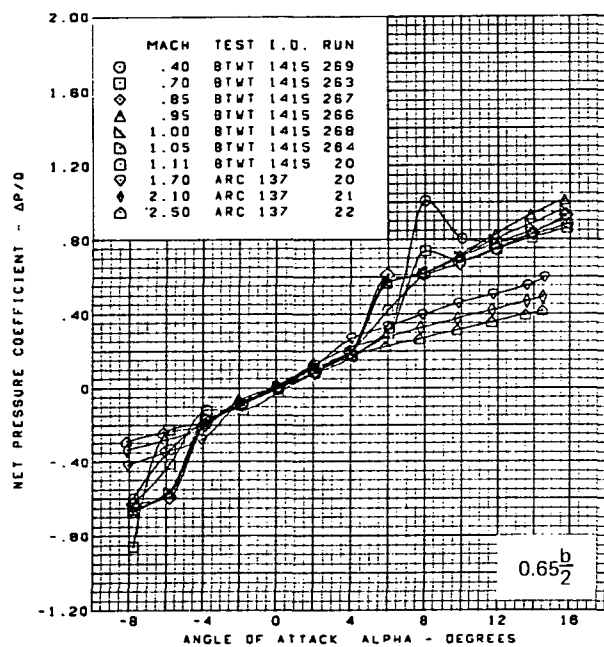
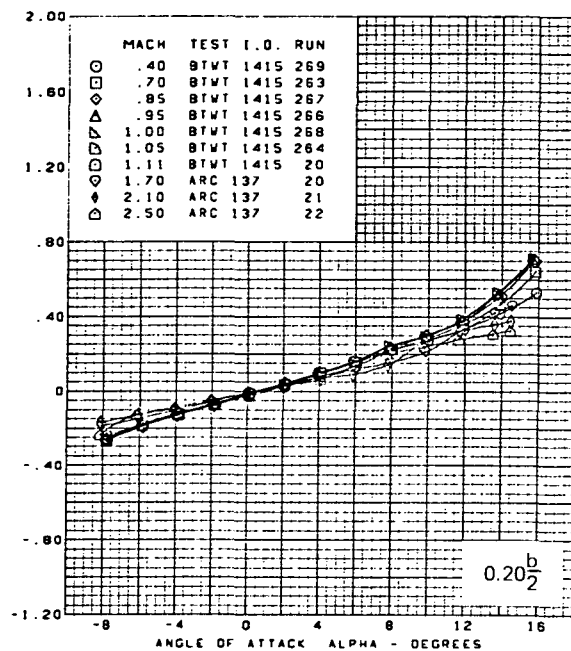
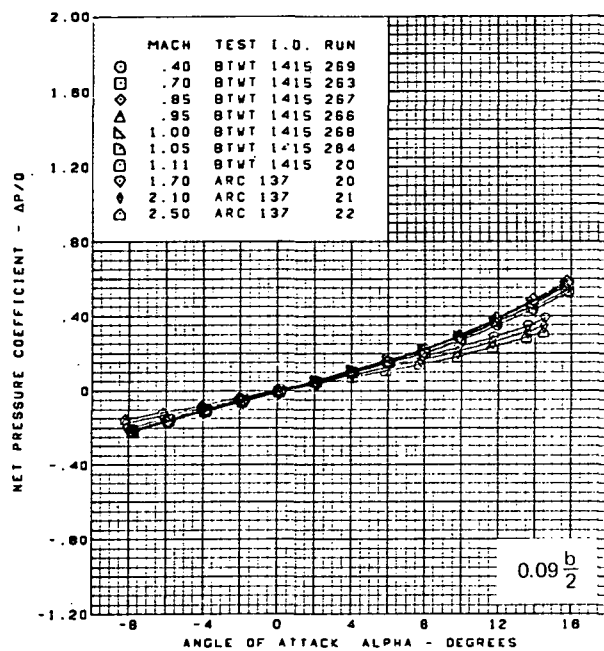


Flat wing, rounded L.E.  
 L.E. deflection, full span =  $0.0^\circ$   
 T.E. deflection, full span =  $0.0^\circ$



(f) (Concluded)

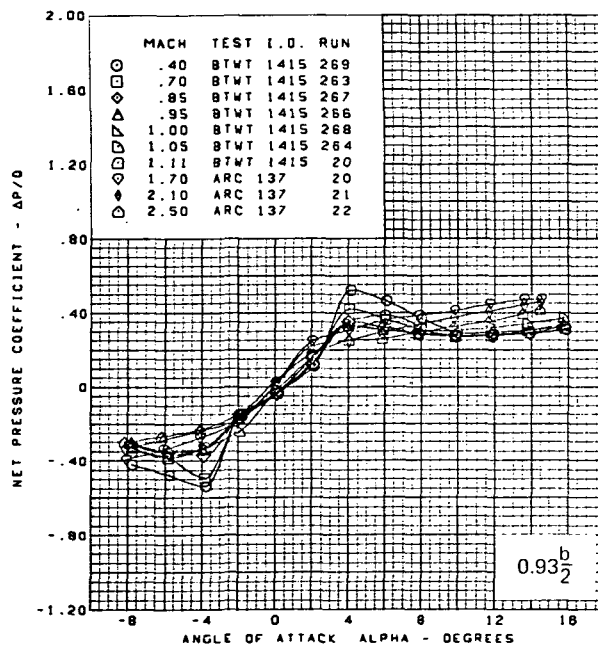
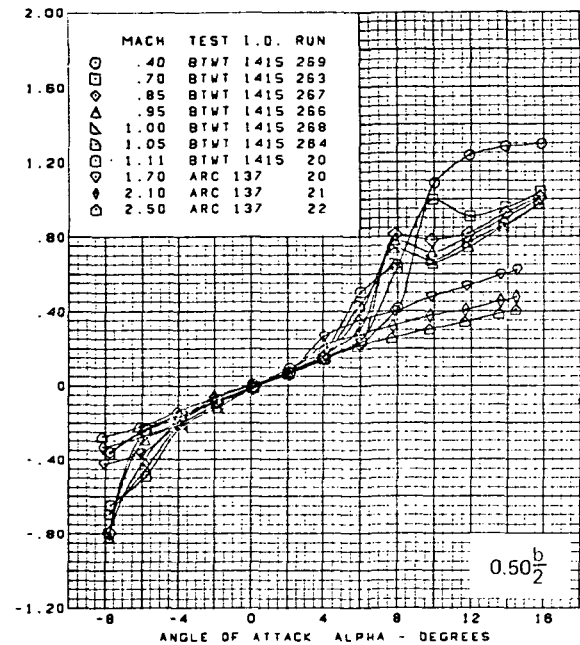
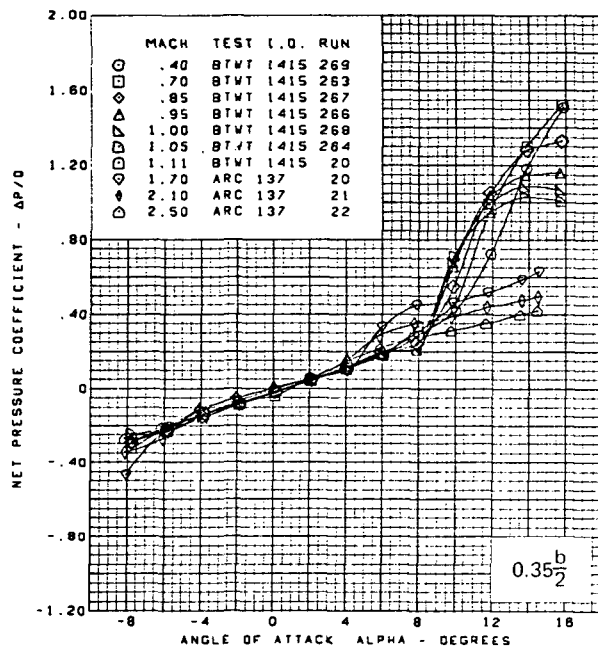
Figure 48.—(Continued)



(g) Net Pressure at  $0.300 \frac{x}{c}$

Figure 48.—(Continued)

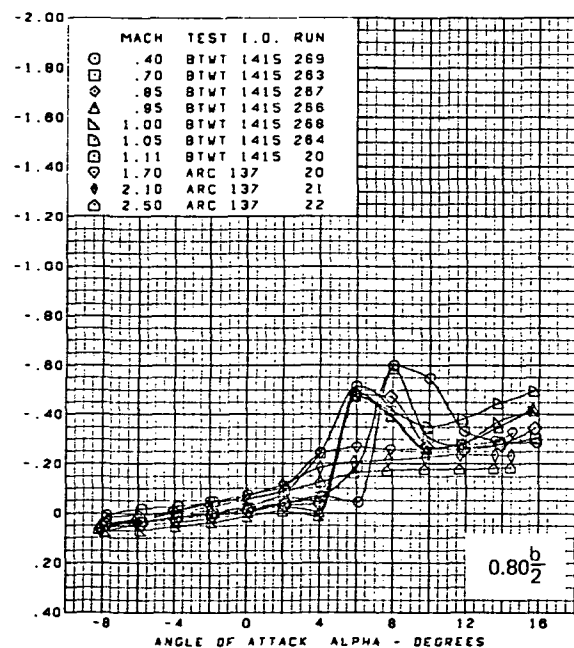
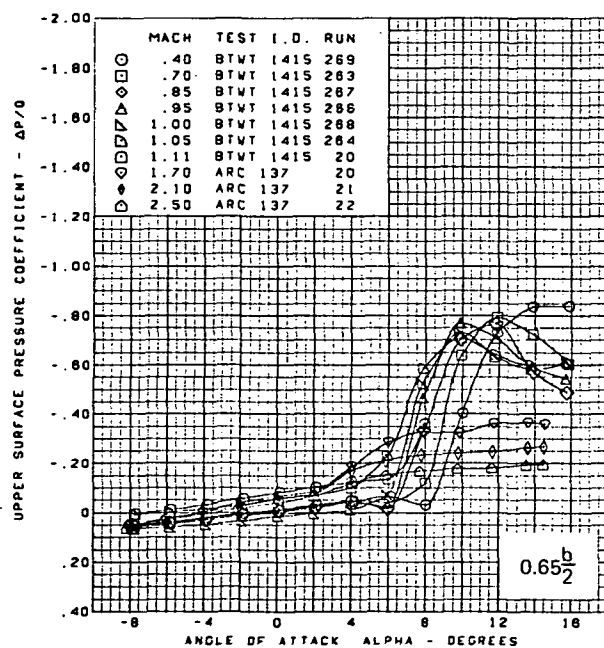
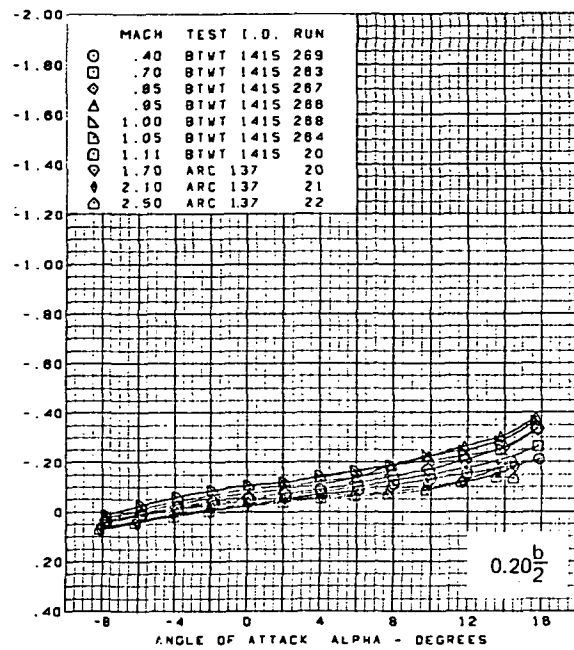
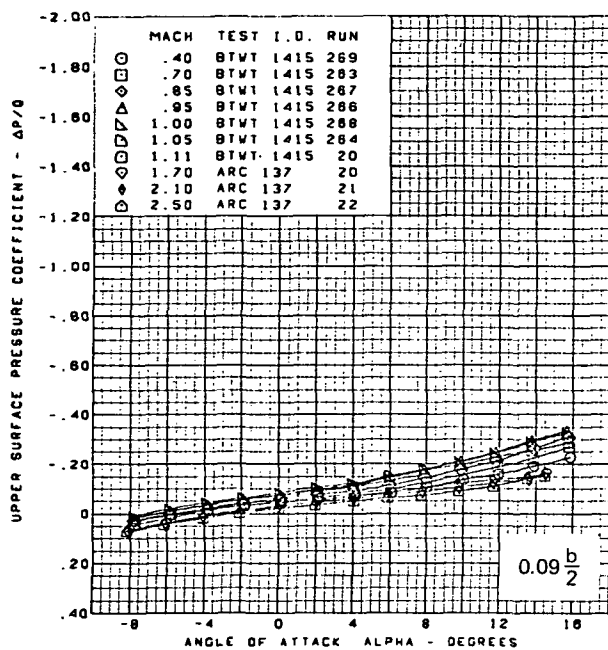




Flat wing, rounded L.E.  
 L.E. deflection, full span =  $0.0^\circ$   
 T.E. deflection, full span =  $0.0^\circ$

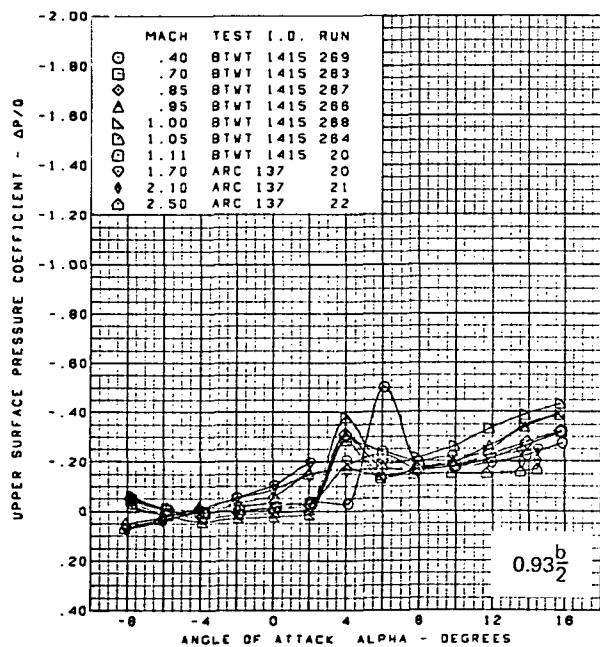
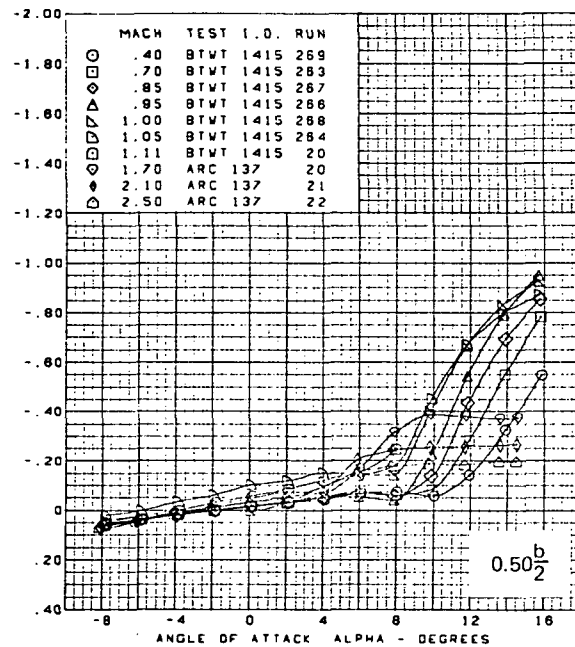
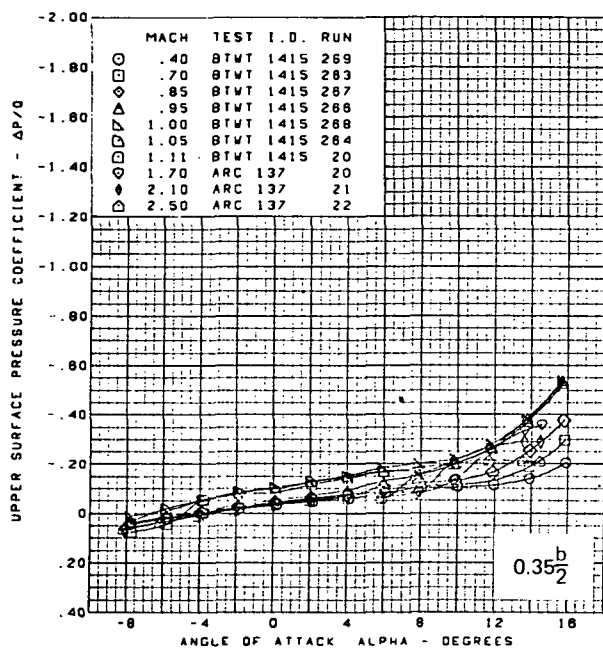
(g) (Concluded)

Figure 48.—(Continued)

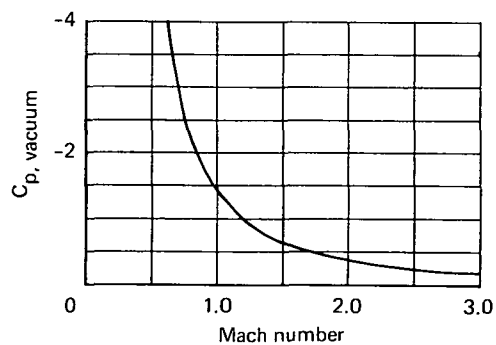


(h) Upper Surface Pressure at  $0.725 \frac{x}{c}$

Figure 48.—(Continued)

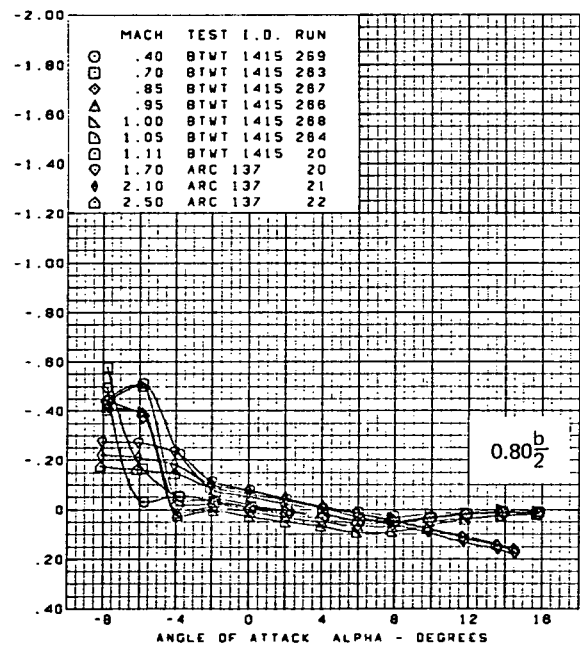
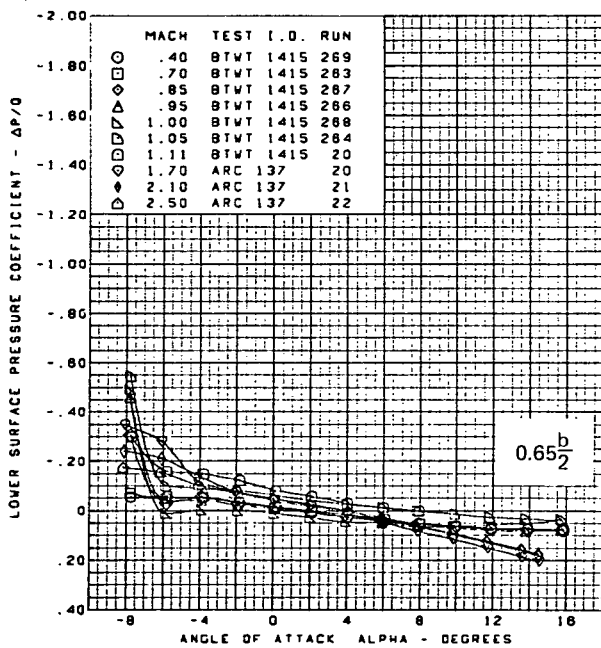
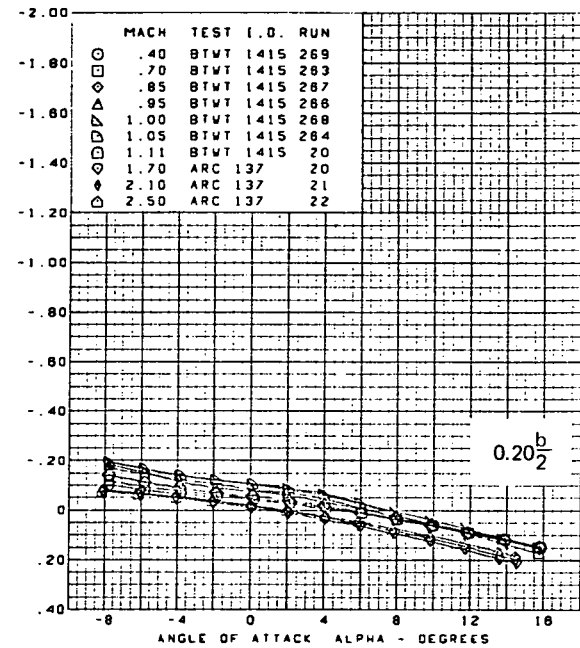
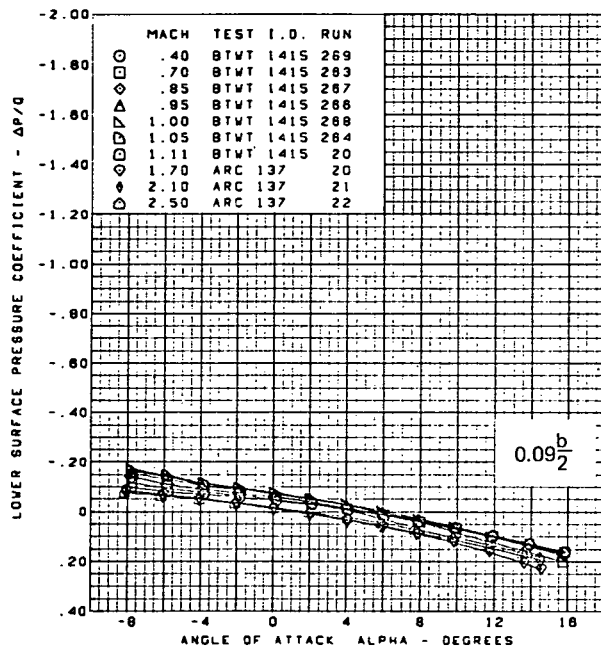


Flat wing, rounded L.E.  
 L.E. deflection, full span =  $0.0^\circ$   
 T.E. deflection, full span =  $0.0^\circ$



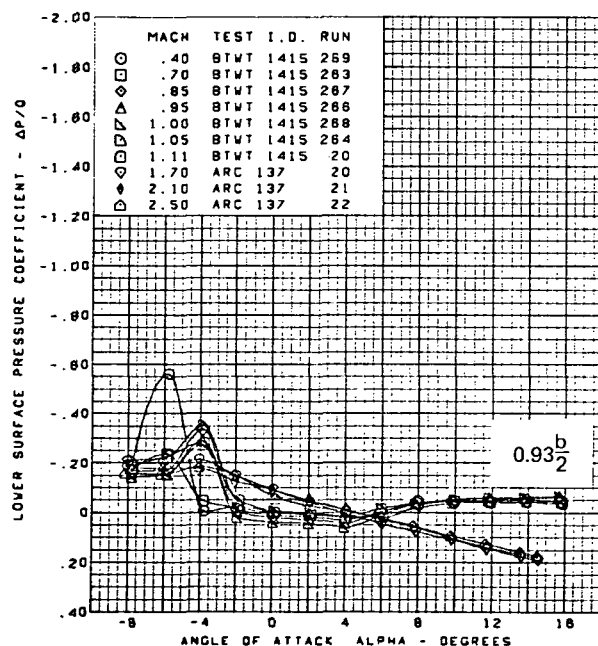
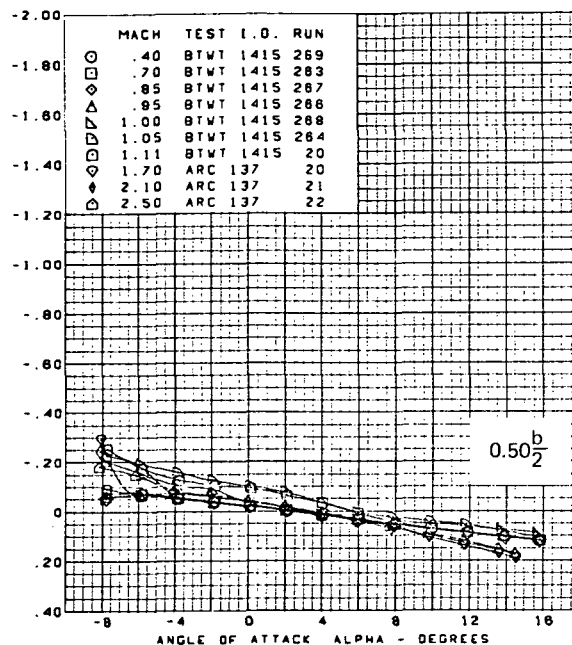
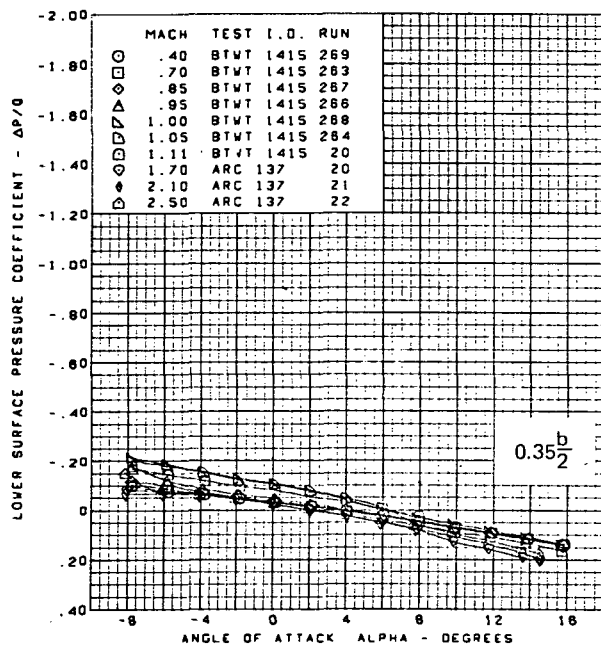
(h) (Concluded)

Figure 48.—(Continued)

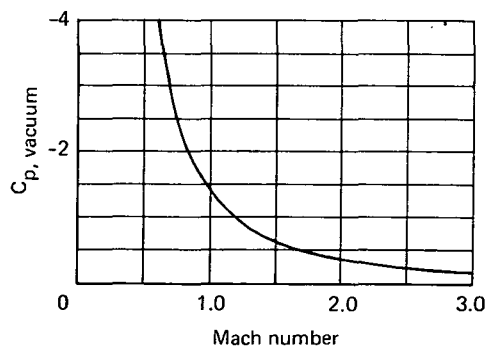


(i) Lower Surface Pressure at  $0.725 \frac{x}{c}$

Figure 48.—(Continued)

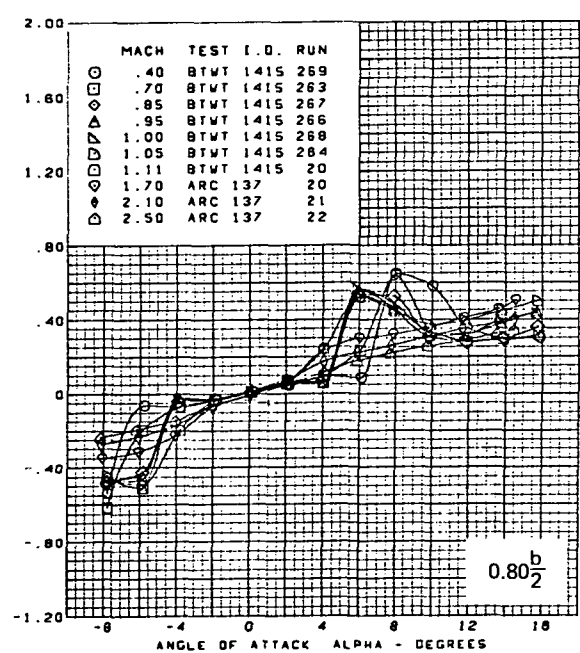
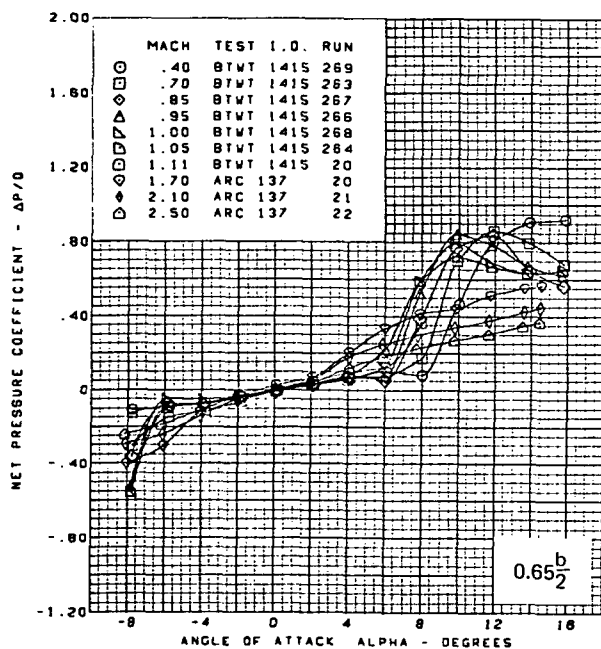
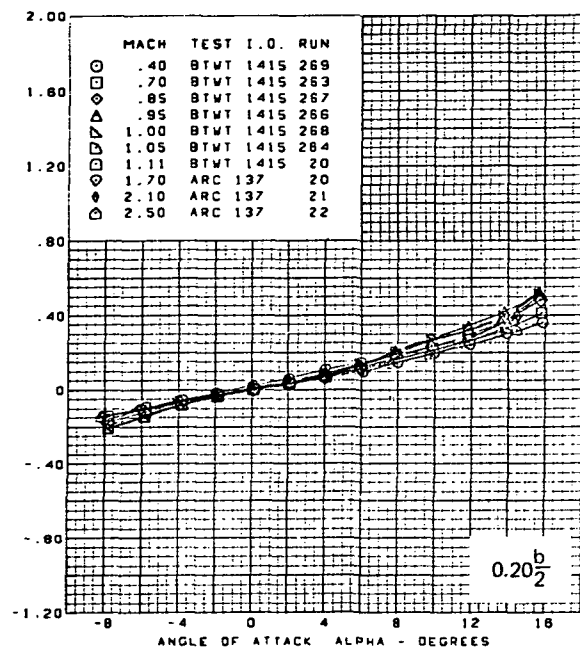
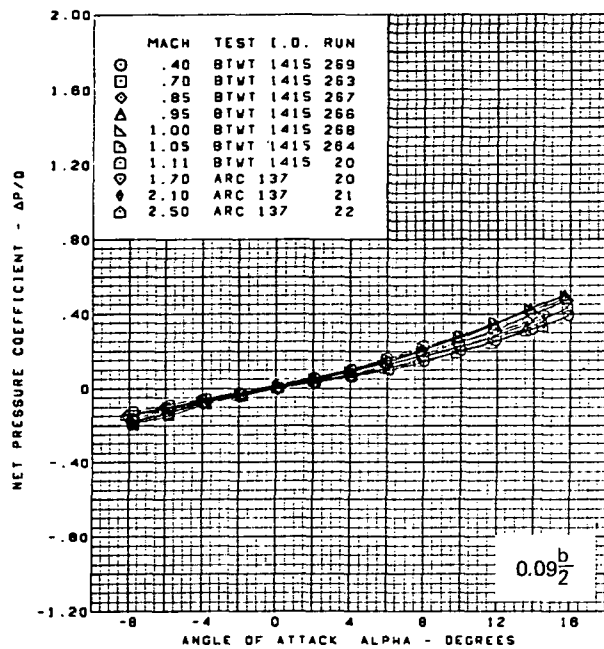


Flat wing, rounded L.E.  
 L.E. deflection, full span =  $0.0^\circ$   
 T.E. deflection, full span =  $0.0^\circ$



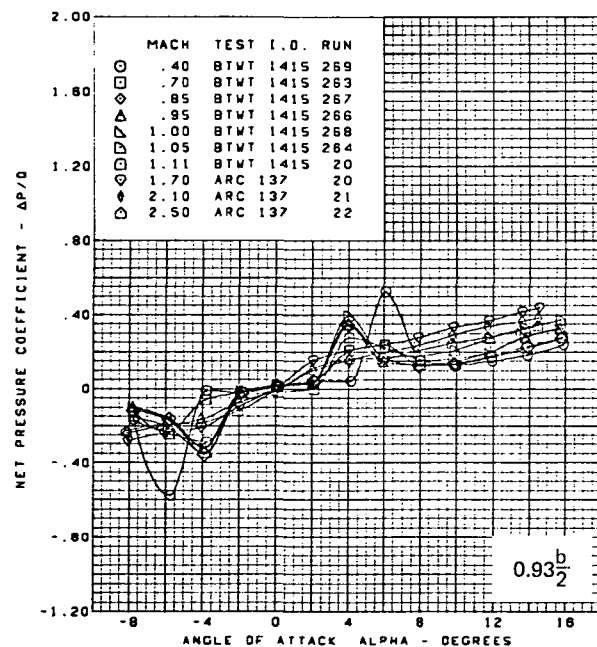
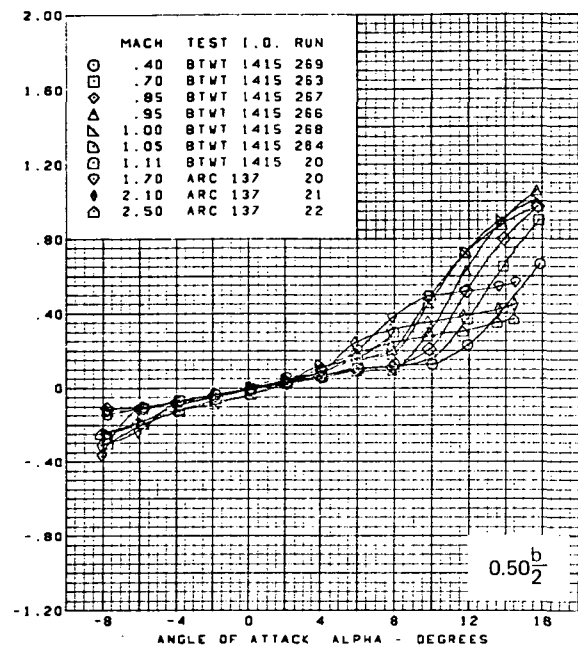
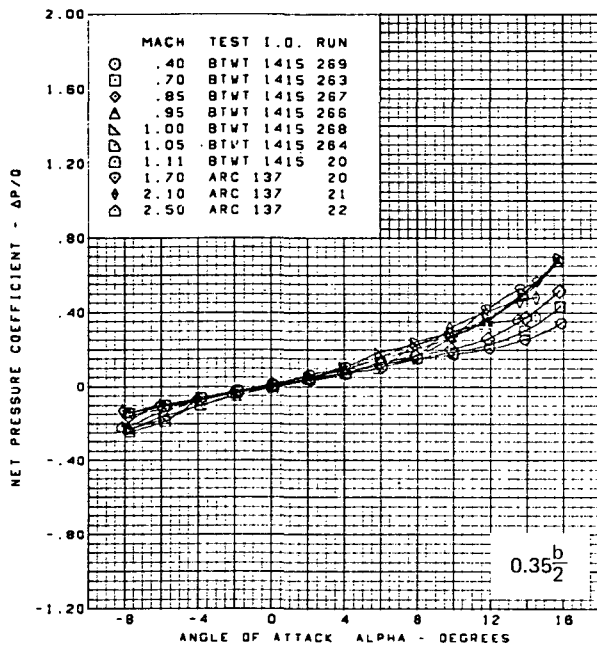
(i) (Concluded)

Figure 48.—(Continued)



(j) Net Pressure at  $0.725 \frac{x}{c}$

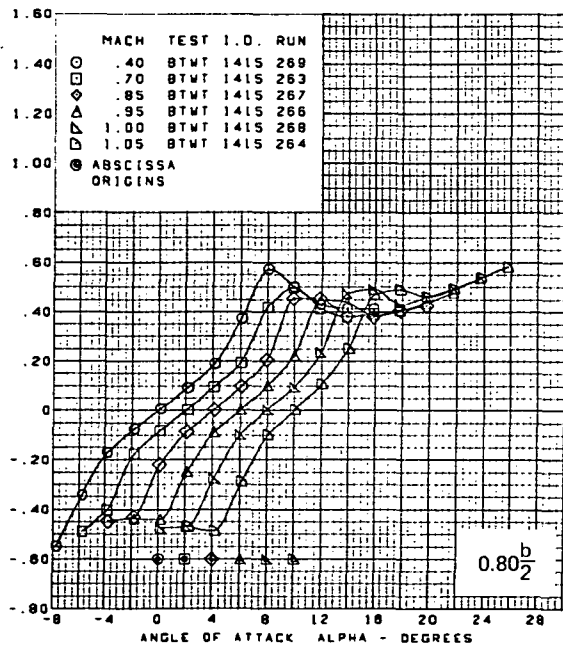
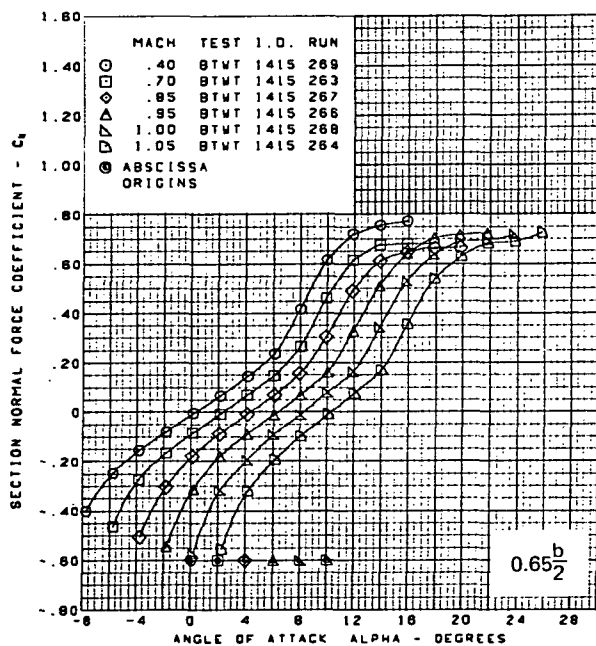
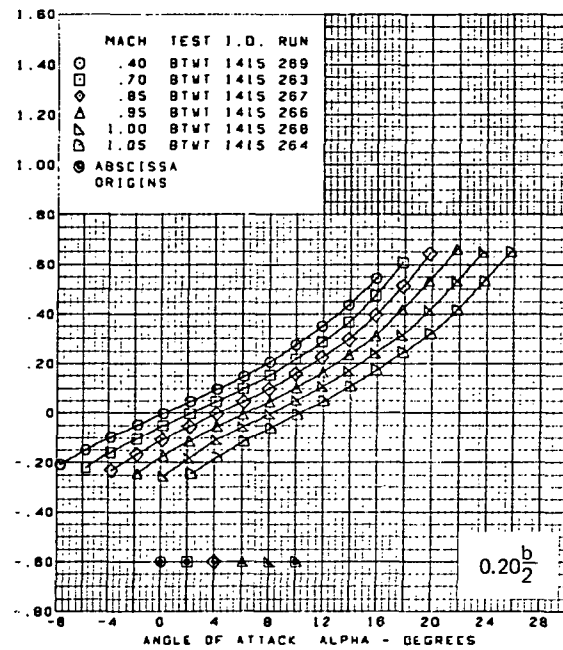
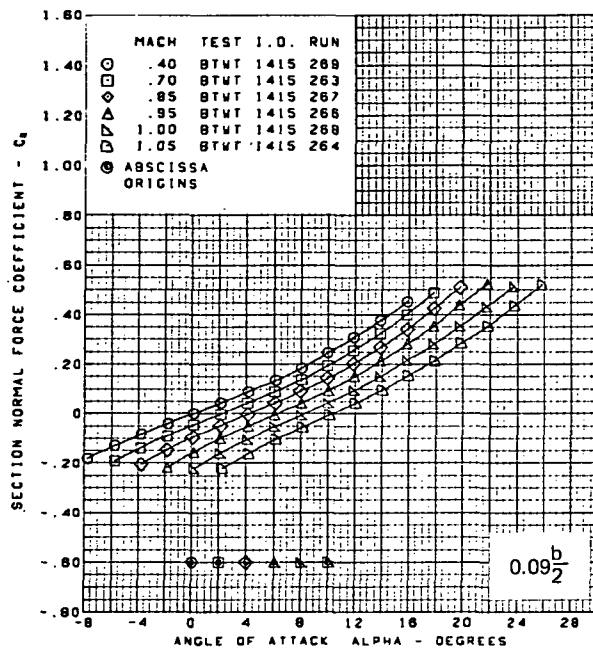
Figure 48.—(Continued)



Flat wing, rounded L.E.  
 L.E. deflection, full span =  $0.0^\circ$   
 T.E. deflection, full span =  $0.0^\circ$

(j) (Concluded)

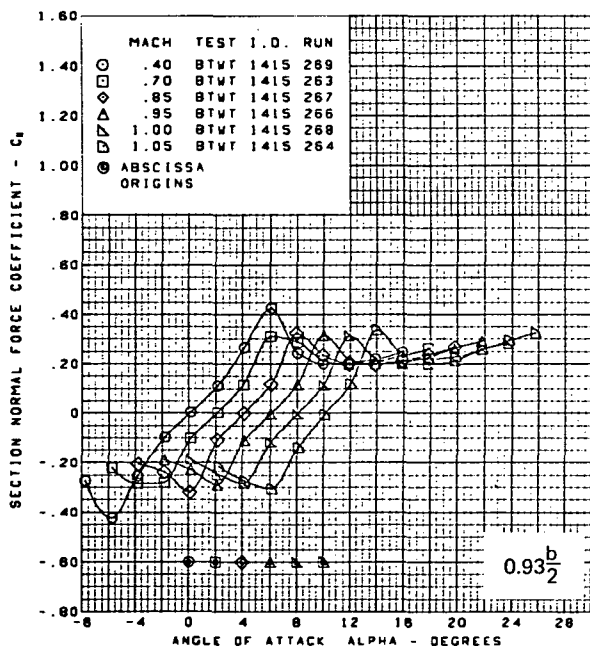
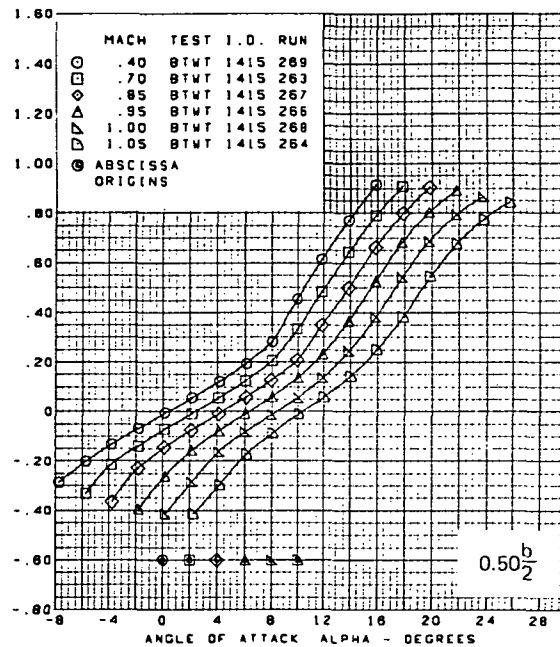
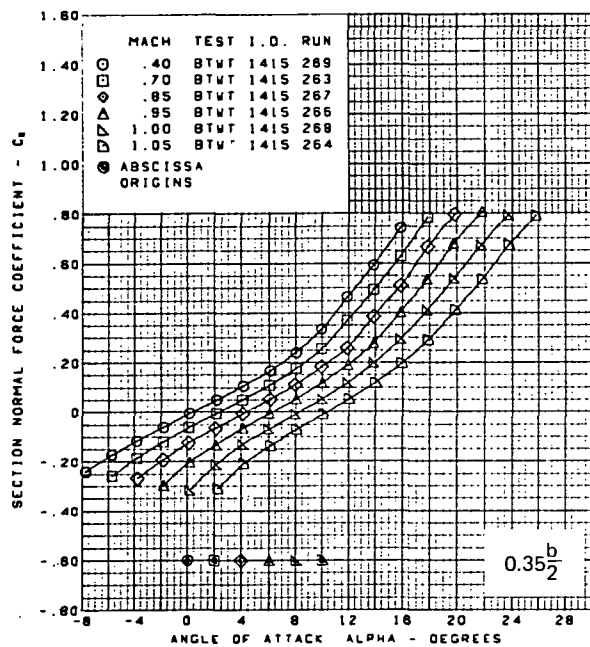
Figure 48.—(Continued)



(k) Section Normal Force Coefficients vs. Angle of Attack,  $M = 0.40$  Through  $1.05$

Figure 48.—(Continued)

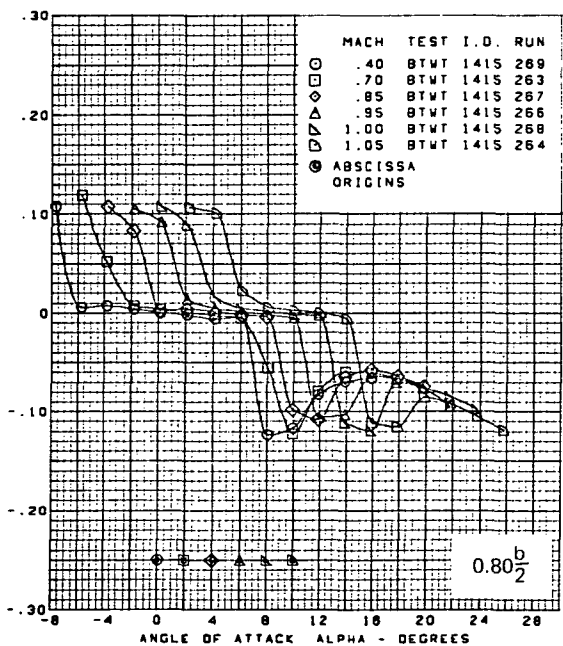
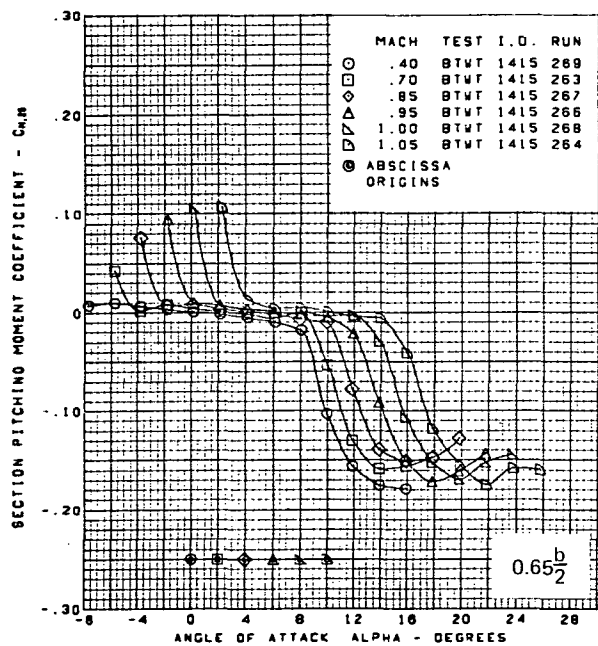
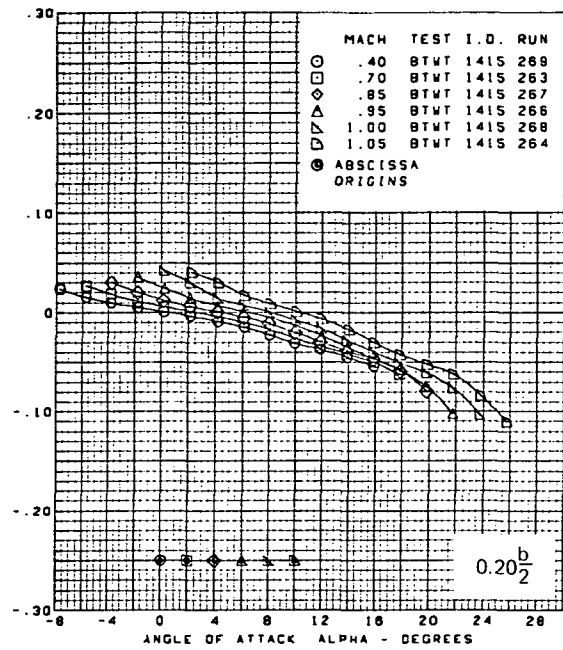
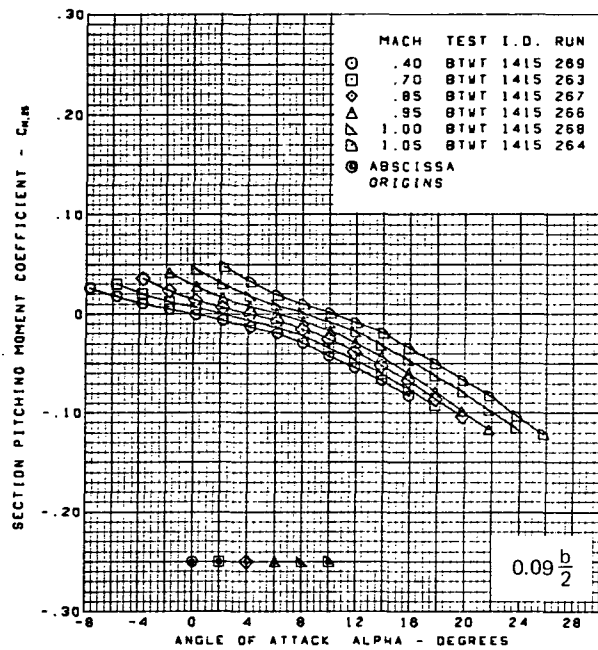




Flat wing, rounded L.E.  
 L.E. deflection, full span =  $0.0^\circ$   
 T.E. deflection, full span =  $0.0^\circ$

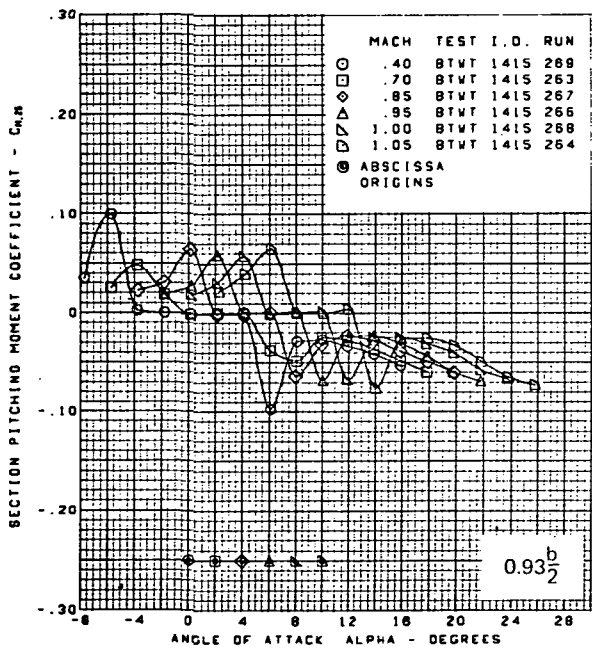
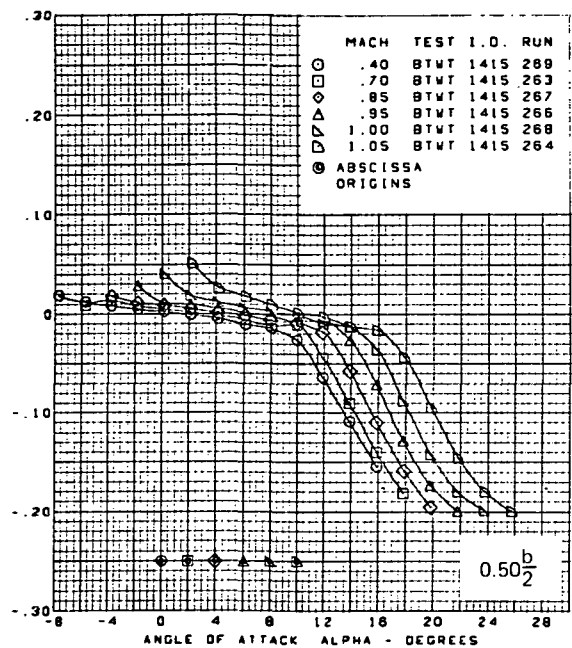
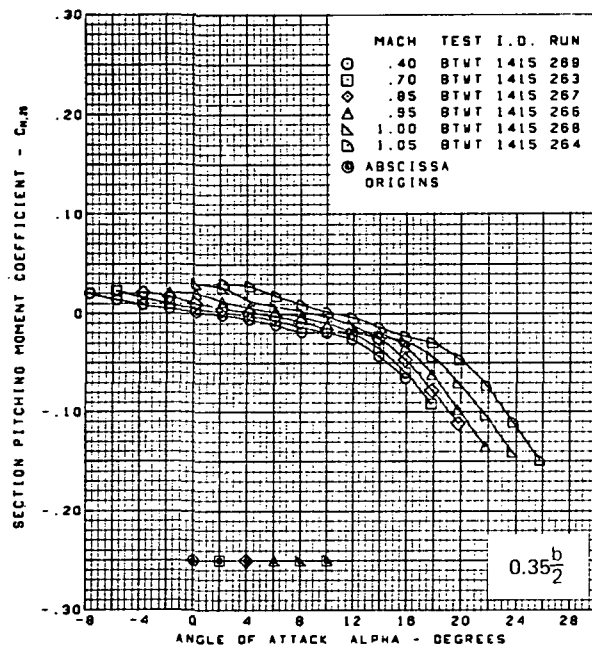
(k) (Concluded)

Figure 48.—(Continued)



(I) Section Pitching Moment Coefficients vs. Angle of Attack,  $M = 0.40$  Through 1.05

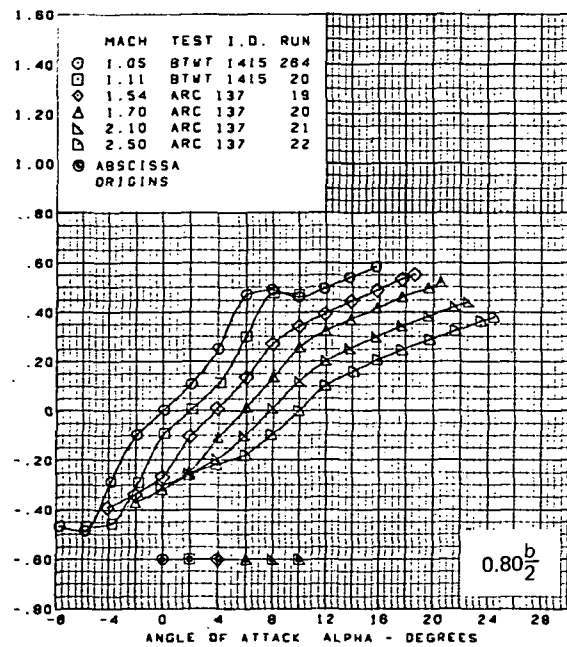
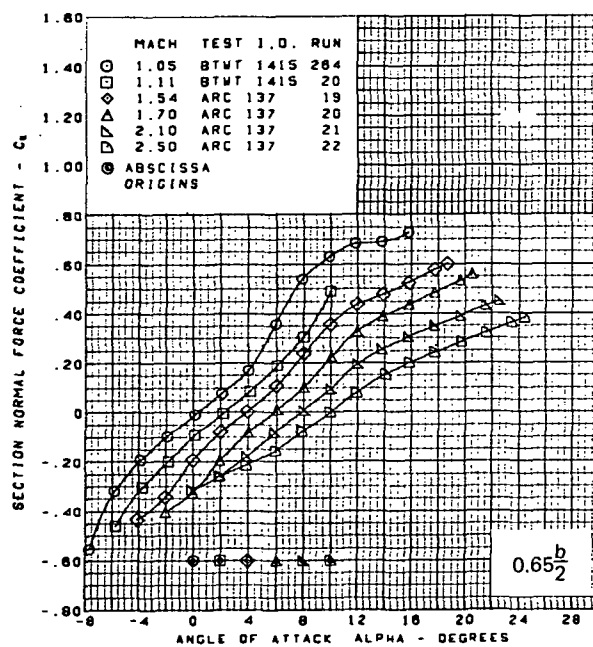
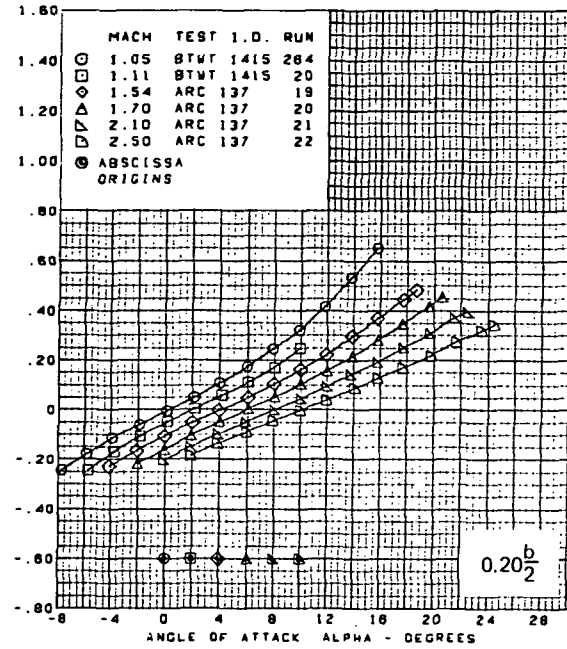
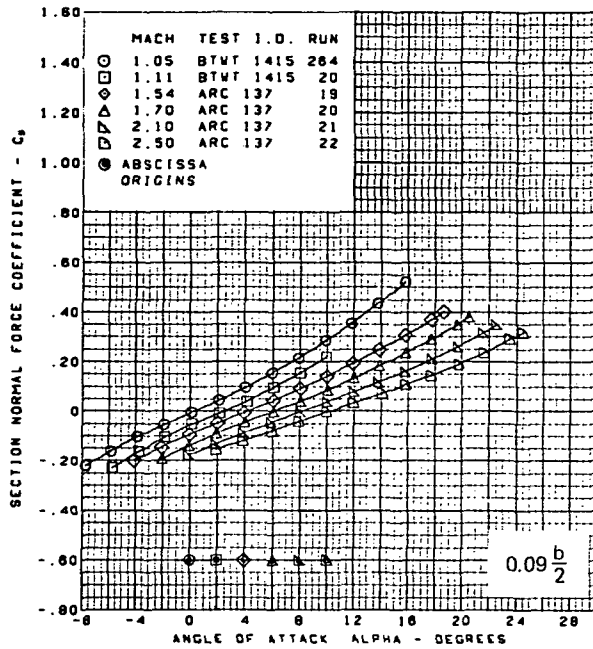
Figure 48.—(Continued)



Flat wing, rounded L.E.  
 L.E. deflection, full span =  $0.0^\circ$   
 T.E. deflection, full span =  $0.0^\circ$

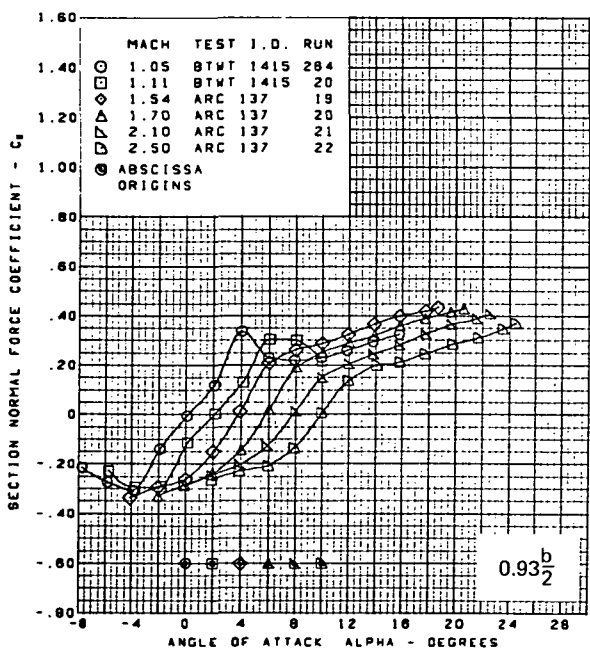
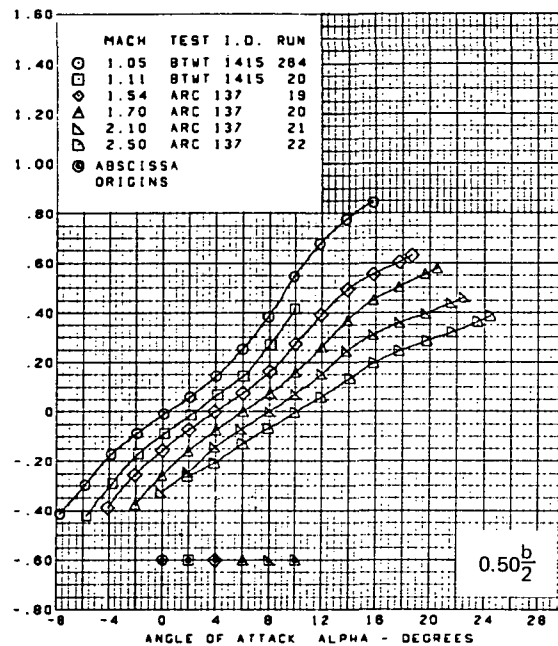
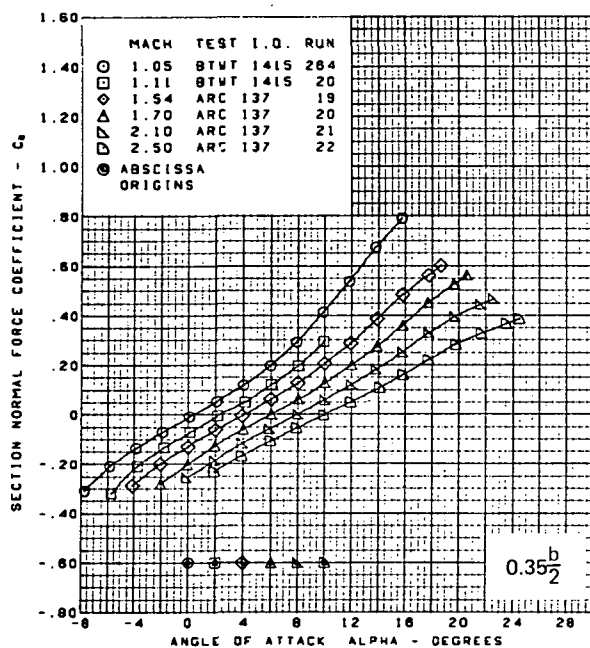
(I) (Concluded)

Figure 48. —(Continued)



(m) Section Normal Force Coefficients vs. Angle of Attack, M = 1.05 Through 2.50

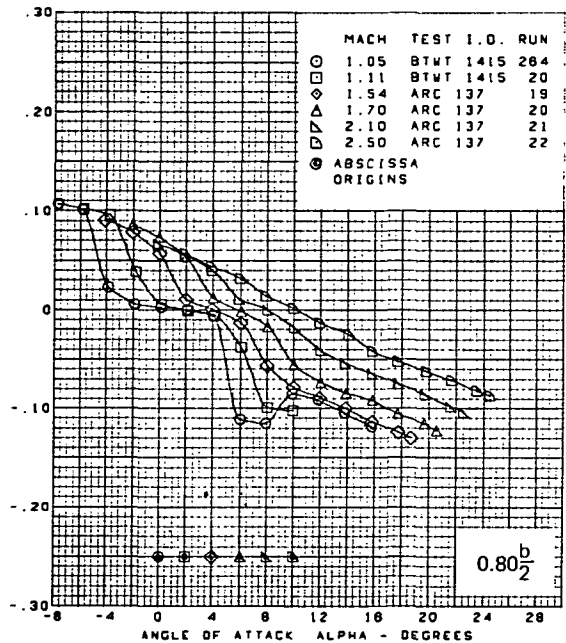
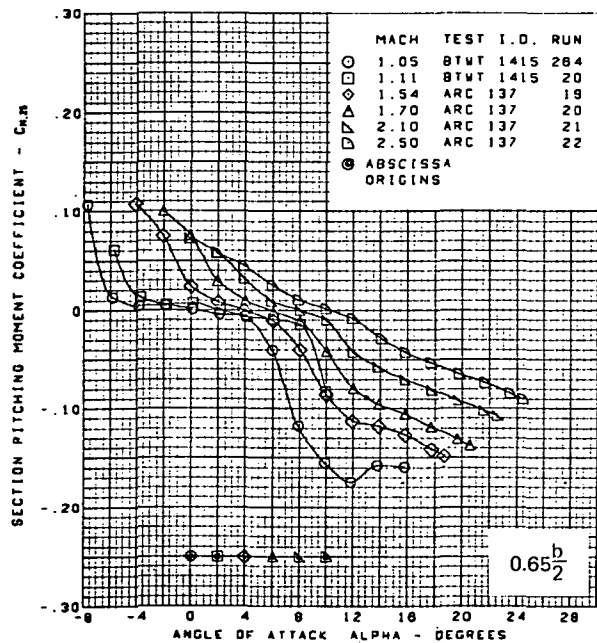
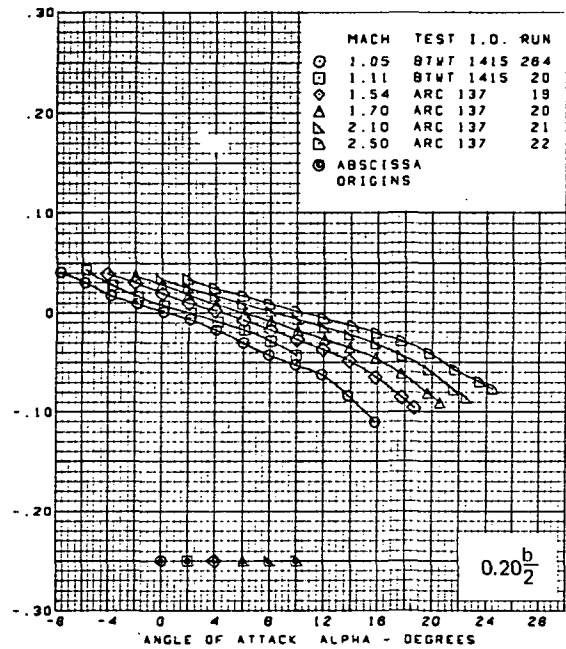
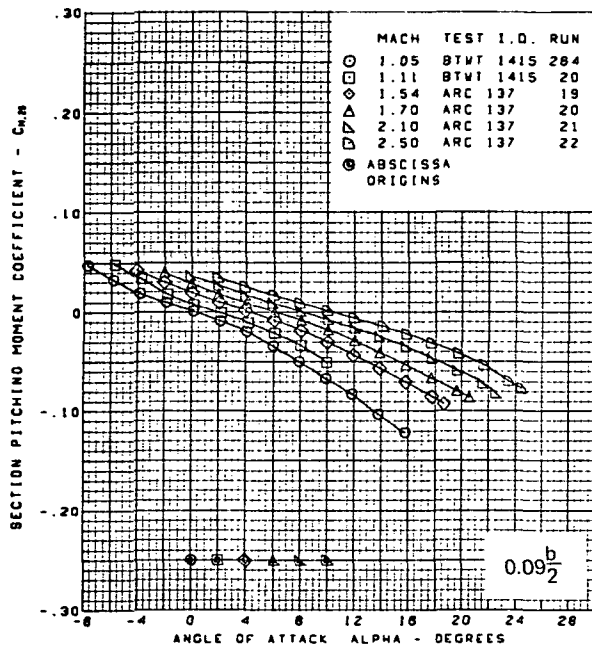
Figure 48.—(Continued)



Flat wing, rounded L.E.  
 L.E. deflection, full span =  $0.0^\circ$   
 T.E. deflection, full span =  $0.0^\circ$

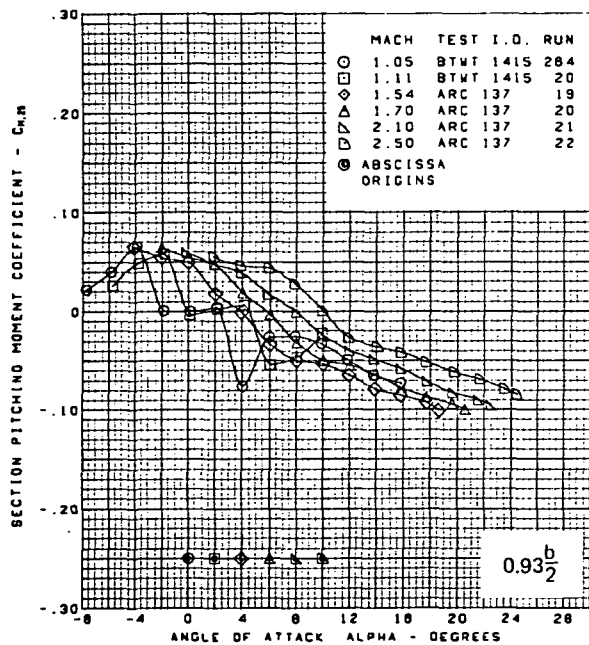
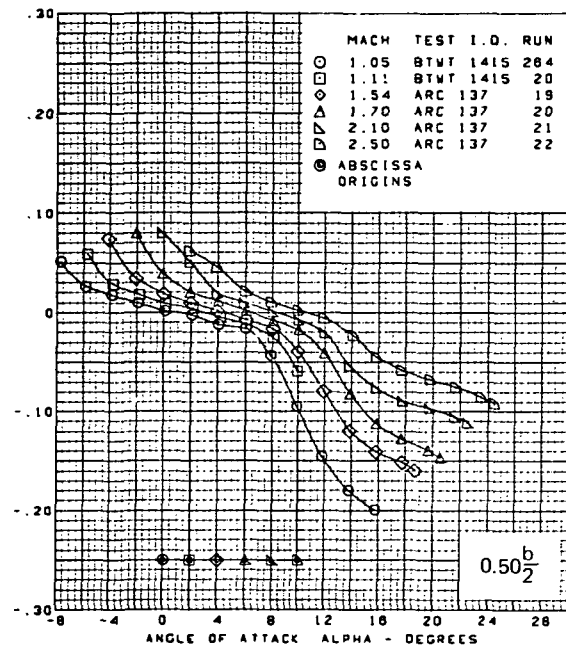
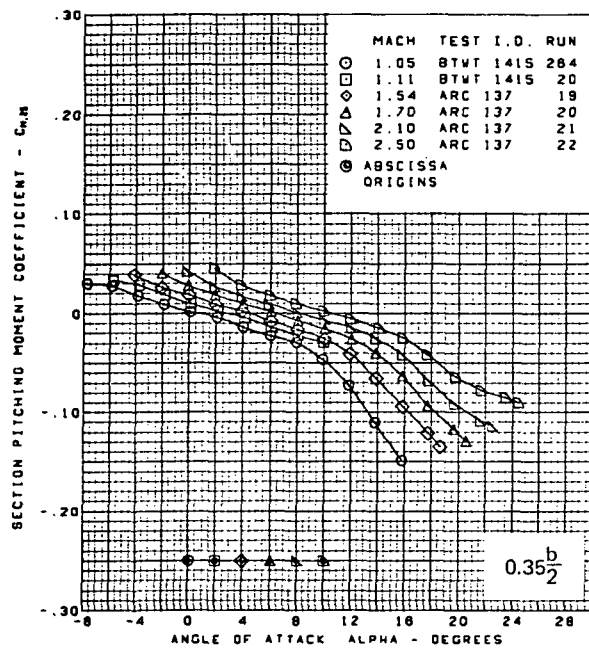
(m) (Concluded)

Figure 48.—(Continued)



(n) Section Pitching Moment Coefficients vs. Angle of Attack,  $M = 1.05$  Through 2.50

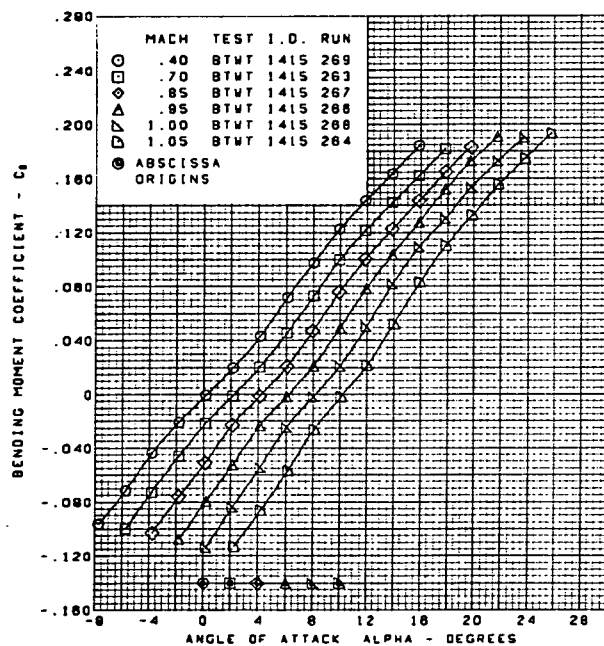
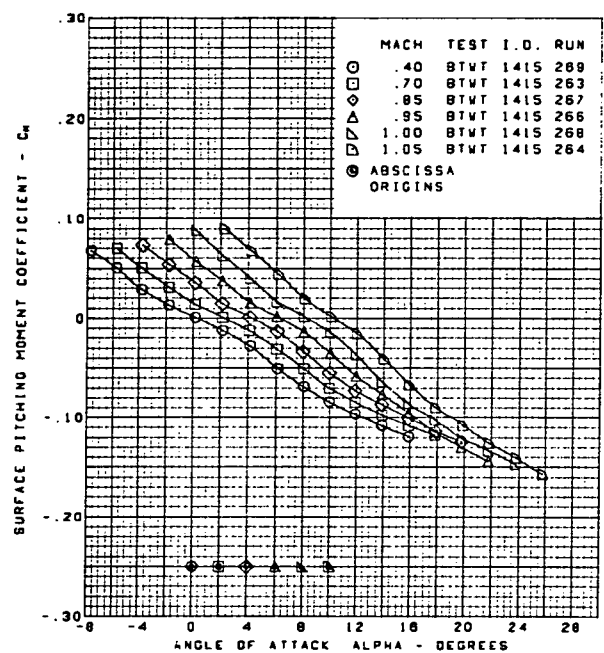
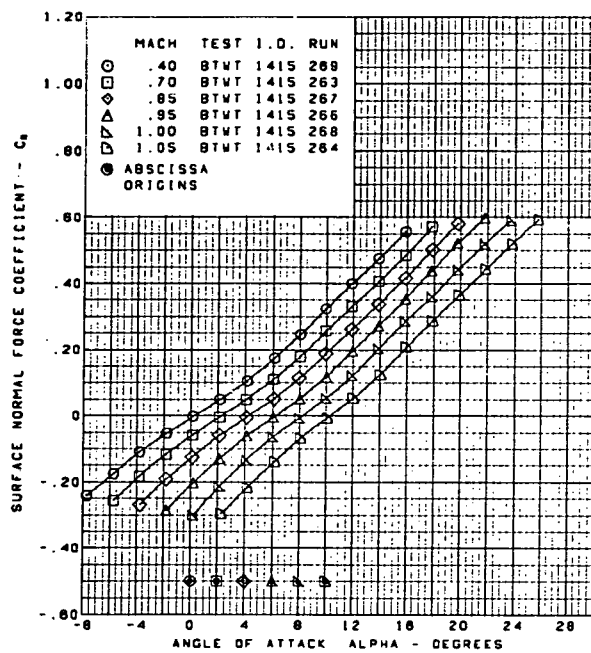
Figure 48.—(Continued)



Flat wing, rounded L.E.  
 L.E. deflection, full span =  $0.0^\circ$   
 T.E. deflection, full span =  $0.0^\circ$

(n) (Concluded)

Figure 48.—(Continued)

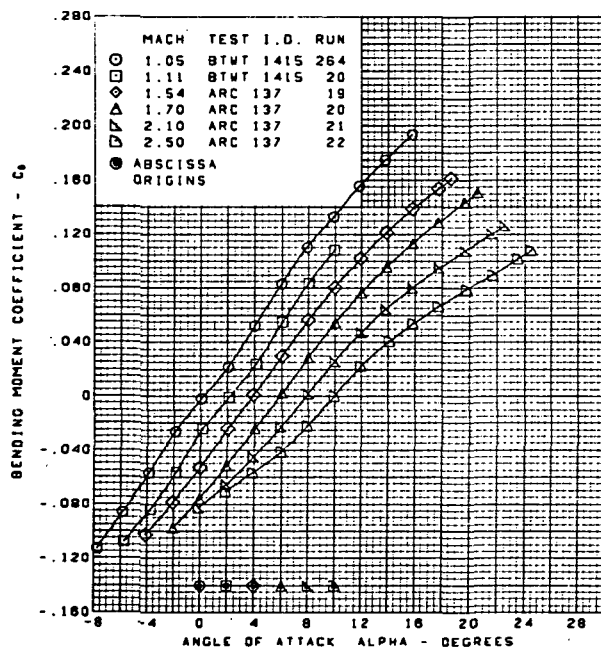
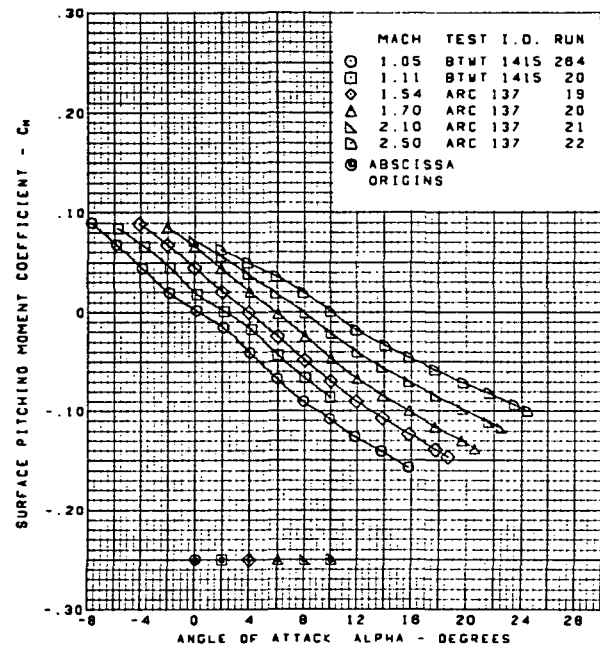
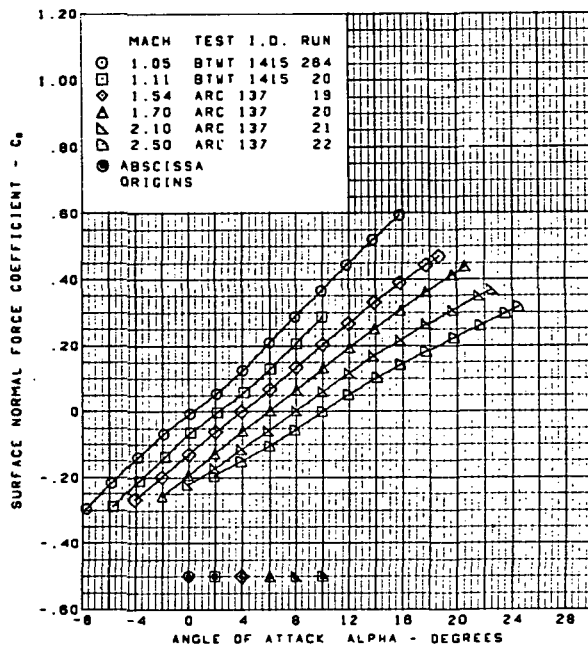


Flat wing, rounded L.E.  
 L.E. deflection, full span =  $0.0^\circ$   
 T.E. deflection, full span =  $0.0^\circ$

(o) Wing Aerodynamic Coefficients vs. Angle of Attack

Figure 48.—(Continued)

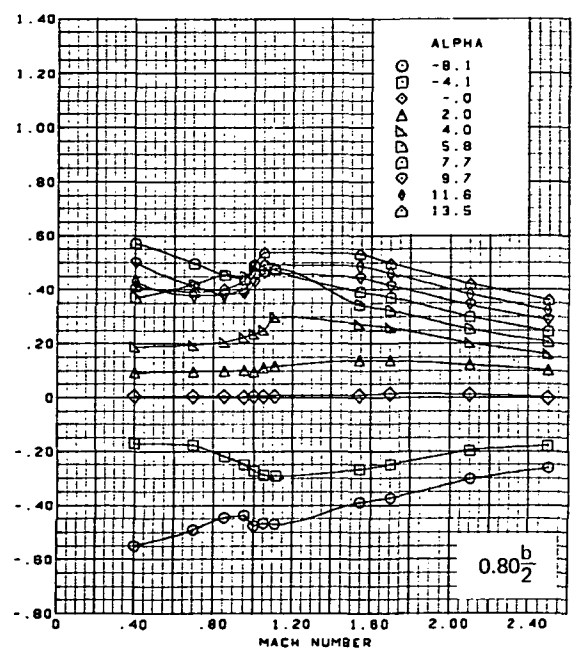
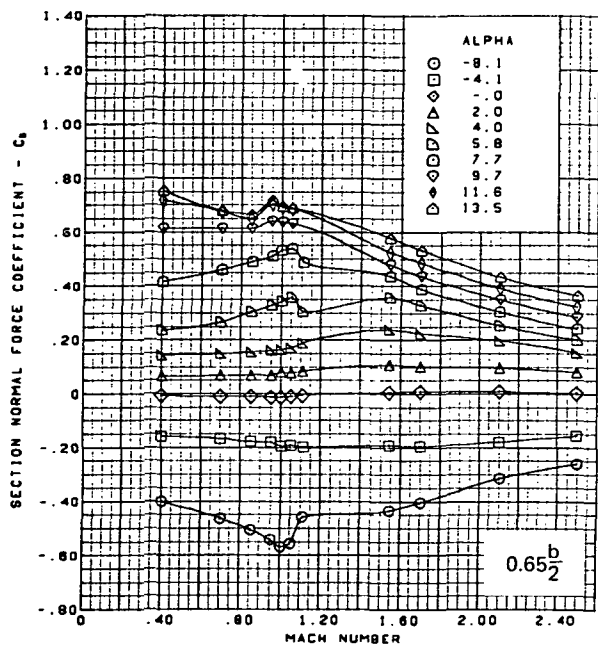
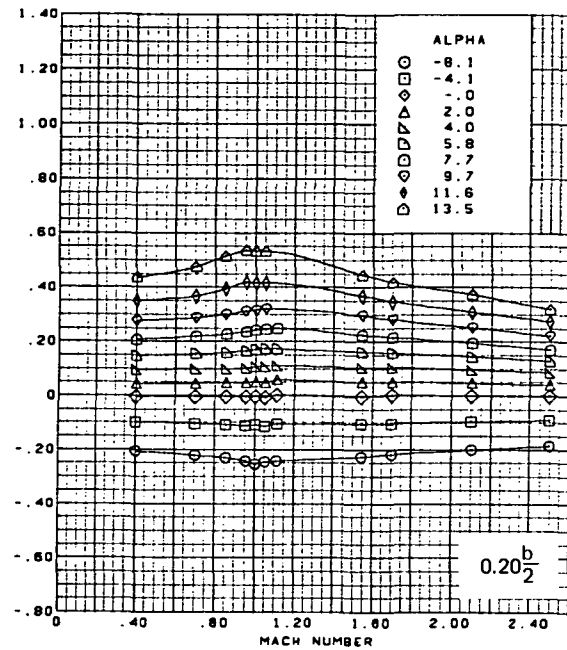
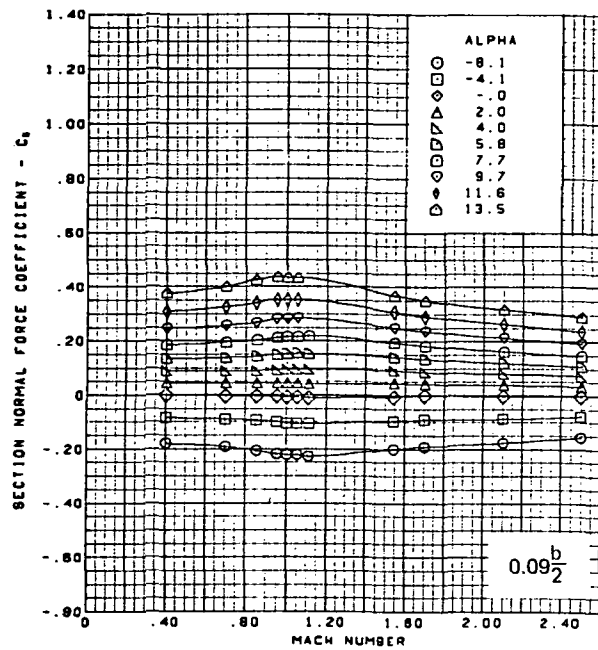




Flat wing, rounded L.E.  
 L.E. deflection, full span =  $0.0^\circ$   
 T.E. deflection, full span =  $0.0^\circ$

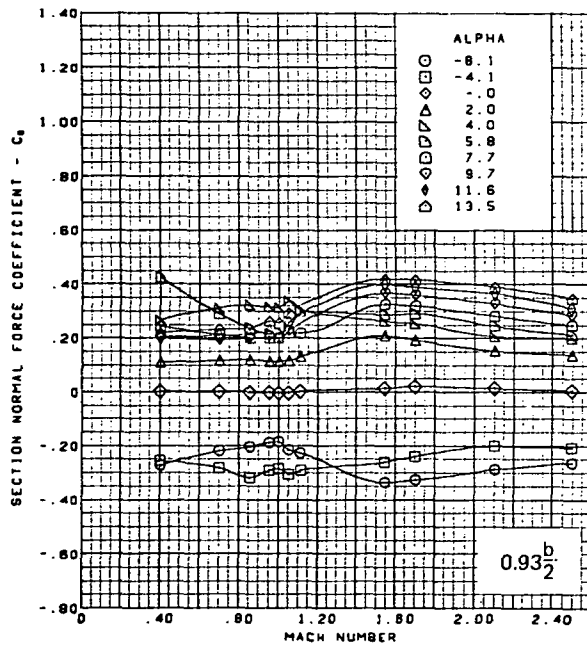
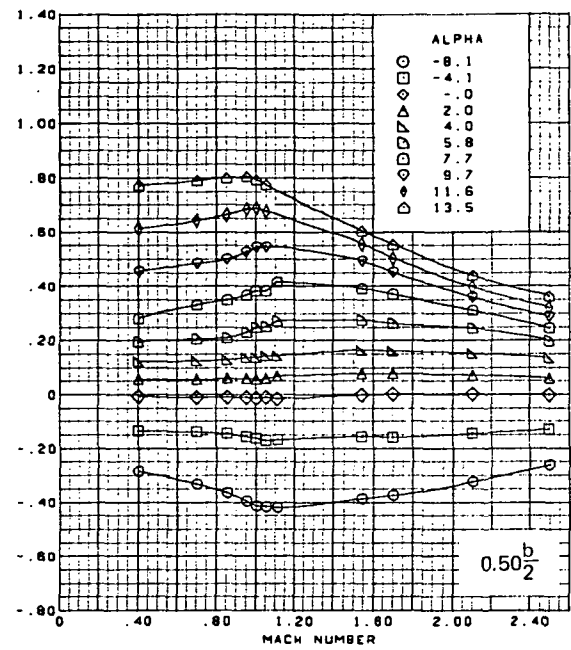
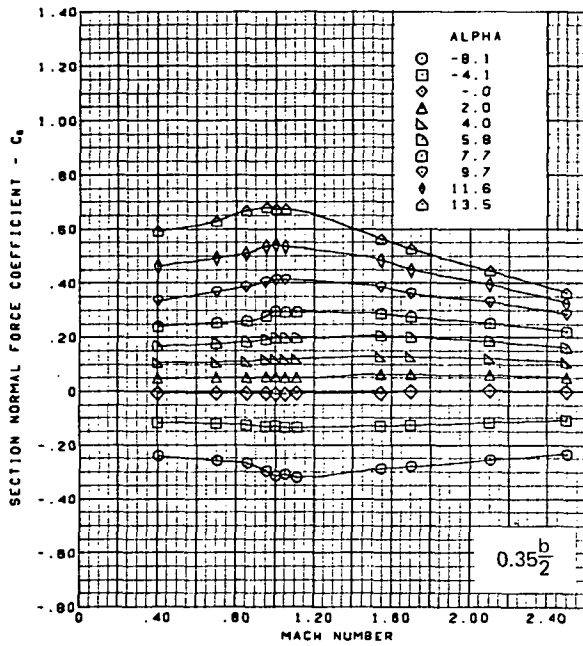
(o) (Concluded)

Figure 48.—(Continued)



(p) Section Aerodynamic Coefficients—Normal Force

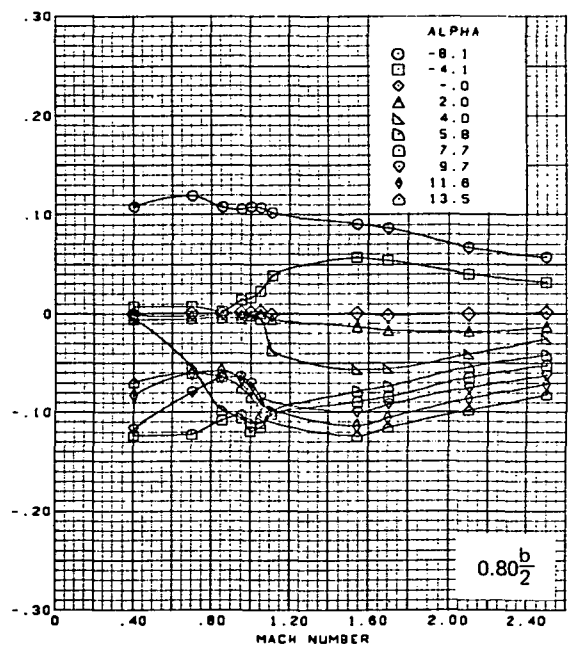
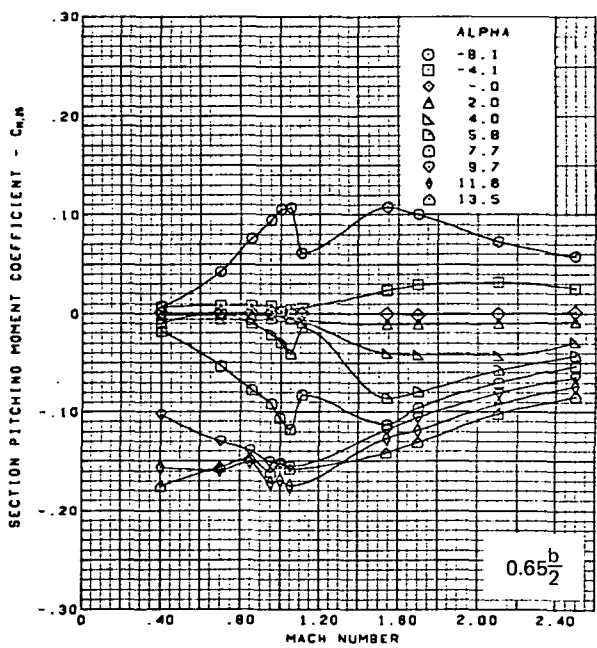
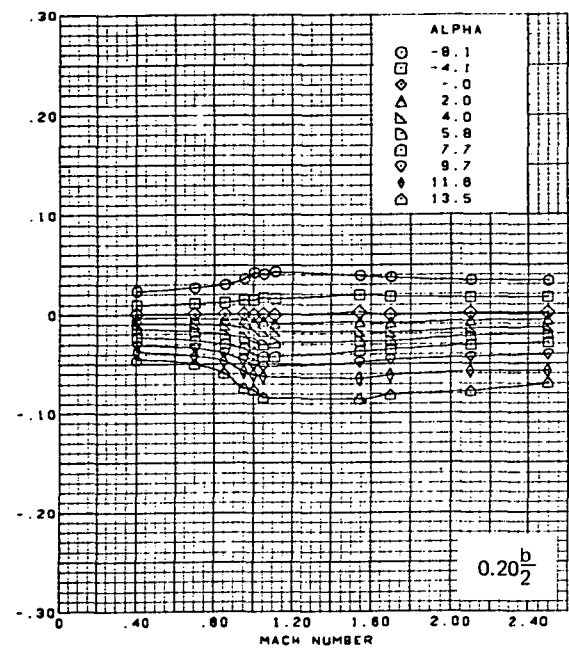
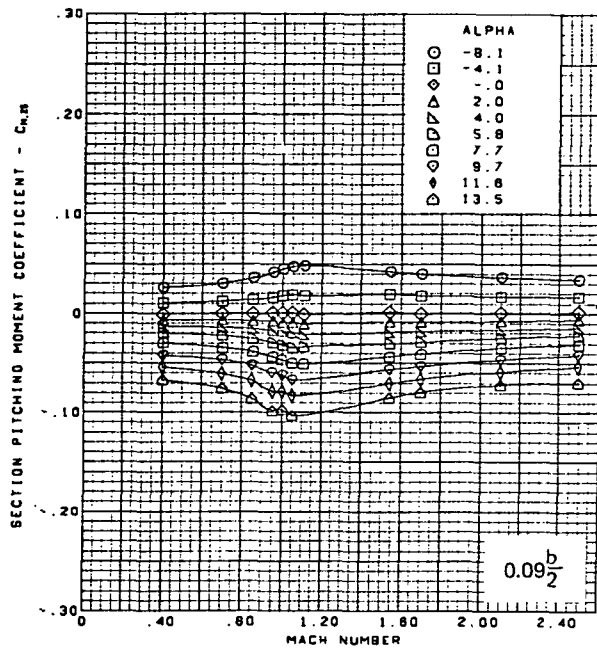
Figure 48.—(Continued)



Flat wing, rounded L.E.  
 L.E. deflection, full span  $\approx 0.0^\circ$   
 T.E. deflection, full span  $\approx 0.0^\circ$

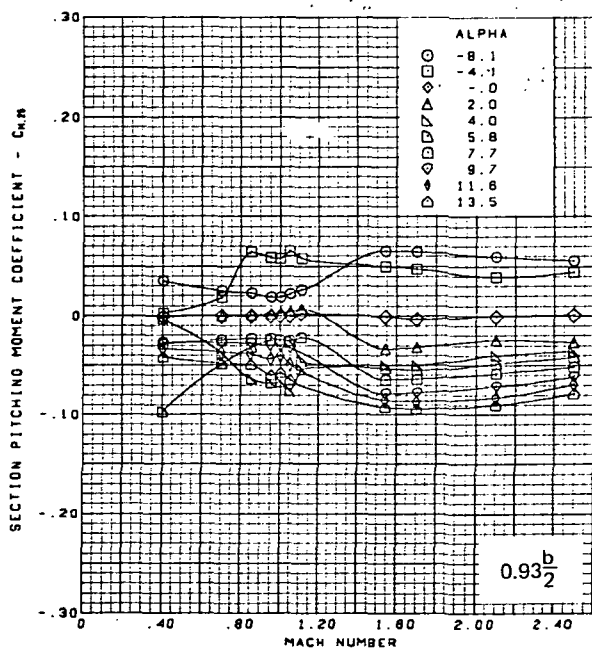
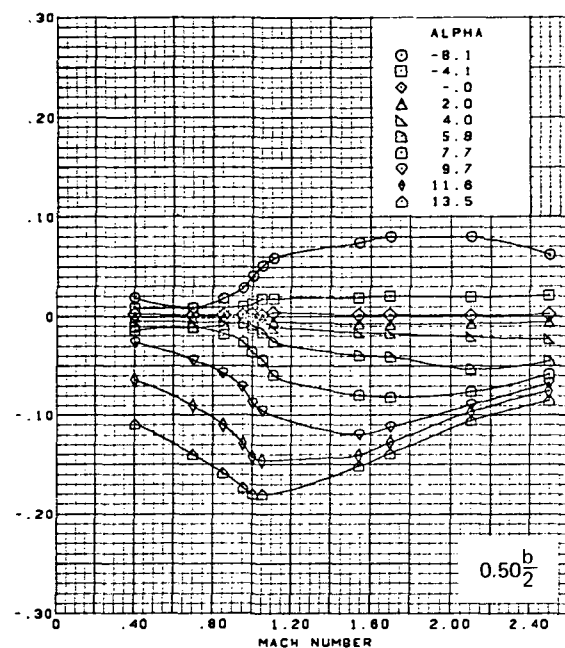
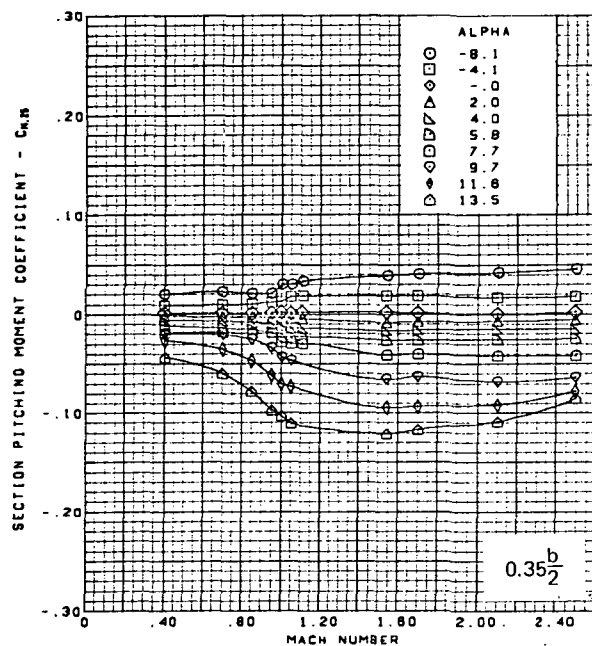
(p) (Concluded)

Figure 48.—(Continued)



(q) Section Aerodynamic Coefficients—Pitching Moment

Figure 48.—(Continued)

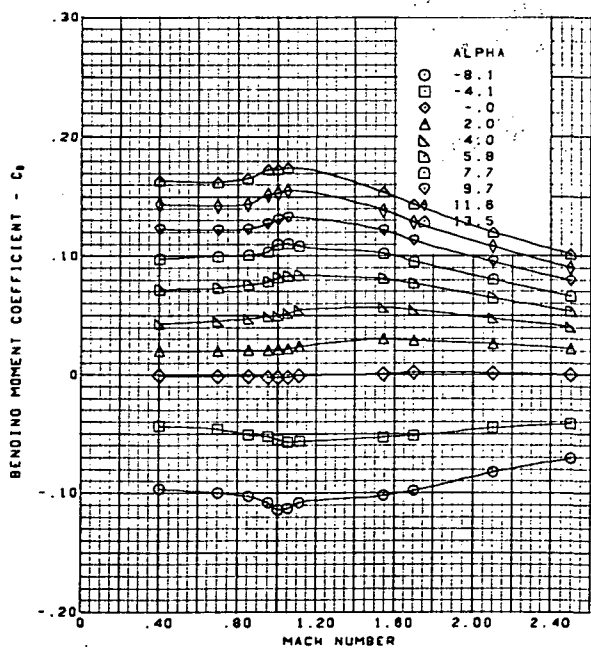
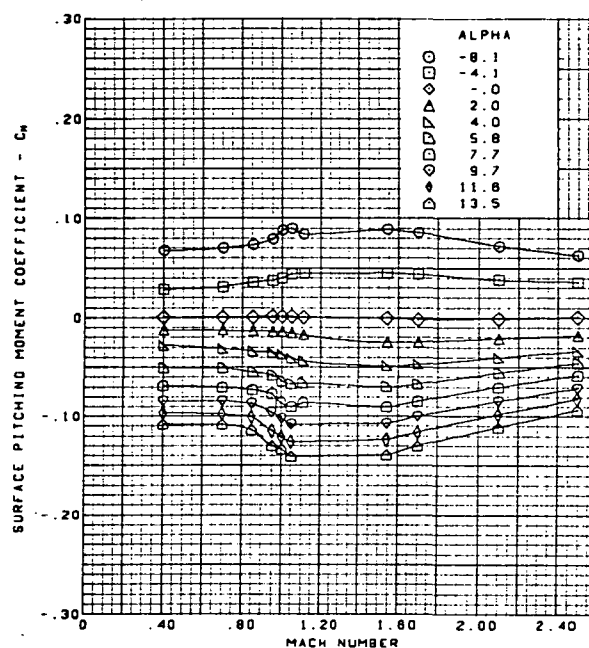
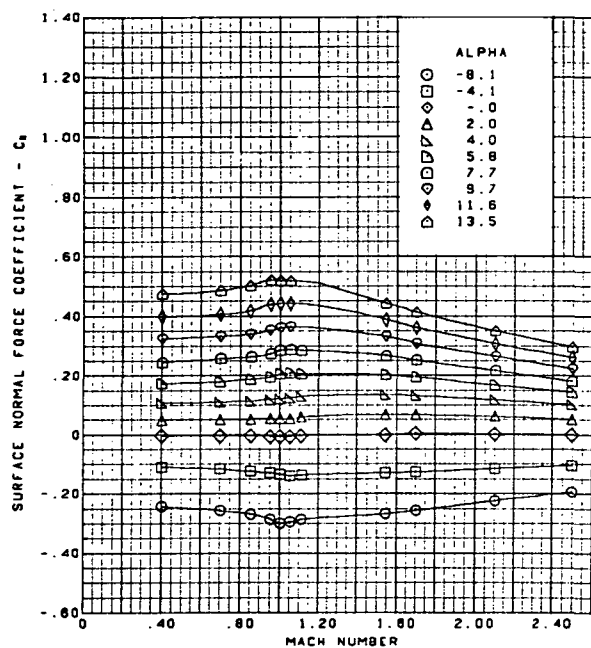


Flat wing, rounded L.E.  
 L.E. deflection, full span =  $0.0^\circ$   
 T.E. deflection, full span =  $0.0^\circ$

(q) (Concluded)

Figure 48.—(Continued)

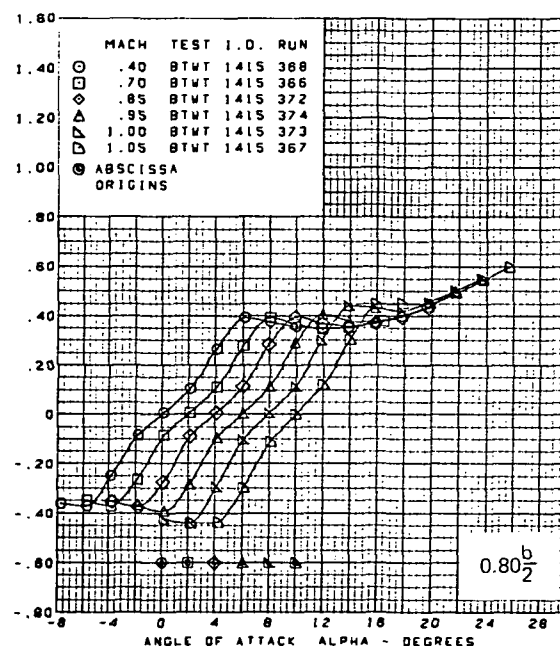
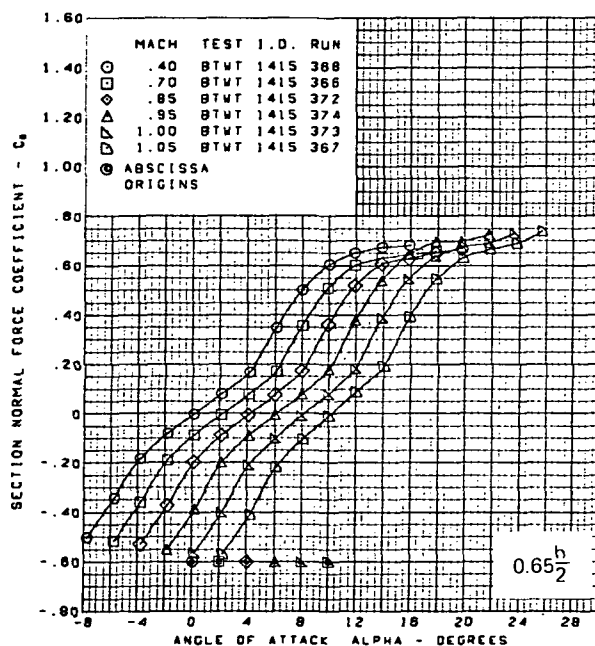
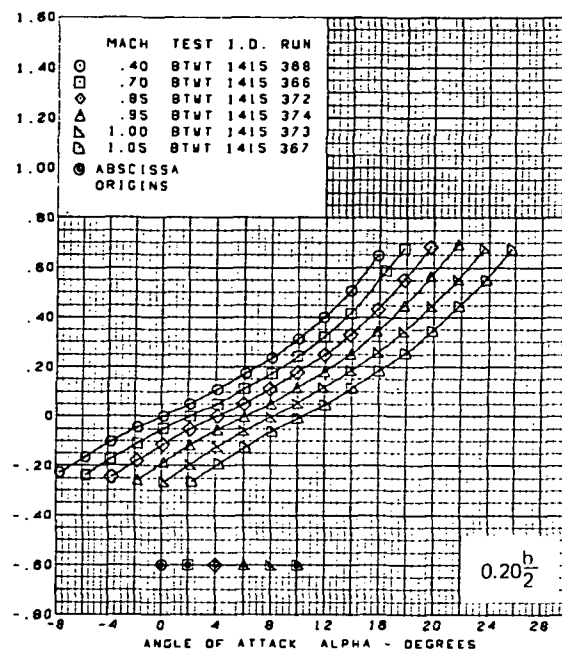
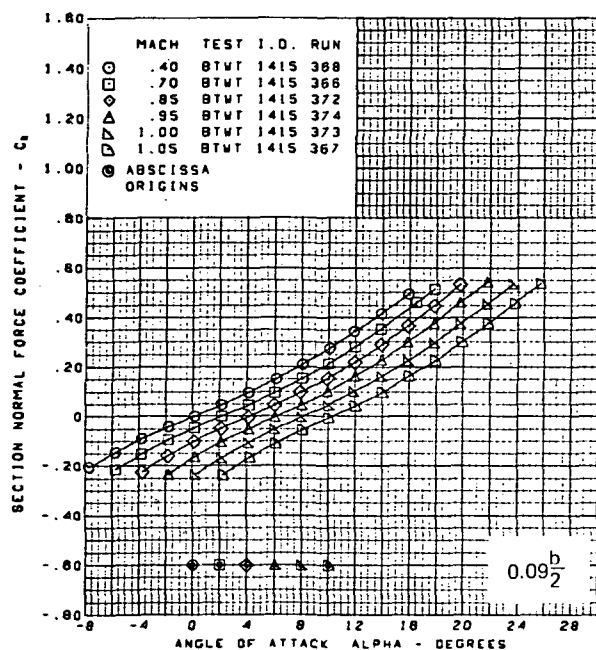
**Page**  
**Intentionally**  
**Left Blank**



Flat wing, rounded L.E.  
 L.E. deflection, full span =  $0.0^\circ$   
 T.E. deflection, full span =  $0.0^\circ$

(r) Wing Aerodynamic Coefficients

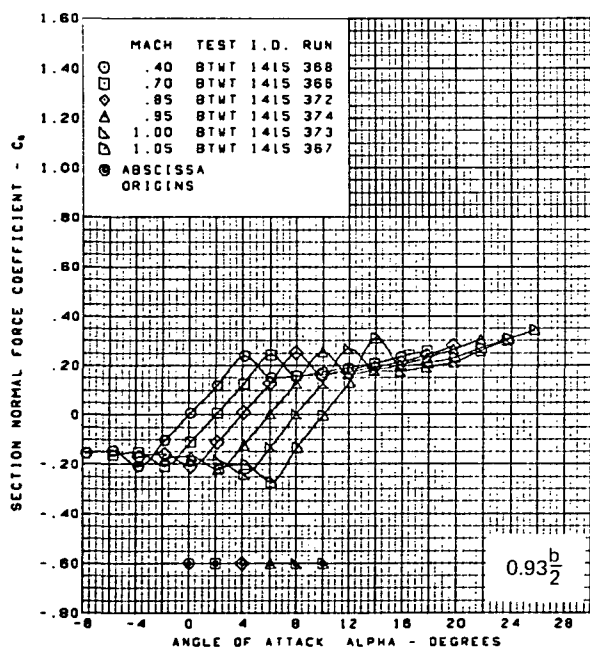
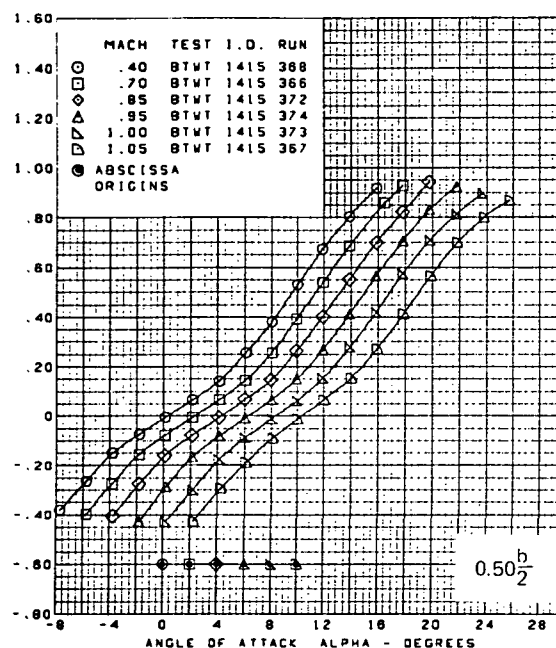
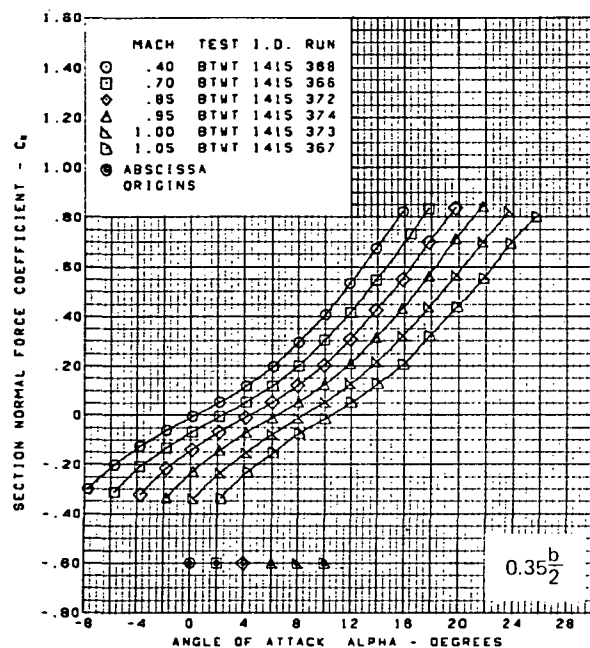
Figure 48.—(Concluded)



(a) Section Normal Force Coefficients vs. Angle of Attack,  $M = 0.40$  Through  $1.05$

Figure 49.—Wing Experimental Data—Effect of Mach Number and Angle of Attack; Flat Wing, Sharp L.E.; L.E. Deflection, Full Span =  $0.0^\circ$ ; T.E. Deflection, Full Span =  $0.0^\circ$

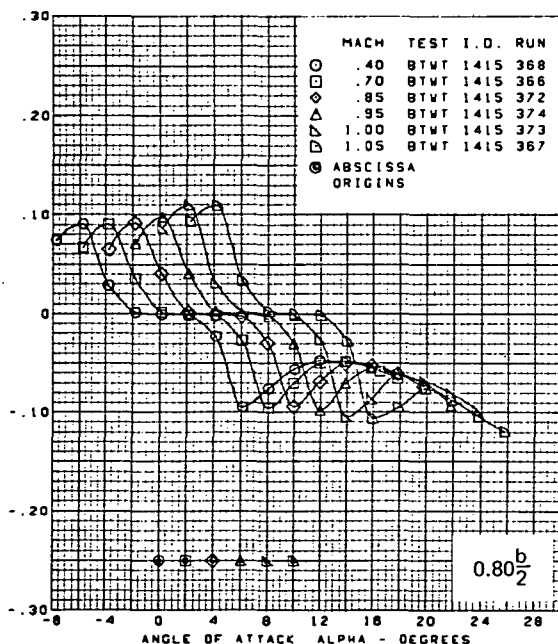
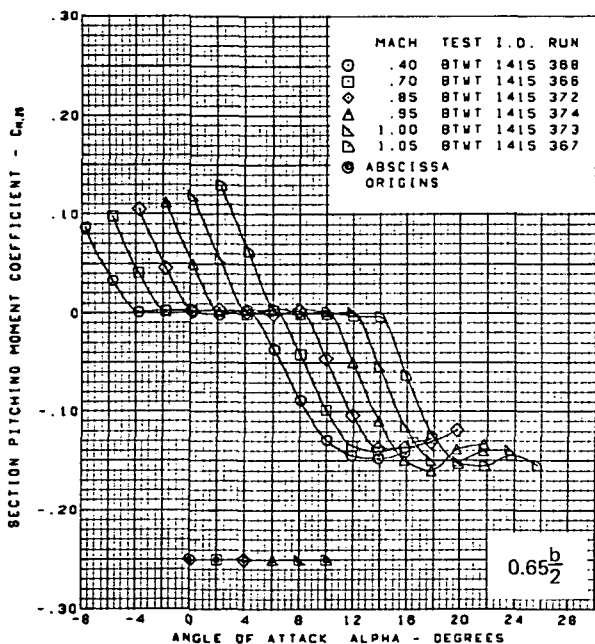
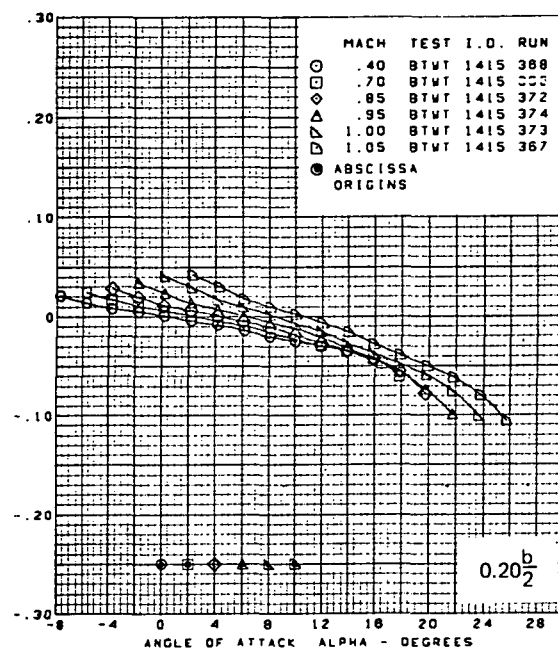
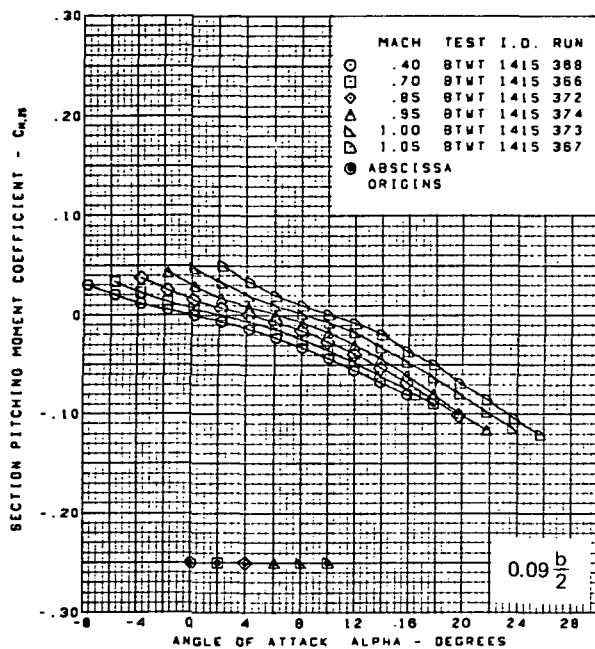




Flat wing, sharp L.E.  
 L.E. deflection, full span = 0.0°  
 T.E. deflection, full span = 0.0°

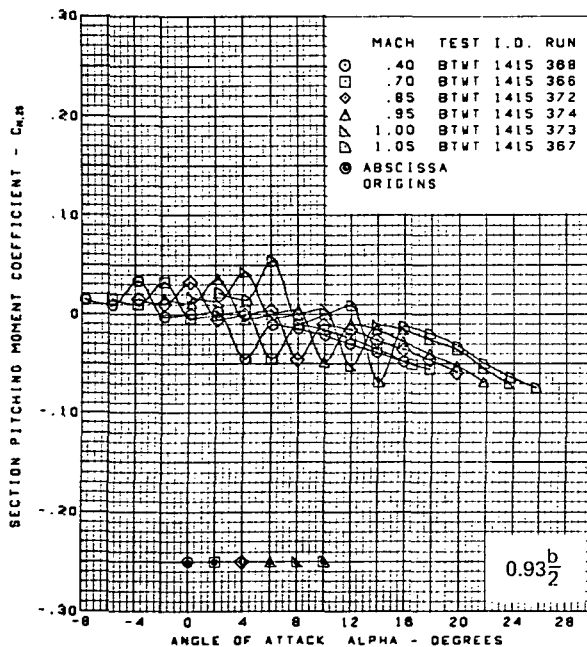
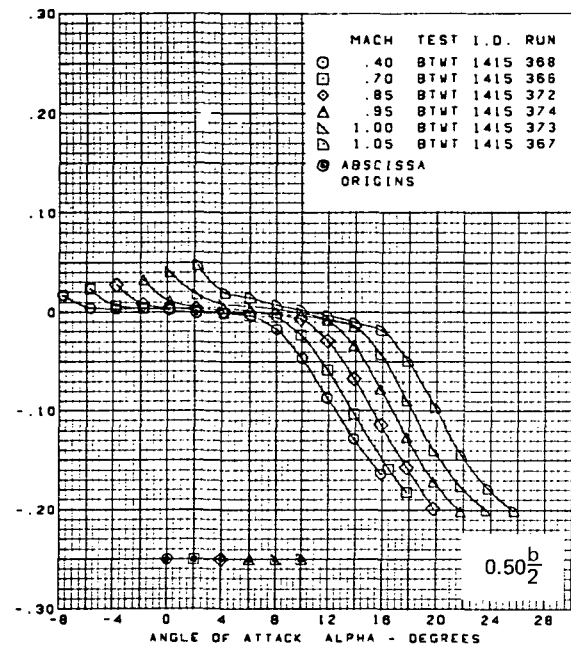
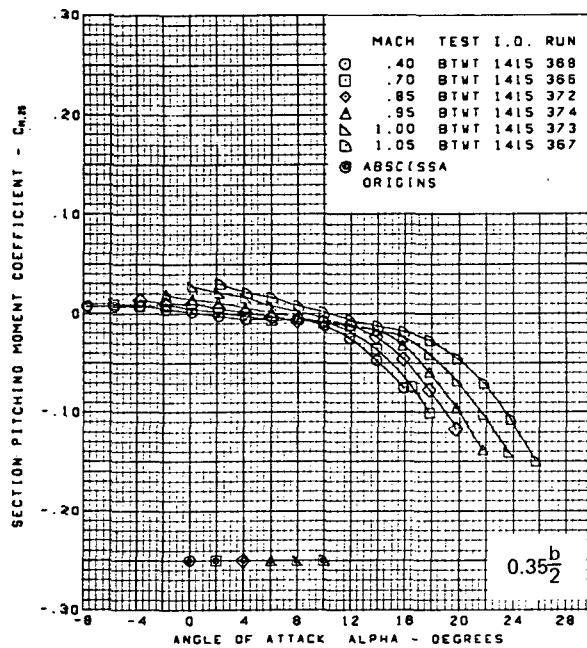
(a) (Concluded)

Figure 49.—(Continued)



(b) Section Pitching Moment Coefficients vs. Angle of Attack,  $M = 0.40$  Through 1.05

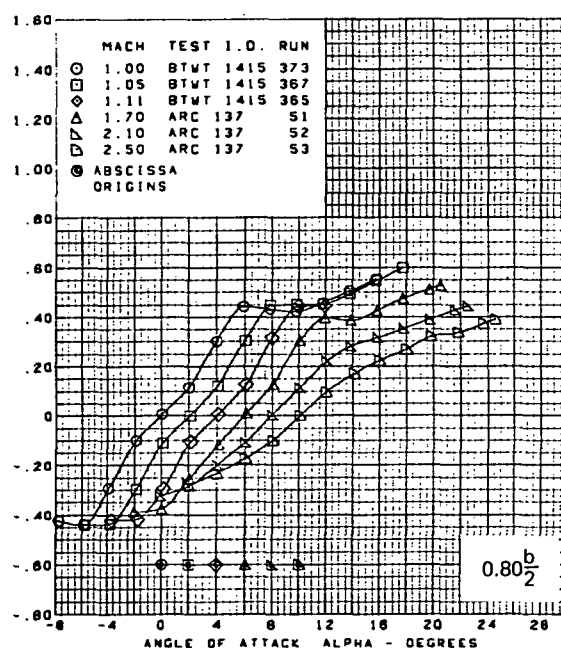
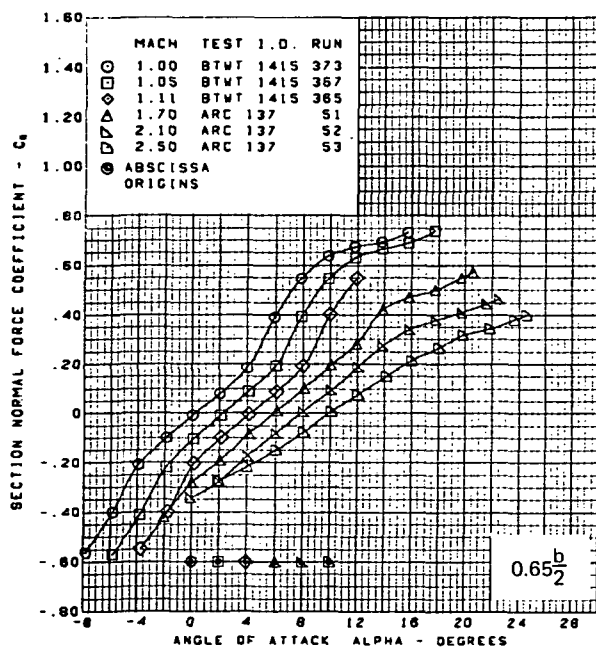
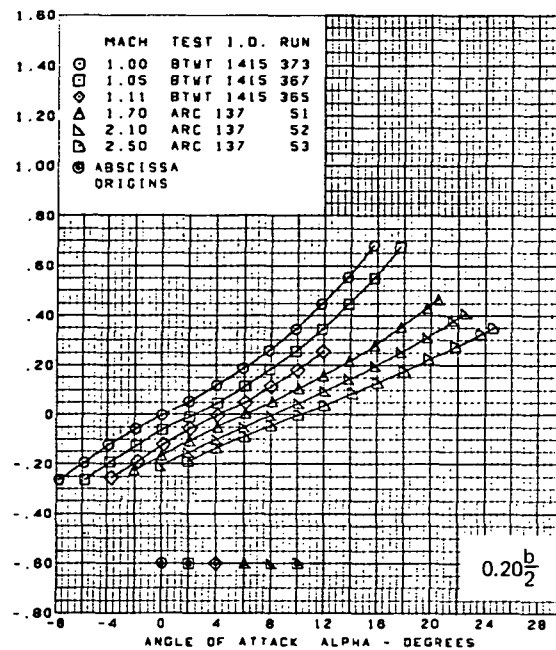
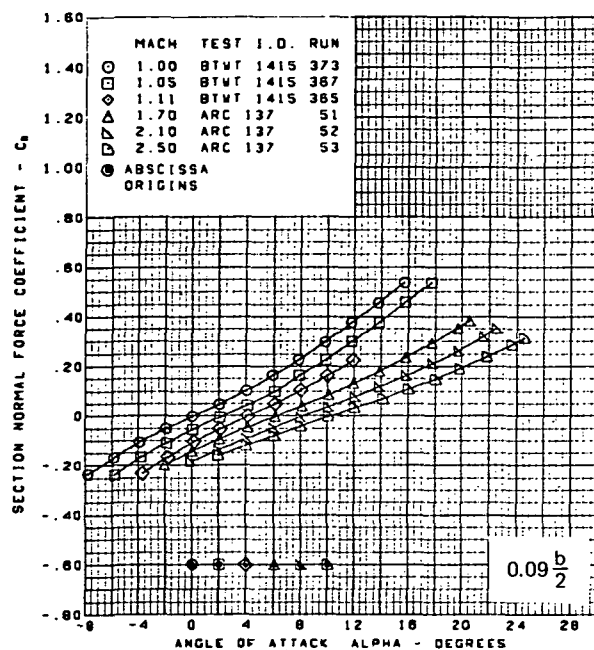
Figure 49.—(Continued)



Flat wing, sharp L.E.  
 L.E. deflection, full span =  $0.0^\circ$   
 T.E. deflection, full span =  $0.0^\circ$

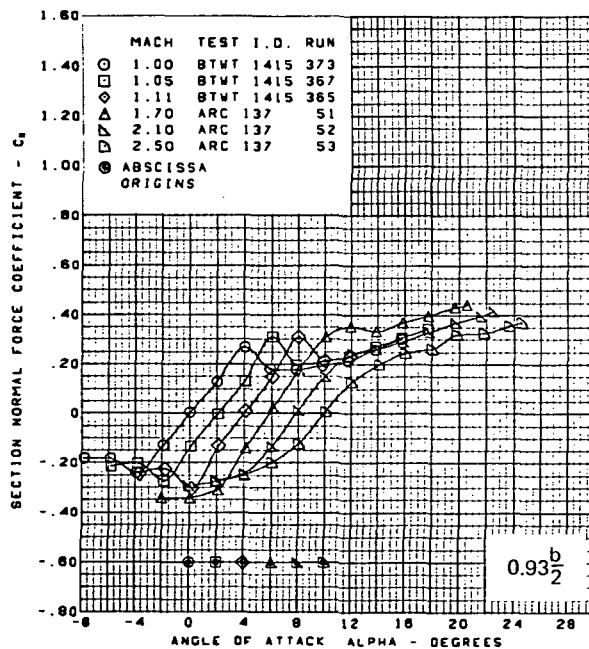
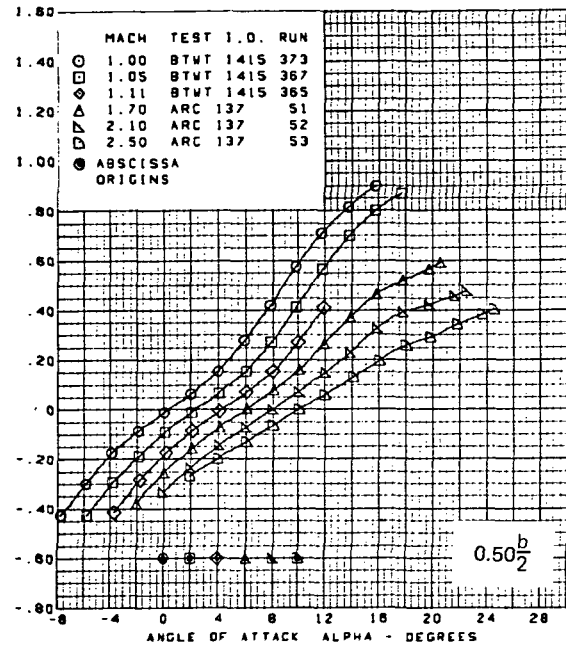
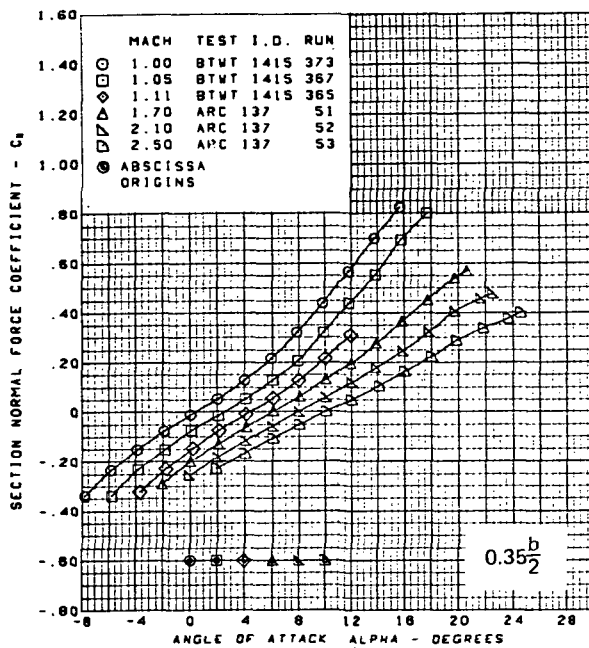
(b) (Concluded)

Figure 49. —(Continued)



(c) Section Normal Force Coefficients vs. Angle of Attack,  $M = 1.00$  Through 2.50

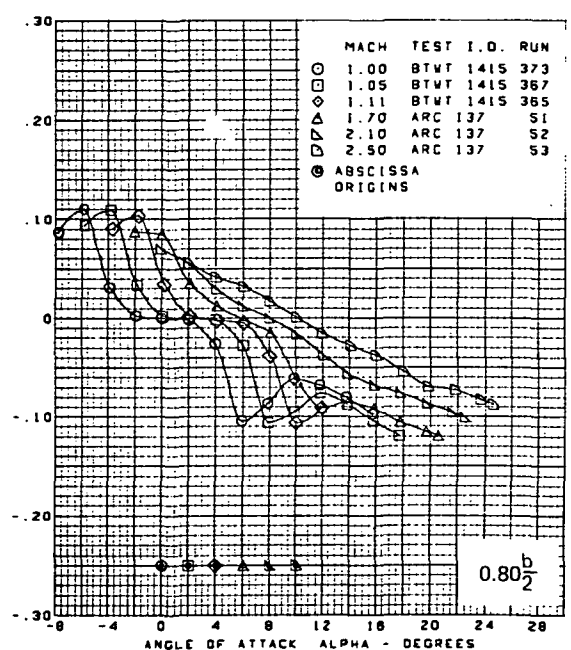
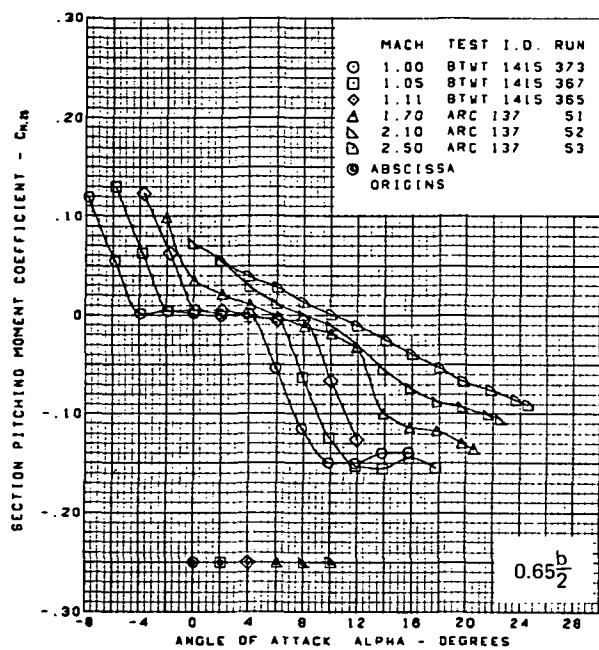
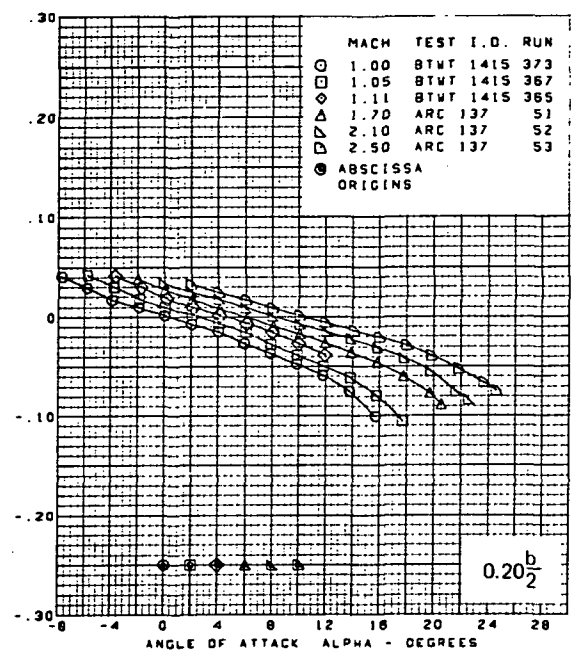
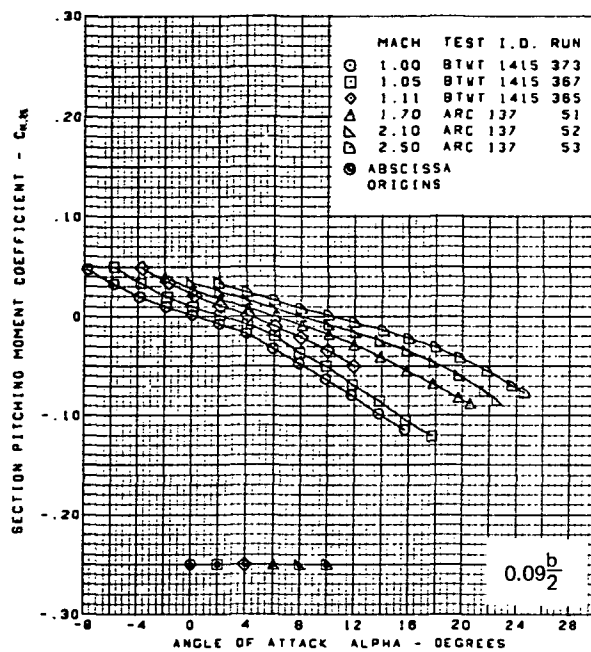
Figure 49.—(Continued)



Flat wing, sharp L.E.  
 L.E. deflection, full span =  $0.0^\circ$   
 T.E. deflection, full span =  $0.0^\circ$

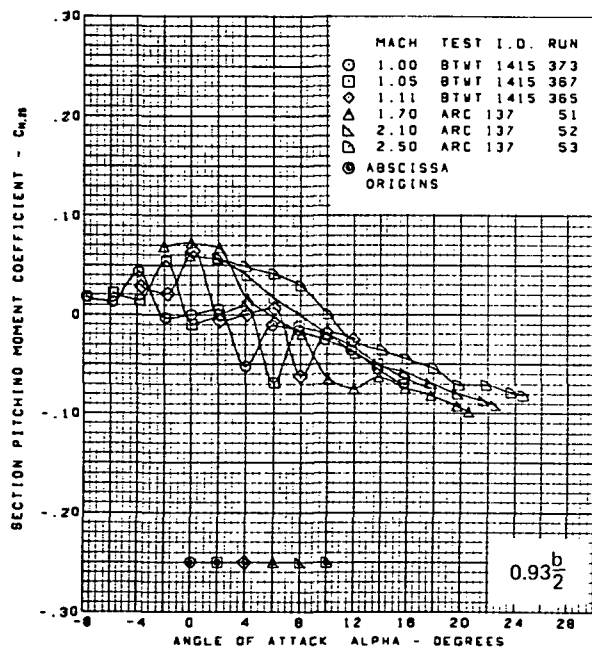
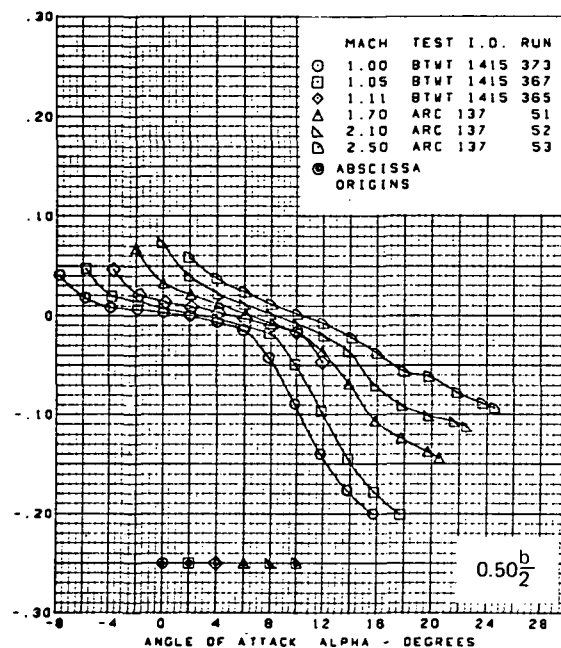
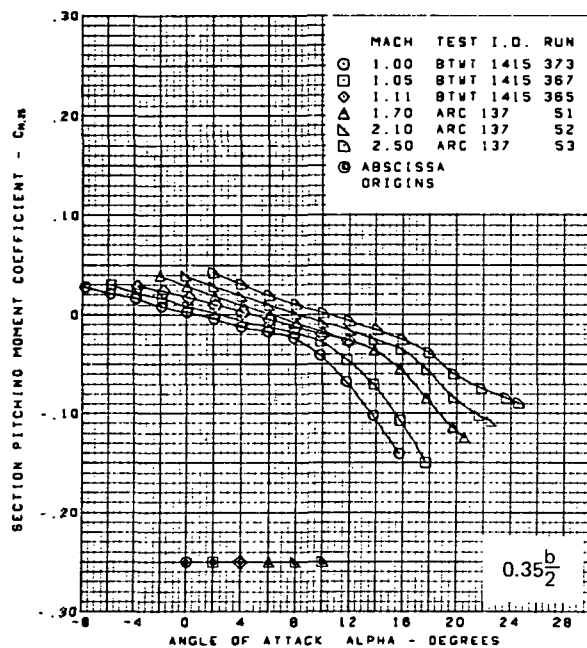
(c) (Concluded)

Figure 49.—(Continued)



(d) Section Pitching Moment Coefficients vs. Angle of Attack,  $M = 1.00$  Through 2.50

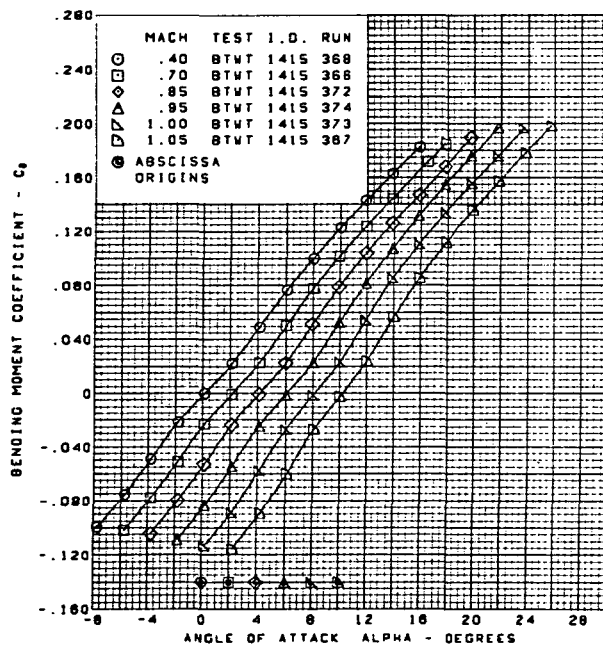
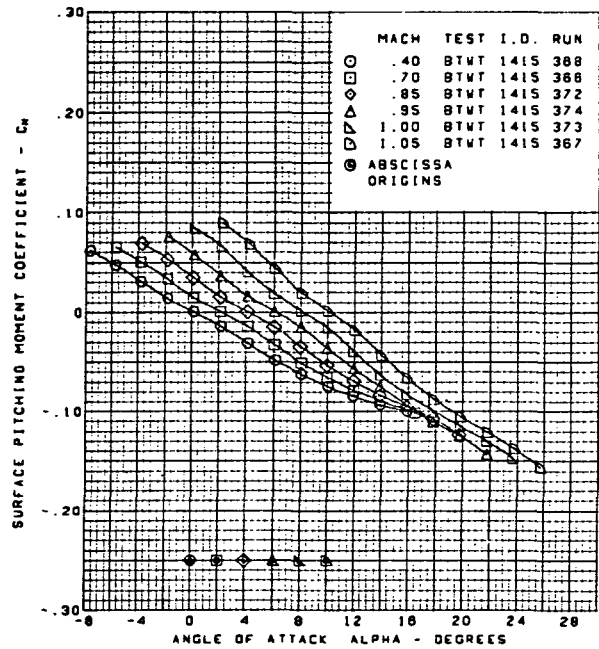
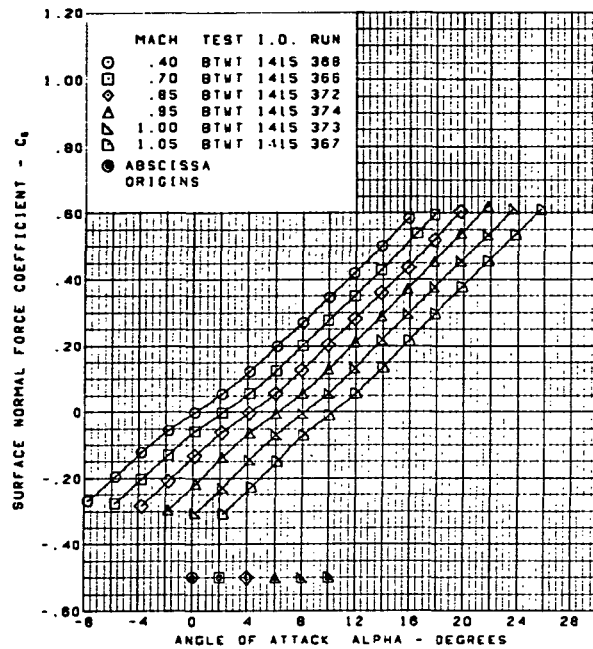
Figure 49. —(Continued)



Flat wing, sharp L.E.  
 L.E. deflection, full span =  $0.0^\circ$   
 T.E. deflection, full span =  $0.0^\circ$

(d) (Concluded)

Figure 49. —(Continued)

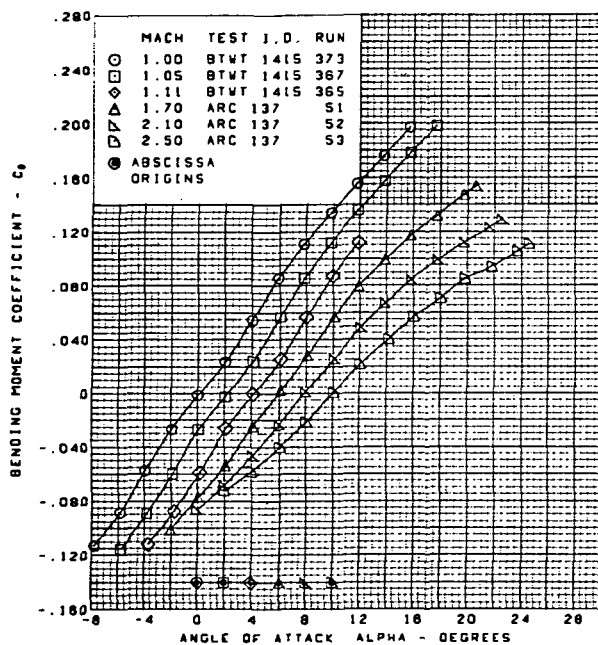
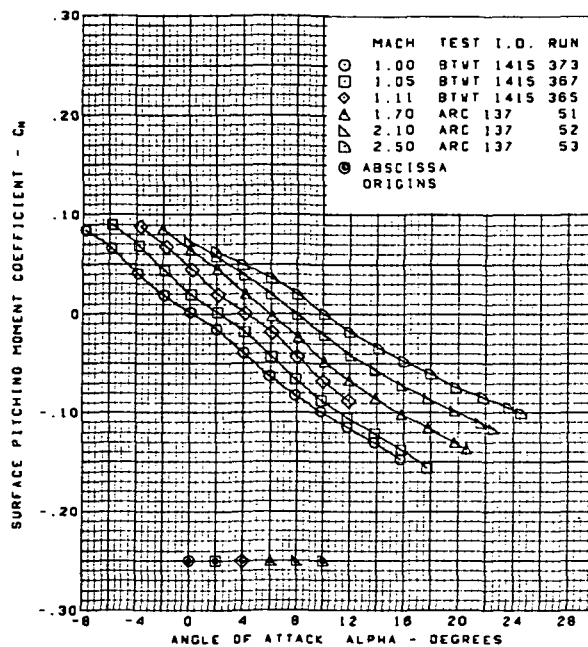
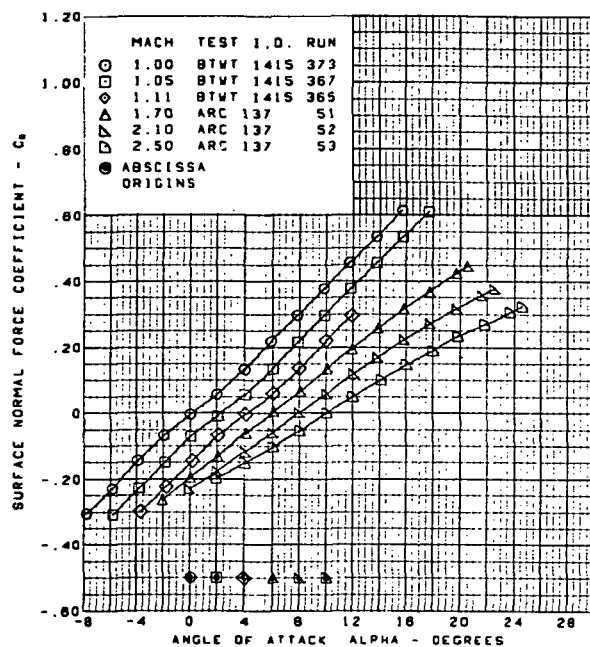


Flat wing, sharp L.E.  
 L.E. deflection, full span =  $0.0^\circ$   
 T.E. deflection, full span =  $0.0^\circ$

(e) Wing Aerodynamic Coefficients vs. Angle of Attack

Figure 49.—(Continued)

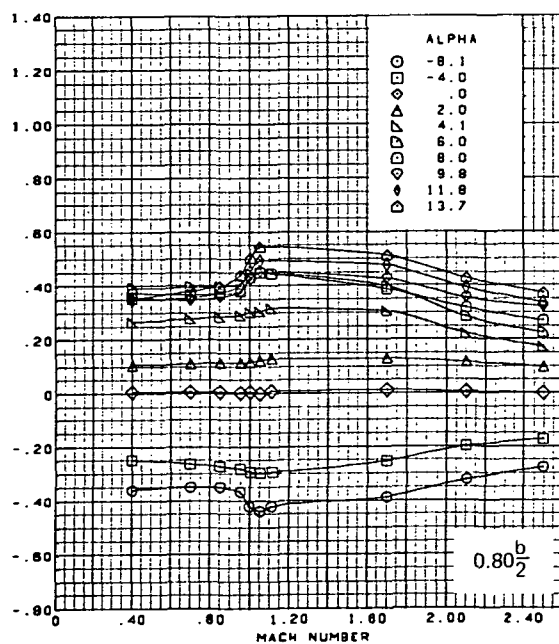
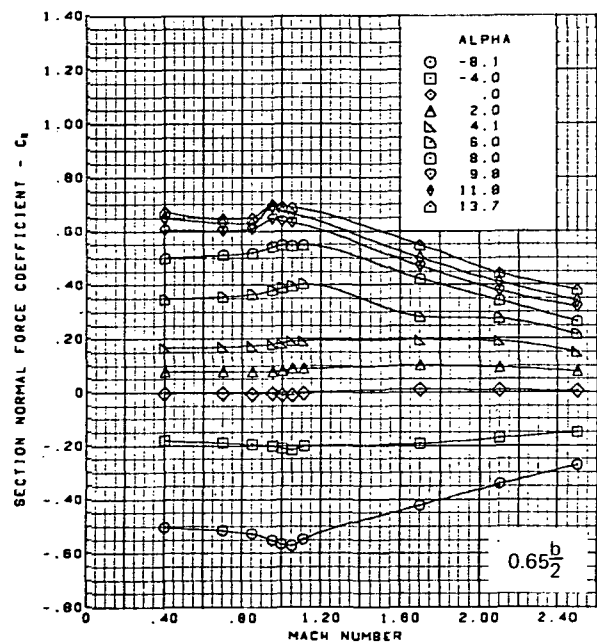
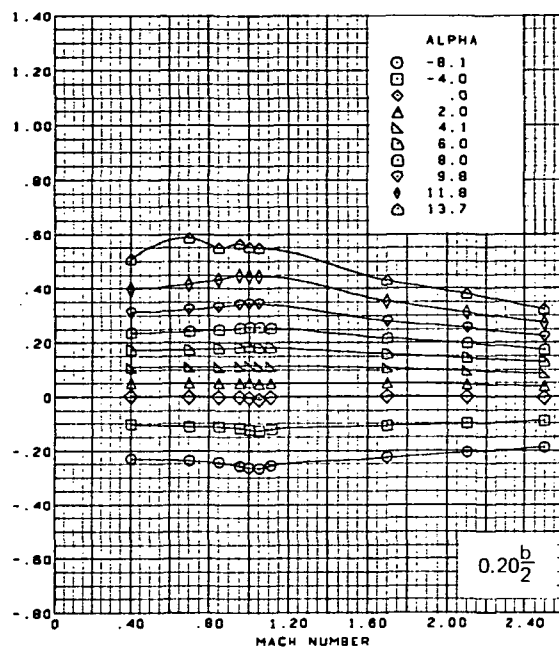
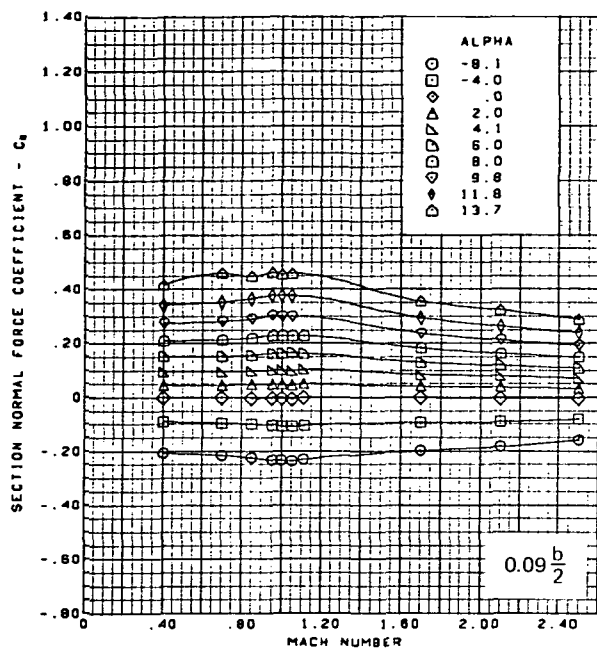




Flat wing, sharp L.E.  
 L.E. deflection, full span =  $0.0^\circ$   
 T.E. deflection, full span =  $0.0^\circ$

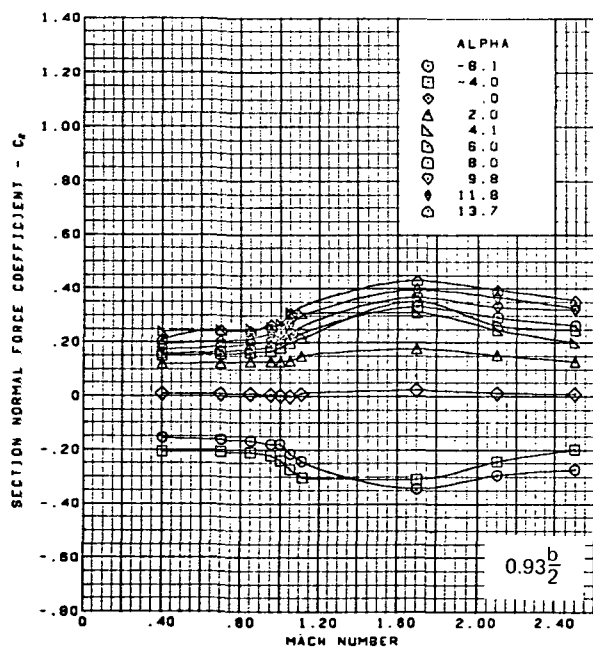
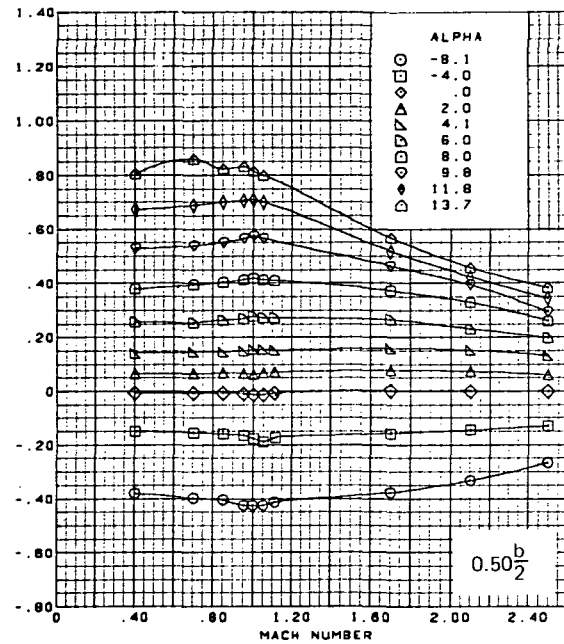
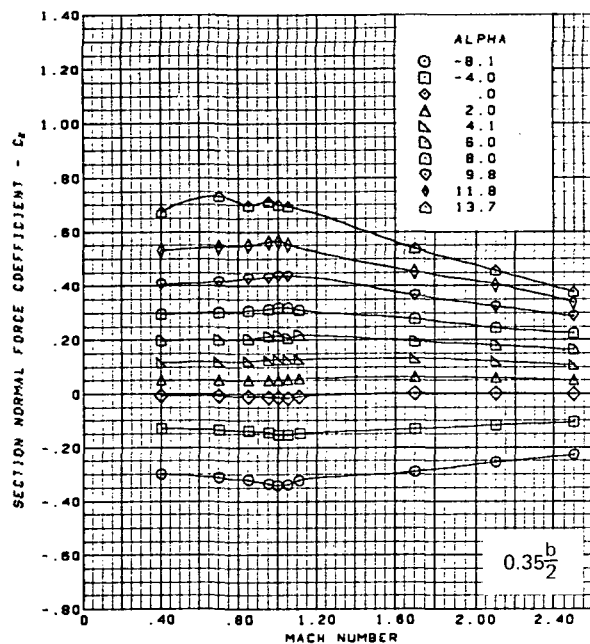
(e) (Concluded)

Figure 49. —(Continued)



(f) Section Aerodynamic Coefficients—Normal Force

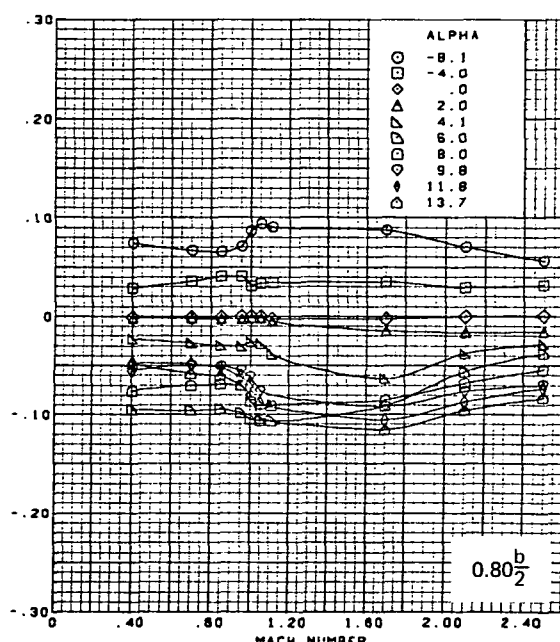
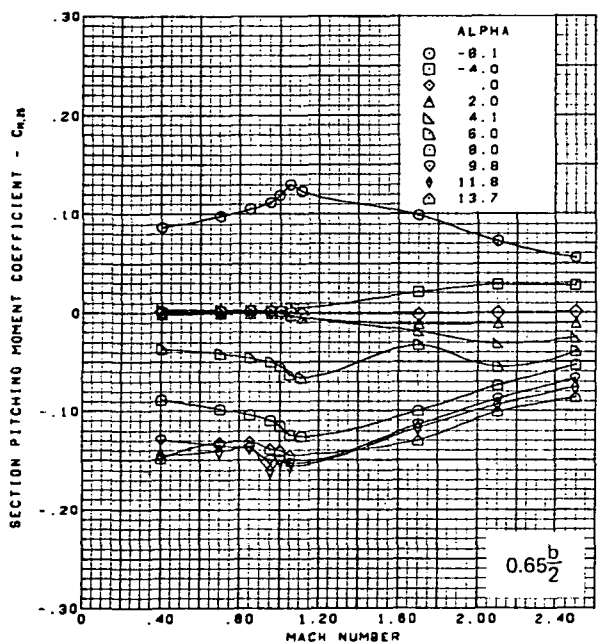
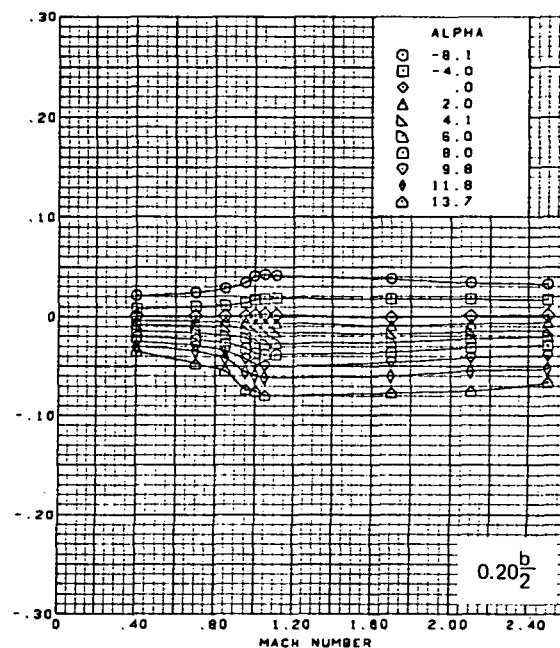
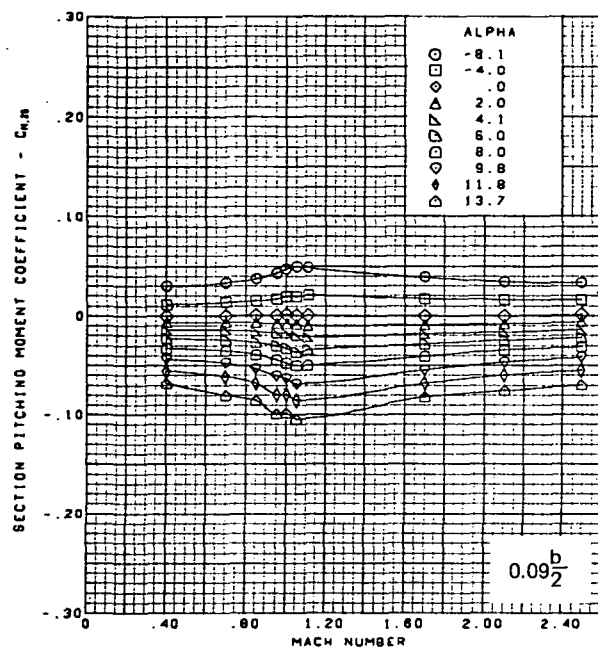
Figure 49. —(Continued)



Flat wing, sharp L.E.  
 L.E. deflection, full span =  $0.0^\circ$   
 T.E. deflection, full span =  $0.0^\circ$

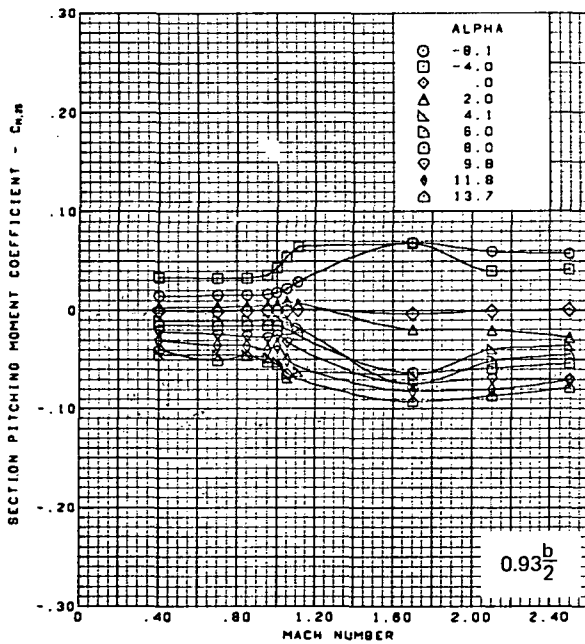
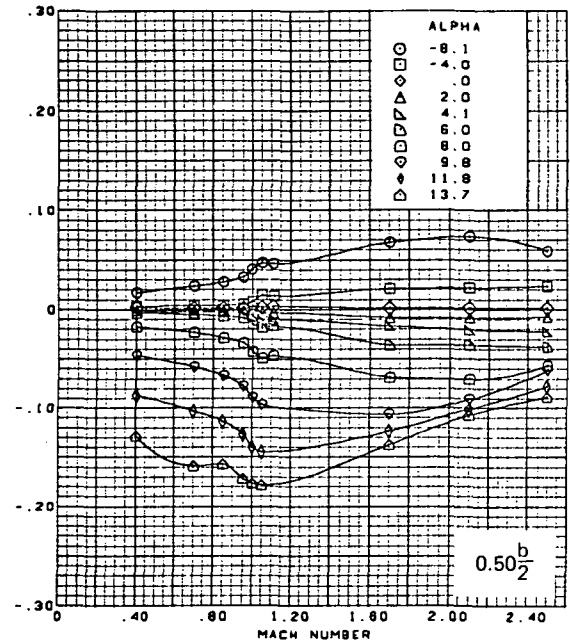
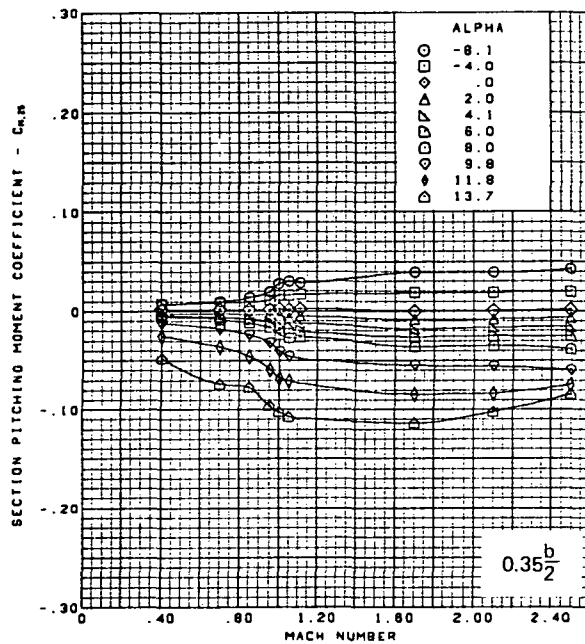
(f) (Concluded)

Figure 49.-(Continued)



(g) Section Aerodynamic Coefficients—Pitching Moment

Figure 49.—(Continued)

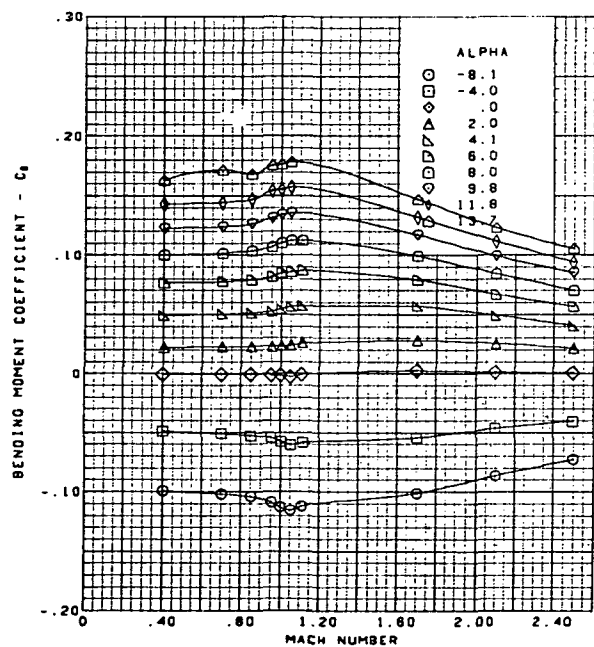
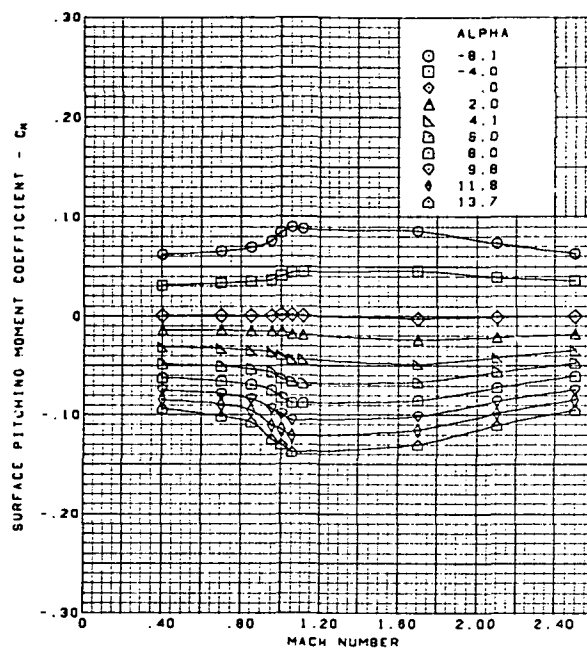
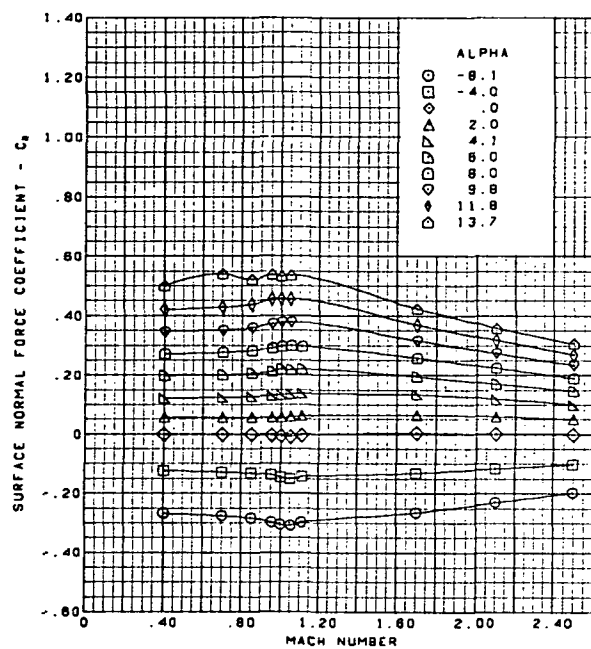


Flat wing, sharp L.E.  
 L.E. deflection, full span =  $0.0^\circ$   
 T.E. deflection, full span =  $0.0^\circ$

(g) (Concluded)

Figure 49.—(Continued)

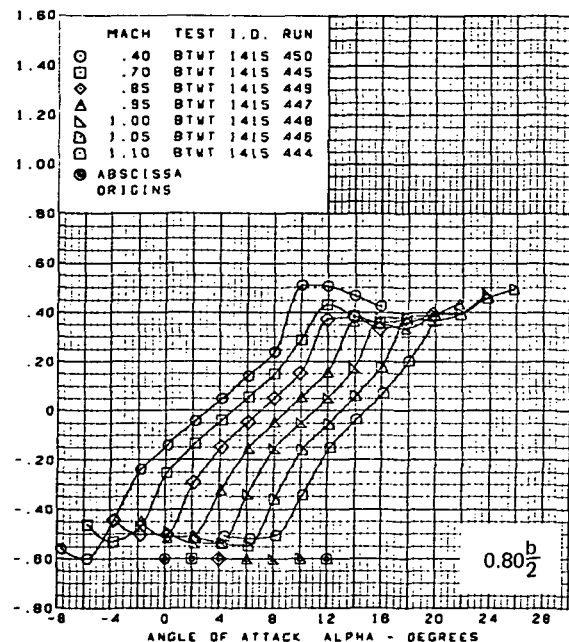
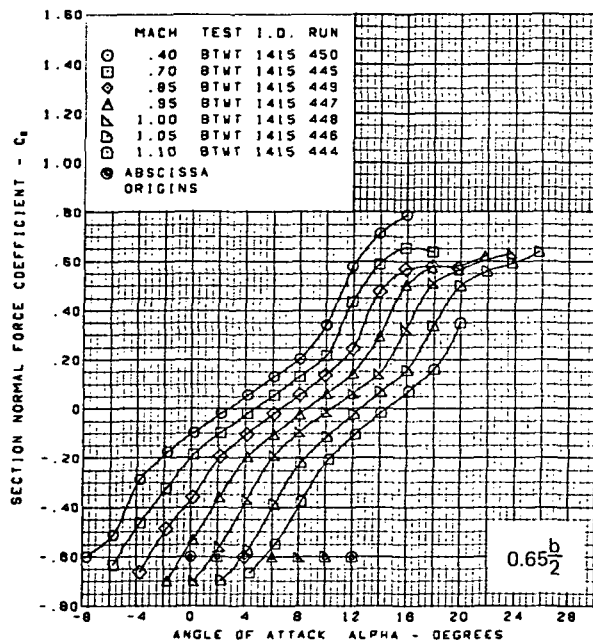
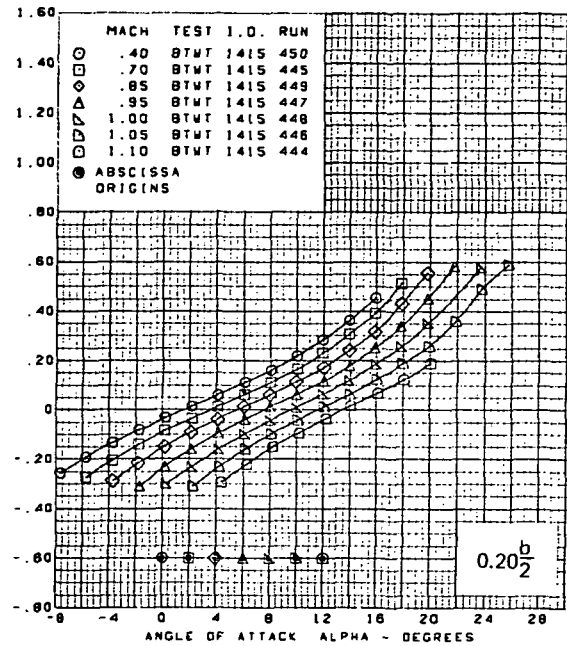
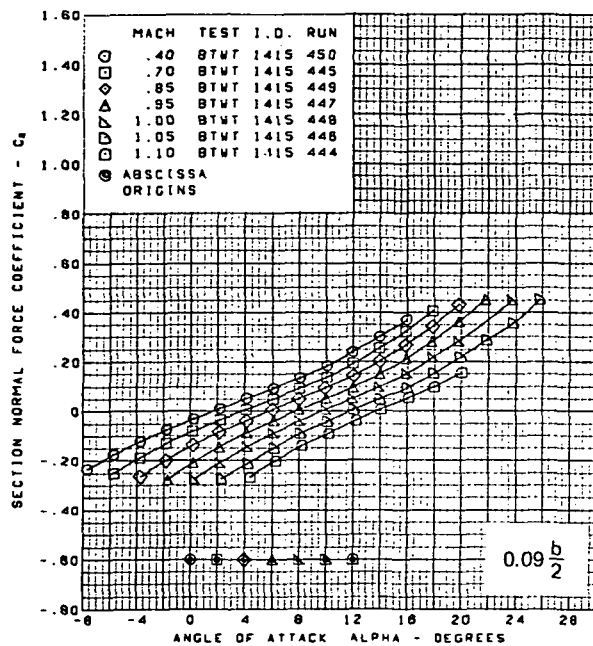
**Page  
Intentionally  
Left Blank**



Flat wing, sharp L.E.  
 L.E. deflection, full span =  $0.0^\circ$   
 T.E. deflection, full span =  $0.0^\circ$

(h) Wing Aerodynamic Coefficients

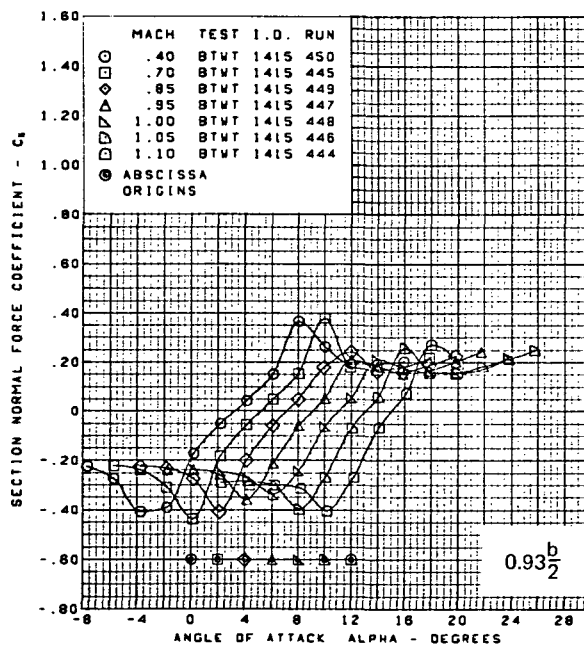
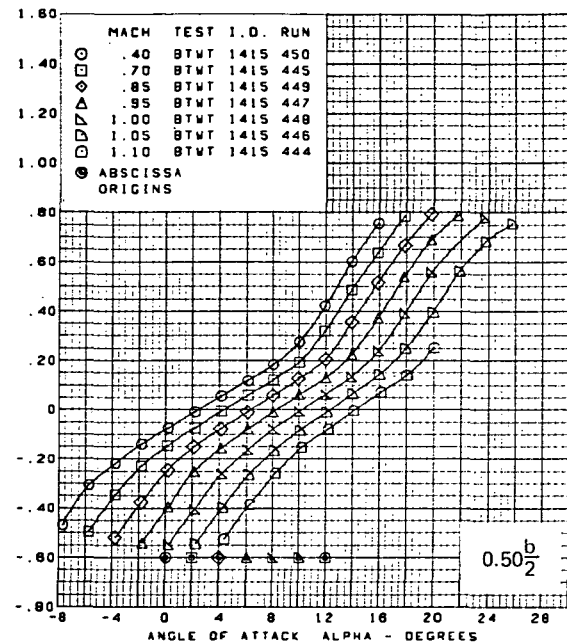
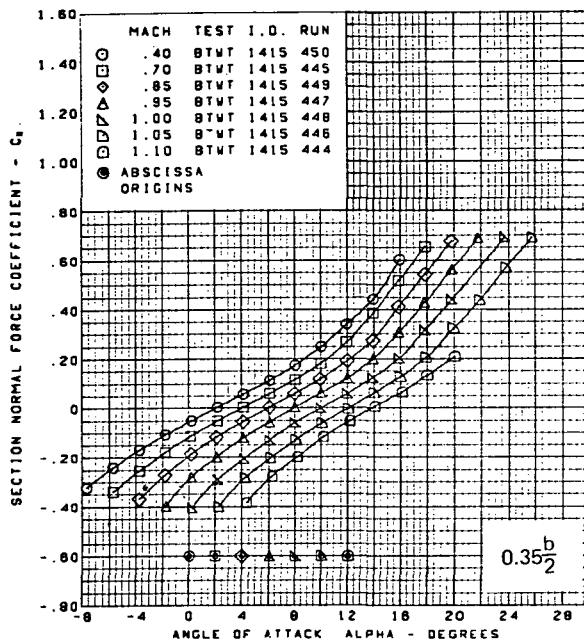
Figure 49.—(Concluded)



(a) Section Normal Force Coefficients vs. Angle of Attack,  $M = 0.40$  Through  $1.10$

Figure 50.—Wing Experimental Data—Effect of Mach Number and Angle of Attack; Twisted Wing, Rounded L.E.; L.E. Deflection, Full Span =  $0.0^\circ$ ; T.E. Deflection, Full Span =  $0.0^\circ$

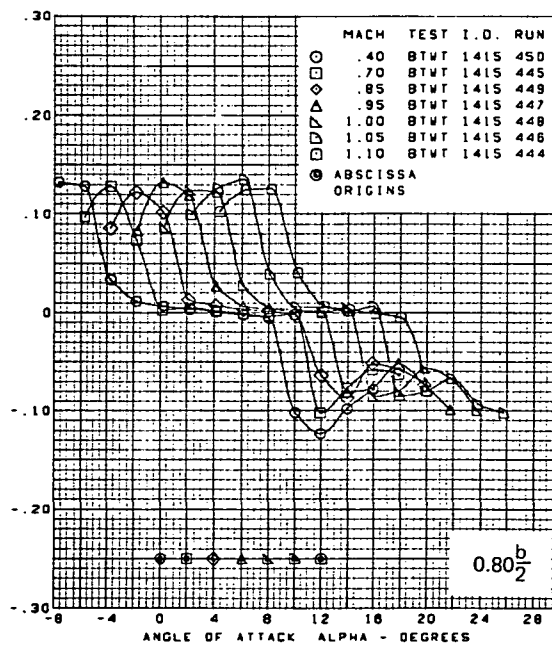
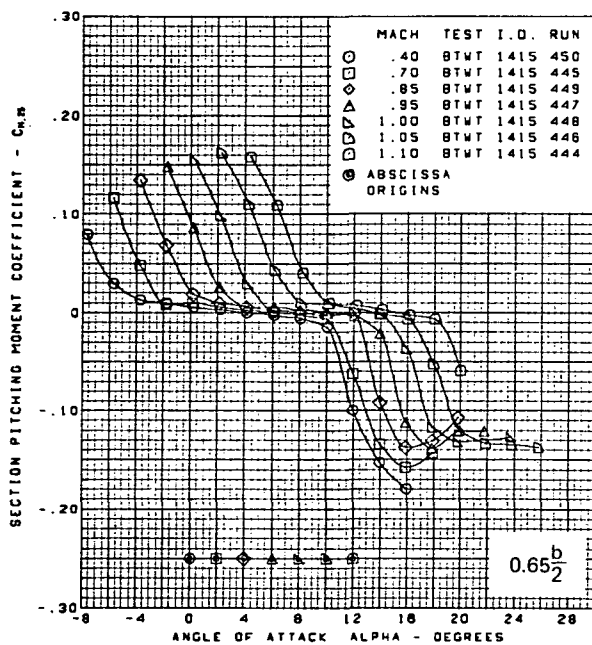
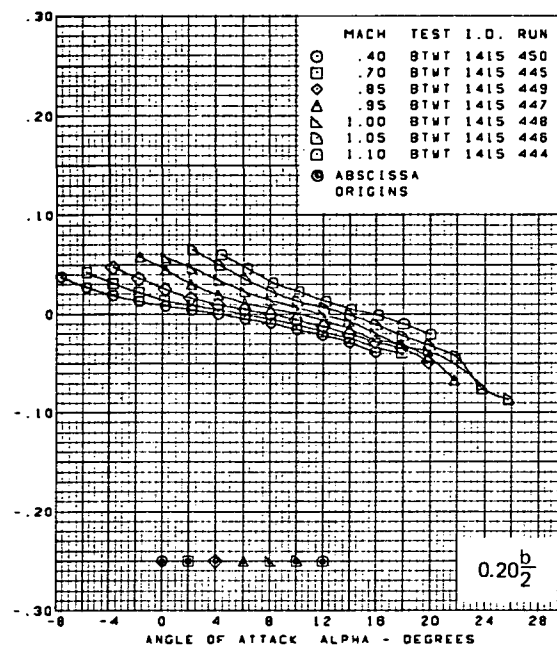
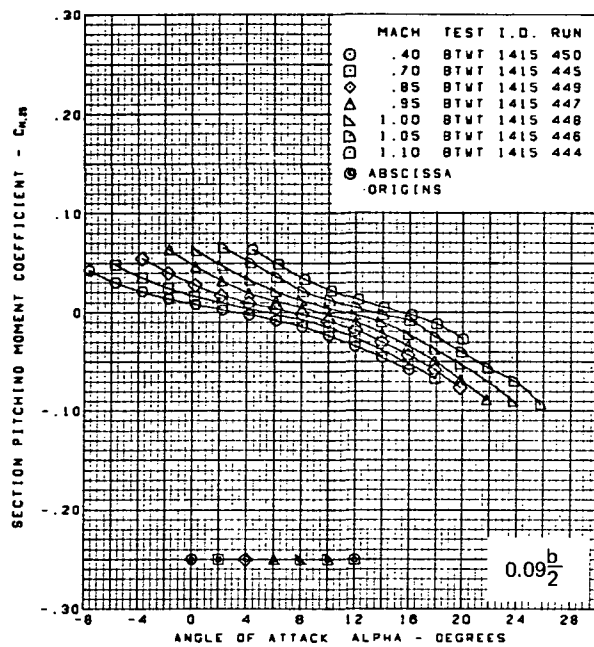




Twisted wing, rounded L.E.  
 L.E. deflection, full span =  $0.0^\circ$   
 T.E. deflection, full span =  $0.0^\circ$

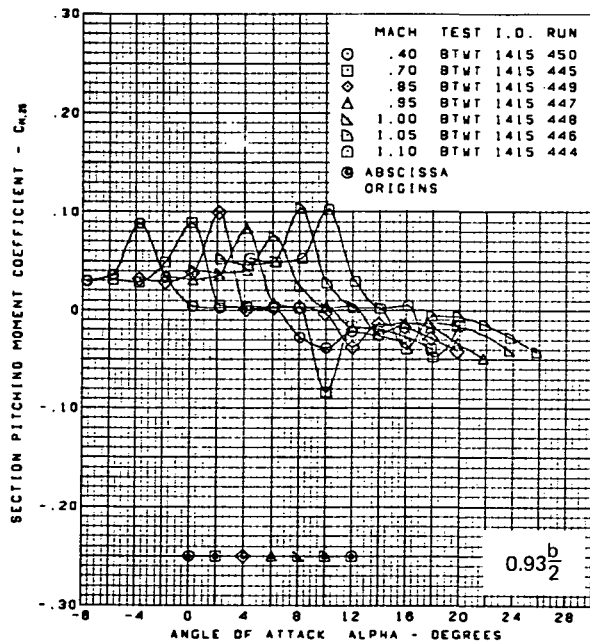
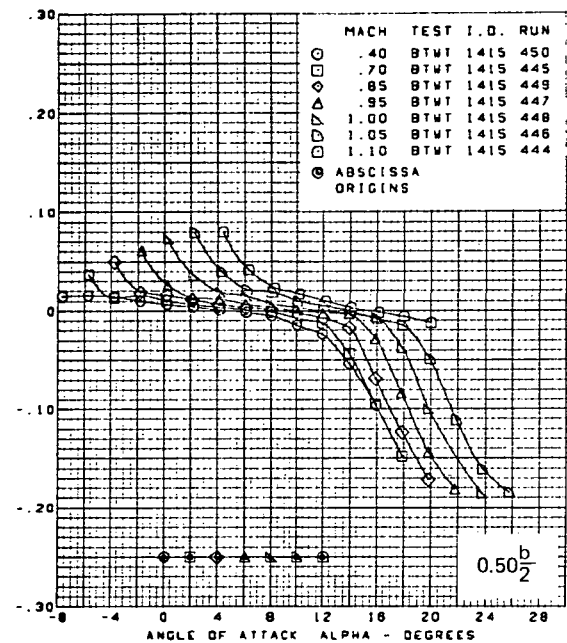
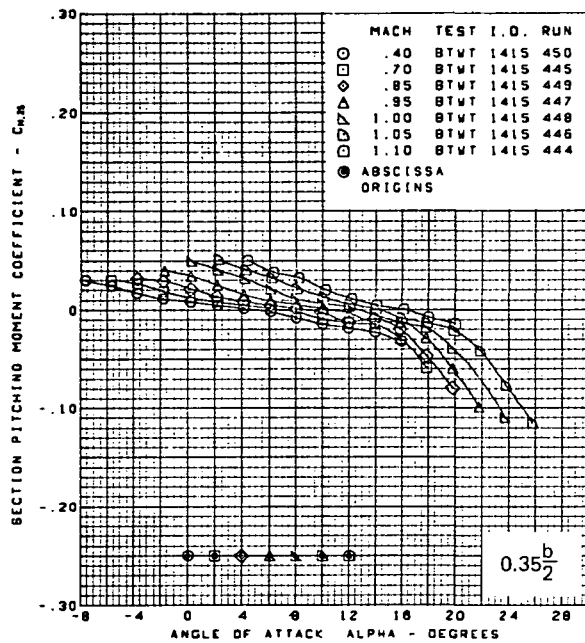
(a) (Concluded)

Figure 50.-(Continued)



(b) Section Pitching Moment Coefficients vs. Angle of Attack,  $M = 0.40$  Through 1.10

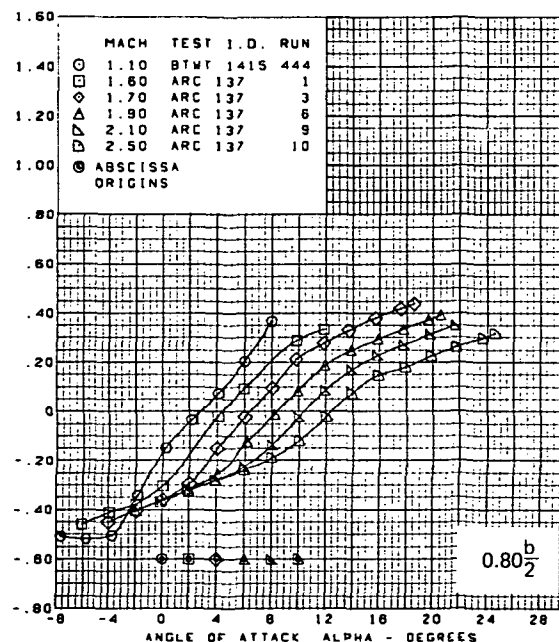
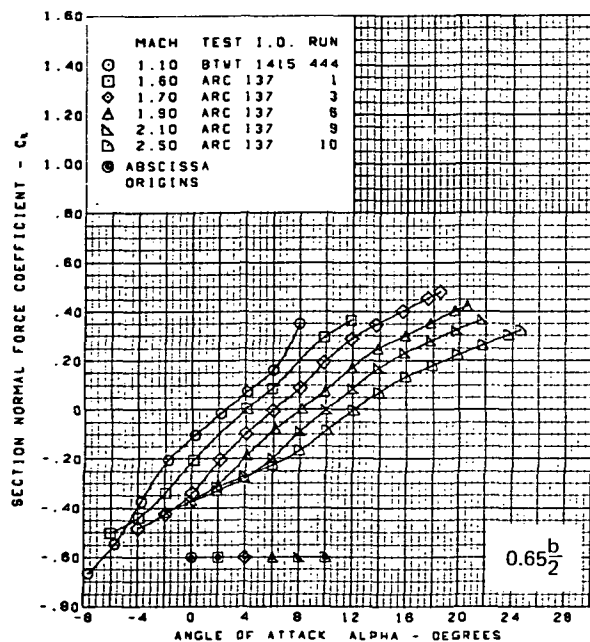
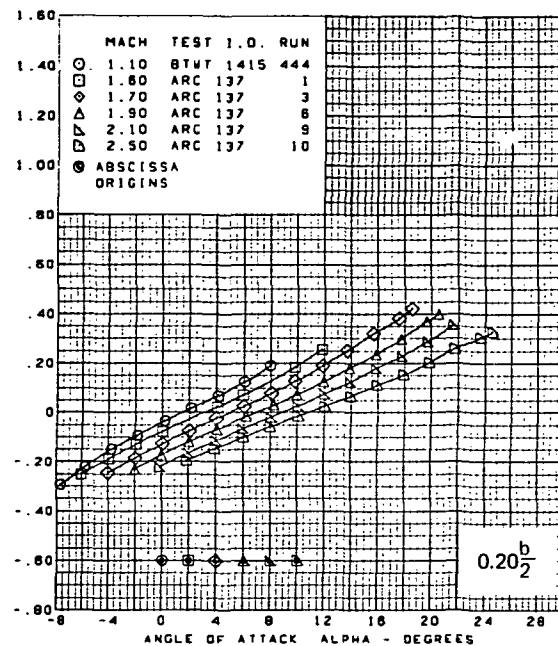
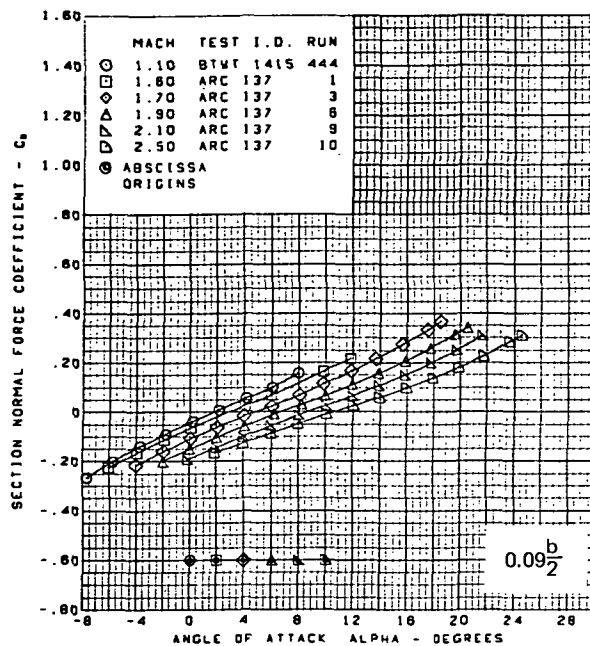
Figure 50.-(Continued)



Twisted wing, rounded L.E.  
 L.E. deflection, full span =  $0.0^\circ$   
 T.E. deflection, full span =  $0.0^\circ$

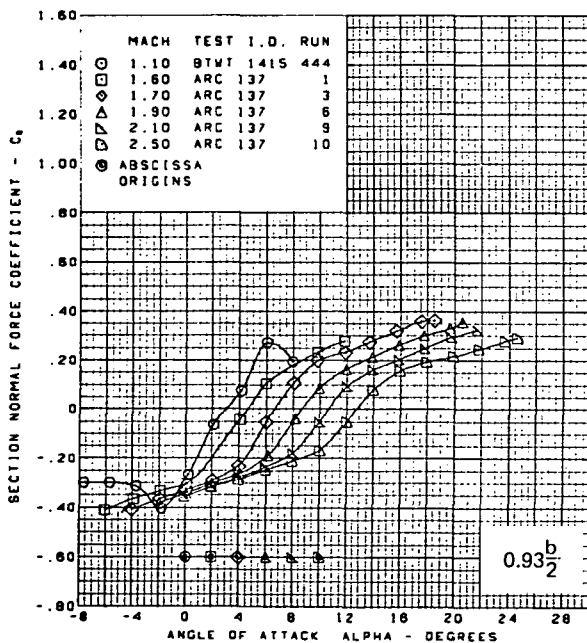
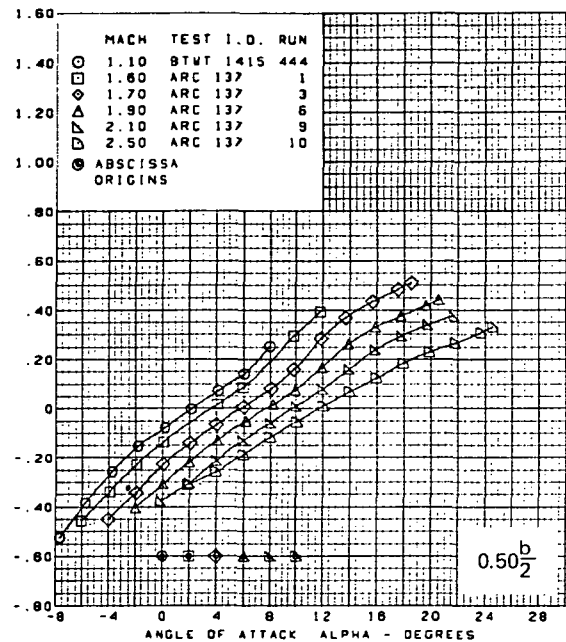
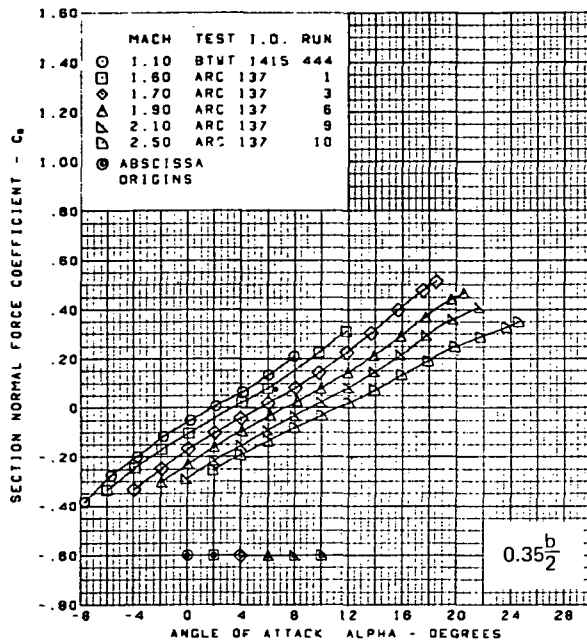
(b) (Concluded)

Figure 50.-(Continued)



(c) Section Normal Force Coefficients vs. Angle of Attack,  $M = 1.10$  Through  $2.50$

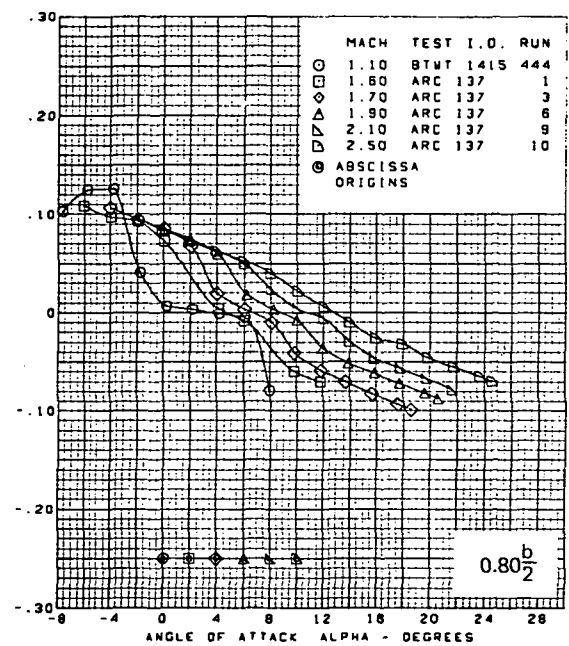
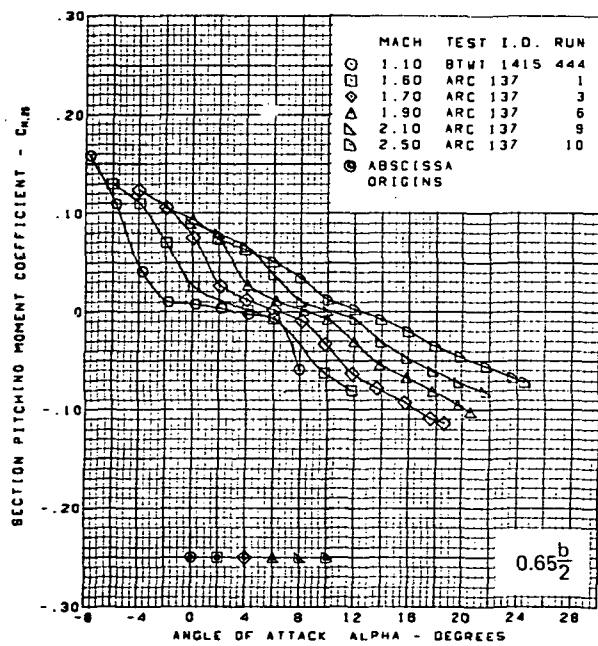
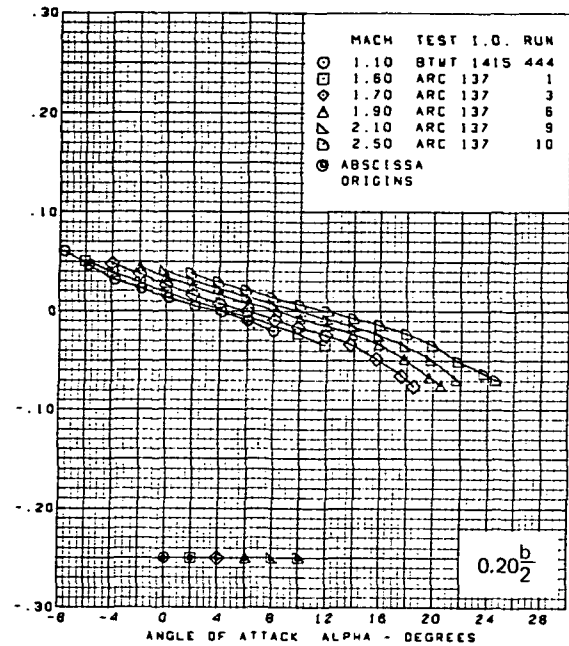
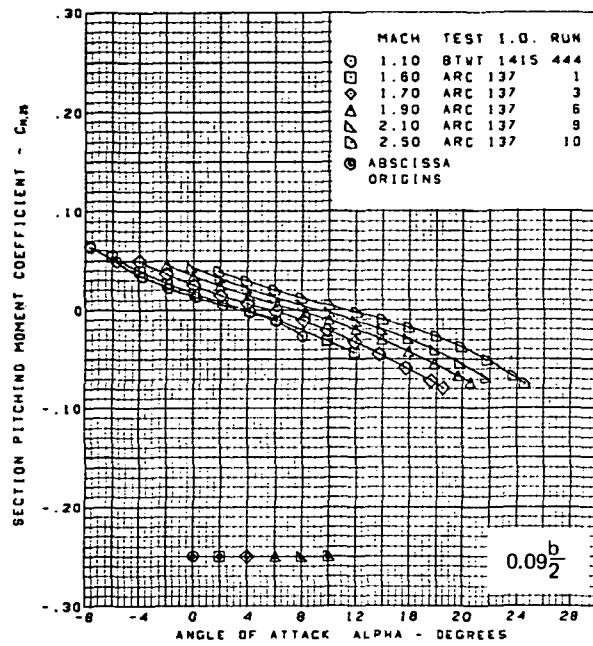
Figure 50.—(Continued)



Twisted wing, rounded L.E.  
 L.E. deflection, full span =  $0.0^\circ$   
 T.E. deflection, full span =  $0.0^\circ$

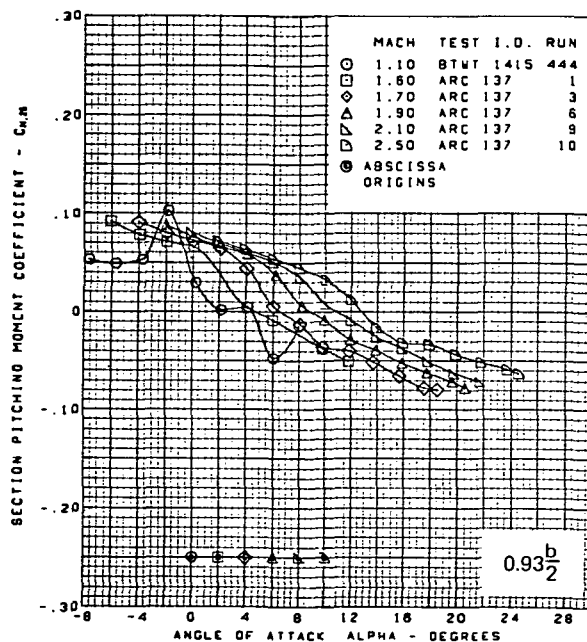
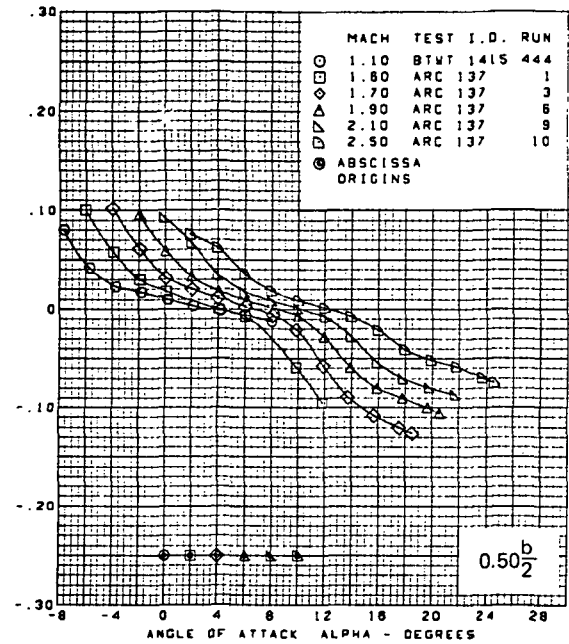
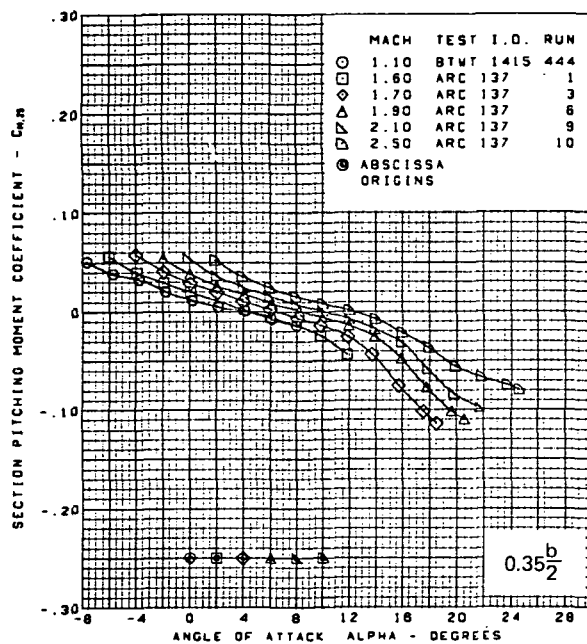
(c) (Concluded)

Figure 50.—(Continued)



(d) Section Pitching Moment Coefficients vs. Angle of Attack,  $M = 1.10$  Through 2.50

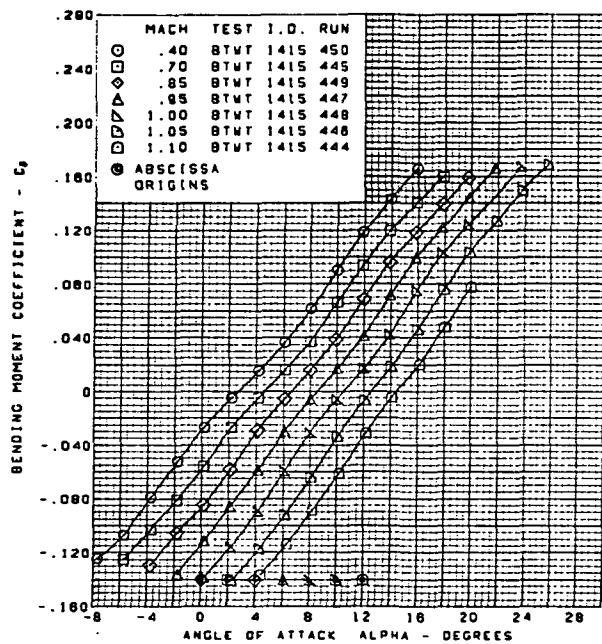
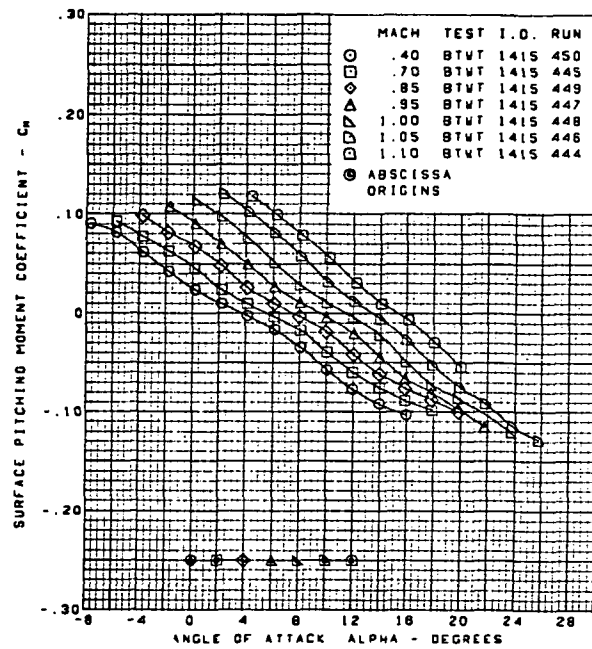
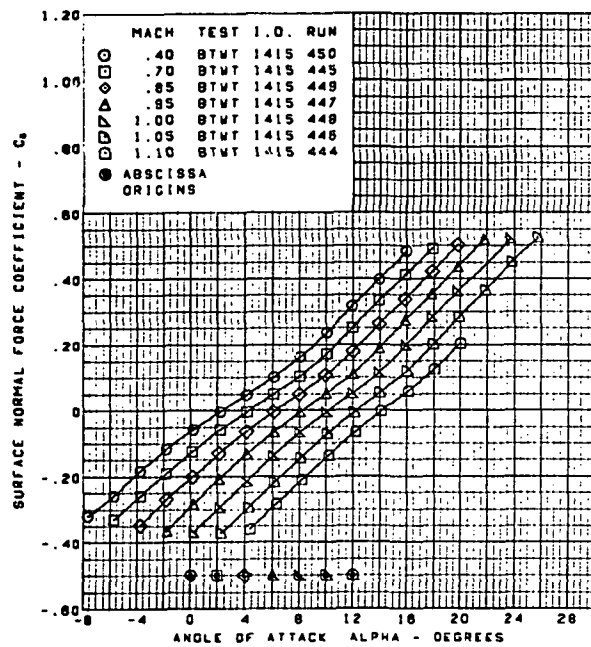
Figure 50.—(Continued)



Twisted wing, rounded L.E.  
 L.E. deflection, full span =  $0.0^\circ$   
 T.E. deflection, full span =  $0.0^\circ$

(d) (Concluded)

Figure 50.—(Continued)

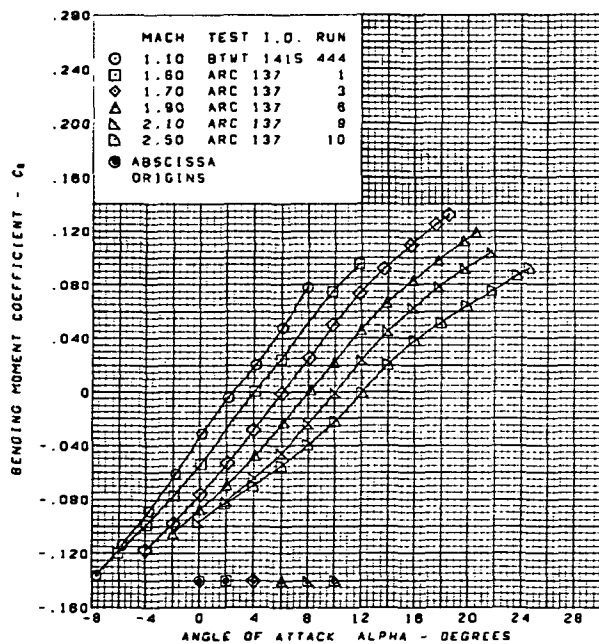
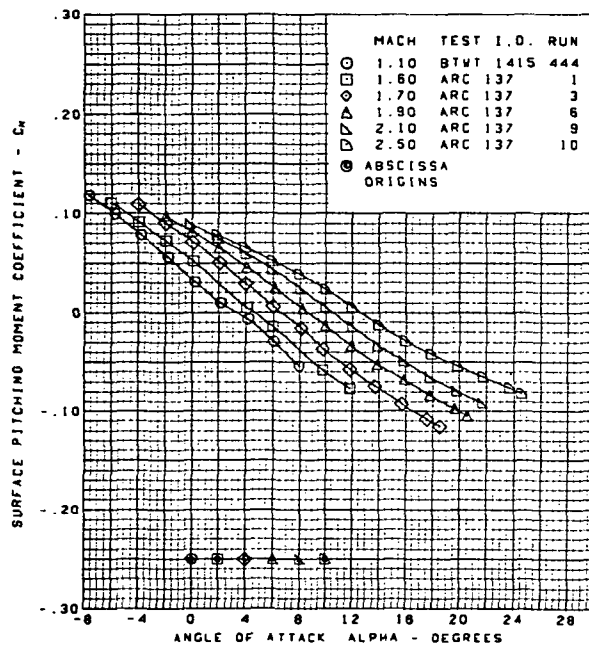
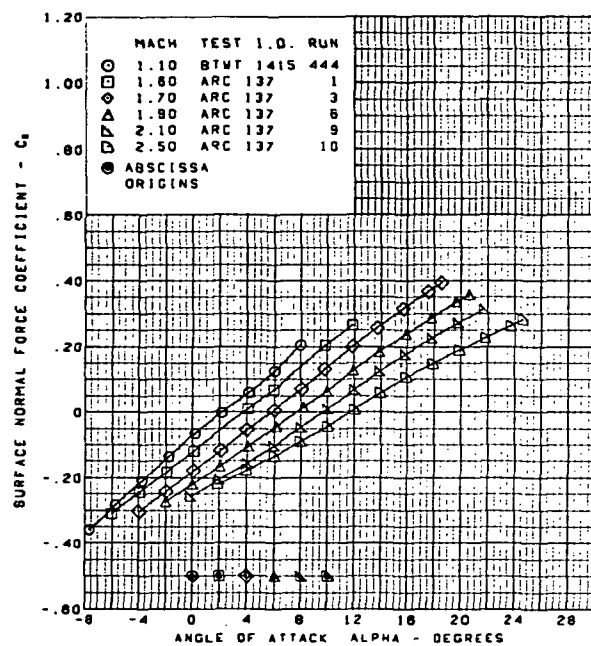


Twisted wing, rounded L.E.  
 L.E. deflection, full span =  $0.0^\circ$   
 T.E. deflection, full span =  $0.0^\circ$

(e) Wing Aerodynamic Coefficients vs. Angle of Attack

Figure 50.—(Continued)

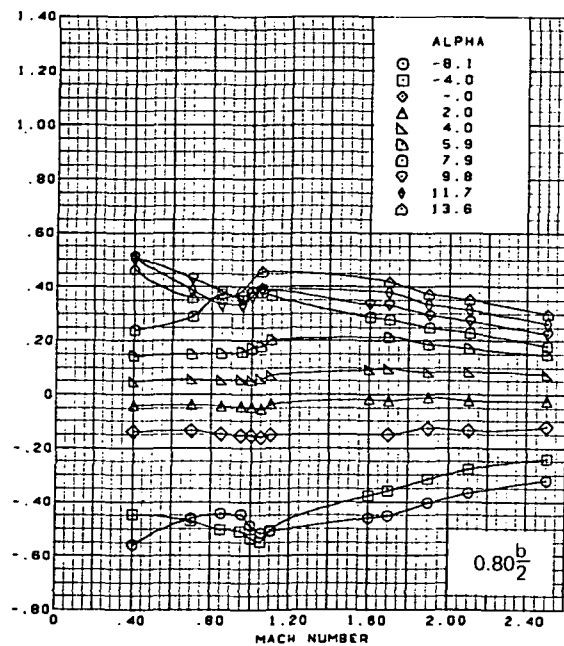
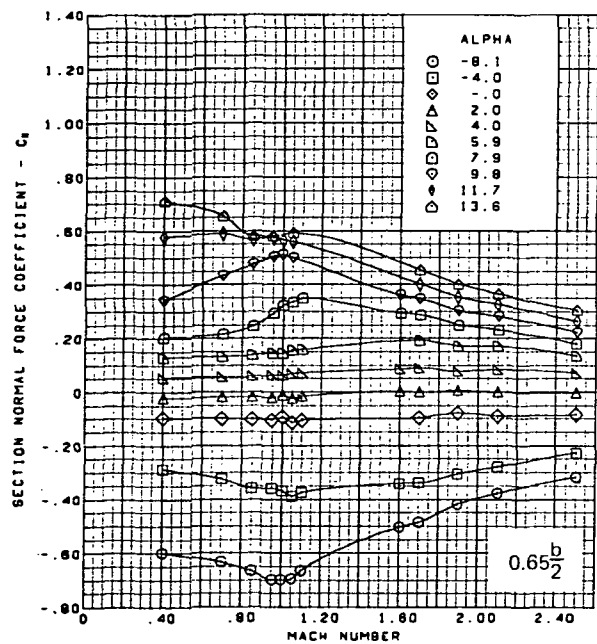
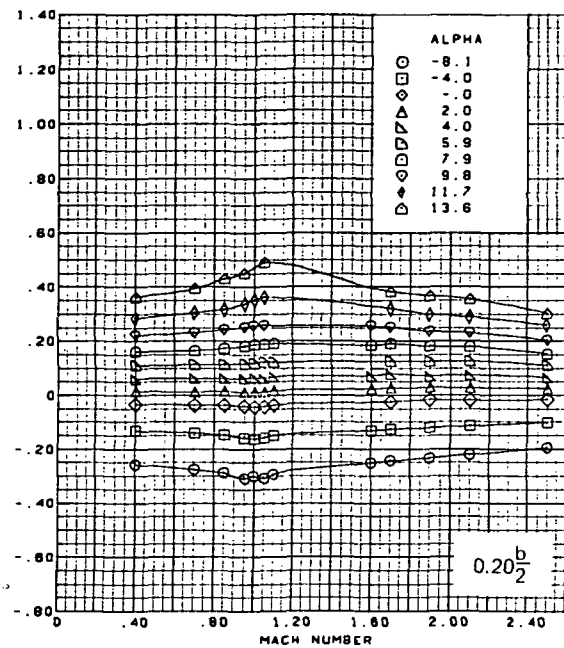
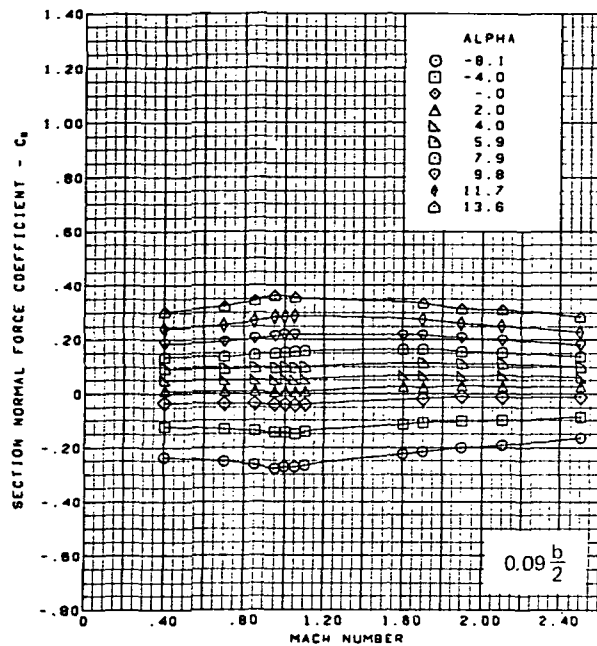




Twisted wing, rounded L.E.  
 L.E. deflection, full span =  $0.0^\circ$   
 T.E. deflection, full span =  $0.0^\circ$

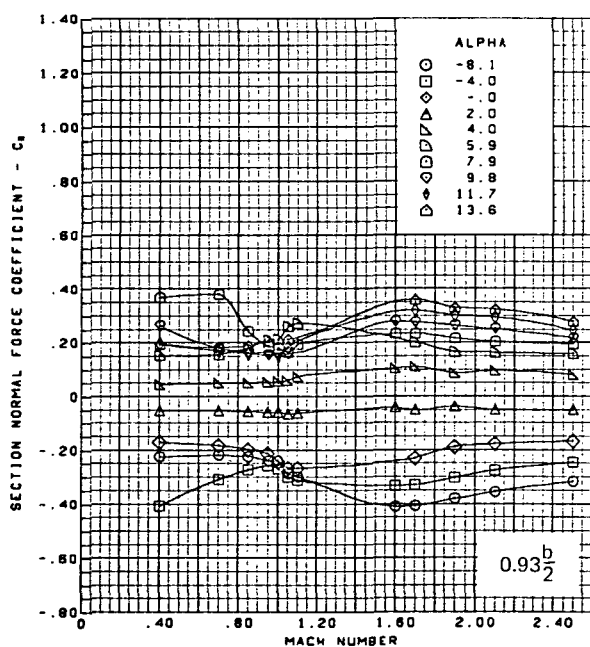
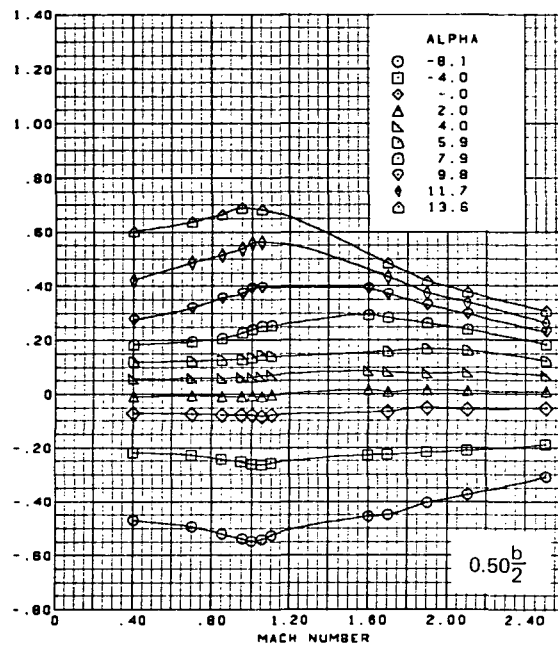
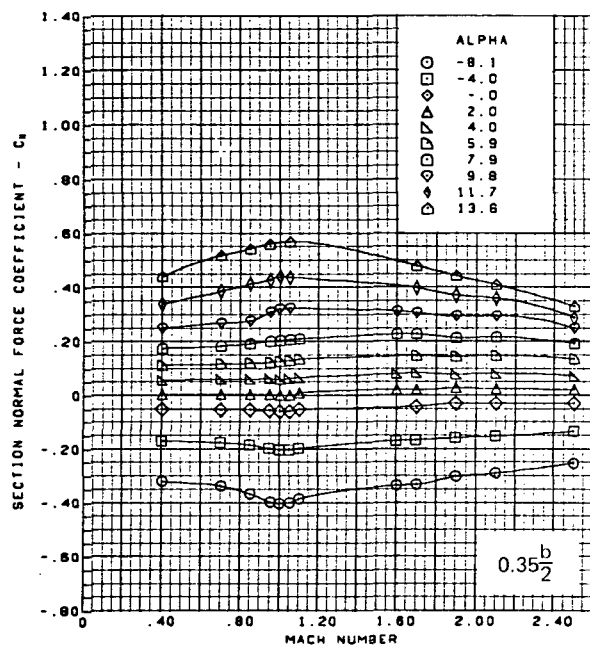
(e) (Concluded)

Figure 50.—(Continued)



(f) Section Aerodynamic Coefficients—Normal Force

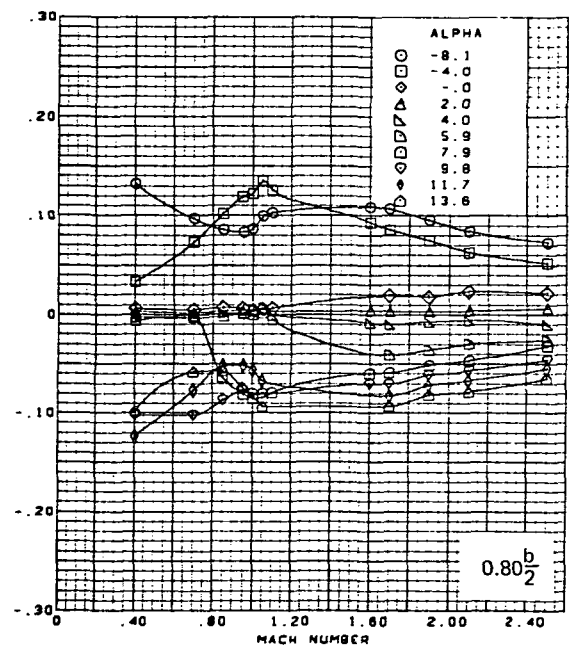
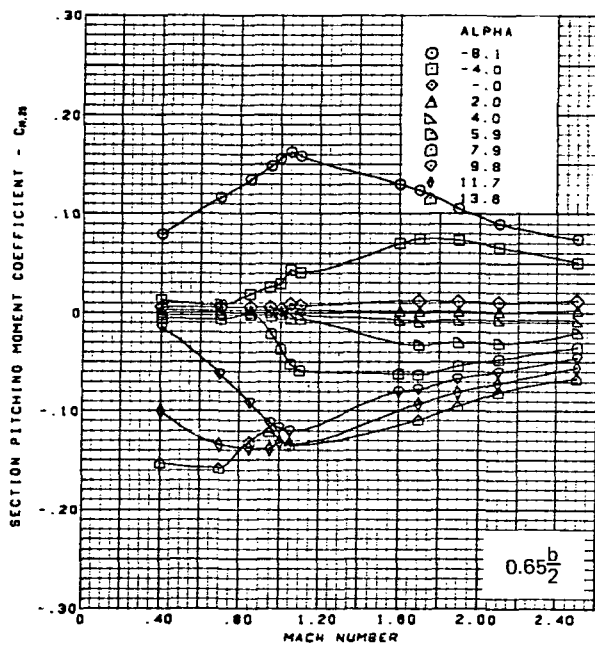
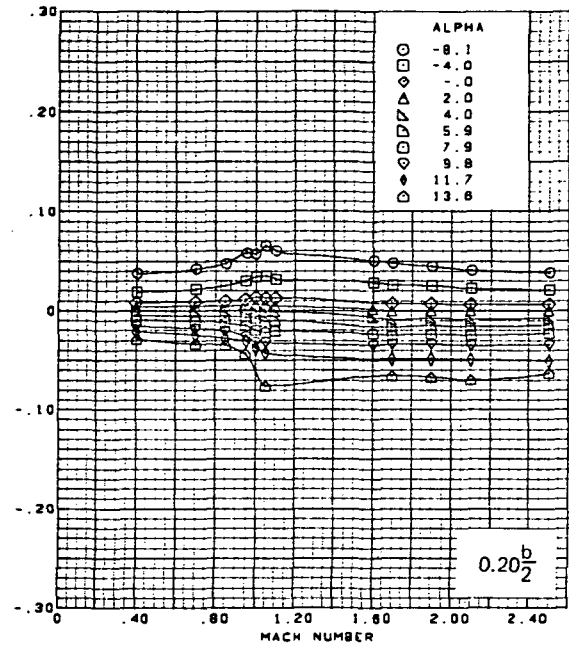
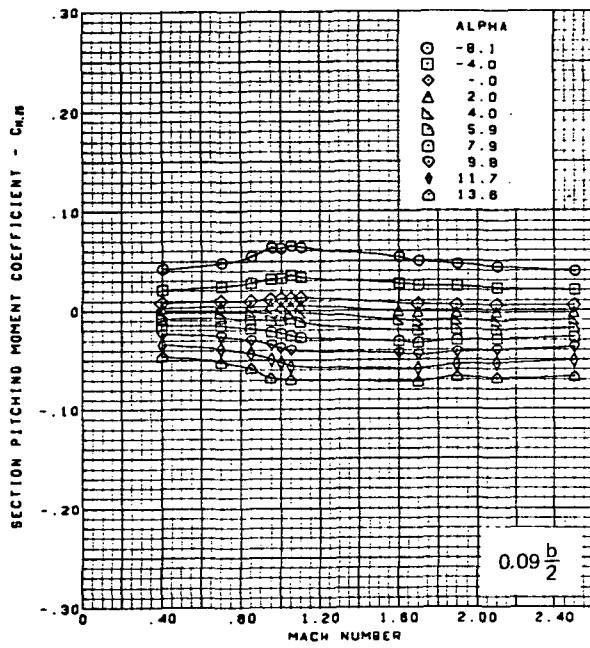
Figure 50.—(Continued)



Twisted wing, rounded L.E.  
 L.E. deflection, full span =  $0.0^\circ$   
 T.E. deflection, full span =  $0.0^\circ$

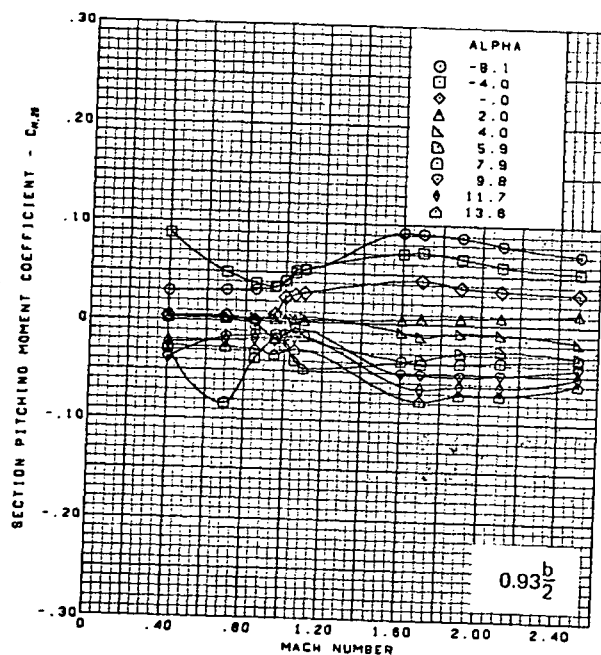
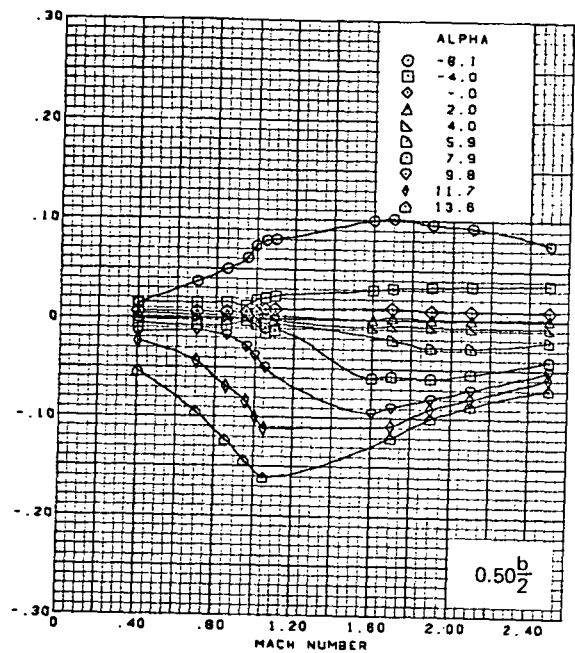
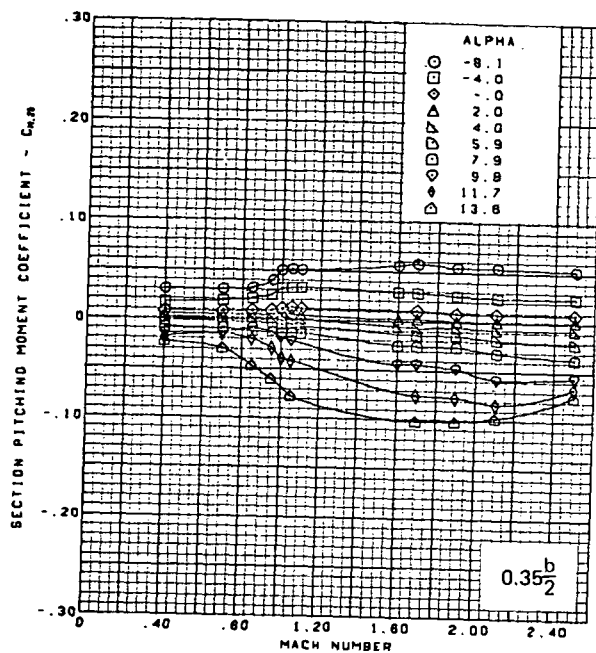
(f) (Concluded)

Figure 50. —(Continued)



(g) Section Aerodynamic Coefficients—Pitching Moment

Figure 50.—(Continued)

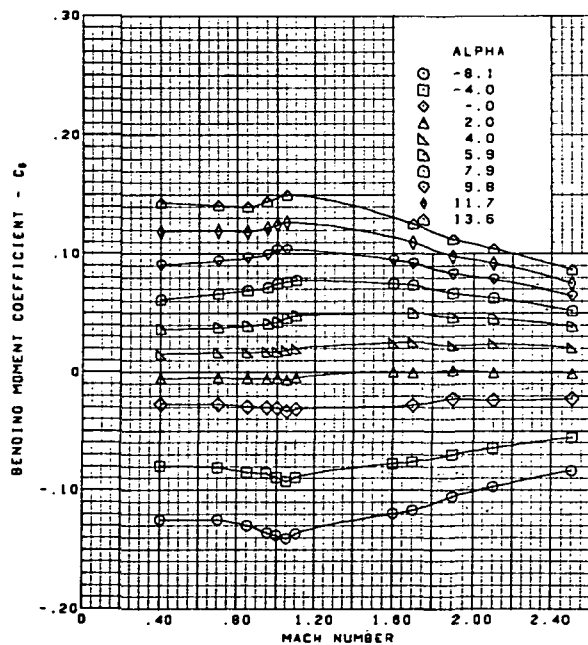
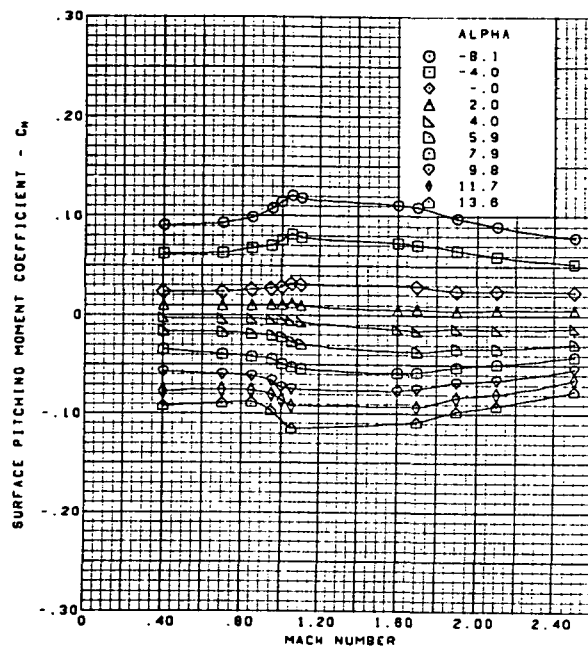
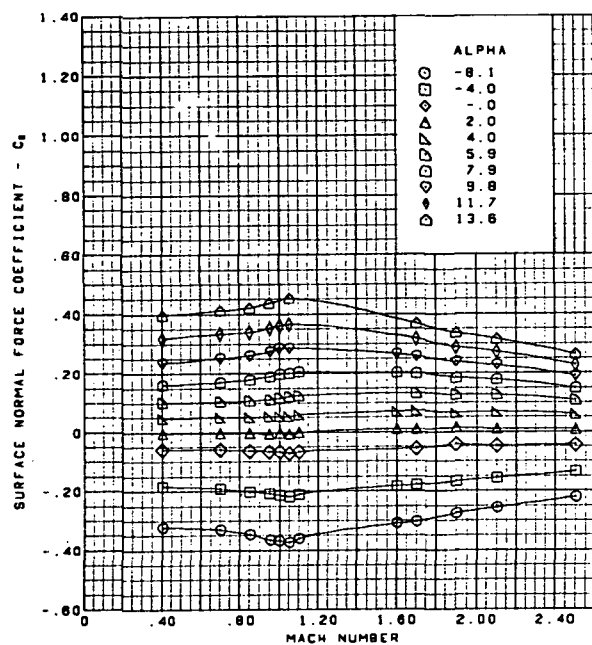


Twisted wing, rounded L.E.  
 L.E. deflection, full span = 0.0°  
 T.E. deflection, full span = 0.0°

(g) (Concluded)

Figure 50.—(Continued)

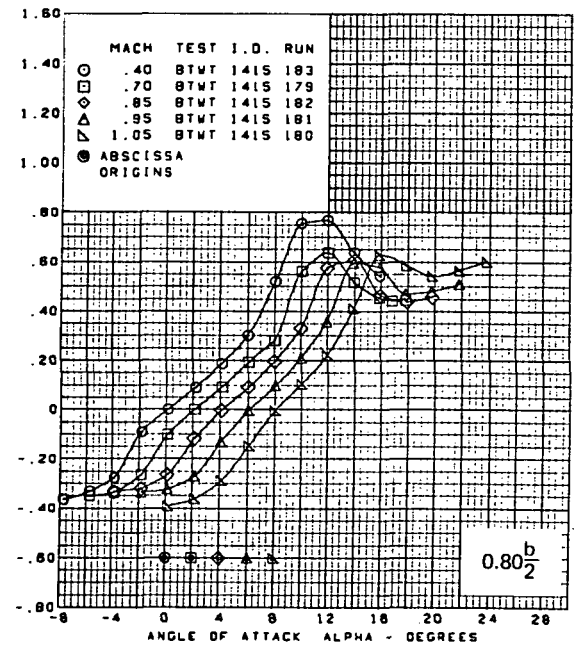
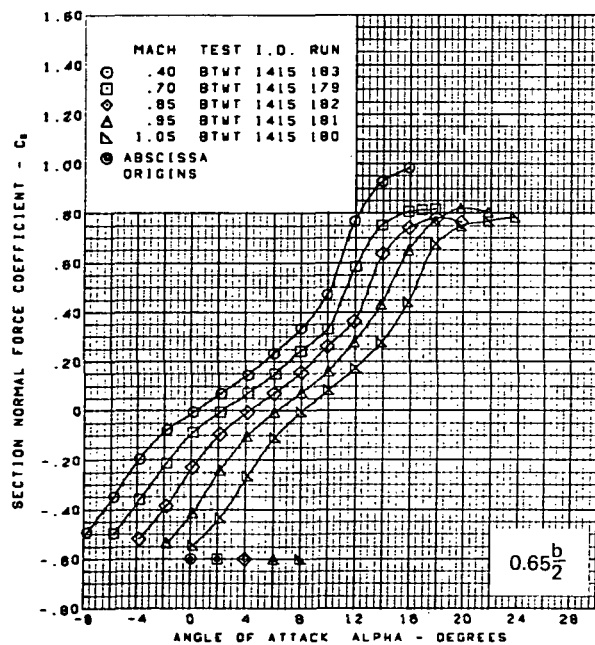
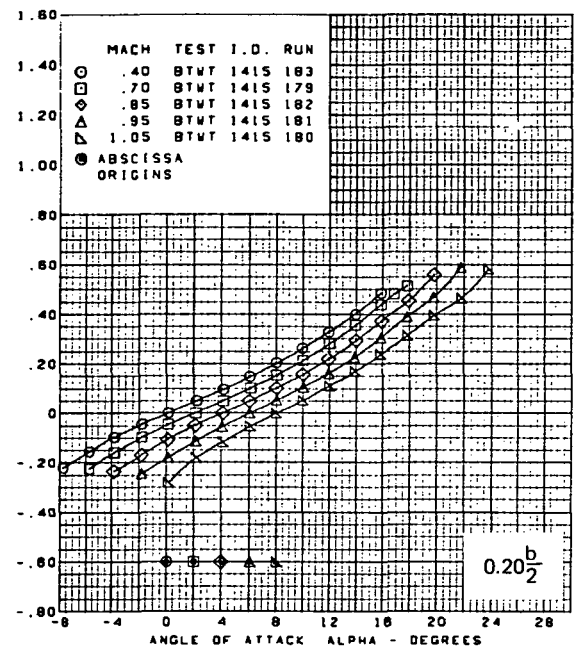
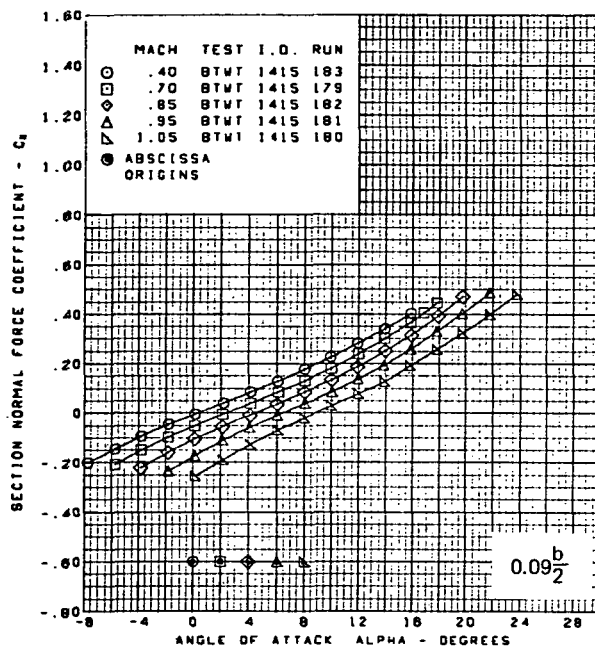
**Page  
Intentionally  
Left Blank**



Twisted wing, rounded L.E.  
 L.E. deflection, full span =  $0.0^\circ$   
 T.E. deflection, full span =  $0.0^\circ$

(h) Wing Aerodynamic Coefficients

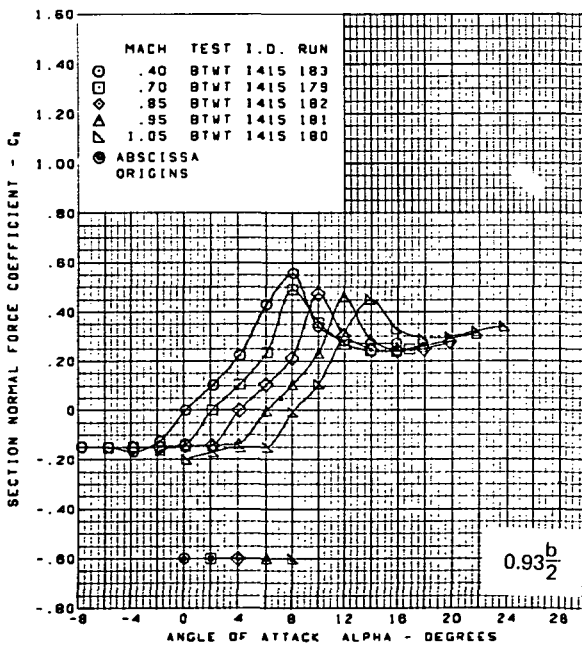
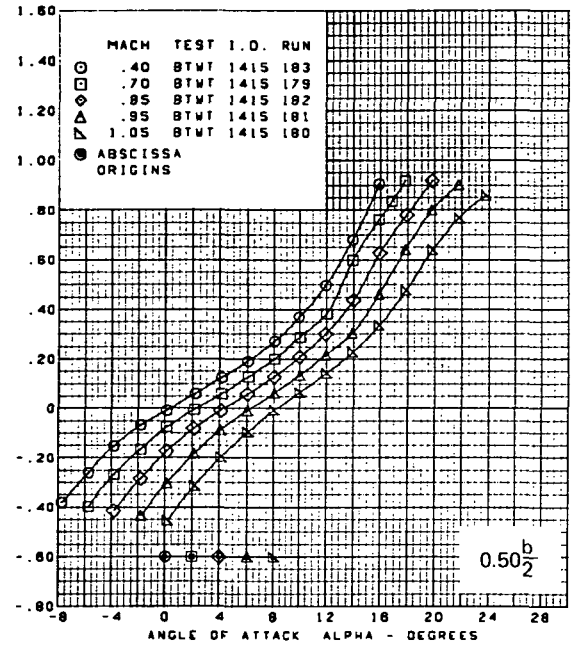
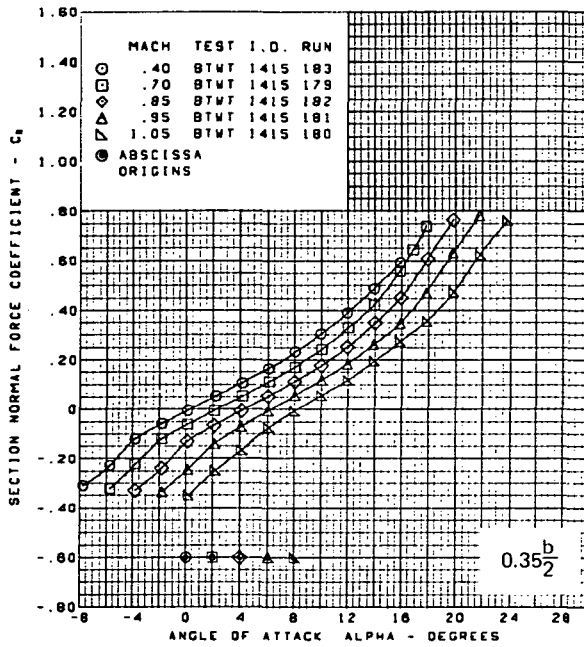
Figure 50.—(Concluded)



(a) Section Normal Force Coefficients vs. Angle of Attack,  $M = 0.40$  Through  $1.05$

Figure 51.—Wing Experimental Data—Effect of Mach Number and Angle of Attack; Flat Wing, Rounded L.E.; L.E. Deflection, Full Span =  $5.1^\circ$ ; T.E. Deflection, Full Span =  $0.0^\circ$

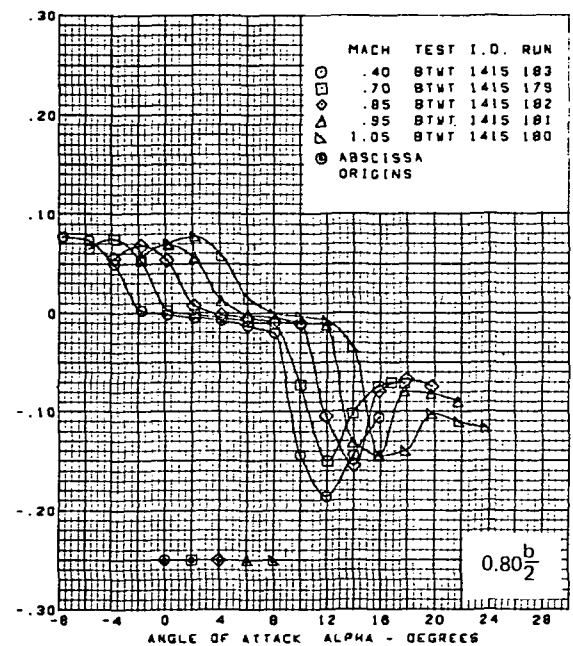
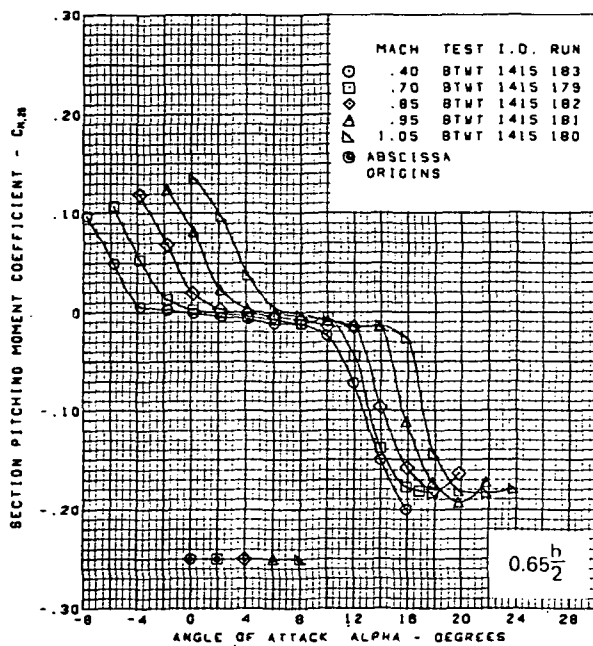
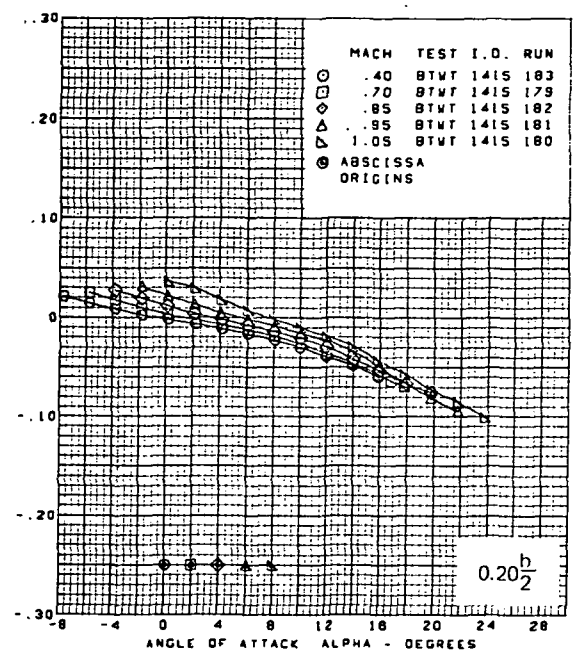
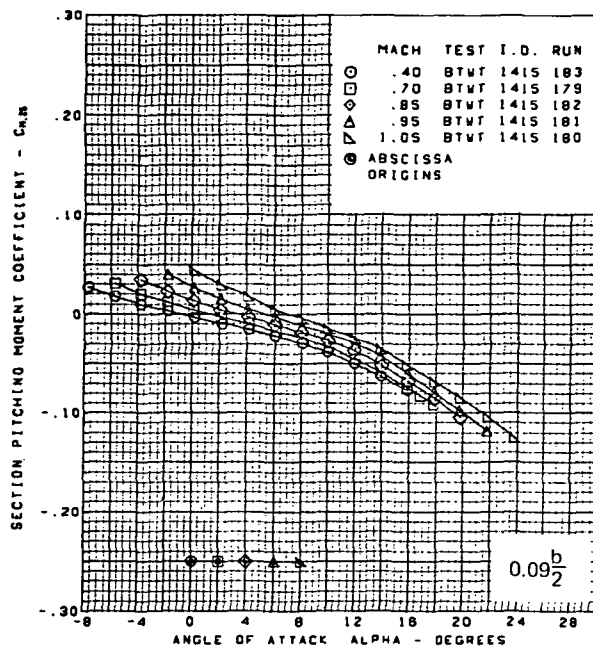




Flat wing, rounded L.E.  
 L.E. deflection, full span =  $5.1^\circ$   
 T.E. deflection, full span =  $0.0^\circ$

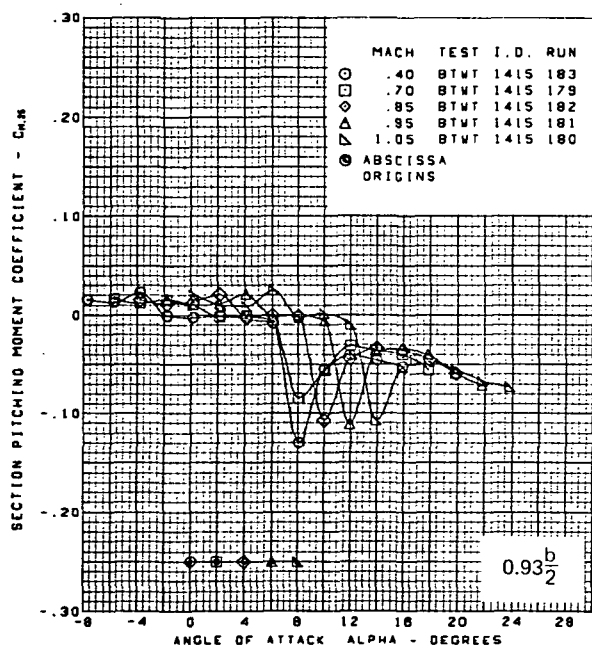
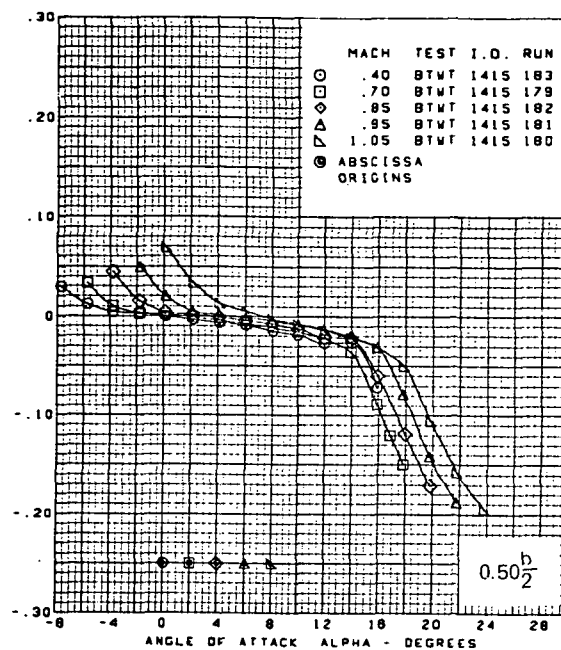
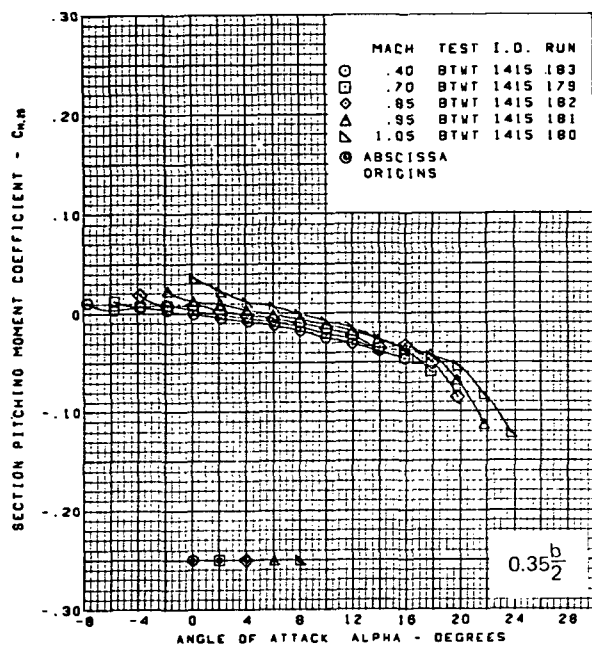
(a) (Concluded)

Figure 51.—(Continued)



(b) Section Pitching Moment Coefficients vs. Angle of Attack,  $M = 0.40$  Through 1.05

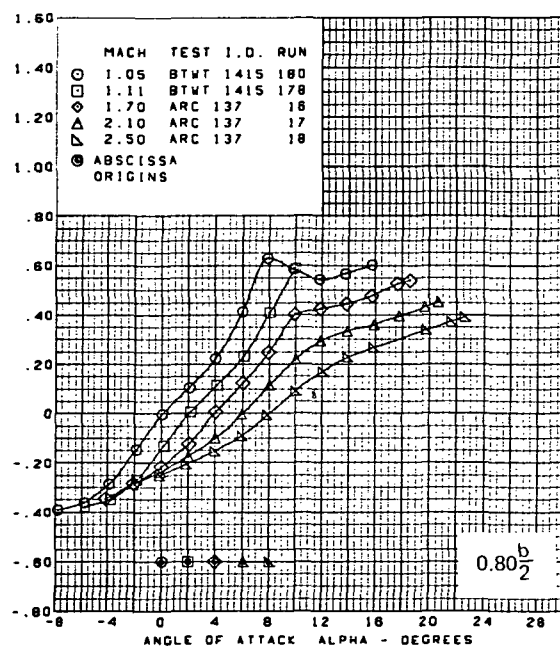
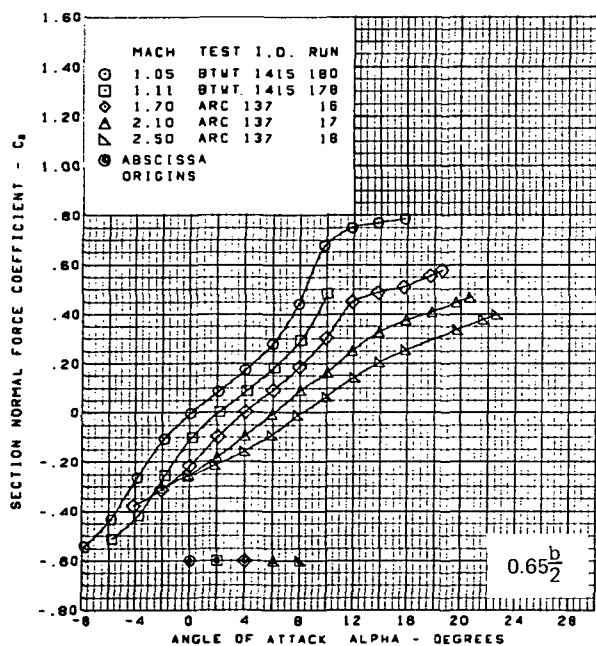
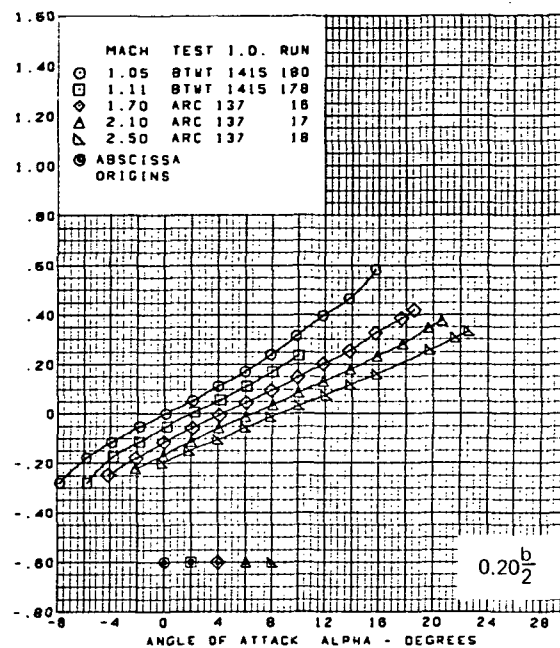
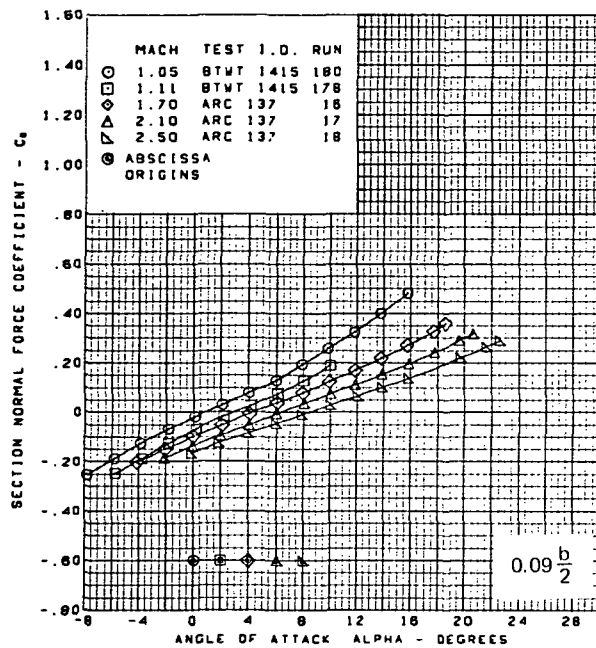
Figure 51. —(Continued)



Flat wing, rounded L.E.  
 L.E. deflection, full span =  $5.1^\circ$   
 T.E. deflection, full span =  $0.0^\circ$

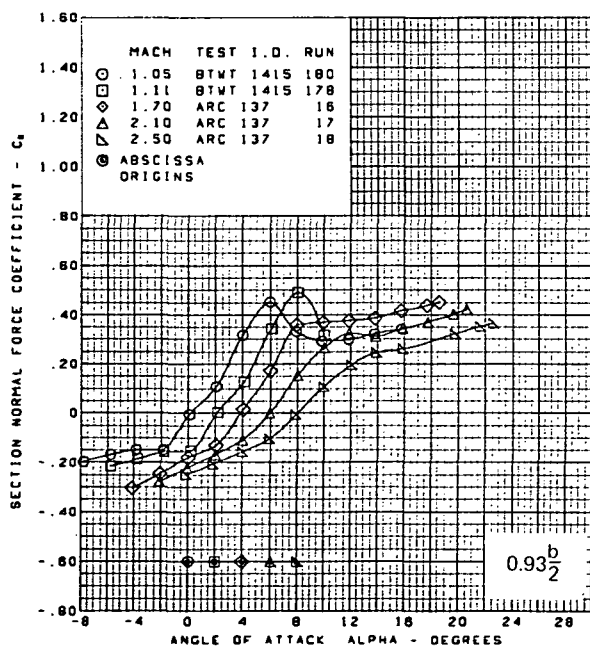
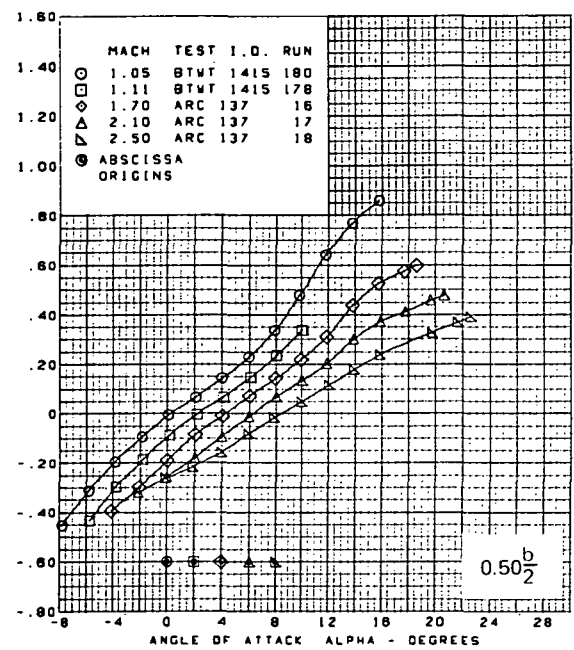
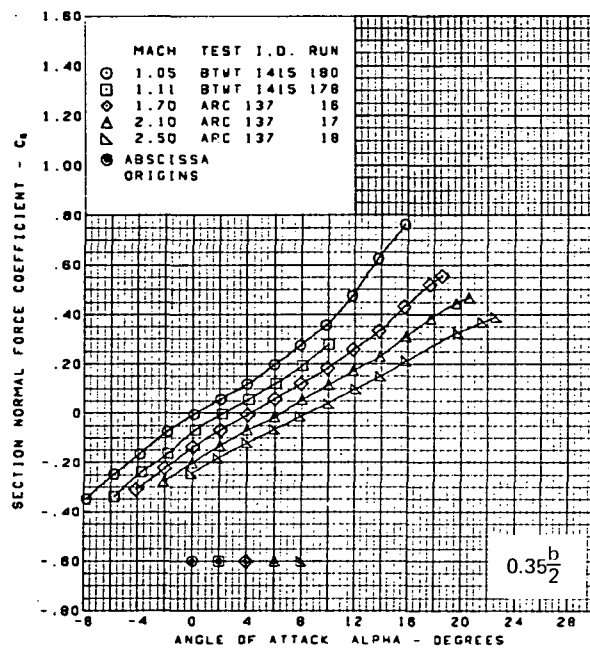
(b) (Concluded)

Figure 51.—(Continued)



(c) Section Pitching Moment Coefficients vs. Angle of Attack,  $M = 1.05$  Through 2.50

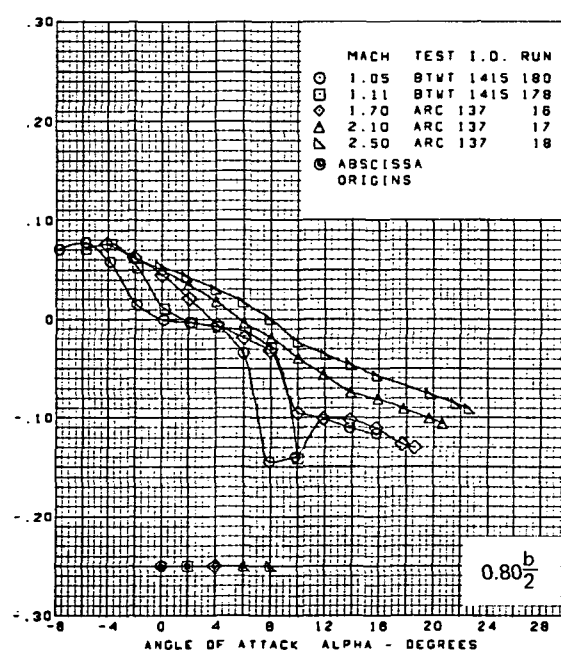
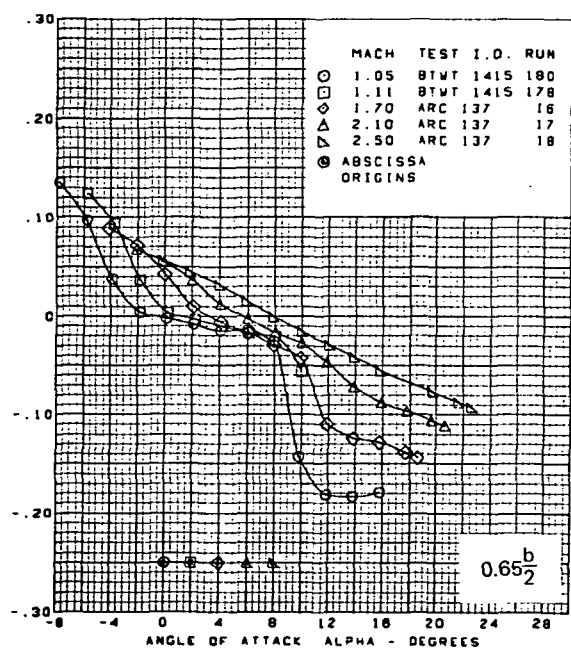
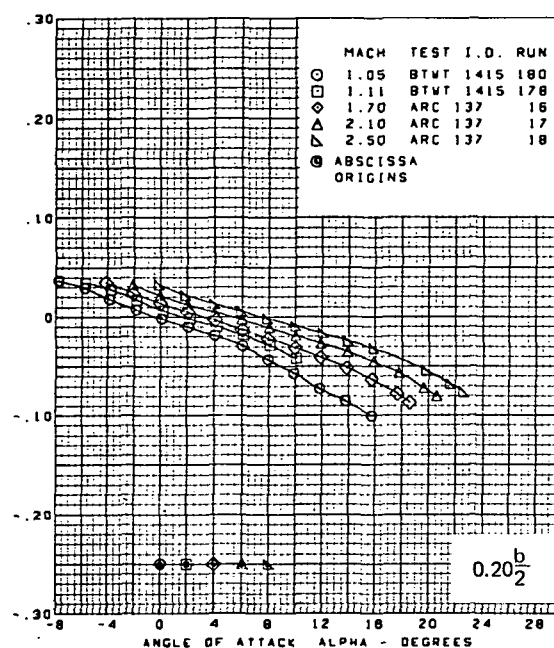
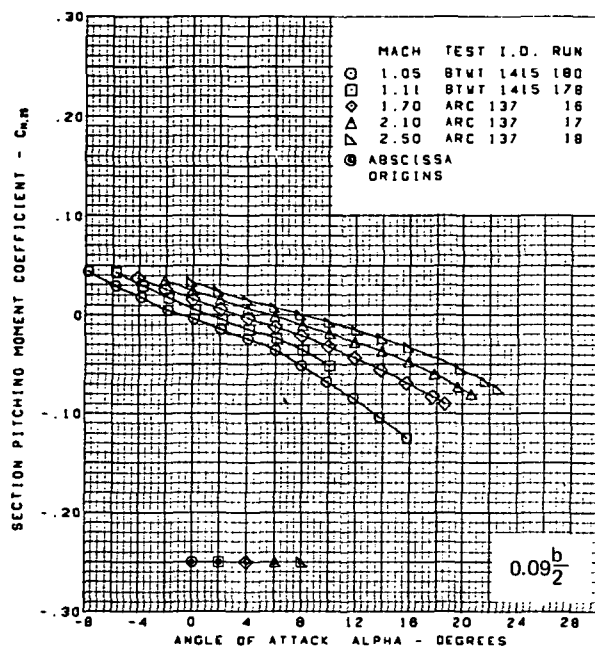
Figure 51.-(Continued)



Flat wing, rounded L.E.  
 L.E. deflection, full span =  $5.1^\circ$   
 T.E. deflection, full span =  $0.0^\circ$

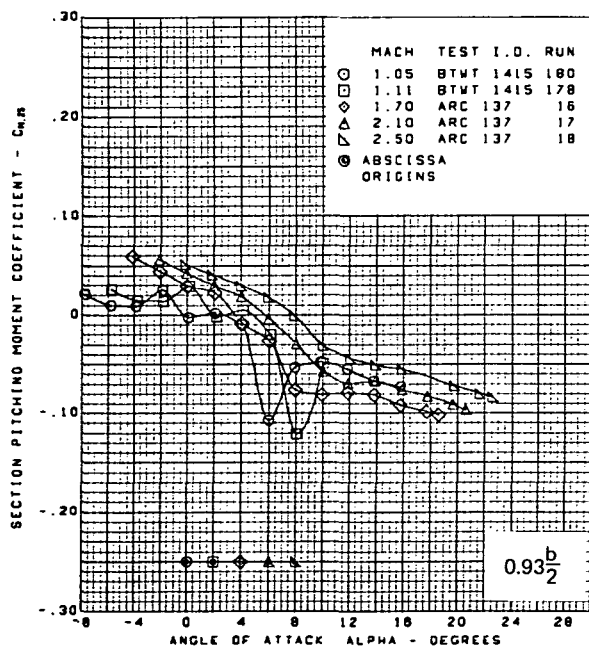
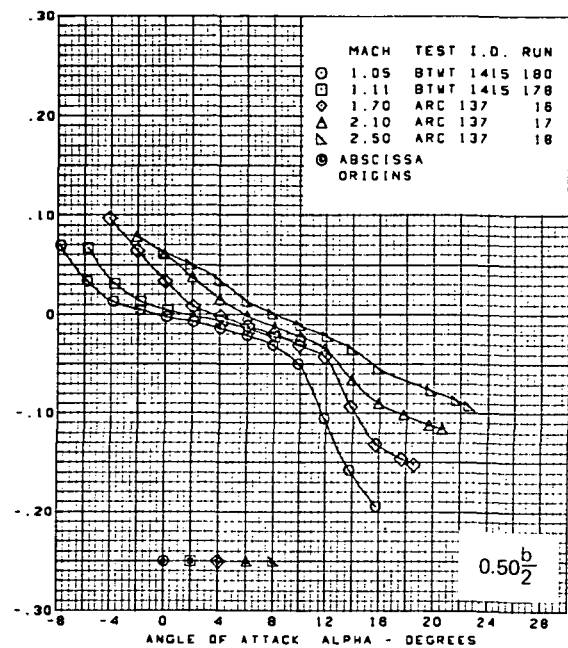
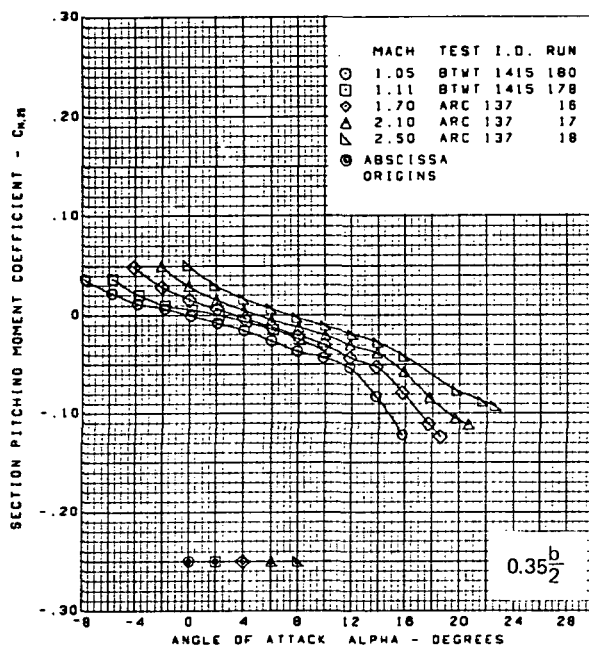
(c) (Concluded)

Figure 51. —(Continued)



(d) Section Pitching Moment Coefficients vs. Angle of Attack,  $M = 1.05$  Through 2.50

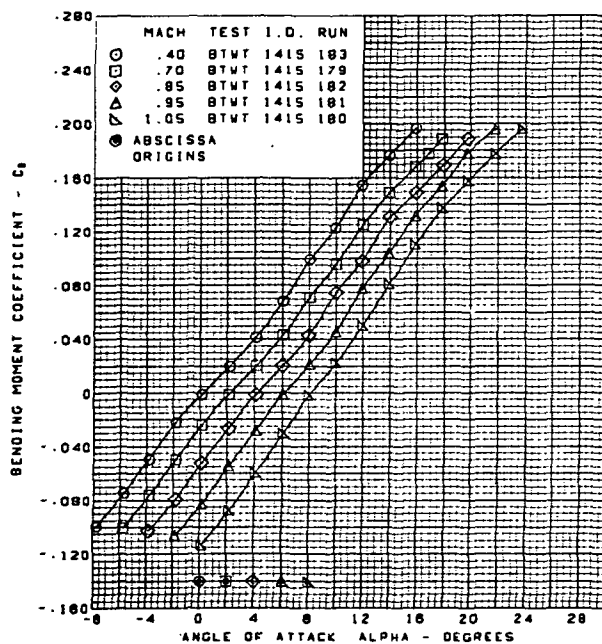
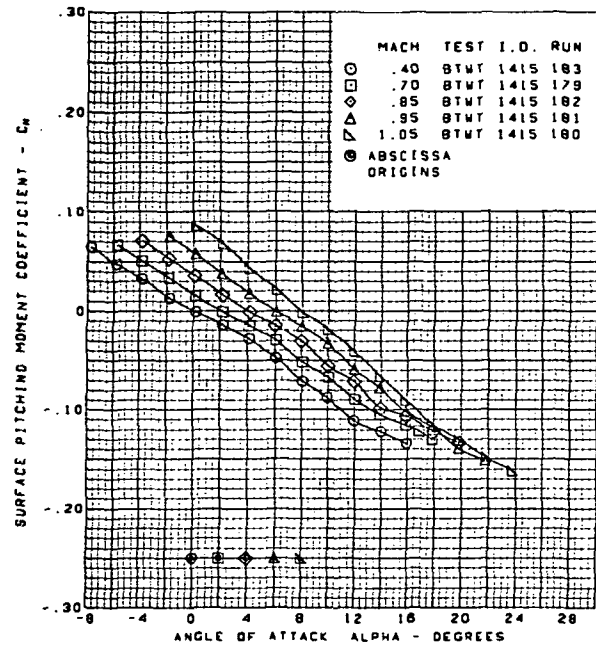
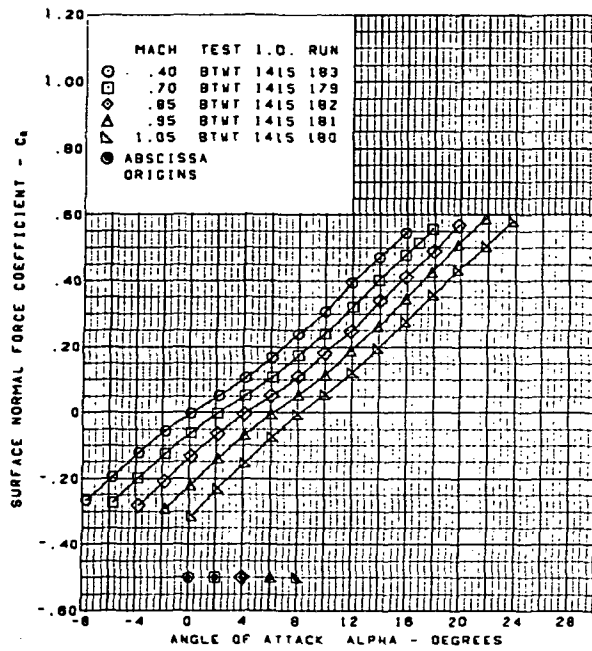
Figure 51.—(Continued)



Flat wing, rounded L.E.  
 L.E. deflection, full span =  $5.1^\circ$   
 T.E. deflection, full span =  $0.0^\circ$

(d) (Concluded)

Figure 51. —(Continued)

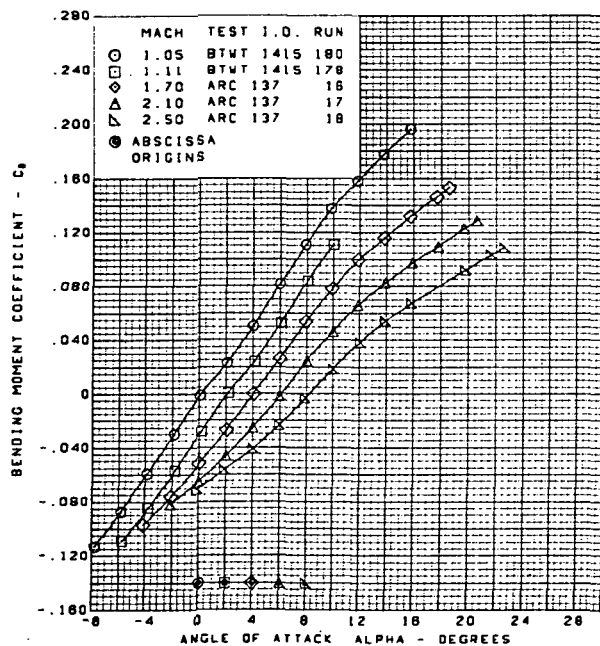
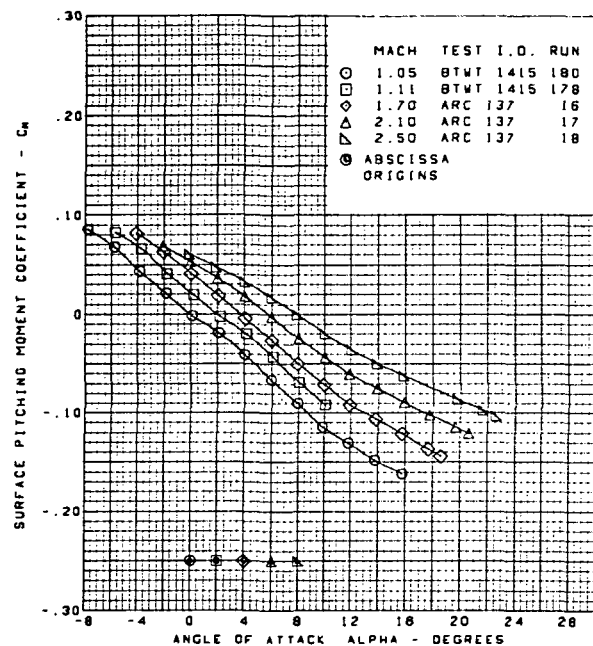
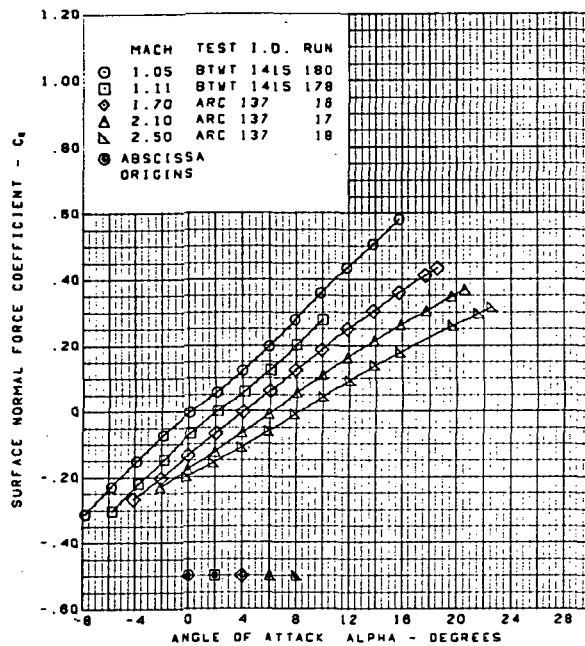


Flat wing, rounded L.E.  
 L.E. deflection, full span =  $5.1^\circ$   
 T.E. deflection, full span =  $0.0^\circ$

(e) Wing Aerodynamic Coefficients vs. Angle of Attack

Figure 51.—(Continued)

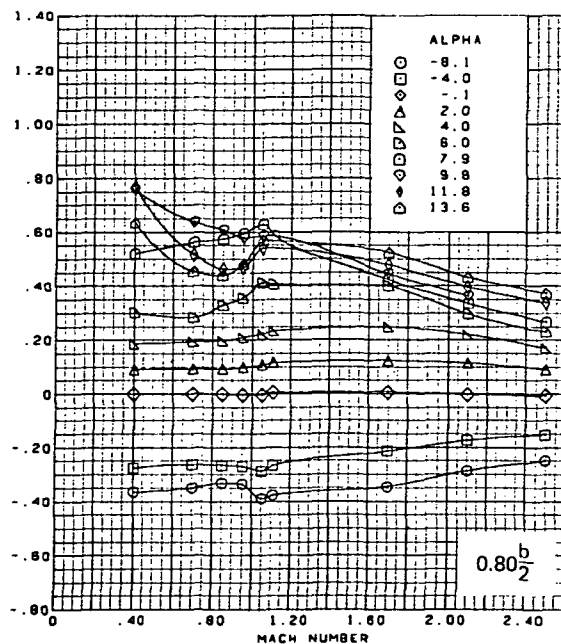
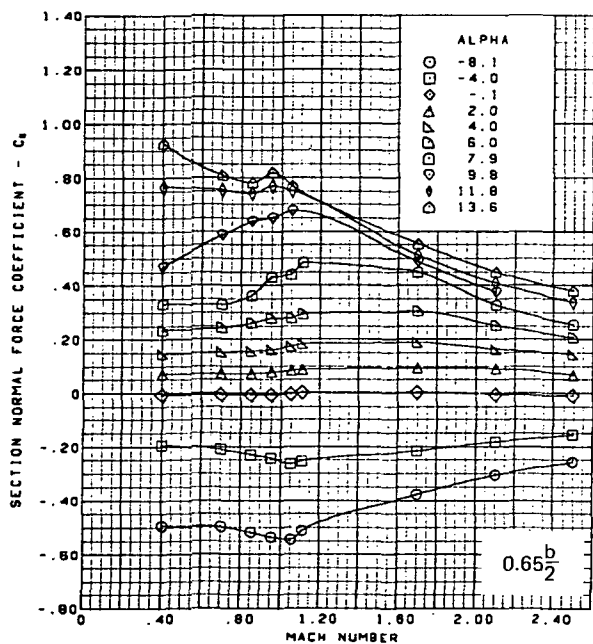
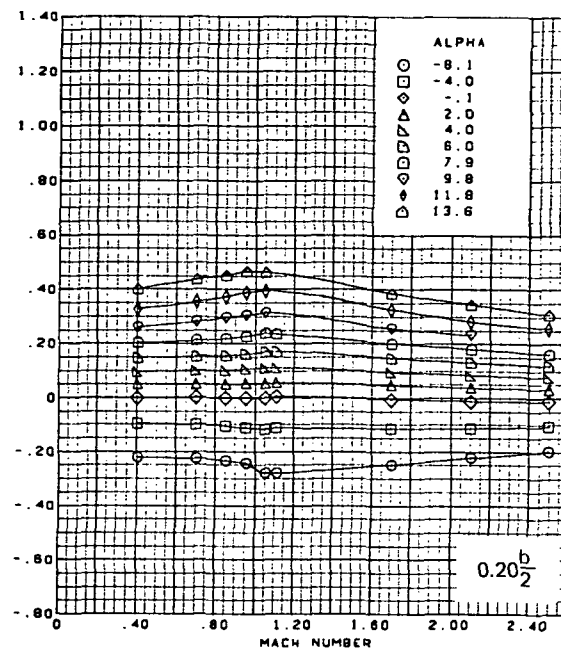
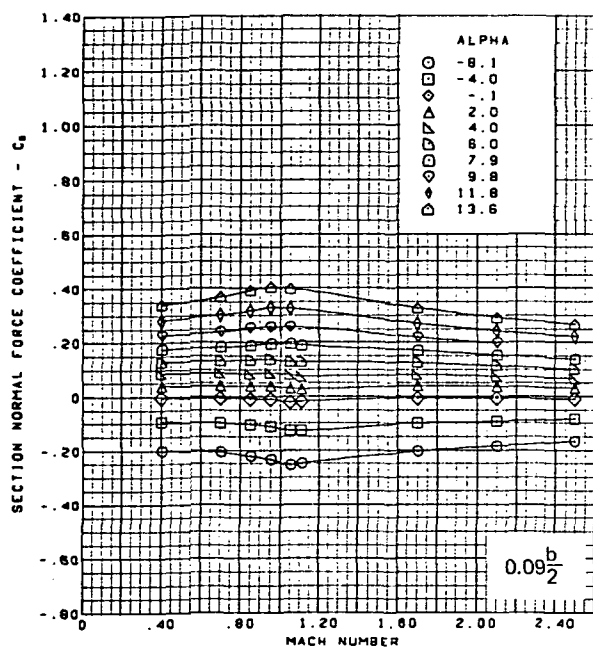




Flat wing, rounded L.E.  
 L.E. deflection, full span =  $5.1^\circ$   
 T.E. deflection, full span =  $0.0^\circ$

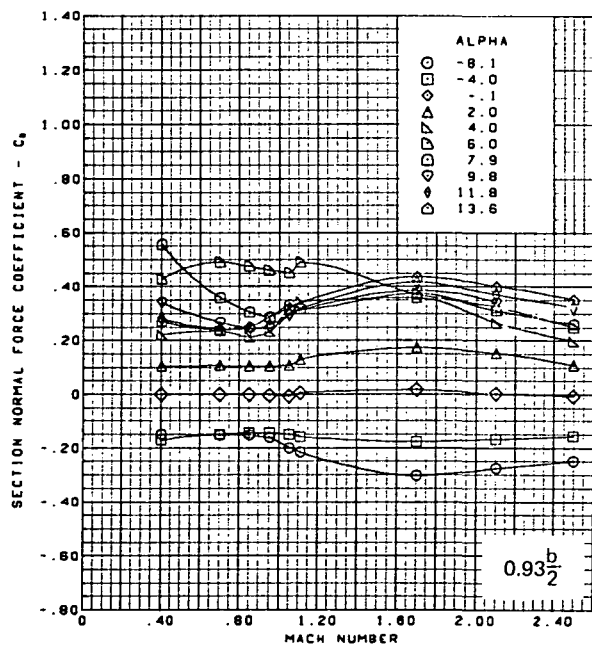
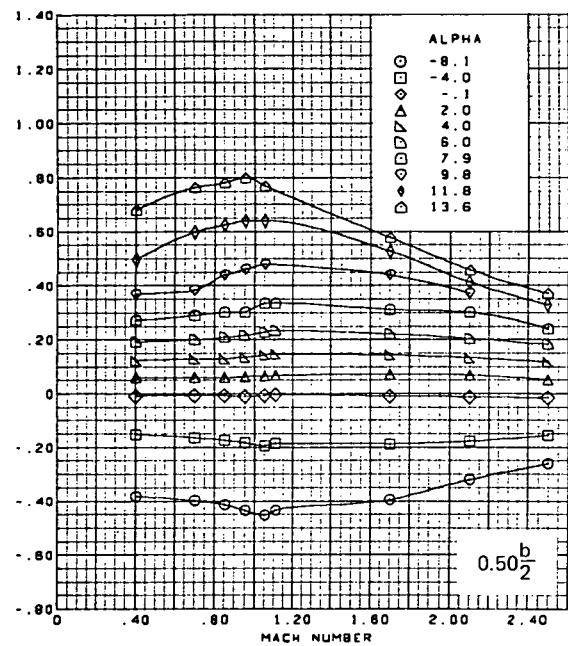
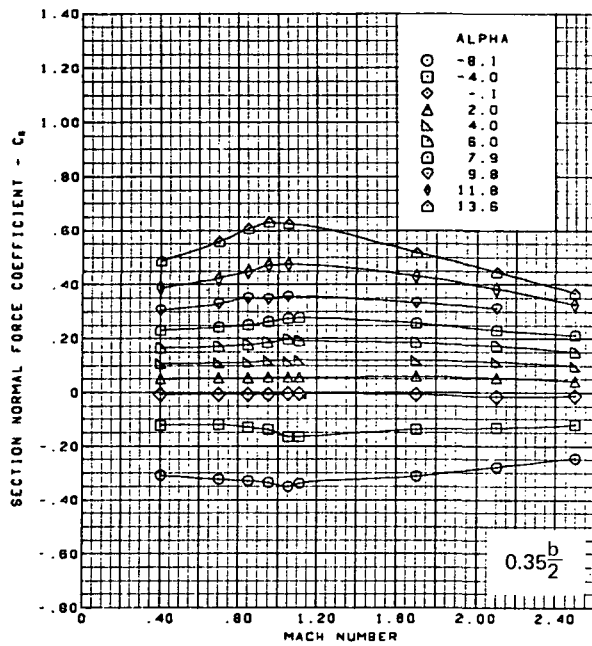
(e) (Concluded)

Figure 51.—(Continued)



(f) Section Aerodynamic Coefficients—Normal Force

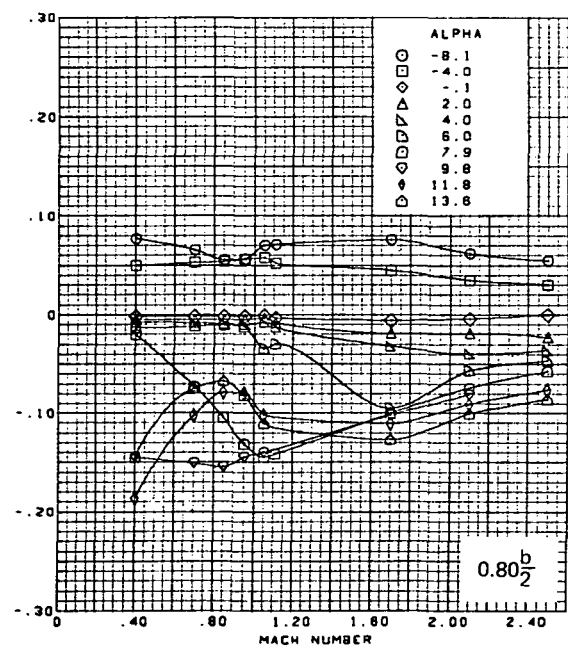
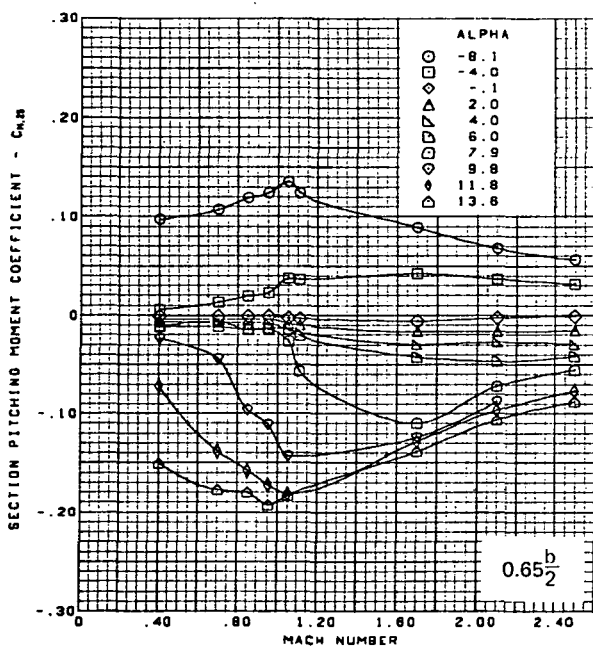
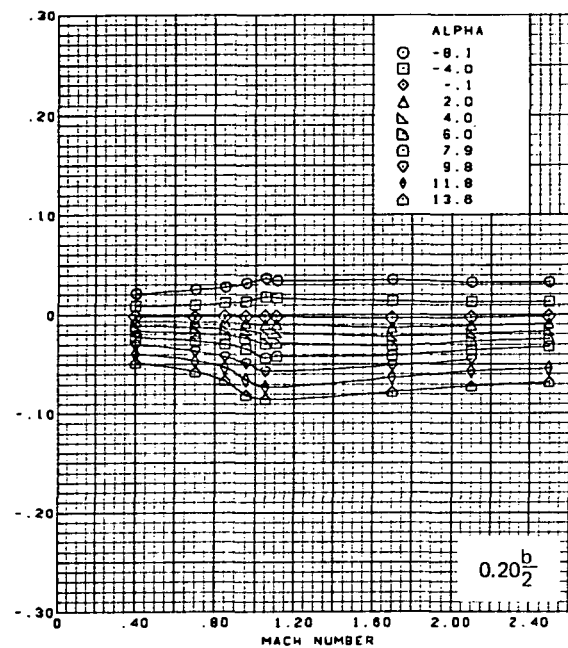
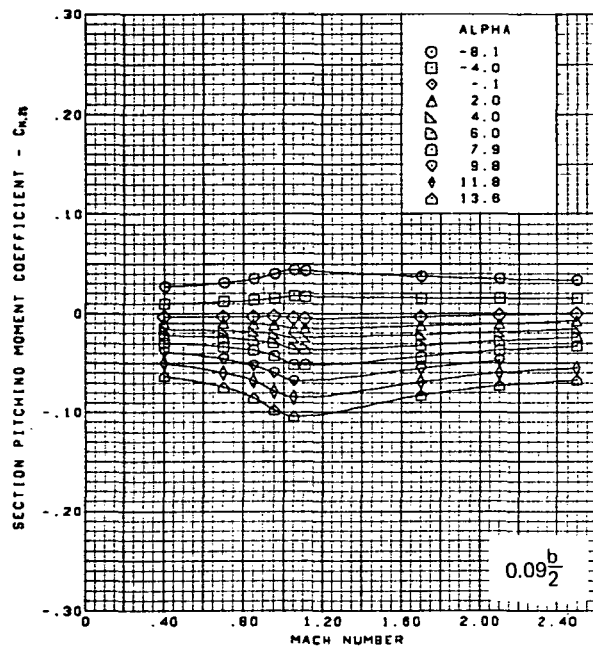
Figure 51.—(Continued)



Flat wing, rounded L.E.  
 L.E. deflection, full span =  $5.1^\circ$   
 T.E. deflection, full span =  $0.0^\circ$

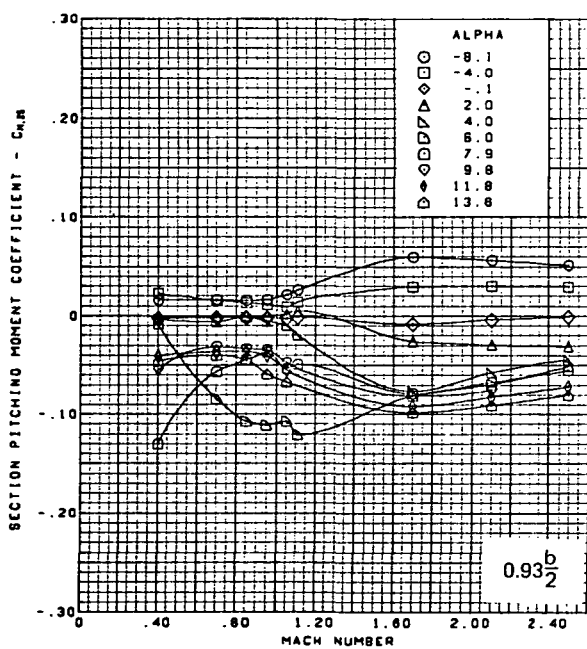
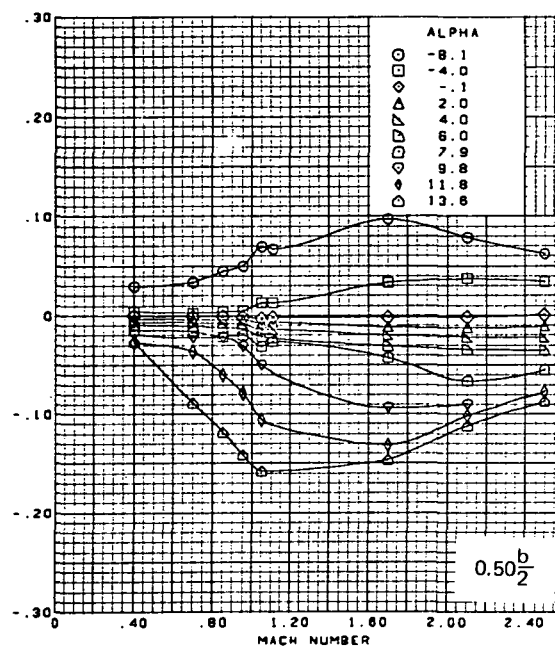
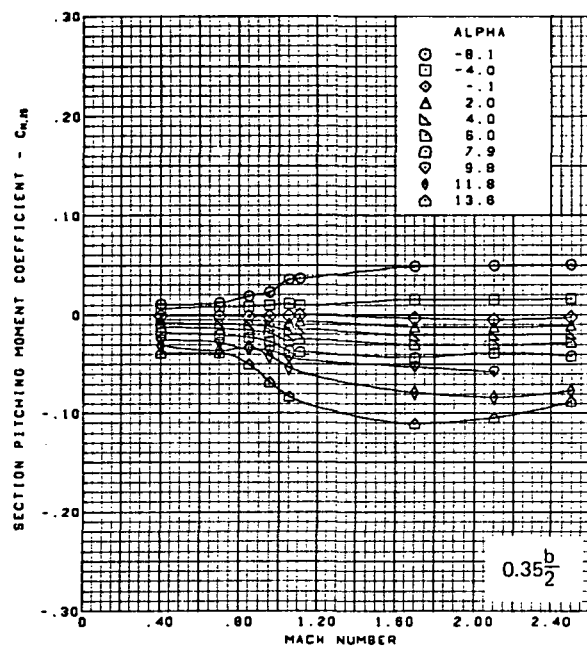
(f) (Concluded)

Figure 51.—(Continued)



(g) Section Aerodynamic Coefficients—Pitching Moment

Figure 51.—(Continued)

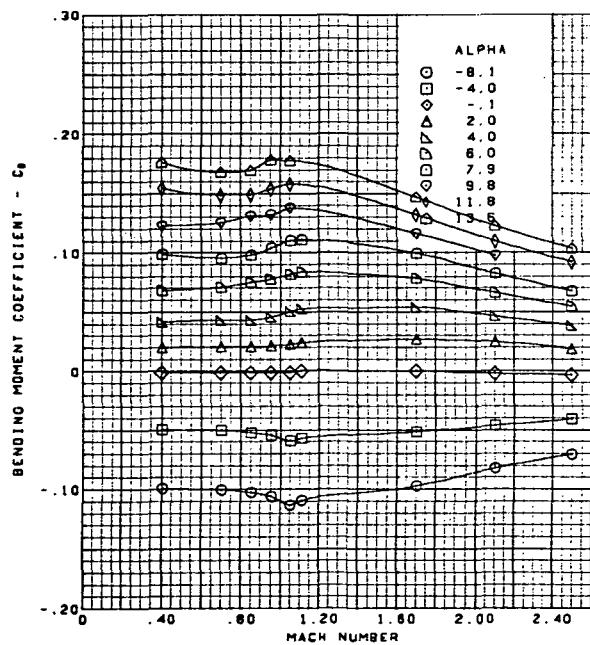
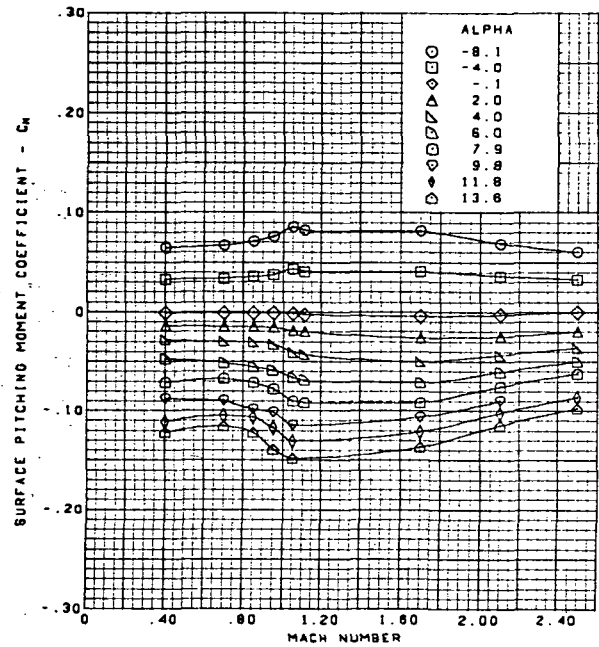
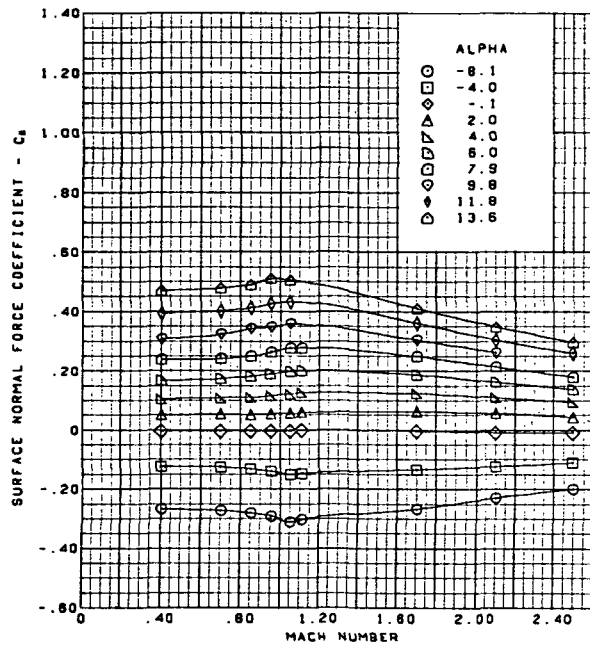


Flat wing, rounded L.E.  
 L.E. deflection, full span =  $5.1^\circ$   
 T.E. deflection, full span =  $0.0^\circ$

(g) (Concluded)

Figure 51.—(Continued)

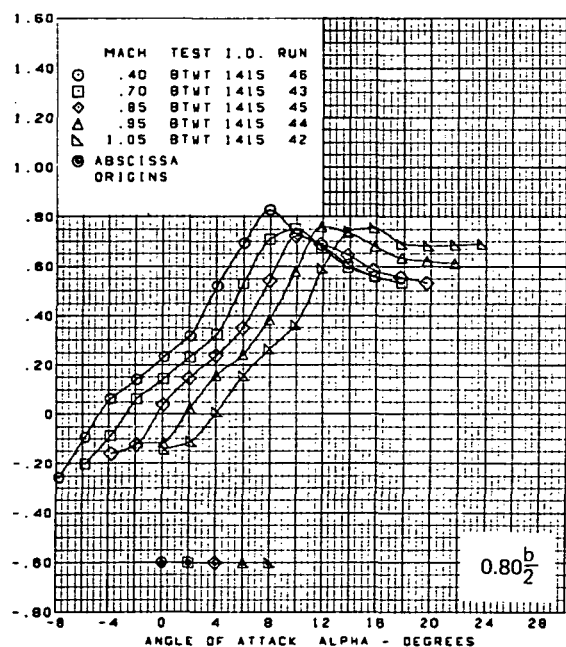
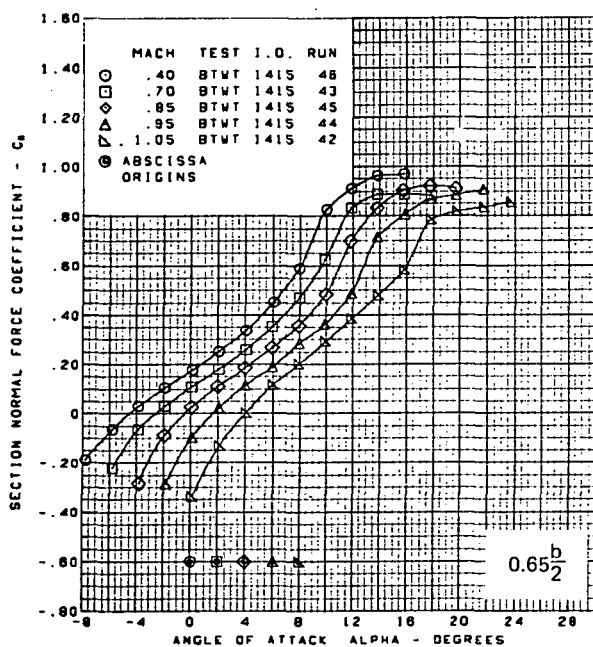
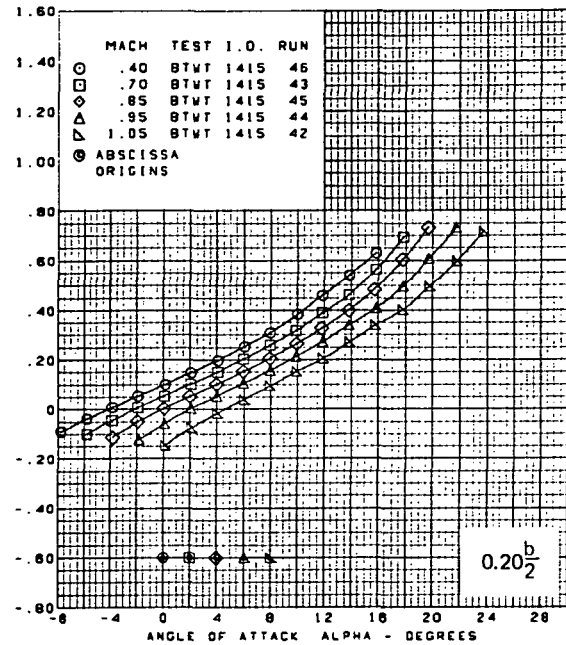
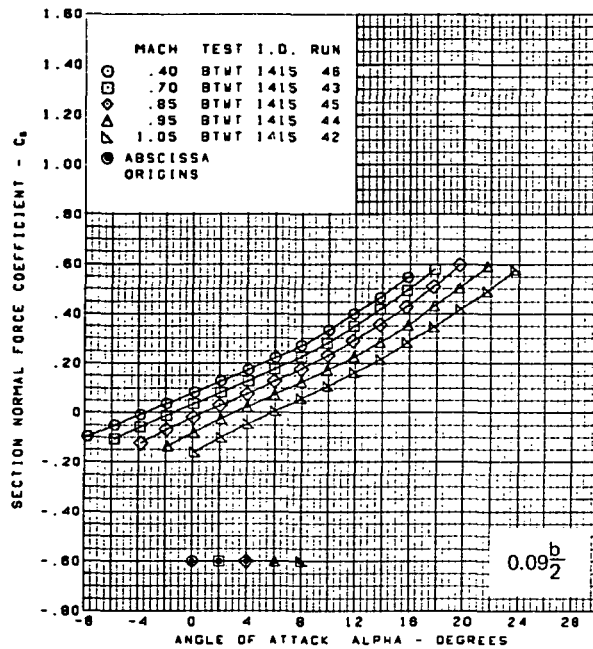
**Page  
Intentionally  
Left Blank**



Flat wing, rounded L.E.  
 L.E. deflection, full span =  $5.1^\circ$   
 T.E. deflection, full span =  $0.0^\circ$

(h) Wing Aerodynamic Coefficients

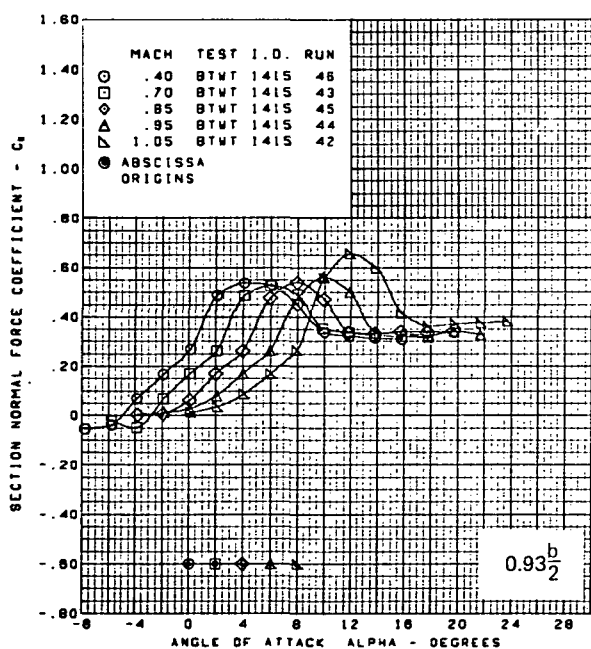
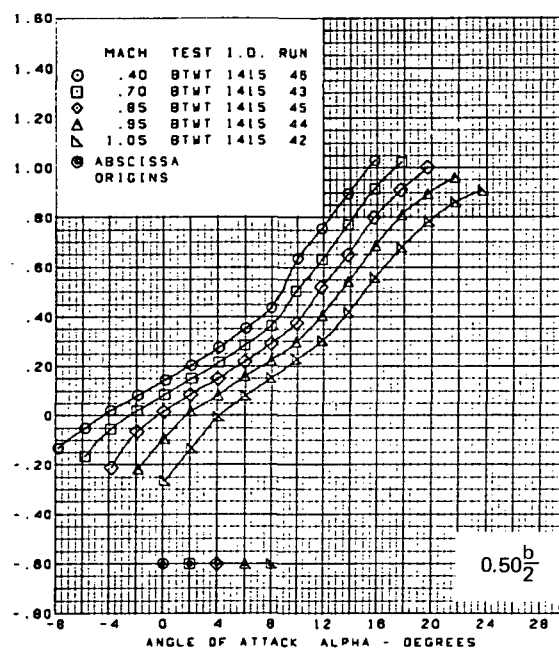
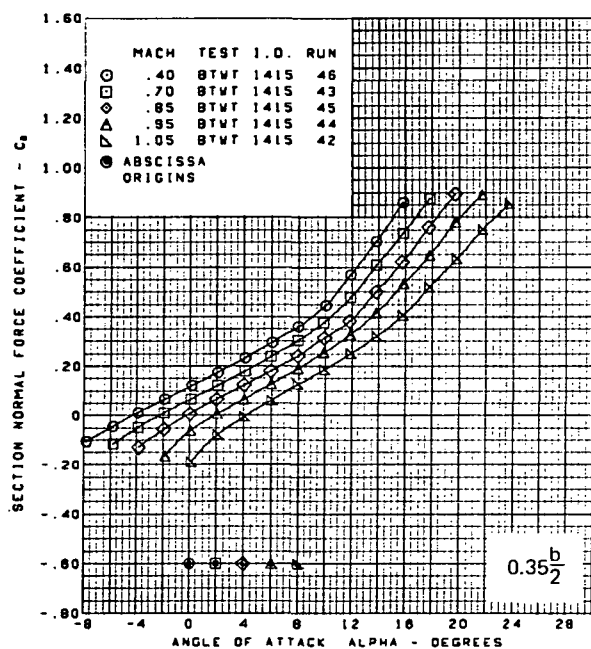
Figure 51.—(Concluded)



(a) Section Normal Force Coefficients vs. Angle of Attack,  $M = 0.40$  Through  $1.05$

Figure 52. —Wing Experimental Data—Effect of Mach Number and Angle of Attack; Flat Wing, Rounded L.E.; L.E. Deflection, Full Span =  $0.0^\circ$ ; T.E. Deflection, Full Span =  $8.3^\circ$

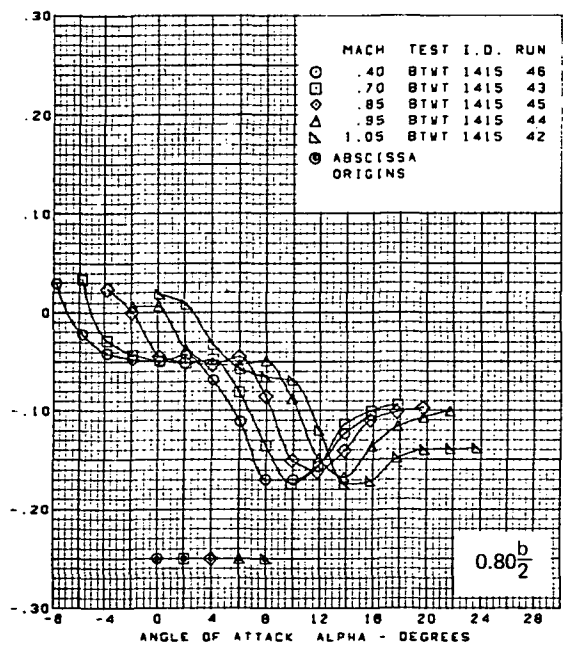
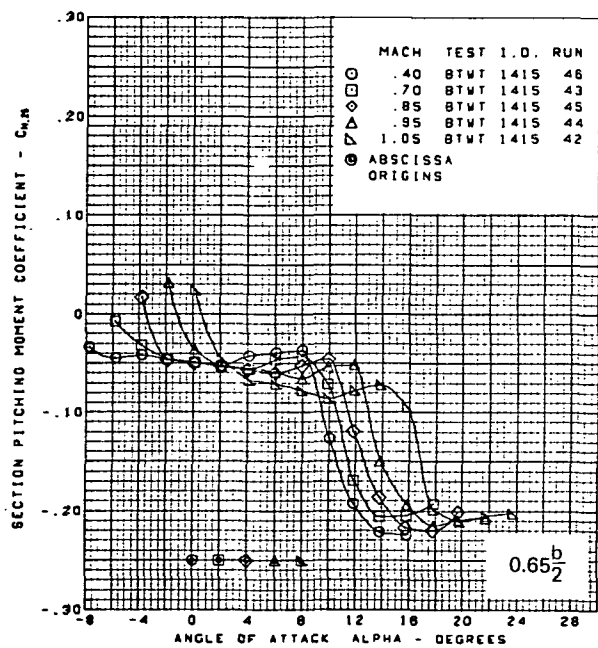
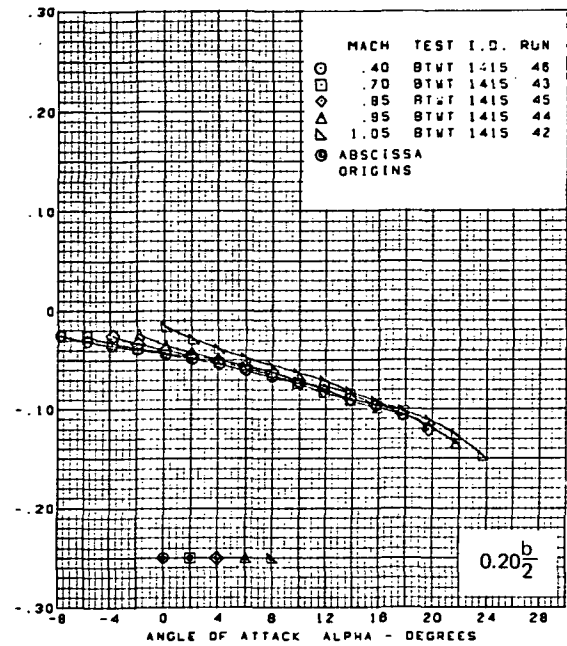
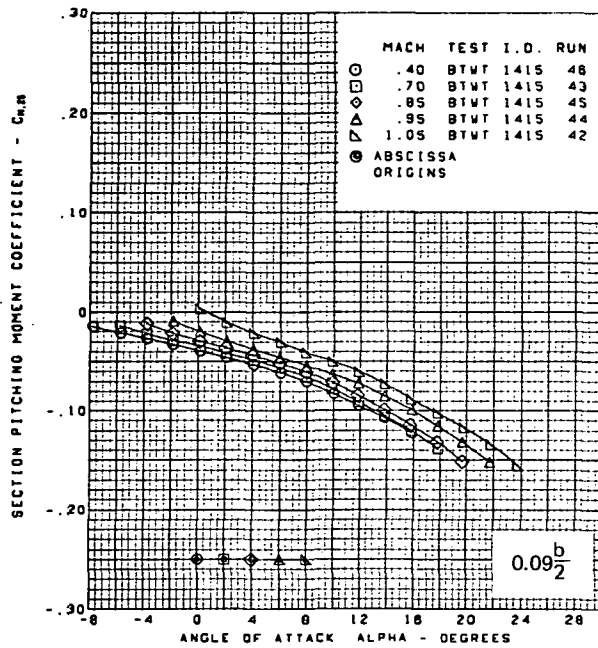




Flat wing, rounded L.E.  
 L.E. deflection, full span =  $0.0^\circ$   
 T.E. deflection, full span =  $8.3^\circ$

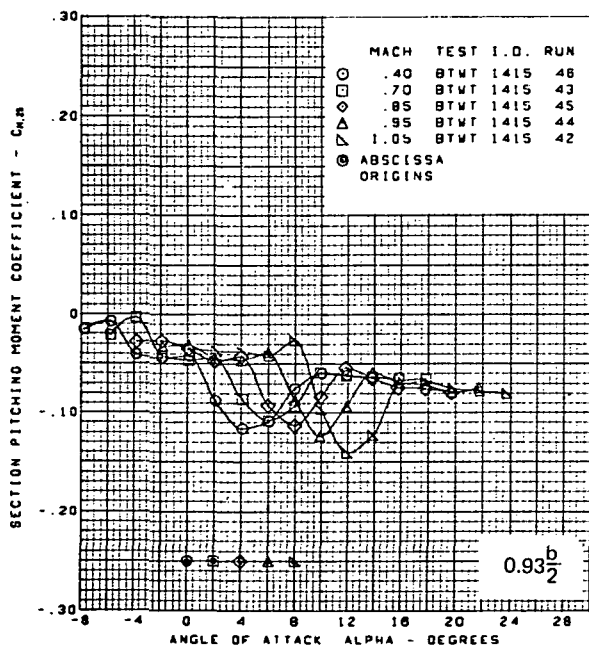
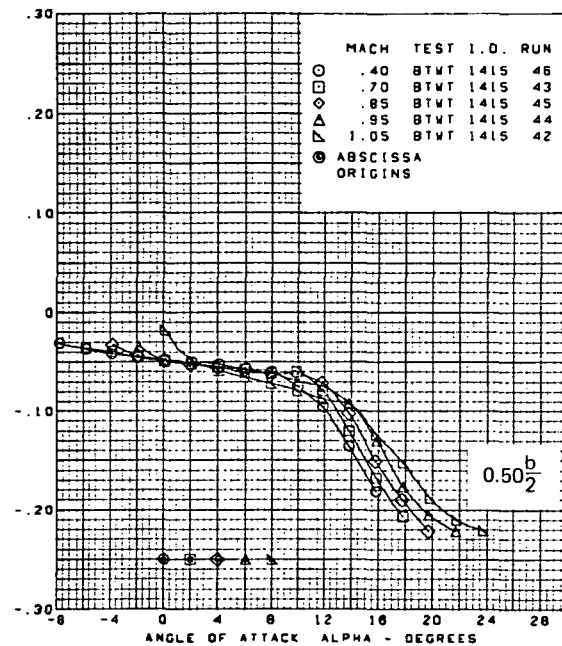
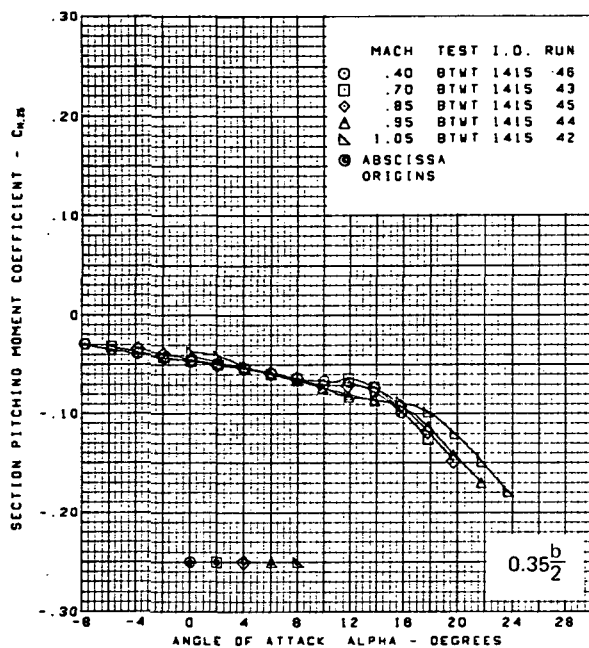
(a) (Concluded)

Figure 52.—(Continued)



(b) Section Pitching Moment Coefficients vs. Angle of Attack,  $M=0.40$  Through 1.05

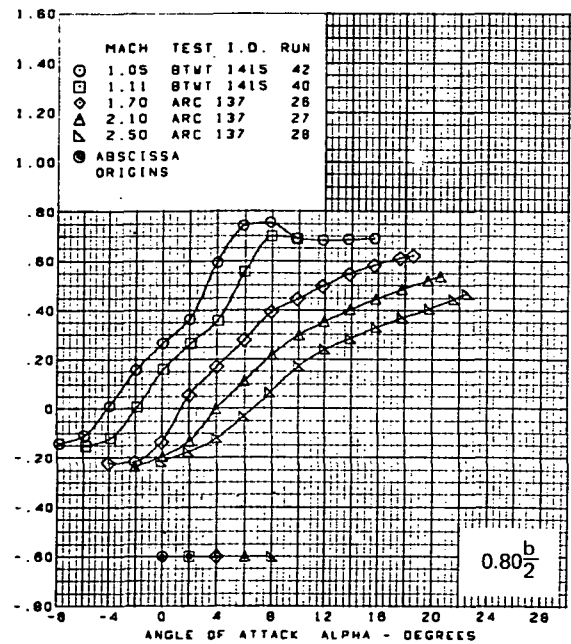
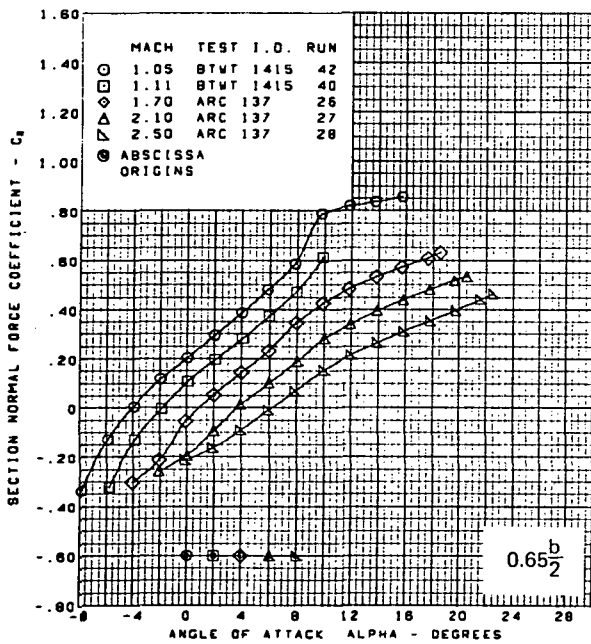
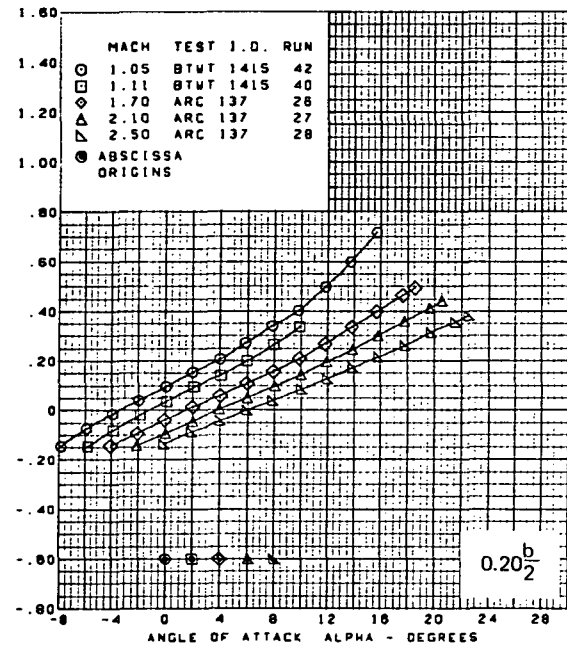
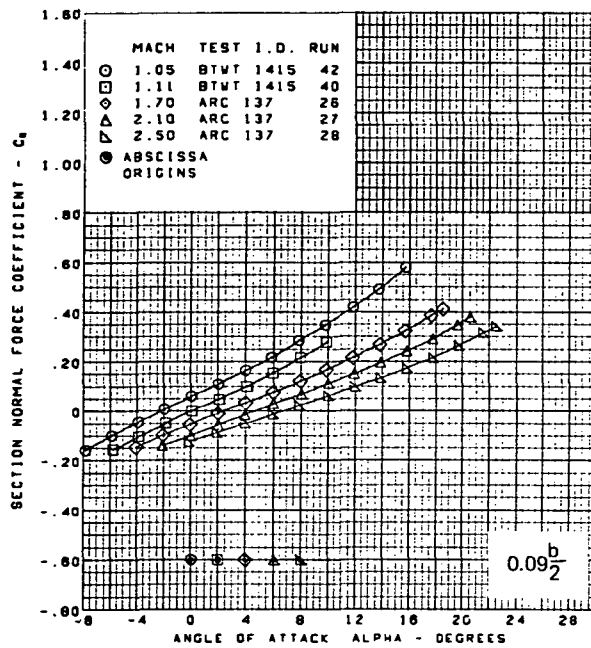
Figure 52.-(Continued)



Flat wing, rounded L.E.  
 L.E. deflection, full span =  $0.0^\circ$   
 T.E. deflection, full span =  $8.3^\circ$

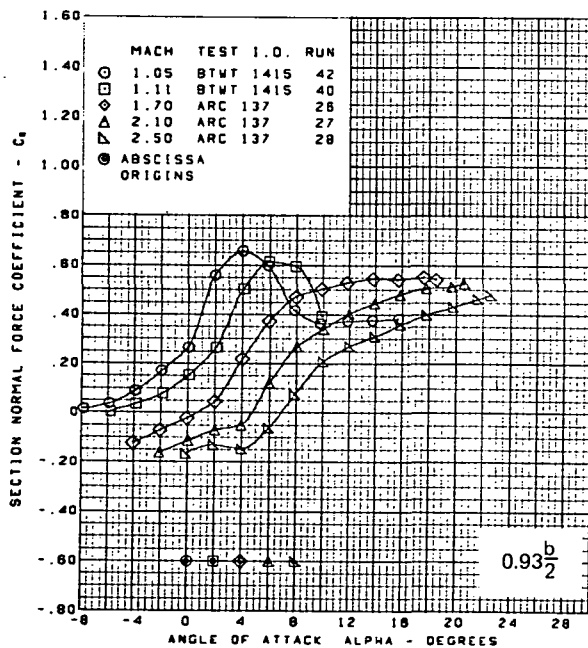
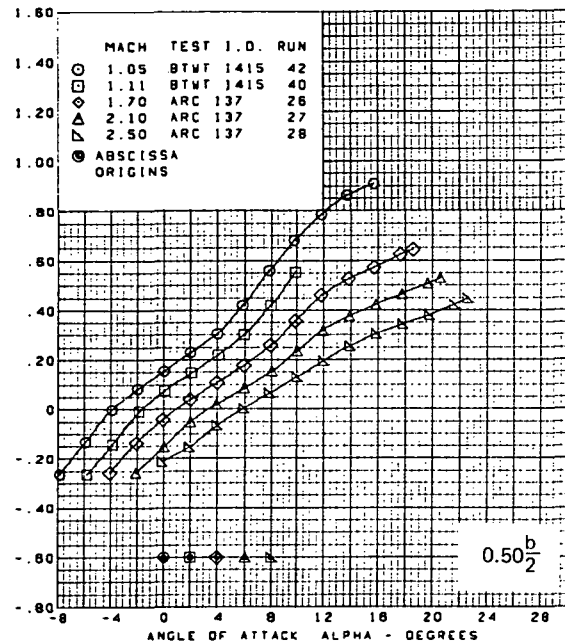
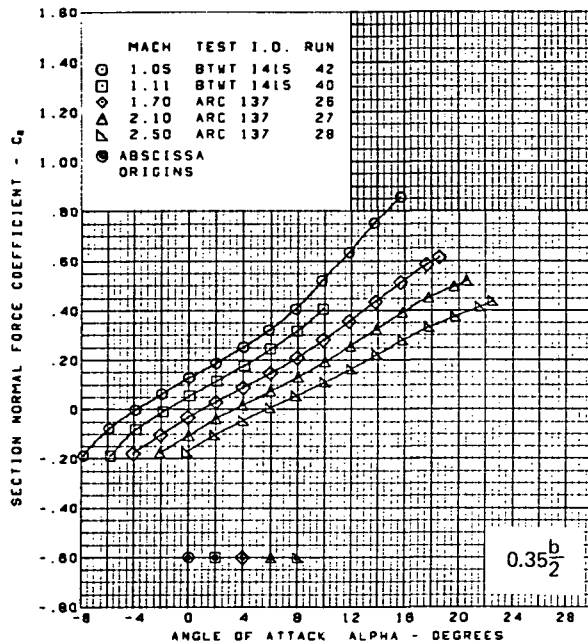
(b) (Concluded)

Figure 52.—(Continued)



(c) Section Normal Force Coefficients vs. Angle of Attack,  $M=1.05$  Through 2.50

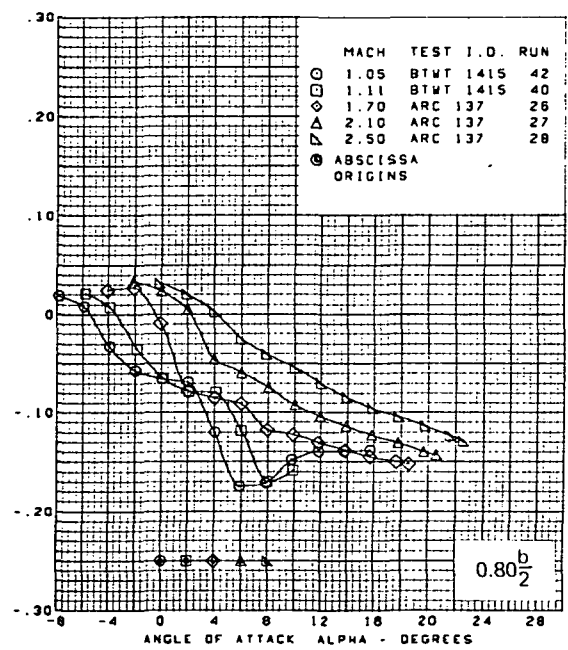
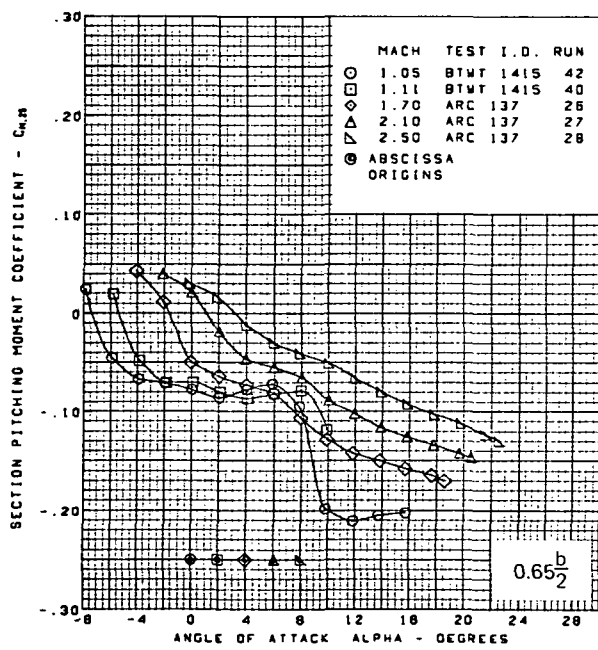
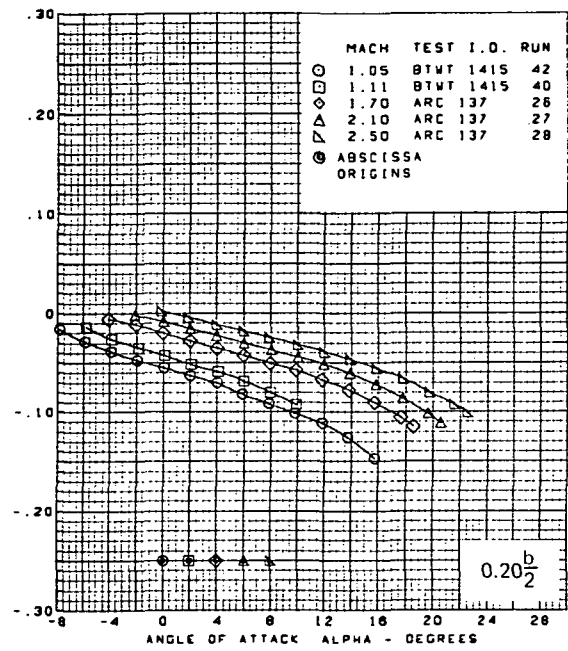
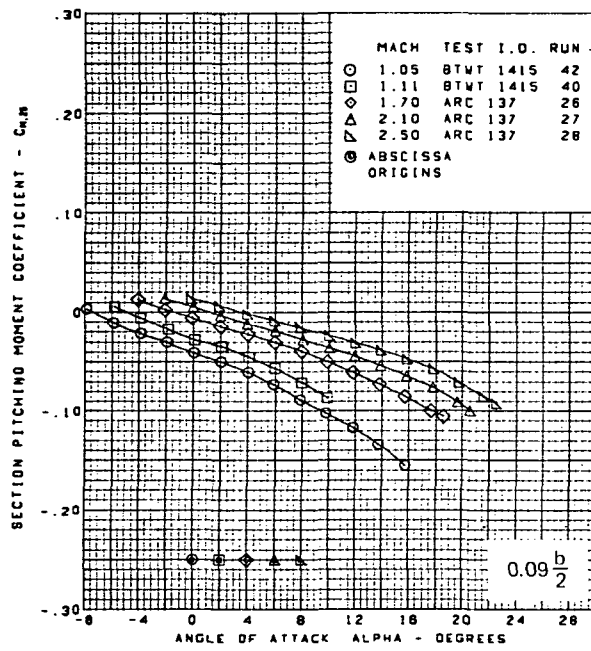
Figure 52. —(Continued)



Flat wing, rounded L.E.  
 L.E. deflection, full span =  $0.0^\circ$   
 T.E. deflection, full span =  $8.3^\circ$

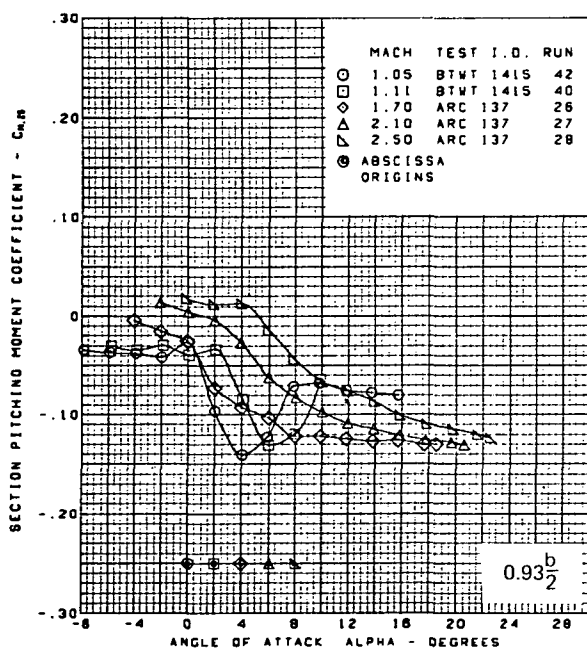
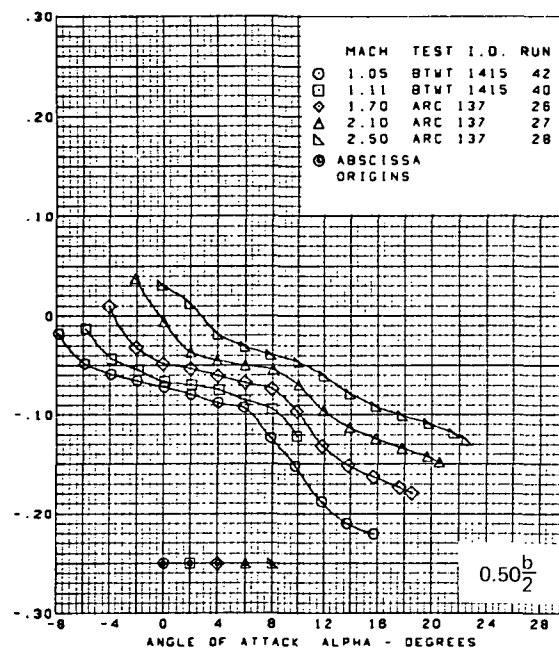
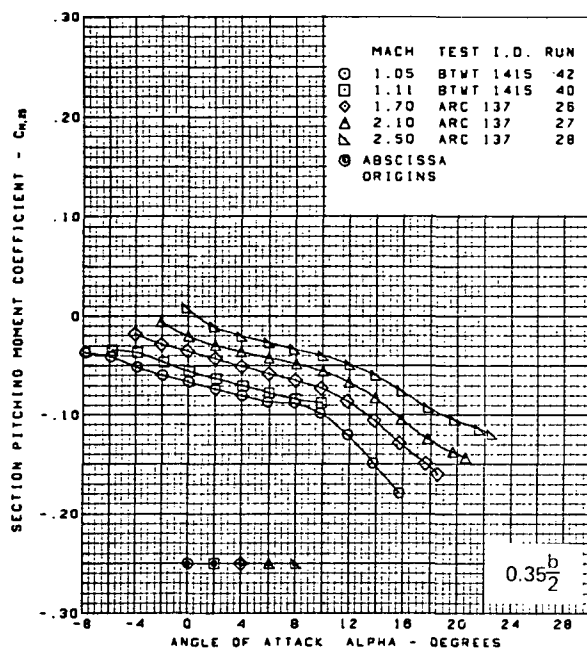
(c) (Concluded)

Figure 52.—(Continued)



(d) Section Pitching Moment Coefficients vs. Angle of Attack,  $M = 1.05$  Through 2.50

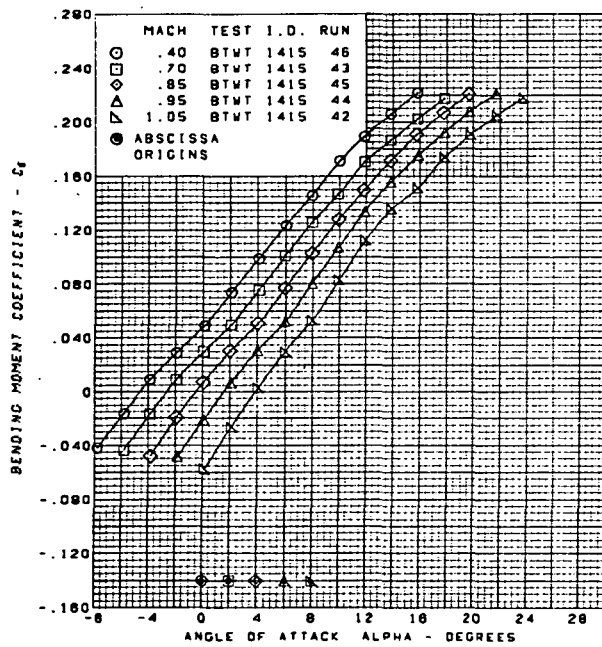
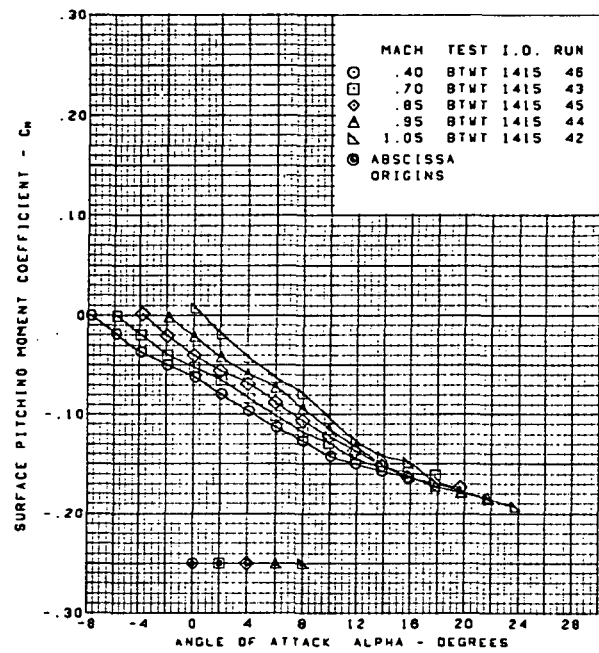
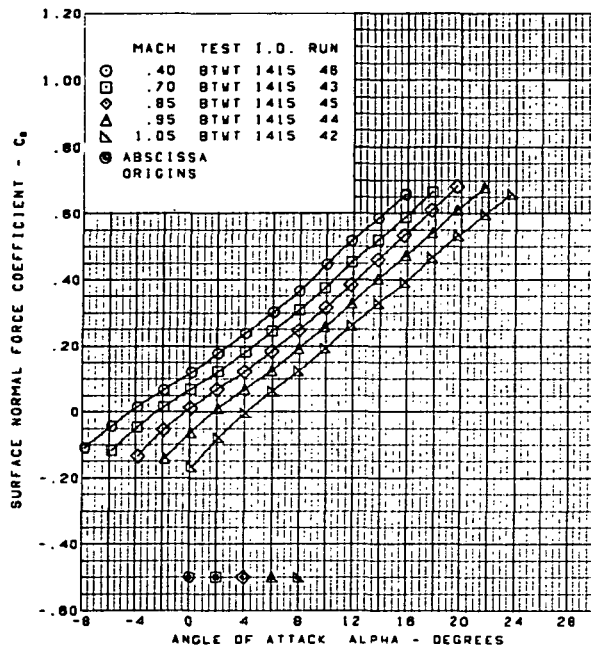
Figure 52.—(Continued)



Flat wing, rounded L.E.  
 L.E. deflection, full span =  $0.0^\circ$   
 T.E. deflection, full span =  $8.3^\circ$

(d) (Concluded)

Figure 52.—(Continued)

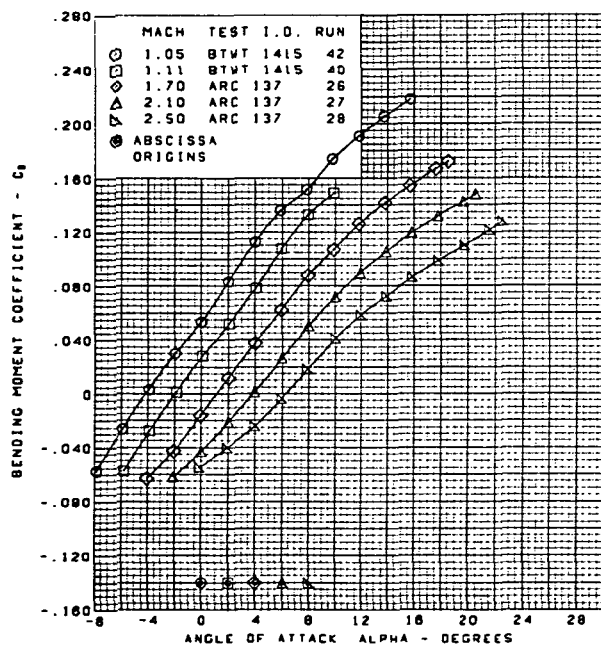
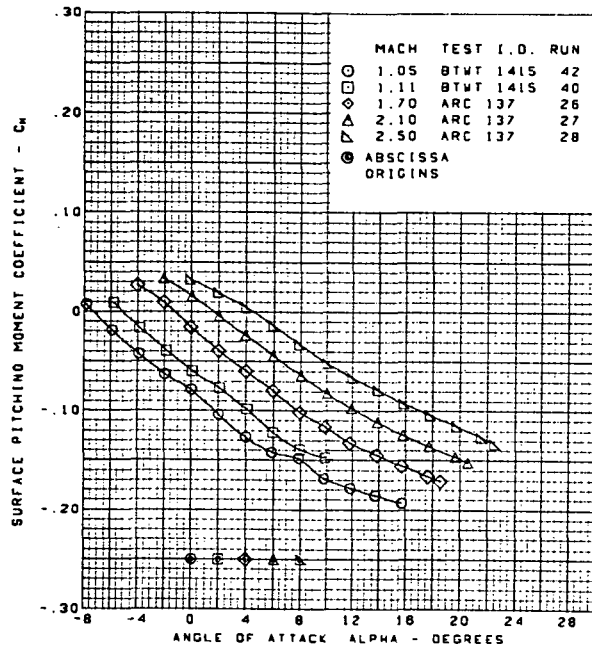
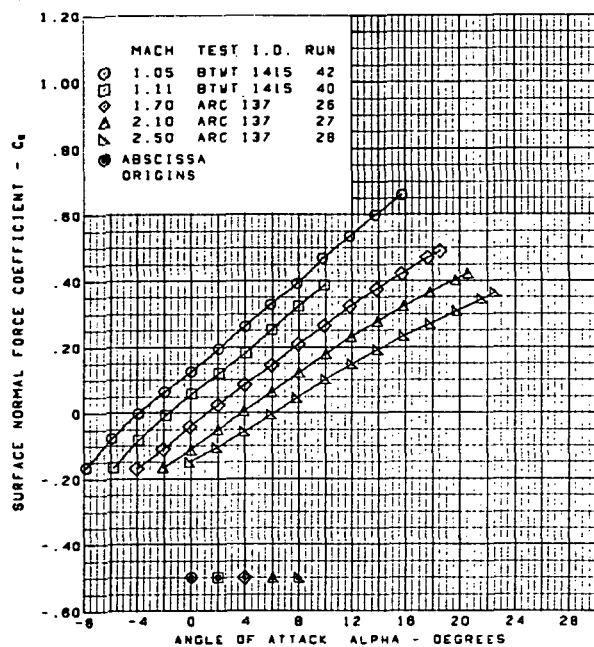


Flat wing, rounded L.E.  
 L.E. deflection, full span =  $0.0^\circ$   
 T.E. deflection, full span =  $8.3^\circ$

(e) Wing Aerodynamic Coefficients vs. Angle of Attack

Figure 52.—(Continued)

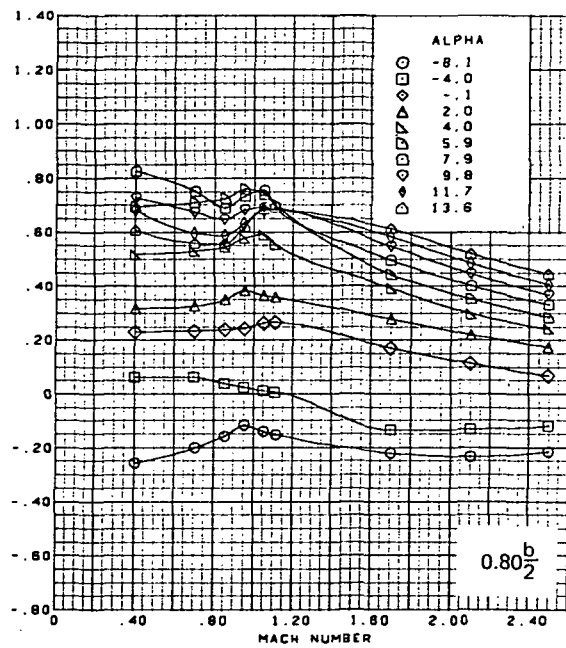
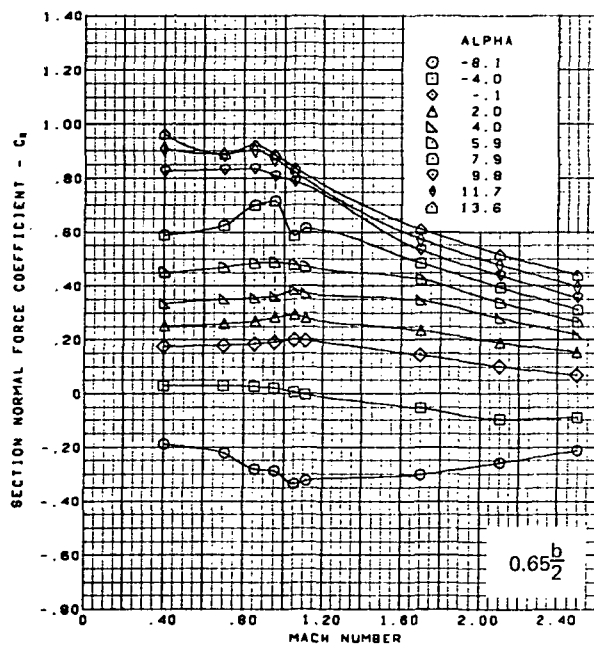
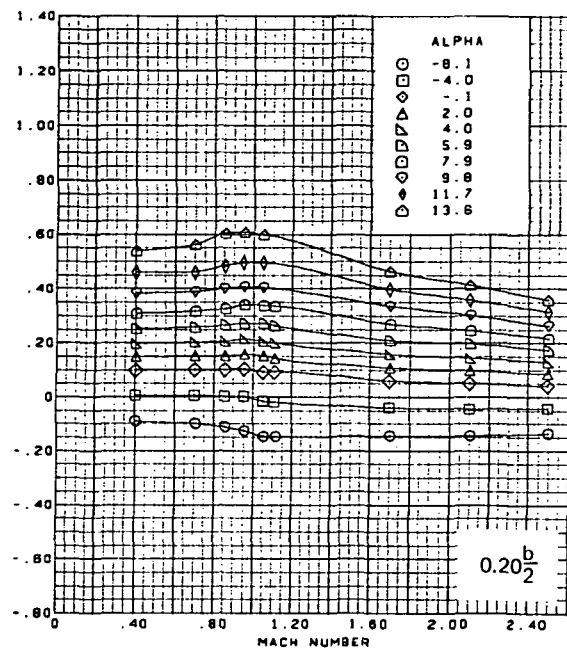
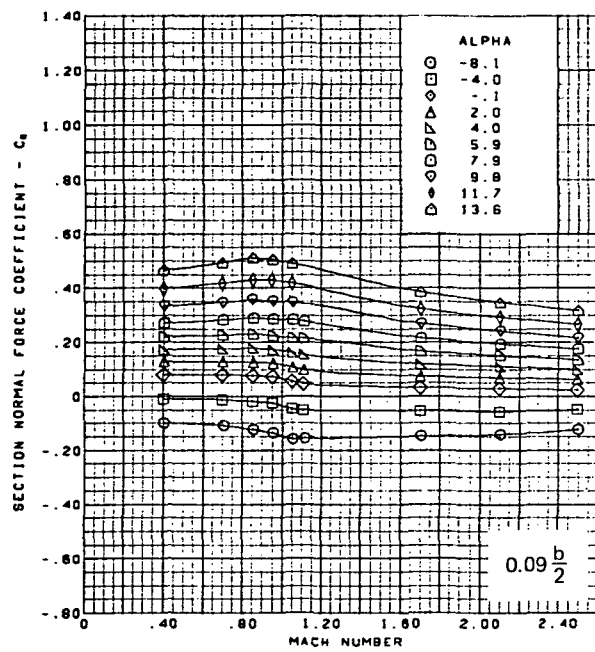




Flat wing, rounded L.E.  
 L.E. deflection, full span =  $0.0^\circ$   
 T.E. deflection, full span =  $8.3^\circ$

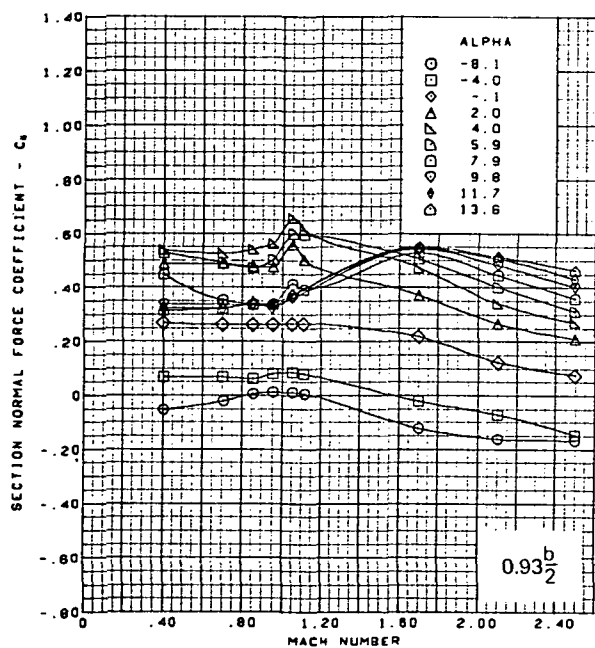
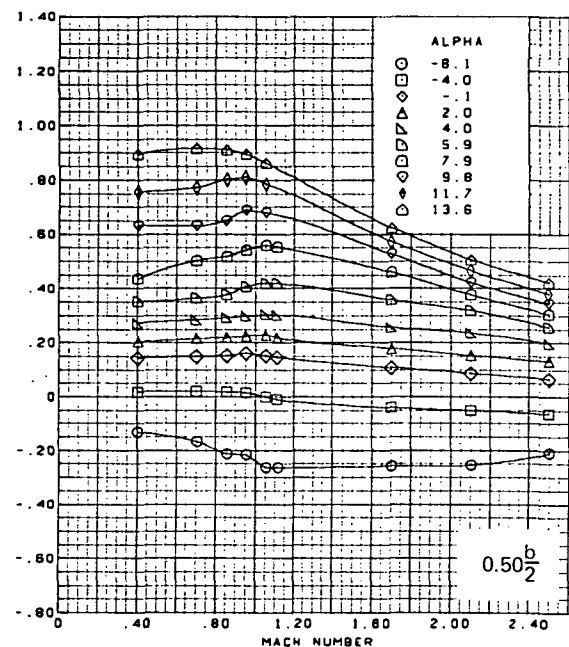
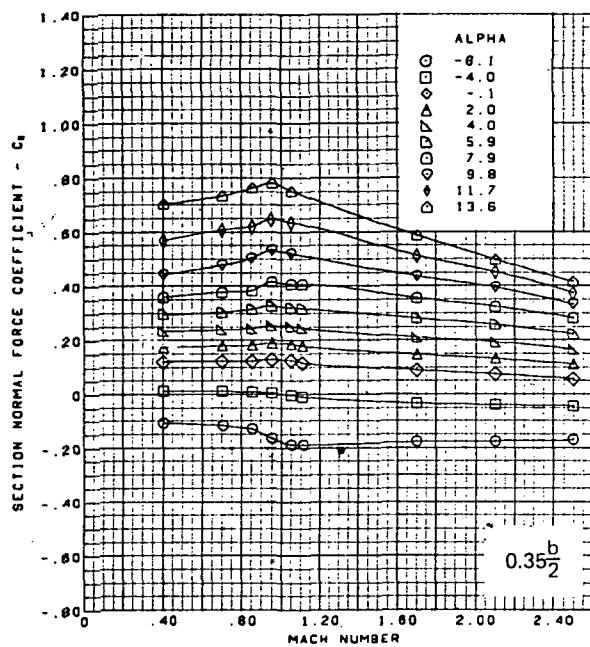
(e) (Concluded)

Figure 52.—(Continued)



(f) Section Aerodynamic Coefficients—Normal Force

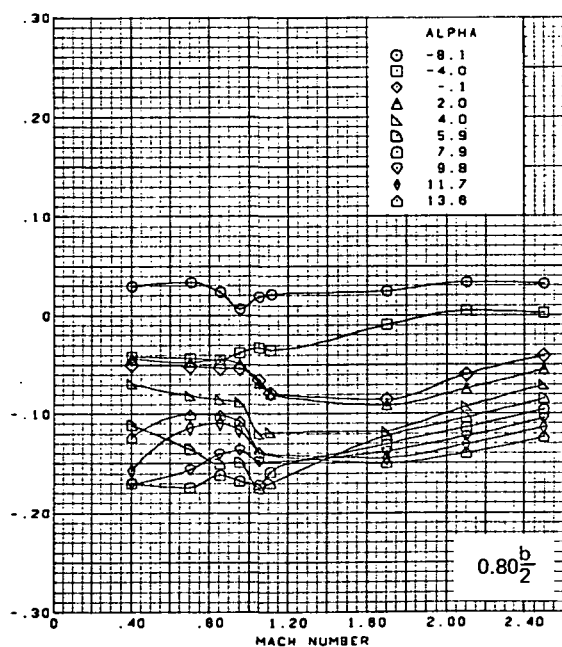
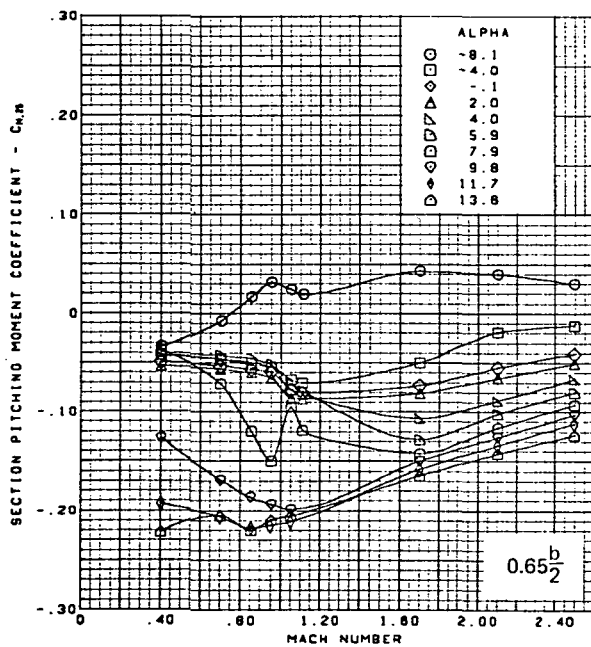
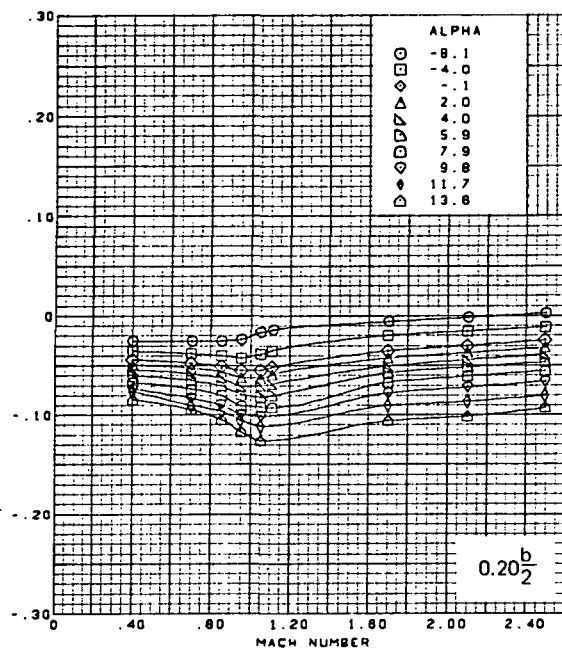
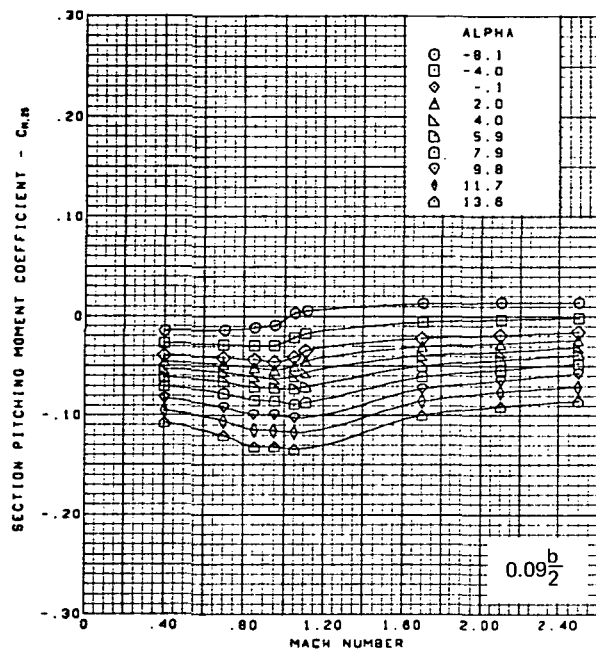
Figure 52.—(Continued)



Flat wing, rounded L.E.  
 L.E. deflection, full span =  $0.0^\circ$   
 T.E. deflection, full span =  $8.3^\circ$

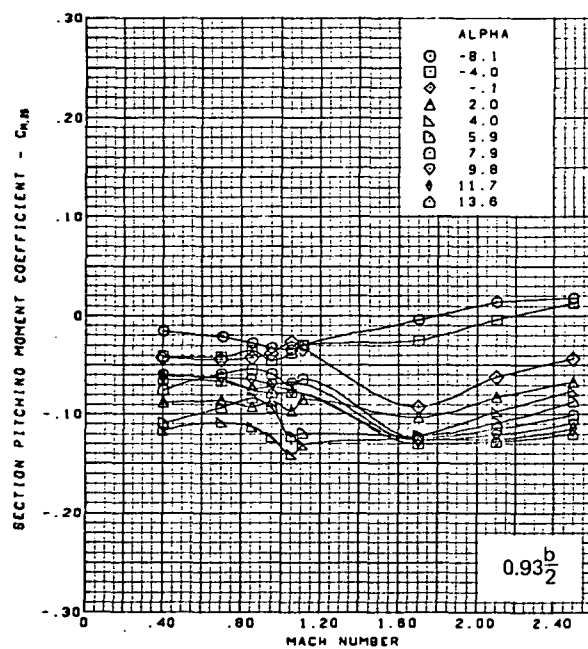
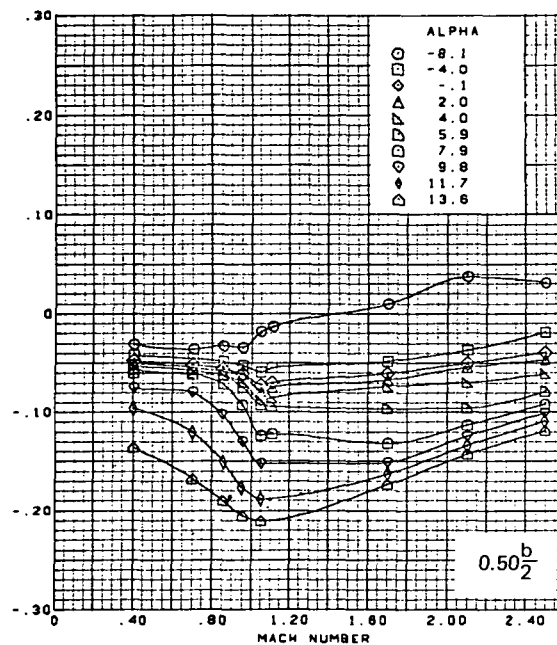
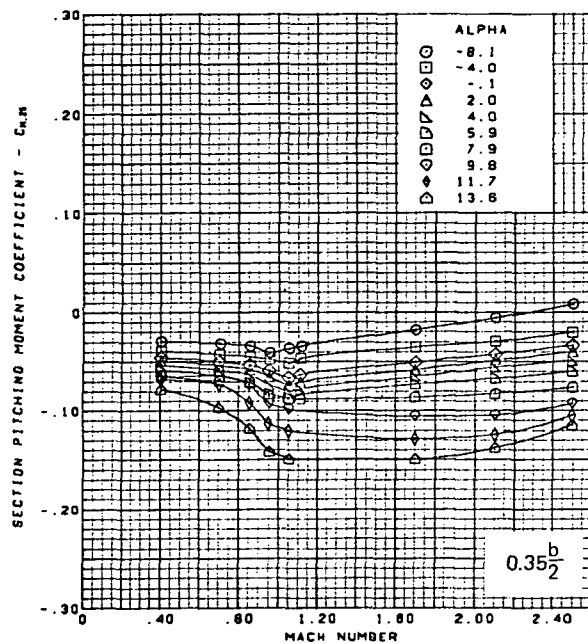
(f) (Concluded)

Figure 52.—(Continued)



(g) Section Aerodynamic Coefficients—Pitching Moment

Figure 52.—(Continued)

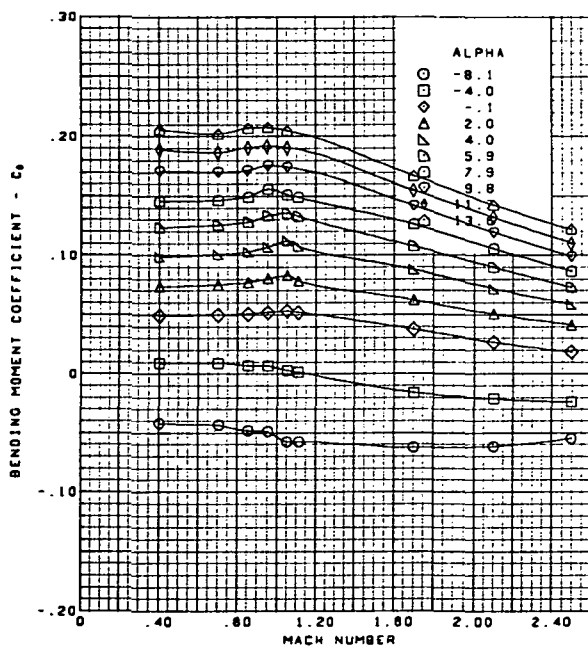
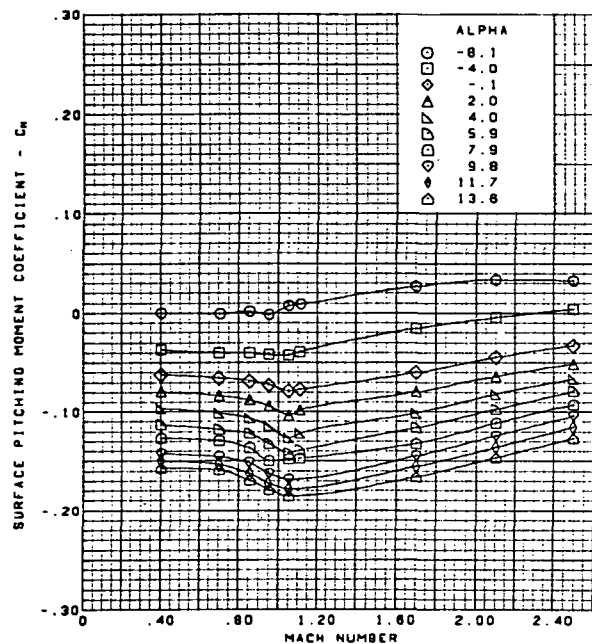
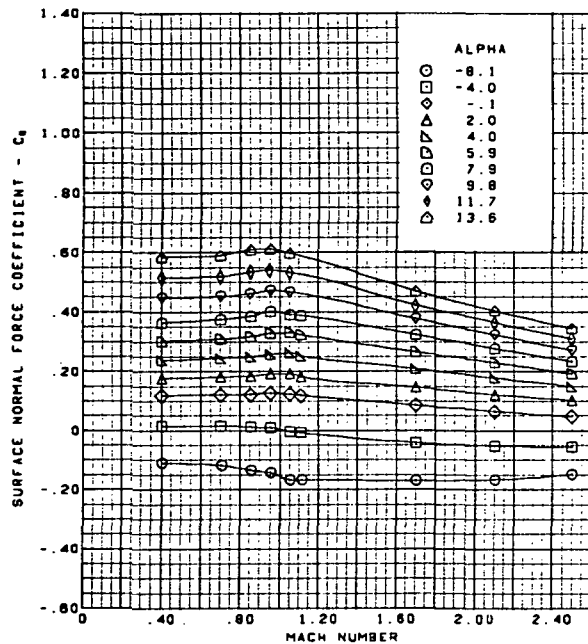


Flat wing, rounded L.E.  
 L.E. deflection, full span =  $0.0^\circ$   
 T.E. deflection, full span =  $8.3^\circ$

(g) (Concluded)

Figure 52.—(Continued)

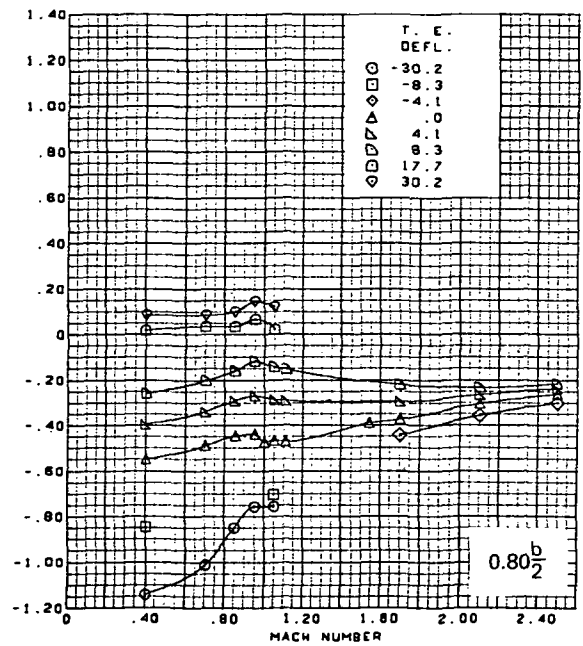
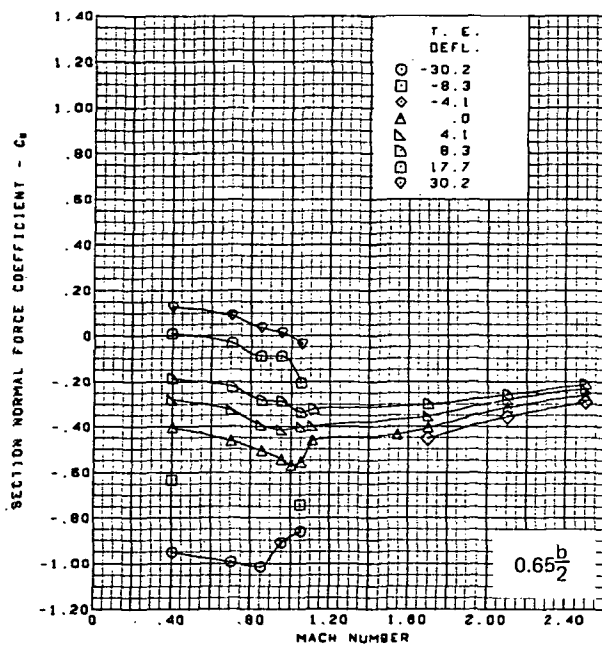
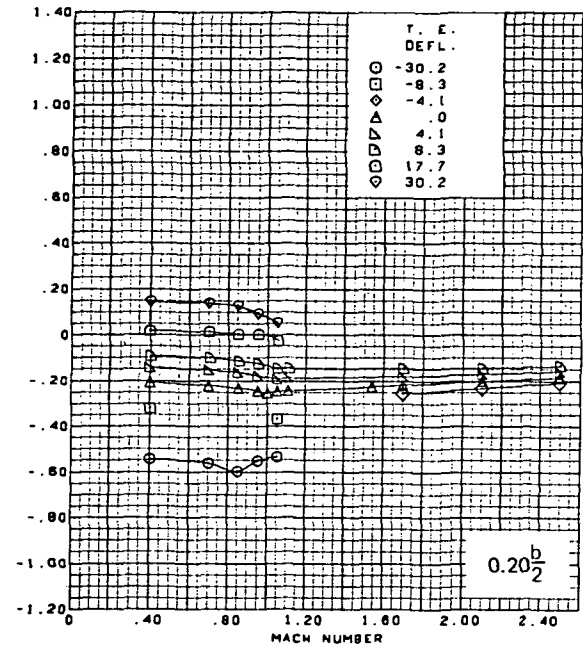
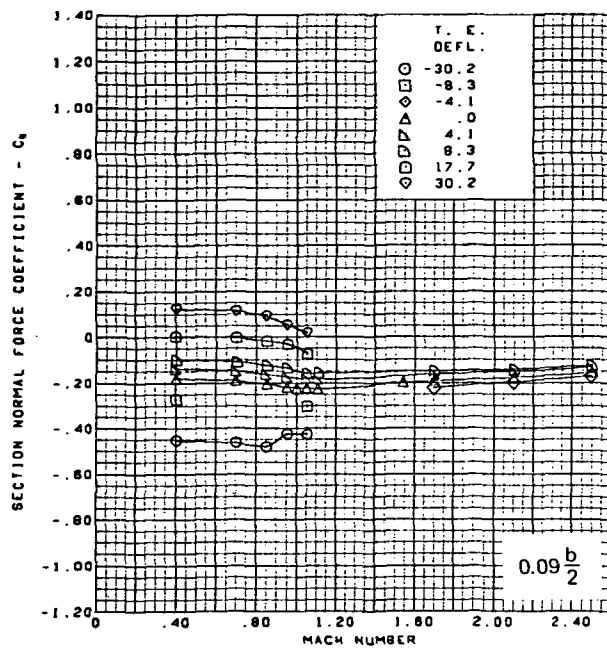
**Page  
Intentionally  
Left Blank**



Flat wing, rounded L.E.  
 L.E. deflection, full span =  $0.0^\circ$   
 T.E. deflection, full span =  $8.3^\circ$

(h) Wing Aerodynamic Coefficients

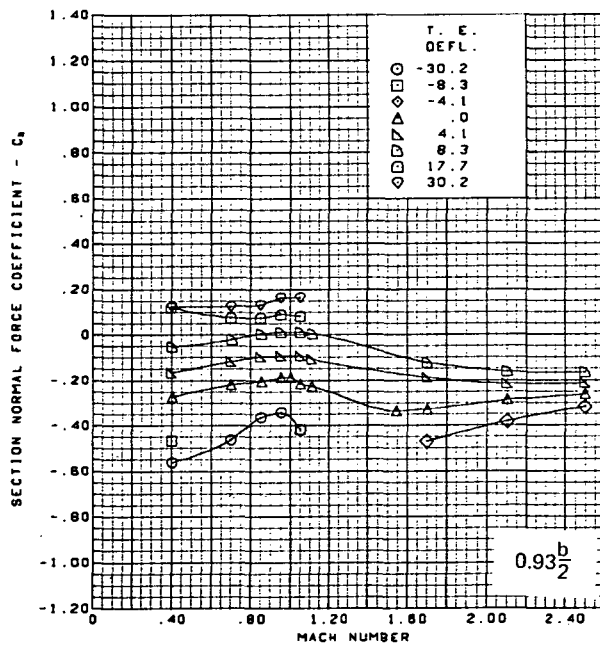
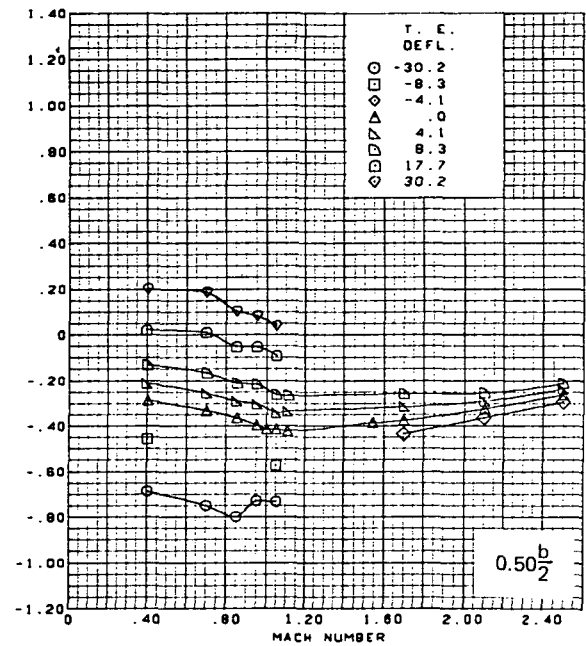
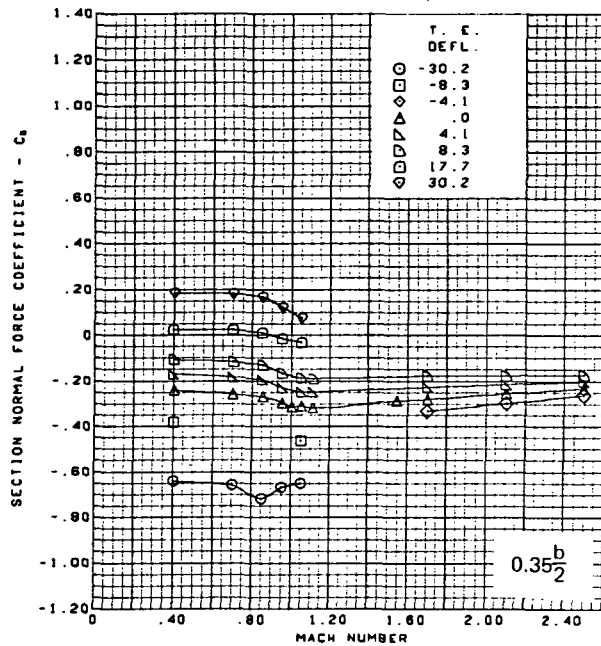
Figure 52.—(Concluded)



(a) Section Normal Force Coefficients,  $\alpha = -8^\circ$

Figure 53.—Wing Experimental Data—Effect of T.E. Control Surface Deflection With Mach Number and Angle of Attack; Flat Wing, Rounded L.E.; L.E. Deflection, Full Span =  $0.0^\circ$

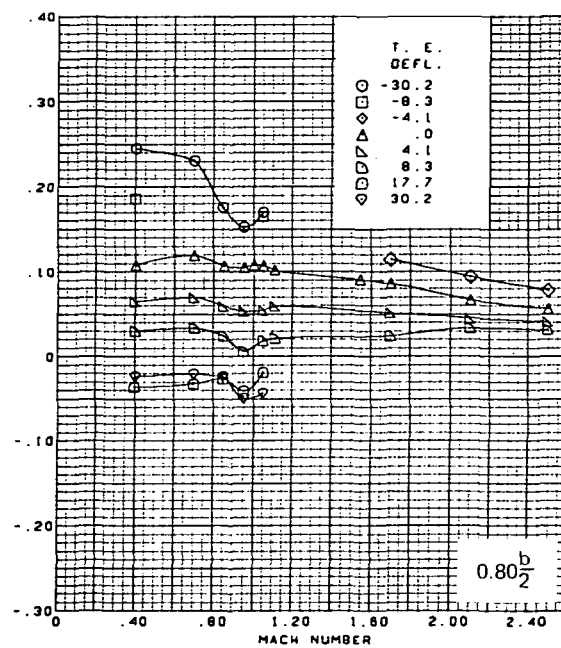
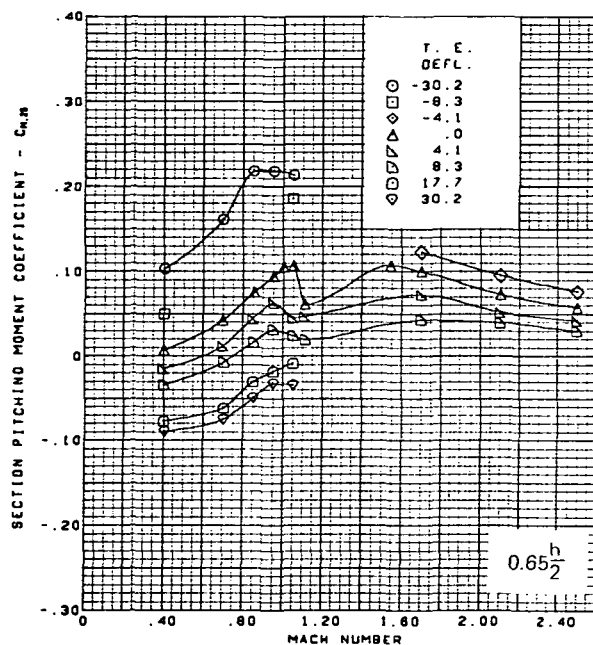
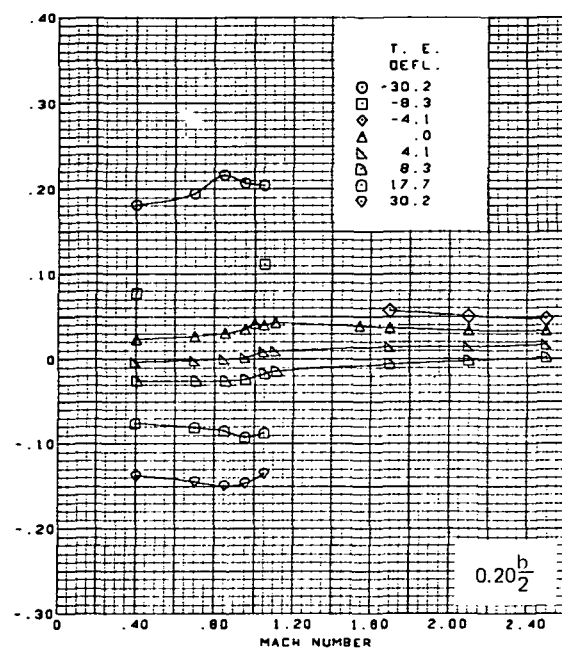
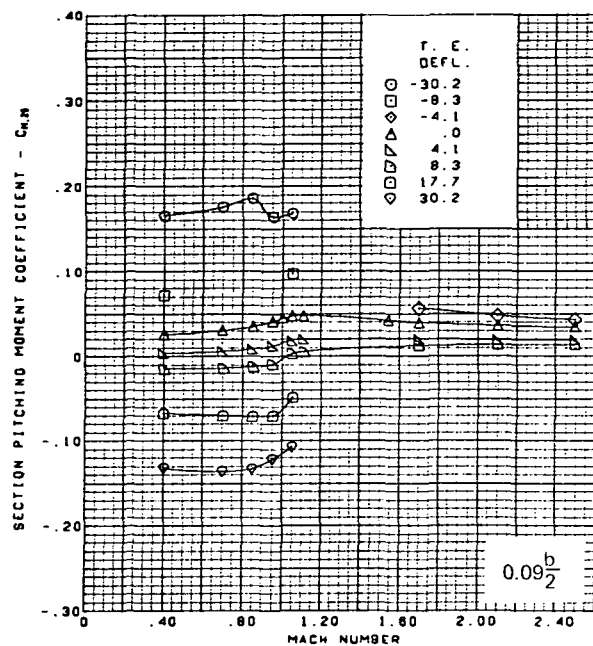




Flat wing, rounded L.E.  
L.E. deflection, full span =  $0.0^\circ$

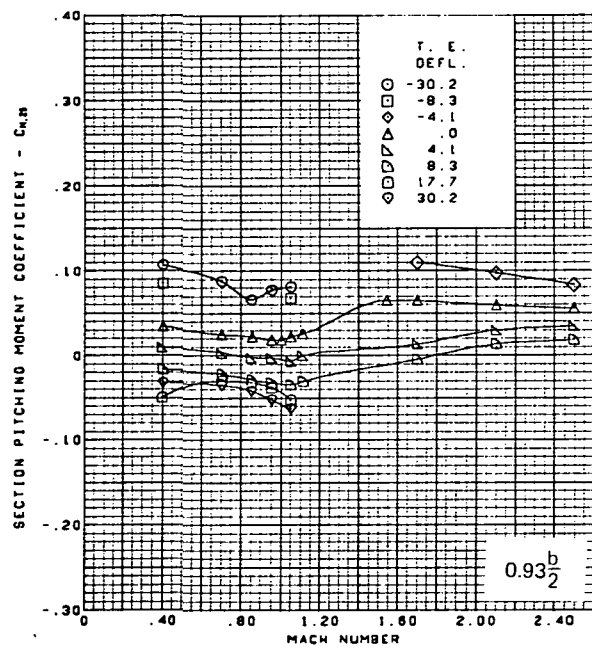
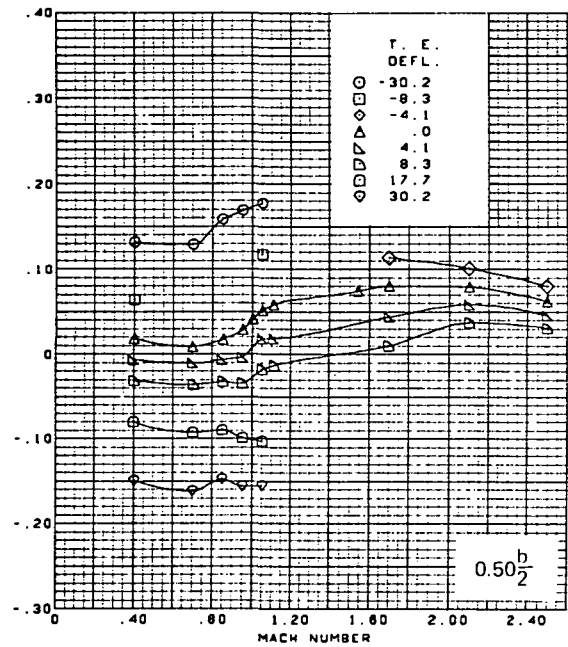
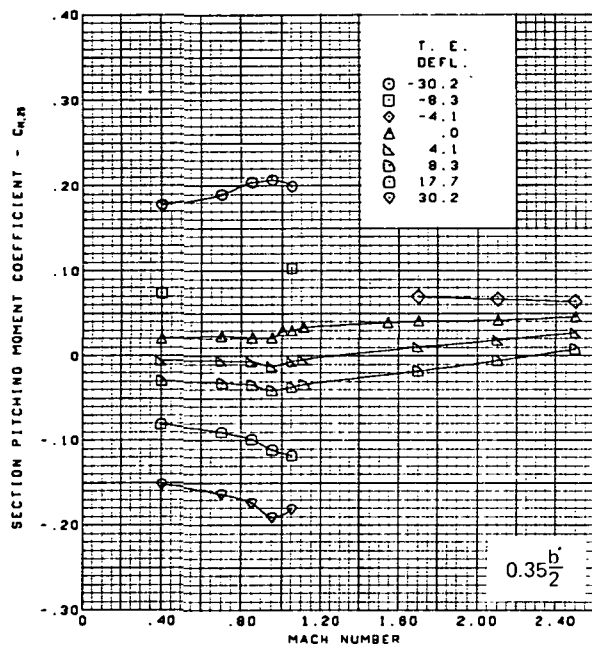
(a) (Concluded)

Figure 53.—(Continued)



(b) Section Pitching Moment Coefficients,  $\alpha = -8^\circ$

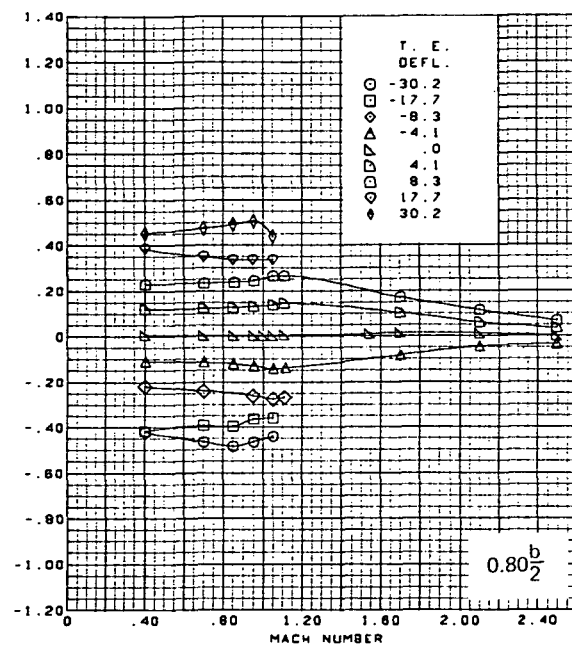
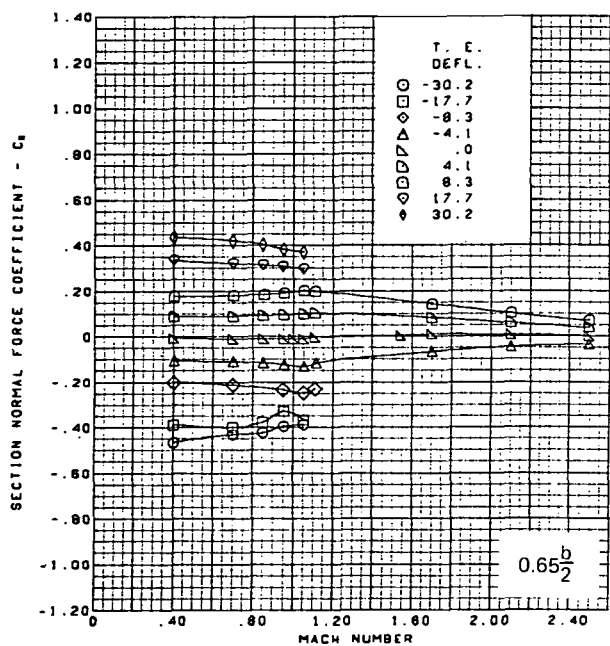
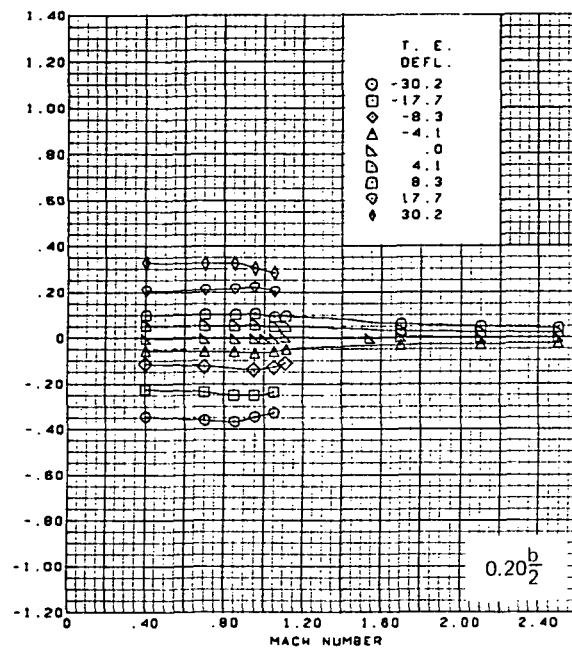
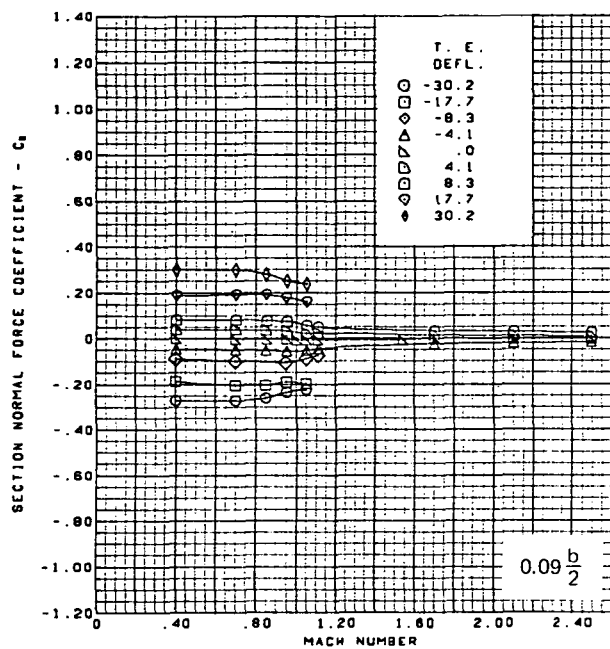
Figure 53.—(Continued)



Flat wing, rounded L.E.  
L.E. deflection, full span =  $0.0^\circ$

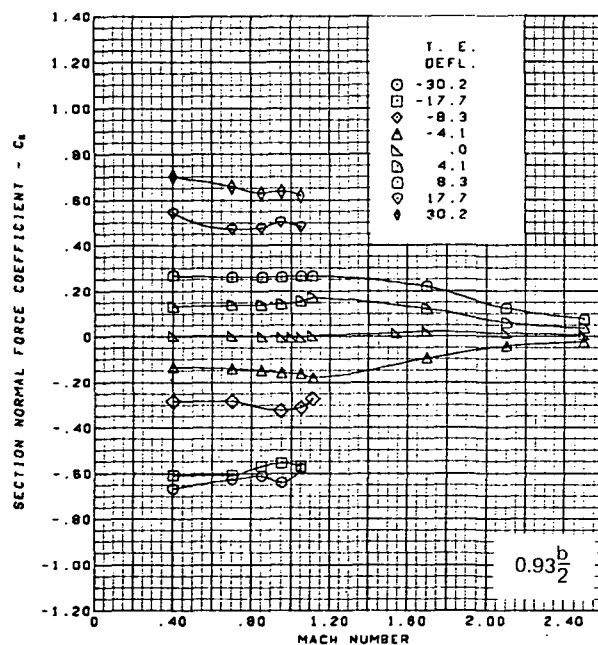
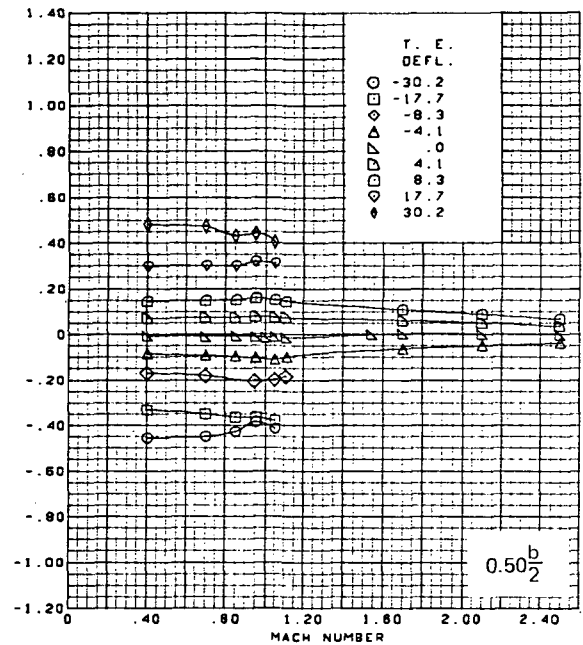
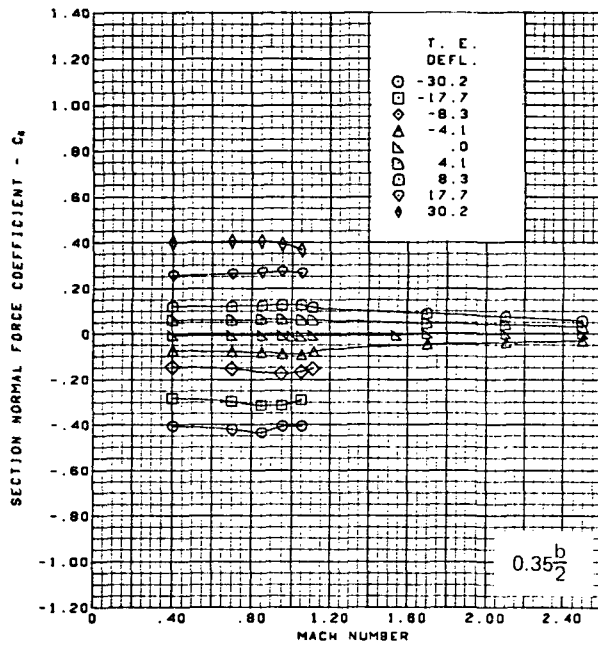
(b) (Concluded)

Figure 53.—(Continued)



(c) Section Normal Force Coefficients,  $\alpha = 0^\circ$

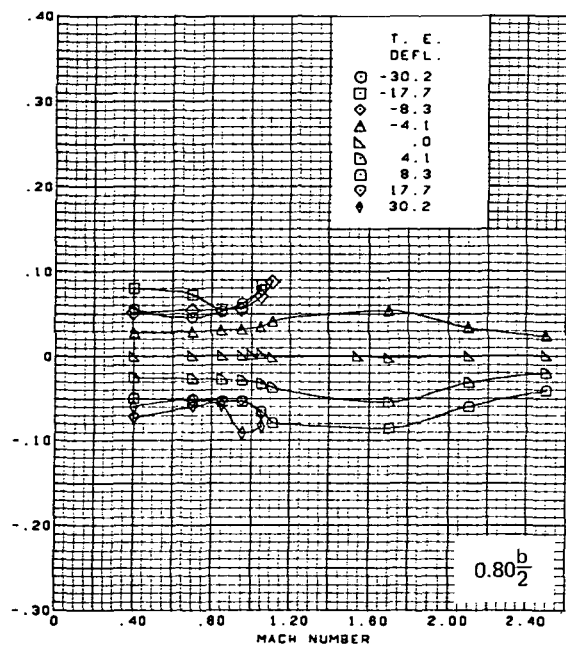
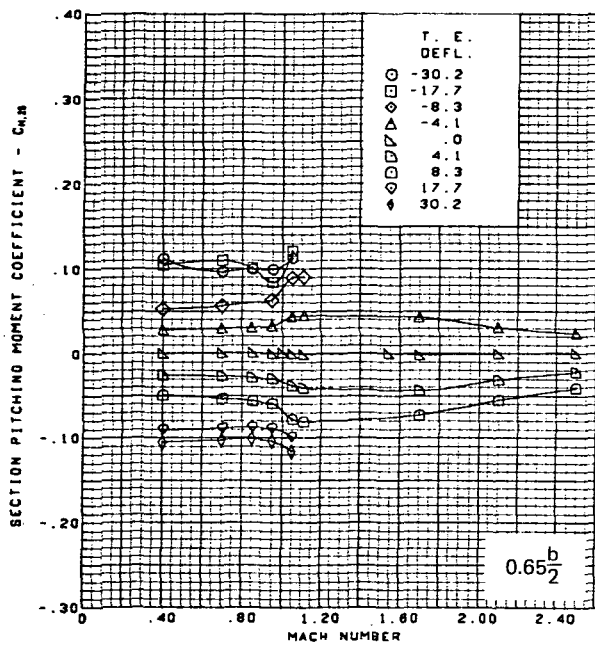
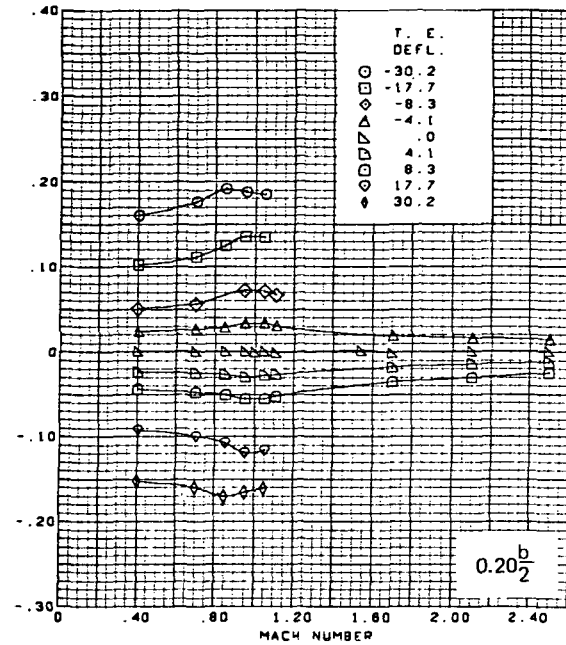
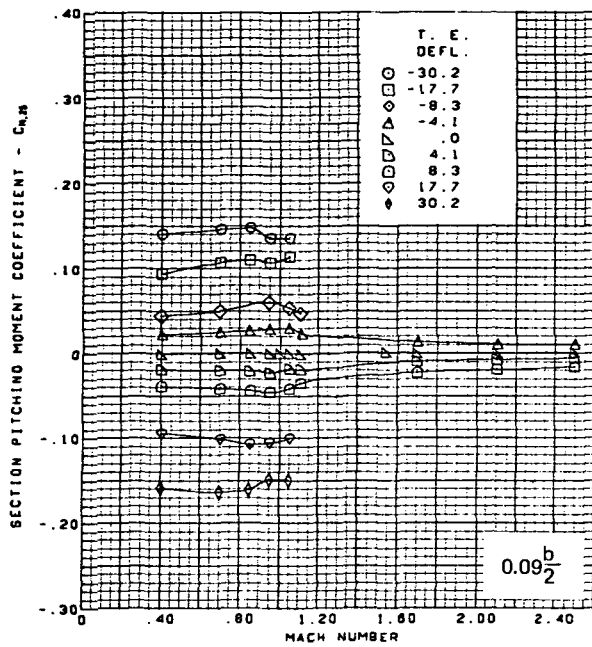
Figure 53.—(Continued)



Flat wing, rounded L.E.  
L.E. deflection, full span =  $0.0^\circ$

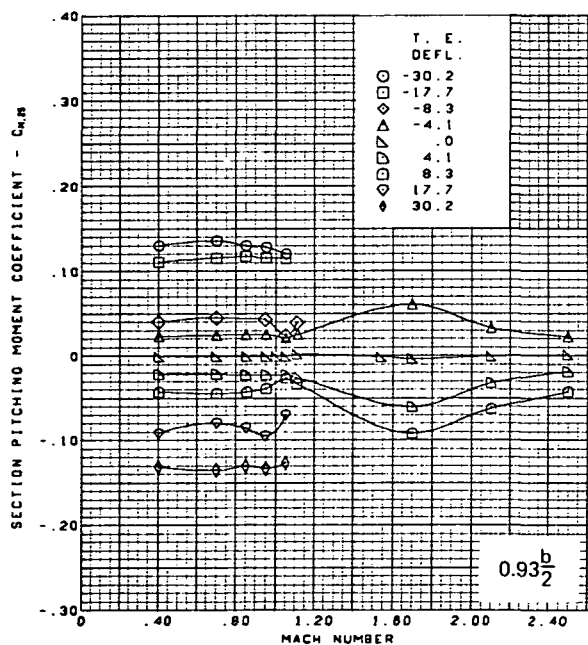
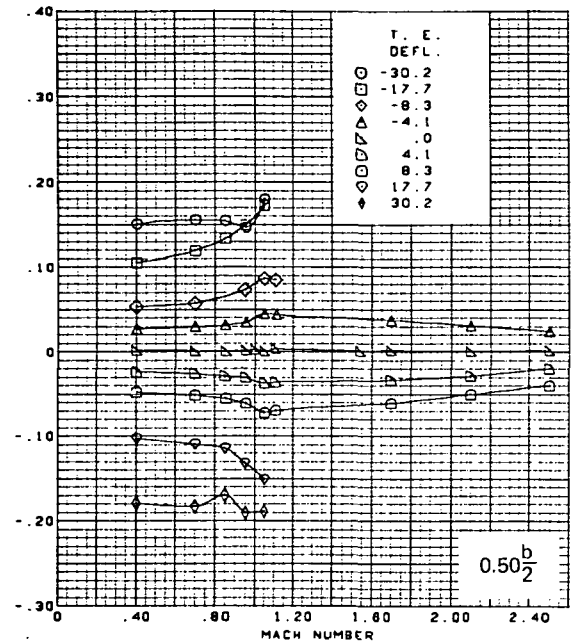
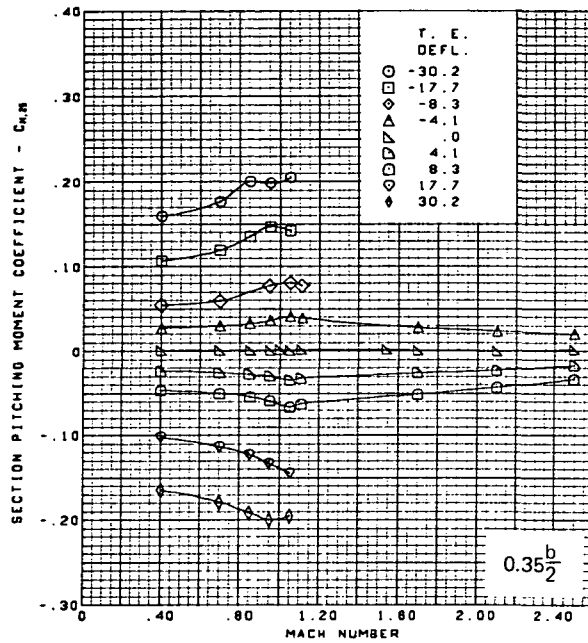
(c) (Concluded)

Figure 53.—(Continued)



(d) Section Pitching Moment Coefficients,  $\alpha = 0^\circ$

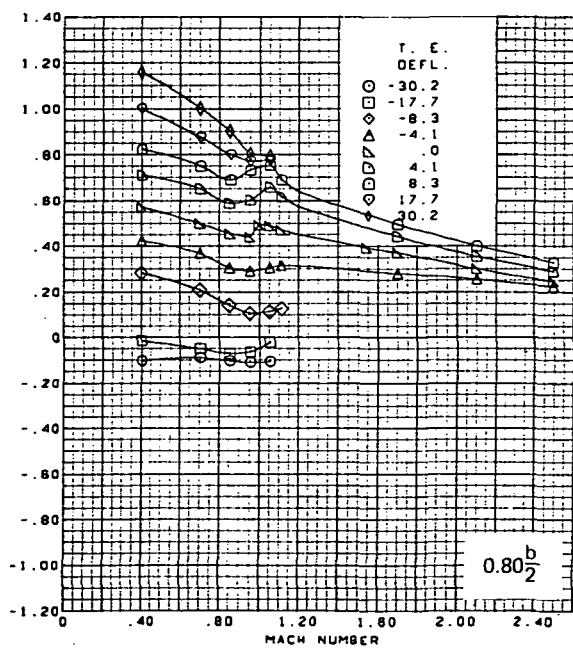
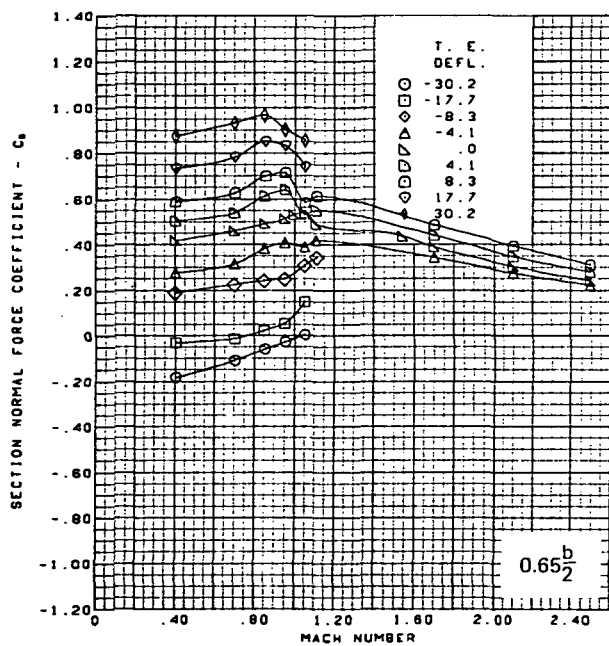
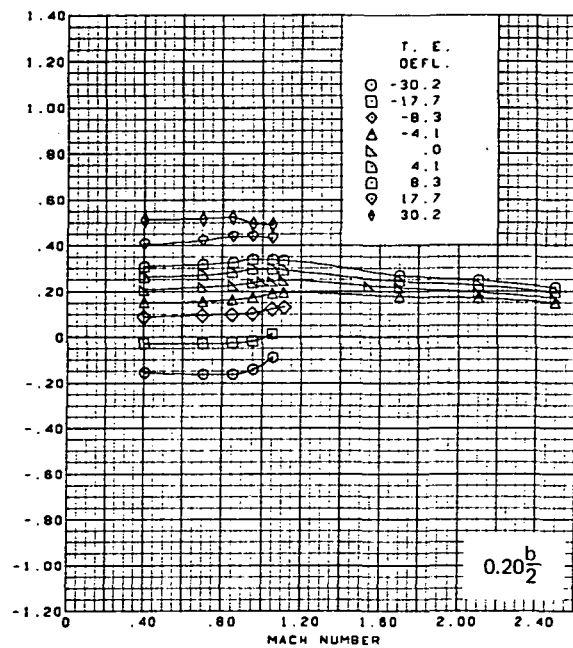
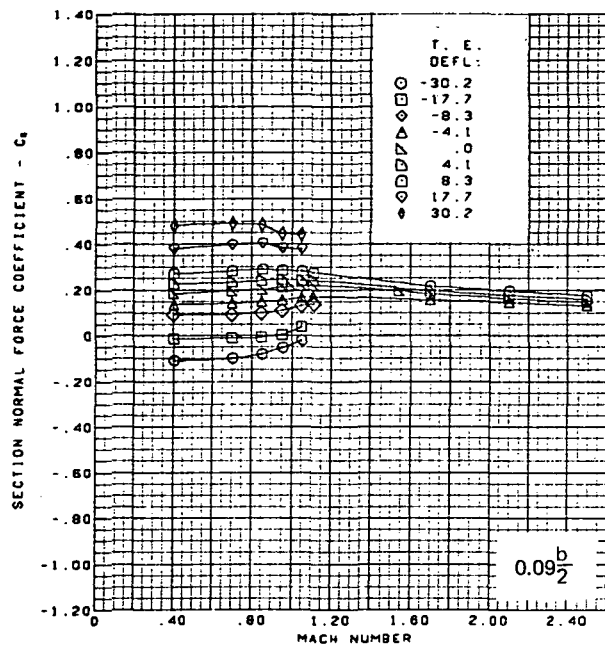
Figure 53.—(Continued)



Flat wing, rounded L.E.  
L.E. deflection, full span =  $0.0^\circ$

(d) (Concluded)

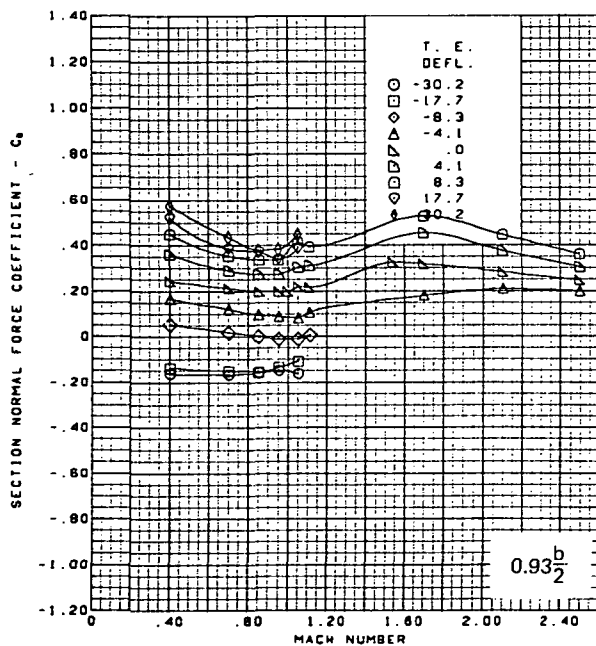
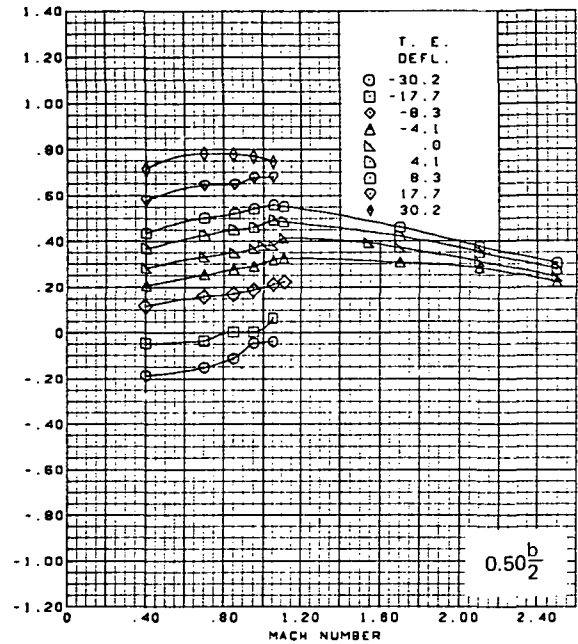
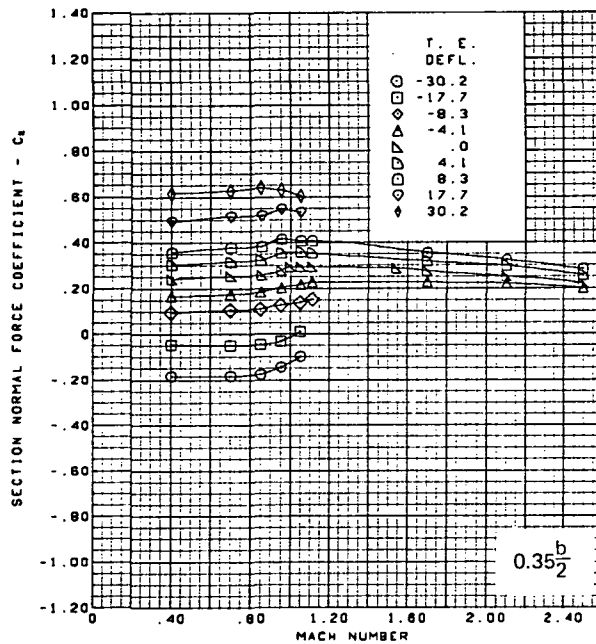
Figure 53.—(Continued)



(e) Section Normal Force Coefficients,  $\alpha = 8^\circ$

Figure 53.—(Continued)

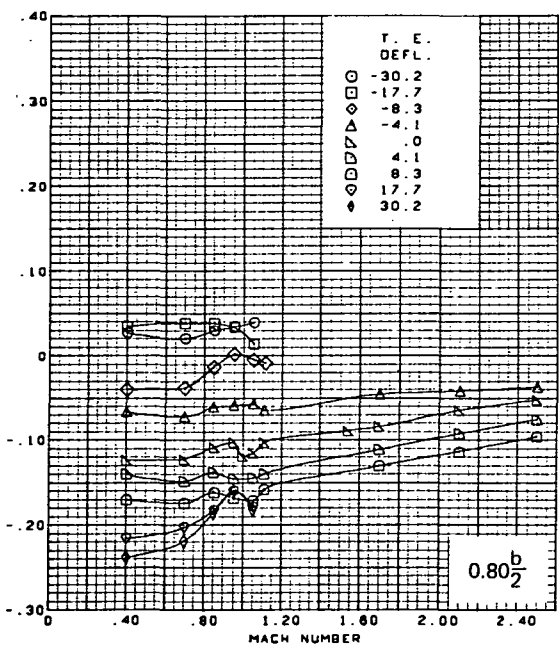
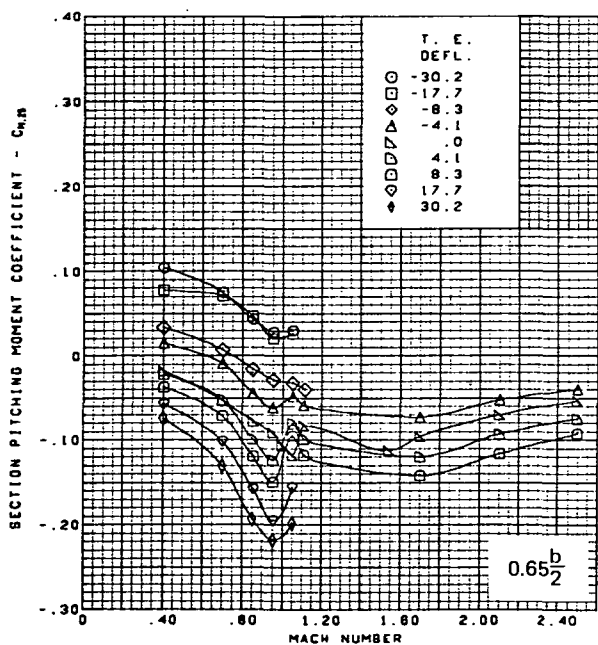
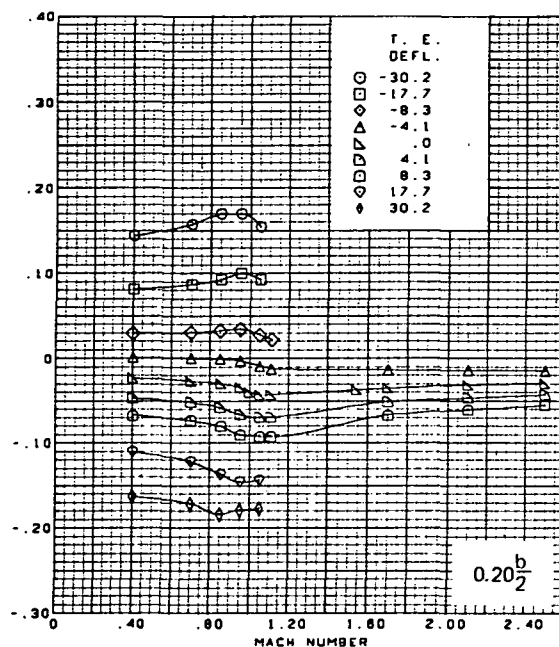
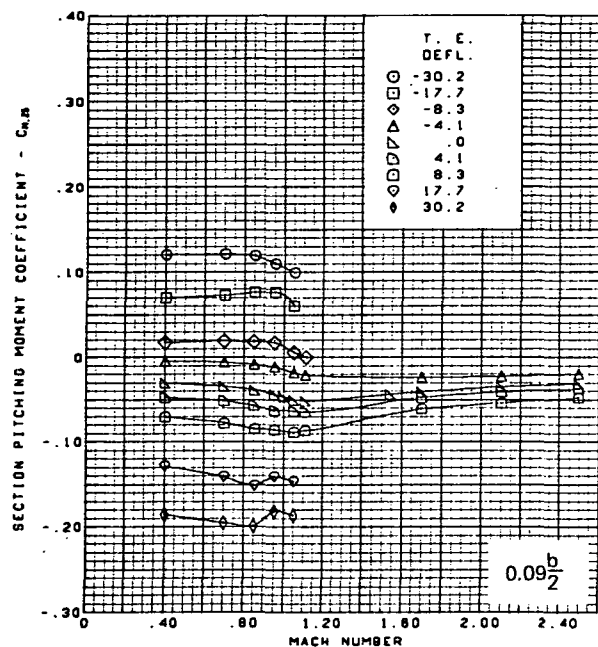




Flat wing, rounded L.E.  
L.E. deflection, full span =  $0.0^\circ$

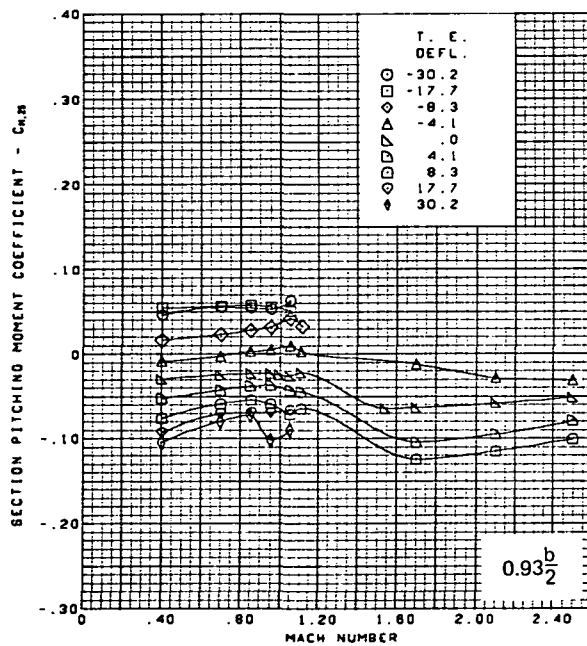
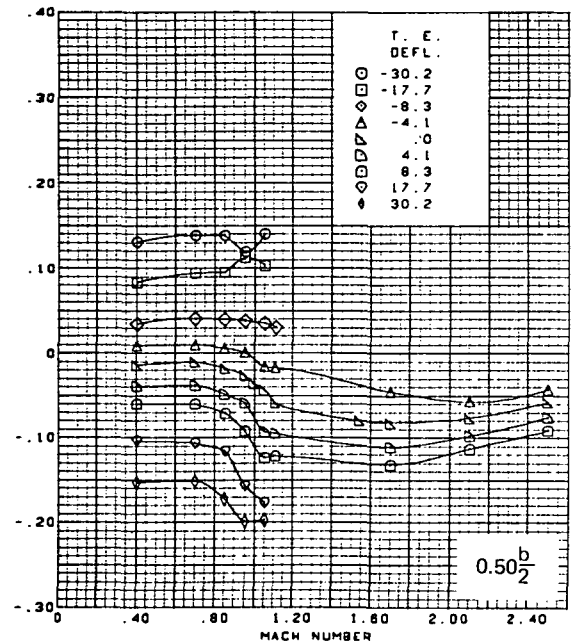
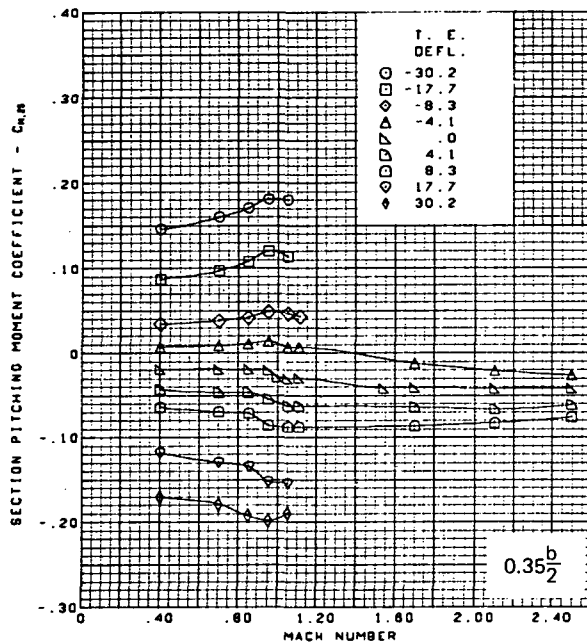
(e) (Concluded)

Figure 53.—(Continued)



(f) Section Pitching Moment Coefficients,  $\alpha = 8^\circ$

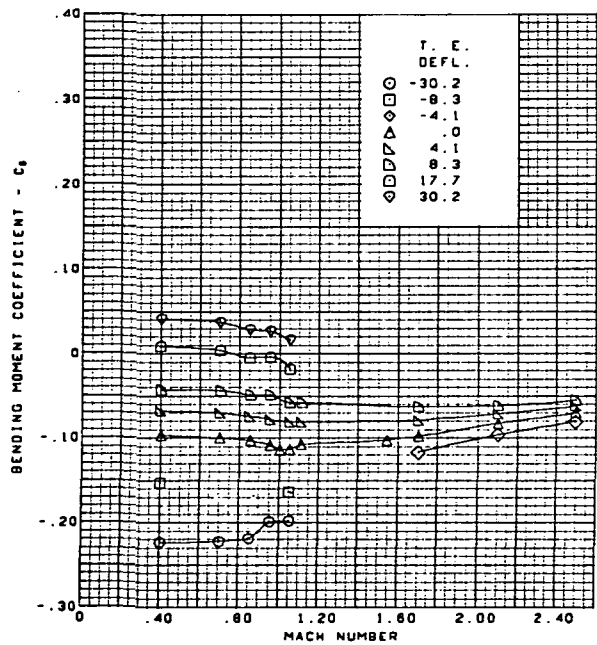
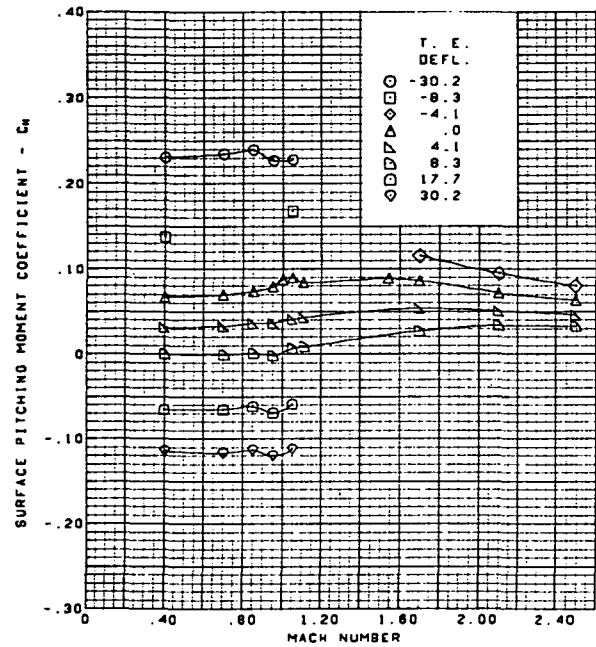
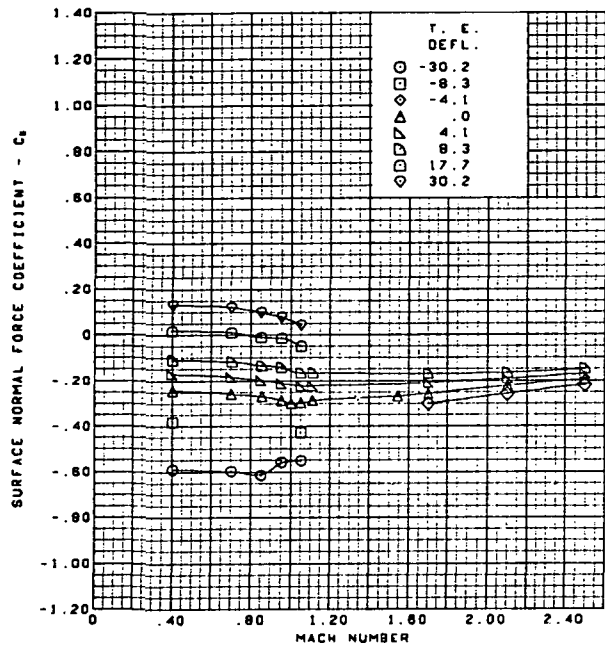
Figure 53.—(Continued)



Flat wing, rounded L.E.  
L.E. deflection, full span =  $0.0^\circ$

(f) (Concluded)

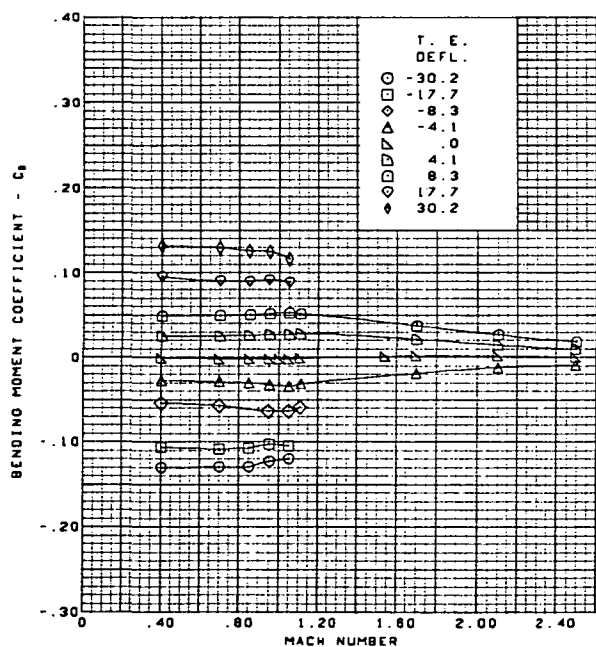
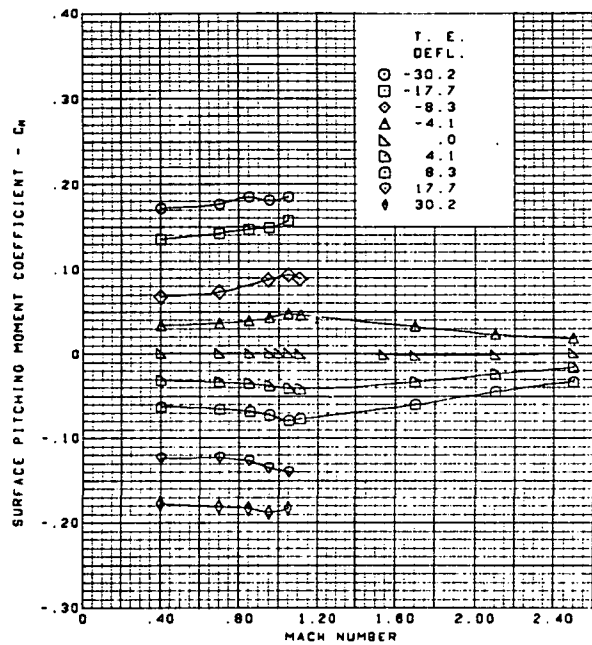
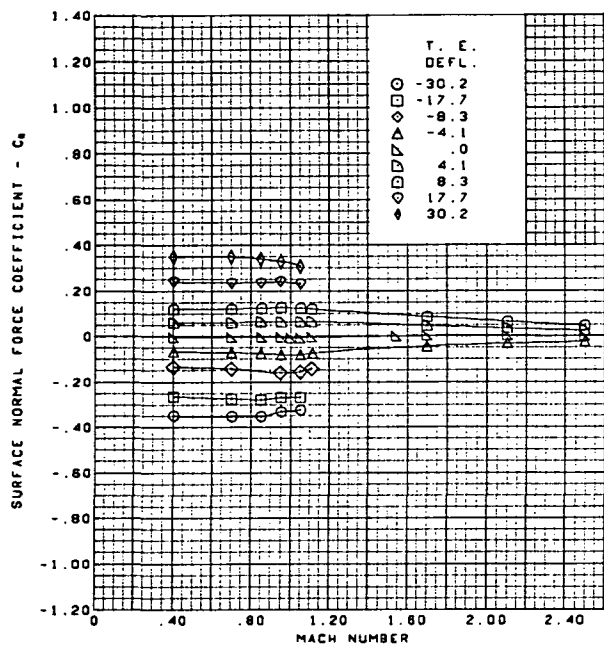
Figure 53.—(Continued)



Flat wing, rounded L.E.  
L.E. deflection, full span =  $0.0^\circ$

(g) Wing Aerodynamic Coefficients,  $\alpha = -8^\circ$

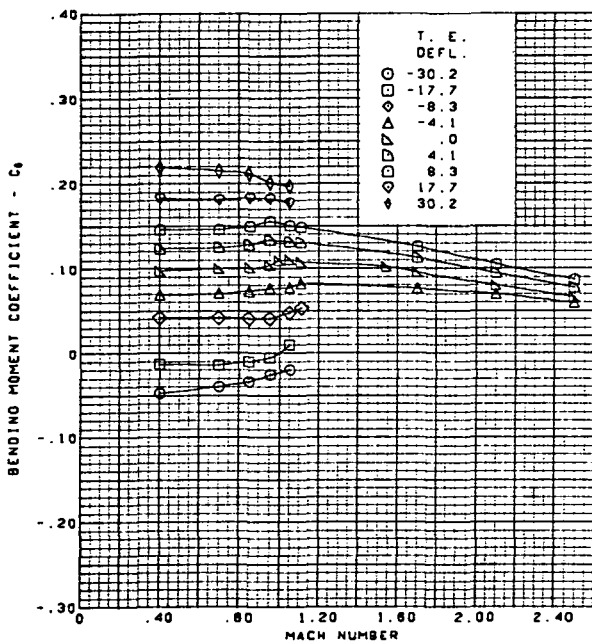
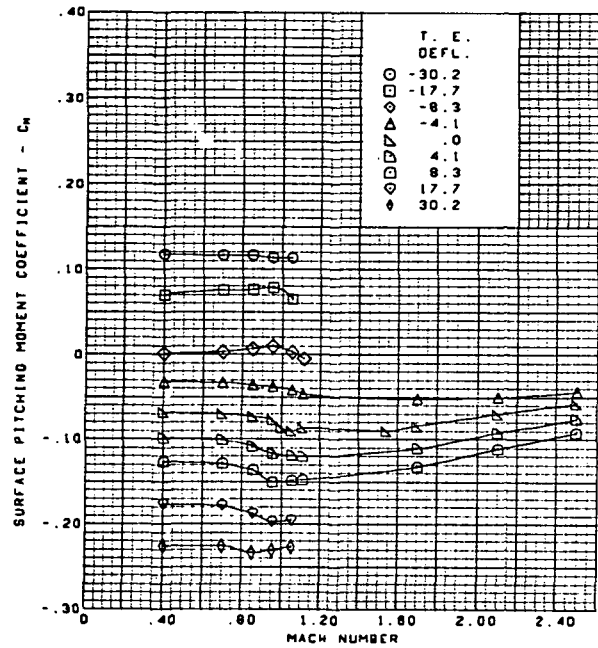
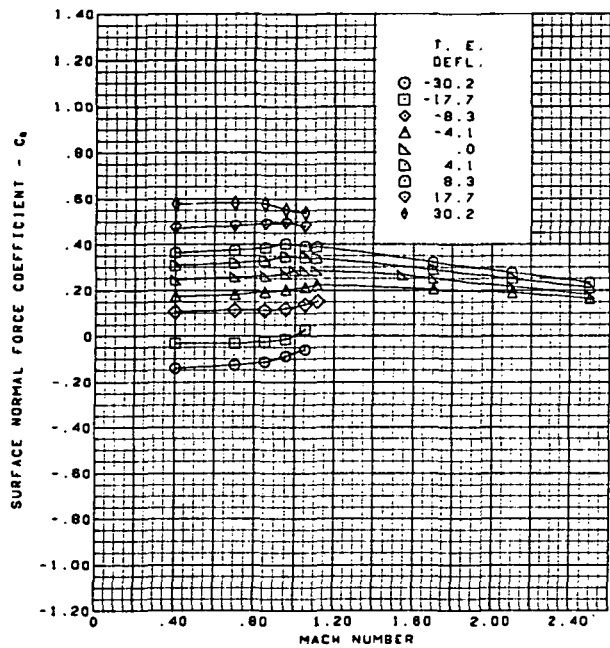
Figure 53.—(Continued)



Flat wing, rounded L.E.  
L.E. deflection, full span =  $0.0^\circ$

(h) Wing Aerodynamic Coefficients,  $\alpha = 0^\circ$

Figure 53.—(Continued)



Flat wing, rounded L.E.  
L.E. deflection, full span =  $0.0^\circ$

(i) Wing Aerodynamic Coefficients,  $\alpha = 8^\circ$

Figure 53.—(Concluded)

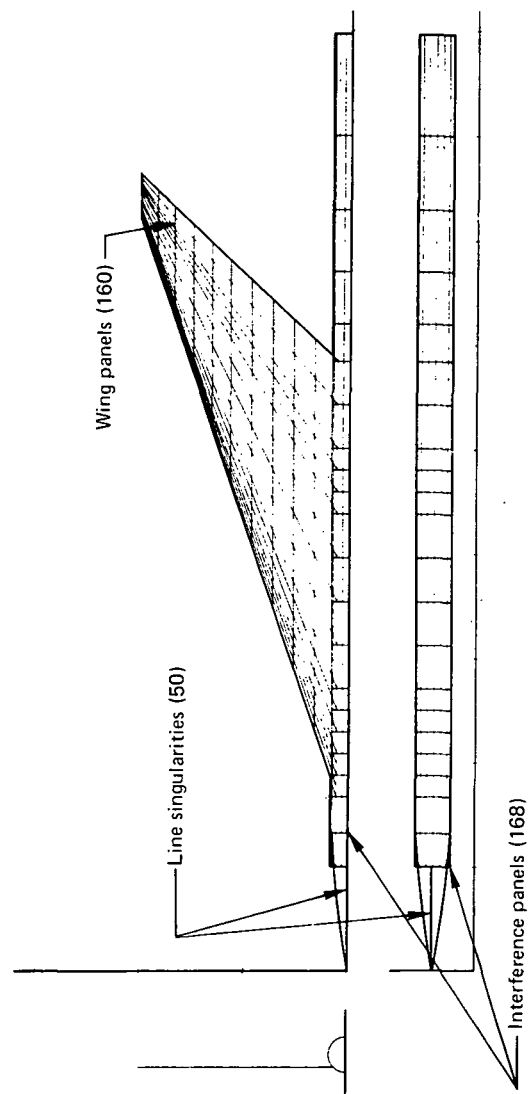
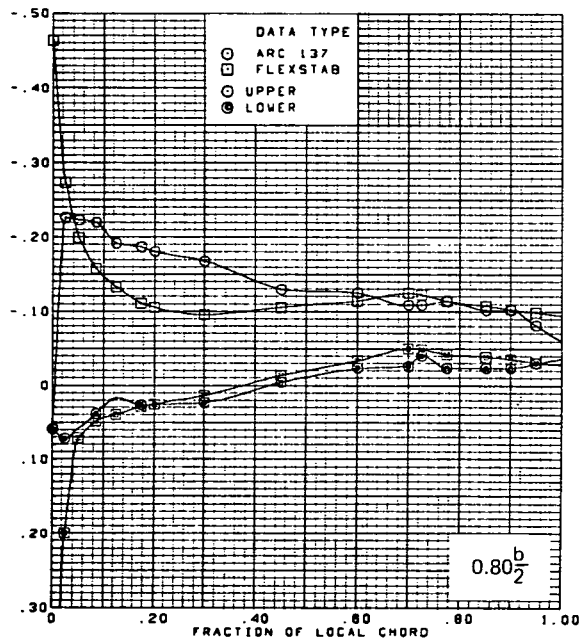
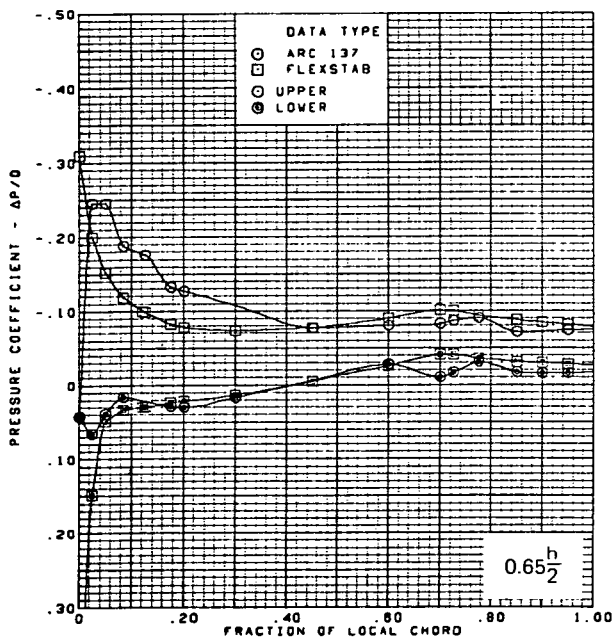
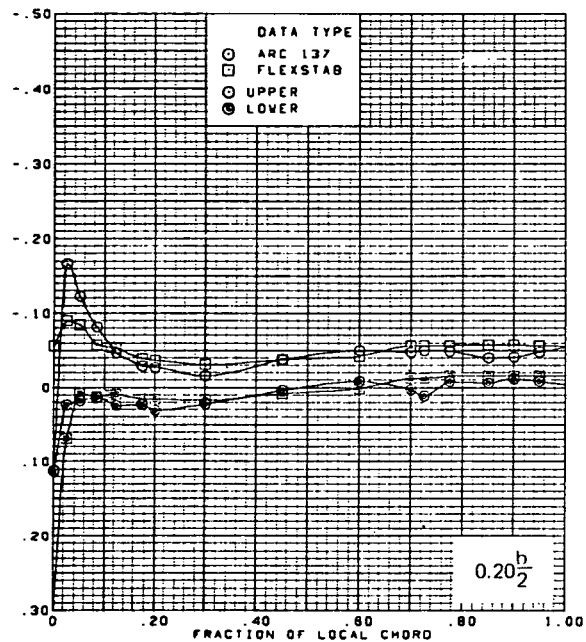
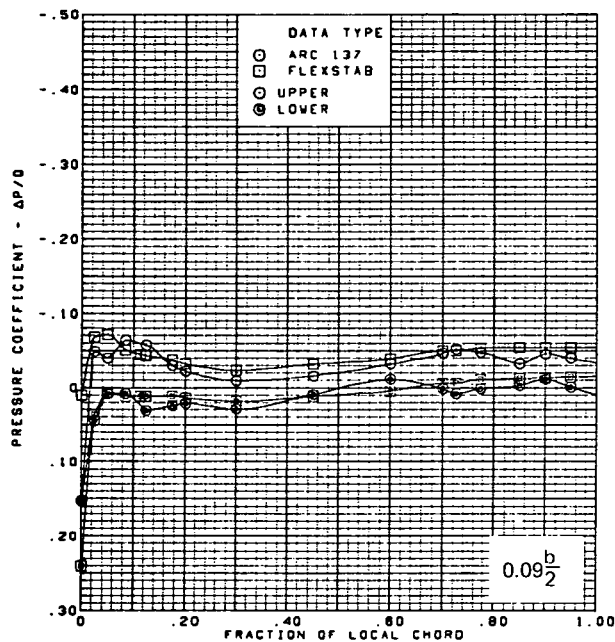


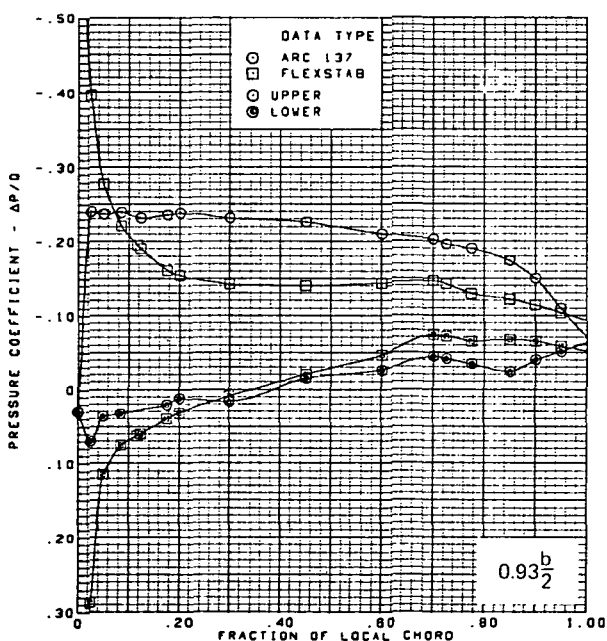
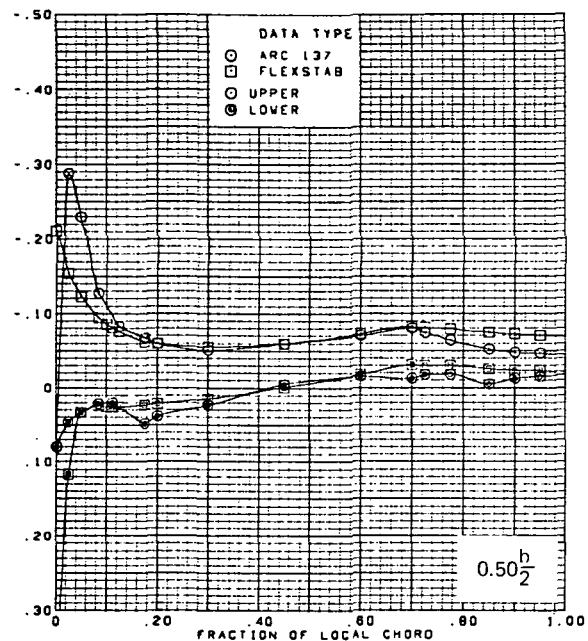
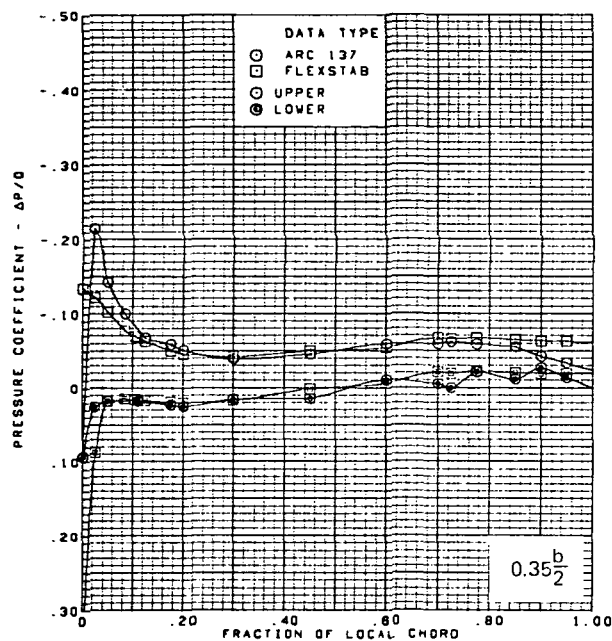
Figure 54.—Paneling for FLEXSTAB Computer Program



(a) Surface Chordwise Pressure Distributions,  $\alpha = 2^\circ$

Figure 55.—Wing Theory-to-Experiment Comparison—Flat Wing, Rounded L.E.; L.E. Deflection, Full Span =  $0.0^\circ$ ; T.E. Deflection, Full Span =  $0.0^\circ$ ;  $M = 1.70$



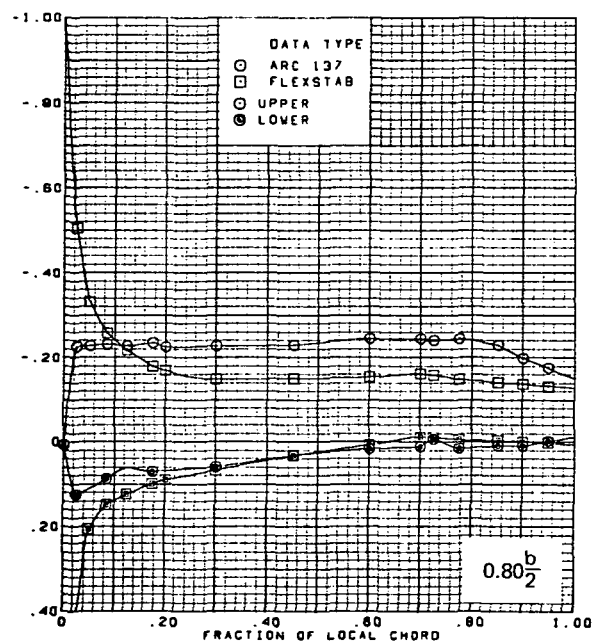
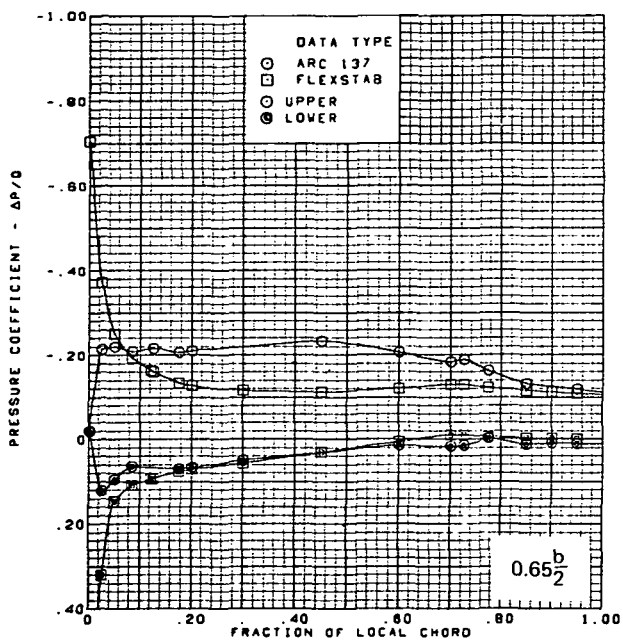
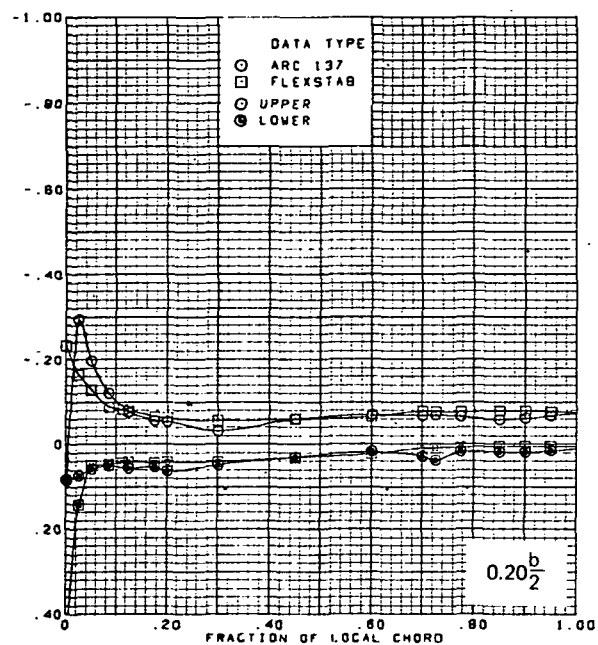
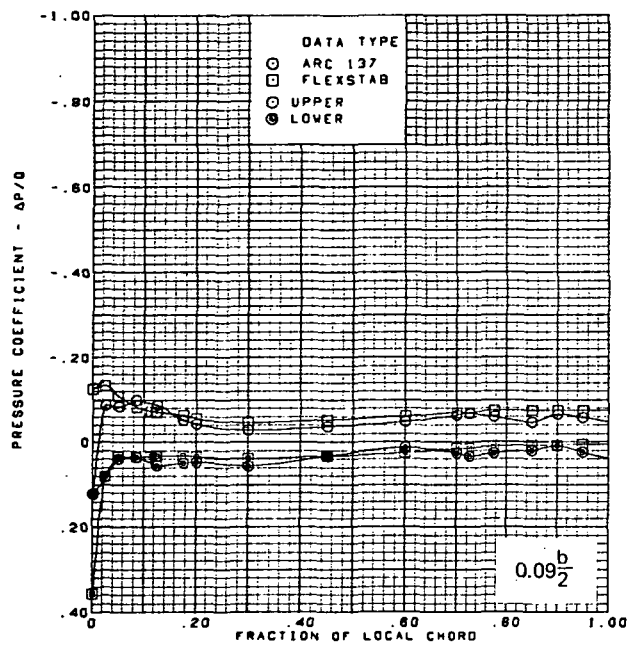


$M = 1.70$  (run 20)  
 $\alpha = 2^\circ$   
 Flat wing, rounded L.E.  
 L.E. deflection, full span =  $0.0^\circ$   
 T.E. deflection, full span =  $0.0^\circ$

Note:  $C_{p, \text{vacuum}} = -0.49$

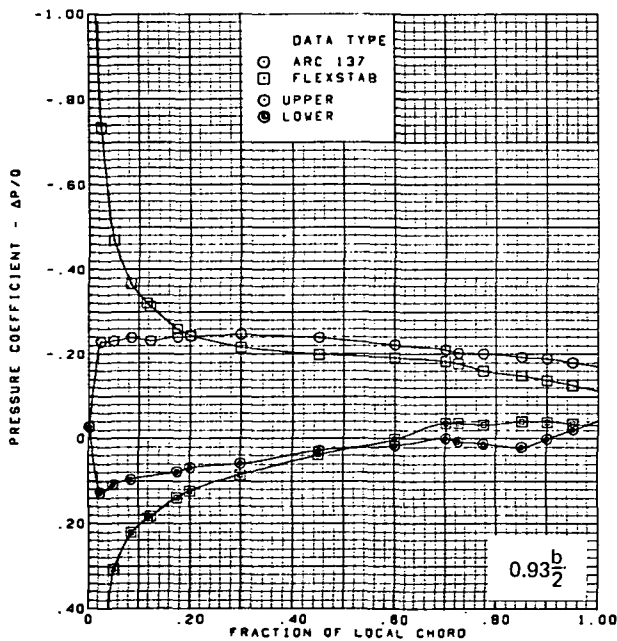
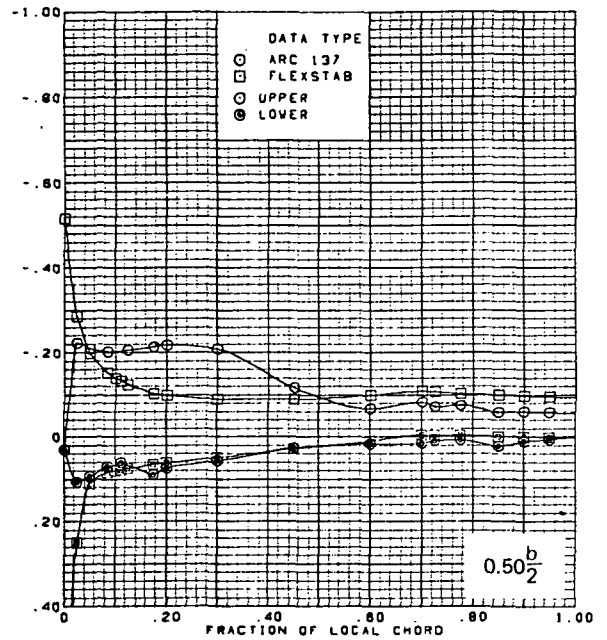
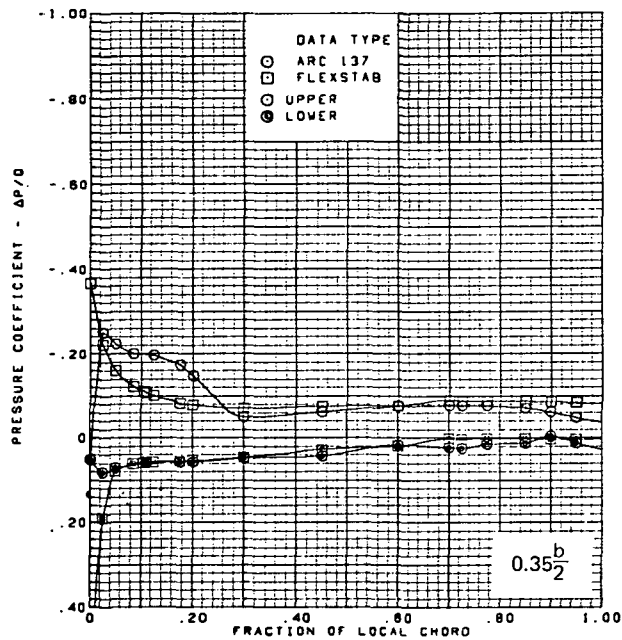
(a) (Concluded)

Figure 55.—(Continued)



(b) Surface Chordwise Pressure Distributions,  $\alpha = 4^\circ$

Figure 55.—(Continued)

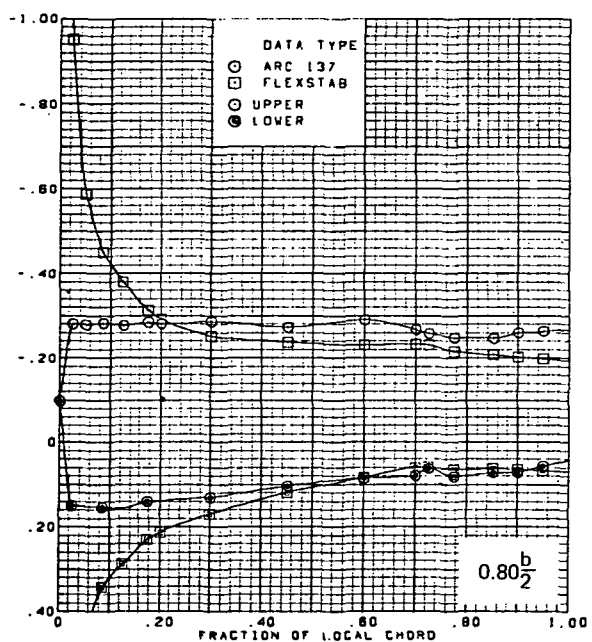
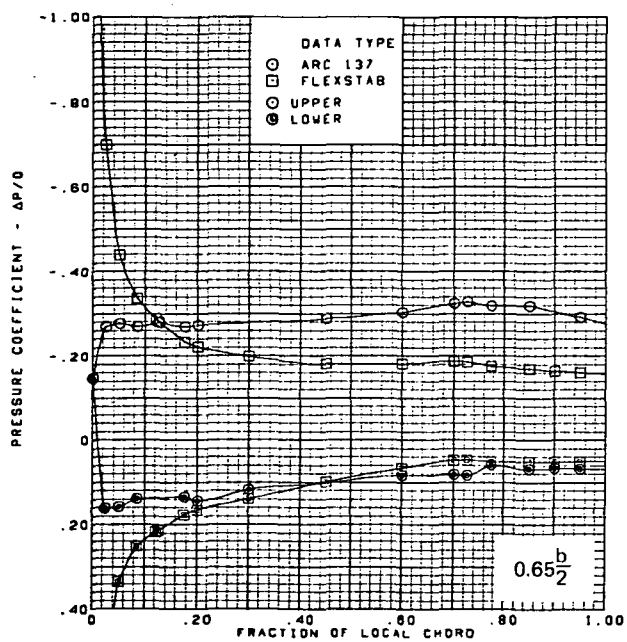
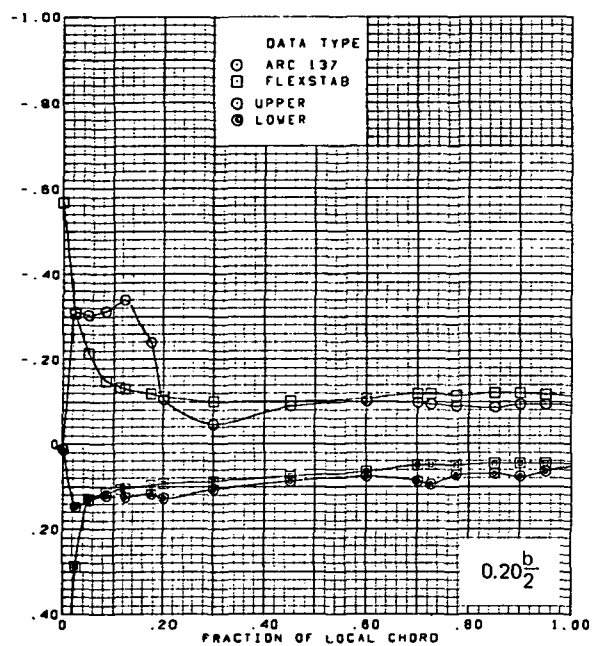
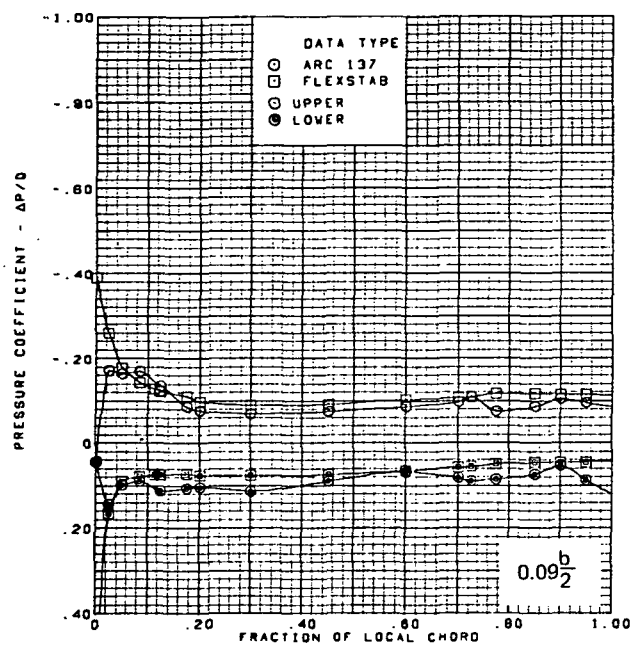


$M = 1.70$  (run 20)  
 $\alpha = 4^\circ$   
 Flat wing, rounded L.E.  
 L.E. deflection, full span =  $0.0^\circ$   
 T.E. deflection, full span =  $0.0^\circ$

Note:  $C_{p, \text{vacuum}} = -0.49$

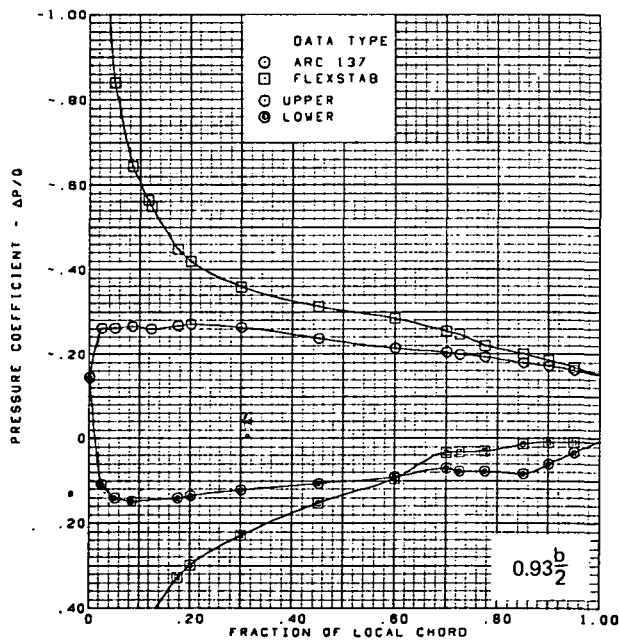
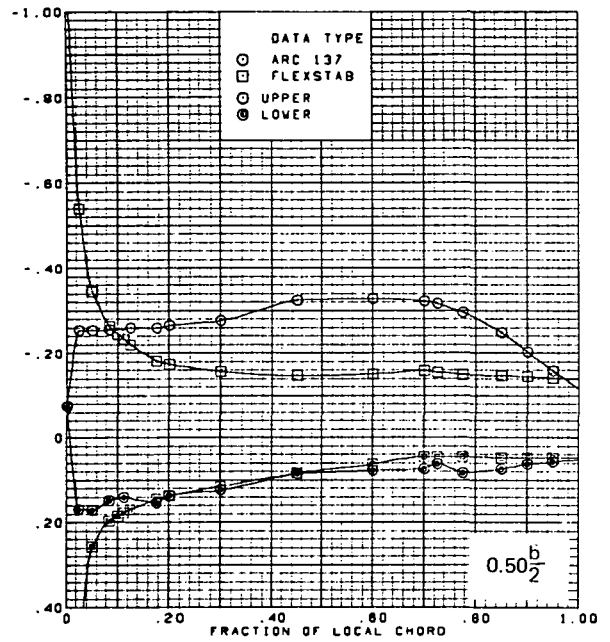
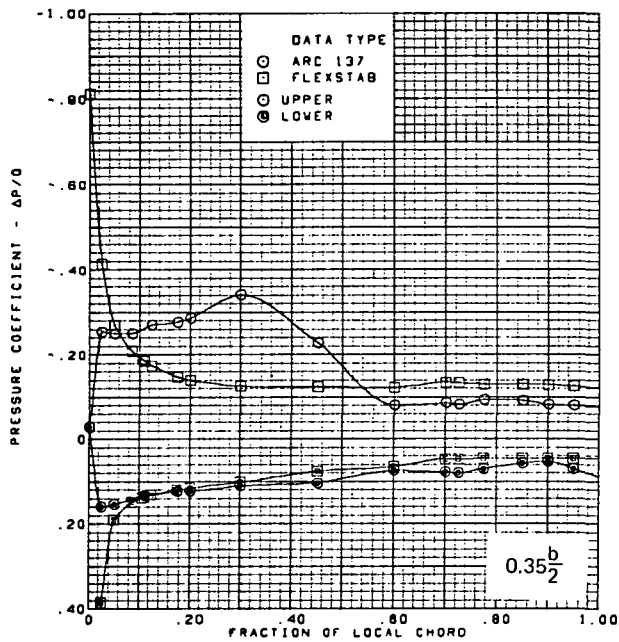
(b) (Concluded)

Figure 55.—(Continued)



(c) Surface Chordwise Pressure Distributions,  $\alpha = 8^\circ$

Figure 55.—(Continued)

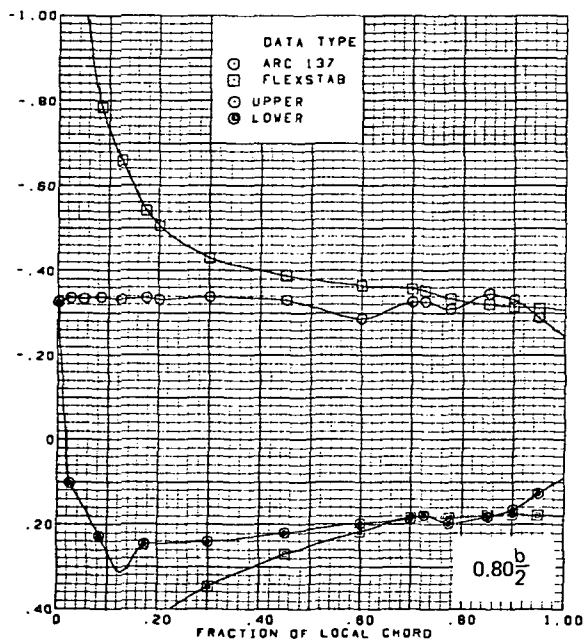
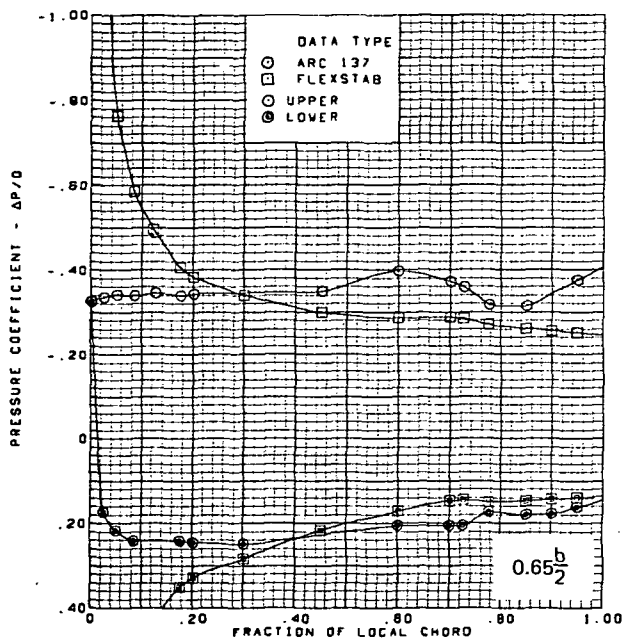
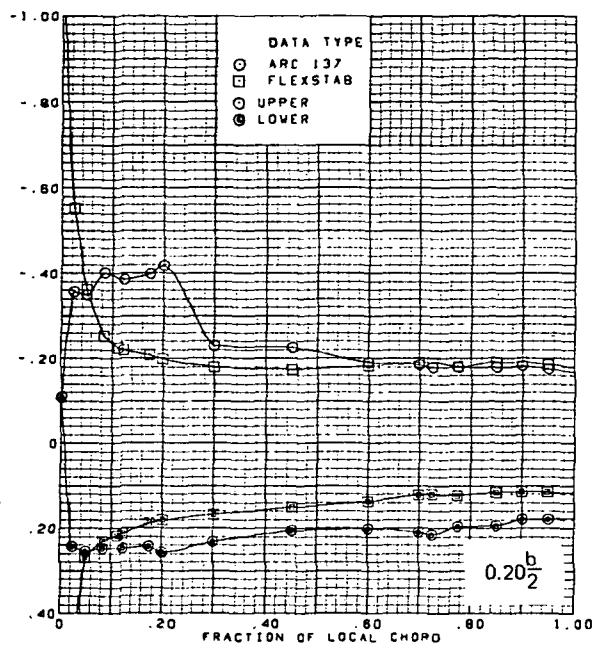
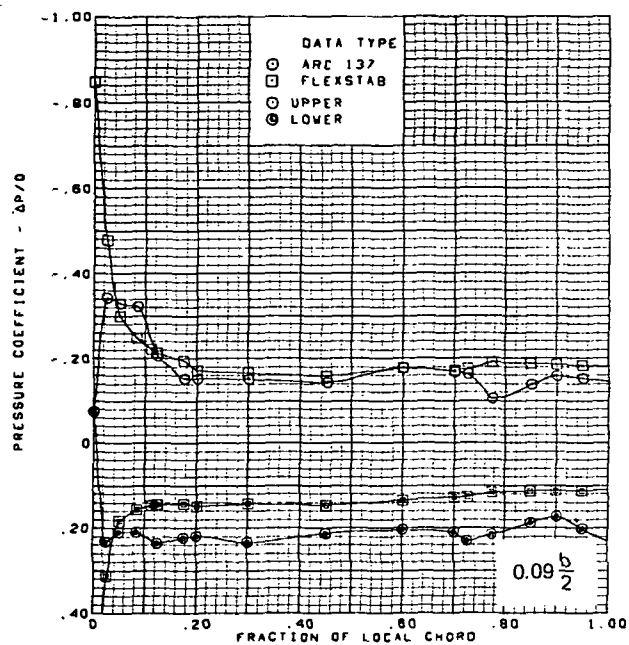


$M = 1.70$  (run 20)  
 $\alpha = 8^\circ$   
 Flat wing, rounded L.E.  
 L.E. deflection, full span =  $0.0^\circ$   
 T.E. deflection, full span =  $0.0^\circ$

Note:  $C_{p, \text{vacuum}} = -0.49$

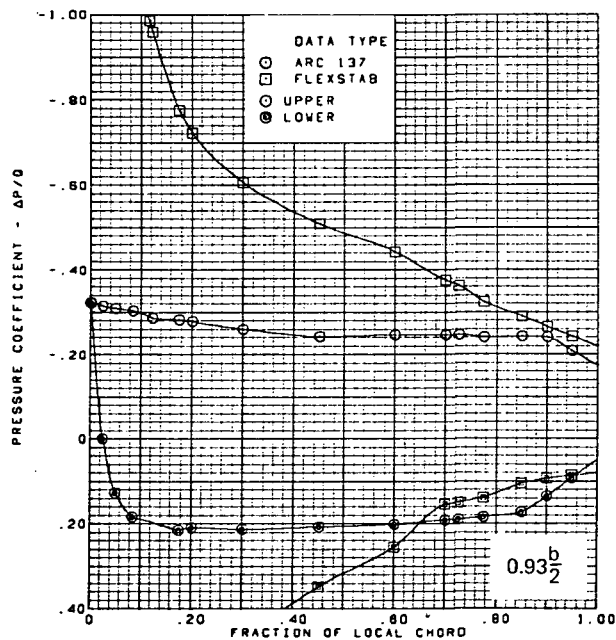
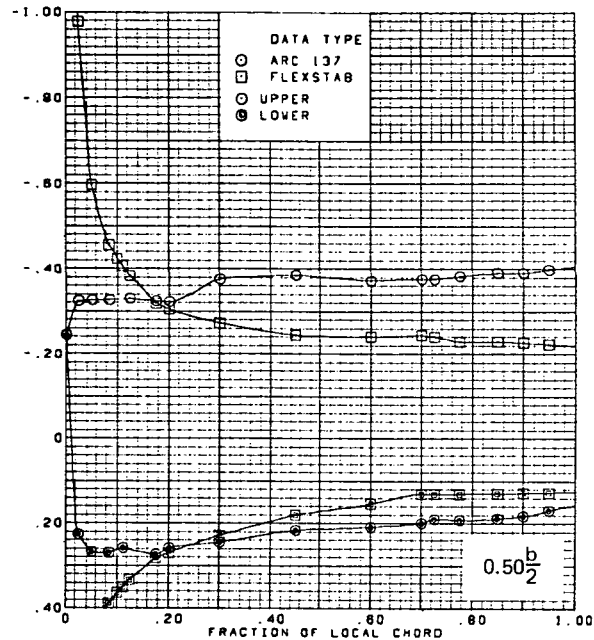
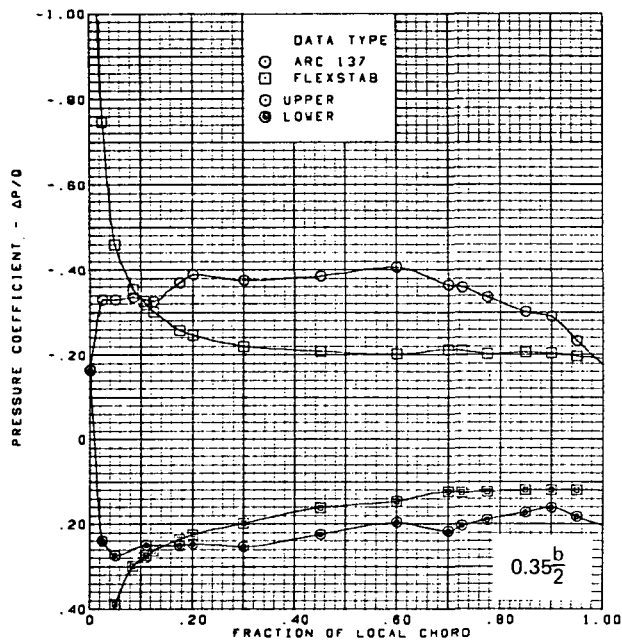
(c) (Concluded)

Figure 55.—(Continued)



(d) Surface Chordwise Pressure Distributions,  $\alpha = 15^\circ$

Figure 55.—(Continued)

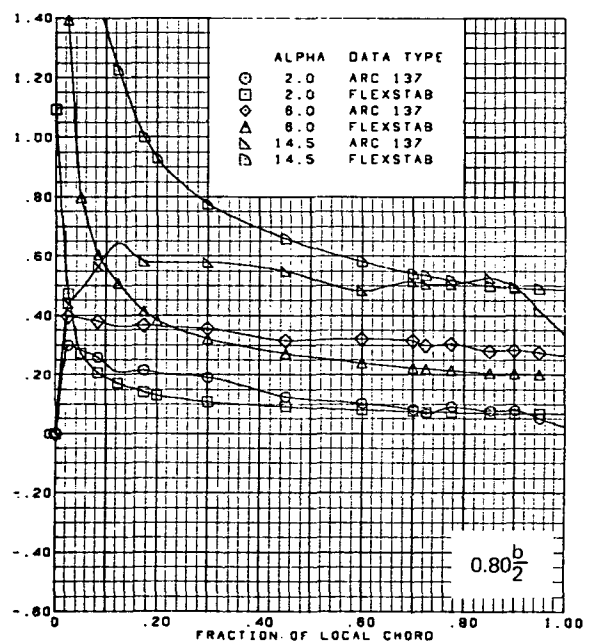
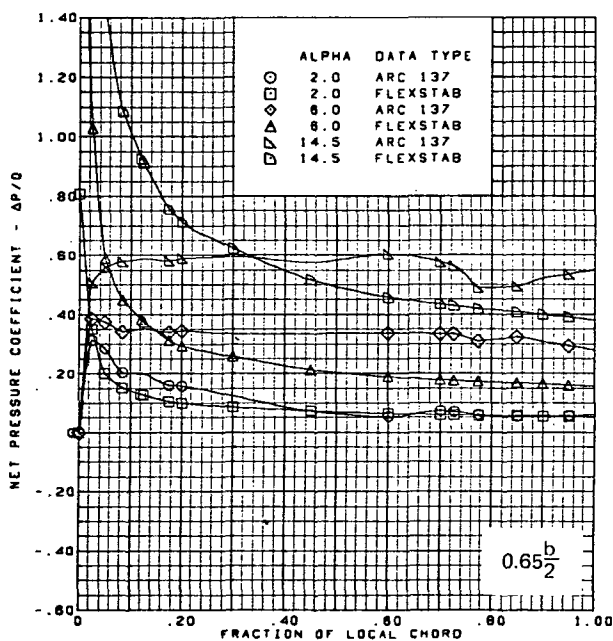
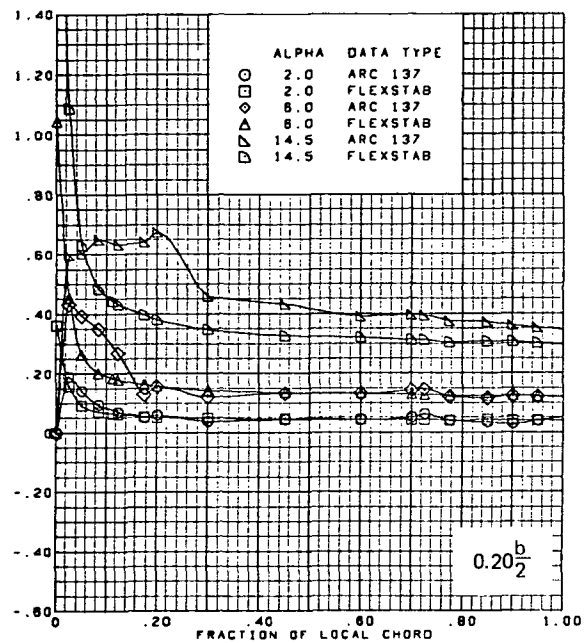
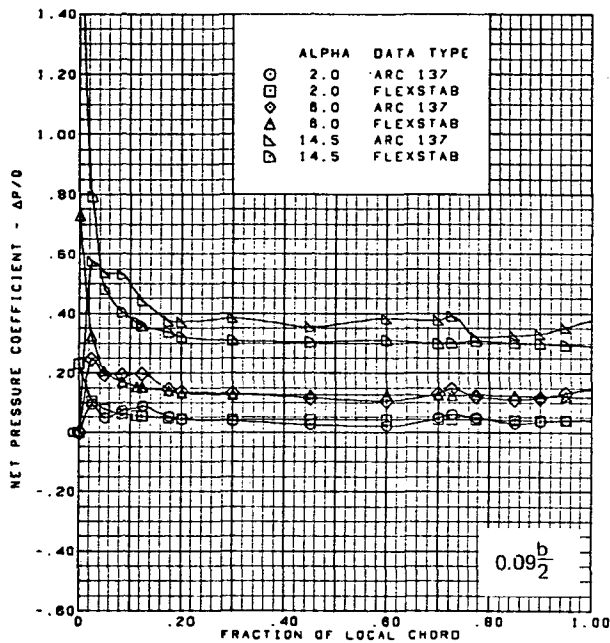


$M = 1.70$  (run 20)  
 $\alpha = 15^\circ$   
 Flat wing, rounded L.E.  
 L.E. deflection, full span =  $0.0^\circ$   
 T.E. deflection, full span =  $0.0^\circ$

Note:  $C_{p, \text{vacuum}} = -0.49$

(d) (Concluded)

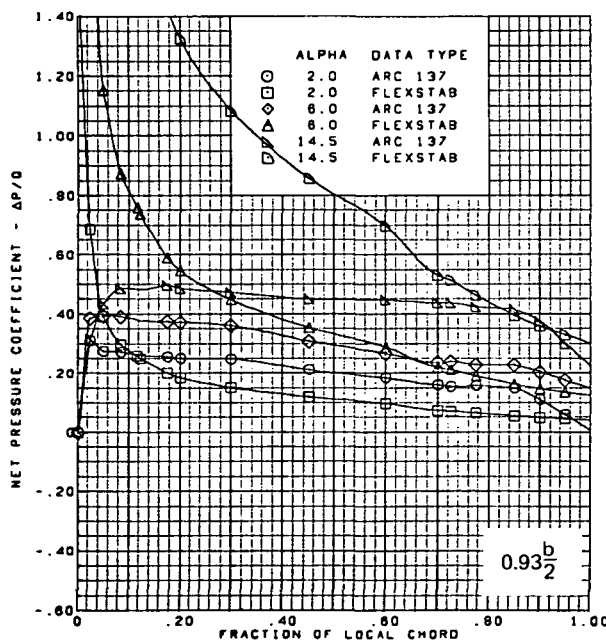
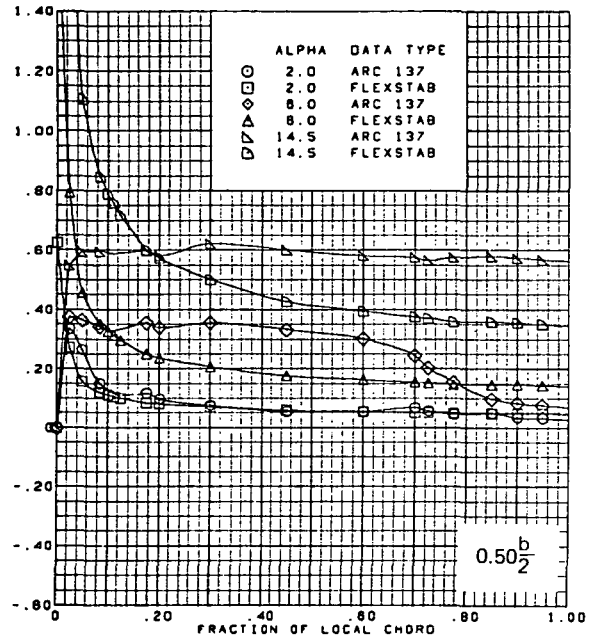
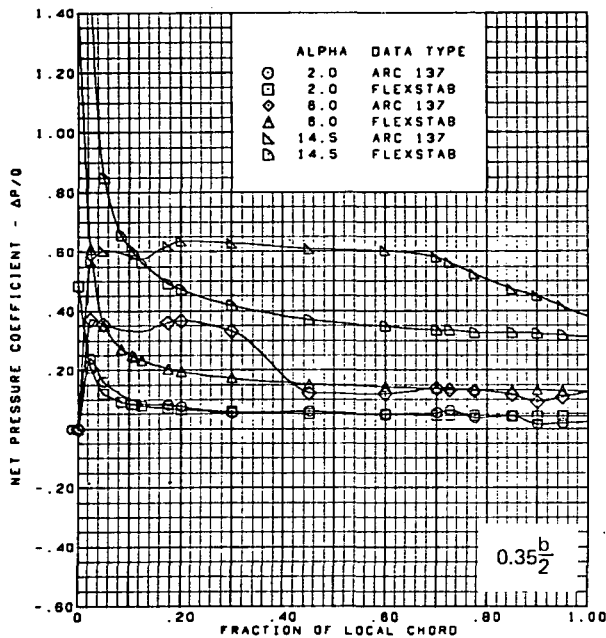
Figure 55.—(Continued)



(e) Net Chordwise Pressure Distributions,  $\alpha = 2^\circ, 6^\circ, 15^\circ$

Figure 55.—(Continued)

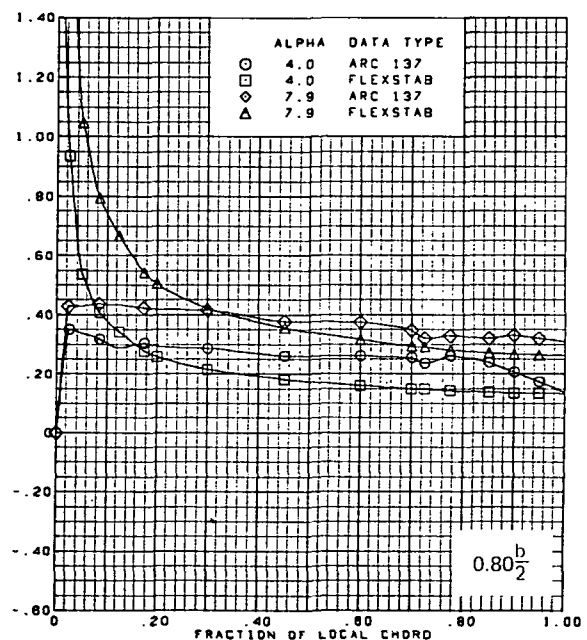
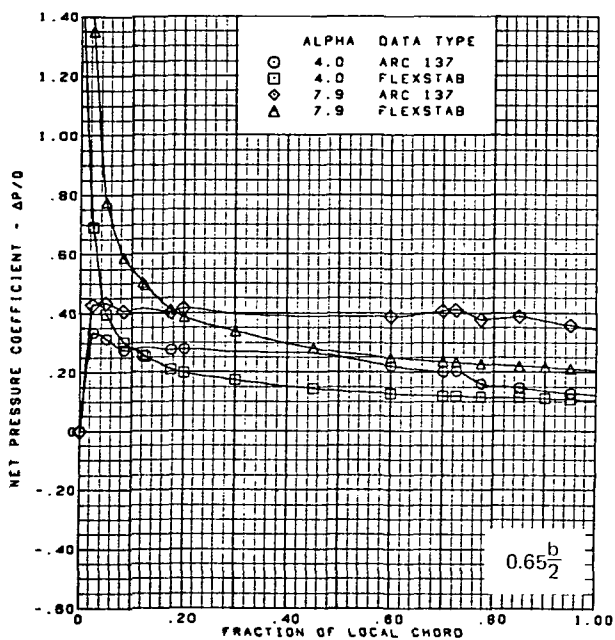
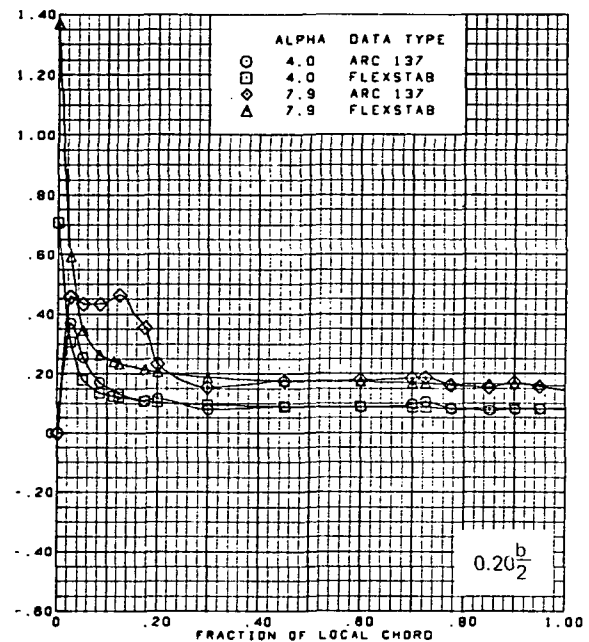
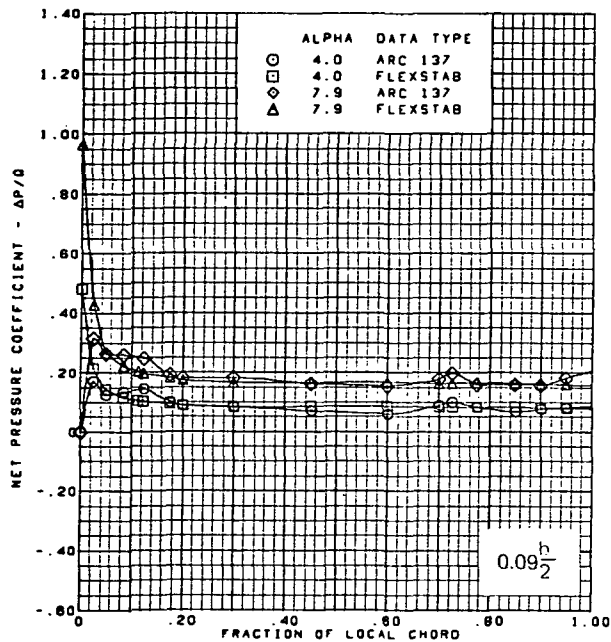




$M = 1.70$  (run 20)  
 Flat wing, rounded L.E.  
 L.E. deflection, full span =  $0.0^\circ$   
 T.E. deflection, full span =  $0.0^\circ$

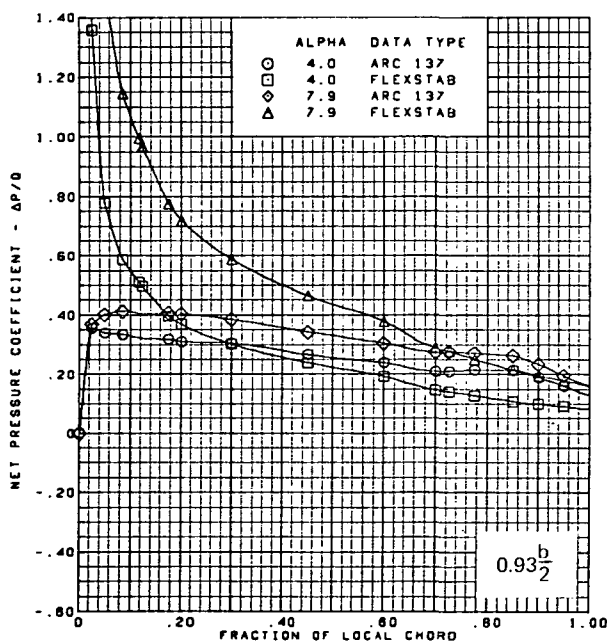
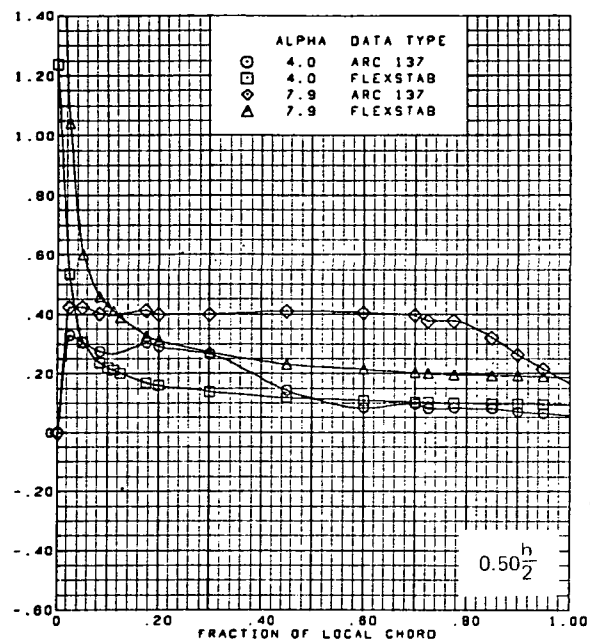
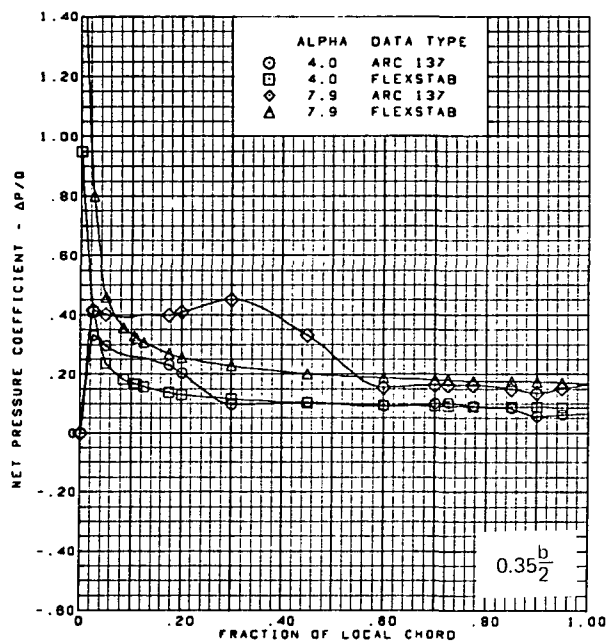
(e) (Concluded)

Figure 55.—(Continued)



(f) Net Chordwise Pressure Distributions,  $\alpha = 4^\circ, 8^\circ$

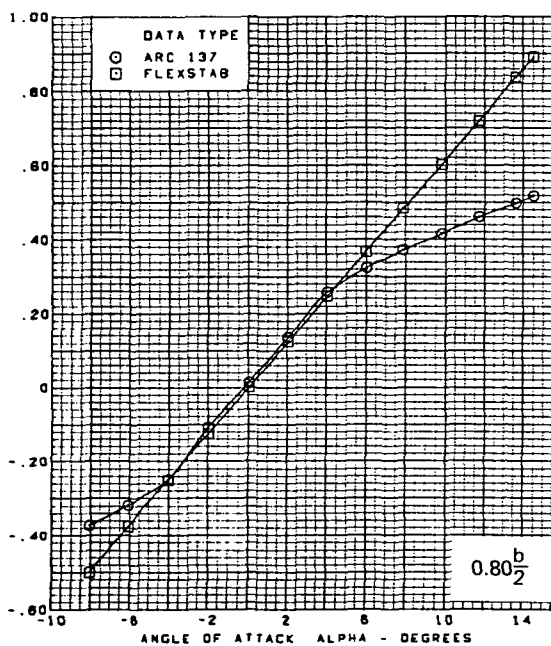
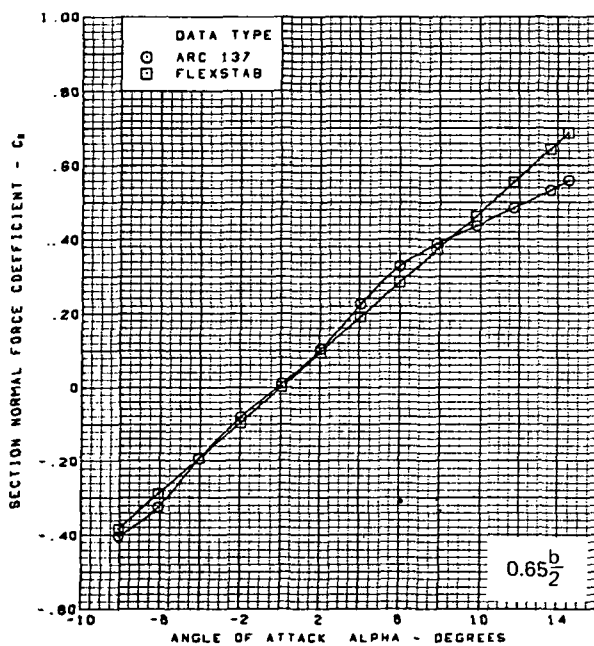
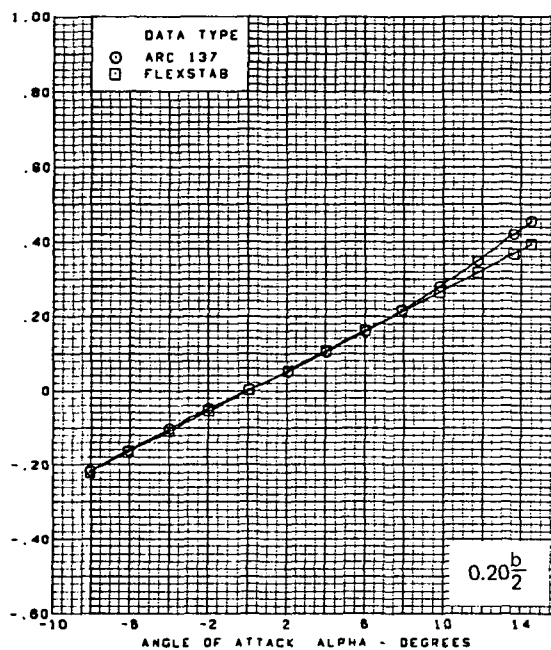
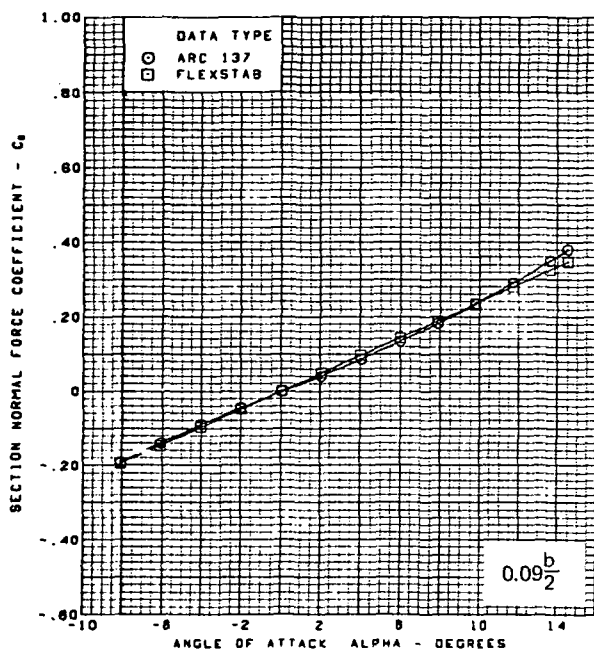
Figure 55.—(Continued)



$M = 1.70$  (run 20)  
 Flat wing, rounded L.E.  
 L.E. deflection, full span =  $0.0^\circ$   
 T.E. deflection, full span =  $0.0^\circ$

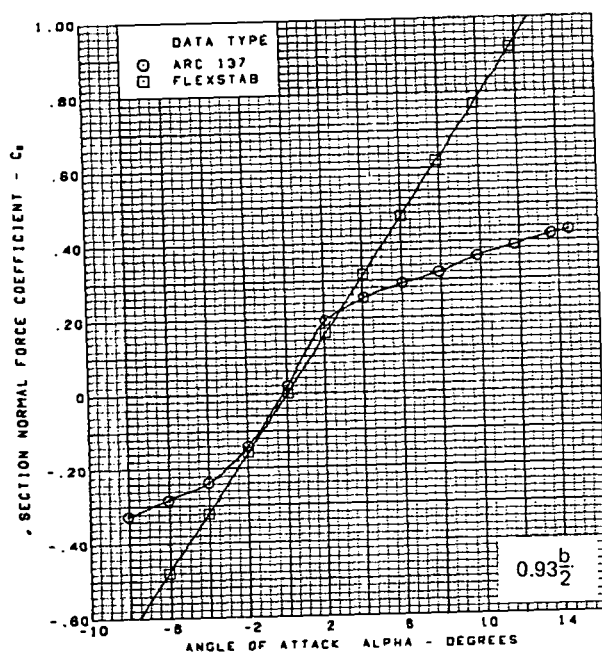
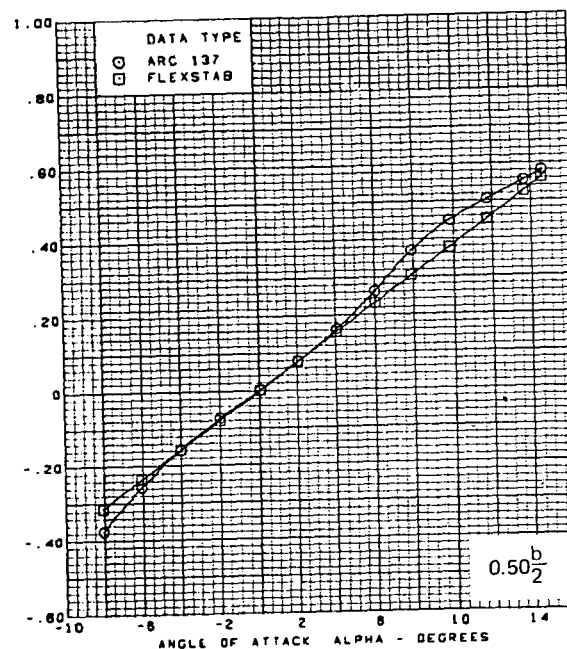
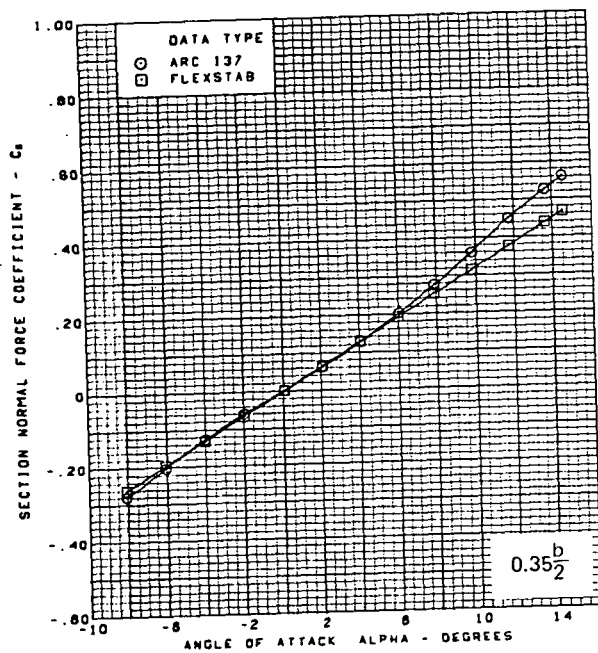
(f) (Concluded)

Figure 55.—(Continued)



(g) Section Aerodynamic Coefficients—Normal Force

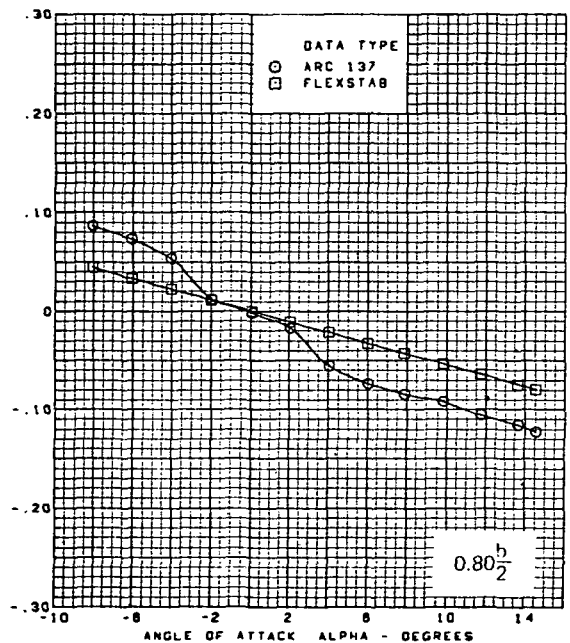
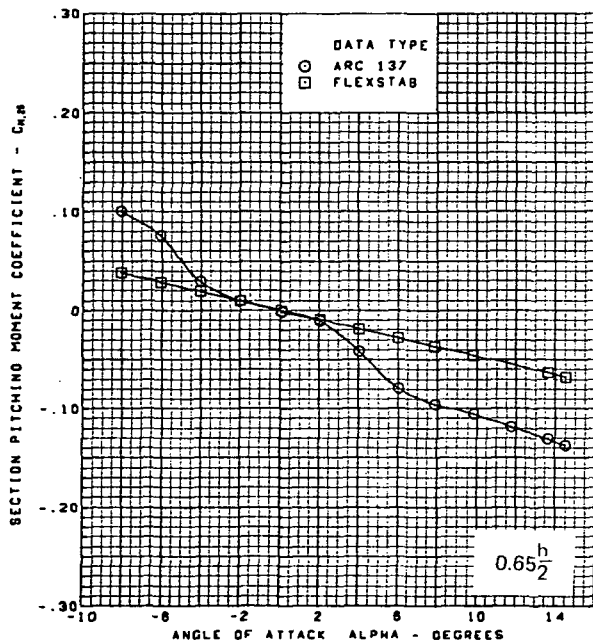
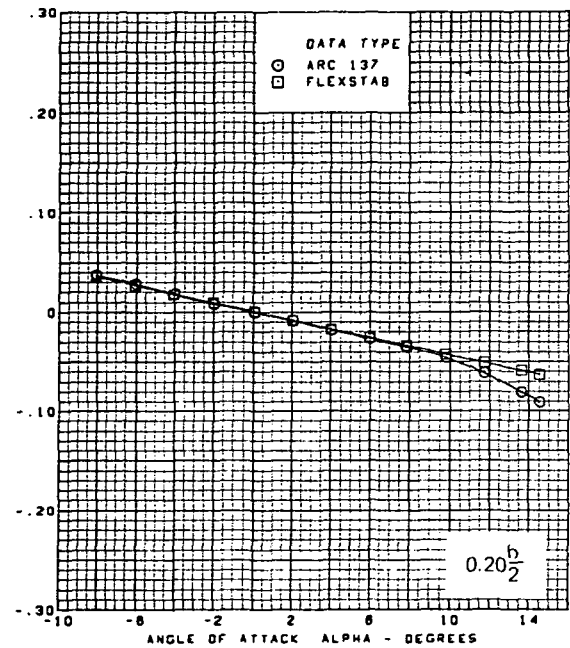
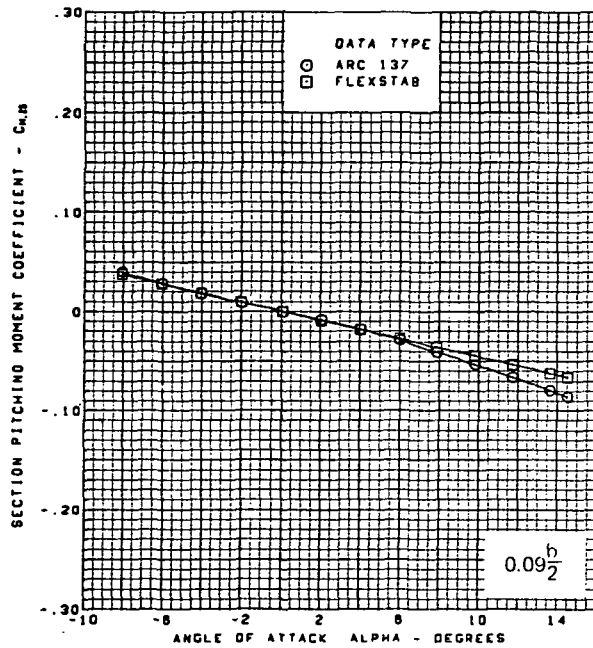
Figure 55.—(Continued)



$M = 1.70$  (run 20)  
 Flat wing, rounded L.E.  
 L.E. deflection, full span =  $0.0^\circ$   
 T.E. deflection, full span =  $0.0^\circ$

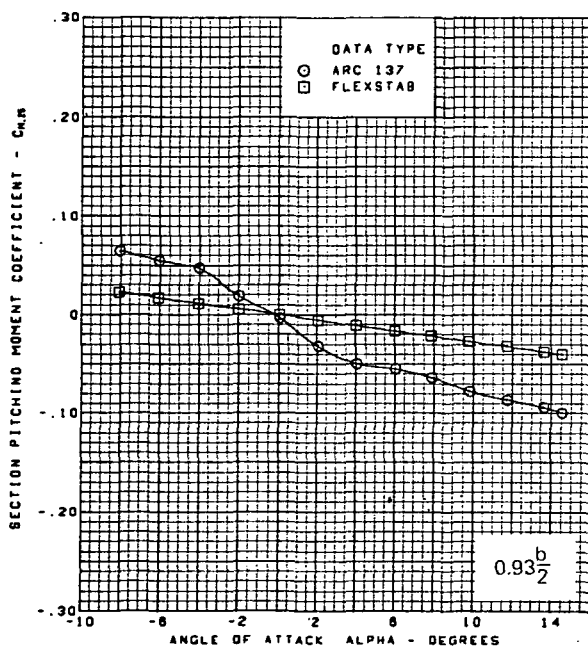
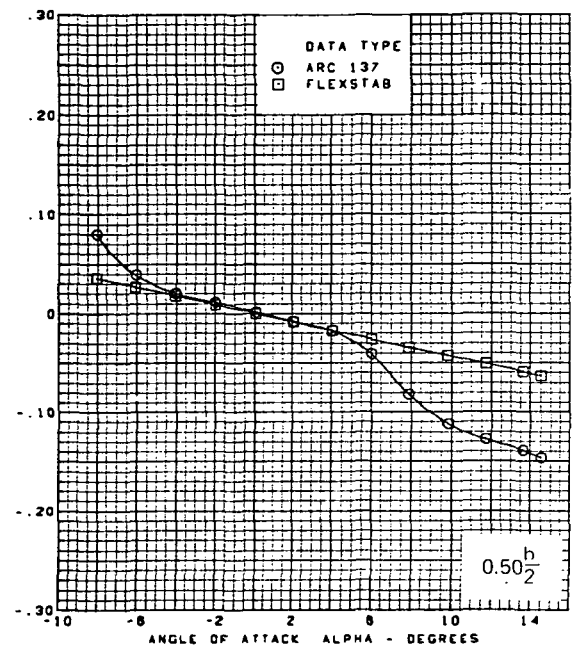
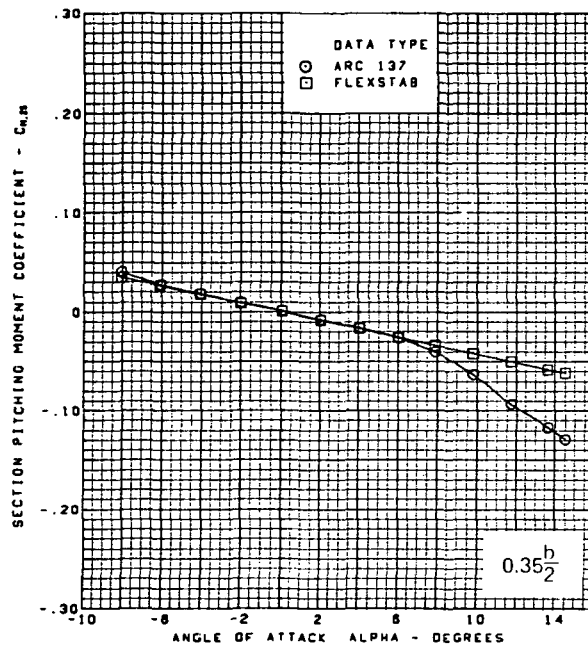
(g) (Concluded)

Figure 55. —(Continued)



(h) Section Aerodynamic Coefficients—Pitching Moment

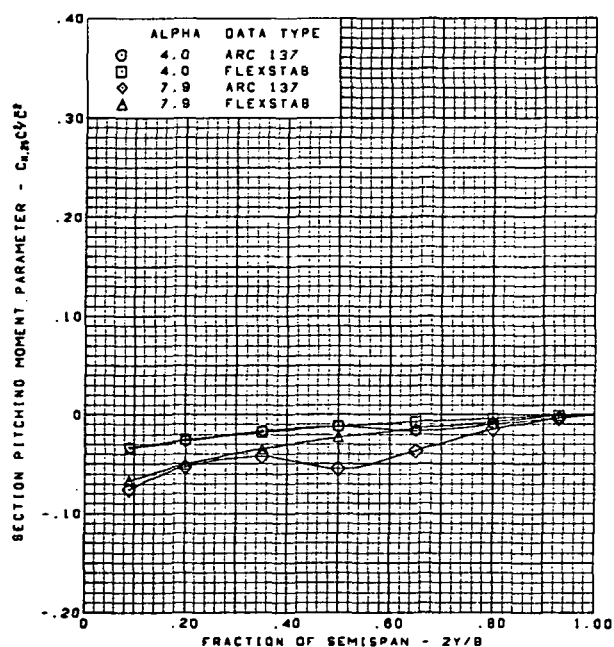
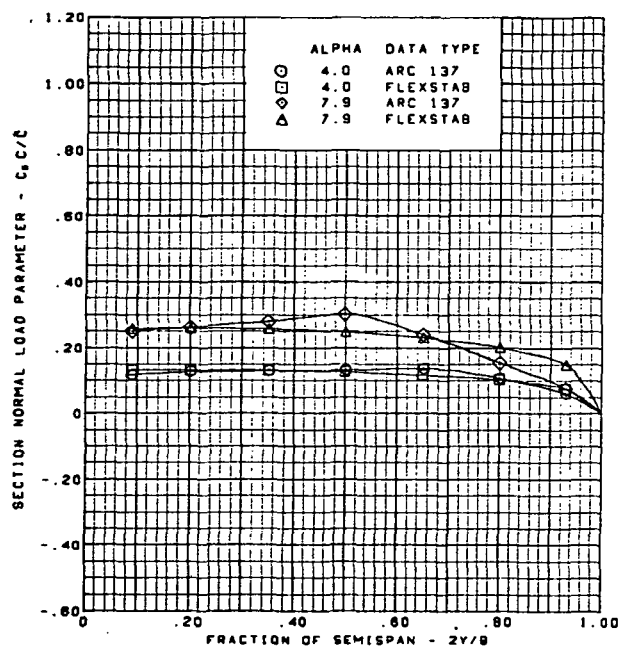
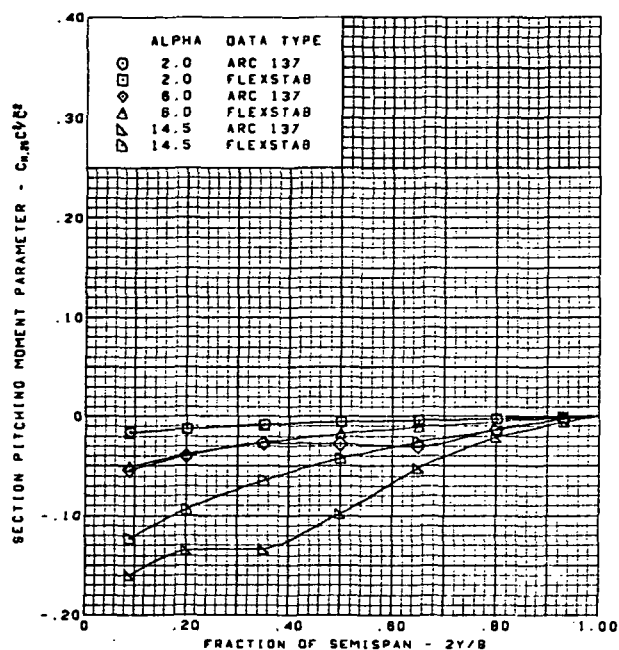
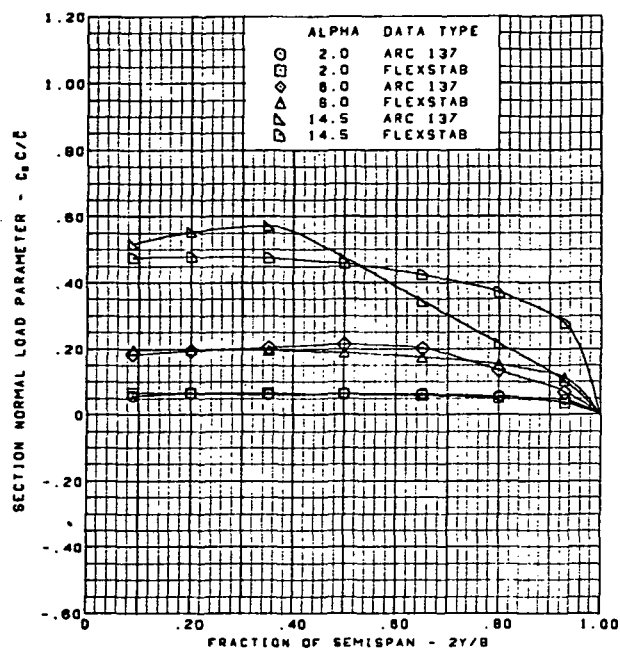
Figure 55.—(Continued)



$M = 1.70$  (run 20)  
 Flat wing, rounded L.E.  
 L.E. deflection, full span =  $0.0^\circ$   
 T.E. deflection, full span =  $0.0^\circ$

(h) (Concluded)

Figure 55.—(Continued)

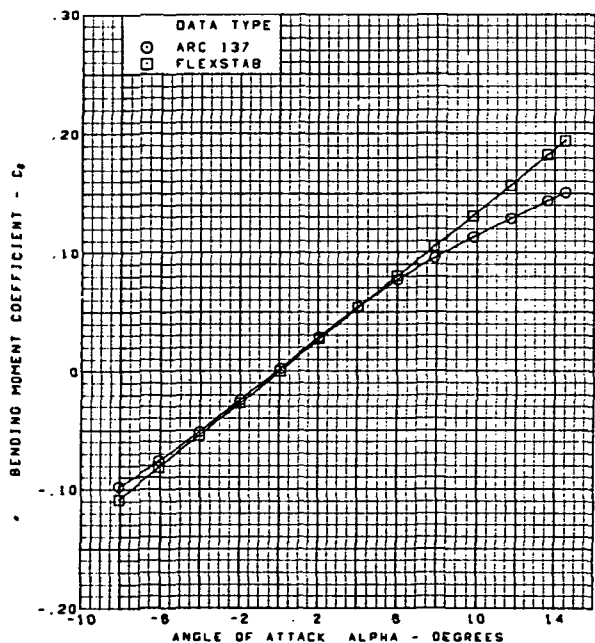
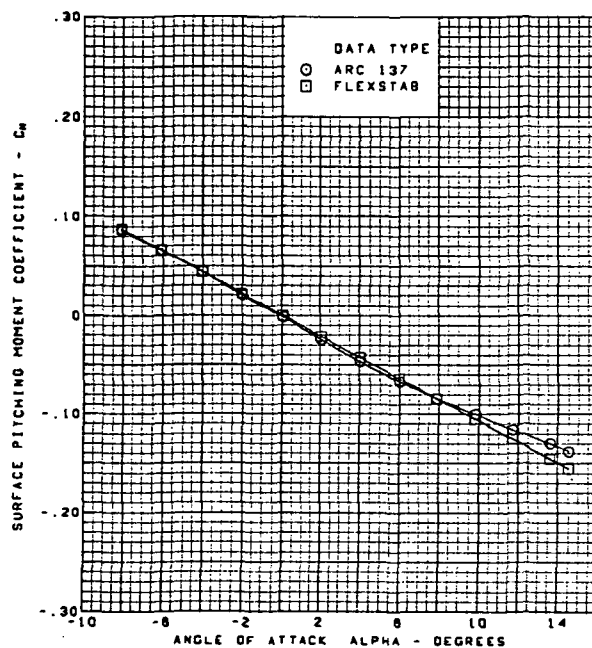
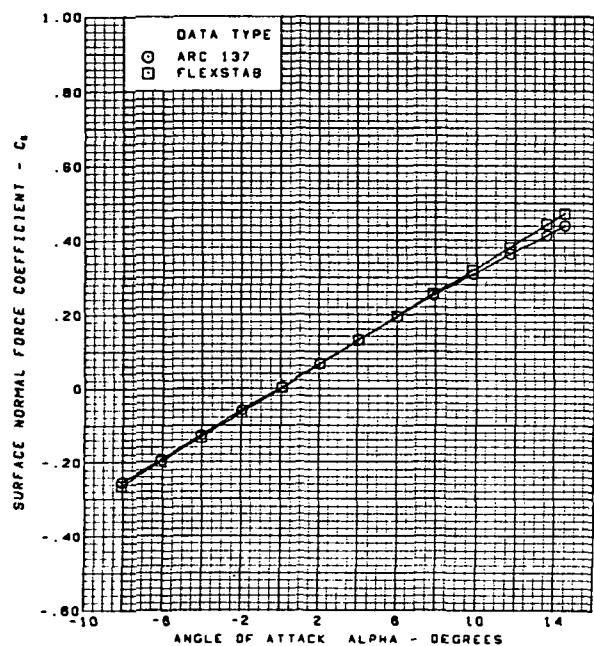


M = 1.70 (run 20)  
 Flat wing, rounded L.E.  
 L.E. deflection, full span =  $0.0^\circ$   
 T.E. deflection, full span =  $0.0^\circ$

(i) Spanload Distributions

Figure 55.—(Continued)

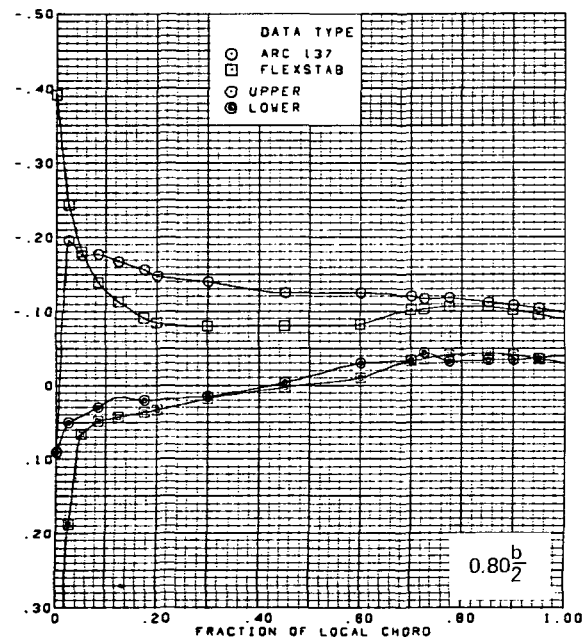
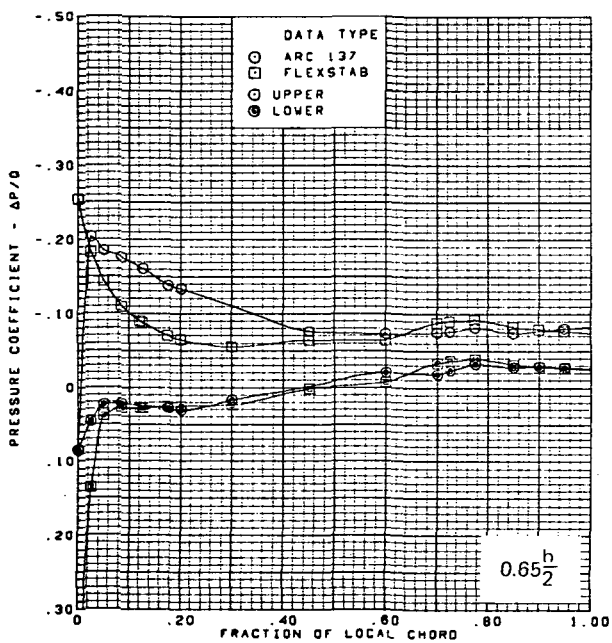
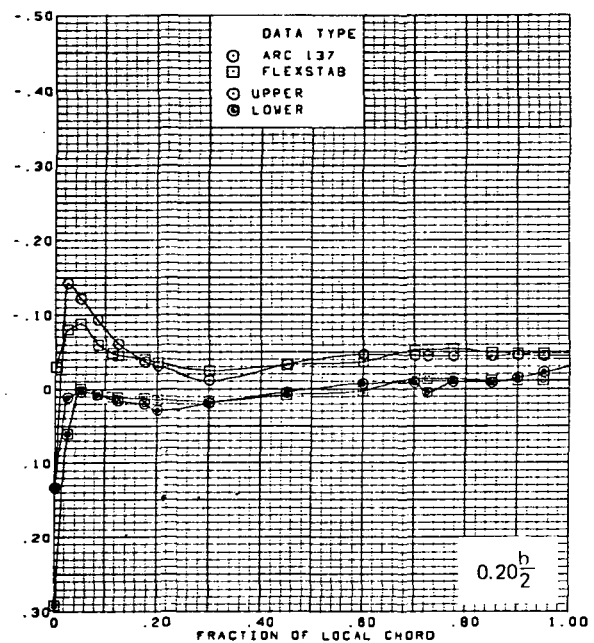
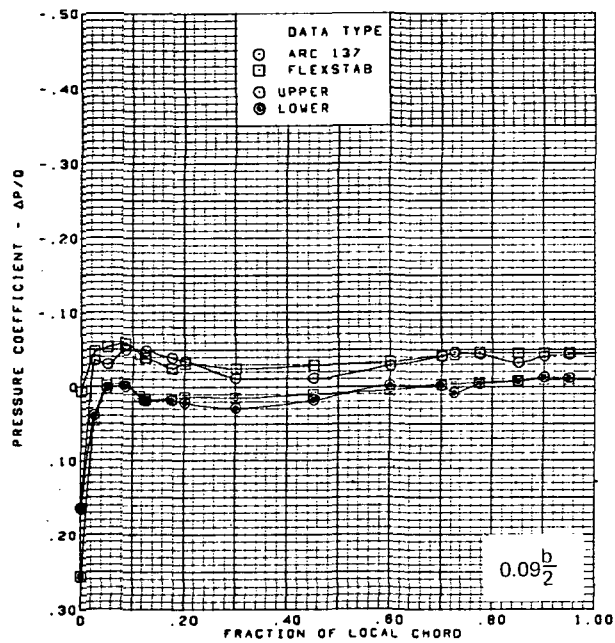




M = 1.70 ( run 20 )  
 Flat wing, rounded L.E.  
 L.E. deflection, full span = 0.0°  
 T.E. deflection, full span = 0.0°

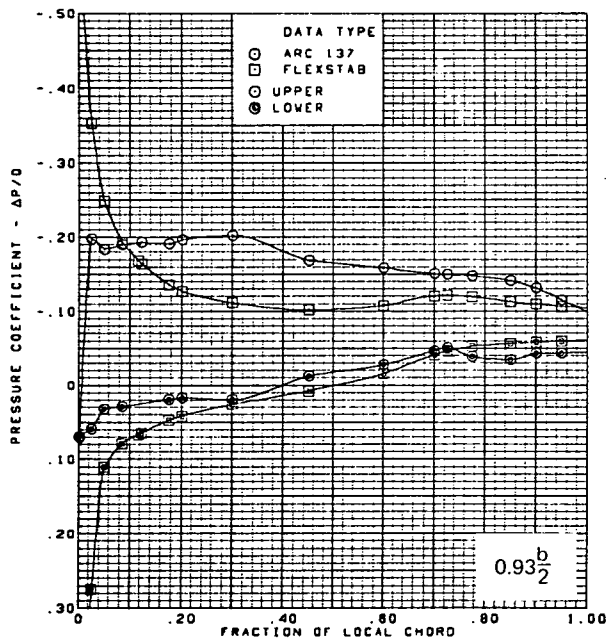
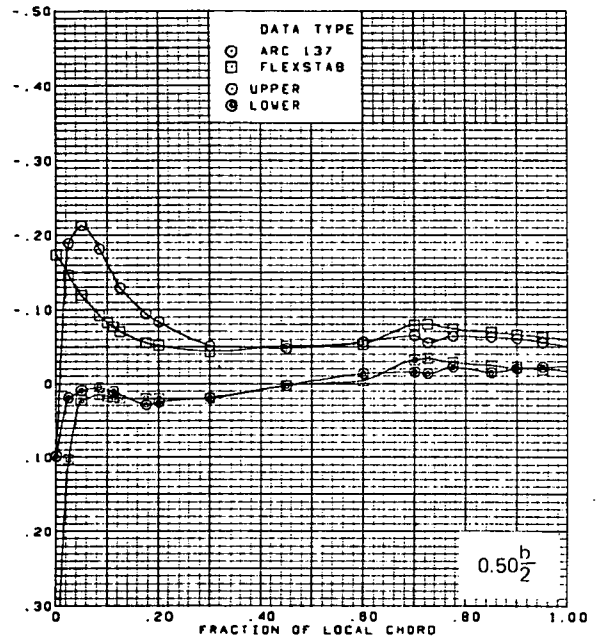
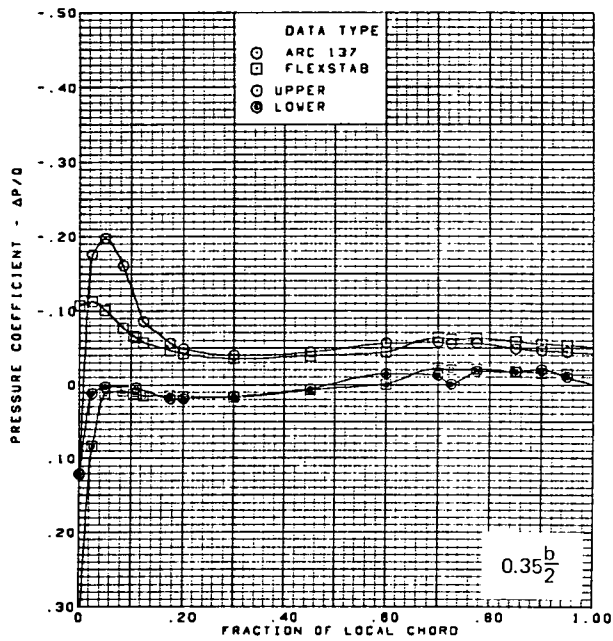
(j) Wing Aerodynamic Coefficients

Figure 55.—(Concluded)



(b) Surface Chordwise Pressure Distributions,  $\alpha = 2^\circ$

Figure 56.—Wing Theory-to-Experiment Comparison—Flat Wing, Rounded L.E.; L.E. Deflection, Full Span =  $0.0^\circ$ ; T.E. Deflection, Full Span =  $0.0^\circ$ ;  $M = 2.10$

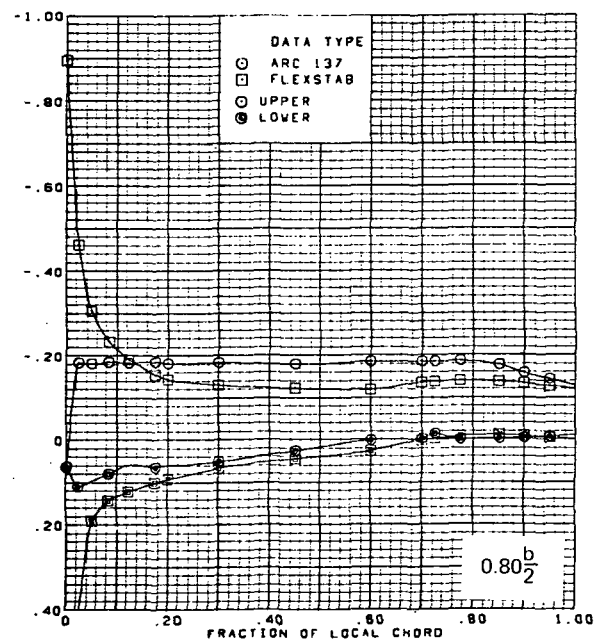
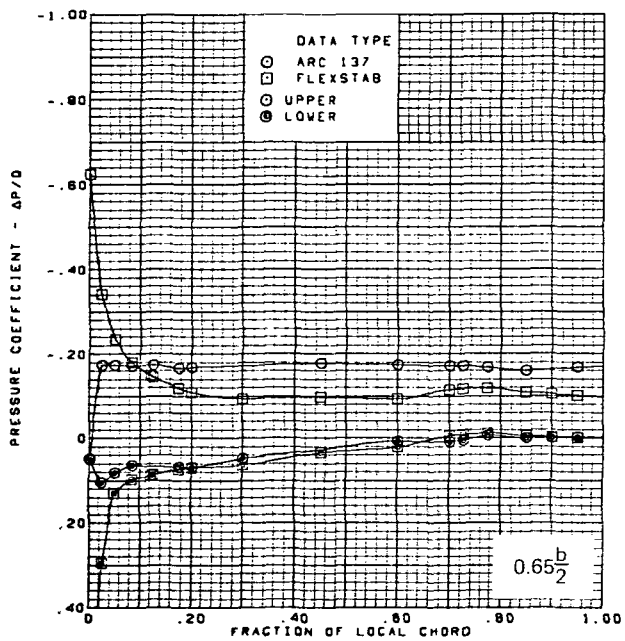
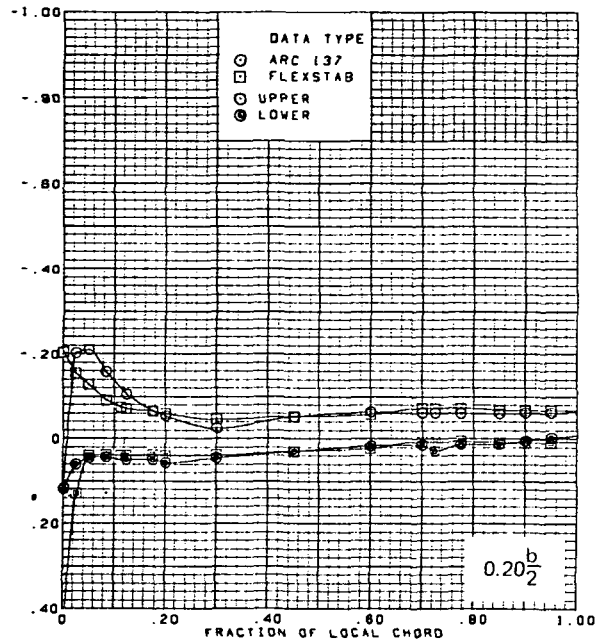
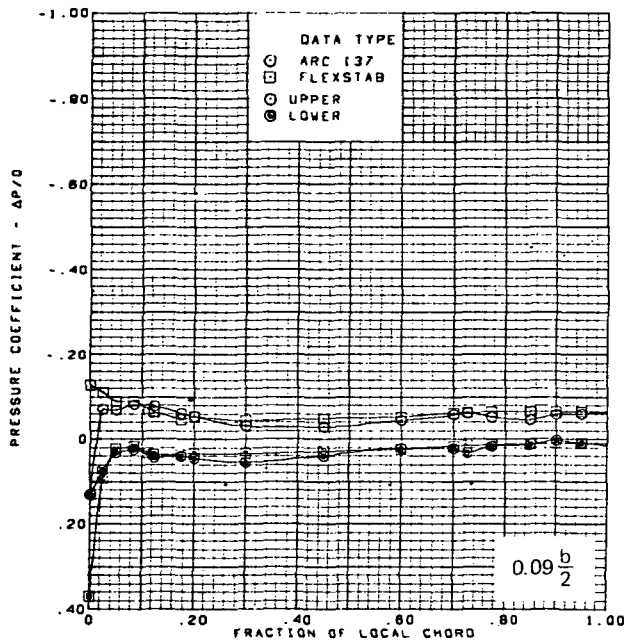


$M = 2.10$  (run 21)  
 $\alpha = 2^\circ$   
 Flat wing, rounded L.E.  
 L.E. deflection, full span =  $0.0^\circ$   
 T.E. deflection, full span =  $0.0^\circ$

Note:  $C_{p, \text{vacuum}} = -0.32$

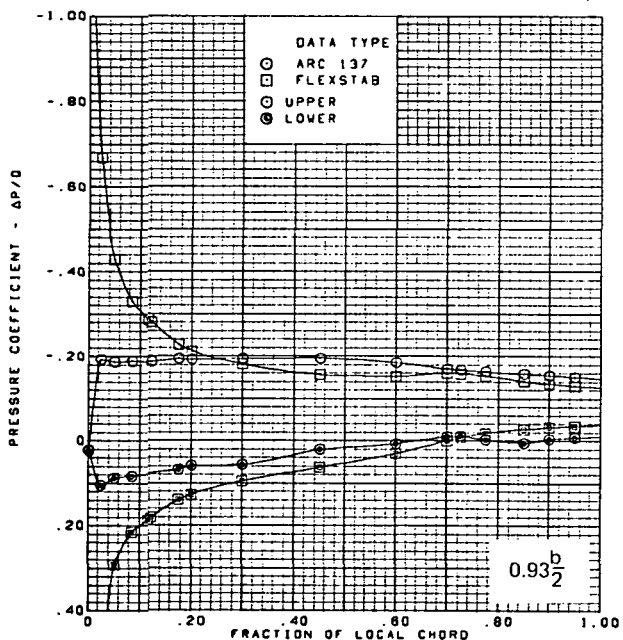
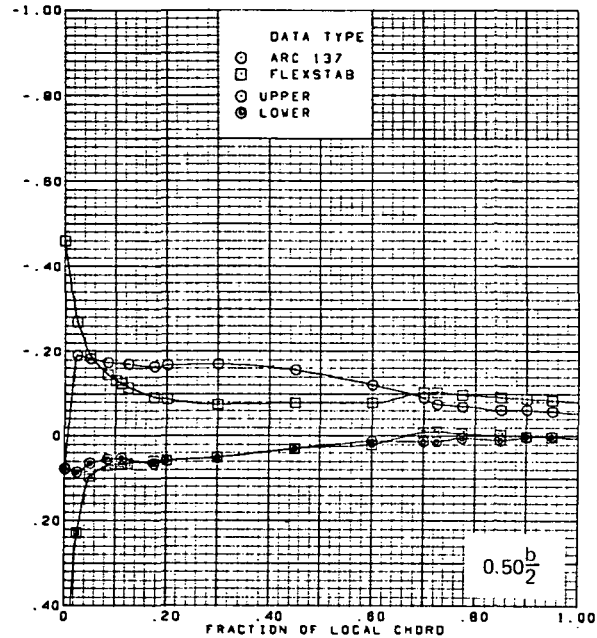
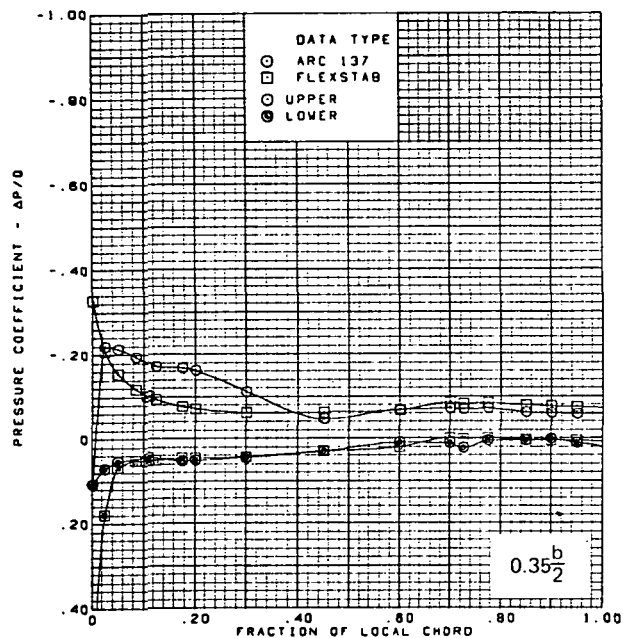
(a) (Concluded)

Figure 56.—(Continued)



(b) Surface Chordwise Pressure Distributions,  $\alpha = 4^\circ$

Figure 56. —(Continued)

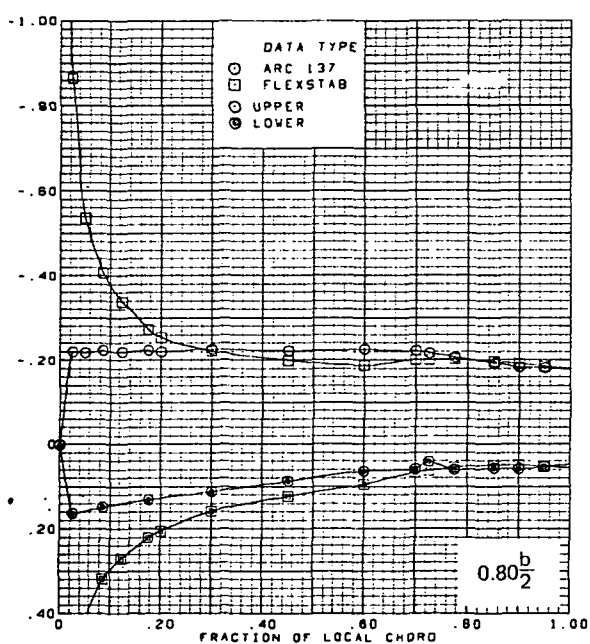
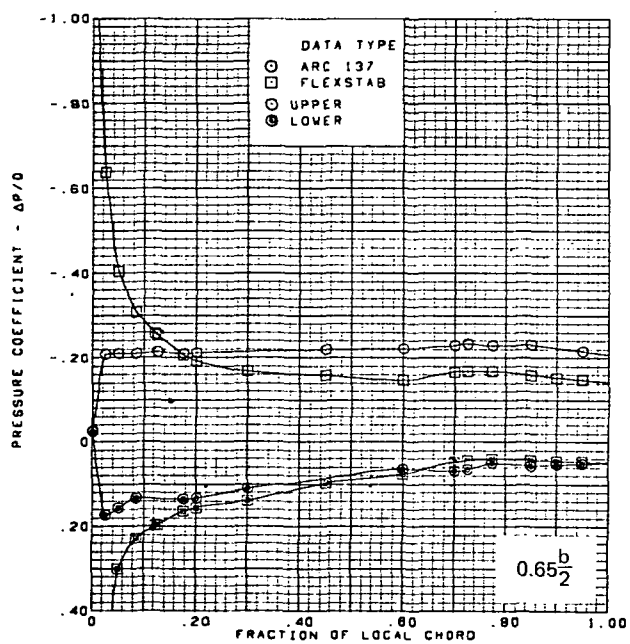
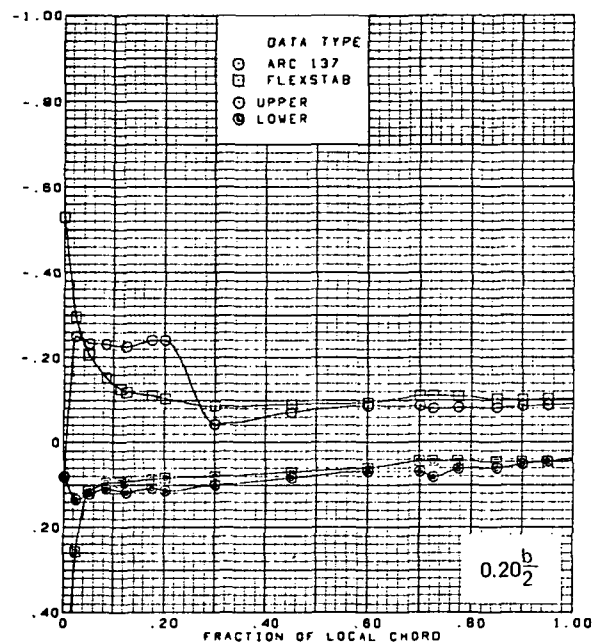
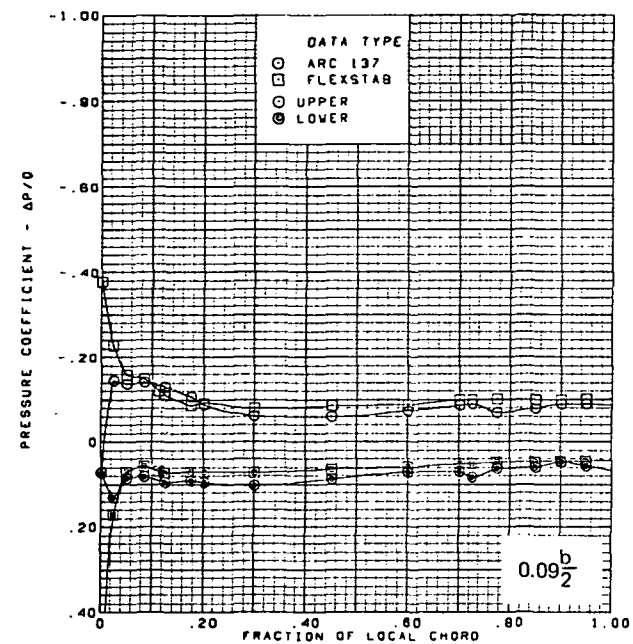


$M = 2.10$  (run 21)  
 $\alpha = 4^\circ$   
 Flat wing, rounded L.E.  
 L.E. deflection, full span =  $0.0^\circ$   
 T.E. deflection, full span =  $0.0^\circ$

Note:  $C_{p, \text{vacuum}} = -0.32$

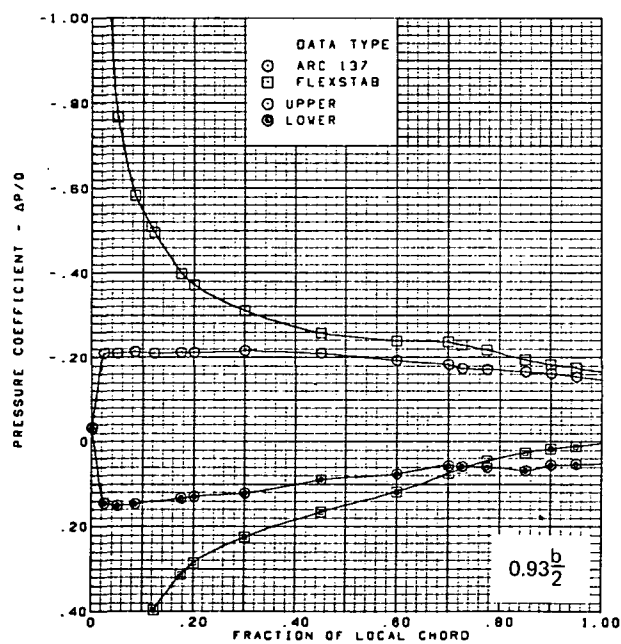
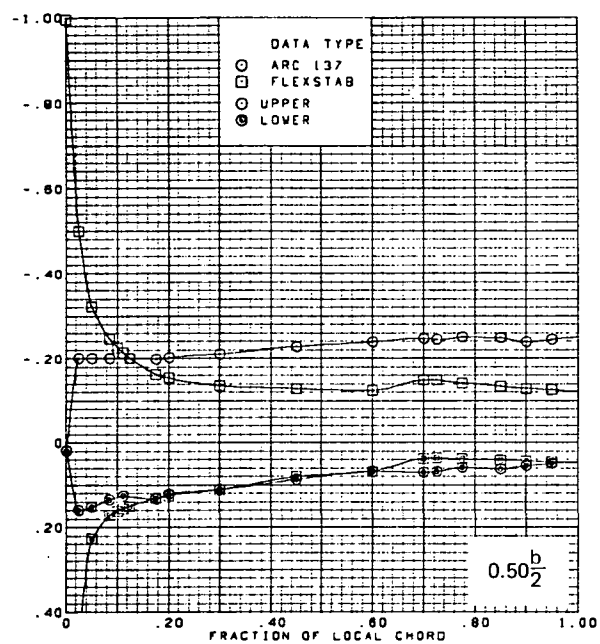
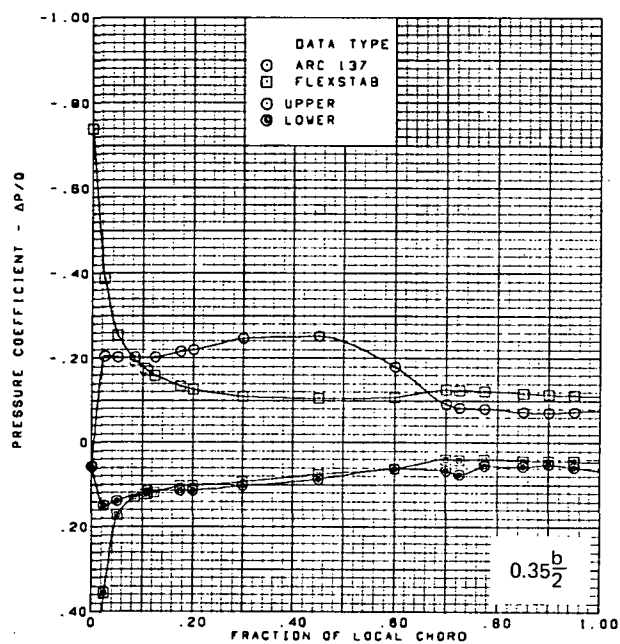
(b) (Concluded)

Figure 56.—(Continued)



(c) Surface Chordwise Pressure Distributions,  $\alpha = 8^\circ$

Figure 56.—(Continued)

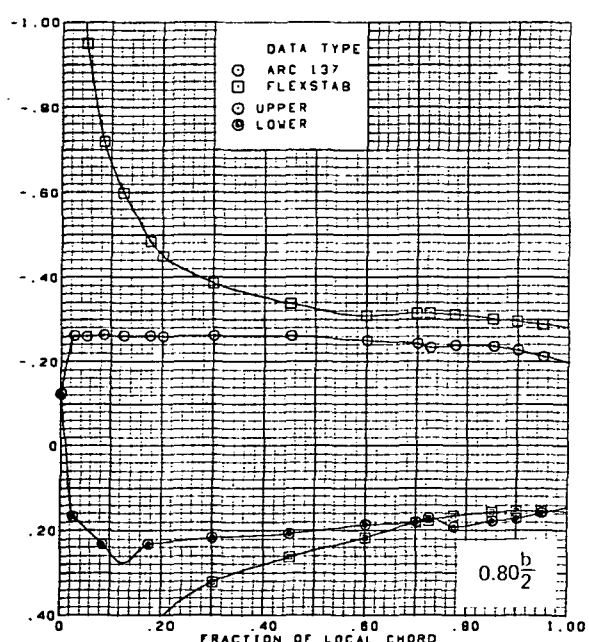
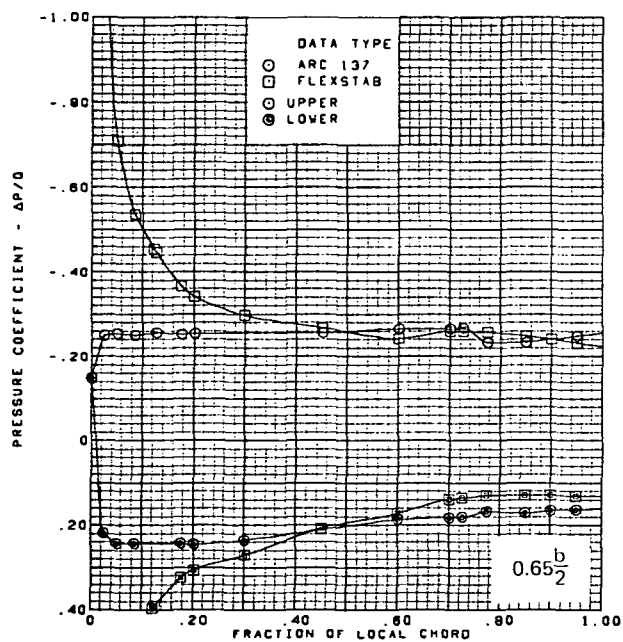
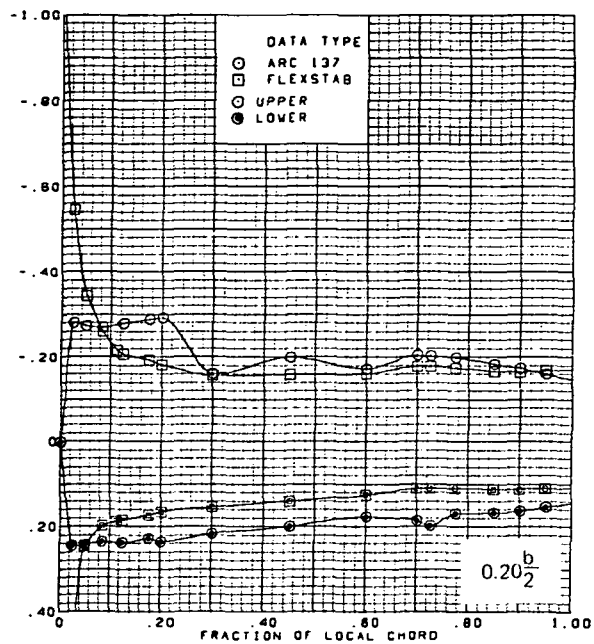
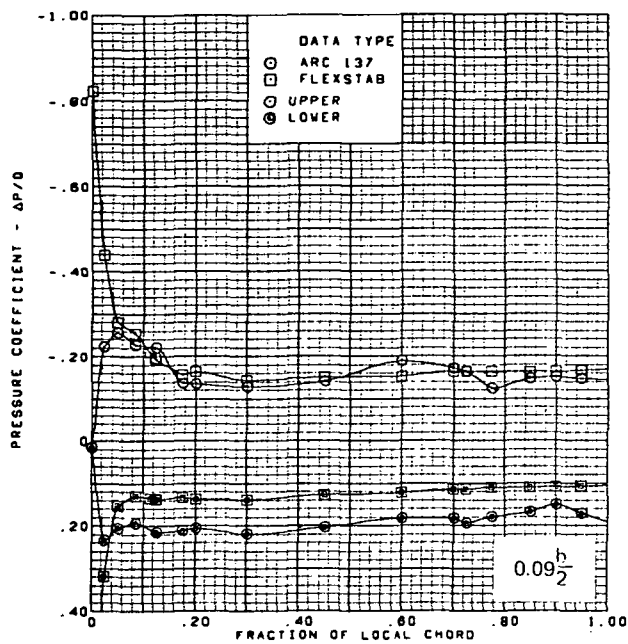


$M = 2.10$  (run 21)  
 $\alpha = 8^\circ$   
 Flat wing, rounded L.E.  
 L.E. deflection, full span =  $0.0^\circ$   
 T.E. deflection, full span =  $0.0^\circ$

Note:  $C_{p, \text{vacuum}} = -0.32$

(c) (Concluded)

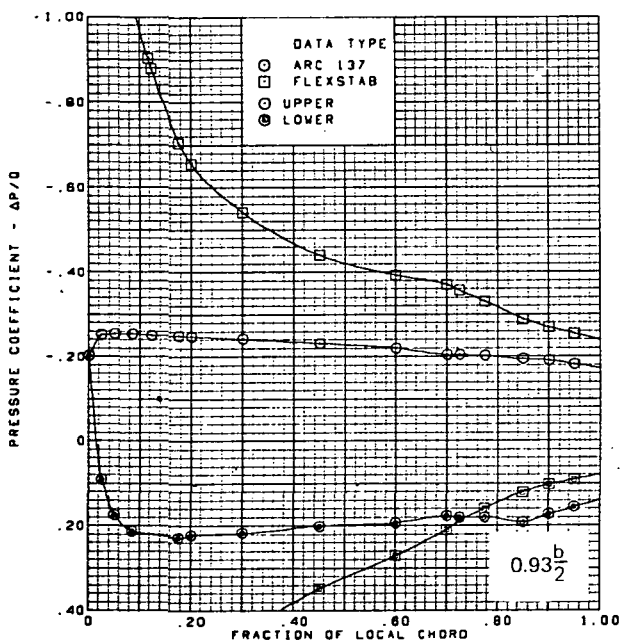
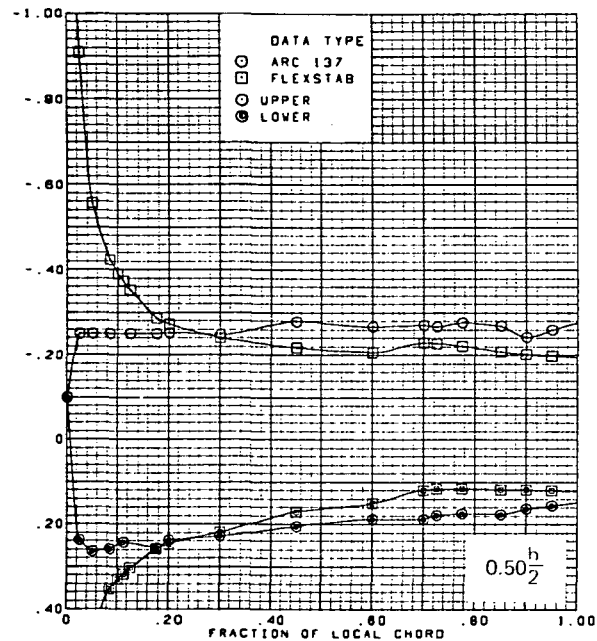
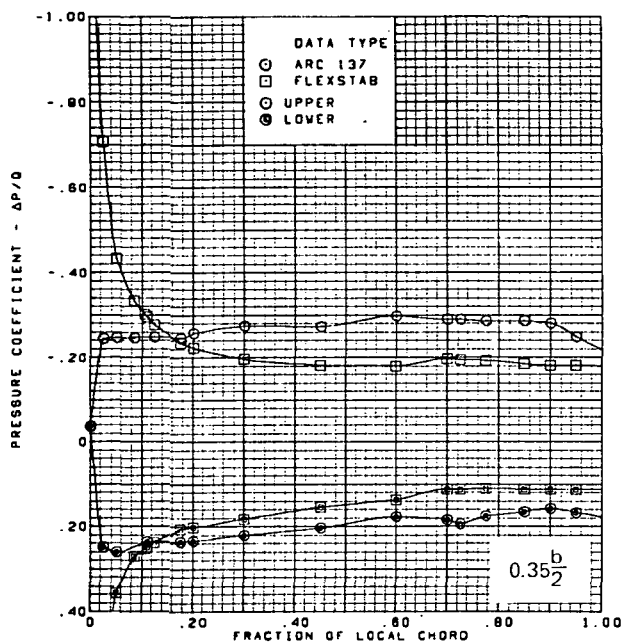
Figure 56.—(Continued)



(d) Surface Chordwise Pressure Distributions,  $\alpha = 15^\circ$

Figure 56: --(Continued)



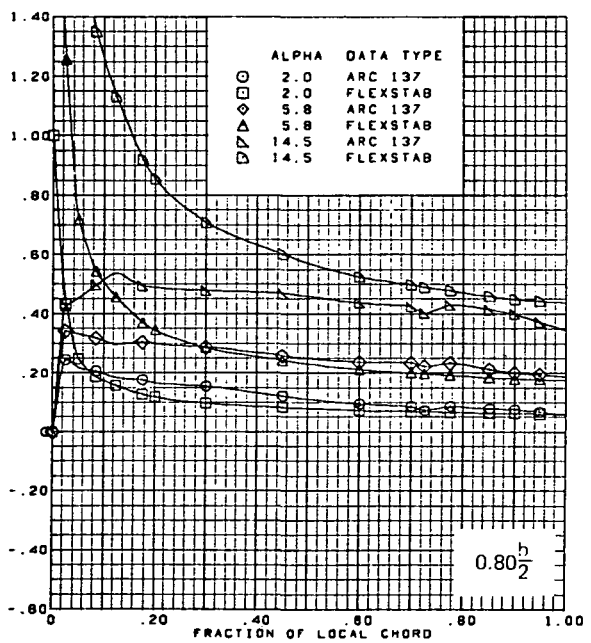
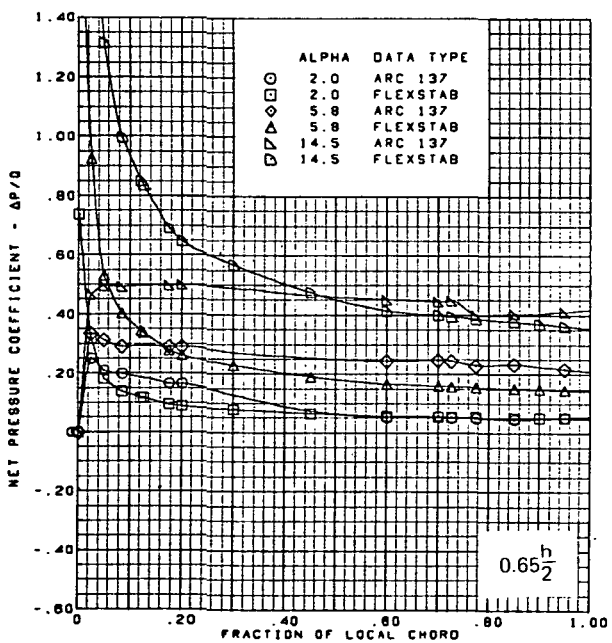
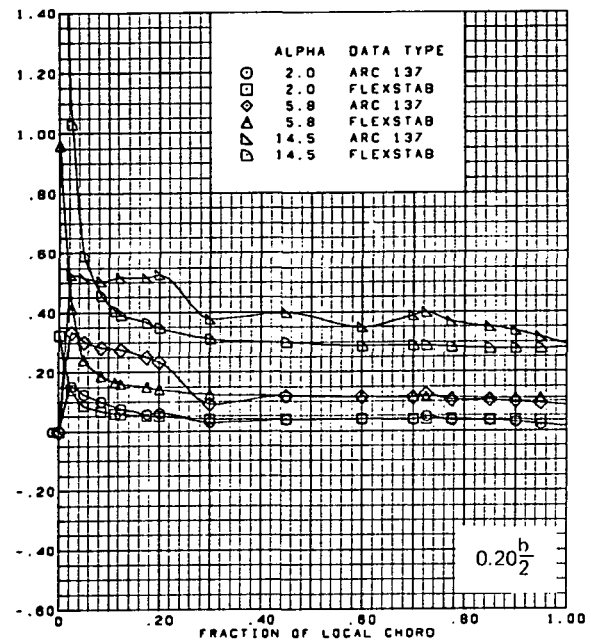
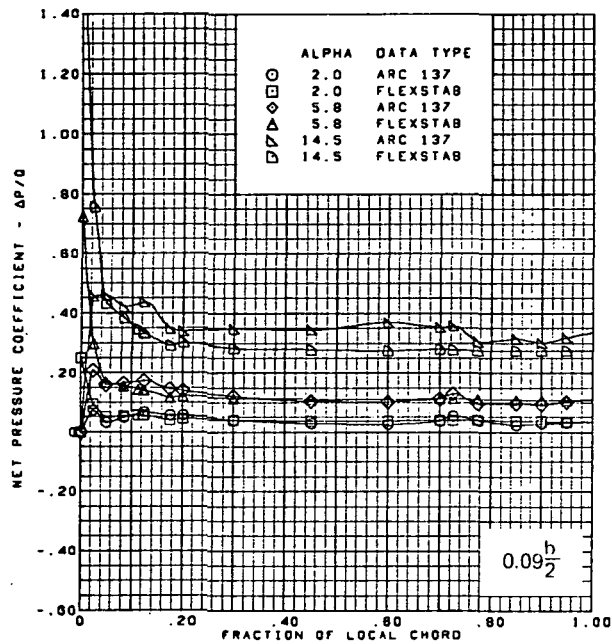


$M = 2.10$  (run 21)  
 $\alpha = 15^\circ$   
 Flat wing, rounded L.E.  
 L.E. deflection, full span =  $0.0^\circ$   
 T.E. deflection, full span =  $0.0^\circ$

Note:  $C_{p, \text{vacuum}} = -0.32$

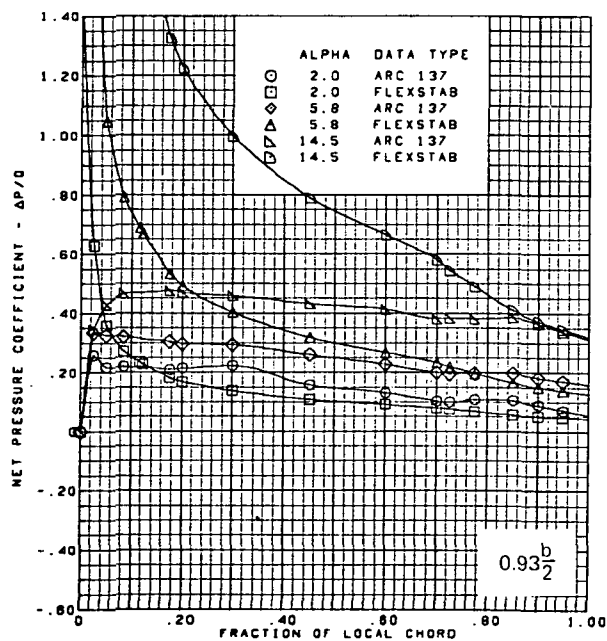
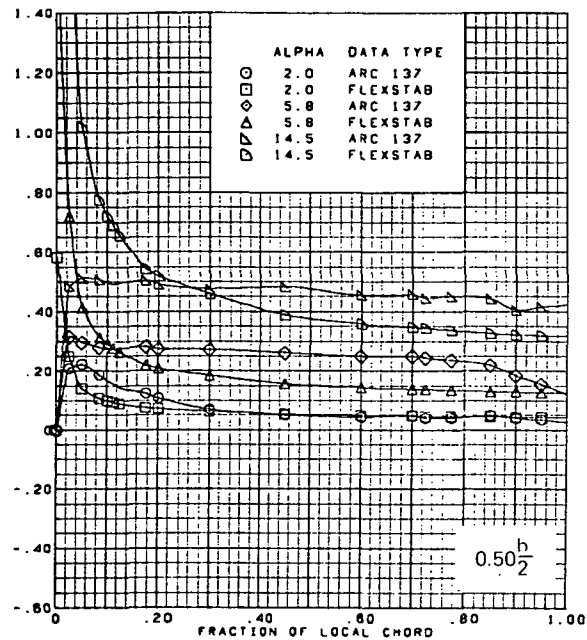
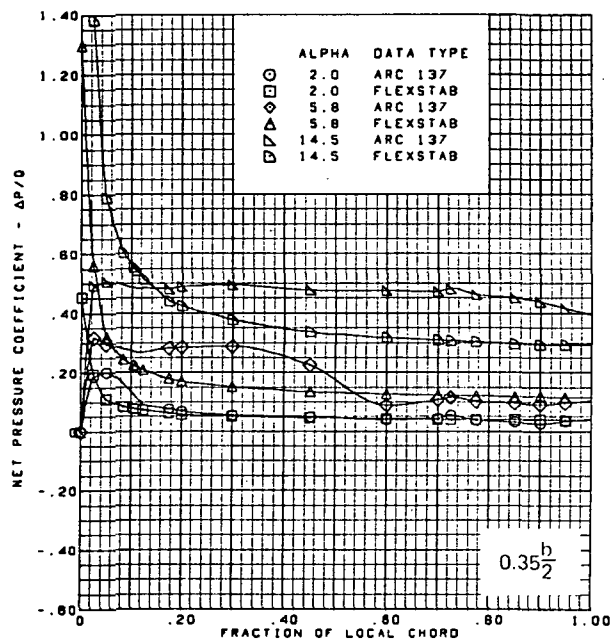
(d) (Concluded)

Figure 56.—(Continued)



(e) Net Chordwise Pressure Distributions,  $\alpha = 2^\circ, 6^\circ, 15^\circ$

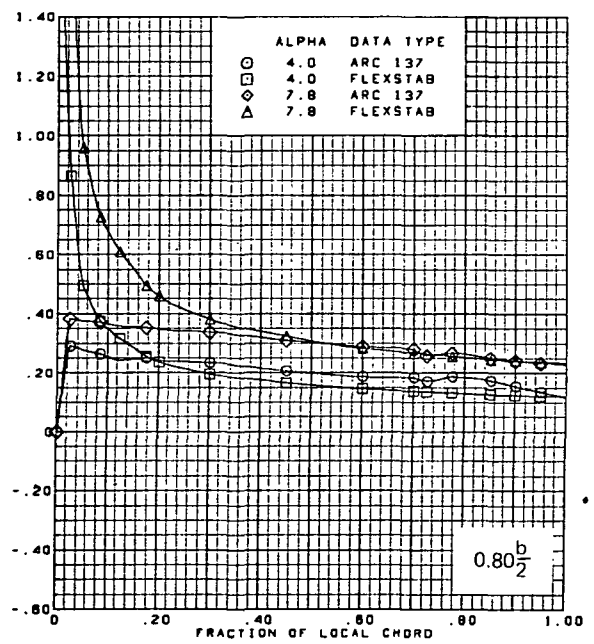
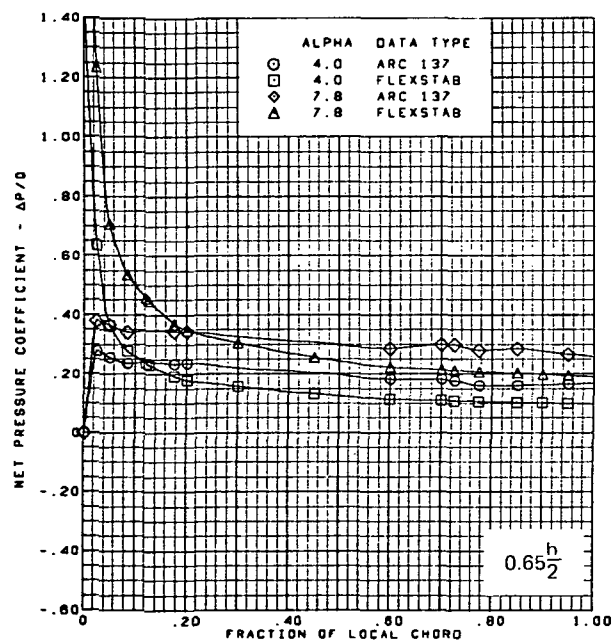
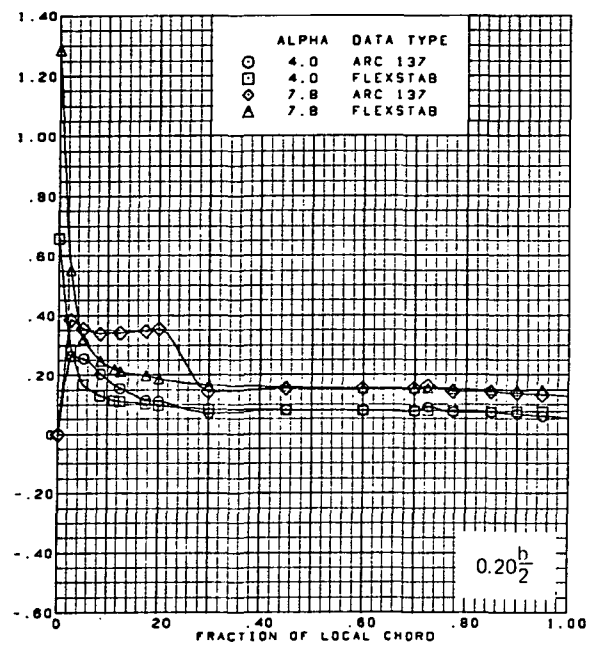
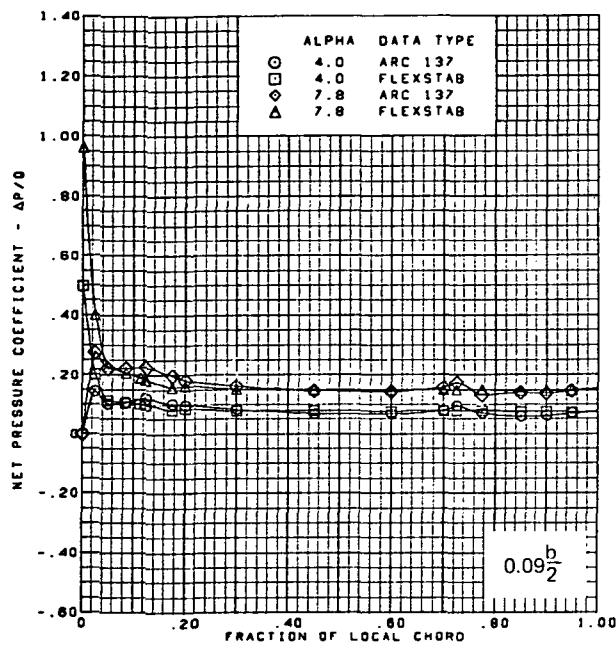
Figure 56.—(Continued)



$M = 2.10$  (run 21)  
 Flat wing, rounded L.E.  
 L.E. deflection, full span =  $0.0^\circ$   
 T.E. deflection, full span =  $0.0^\circ$

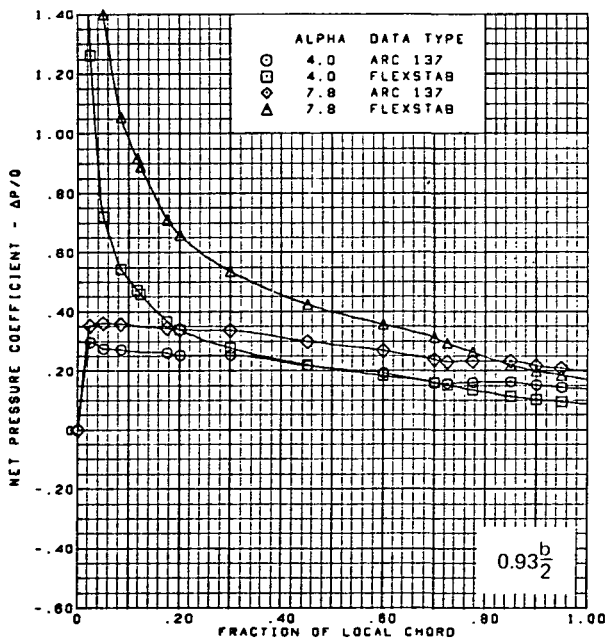
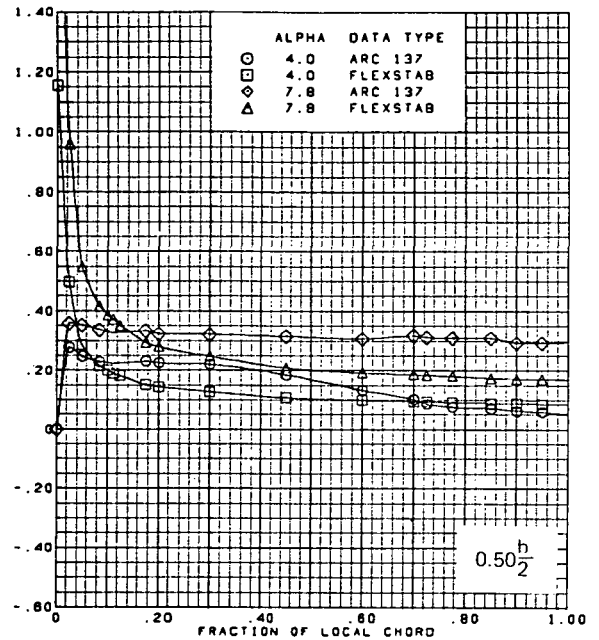
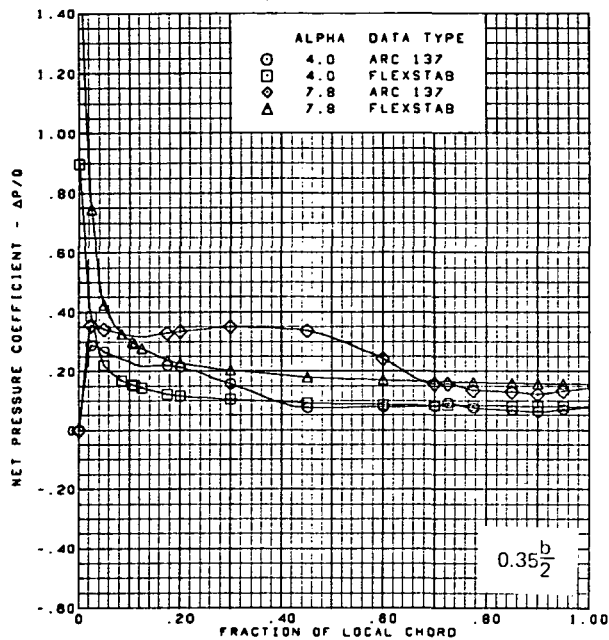
(e) (Concluded)

Figure 56.—(Continued)



(f) Net Chordwise Pressure Distributions,  $\alpha = 4^\circ, 8^\circ$

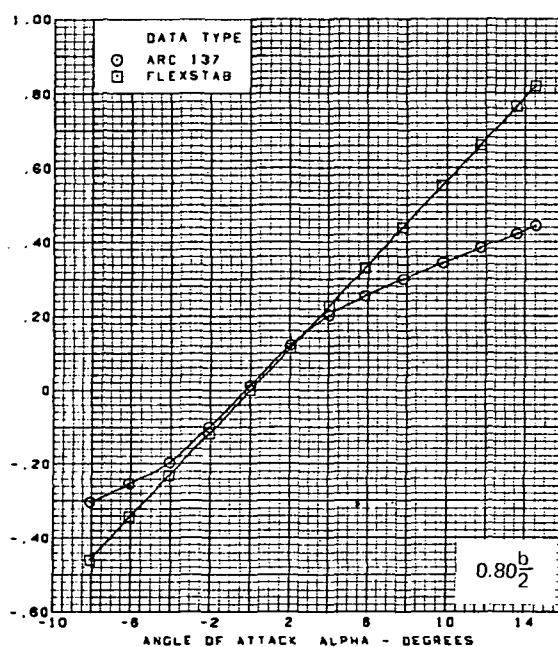
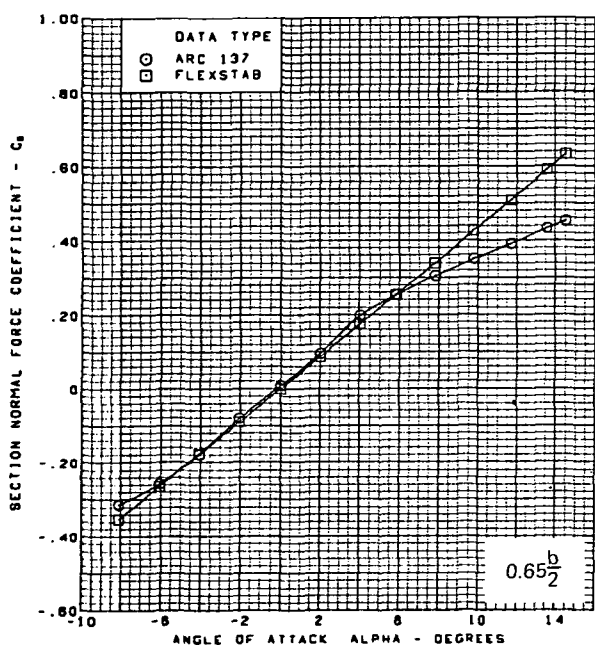
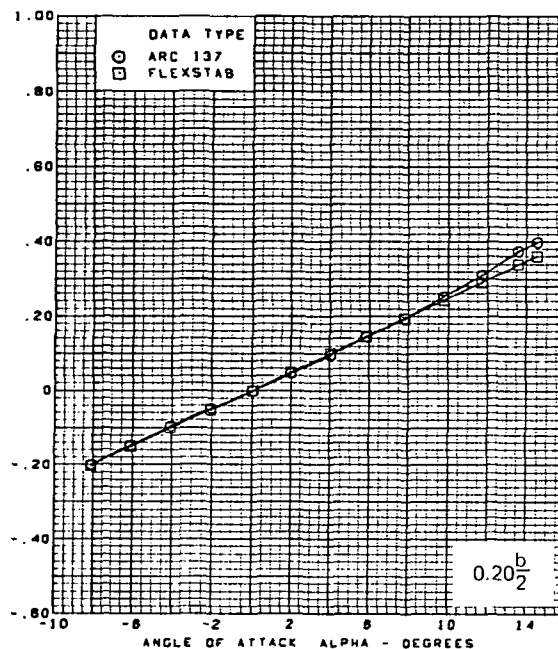
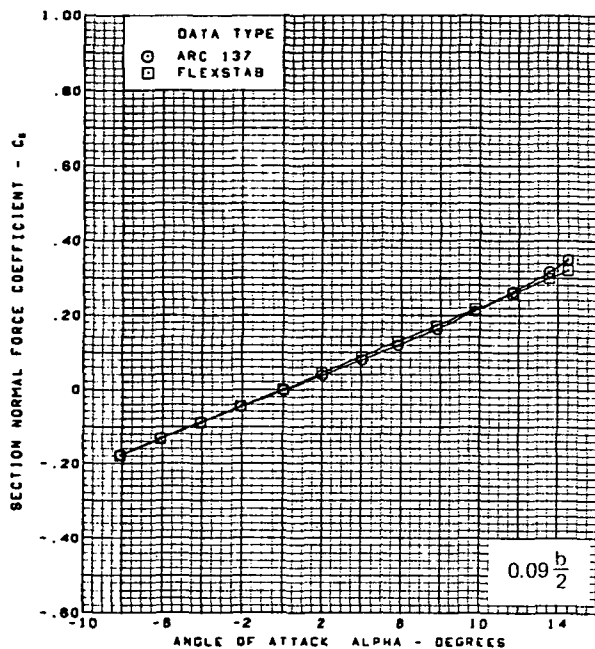
Figure 56.—(Continued)



$M = 2.10$  (run 21)  
 Flat wing, rounded L.E.  
 L.E. deflection, full span =  $0.0^\circ$   
 T.E. deflection, full span =  $0.0^\circ$

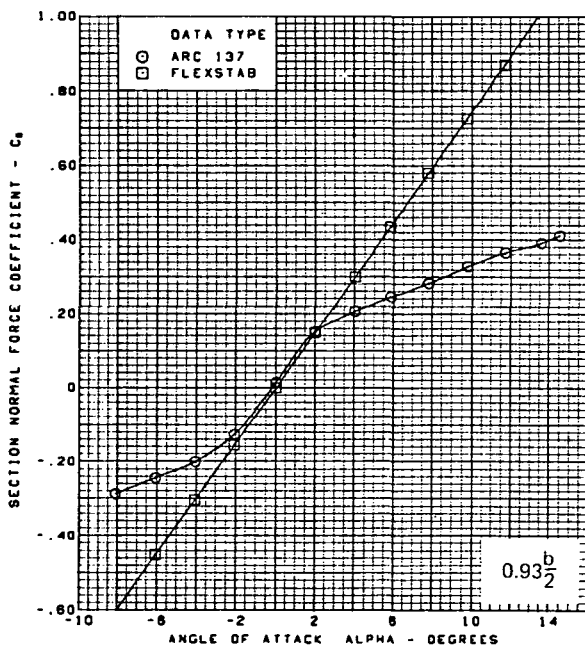
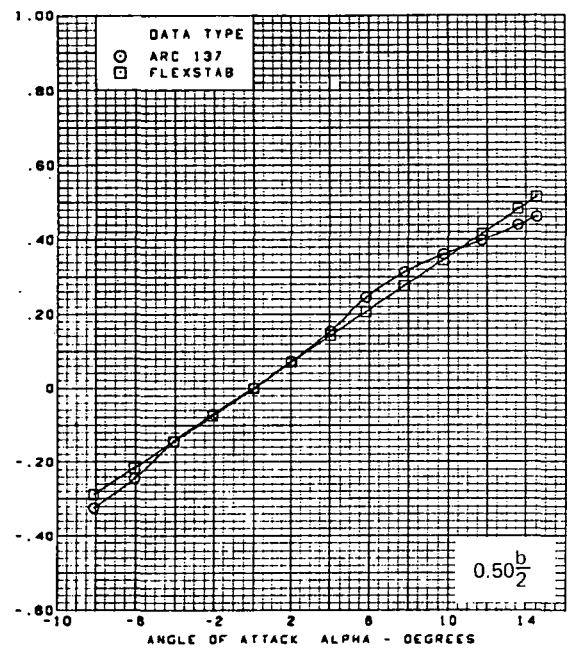
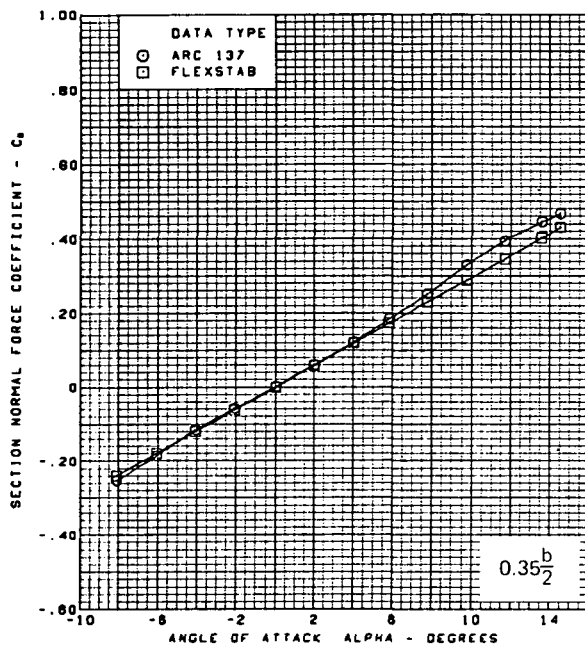
(f) (Concluded)

Figure 56.—(Continued)



(g) Section Aerodynamic Coefficients—Normal Force

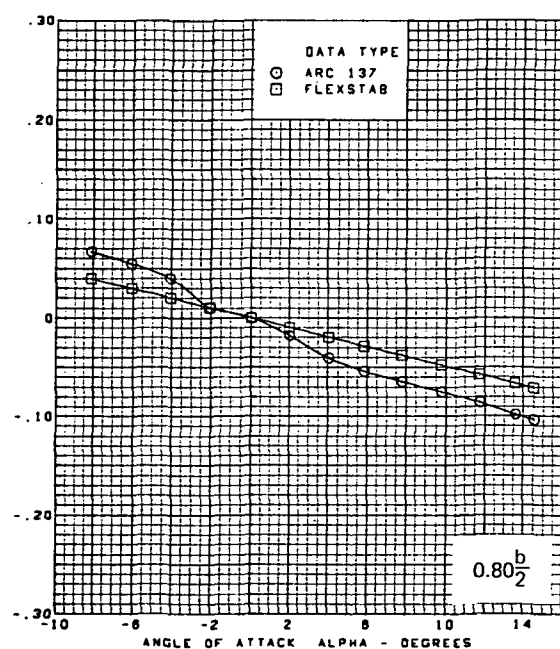
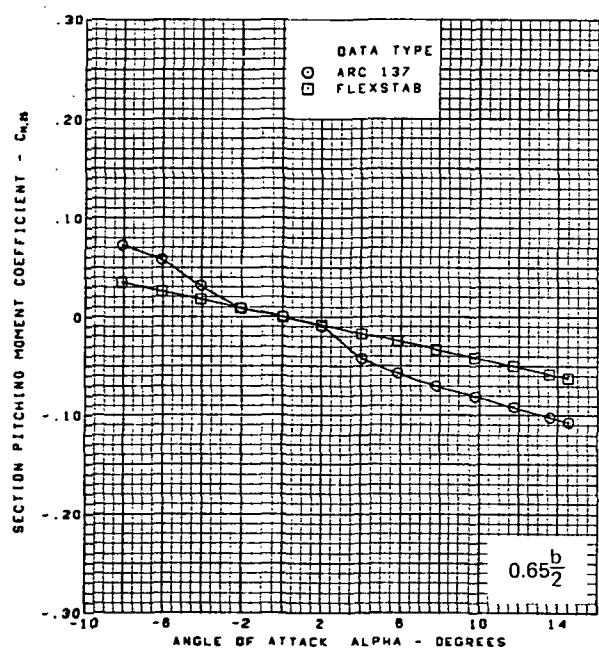
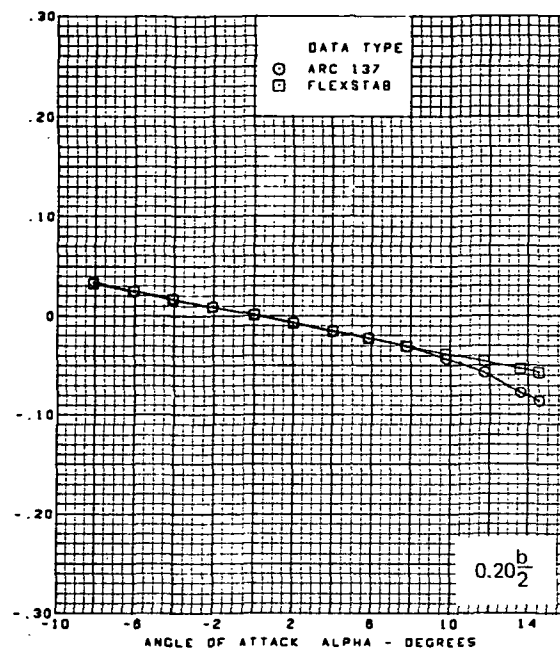
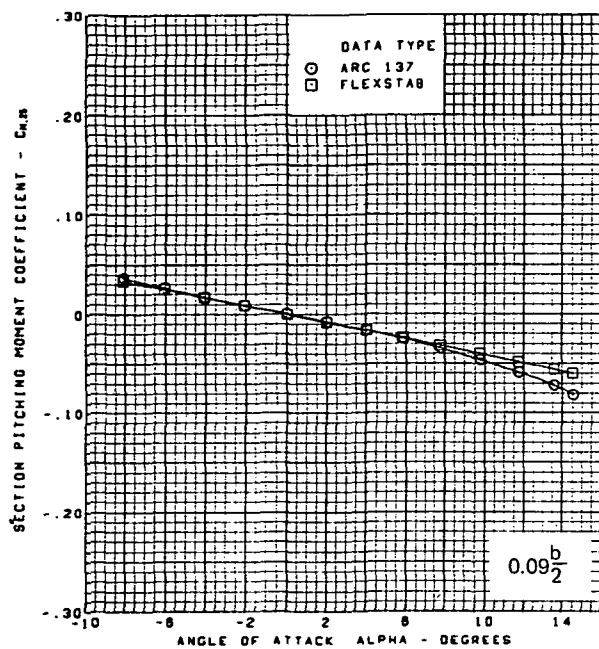
Figure 56.—(Continued)



M = 2.10 (run 21)  
Flat wing, rounded L.E.  
L.E. deflection, full span =  $0.0^\circ$   
T.E. deflection, full span =  $0.0^\circ$

(g) (Concluded)

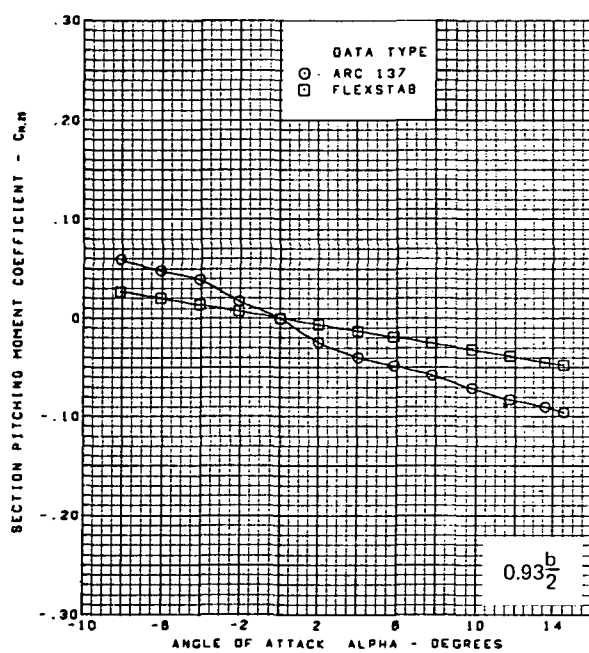
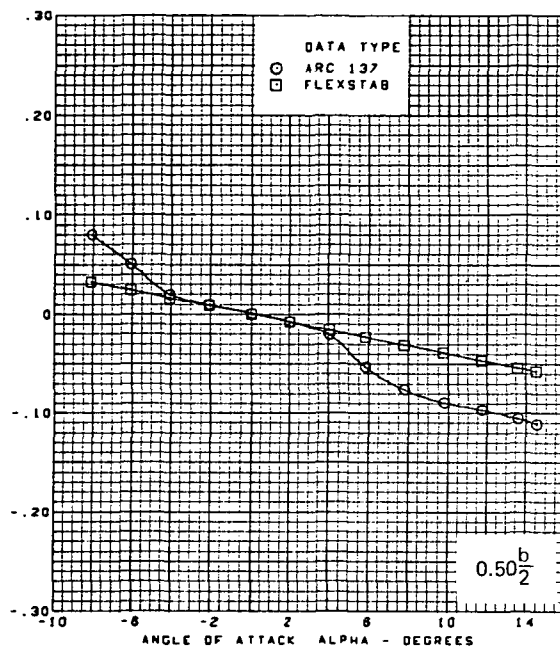
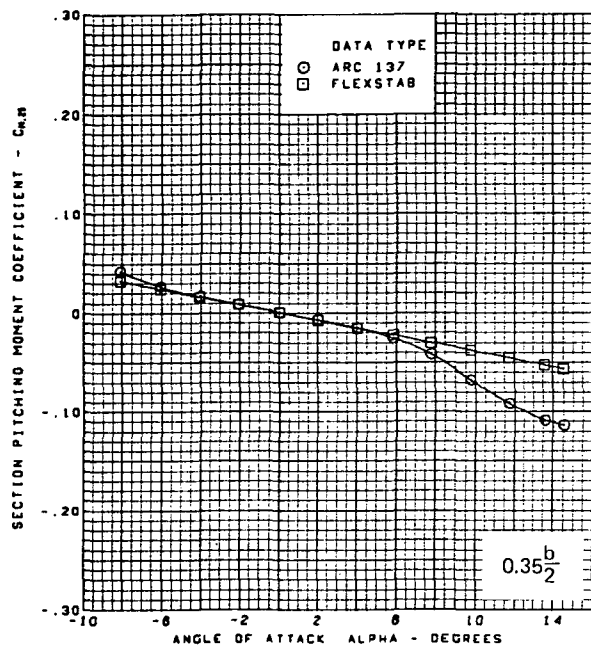
Figure 56. —(Continued)



(h) Section Aerodynamic Coefficients--Pitching Moment

Figure 56. --(Continued)

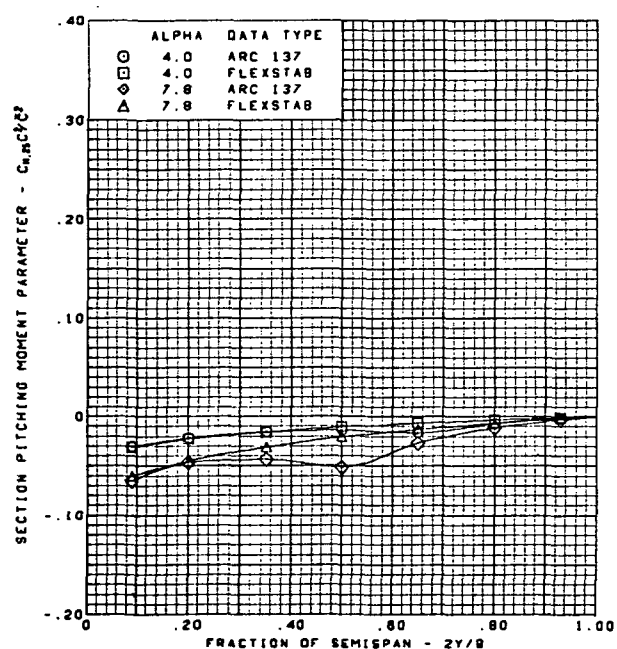
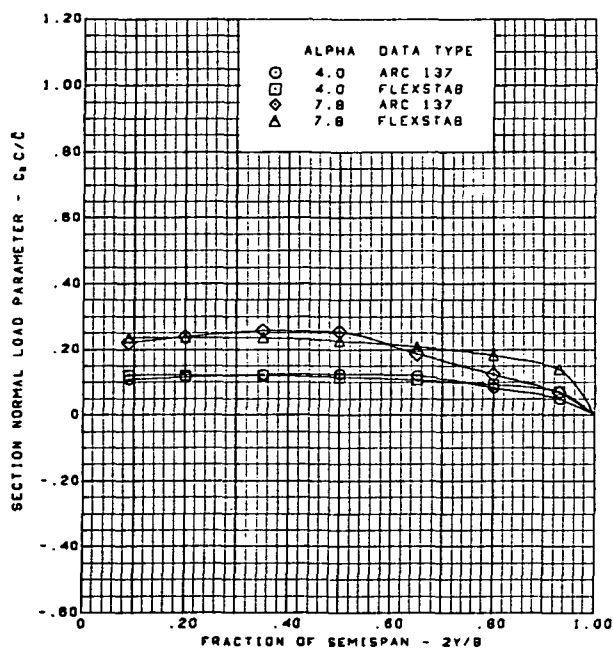
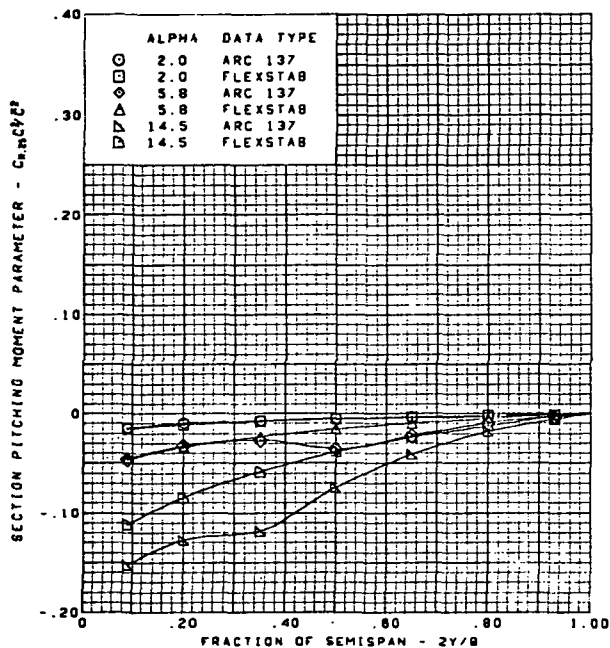
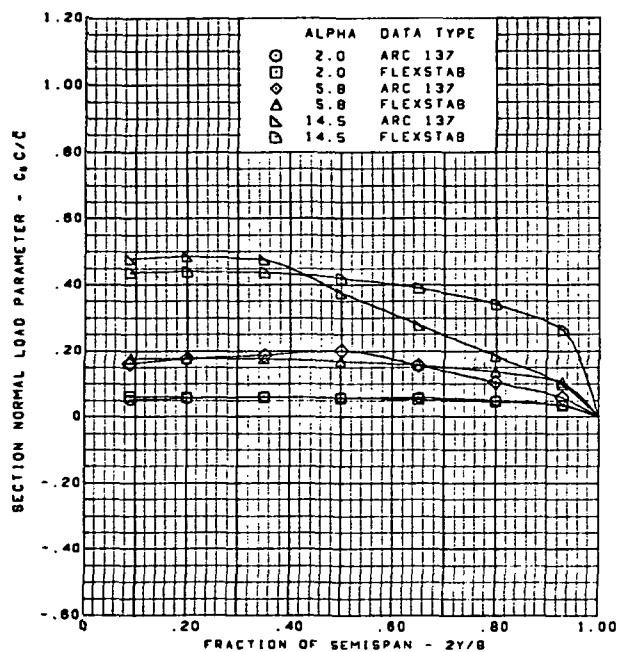




M = 2.10 (run 21)  
 Flat wing, rounded L.E.  
 L.E. deflection, full span =  $0.0^\circ$   
 T.E. deflection, full span =  $0.0^\circ$

(h) (Concluded)

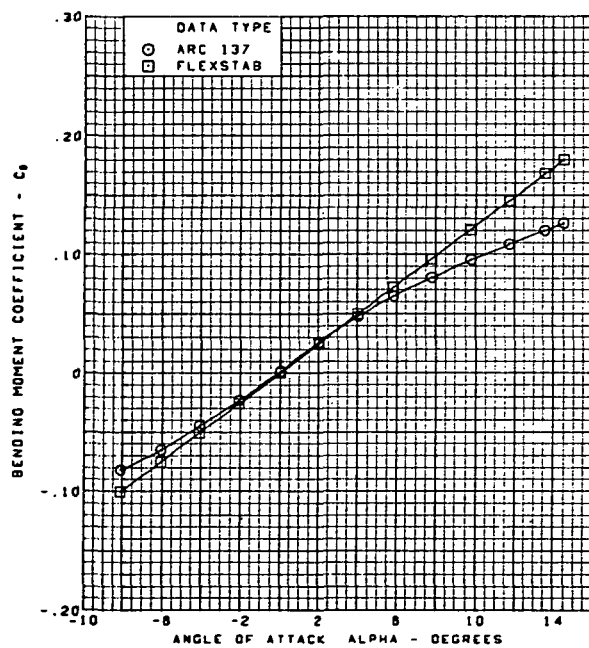
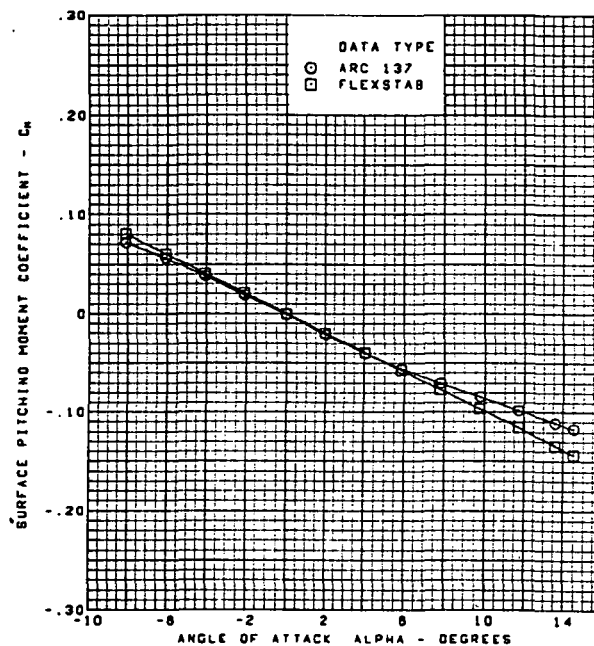
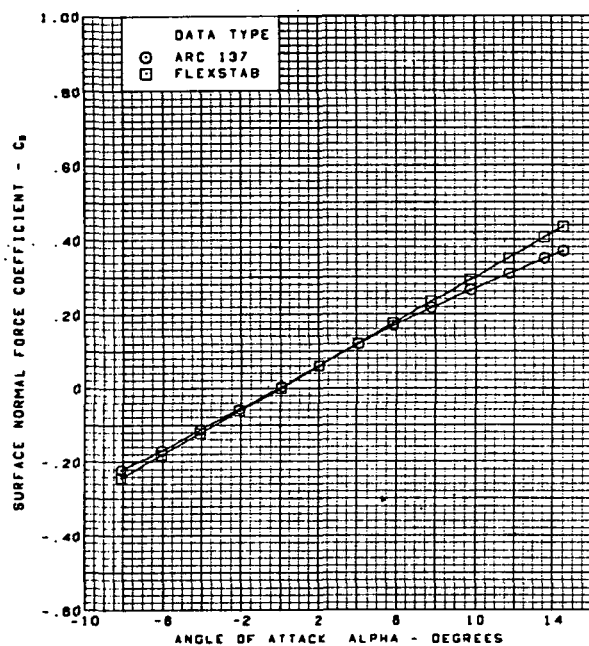
Figure 56. —(Continued)



M = 2.10 (run 21)  
 Flat wing, rounded L.E.  
 L.E. deflection, full span =  $0.0^\circ$   
 T.E. deflection, full span =  $0.0^\circ$

(i) Spanload Distributions

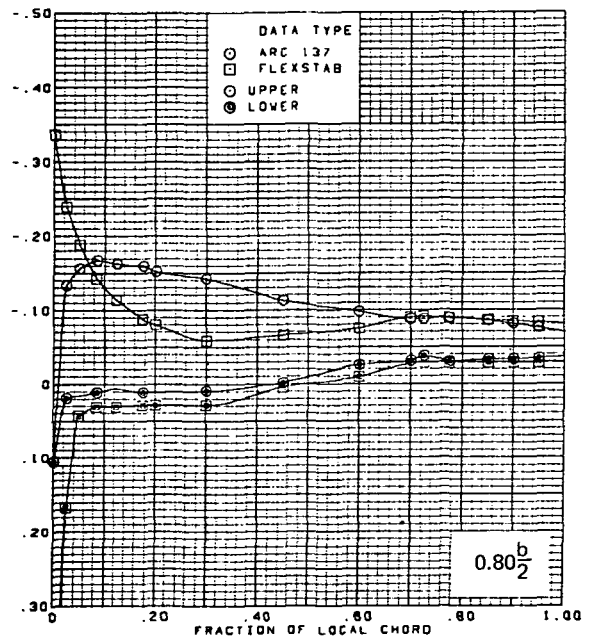
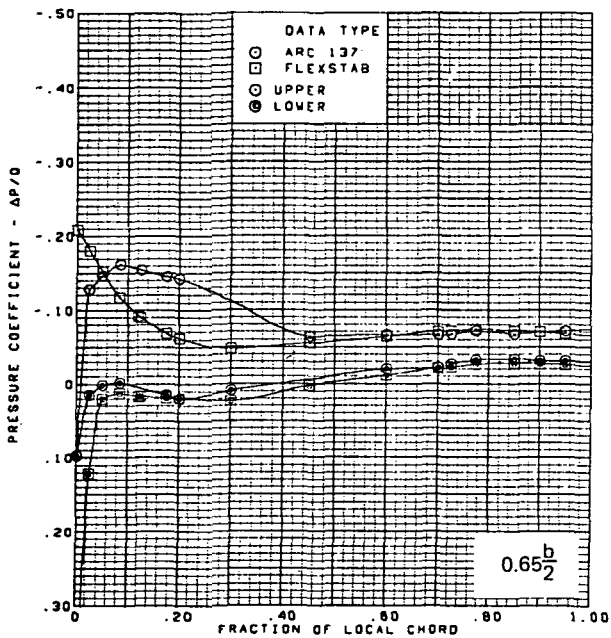
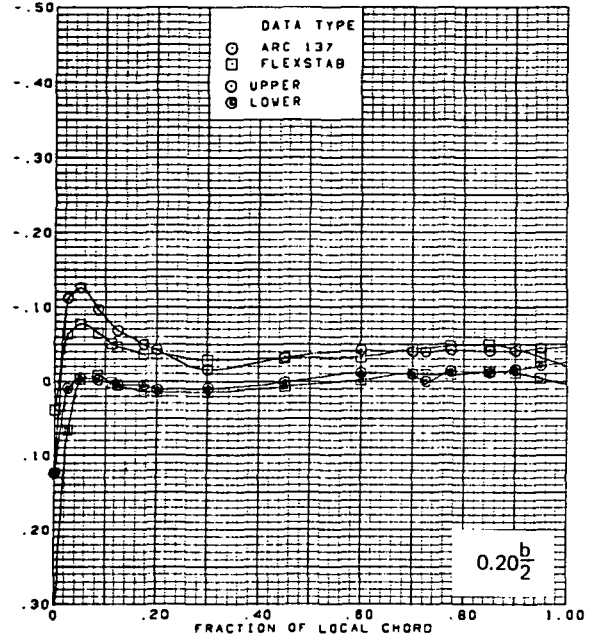
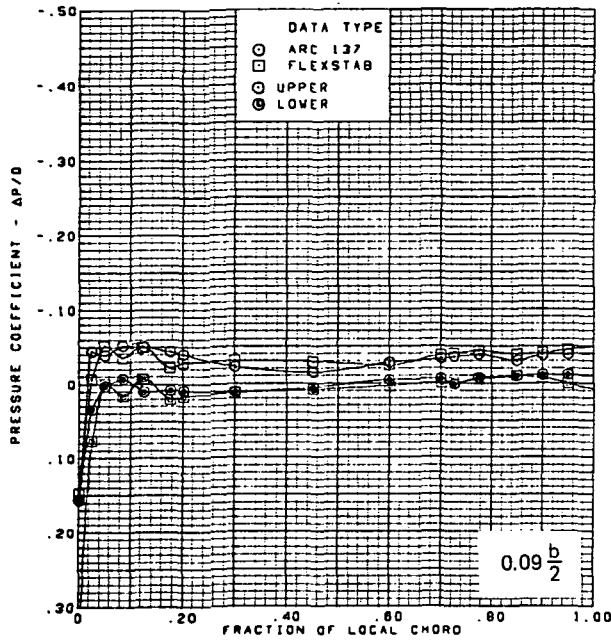
Figure 56. —(Continued)



$M = 2.10$  (run 21)  
 Flat wing, rounded L.E.  
 L.E. deflection, full span =  $0.0^\circ$   
 T.E. deflection, full span =  $0.0^\circ$

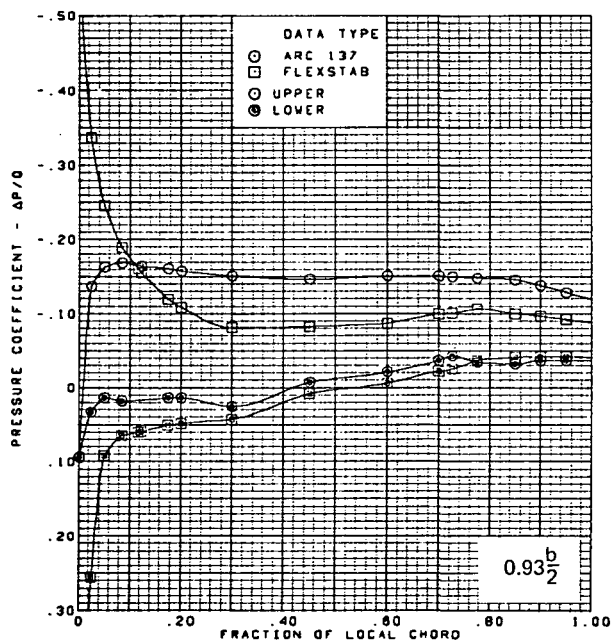
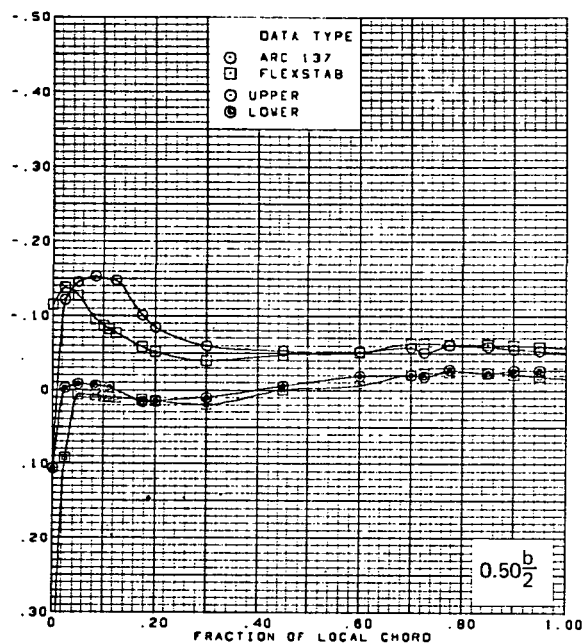
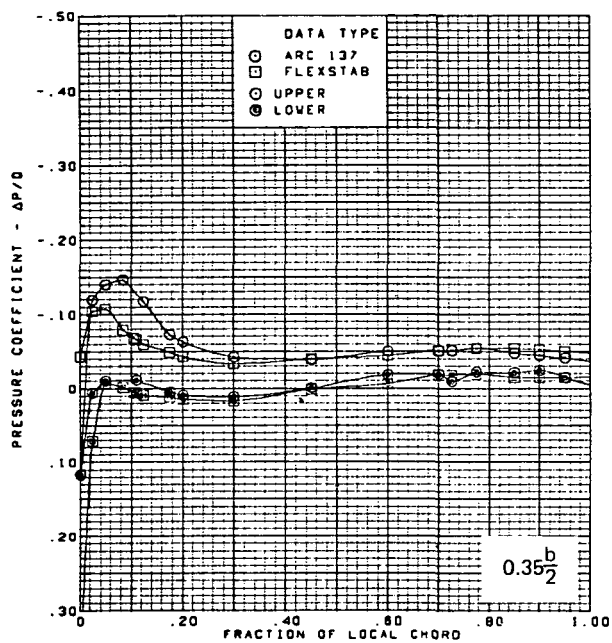
(j) Wing Aerodynamic Coefficients

Figure 56.—(Concluded)



(a) Surface Chordwise Pressure Distributions,  $\alpha = 2^\circ$

Figure 57.—Wing Theory-to-Experiment Comparison—Flat Wing, Rounded L.E.; L.E. Deflection, Full Span =  $0.0^\circ$ ; T.E. Deflection, Full Span =  $0.0^\circ$ ;  $M = 2.50$

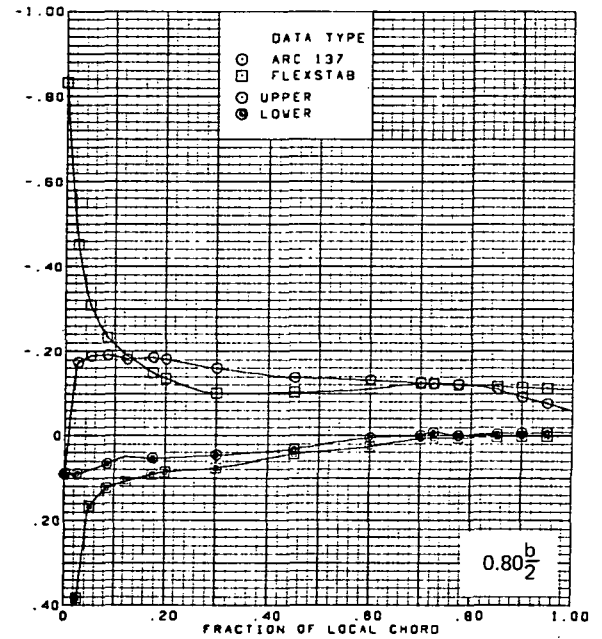
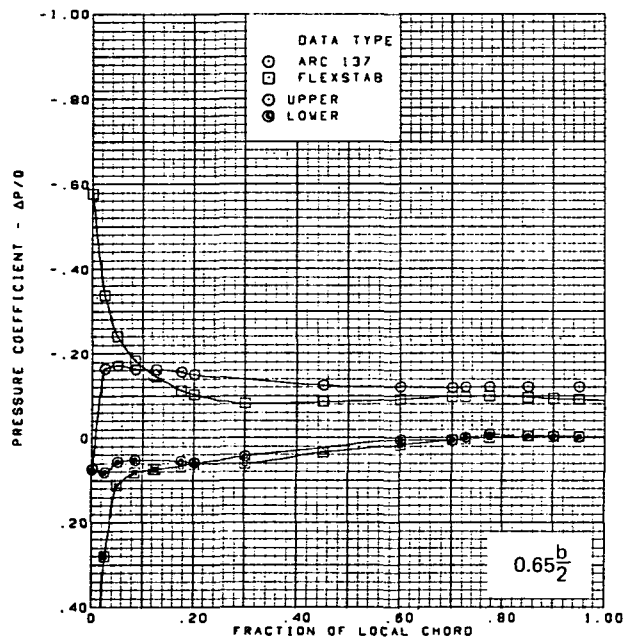
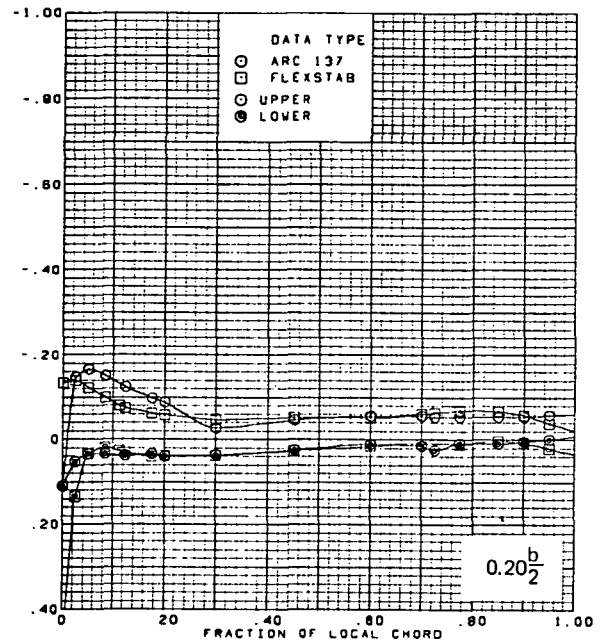
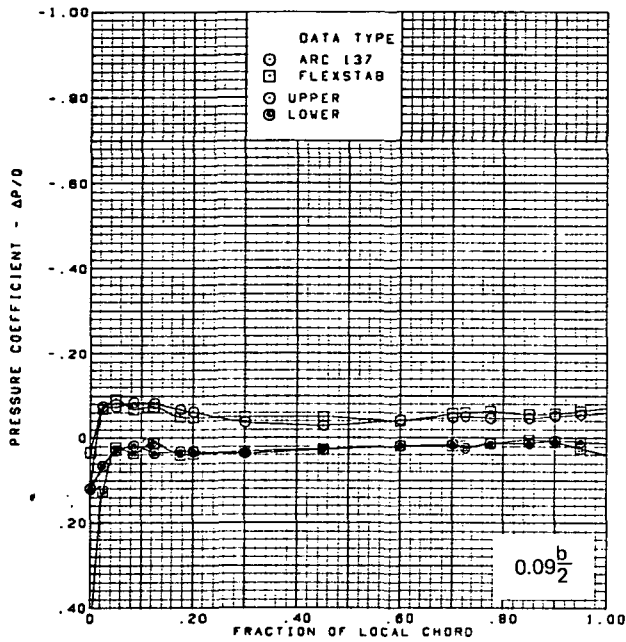


$M = 2.50$  (run 22)  
 $\alpha = 2^\circ$   
 Flat wing, rounded L.E.  
 L.E. deflection, full span =  $0.0^\circ$   
 T.E. deflection, full span =  $0.0^\circ$

Note:  $C_{p, \text{vacuum}} = -0.23$

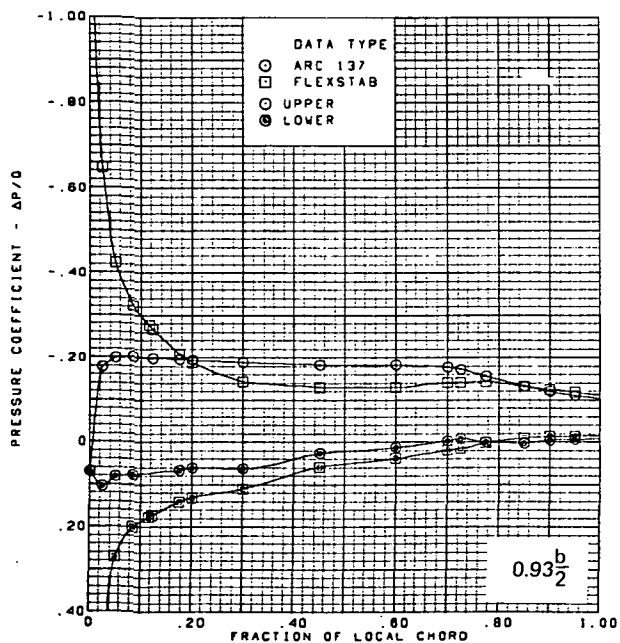
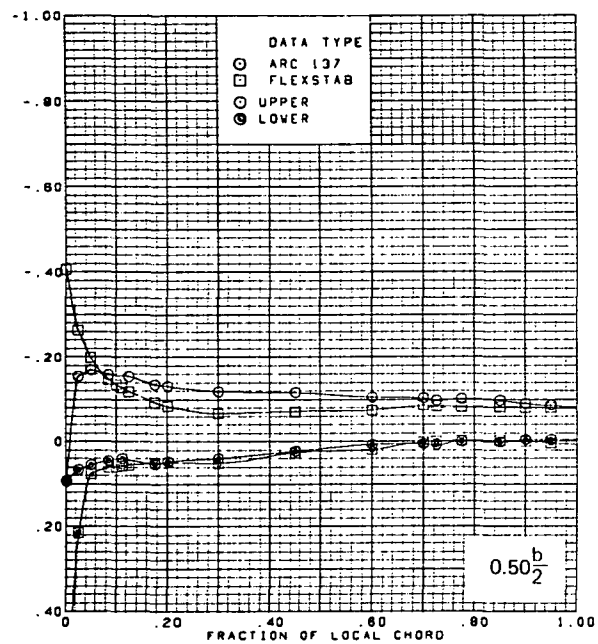
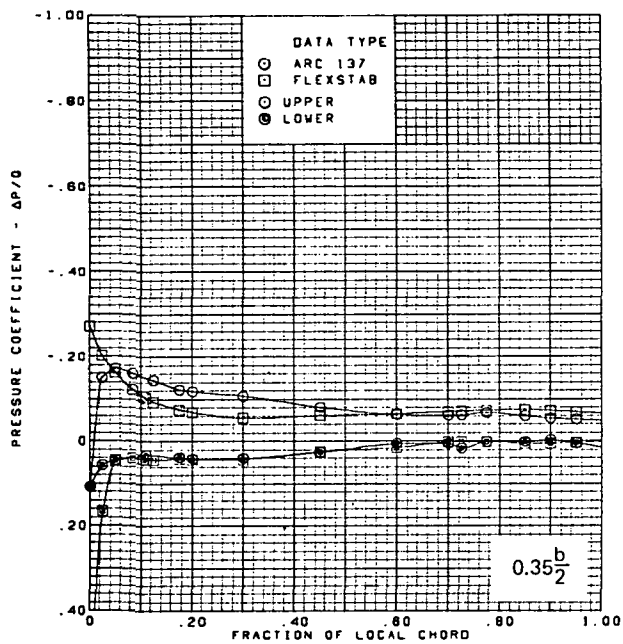
(a) (Concluded)

Figure 57.—(Continued)



(b) Surface Chordwise Pressure Distributions,  $\alpha = 4^\circ$

Figure 57.—(Continued)

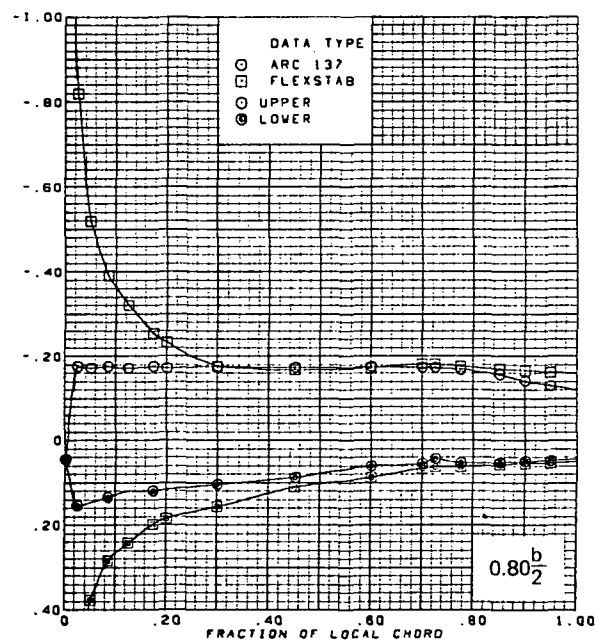
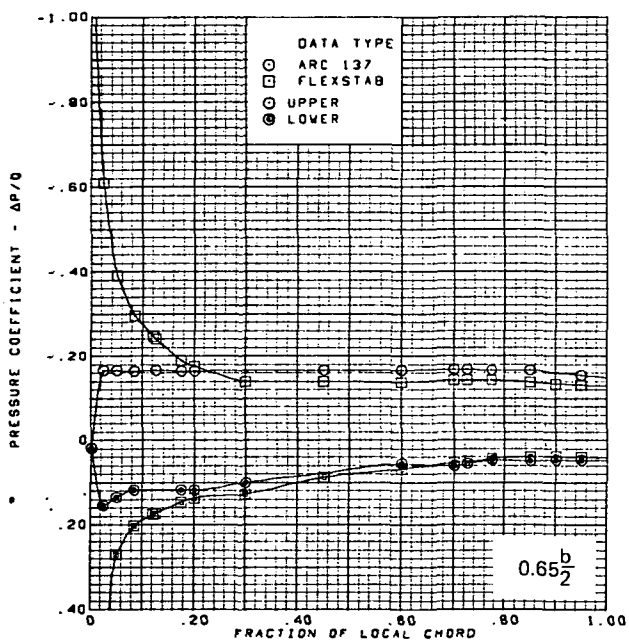
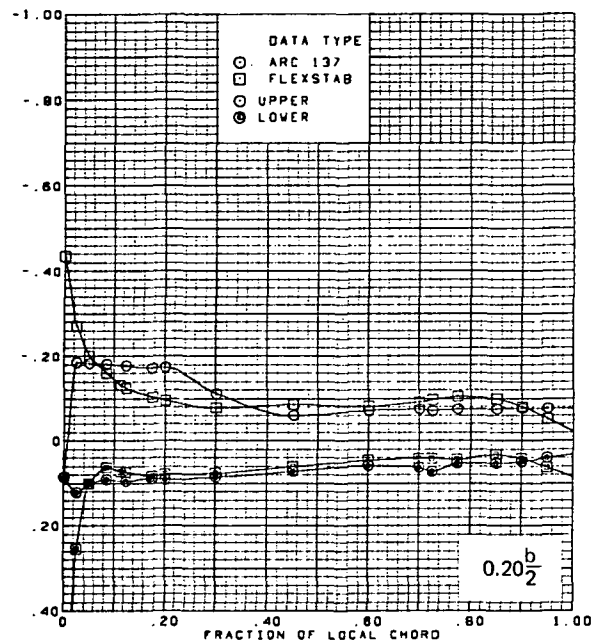
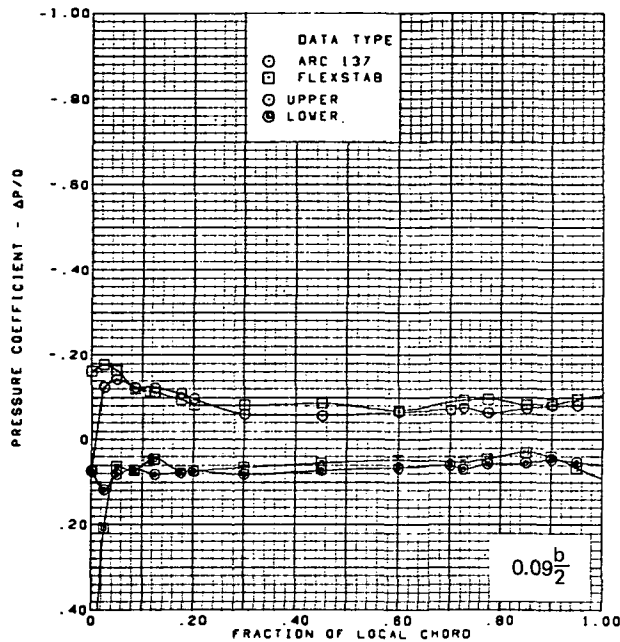


$M = 2.50$  (run 22)  
 $\alpha = 4^\circ$   
 Flat wing, rounded L.E.  
 L.E. deflection, full span =  $0.0^\circ$   
 T.E. deflection, full span =  $0.0^\circ$

Note:  $C_{p, \text{vacuum}} = -0.23$

(b) (Concluded)

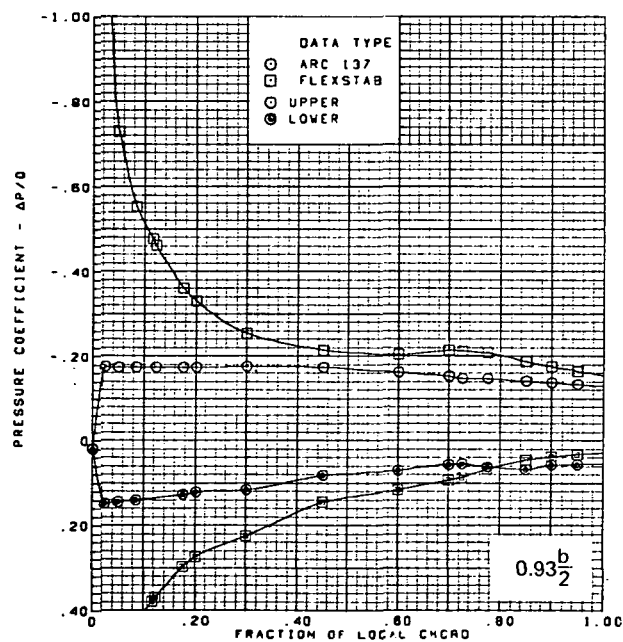
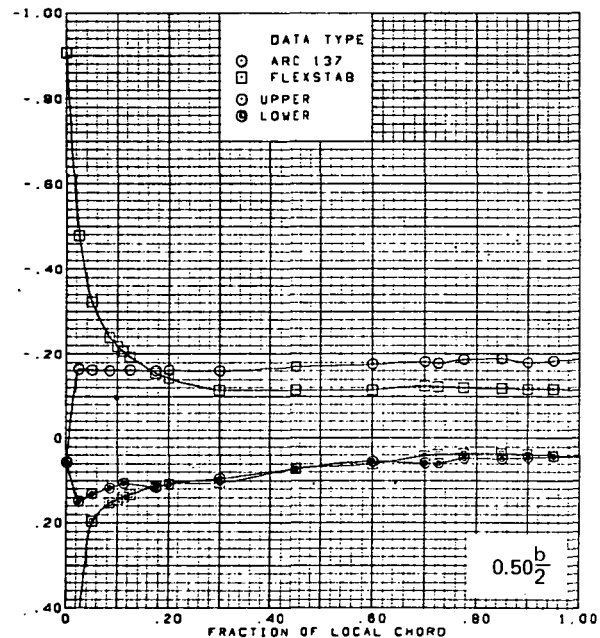
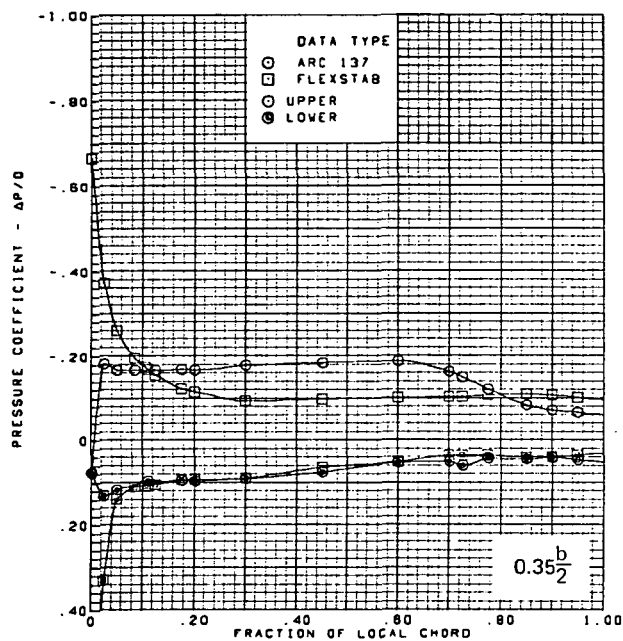
Figure 57.—(Continued)



(c) Surface Chordwise Pressure Distributions,  $\alpha = 8^\circ$

Figure 57.—(Continued)



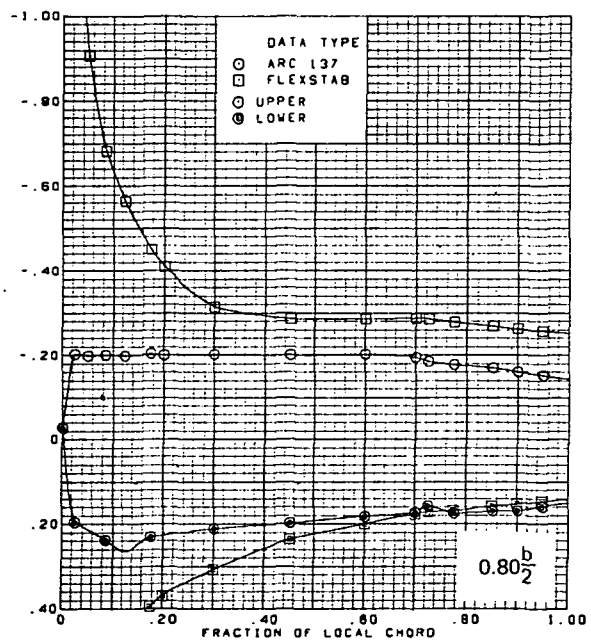
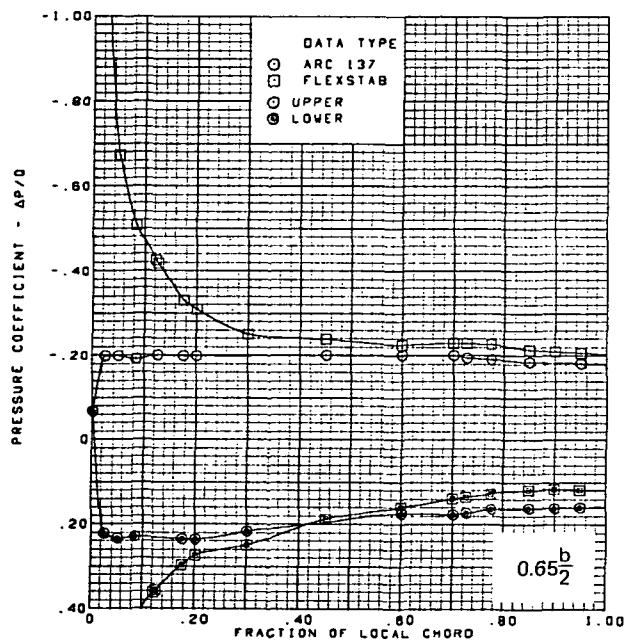
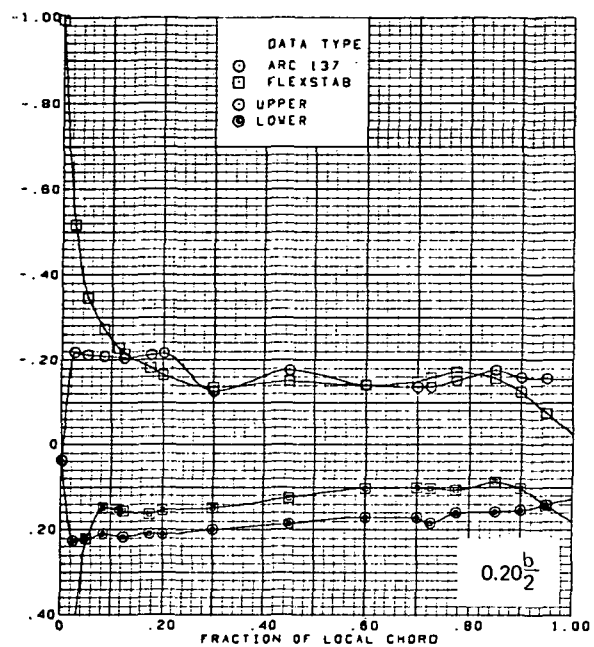
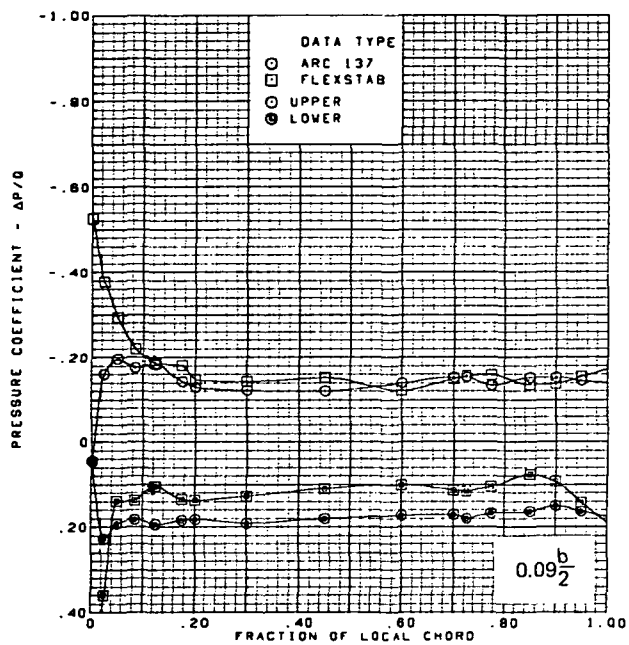


$M = 2.50$  (run 22)  
 $\alpha = 8^\circ$   
 Flat wing, rounded L.E.  
 L.E. deflection, full span =  $0.0^\circ$   
 T.E. deflection, full span =  $0.0^\circ$

Note:  $C_{p, \text{vacuum}} = -0.23$

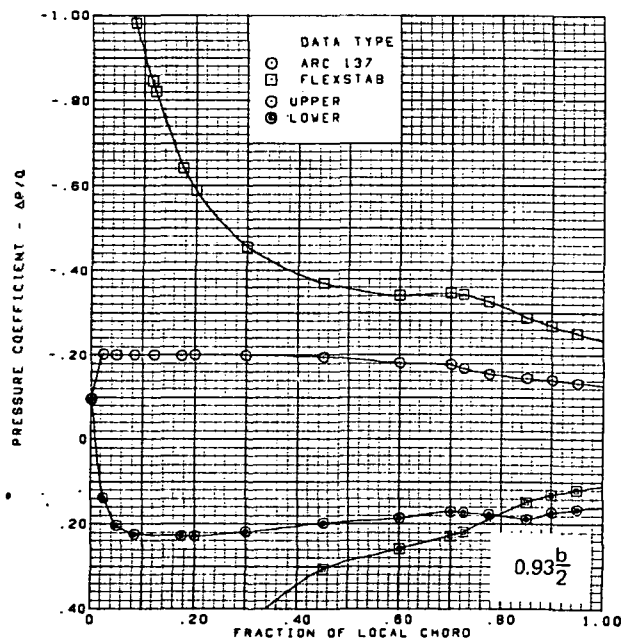
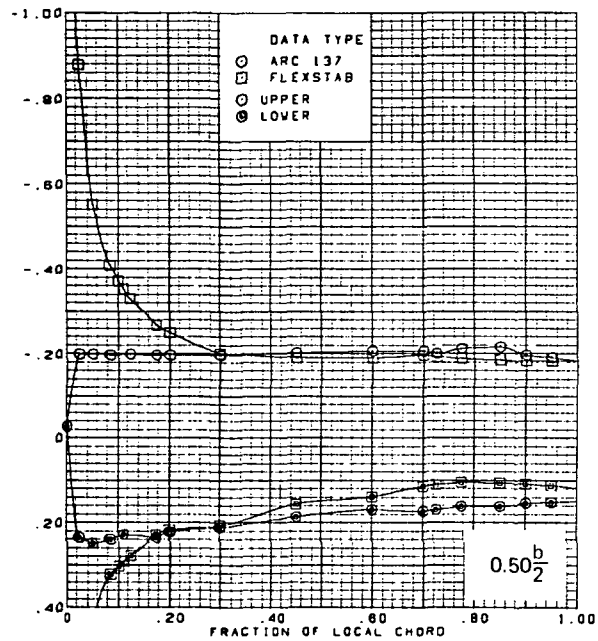
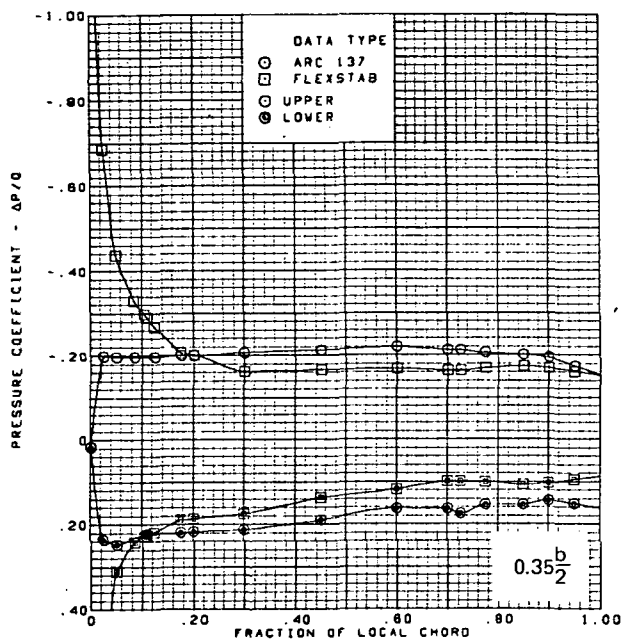
(c) (Concluded)

Figure 57.—(Continued)



(d) Surface Chordwise Pressure Distributions,  $\alpha = 15^\circ$

Figure 57.—(Continued)

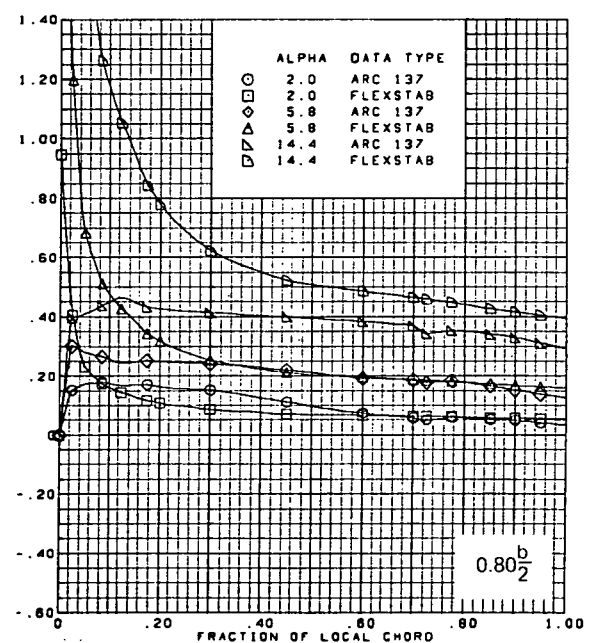
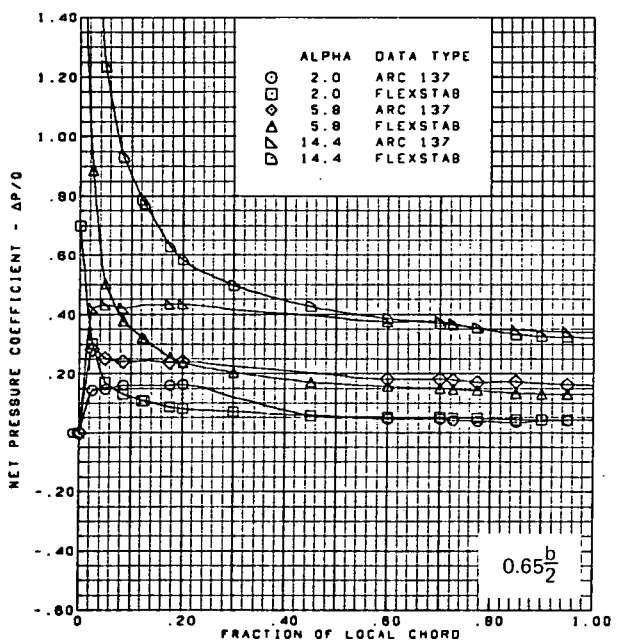
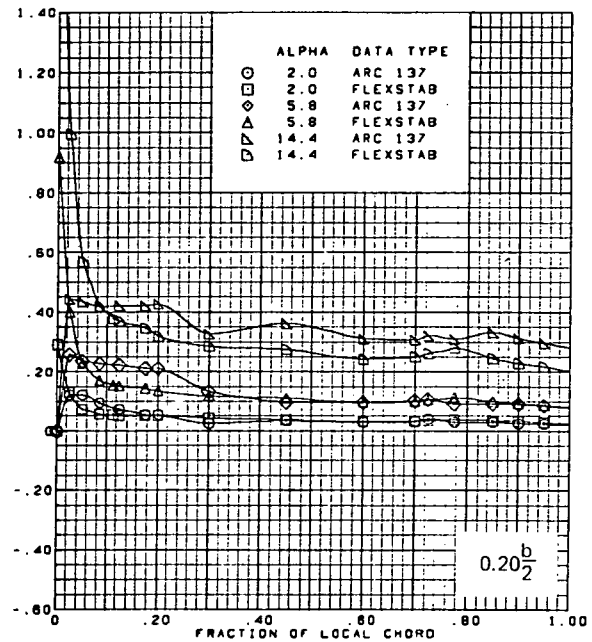
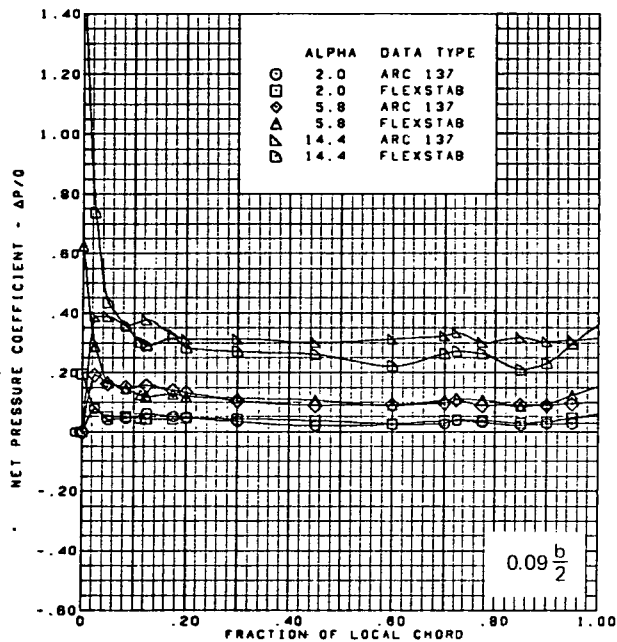


$M = 2.50$  (run 22)  
 $\alpha = 15^\circ$   
 Flat wing, rounded L.E.  
 L.E. deflection, full span =  $0.0^\circ$   
 T.E. deflection, full span =  $0.0^\circ$

Note:  $C_{p, \text{vacuum}} = -0.23$

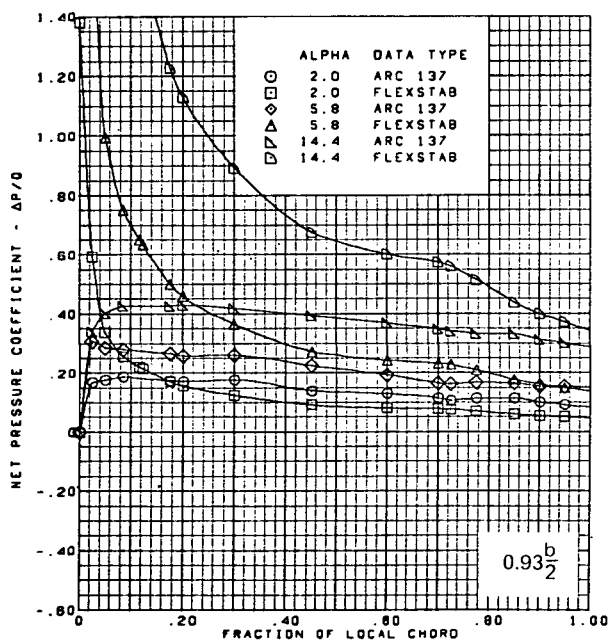
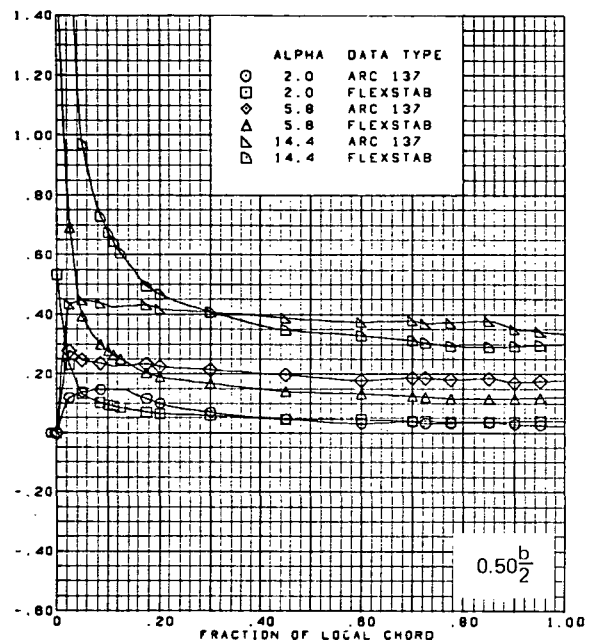
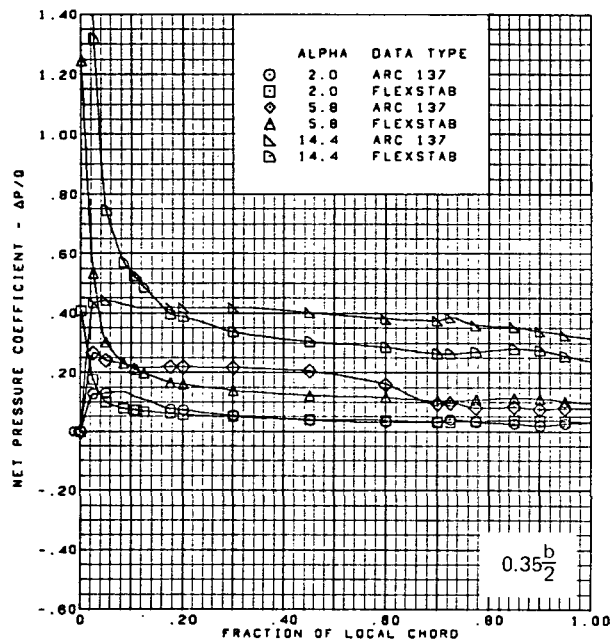
(d) (Concluded)

Figure 57.—(Continued)



(e) Net Chordwise Pressure Distributions,  $\alpha = 2^\circ, 6^\circ, 15^\circ$

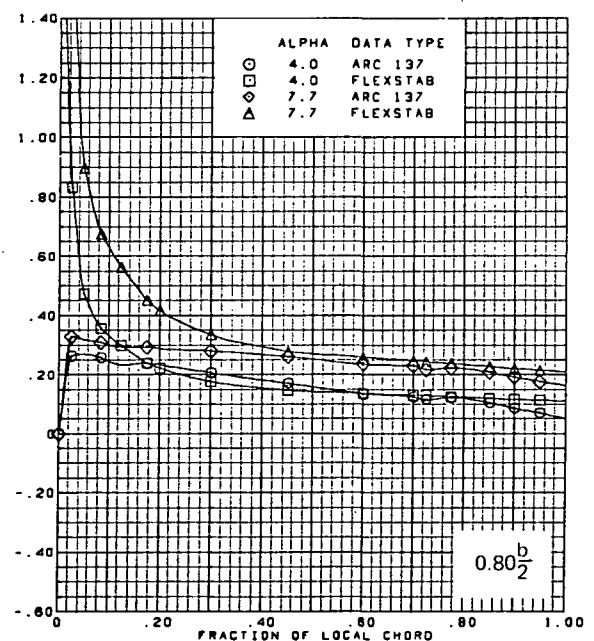
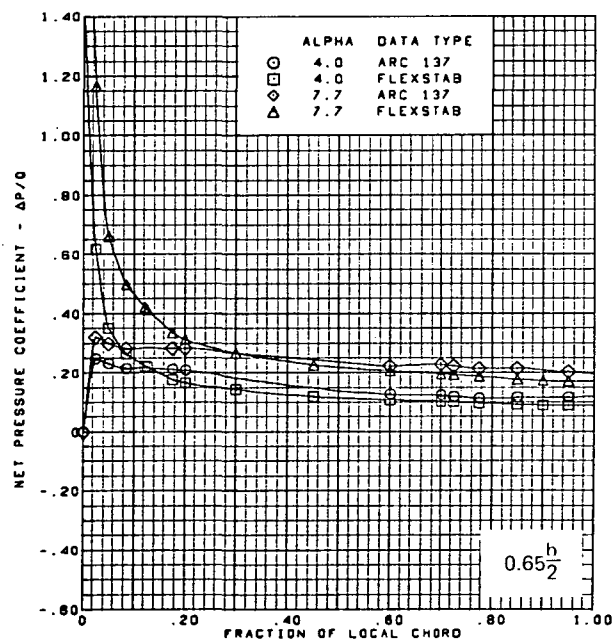
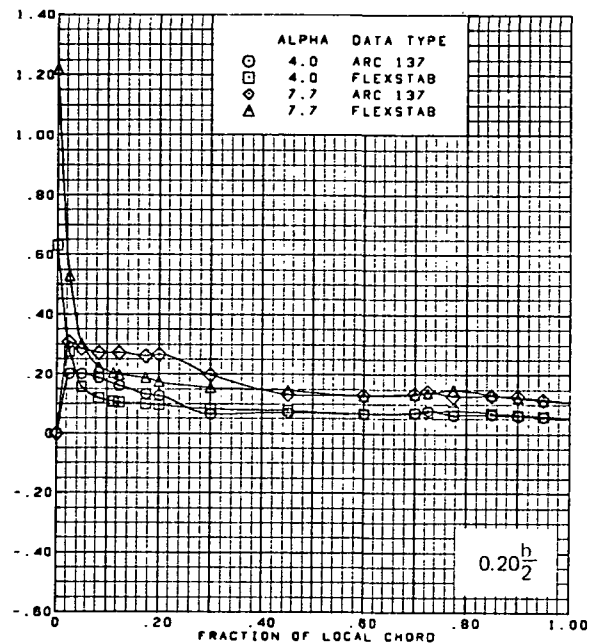
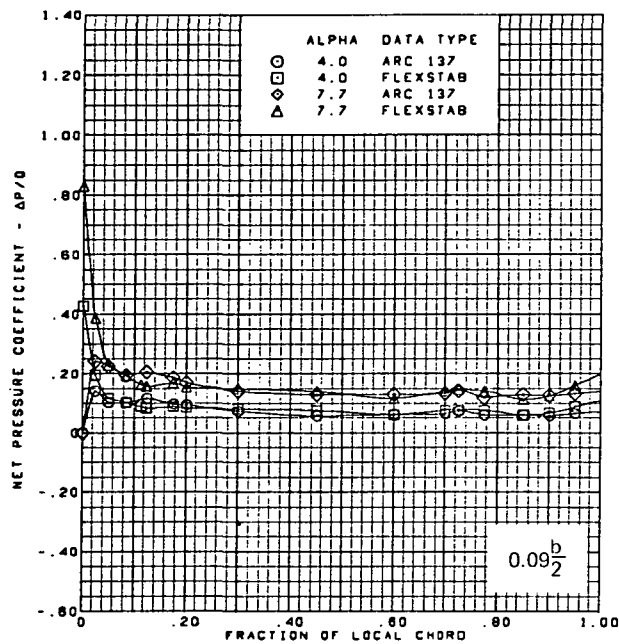
Figure 57.—(Continued)



$M = 2.50$  (run 22)  
 Flat wing, rounded L.E.  
 L.E. deflection, full span =  $0.0^\circ$   
 T.E. deflection, full span =  $0.0^\circ$

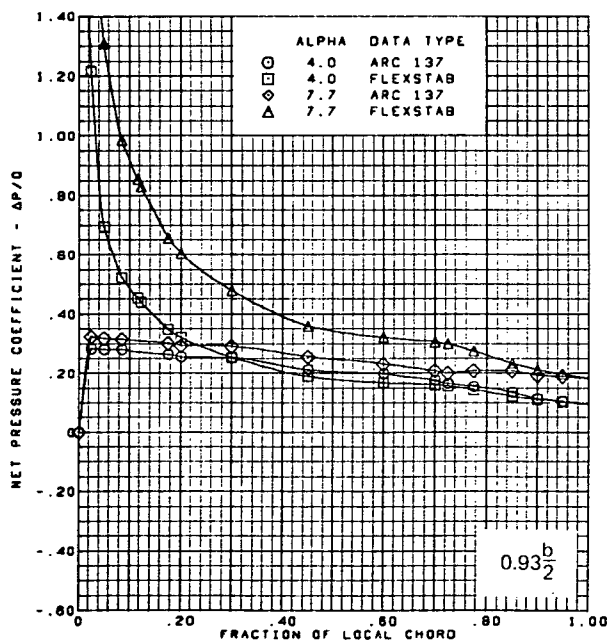
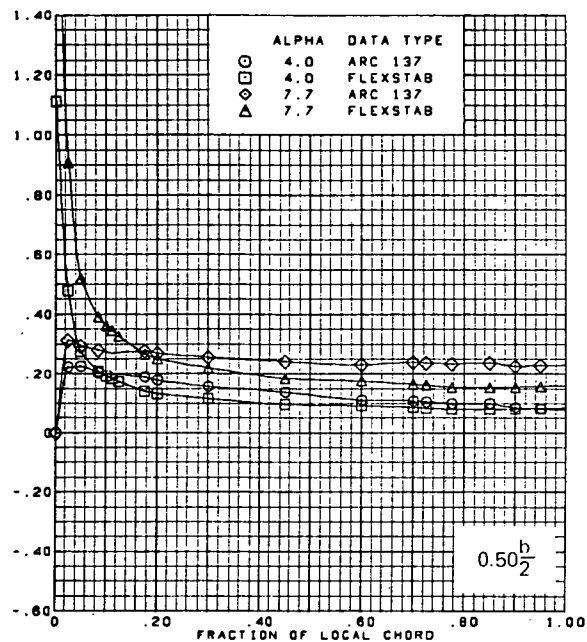
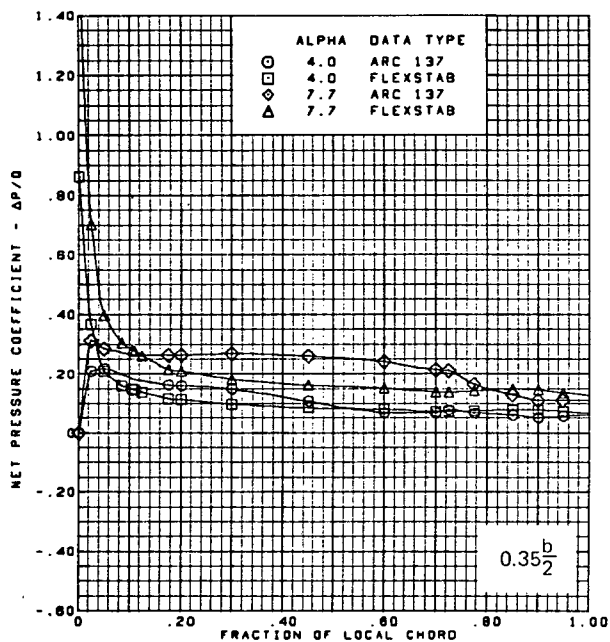
(e) (Concluded)

Figure 57.—(Continued)



(f) Net Chordwise Pressure Distributions,  $\alpha = 4^\circ$ ,  $\alpha = 8^\circ$

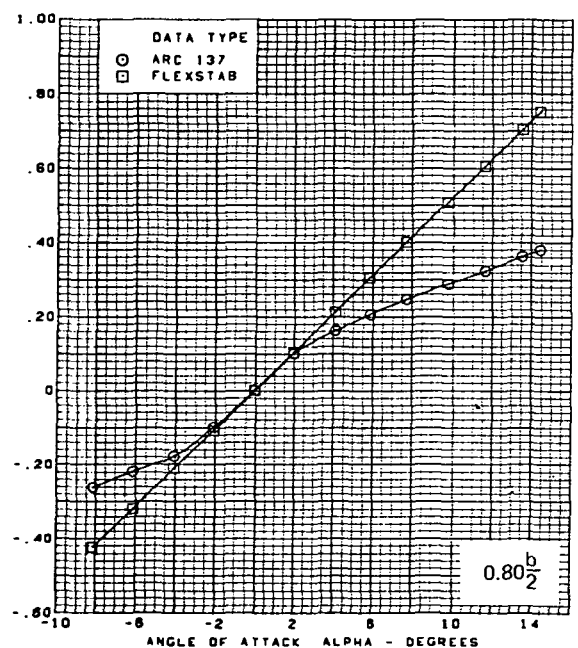
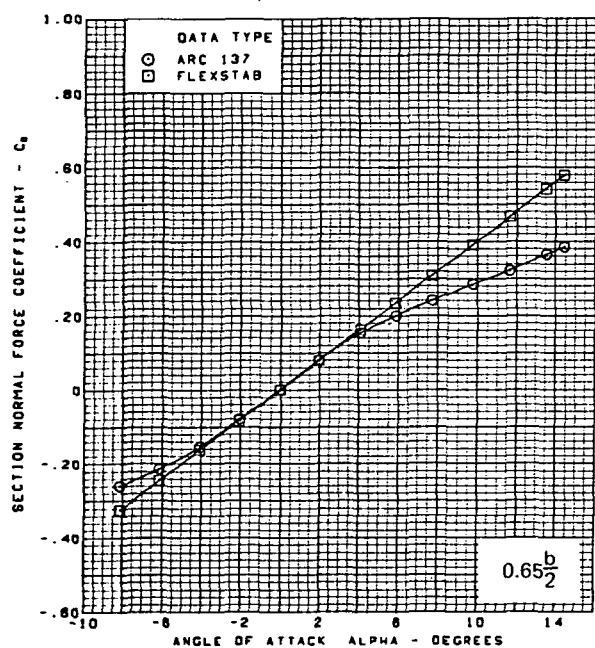
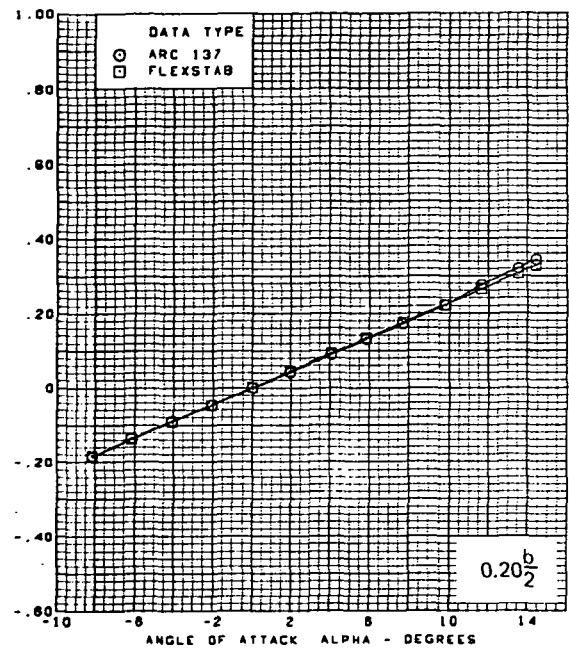
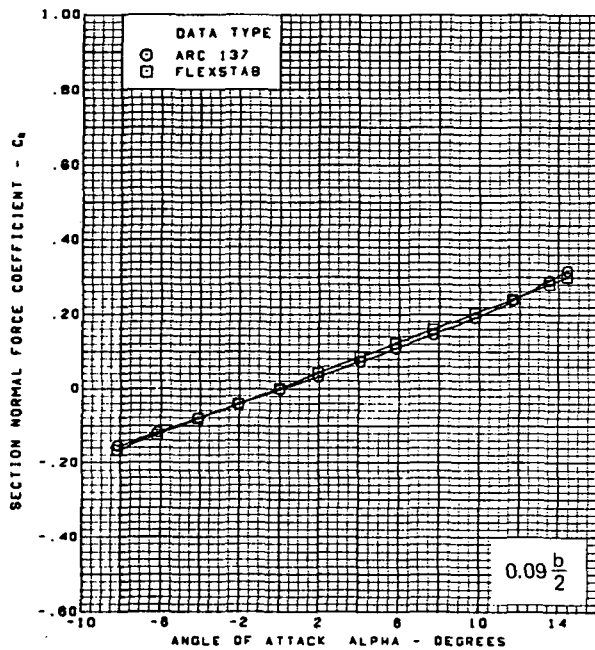
Figure 57.—(Continued)



$M = 2.50$  (run 22)  
 Flat wing, rounded L.E.  
 L.E. deflection, full span =  $0.0^\circ$   
 T.E. deflection, full span =  $0.0^\circ$

(f) (Concluded)

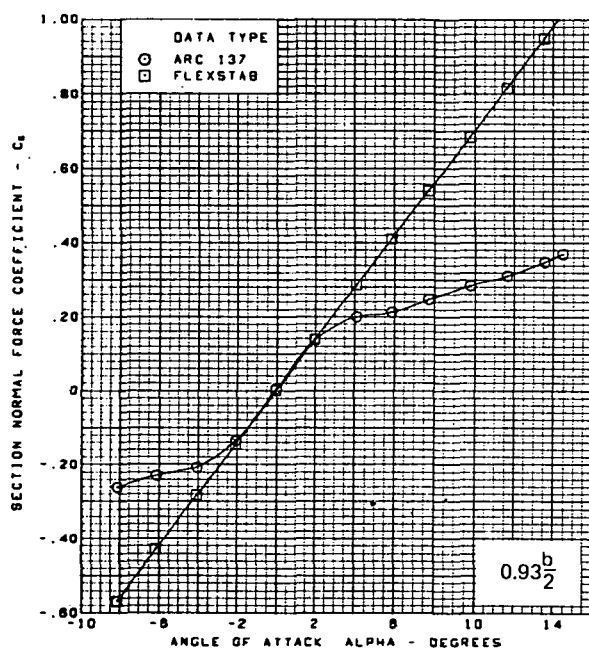
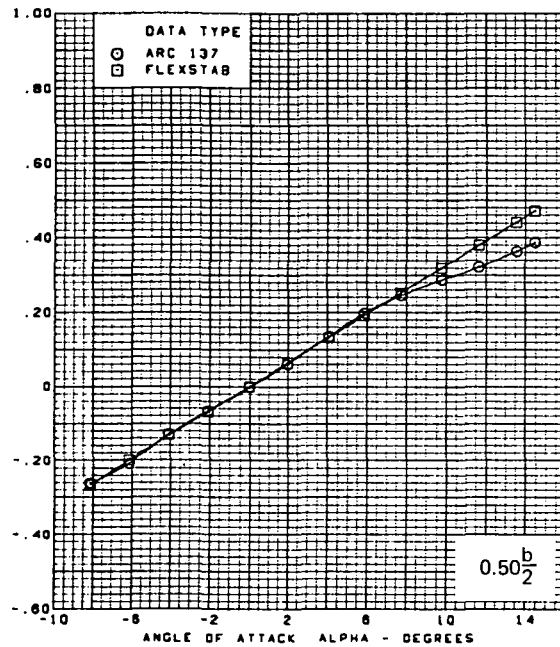
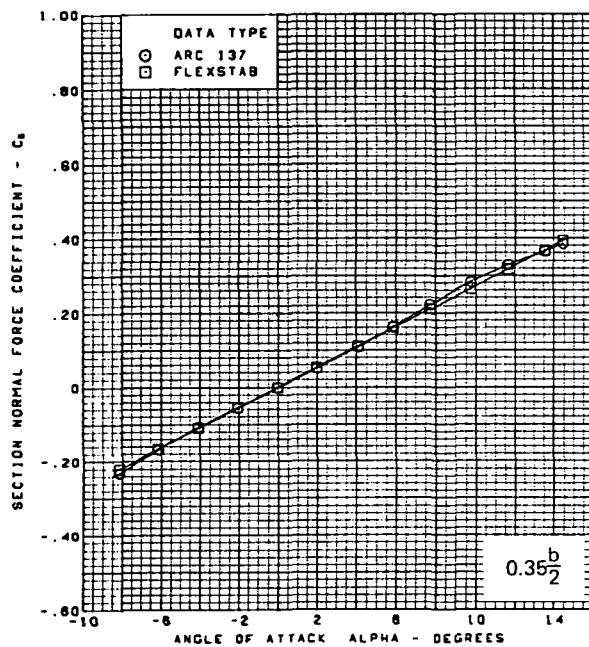
Figure 57.—(Continued)



(g) Section Aerodynamic Coefficients—Normal Force

Figure 57.—(Continued)

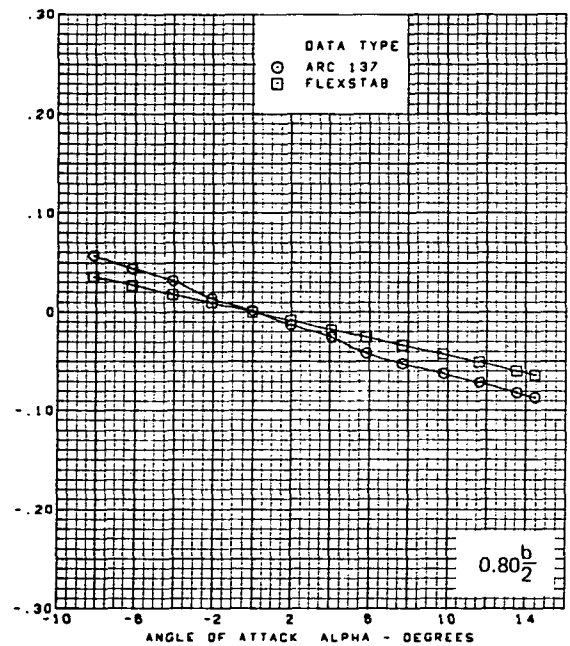
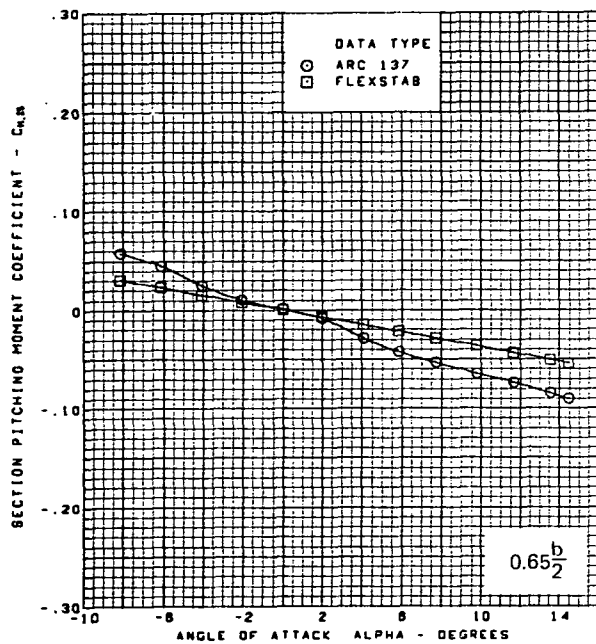
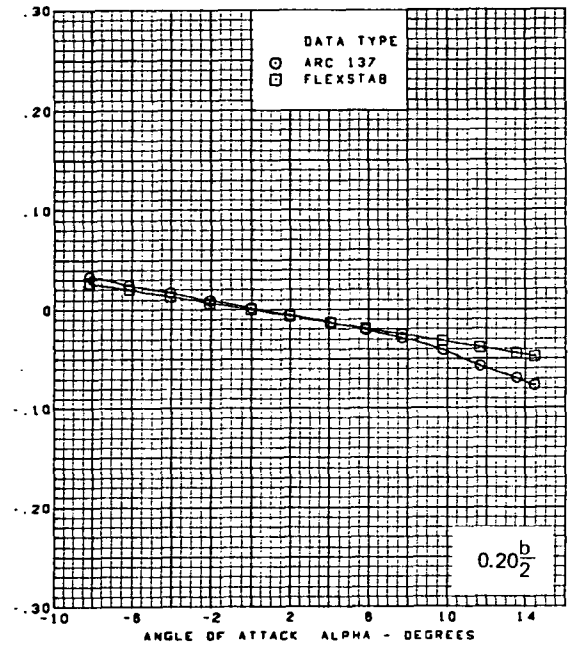
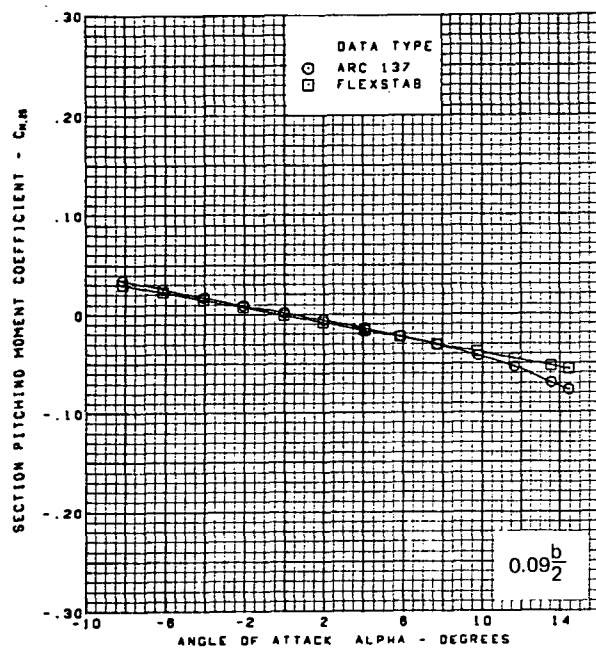




M = 2.50 (run 22)  
 Flat wing, rounded L.E.  
 L.E. deflection, full span =  $0.0^\circ$   
 T.E. deflection, full span =  $0.0^\circ$

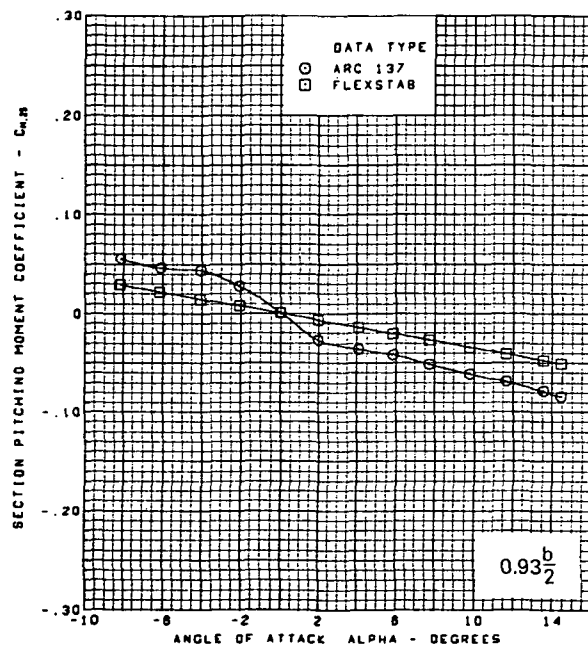
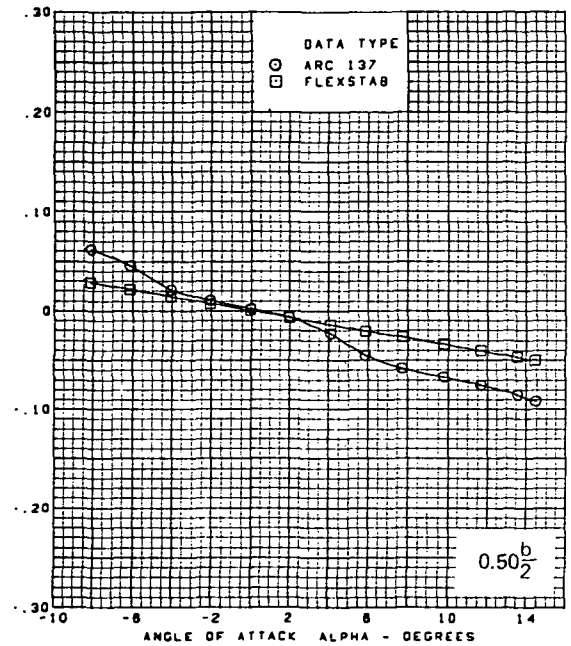
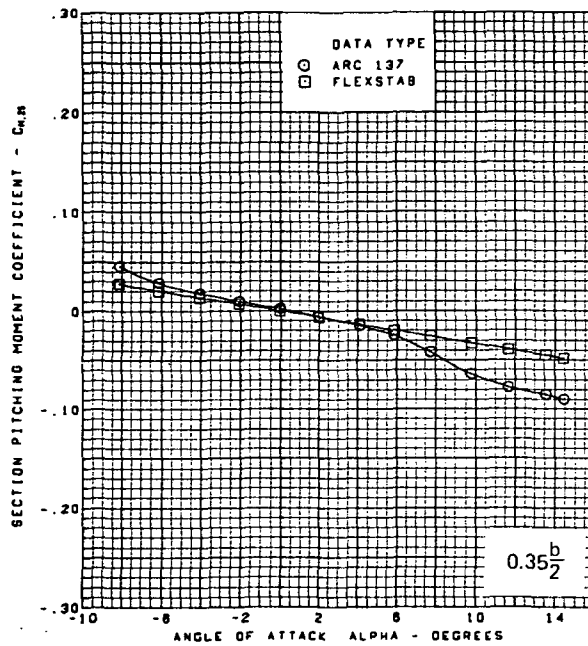
(g) (Concluded)

Figure 57.—(Continued)



(h) Section Aerodynamic Coefficients—Pitching Moment.

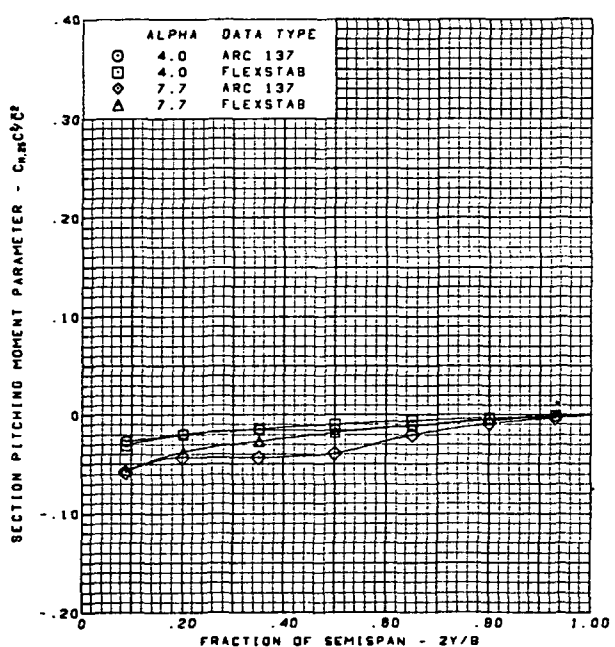
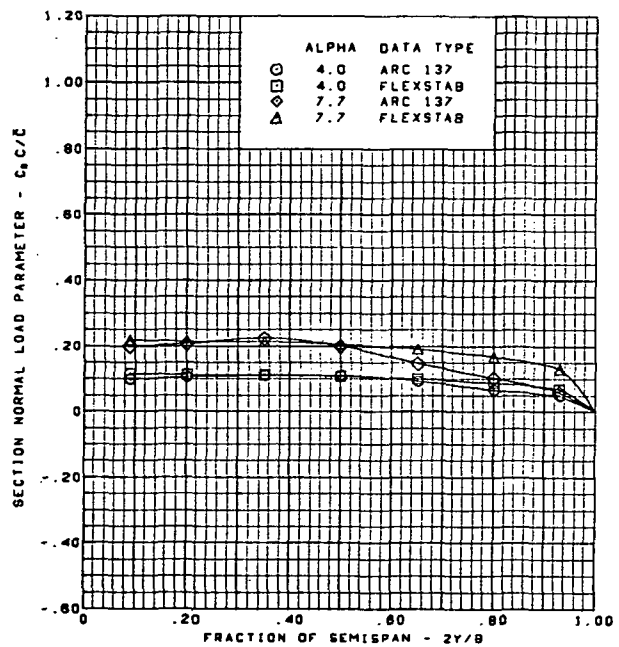
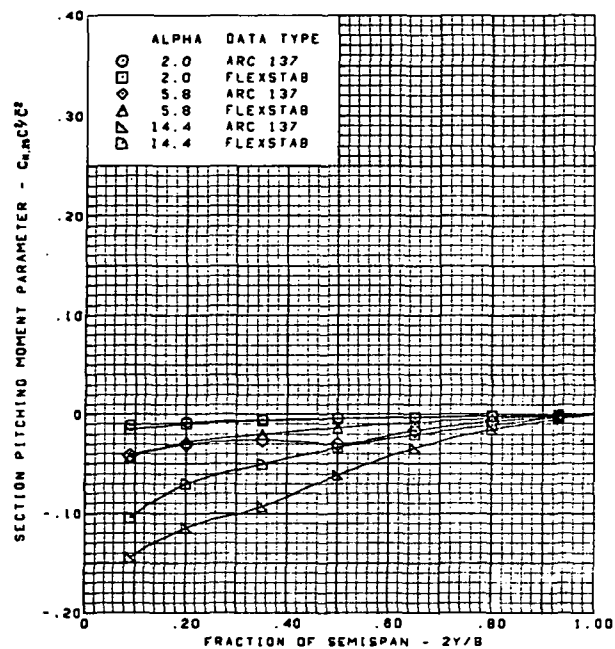
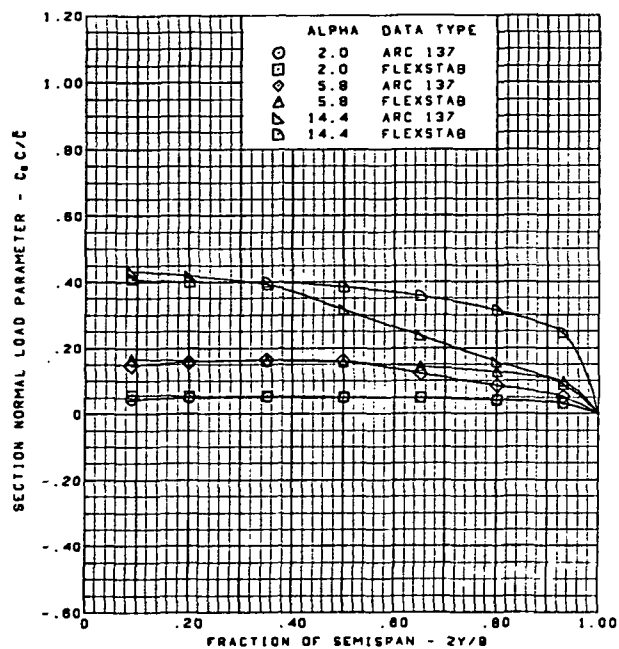
Figure 57.—(Continued)



M = 2.50 (run 22)  
 Flat wing, rounded L.E.  
 L.E. deflection, full span =  $0.0^\circ$   
 T.E. deflection, full span =  $0.0^\circ$

(h) (Concluded)

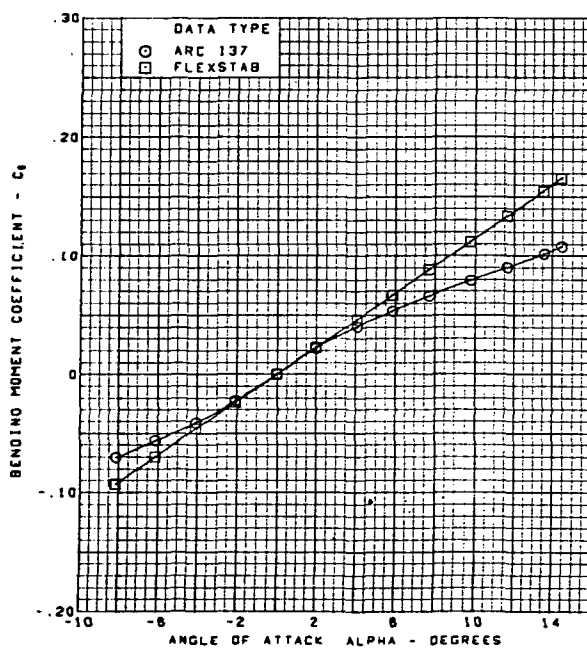
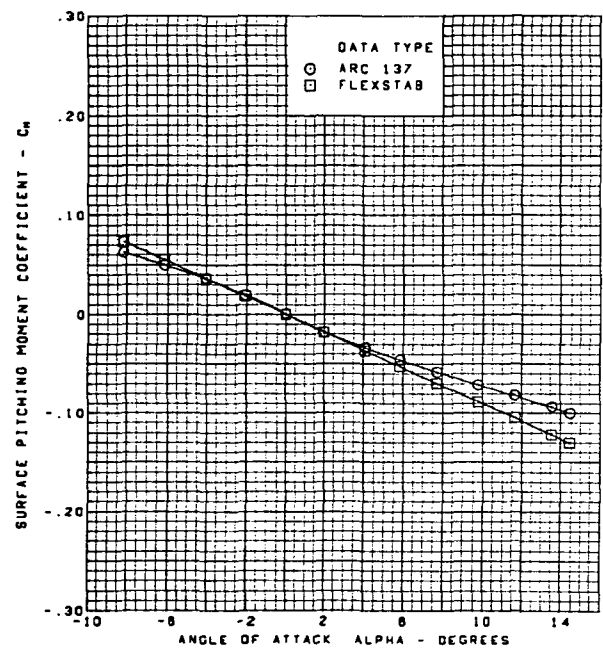
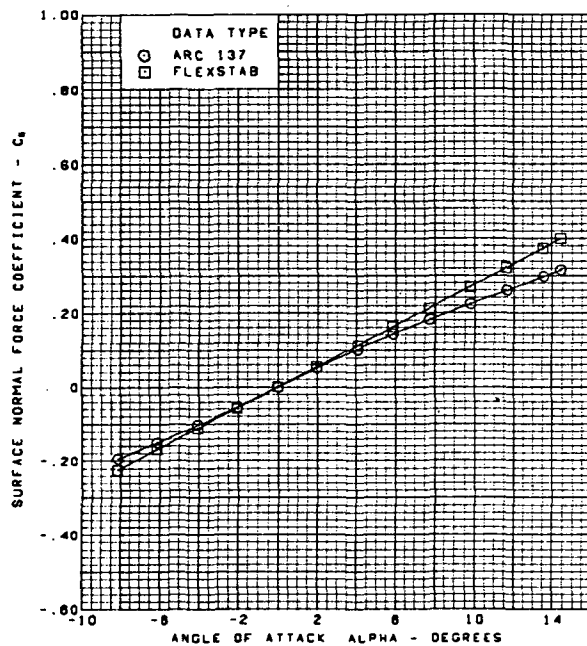
Figure 57.—(Continued)



$M = 2.50$  (run 22)  
 Flat wing, rounded L.E.  
 L.E. deflection, full span =  $0.0^\circ$   
 T.E. deflection, full span =  $0.0^\circ$

(i) Spanload Distributions

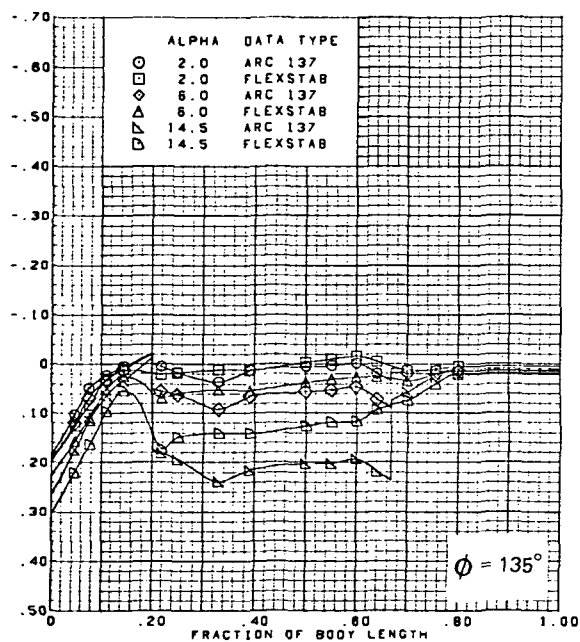
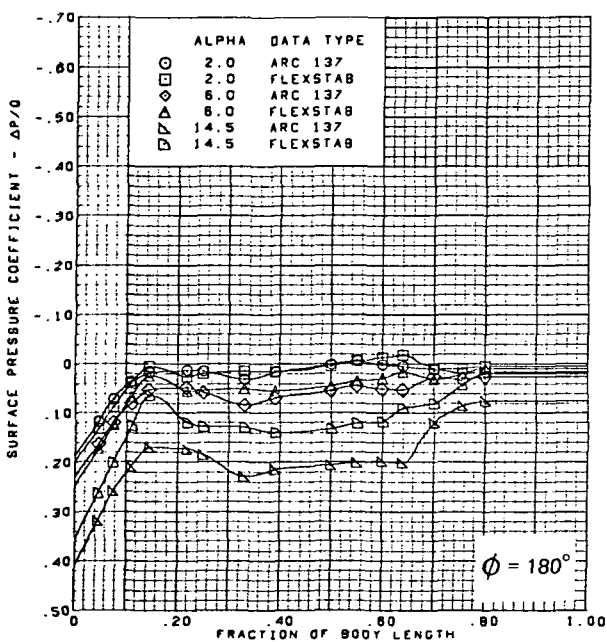
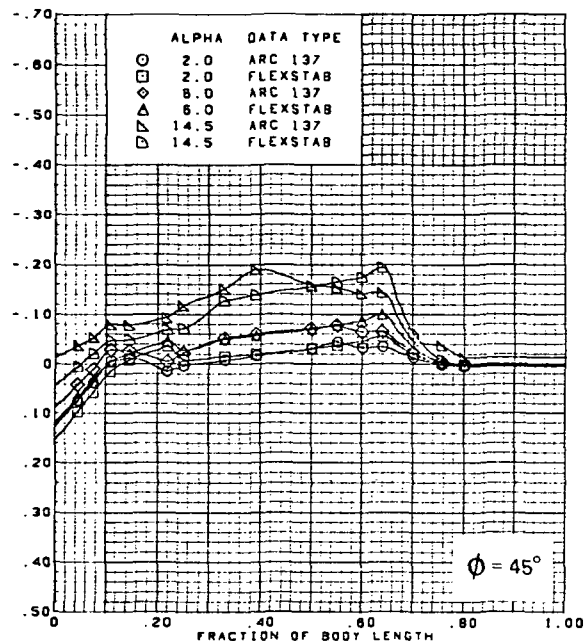
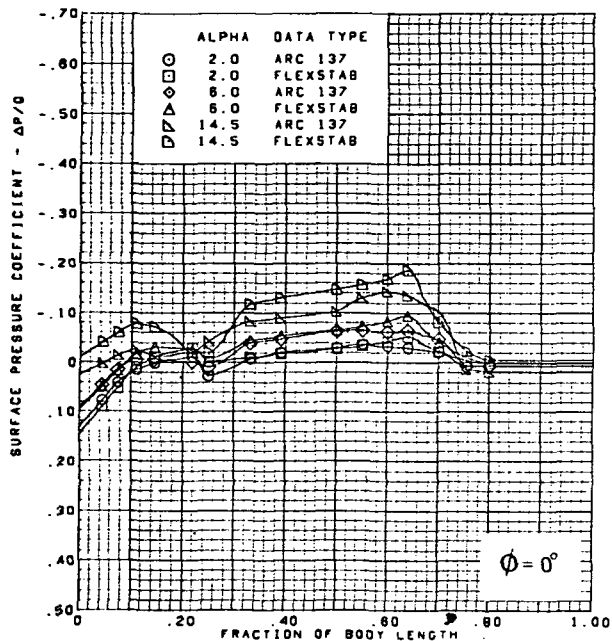
Figure 57.—(Continued)



$M = 2.50$  (run 22)  
 Flat wing, rounded L.E.  
 L.E. deflection, full span =  $0.0^\circ$   
 T.E. deflection, full span =  $0.0^\circ$

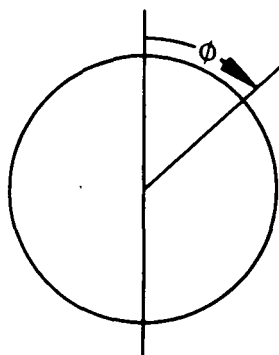
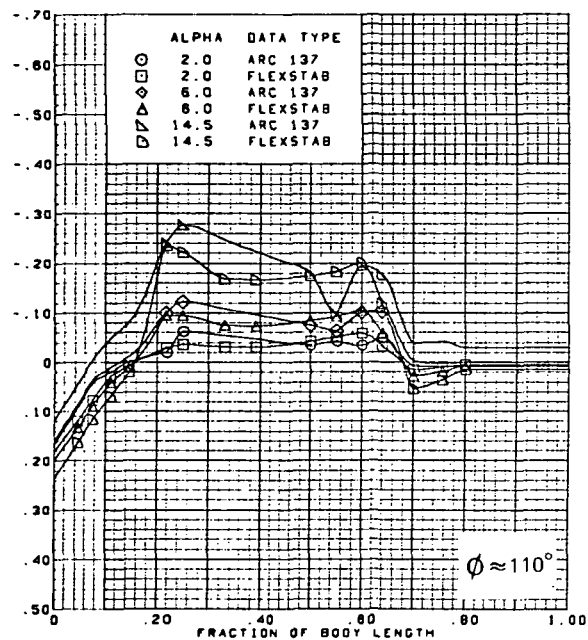
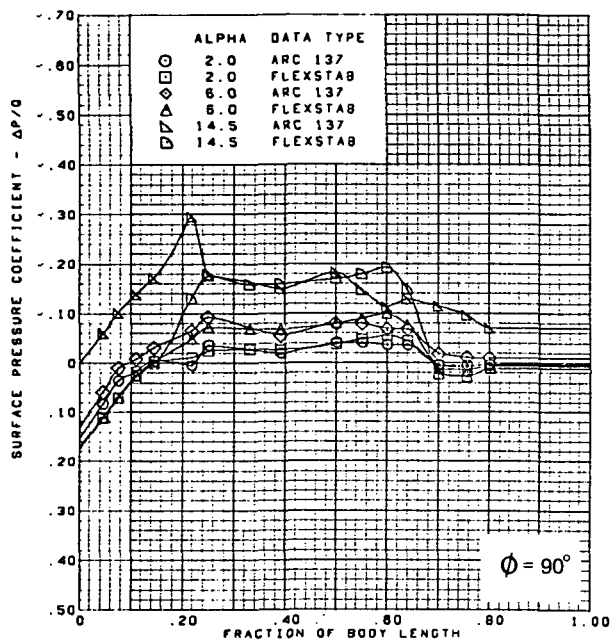
(j) Wing Aerodynamic Coefficients

Figure 57.—(Concluded)



(a)  $\alpha = 2^\circ, 6^\circ, 15^\circ$

Figure 58.—Body Theory-to-Experiment Comparison—Flat Wing, Rounded L.E.; L.E. Deflection, Full Span =  $0.0^\circ$ ; T.E. Deflection, Full Span =  $0.0^\circ$ ;  $M = 1.70$

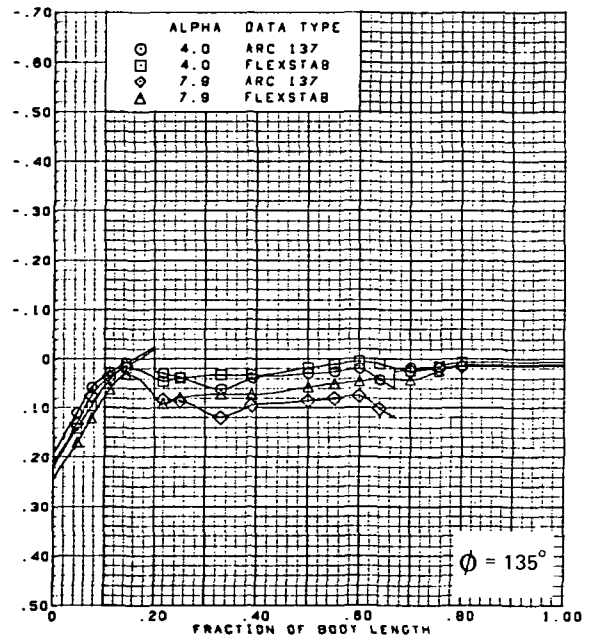
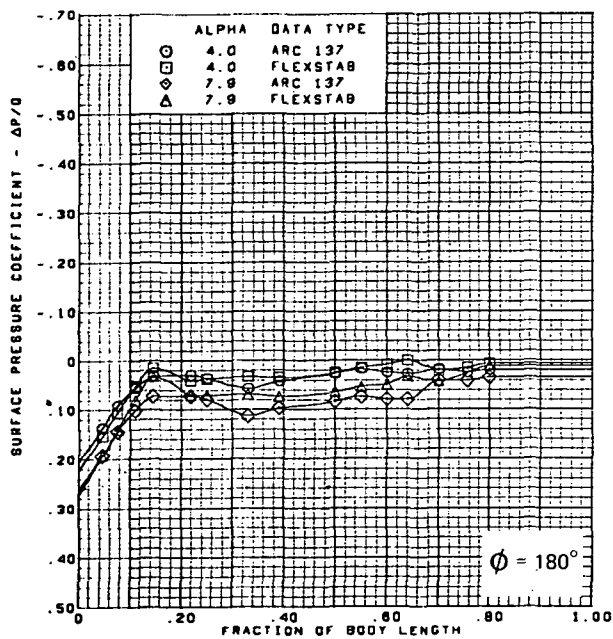
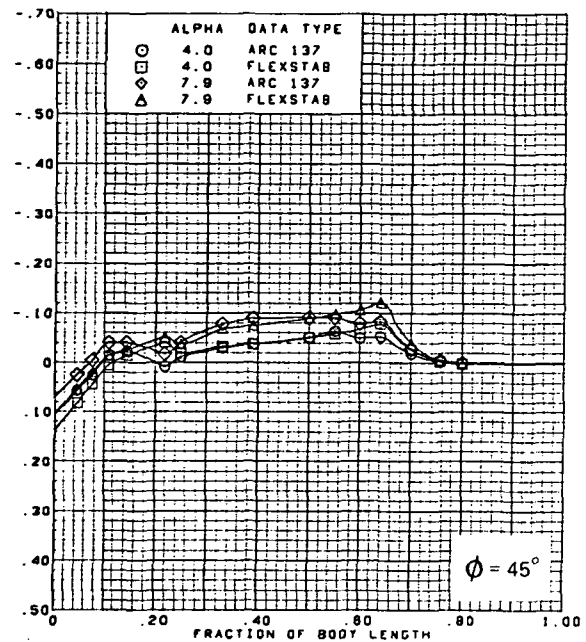
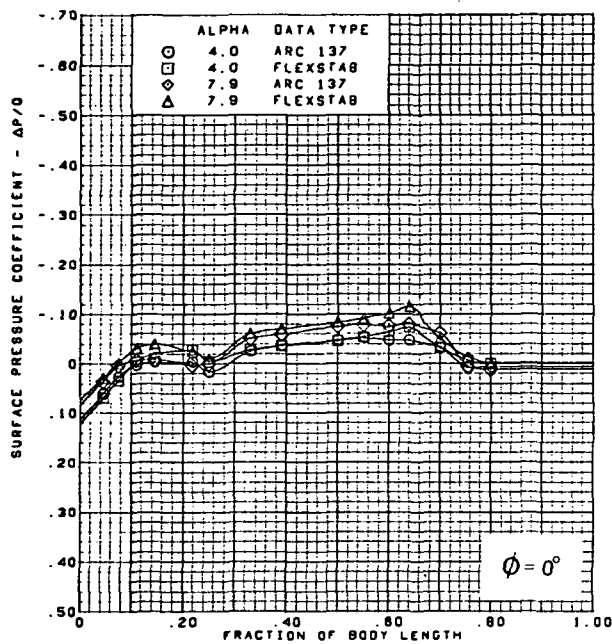


M = 1.70 (run 20)  
 Flat wing, rounded L.E.  
 L.E. deflection, full span =  $0.0^\circ$   
 T.E. deflection, full span =  $0.0^\circ$

Note:  $C_{p, \text{vacuum}} = -0.49$

(a) (Concluded)

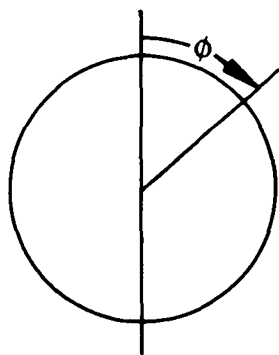
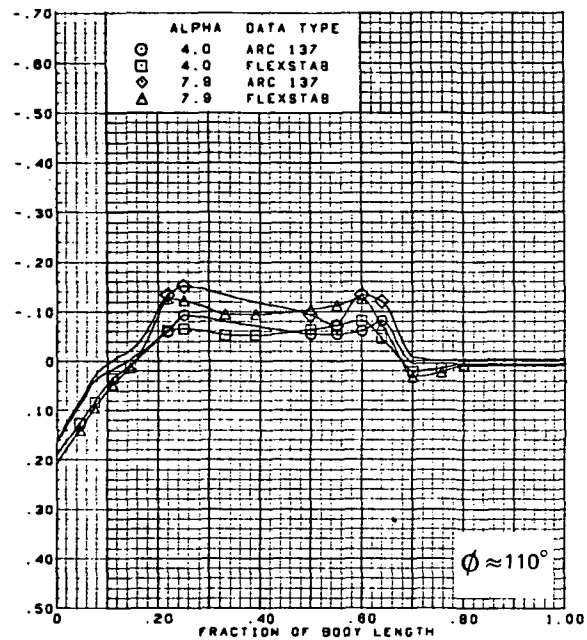
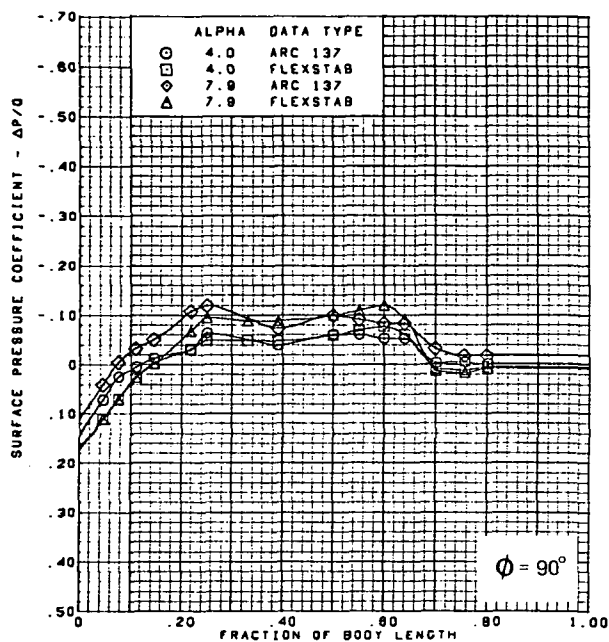
Figure 58.—(Continued)



(b)  $\alpha = 4^\circ, 8^\circ$

Figure 58.—(Continued)



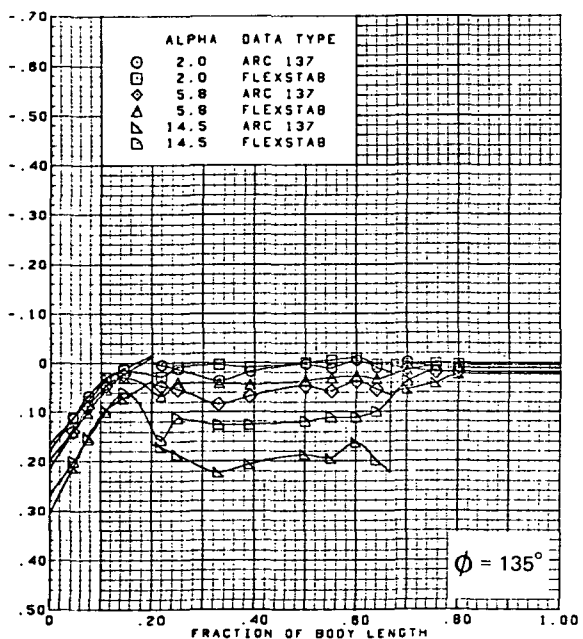
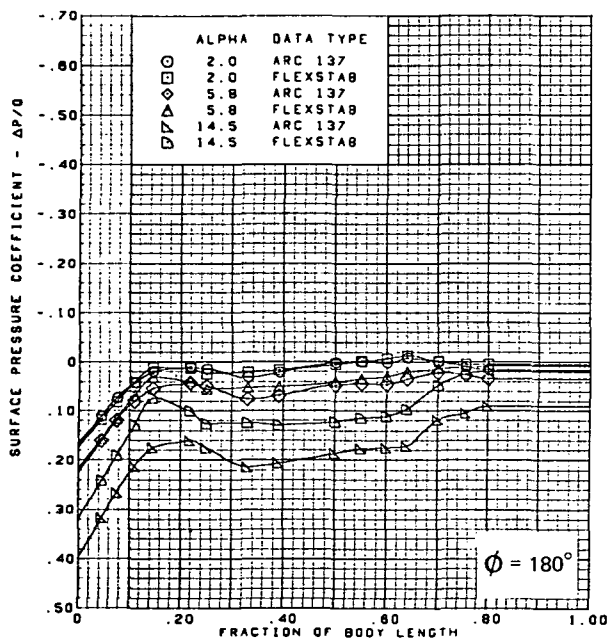
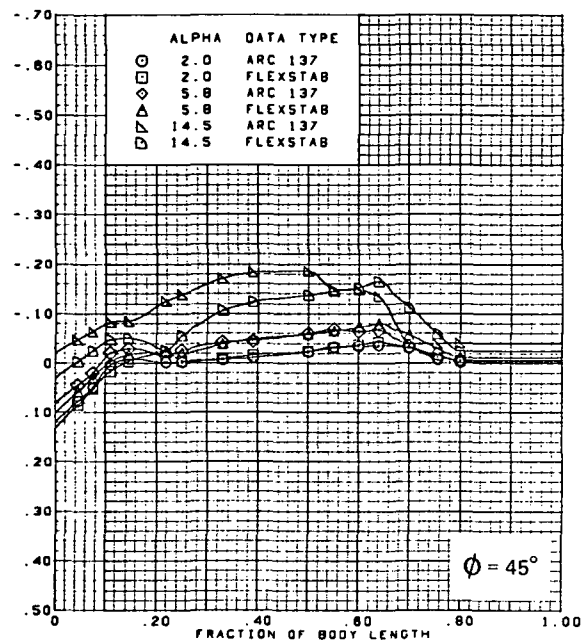
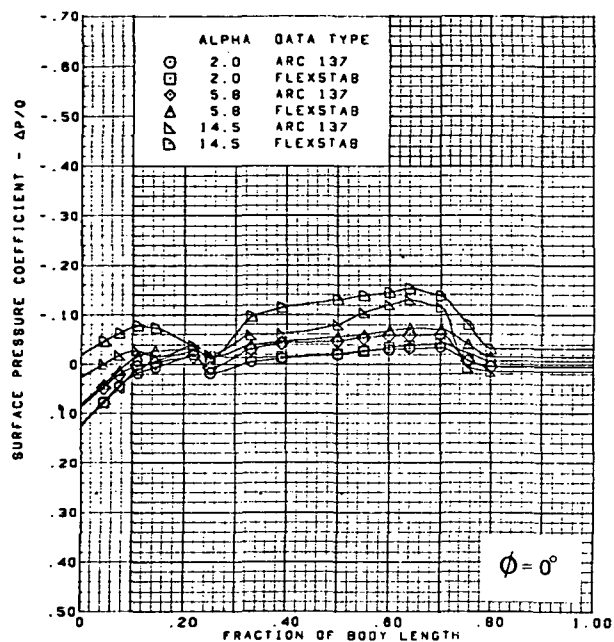


M = 1.70 (run 20)  
 Flat wing, rounded L.E.  
 L.E. deflection, full span =  $0.0^\circ$   
 T.E. deflection, full span =  $0.0^\circ$

Note:  $C_{p, \text{vacuum}} = -0.49$

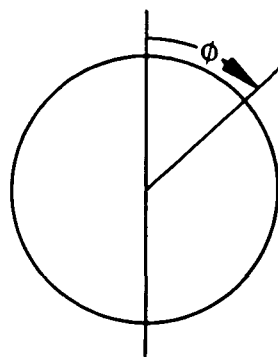
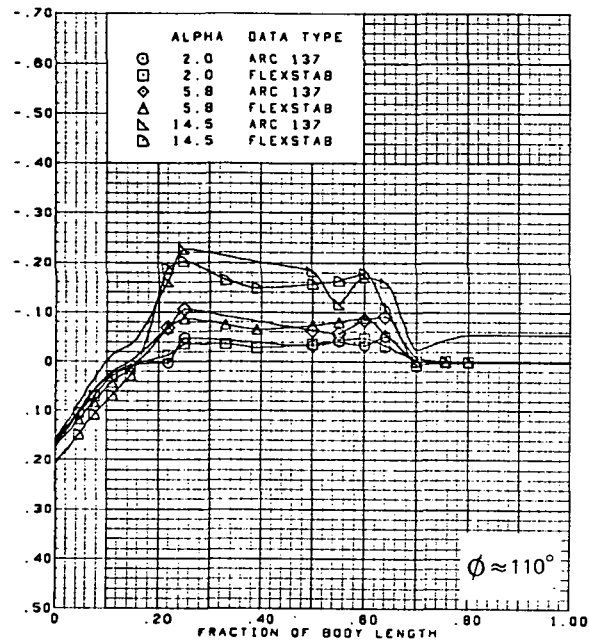
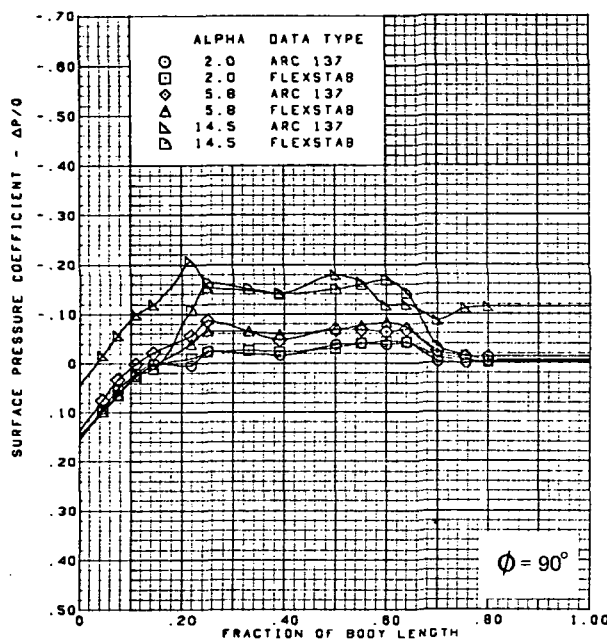
(b) (Concluded)

Figure 58. —(Concluded)



(a)  $\alpha = 2^\circ, 6^\circ, 15^\circ$

Figure 59.—Body Theory-to-Experiment Comparison—Flat Wing, Rounded L.E.; L.E. Deflection, Full Span =  $0.0^\circ$ ; T.E. Deflection, Full Span =  $0.0^\circ$ ;  $M = 2.10$

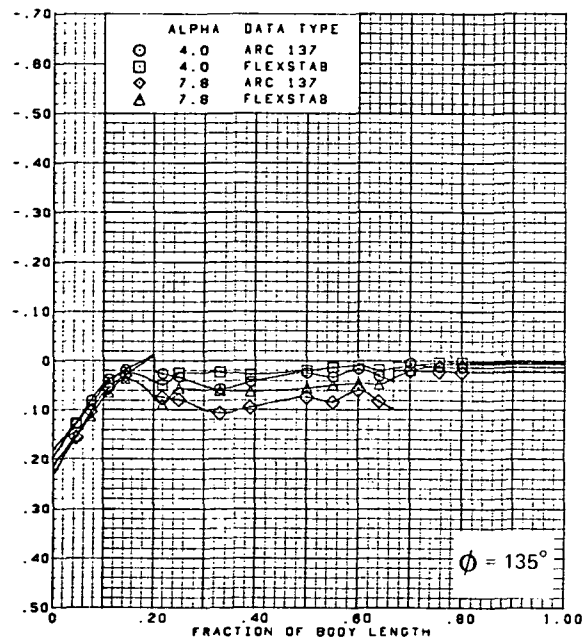
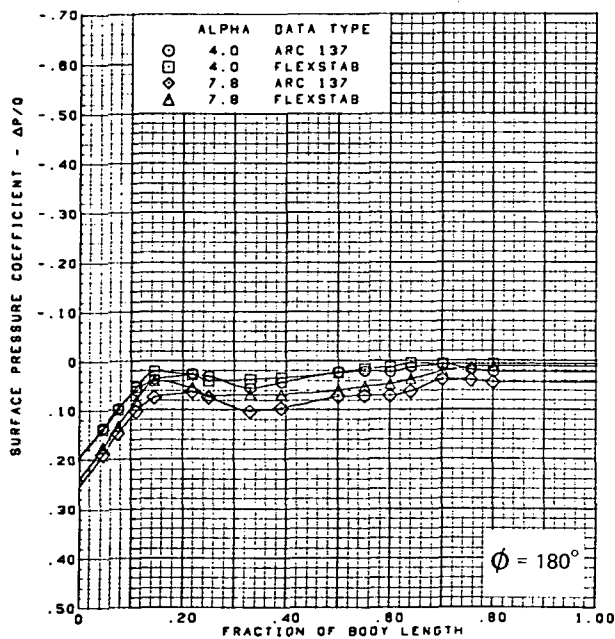
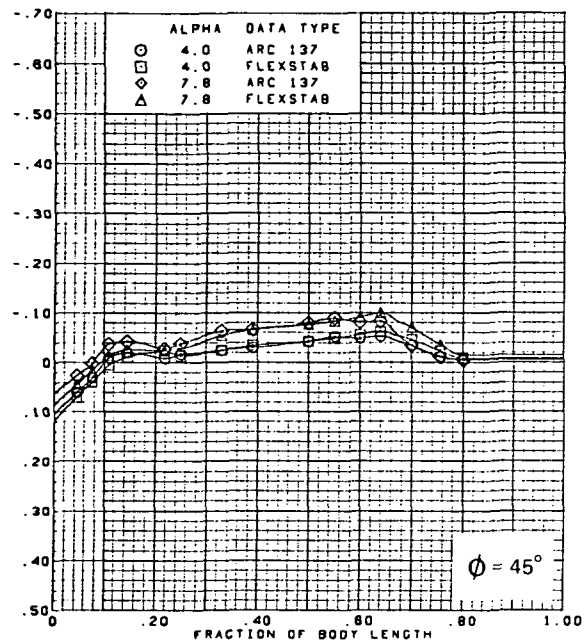
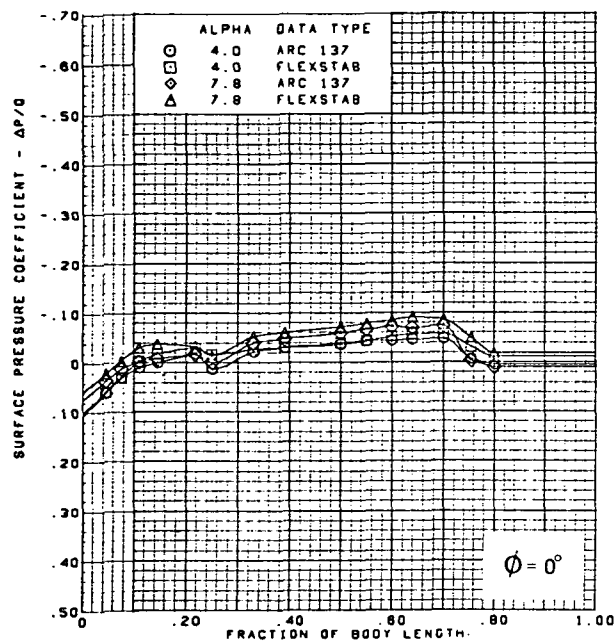


$M = 2.10$  (run 21)  
 Flat wing, rounded L.E.  
 L.E. deflection, full span =  $0.0^\circ$   
 T.E. deflection, full span =  $0.0^\circ$

Note:  $C_{p, \text{vacuum}} = -0.32$

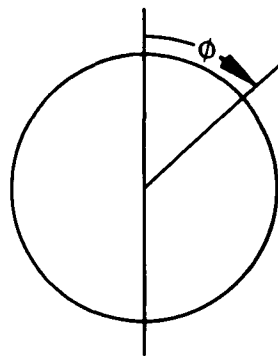
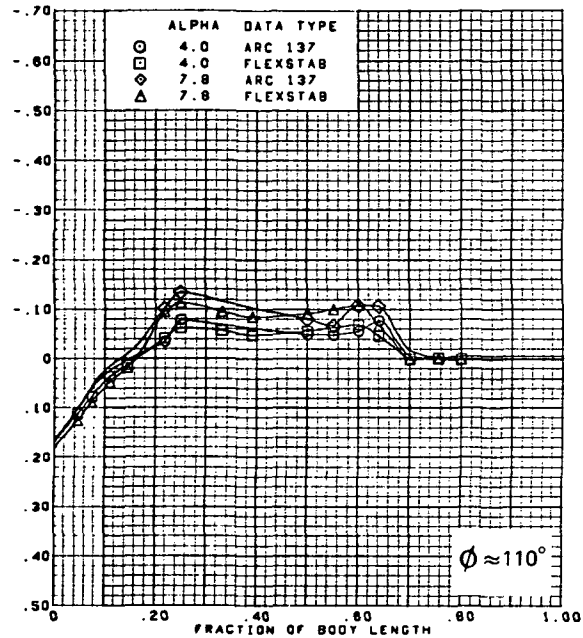
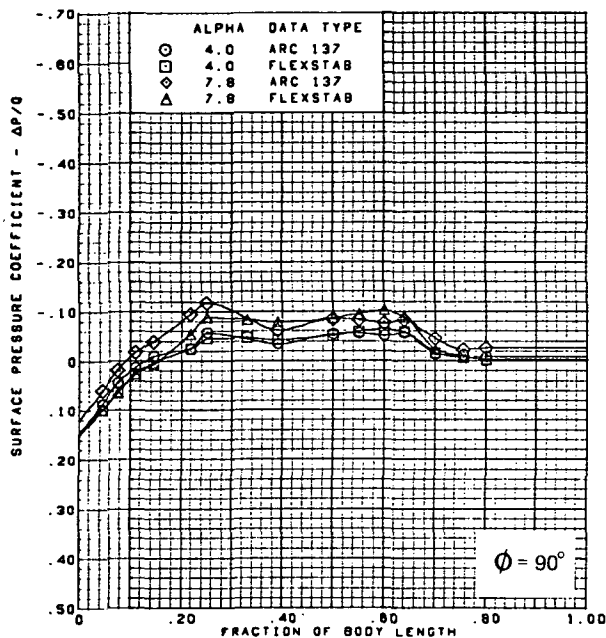
(a) (Concluded)

Figure 59.—(Continued)



(b)  $\alpha = 4^\circ, 8^\circ$

Figure 59.-(Continued)

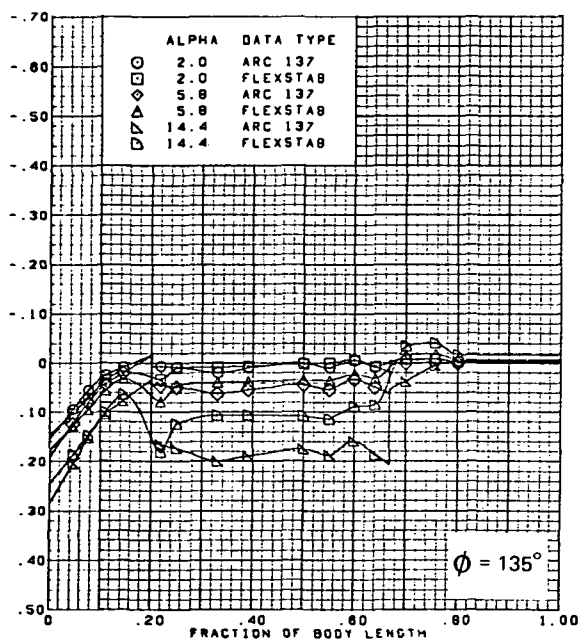
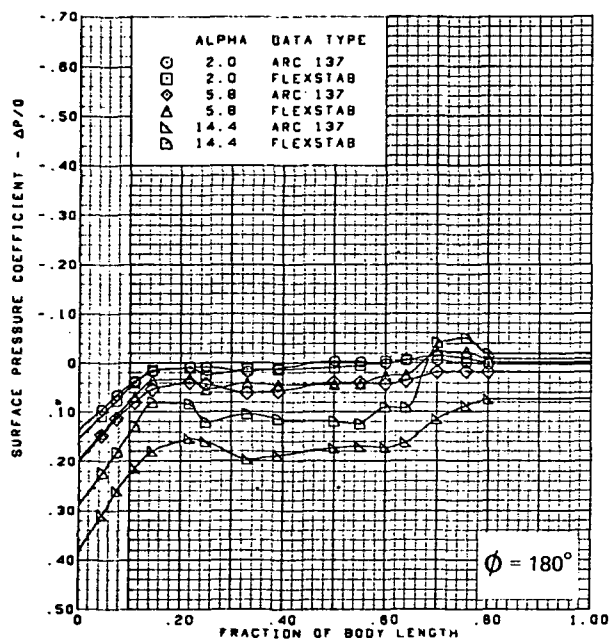
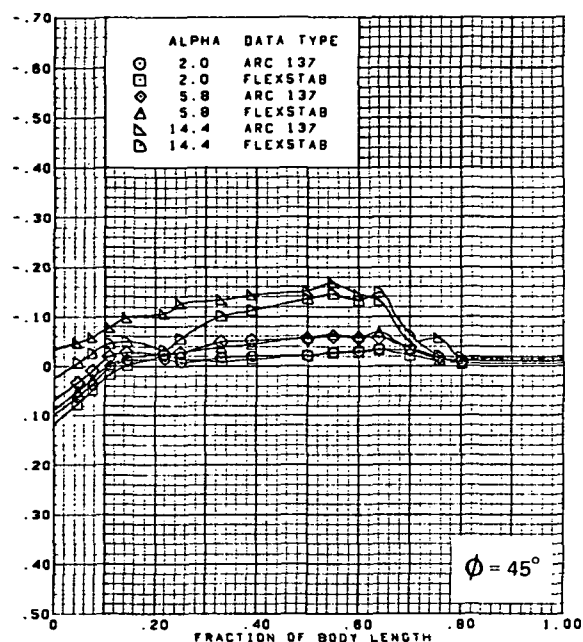
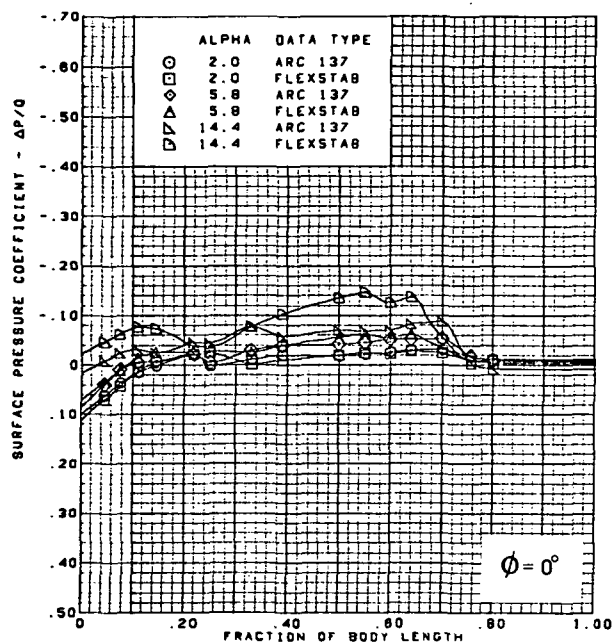


M = 2.10 (run 21)  
 Flat wing, rounded L.E.  
 L.E. deflection, full span =  $0.0^\circ$   
 T.E. deflection, full span =  $0.0^\circ$

Note:  $C_{p, \text{vacuum}} = -0.32$

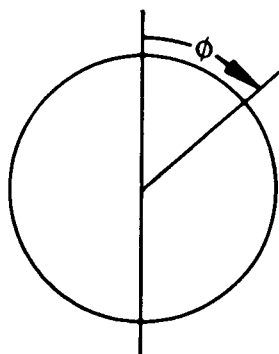
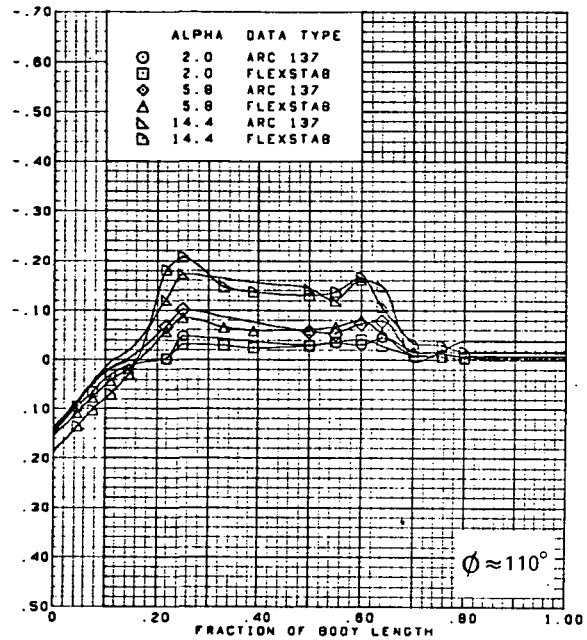
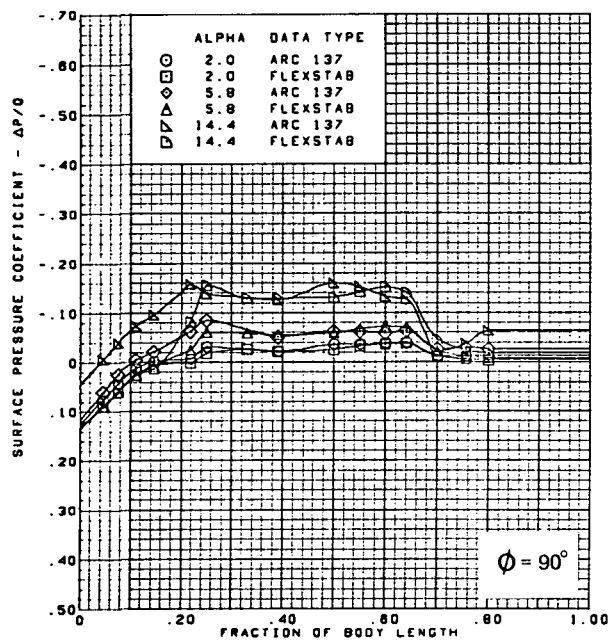
(b) (Concluded)

Figure 59.—(Concluded)



(a)  $\alpha = 2^\circ, 6^\circ, 15^\circ$

Figure 60.—Body Theory-to-Experiment Comparison—Flat Wing, Rounded L.E.; L.E. Deflection, Full Span =  $0.0^\circ$ ; T.E. Deflection, Full Span =  $0.0^\circ$ ;  $M = 2.50$

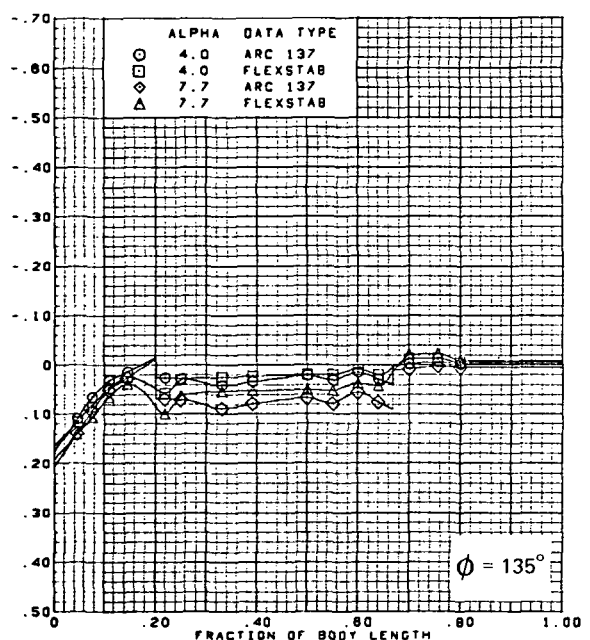
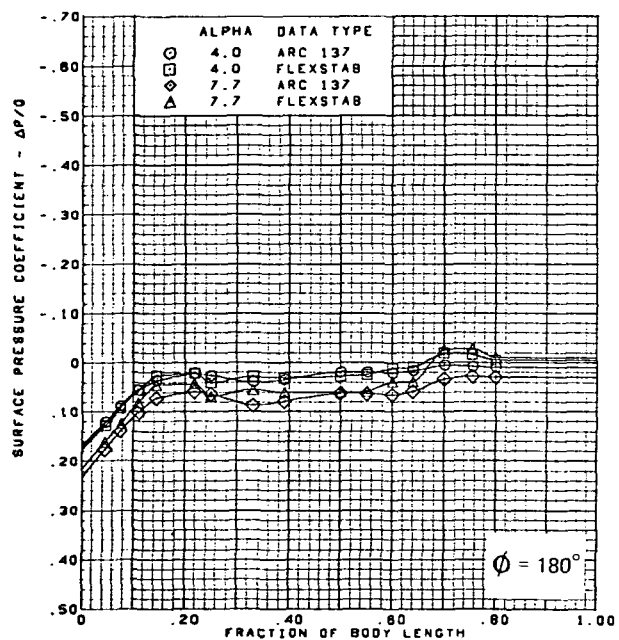
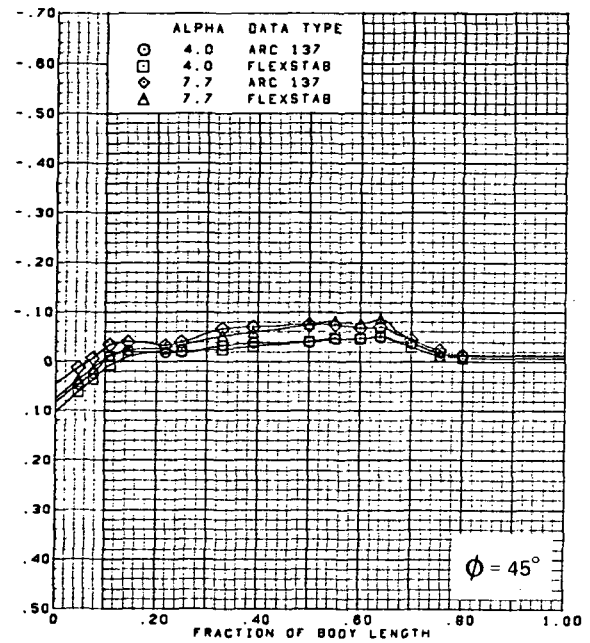
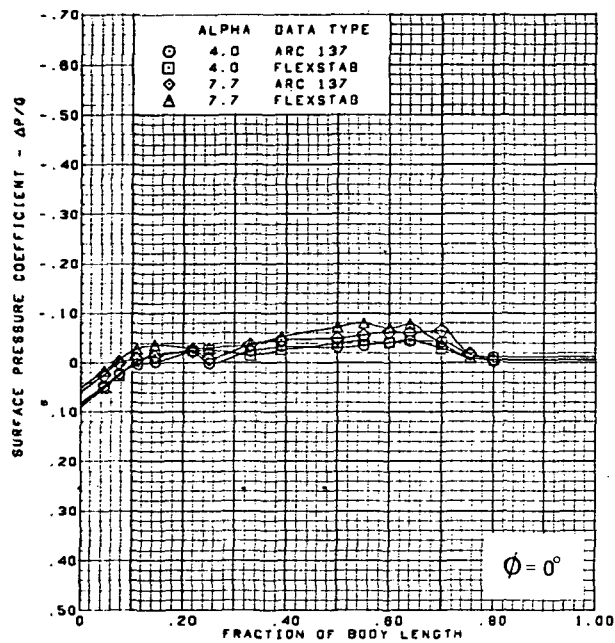


M = 2.50 (run 22)  
 Flat wing, rounded L.E.  
 L.E. deflection, full span =  $0.0^\circ$   
 T.E. deflection, full span =  $0.0^\circ$

Note:  $C_{p, \text{vacuum}} = -0.23$

(a) (Concluded)

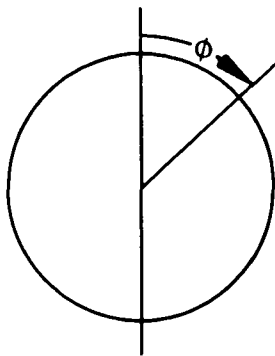
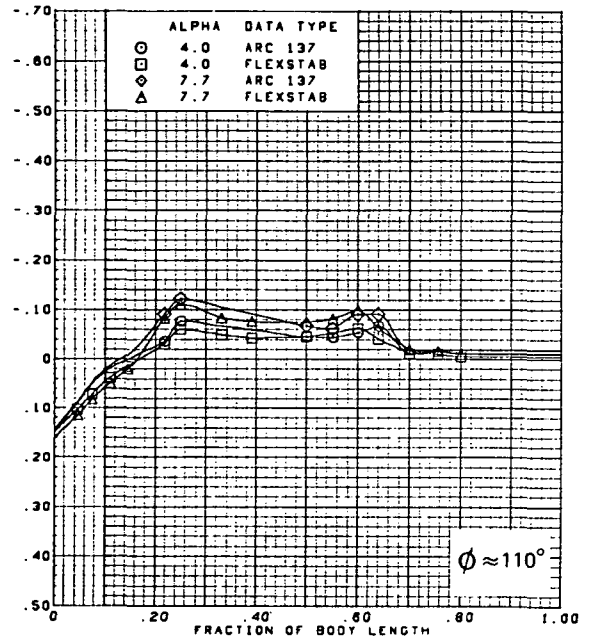
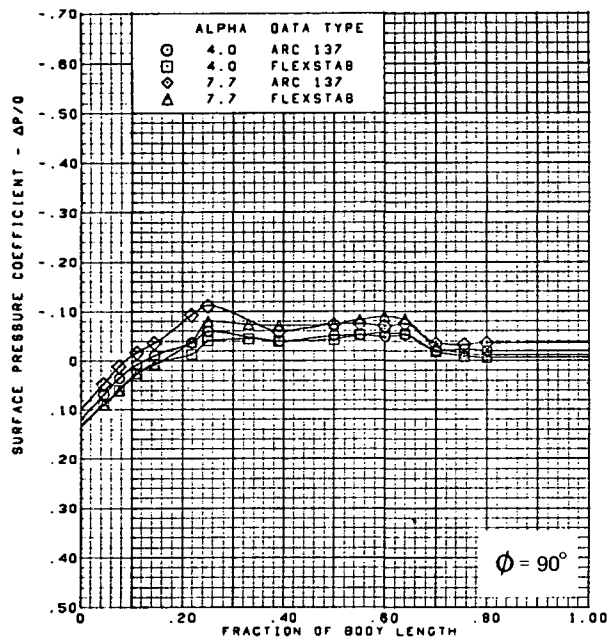
Figure 60.—(Continued)



(b)  $\alpha = 4^\circ, 8^\circ$

Figure 60. —(Continued)



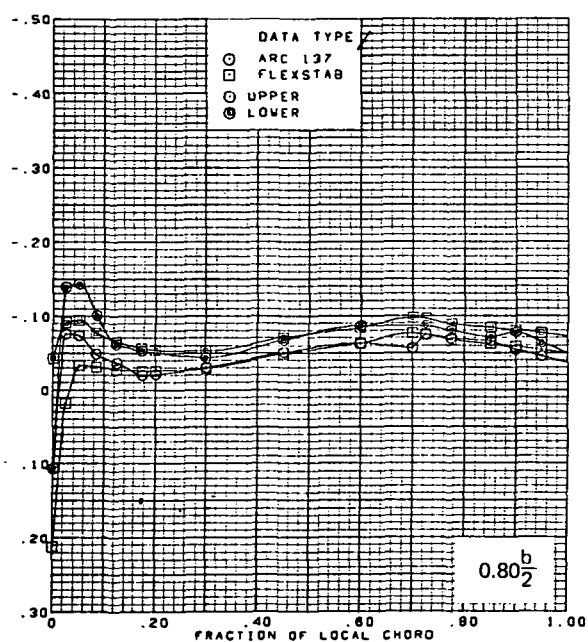
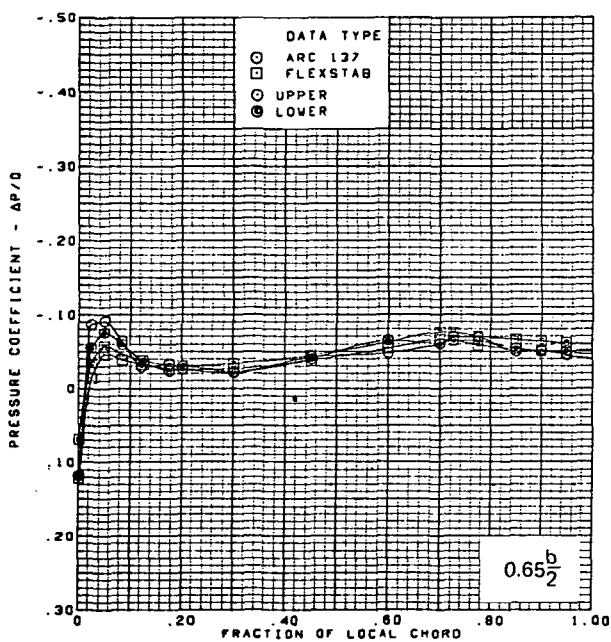
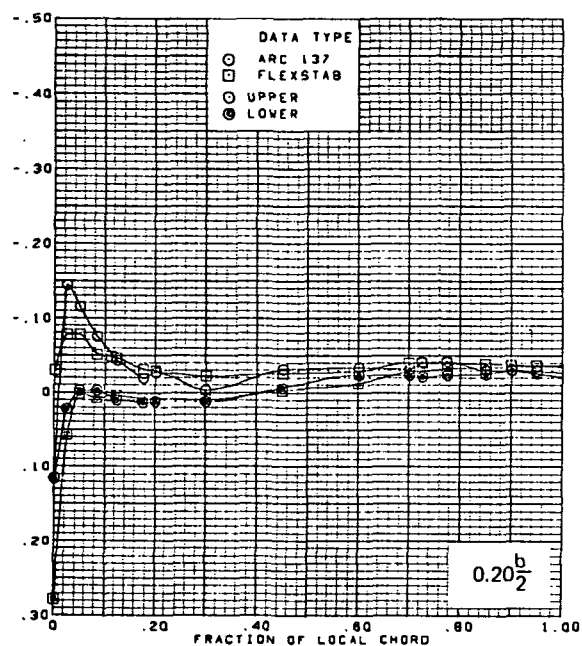
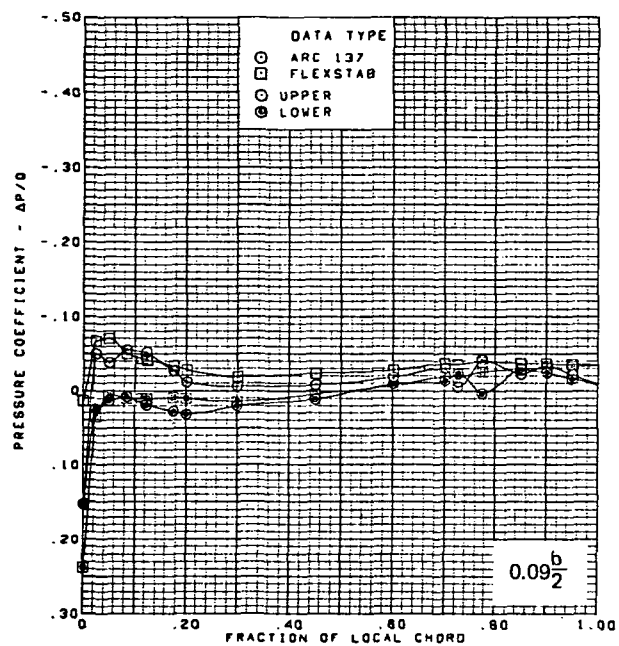


$M = 2.50$  (run 22)  
 Flat wing, rounded L.E.  
 L.E. deflection, full span =  $0.0^\circ$   
 T.E. deflection, full span =  $0.0^\circ$

Note:  $C_{p, \text{vacuum}} = -0.23$

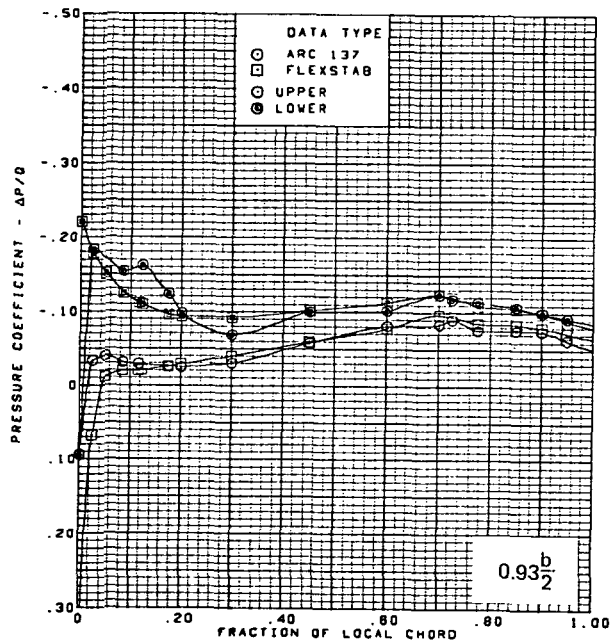
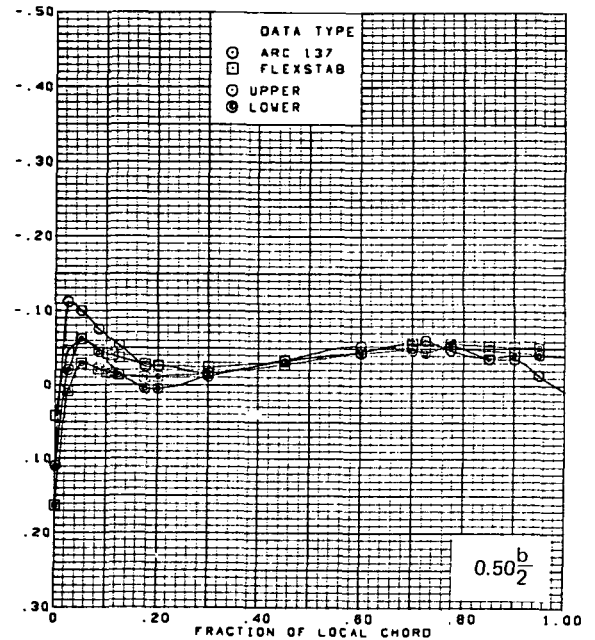
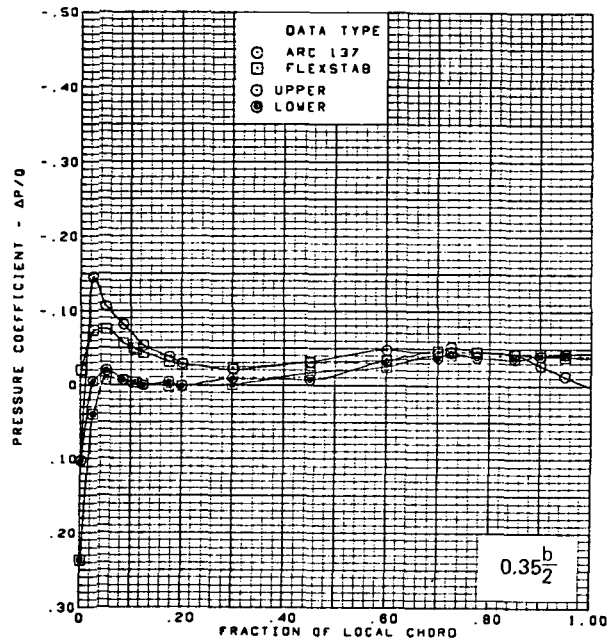
(b) (Concluded)

Figure 60.—(Concluded)



(a) Surface Chordwise Pressure Distributions,  $\alpha = 2^\circ$

Figure 61.—Wing Theory-to-Experiment Comparison—Twisted Wing, Rounded L.E.; L.E. Deflection, Full Span =  $0.0^\circ$ ; T.E. Deflection, Full Span =  $0.0^\circ$ ;  $M = 1.70$

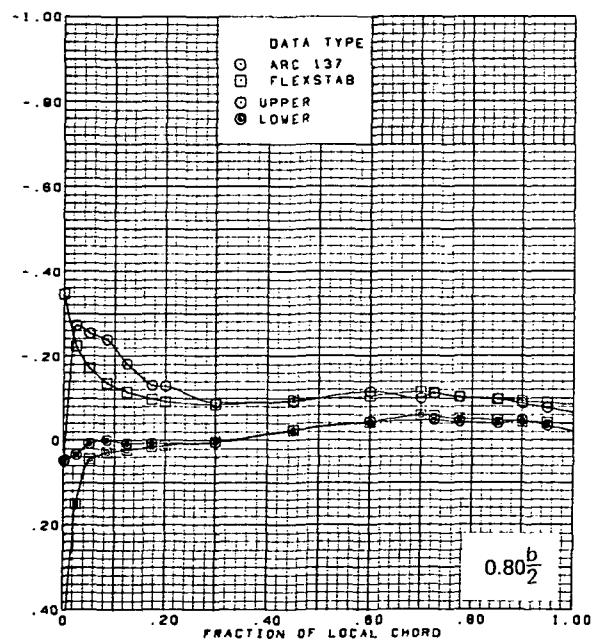
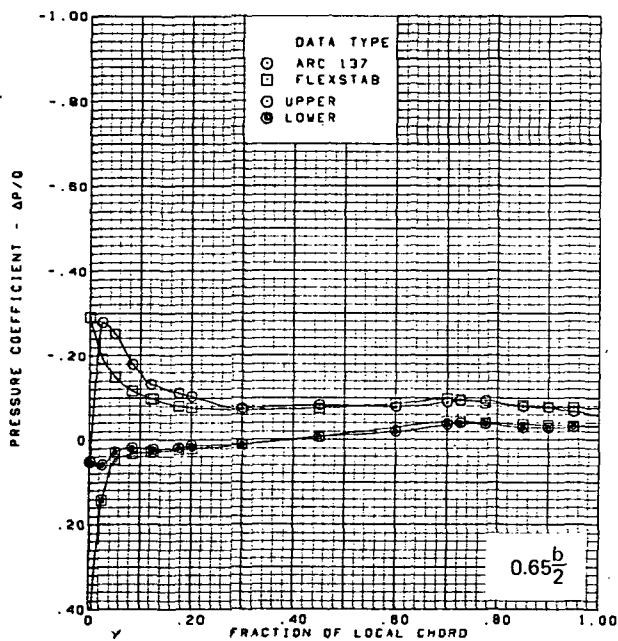
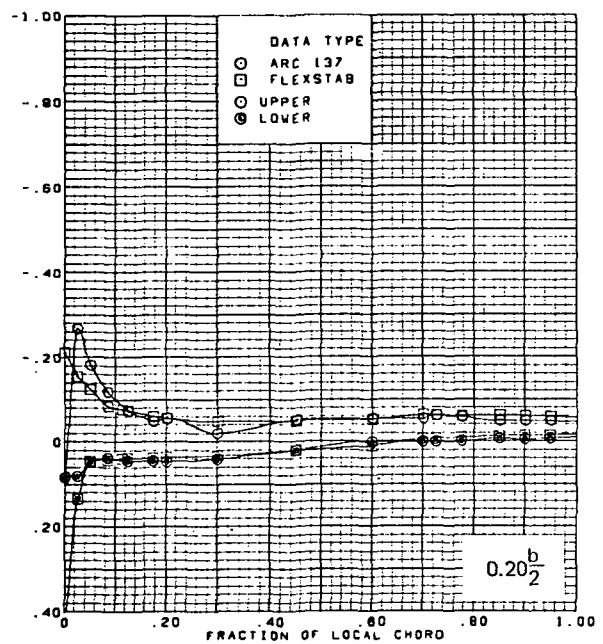
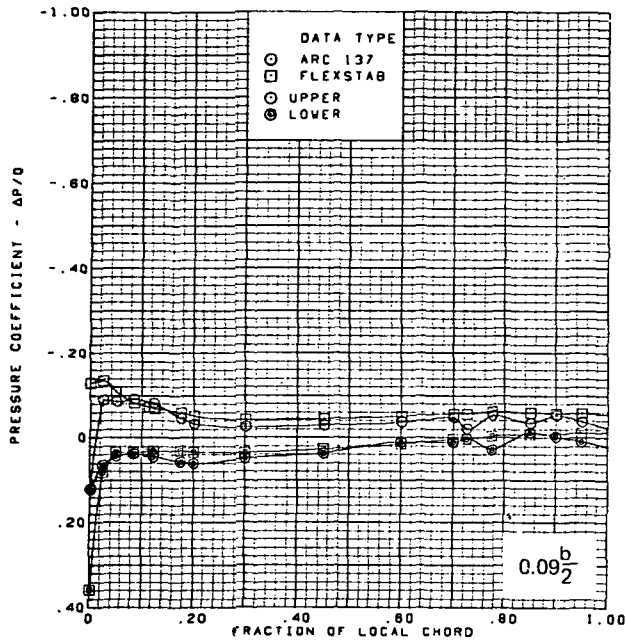


$M = 1.70$  (run 3)  
 $\alpha = 2^\circ$   
 Twisted wing, rounded L.E.  
 L.E. deflection, full span =  $0.0^\circ$   
 T.E. deflection, full span =  $0.0^\circ$

Note:  $C_{p, \text{vacuum}} = -0.49$

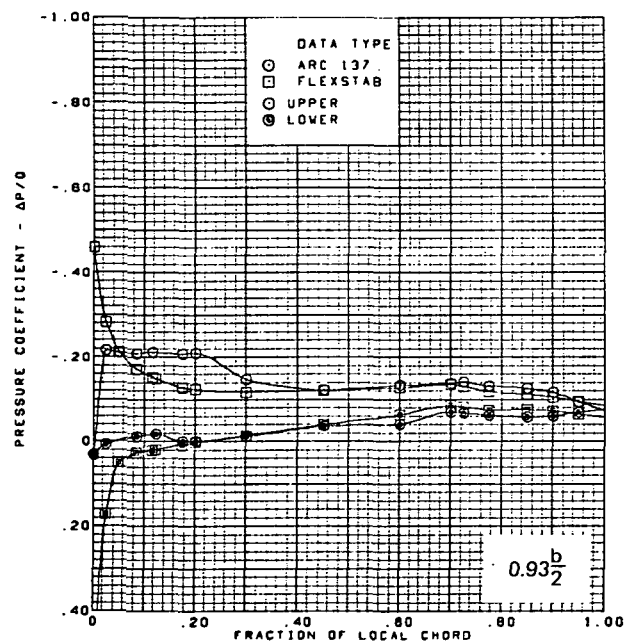
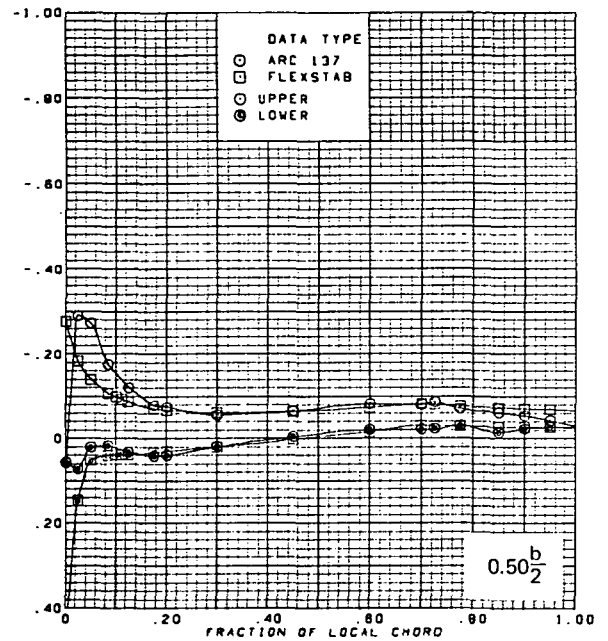
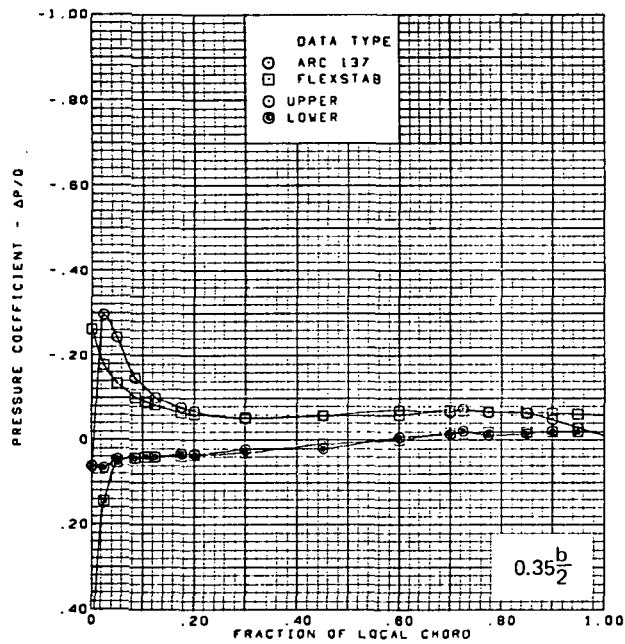
(a) (Concluded)

Figure 61.—(Continued)



(b) Surface Chordwise Pressure Distributions,  $\alpha = 4^\circ$

Figure 61. —(Continued)

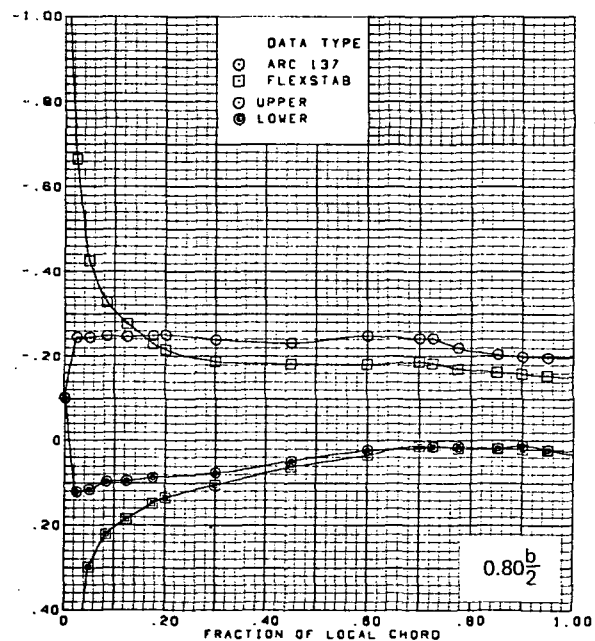
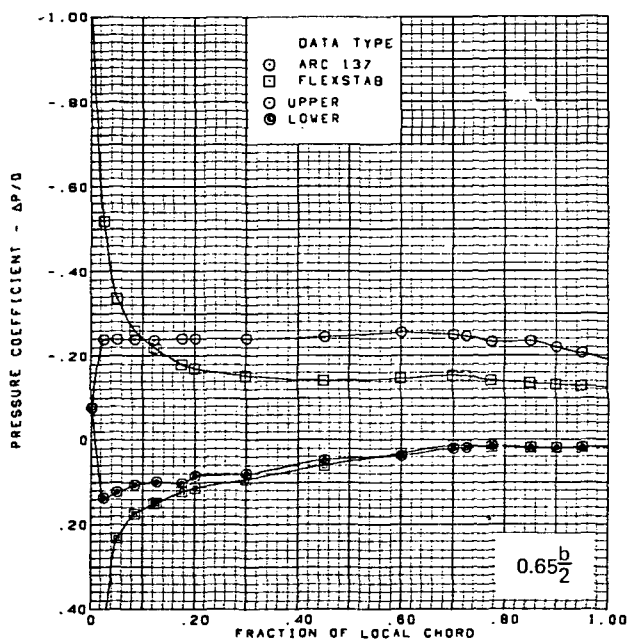
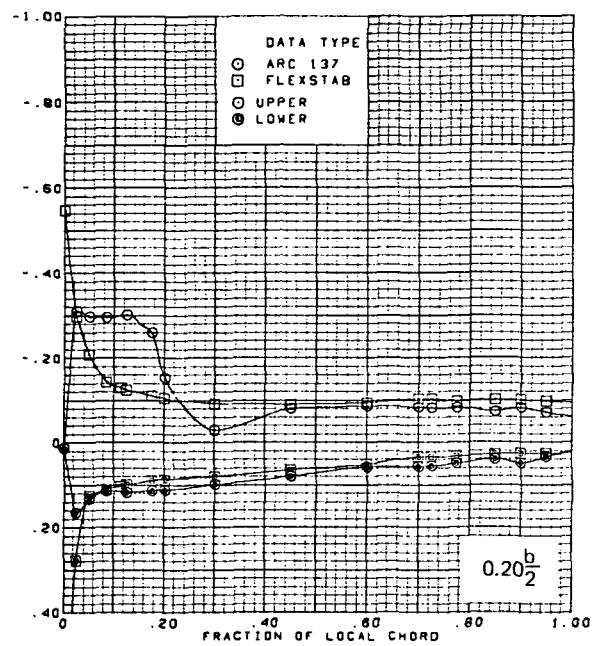
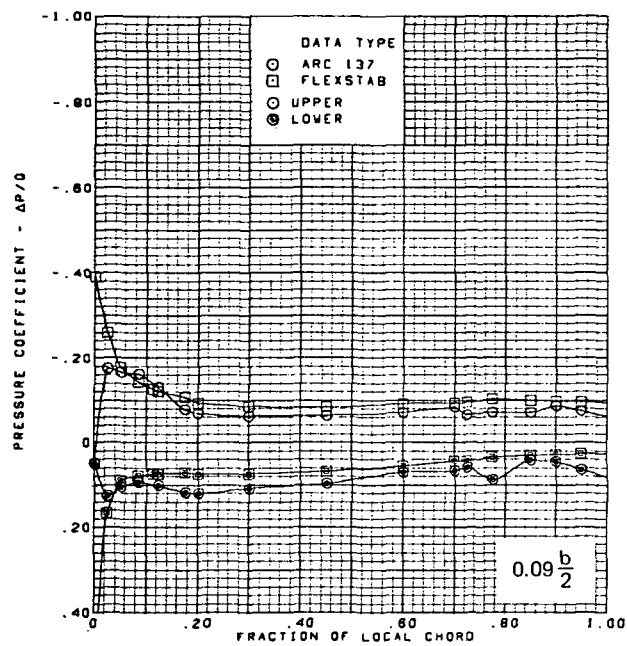


$M = 1.70$  (run 3)  
 $\alpha = 4^\circ$   
 Twisted wing, rounded L.E.  
 L.E. deflection, full span =  $0.0^\circ$   
 T.E. deflection, full span =  $0.0^\circ$

Note:  $C_{p, \text{vacuum}} = -0.49$

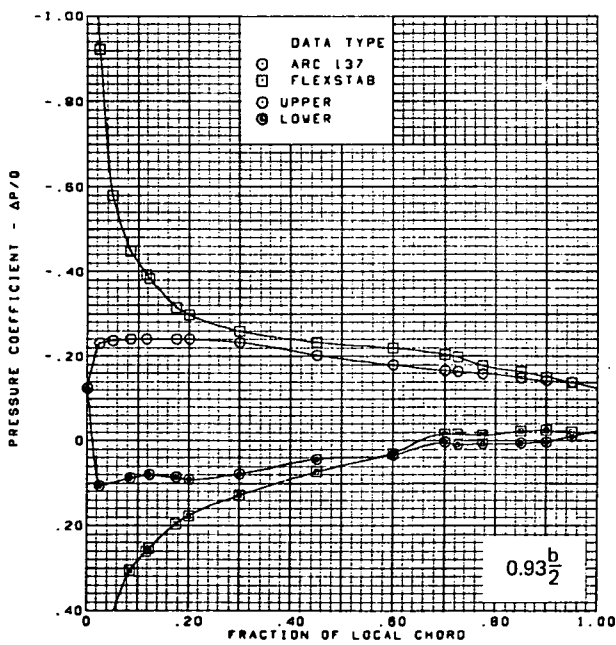
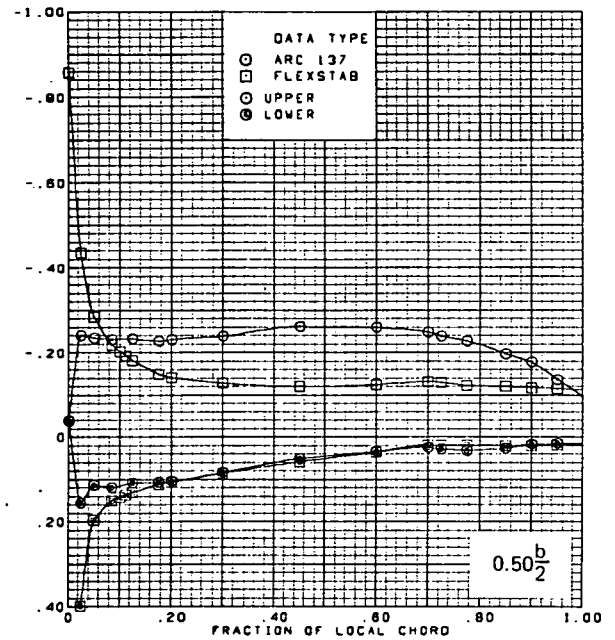
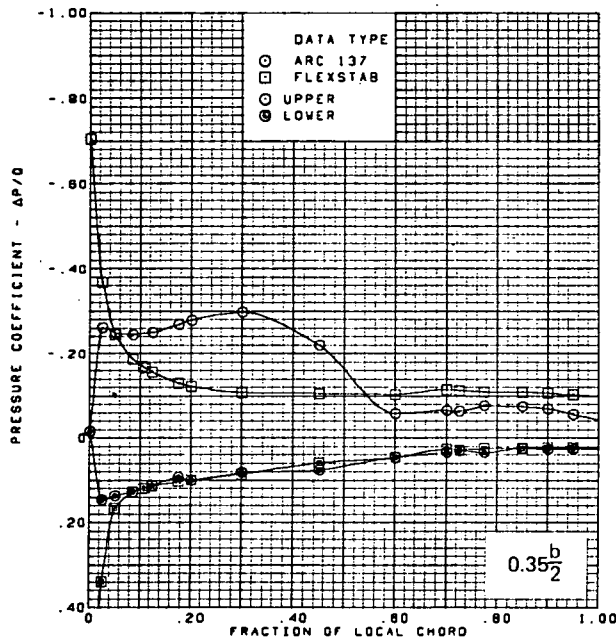
(b) (Concluded)

Figure 61.—(Continued)



(c) Surface Chordwise Pressure Distributions,  $\alpha = 8^\circ$

Figure 61.—(Continued)

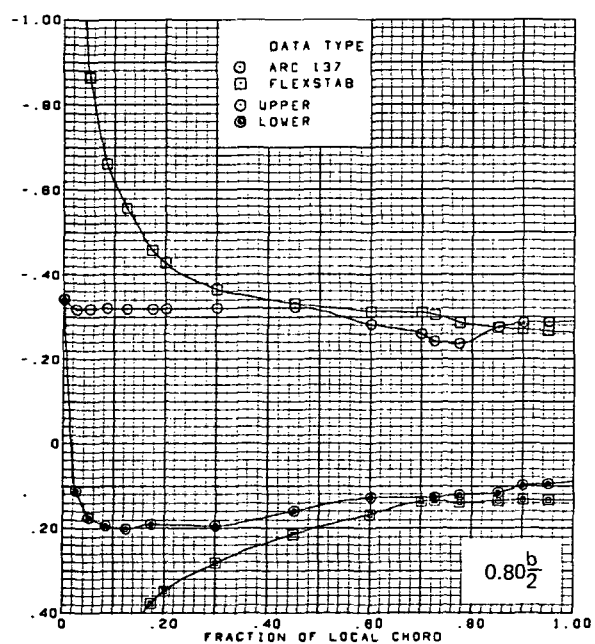
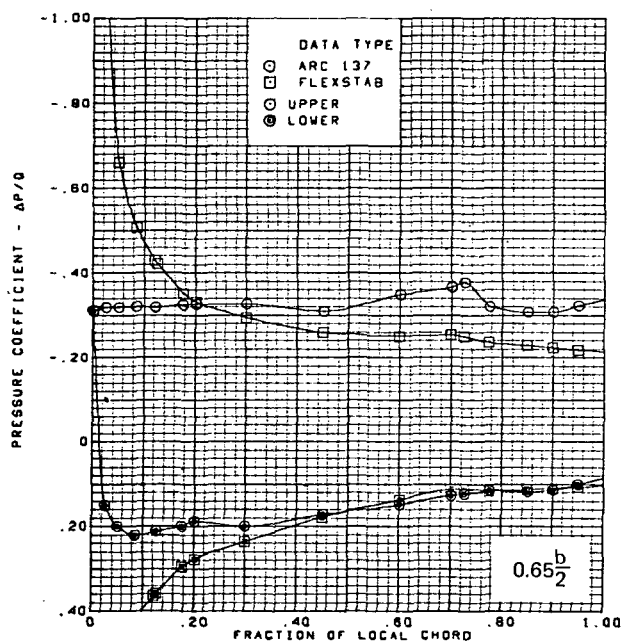
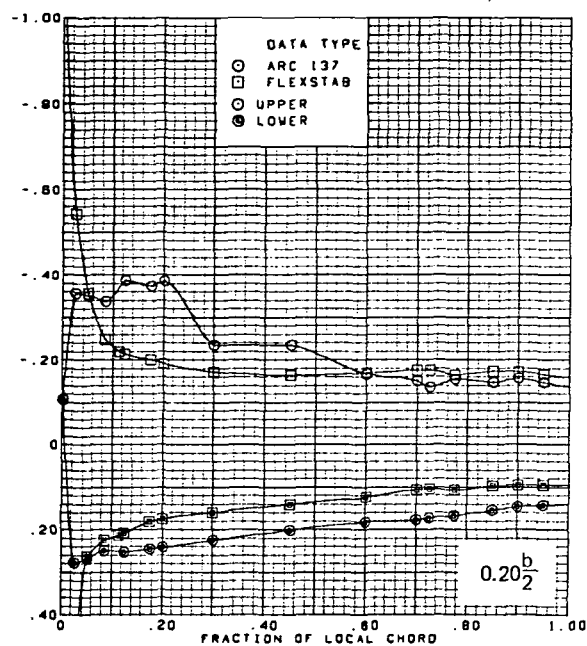
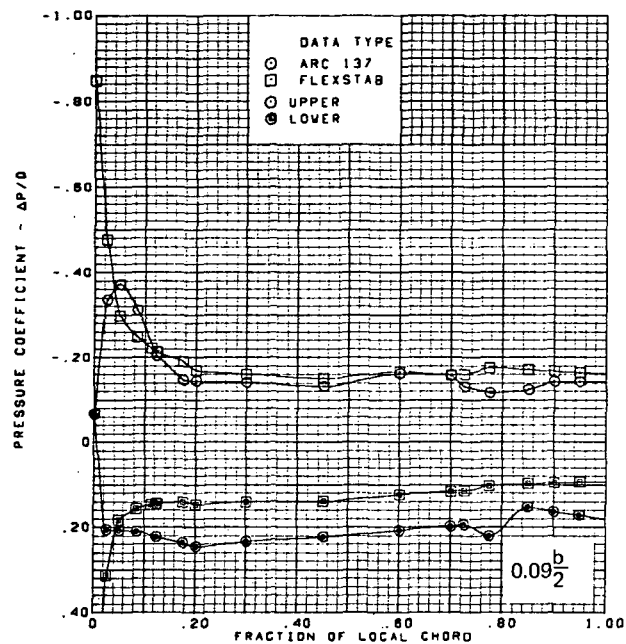


$M = 1.70$  (run 3)  
 $\alpha = 8^\circ$   
 Twisted wing, rounded L.E.  
 L.E. deflection, full span =  $0.0^\circ$   
 T.E. deflection, full span =  $0.0^\circ$

Note:  $C_{p, \text{vacuum}} = -0.49$

(c) (Concluded)

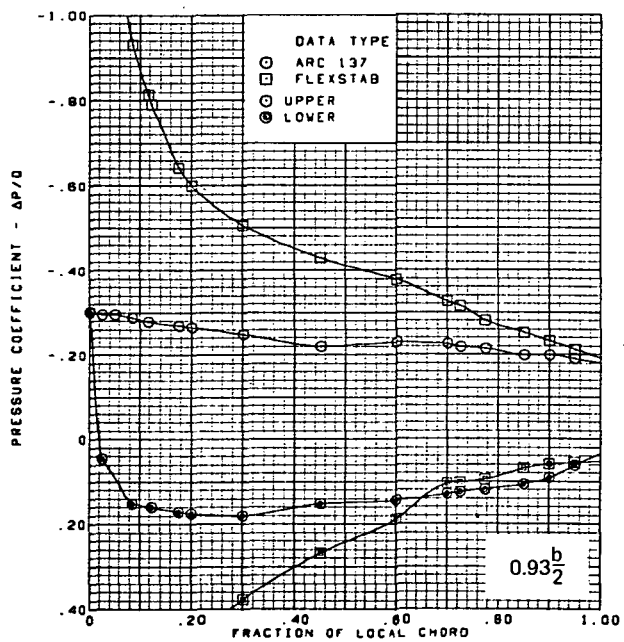
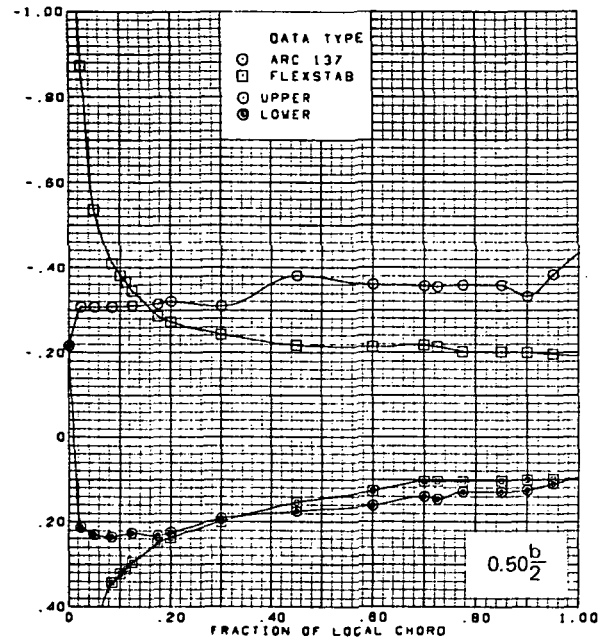
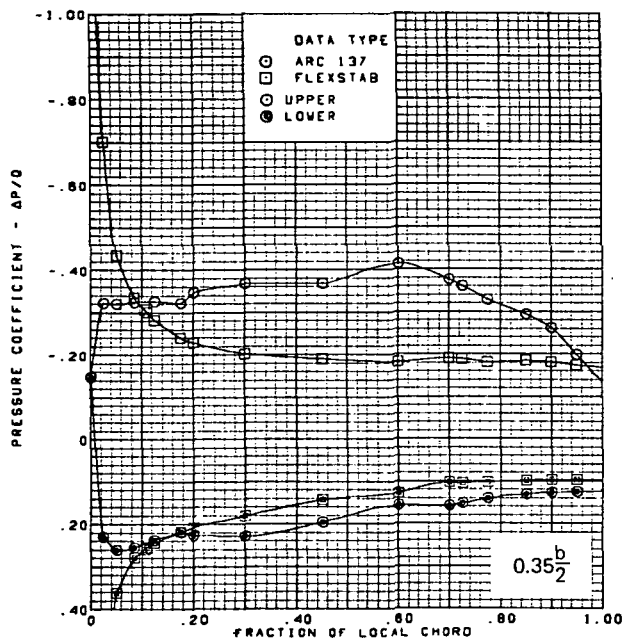
Figure 61.—(Continued)



(d) Surface Chordwise Pressure Distributions,  $\alpha = 15^\circ$

Figure 61. —(Continued)



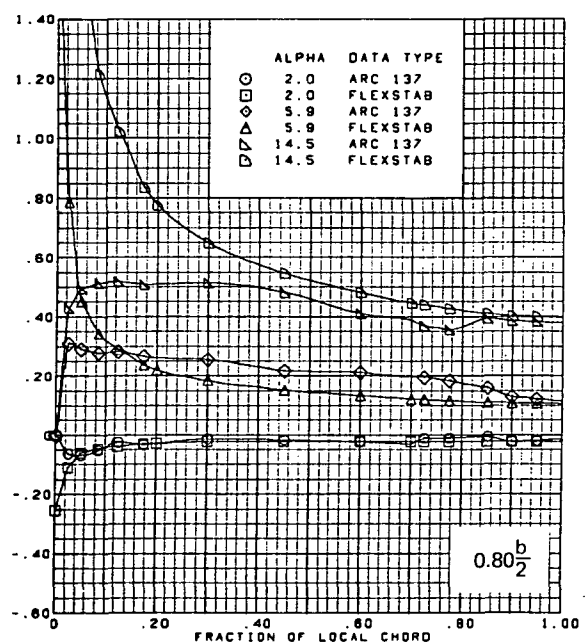
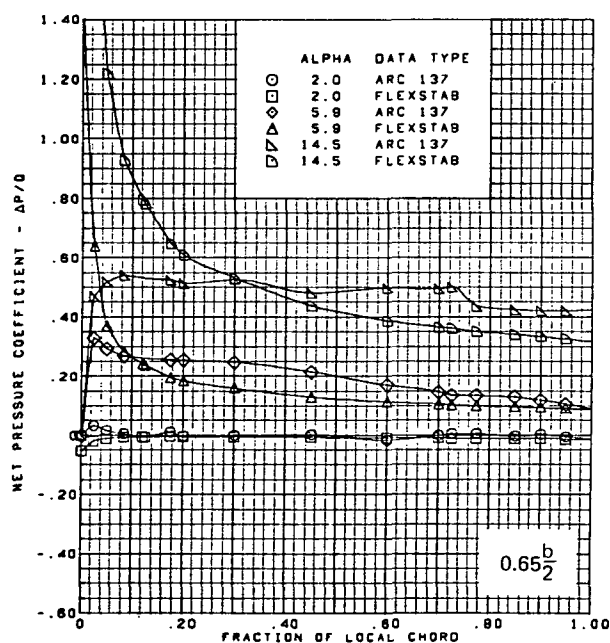
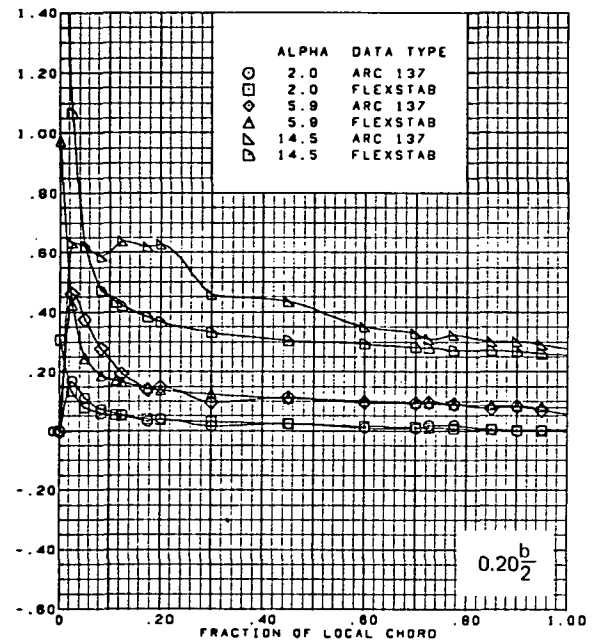
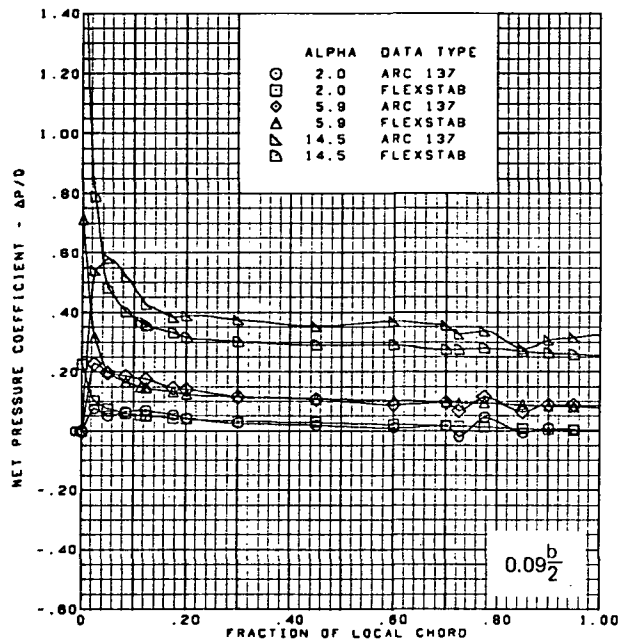


$M = 1.70$  (run 3)  
 $\alpha = 15^\circ$   
 Twisted wing, rounded L.E.  
 L.E. deflection, full span =  $0.0^\circ$   
 T.E. deflection, full span =  $0.0^\circ$

Note:  $C_{p, \text{vacuum}} = -0.49$

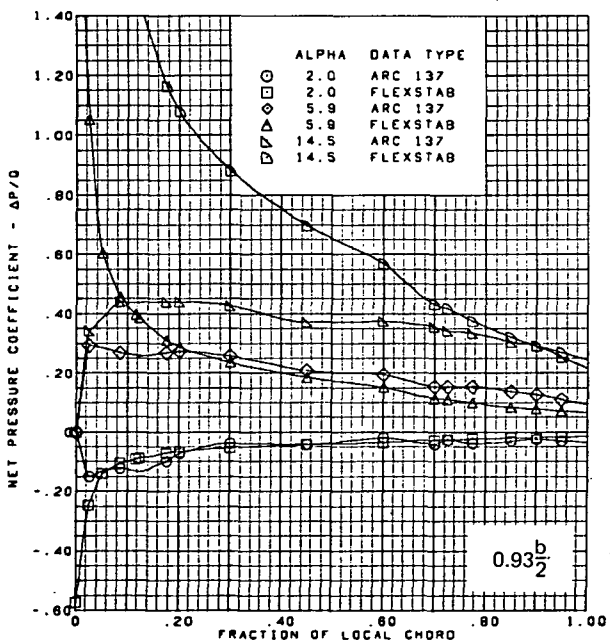
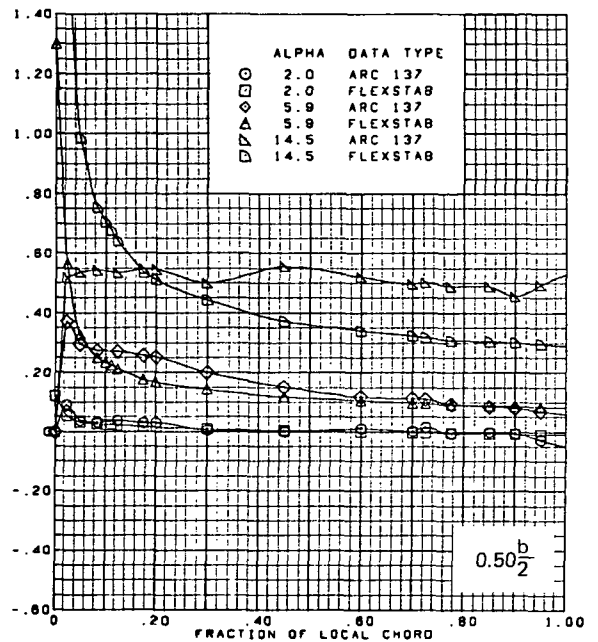
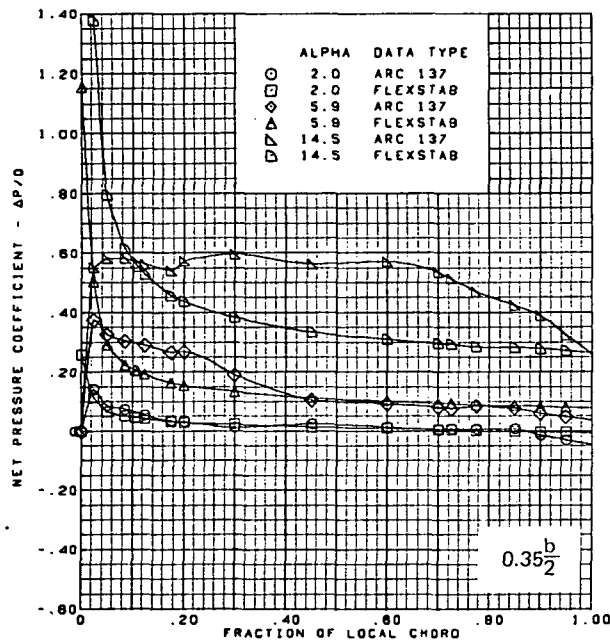
(d) (Concluded)

Figure 61. —(Continued)



(e) Net Chordwise Pressure Distributions,  $\alpha = 2^\circ, 6^\circ, 15^\circ$

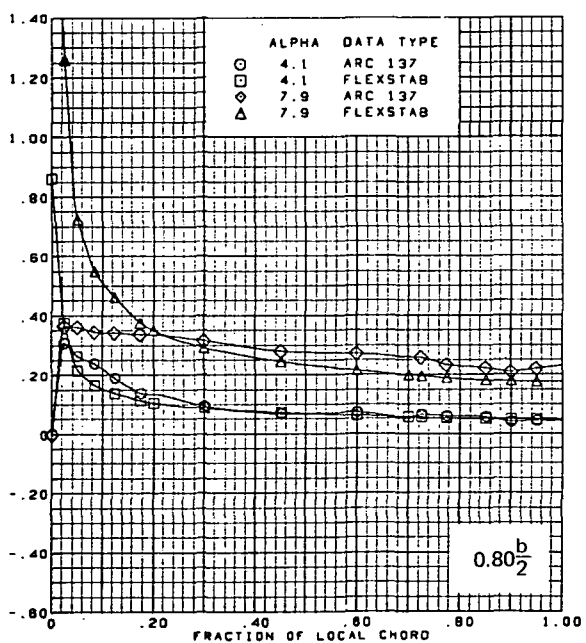
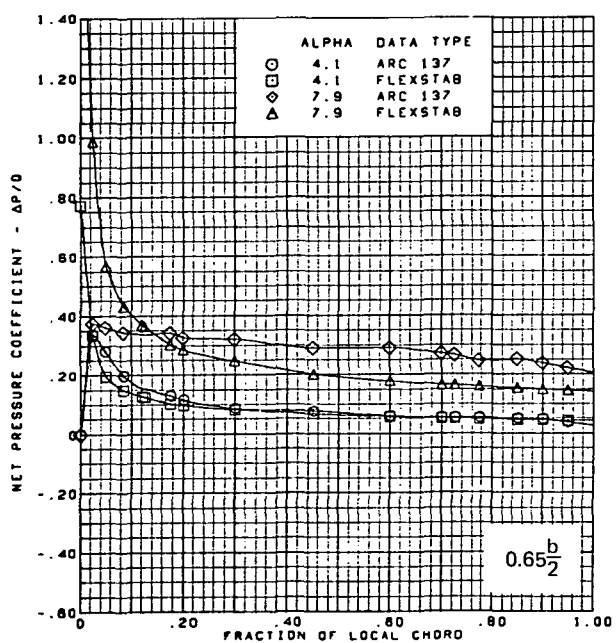
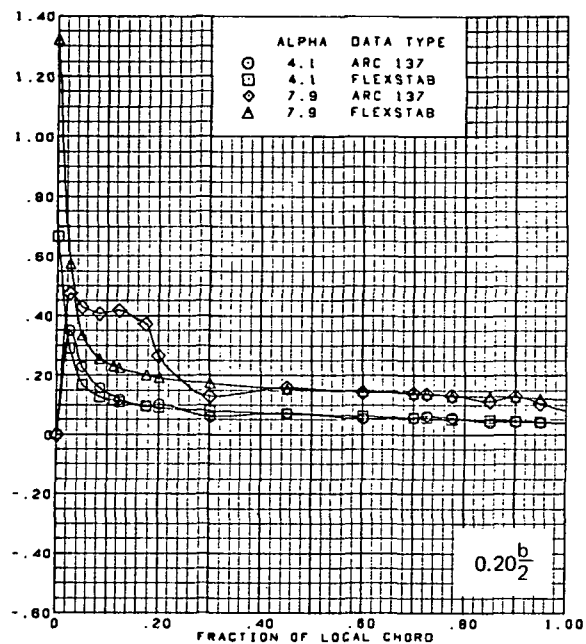
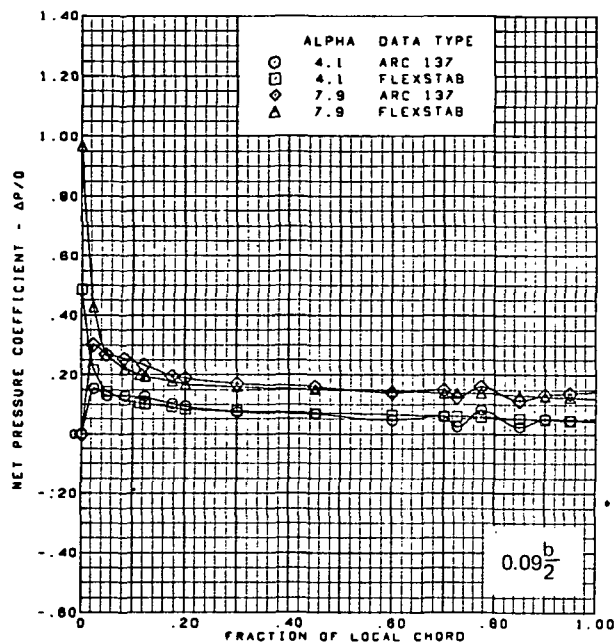
Figure 61.-(Continued)



M = 1.70 (run 3)  
 Twisted wing, rounded L.E.  
 L.E. deflection, full span =  $0.0^\circ$   
 T.E. deflection, full span =  $0.0^\circ$

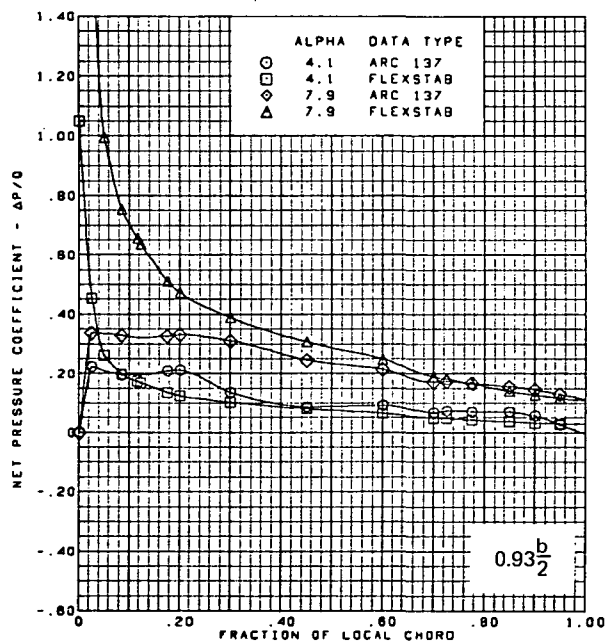
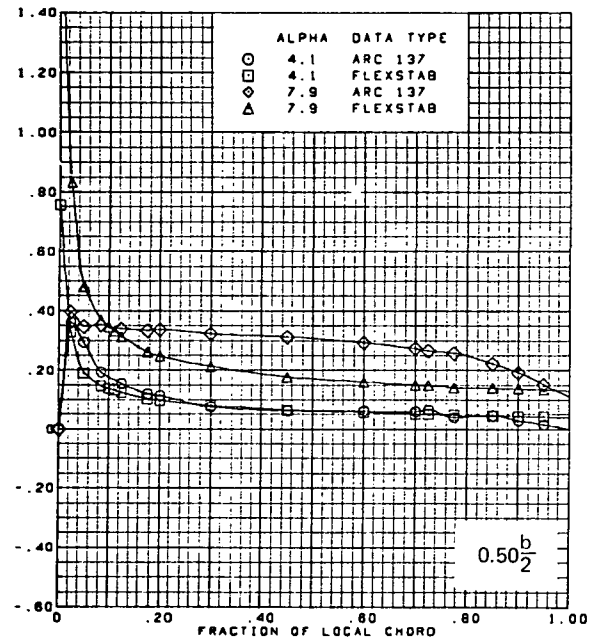
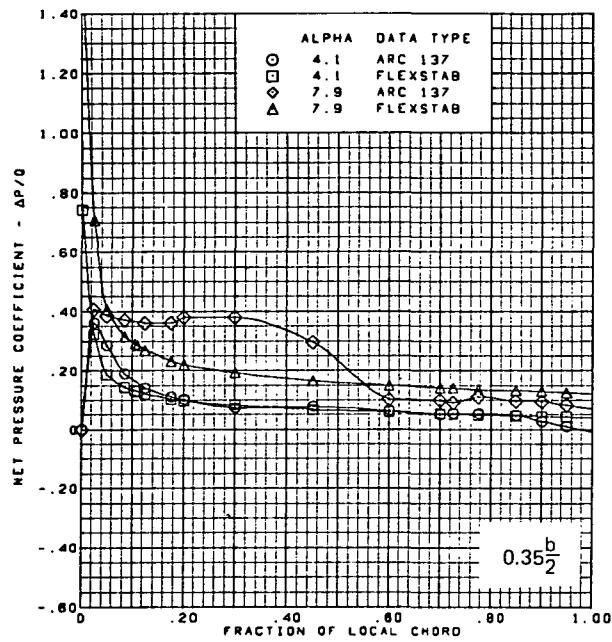
(e) (Concluded)

Figure 61.—(Continued)



(f) Net Chordwise Pressure Distributions,  $\alpha = 4^\circ, 8^\circ$

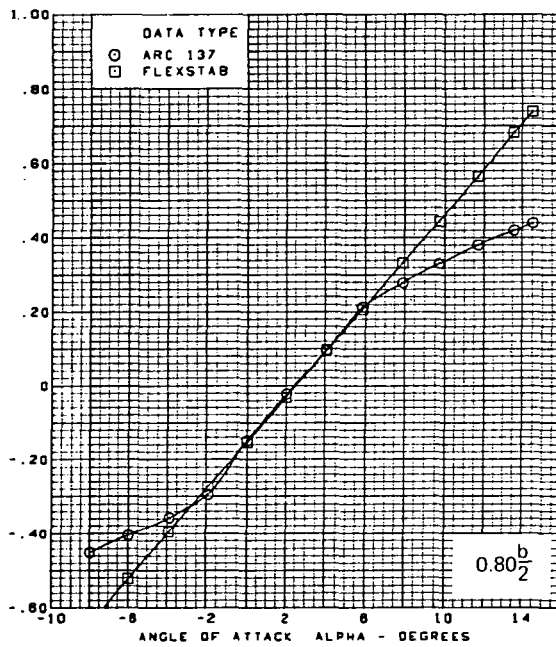
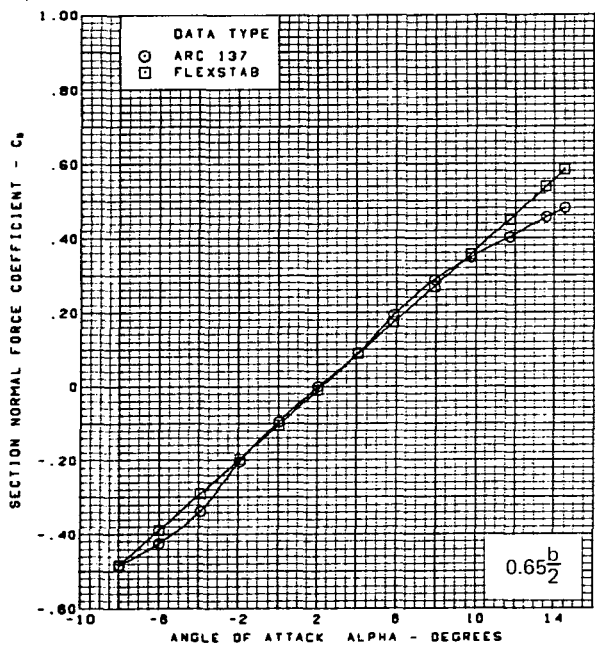
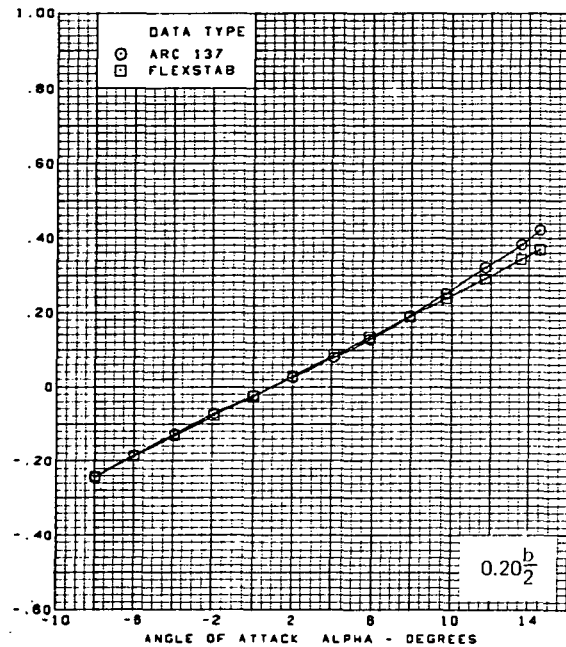
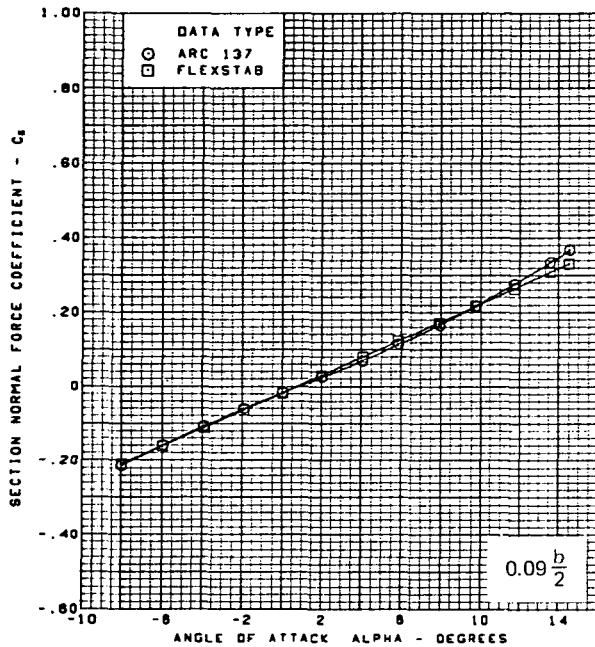
Figure 61.—(Continued)



$M = 1.70$  (run 3)  
 Twisted wing, rounded L.E.  
 L.E. deflection, full span =  $0.0^\circ$   
 T.E. deflection, full span =  $0.0^\circ$

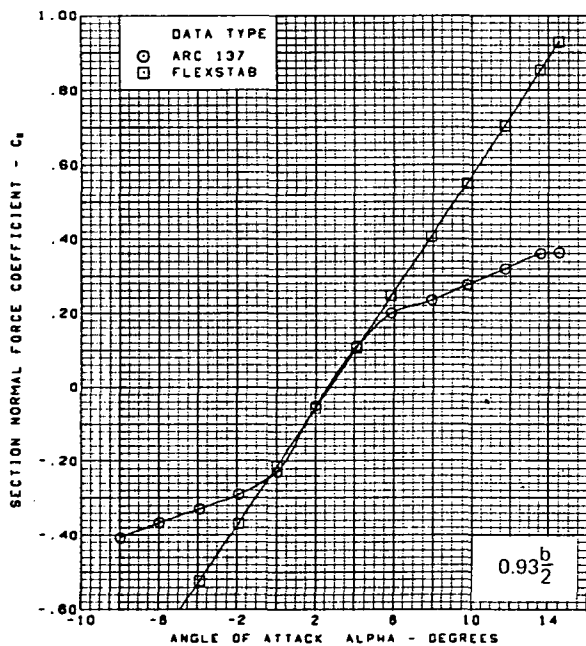
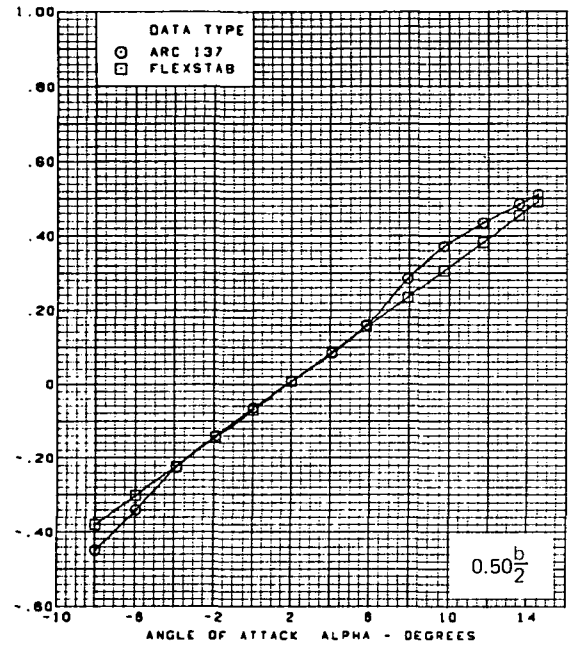
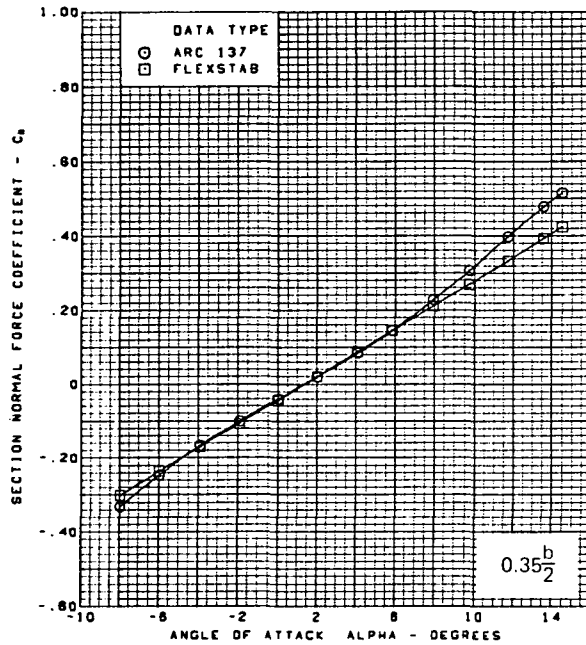
(f) (Concluded)

Figure 61.-(Continued)



(g) Section Aerodynamic Coefficients - Normal Force

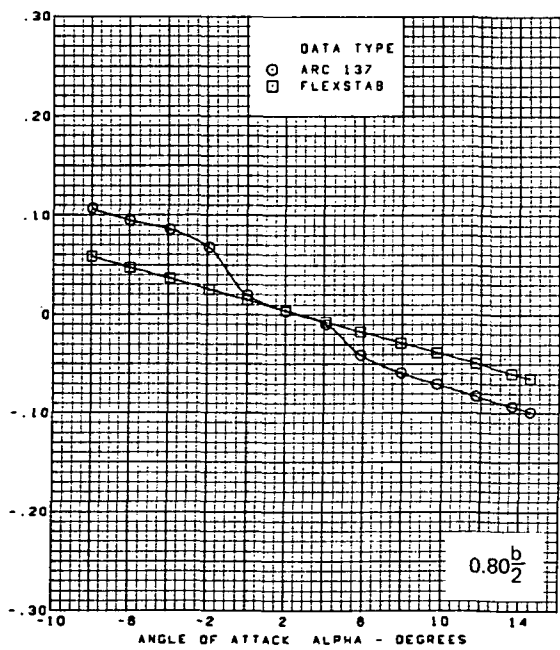
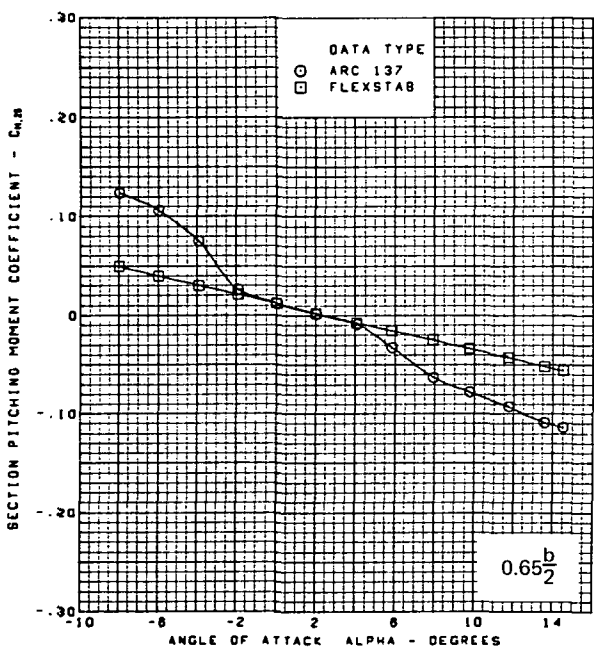
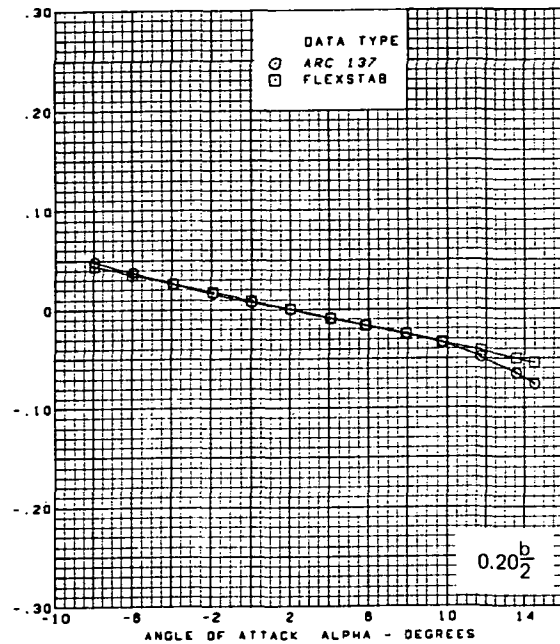
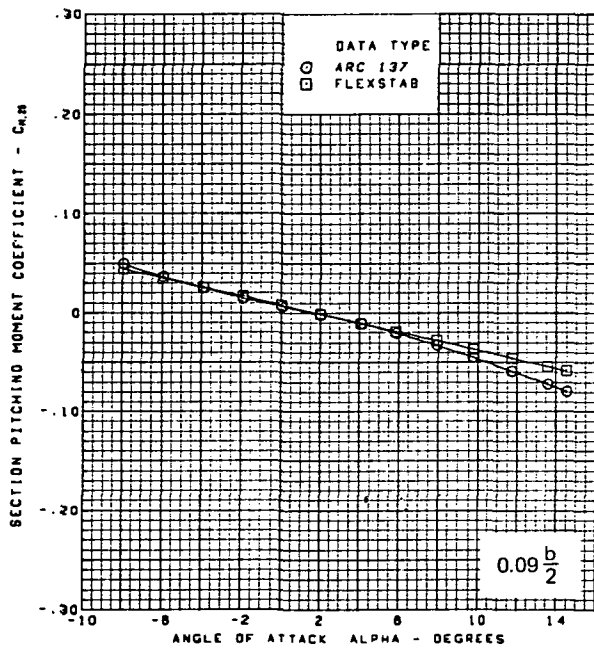
Figure 61.—(Continued)



M = 1.70 (run 3)  
 Twisted wing, rounded L.E.  
 L.E. deflection, full span =  $0.0^\circ$   
 T.E. deflection, full span =  $0.0^\circ$

(g) (Concluded)

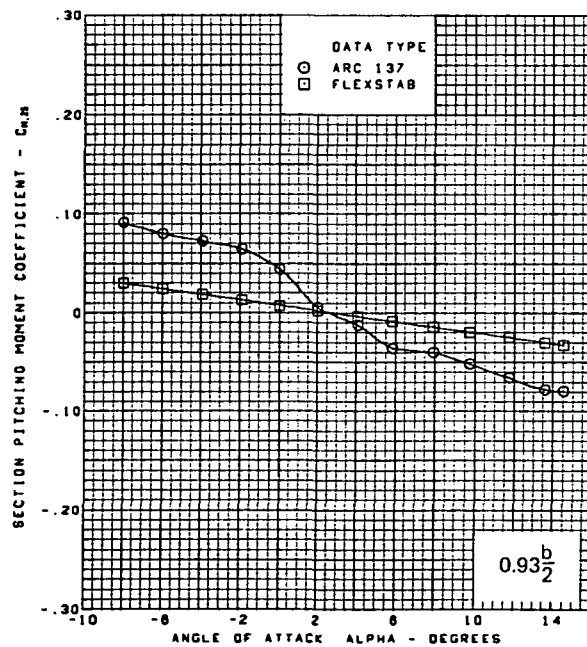
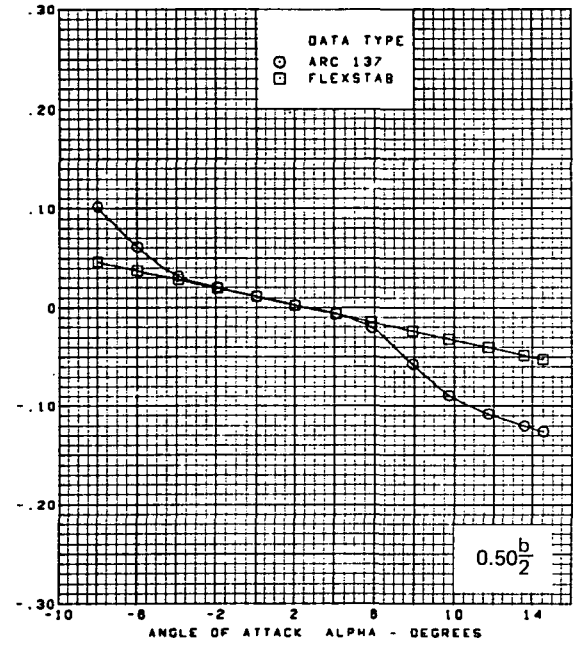
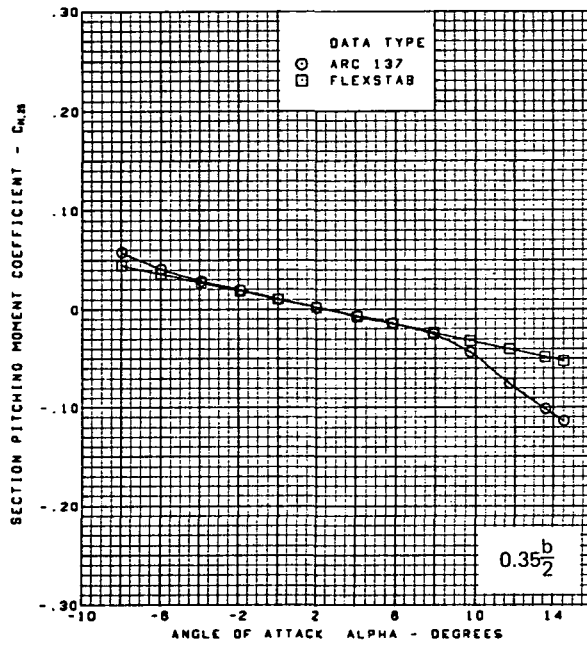
Figure 61.—(Continued)



(h) Section Aerodynamic Coefficients - Pitching Moment

Figure 61.—(Continued)

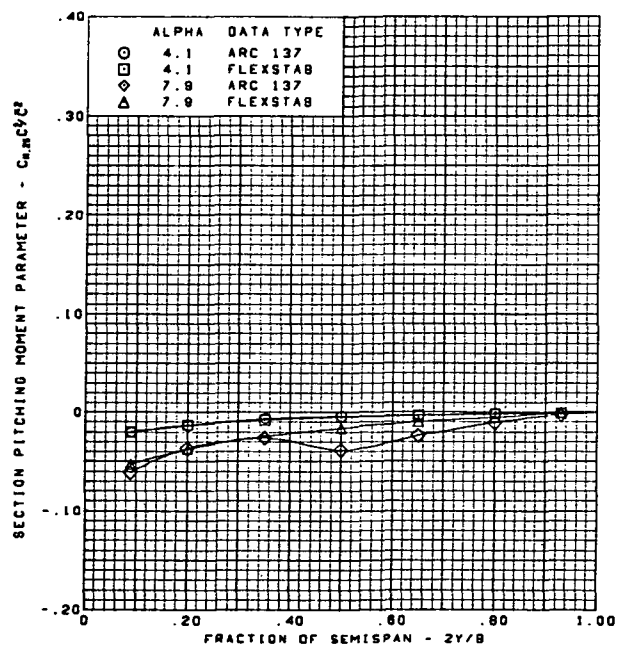
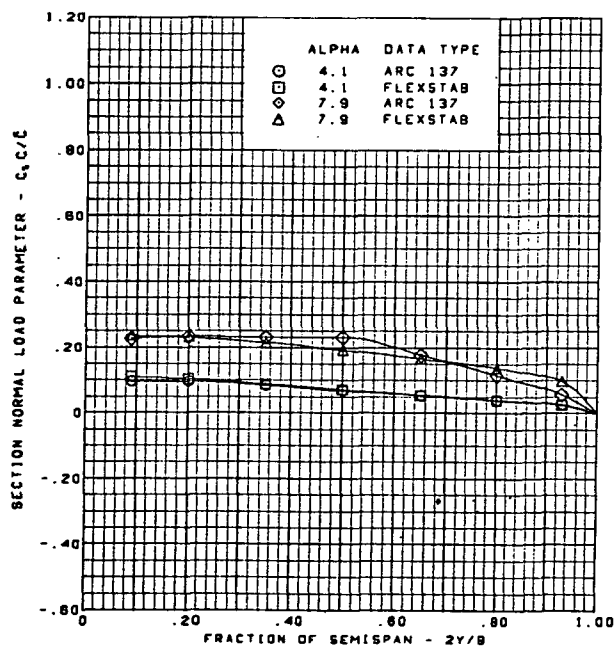
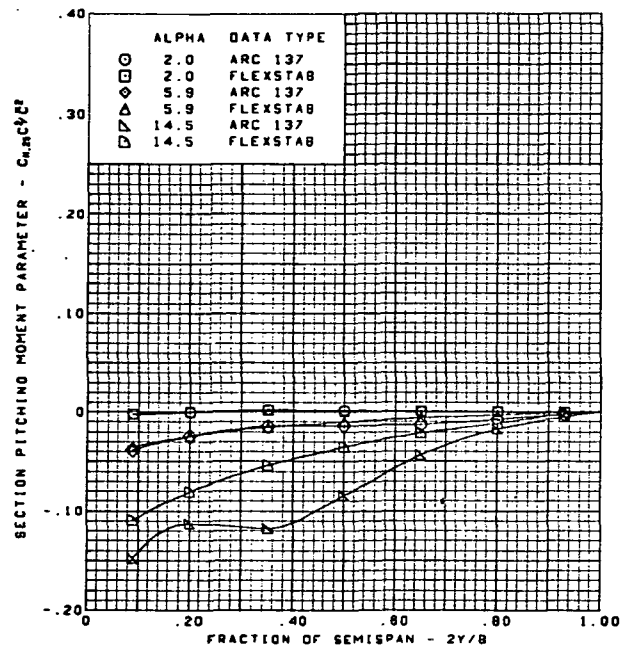
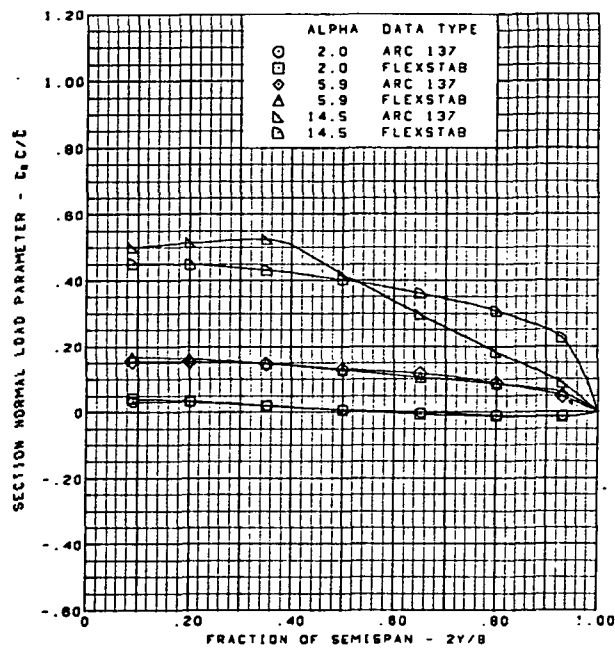




$M = 1.70$  (run 3)  
 Twisted wing, rounded L.E.  
 L.E. deflection, full span =  $0.0^\circ$   
 T.E. deflection, full span =  $0.0$

(h) (Concluded)

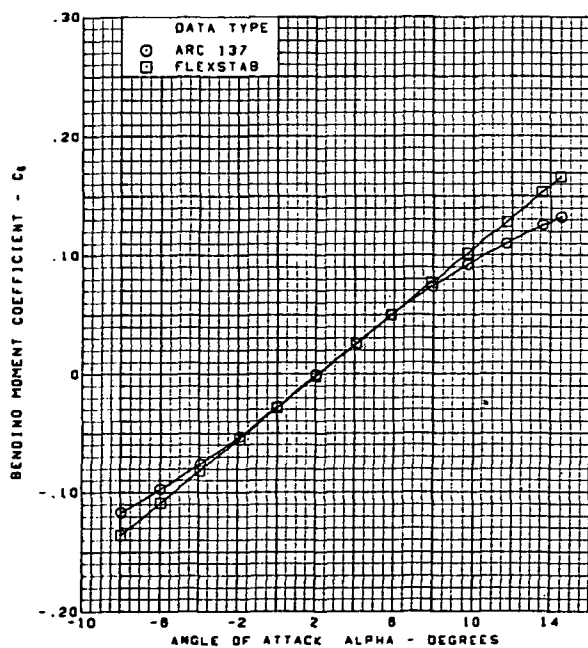
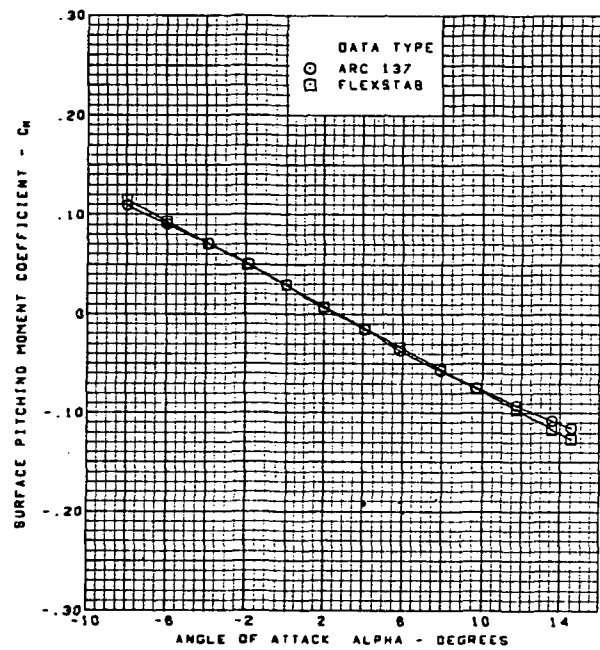
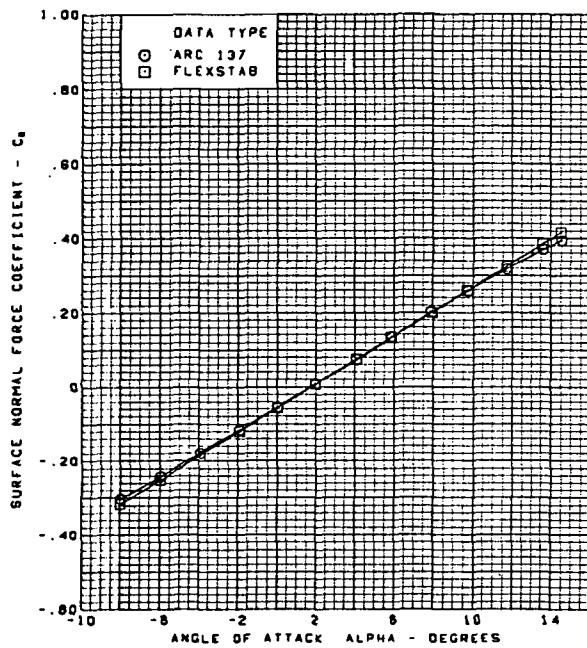
Figure 61.—(Continued)



M = 1.70 (run 3)  
 Twisted wing, rounded L.E.  
 L.E. deflection, full span = 0.0°  
 T.E. deflection, full span = 0.0°

(i) Spanload Distributions

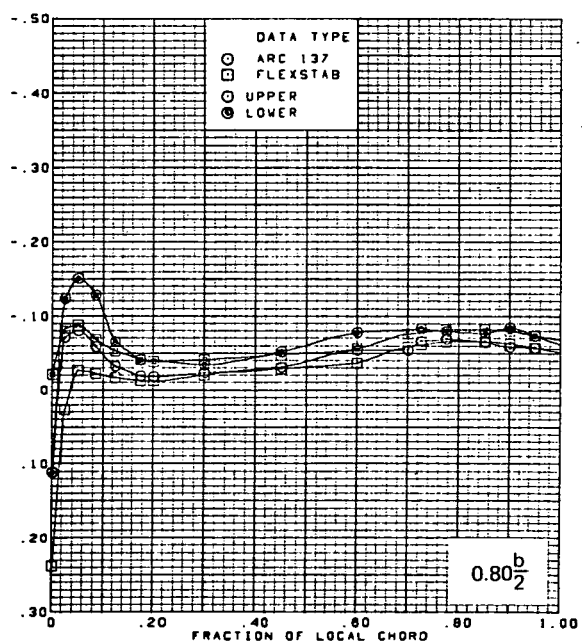
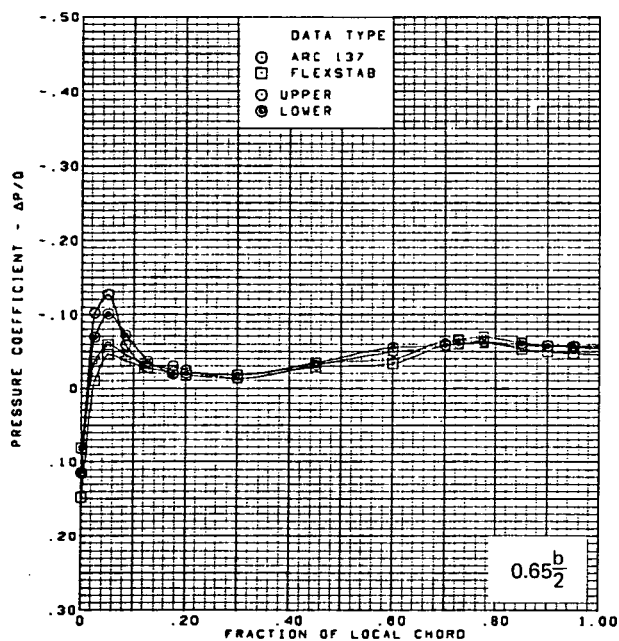
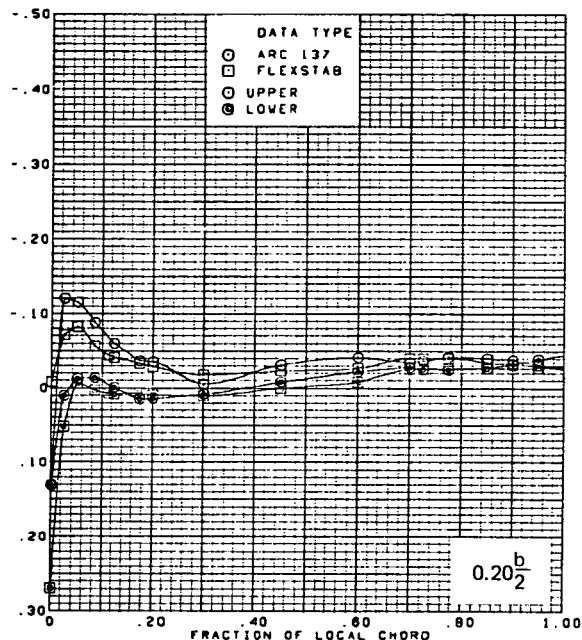
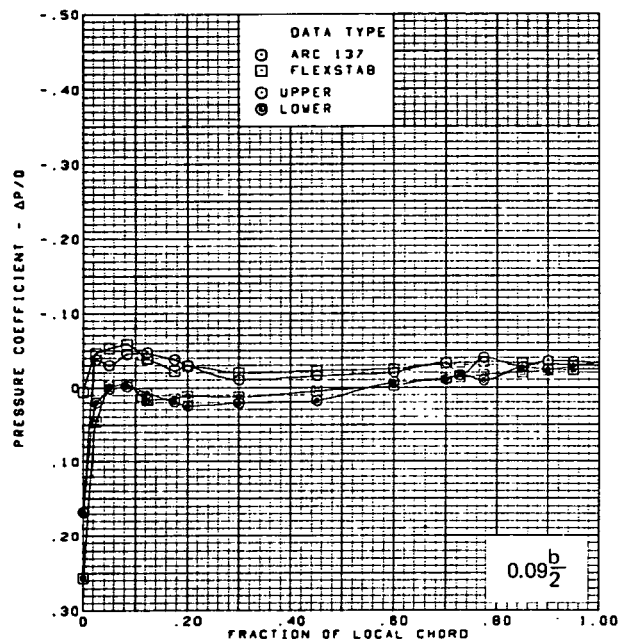
Figure 61.—(Continued)



$M = 1.70$  (run 3)  
 Twisted wing, rounded L.E.  
 L.E. deflection, full span =  $0.0^\circ$   
 T.E. deflection, full span =  $0.0^\circ$

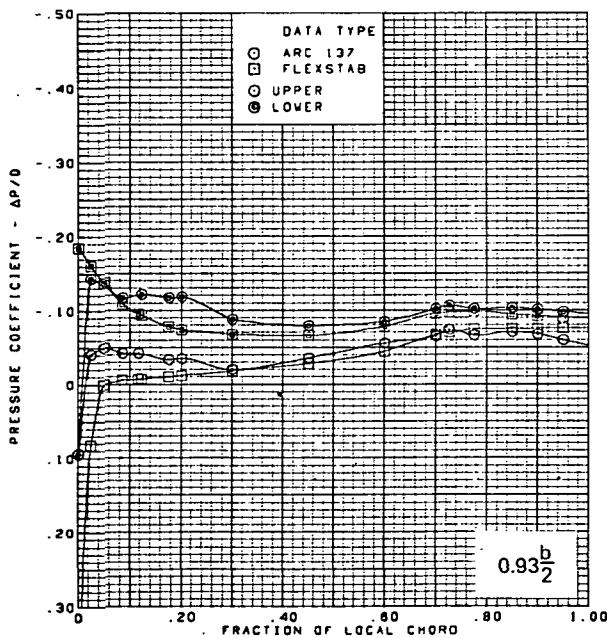
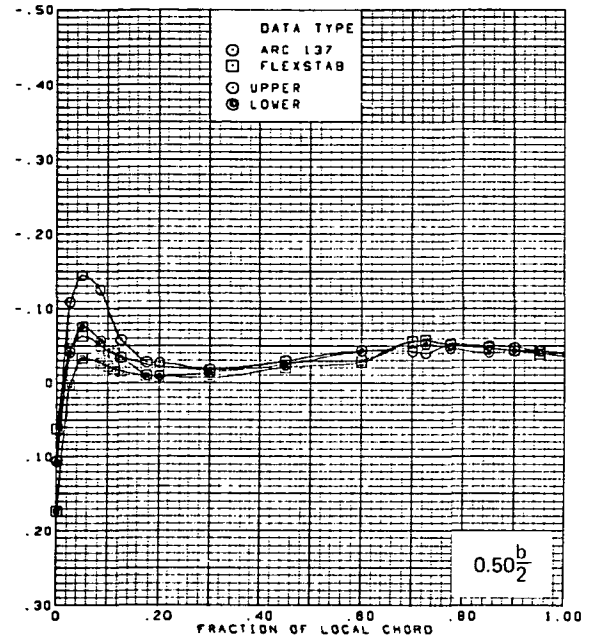
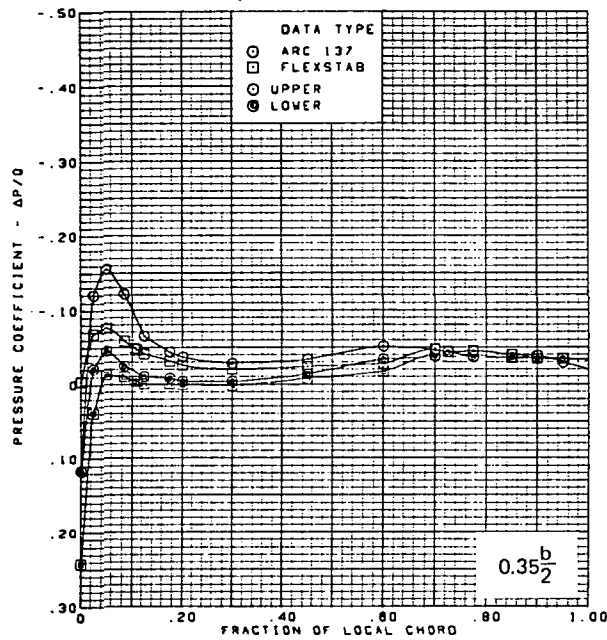
(j) Wing Aerodynamic Coefficients

Figure 61.—(Concluded)



(a) Surface Chordwise Pressure Distributions,  $\alpha = 2^\circ$

Figure 62.—Wing Theory-to-Experiment Comparison—Twisted Wing, Rounded L.E.; L.E. Deflection, Full Span =  $0.0^\circ$ ; T.E. Deflection, Full Span =  $0.0^\circ$ ;  $M = 2.10$

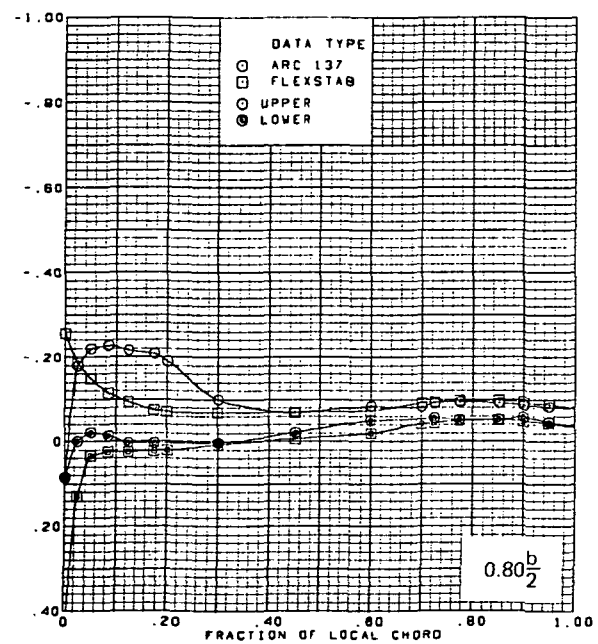
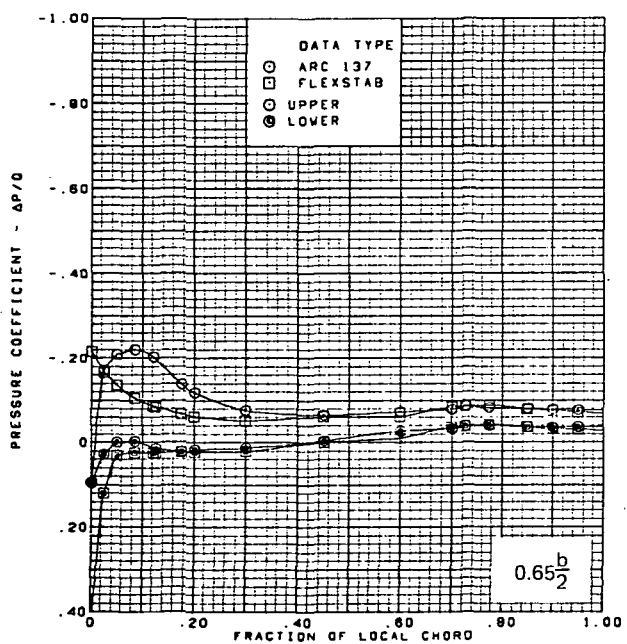
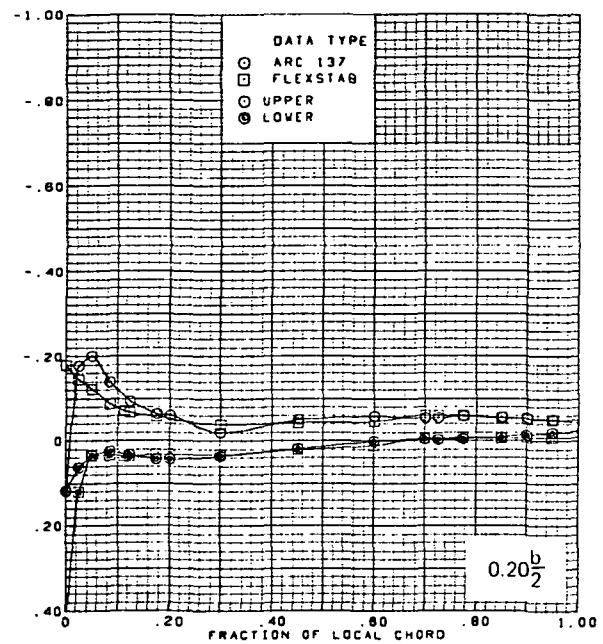
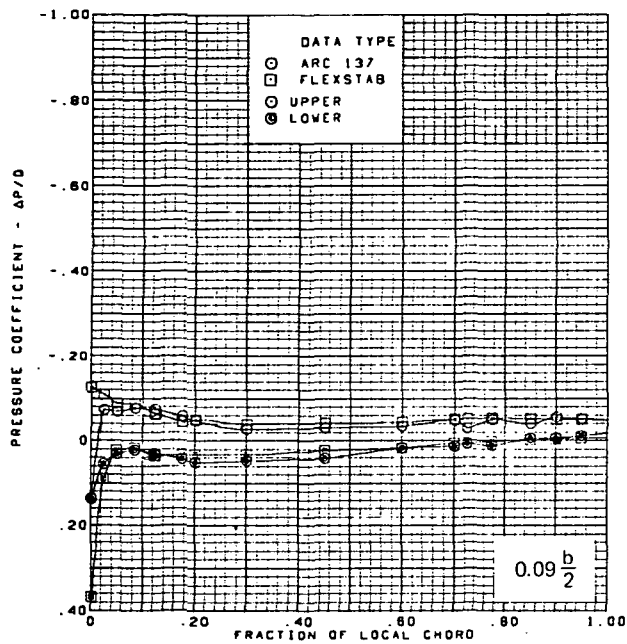


$M = 2.10$  (run 9)  
 $\alpha = 2^\circ$   
 Twisted wing, rounded L.E.  
 L.E. deflection, full span =  $0.0^\circ$   
 T.E. deflection, full span =  $0.0^\circ$

Note:  $C_{p, \text{vacuum}} = -0.32$

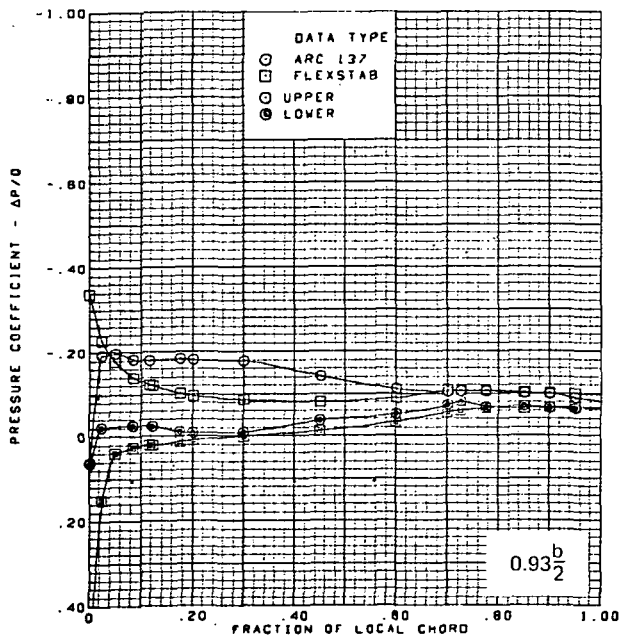
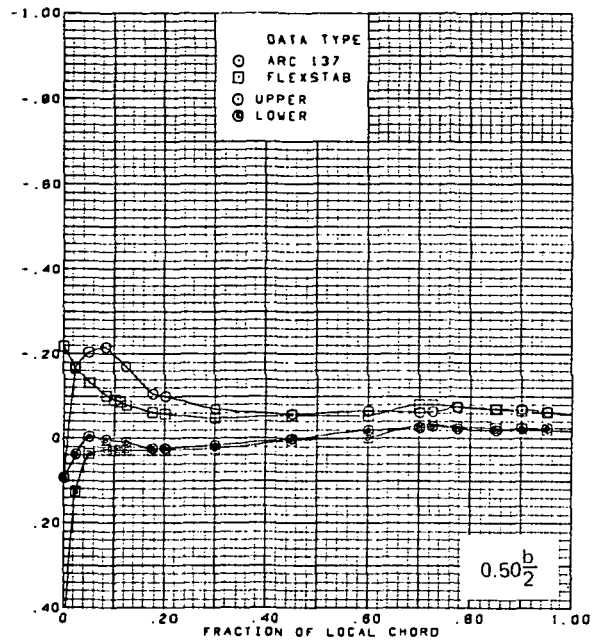
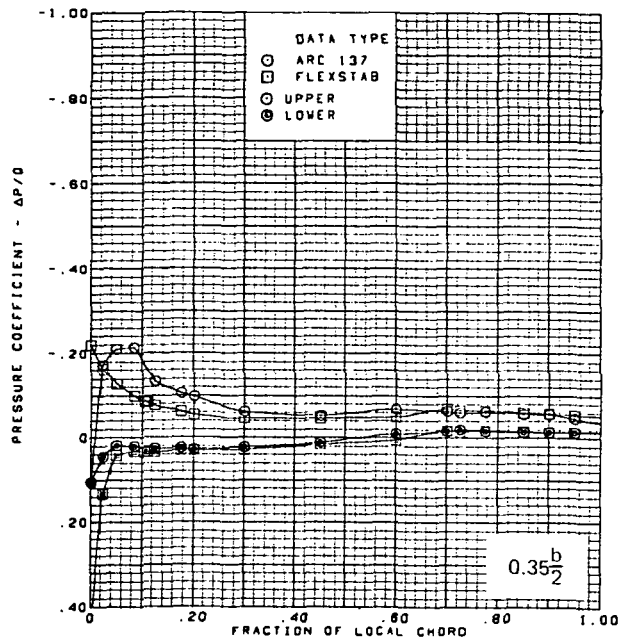
(a) (Concluded)

Figure 62.-(Continued)



(b) Surface Chordwise Pressure Distributions,  $\alpha = 4^\circ$

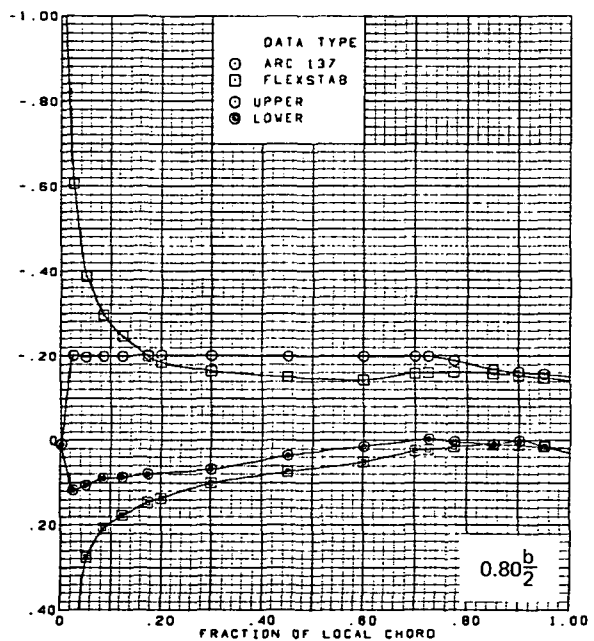
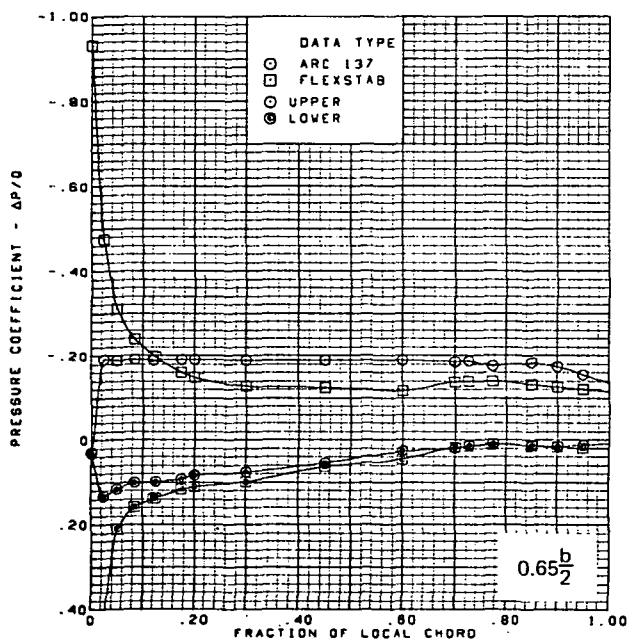
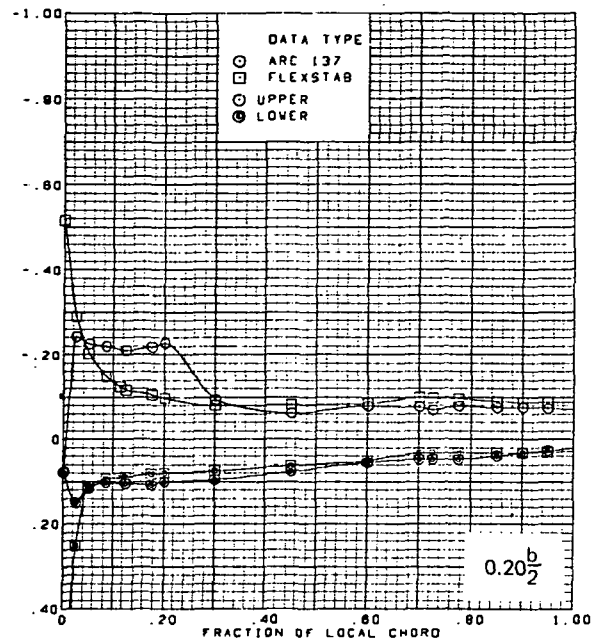
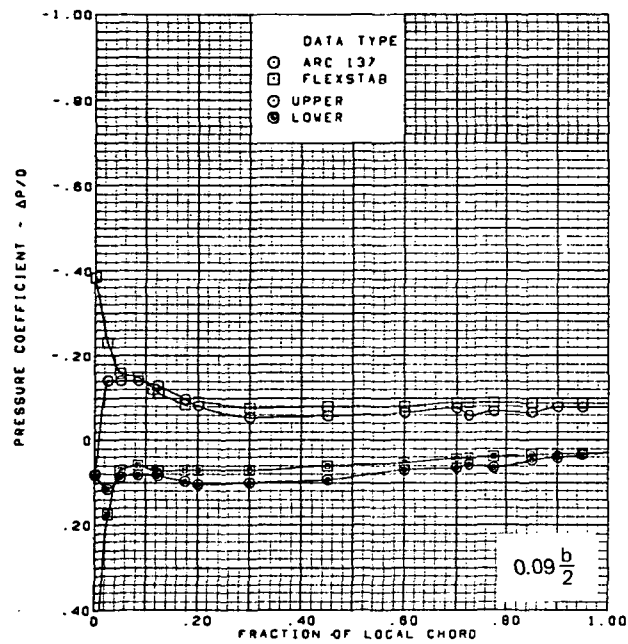
Figure 62.—(Continued)



$M = 2.10$  (run 9)  
 $\alpha = 4^\circ$   
 Twisted wing, rounded L.E.  
 L.E. deflection, full span =  $0.0^\circ$   
 T.E. deflection, full span =  $0.0^\circ$   
 Note:  $C_{p, \text{vacuum}} = -0.32$

(b) (Concluded)

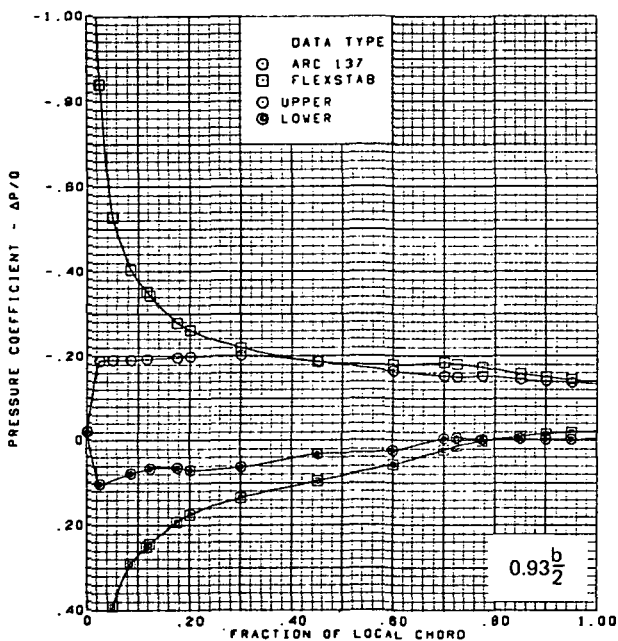
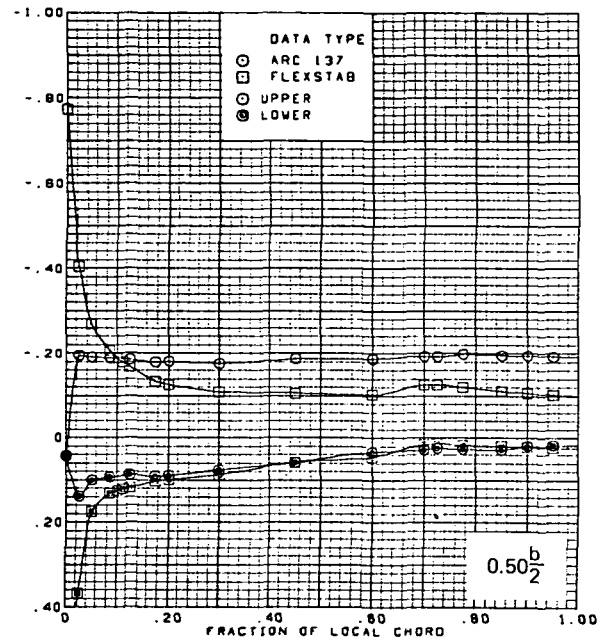
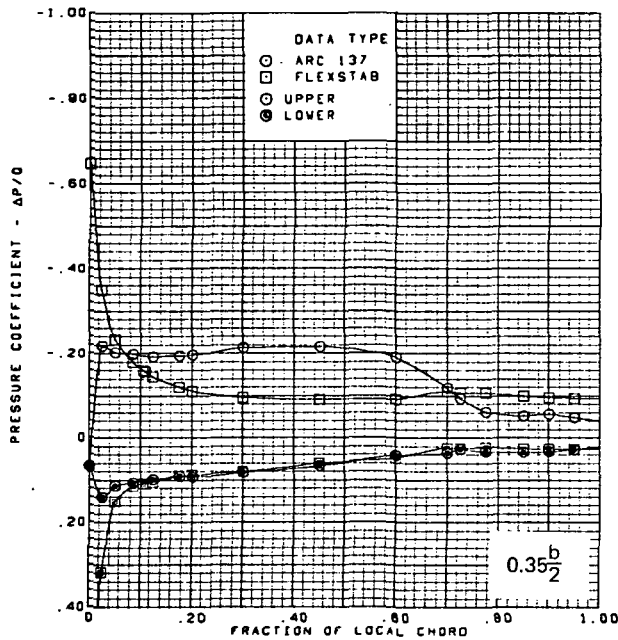
Figure 62.—(Continued)



(c) Surface Chordwise Pressure Distributions,  $\alpha = 8^\circ$

Figure 62.-(Continued)

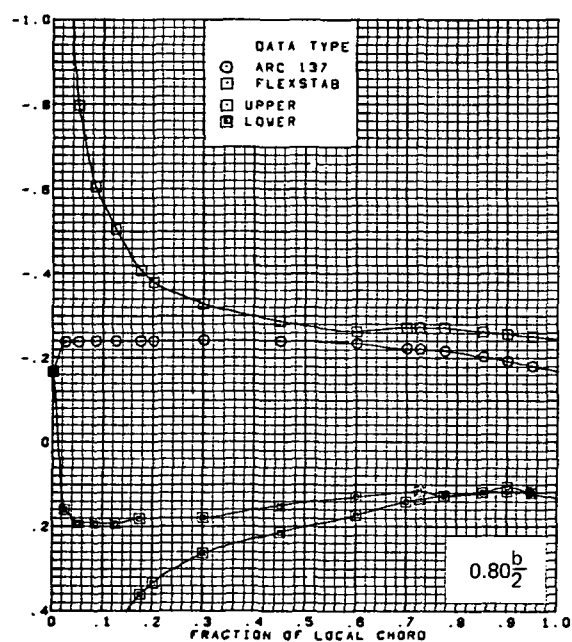
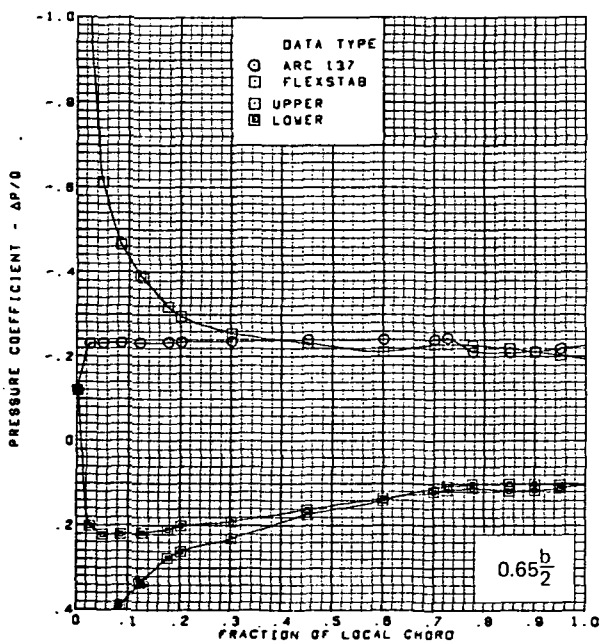
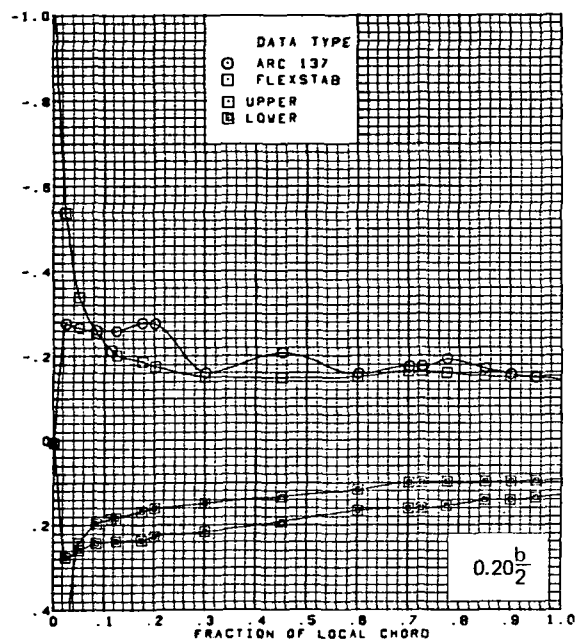
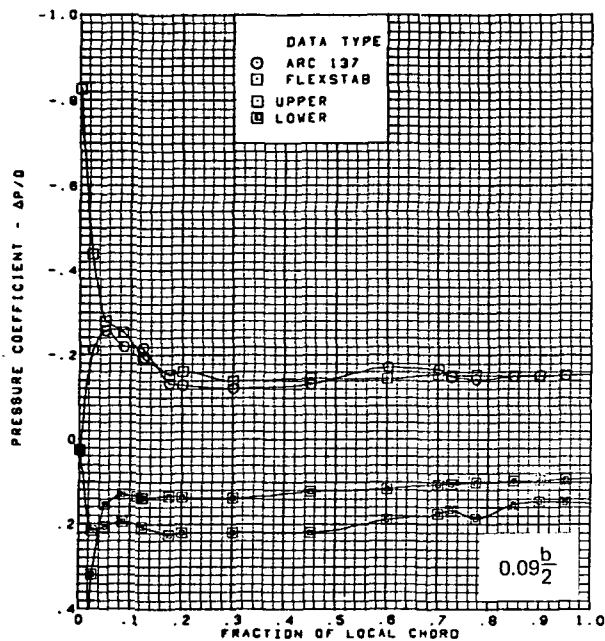




$M = 2.10$  (run 9)  
 $\alpha = 8^\circ$   
 Twisted wing, rounded L.E.  
 L.E. deflection, full span =  $0.0^\circ$   
 T.E. deflection, full span =  $0.0^\circ$   
 Note:  $C_{p, \text{vacuum}} = -0.32$

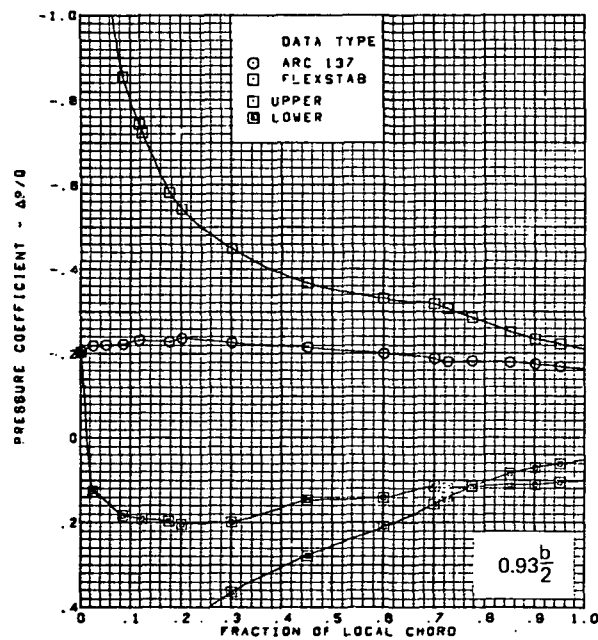
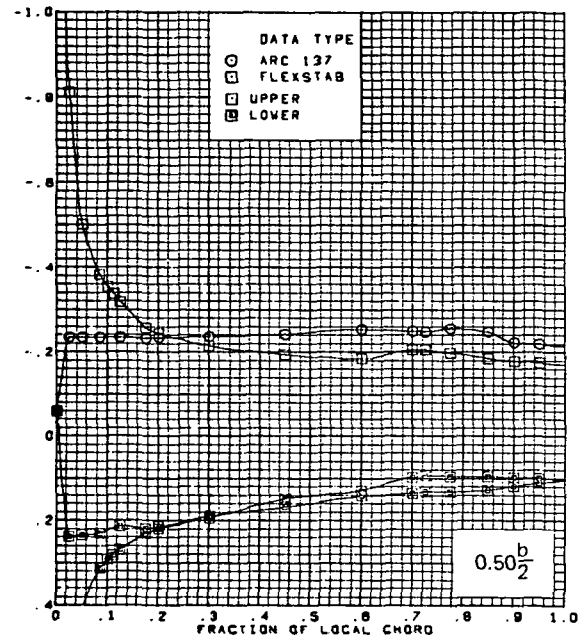
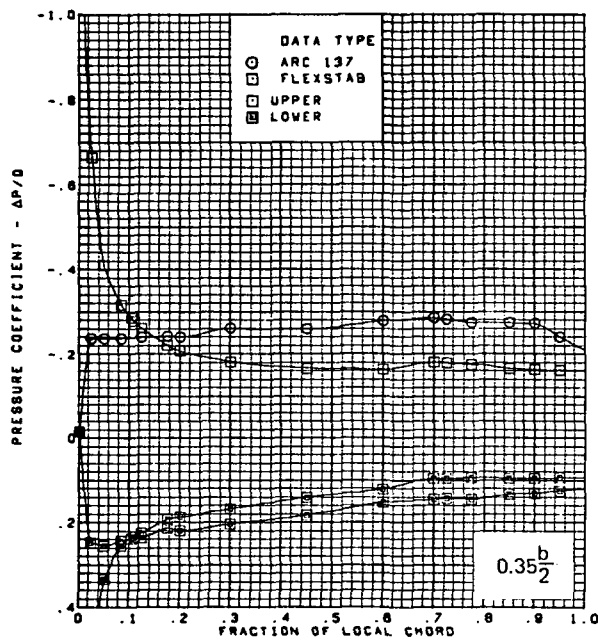
(c) (Concluded)

Figure 62.—(Continued)



(d) Surface Chordwise Pressure Distributions,  $\alpha = 15^\circ$

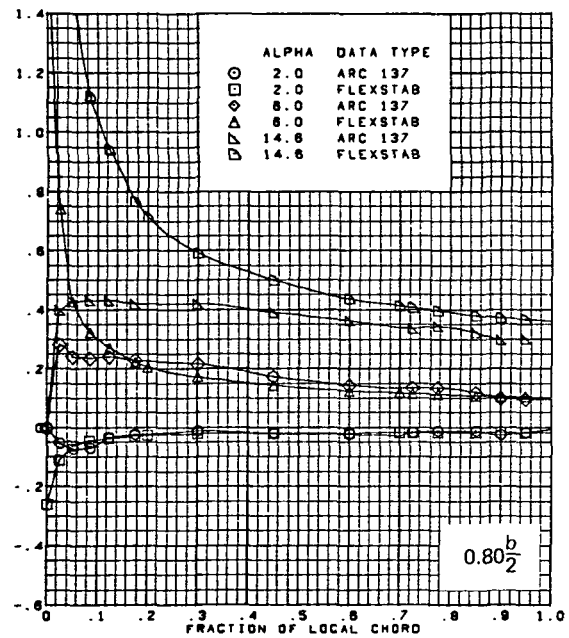
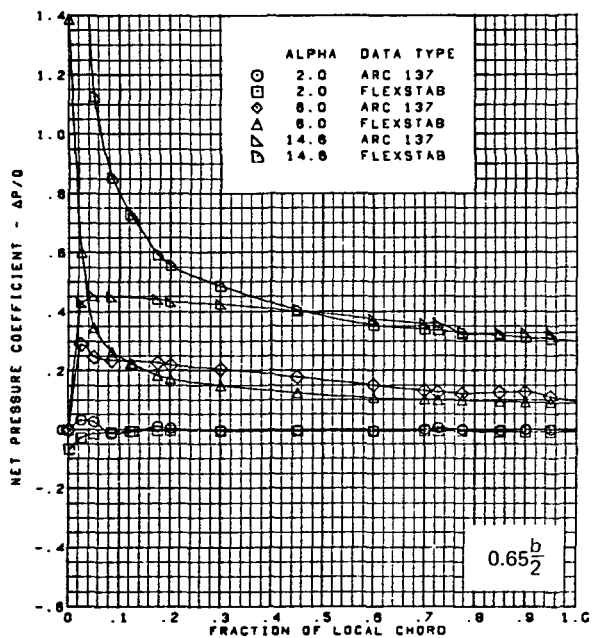
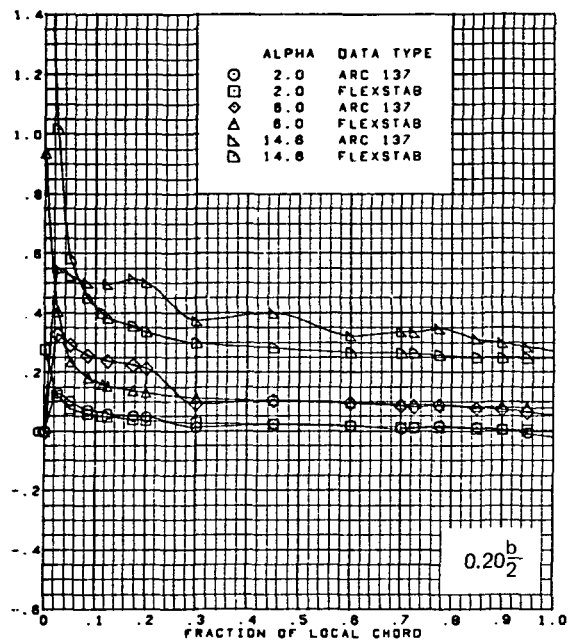
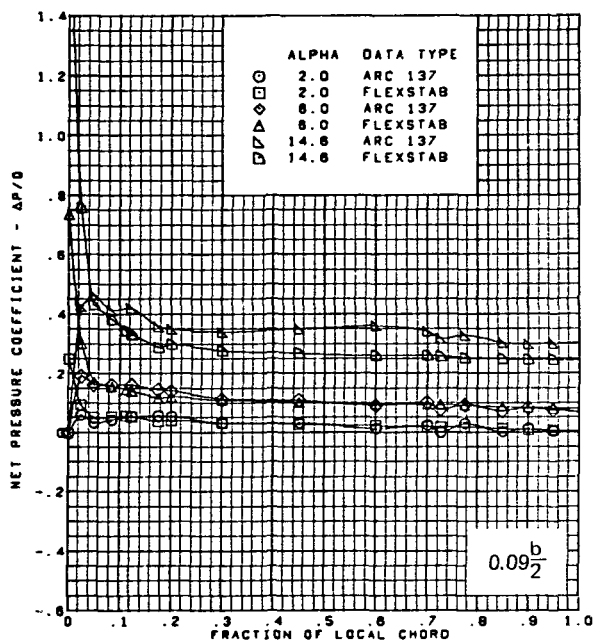
Figure 62.—(Continued)



$M = 2.10$  (run 9)  
 $\alpha = 15^\circ$   
 Twisted wing, rounded L.E.  
 L.E. deflection, full span =  $0.0^\circ$   
 T.E. deflection, full span =  $0.0^\circ$   
 Note:  $C_{p, \text{vacuum}} = -0.32$

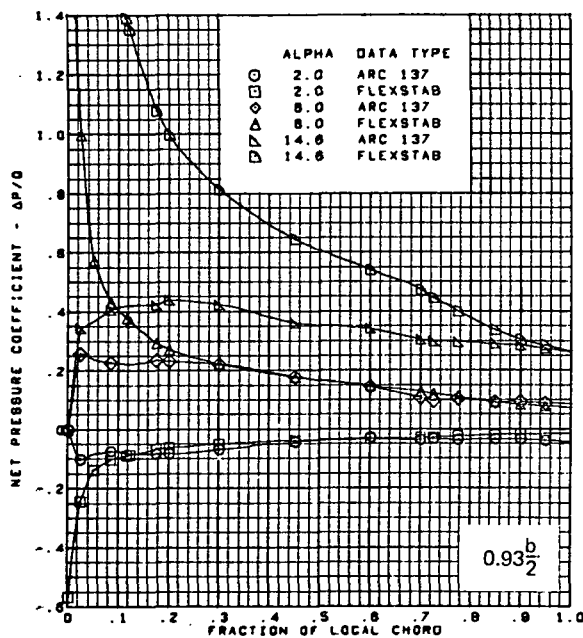
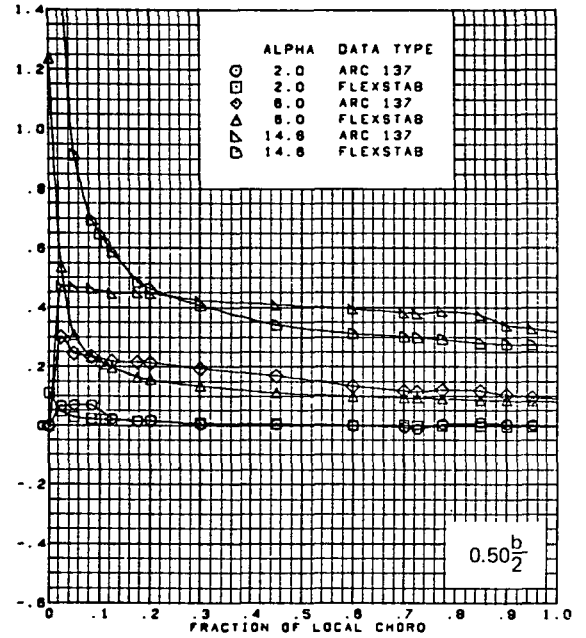
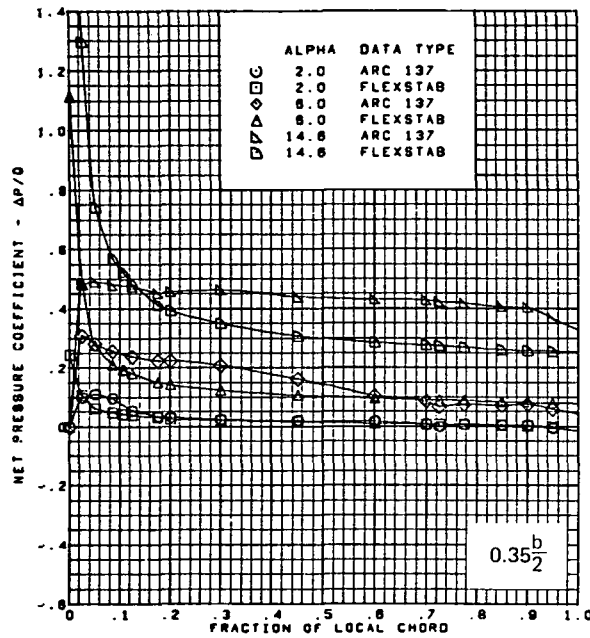
(d) (Concluded)

Figure 62.—(Continued)



(e) Net Chordwise Pressure Distributions,  $\alpha = 2^\circ, 6^\circ, 15^\circ$

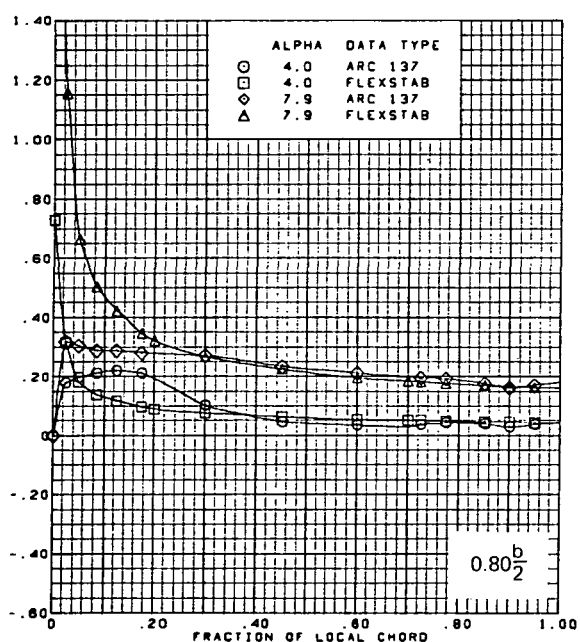
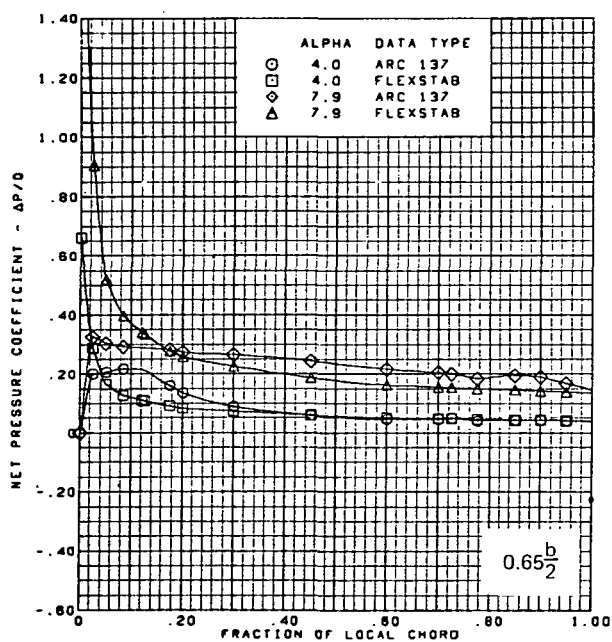
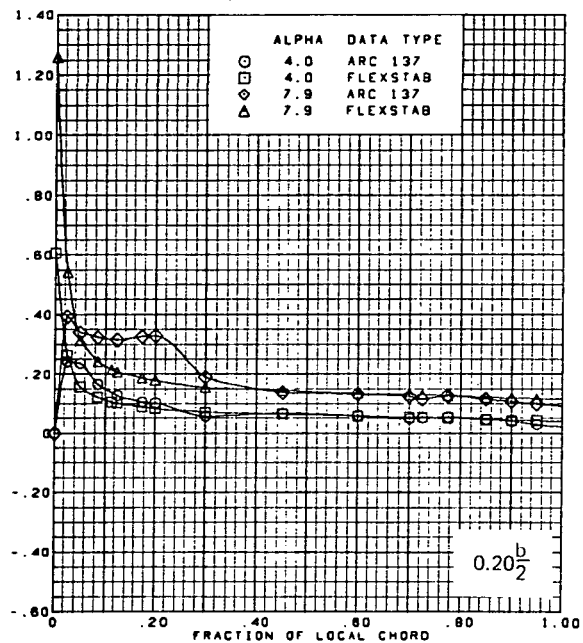
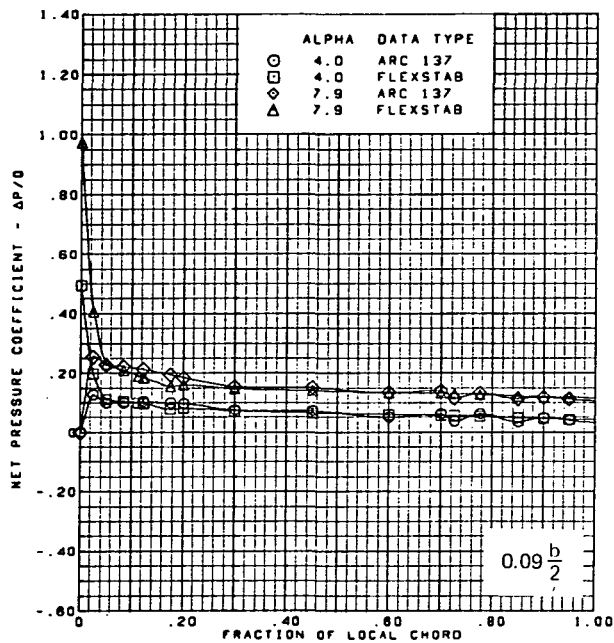
Figure 62.—(Continued)



M = 2.10 (run 9)  
 Twisted wing, rounded L.E.  
 L.E. deflection, full span =  $0.0^\circ$   
 T.E. deflection, full span =  $0.0^\circ$

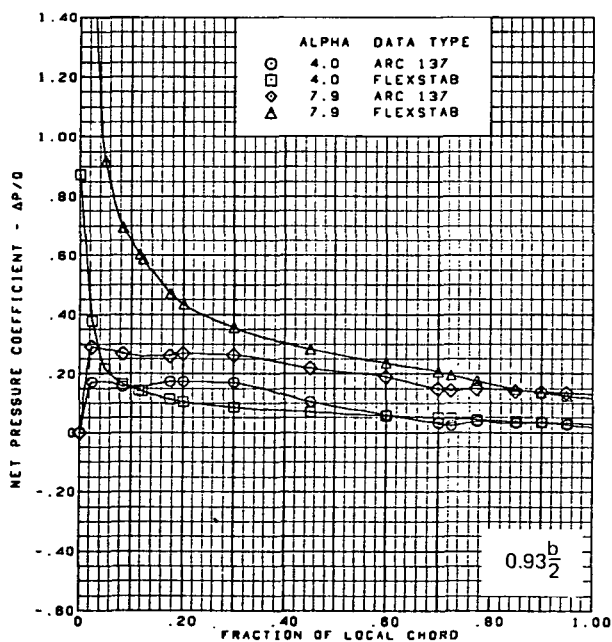
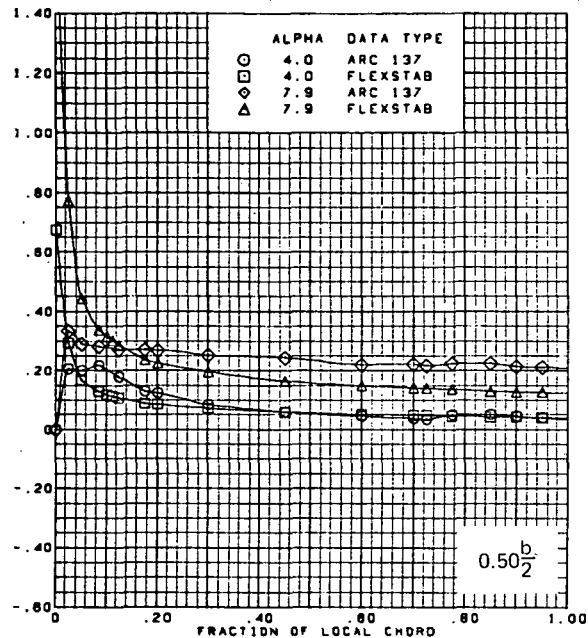
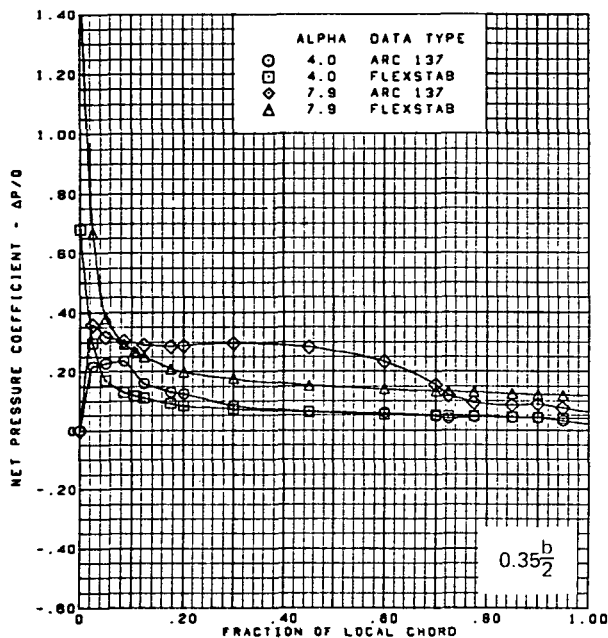
(e) (Concluded)

Figure 62.—(Continued)



(f) Net Chordwise Pressure Distributions,  $\alpha = 4^\circ, 8^\circ$

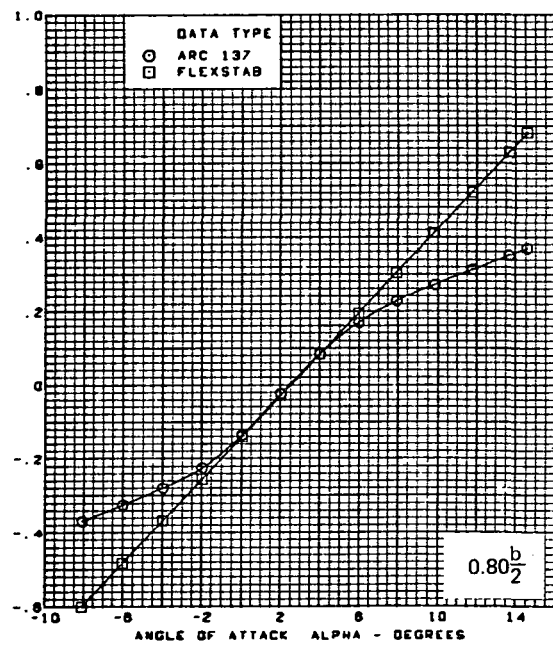
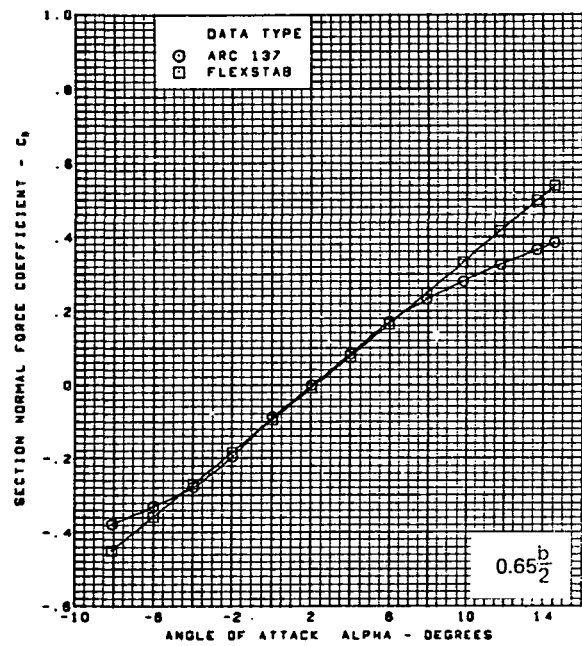
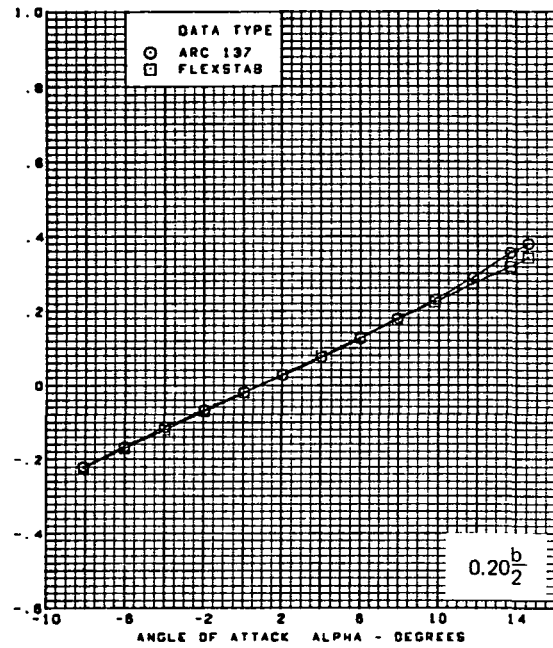
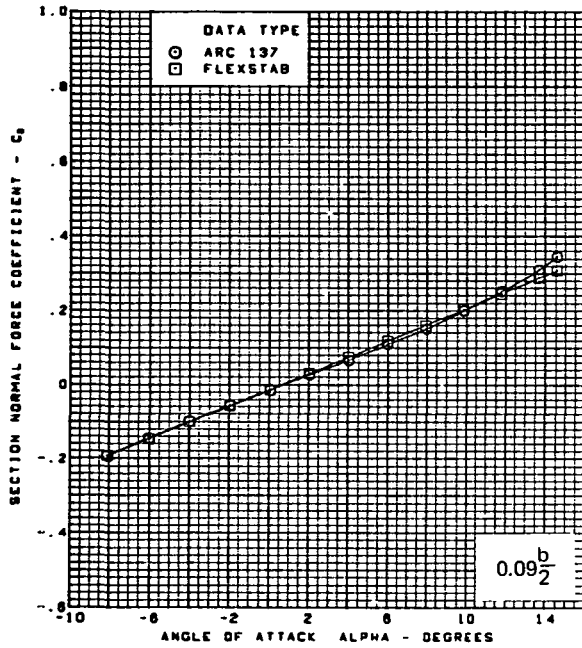
Figure 62.-(Continued)



$M = 2.10$  (run 9)  
 Twisted wing, rounded L.E.  
 L.E. deflection, full span =  $0.0^\circ$   
 T.E. deflection, full span =  $0.0^\circ$

(f) (Concluded)

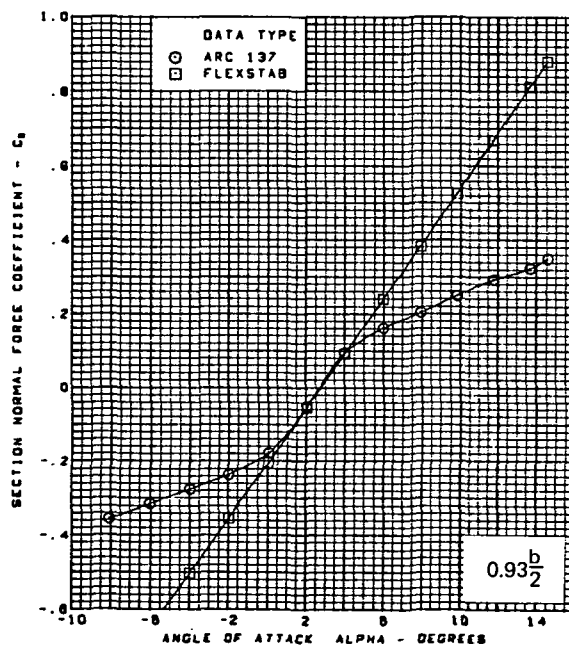
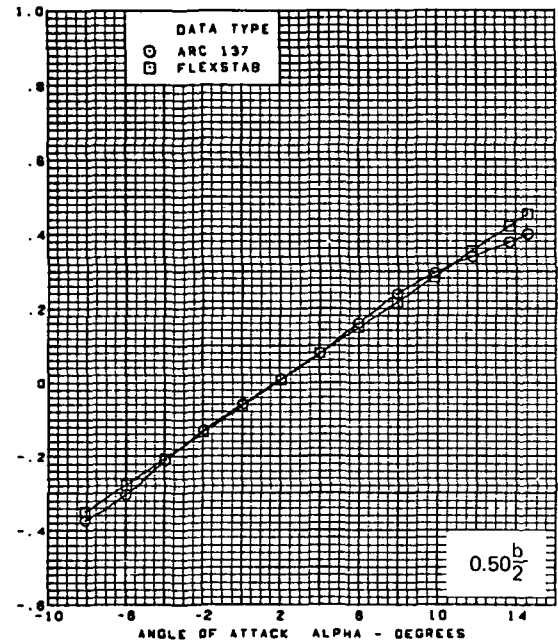
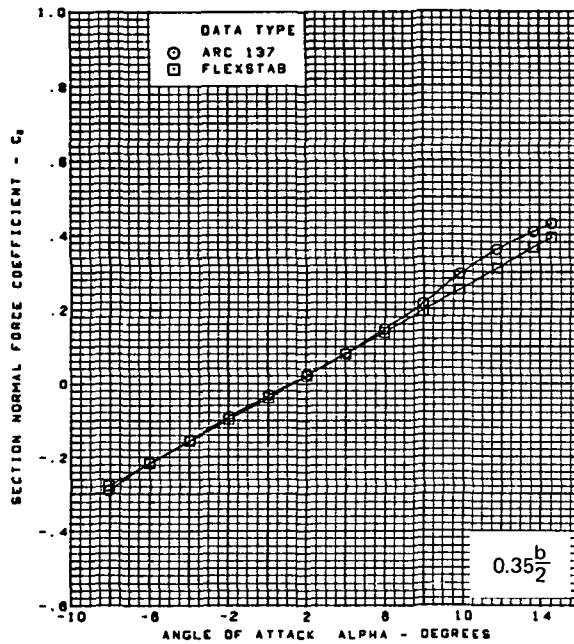
Figure 62.—(Continued)



(g) Section Aerodynamic Coefficients—Normal Force

Figure 62.—(Continued)

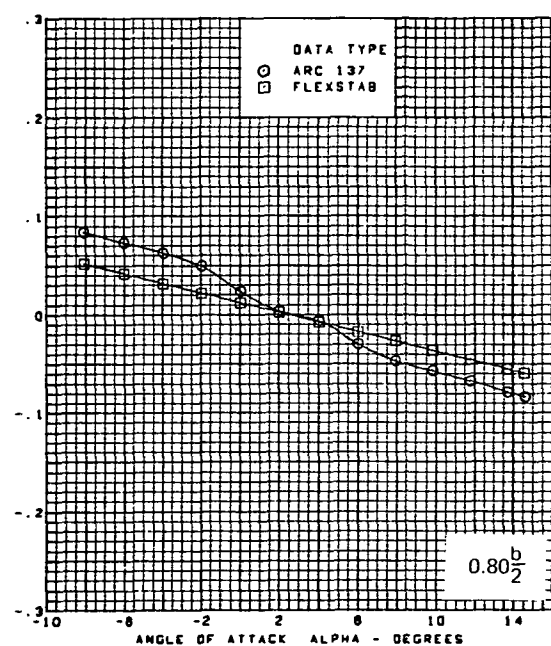
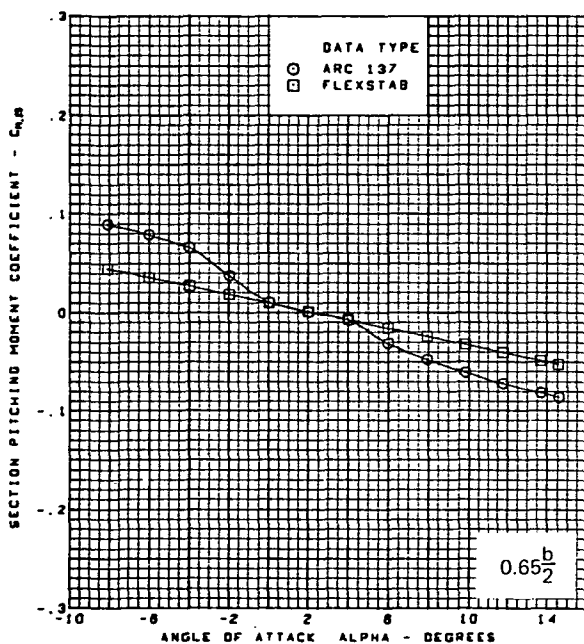
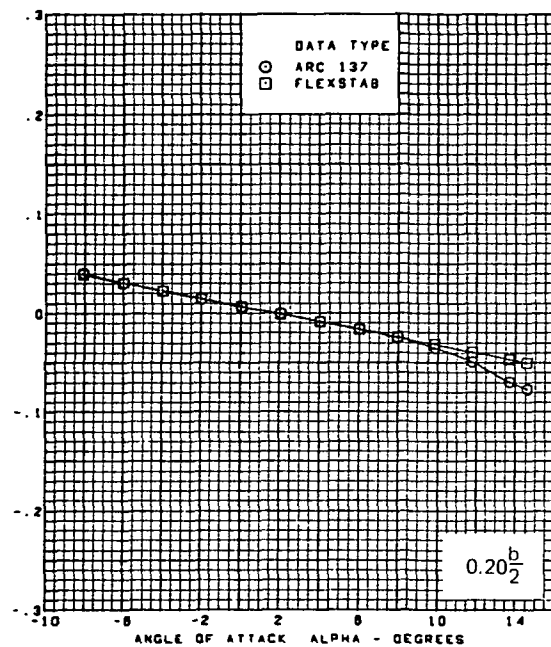
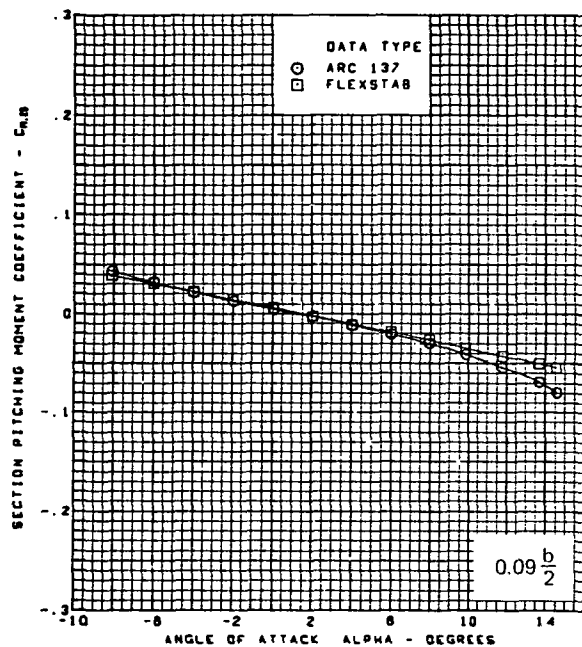




M = 2.10 (run 9)  
 Twisted wing, rounded L.E.  
 L.E. deflection, full span =  $0.0^\circ$   
 T.E. deflection, full span =  $0.0^\circ$

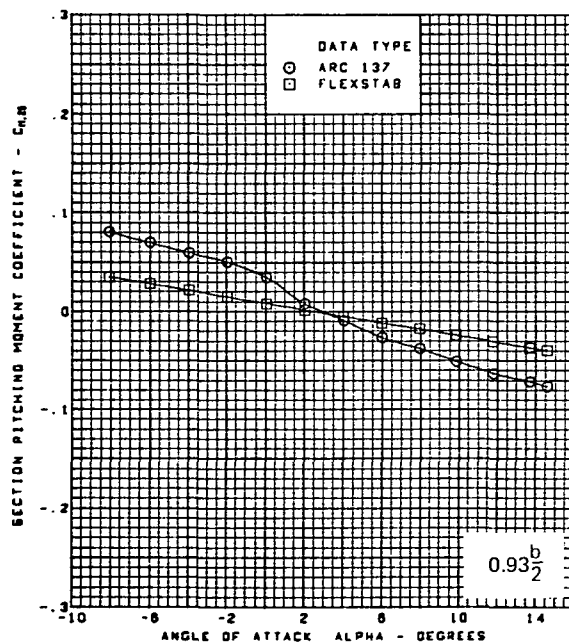
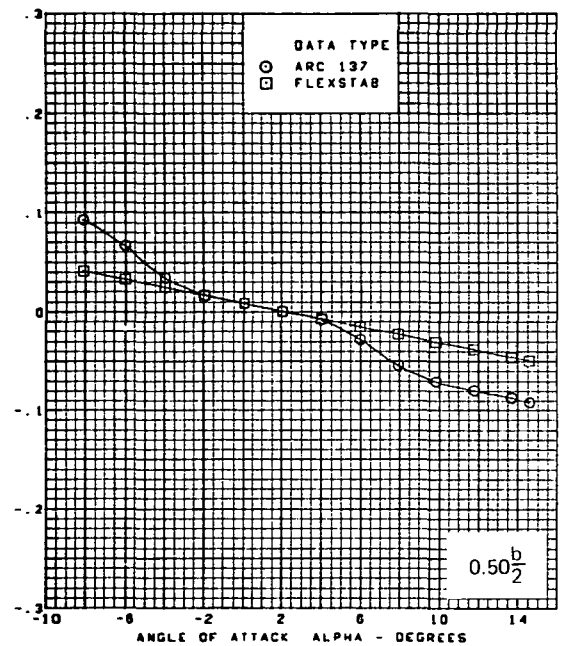
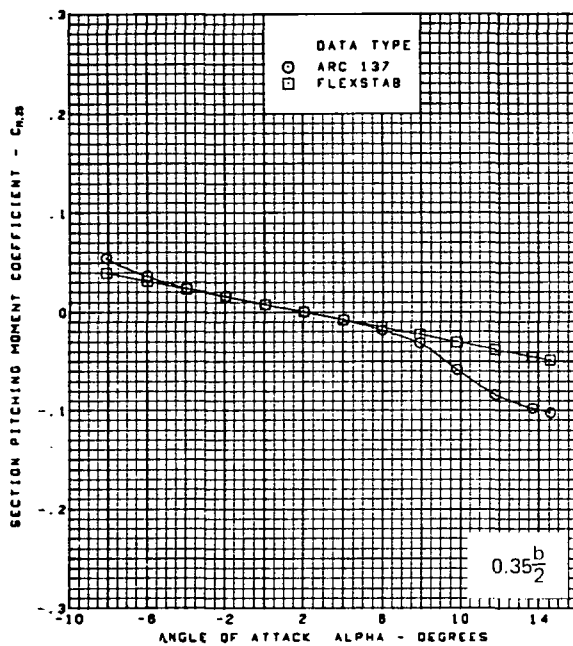
(g) (Concluded)

Figure 62.—(Continued)



(h) Section Aerodynamic Coefficients—Pitching Moment

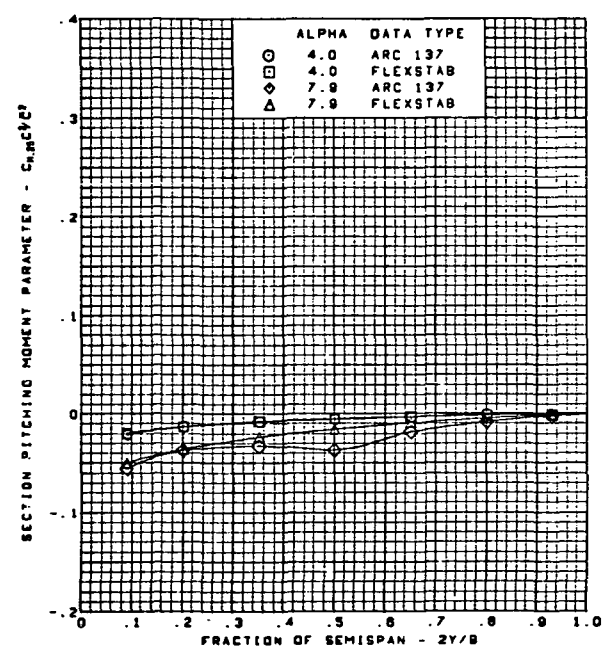
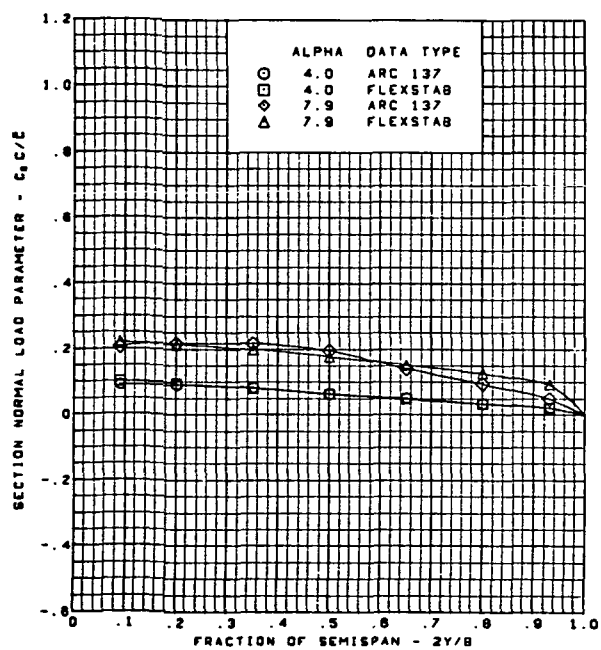
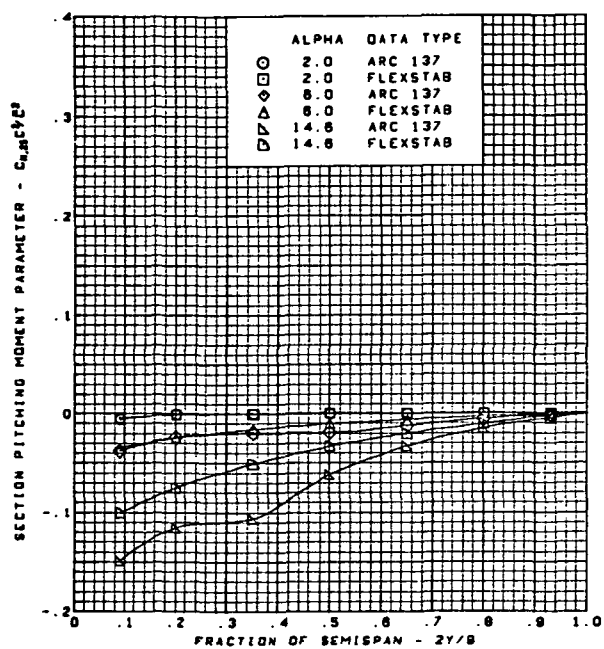
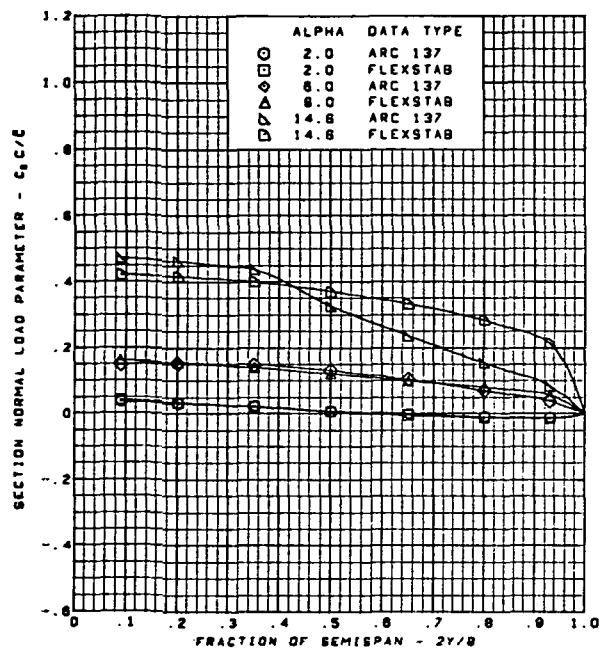
Figure 62.—(Continued)



M = 2.10 (run 9)  
 Twisted wing, rounded L.E.  
 L.E. deflection, full span =  $0.0^\circ$   
 T.E. deflection, full span =  $0.0^\circ$

(h) (Concluded)

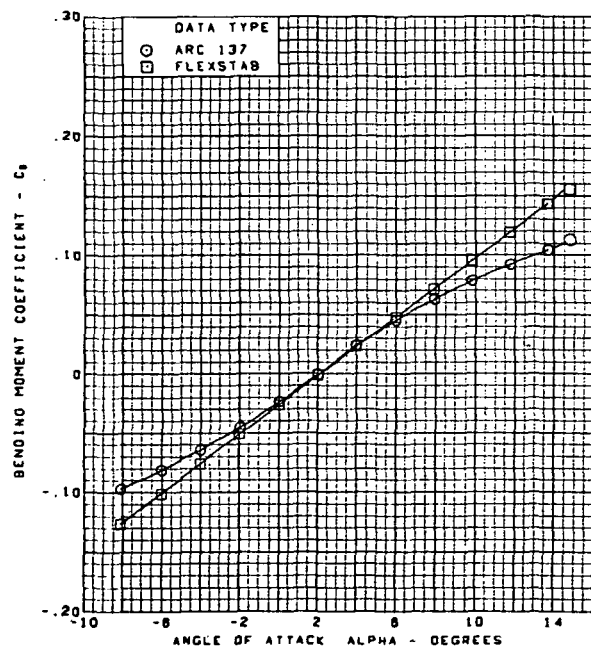
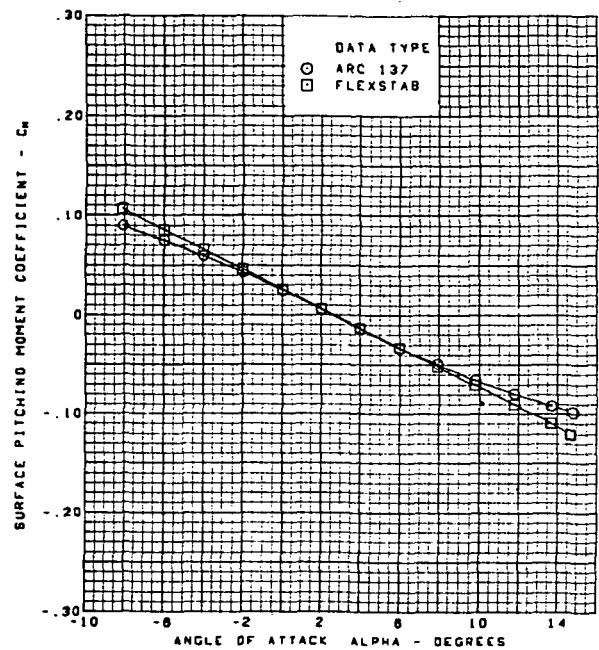
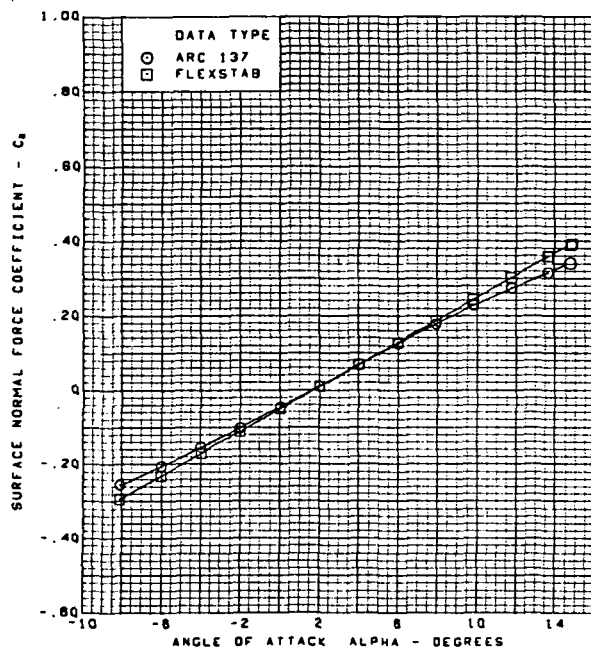
Figure 62.—(Continued)



M = 2.10 (run 9)  
 Twisted wing, rounded L.E.  
 L.E. deflection, full span =  $0.0^\circ$   
 T.E. deflection, full span =  $0.0^\circ$

(i) Spanload Distributions

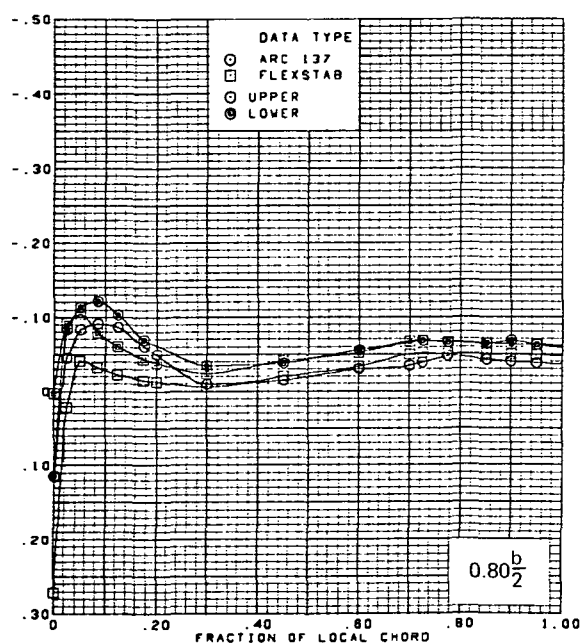
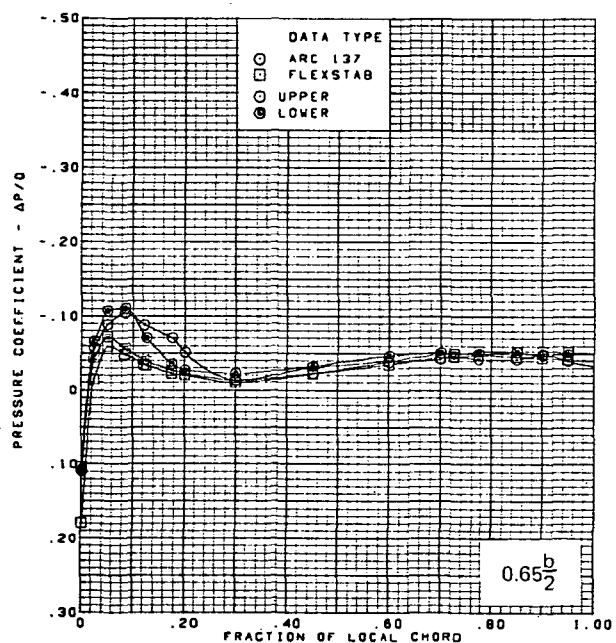
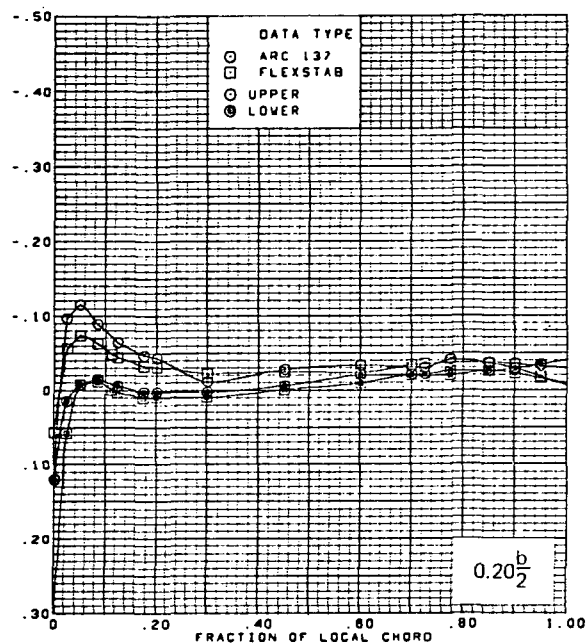
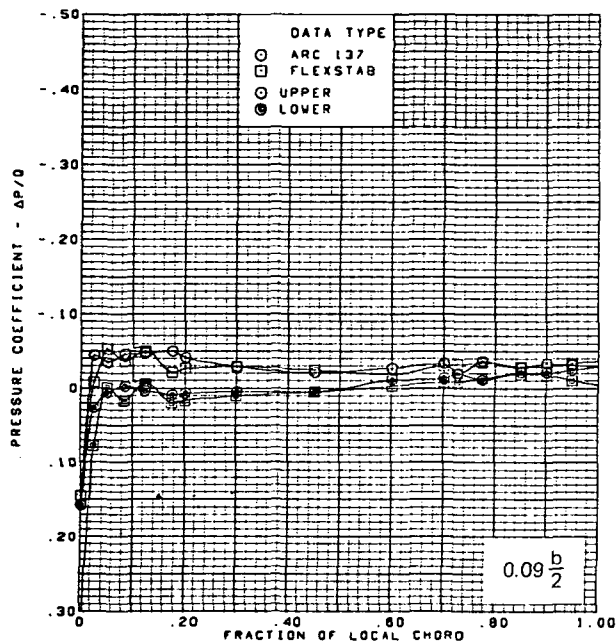
Figure 62.—(Continued)



M = 2.10 (run 9)  
 Twisted wing, rounded L.E.  
 L.E. deflection, full span =  $0.0^\circ$   
 T.E. deflection, full span =  $0.0^\circ$

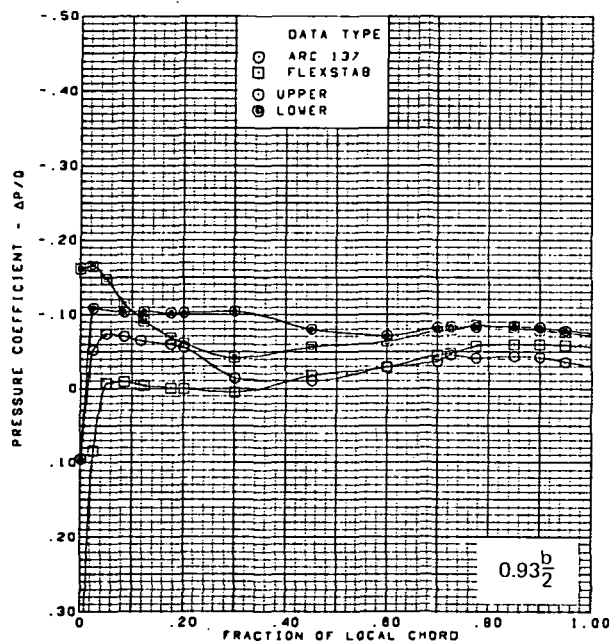
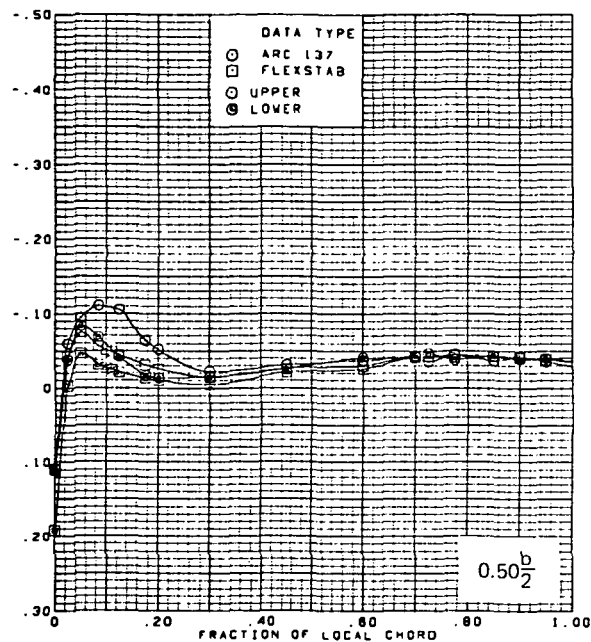
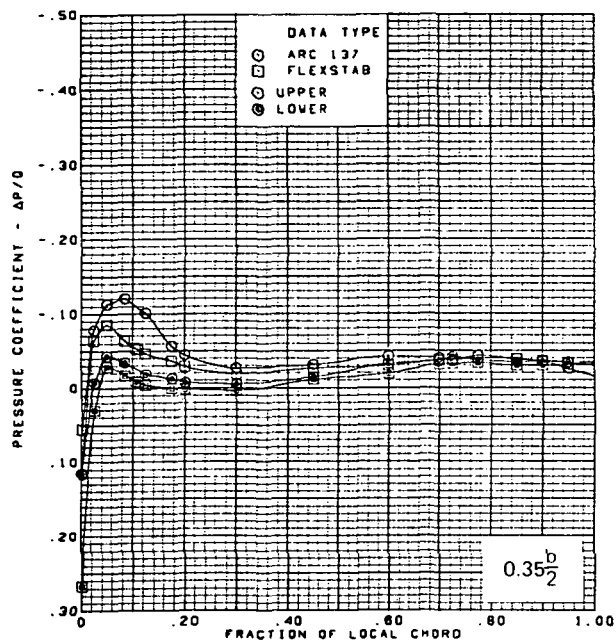
(j) Wing Aerodynamic Coefficients

Figure 62.—(Concluded)



(a) Surface Chordwise Pressure Distributions,  $\alpha = 2^\circ$

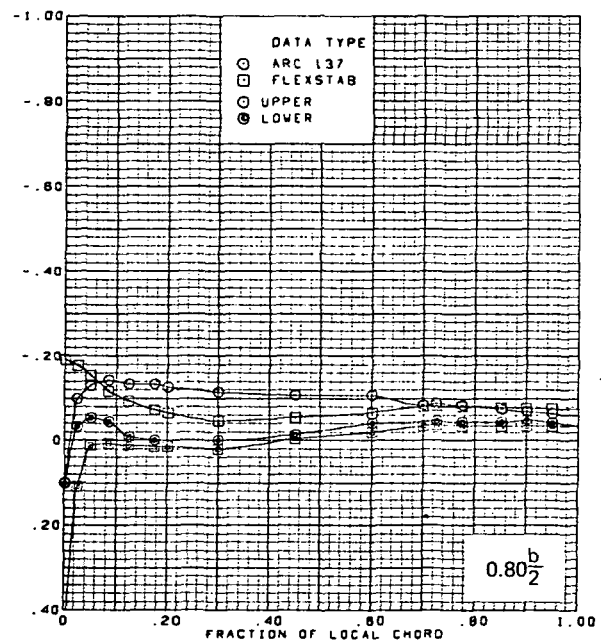
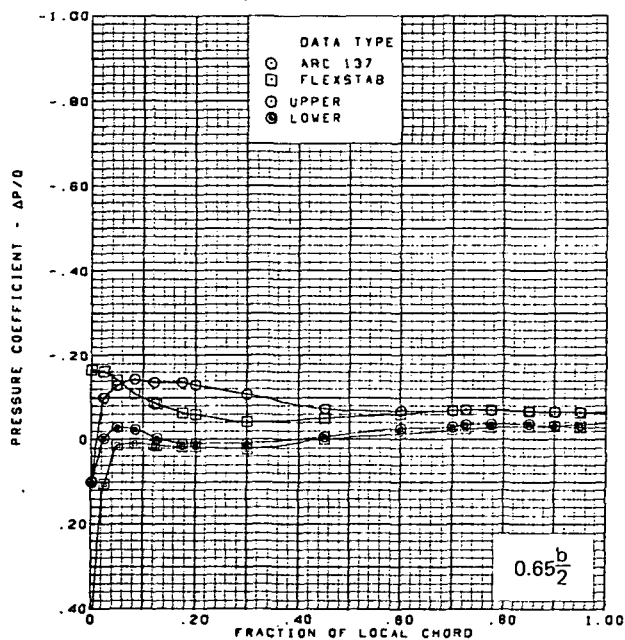
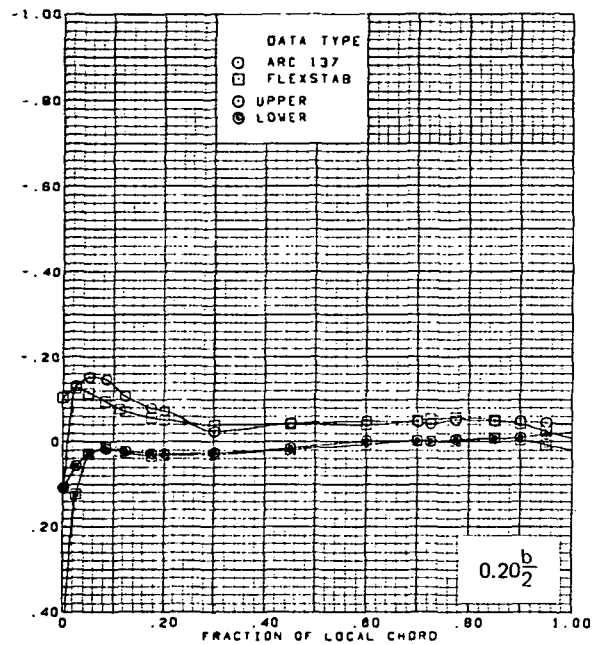
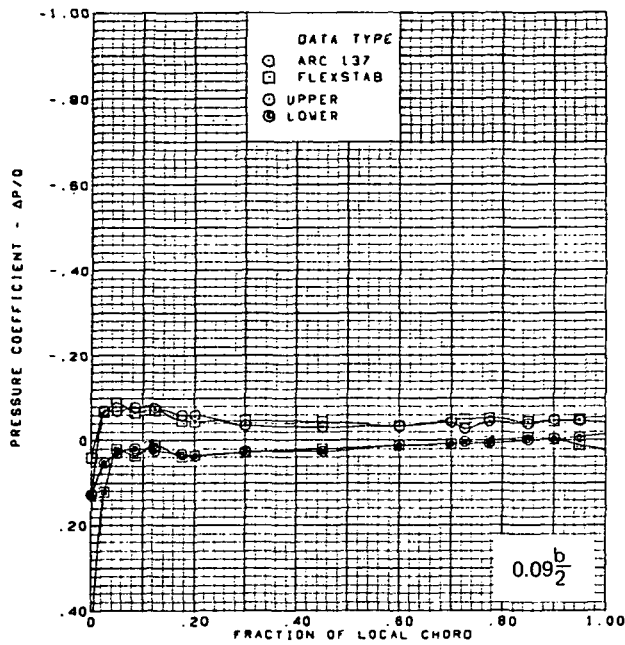
Figure 63.—Wing Theory-to-Experiment Comparison—Twisted Wing, Rounded L.E.; L.E. Deflection, Full Span =  $0.0^\circ$ ; T.E. Deflection, Full Span =  $0.0^\circ$ ;  $M = 2.50$



$M = 2.50$  (run 10)  
 $\alpha = 2^\circ$   
 Twisted wing, rounded L.E.  
 L.E. deflection, full span =  $0.0^\circ$   
 T.E. deflection, full span =  $0.0^\circ$   
 Note:  $C_{p, \text{vacuum}} = -0.23$

(a) (Concluded)

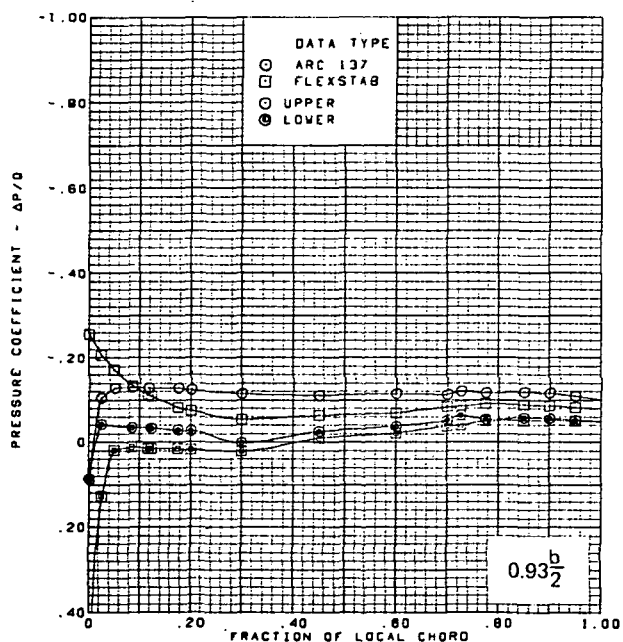
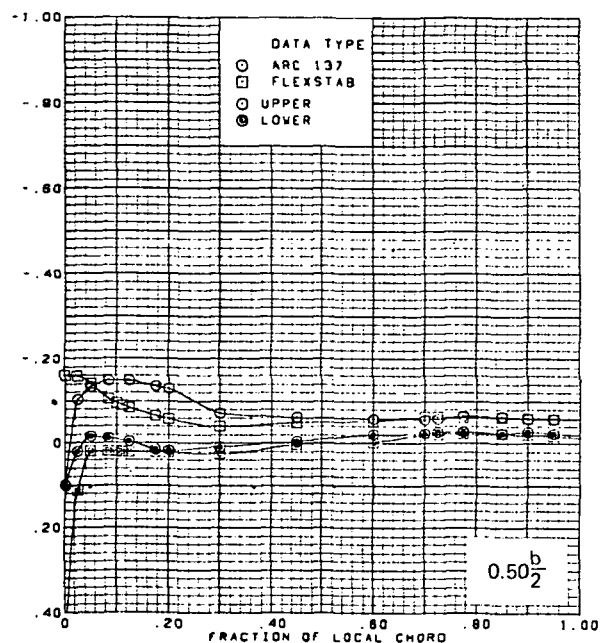
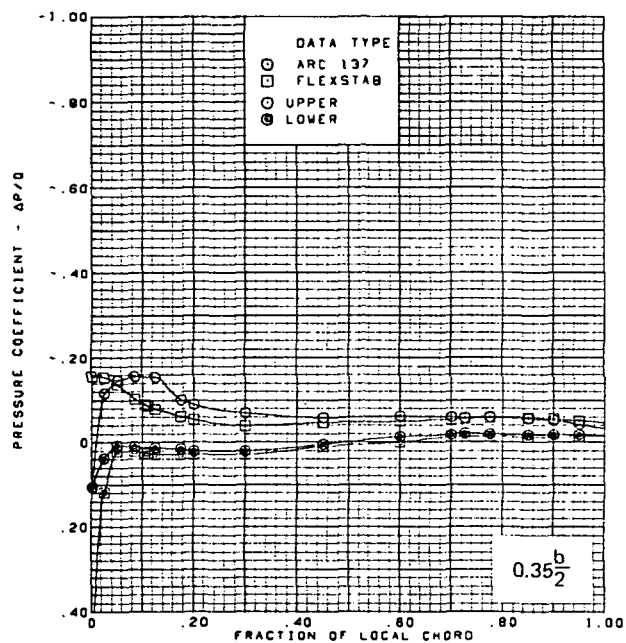
Figure 63.—(Continued)



(b) Surface Chordwise Pressure Distributions,  $\alpha = 4^\circ$

Figure 63.-(Continued)

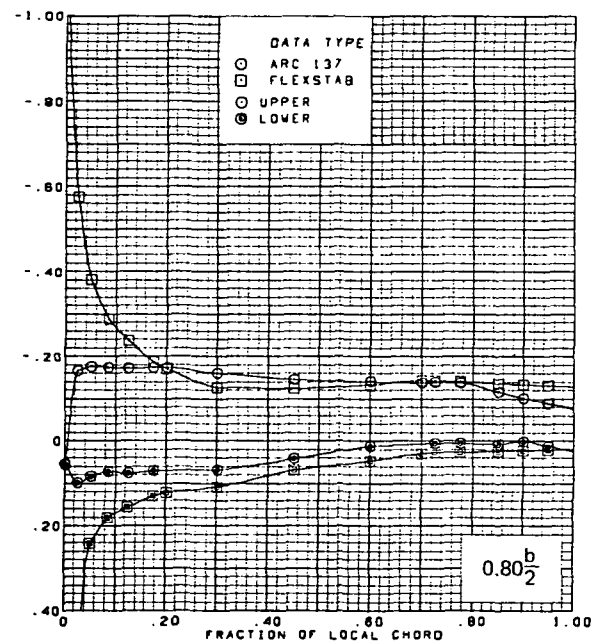
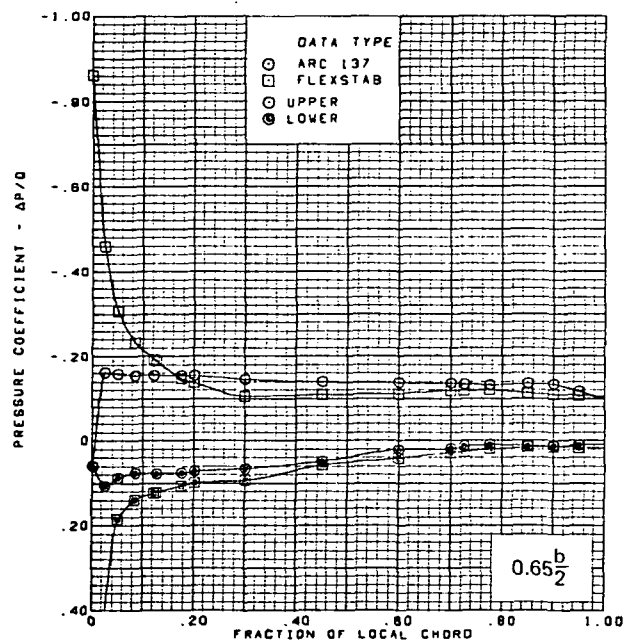
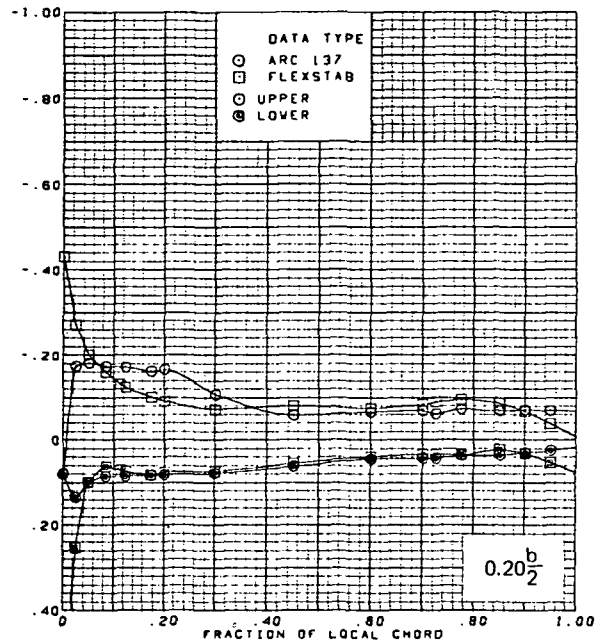
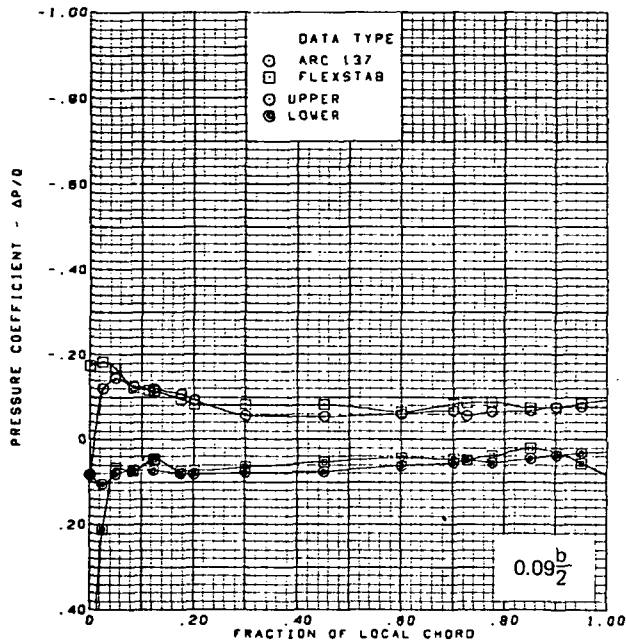




$M = 2.50$  (run 10)  
 $\alpha = 4^\circ$   
 Twisted wing, rounded L.E.  
 L.E. deflection, full span =  $0.0^\circ$   
 T.E. deflection, full span =  $0.0^\circ$   
 Note:  $C_{p, \text{vacuum}} = -0.23$

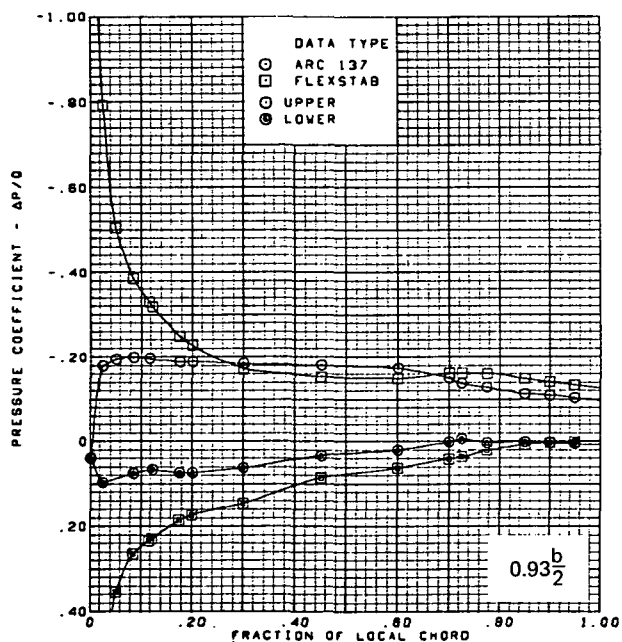
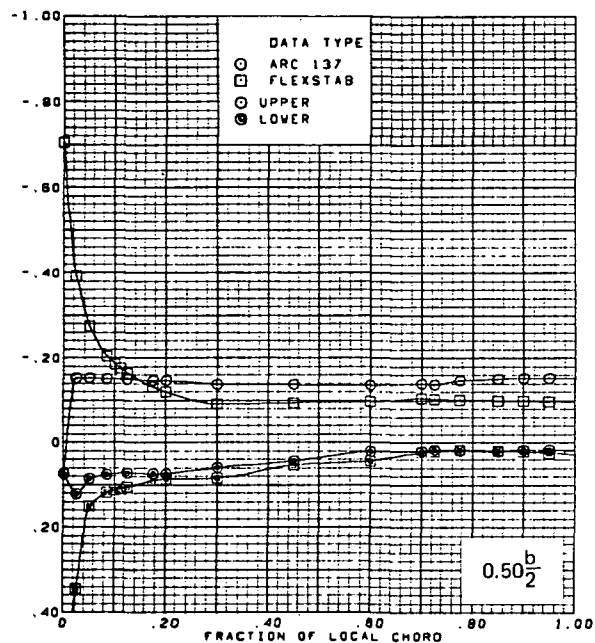
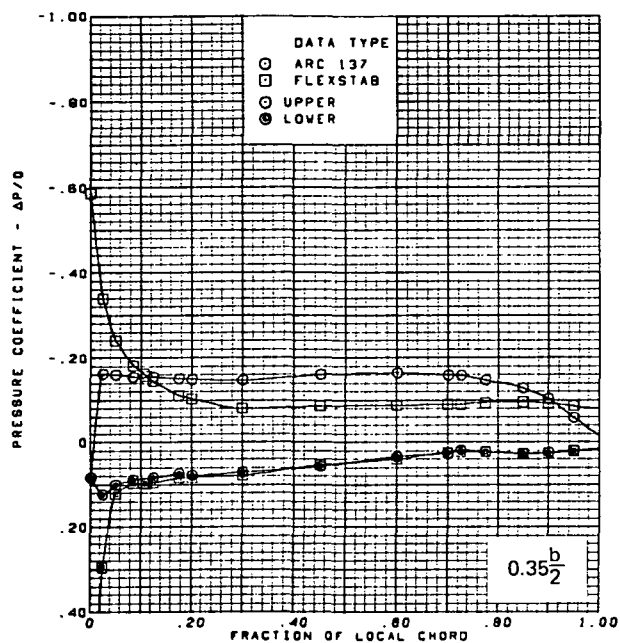
(b) (Concluded)

Figure 63.—(Continued)



(c) Surface Chordwise Pressure Distributions,  $\alpha = 8^\circ$

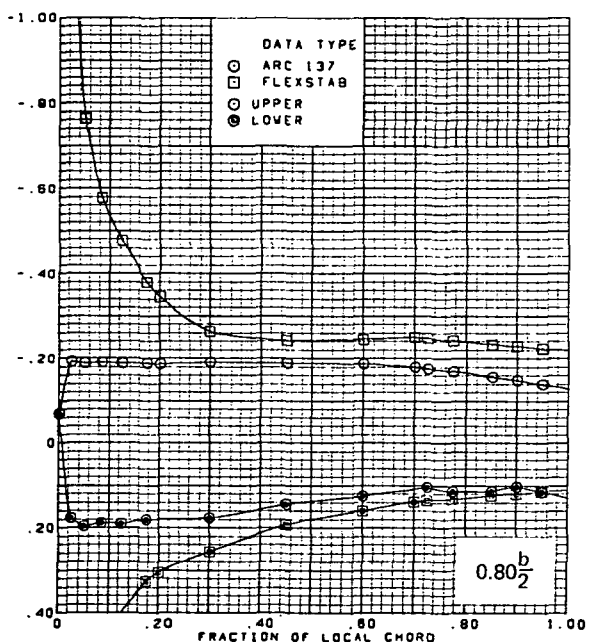
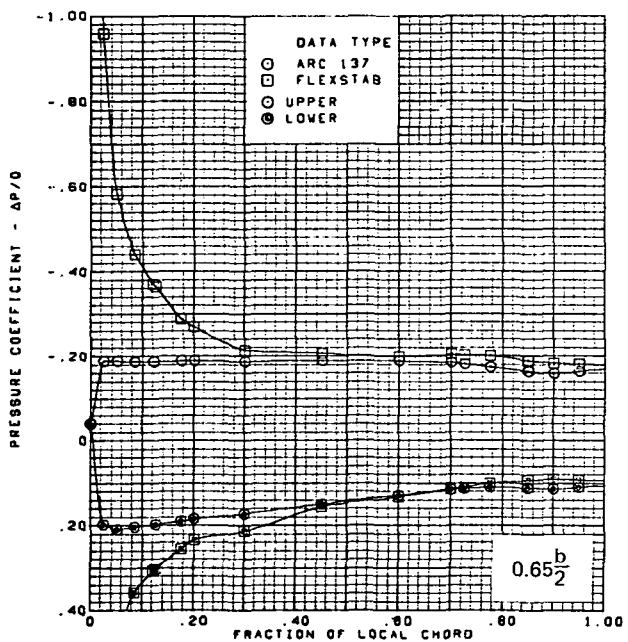
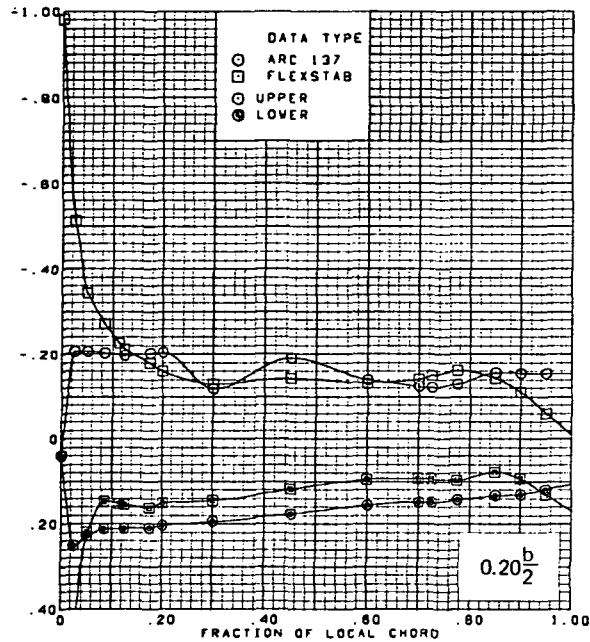
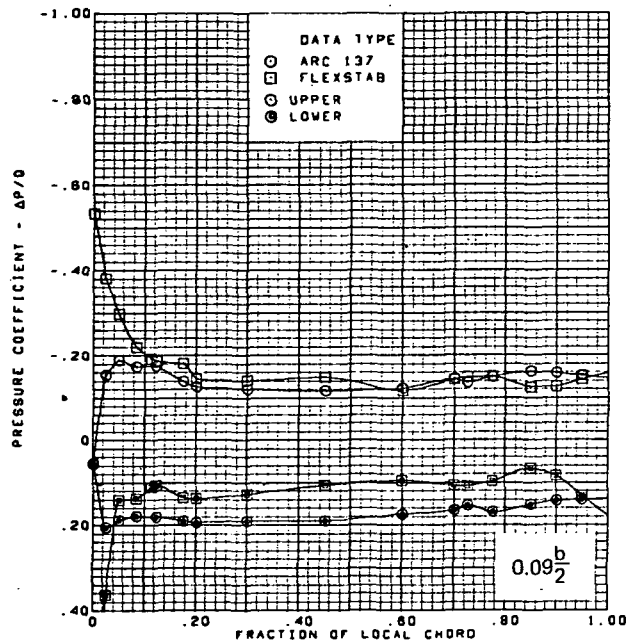
Figure 63.—(Continued)



$M = 2.50$  (run 10)  
 $\alpha = 8^\circ$   
 Twisted wing, rounded L.E.  
 L.E. deflection, full span =  $0.0^\circ$   
 T.E. deflection, full span =  $0.0^\circ$   
 Note:  $C_{p, \text{vacuum}} = -0.23$

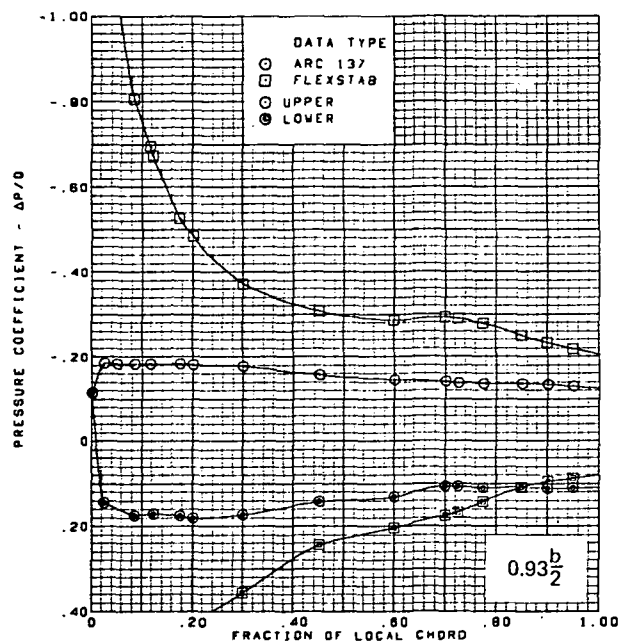
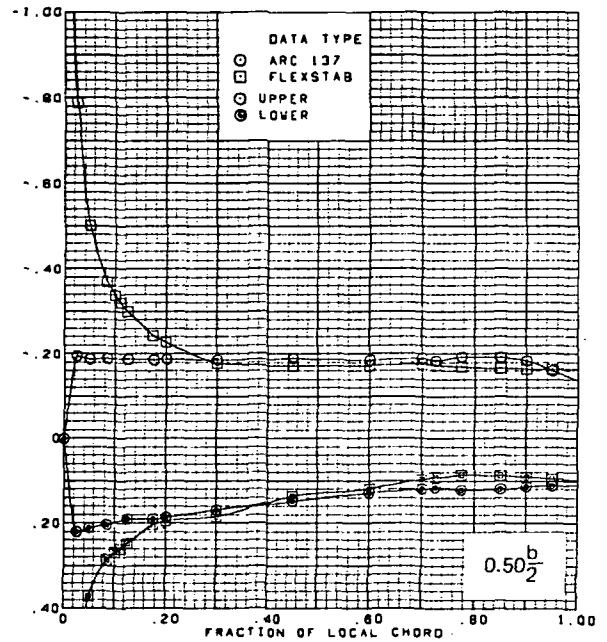
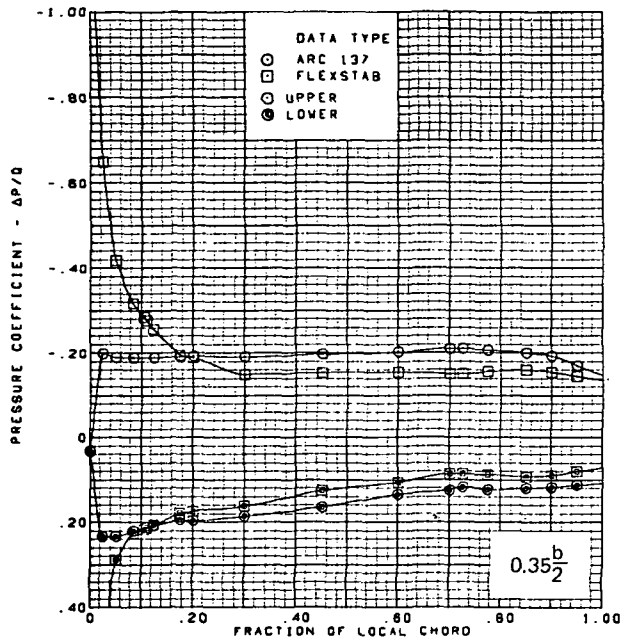
(c) (Concluded)

Figure 63.—(Continued)



(d) Surface Chordwise Pressure Distributions,  $\alpha = 15^\circ$

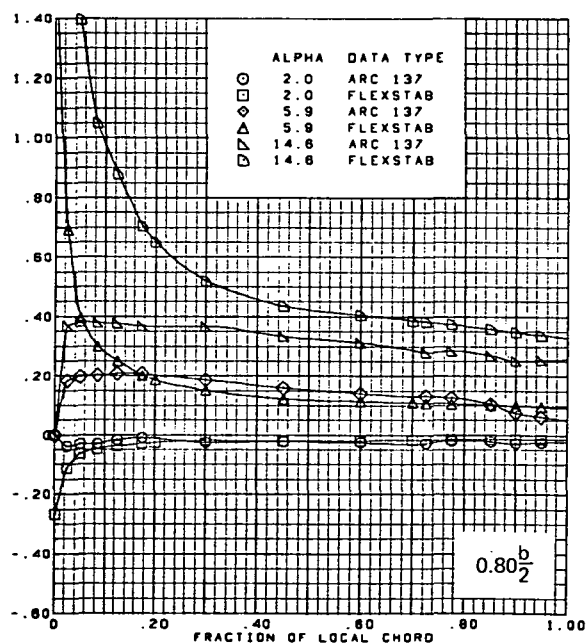
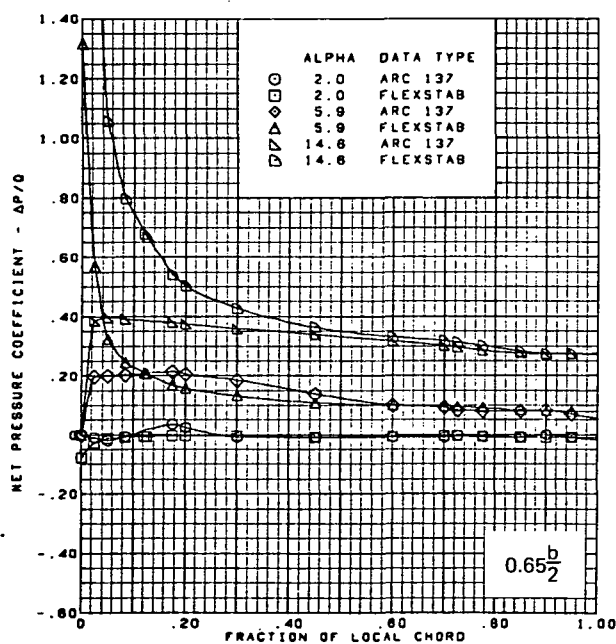
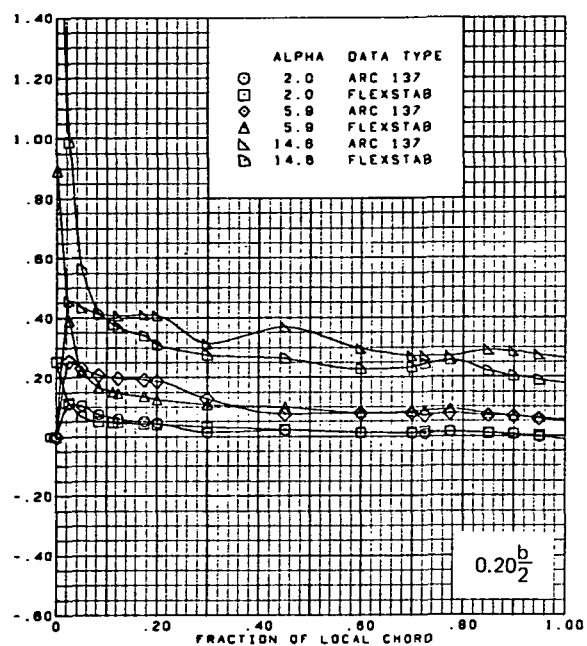
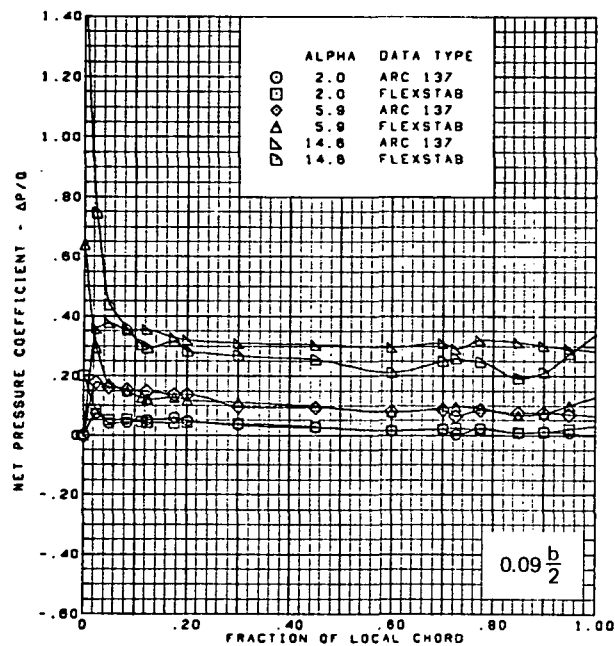
Figure 63.—(Continued)



$M = 2.50$  (run 10)  
 $\alpha = 15^\circ$   
 Twisted wing, rounded L.E.  
 L.E. deflection, full span =  $0.0^\circ$   
 T.E. deflection, full span =  $0.0^\circ$   
 Note:  $C_{p, \text{vacuum}} = -0.23$

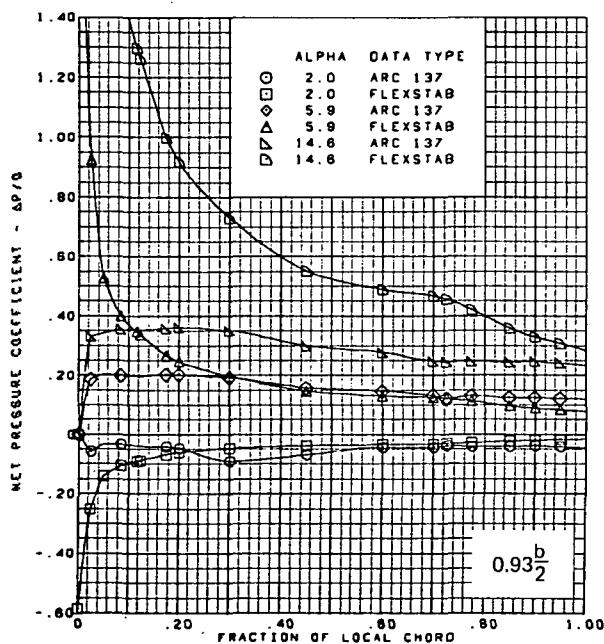
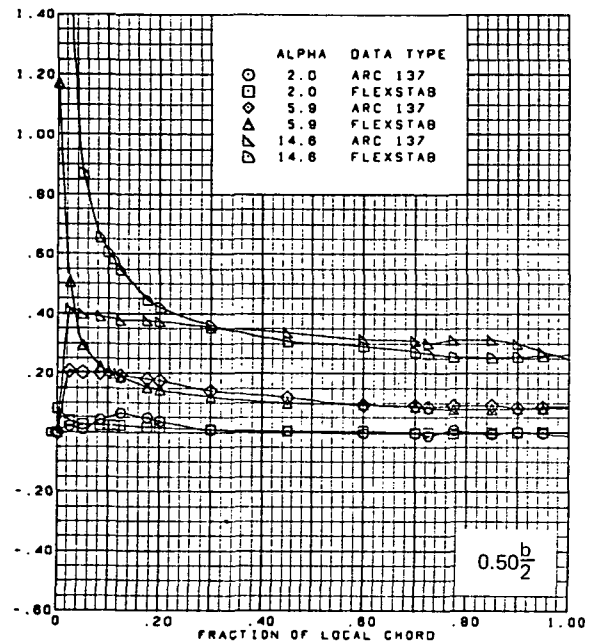
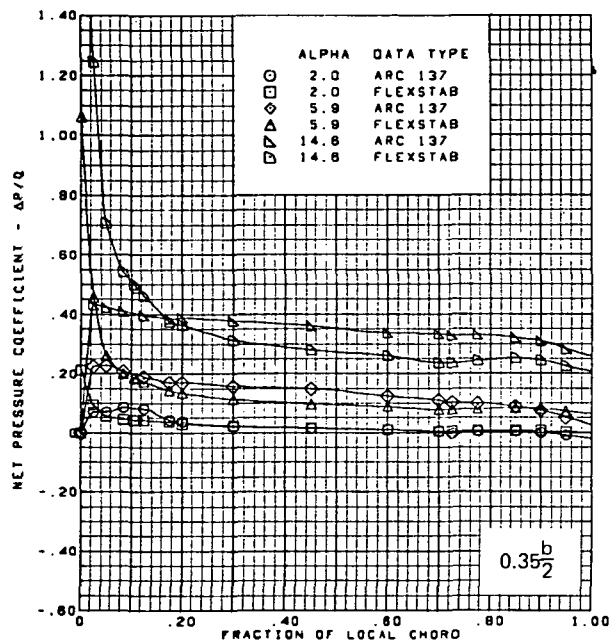
(d) (Concluded).

Figure 63. —(Continued)



(e) Net Chordwise Pressure Distributions,  $\alpha = 2^\circ, 6^\circ, 15^\circ$

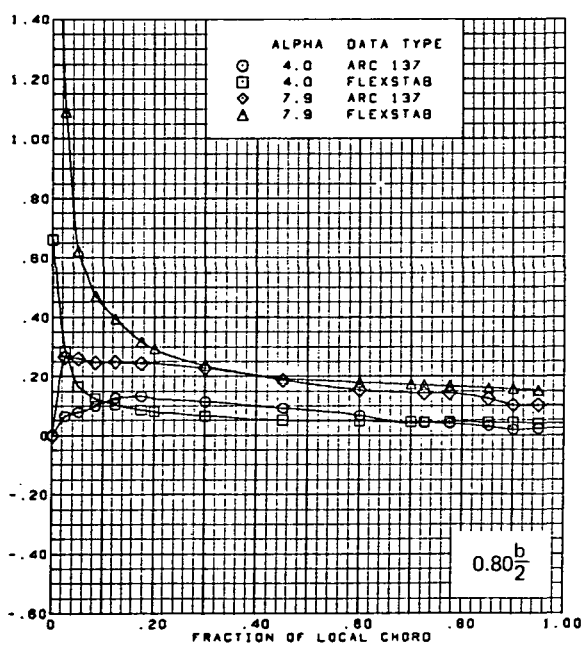
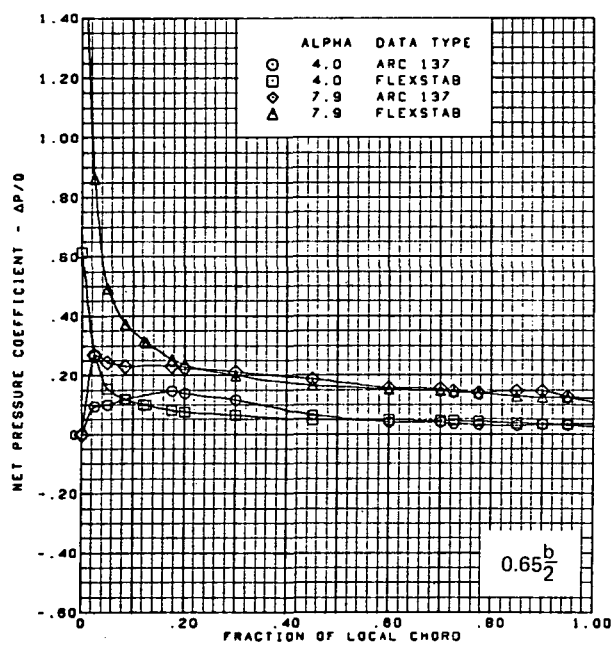
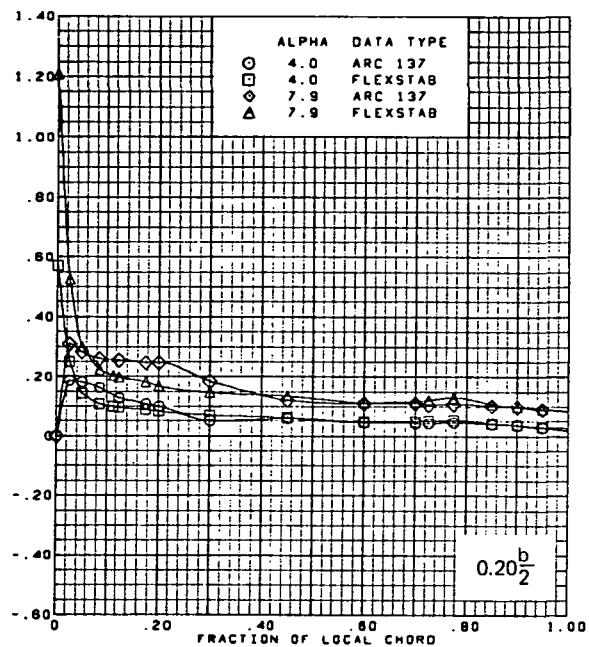
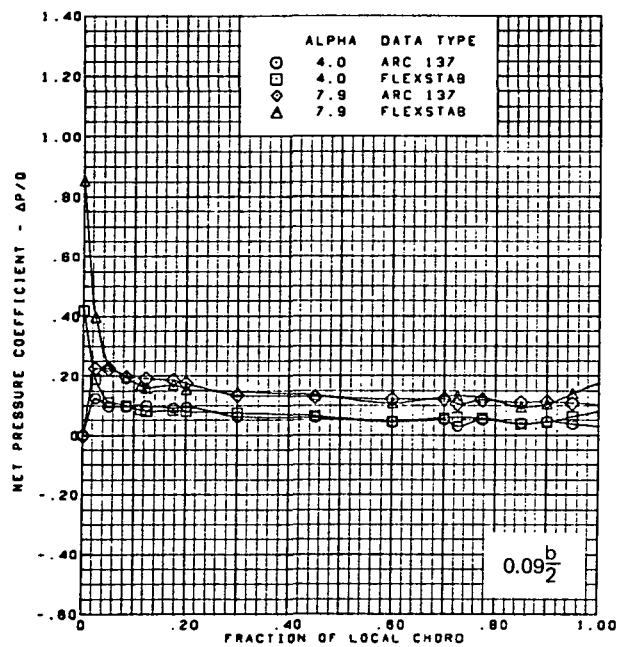
Figure 63.—(Continued)



$M = 2.50$  (run 10)  
 Twisted wing, rounded L.E.  
 L.E. deflection, full span =  $0.0^\circ$   
 T.E. deflection, full span =  $0.0^\circ$

(e) (Concluded)

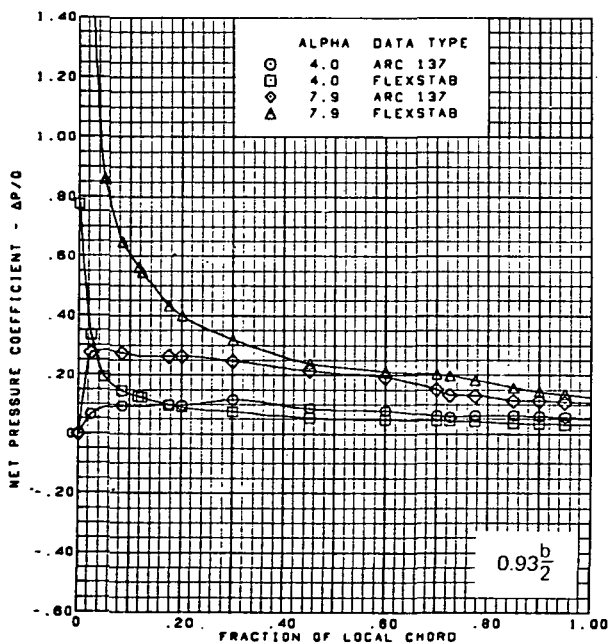
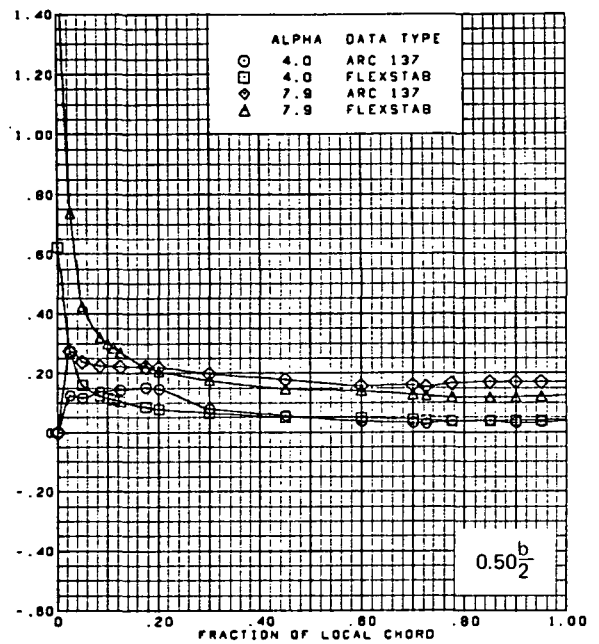
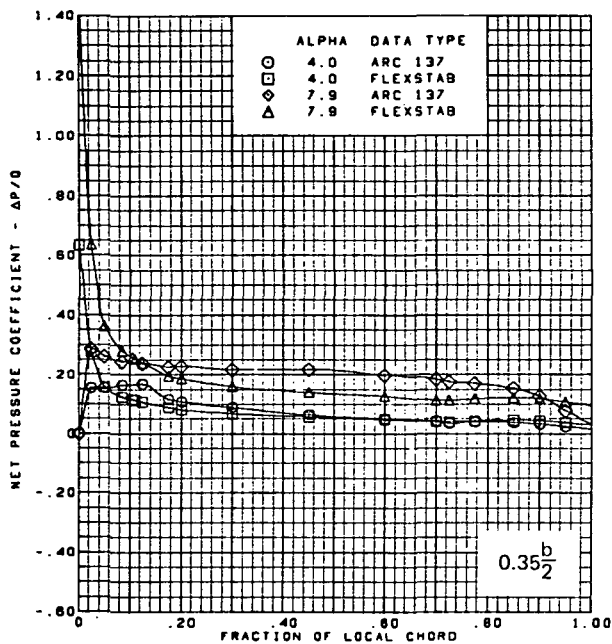
Figure 63.—(Continued)



(f) Net Chordwise Pressure Distributions,  $\alpha = 4^\circ, 8^\circ$

Figure 63.—(Continued)

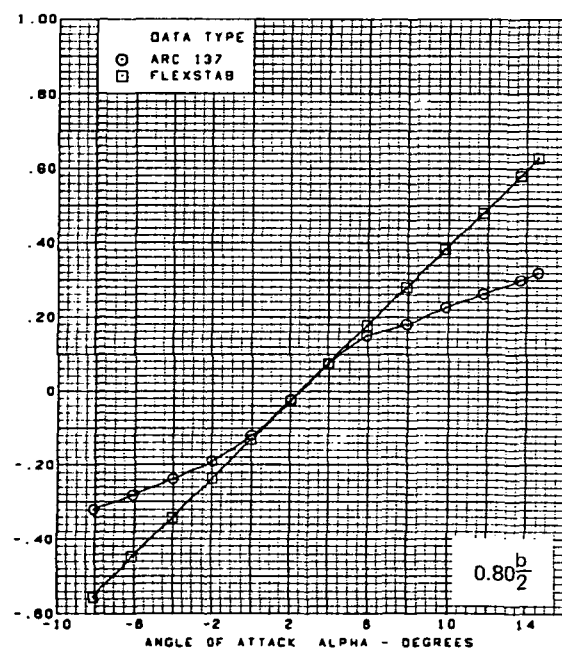
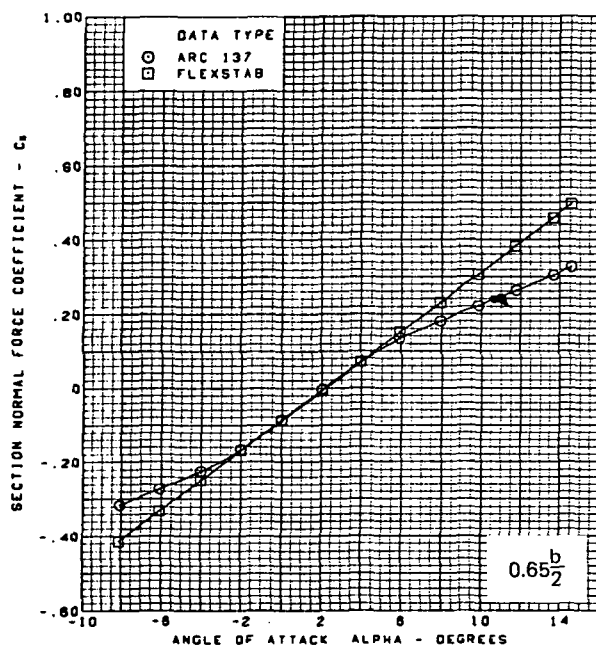
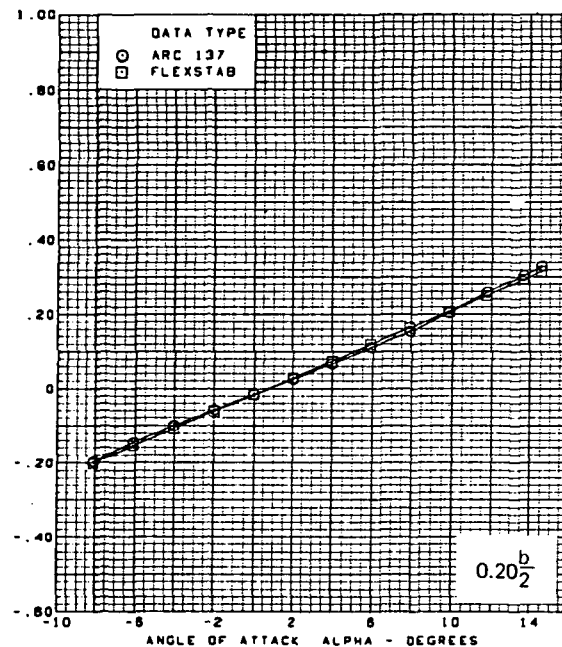
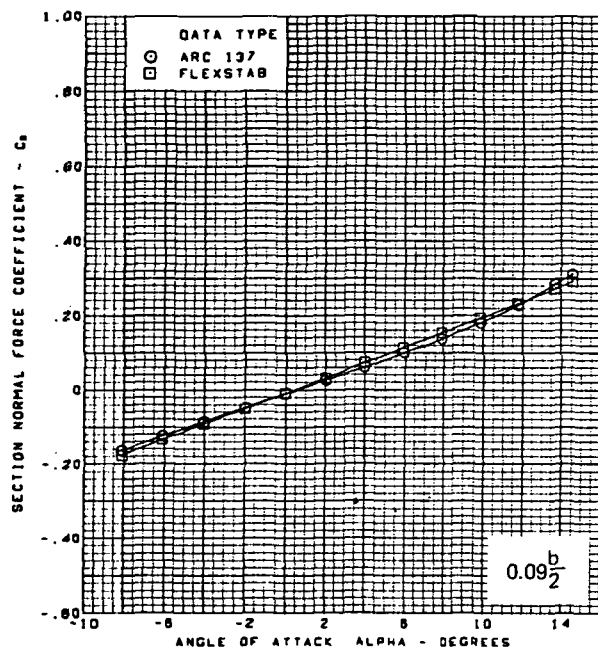




$M = 2.50$  (run 10)  
 Twisted wing, rounded L.E.  
 L.E. deflection, full span =  $0.0^\circ$   
 T.E. deflection, full span =  $0.0^\circ$

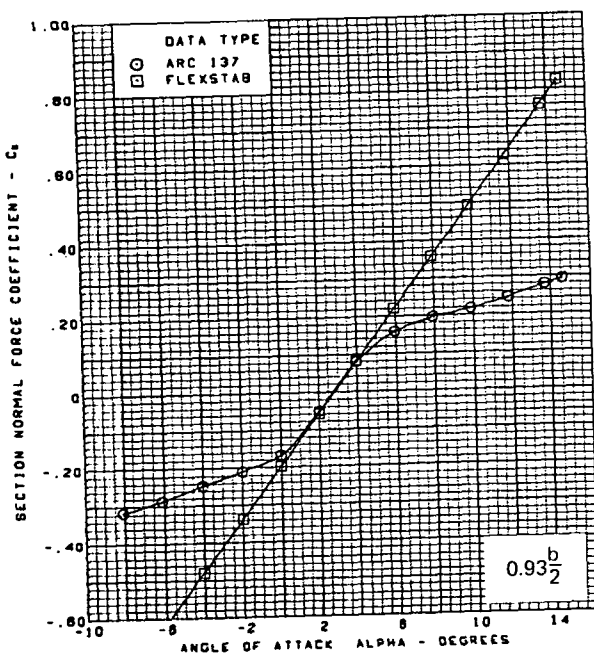
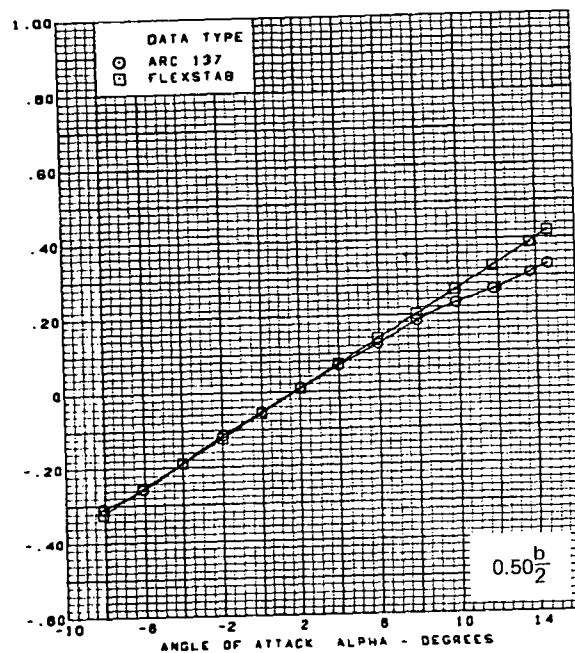
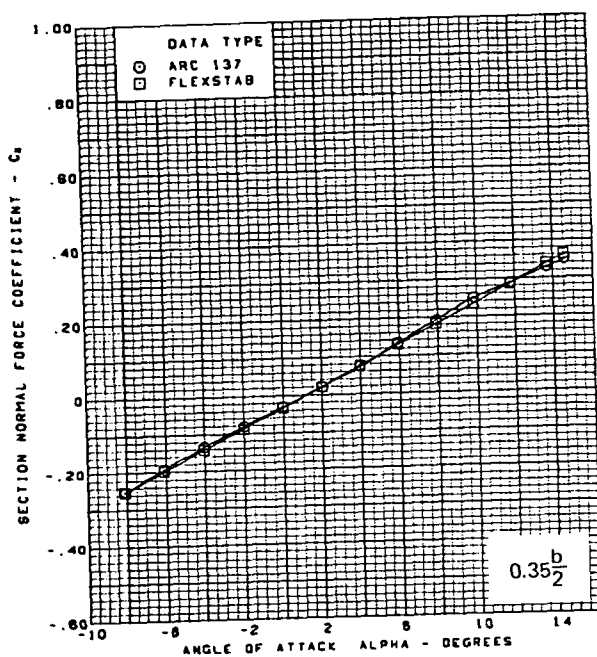
(f) (Concluded)

Figure 63.—(Continued)



(g) Section Aerodynamic Coefficients—Normal Force

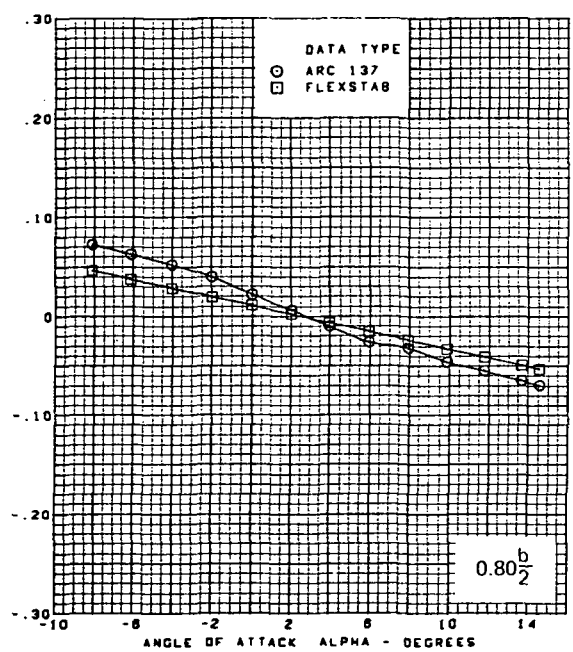
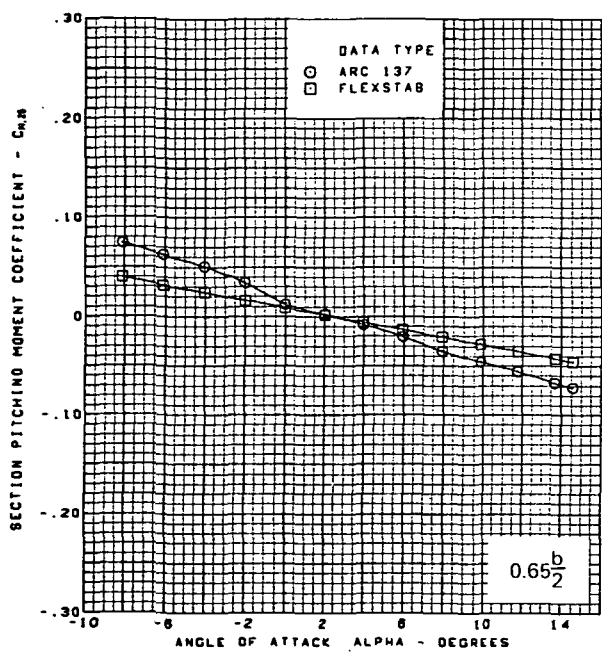
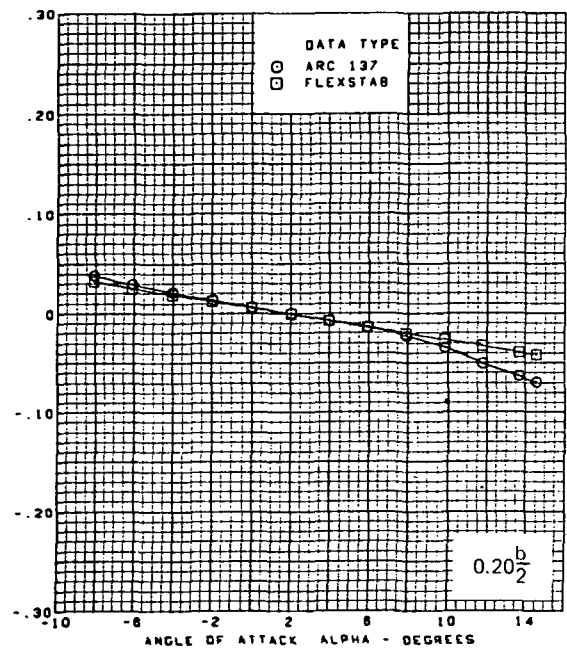
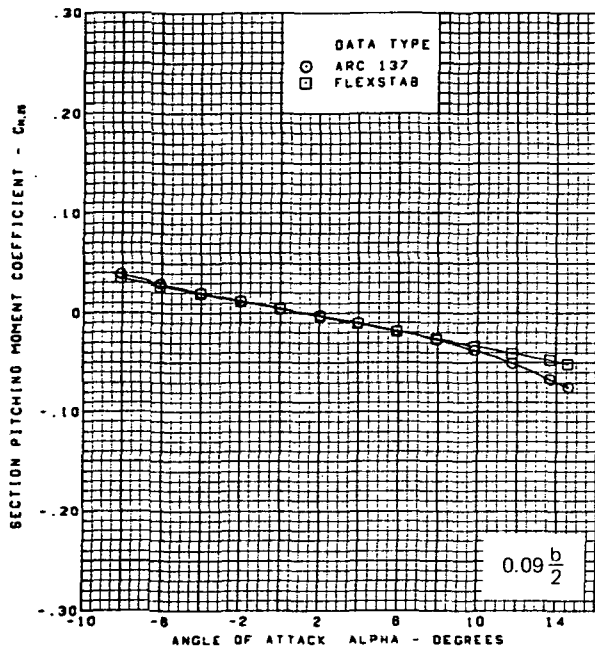
Figure 63.—(Continued)



M = 2.50 (run 10)  
 Twisted wing, rounded L.E.  
 L.E. deflection, full span =  $0.0^\circ$   
 T.E. deflection, full span =  $0.0^\circ$

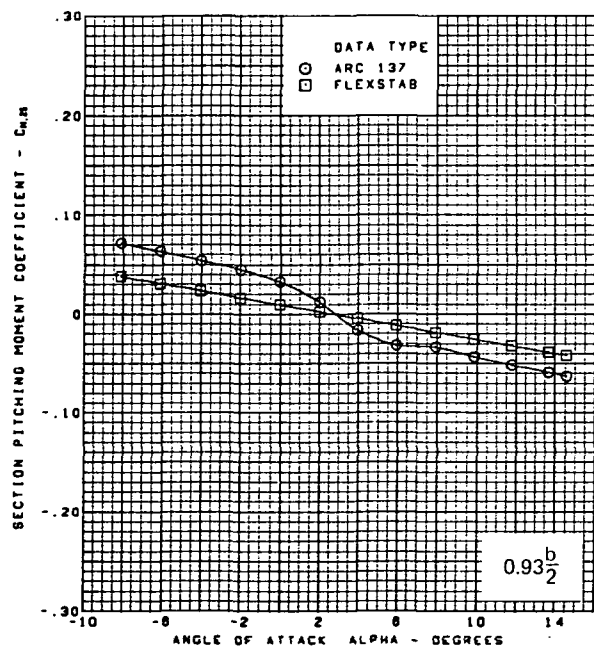
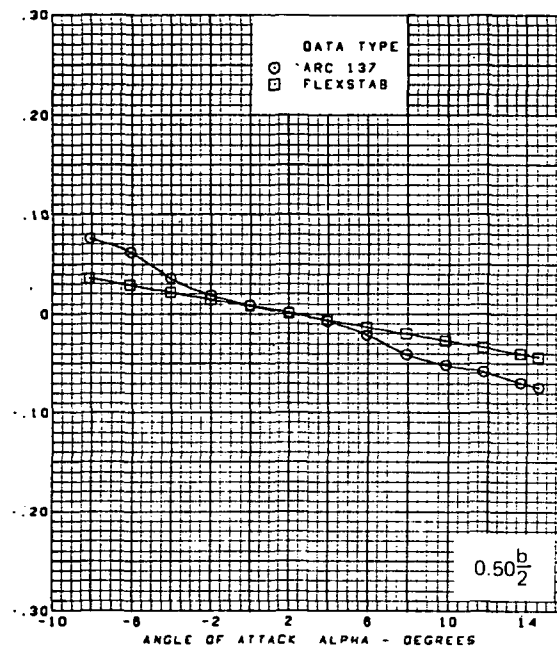
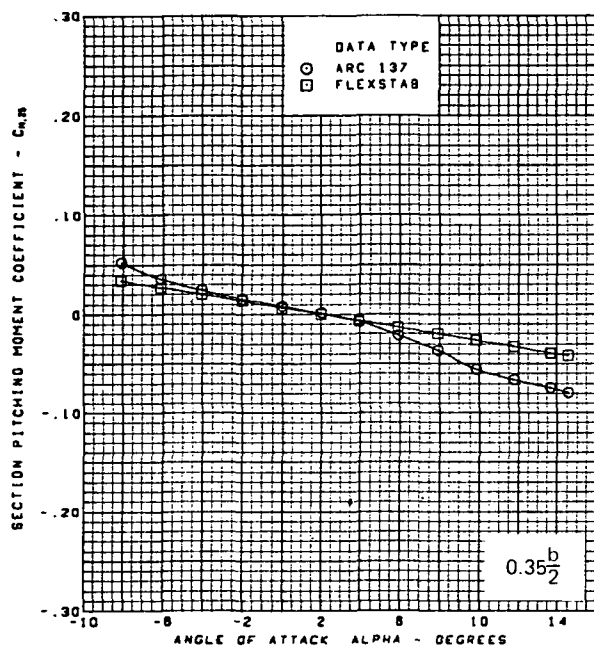
(g) (Concluded)

Figure 63.-(Continued)



(h) Section Aerodynamic Coefficients—Pitching Moment

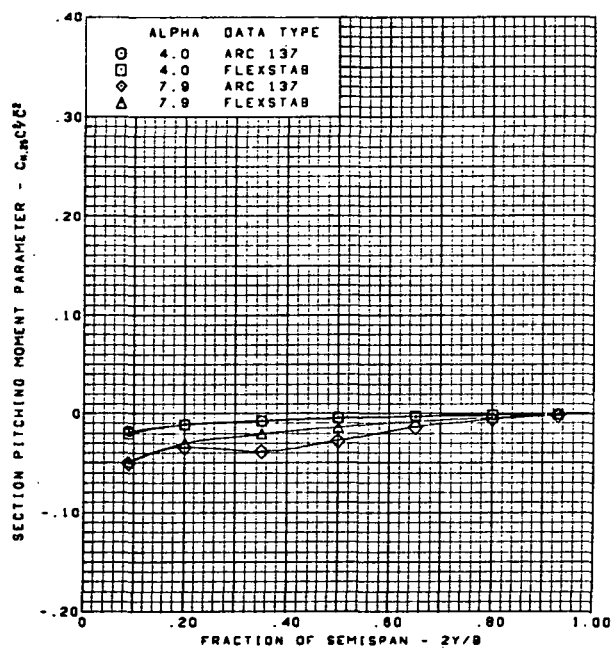
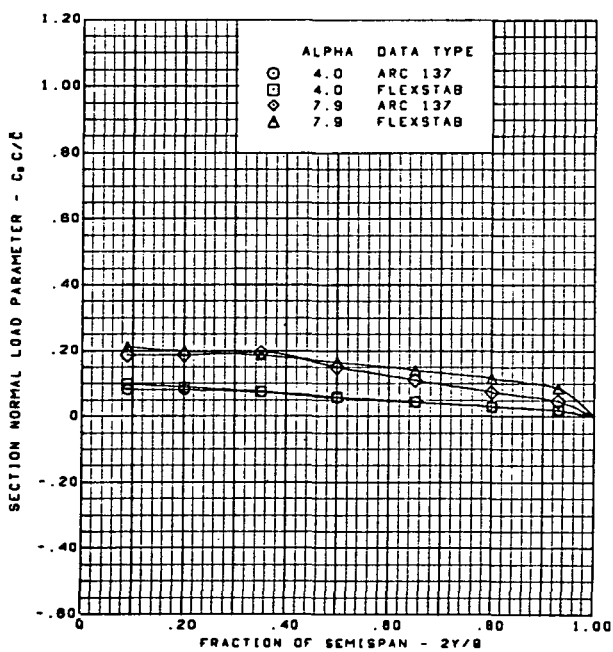
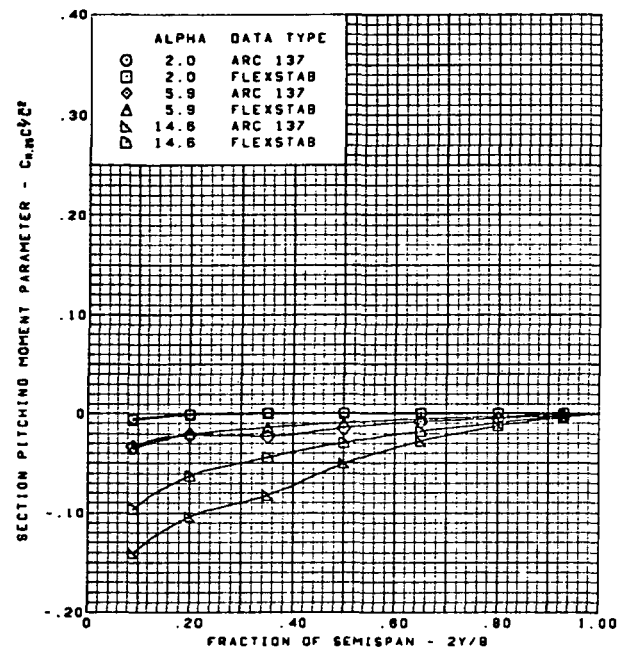
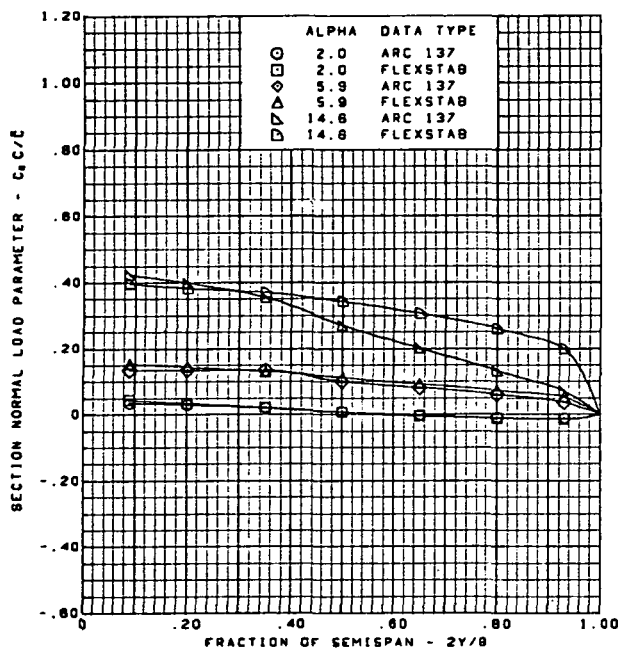
Figure 63.—(Continued)



$M = 2.50$  (run 10)  
 Twisted wing, rounded L.E.  
 L.E. deflection, full span =  $0.0^\circ$   
 T.E. deflection, full span =  $0.0^\circ$

(h) (Concluded)

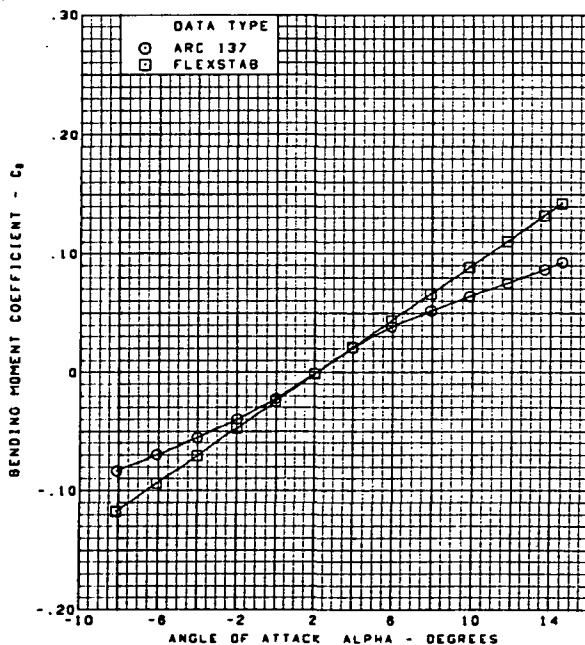
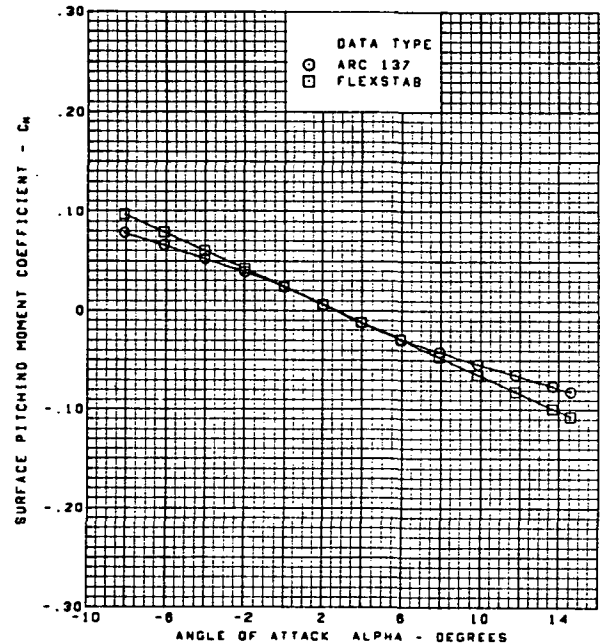
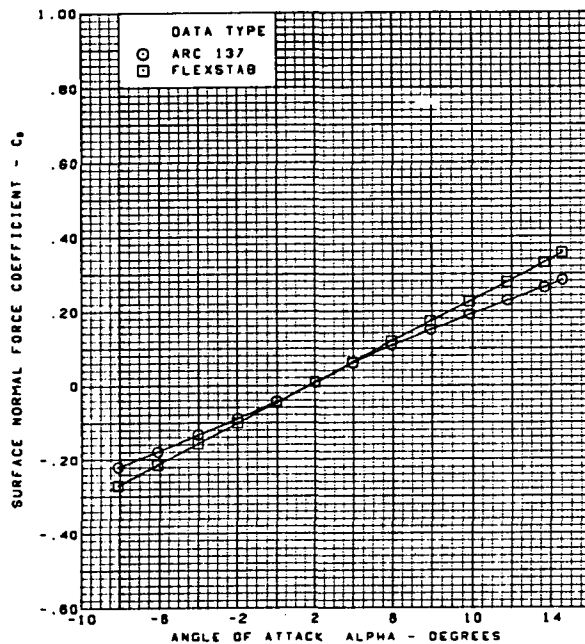
Figure 63.—(Continued)



M = 2.50 (run 10)  
 Twisted wing, rounded L.E.  
 L.E. deflection, full span =  $0.0^\circ$   
 T.E. deflection, full span =  $0.0^\circ$

(i) Spanload Distributions

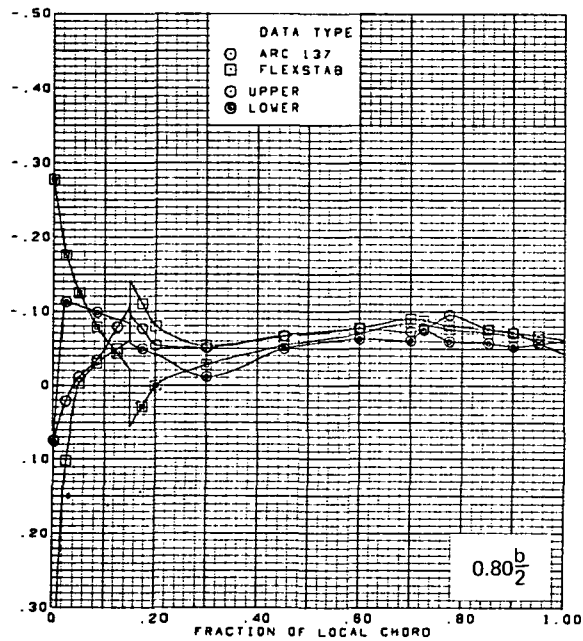
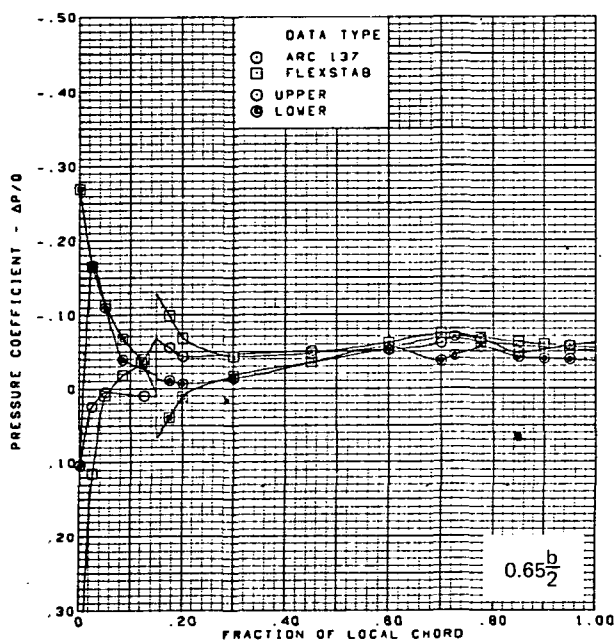
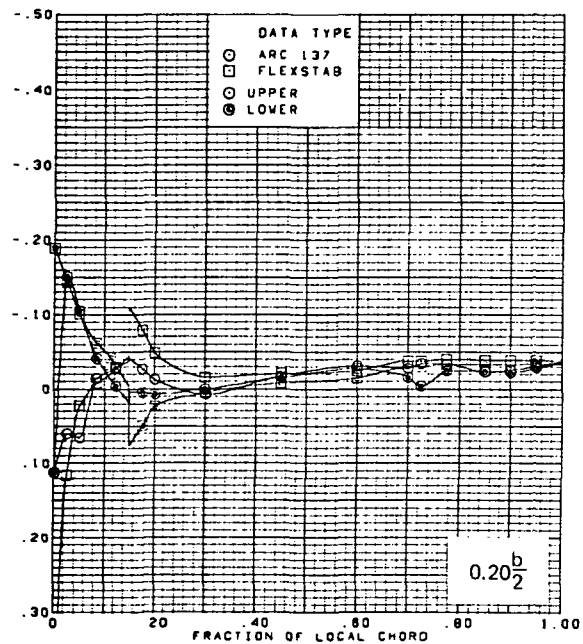
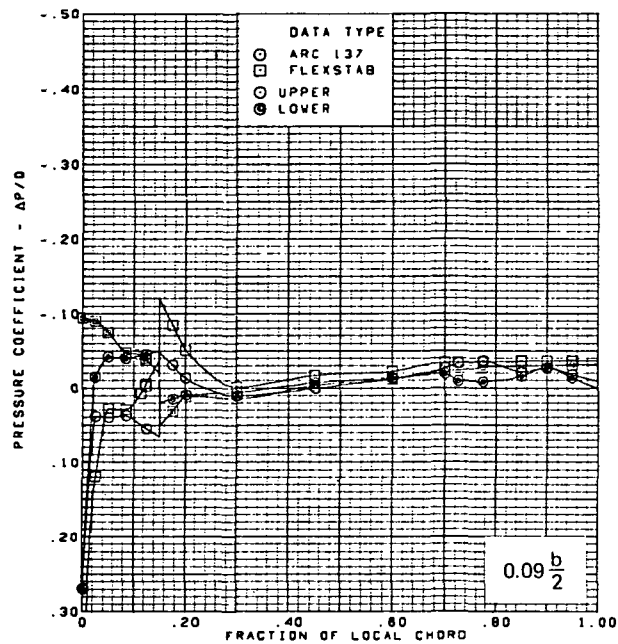
Figure 63. — (Continued)



$M = 2.50$  (run 10)  
Twisted wing, rounded L.E.  
L.E. deflection, full span =  $0.0^\circ$   
T.E. deflection, full span =  $0.0^\circ$

(j) Wing Aerodynamic Coefficients

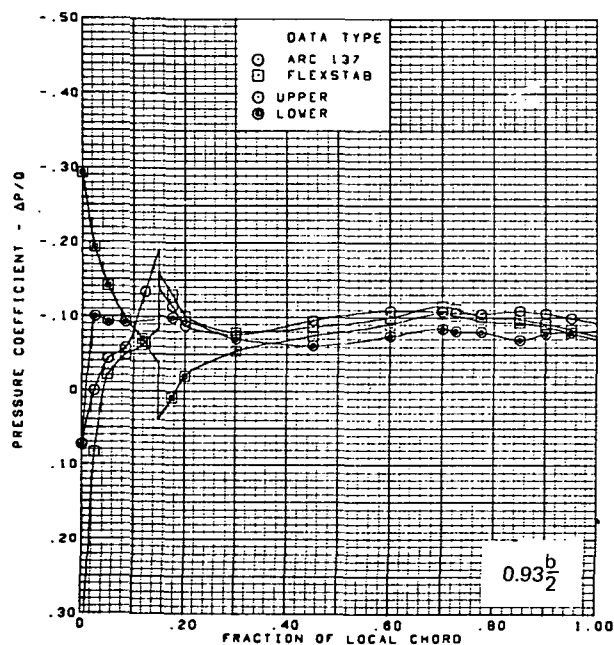
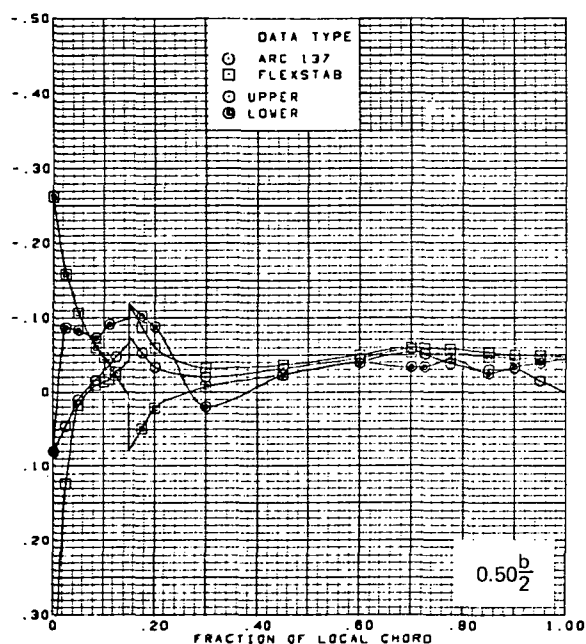
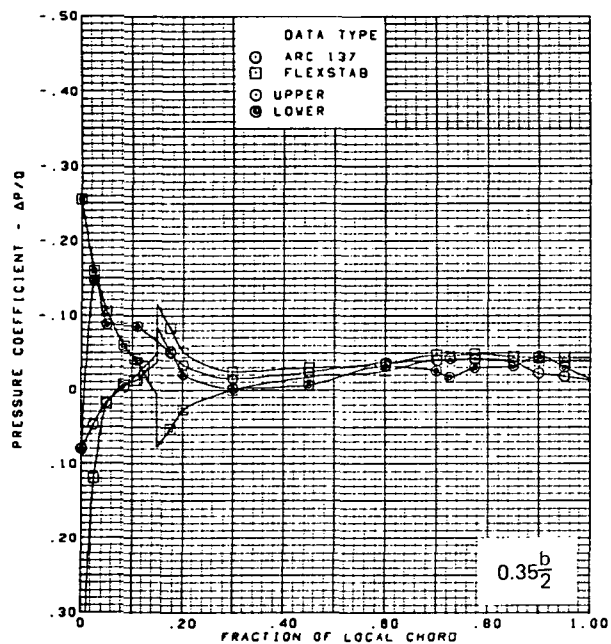
Figure 63.—(Concluded)



(a) Surface Chordwise Pressure Distributions,  $\alpha = 0^\circ$

Figure 64. -Wing Theory-to-Experiment Comparison—Flat Wing, Rounded L.E.; L.E. Deflection, Full Span =  $5.1^\circ$ ; T.E. Deflection, Full Span =  $0.0^\circ$ ;  $M = 1.70$

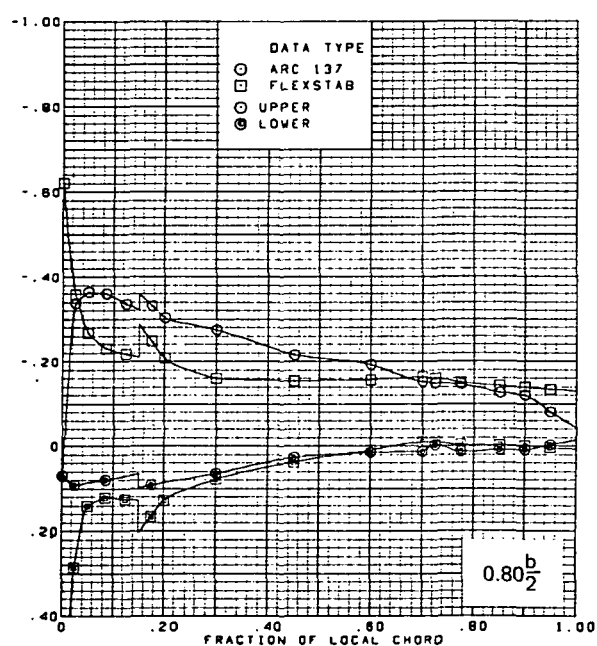
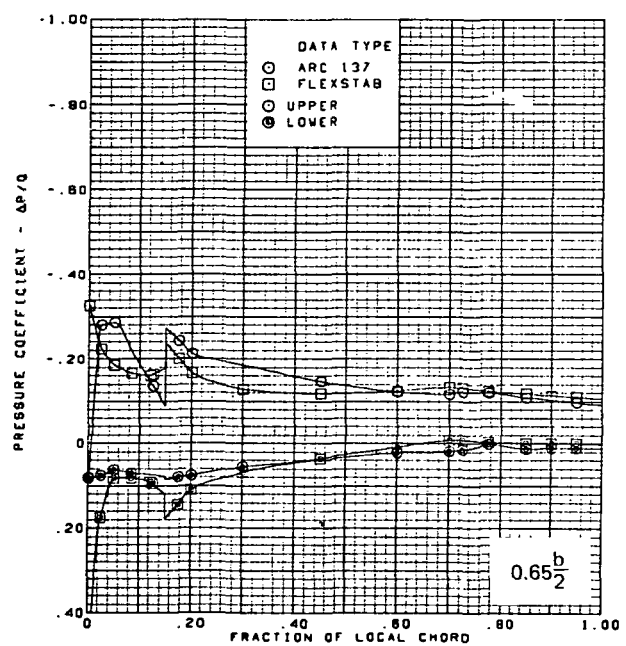
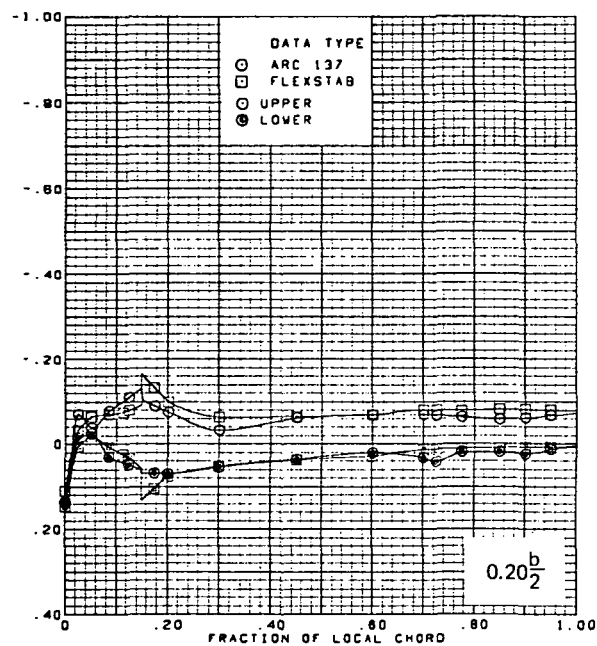
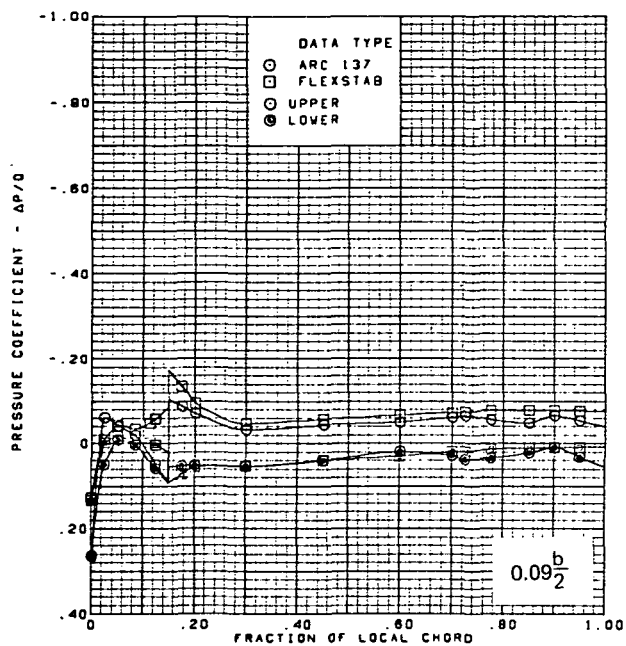




$M = 1.70$  (run 16)  
 $\alpha = 0^\circ$   
 Flat wing, rounded L.E.  
 L.E. deflection, full span =  $5.1^\circ$   
 T.E. deflection, full span =  $0.0^\circ$   
 Note:  $C_{p, \text{vacuum}} = -0.49$

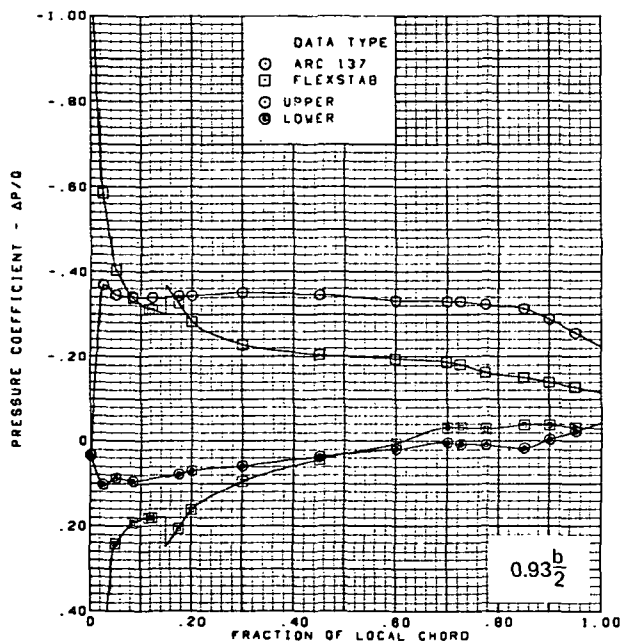
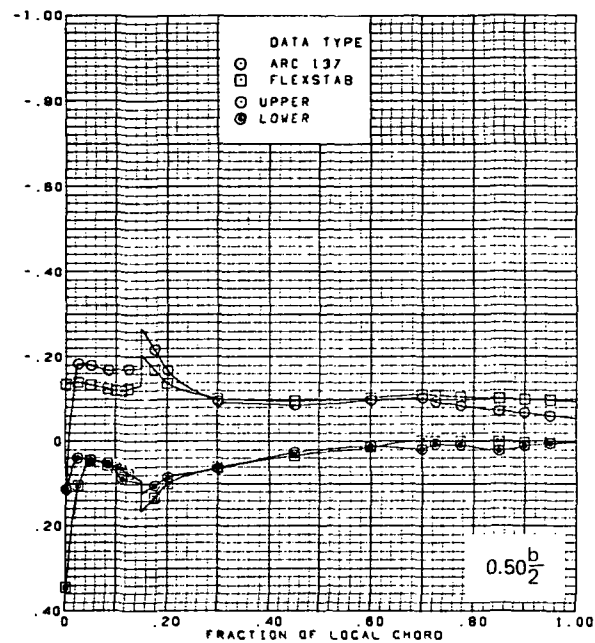
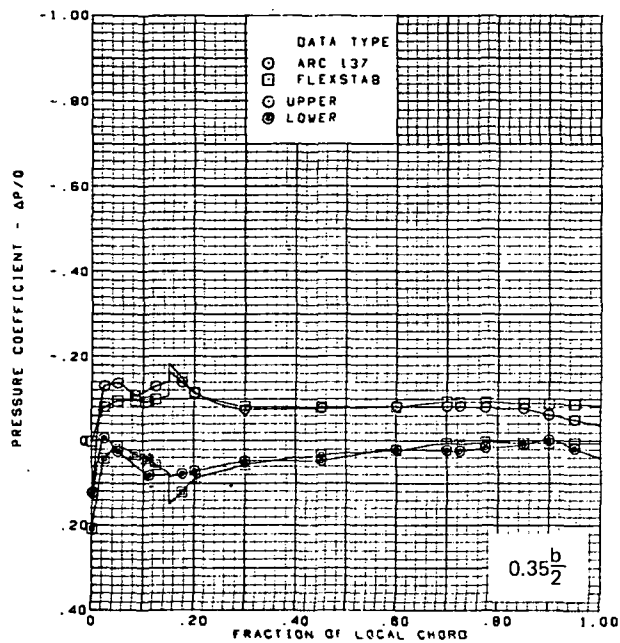
(a) (Concluded)

Figure 64.—(Continued)



(b) Surface Chordwise Pressure Distributions,  $\alpha = 4^\circ$

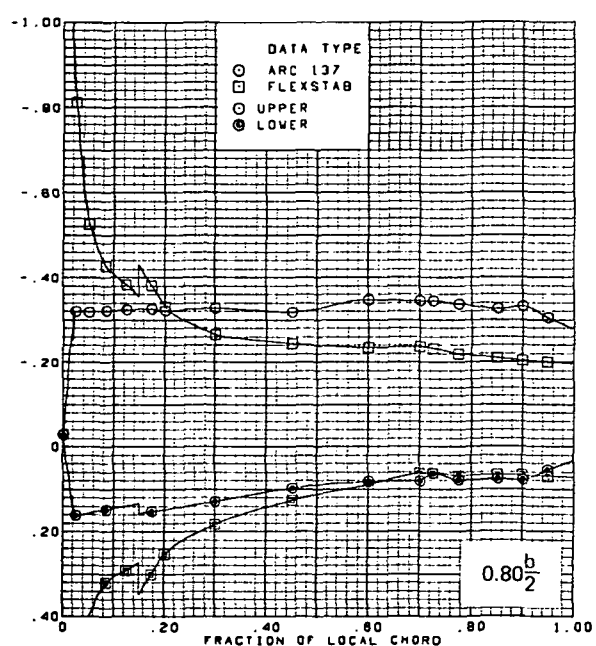
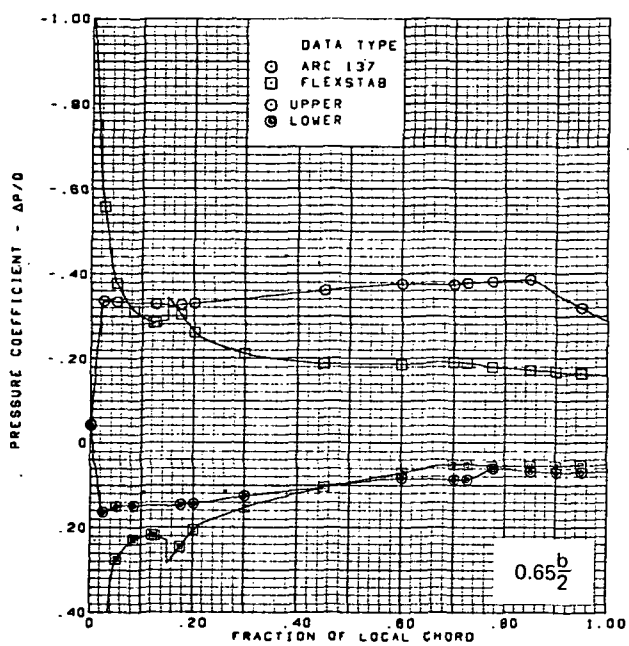
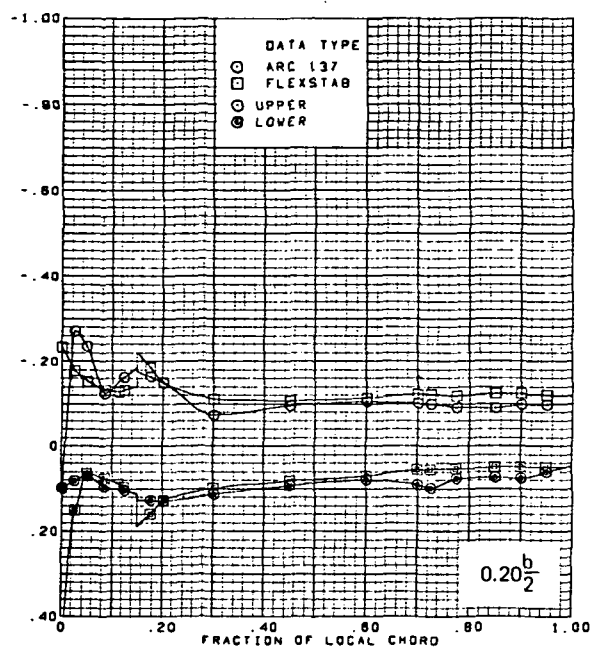
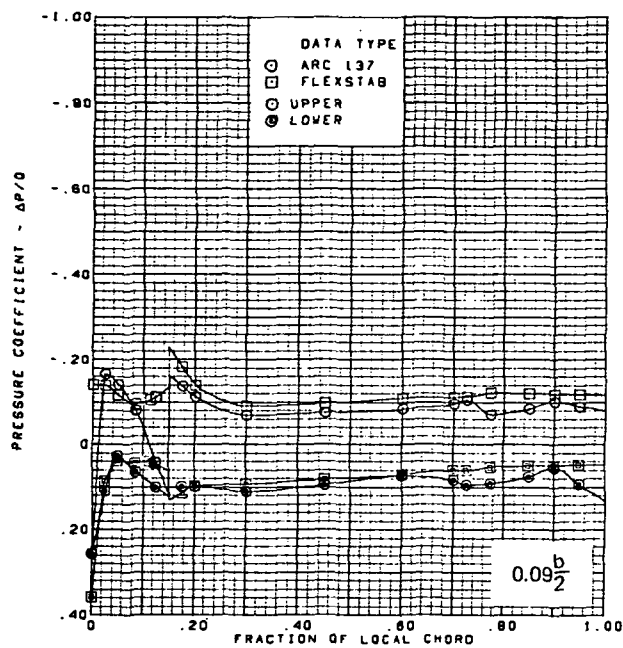
Figure 64. -(Continued)



$M = 1.70$  (run 16)  
 $\alpha = 4^\circ$   
 Flat wing, rounded L.E.  
 L.E. deflection, full span =  $5.1^\circ$   
 T.E. deflection, full span =  $0.0^\circ$   
 Note:  $C_{p, \text{vacuum}} = -0.49$

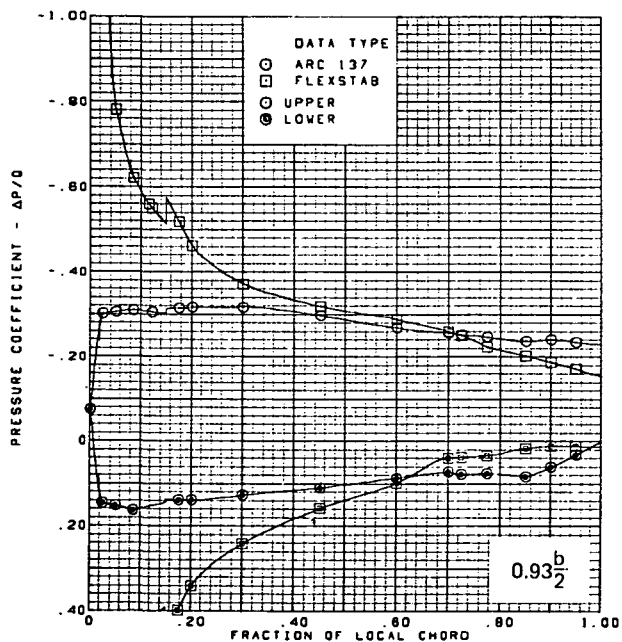
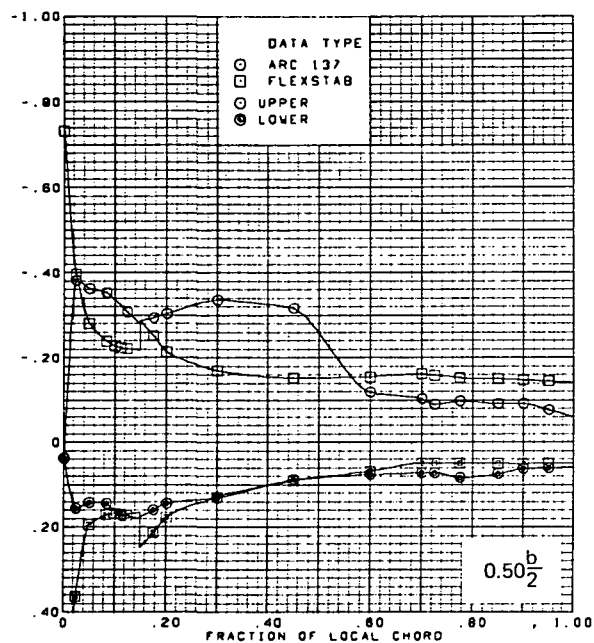
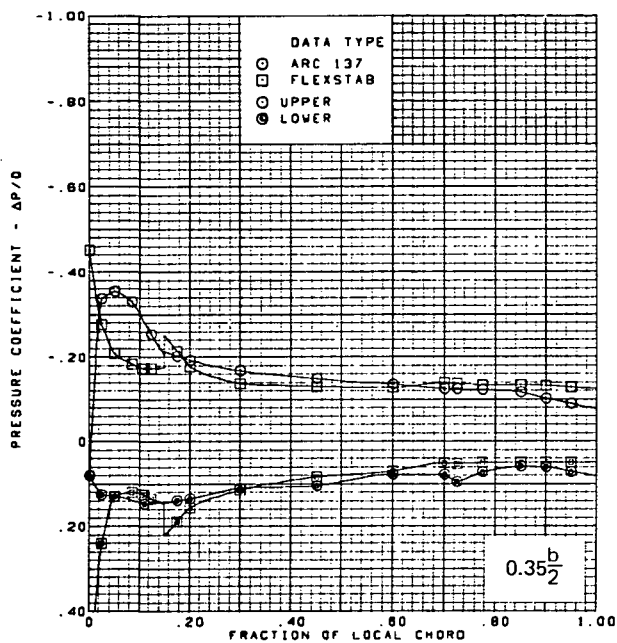
(b) (Concluded)

Figure 64. -(Continued)



(c) Surface Chordwise Pressure Distributions,  $\alpha = 8^\circ$

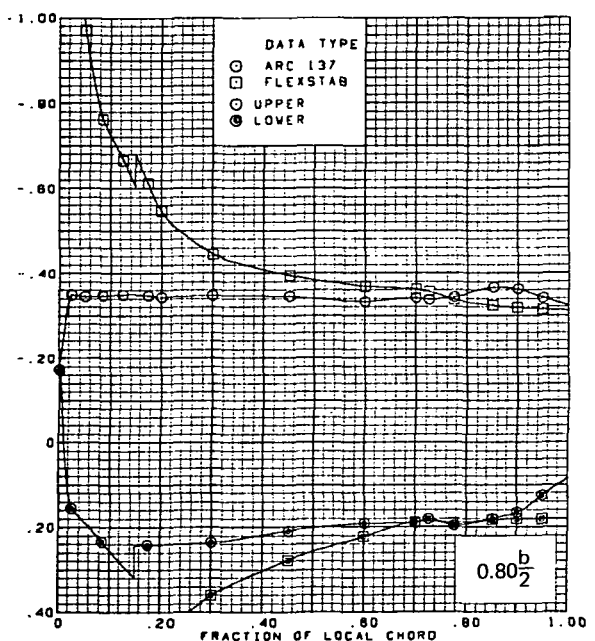
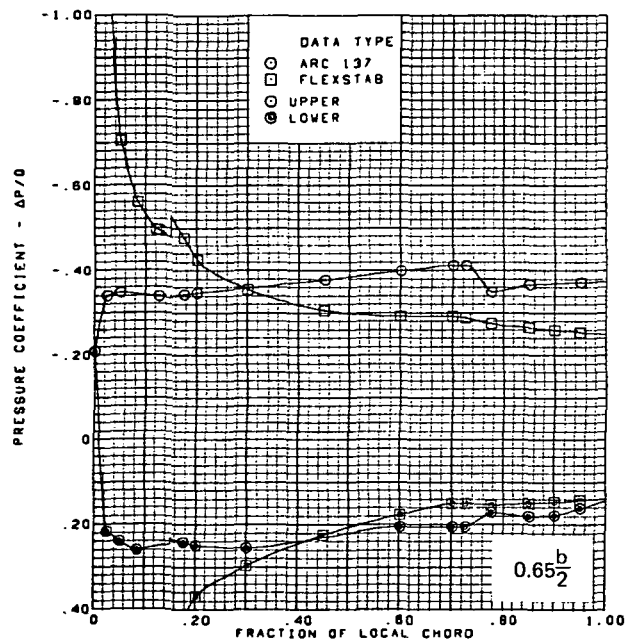
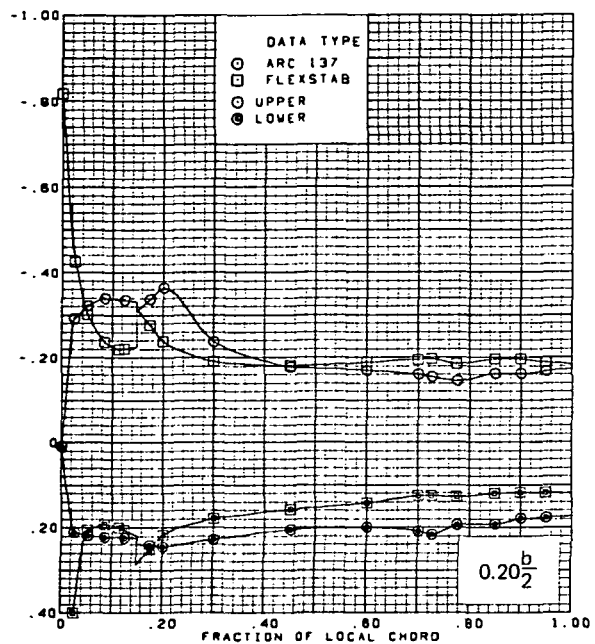
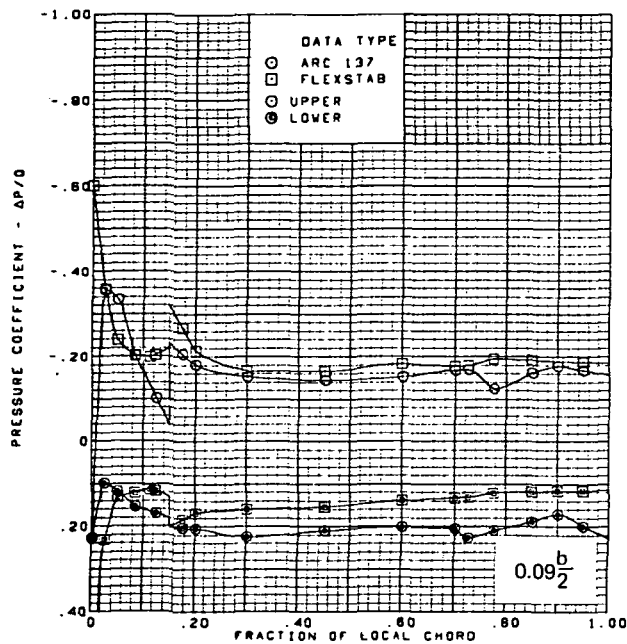
Figure 64. -(Concluded)



$M = 1.70$  (run 16)  
 $\alpha = 8^\circ$   
 Flat wing, rounded L.E.  
 L.E. deflection, full span =  $5.1^\circ$   
 T.E. deflection, full span =  $0.0^\circ$   
 Note:  $C_{p, \text{vacuum}} = -0.49$

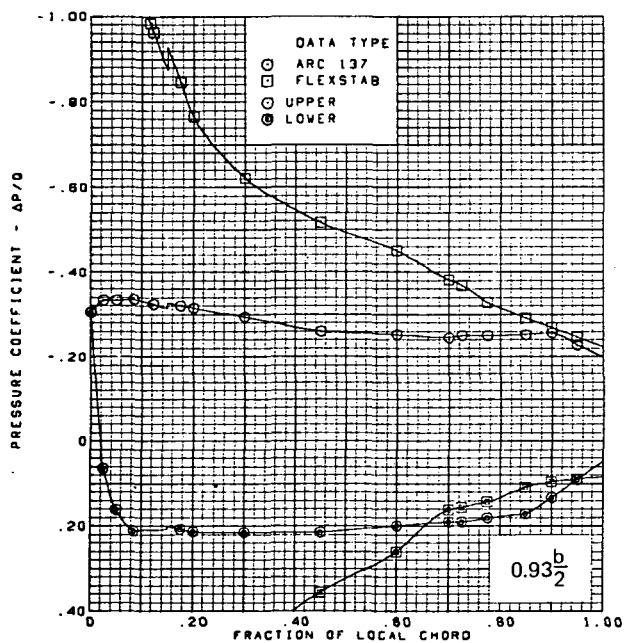
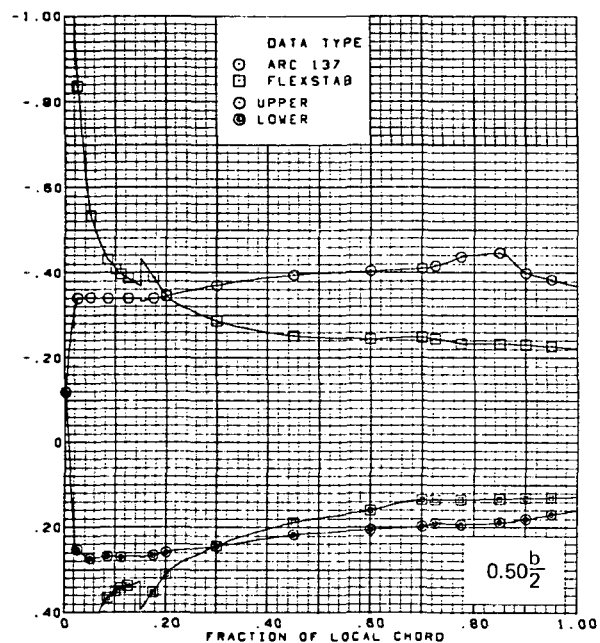
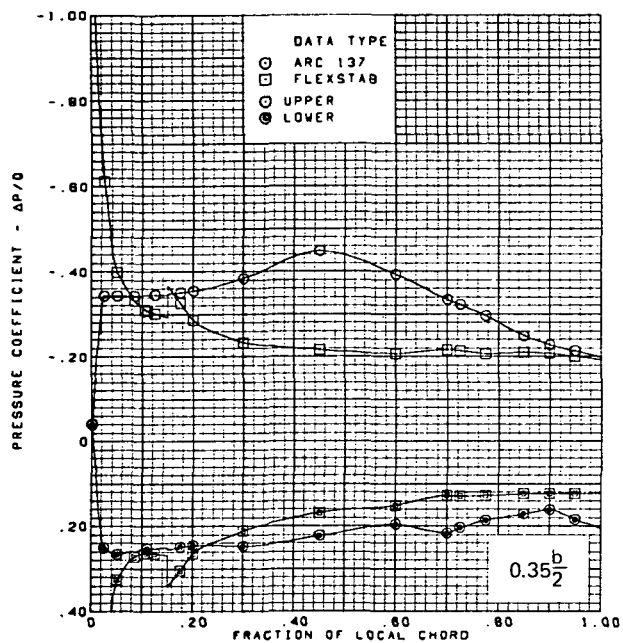
(c) (Concluded)

Figure 64. -(Continued)



(d) Surface Chordwise Pressure Distributions,  $\alpha = 15^\circ$

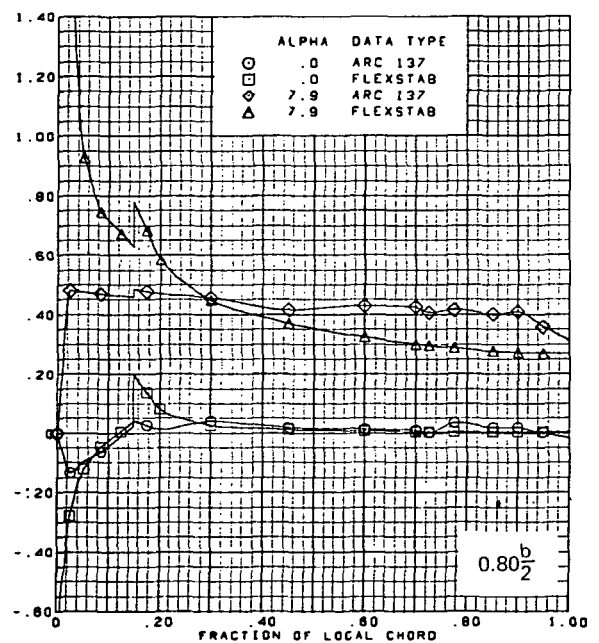
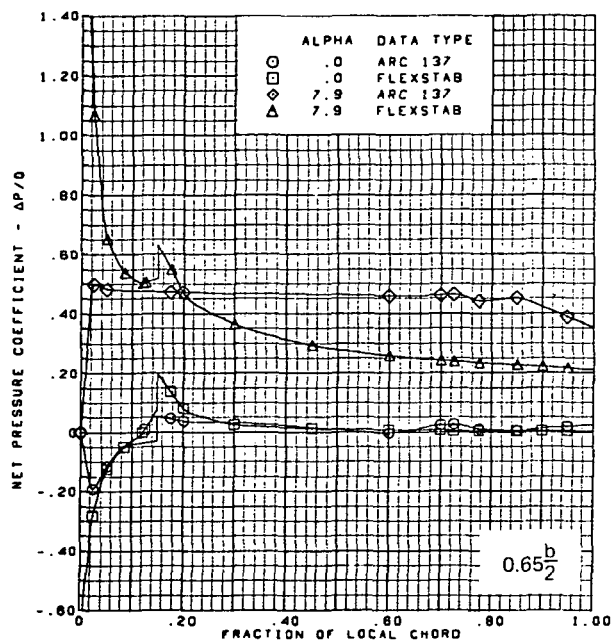
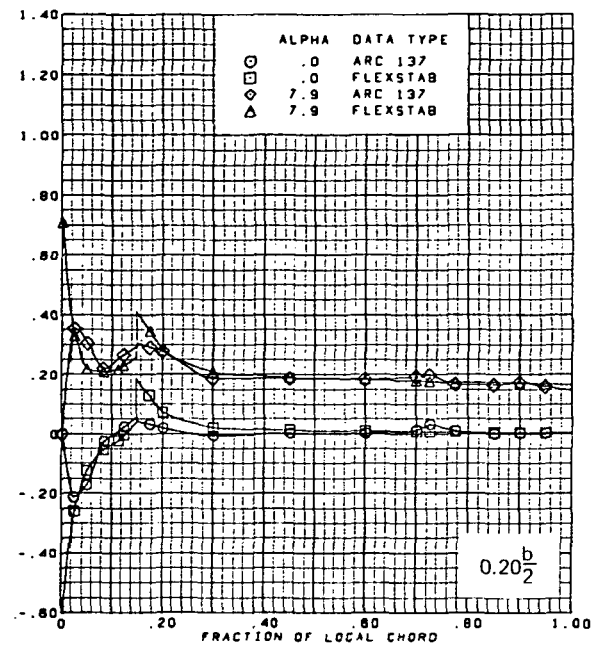
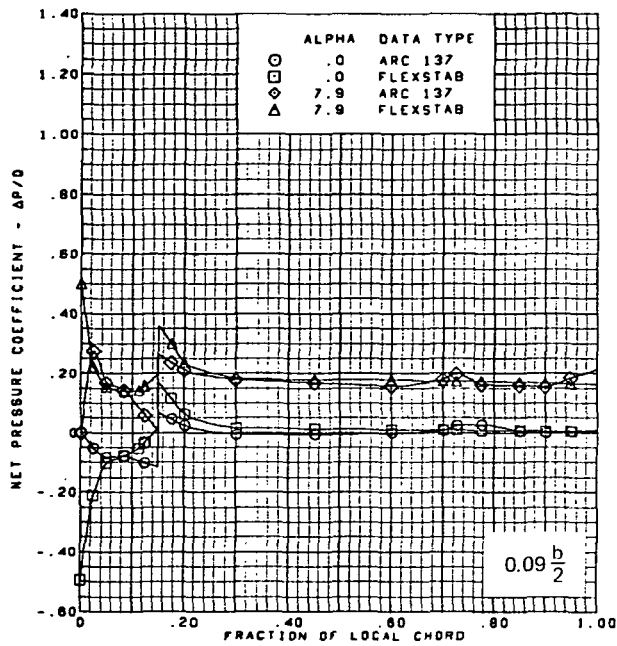
Figure 64. —(Continued)



$M = 1.70$  (run 16)  
 $\alpha = 15^\circ$   
 Flat wing, rounded L.E.  
 L.E. deflection, full span  $\approx 5.1^\circ$   
 T.E. deflection, full span  $\approx 0.0^\circ$   
 Note:  $C_{p, \text{vacuum}} = -0.49$

(d) (Concluded)

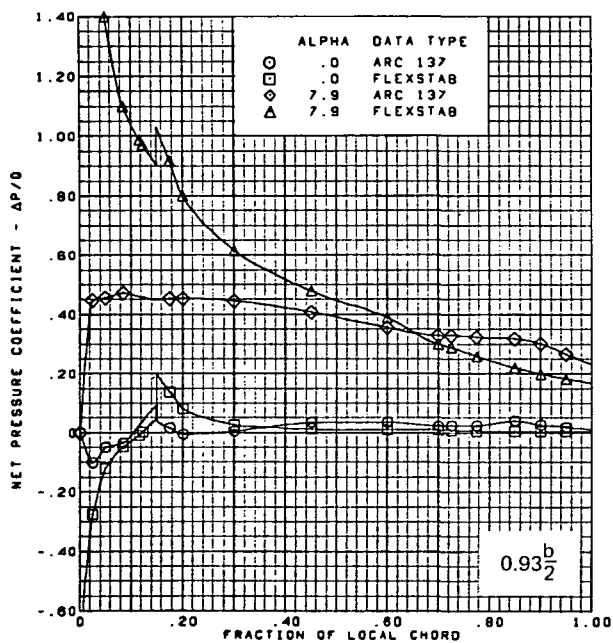
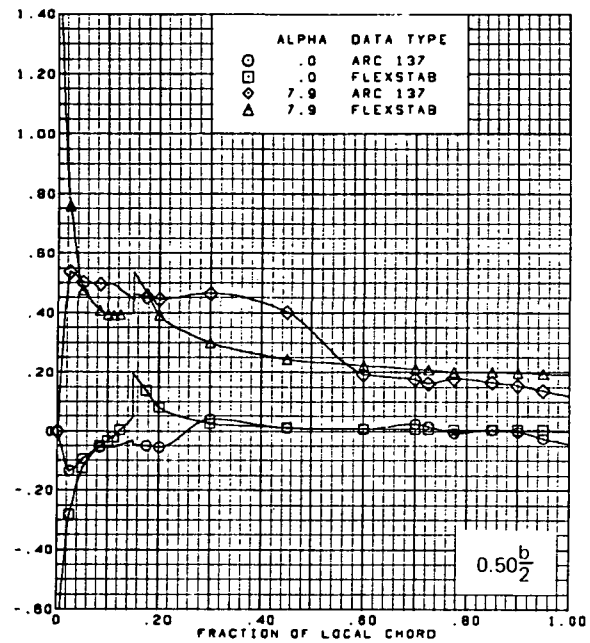
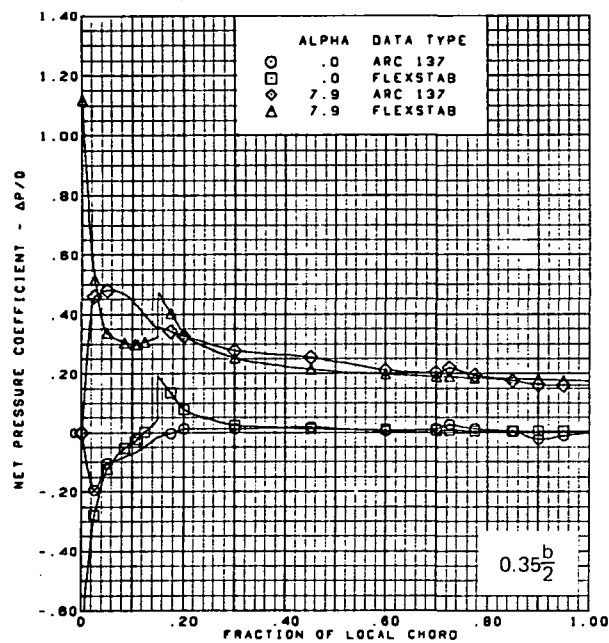
Figure 64. -(Continued)



(e) Net Chordwise Pressure Distributions,  $\alpha = 0^\circ, 8^\circ$

Figure 64. -(Continued)

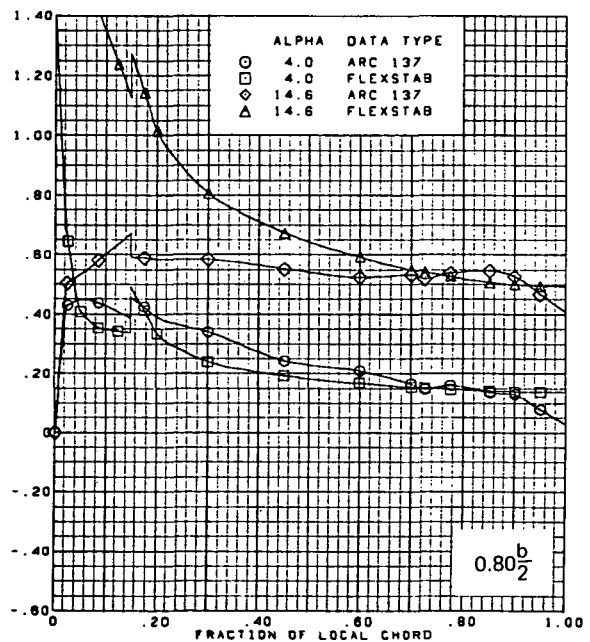
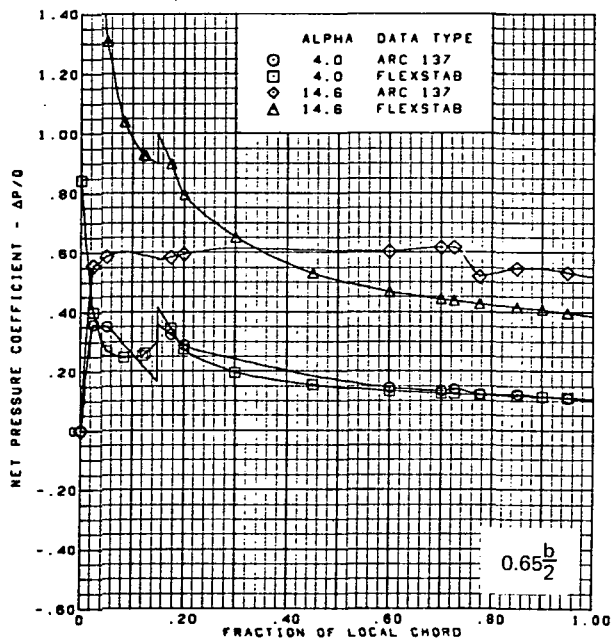
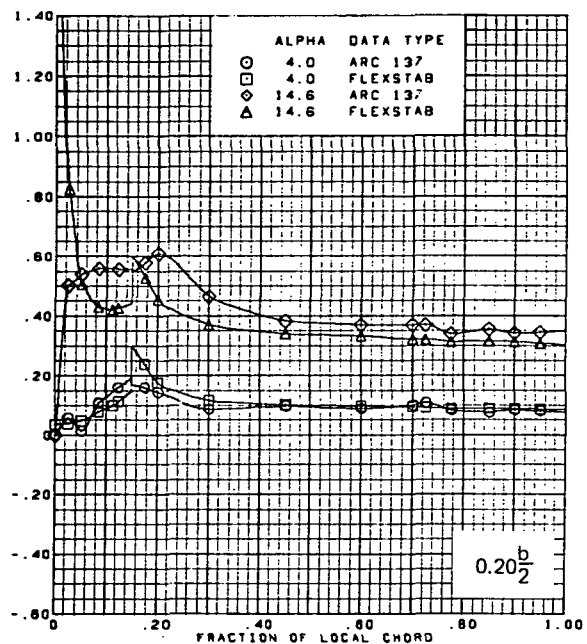
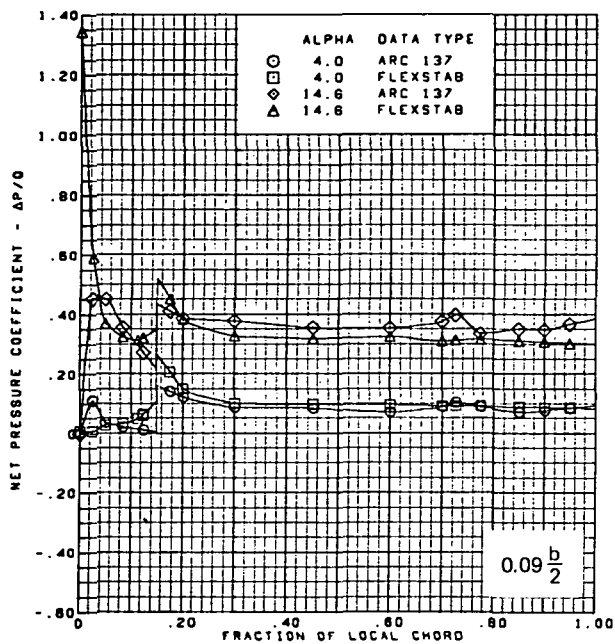




M = 1.70 (run 16)  
 Flat wing, rounded L.E.  
 L.E. deflection, full span =  $5.1^\circ$   
 T.E. deflection, full span =  $0.0^\circ$

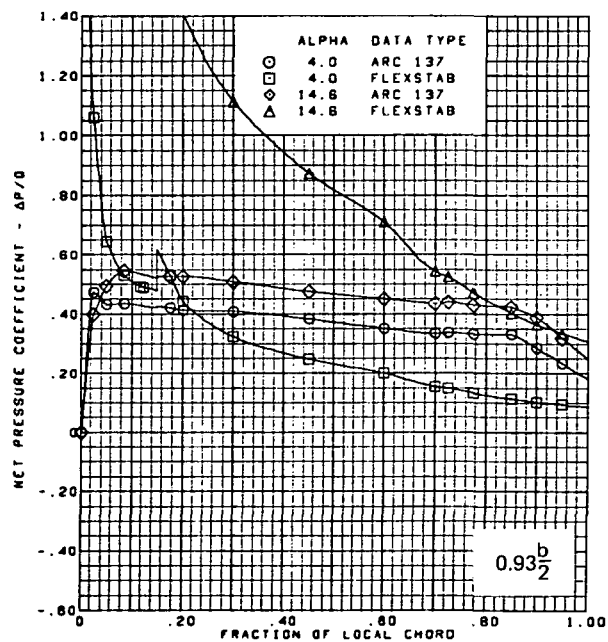
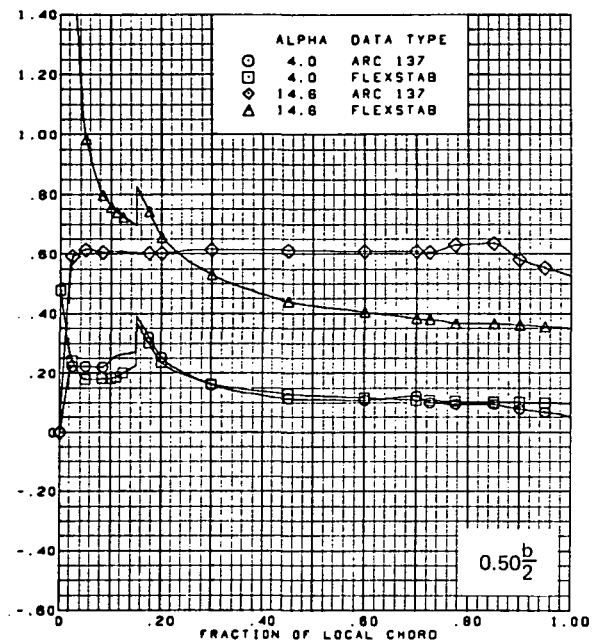
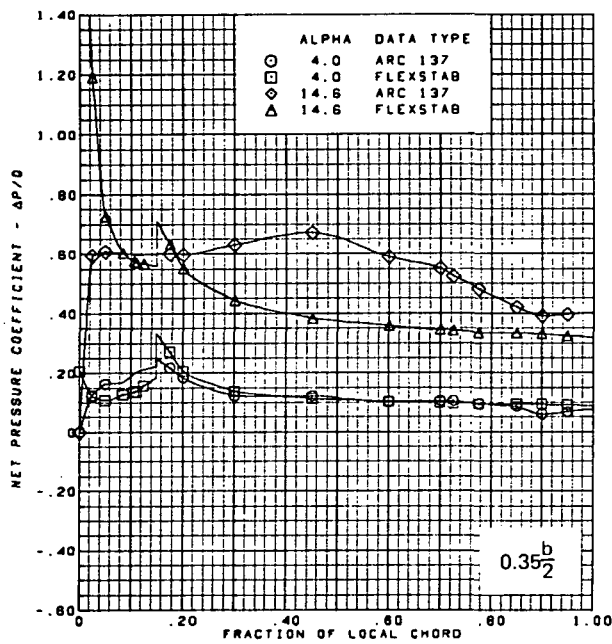
(e) (Concluded)

Figure 64. —(Continued)



(f) Net Chordwise Pressure Distributions,  $\alpha = 4^\circ, 15^\circ$

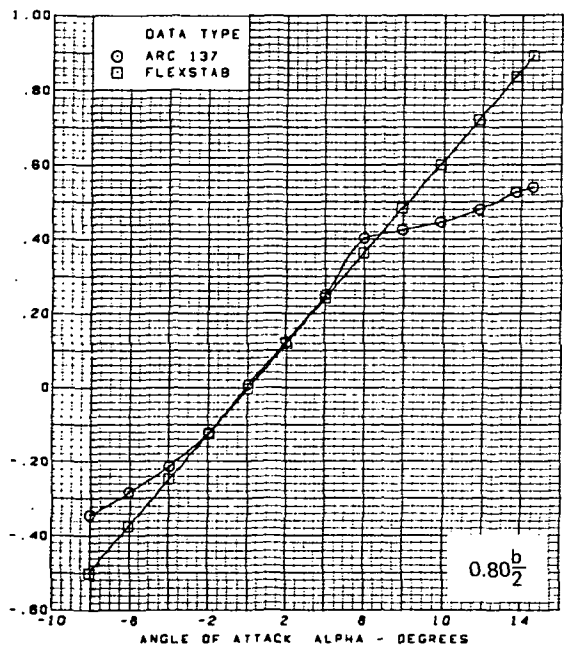
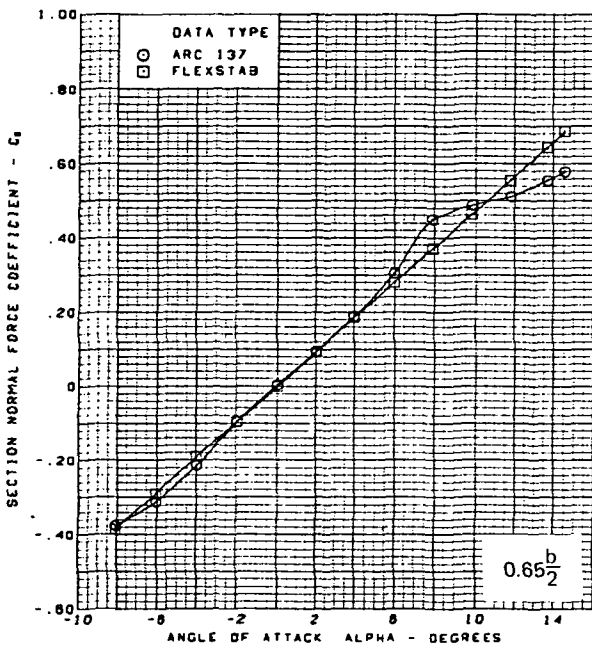
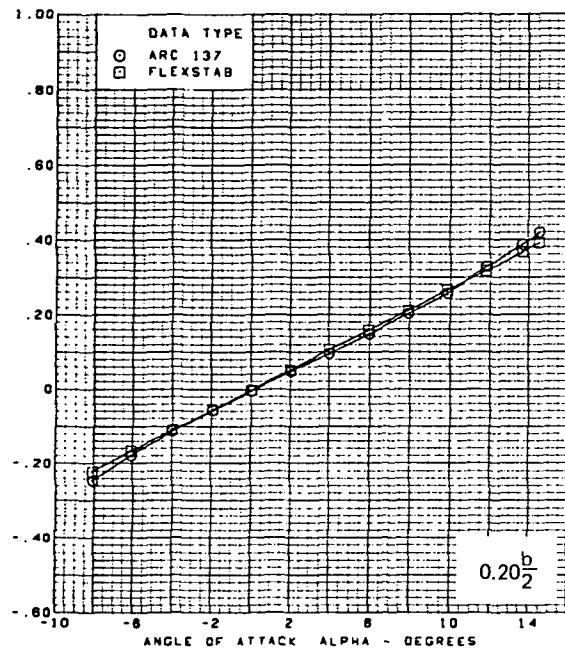
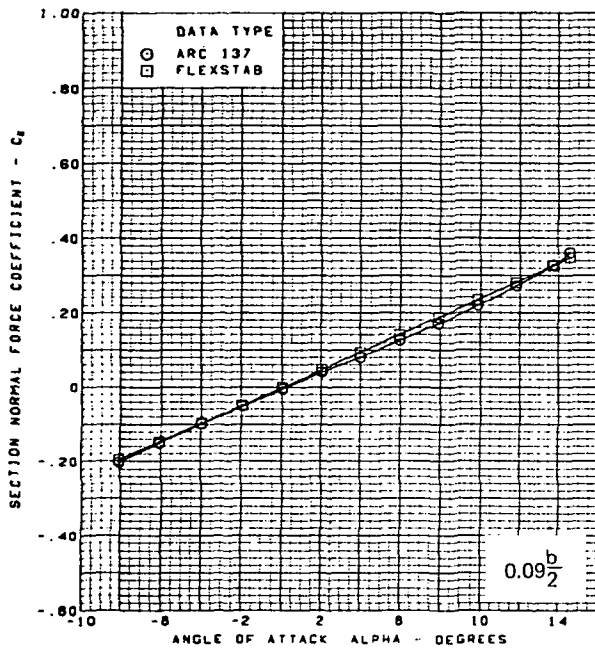
Figure 64. —(Continued)



$M = 1.70$  (run 16)  
 Flat wing, rounded L.E.  
 L.E. deflection, full span =  $5.1^\circ$   
 T.E. deflection, full span =  $0.0^\circ$

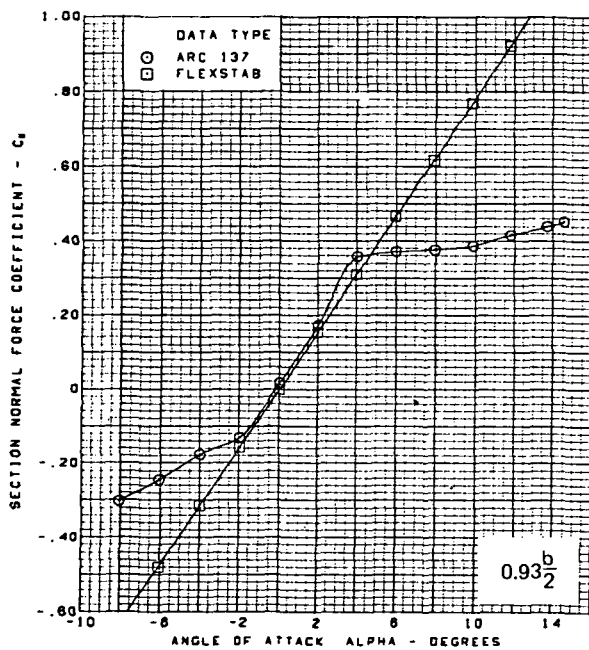
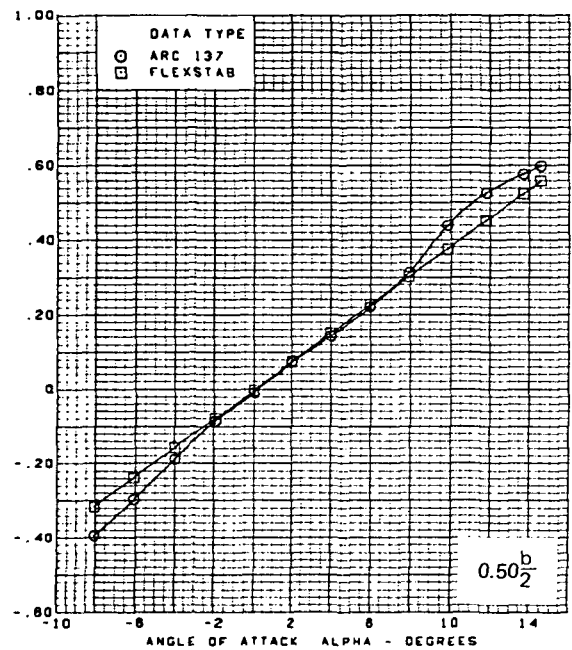
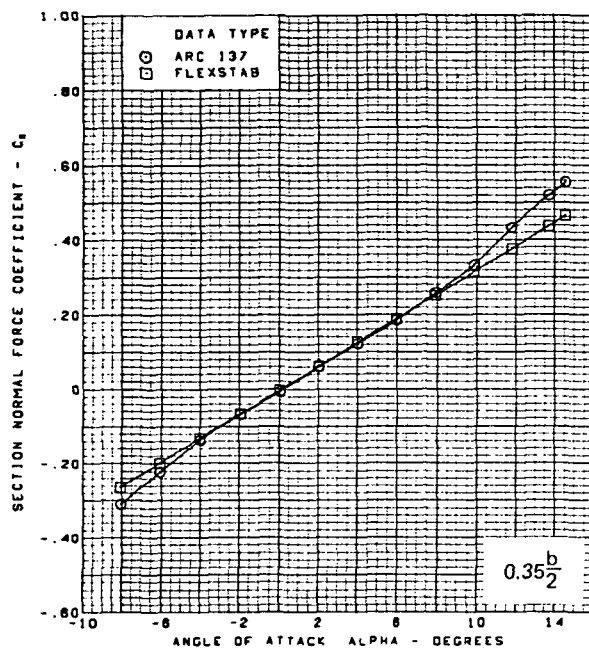
(f) (Concluded)

Figure 64. —(Continued)



(g) Section Aerodynamic Coefficients—Normal Force

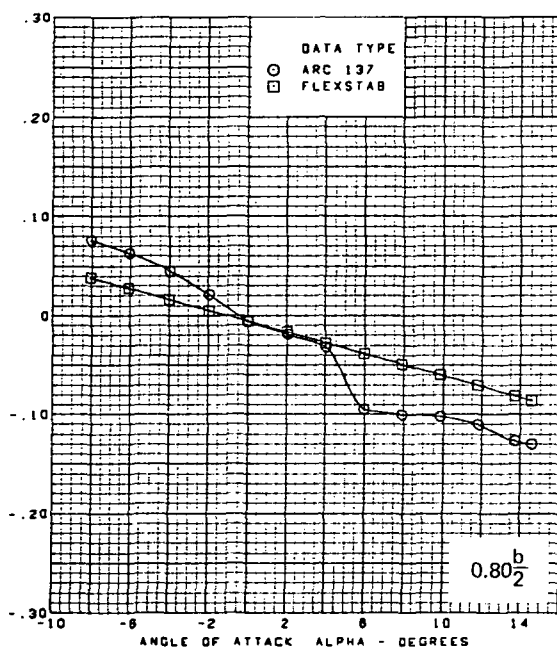
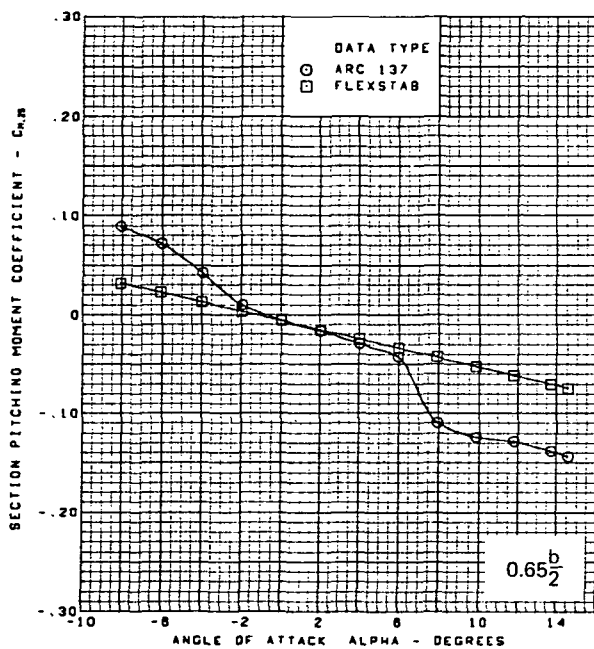
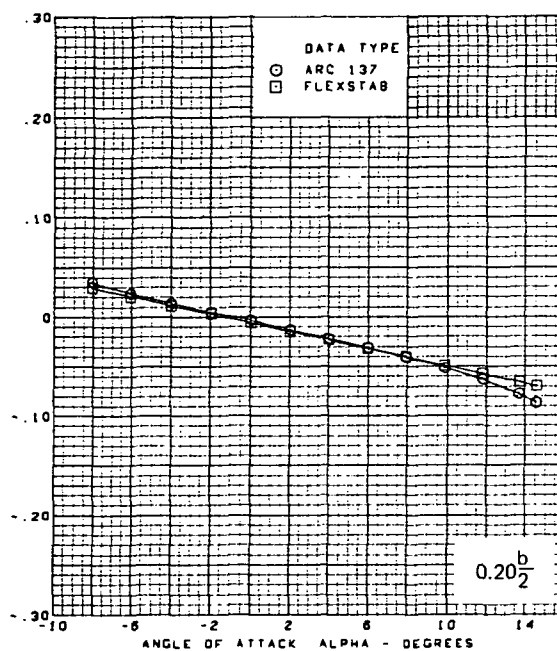
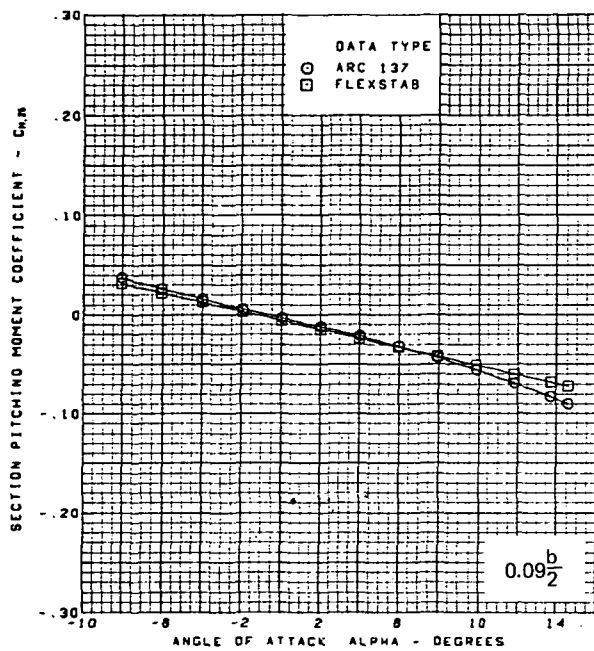
Figure 64. —(Continued)



M = 1.70 (run 16)  
 Flat wing, rounded L.E.  
 L.E. deflection, full span =  $5.1^\circ$   
 T.E. deflection, full span =  $0.0^\circ$

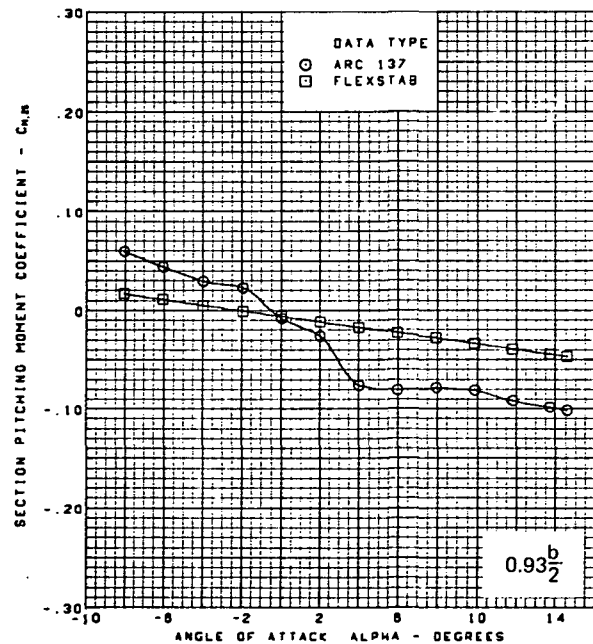
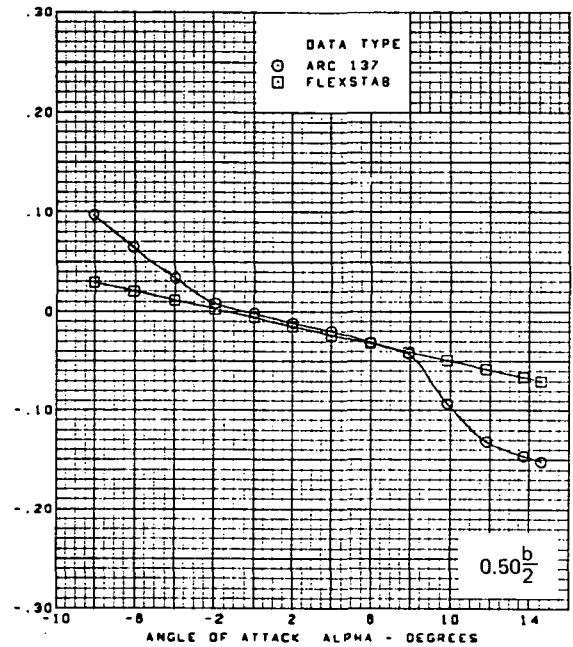
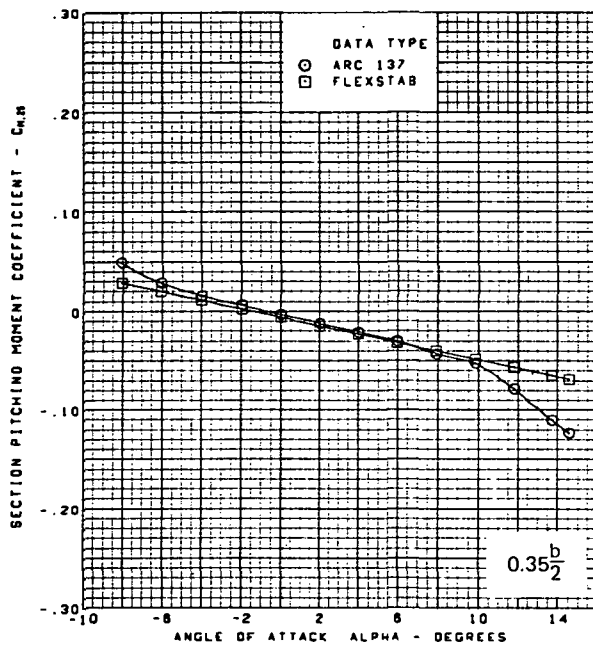
(g) (Concluded)

Figure 64. —(Continued)



(h) Section Aerodynamic Coefficients—Pitching Moment

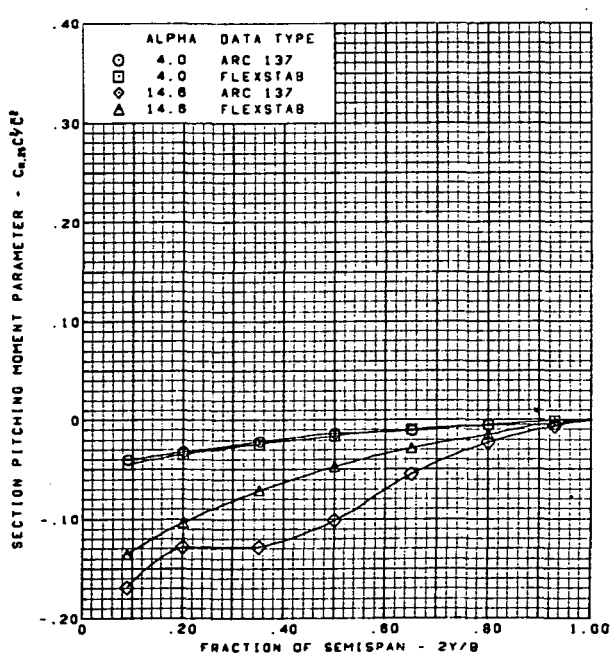
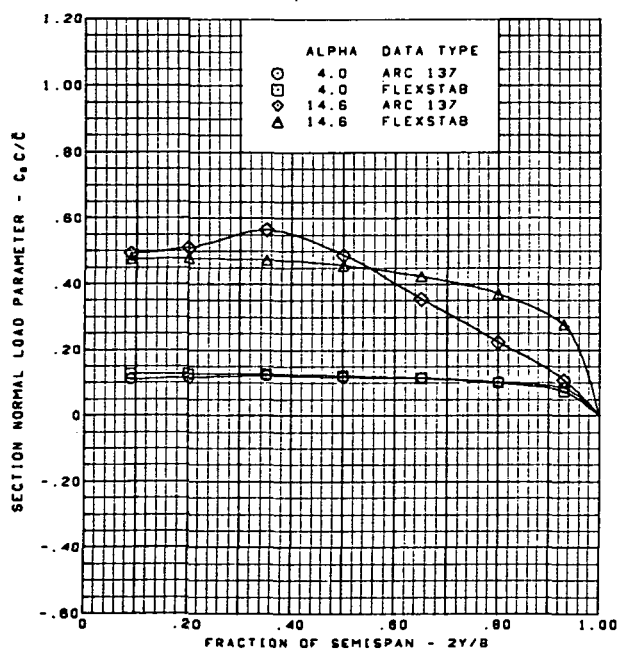
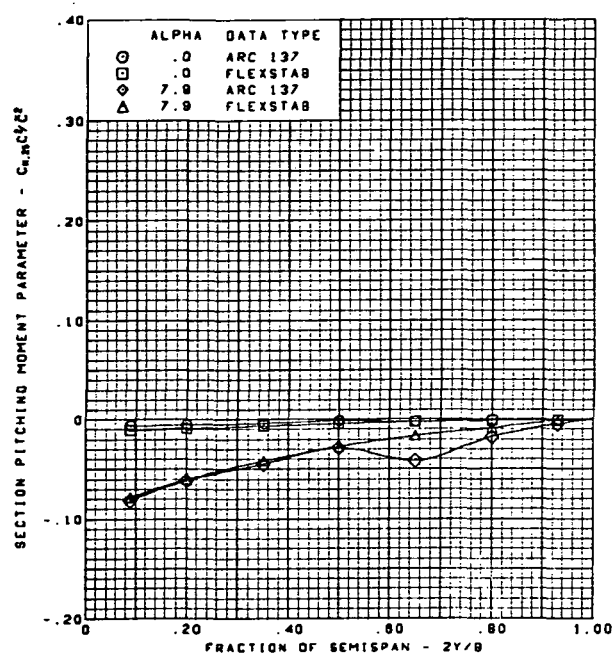
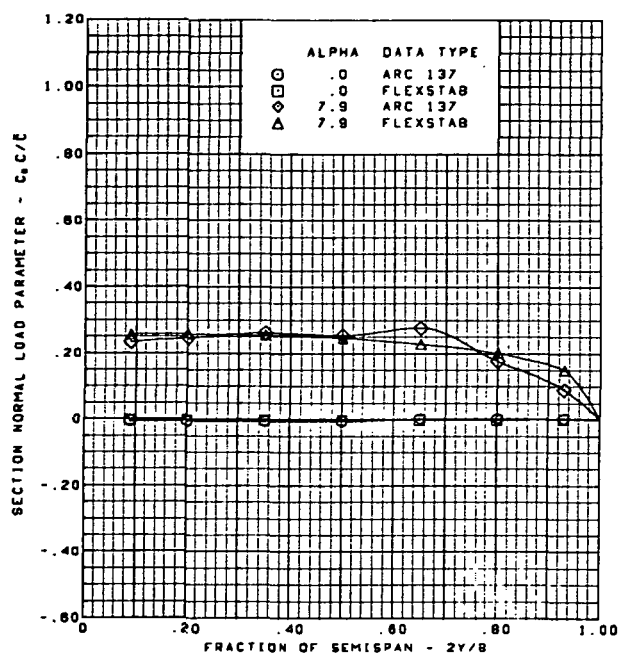
Figure 64. —(Continued)



M = 1.70 (run 16)  
 Flat wing, rounded L.E.  
 L.E. deflection, full span =  $5.1^\circ$   
 T.E. deflection, full span =  $0.0^\circ$

(h) (Concluded)

Figure 64. -(Continued)

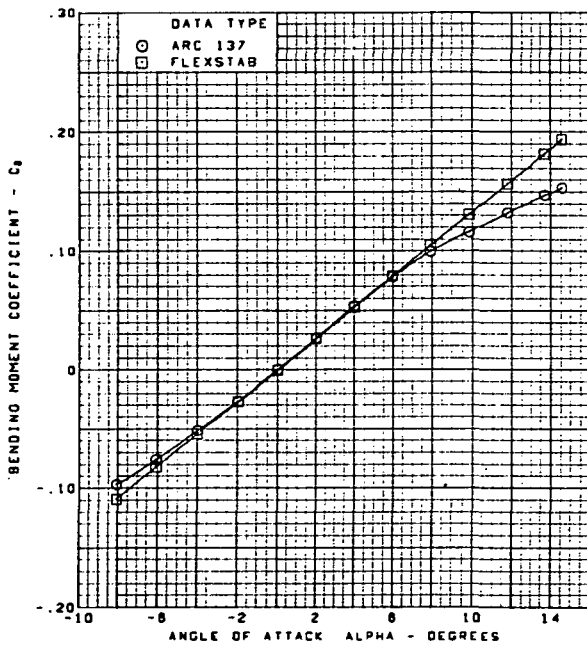
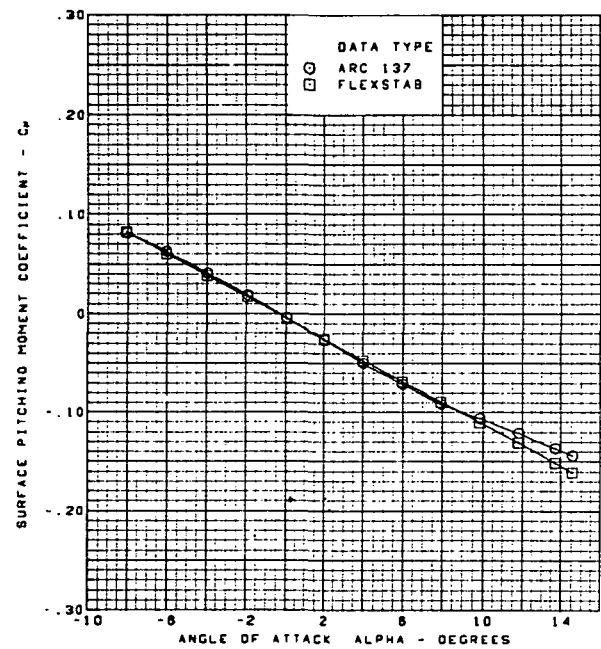
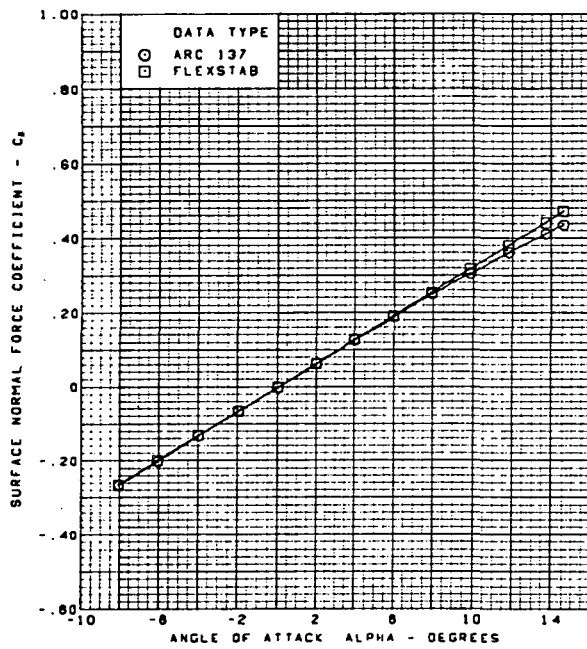


M = 1.70 (run 16)  
 Flat wing, rounded L.E.  
 L.E. deflection, full span = 5.1°  
 T.E. deflection, full span = 0.0°

(i) Spanload Distributions

Figure 64. -(Continued)

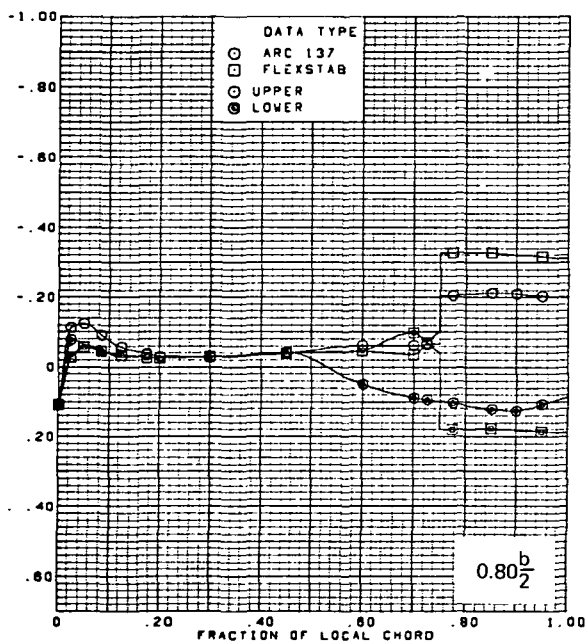
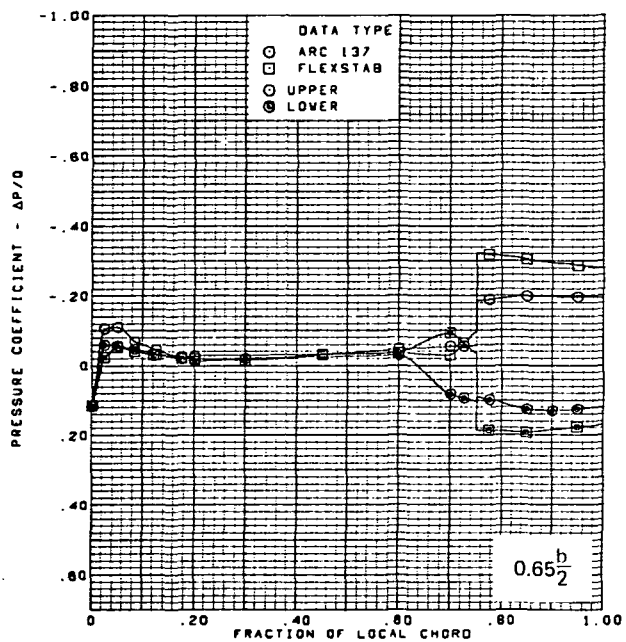
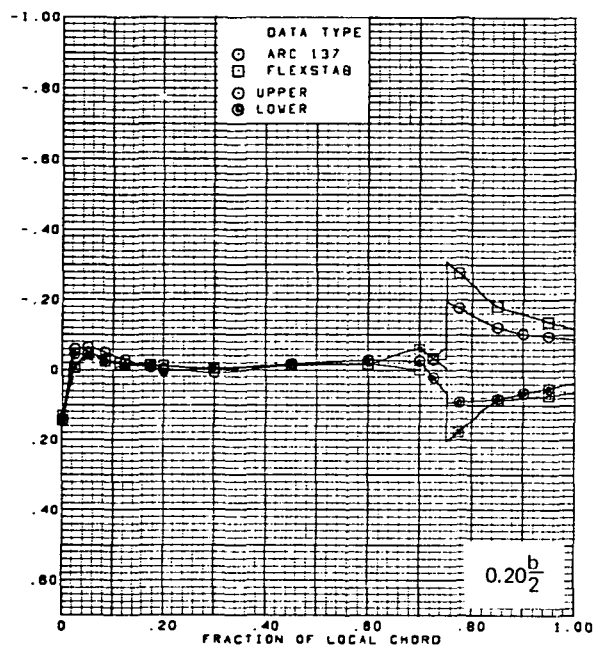
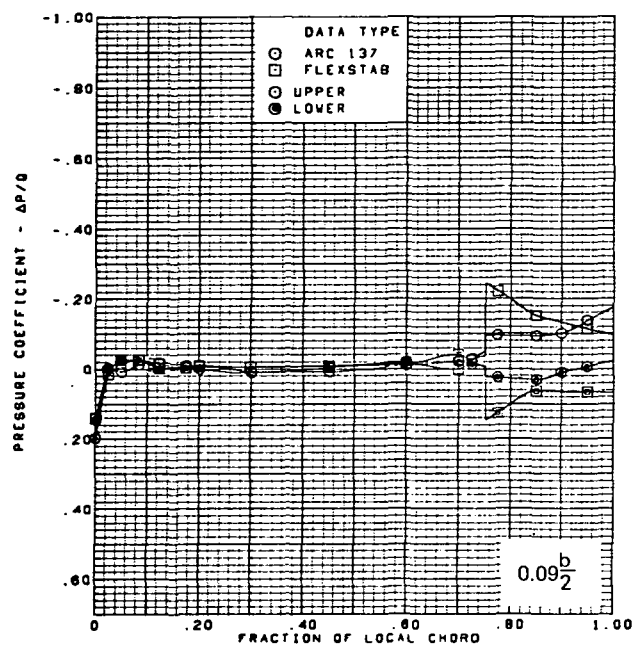




$M = 1.70$  (run 16)  
 Flat wing, rounded L.E.  
 L.E. deflection, full span =  $5.1^\circ$   
 T.E. deflection, full span =  $0.0^\circ$

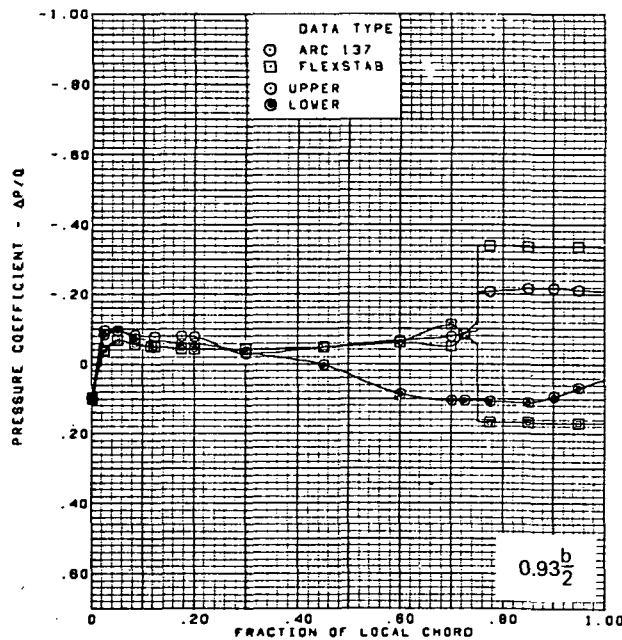
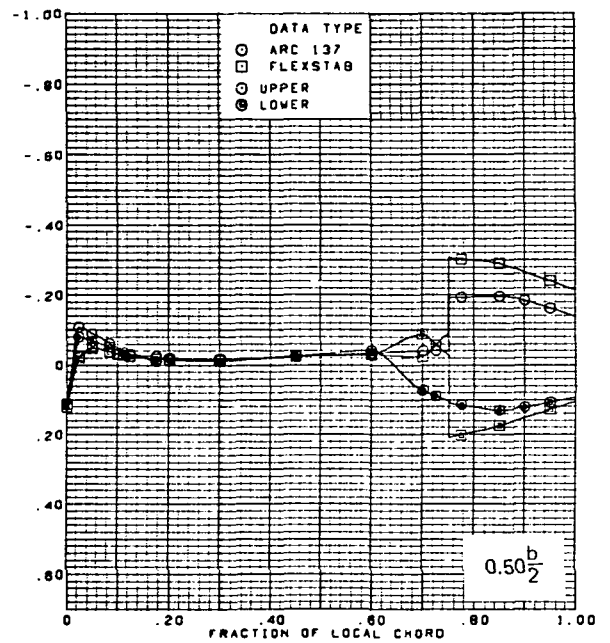
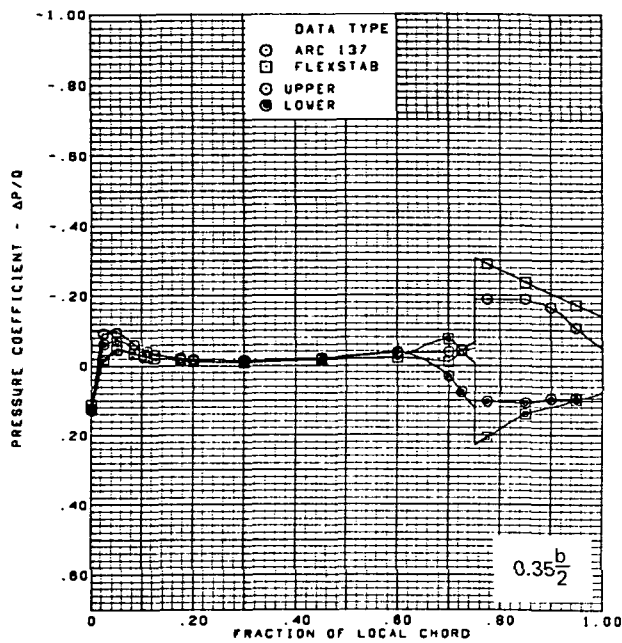
(j) Wing Aerodynamic Coefficients

Figure 64. —(Concluded)



(a) Surface Chordwise Pressure Distributions,  $\alpha = 0^\circ$

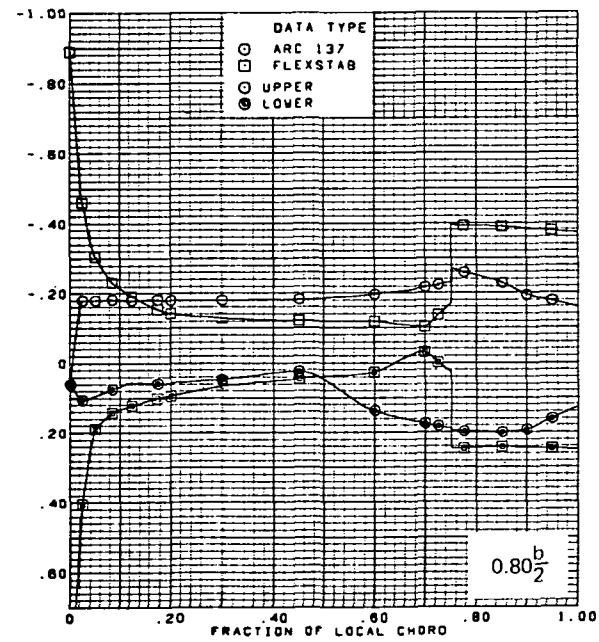
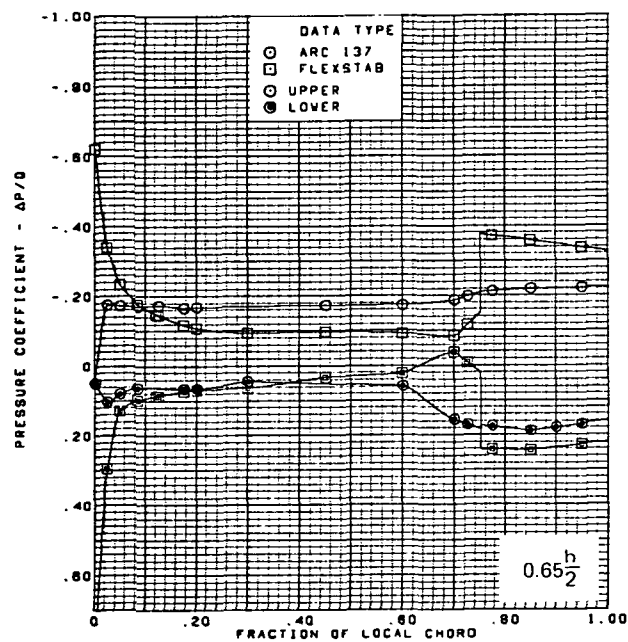
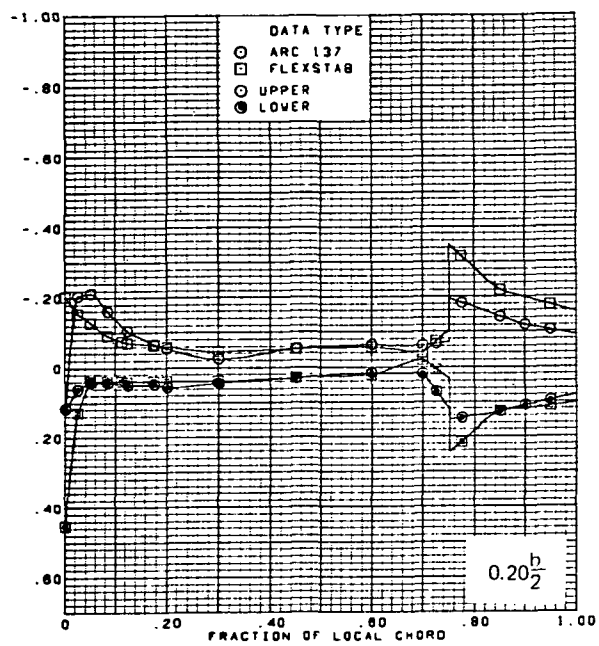
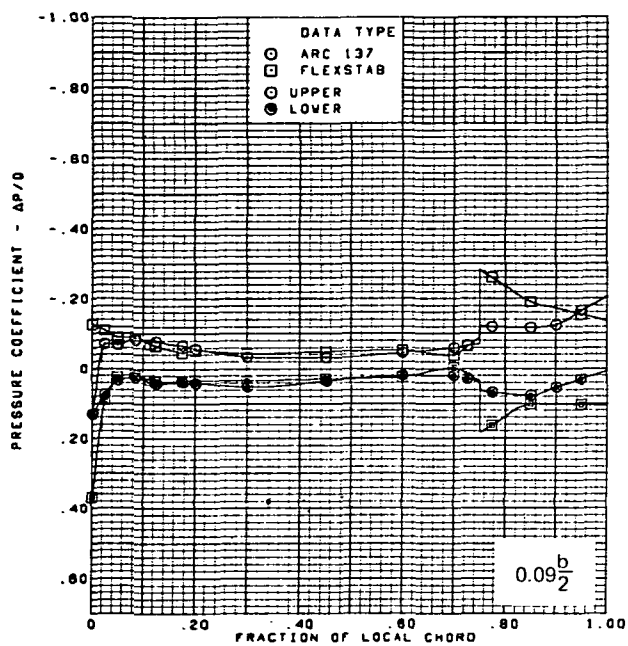
Figure 65.—Wing Theory-to-Experiment Comparison—Flat Wing, Rounded L.E.; L.E. Deflection, Full Span =  $0.0^\circ$ ; T.E. Deflection, Full Span =  $8.3^\circ$ ;  $M = 2.10$



$M = 2.10$  (run 27)  
 $\alpha = 0^\circ$   
 Flat wing, rounded L.E.  
 L.E. deflection, full span =  $0.0^\circ$   
 T.E. deflection, full span =  $8.3^\circ$   
 Note:  $C_{p, \text{vacuum}} = -0.32$

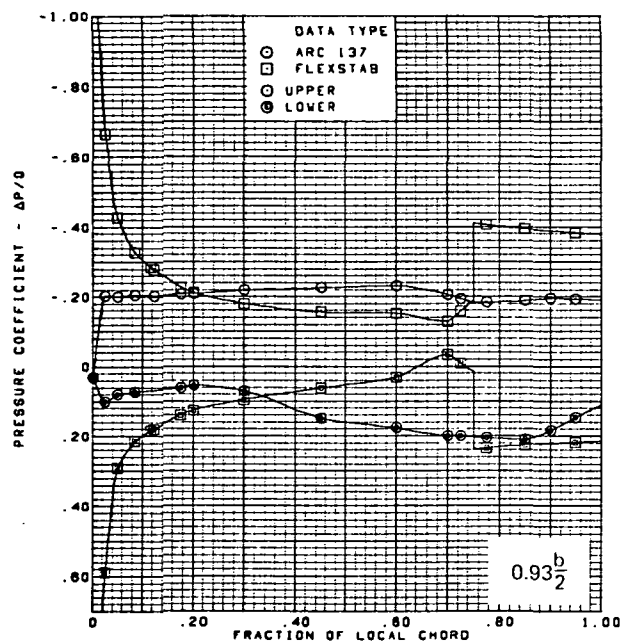
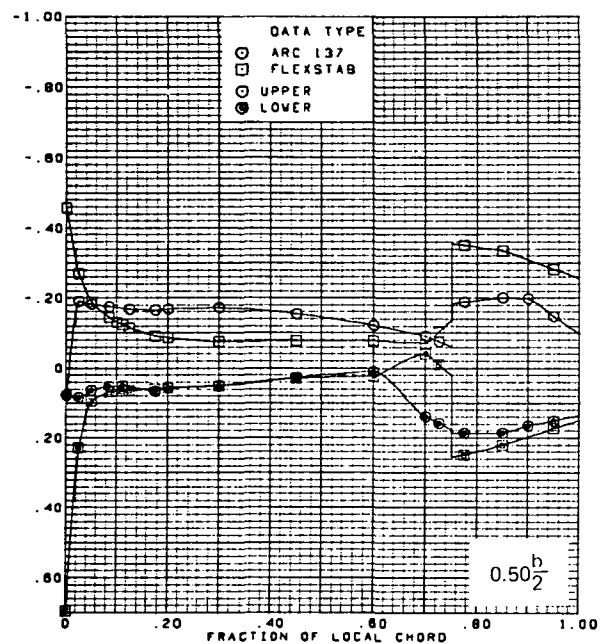
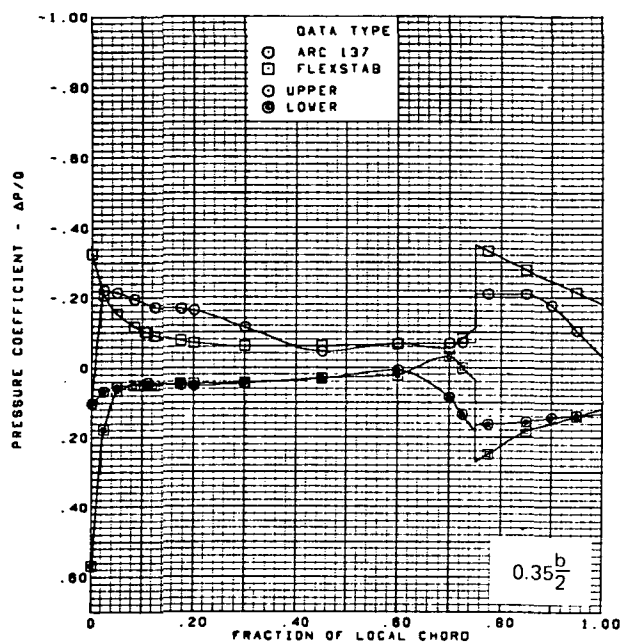
(a) (Concluded)

Figure 65.-(Continued)



(b) Surface Chordwise Pressure Distributions,  $\alpha = 4^\circ$

Figure 65.-(Continued)

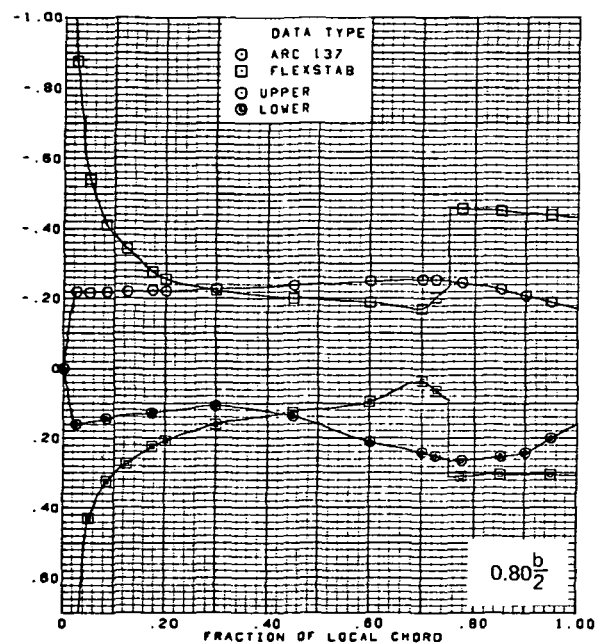
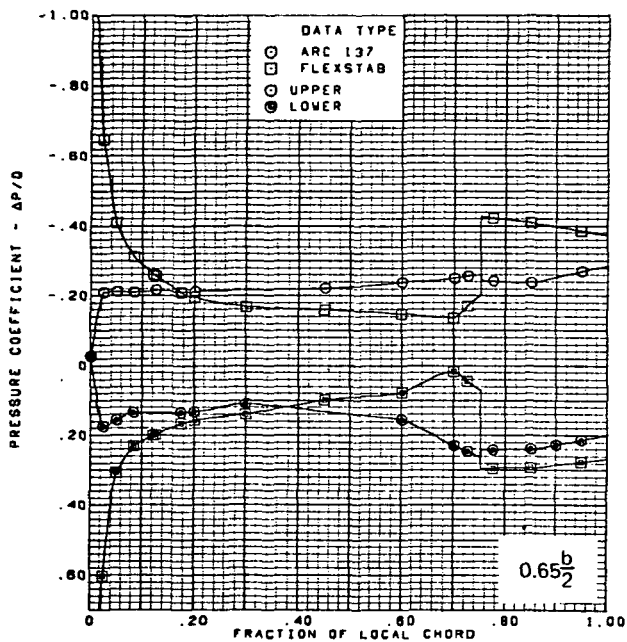
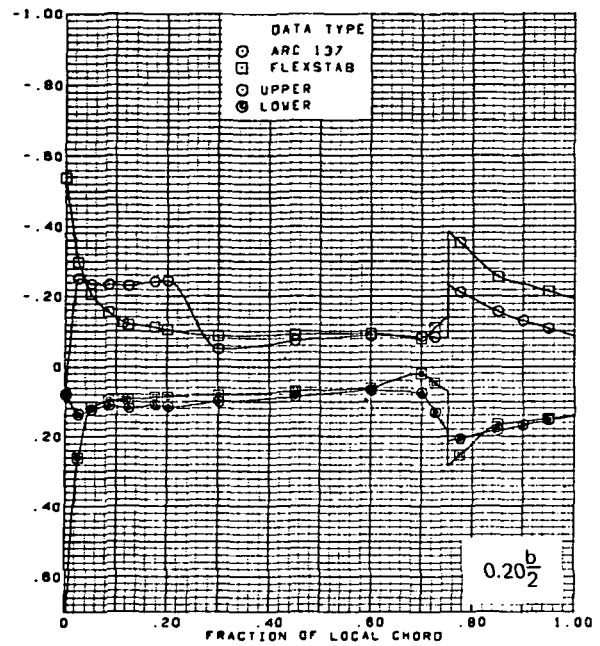
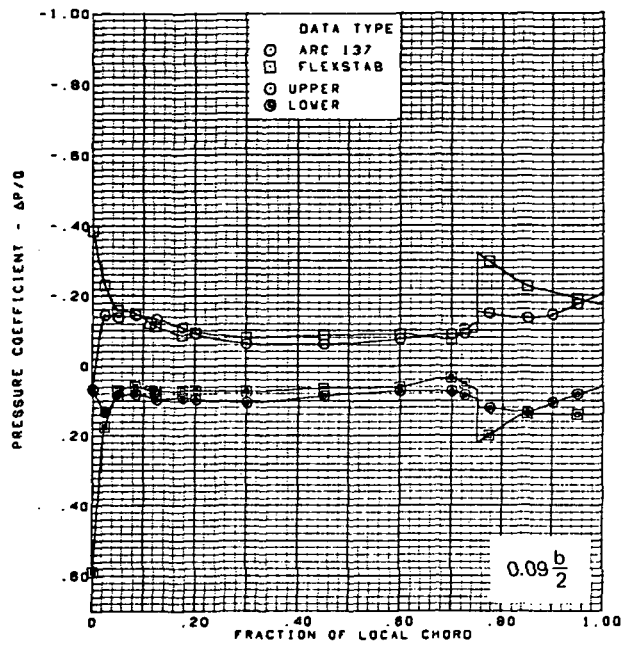


$M = 2.10$  (run 27)  
 $\alpha = 4^\circ$   
 Flat wing, rounded L.E.  
 L.E. deflection, full span =  $0.0^\circ$   
 T.E. deflection, full span =  $8.3^\circ$

Note:  $C_{p, \text{vacuum}} = -0.32$

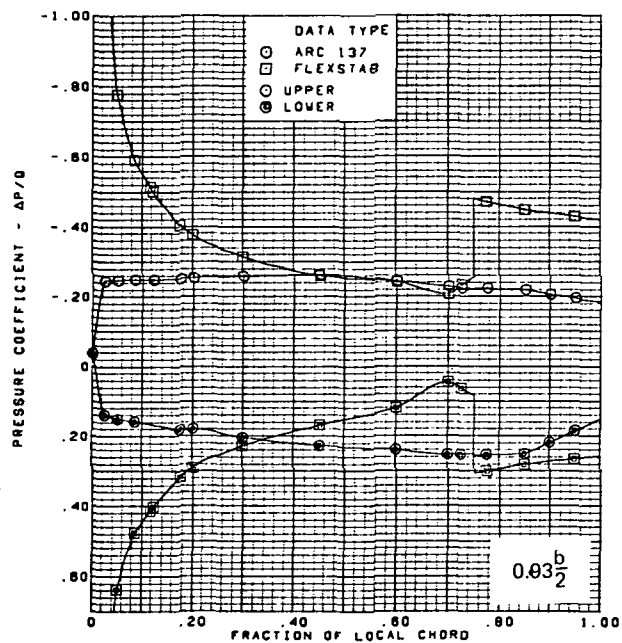
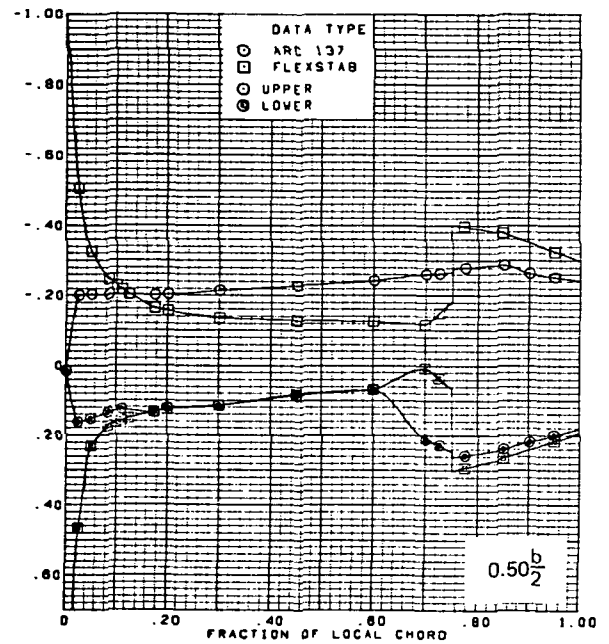
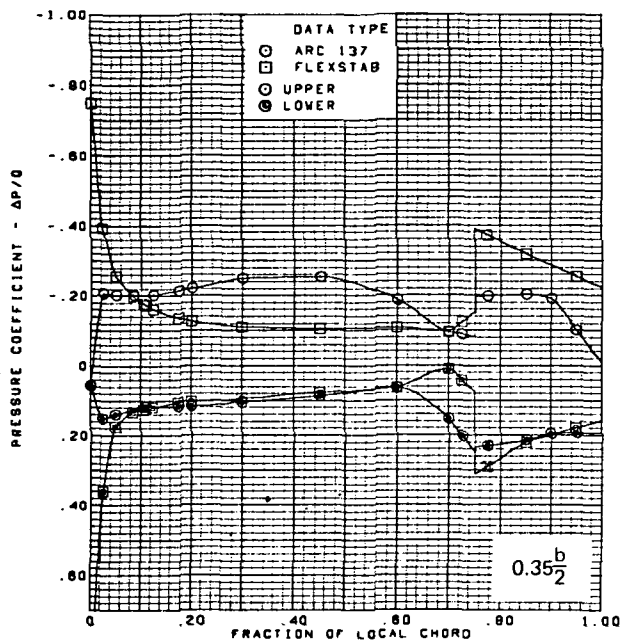
(b) (Concluded)

Figure 65.—(Continued)



(c) Surface Chordwise Pressure Distributions,  $\alpha = 8^\circ$

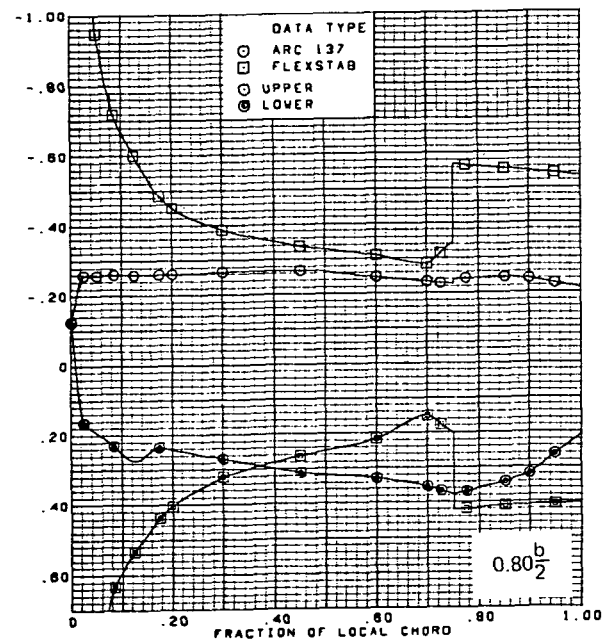
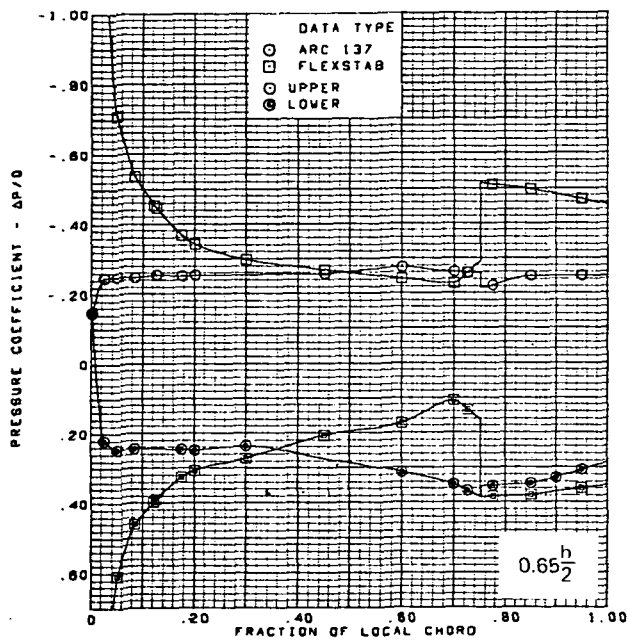
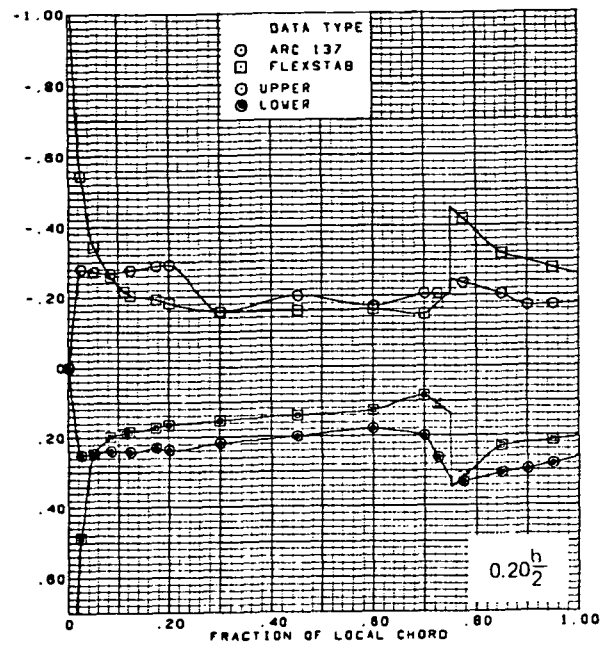
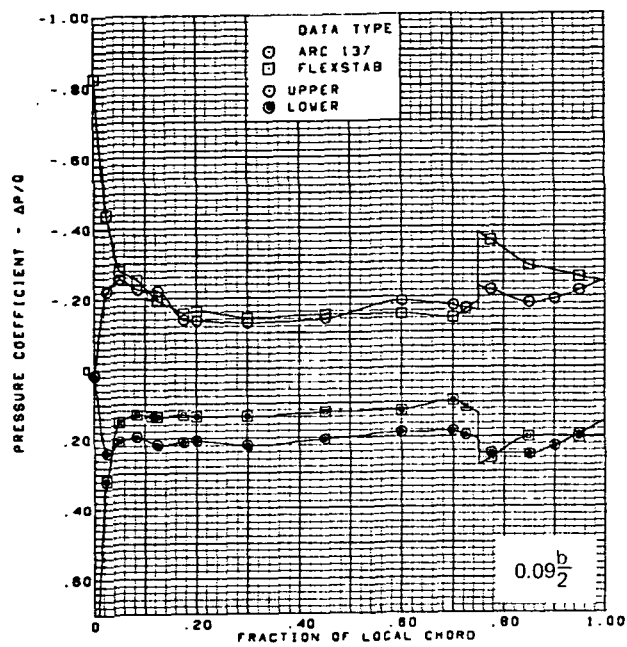
Figure 65.—(Continued)



$M = 2.10$  (run 27)  
 $\alpha = 8^\circ$   
 Flat wing, rounded L.E.  
 L.E. deflection, full span =  $0.0^\circ$   
 T.E. deflection, full span =  $8.3^\circ$   
 Note:  $C_{p, \text{vacuum}} = -0.32$

(c) (Concluded)

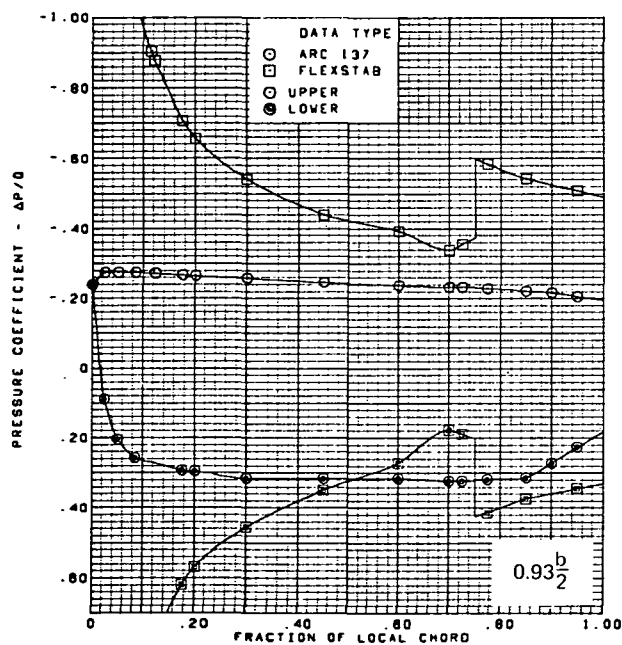
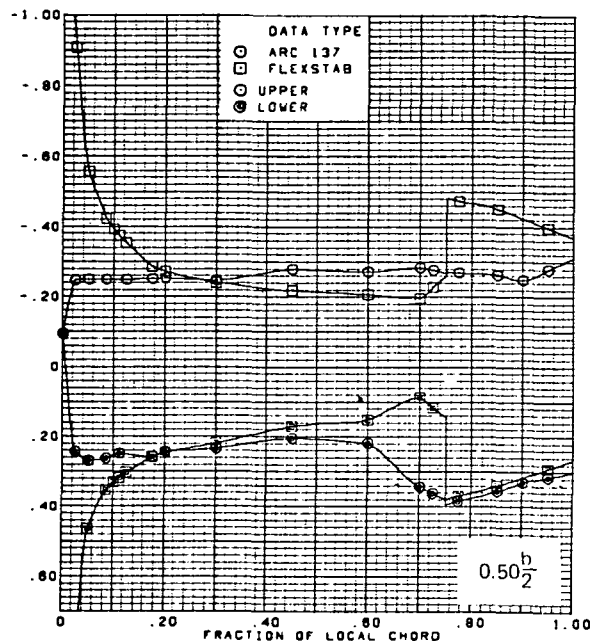
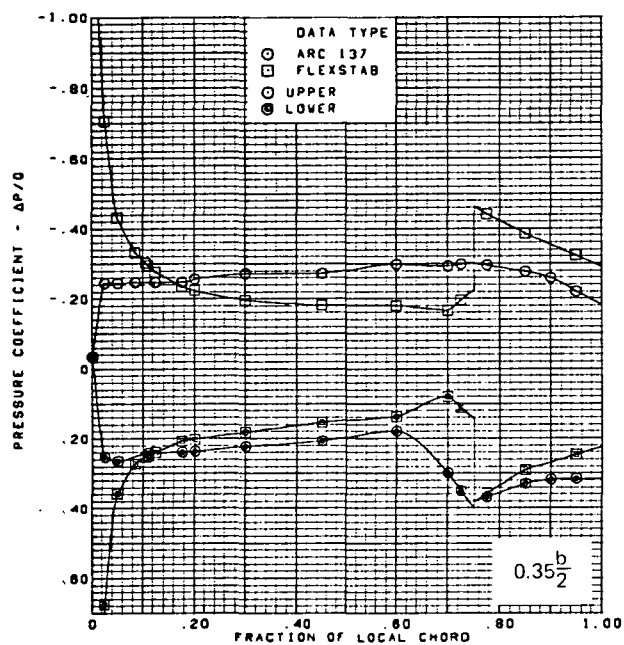
Figure 65.—(Continued)



(d) Surface Chordwise Pressure Distributions,  $\alpha = 15^\circ$

Figure 65.—(Continued)

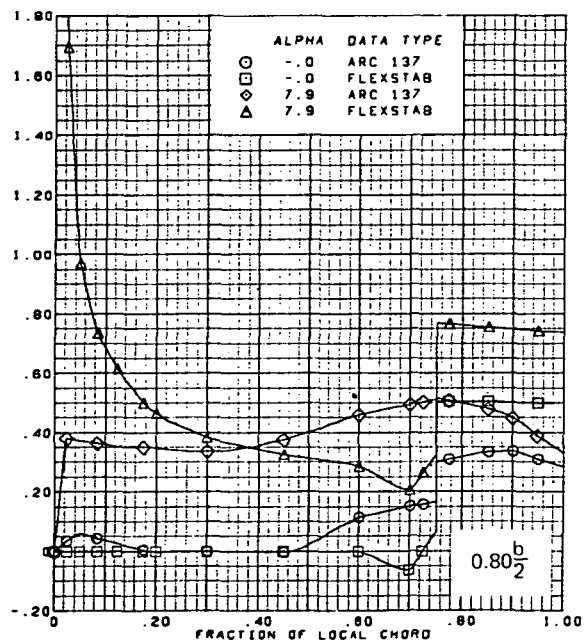
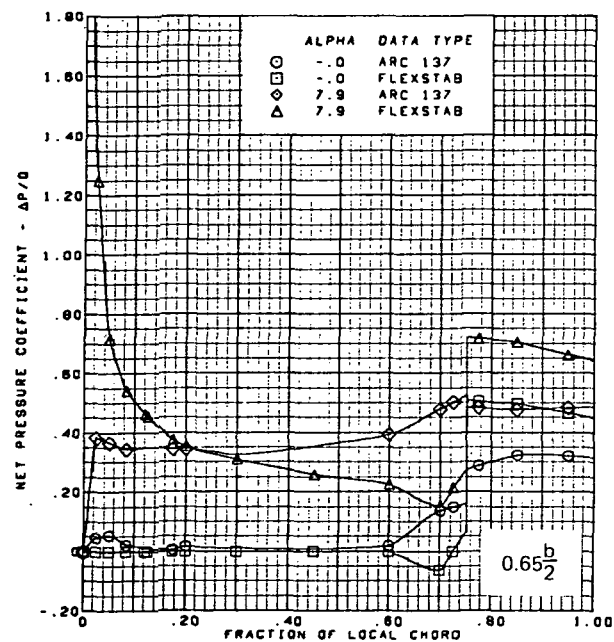
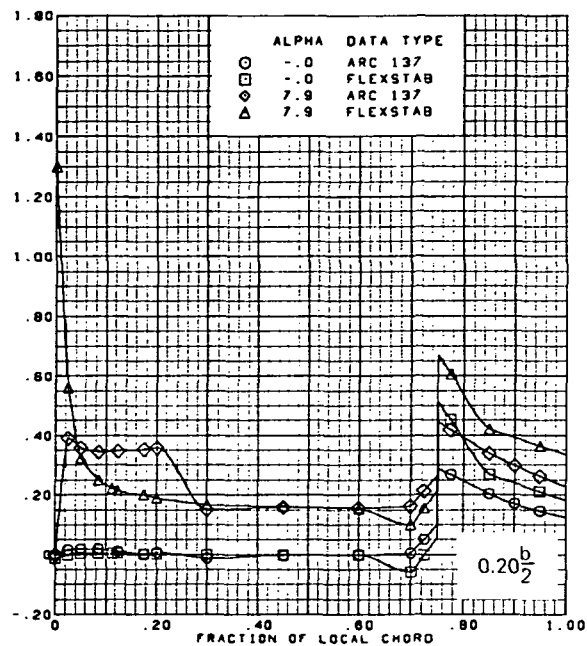
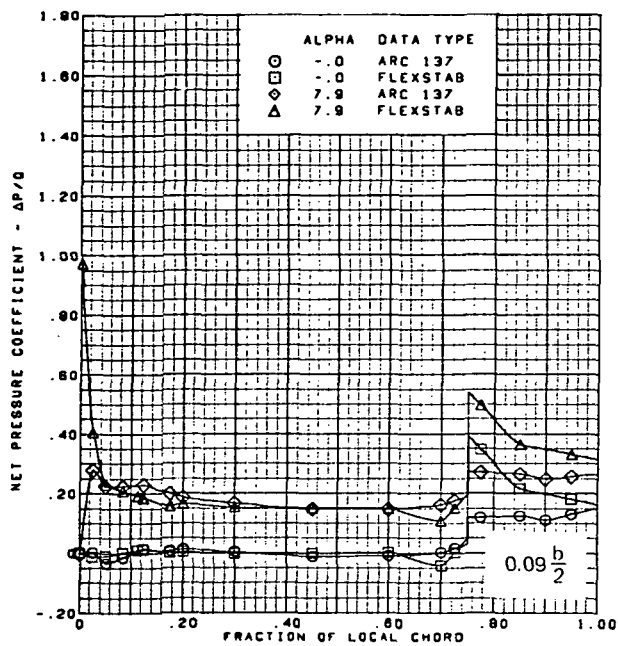




$M = 2.10$  (run 27)  
 $\alpha = 15^\circ$   
 Flat wing, rounded L.E.  
 L.E. deflection, full span =  $0.0^\circ$   
 T.E. deflection, full span =  $8.3^\circ$   
 Note:  $C_{p, \text{vacuum}} = -0.32$

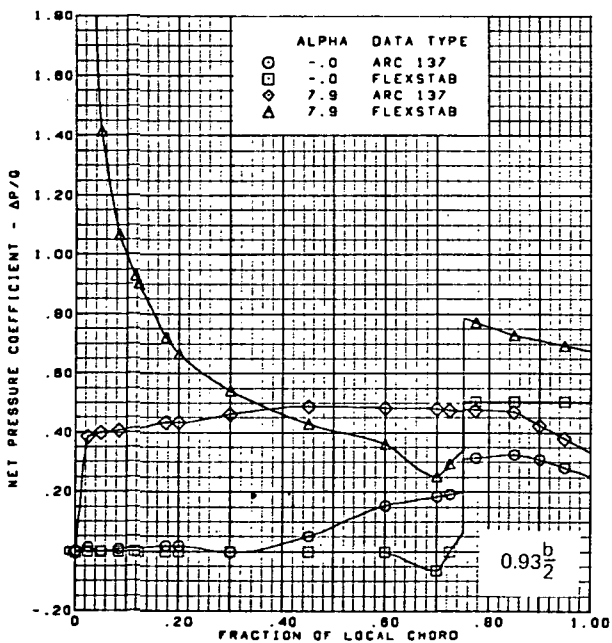
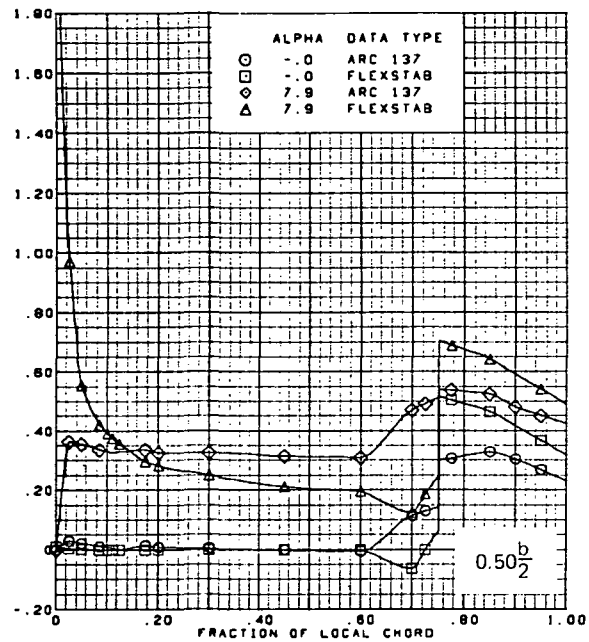
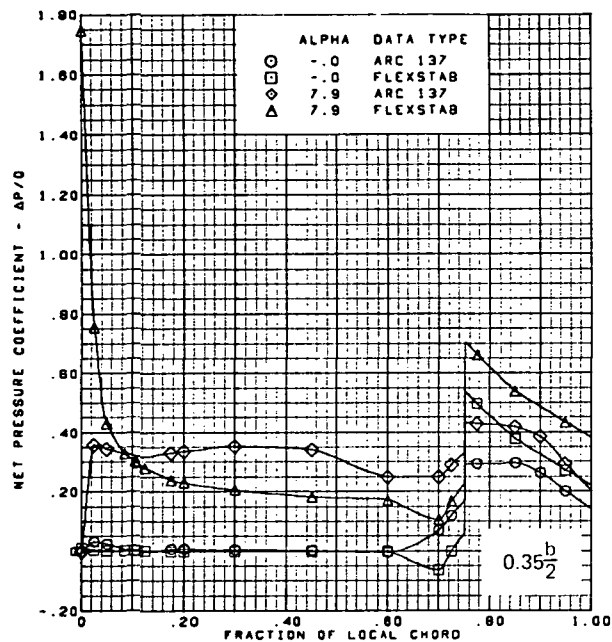
(d) (Concluded)

Figure 65.—(Continued)



(e) Net Chordwise Pressure Distributions,  $\alpha = 0^\circ, 8^\circ$

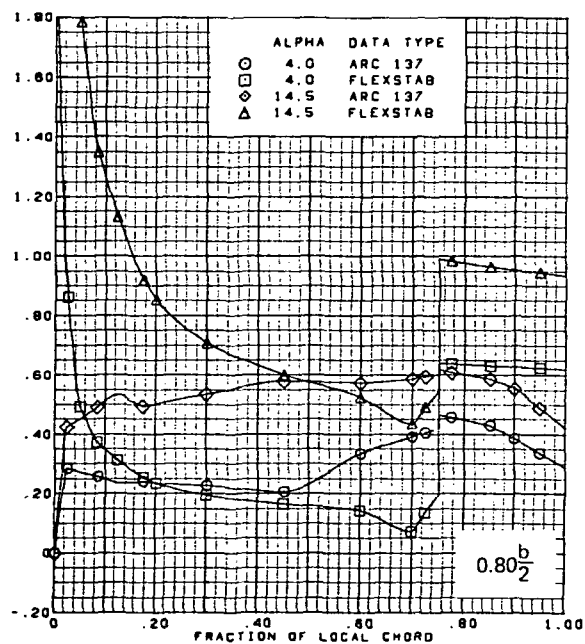
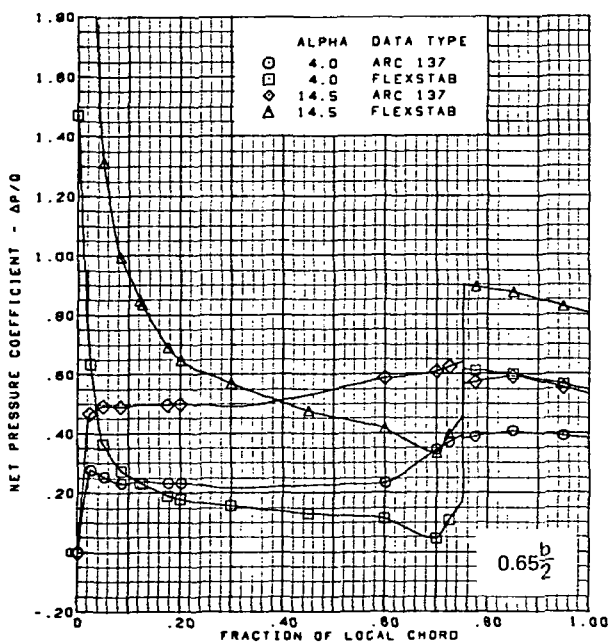
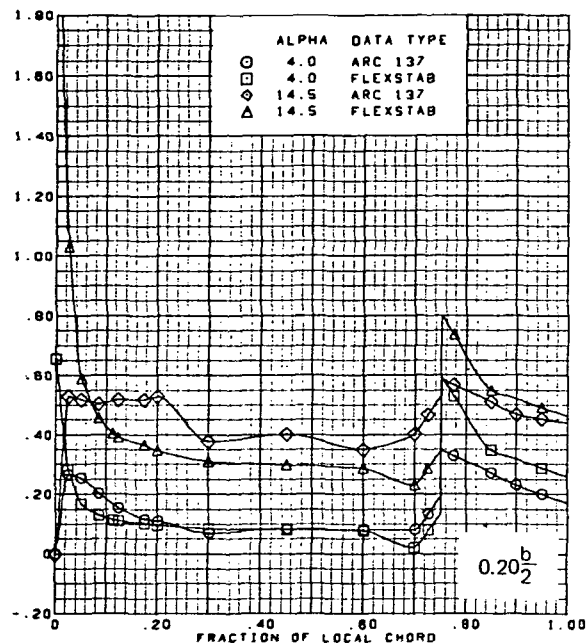
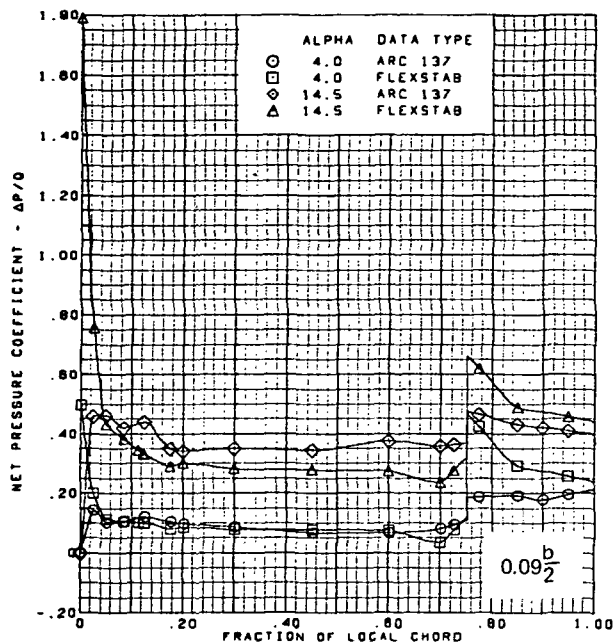
Figure 65.—(Continued)



M = 2.10 (run 27)  
 Flat wing, rounded L.E.  
 L.E. deflection, full span =  $0.0^\circ$   
 T.E. deflection, full span =  $8.3^\circ$

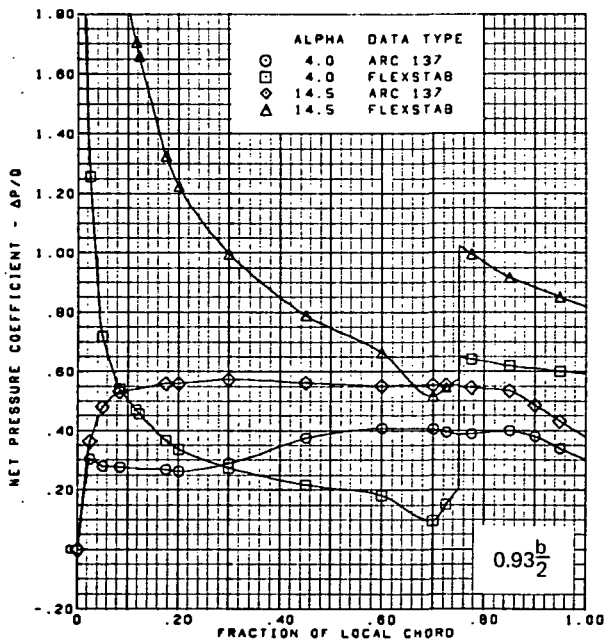
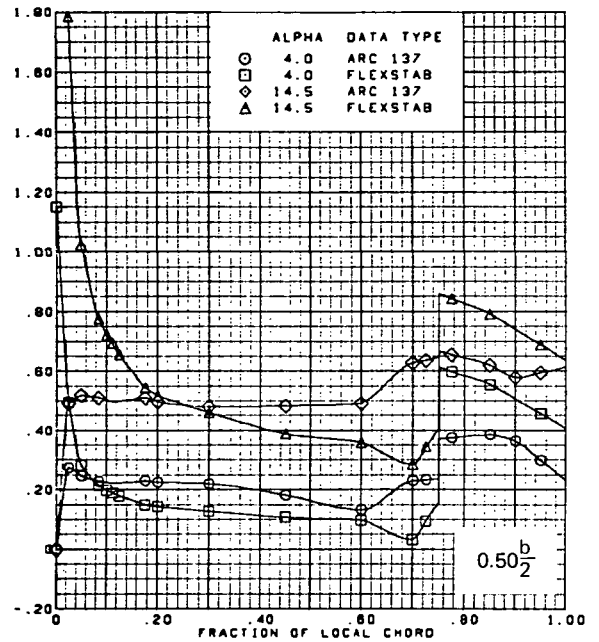
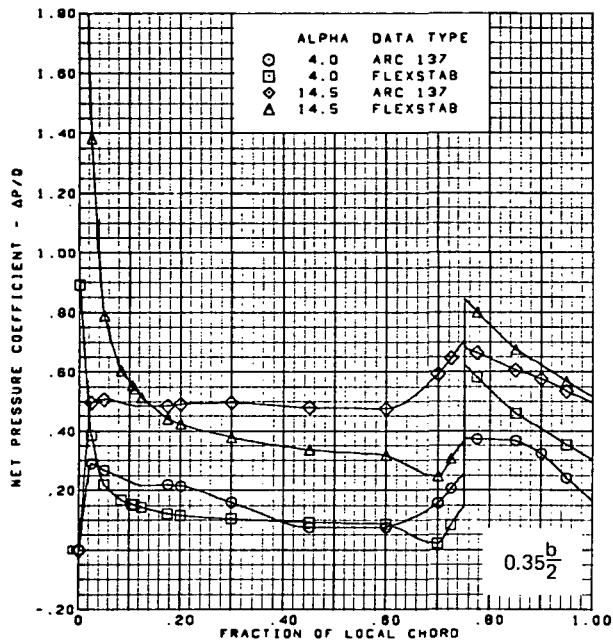
(e) (Concluded)

Figure 65.—(Continued)



(f) Net Chordwise Pressure Distributions,  $\alpha = 4^\circ, 15^\circ$

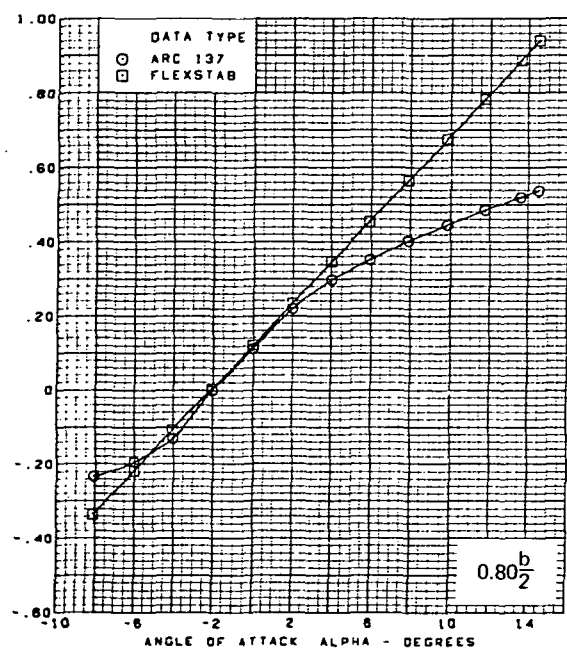
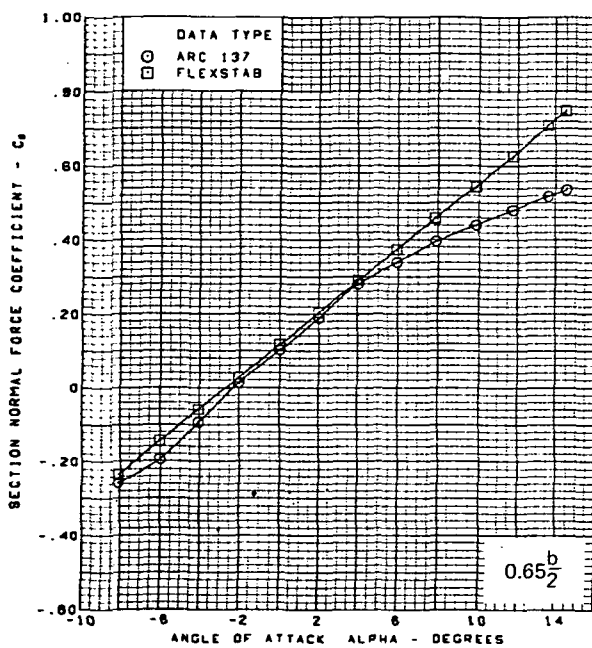
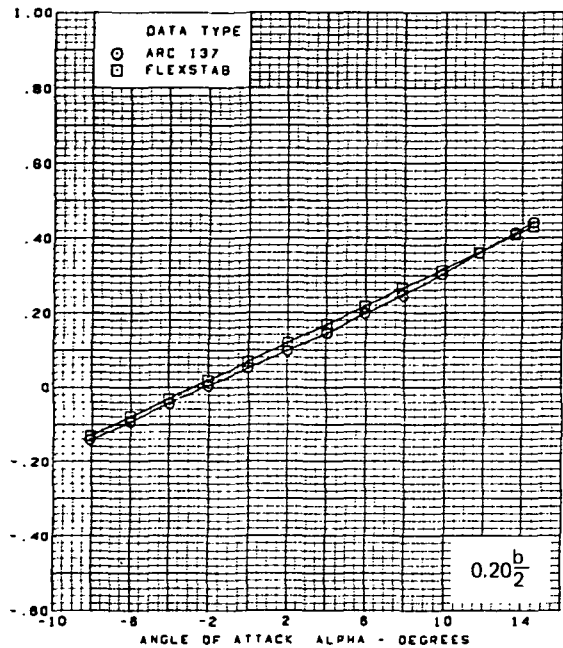
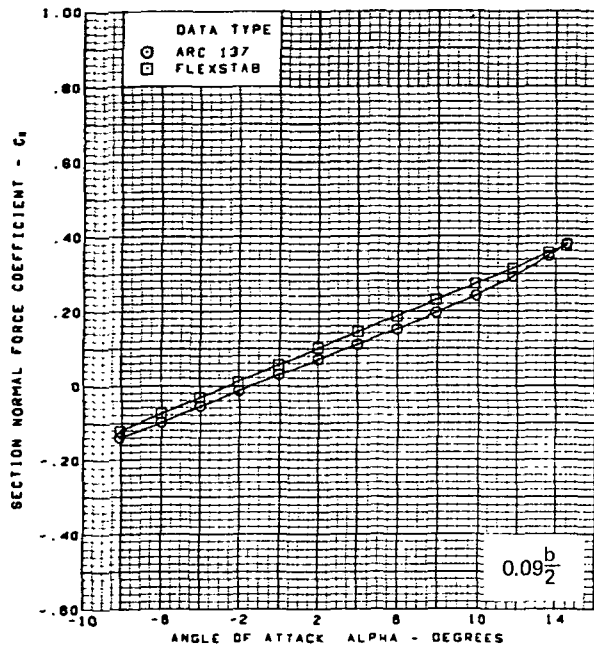
Figure 65.—(Continued)



$M = 2.10$  (run 27)  
 Flat wing, rounded L.E.  
 L.E. deflection, full span =  $0.0^\circ$   
 T.E. deflection, full span =  $8.3^\circ$

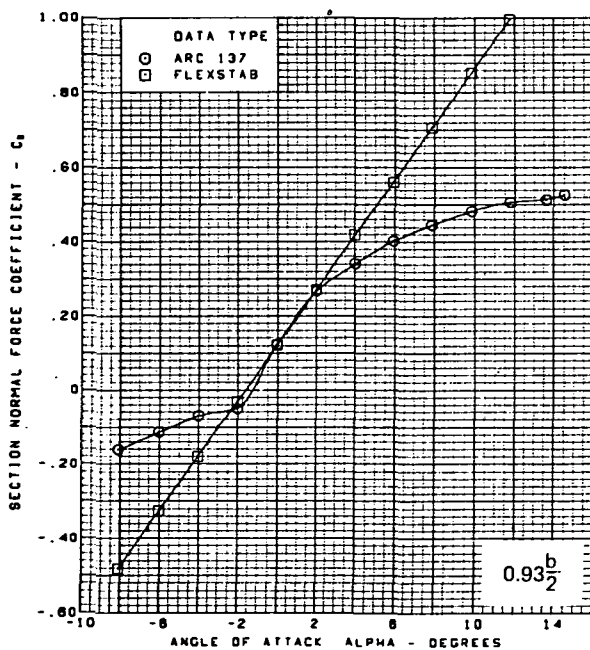
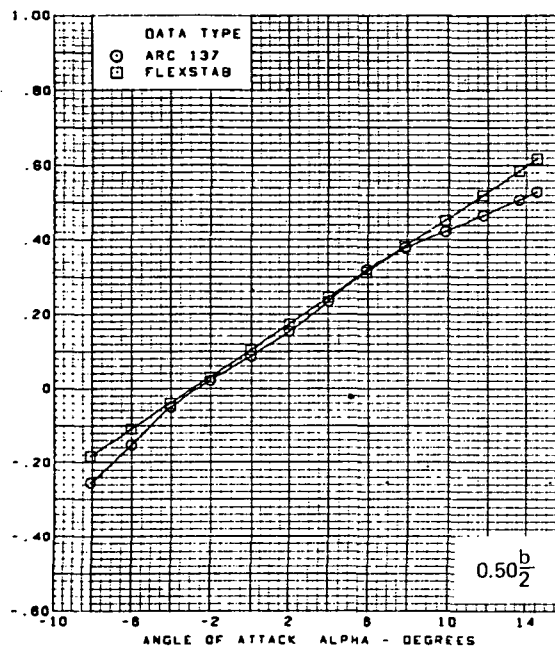
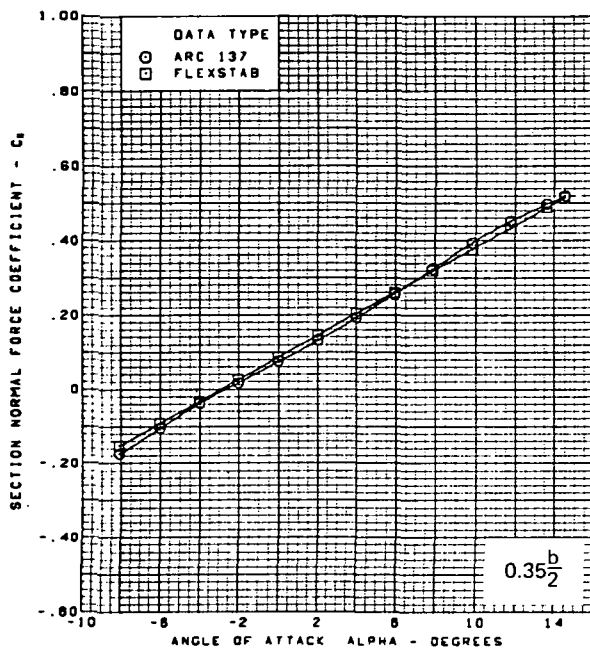
(f) (Concluded)

Figure 65.—(Continued)



(g) Section Aerodynamic Coefficients—Normal Force

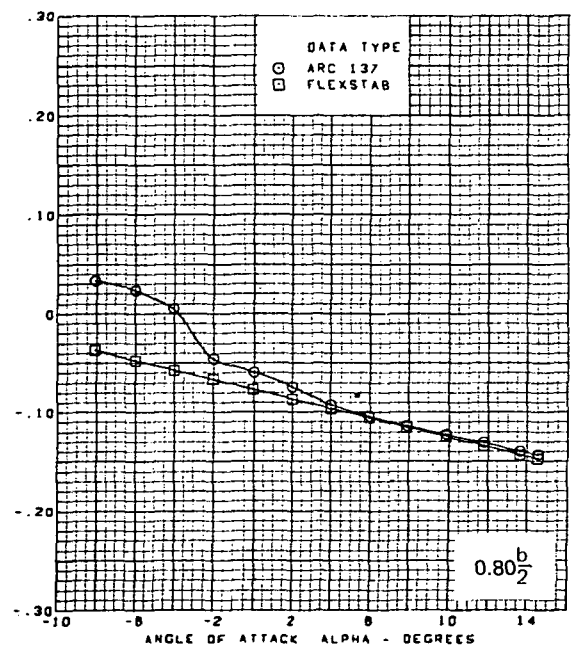
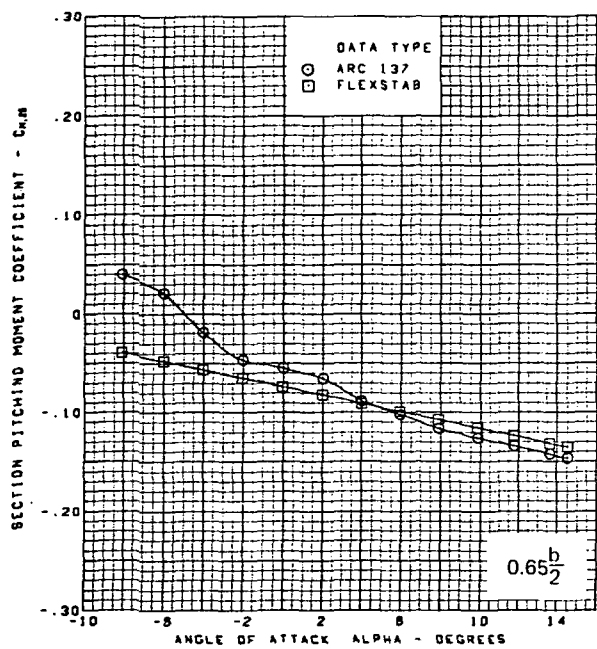
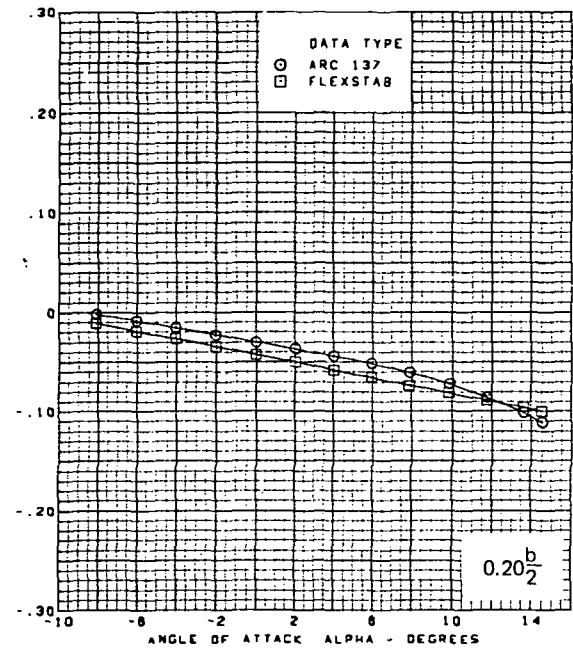
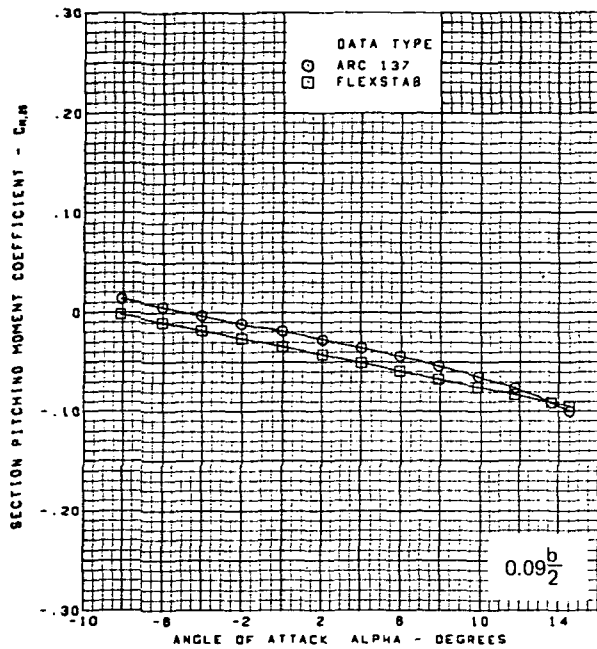
Figure 65.—(Continued)



$M = 2.10$  (run 27)  
 Flat wing, rounded L.E.  
 L.E. deflection, full span =  $0.0^\circ$   
 T.E. deflection, full span =  $8.3^\circ$

(g) (Concluded)

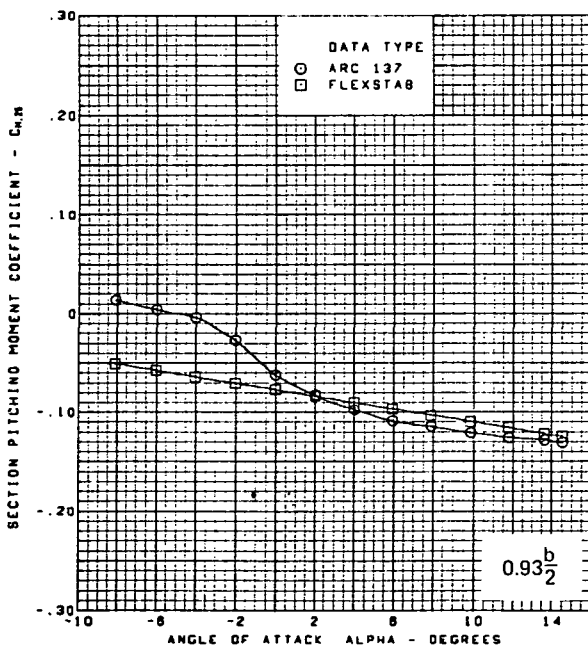
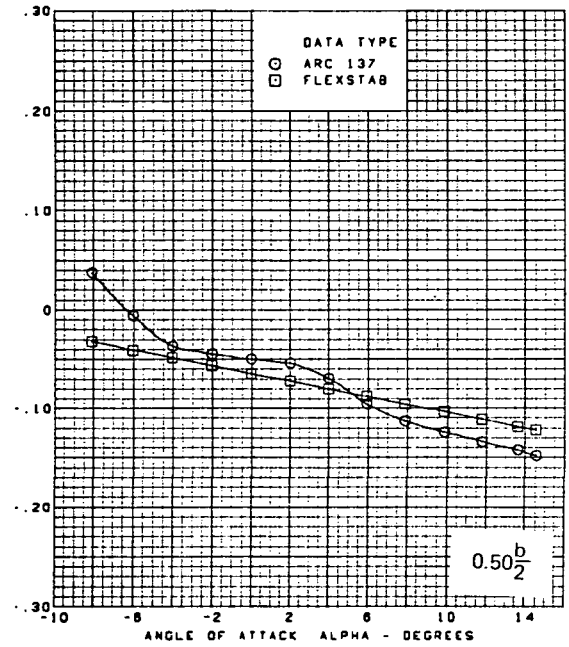
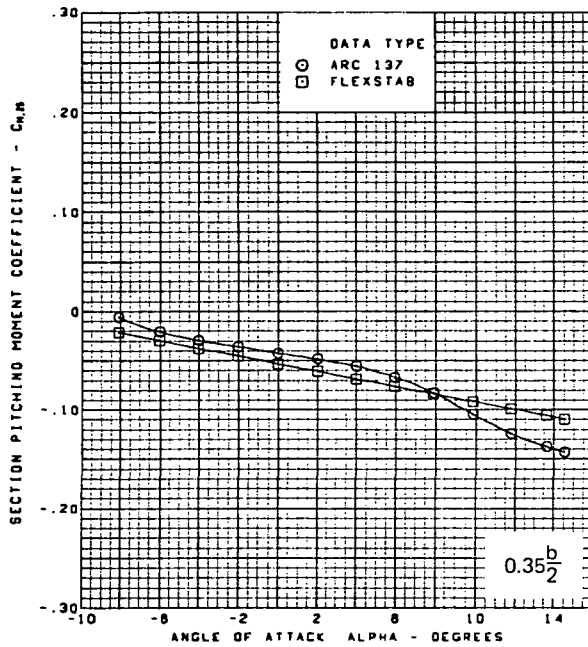
Figure 65.—(Continued)



(h) Section Aerodynamic Coefficients—Pitching Moment

Figure 65.—(Continued)

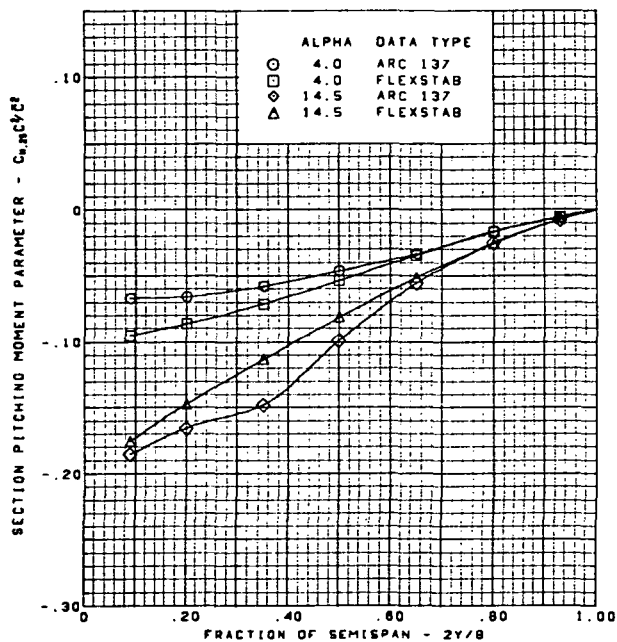
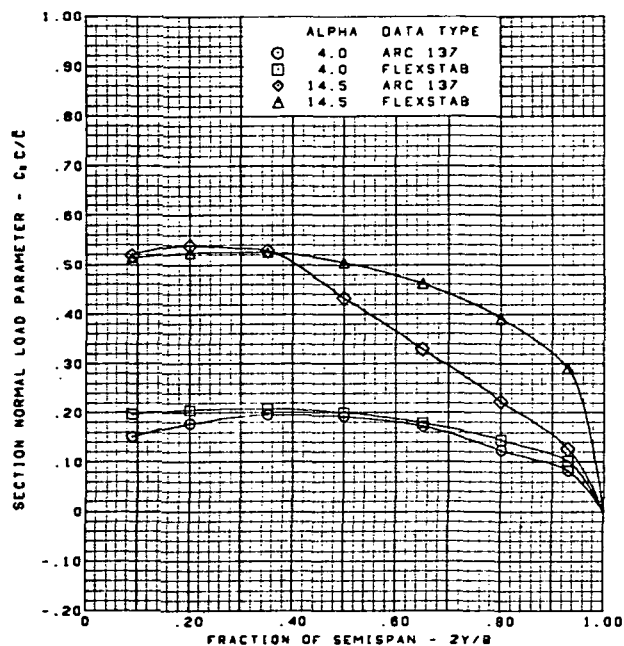
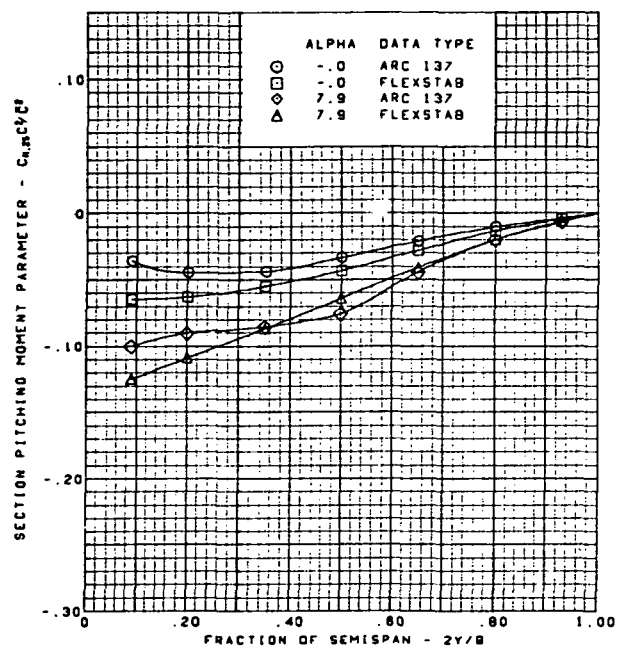
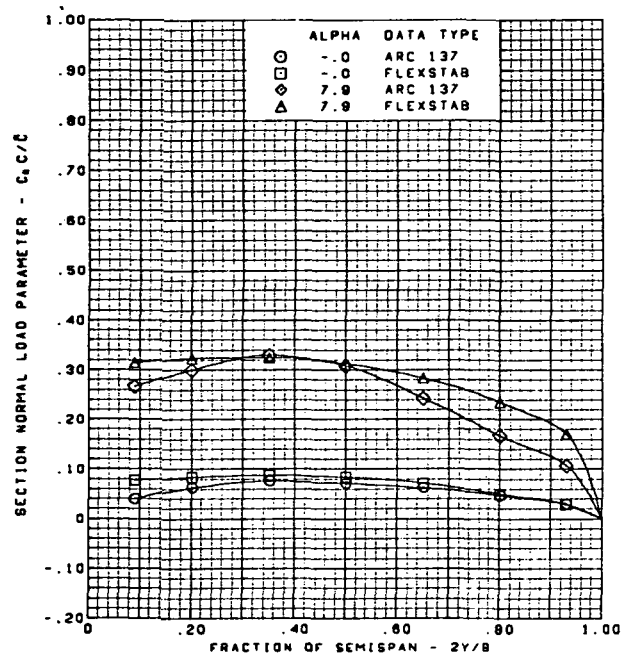




M = 2.10 (run 27)  
 Flat wing, rounded L.E.  
 L.E. deflection, full span =  $0.0^\circ$   
 T.E. deflection, full span =  $8.3^\circ$

(h) (Concluded)

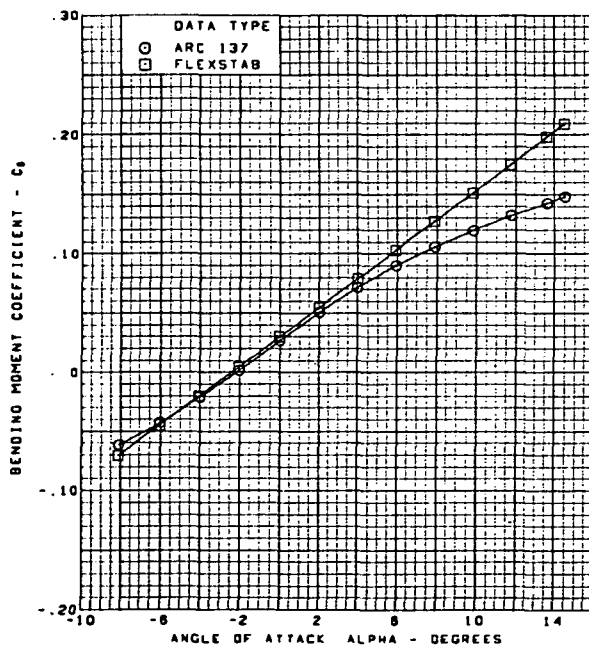
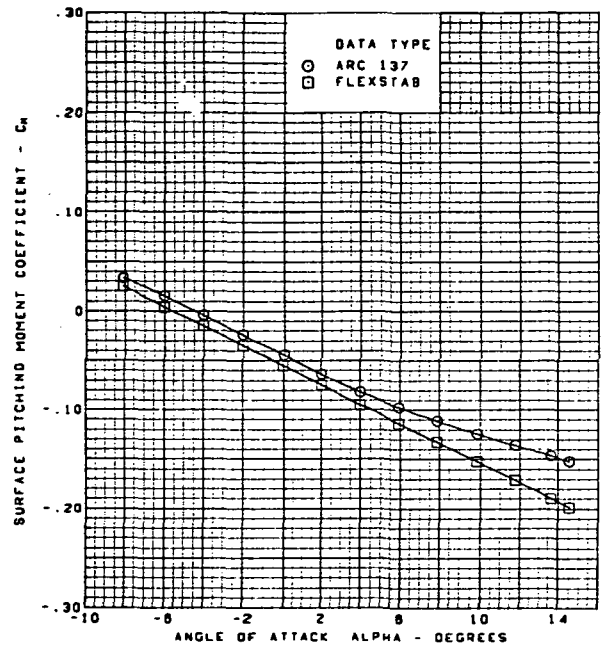
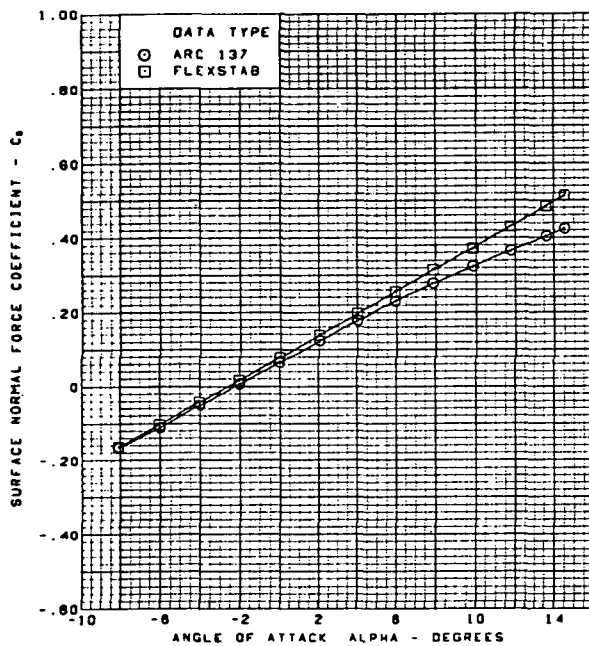
Figure 65.—(Continued)



$M = 2.10$  (run 27)  
 Flat wing, rounded L.E.  
 L.E. deflection, full span =  $0.0^\circ$   
 T.E. deflection, full span =  $8.3^\circ$

(i) Spanload Distributions

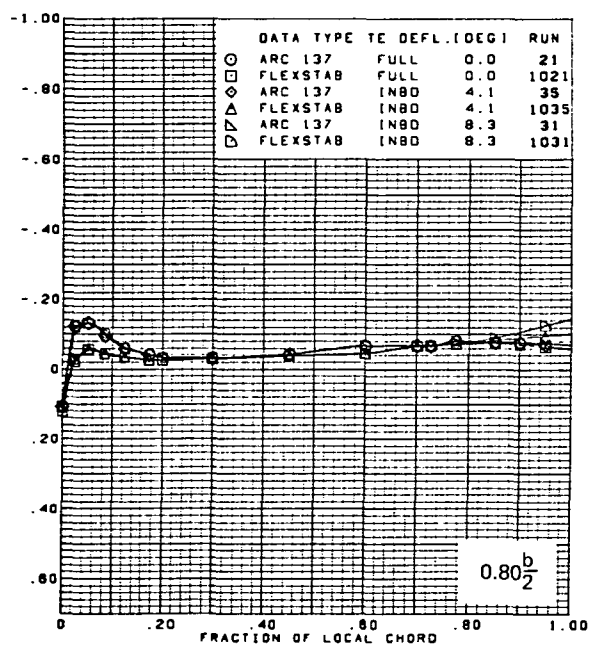
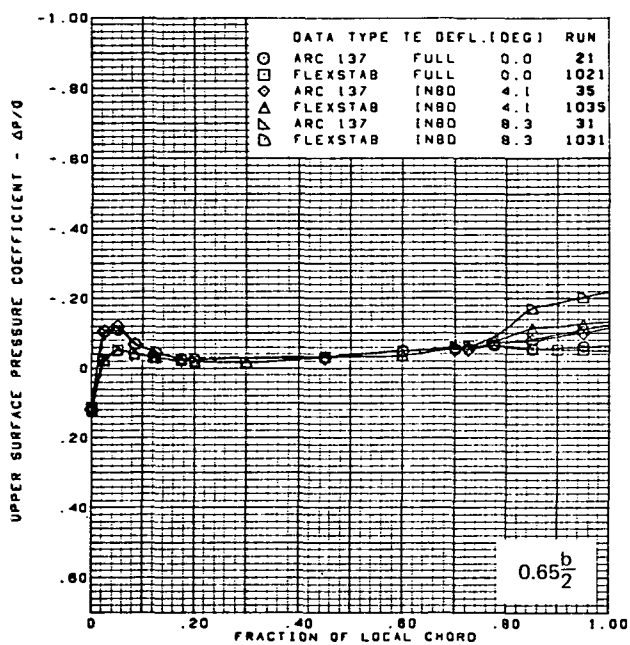
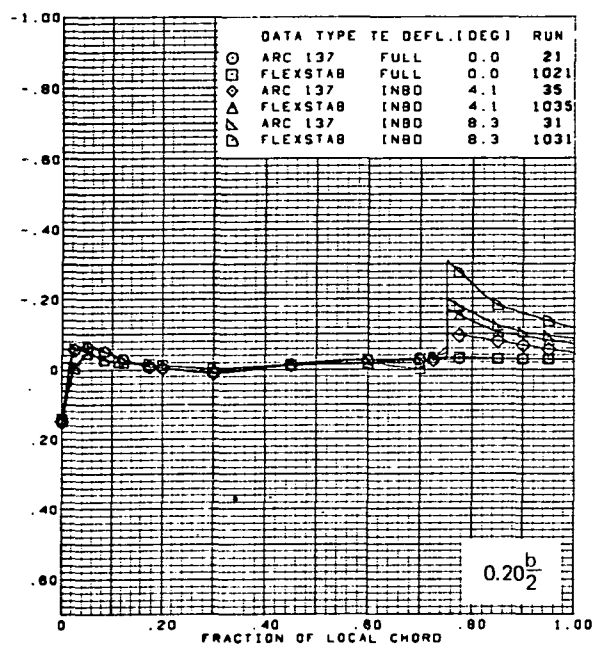
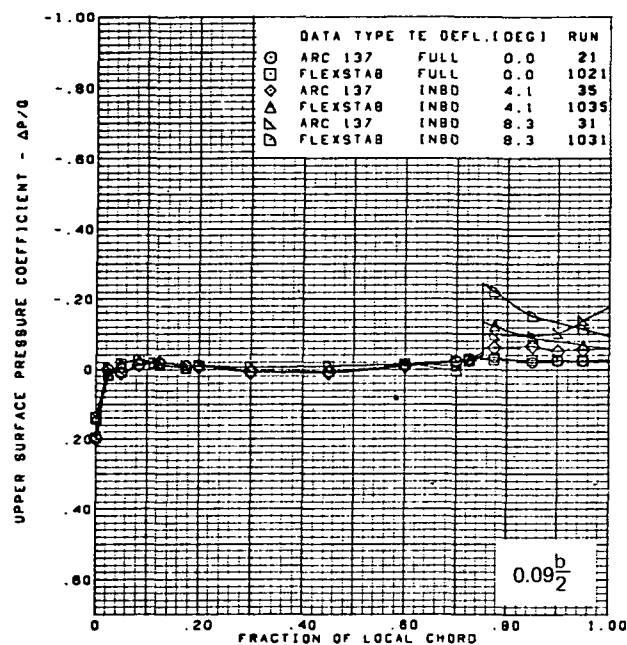
Figure 65.—(Continued)



$M = 2.10$  (run 27)  
 Flat wing, rounded L.E.  
 L.E. deflection, full span =  $0.0^\circ$   
 T.E. deflection, full span =  $8.3^\circ$

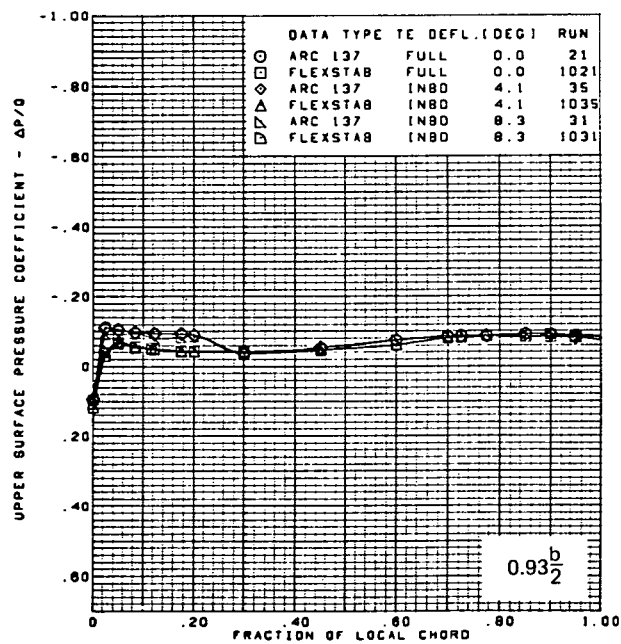
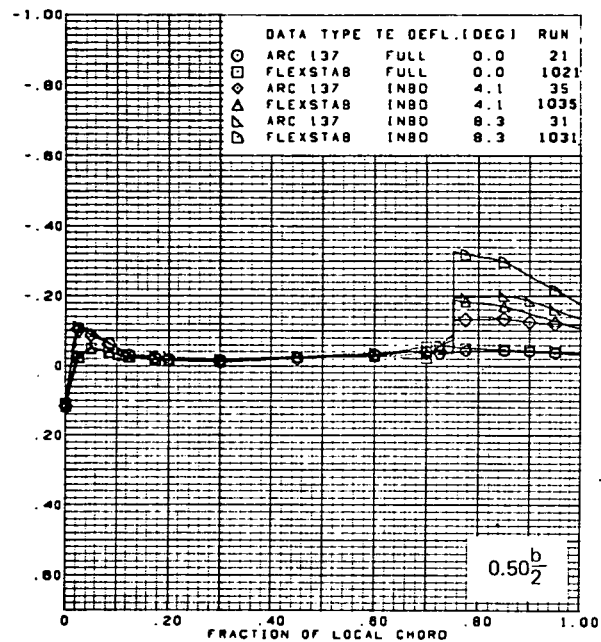
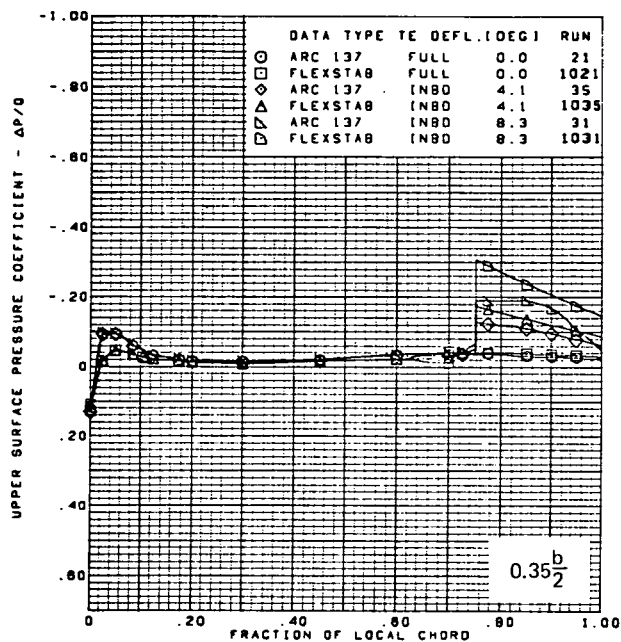
(j) Wing Aerodynamic Coefficients

Figure 65.—(Concluded)



(a) Upper Surface Chordwise Pressure Distributions,  $\alpha = 0^\circ$

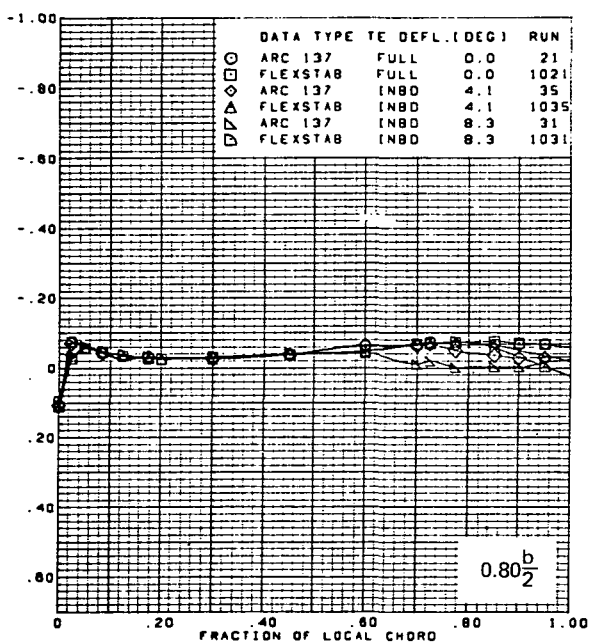
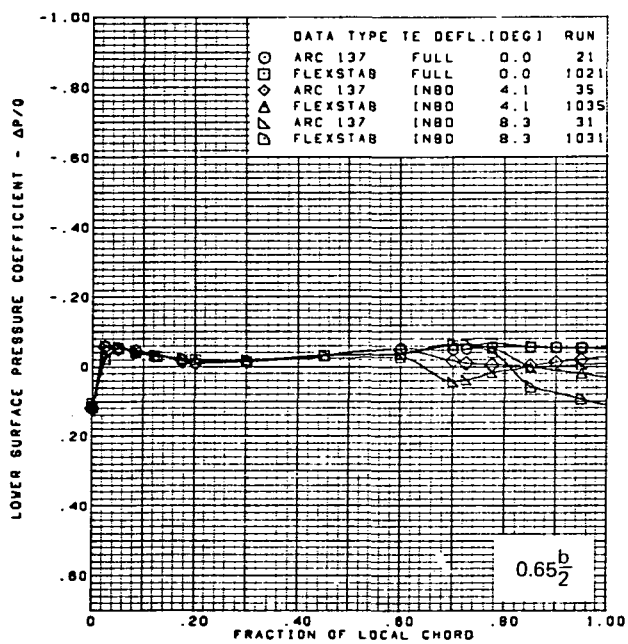
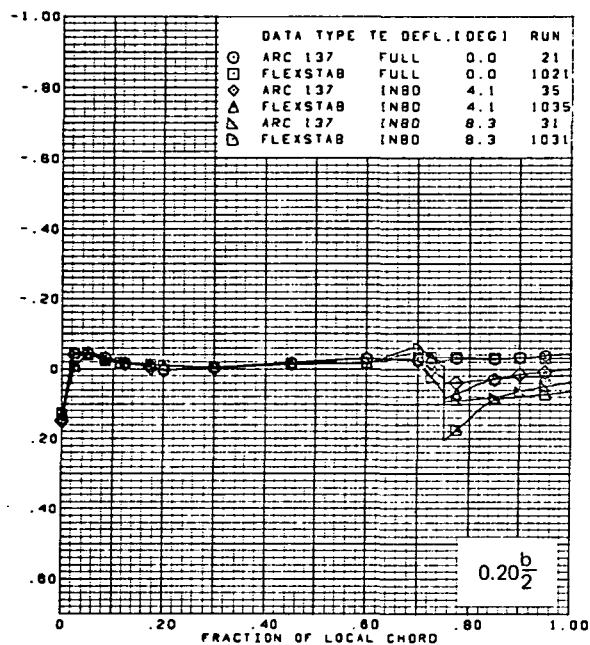
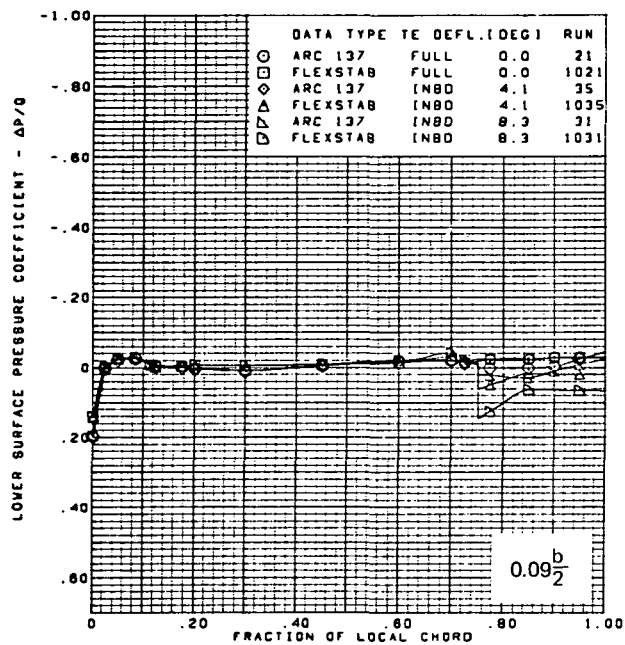
Figure 66. —Wing Theory-to-Experiment Comparison—Flat Wing, Rounded L.E.; L.E. Deflection, Full Span =  $0.0^\circ$ ; T.E. Deflection, Outboard =  $0.0^\circ$ ;  $M = 2.10$



$M = 2.10$   
 $\alpha = 0^\circ$   
 Flat wing, rounded L.E.  
 L.E. deflection, full span =  $0.0^\circ$   
 T.E. deflection, outboard =  $0.0^\circ$   
 Note:  $C_{p, \text{vacuum}} = -0.32$

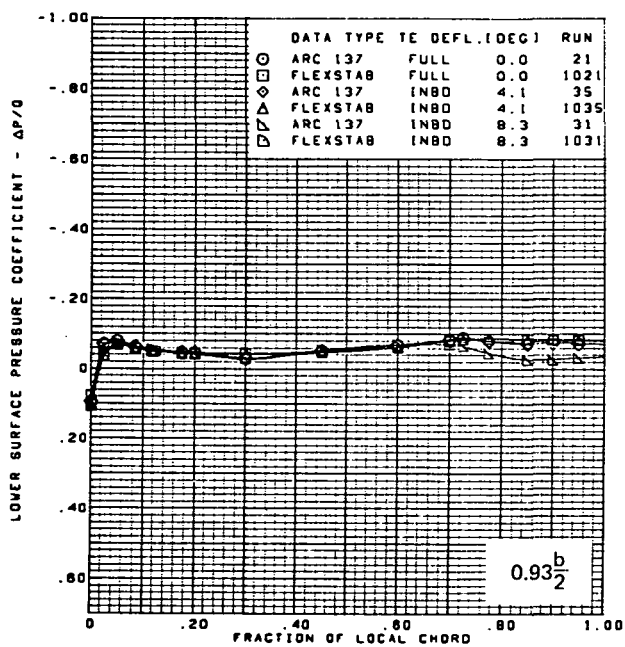
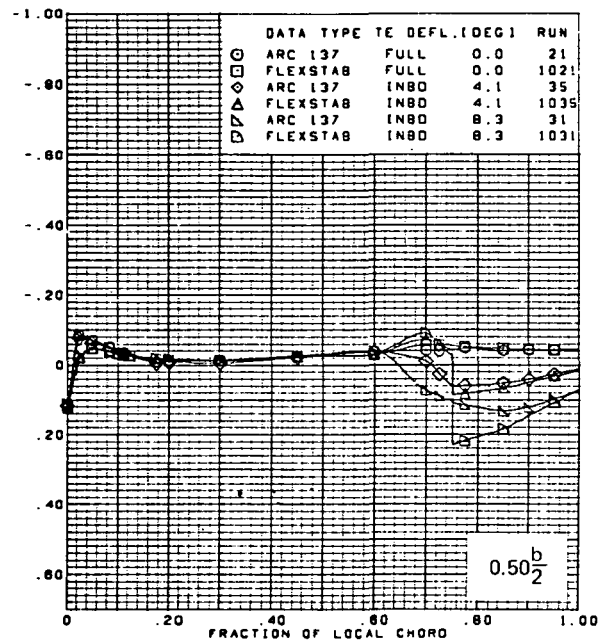
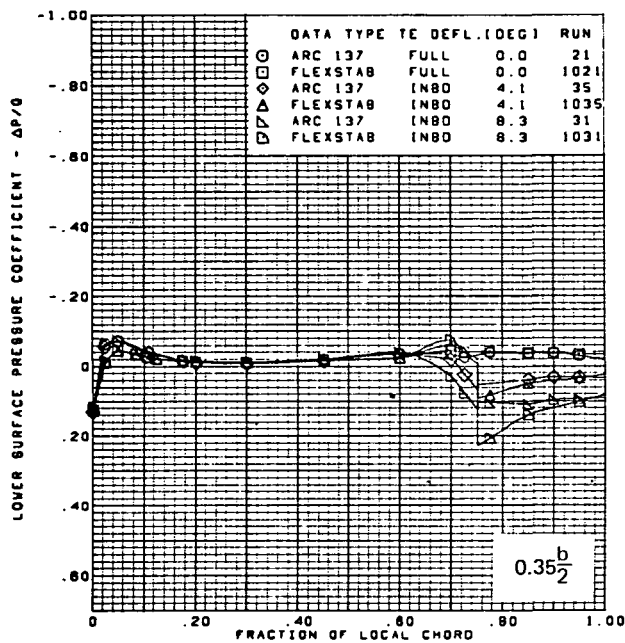
(a) (Concluded)

Figure 66.—(Continued)



(b) Lower Surface Chordwise Pressure Distributions,  $\alpha = 0^\circ$

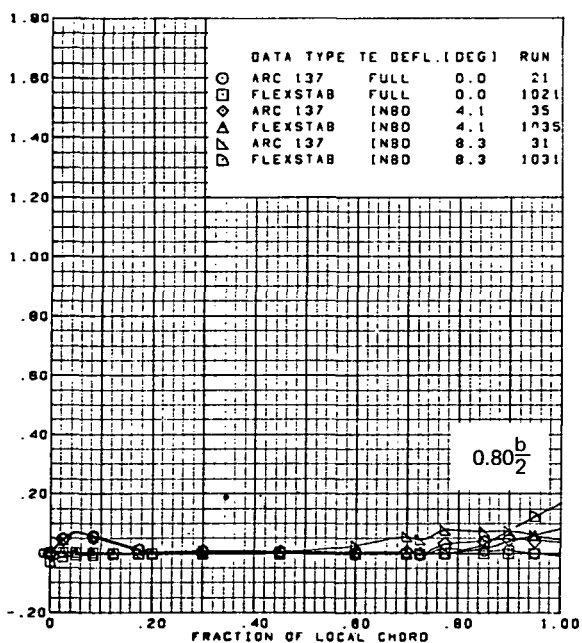
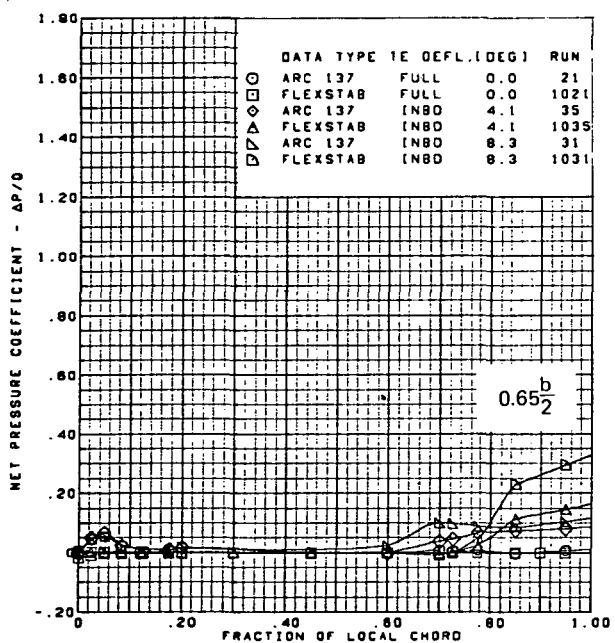
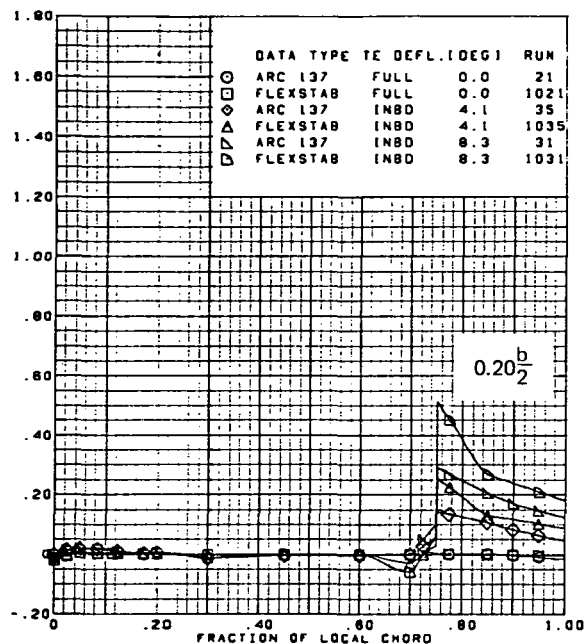
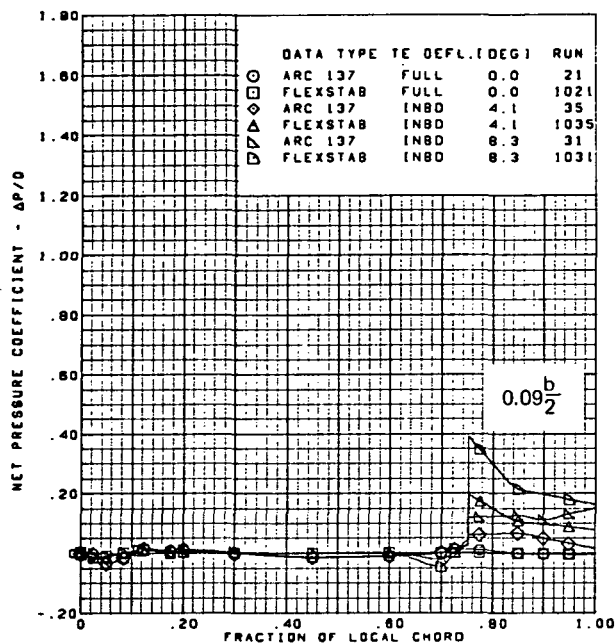
Figure 66. —(Continued)



$M = 2.10$   
 $\alpha = 0^\circ$   
 Flat wing, rounded L.E.  
 L.E. deflection, full span =  $0.0^\circ$   
 T.E. deflection, outboard =  $0.0^\circ$   
 Note:  $C_{p, \text{vacuum}} = -0.32$

(b) (Concluded)

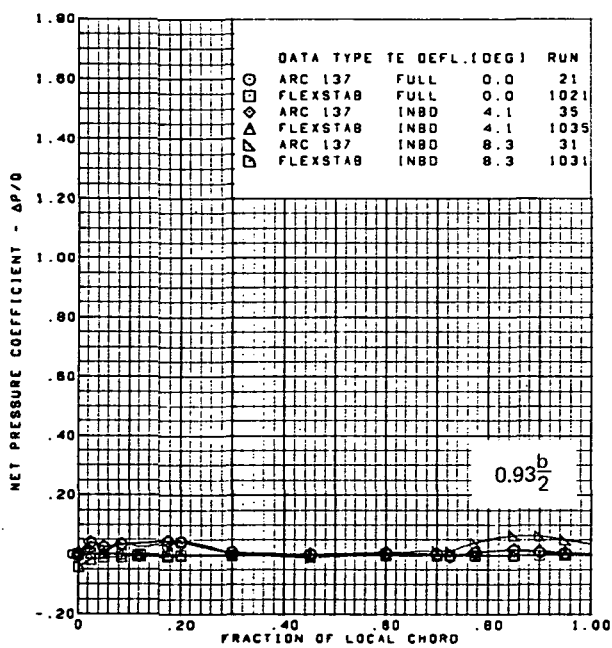
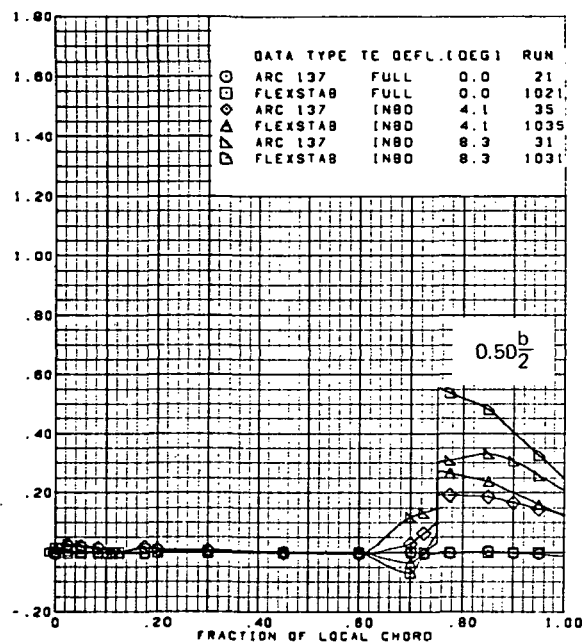
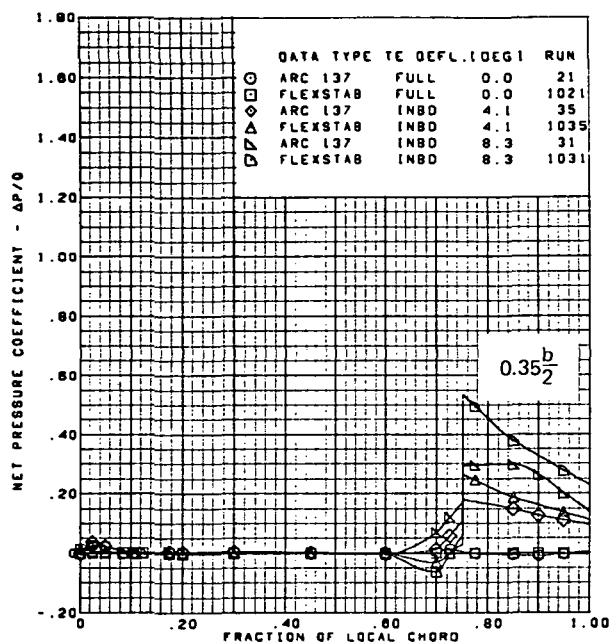
Figure 66. —(Continued)



(c) Net Chordwise Pressure Distributions,  $\alpha = 0^\circ$

Figure 66. —(Continued)

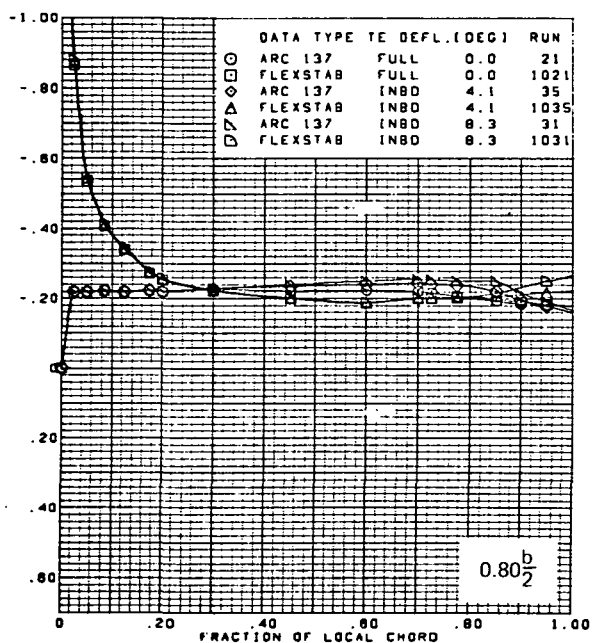
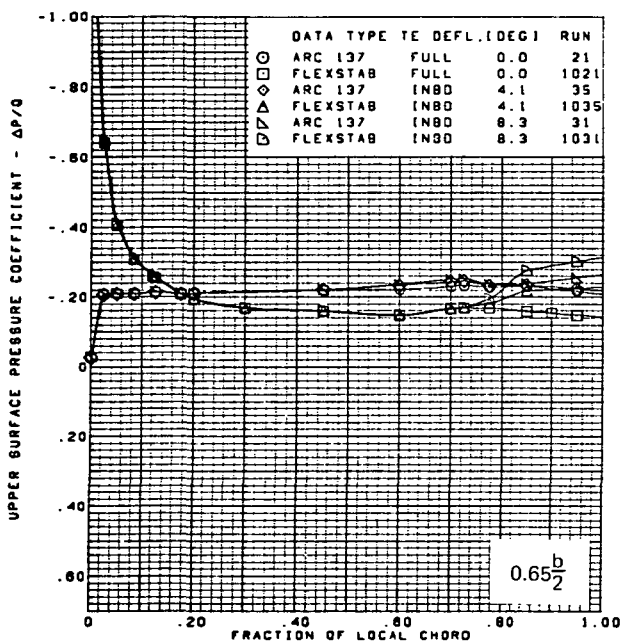
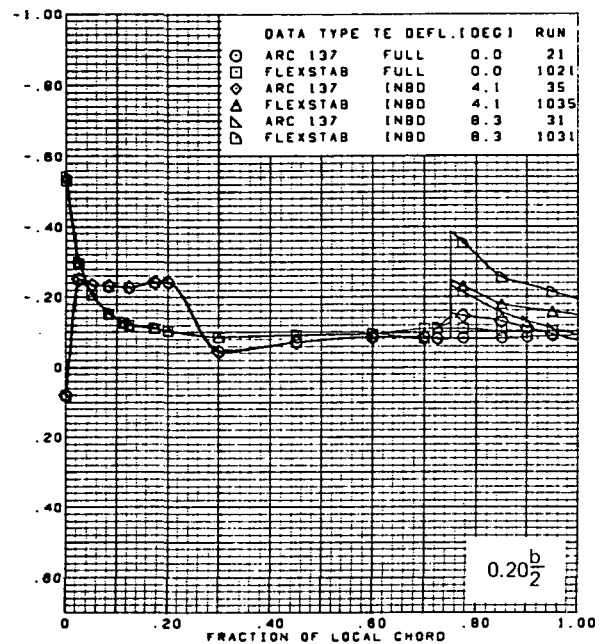
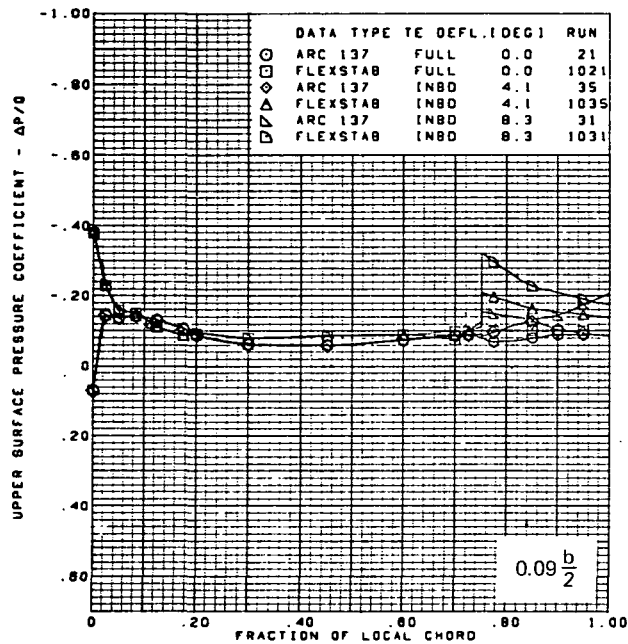




$M = 2.10$   
 $\alpha = 0^\circ$   
 Flat wing, rounded L.E.  
 L.E. deflection, full span =  $0.0^\circ$   
 T.E. deflection, outboard =  $0.0^\circ$

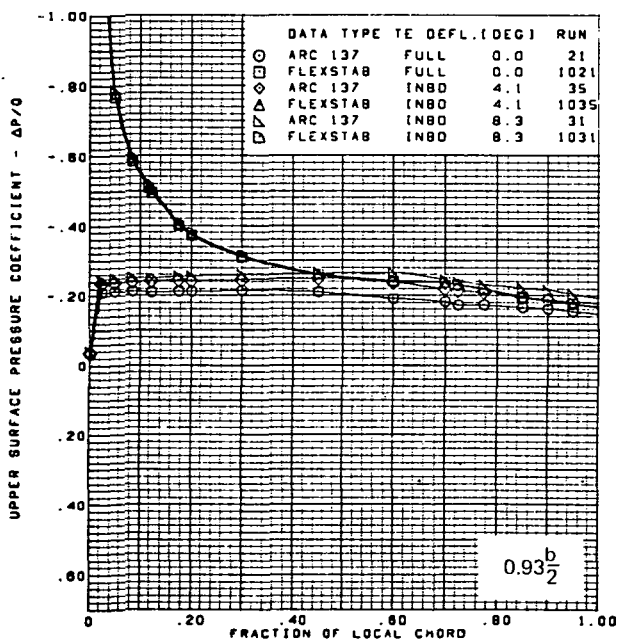
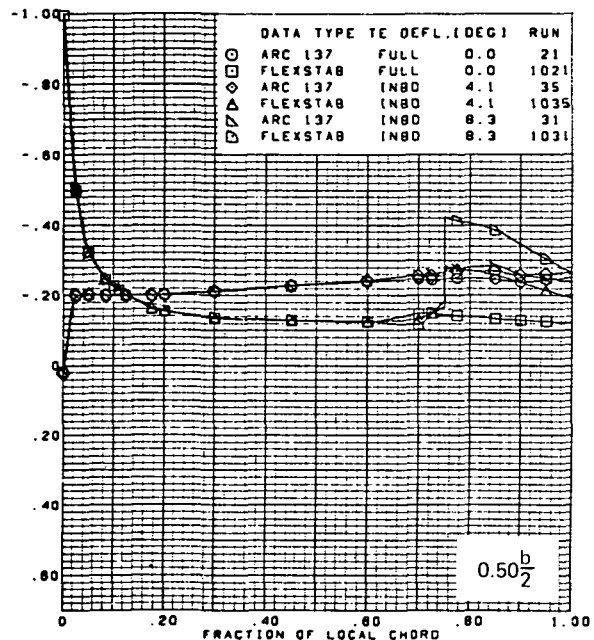
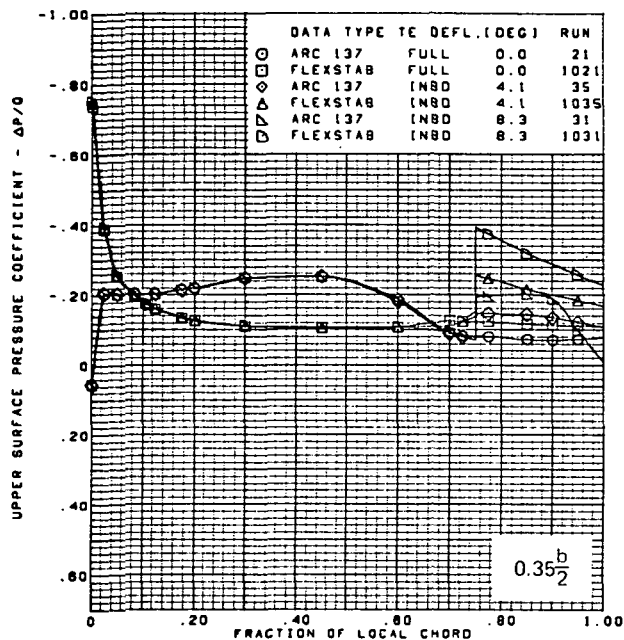
(c) (Concluded)

Figure 66.—(Continued)



(d) Upper Surface Chordwise Pressure Distributions,  $\alpha = 8^\circ$

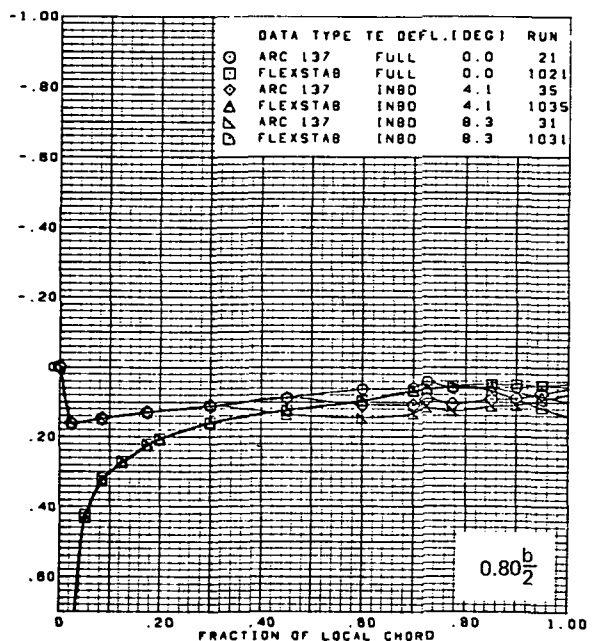
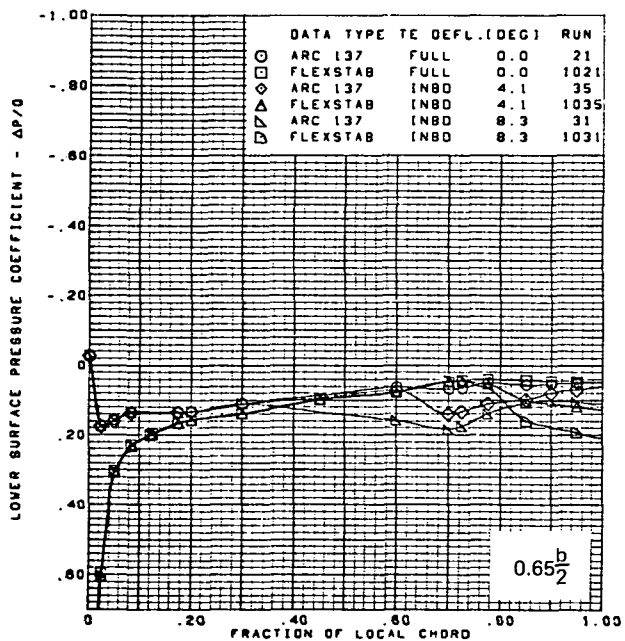
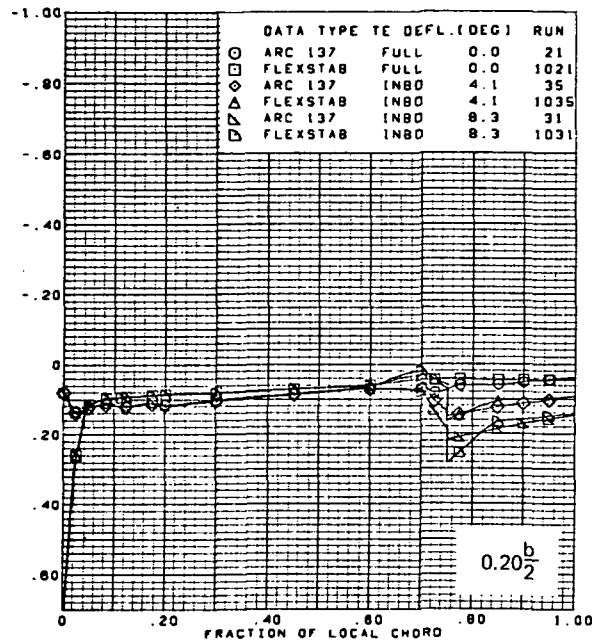
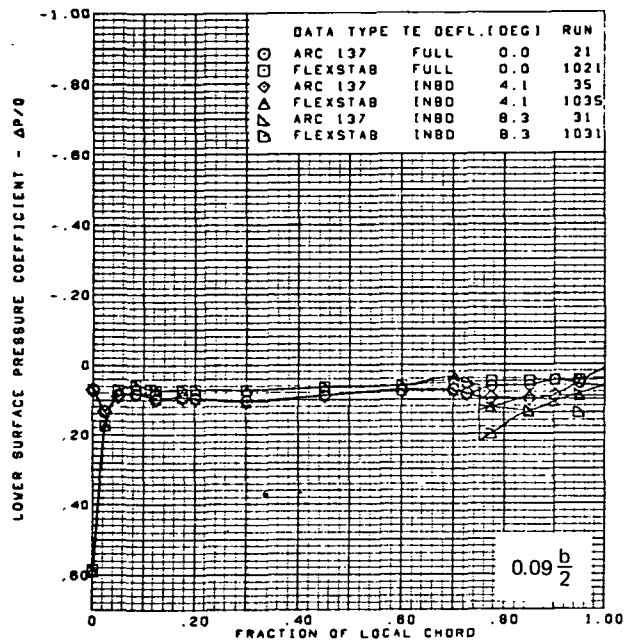
Figure 66.—(Continued)



$M = 2.10$   
 $\alpha = 8^\circ$   
 Flat wing, rounded L.E.  
 L.E. deflection, full span =  $0.0^\circ$   
 T.E. deflection, outboard =  $0.0^\circ$   
 Note:  $C_{p, \text{vacuum}} = -0.32$

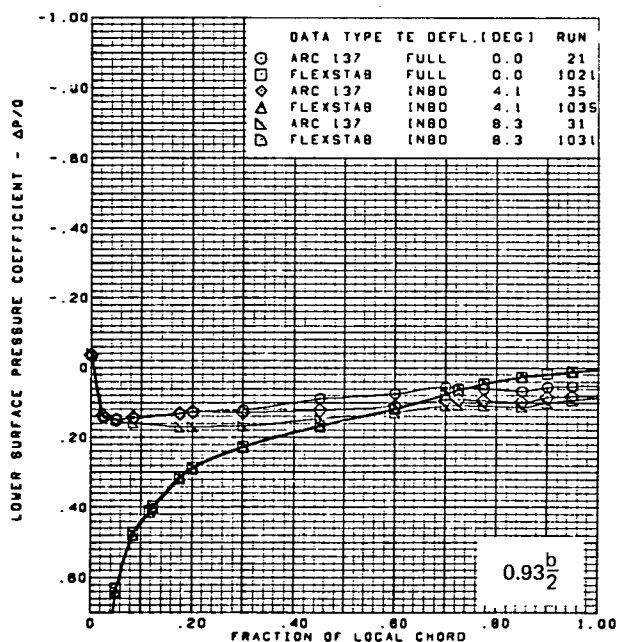
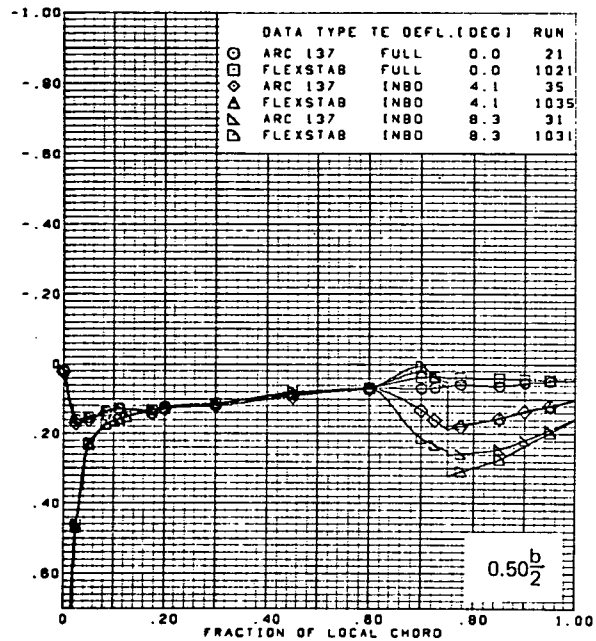
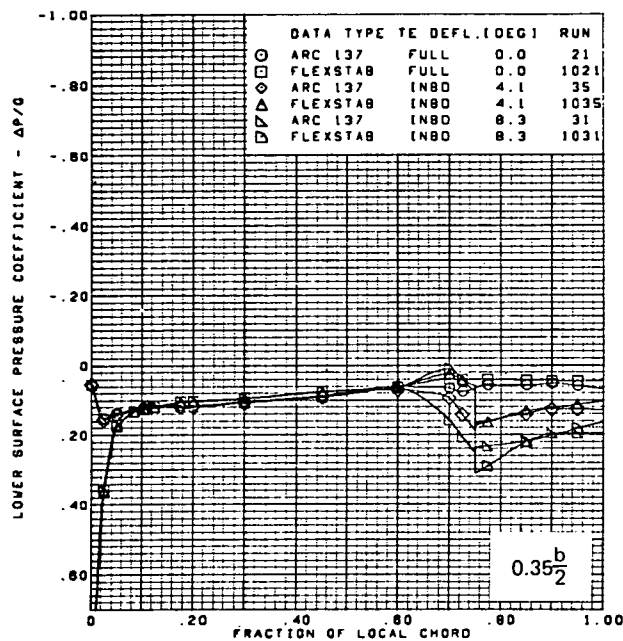
(d) (Concluded)

Figure 66.-(Continued)



(e) Lower Surface Chordwise Pressure Distributions,  $\alpha = 8^\circ$

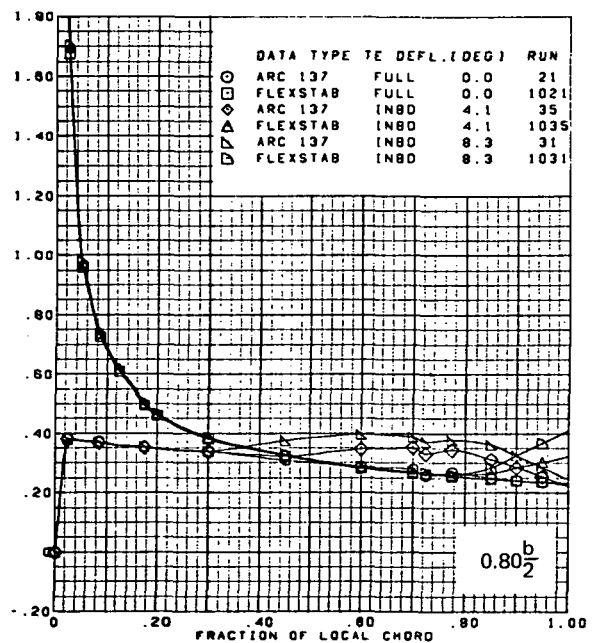
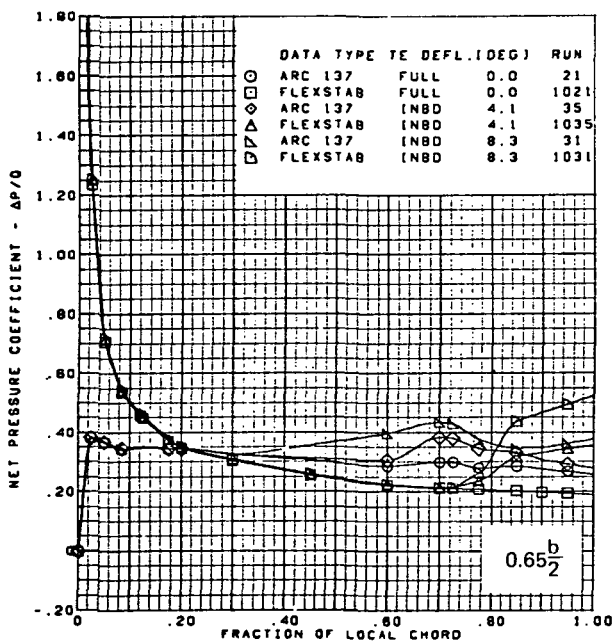
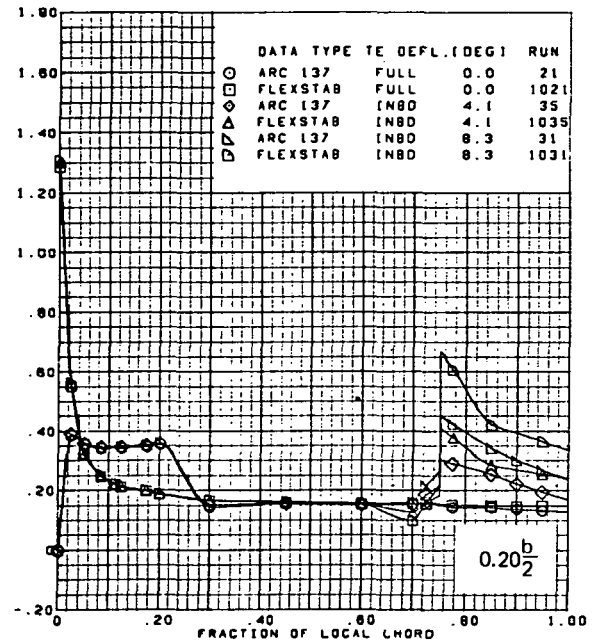
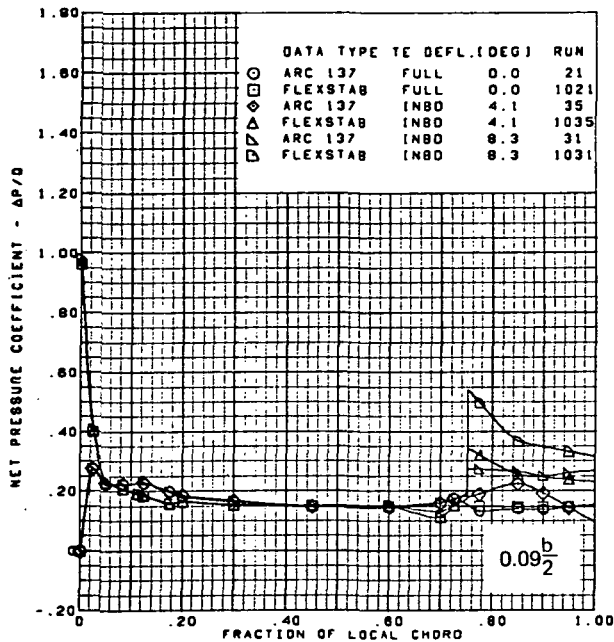
Figure 66.—(Continued)



$M = 2.10$   
 $\alpha = 8^\circ$   
 Flat wing, rounded L.E.  
 L.E. deflection, full span =  $0.0^\circ$   
 T.E. deflection, outboard =  $0.0^\circ$   
 None:  $C_{p, \text{vacuum}} = -0.32$

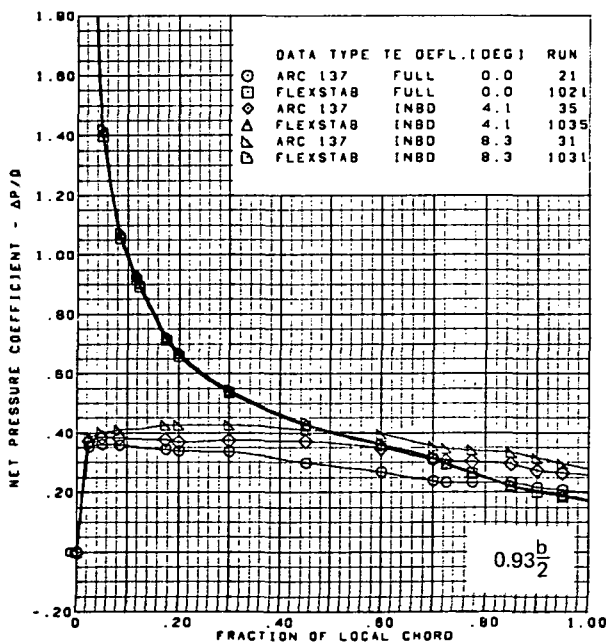
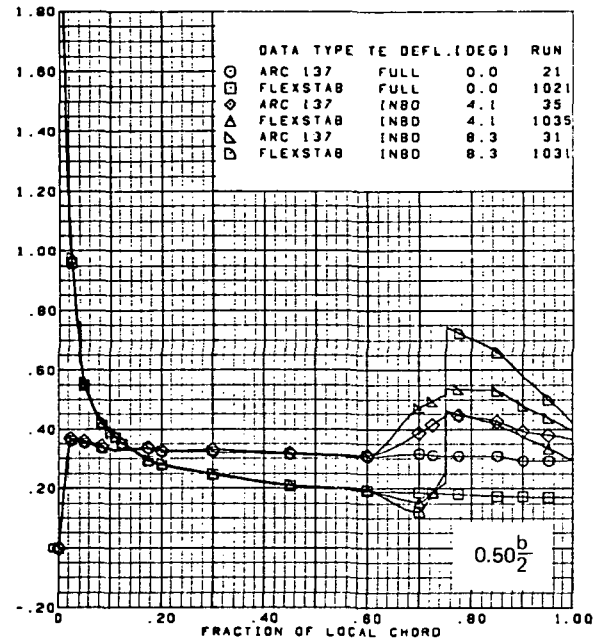
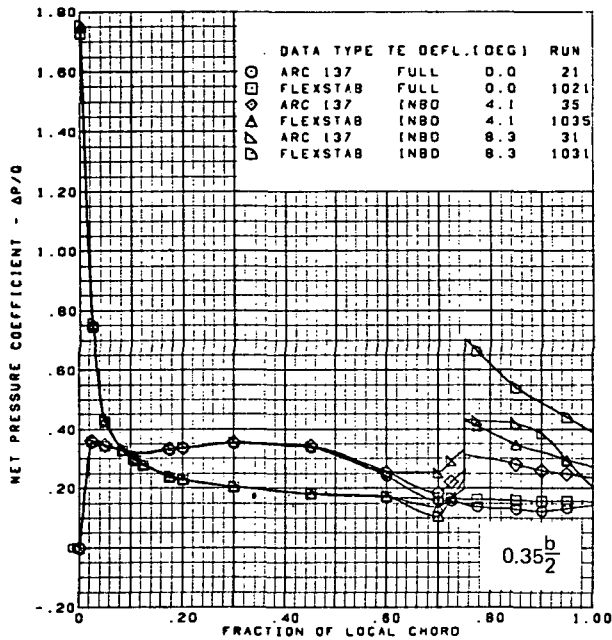
(e) (Concluded)

Figure 66.—(Continued)



(f) Net Chordwise Pressure Distributions,  $\alpha = 8^\circ$

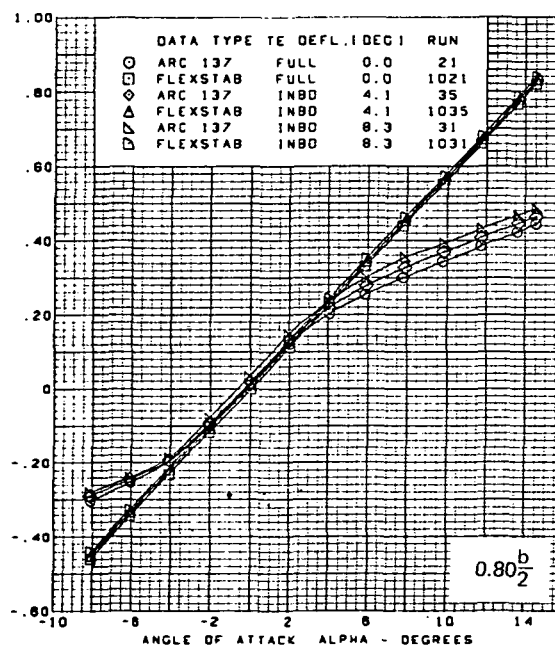
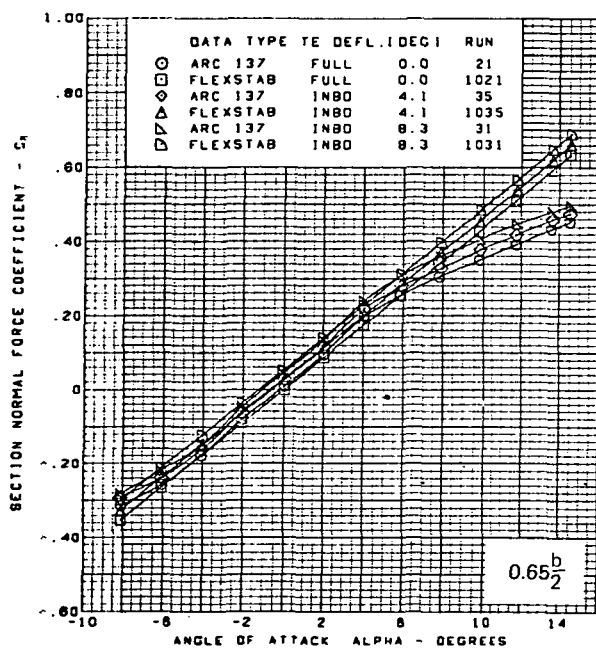
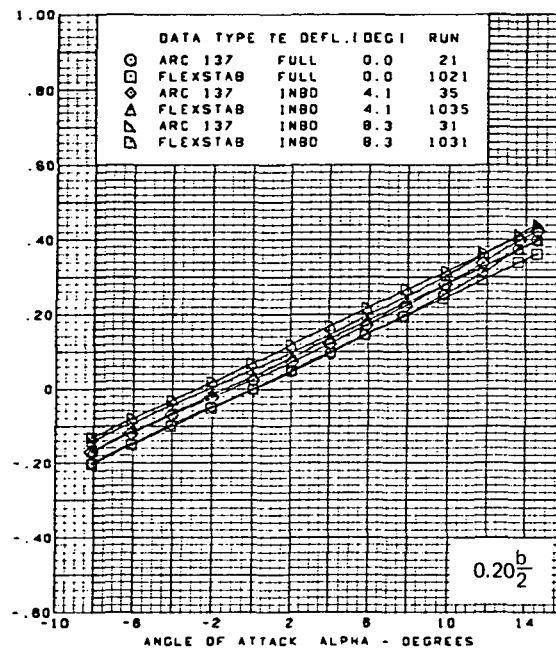
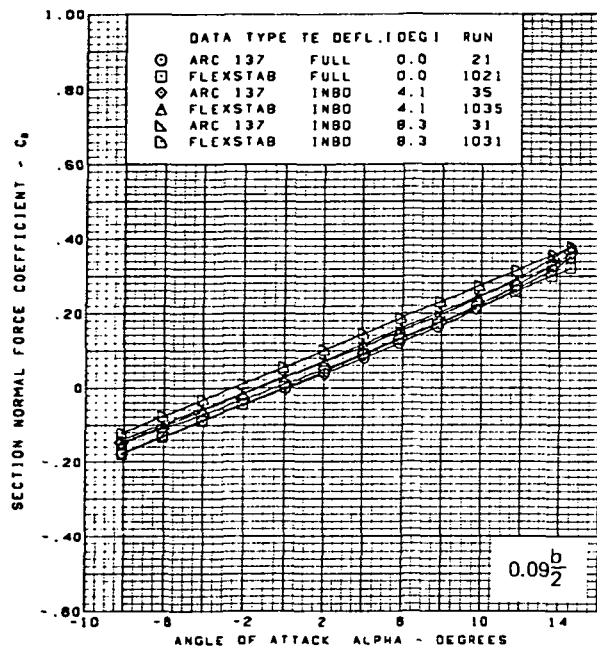
Figure 66. —(Continued)



M = 2.10  
 $\alpha = 8^\circ$   
 Flat wing, rounded L.E.  
 L.E. deflection, full span =  $0.0^\circ$   
 T.E. deflection, outboard =  $0.0^\circ$

(f) (Concluded)

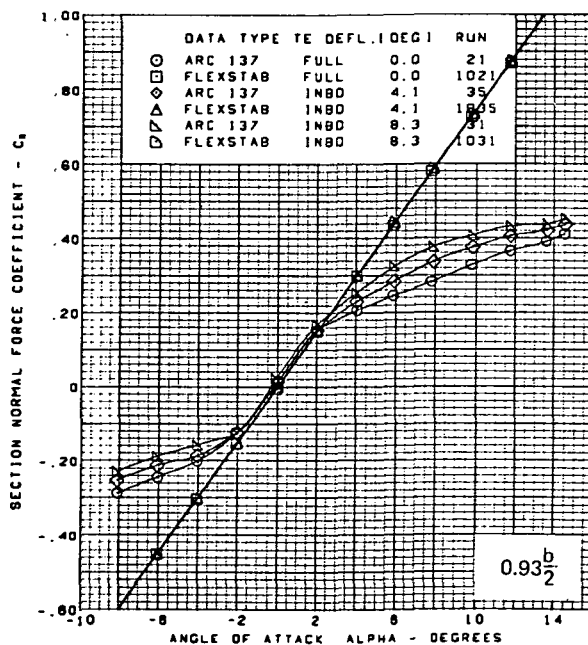
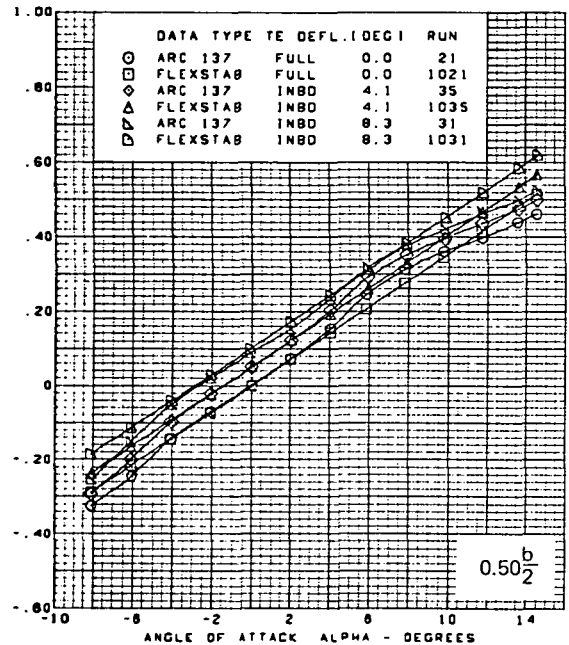
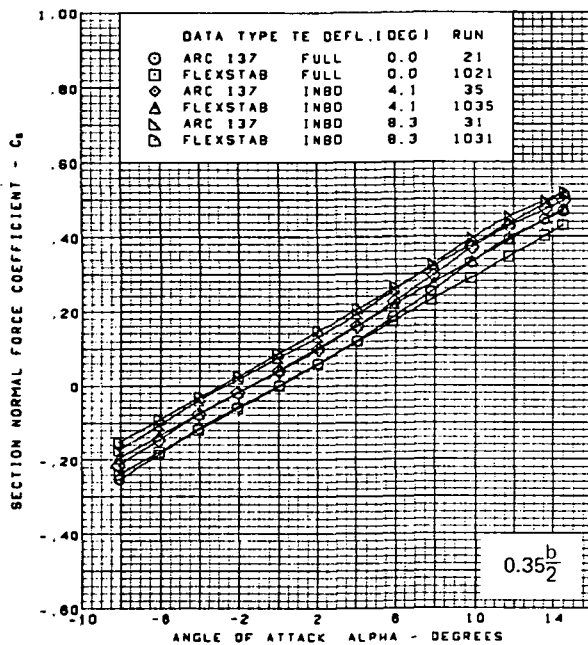
Figure 66.—(Continued)



(g) Section Aerodynamic Coefficients—Normal Force

Figure 66.—(Continued)

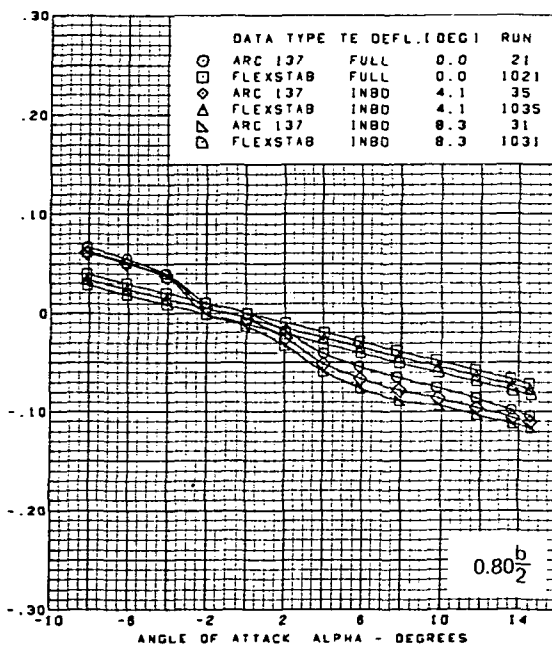
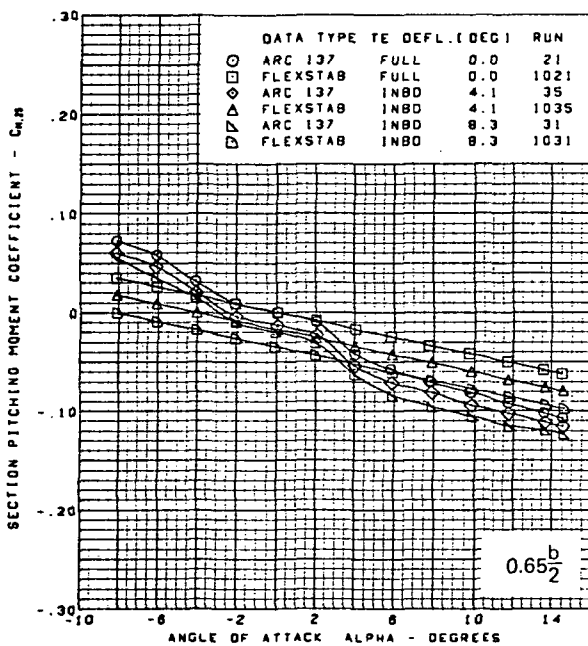
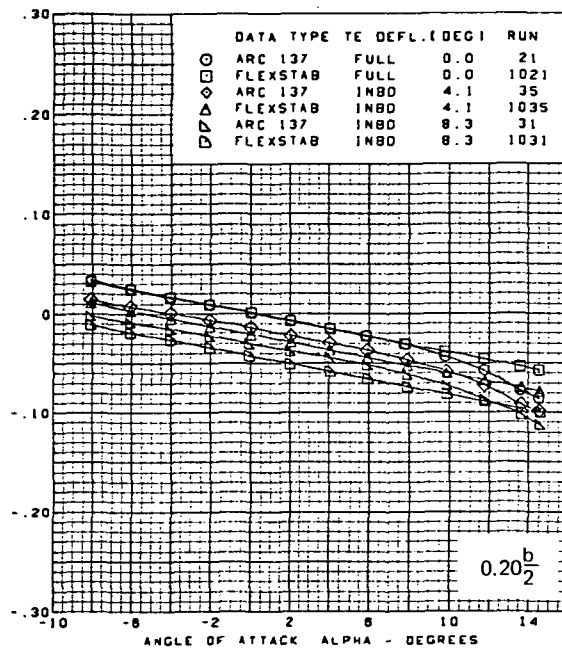
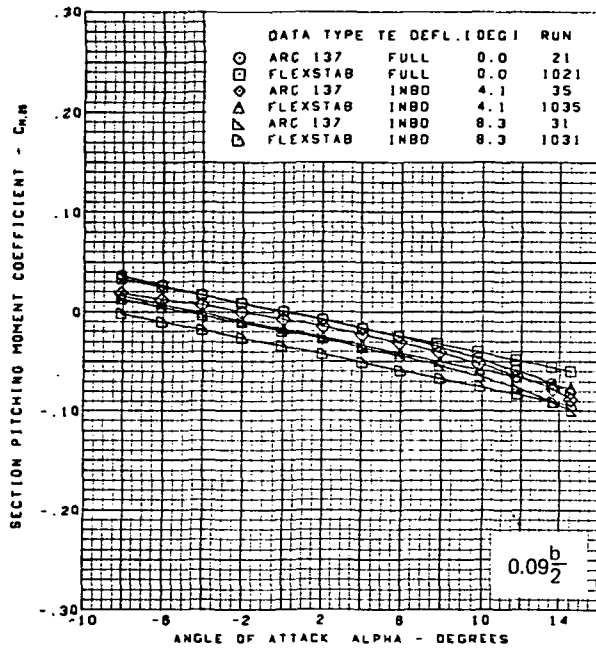




M = 2.10  
 Flat wing, rounded L.E.  
 L.E. deflection, full span = 0.0°  
 T.E. deflection, outboard = 0.0°

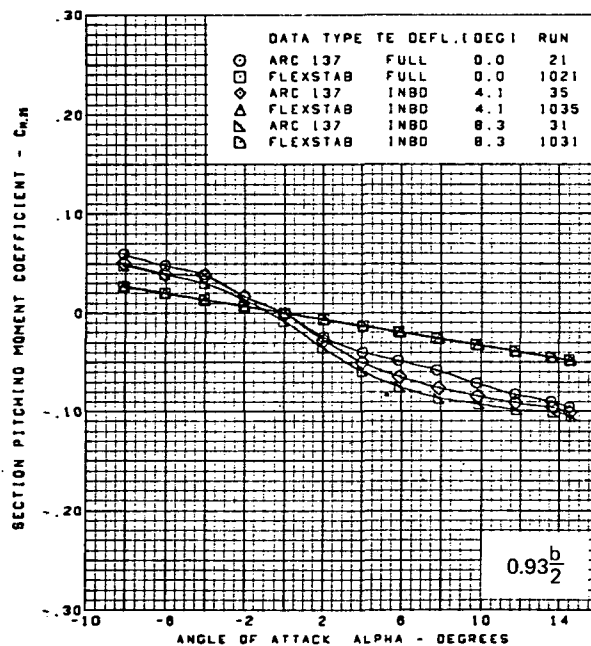
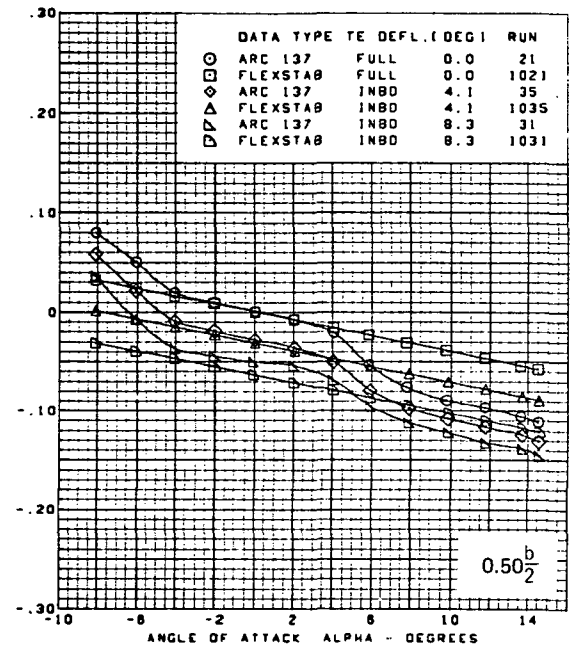
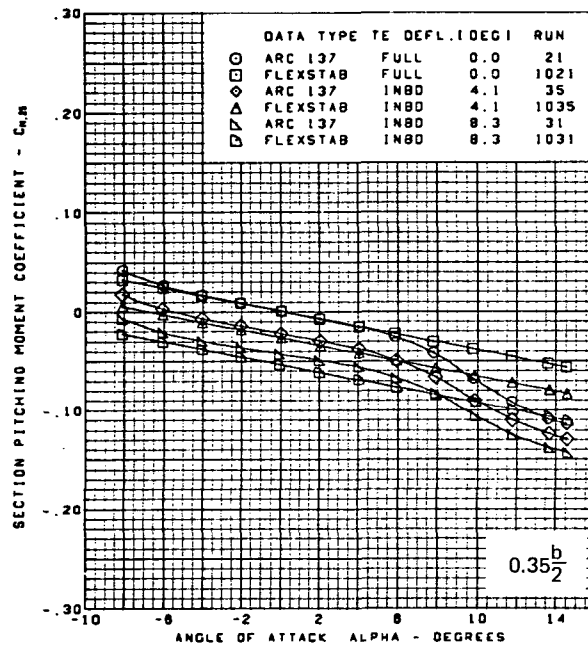
(g) (Concluded)

Figure 66.-(Continued)



(h) Section Aerodynamic Coefficients—Pitching Moment

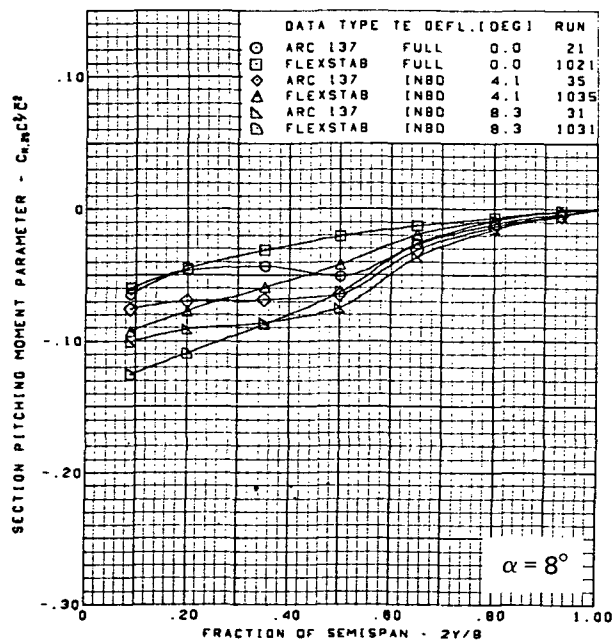
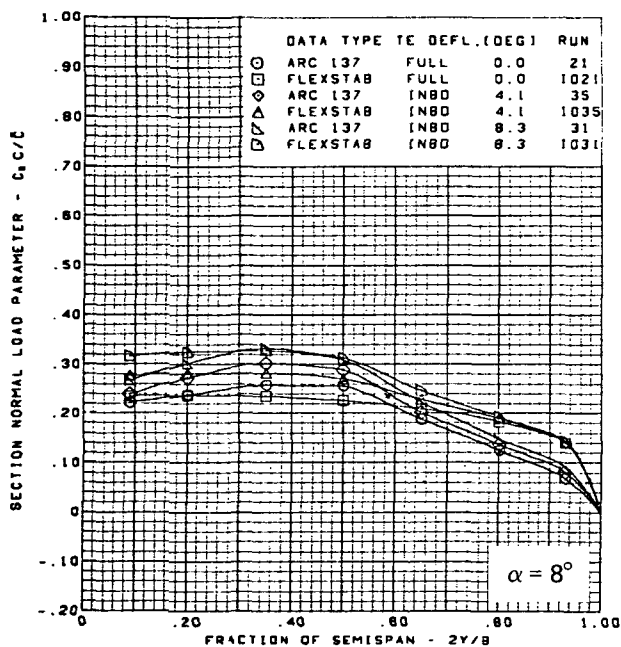
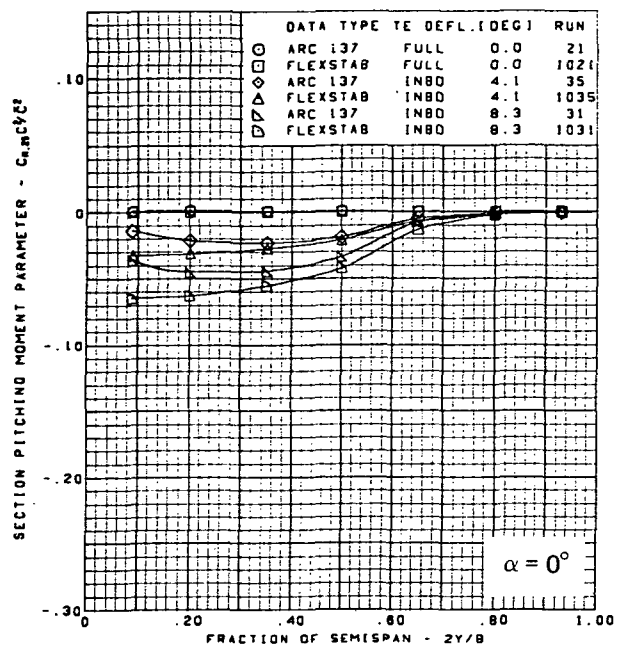
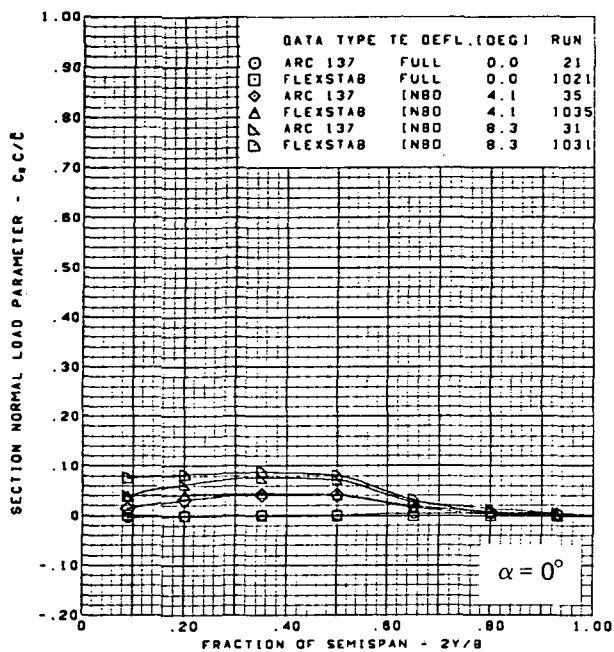
Figure 66.—(Continued)



M = 2.10  
 Flat wing, rounded L.E.  
 L.E. deflection, full span = 0.0°  
 T.E. deflection, outboard = 0.0°

(h) (Concluded)

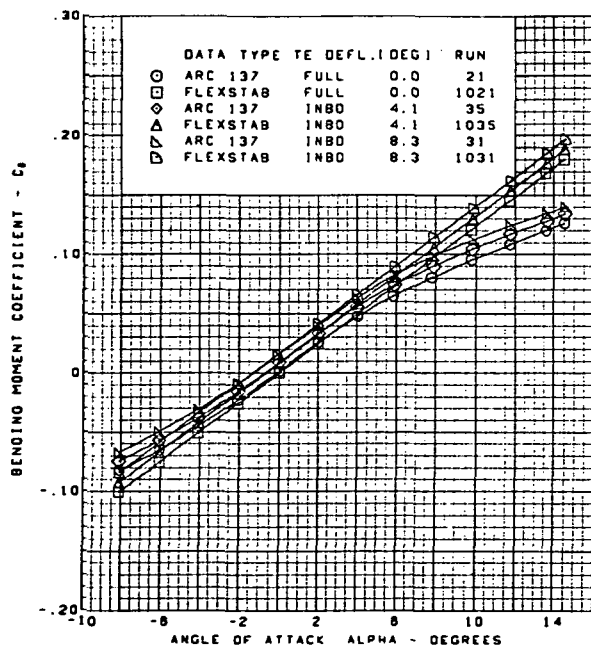
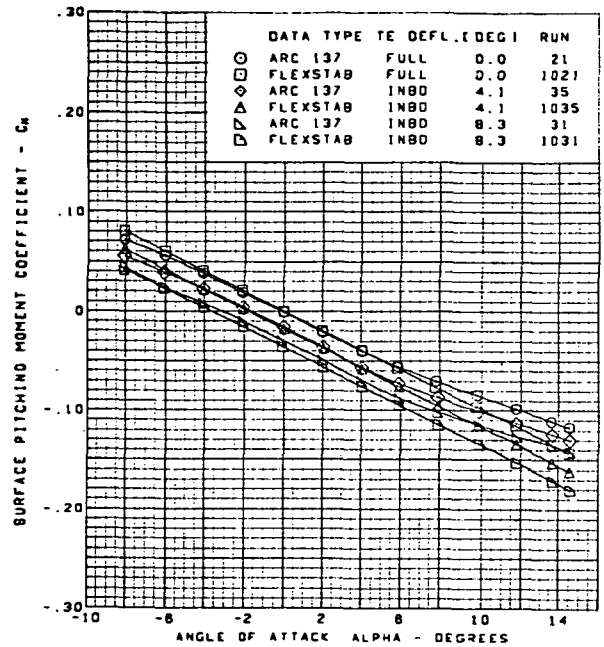
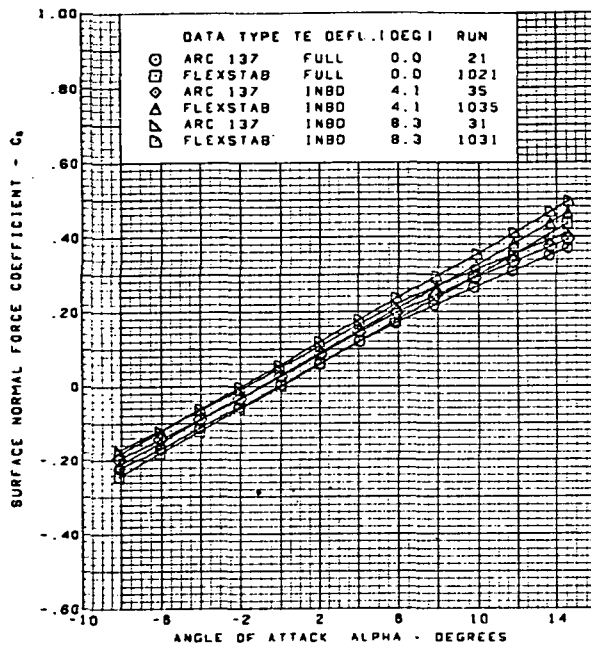
Figure 66.-(Continued)



$M = 2.10$   
 Flat wing, rounded L.E.  
 L.E. deflection, full span  $= 0.0^\circ$   
 T.E. deflection, outboard  $= 0.0^\circ$

(i) Spanload Distributions

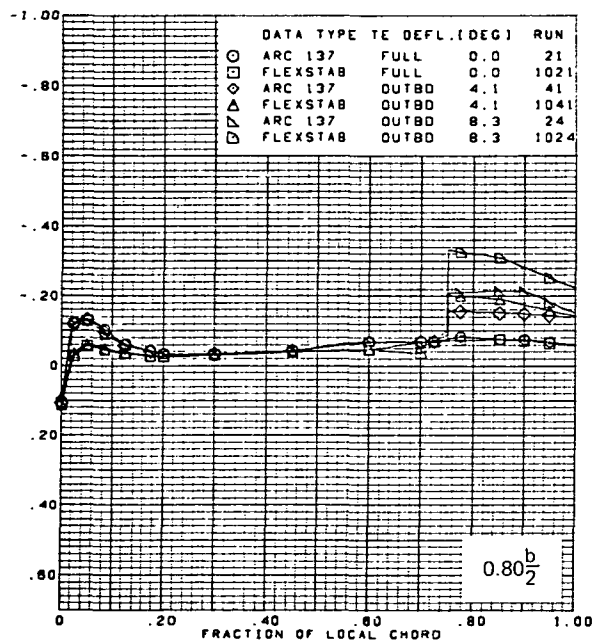
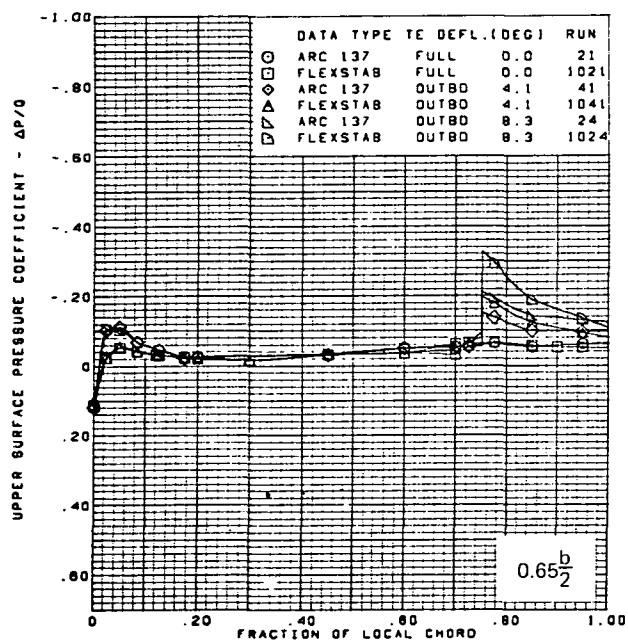
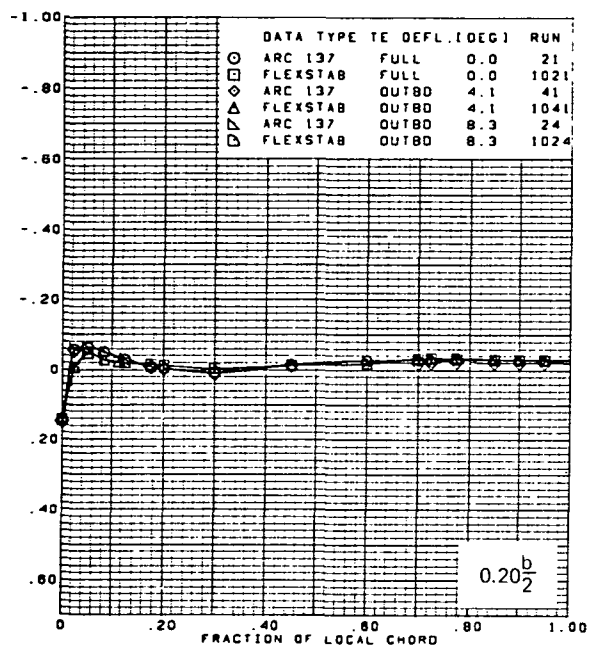
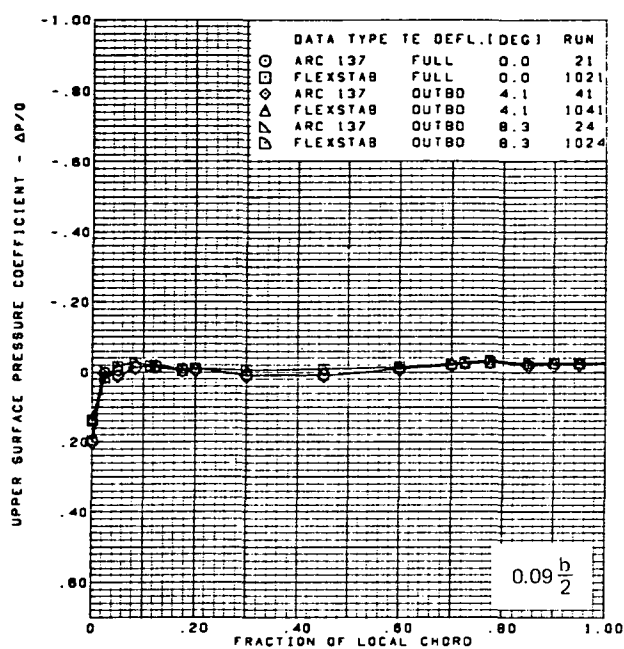
Figure 66. —(Continued)



$M = 2.10$   
 Flat wing, rounded L.E.  
 L.E. deflection, full span  $\approx 0.0^\circ$   
 T.E. deflection, outboard  $\approx 0.0^\circ$

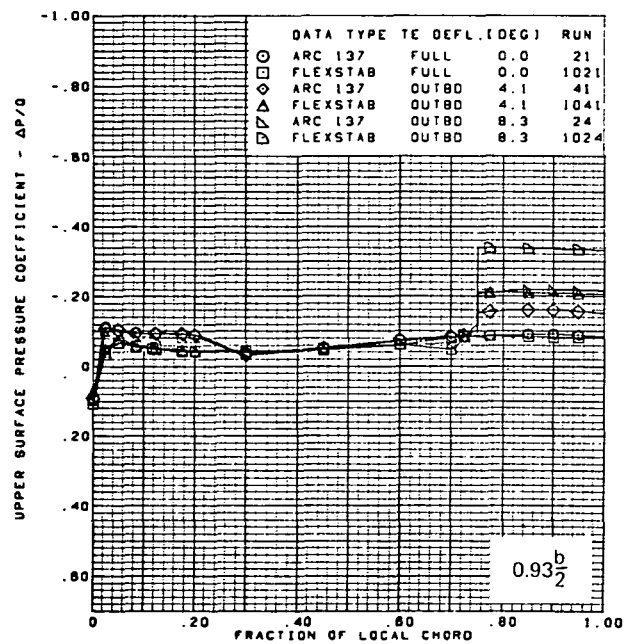
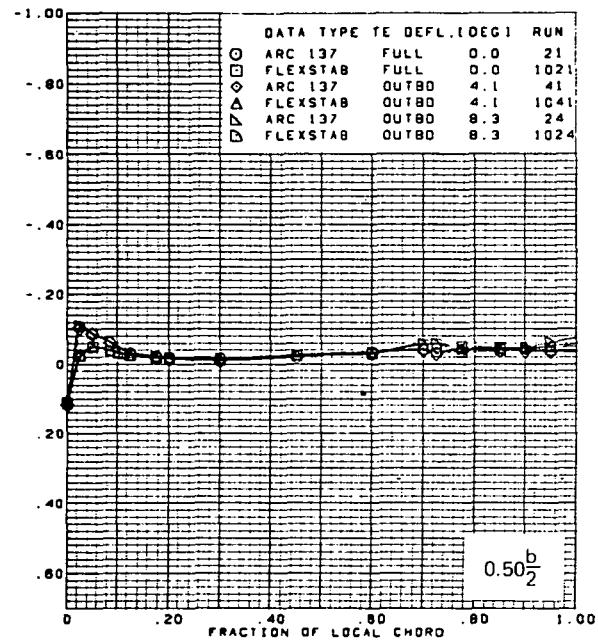
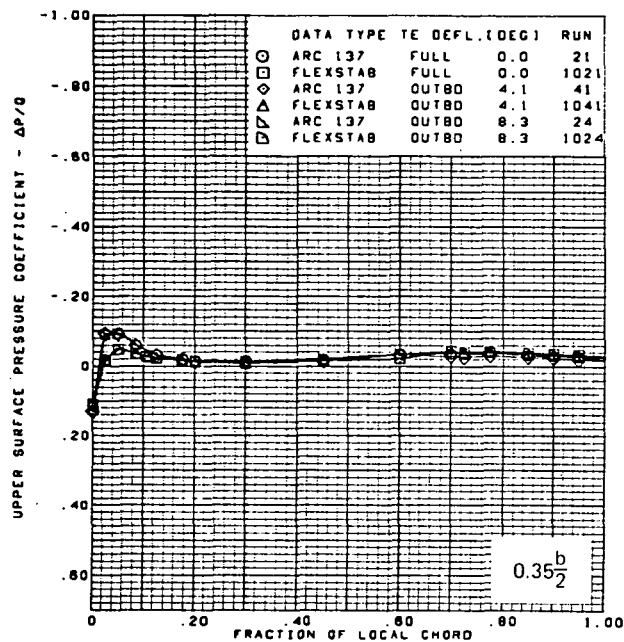
(j) Wing Aerodynamic Coefficients

Figure 66 —(Concluded)



(a) Upper Surface Chordwise Pressure Distributions,  $\alpha = 0^\circ$

Figure 67.—Wing Theory-to-Experiment Comparison—Flat Wing, Rounded L.E.; L.E. Deflection, Full Span =  $0.0^\circ$ ; T.E. Deflection; Inboard =  $0.0^\circ$ ;  $M = 2.10$



$M = 2.10$

$\alpha = 0^\circ$

Flat wing, rounded L.E.

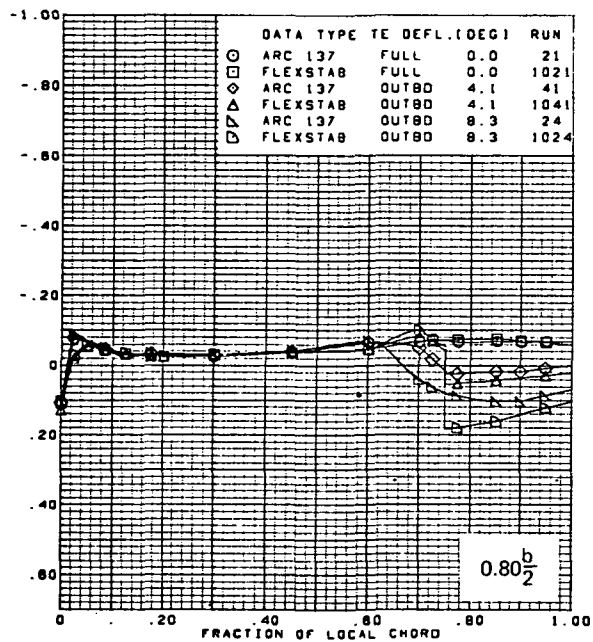
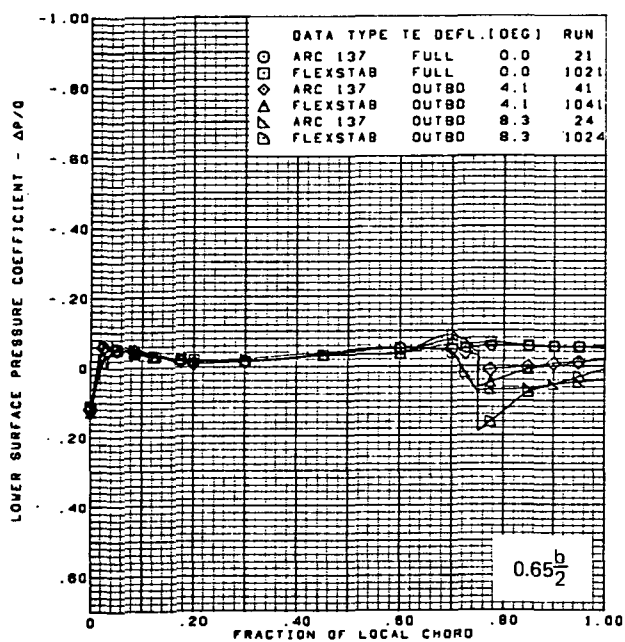
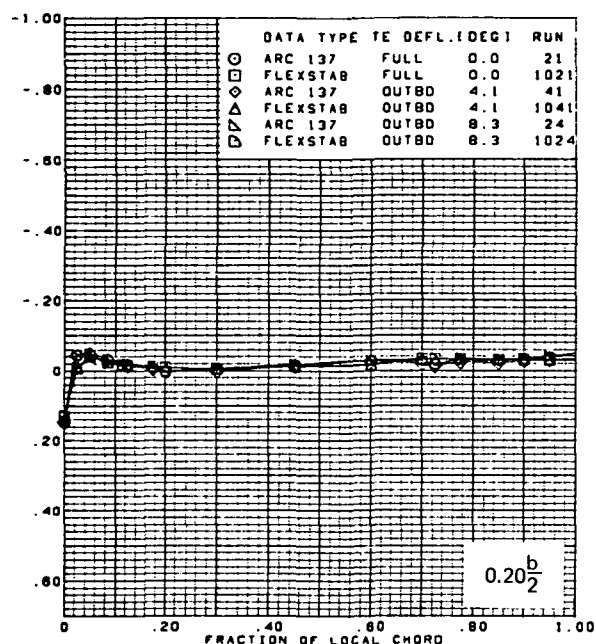
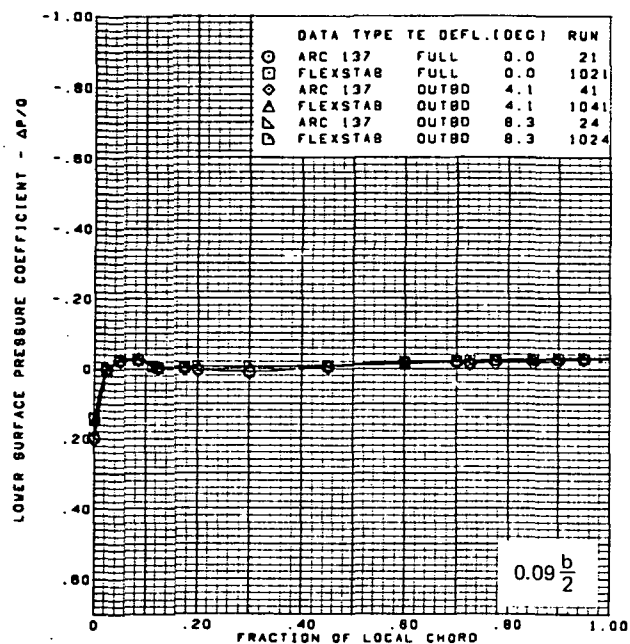
L.E. deflection, full span =  $0.0^\circ$

T.E. deflection, inboard =  $0.0^\circ$

Note:  $C_{p, \text{vacuum}} = -0.32$

(a) (Concluded)

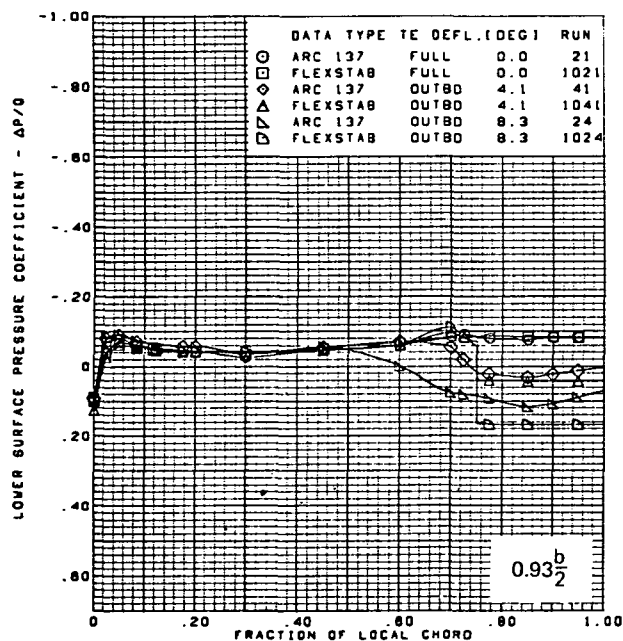
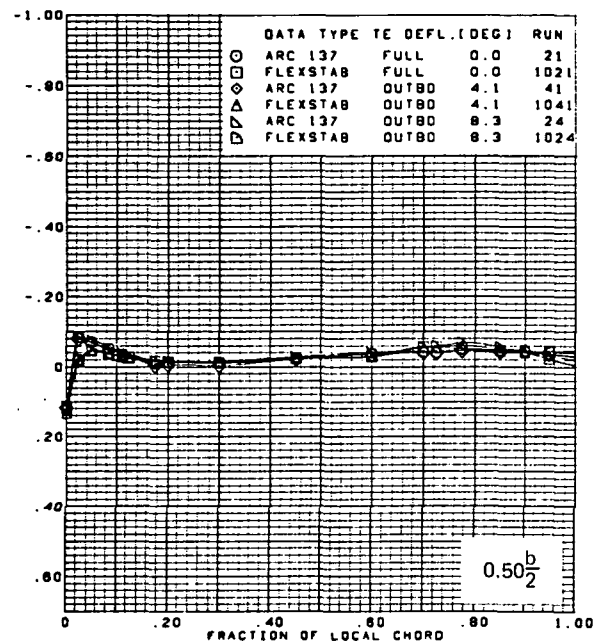
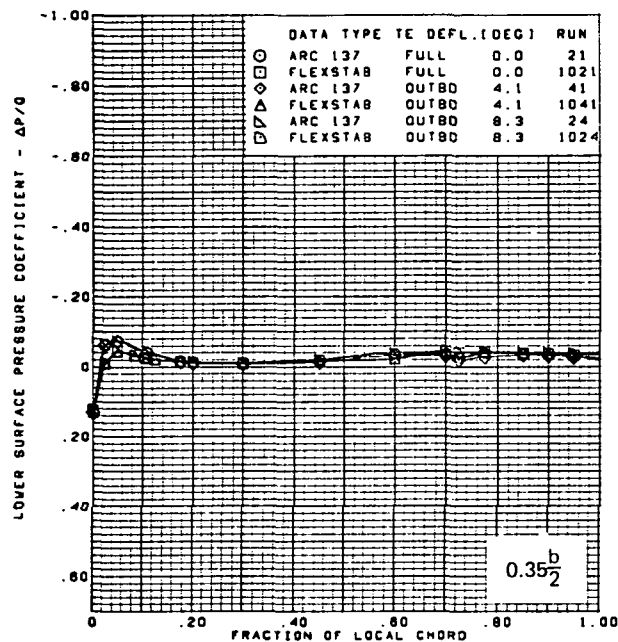
Figure 67.—(Continued)



(b) Lower Surface Chordwise Pressure Distributions,  $\alpha = 0^\circ$

Figure 67. —(Continued)

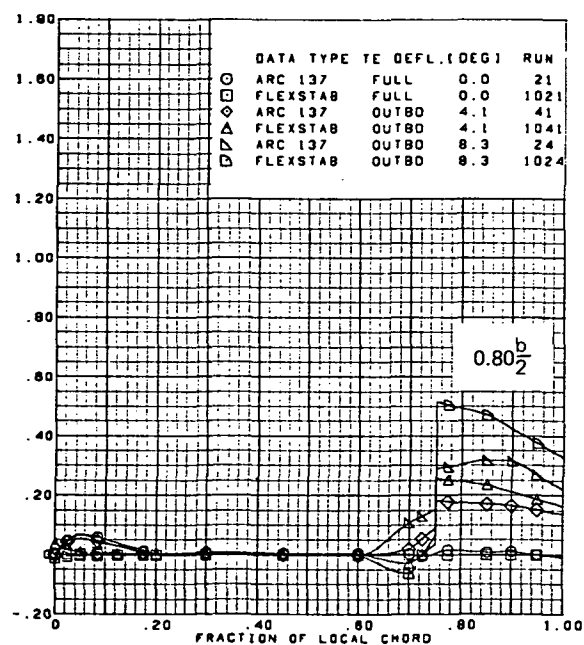
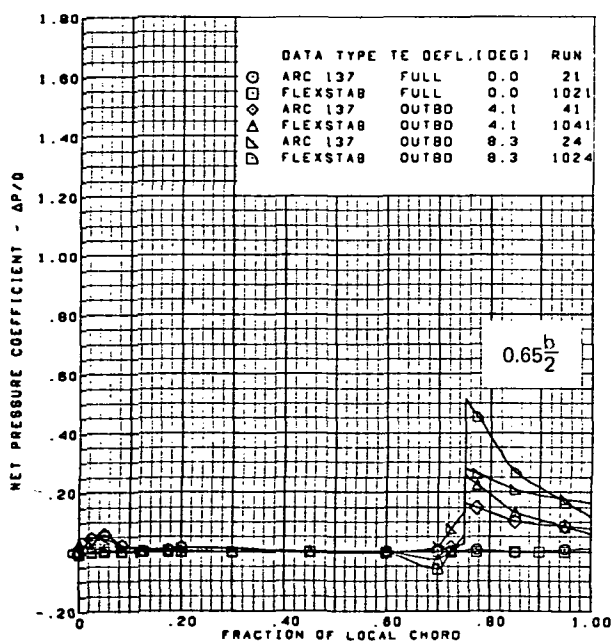
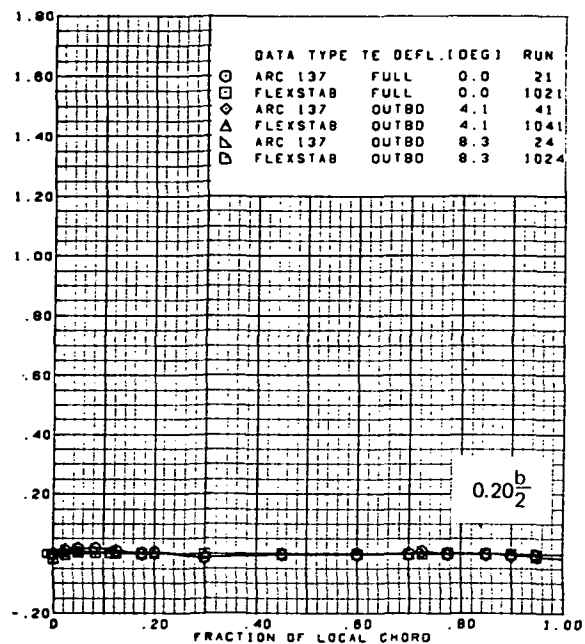
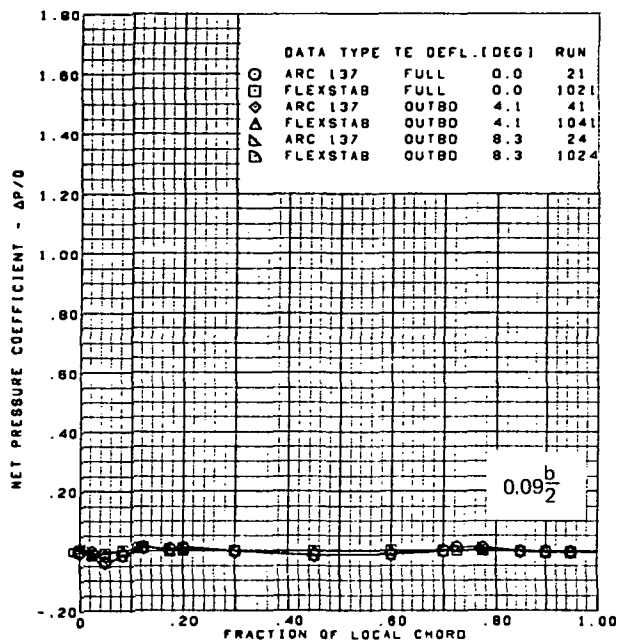




$M = 2.10$   
 $\alpha = 0^\circ$   
 Flat wing, rounded L.E.  
 L.E. deflection, full span =  $0.0^\circ$   
 T.E. deflection, inboard =  $0.0^\circ$   
 Note:  $C_{p, \text{vacuum}} = -0.32$

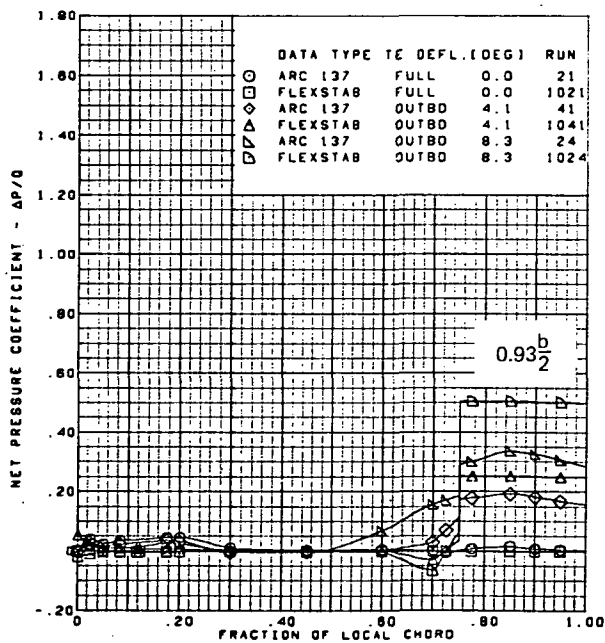
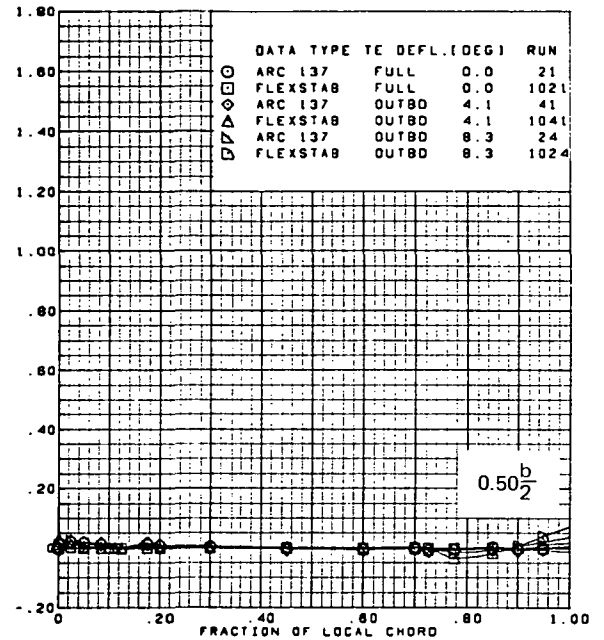
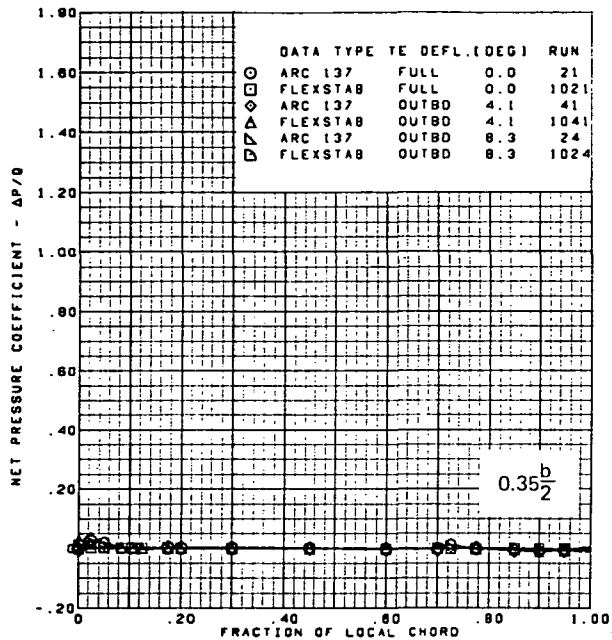
(b) (Concluded)

Figure 67.—(Continued)



(c) Net Chordwise Pressure Distributions,  $\alpha = 0^\circ$

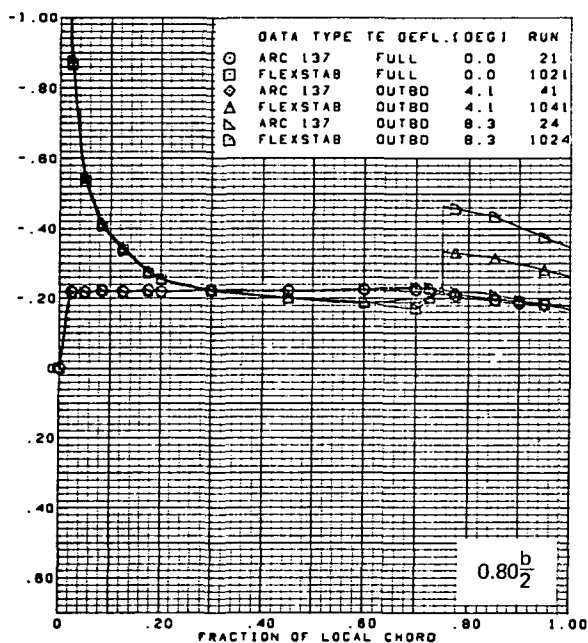
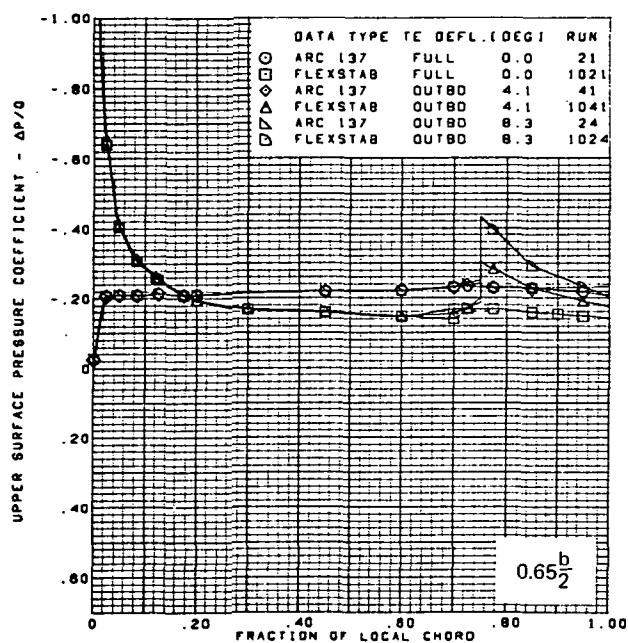
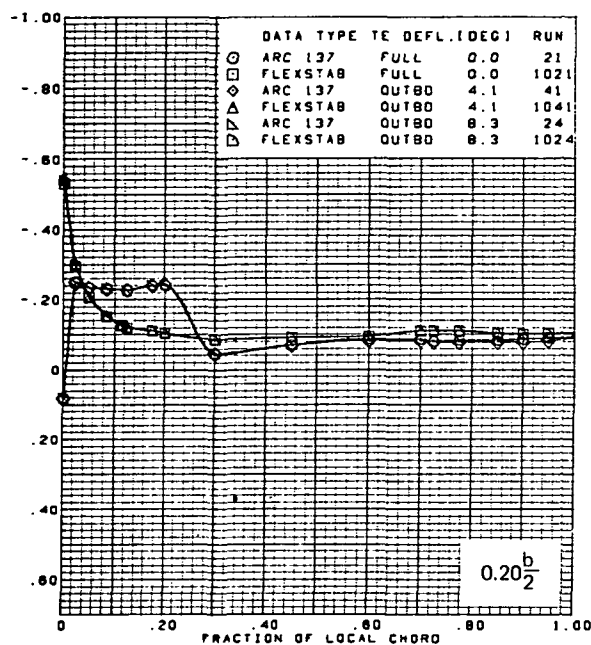
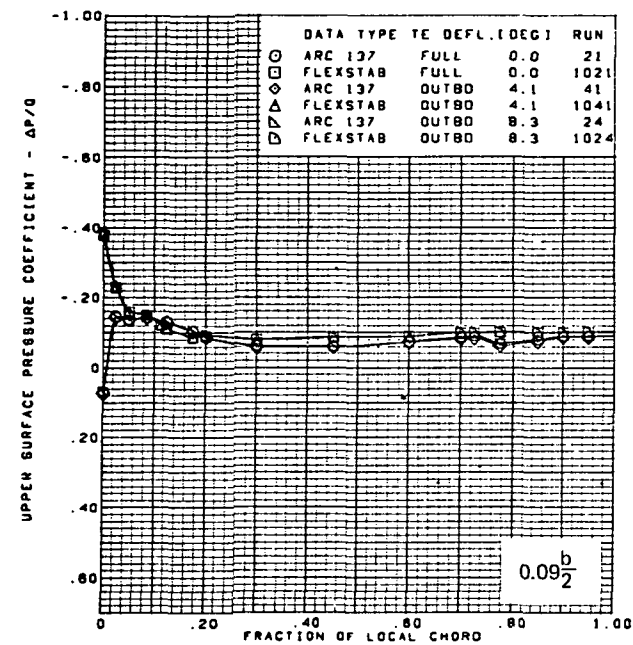
Figure 67. —(Continued)



$M = 2.10$   
 $\alpha = 0^\circ$   
 Flat wing, rounded L.E.  
 L.E. deflection, full span =  $0.0^\circ$   
 T.E. deflection, inboard =  $0.0^\circ$

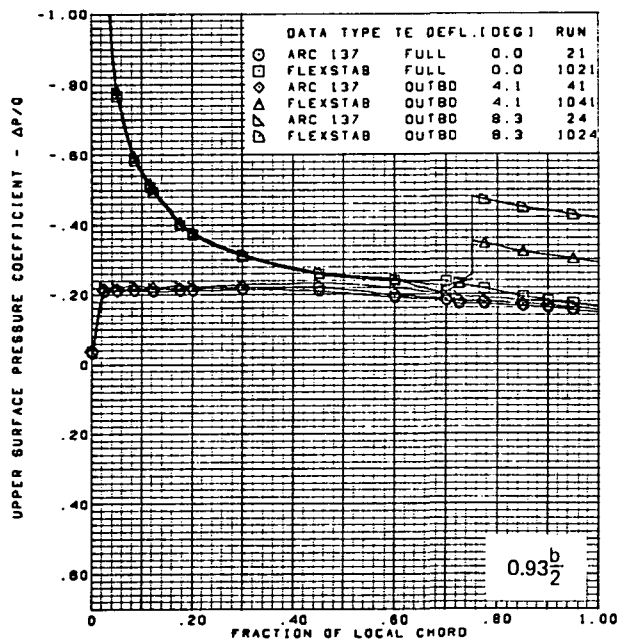
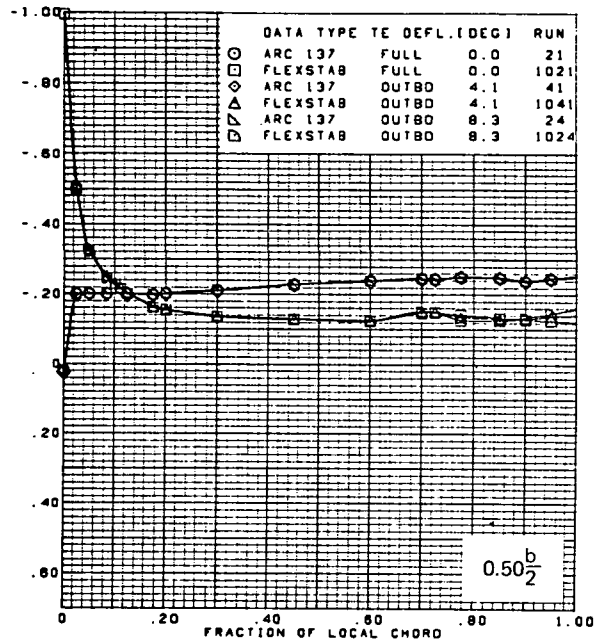
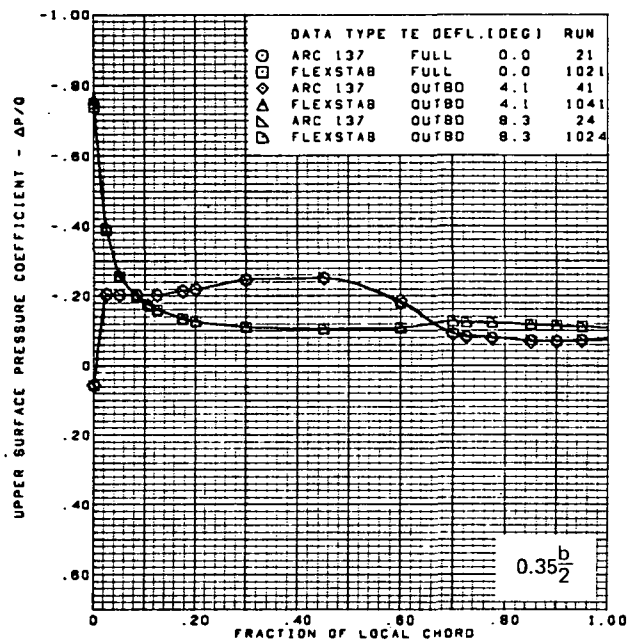
(c) (Concluded)

Figure 67.—(Continued)



(d) Upper Surface Chordwise Pressure Distributions,  $\alpha = 8^\circ$

Figure 67.—(Continued)

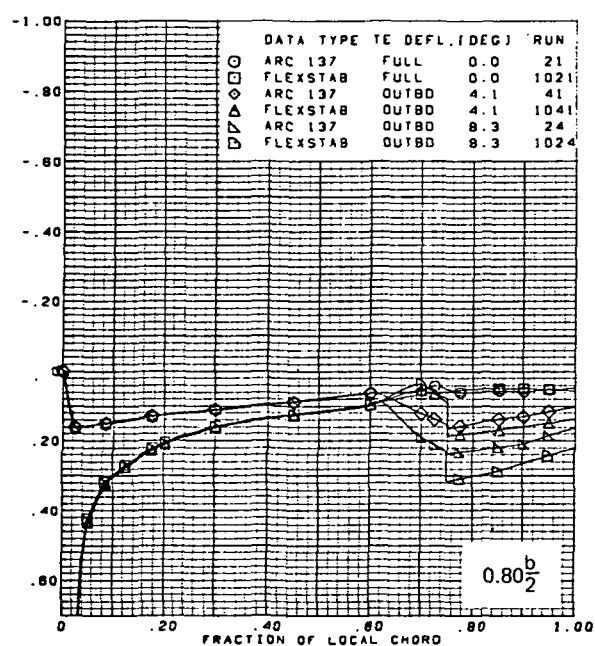
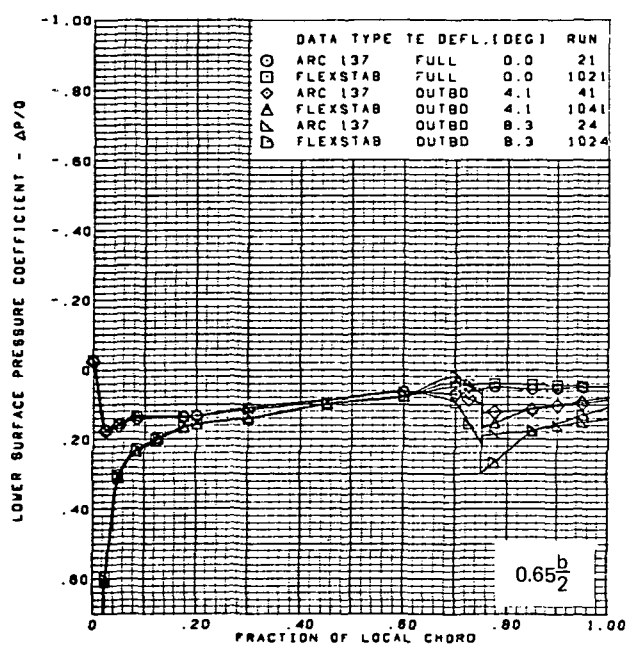
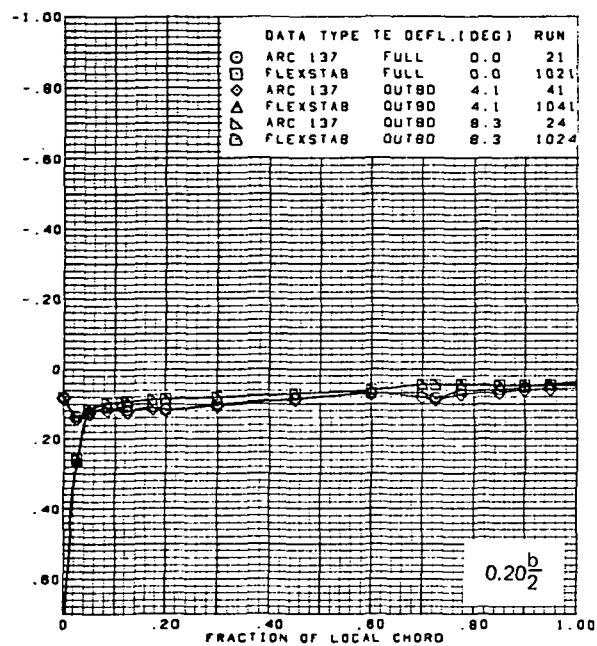
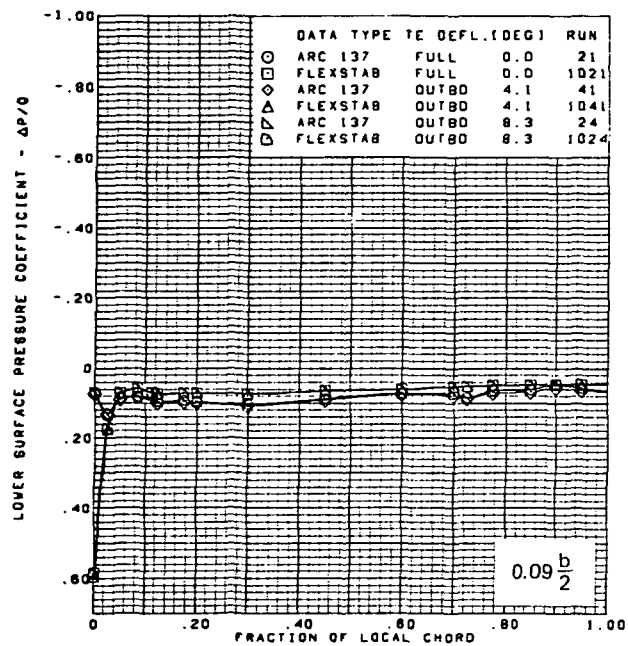


$M = 2.10$   
 $\alpha = 8^\circ$   
 Flat wing, rounded L.E.  
 L.E. deflection, full span =  $0.0^\circ$   
 T.E. deflection, inboard =  $0.0^\circ$

Note:  $C_{p, \text{vacuum}} = -0.32$

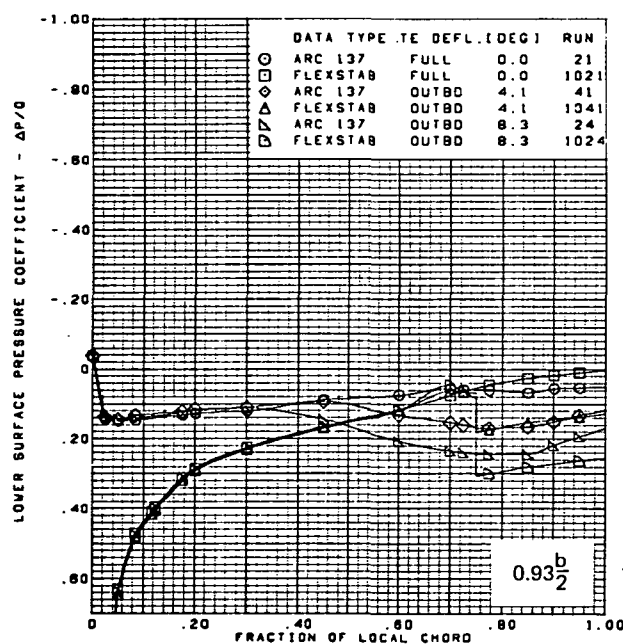
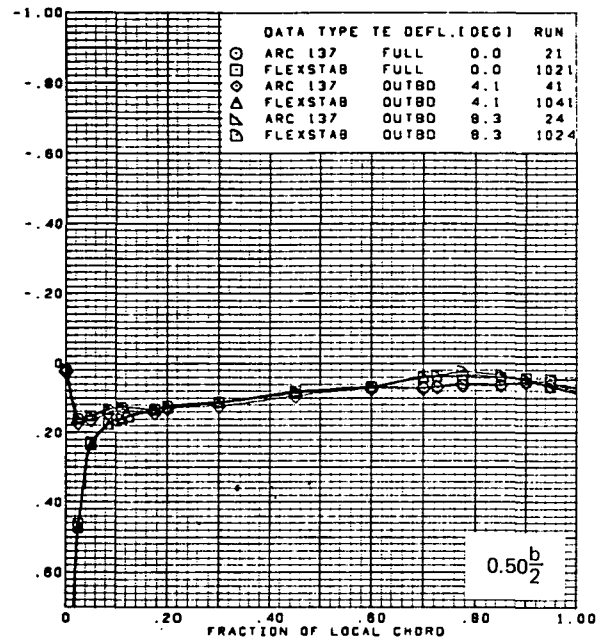
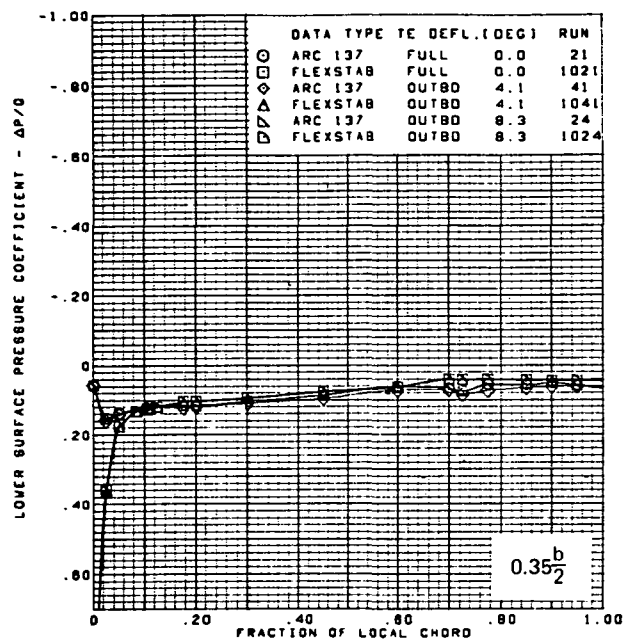
(d) (Concluded)

Figure 67.— (Continued)



(e) Lower Surface Chordwise Pressure Distributions,  $\alpha = 8^\circ$

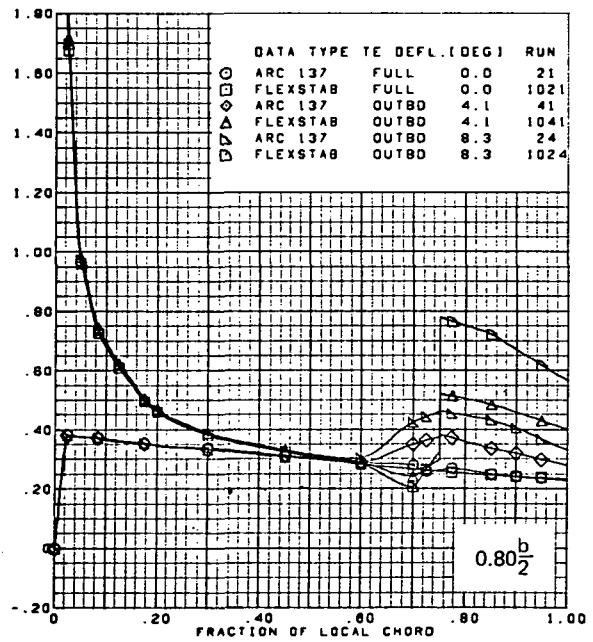
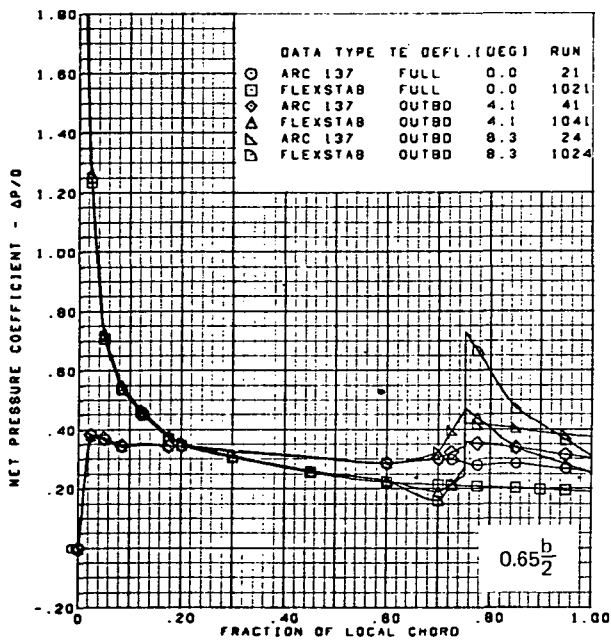
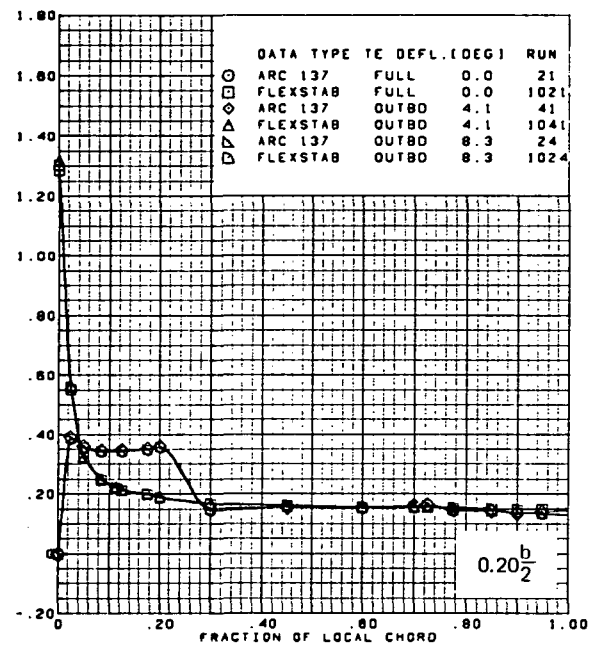
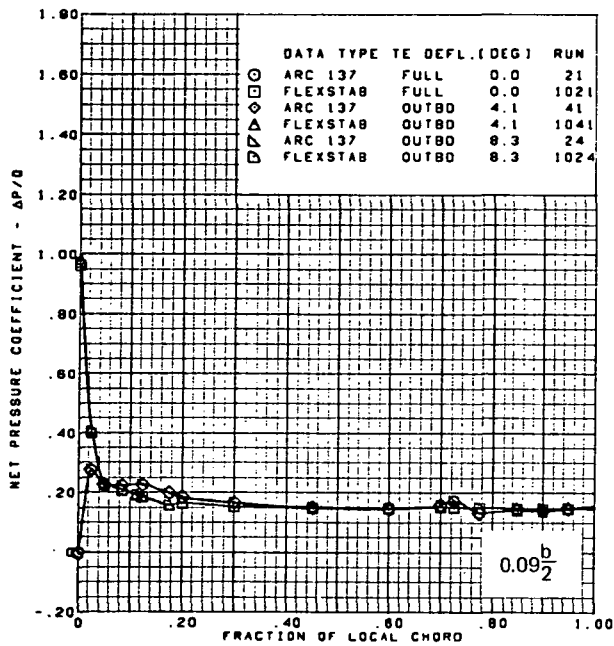
Figure 67. —(Continued)



$M = 2.10$   
 $\alpha = 8^\circ$   
 Flat wing, rounded L.E.  
 L.E. deflection, full span =  $0.0^\circ$   
 T.E. deflection, inboard =  $0.0^\circ$   
 Note:  $C_{p, \text{vacuum}} = -0.32$

(e) (Concluded)

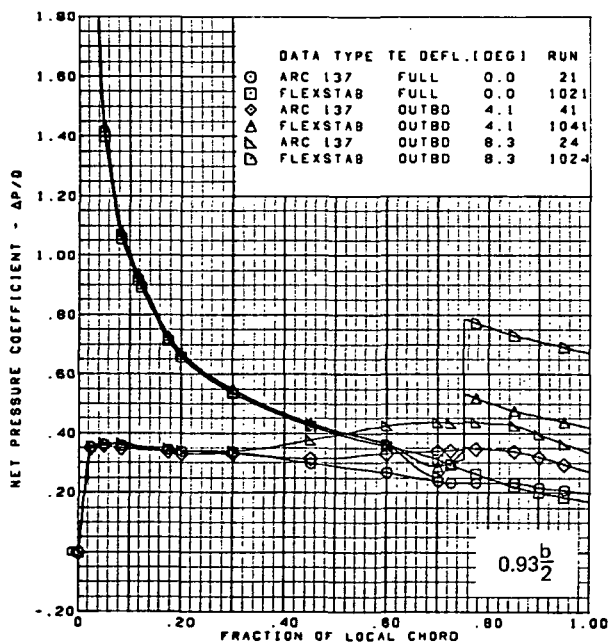
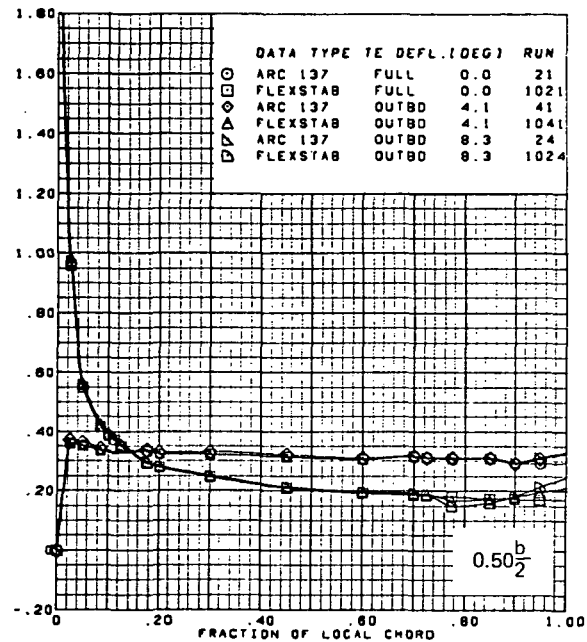
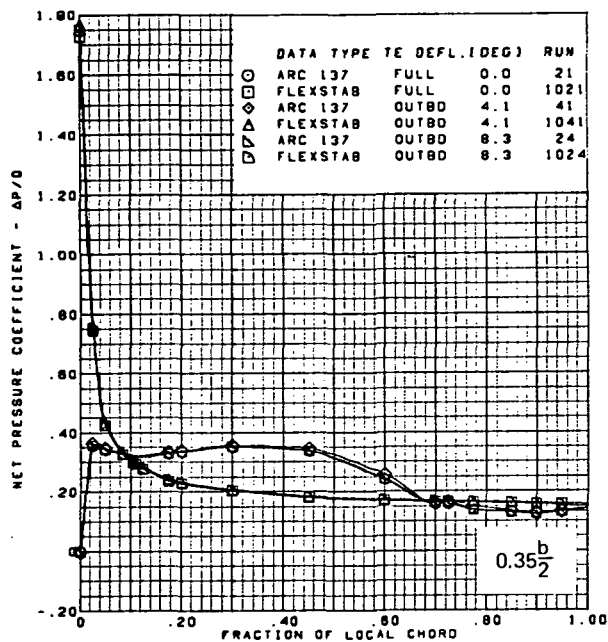
Figure 67.—(Continued)



(f) Net Chordwise Pressure Distributions,  $\alpha = 8^\circ$

Figure 67.—(Continued)

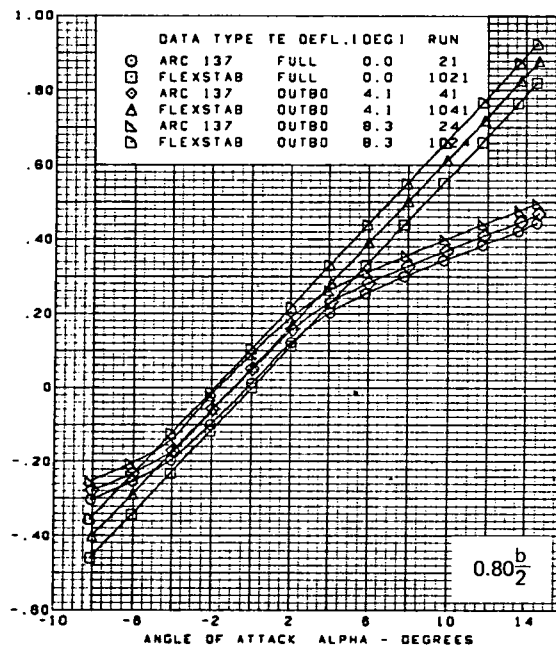
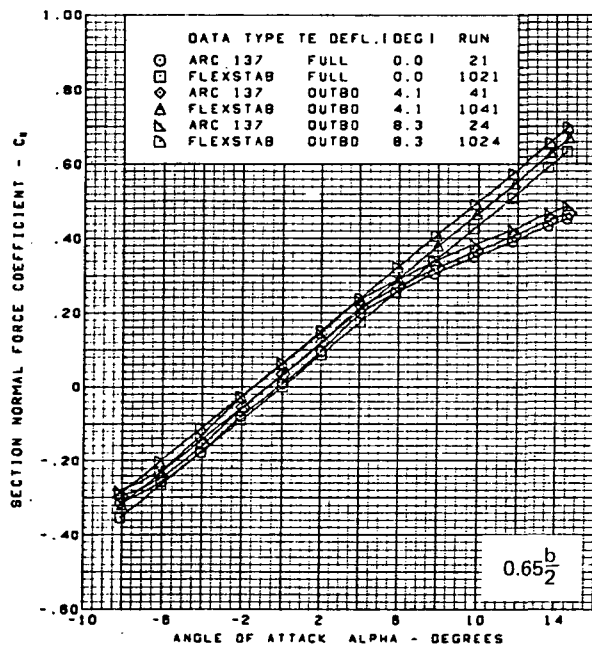
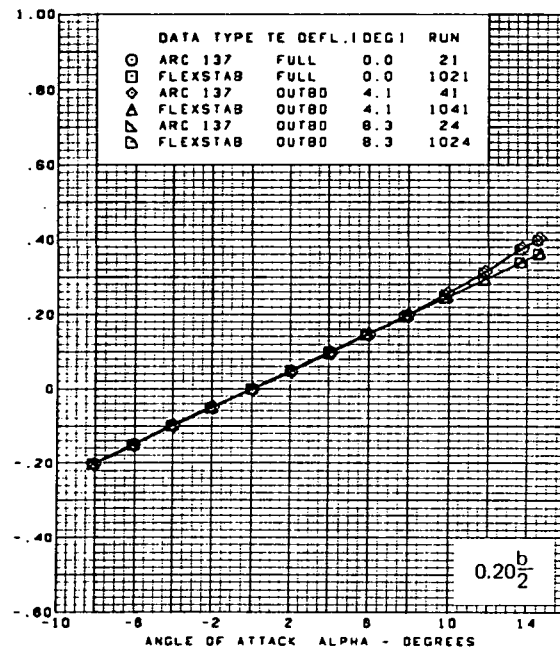
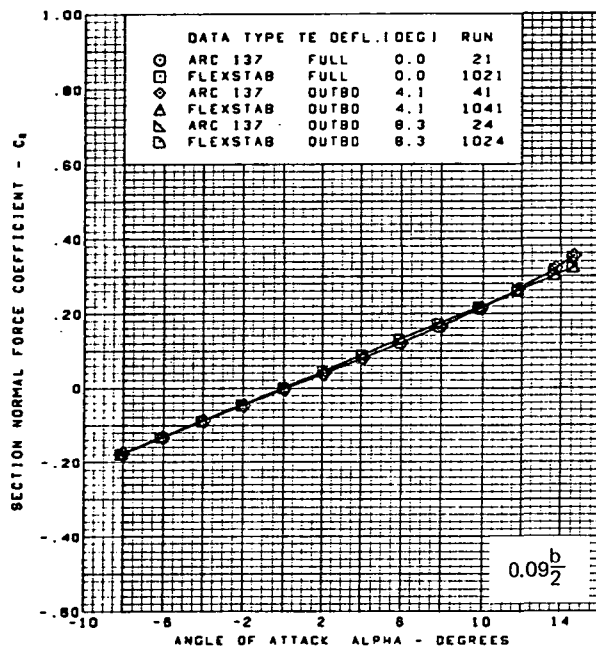




$M = 2.10$   
 $\alpha = 8^\circ$   
 Flat wing, rounded L.E.  
 L.E. deflection, full span =  $0.0^\circ$   
 T.E. deflection, inboard =  $0.0^\circ$

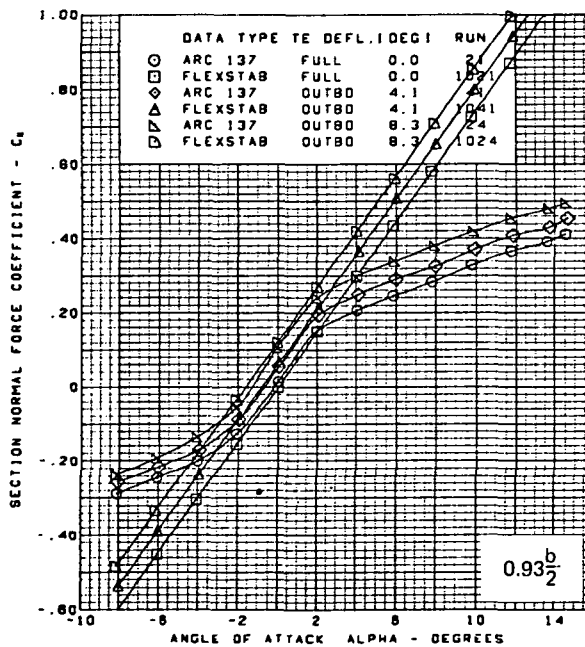
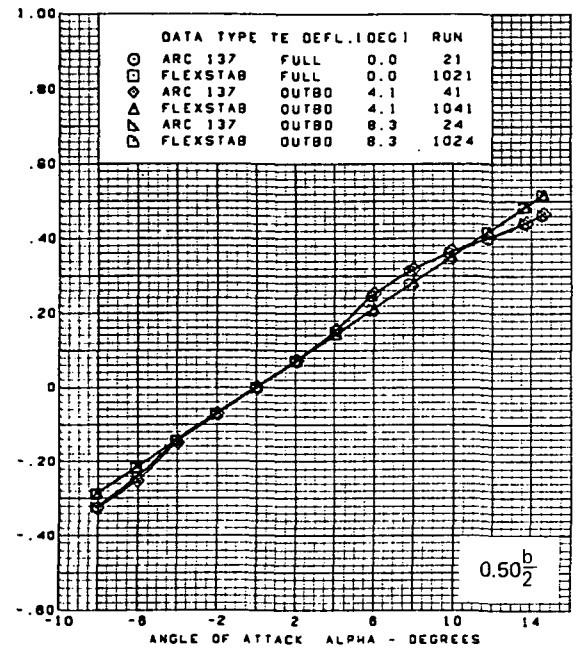
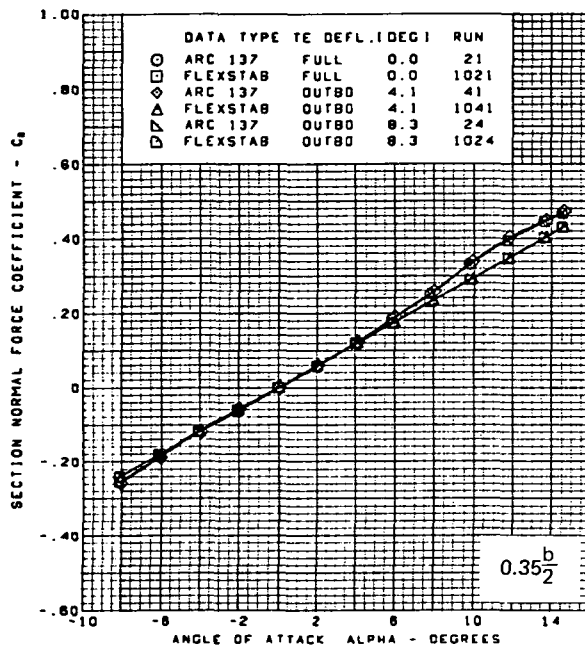
(f) (Concluded)

Figure 67.—(Continued)



(g) Section Aerodynamic Coefficients—Normal Force

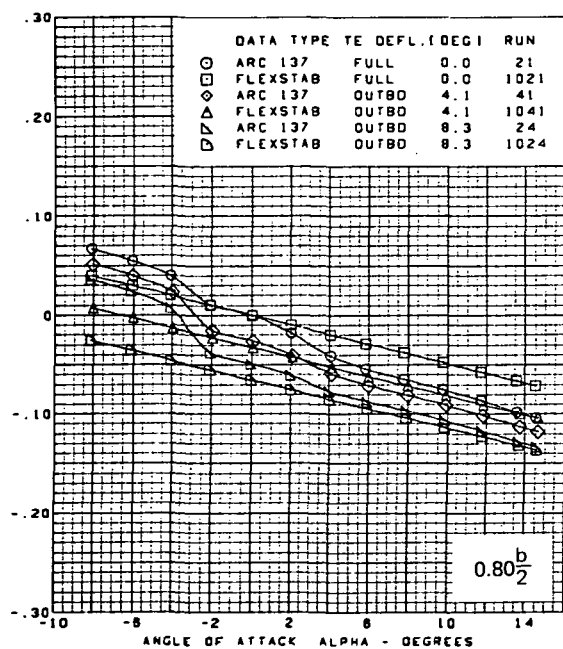
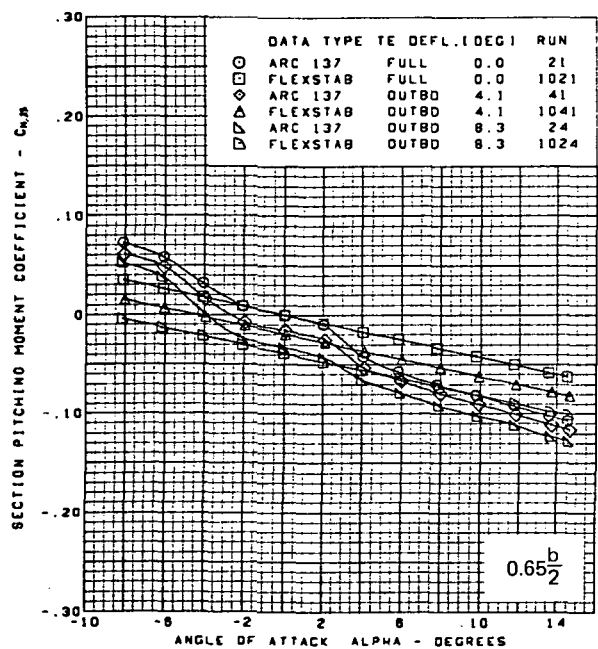
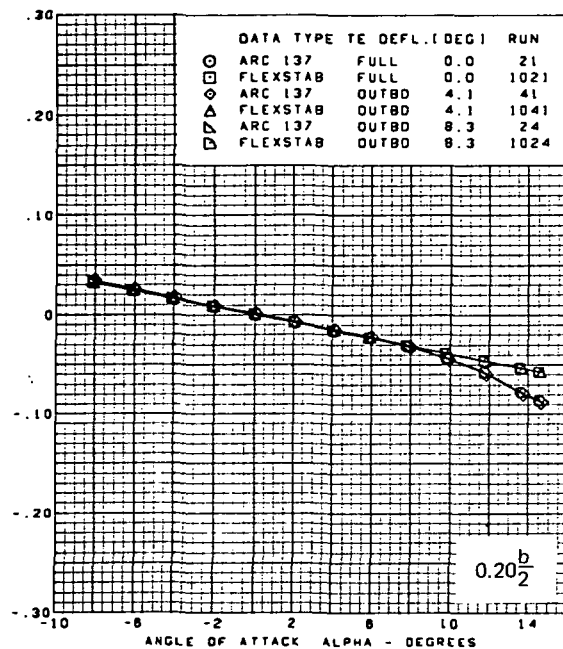
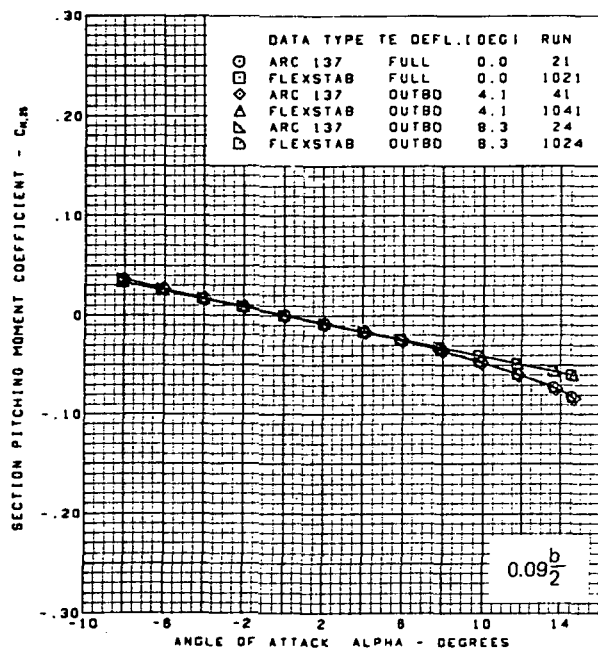
Figure 67.—(Continued)



M = 2.10  
 Flat wing, rounded L.E.  
 L.E. deflection, full span =  $0.0^\circ$   
 T.E. deflection, inboard =  $0.0^\circ$

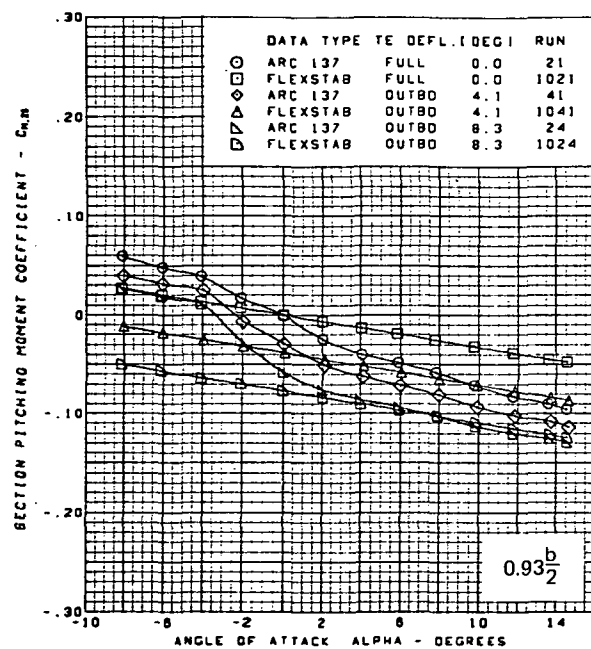
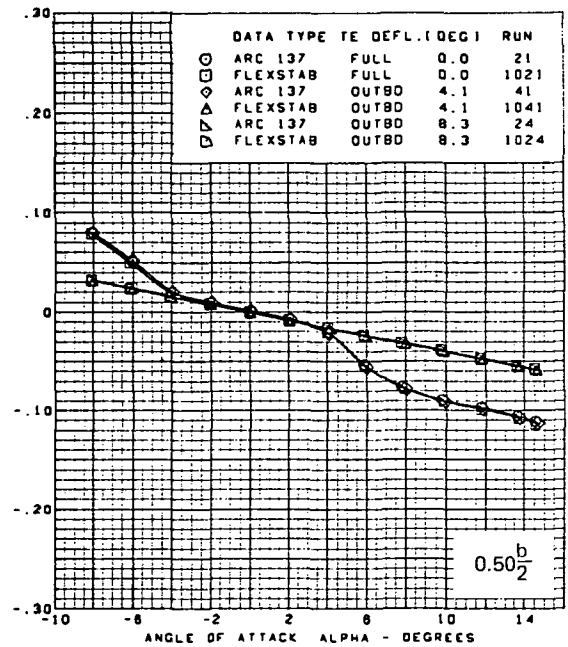
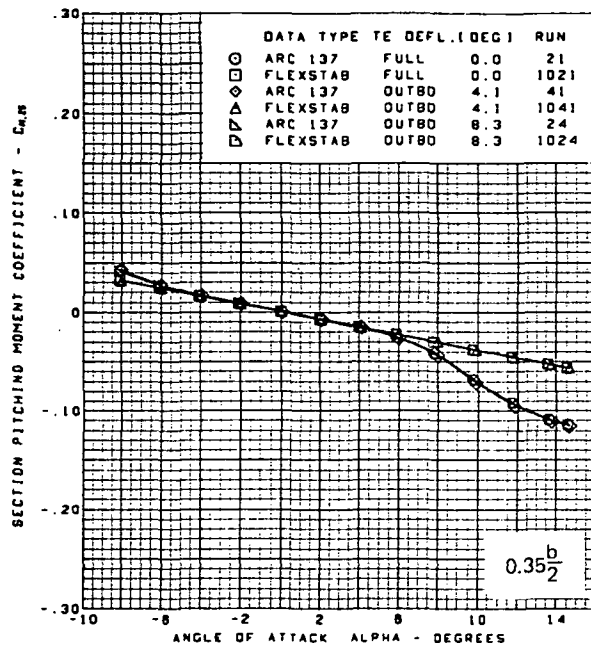
(g) (Concluded)

Figure 67.—(Continued)



(h) Section Aerodynamic Coefficients—Pitching Moment

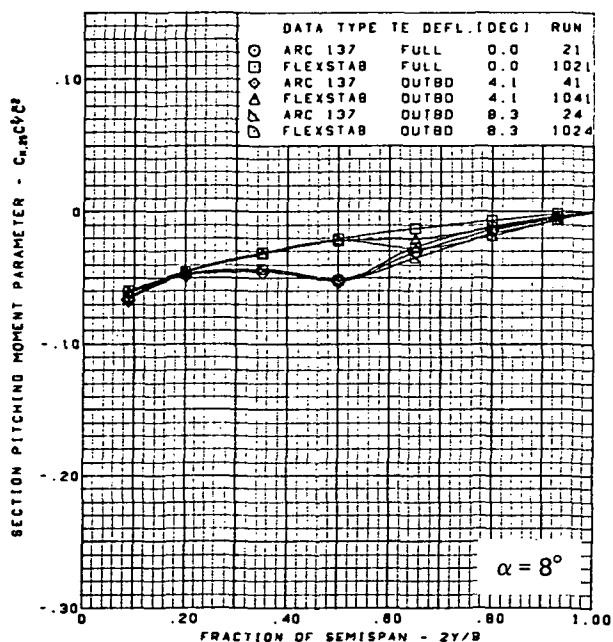
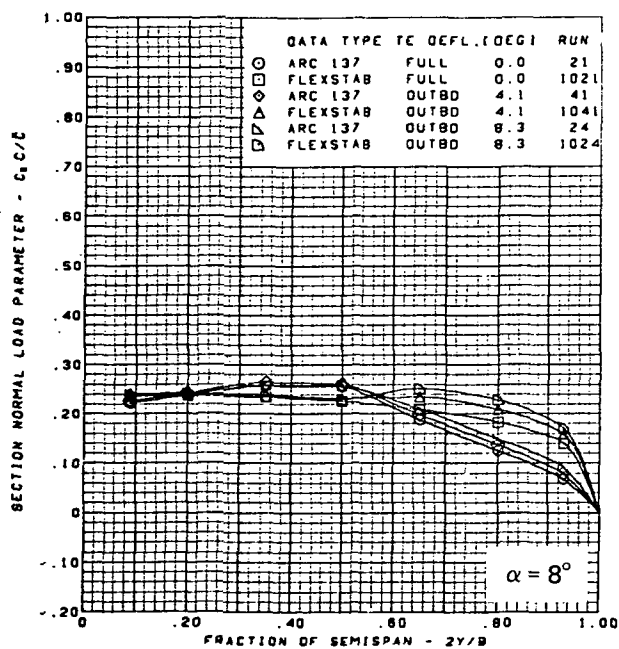
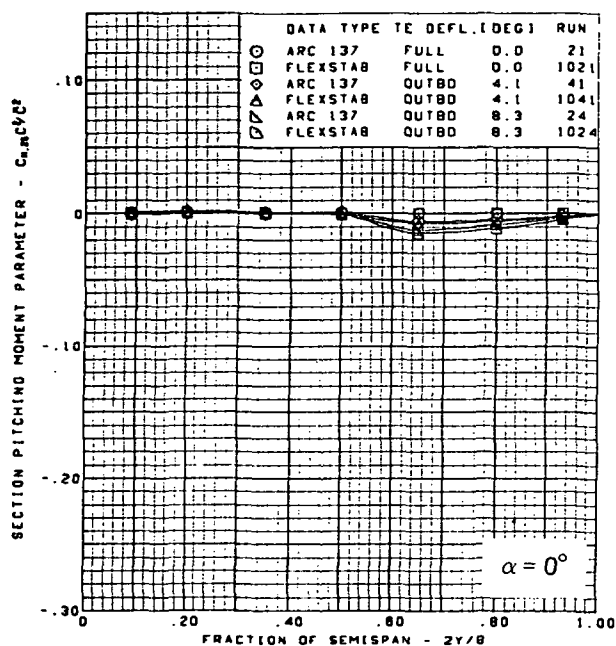
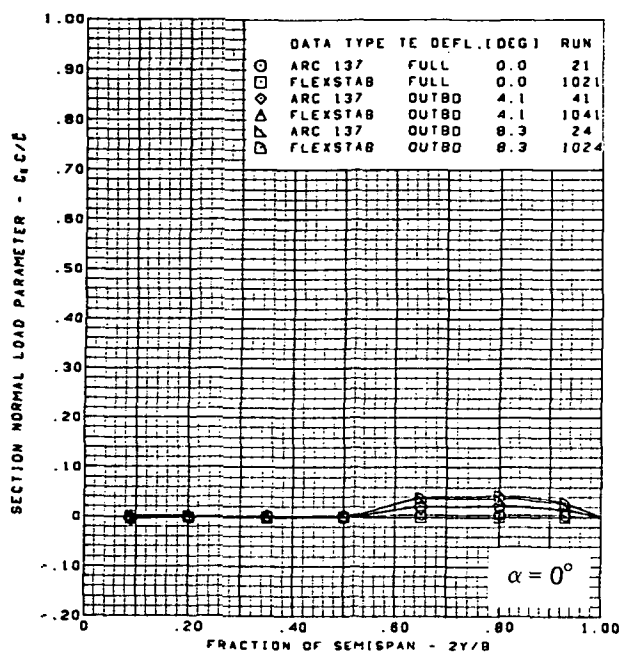
Figure 67.—(Continued)



$M = 2.10$   
 Flat wing, rounded L.E.  
 L.E. deflection, full span =  $0.0^\circ$   
 T.E. deflection, inboard =  $0.0^\circ$

(h) (Concluded)

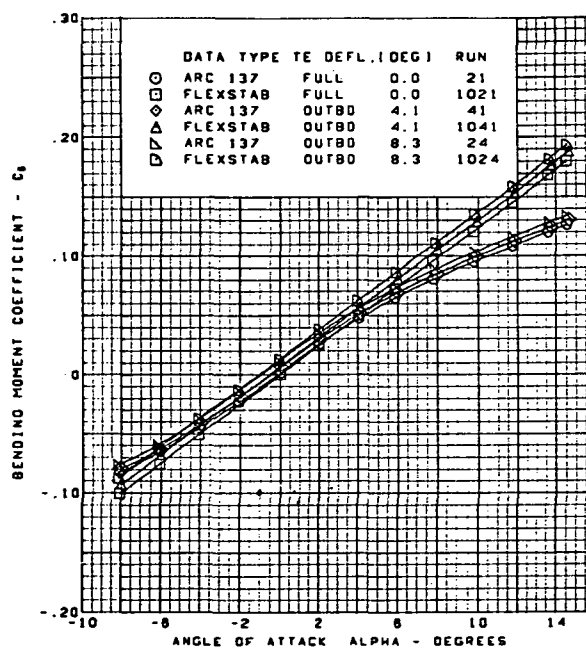
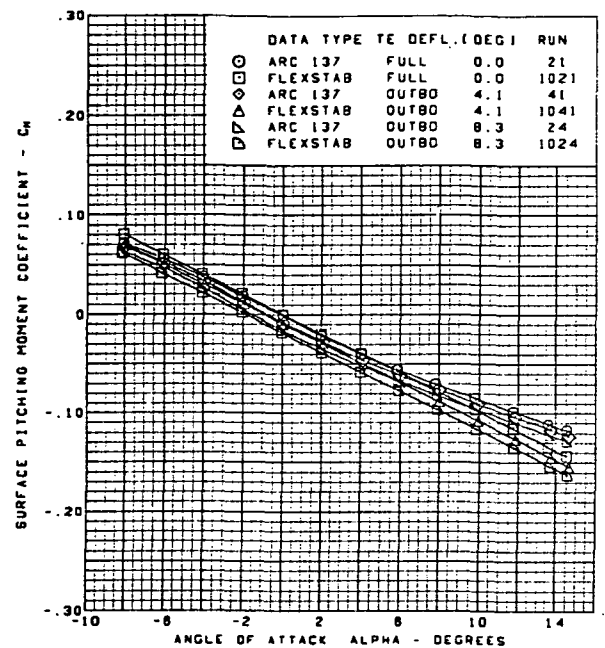
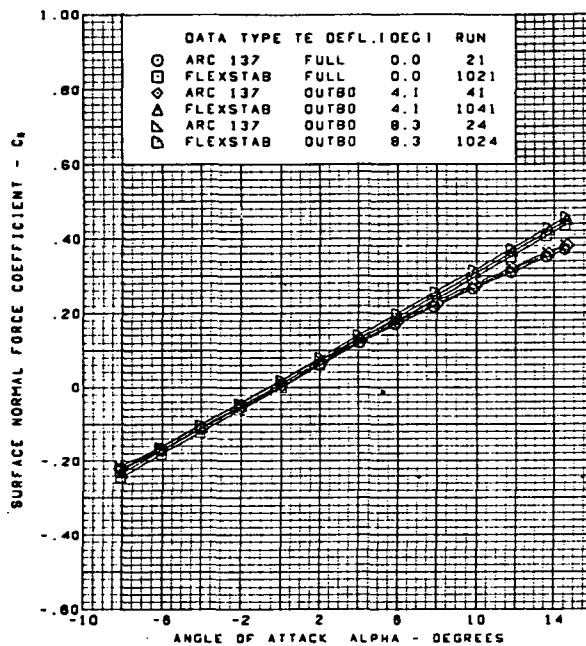
Figure 67.—(Continued)



$M = 2.10$   
 Flat wing, rounded L.E.  
 L.E. deflection, full span =  $0.0^\circ$   
 T.E. deflection, inboard =  $0.0^\circ$

(i) Spanload Distributions

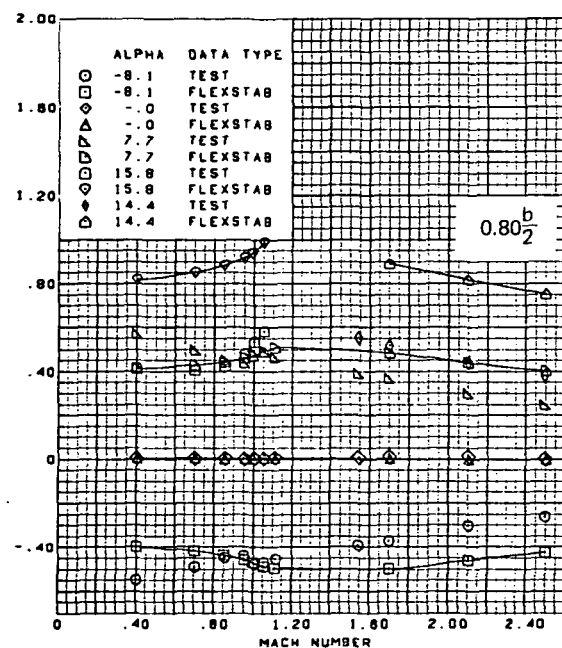
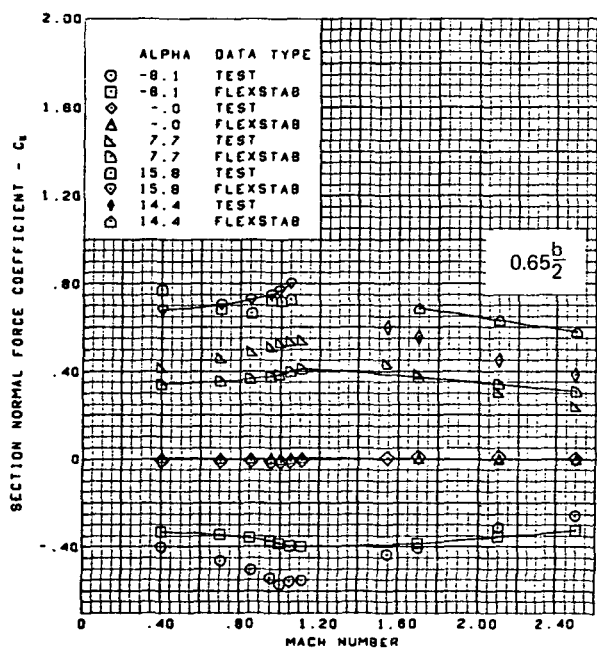
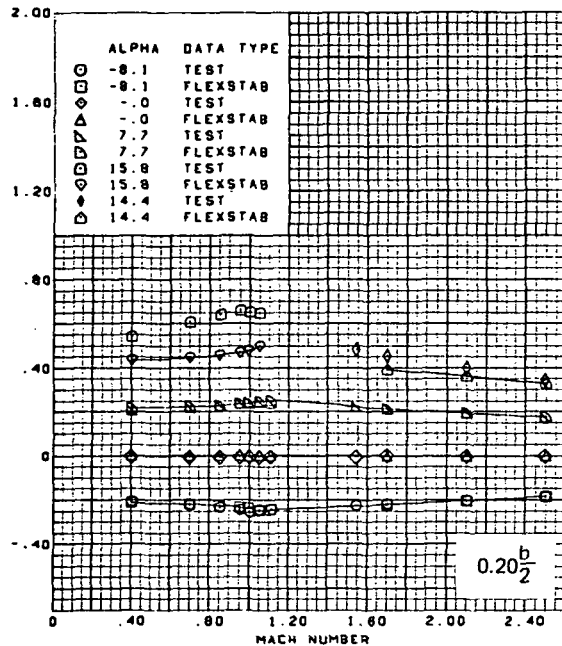
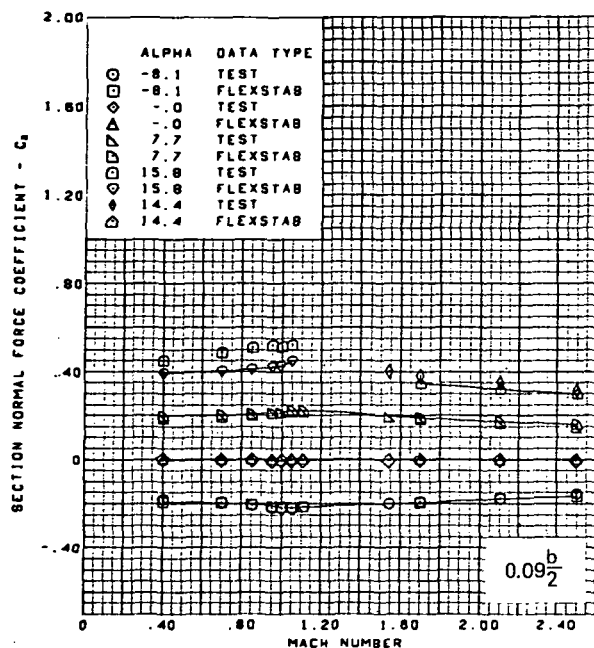
Figure 67.—(Continued)



$M = 2.10$   
 Flat wing, rounded L.E.  
 L.E. deflection, full span =  $0.0^\circ$   
 T.E. deflection, inboard =  $0.0^\circ$

(j) Wing Aerodynamic Coefficients

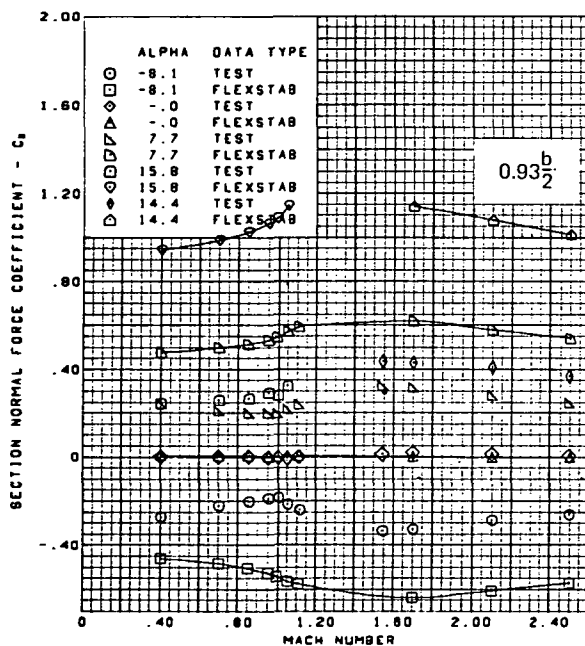
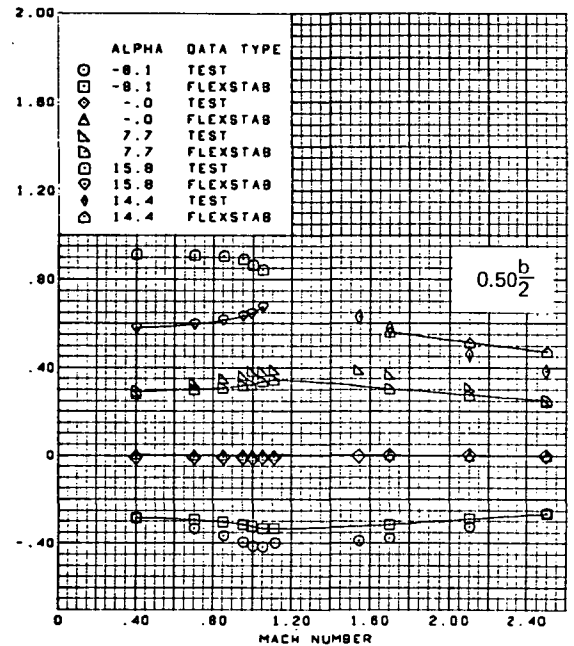
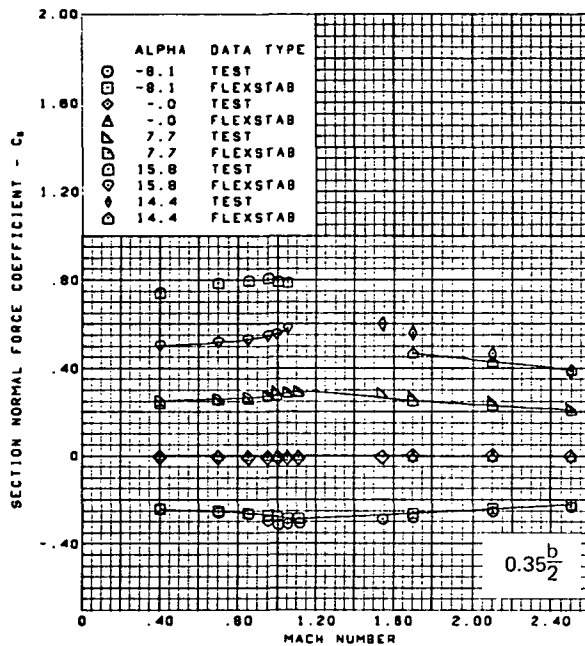
Figure 67.—(Concluded)



(a) Section Aerodynamic Coefficients—Normal Force

Figure 68.—Wing Theory-to-Experiment Comparison —Effect of Mach Number and Angle of Attack;  
Flat Wing, Rounded L.E.; L.E. Deflection, Full Span =  $0.0^\circ$ ; T.E. Deflection, Full Span =  $0.0^\circ$

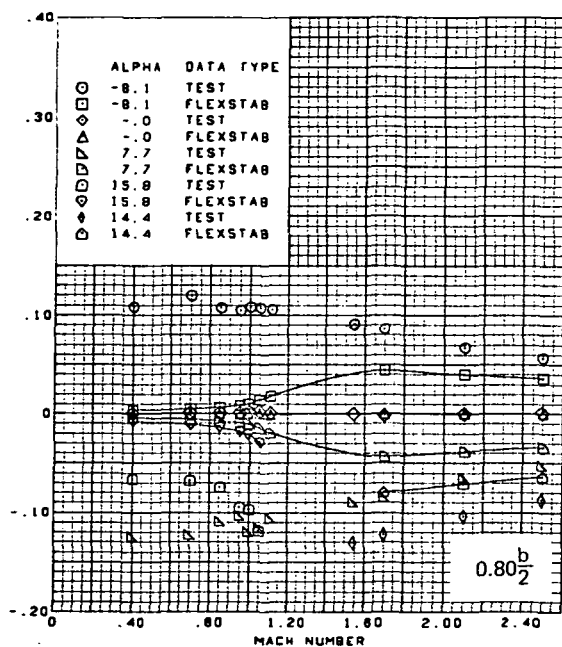
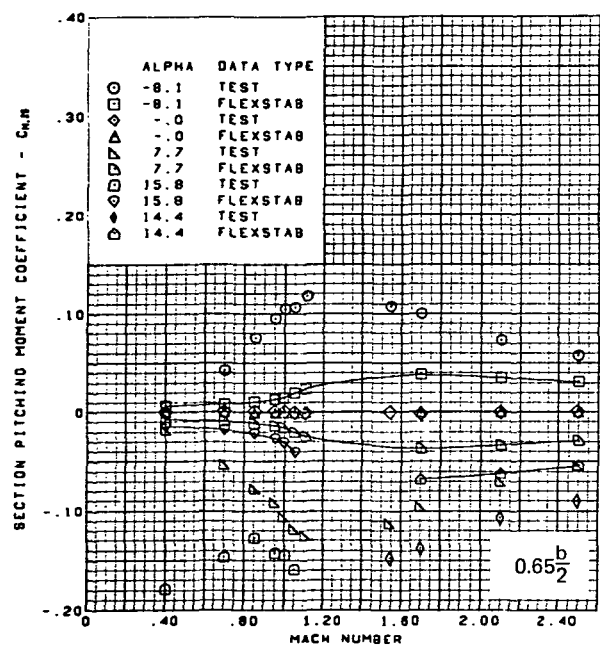
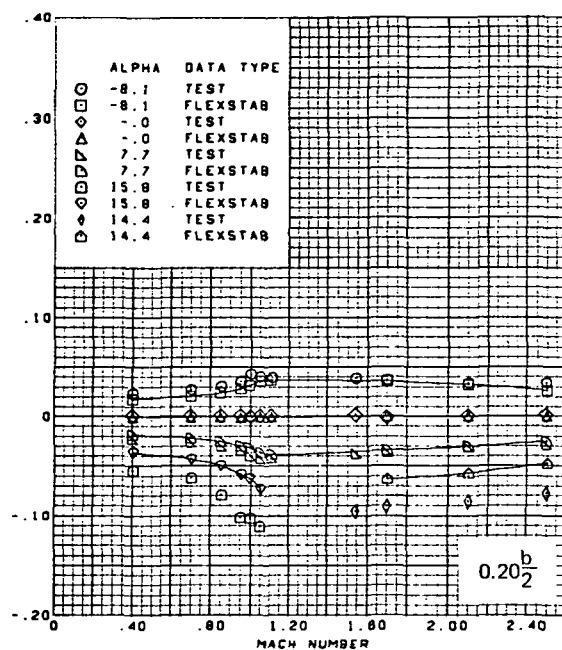
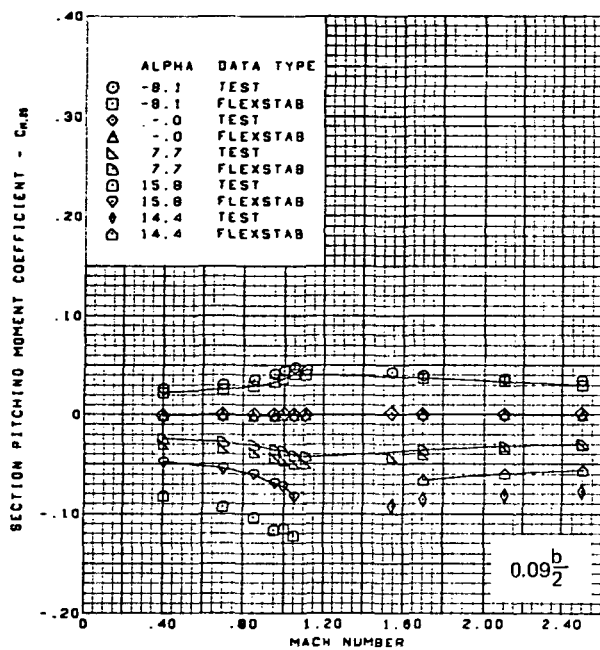




Flat wing, rounded L.E.  
 L.E. deflection, full span =  $0.0^\circ$   
 T.E. deflection, full span =  $0.0^\circ$

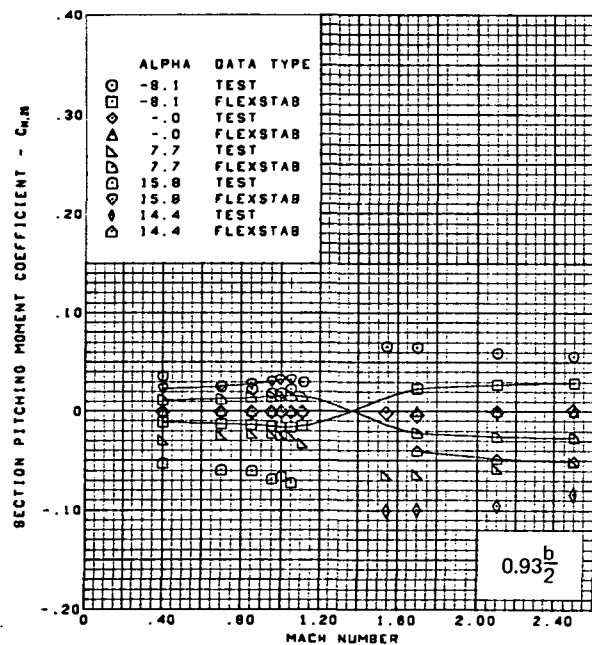
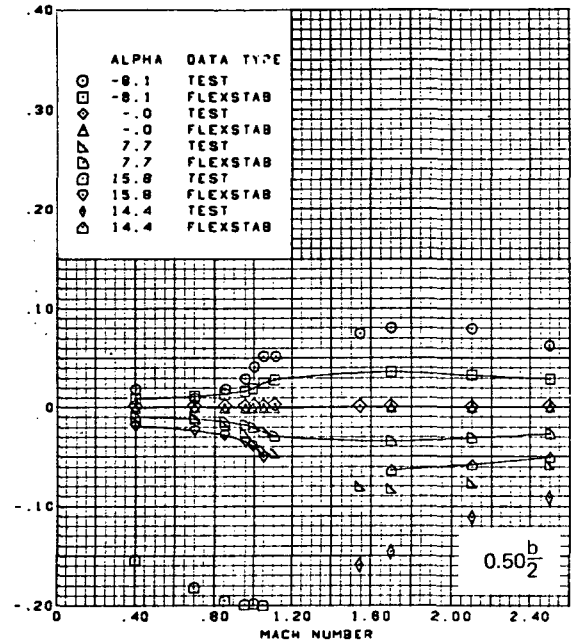
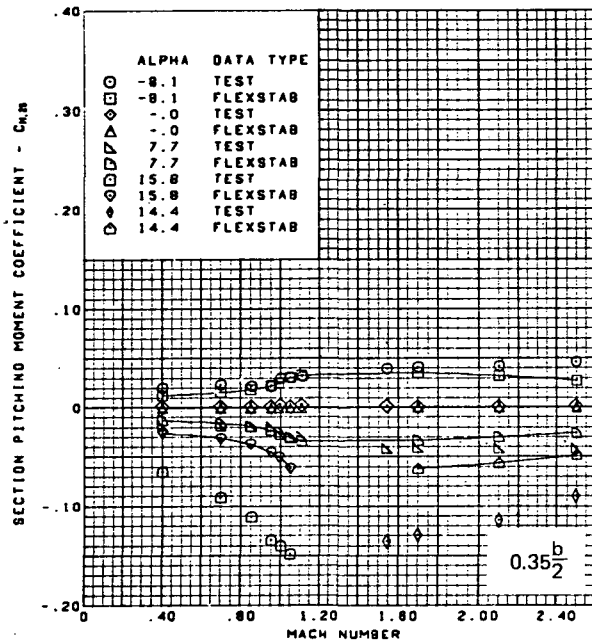
(a) (Concluded)

Figure 68.—(Continued)



(b) Section Aerodynamic Coefficients—Pitching Moment

Figure 68.—(Continued)

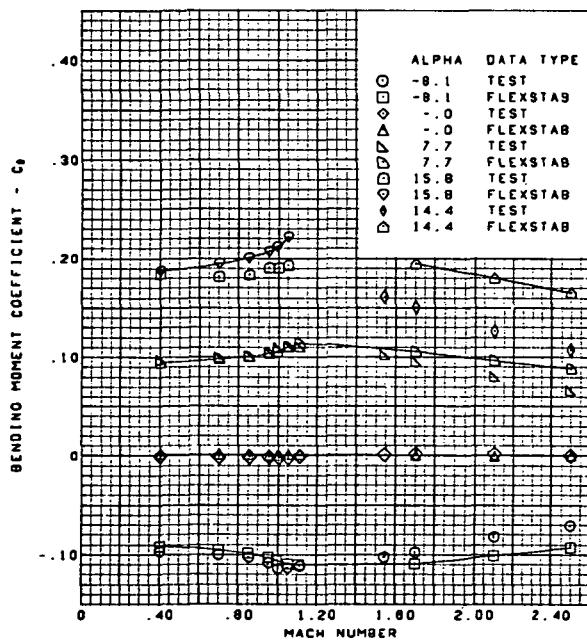
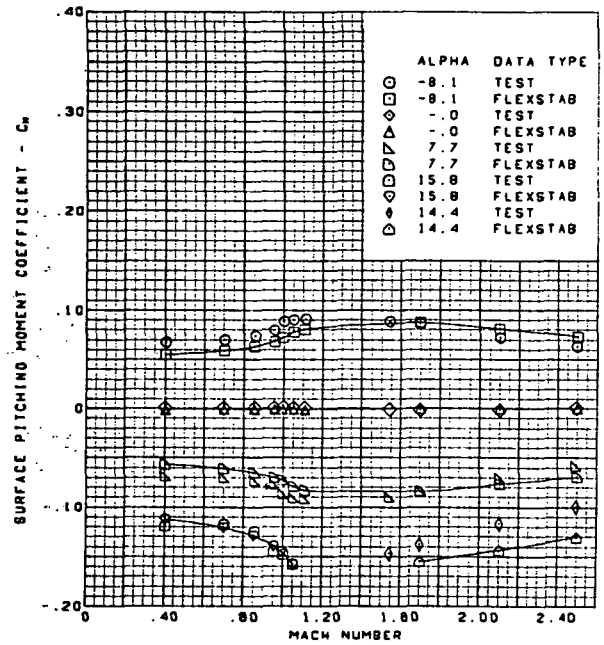
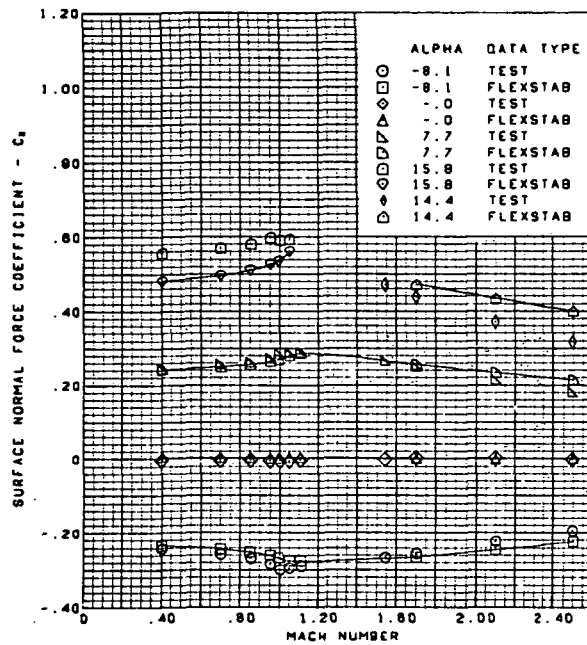


Flat wing, rounded L.E.  
 L.E. deflection, full span =  $0.0^\circ$   
 T.E. deflection, full span =  $0.0^\circ$

(b) (Concluded)

Figure 68.—(Continued)

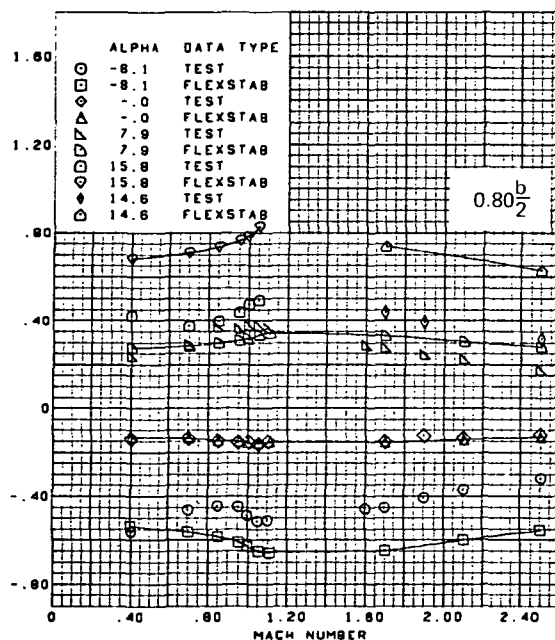
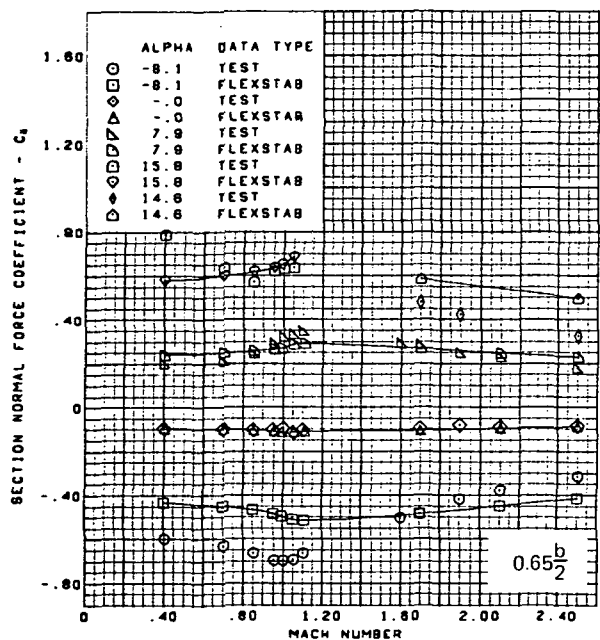
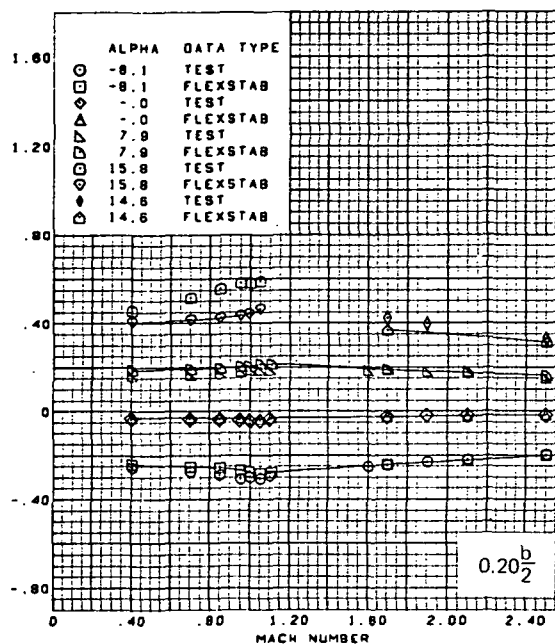
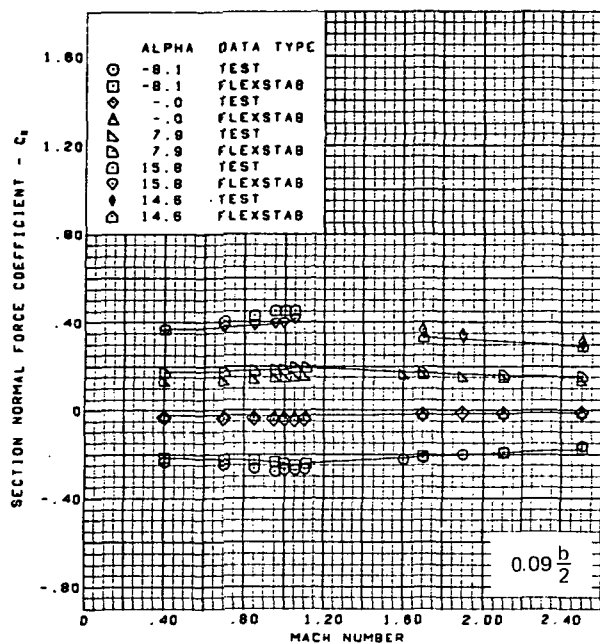
**Page  
Intentionally  
Left Blank**



Flat wing, rounded L.E.  
 L.E. deflection, full span =  $0.0^\circ$   
 T.E. deflection, full span =  $0.0^\circ$

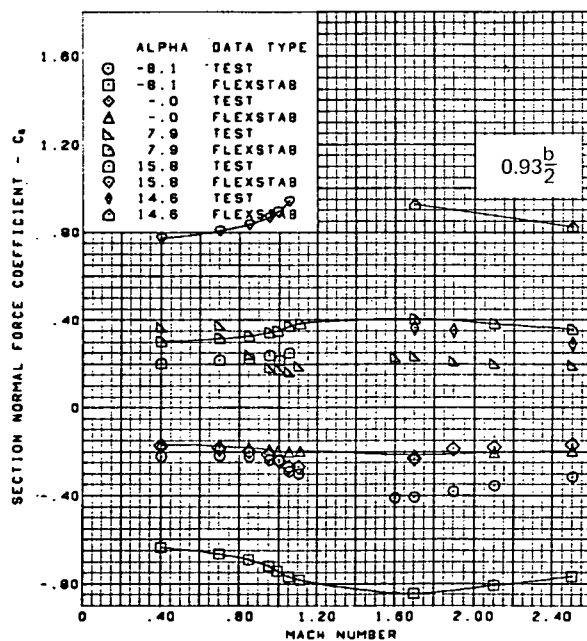
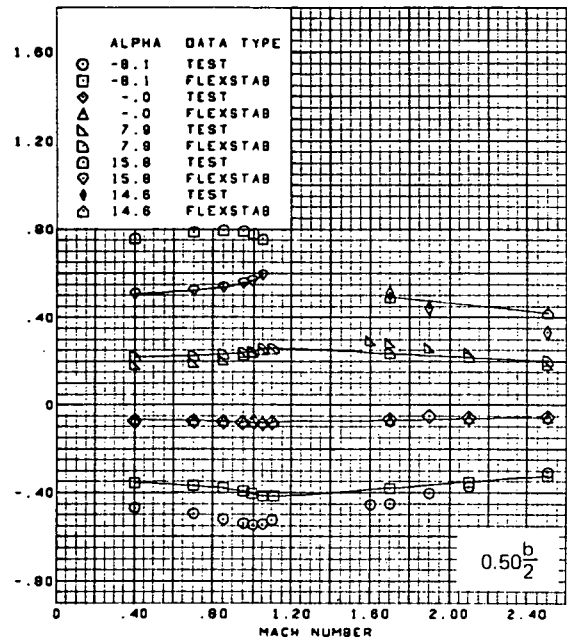
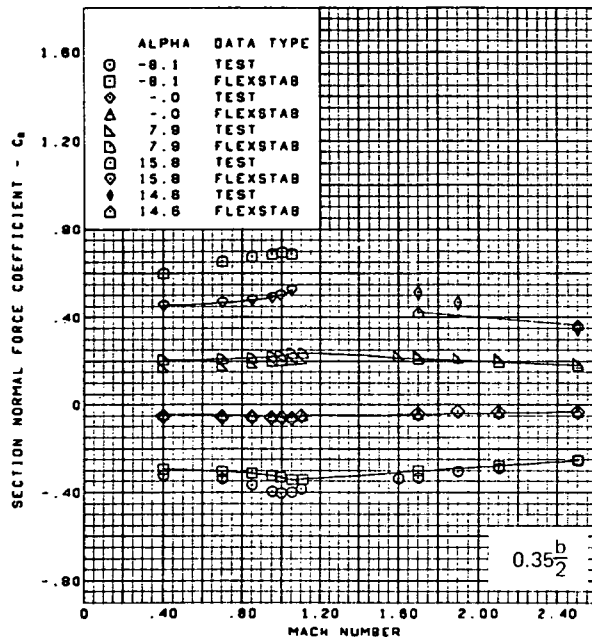
(c) Wing Aerodynamic Coefficients

Figure 68.—(Concluded)



(a) Section Aerodynamic Coefficients—Normal Force

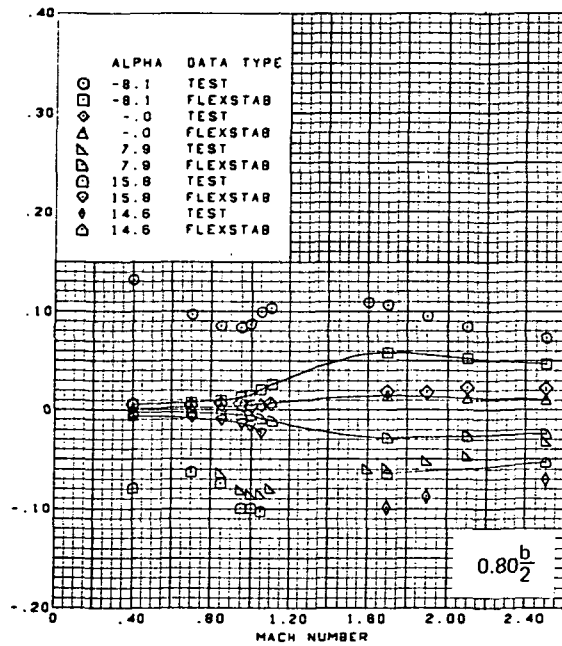
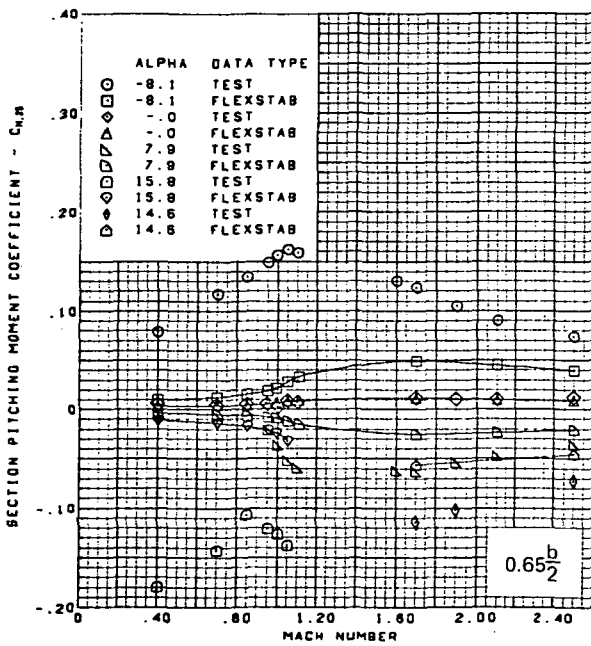
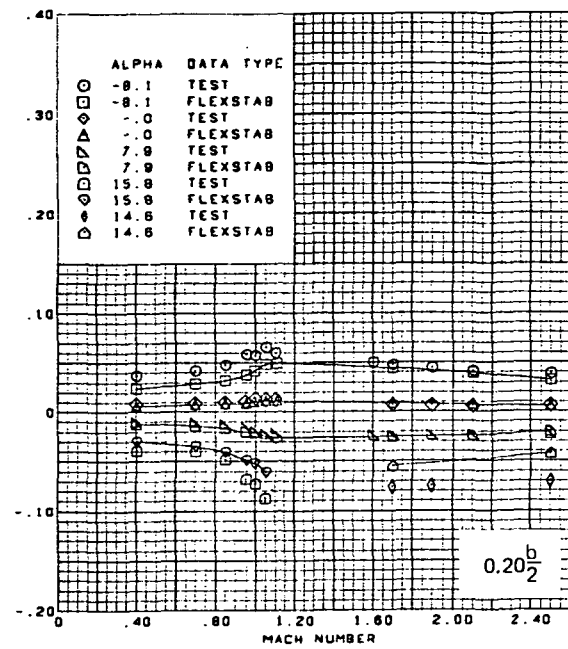
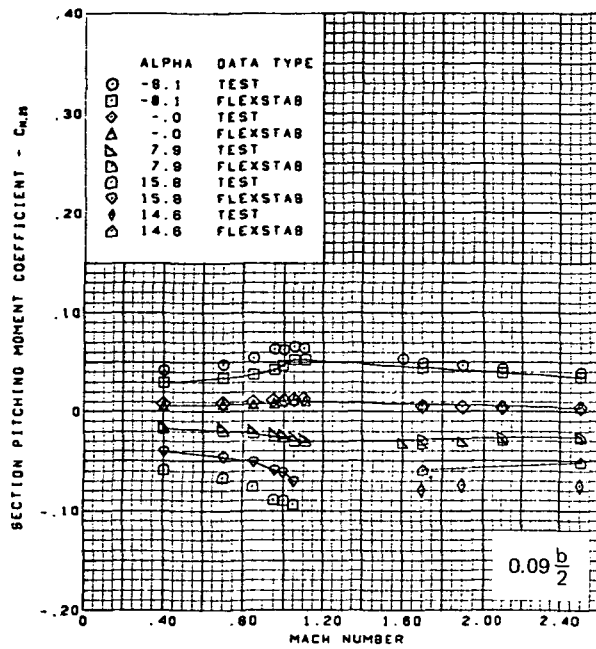
Figure 69.—Wing Theory-to-Experiment Comparison —Effect of Mach Number and Angle of Attack; Twisted Wing, Rounded L.E.; L.E. Deflection, Full Span =  $0.0^\circ$ ; T.E. Deflection, Full Span =  $0.0^\circ$



Twisted wing, rounded L.E.  
 L.E. deflection, full span =  $0.0^\circ$   
 T.E. deflection, full span =  $0.0^\circ$

(a) (Concluded)

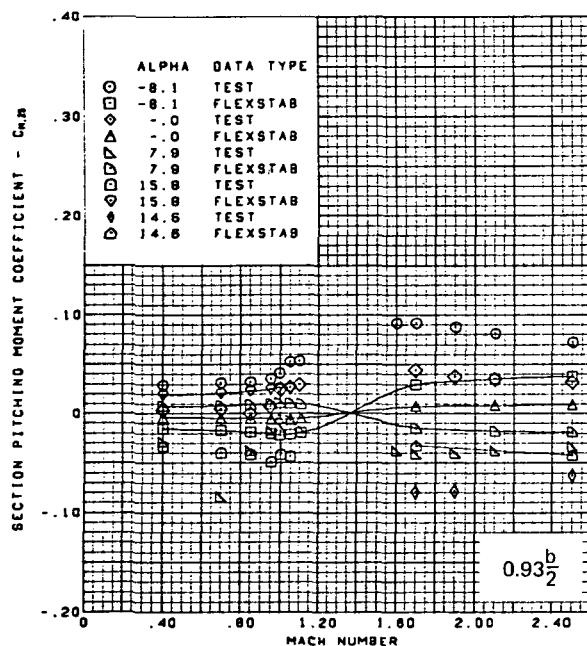
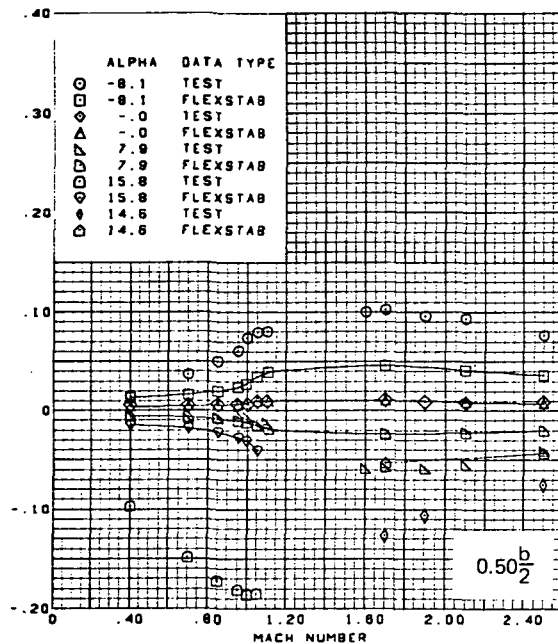
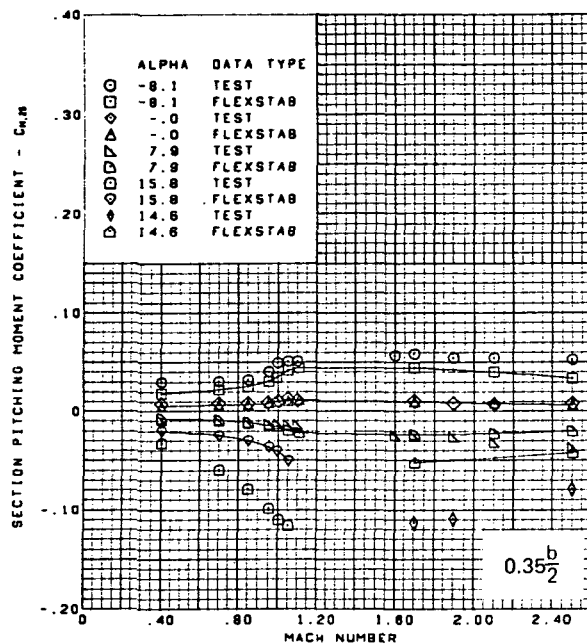
Figure 69.—(Continued)



(b) Section Aerodynamic Coefficients—Pitching Moment

Figure 69.—(Continued)



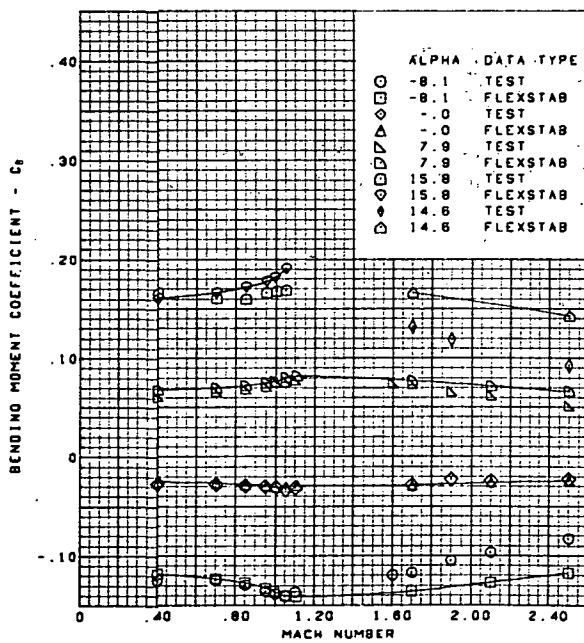
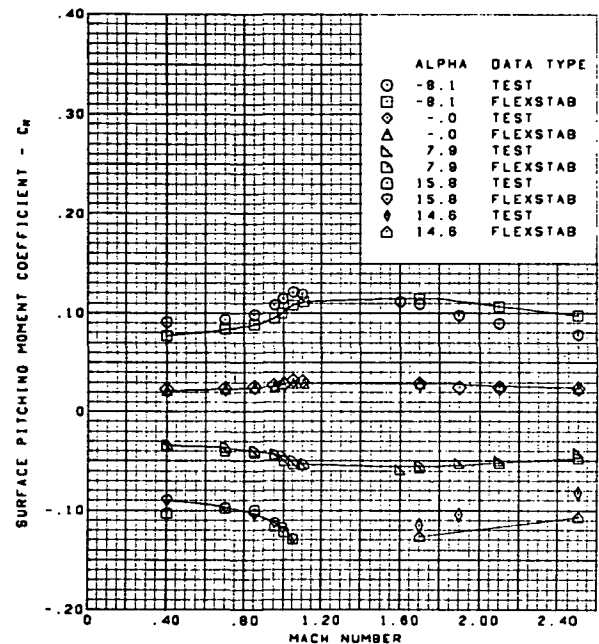
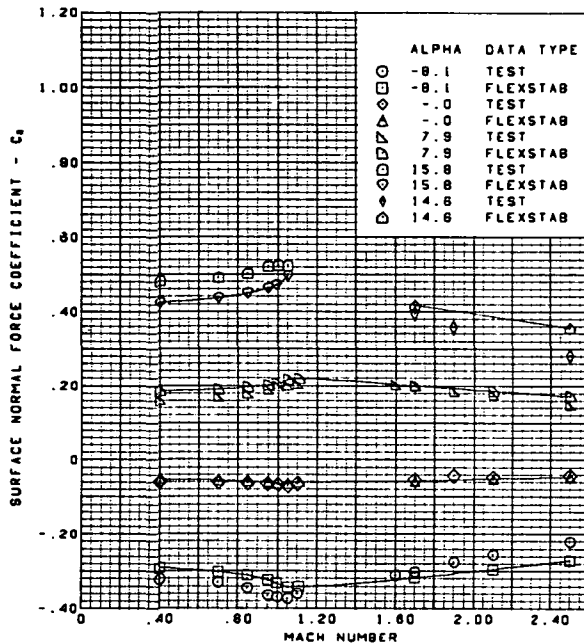


Twisted wing, rounded L.E.  
 L.E. deflection, full span =  $0.0^\circ$   
 T.E. deflection, full span =  $0.0^\circ$

(b) (Concluded)

Figure 69.—(Continued)

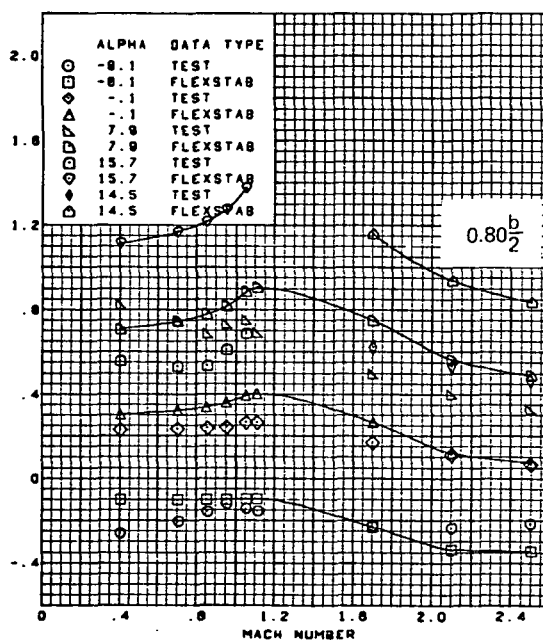
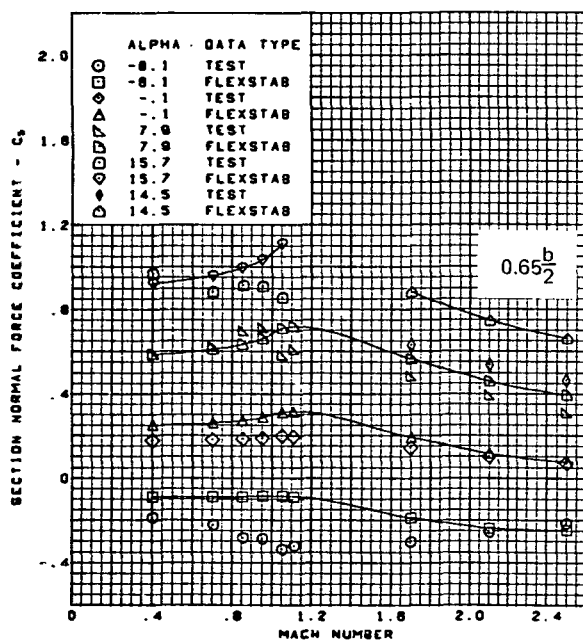
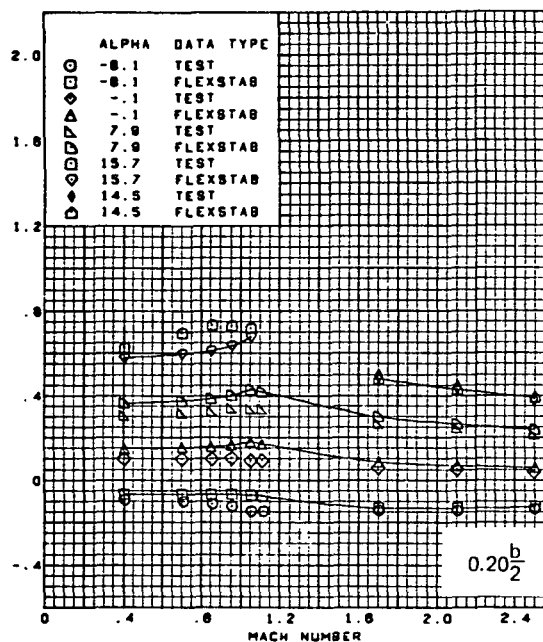
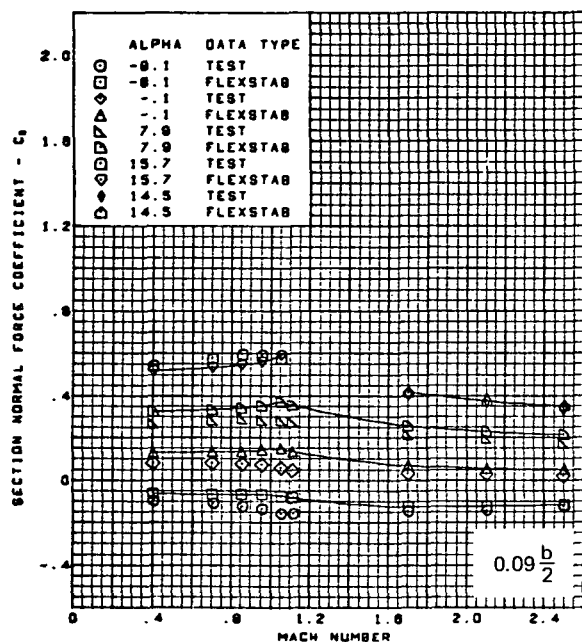
**Page  
Intentionally  
Left Blank**



Twisted wing, rounded L.E.  
L.E. deflection, full span = 0.0°  
T.E. deflection, full span = 0.0°

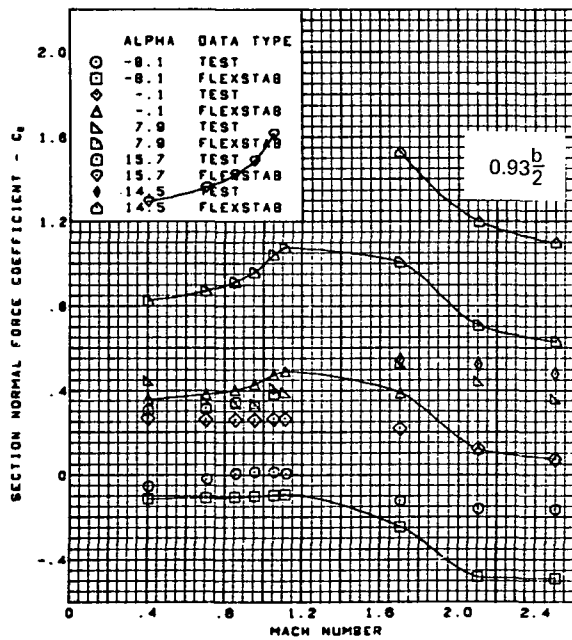
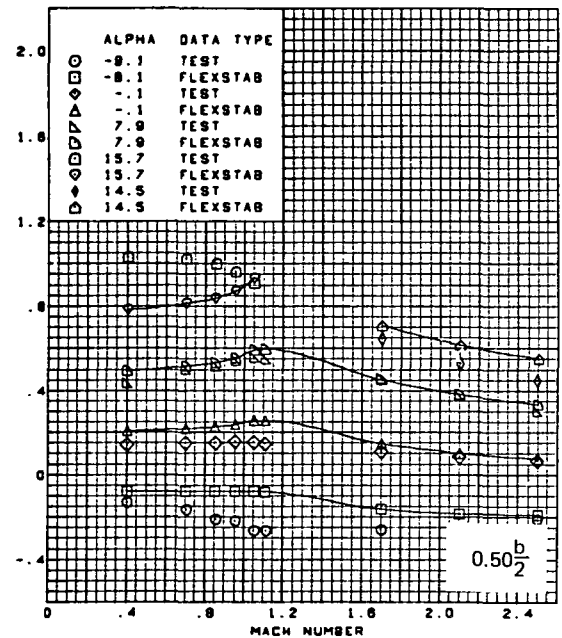
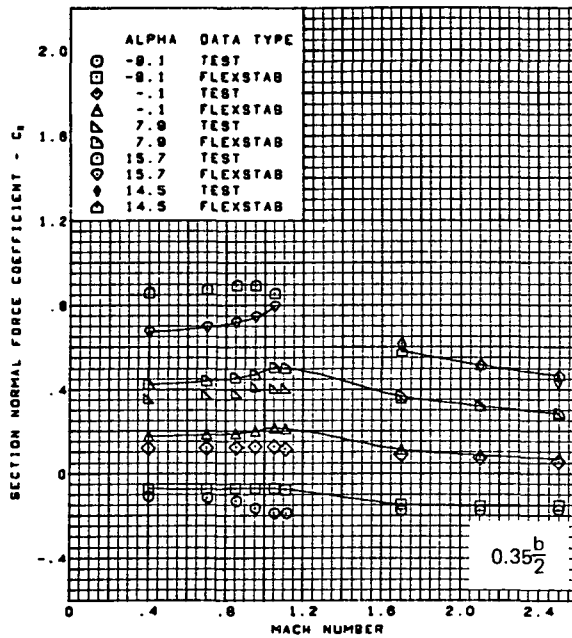
(c) Wing Aerodynamic Coefficients

Figure 69.—(Concluded)



(a) Section Aerodynamic Coefficients—Normal Force

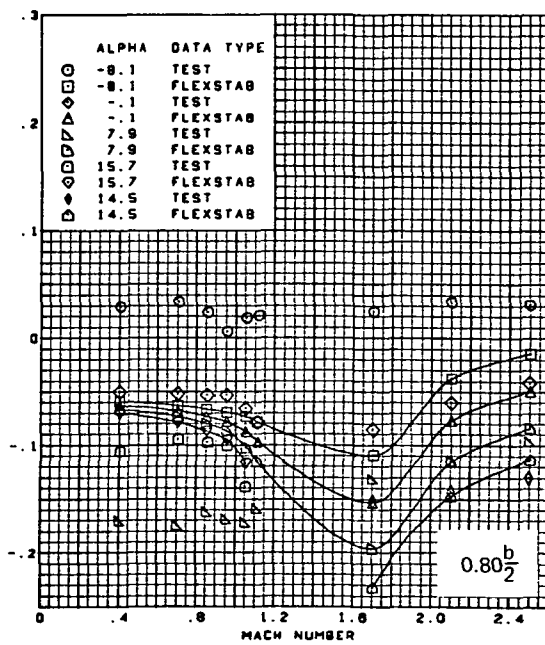
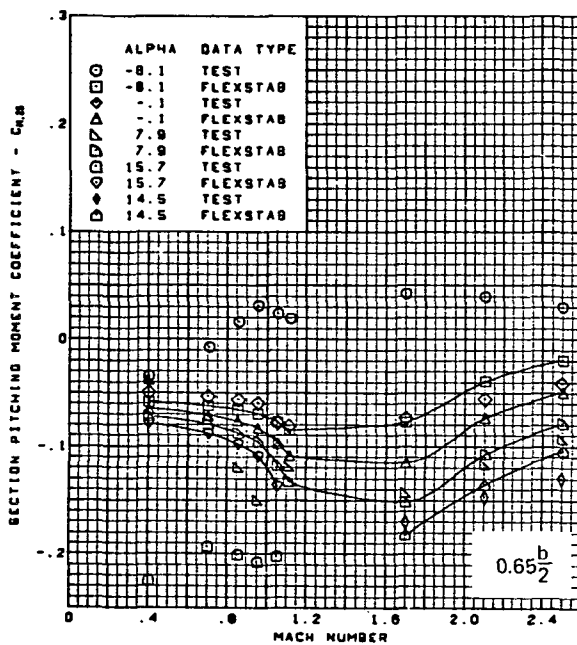
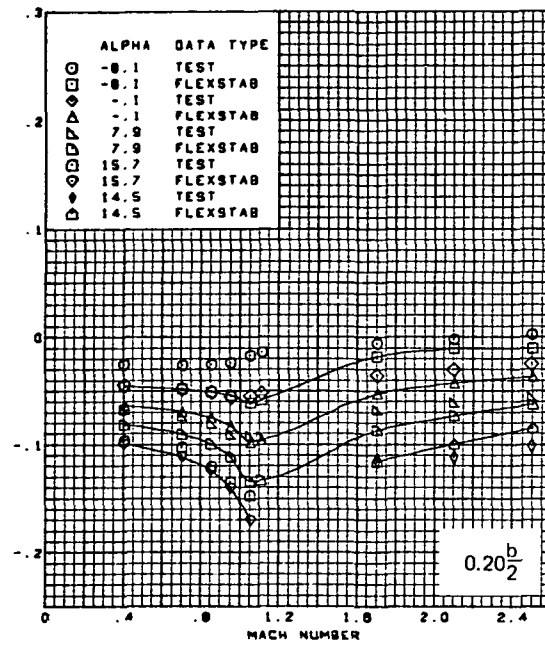
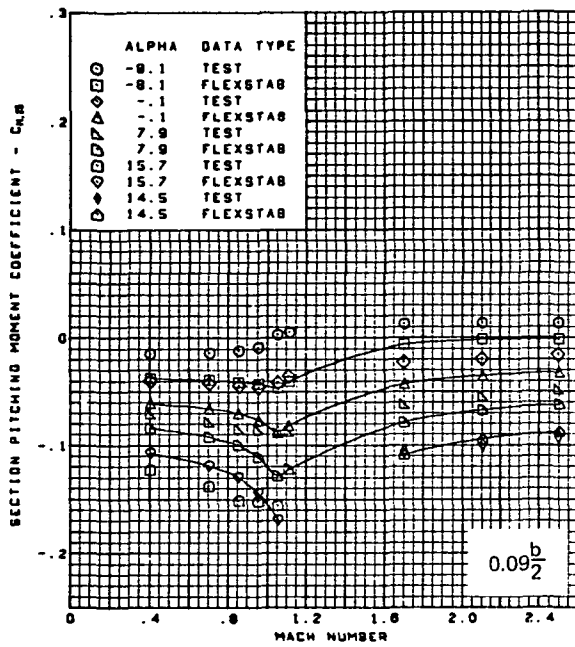
Figure 70.—Wing Theory-to-Experiment Comparison —Effect of Mach Number and Angle of Attack; Flat Wing, Rounded L.E.; L.E. Deflection, Full span =  $0.0^\circ$ ; T.E. Deflection, Full Span =  $8.3^\circ$



Flat wing, rounded L.E.  
 L.E. deflection, full span = 0.0°  
 T.E. deflection, full span = 8.3°

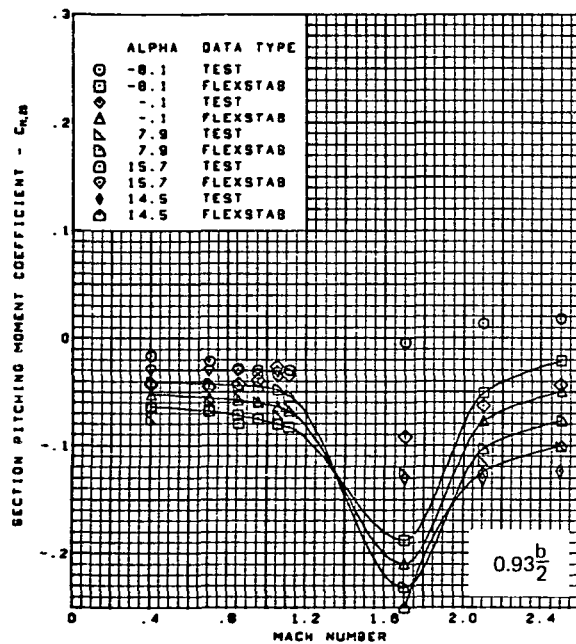
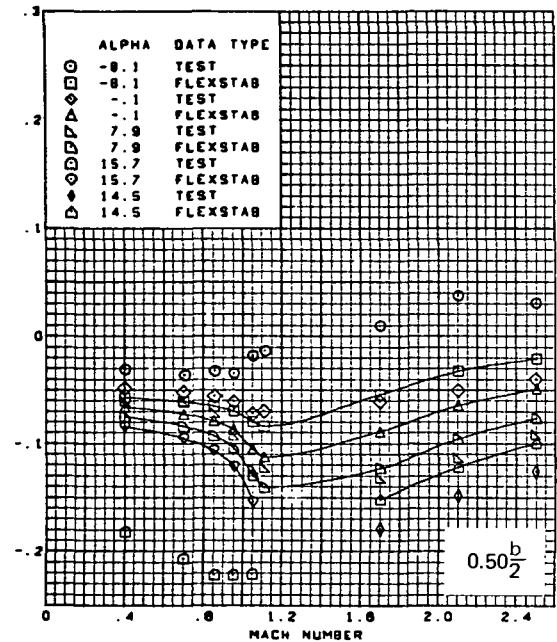
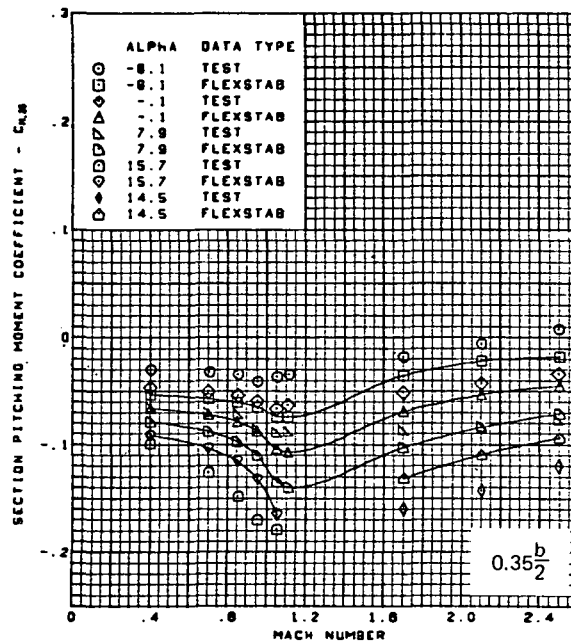
(a) (Concluded)

Figure 70.—(Continued)



(b) Section Aerodynamic Coefficients—Pitching Moment

Figure 70.—(Continued)



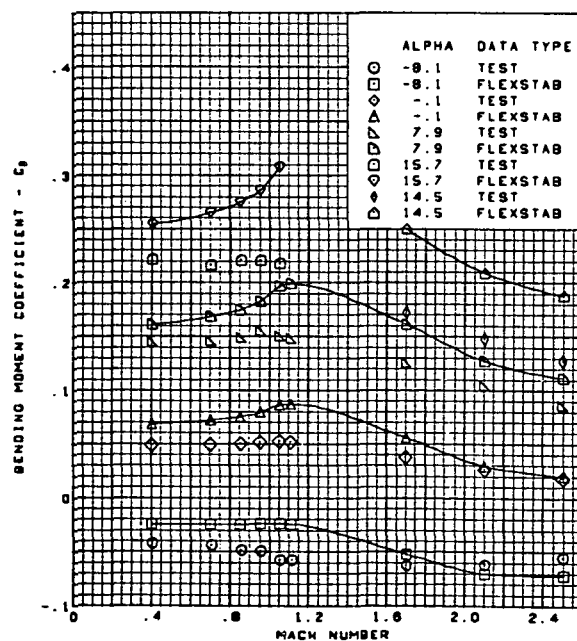
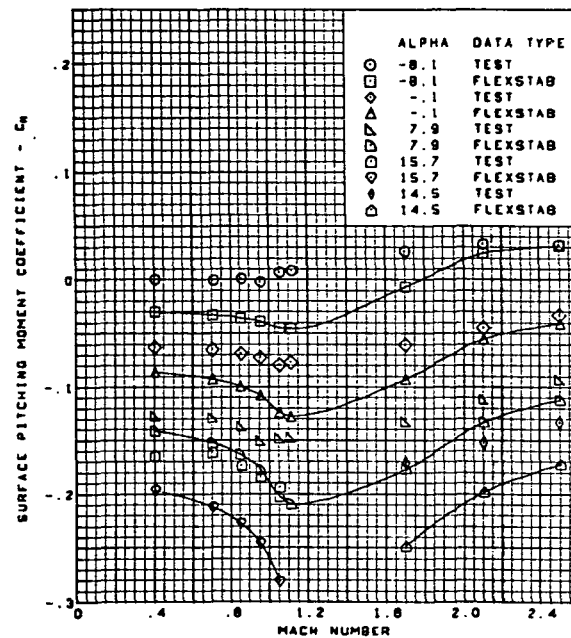
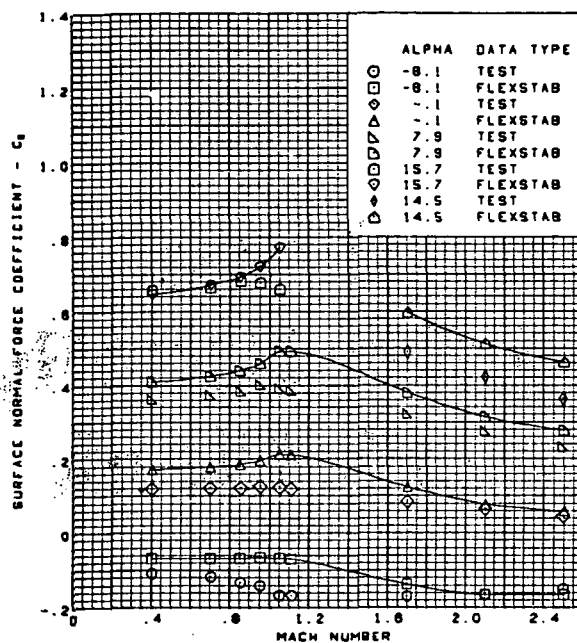
Flat wing, rounded L.E.  
 L.E. deflection, full span =  $0.0^\circ$   
 T.E. deflection, full span =  $8.3^\circ$

(b) (Concluded)

Figure 70.—(Continued)

**Page  
Intentionally  
Left Blank**

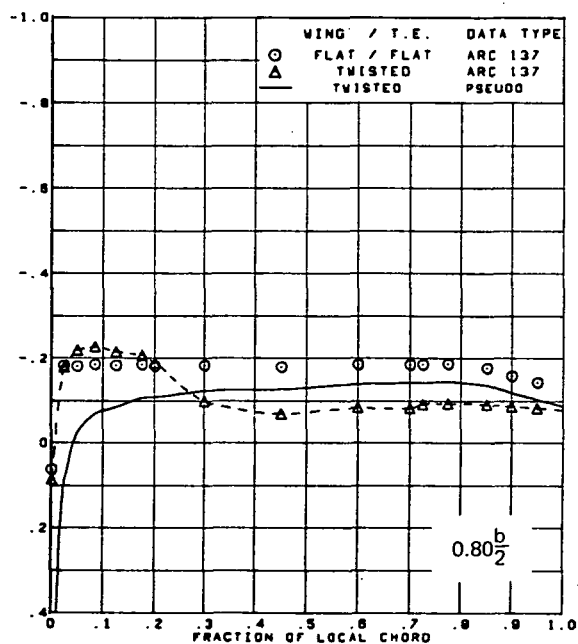
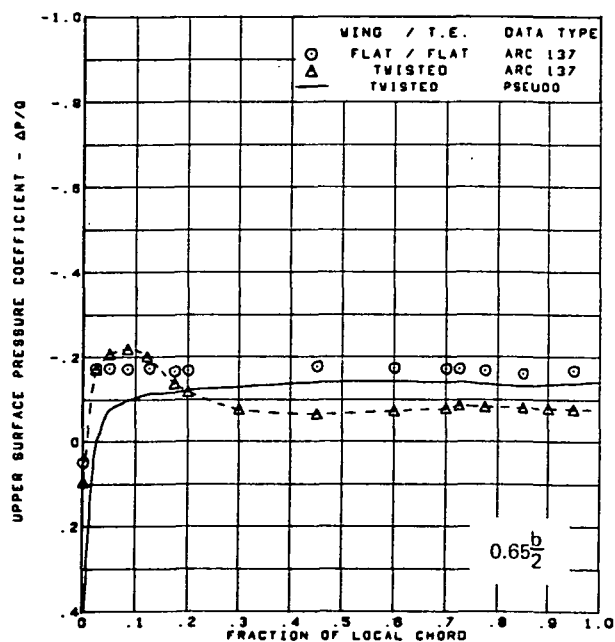
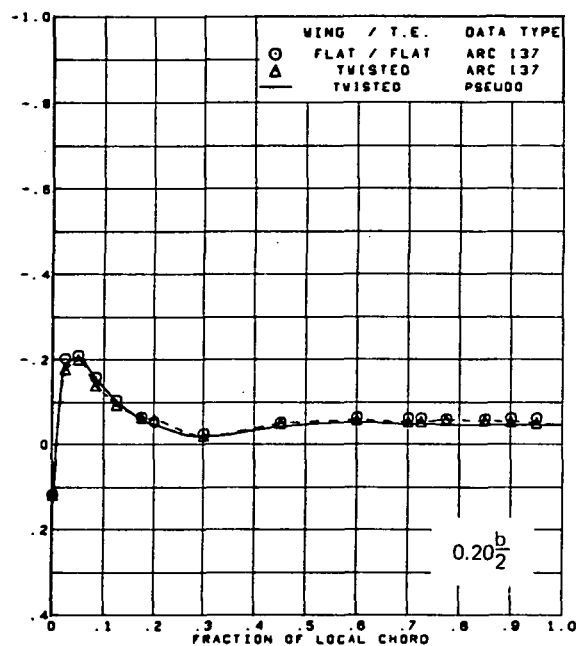
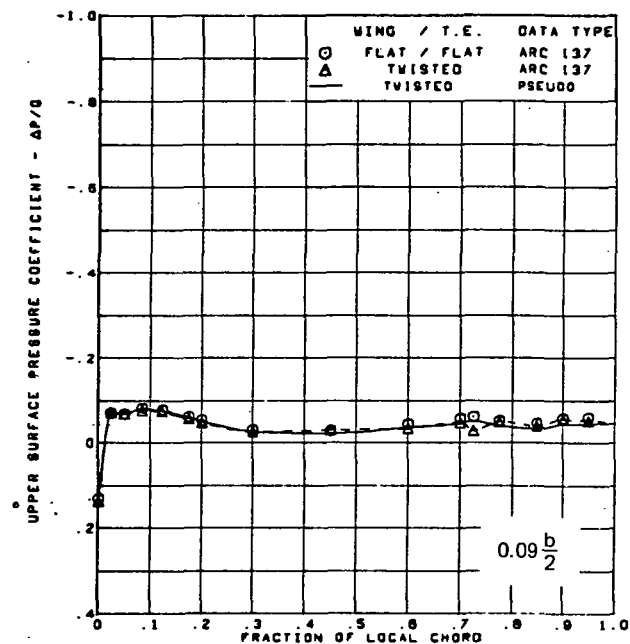




Flat wing, rounded L.E.  
 L.E. deflection, full span =  $0.0^\circ$   
 T.E. deflection, full span =  $8.3^\circ$

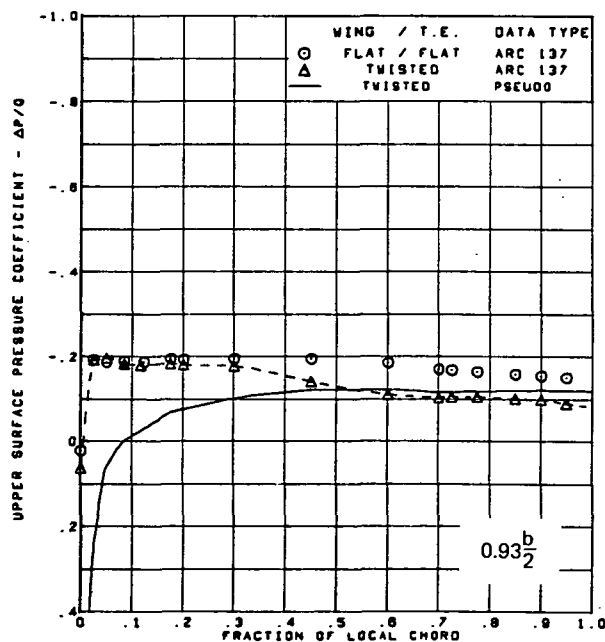
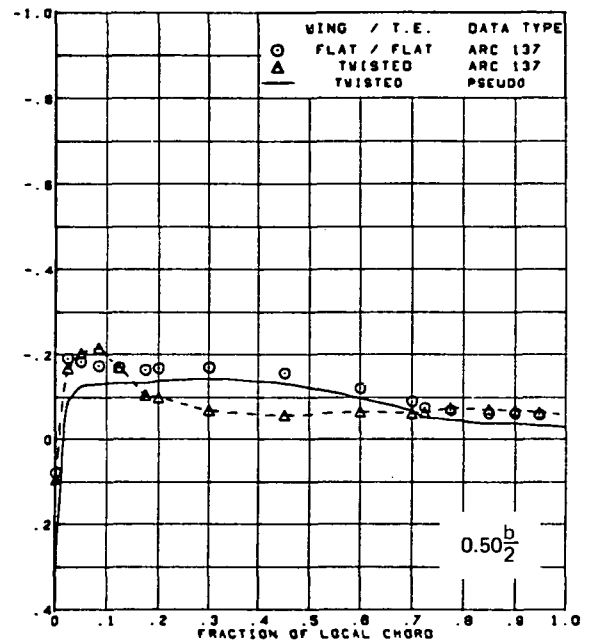
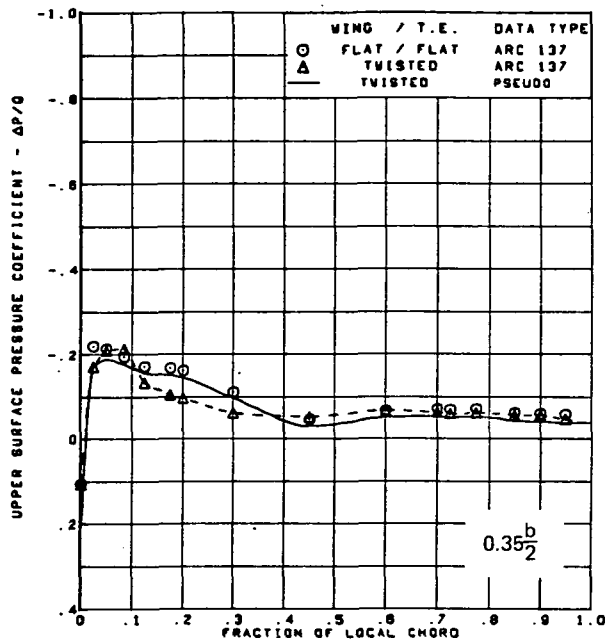
(c) Wing Aerodynamic Coefficients

Figure 70.—(Concluded)



(a) Upper Surface Chordwise Pressure Distributions,  $\alpha = 4^\circ$

Figure 71.—Pseudo Aeroelastic Predictions; Rounded L.E.; L.E. Deflection, Full Span =  $0.0^\circ$ ;  
 T.E. Deflection, Full Span =  $0.0^\circ$ ;  $M = 2.10$

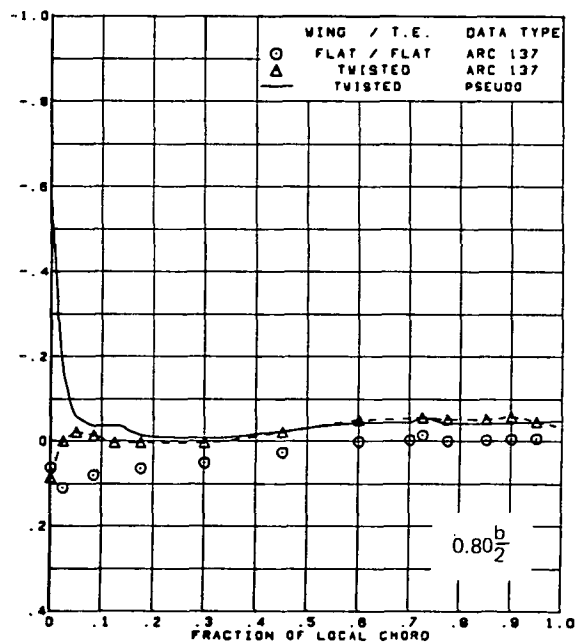
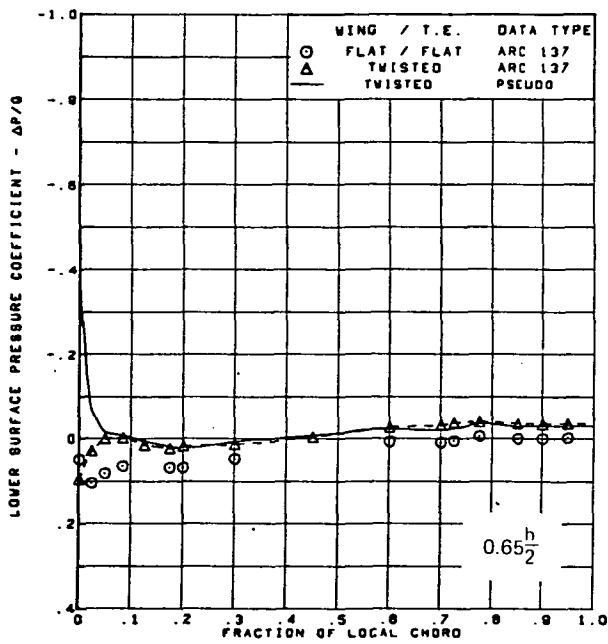
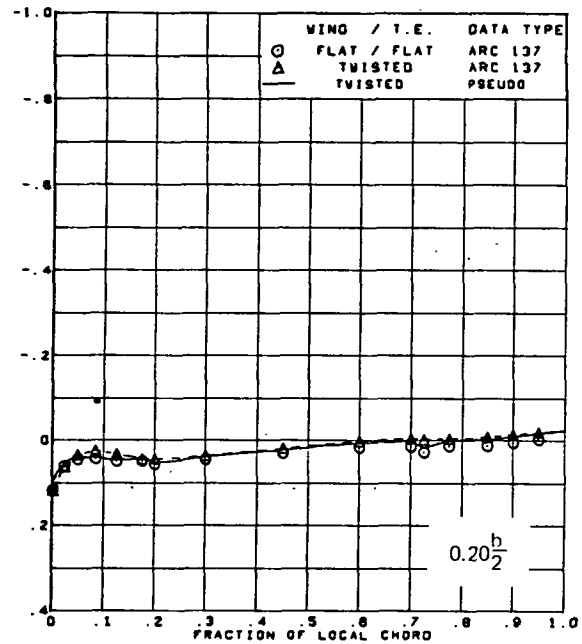
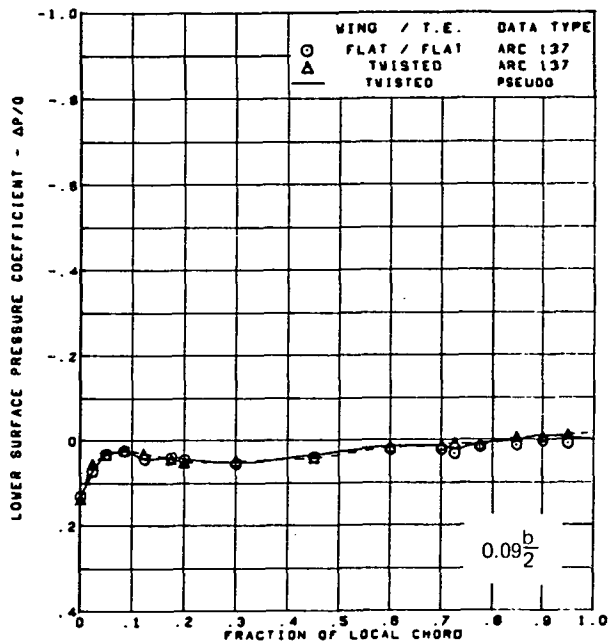


$M = 2.10$   
 $\alpha = 4^\circ$   
 Rounded L.E.  
 L.E. deflection, full span =  $0.0^\circ$   
 T.E. deflection, full span =  $0.0^\circ$

Note:  $C_{p, \text{vacuum}} = -0.32$

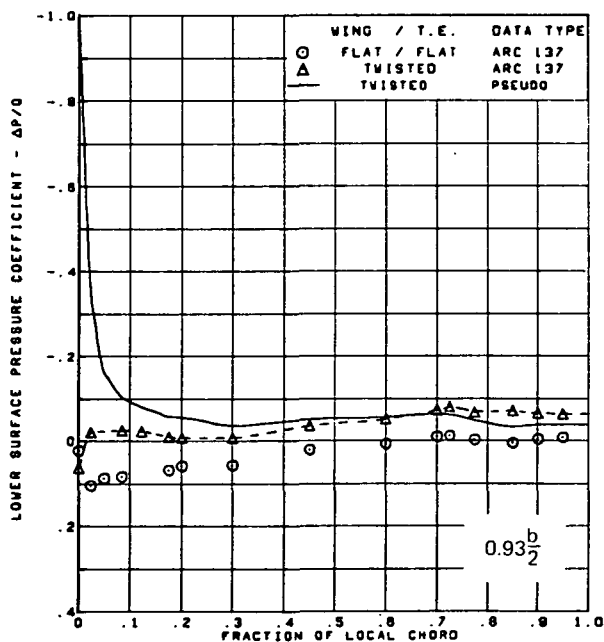
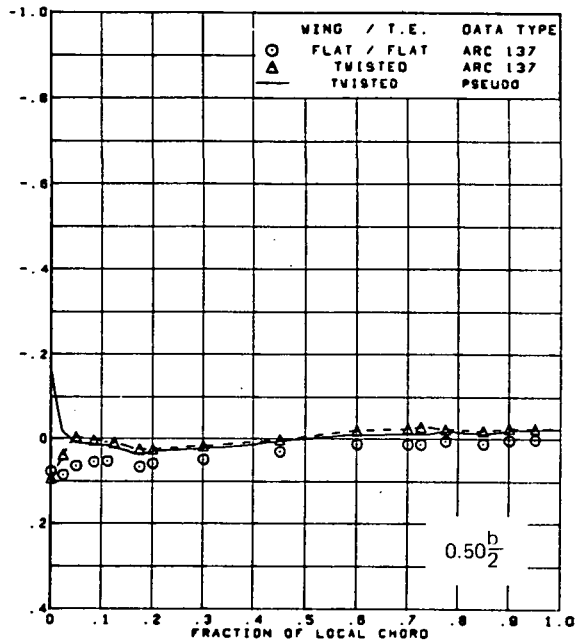
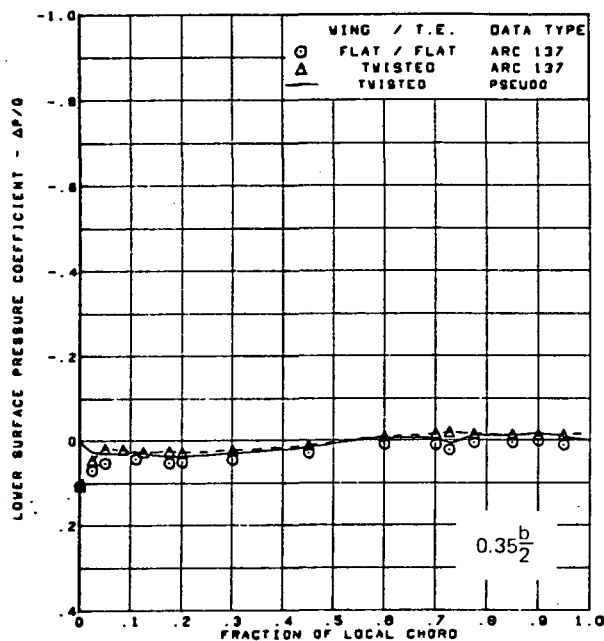
(a) (Concluded)

Figure 71.—(Continued)



(b) Lower Surface Chordwise Pressure Distributions,  $\alpha = 4^\circ$

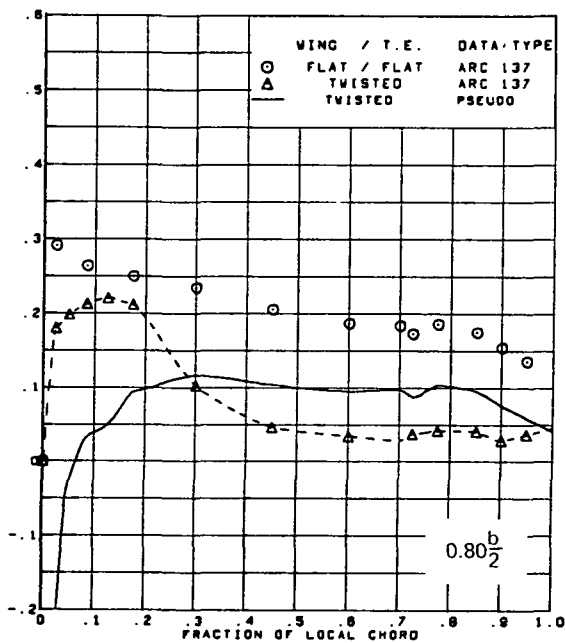
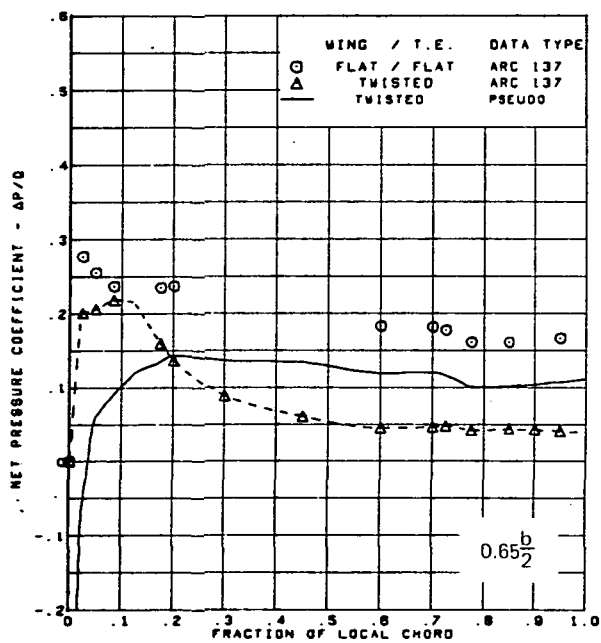
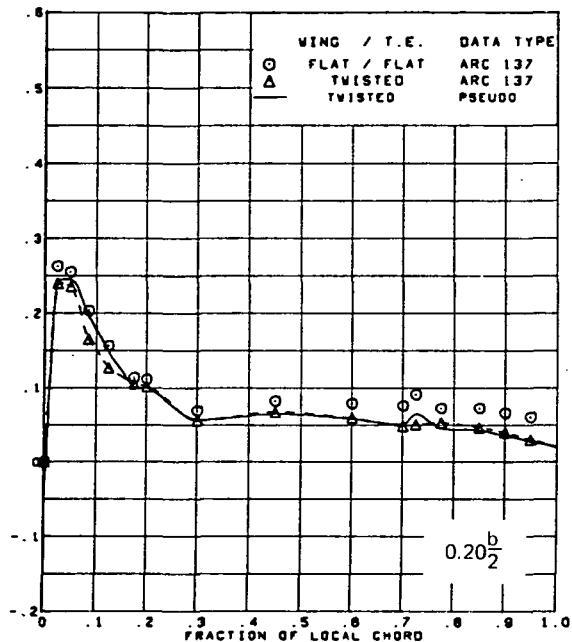
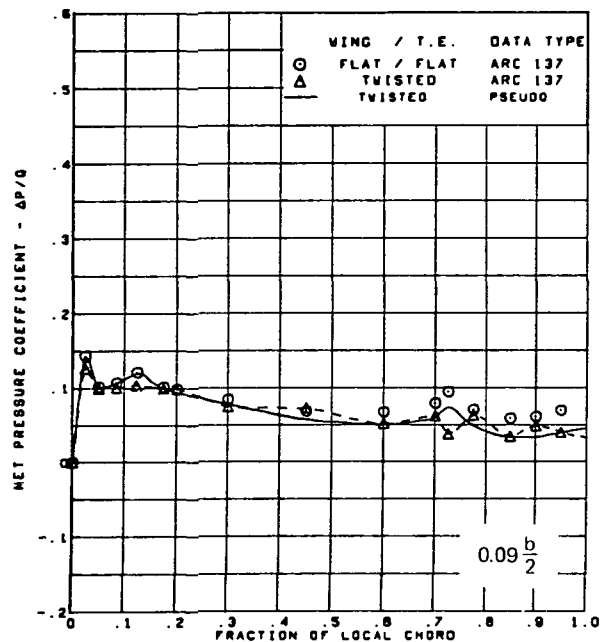
Figure 71.—(Continued)



$M = 2.10$   
 $\alpha = 4^\circ$   
 Rounded L.E.  
 L.E. deflection, full span =  $0.0^\circ$   
 T.E. deflection, full span =  $0.0^\circ$   
 Note:  $C_{p, \text{vacuum}} = -0.32$

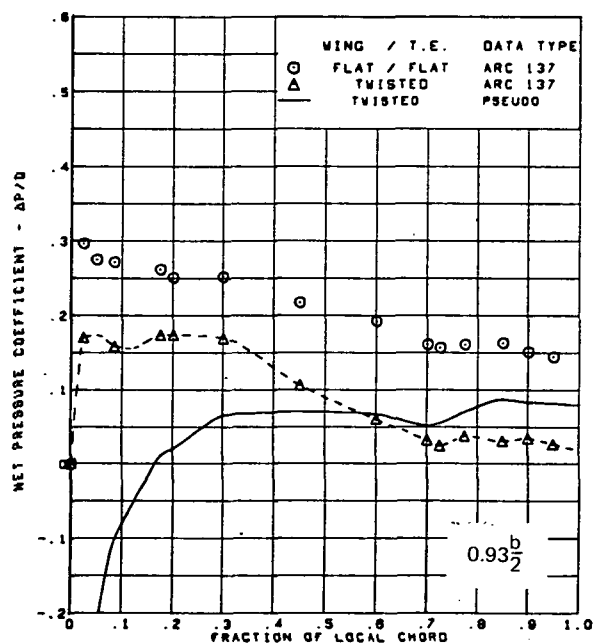
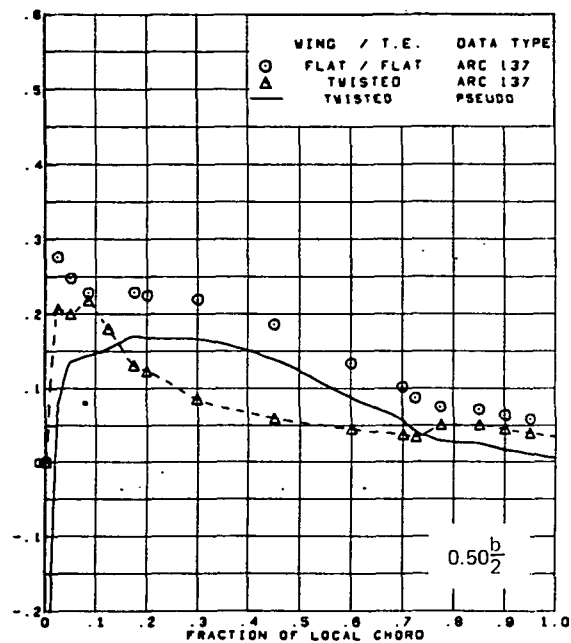
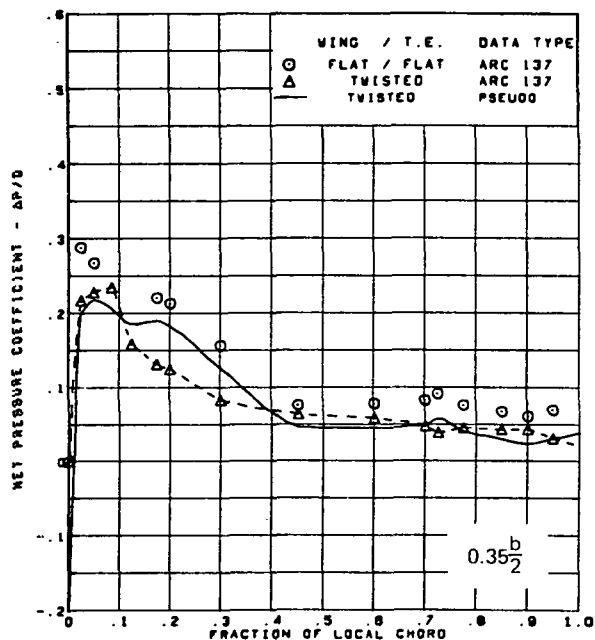
(b) (Concluded)

Figure 71.—(Continued)



(c) Net Chordwise Pressure Distributions,  $\alpha = 4^\circ$

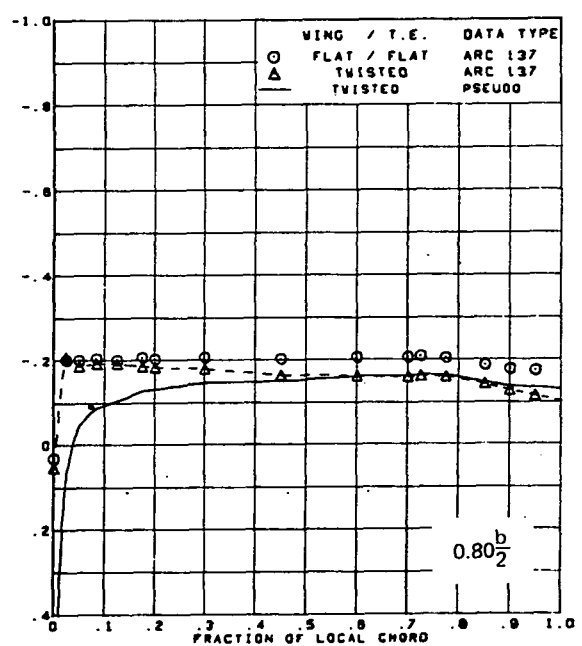
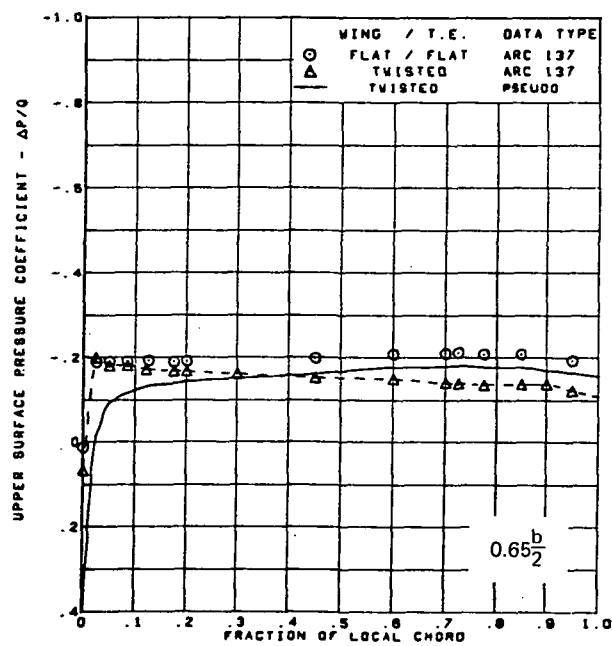
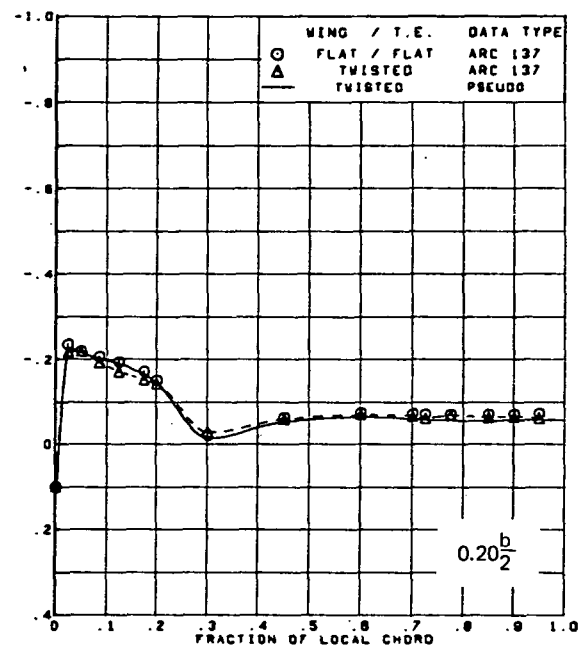
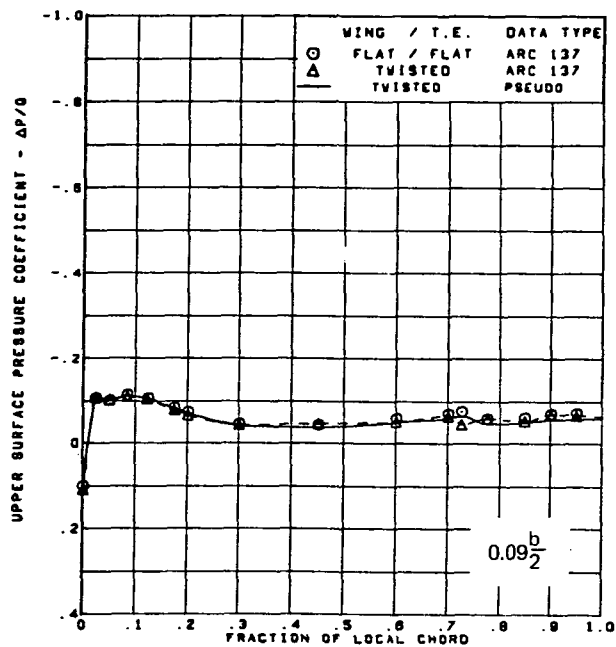
Figure 71.—(Continued)



$M = 2.10$   
 $\alpha = 4^\circ$   
 Rounded L.E.  
 L.E. deflection, full span =  $0.0^\circ$   
 T.E. deflection, full span =  $0.0^\circ$

(c) (Concluded)

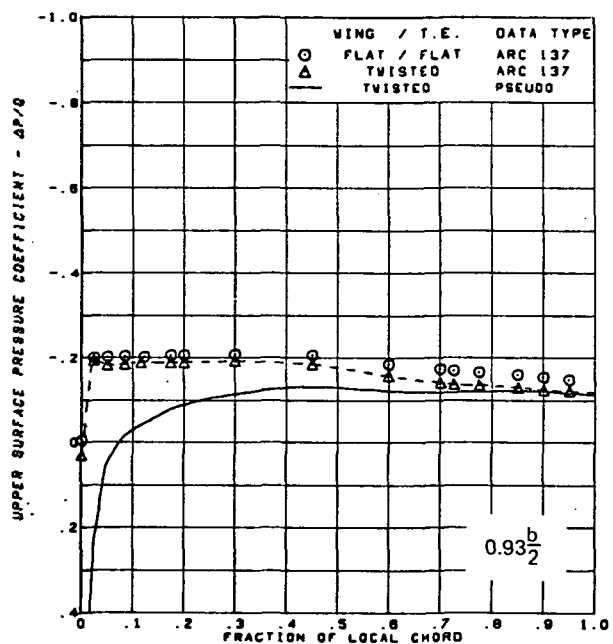
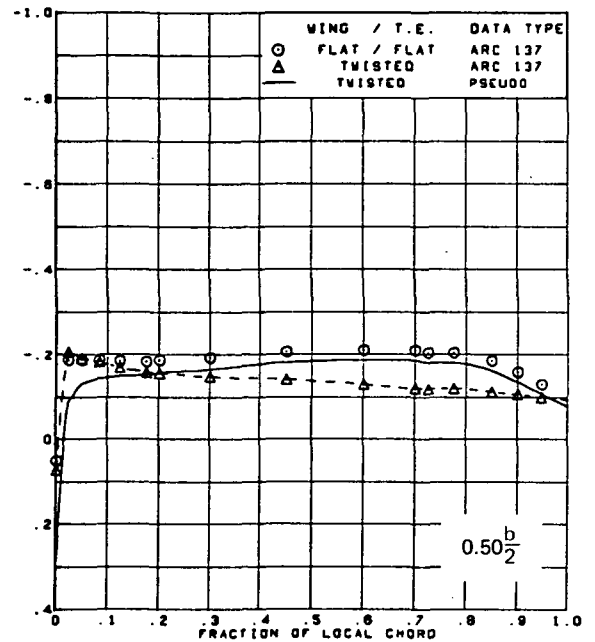
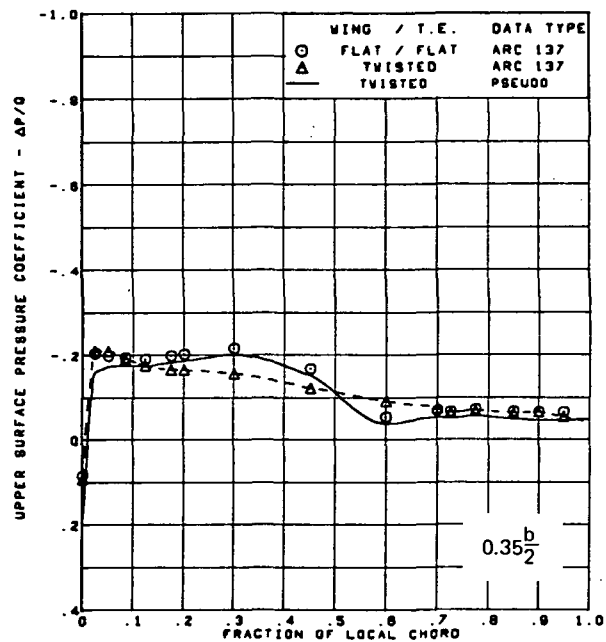
Figure 71.—(Continued)



(d) Upper Surface Chordwise Pressure Distributions,  $\alpha = 6^\circ$

Figure 71.—(Continued)



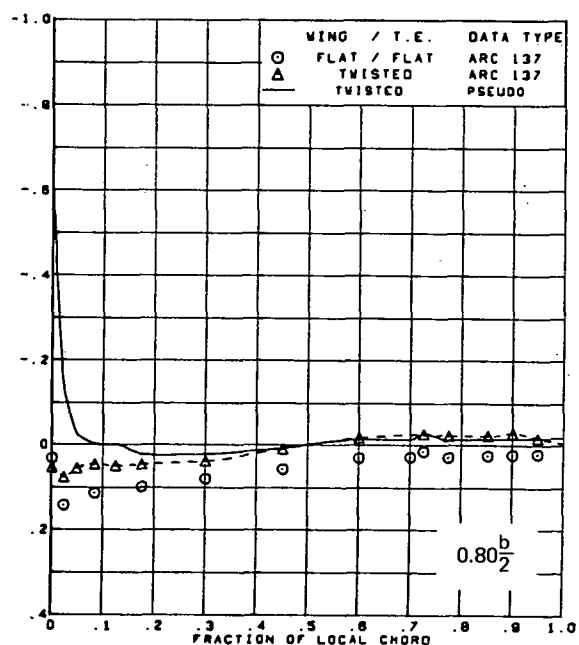
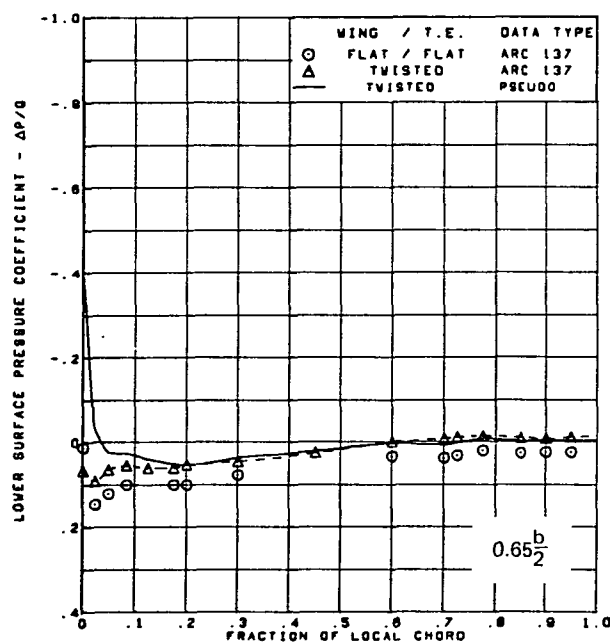
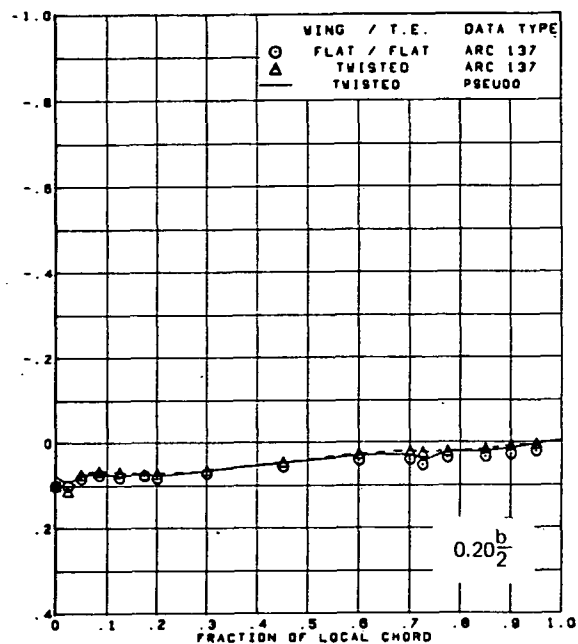
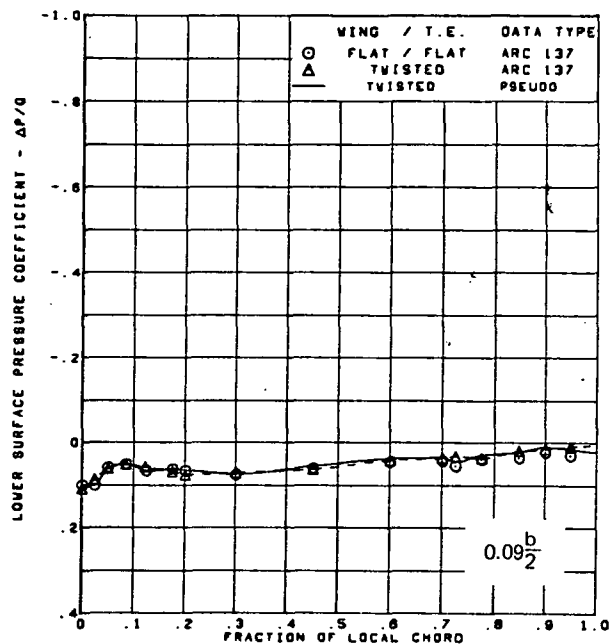


$M = 2.10$   
 $\alpha = 6^\circ$   
 Rounded L.E.  
 L.E. deflection, full span =  $0.0^\circ$   
 T.E. deflection, full span =  $0.0^\circ$

Note:  $C_{p, \text{vacuum}} = -0.32$

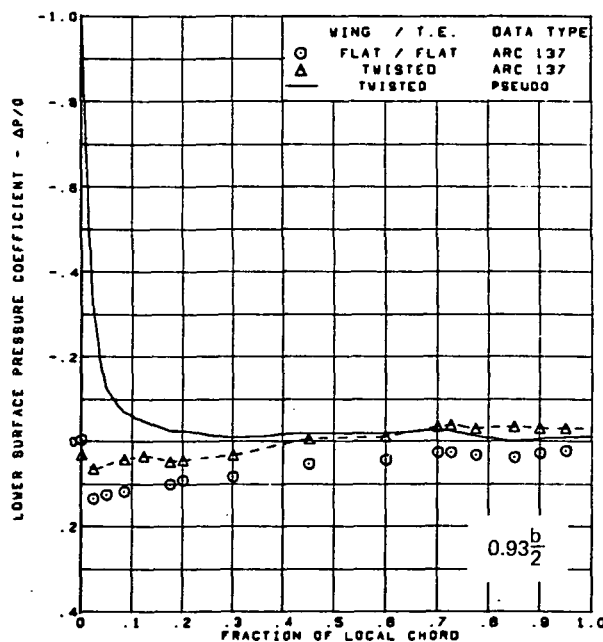
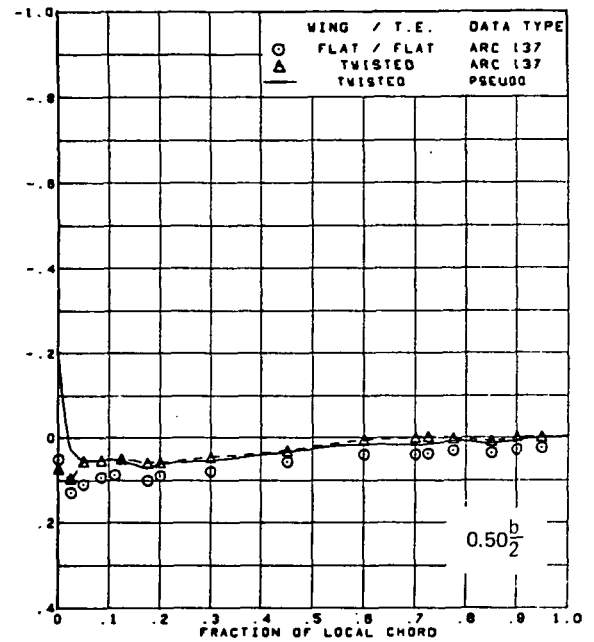
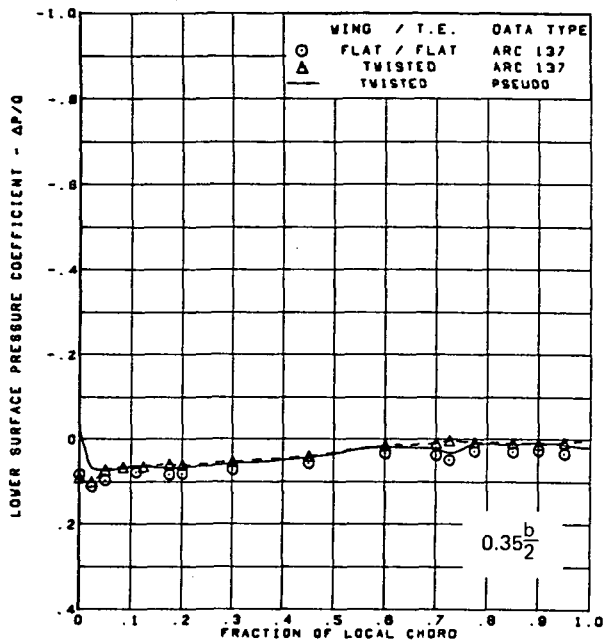
(d) (Concluded)

Figure 71.—(Continued)



(e) Lower Surface Chordwise Pressure Distributions,  $\alpha = 6^\circ$

Figure 71.—(Continued)

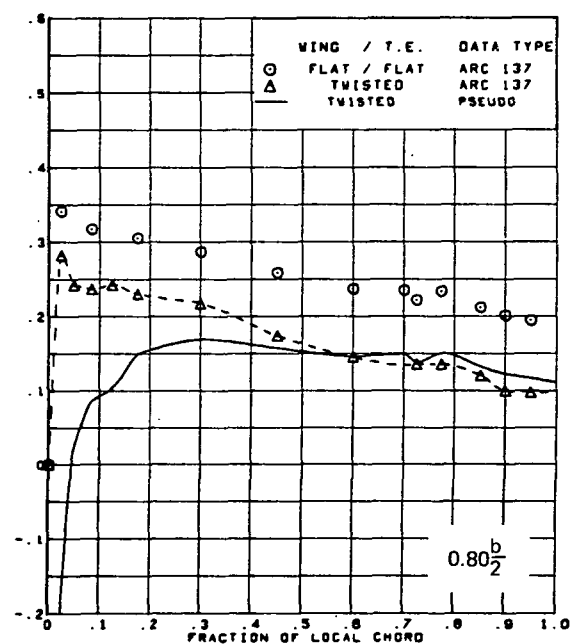
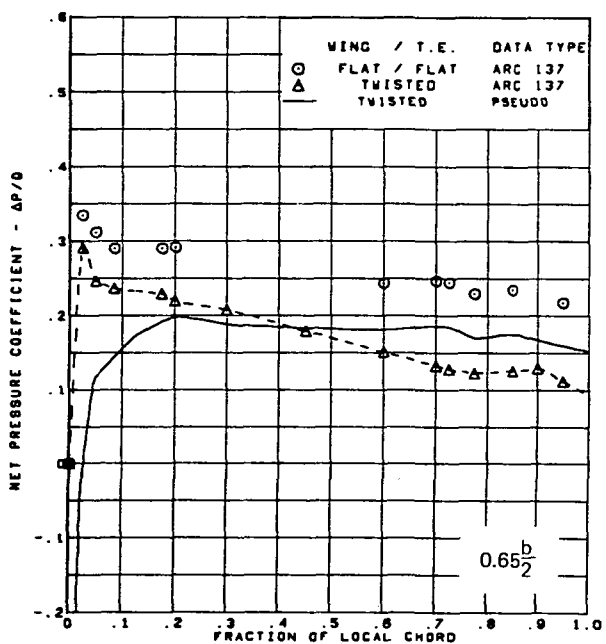
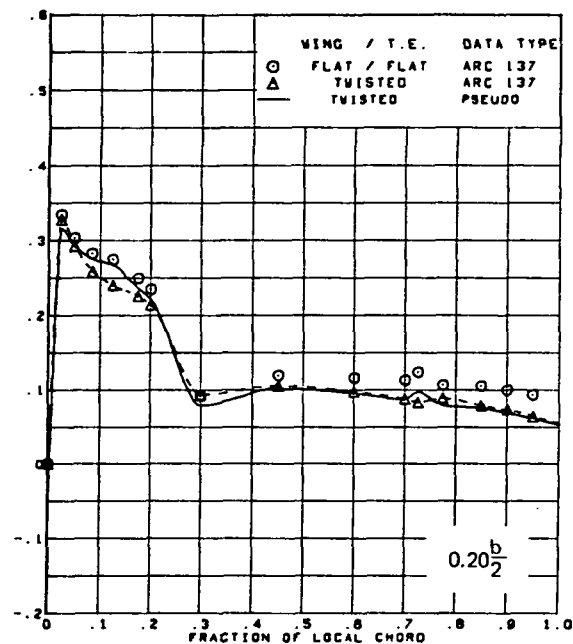
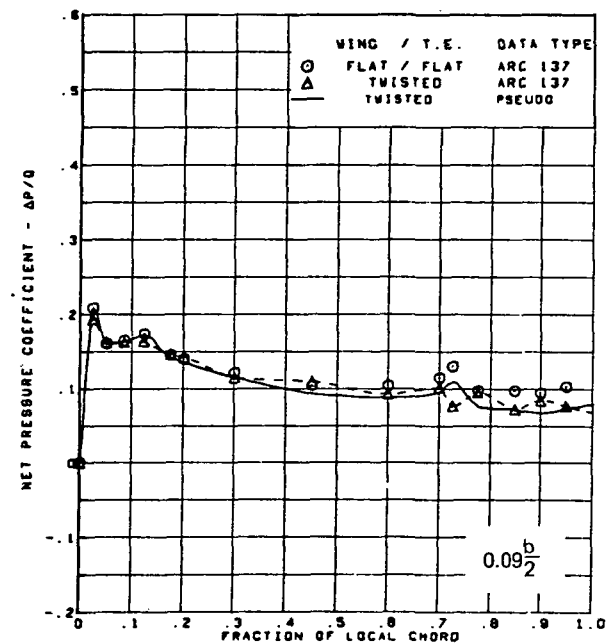


$M = 2.10$   
 $\alpha = 6^\circ$   
 Rounded L.E.  
 L.E. deflection, full span =  $0.0^\circ$   
 T.E. deflection, full span =  $0.0^\circ$

Note:  $C_{p, \text{vacuum}} = -0.32$

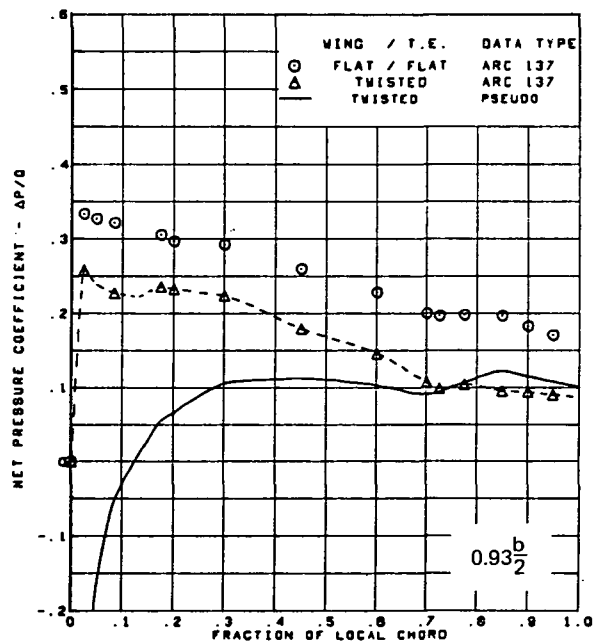
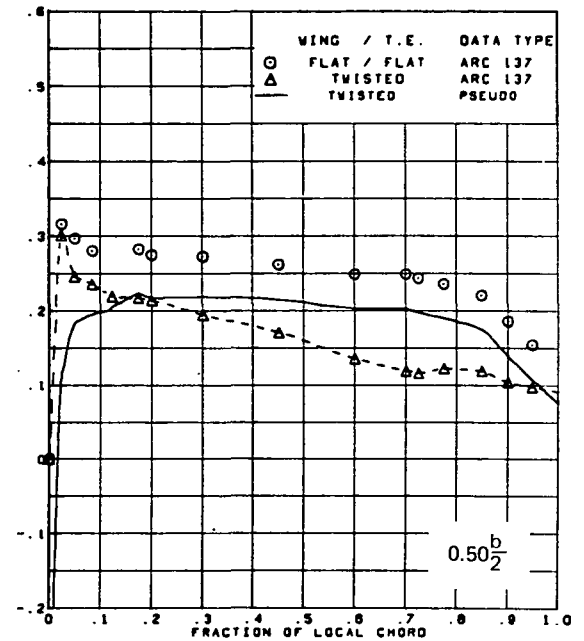
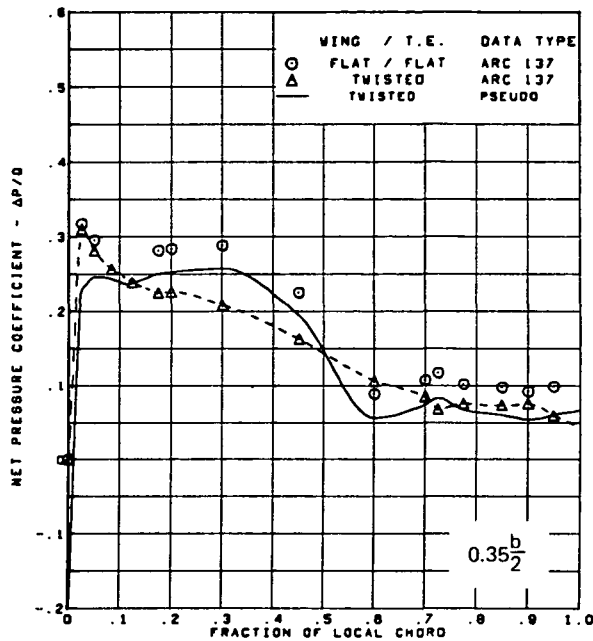
(e) (Concluded)

Figure 71.—(Continued)



(f) Net Chordwise Pressure Distributions,  $\alpha = 6^\circ$

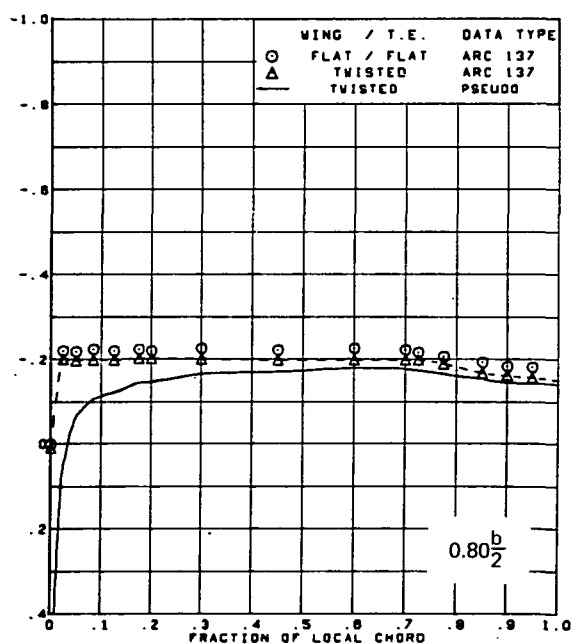
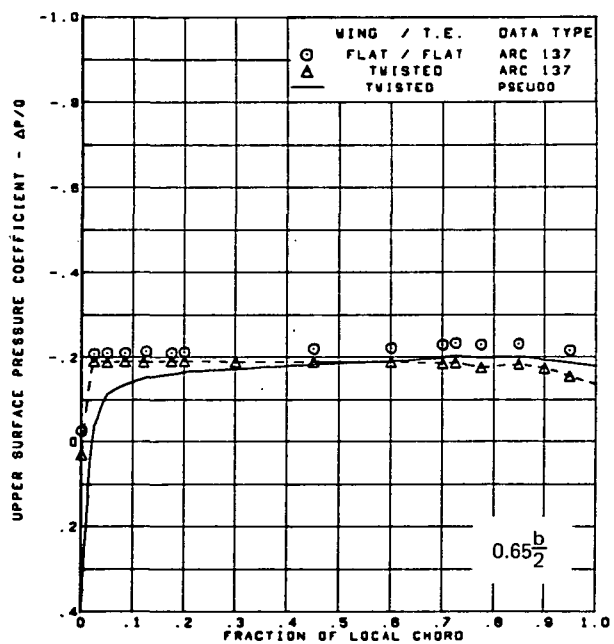
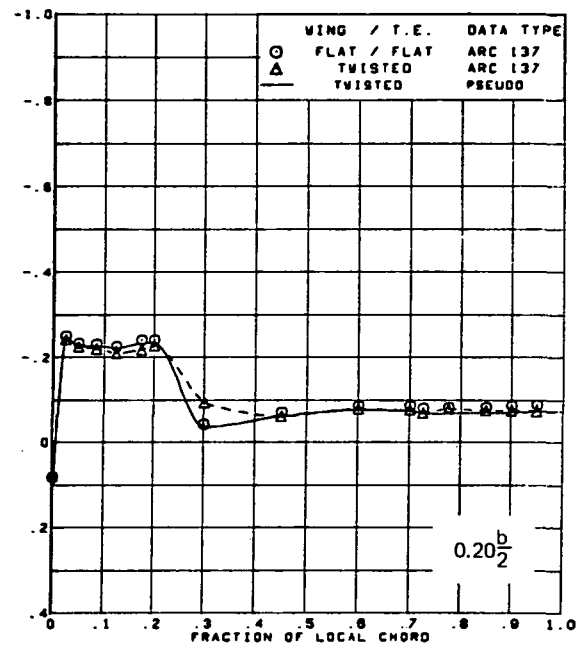
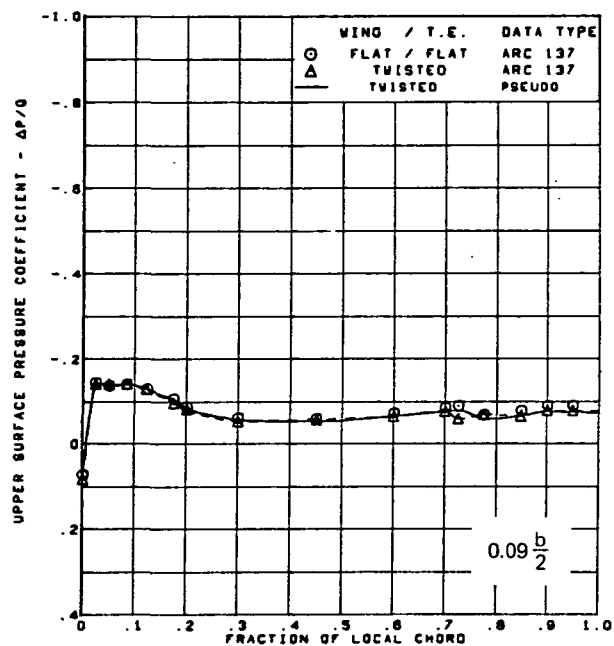
Figure 71.—(Continued)



$M = 2.10$   
 $\alpha = 6^\circ$   
 Rounded L.E.  
 L.E. deflection, full span =  $0.0^\circ$   
 T.E. deflection, full span =  $0.0^\circ$

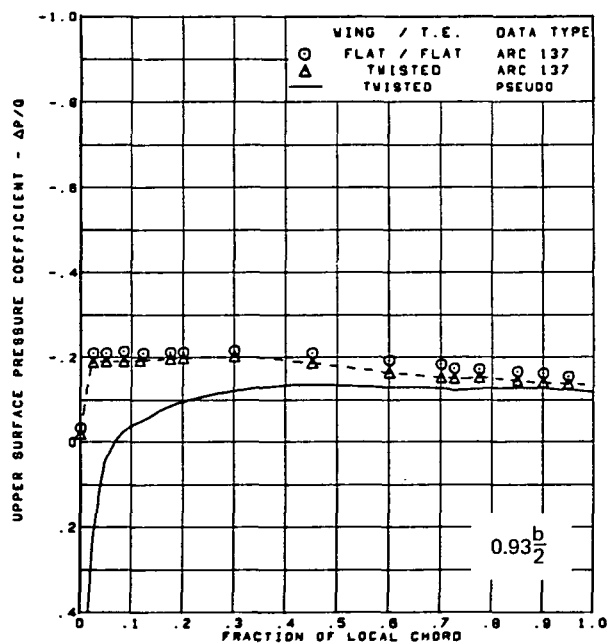
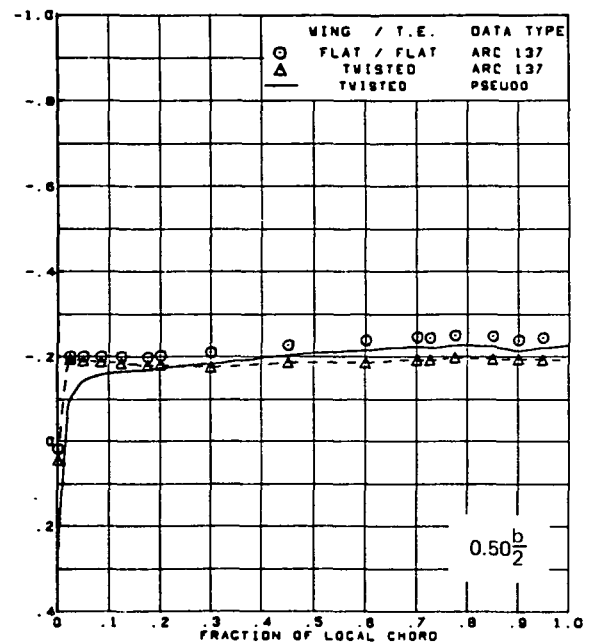
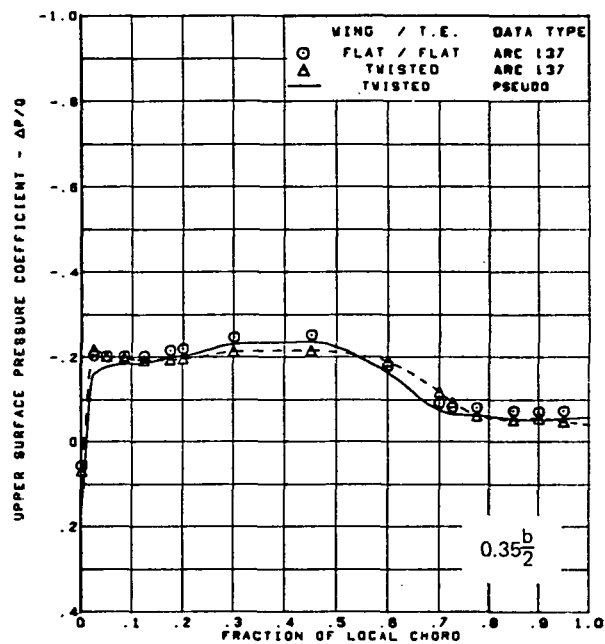
(f) (Concluded)

Figure 71.—(Continued)



(g) Upper Surface Chordwise Pressure Distributions,  $\alpha = 8^\circ$

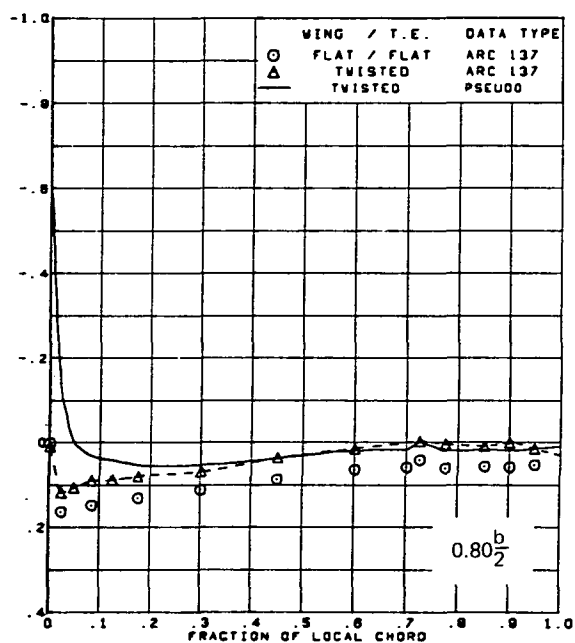
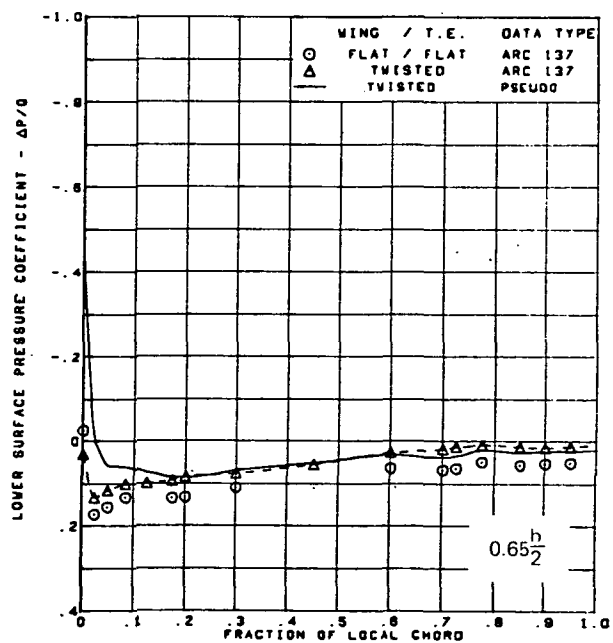
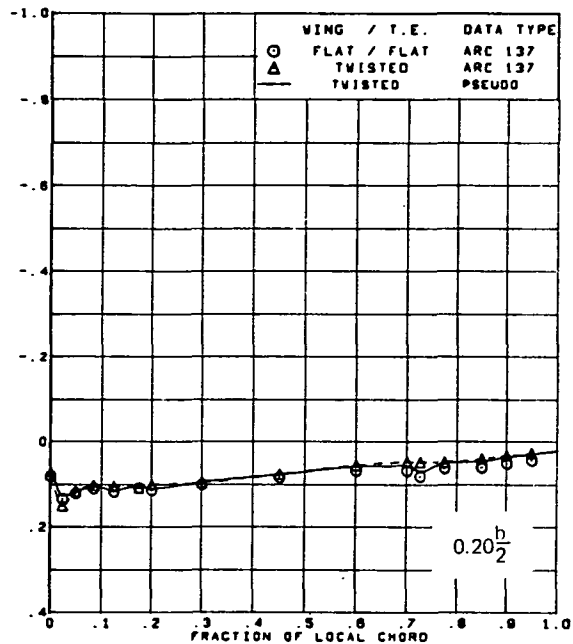
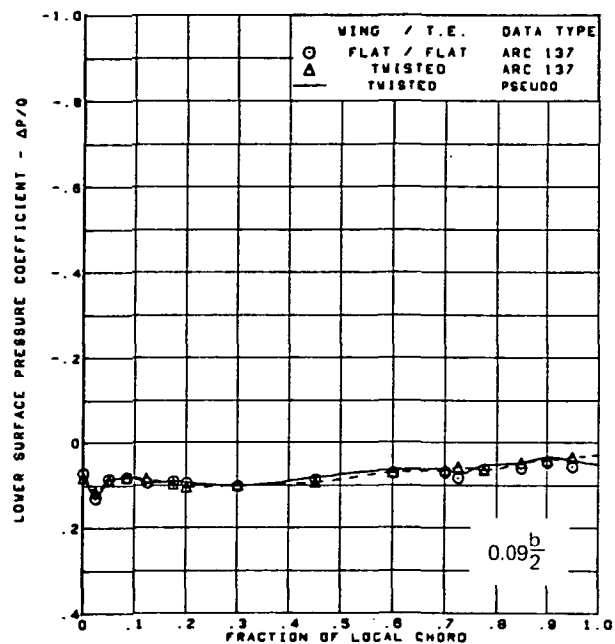
Figure 71.—(Continued)



$M = 2.10$   
 $\alpha = 8^\circ$   
 Rounded L.E.  
 L.E. deflection, full span =  $0.0^\circ$   
 T.E. deflection, full span =  $0.0^\circ$   
 Note:  $C_{p, \text{vacuum}} = -0.32$

(g) (Concluded)

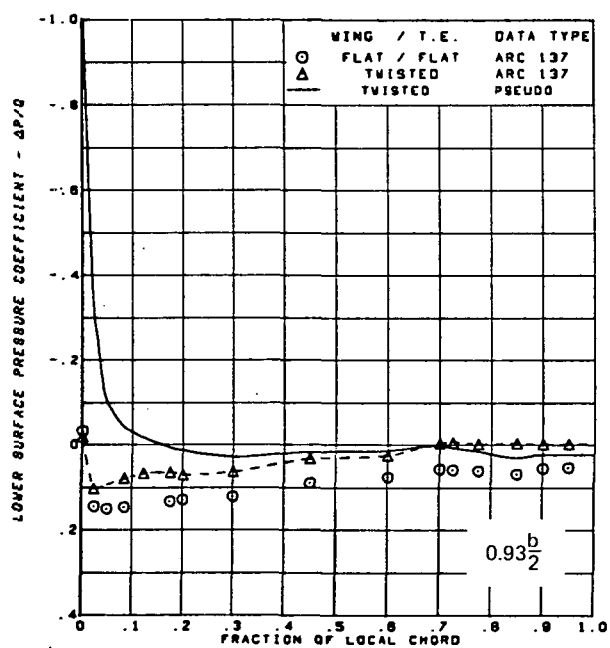
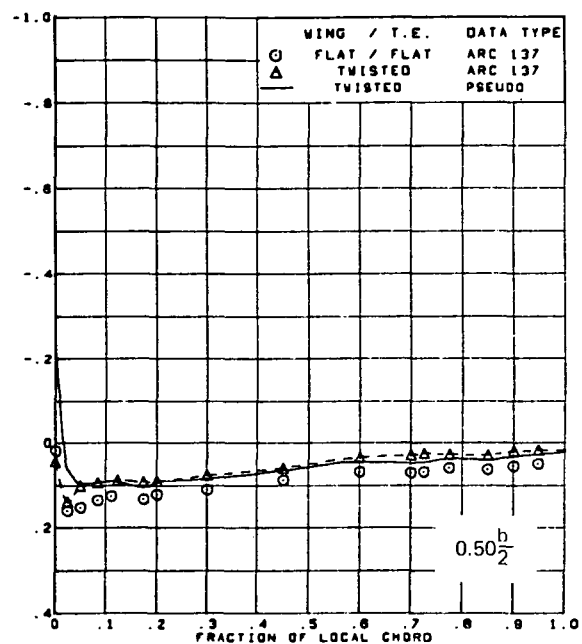
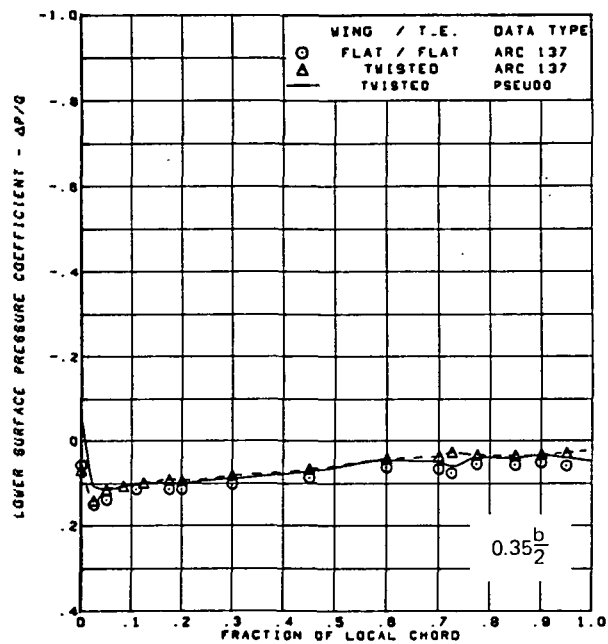
Figure 71.—(Continued)



(h) Lower Surface Chordwise Pressure Distributions,  $\alpha = 8^\circ$

Figure 71.—(Continued)

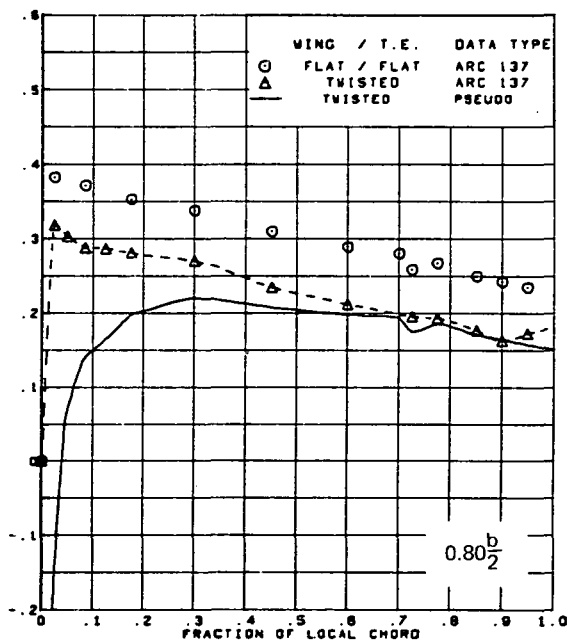
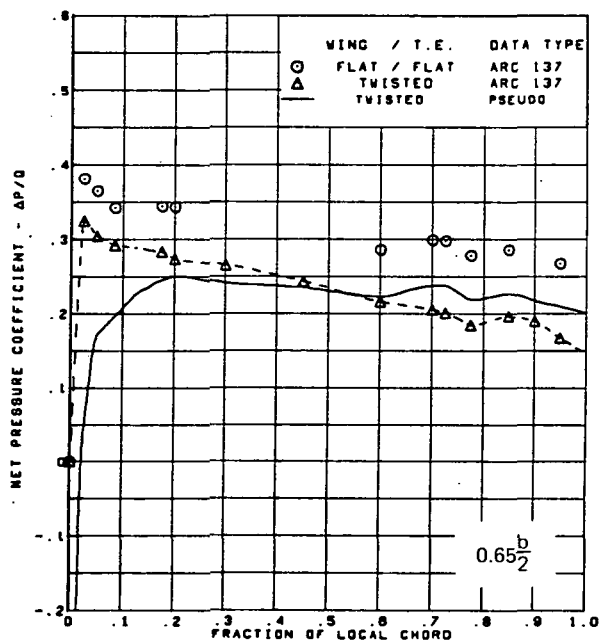
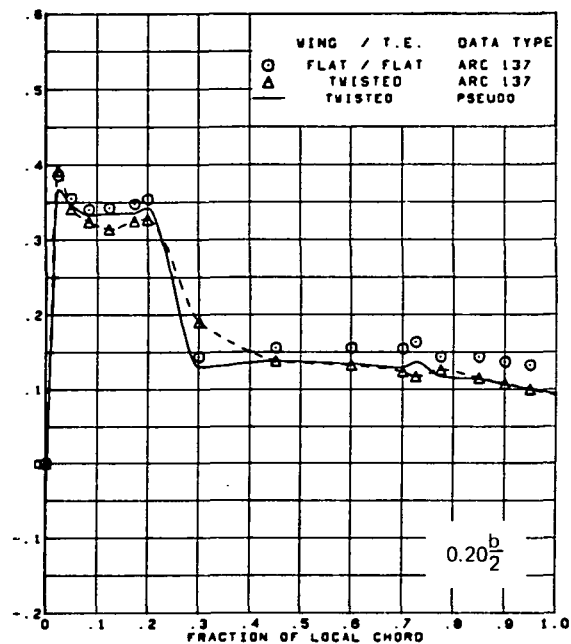
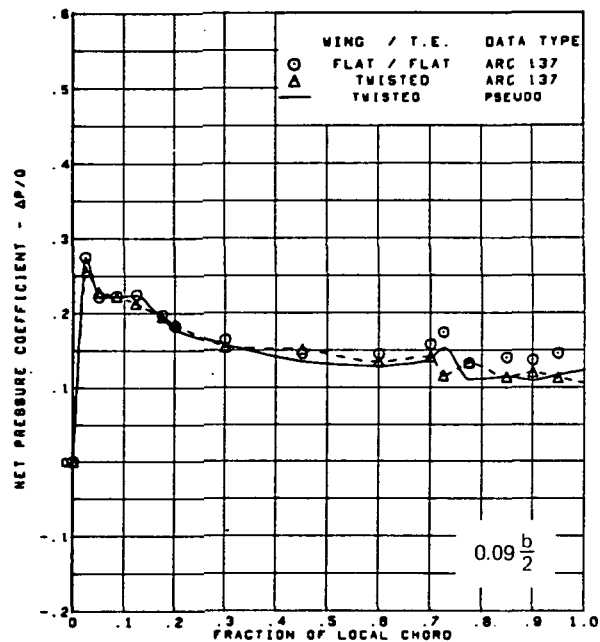




$M = 2.10$   
 $\alpha = 8^\circ$   
 Rounded L.E.  
 L.E. deflection, full span =  $0.0^\circ$   
 T.E. deflection, full span =  $0.0^\circ$   
 Note:  $C_{p, \text{vacuum}} = -0.32$

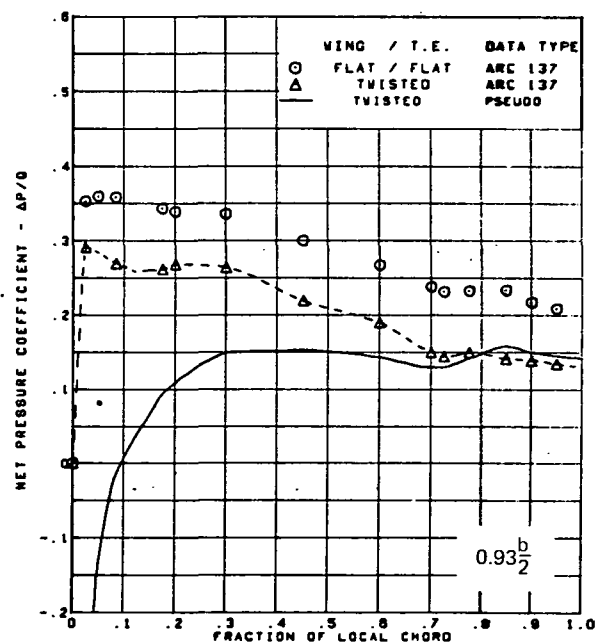
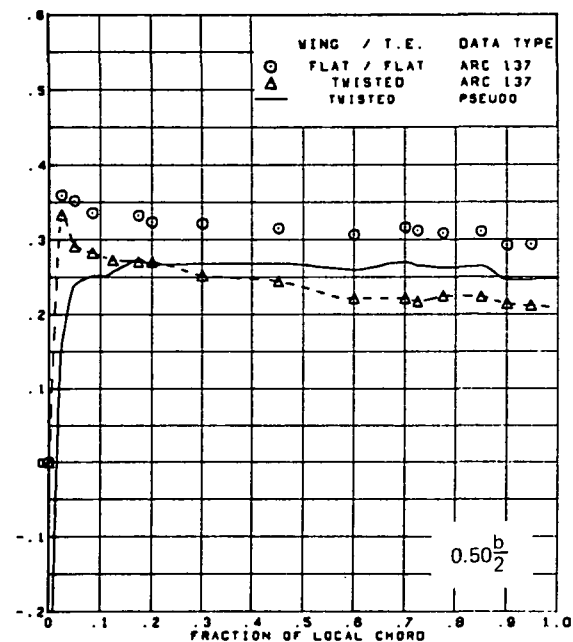
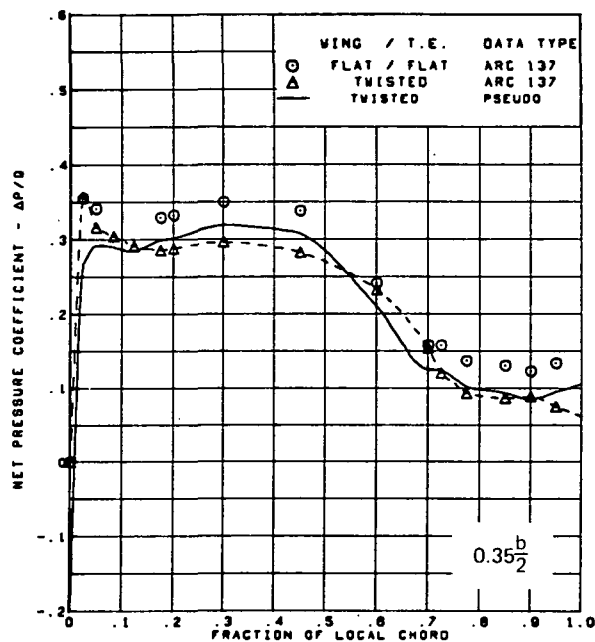
(h) (Concluded)

Figure 71.—(Continued)



(i) Net Chordwise Pressure Distributions,  $\alpha = 8^\circ$

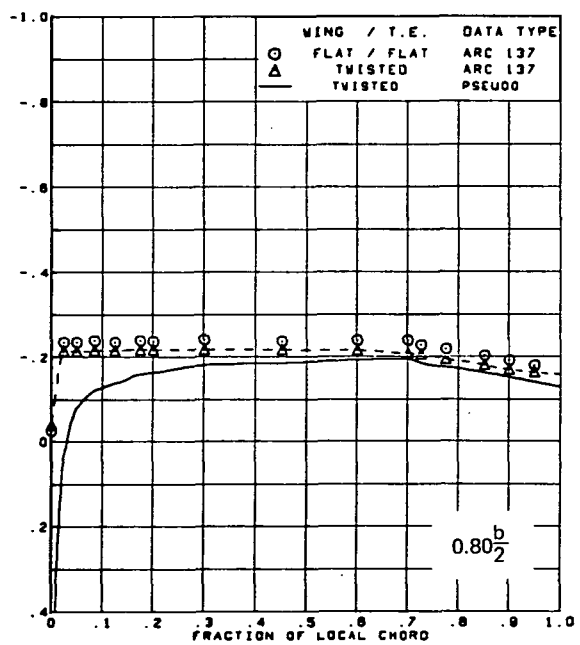
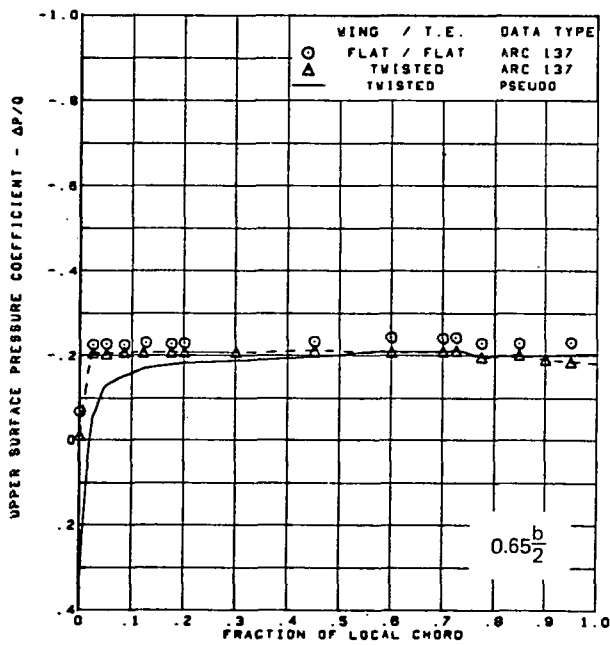
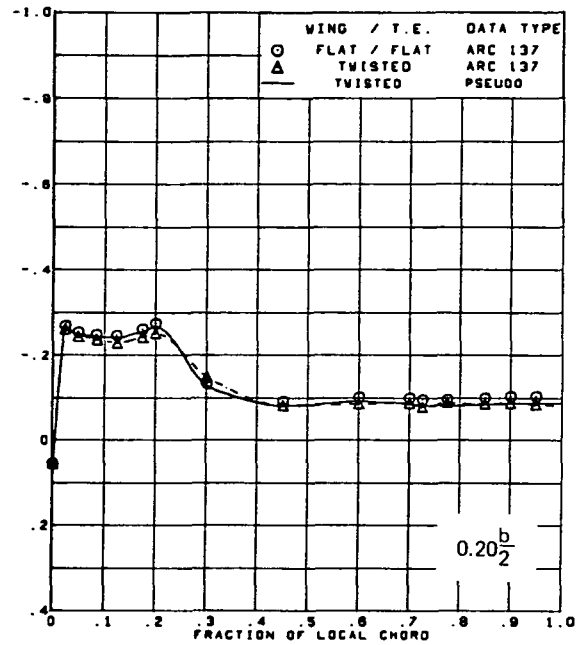
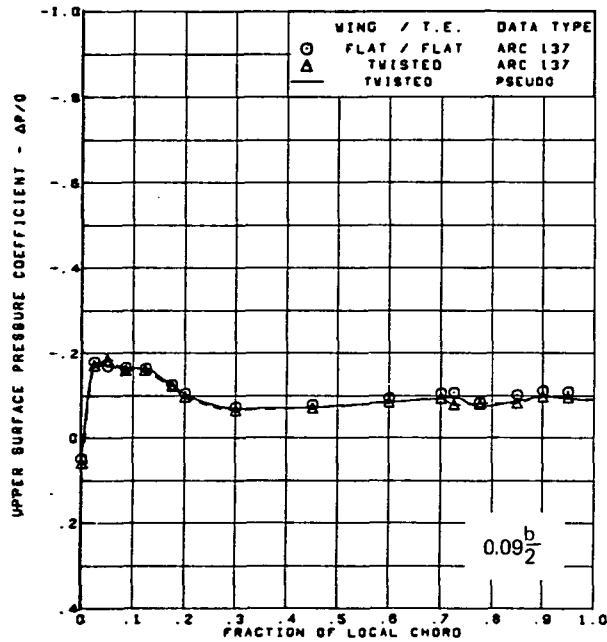
Figure 71.—(Continued)



$M = 2.10$   
 $\alpha = 8^\circ$   
 Rounded L.E.  
 L.E. deflection, full span =  $0.0^\circ$   
 T.E. deflection, full span =  $0.0^\circ$

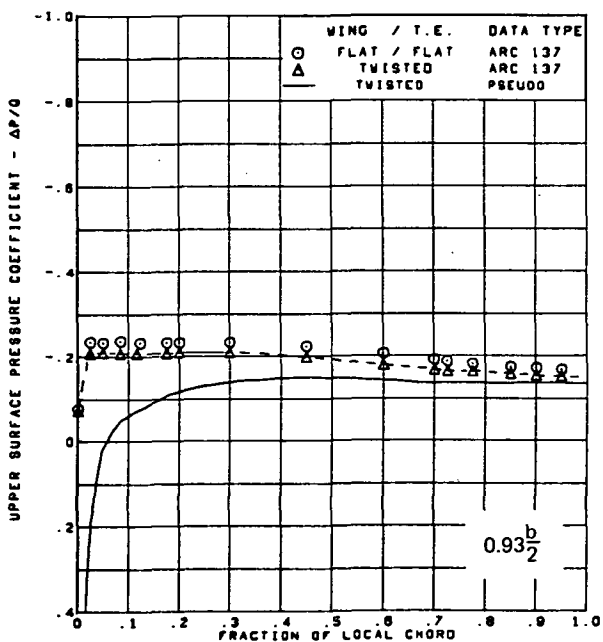
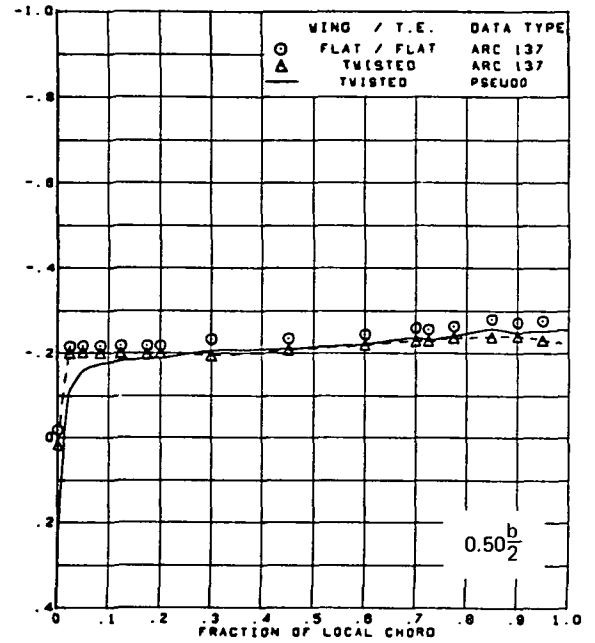
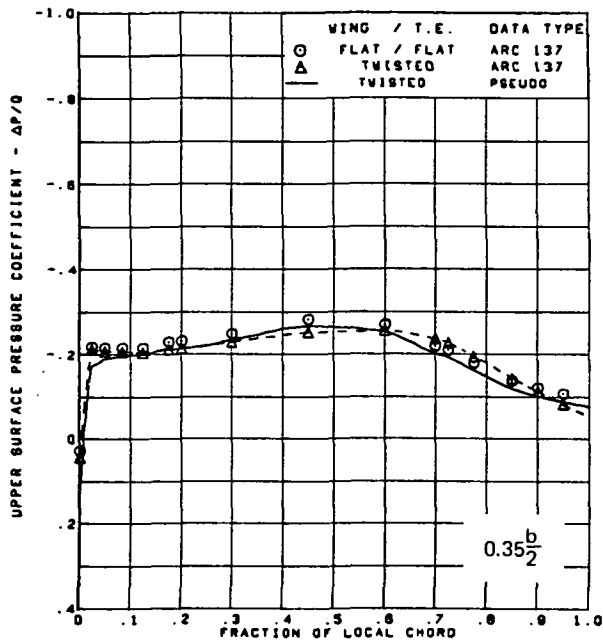
(i) (Concluded)

Figure 71.—(Continued)



(j) Upper Surface Chordwise Pressure Distributions,  $\alpha = 10^\circ$

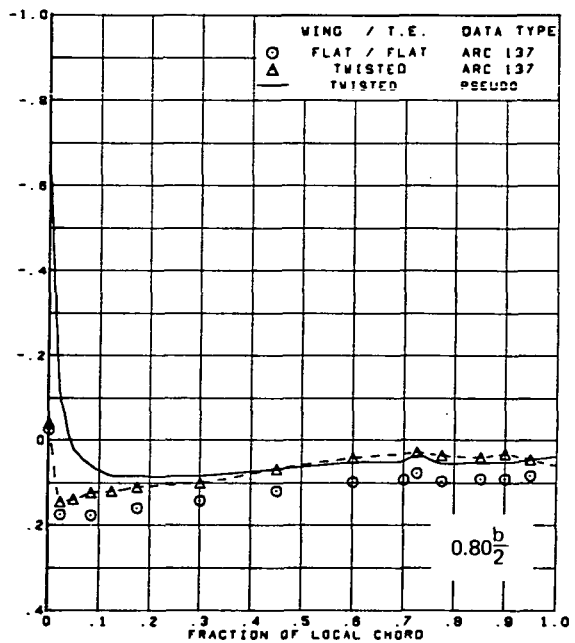
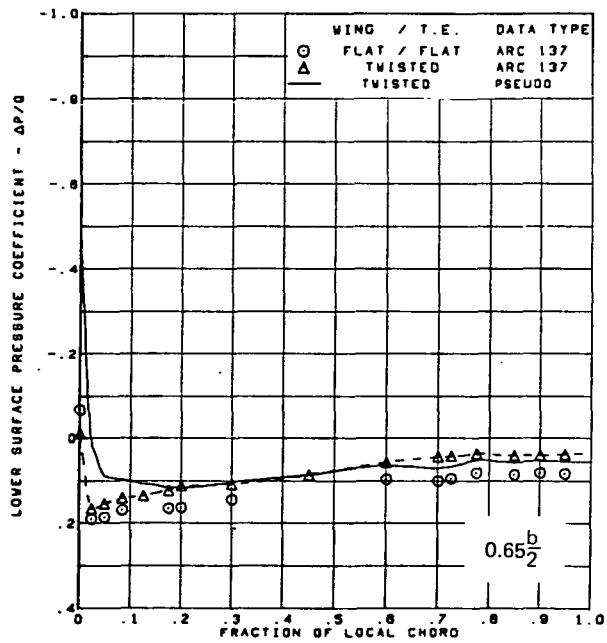
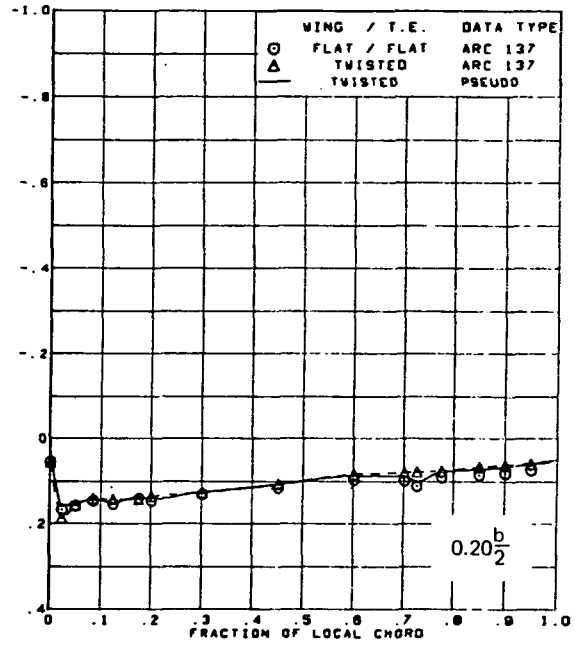
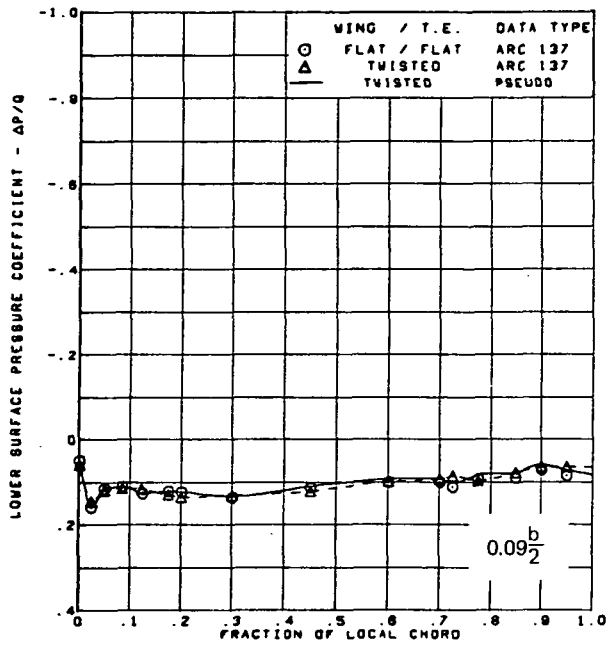
Figure 71.—(Continued)



$M = 2.10$   
 $\alpha = 10^\circ$   
 Rounded L.E.  
 L.E. deflection, full span =  $0.0^\circ$   
 T.E. deflection, full span =  $0.0^\circ$   
 Note:  $C_{p, \text{vacuum}} = -0.32$

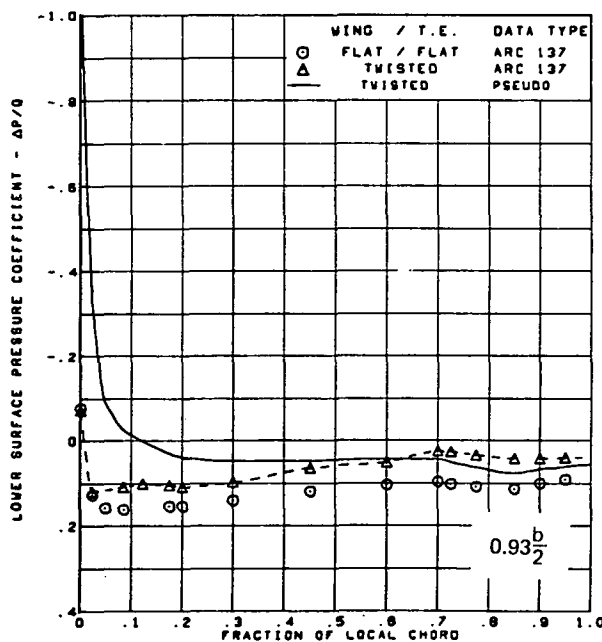
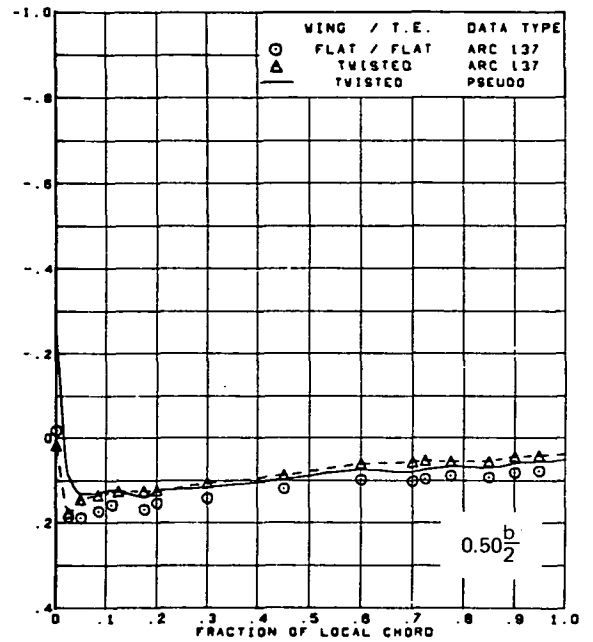
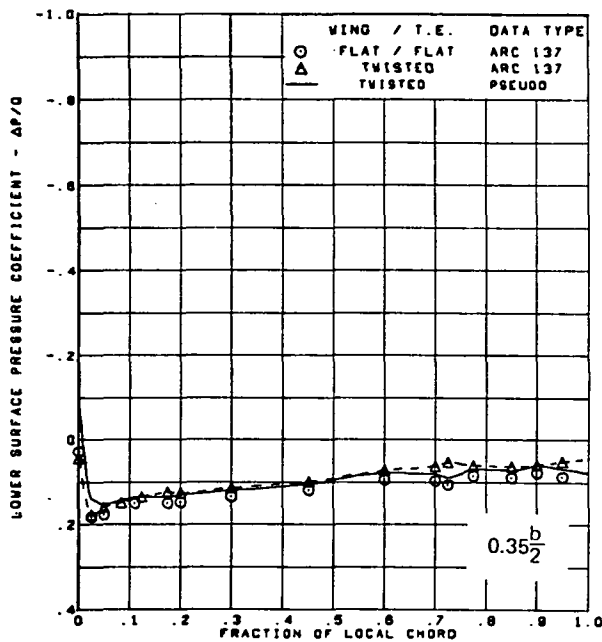
(j) (Concluded)

Figure 71.—(Continued)



(k) Lower Surface Chordwise Pressure Distributions,  $\alpha = 10^\circ$

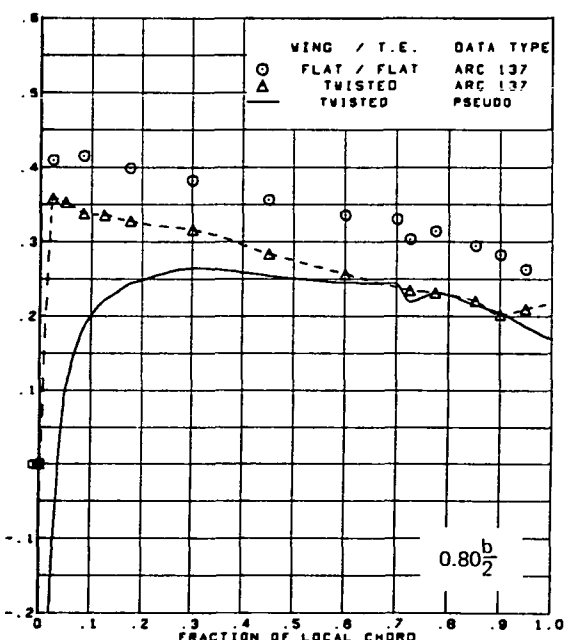
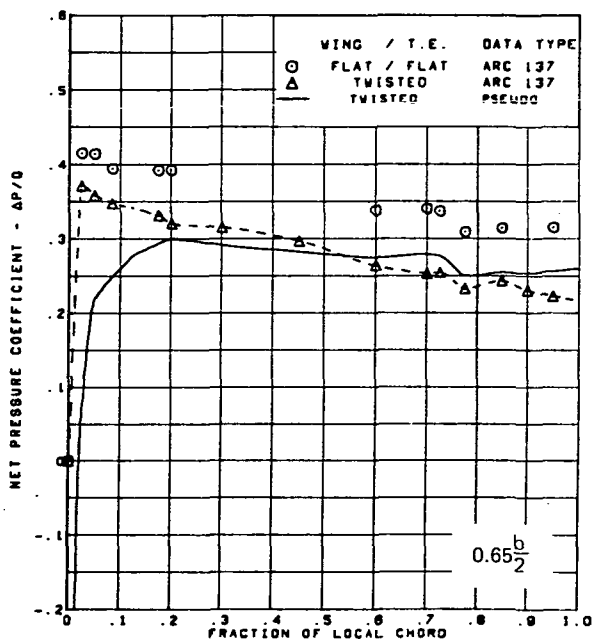
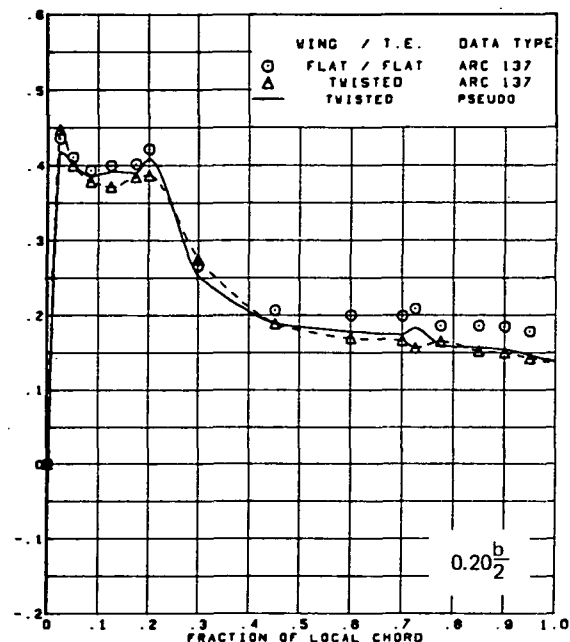
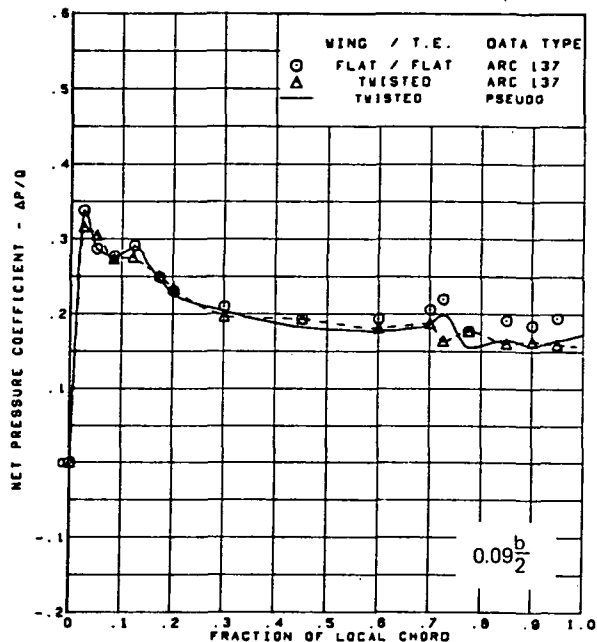
Figure 71.—(Continued)



$M = 2.10$   
 $\alpha = 10^\circ$   
 Rounded L.E.  
 L.E. deflection, full span =  $0.0^\circ$   
 T.E. deflection, full span =  $0.0^\circ$   
 Note:  $C_{p, \text{vacuum}} = -0.32$

(k) (Concluded)

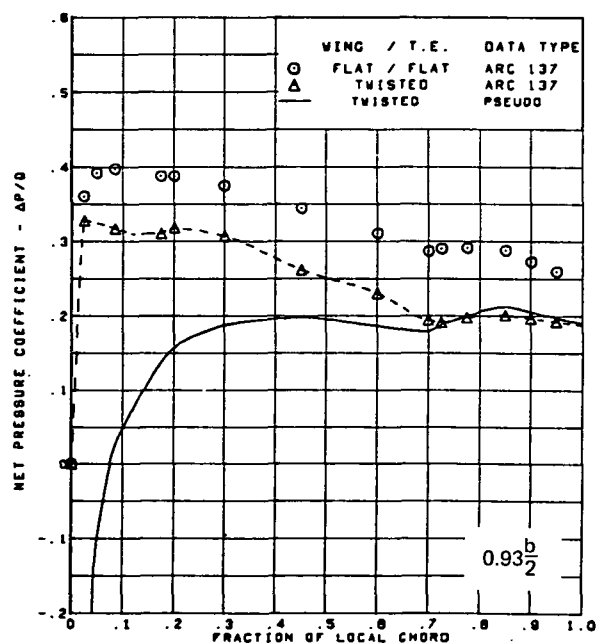
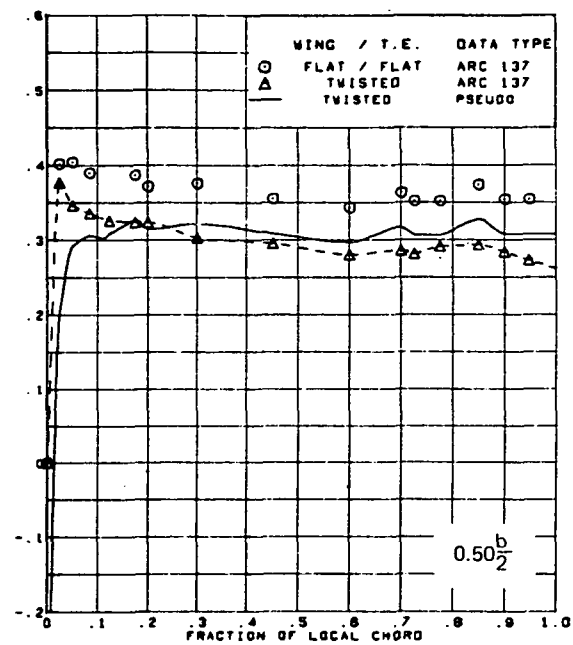
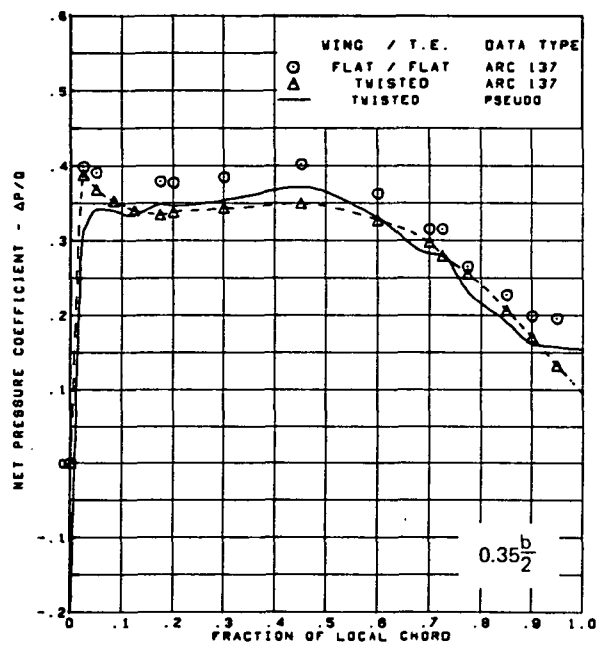
Figure 71.—(Continued)



(I) Net Chordwise Pressure Distributions,  $\alpha = 10^\circ$

Figure 71.—(Continued)

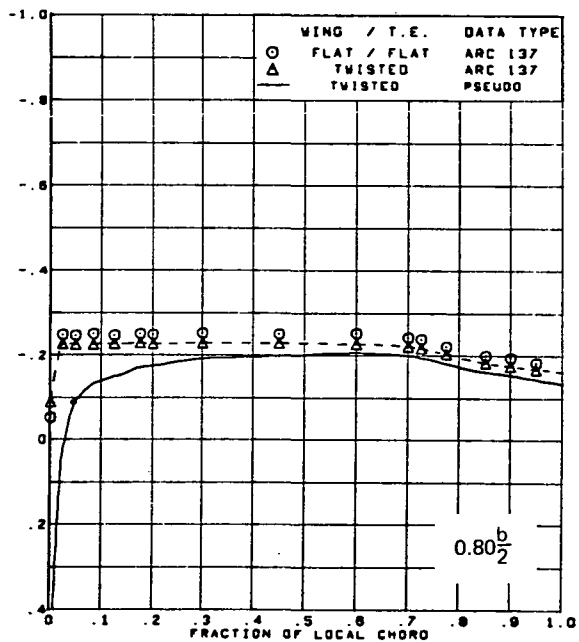
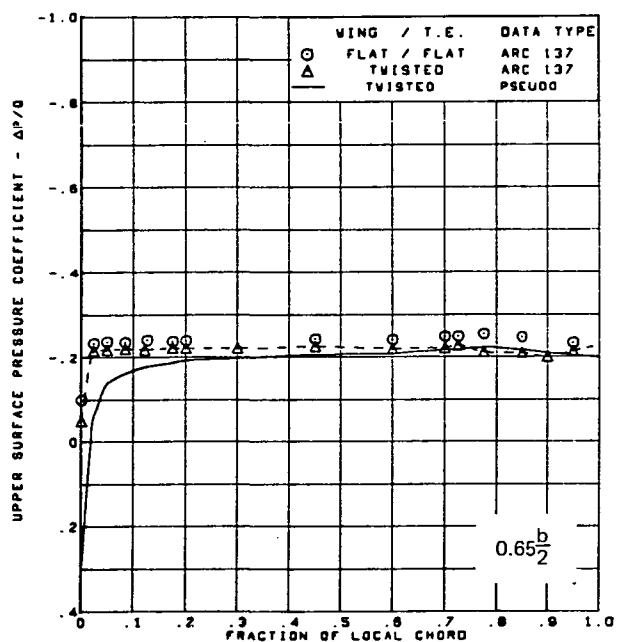
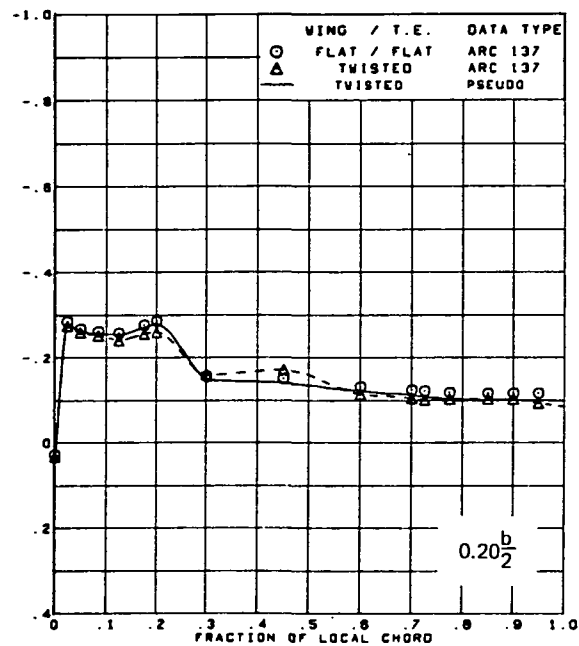
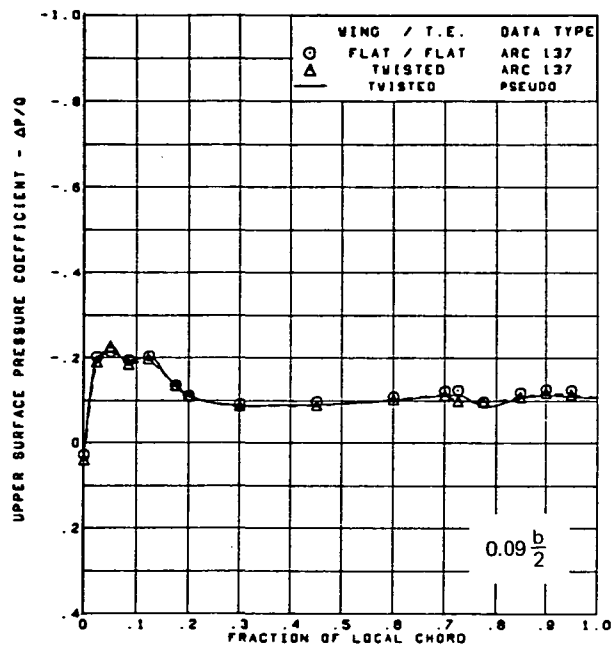




$M = 2.10$   
 $\alpha = 10^\circ$   
 Rounded L.E.  
 L.E. deflection, full span =  $0.0^\circ$   
 T.E. deflection, full span =  $0.0^\circ$

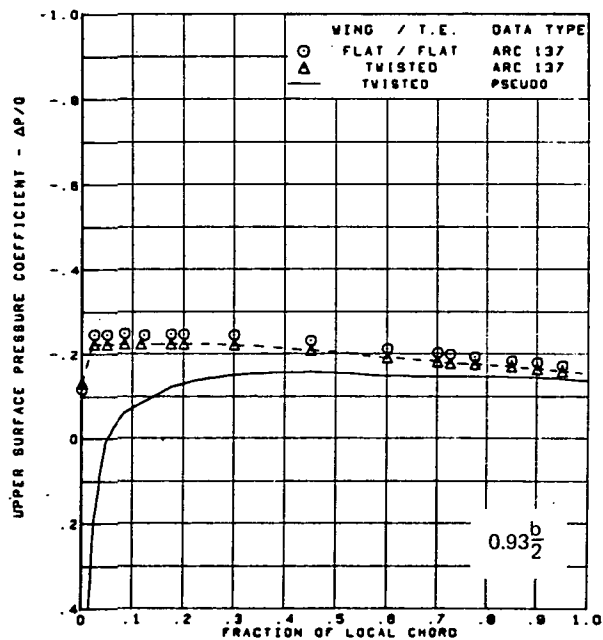
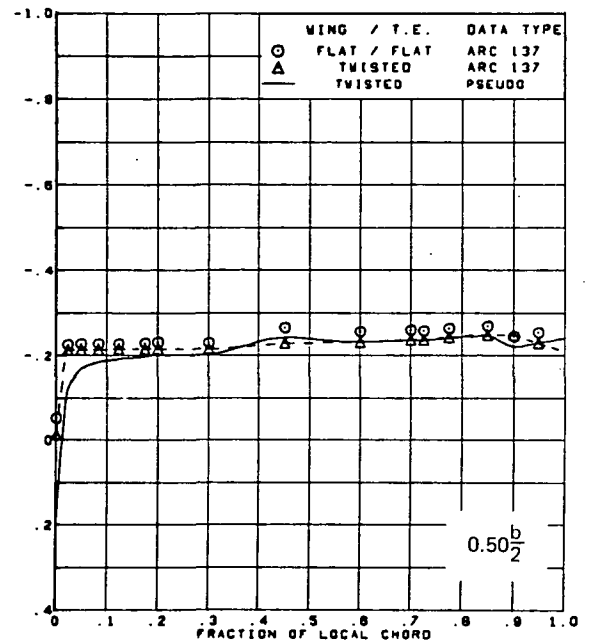
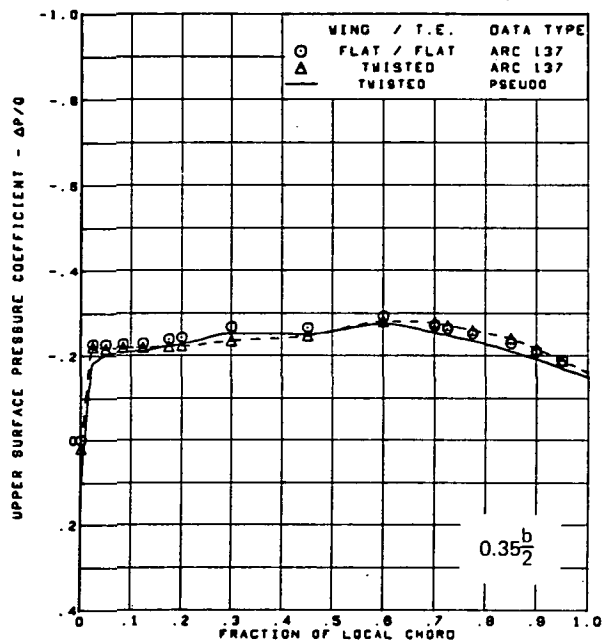
(1) (Concluded)

Figure 71.—(Continued)



(m) Upper Surface Chordwise Pressure Distributions,  $\alpha = 12^\circ$

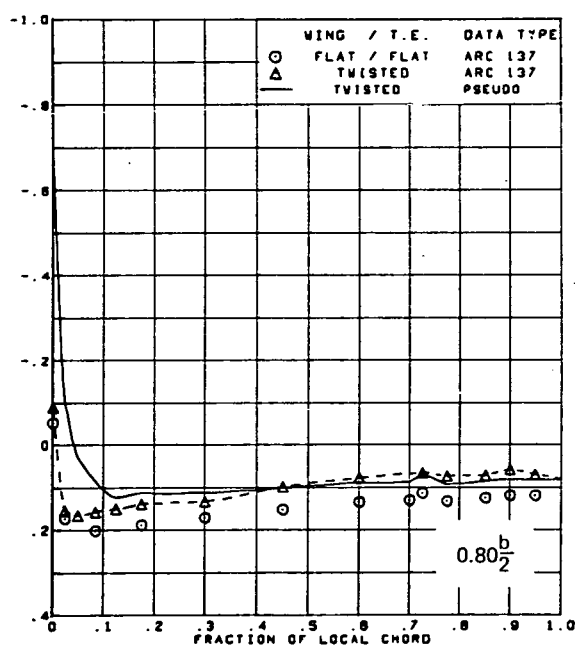
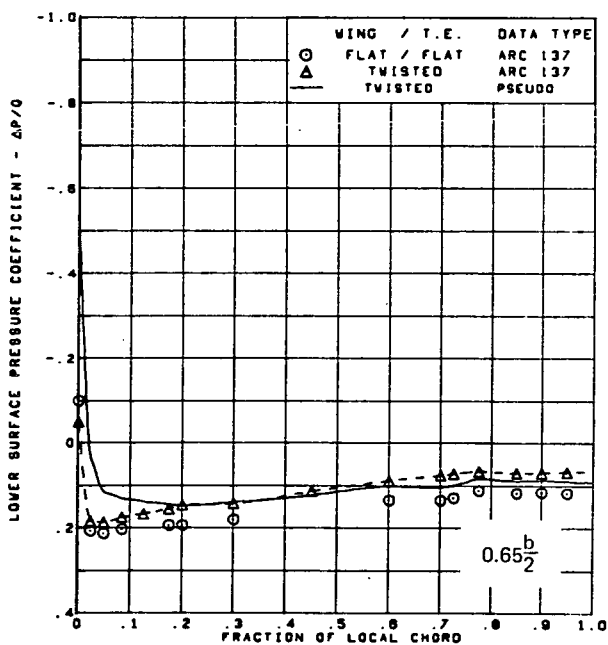
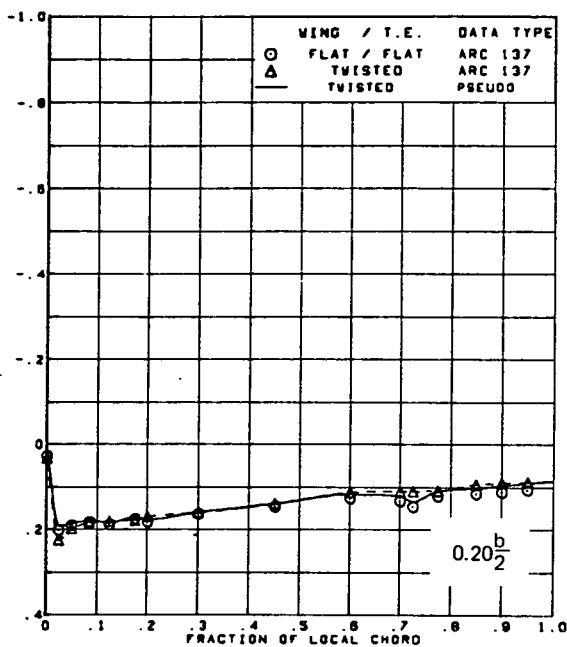
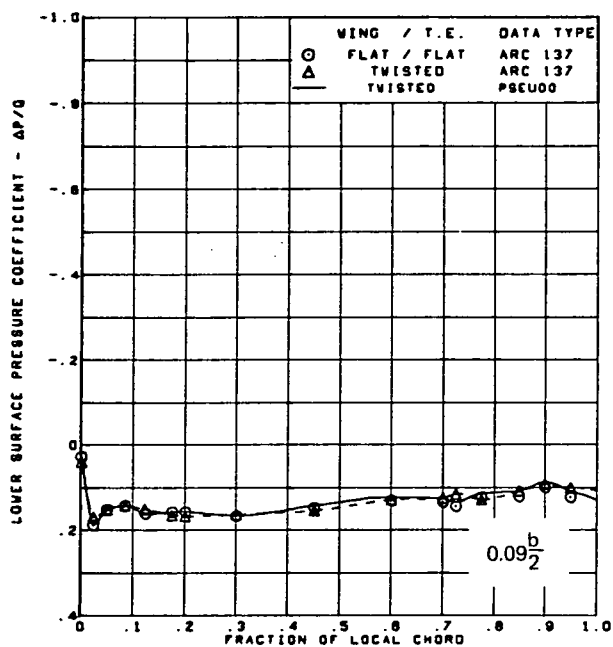
Figure 71.—(Continued)



$M = 2.10$   
 $\alpha = 12^\circ$   
 Rounded L.E.  
 L.E. deflection, full span =  $0.0^\circ$   
 T.E. deflection, full span =  $0.0^\circ$   
 Note:  $C_{p, \text{vacuum}} = -0.32$

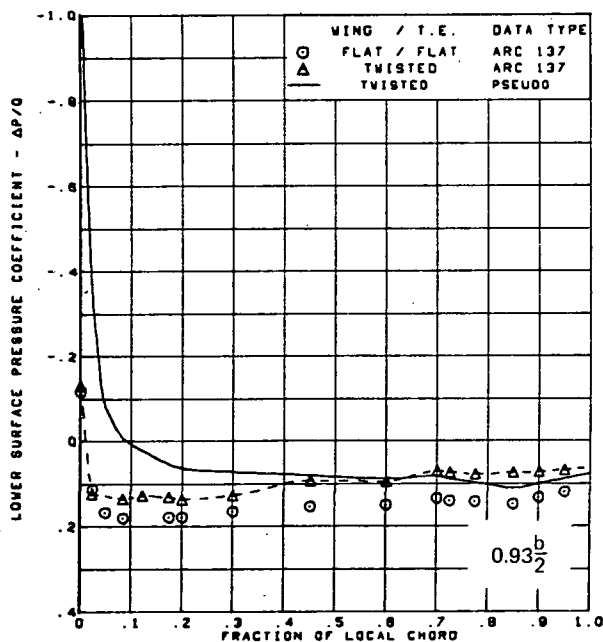
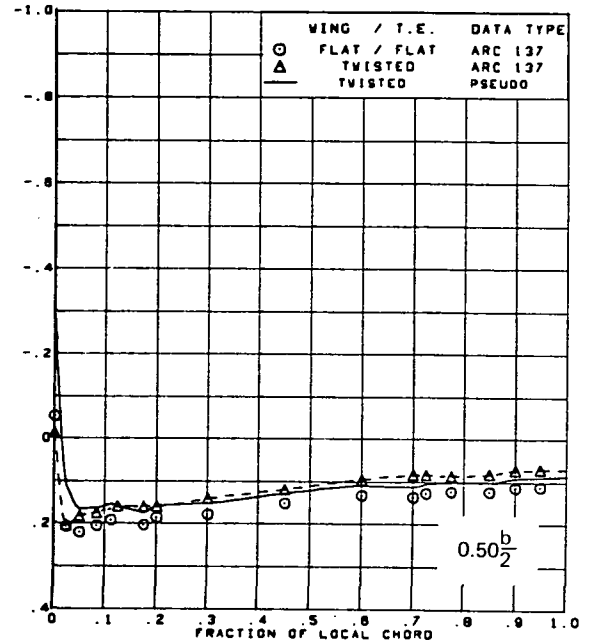
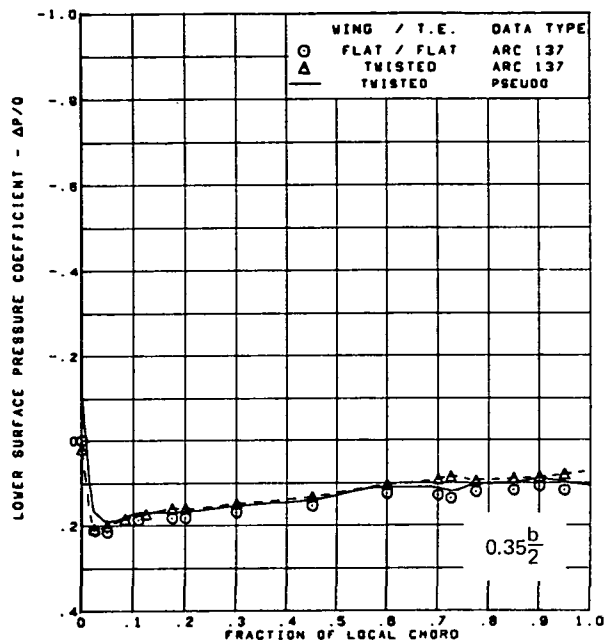
(m) (Concluded)

Figure 71.—(Continued)



(n) Lower Surface Chordwise Pressure Distributions,  $\alpha = 12^\circ$

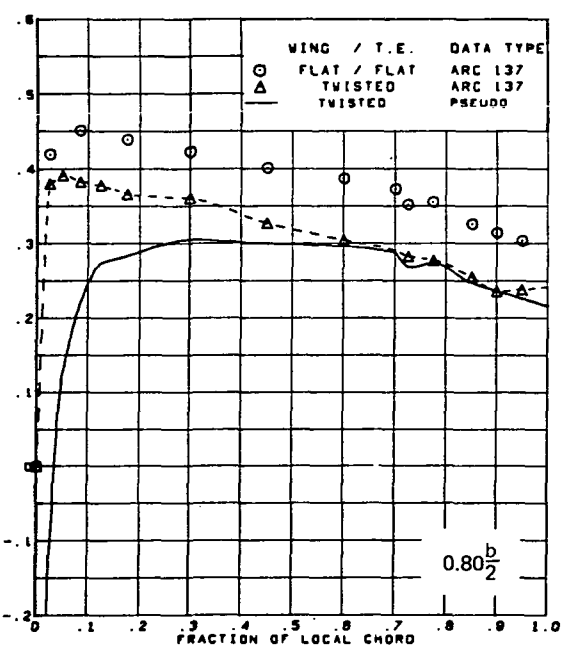
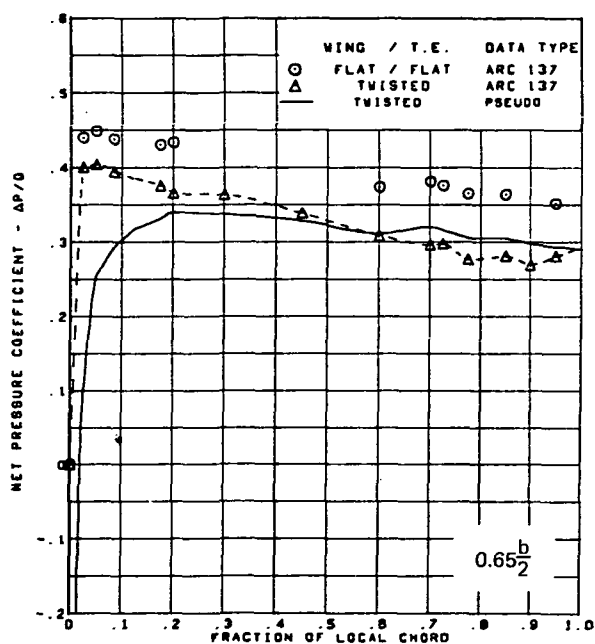
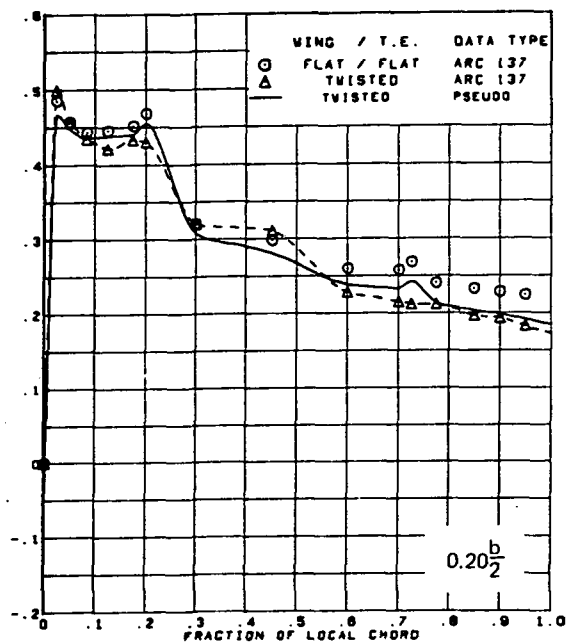
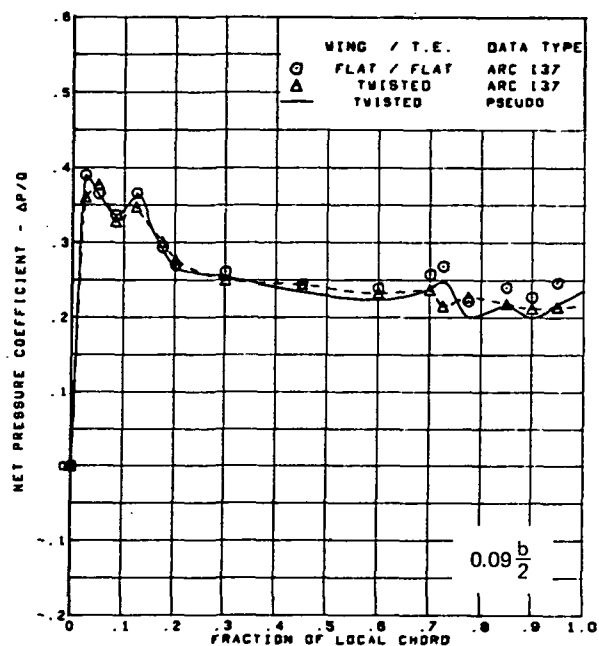
Figure 71.—(Continued)



$M = 2.10$   
 $\alpha = 12^\circ$   
 Rounded L.E.  
 L.E. deflection, full span =  $0.0^\circ$   
 T.E. deflection, full span =  $0.0^\circ$   
 Note:  $C_{p, \text{vacuum}} = -0.32$

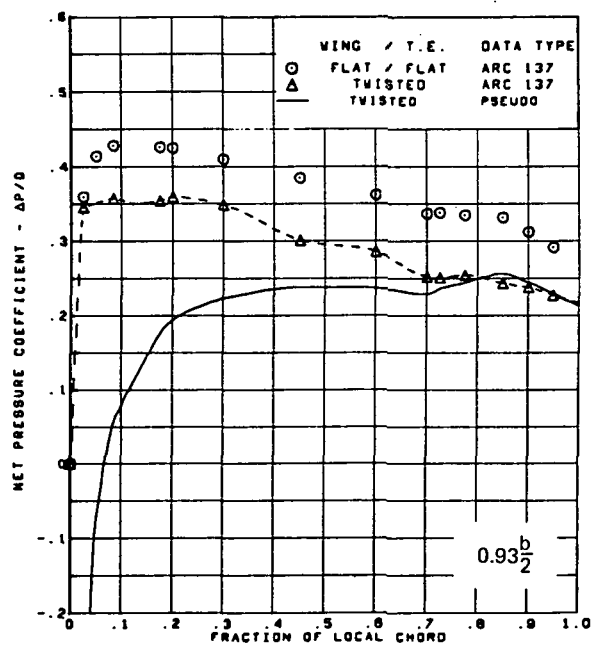
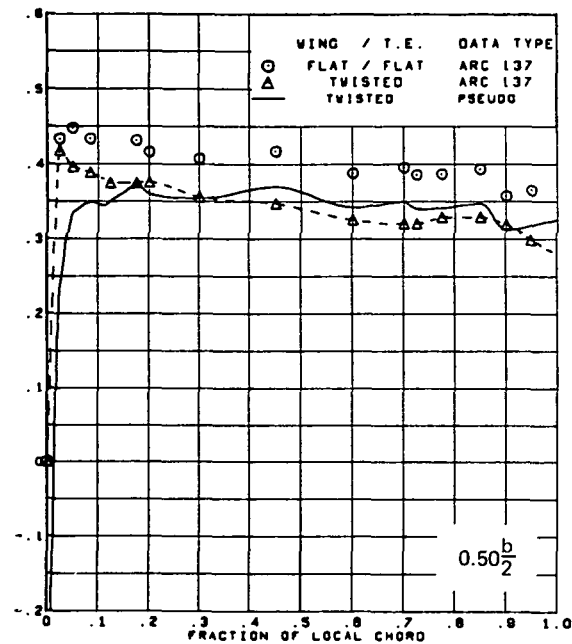
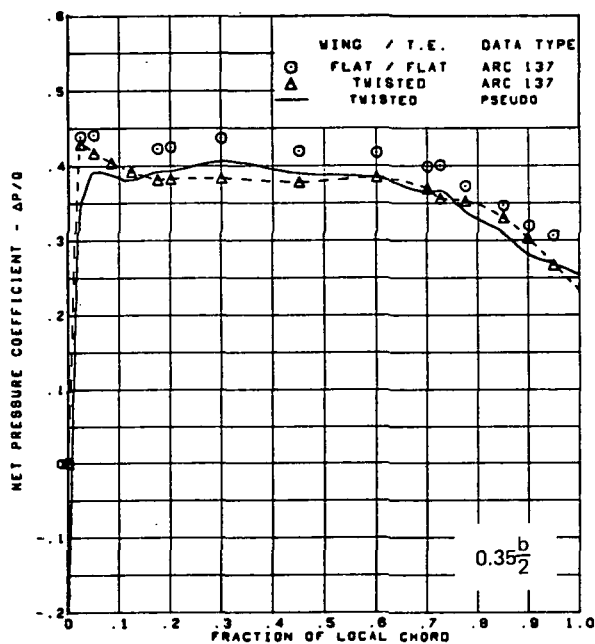
(n) (Concluded)

Figure 71.—(Continued)



(a) Net Chordwise Pressure Distributions,  $\alpha = 12^\circ$

Figure 71.—(Continued)



$M = 2.10$   
 $\alpha = 12^\circ$   
 Rounded L.E.  
 L.E. deflection, full span =  $0.0^\circ$   
 T.E. deflection, full span =  $0.0^\circ$

(o) (Concluded)

Figure 71.—(Concluded)